Enantioselective Pd(0)-Catalyzed Activation of Secondary C(sp^3)−H Bonds and Mechanistic Studies

Inauguraldissertation

zur

Erlangung der Würde eines Doktors der Philosophie

vorgelegt der

Philosophisch-Naturwissenschaftlichen Fakultät

der Universität Basel

von

Marco Zuccarello

2022

Originaldokument gespeichert auf dem Dokumentenserver der Universität Basel
edoc.unibas.ch

Genehmigt von der Philosophisch-Naturwissenschaftlichen Fakultät

Auf Antrag von

Prof. Dr. Olivier Baudoin

Prof. Dr. Christof Sparr

Prof. Dr. Clément Mazet

Basel, den 18.10.2022

Prof. Dr. Marcel Mayor

Acknowledgements

I would like to acknowledge my supervisor Prof. Dr. Olivier Baudoin for accepting me as a Master student and for my Doctoral studies. The stay in his group at the University of Basel has allowed me to work on interesting and challenging chemistry and therefore grow as a chemist and as a person.

I would like to thank Prof. Dr. Christof Sparr for the great support as second supervisor throughout my PhD studies. I am grateful for the interesting and helpful inputs that made me think “outside the box” and overcome many obstacles.

I thank Prof. Dr. Clément Mazet for accepting the co-examination of this doctoral thesis and Prof. Dr. Andreas Pfaltz for chairing the PhD defence.

I thank Dr. Matthew Wheatley for tirelessly proofreading the present Doctoral thesis. Since you joined the Baudoin group, it has been a blast to work with you. Thank you for the great chemistry discussions and for the numerous laughter we had together.

I am grateful to my brother Dr. Giuseppe Zuccarello, who also greatly contributed to the proofreading of this Manuscript. Having a chemist in the family is a luxury that not everyone can have. Thank you not only for the great support and discussions in chemistry but also for having the right answer for all my questions in life.

I would like to express my gratitude to Dr. Stefania Vergura for proofreading one of the chapters and for the great time we had inside and outside the lab. Despite our “difficult” start, I much enjoyed working with you and I am happy that our paths crossed in the Baudoin group.

I thank Dr. Romain Melot, who supervised me during my Master project and for the further collaboration at the start of my PhD studies. I was very lucky to learn from a very talented and creative chemist, which greatly facilitated the beginning of my PhD studies.

With that, I would also express my gratitude to David Savary and Yann Baumgartner, who were always available for discussions during my Master and Doctoral studies. I really much enjoyed also the time outside the lab with the both of you and I am looking forward to many more years of friendship.

The stay in the lab 208 was unique and I will keep it as a special memory. In particular, I would like to thank Dr. Antonin Clemenceau with whom I had a fresh new start in a somewhat tired lab. Then, I thank Takeru Miyakoshi, who joined shortly after, for the great moments and for teaching me many things about the Japanese culture. It helped me to stay calm and keep a clear mind in difficult situations. I would also like to thank Rafael Lombardi who joined the lab the last and kept the high standards. Your readiness to help others is unique and the time with you inside but also outside the lab has always been great.

I am grateful for the time I spent with past and present group members. Your contributions have been key to the success of this thesis.

The Secretaries Marina Mambelli-Johnson and Nathalie Plattner-Longhi have never hesitated to support me with important bureaucracy that unfortunately still remains a part of a PhD study. I therefore thank you for your great helpfulness.

I thank the “Werkstatt-Team” consisting of Hisni Meha, Andreas Sohler and Marcus Ast, who worked tirelessly on the maintenance of the building, making sure that our research would never come to a stop.

Ringrazio I miei genitori Lina Cuturi e Antonino Zuccarello per il loro sostegno durante il dottorato. Grazie per tutti i sacrifici che avete fatto per me durante tutta la mia vita rendendo possibile di portare a termine tutti i miei studi fino al giorno d‘oggi.

The results discussed in this doctoral thesis were published in:

R. Melot[‡], **M. Zuccarello**[‡], D. Cavalli, N. Niggli, M. Devereux, T. Bürgi, O. Baudoin "Palladium(0)-Catalyzed Enantioselective Intramolecular Arylation of Enantiotopic Secondary C−H Bonds" *Angew. Chem. Int. Ed.* **2021**, *60*, 7245−7250. ([‡] Denotes equal contribution)

Table of contents

Prologue 1

List of abbreviations 3

Abstract 5

General Objectives 7

Chapter 1: Introduction 9

1.1 General aspects 9

1.1.1 Cross-coupling reactions to form C−C and C−X Bonds 9

1.1.2 The Hoffmann-Löffler-Freytag reaction-early advances in C−H bond functionalization 9

1.1.3 Transition metal-catalyzed C−H functionalization 10

1.2 Pd-catalyzed C−H bond activation 13

1.2.1 Pd(0)-catalyzed intramolecular C(sp^2)−H bond activation for the formation of small- to medium-sized rings 14

1.2.2 Pd(0)-catalyzed intramolecular C(sp^3)−H bond activation 22

Chapter 2: Palladium(0)-catalyzed enantioselective intramolecular arylation of enantiotopic secondary C−H bonds for the synthesis of chiral indanes 29

2.1 Introduction: Pd(0)-catalyzed enantioselective activation of C(sp^3)−H bonds 29

2.1.1 Activation of methyl and methylene C−H bonds 29

2.2 Enantioselective Pd(0)-catalyzed intramolecular activation of methylene C−H bonds 35

2.2.1 Optimization of reaction conditions 35

2.2.2 Scope of the Pd(0)-catalyzed asymmetric synthesis of indanes 42

2.2.3 Evaluation of steric properties of IBioxR ligands 46

2.2.4 Application of enantioselective Pd(0)-catalyzed C(sp^3)−H bond activation in total synthesis of natural products 48

2.3 Expansion of enantioselective Pd(0)-catalyzed activation of secondary C−H bonds to different substrate families 50

2.4 Conclusion 53

Chapter 3: The effect of α-substitution on the reactivity of Pd(0)-catalyzed C(sp^3)−H activation for the formation of indanes 55

3.1 Introduction 55

3.2 The effect of α-substitution on the reactivity of Pd(0)-catalyzed C(sp^3)−H arylation 58

3.2.1 Optimization of the catalytic system. 58

3.2.2 Mechanistic aspects of the Pd(0)-catalyzed methylene C(sp^3)−H bond activation: KIE, orders in reaction components and stirring rate experiments 60

3.2.3 Influence of α-substitution on the reactivity of methylene C(sp^3)−H bonds 64

3.2.4 DFT calculations 65

3.3 Conclusion 67

Chapter 4: Enantioselective remote C(sp^3)−H activation by 1,4-Pd shift 69

4.1 Introduction 69

4.2 Studies on Pd(0)-catalyzed enantioselective remote C(sp^3)−H activation 73

4.2.1 Enantioselective synthesis of oxygen containing heterocycles. 73

4.2.2 Synthesis of chromanones 75

4.3 Conclusion 77

5. General conclusions 79

6. Experimental part 81

6.1 Palladium(0)-catalyzed enantioselective intramolecular arylation of enantiotopic secondary C−H bonds for the synthesis of chiral indanes 82

6.1.1 Synthesis of IBioxR ligands and well-defined Pd-complexes 82

6.1.2 Substrates synthesis 89

6.1.3 Enantioselective C(sp^3)–H arylation 104

6.1.4 Effect of the ligand structure on the enantioselectivity 115

6.1.5 Determination of absolute configuration of 2.45c, 2.45t and 2.45ja by VCD spectroscopy 116

6.1.6 Synthesis of new substrates for enantioselective C(sp^3)−H activation 126

6.2 The effect of α-substitution on the reactivity of Pd(0)-catalyzed C(sp^3)−H activation for the formation of indanes 130

6.2.1 Catalyst preparation 130

6.2.2 Substrate and reference for proto-dehalogenation synthesis 131

6.2.3 Product syntheses 137

6.2.4 Kinetic experiments 141

6.3 Enantioselective remote C(sp^3)−H activation by 1,4-Pd shift 150

6.3.1 Substrate synthesis 150

7. References 153

8. Spectra 161

Prologue

The present doctoral thesis is subdivided into five main parts including one chapter on general introduction, three chapters describing research results and one general conclusion. At the beginning of each research chapter, a specific introduction into the topic is provided followed by results and discussion and a conclusion. The structures and references are numbered continuously throughout the thesis. The experimental section is found at the end of the thesis.

Chapter 1: gives an introduction on fundamental aspects of transition metal catalyzed C−H activation and summarizes the most successful and pivotal examples for the development of the intramolecular Pd(0)-catalyzed C−H activation reaction to form small- and medium-sized rings.

Chapter 2: presents the design and optimization of a new Pd(0)/NHC* catalytic system for the activation of secondary C−H bonds to form chiral indanes. The project was developed in collaboration with Romain Melot, Diana Cavalli and Nadja Niggli. The presented results are published in *Angew. Chem. Int. Ed.* **2021**, *60*, 7245−7250.

Chapter 3: discusses the influence of α-substituents on the reactivity of C(sp^3)−H bonds based on differences in initial rates. Kinetic analysis of the reaction showed that the C−H abstraction step is rate-limiting, thus confirming that the comparison is relevant. The study was conducted in collaboration with Dr. Matthew Wheatley and his results are included in the chapter. At the time of writing this thesis, the manuscript is in preparation.

Chapter 4: describes preliminary results on the optimization of an enantioselective Pd(0)/L* catalytic system to activate remote C(sp^3)−H bonds enabled by 1,4-Pd shift. This strategy has seen significant developments over the past 5 years and complements the direct Pd(0)-catalyzed C−H activation methods in terms of structures that can be prepared.

A **General conclusion** is provided at the end of this thesis.

List of abbreviations

$\%V_{\mathrm{Bur}}$	Percentage of buried volume
$\%V_{\mathrm{Bur(QD)}}$	Quadrant difference buried volume
Ac	Acetyl
Alk	Alkyl
AMLA	Ambiphylic Metal-Ligand Activation
Ar	Aryl
Boc	*ter*-Butyloxycarbonyl
CAAC	Cyclic Alkyl Amino Carbene
CMD	Concerted Metalation Deprotonation
Cp	Cyclopentadiene
CPME	Cyclopentyl methyl ether
*c*Pr	Cyclopropyl
Cy	Cyclohexyl
dba	Dibenzylideneacetone
DCE	1,2-dichloroethane
DFT	Density Functional Theory
DG	Directing group
DMAP	*N*,*N*-dimethylaminopyridine
DMBA	1,3-Dimethylbarbituric acid
DMF	*N*,*N*-dimethylformamide
DMSO	Dimethylsulfoxide
DTP	Dithiodiketopiperazine
EDG	Electron Donating Group
ESI	Electronspray Ionization
EWH	Electron Withdrawing Group
GC-MS	Gas Chromatography-Mass Spectrometry
HAT	Hydrogen Atom Transfer
HRMS	High Resolution Mass Spectrometry
*i*Pr	Isopropyl
KIE	Kinetic Isotope Effect
L	Ligand
LG	Leaving Group

M	Metal
Mes	Mesityl
Mp	Melting point
NHC	*N*-Heterocyclic Carbene
NMR	Nuclear Magnetic Resonance
PG	Protecting Group
PIP	2-(Pyridine-2-yl)isopropyl
Piv	*tert*-Butyl Carboxyl
PMP	*p*-methoxy phenyl
*t*Bu	tert-Butyl
THF	Tetrahydrofuran
TM	Transition Metal
TLC	Thin layer chromatography
TS	Transition State
VCD	Vibrational Circular Dichroism
VTNA	Variable Time Normalization Analysis

Abstract

Direct transition metal catalyzed C−H bond functionalization has emerged as a powerful strategy to form new C−C or C−X bonds over the past decades. Advantages such as no requirement for pre-functionalization of the reagents and therefore the reduced metal waste makes it an attractive alternative to the well-established cross-coupling reactions. In this regard, Pd(0)-catalyzed C(sp^3)−H activation has been applied in the past for the construction of complex molecules and in numerous total syntheses of natural products. In addition, elegant enantioselective methodologies have granted access to important scalemic products for the pharmaceutical and agrochemical industry. However, most of these methods rely on the desymmetrization of prochiral alkyl groups leading to the formation of the stereogenic center distal to the activation site. The activation of enantiotopic secondary C−H bonds remains underdeveloped, mainly attributed to their low intrinsic reactivity, with only one report on the synthesis of β-lactams.

To address this long-standing challenge, a highly reactive Pd/NHC catalytic system was design and optimized for the synthesis of chiral indanes. A variety of products were obtained in good to high yields and high enantioselectivities using IBioxR NHC ligands developed by the Glorius group. Furthermore, the first synthesis of chiral 3^{ary} amides by Pd(0)-catalyzed C(sp^3)−H activation was described in consistent high enantioselectivites. Moreover, a stereochemical analysis provided valuable insights on the relationship between ligand structure and enantioinduction.

Mechanistic studies were performed on the newly developed Pd/NHC catalyzed activation of methylene C−H bonds to examine the selectivity trends observed in the course of the development of the Pd(0)-catalyzed C(sp^3)−H activation reaction. For instance, primary C−H bonds are preferentially activated over secondary C−H bonds or the selectivity between C−H bonds is altered by changing the substituent in α-position. In contrast to C(sp^2)−H bond activation, where the use of Hammet plots has helped to quantify the influence of substituents with different electronic properties on the C−H activation process, the design and development of new C(sp^3)−H activation methods has been mainly guided by chemical intuition. In this context, a reactivity scale was constructed putting C(sp^3)−H bonds differing in α-substitution on a series of most to least reactive by performing initial rate experiments. Prior kinetic isotope studies and kinetic analysis of the reaction to obtain the orders in reaction components confirmed the C−H activation step to be rate-limiting, thus suggesting that the comparison of the different C−H bonds is significant.

The activation of remote C(sp^3)−H bonds enabled by 1,4-Pd shift has experienced significant growth in the past 5 years. With this strategy new type of complex molecules, lacking structural motifs promoting the ring closure otherwise required for direct C−H activation, could be synthesized. Nevertheless, no enantioselective methods are reported to this date. To this end, new substrates were designed and synthesized and preliminary screening of chiral ligand families previously applied in direct enantioselective Pd(0)-catalyzed C−H activation was undertaken to contribute to the progress of asymmetric remote C(sp^3)−H activation.

General Objectives

The objectives of this Doctoral Thesis include the development of an enantioselective method for the activation of secondary C−H bonds under Pd(0) catalysis and the study of the operative mechanism. In particular, our investigations focused on:

- The synthesis of enantioenriched indanes and amides featuring a tertiary α-stereogenic center using chiral IBiox-type ligands.

- The correlation between steric properties of the ligands and enantioselectivity.

- The effect of α-substitution on the reaction rate employing the visual kinetic analysis method variable time normalization.

Chapter 1: Introduction

1.1 General aspects

1.1.1 Cross-coupling reactions to form C−C and C−X Bonds

Synthetic organic chemistry is driven by the formation of new chemical bonds to construct highly complex molecules from simple and abundant building blocks. In particular, the formation of C−C bonds is of central importance. A major historical milestone was set with the discovery of catalytic cross-coupling reactions complementing classical functional group interconversion chemistry. In fact, the pioneering efforts by Heck, Suzuki and Negishi on Pd-catalyzed cross-couplings was awarded with the Nobel prize in 2010.[1,2] The general catalytic cycle for this transformation starts with the oxidative addition of the active M^0 species into the carbon−halogen (or pseudo halogen) bond of substrate **1.1** leading to the formation of oxidative addition complex **1.2** (Scheme 1.1). Then, transmetalation with a nucleophilic coupling partner, typically of structure R−Y, gives intermediate **1.3**, which upon reductive elimination is transformed to the desired product and the catalytic active M^0 species is restored.

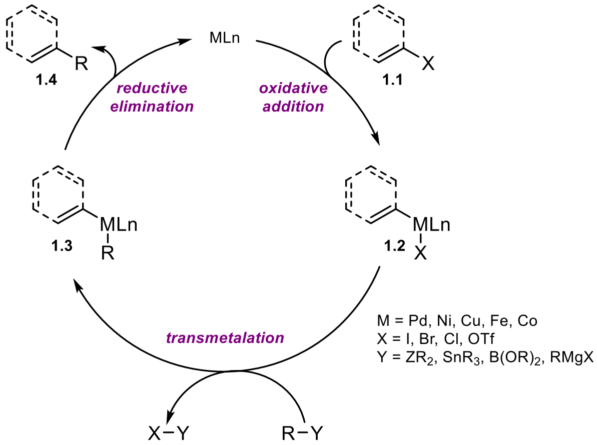

M = Pd, Ni, Cu, Fe, Co
X = I, Br, Cl, OTf
Y = ZR_2, SnR_3, $B(OR)_2$, RMgX

Scheme 1.1: General catalytic cycle for cross-coupling reactions.

To date, cross-coupling reactions have been expanded to C−heteroatom bond formation[3,4] and catalysts based on transition metals such as Ni,[2] Co,[5] Fe[2] and Cu[3,4,6,7] have been employed with numerous applications in the total synthesis of natural products,[8] medicinal chemistry, agricultural chemistry and ton-scale industrial processes. However, despite the great utility of this extremely powerful tool, major drawbacks include the use of expensive metal-containing reagents and the high quantities of toxic metal waste that comes with it. Thus, finding more environmentally friendly and cheaper alternatives has been a long-standing challenge.

1.1.2 The Hoffmann-Löffler-Freytag reaction-early advances in C−H bond functionalization

Organic molecules consist of linear or cyclic consecutive hydrocarbon motifs, interrupted by heteroatoms such as nitrogen, oxygen, sulfur and phosphorus. Thus, C−H bonds are omnipresent in organic chemistry and their direct and selective functionalization to form new C−C, C−O, C−N and C−X bonds constitute a step economical and sustainable alternative to cross-coupling chemistry. Molecular diversity can be easily achieved by selective functionalization of distinct C−H bonds based on electronic and steric properties on a complex precursor, facilitating late-stage functionalisation of active compounds.[9,10] Additionally, direct C−H functionalization eliminates the preparation of metal containing coupling partners as required for cross-couplings, thus significantly reducing, synthetic steps, toxic waste and costs. Early advances in C−H bond functionalization were made by Hoffmann showing that homolysis of bromo- and chloroamines led to cyclization with methylene or methyl groups. Homolysis of the N−Br bond on substrate **1.5** forms a highly reactive *N*-centered radical, which subsequently triggers a 1,5 hydrogen atom transfer (HAT) to form **1.7** after recombination. The ring is then closed by nucleophilic substitution completing the synthesis of nicotine (**1.8**, Scheme 1.2a). Similarly, conanine alkaloids were prepared by Buchsacher and Jeger[11] by subjecting substrate **1.9** to a mixture of sulfuric and acetic acid. Although this reaction proceeds through an unstable primary radical intermediate **1.11**, the 1,5-HAT is facilitated by the structural preorganisation of the molecule (Scheme 1.2b). In the same year, Corey reported the synthesis of the structural related dehydroconessine employing similar reaction conditions.[12]

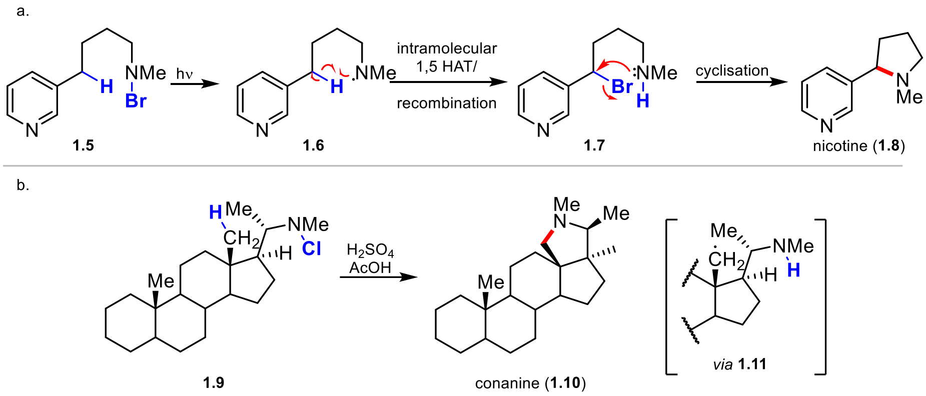

Scheme 1.2: Early applications of the Hoffmann-Löffler-Freytag reaction.

This transformation, to date known as the Hoffman-Löffler-Freytag reaction, set the fundament for the consideration of inherently inert C−H bonds as a retron for various functional groups.

1.1.3 Transition metal-catalyzed C−H functionalization

1.1.3.1 general mechanisms

In the past decades, transition metal-catalyzed C−H functionalization has experienced significant advancement as it constitutes an elegant strategy to introduce molecular complexity starting from simple substrates. However, as most organic molecules possess several C−H bonds, the selective functionalization of one C−H bond over the other remains highly challenging. As described by Sanford,[13] two main mechanisms are operative in transition metal-catalyzed C−H functionalization. (1) In the *"inner-sphere"* mechanism, an organometallic intermediate of structure **1.13** is formed after C−H bond cleavage (Scheme 1.3a). Regio- and stereoselectivity of functionalization are driven by structural and electronic properties of the formed intermediate. In this type of transformation high selectivity for the less hindered C−H bond is observed. However, the selectivity can be influenced not only by the mechanism of the C−H bond cleavage but also the ligand environment on the metal centre. This mechanism is encountered in C−H activation processes but also in the oxidative addition into C−H bonds and σ-bond metathesis.[14]

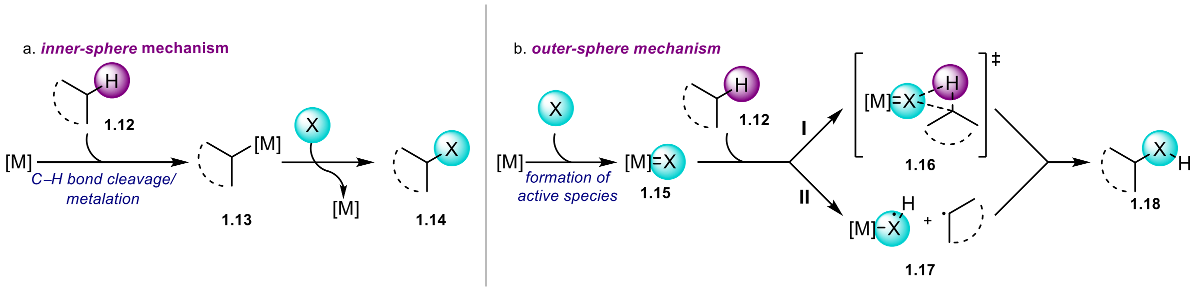
a. inner-sphere mechanism
H
1.12
[M]
C−H bond cleavage/ metalation
[M]
1.13
X
[M]
X
1.14
b. outer-sphere mechanism
X
[M]
formation of active species
[M]=X
1.15
H
1.12
I
II
[M]=X
H
1.16
‡
[M]-X
H
1.17
X
H
1.18

Scheme 1.3: a. Inner-sphere mechanism. b. Outer-sphere mechanism.

(2) The *"outer-sphere"* mechanism is reminiscent of biological oxidation reactions catalyzed by cytochrome P450 and methane monooxygenase.[15,16] Initially, a high oxidation state metal complex **1.15** is formed possessing an activated ligand X (Scheme 1.3b). The ligand then reacts with the C−H bond of substrate **1.12** either by direct insertion (path **I**) or H-atom abstraction/rebound (path **II**). As opposed to the inner-sphere mechanism, the substrate directly reacts with the ligand and not with the metal center. In this case the selectivity is driven by the build-up of cationic or radical character and therefore weaker bonds such as benzylic, allylic, 3^{ary} or in α-position to heteroatoms are cleaved preferentially. Typical reactions proceeding over an outer-sphere mechanism are carbenoid [17,18]/nitrenoid[19,20] C−H insertion[17,18] and C−H bond oxidation.[21,22]

1.1.3.2 Transition metal-catalyzed C−H bond activation

Labinger and Bercaw[23] defined C−H bond activation as a process where a distinct C−[M] bond is formed after cleavage of a C−H bond. Thus, C−H activation falls into the category of inner-sphere mechanisms of C−H functionalization (see section 1.1.3.1, Scheme 1.3a). Depending on the nature of the substrate, five different mechanisms have been widely accepted.[24,25] (1) In the *oxidative addition* mechanism the metal species oxidatively inserts into the carbon-hydrogen bond of **1.12** leading to transition metal intermediate **1.20** (Scheme 1.4a).

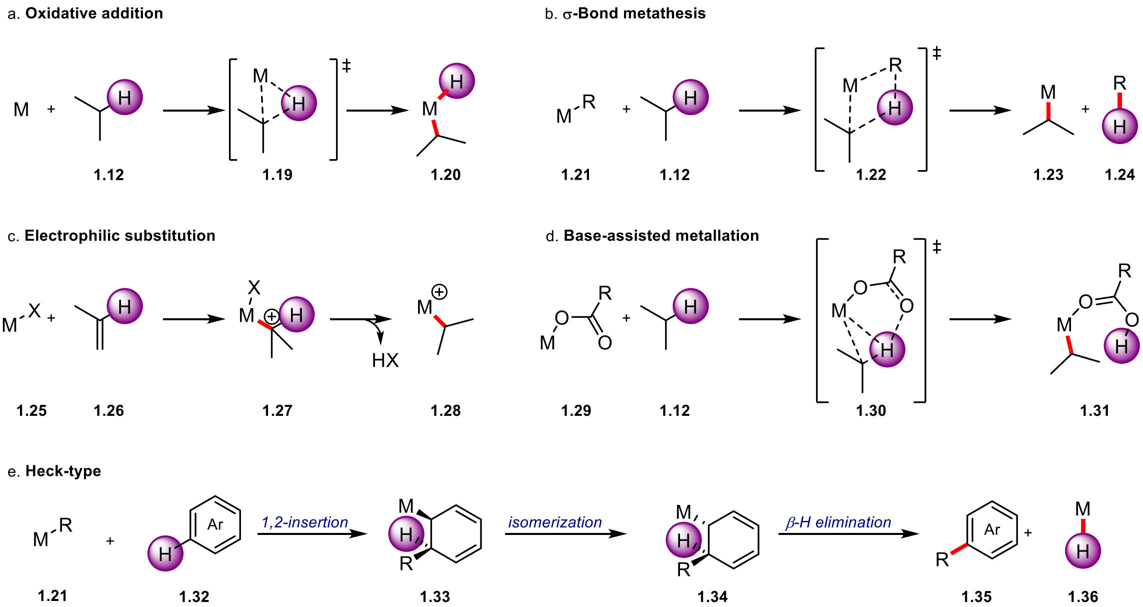
a. Oxidative addition
M
H
1.12
M
H
‡
1.19
H
M
1.20
b. σ-Bond metathesis
M R
1.21
H
1.12
M
R
H
‡
1.22
M
1.23
R
H
1.24
c. Electrophilic substitution
M X
1.25
H
1.26
X
M
H
1.27
HX
M
1.28
d. Base-assisted metallation
O R O M
1.29
H
1.12
R O O M H
‡
1.30
R O O M H
1.31
e. Heck-type
M R
1.21
Ar
H
1.32
1,2-insertion
M H R
1.33
isomerization
M H R
1.34
β-H elimination
Ar R
1.35
M H
1.36

Scheme 1.4: Mechanisms of C−H bond activation.

(2) *σ-Bond metathesis* proceeds through 4-membered transition state **1.22** leading to the formation of intermediates **1.23** and **1.24**. This pathway is generally preferred by early transition metals (Scheme 1.4b). (3) During the

electrophilic substitution mechanism the metal species is attacked by aromatic or unsaturated substrate **1.26** forming a positively charged metal intermediate **1.27**. Abstraction of the proton gives structure **1.28**. (4) In the *base assisted mechanism* a carboxylate or carbonate ligand is involved in the proton abstraction over a concerted process forming cyclic transition state **1.30**. To date, this mechanism is known as concerted metalation deprotonation (CMD) or ambiphilic metal−ligand activation (AMLA).[26,27] Finally, (5) the *Heck-type* mechanism begins with 1,2-insertion of organometallic species **1.21** into aromatic structures of type **1.32** leading to intermediate **1.33**. After isomerization, structure **1.34** is formed with the metal and hydrogen substituents in *syn* relationship to each other. β-H Elimination gives then functionalized product **1.35** and metal-hydride species **1.36**.

Additionally, transition metal catalyzed C−H activation reactions can be further subdivided in three different classes.[28] (1) *Directed C−H activation* reactions rely on the coordination of the active catalyst to a Lewis-basic acceptor tethered to the substrate (**1.37**). Upon coordination of the metal structure **1.38** is formed which is transformed to product **1.39** by functionalization (Figure 1.1a). Typically, monodentate amides, pyridines, esters or imines as well as bidentate directing groups are utilized to ensure selectivity.[29] This strategy, although not ideal as often the directing group is not part of the desired product, it is the most widespread one. However, recent efforts have been focused on the use of transient directing groups, which are attached to the substrate *in situ* and cleaved after C−H activation.[30–35] (2) *Non-directed* or *undirected C−H activation* exploits the innate reactivity of the substrate. Selectivity is thereby guided by factors such as electronic properties of the C−H bond and steric hindrance. This method is more attractive since the installation and removal of a directing group can be avoided. Instead, the metal catalyst interacts directly with the C−H bond of substrate **1.40** forming metal complex **1.41**. Product **1.14** is then obtained after functionalization (Figure 1.1b). However, this transformation suffers from major drawbacks such as high catalyst loadings, harsh conditions and often difficult separations due to lower selectivity leading to mixtures of unseparable products. (3) Finally, in the third type of activation reactions the transition metal catalyst oxidatively inserts into a C−LG (LG = leaving group, halogens or pseudohalogens) bond of the substrate to form complex **1.43**, hence the name *oxidative addition-induced C−H activation* (Figure 1.1c). The oxidation state of the metal is thereby increased by two units and an external base is used to abstract the desired proton and form metalated complex **1.44**. Upon functionalization and reductive elimination product **1.45** is formed and the metal catalyst is reduced to its initial oxidation state.[25,36]

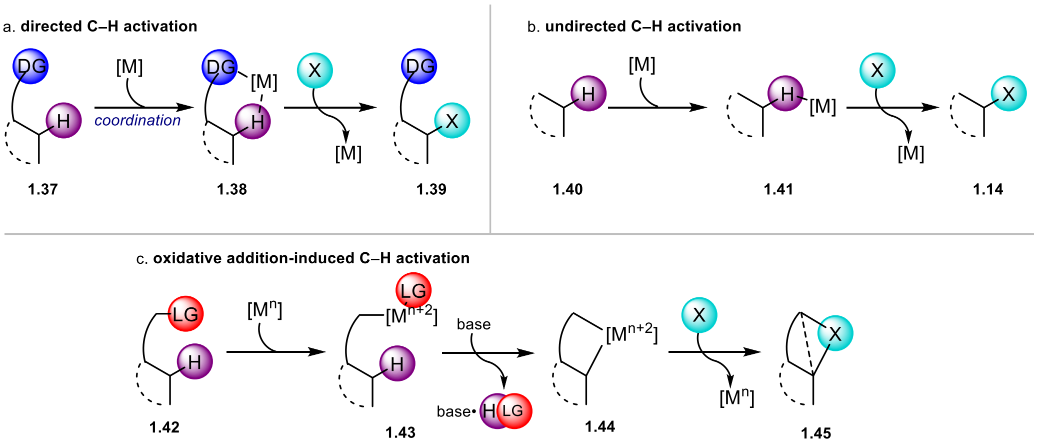
a. directed C–H activation
DG
H
[M]
coordination
[M]
X
1.37
1.38
1.39
b. undirected C–H activation
1.40
1.41
1.14
c. oxidative addition-induced C–H activation
LG
[Mn]
[Mn+2]
base
base•H LG
1.42
1.43
1.44
1.45

Figure 1.1: Different classes of C−H bond activation reactions. a Directed C−H activation b. Undirected C−H activation. c. Oxidative addition-induced C−H activation.

1.2 Pd-catalyzed C−H bond activation

Palladium is arguably one of the most widely used transition metals for C−H bond activation reactions and has been thoroughly reviewed in several articles.[36–39] This is mainly attributed to its ability to operate under several catalytic manifolds such as Pd(II)-Pd(0), Pd(II)-Pd(IV), and Pd(0)-Pd(II) among others.[38] The two first are more widespread in directed C−H activation reactions. Tipically, the Pd(II)-Pd(0) catalytic cycle starts with the activation of the C−H bond of substrate **1.47** leading to palladated species **1.48**. Ligand exchange, usually by trans metalation gives intermediate **1.50** from which product **1.51** is formed by reductive elimination (Scheme 1.5a). The resulting Pd(0) species is oxidized to regenerate catalytic active Pd(II) by an external oxidant. Similarly, the first step in the Pd(II)-(IV) manifold is the C−H activation of substrate **1.47** giving intermediate **1.48**. The functional group is then introduced to the catalyst by an oxidative process leading to Pd(IV) intermediate **1.56**. Product **1.51** is formed by reductive elimination releasing the catalytically active Pd(II) species (Scheme 1.5b).

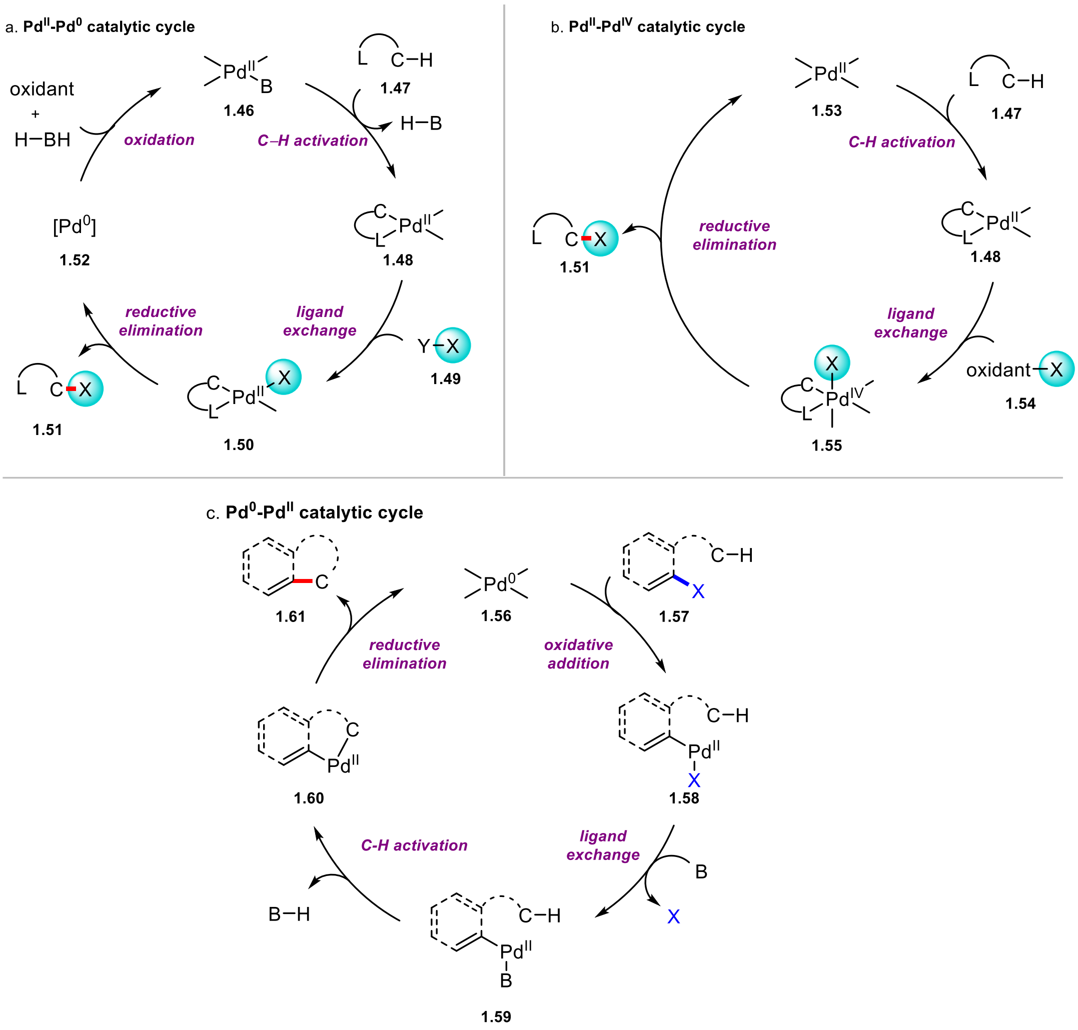
a. Pd^II-Pd^0 catalytic cycle
Pd^II B
1.46
L C−H
1.47
H−B
oxidant
+
H−BH
oxidation
C–H activation
[Pd^0]
1.52
C Pd^II L
1.48
reductive elimination
ligand exchange
Y−X
1.49
L C X
1.51
C Pd^II L X
1.50
b. Pd^II-Pd^IV catalytic cycle
Pd^II
1.53
L C−H
1.47
C-H activation
L C X
1.51
reductive elimination
C Pd^II L
1.48
ligand exchange
oxidant−X
1.54
X C Pd^IV L
1.55
c. Pd^0-Pd^II catalytic cycle
C
1.61
Pd^0
1.56
C−H X
1.57
reductive elimination
oxidative addition
C Pd^II
1.60
C−H Pd^II X
1.58
C-H activation
ligand exchange
B
X
B−H
C−H Pd^II B
1.59

Scheme 1.5: Catalytic cycles of Pd-catalyzed C−H activation. a Pd(II)-Pd(0) catalysis. b. Pd(II)-Pd(IV) catalysis. c. Pd(0)-Pd(II) catalysis.

The Pd(0)-Pd(II) manifold is generally operative in non-directed or intramolecular oxidative addition induced C−H activation (Scheme 1.5c). in this particular case the catalytic cycle begins with the oxidative addition of the Pd(0) species into C−X bond (X = (pseudo-) halogen) of substrate **1.57** generating Pd(II) intermediate **1.58**. After ligand exchange, C−H bond activation leads to cyclopalladated species **1.60** from which the product is obtained by reductive elimination with concomitant reduction of the Pd(II) to the active Pd(0) species. Notably, in all three cases the C−H activation reaction occurs from the Pd(II) species. Although the three manifolds are well established in C−H activation transformations,[24,39] the main focus of this introduction is the Pd(0)-Pd(II)-catalyzed intramolecular C−H activation.

1.2.1 Pd(0)-catalyzed intramolecular C(sp^2)−H bond activation for the formation of small- to medium-sized rings

The first example of Pd(0)-catalyzed activation of C(sp^2)−H bonds was reported by Ames in 1982.[40] Reacting cinnoquinoline **1.62a** in presence of catalytic Pd(OAc)$_2$ and ethyl acrylate gave dibenzofuranyl **1.63a** in 19% yield instead of the expected alkenlyation at the 3-position (Scheme 1.6). A similar reaction outcome was observed with **1.62b** giving product **1.63b** in 55% yield. In absence of ethyl acrylate no product formation was observed presumably, because the acrylate is responsible for the reduction of the Pd(II) precatalyst to the Pd(0) active species. Later, examples for the formation of 5 and 6 membered rings from the corresponding aryl iodides and arylbromide precursors were presented.[41,42] Substituted dibenzofurans (**1.64a-c**), carbazole-1-carboxylic acid **1.65**, fluorenone **1.66**, lactone **1.67** and lactam **1.68** were prepared in good to high yields.

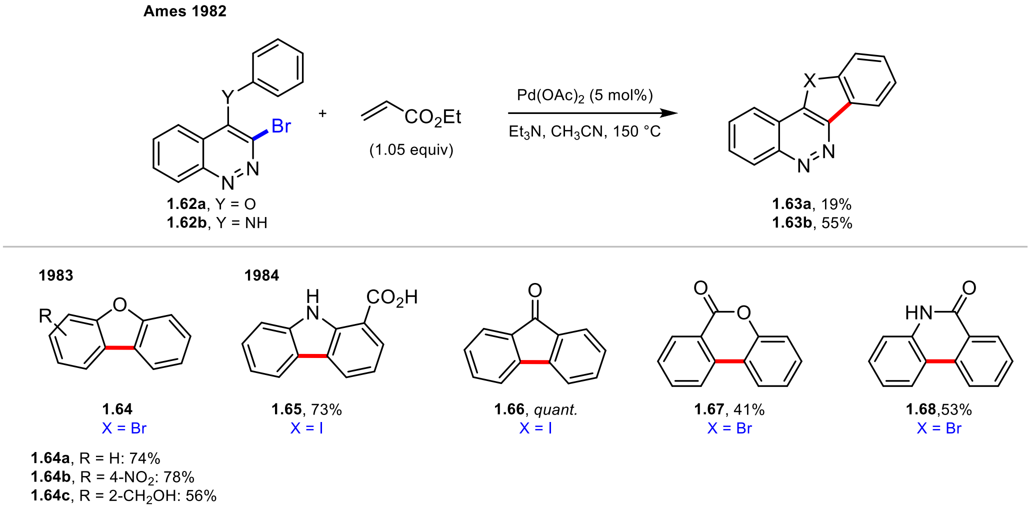
Ames 1982
Y
Br
N
N
+
CO$_2$Et
(1.05 equiv)
Pd(OAc)$_2$ (5 mol%)
Et$_3$N, CH$_3$CN, 150 °C
X
N
N
1.62a, Y = O
1.62b, Y = NH
1.63a, 19%
1.63b, 55%
1983
R
O
1.64
X = Br
1.64a, R = H: 74%
1.64b, R = 4-NO$_2$: 78%
1.64c, R = 2-CH$_2$OH: 56%
1984
H
N
CO$_2$H
1.65, 73%
X = I
O
1.66, quant.
X = I
O
O
1.67, 41%
X = Br
HN
O
1.68,53%
X = Br

Scheme 1.6: early contributions to Pd(0)-catalyzed C(sp^2)−H activation.

The first application in the total synthesis of ancistrocladisine (**1.72**) was reported by the Bringmann group in 1989 (Scheme 1.7). Starting from substituted phenol **1.69**, substrate **1.70** for the Pd(0)-catalyzed C(sp^2)−H activation was reached by Pictet-Spengler reaction with acetaldehyde and acylation of the phenol with the corresponding naphthoyl chloride. Subjecting **1.70** to catalytic amount of Pd(PPh$_3$)$_2$Cl in presence of NaOAc afforded **1.71** in 87% yield. The synthesis was completed by opening of the lactone ring, epimerization

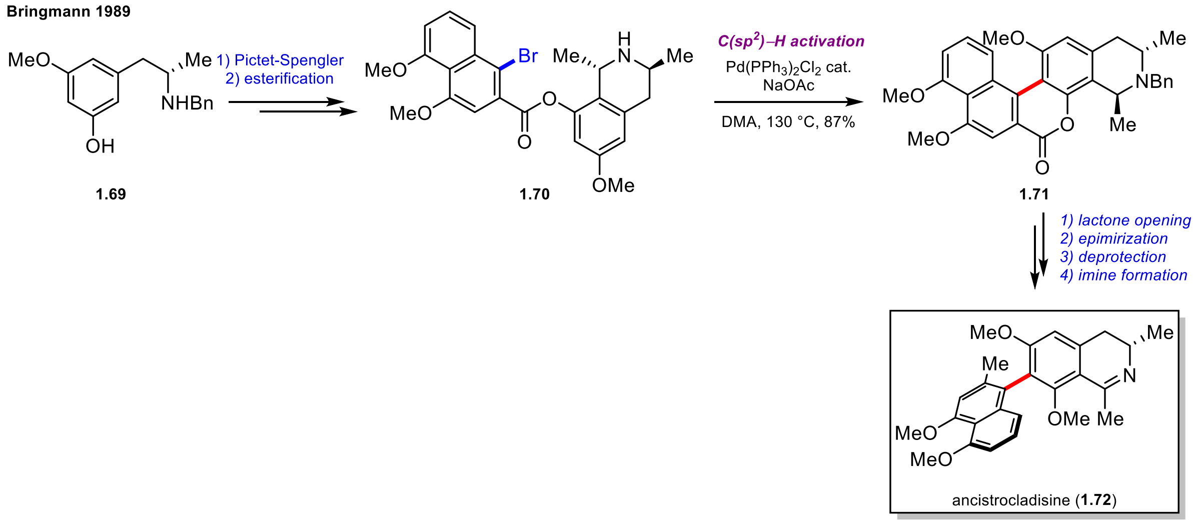
Bringmann 1989
1) Pictet-Spengler
2) esterification
C(sp2)–H activation
Pd(PPh3)2Cl2 cat.
NaOAc
DMA, 130 °C, 87%
1) lactone opening
2) epimirization
3) deprotection
4) imine formation
1.69
1.70
1.71
ancistrocladisine (1.72)

Scheme 1.7: First application of Pd(0)-catalyzed C(sp^2)−H activation: total synthesis of ancistrocladisine (**1.72**).

deprotection and imine formation. Although other examples of applications into the synthesis of important natural products were demonstrated by the Bringmann group[43,44] the scope of the method is limited and relies on harsh conditions including temperatures up to 190 °C.

Fagnou introduced the use of Buchwald-type ligands for the intramolecular arylation of C(sp^2)−H bonds.[45] Susbtrates of type **1.73** readily cyclised to tricyclic products **1.74** with high efficiency under catalyst loadings as low as 0.1 mol% Pd(OAc)$_2$ and 0.2 mol% of ligand **L1.1** (Scheme 1.8a). A broad scope of products featuring electron-donating (**1.74b**) and -withdrawing (**1.74c**) groups on the aromatic ring was presented. Additionally, the oxygen on the tether could be changed to a nitrogen or carbon (**1.74d**). The formation of a 7-membered ring (**1.74f**) was achieved by introducing an electron-withdrawing group in position of the dimethyl amino group on the biaryl ligand.

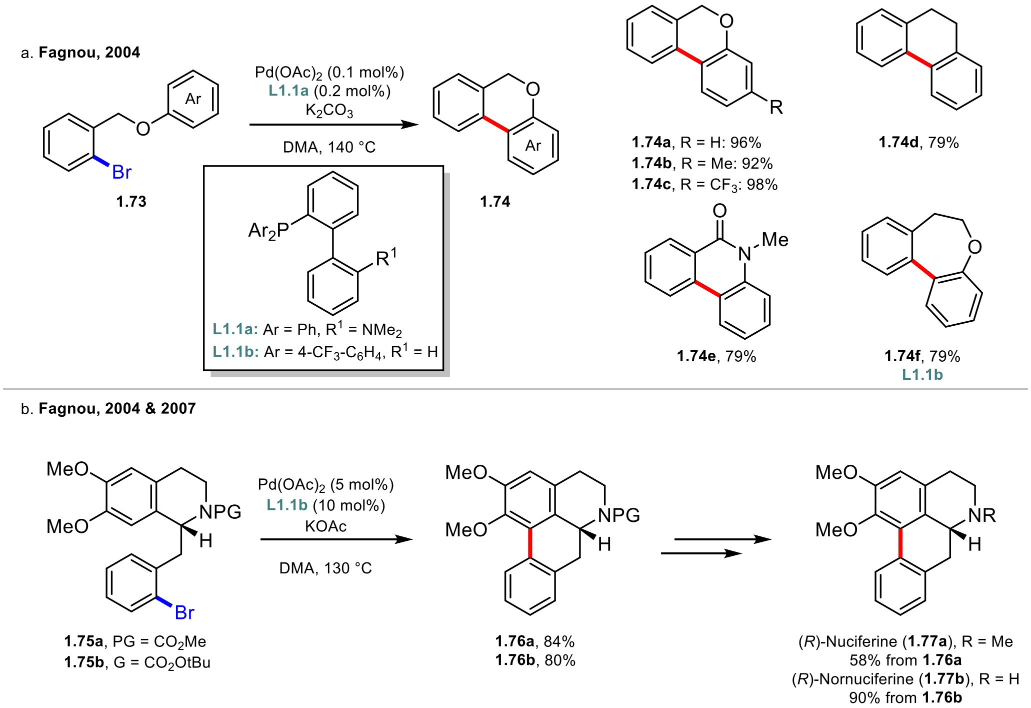
a. Fagnou, 2004
Pd(OAc)2 (0.1 mol%)
L1.1a (0.2 mol%)
K2CO3
DMA, 140 °C
1.73
1.74
L1.1a: Ar = Ph, R1 = NMe2
L1.1b: Ar = 4-CF3-C6H4, R1 = H
1.74a, R = H: 96%
1.74b, R = Me: 92%
1.74c, R = CF3: 98%
1.74d, 79%
1.74e, 79%
1.74f, 79%
L1.1b
b. Fagnou, 2004 & 2007
Pd(OAc)2 (5 mol%)
L1.1b (10 mol%)
KOAc
DMA, 130 °C
1.75a, PG = CO2Me
1.75b, G = CO2OtBu
1.76a, 84%
1.76b, 80%
(R)-Nuciferine (1.77a), R = Me
58% from 1.76a
(R)-Nornuciferine (1.77b), R = H
90% from 1.76b

Scheme 1.8: a. Highly efficient C(sp^2)−H arylation using Buchwald-type ligands. b. Application in total synthesis of (*R*)-Nuciferine (**1.77a**) and (*R*)-Nornuciferine (**1.77b**).

This improved protocol was applied in the total synthesis of aporphine alkaloids (Scheme 1.8b).[46,47] From substrates **1.75a** and **1.70b** differing in the protecting group of the amine, the corresponding tetracyclic cores **1.76a** and **1.76b** were obtained by C(sp^2)−H activation in 84% and 80% yield respectively. (*R*)-Nuciferine (**1.77a**) was then accessed by reduction of the CO_2Me protecting group of **1.76a** with $LiAlH_4$. Similarly, deprotection of the CO_2*t*Bu group on **1.76b** gave (*R*)-Nornuciferine (**1.77b**) in remarkable 90% yield. After this report, the field experienced a strong growth and several methods relying on the Pd(0)-catalyzed activation of C(sp^2)−H activation were disclosed.[25,48]

An important milestone was reached with a thorough mechanistic study of Echavarren and Maseras on the formation of phenanthrenes.[49,50] Subjecting substrates of type **1.78** under the conditions optimized by Fagnou and subsequent treatment with DDQ gave either product **1.79** or **1.80** depending on the nature of the R substituent on the aromatic ring (Scheme 1.9). It was found that when R was electron-withdrawing cyclisation preferentially occurred with the substituted aromatic ring giving product **1.79**. Conversely, product **1.80** was observed when R was of electron-donating nature. This is in disagreement with the electrophilic palladation mechanism originally thought to be operative. With density functional theory (DFT) calculations direct σ-bond metathesis (**TS1**) could be ruled out based on the high energy of 43.3 kcal mol^{-1}. Instead, a base-assisted proton abstraction mechanism either inter- or intramolecular (**TS2** and **TS3**) was found plausible.

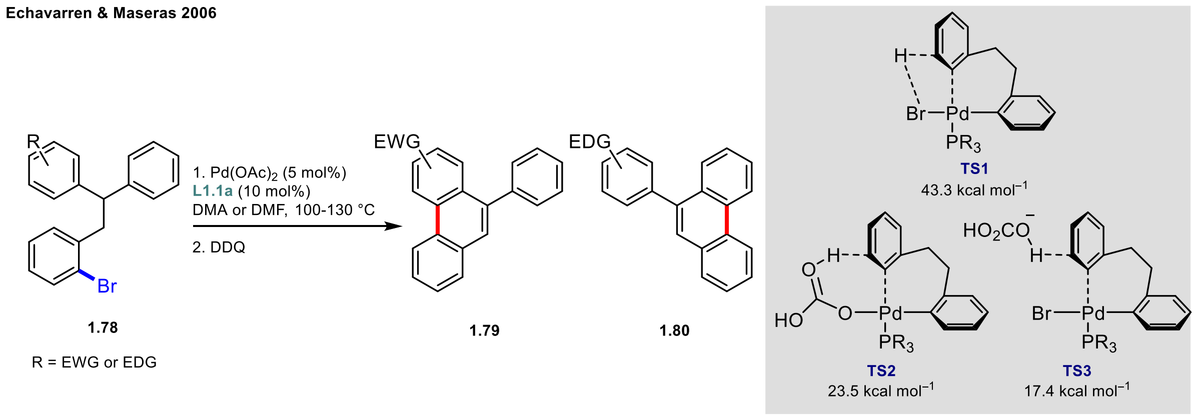

Scheme 1.9: Formation of phenanthrenes **1.79** and **1.80** and calculated transition states for C(sp^2)−H arylation.

Enantioselective C(sp^2)−H activation methods rely on the desymmetrization of prochiral substrates forming the stereogenic center distal to the C−H activation site or on the formation of a chiral axis or plane. The first example of asymmetric C(sp^2)−H activation was reported by the Cramer group in 2009.[51] Alkenyl triflates **1.81**, easily accessed from ketone precursors, were subjected to Pd(0) catalysis with chiral taddol-based phosphoramidite ligand **L1.2a** furnishing indanes **1.82** in high yields and enantioselectivities (Scheme 1.10a). Later the desymmetrization of arylbromide substrates of type **1.83** to form 7-membered rings using a similar phosphoramidite ligand **L1.2b** was demonstrated by the same group. In this case, the reaction proceeds through a thermodynamically unfavoured 8-membered palladacycle. Dibenzazepinone products **1.84** featuring a quaternary stereogenic center were obtained in excellent yields and enantioselectivities.

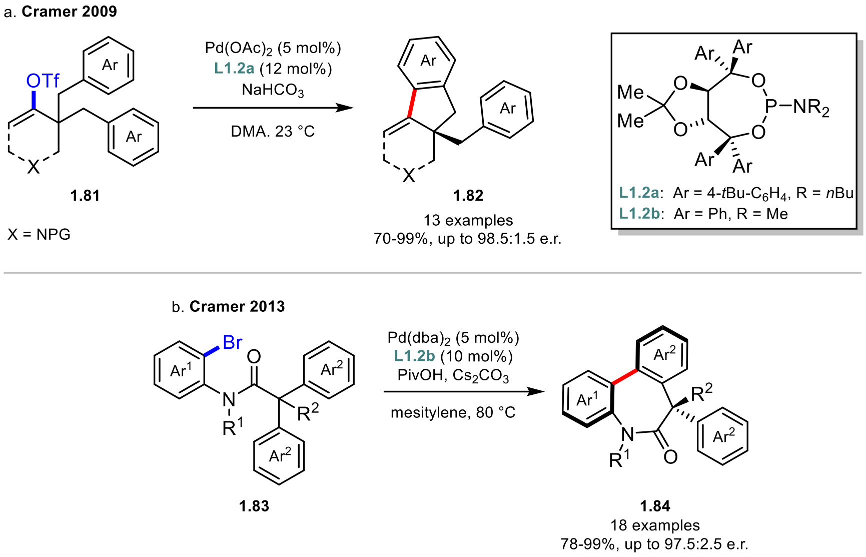
a. Cramer 2009
OTf
Ar
Ar
X
1.81
X = NPG
Pd(OAc)$_2$ (5 mol%)
L1.2a (12 mol%)
NaHCO$_3$
DMA. 23 °C
Ar
Ar
X
1.82
13 examples
70-99%, up to 98.5:1.5 e.r.
Ar, Ar
Me
Me
O
O
O
P−NR$_2$
O
Ar Ar
L1.2a: Ar = 4-tBu-C$_6$H$_4$, R = nBu
L1.2b: Ar = Ph, R = Me
b. Cramer 2013
Br
Ar^1
O
N
R^1
Ar^2
R^2
Ar^2
1.83
Pd(dba)$_2$ (5 mol%)
L1.2b (10 mol%)
PivOH, Cs$_2$CO$_3$
mesitylene, 80 °C
Ar^2
Ar^1
R^2
Ar^2
N
R^1
O
1.84
18 examples
78-99%, up to 97.5:2.5 e.r.

Scheme 1.10: First report of enantioselective C(sp^2)−H activation.

The Baudoin group reported the use of bifunctional ligands for enantioselective C(sp^2)−H activation. Binapthalene derived phosphine ligands **L1.3** featuring a carboxylic acid substituent on the aromatic scaffold are responsible for both, proton abstraction and enantioinduction (Scheme 1.11a). Substrates **1.85** were efficiently converted to dihydrophenanthridines **1.86** with high selectivities of up to 98.5:1.5 e.r. It was found that the length of the linker of the carboxylic acid to the aromatic ring has an impact on the enantioselectivity. The e.r. value decreased with increasing chain length of the linker. The control experiments with 1.0 equivalent of the potassium salt derived from ligand **L1.3a** omitting Cs_2CO_3 showed that the product was formed in in comparable yield and selectivity. This result suggests that the ligand is operating in bifunctional mode and that Cs_2CO_3 is not involved in the proton abstraction process. Additionally, parallel kinetic resolution from racemic mixtures of **1.85** bearing different aromatic groups undergoing C−H activation was achieved leading to the formation of two enantioenriched products. A similar protocol was employed in the synthesis of highly strained fluoradenes **1.87** and other warped molecules of type **1.88** by the same group (Scheme 1.11b).

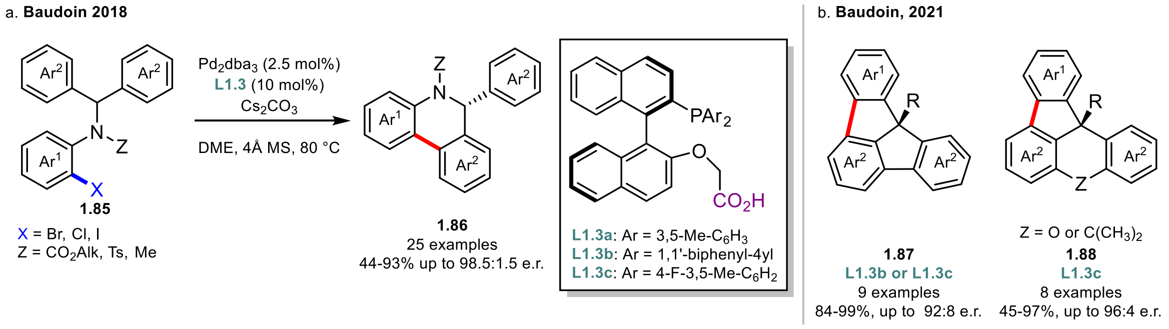
a. Baudoin 2018
Ar^2
Ar^2
N
Z
Ar^1
X
1.85
X = Br, Cl, I
Z = CO$_2$Alk, Ts, Me
Pd$_2$dba$_3$ (2.5 mol%)
L1.3 (10 mol%)
Cs$_2$CO$_3$
DME, 4Å MS, 80 °C
Z
N
Ar^2
Ar^1
Ar^2
1.86
25 examples
44-93% up to 98.5:1.5 e.r.
PAr$_2$
O
CO$_2$H
L1.3a: Ar = 3,5-Me-C$_6$H$_3$
L1.3b: Ar = 1,1'-biphenyl-4yl
L1.3c: Ar = 4-F-3,5-Me-C$_6$H$_2$
b. Baudoin, 2021
Ar^1
R
Ar^2
Ar^2
1.87
L1.3b or L1.3c
9 examples
84-99%, up to 92:8 e.r.
Ar^1
R
Ar^2
Ar^2
Z
Z = O or C(CH$_3$)$_2$
1.88
L1.3c
8 examples
45-97%, up to 96:4 e.r.

Scheme 1.11: Binapthalene-derived bifunctional ligands as enantioinductor and active base.

The use of electrophiles other than aryl- or alkenyl(pseudo-)halides were reported by the Cramer and Tang group. In 2017 the reaction of ketene aminal phosphates **1.89**, which are more stable than triflate derivatives, to chiral isoindolines **1.90** was reported.[52] With electron-rich phospholane ligand **L1.4** high yields and selectivities were obtained at room temperature (Scheme 1.12a). Interestingly, when the reaction was conducted under carboxylate free conditions, i.e. Pd(dba)$_2$ without PivOH, traces of the product were still observed indicating that the diphenyl phosphate anion acts as a poor active base. Moreover, a rare example of Pd(0)-catalyzed parallel kinetic resolution was demonstrated. Shortly after, the same group reported the synthesis of 1*H*-isoindoles **1.92** bearing highly congested quaternary stereogenic centers from perfluoroalkyl-substituted imidoyl chlorides **1.91** (Scheme 1.12b).[53] The products could be further elaborated by reducing or nucleophilicly attacking the imine moiety. The Tang group reported the synthesis of chiral isoindolines **1.94** from carbamoyl chloride precursors of type **1.93** using (*R*)-Antphos previously developed in the sage group. In this case, CO pressure was essential to prevent decarbonylation of the starting materials and ensure high yields and selectivities (Scheme 1.12c).[54]

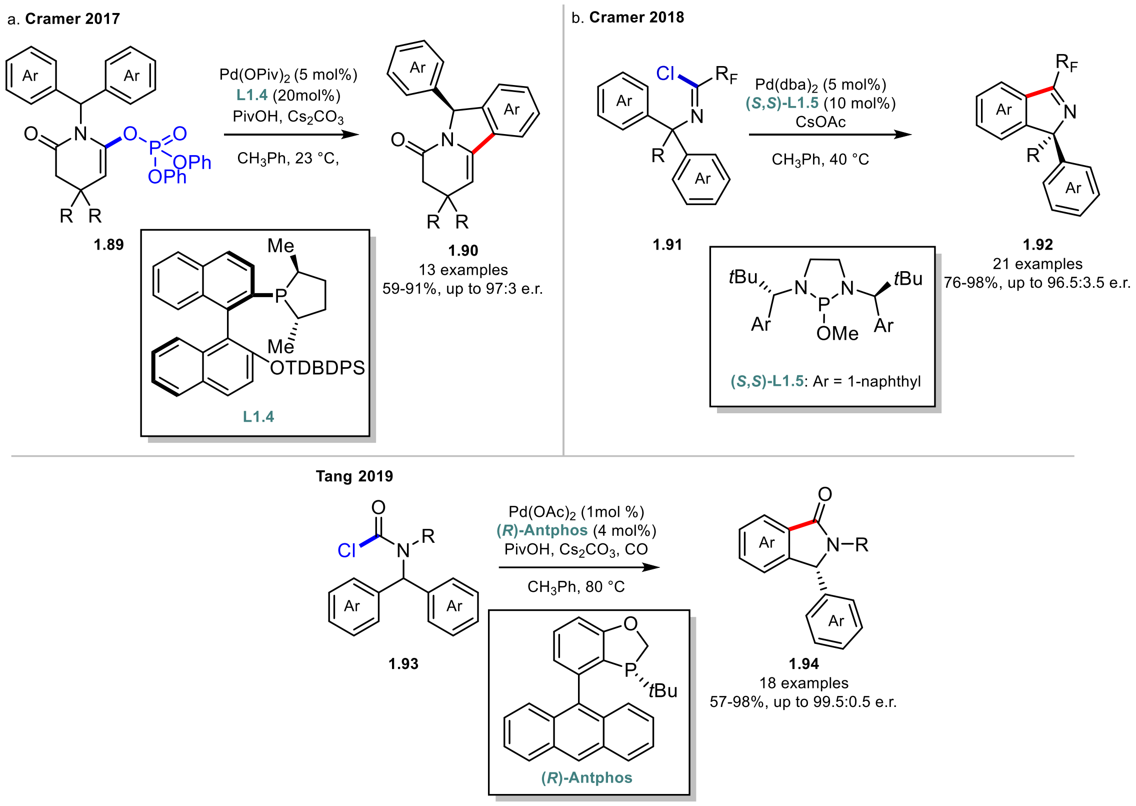
a. Cramer 2017
Pd(OPiv)2 (5 mol%)
L1.4 (20mol%)
PivOH, Cs2CO3
CH3Ph, 23 °C,
1.89
1.90
13 examples
59-91%, up to 97:3 e.r.
L1.4
b. Cramer 2018
Pd(dba)2 (5 mol%)
(S,S)-L1.5 (10 mol%)
CsOAc
CH3Ph, 40 °C
1.91
1.92
21 examples
76-98%, up to 96.5:3.5 e.r.
(S,S)-L1.5: Ar = 1-naphthyl
Tang 2019
Pd(OAc)2 (1mol %)
(R)-Antphos (4 mol%)
PivOH, Cs2CO3, CO
CH3Ph, 80 °C
1.93
1.94
18 examples
57-98%, up to 99.5:0.5 e.r.
(R)-Antphos

Scheme 1.121: Use of alkenylphosphate (a), imidoyl chlorides (b) and acyl chlorides (c) as electrophiles.

In addition to the formation of carbon stereogenic centers, methods to synthesize *Si*- and *P*-stereogenic compounds have been developed over the past decade.[55] An early example is the synthesis of chiral dibenzosiloles **1.96** featuring an *Si*-stereogenic center from triflate precursors **1.95** reported by Hayashi and Shintani.[56] Not only was the bidentate phosphine ligand **(*R*,*S*$_P$)-L1.6** responsible for high enantioselectivities, it also suppressed the formation of achiral **1.97** arising from a 1,5-Pd shift mainly formed with monodentate ligands screened during this study (Scheme 1.13a). In 2015, Duan[57] and Ma[58] simultaneously disclosed the synthesis of *P*-stereogenic phosphinic amides **1.97** by desymmetrization of aryl bromides **1.98** (Scheme 1.13b). With almost identical taddol-derived posphoramidite ligands **L1.2b** and **L1.2b** the products were obtained in excellent yields and enantioselectivities in both cases. Similar tricyclic *P*-stereogenic phosphonates **1.99** were also reported by the Tang group using Antphos-type ligand **L1.6** (Scheme 1.13c). [59]

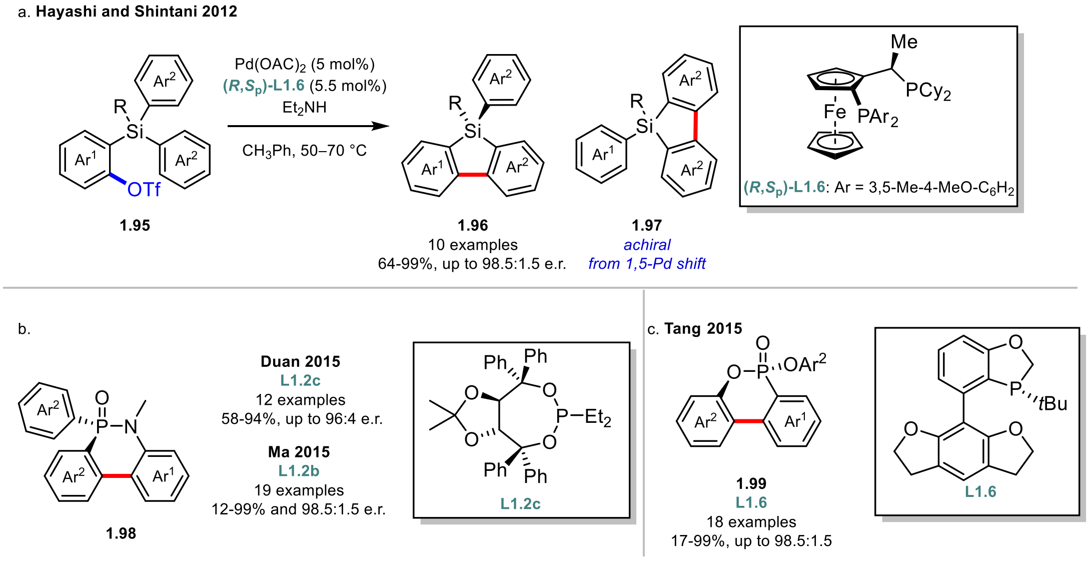
a. Hayashi and Shintani 2012
Pd(OAC)2 (5 mol%)
(R,Sp)-L1.6 (5.5 mol%)
Et2NH
CH3Ph, 50–70 °C
R
Si
Ar1
Ar2
OTf
1.95
1.96
10 examples
64-99%, up to 98.5:1.5 e.r.
1.97
achiral
from 1,5-Pd shift
Me
PCy2
Fe
PAr2
(R,Sp)-L1.6: Ar = 3,5-Me-4-MeO-C6H2
b.
P
N
O
1.98
Duan 2015
L1.2c
12 examples
58-94%, up to 96:4 e.r.
Ma 2015
L1.2b
19 examples
12-99% and 98.5:1.5 e.r.
Ph
P–Et2
L1.2c
c. Tang 2015
O–P
OAr2
1.99
L1.6
18 examples
17-99%, up to 98.5:1.5
tBu
L1.6

Scheme 1.13: Syntheses of *Si*-and *P*-stereogenic compounds: a. benzosiloles **1.96**, b. phosphinic amides **1.98** and c. phosphonates **1.99**.

Cui and Xu,[60] and Duan[61] reported the synthesis of *P*-stereogenic phosphole oxides **1.101** (Scheme 1.14). Bidentate phosphine ligands (*S*,*S*)-Duphos and (*R*)-Segphos furnished the products in high yields and enantioselectivities. Moreover, Duan also demonstrated that chiral binol-derived phosphoric acids and amides can induce enantioselectivity in presence of a non-chiral ligand as a part of the same study.

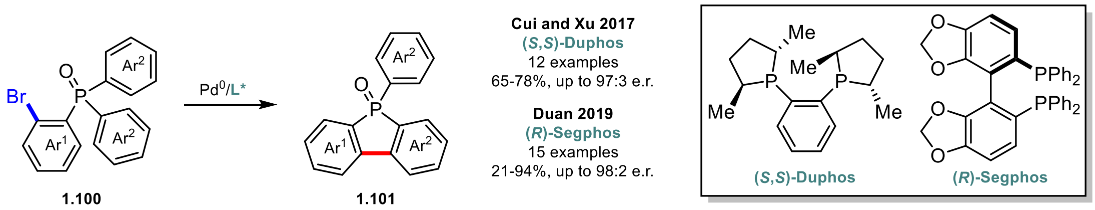
Br
O
P
Ar1
Ar2
1.100
Pd0/L*
1.101
Cui and Xu 2017
(S,S)-Duphos
12 examples
65-78%, up to 97:3 e.r.
Duan 2019
(R)-Segphos
15 examples
21-94%, up to 98:2 e.r.
Me
P
(S,S)-Duphos
PPh2
(R)-Segphos

Scheme 1.14: Enantioselective arylation of phosphine oxides **1.95** to phosphole oxides **1.96**.

The synthesis of planar chiral metallocenes by Pd(0)-catalyzed C(sp^2)−H activation was reported by several groups. The formation of cyclic lactams **1.102** and **1.103** was reported by the Gu group[62] and Liu & Zhao[63] in 2014. Although the protocol of Gu was compatible with both ferrocenes and ruthenocenes, the use of (*R*,*S*$_a$)-OPINAP led to moderate enantioselectivities. Conversely, higher enantioselectivities (up to 97:3 e.r.) were reported by Liu and Zhao employing phosphoramide ligand **L1.2c** (Scheme 1.15a). A major improvement was made by introducing chiral bidentate phosphine ligand BINAP as enantioinductor for the formation of 5-membered rings in the same year. Gu-You[64] and Kang-Gu[65] independently reported the same reaction forming ferrocenes **1.104** and metallocenes **1.105** in excellent yields and enantioselectivities. Later, the synthesis of ferrocenylpyridines **1.106**[66] and C(sp^2)−H alkenylation[67] to form ferrocenes of type **1.107** was reported by the same group (Scheme 1.15b).

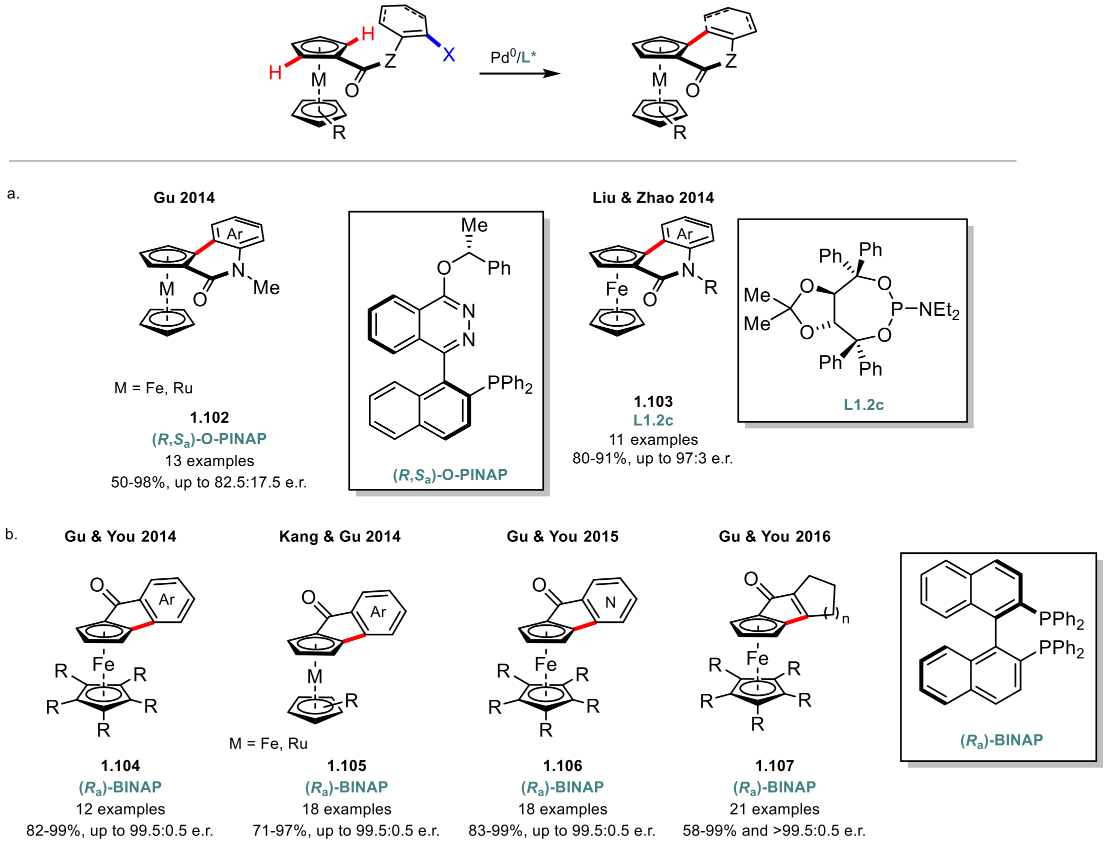
H
H
M
R
Z
X
O
Pd0/L*
a.
Gu 2014
Ar
N
Me
M = Fe, Ru
1.102
(R,Sa)-O-PINAP
13 examples
50-98%, up to 82.5:17.5 e.r.
Me
Ph
PPh2
(R,Sa)-O-PINAP
Liu & Zhao 2014
Fe
1.103
L1.2c
11 examples
80-91%, up to 97:3 e.r.
P−NEt2
L1.2c
b.
Gu & You 2014
1.104
(Ra)-BINAP
12 examples
82-99%, up to 99.5:0.5 e.r.
Kang & Gu 2014
M = Fe, Ru
1.105
(Ra)-BINAP
18 examples
71-97%, up to 99.5:0.5 e.r.
Gu & You 2015
1.106
(Ra)-BINAP
18 examples
83-99%, up to 99.5:0.5 e.r.
Gu & You 2016
n
1.107
(Ra)-BINAP
21 examples
58-99% and >99.5:0.5 e.r.
PPh2
PPh2
(Ra)-BINAP

Scheme 1.15: Synthesis of planar chiral metallocenes. a. Formation of 6-membered rings. b. Formation of 5-membered rings.

The Guiry group presented the synthesis of planar, central and axially chiral ferrocenyl diols by applying the protocol disclosed by Gu and You.[68] Although the preparation of **1.109** from precursor **1.108** by two-fold C−H activation was already reported in the study of the reaction scope, the Guiry group slightly modified the reaction conditions to obtain a quantitative yield. 18 different ferrocenyl diols of type **1.110** were prepared by reacting **1.109** with the corresponding organo-lithium or -Grinard reagents (Scheme 1.16). Ferrocenyl diols **1.110** were applied as catalysts in the asymmetric hetero-Diels-Alder reaction leading to moderate to high enantioselectivities.

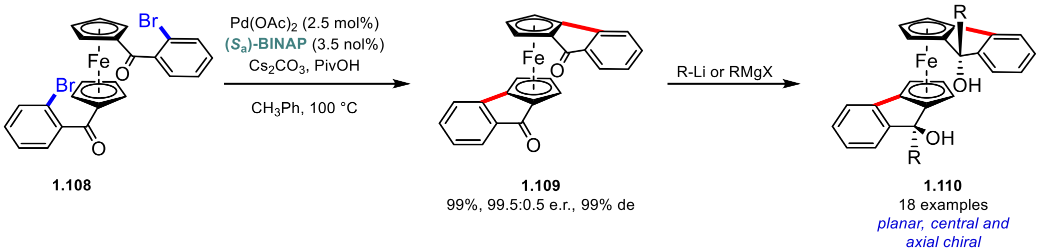
Br
Br
Fe
O
Pd(OAc)2 (2.5 mol%)
(Sa)-BINAP (3.5 nol%)
Cs2CO3, PivOH
CH3Ph, 100 °C
R-Li or RMgX
R
OH
1.108
1.109
99%, 99.5:0.5 e.r., 99% de
1.110
18 examples
planar, central and axial chiral

Scheme 1.16 Synthesis of ferrocenyl diols.

More recently, the Duan group reported the synthesis of planar chiral benzothiophene-fused ferrocenes **1.112**.[69] In the presence of bidentate (*R*)-segphos, ferrocenyls **1.111** were efficiently arylated to the corresponding products in high yields and enantioselectivities. Moreover, planar chiral benzothiophene-fused ferrocene **1.112a** featuring a phosphinoxide substituent on the lower Cp ring was reduced to the corresponding phosphine **1.112aa** and engaged in cross-coupling chemistry. The Suzuki-Miaura coupling between aryl bromide **1.113** and boronic acid **1.114** using **1.112aa** as chiral ligand led to the formation of biaryl **1.115** in good yield and moderate enantioselectivity (Scheme 1.17).

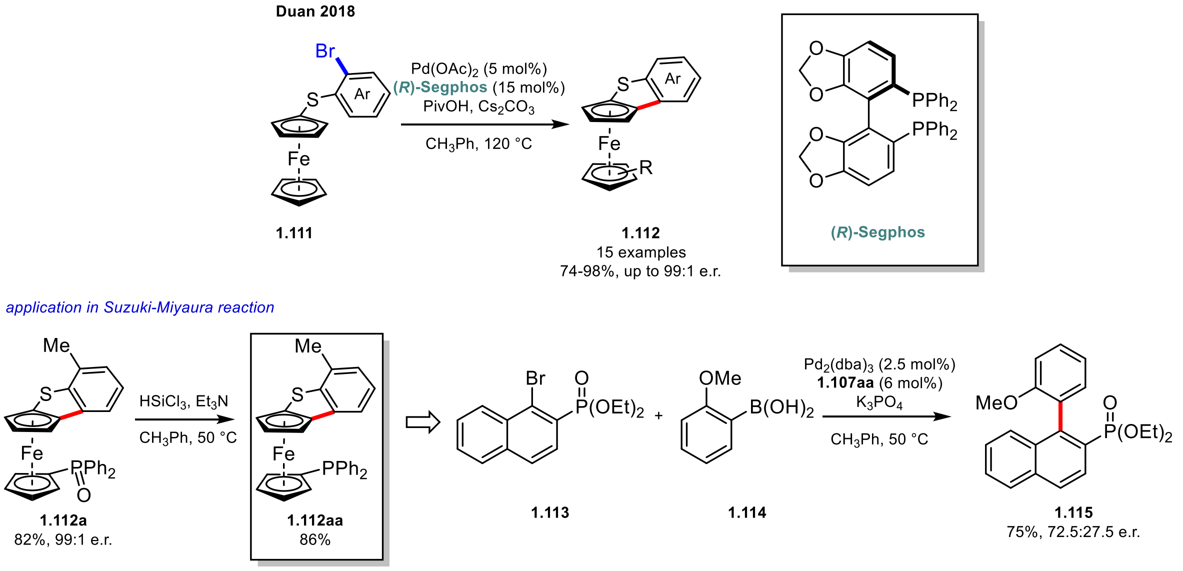
Duan 2018
Br
S
Ar
Fe
Pd(OAc)$_2$ (5 mol%)
(R)-Segphos (15 mol%)
PivOH, Cs$_2$CO$_3$
CH$_3$Ph, 120 °C
R
1.111
1.112
15 examples
74-98%, up to 99:1 e.r.
PPh$_2$
(R)-Segphos
application in Suzuki-Miyaura reaction
Me
HSiCl$_3$, Et$_3$N
CH$_3$Ph, 50 °C
1.112a
82%, 99:1 e.r.
1.112aa
86%
P(OEt)$_2$
OMe
B(OH)$_2$
Pd$_2$(dba)$_3$ (2.5 mol%)
1.107aa (6 mol%)
K$_3$PO$_4$
CH$_3$Ph, 50 °C
MeO
1.113
1.114
1.115
75%, 72.5:27.5 e.r.

Scheme 1.17: Synthesis of of planar chiral benzothiophene-fused ferrocenes **1.107** and application in the Suzuki-Miyaura cross-coupling.

Enantioselective intramolecular Pd(0)-catalyzed C(sp^2)−H activation reactions for the synthesis of molecules with chiral axes are more scarce and only two protocols have been presented in the past 5 years. In 2017 The Gu group demonstrated the atroposelective synthesis of indole-based biaryls **1.117** by dynamic kinetic C−H cyclization of substrates **1.116** (Scheme 1.18a). Using phosphoramite **L1.12d**, high yields of up to 99% and enantioselectivities of 95.5:4.5 were observed. The OMOM substituent on the naphthyl moiety was essential to ensure high enantioselectivities as with the less sterically demanding OMe the rotational barrier was too low. Shortly after, the Cramer group demonstrated the synthesis of axially chiral dibenzazepinones **1.119** using phosphoramidite **L1.2b** (Scheme 1.18b).[70] In contrast to the approach of Gu, in this case, the axis of chirality is formed during the C−H functionalization process by discrimination between enantiotopic faces of a phenyl group. *Ortho* and *meta* substitution on Ar^1 played an important role to ensure high levels of enantioselectivity as non-substituted products racemized withing 2 hours.

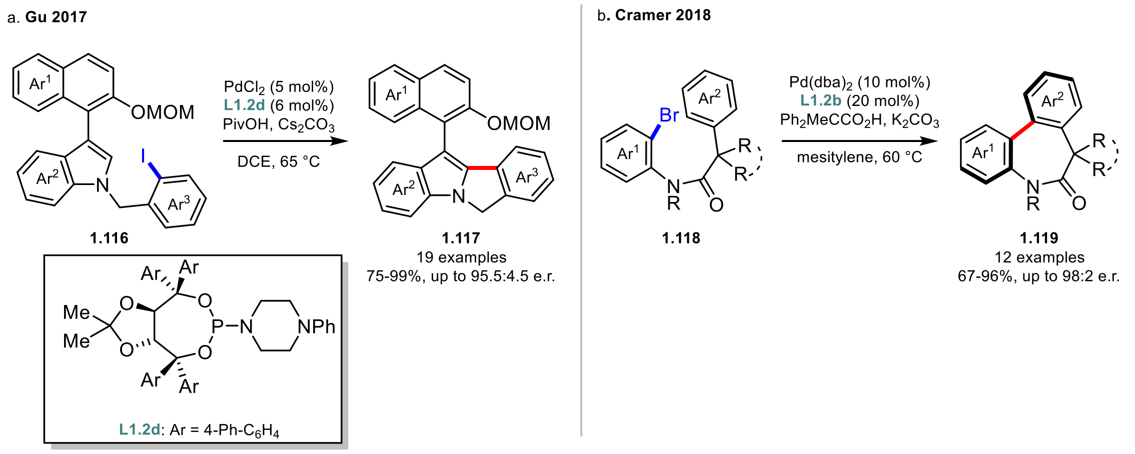
a. Gu 2017
Ar^1
OMOM
I
Ar^2
Ar^3
N
PdCl$_2$ (5 mol%)
L1.2d (6 mol%)
PivOH, Cs$_2$CO$_3$
DCE, 65 °C
1.116
1.117
19 examples
75-99%, up to 95.5:4.5 e.r.
Me
O
Ar
P−N
NPh
L1.2d: Ar = 4-Ph-C$_6$H$_4$
b. Cramer 2018
Br
R
O
Pd(dba)$_2$ (10 mol%)
L1.2b (20 mol%)
Ph$_2$MeCCO$_2$H, K$_2$CO$_3$
mesitylene, 60 °C
1.118
1.119
12 examples
67-96%, up to 98:2 e.r.

Scheme 1.18: Approaches for the synthesis of axially chiral molecules. A. Dynamic kinetic resolution. b. De novo formation of chiral axis.

1.2.2 Pd(0)-catalyzed intramolecular C(sp^3)−H bond activation

The first observation of Pd(0)-catalyzed C(sp^3)−H activation was reported by Dyker in 1992 for the synthesis of structure **1.123** by self-condensation of three molecules of 2-iodoanisole **1.120** (Scheme 1.19).[71] They proposed the formation of cyclopalladated species **1.121** by activation of the OMe group. The new aryl−aryl bond on intermediate **1.122** is presumably formed by oxidative addition of a new molecule of **1.120** on intermediate **1.121** and subsequent reductive elimination leading to an overall 1,5-Pd shift to the OMe group.

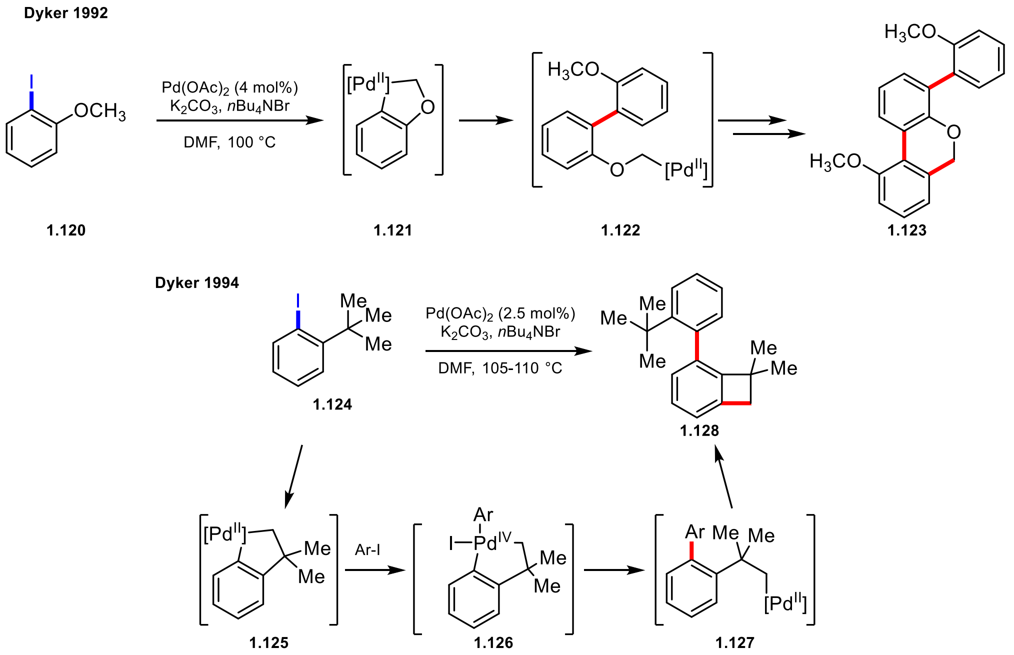

Scheme 1.19: Early C(sp^3)−H activation reactions.

Later, the same group reported the formation of benzocyclobutenes **1.128** by activation of *t*Bu groups. In analogy to the previous report, the activation of the *t*Bu group leads to cyclopalladated species **1.125** followed by oxidative addition of another molecule of starting material to give intermediate **1.126**. Reductive elimination gives structure **1.127** from which product **1.128** is formed by a second C−H activation/reductive elimination sequence.

In 2003, the Baudoin group reported the use of phosphine ligands for Pd(0)-catalyzed C(sp^3)−H activation which prevented the self-condensation of the starting material by suppressing competitive oxidative addition to Pd^{II} intermediates.[72] Depending on the nature of the starting materials **1.129** either olefins **1.130** or benzocyclobutenes **1.131** were formed (Scheme 1.20a). The proposed pathway for the formation of the olefin products proceeds through the formation of 6-membered palladacycle **1.132** and subsequent β-H elimination and reductive elimination. In the case of the benzocyclobutenes direct reductive elimination from 5-membered intermediate **1.133** forges the 4-membered ring. In 2007 the same group reported improved reaction conditions for the selective dehydrogenation of alkanes using the newly designed F-TOTP (tris(5-fluoro-2-mehtylphenyl)phosphane) ligand (Scheme 1.20b).[73] Additionally, with the new reaction conditions product **1.130a** was obtained in 82% yield and was further elaborated to the antihypertensive drug verapamil (**1.134**).

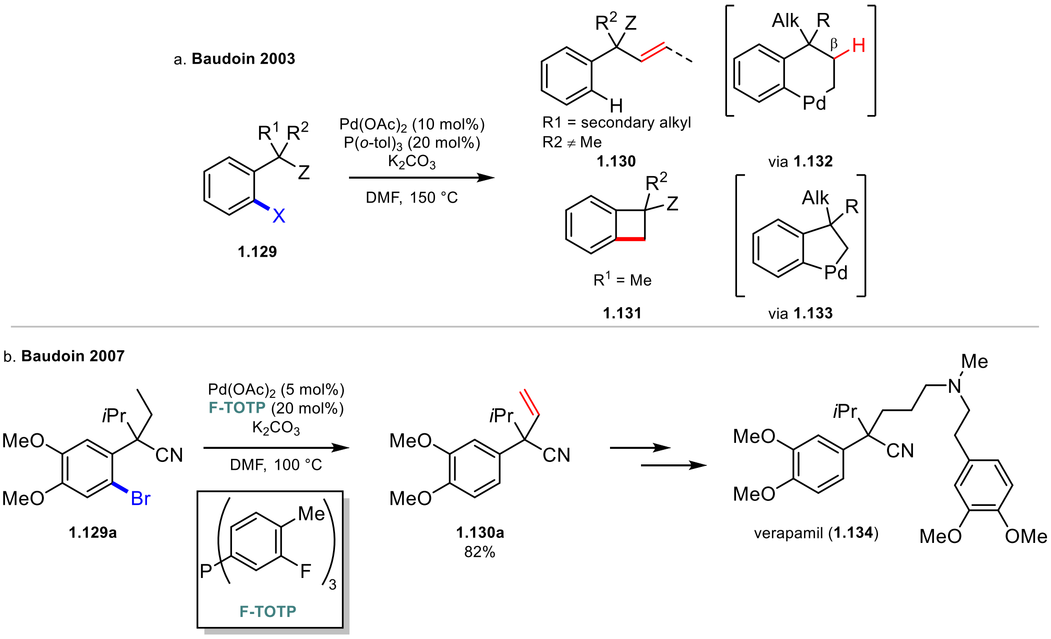
a. Baudoin 2003
R1 R2
Z
X
1.129
Pd(OAc)2 (10 mol%)
P(o-tol)3 (20 mol%)
K2CO3
DMF, 150 °C
R2 Z
H
R1 = secondary alkyl
R2 ≠ Me
1.130
Alk R
β H
Pd
via 1.132
R2
Z
R1 = Me
1.131
Alk R
Pd
via 1.133
b. Baudoin 2007
iPr
MeO
MeO
CN
Br
1.129a
Pd(OAc)2 (5 mol%)
F-TOTP (20 mol%)
K2CO3
DMF, 100 °C
Me
P
F
3
F-TOTP
iPr
MeO
MeO
CN
1.130a
82%
Me
N
iPr
MeO
MeO
CN
verapamil (1.134)
MeO
OMe

Scheme 1.20: a. Preparation of olefins **1.130** or benzocyclobutenes **1.131** by Pd(0)-catalyzed C(sp^3)−H functionalization. b. Application of improved protocol in the synthesis of verapamil (**1.134**).

After the initial report on alkane dehydrogenation of the Baudoin group several, methodologies for the formation of small- to medium-sized rings by arylation of C(sp^3)−H bonds were reported and an overview is given in Scheme 1.21.[36] Examples for the formation of 4-membered rings include the formation of benzocyclobutenes **1.131** from aryl bromide precursors initially reported by the Baudoin group in 2008.[74] Later, similar products were prepared from cheaper and more abundant aryl chlorides.[75] Although benzazetidine intermediates **1.135** could never be isolated, benzoxazines **1.136** were formed by 4π electrocyclic opening of the 4-membered ring followed by a 6π electrocyclization of the aza-*ortho*-xylylene moiety with the carbonyl substituent on the nitrogen atom.[76] The formation of 5-membered rings was demonstrated as well by Baudoin and Fagnou in 2010 giving indanes, indolines or dihydro benzofuranes of type **1.137**. Examples of the more challenging methylene C(sp^3)−H bond activation were reported by the group of Knochel[77] for the synthesis of strained tricyclic structures **1.138** and the Baudoin[73] group to access indanes **1.139**. Electron-rich trialkyl phosphine PCy$_3$ proved to be the ligand of choice for a selection of methods for the formation of 5-membered rings. In fact, dihydrobenzofurans **1.140**,[78] indolines **1.141**,[79] oxindoles **1.142** and sulphonamides **1.143**[80] could be prepared in good to high yields under similar conditions with PCy$_3$ as the ligand. Oxindoles **1.144** were accessed by activation of congested cyclopropyl C(sp^3)−H bonds. Nevertheless, the products were obtained in good to excellent yields up to 14:1 d.r. Examples of 6-membered rings were presented by Knochel[77] (**1.145**) and Shi[81] (**1.146**). Remarkably, in the case of Shi, the unprotected nitrogen was compatible with the reaction conditions. Additionally, the Baudoin group reported the synthesis of tetracyclic structures **1.147** by simultaneous formation of a 6-and a 5-membered ring.[82] This strategy was applied in the total synthesis of lycorine alkaloids. Among others, (±)-lycorane (**1.148**) was prepared in 4 steps with an overall yield of 47%.

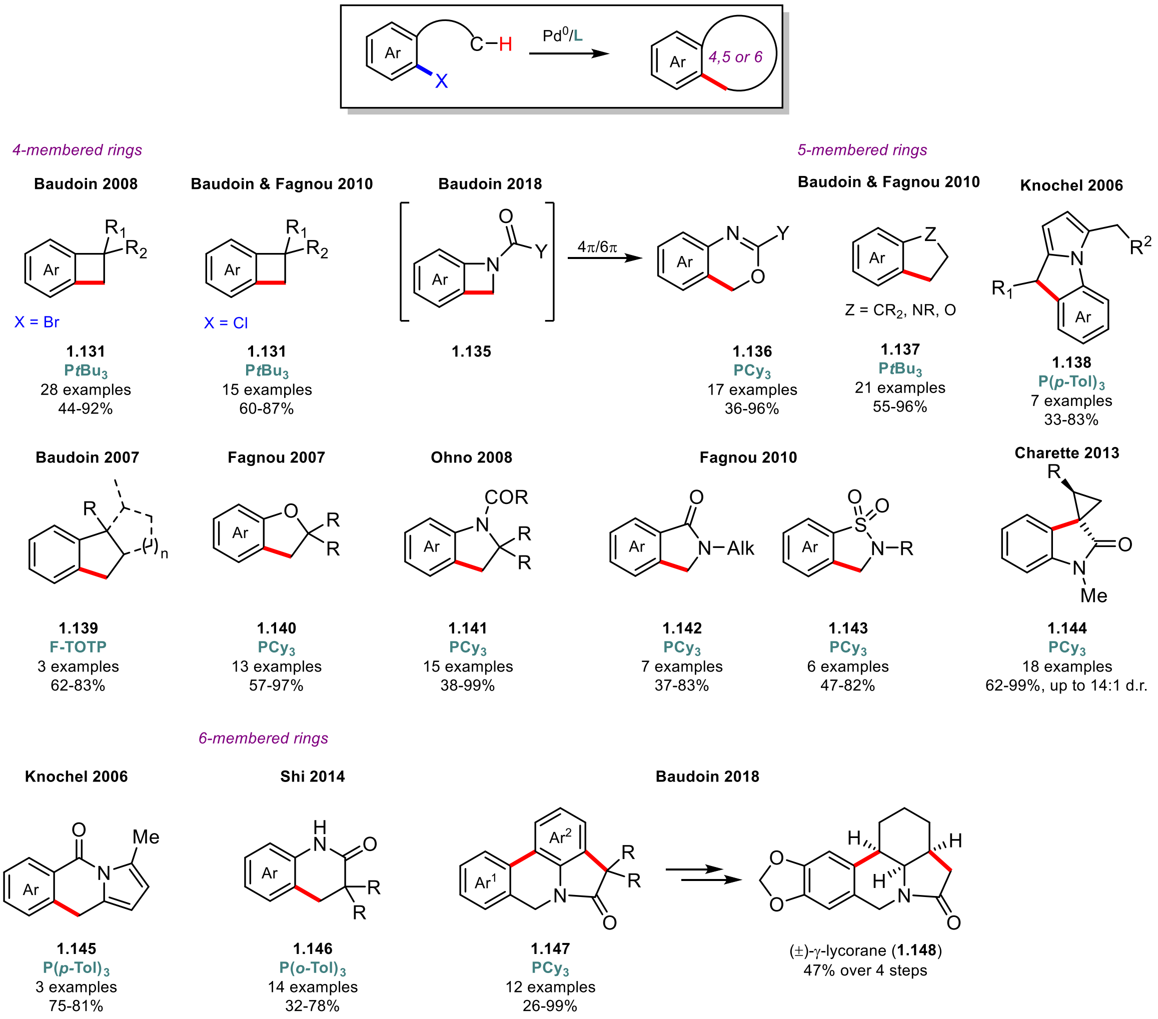
Ar
X
C−H
Pd^0/L
4,5 or 6
4-membered rings
Baudoin 2008
X = Br
1.131
PtBu3
28 examples
44-92%
Baudoin & Fagnou 2010
X = Cl
1.131
PtBu3
15 examples
60-87%
Baudoin 2018
1.135
4π/6π
1.136
PCy3
17 examples
36-96%
5-membered rings
Baudoin & Fagnou 2010
Z = CR2, NR, O
1.137
PtBu3
21 examples
55-96%
Knochel 2006
1.138
P(p-Tol)3
7 examples
33-83%
Baudoin 2007
1.139
F-TOTP
3 examples
62-83%
Fagnou 2007
1.140
PCy3
13 examples
57-97%
Ohno 2008
1.141
PCy3
15 examples
38-99%
Fagnou 2010
1.142
PCy3
7 examples
37-83%
1.143
PCy3
6 examples
47-82%
Charette 2013
1.144
PCy3
18 examples
62-99%, up to 14:1 d.r.
6-membered rings
Knochel 2006
1.145
P(p-Tol)3
3 examples
75-81%
Shi 2014
1.146
P(o-Tol)3
14 examples
32-78%
Baudoin 2018
1.147
PCy3
12 examples
26-99%
(±)-γ-lycorane (1.148)
47% over 4 steps

Scheme 1.21: Examples of Pd(0)-catalyzed C(sp^3)−H activation for the formation of 4-,5-,6-membered rings.

In analogy to Pd(0)-catalyzed C(sp^2)−H activation, other electrophiles were used for the oxidative addition step. For instance, the Takemoto group reported the cyclization of carbamoyl chlorides **1.149** to the corresponding oxindole products **1.150** by activation of a benzylic methyl group (Scheme 1.22).[83] Similarly, the Baudoin group reported the synthesis of strained β-lactams **1.152** from carbamoyl chlorides **1.151**.[84] To prevent in situ decarbonylation of the starting material an excess of COgen was added using a two-chamber system developed by the Skrydstrup group.[85] In contrast to directly purging the reaction with CO as reported by Takemoto, the use of COgen requires fewer safety precautions. An alternative approach for the activation of benzylic C(sp^3)−H bonds was reported by the Cramer group a few years later.[86] Indoles **1.154** were prepared from imidoyl chlorides **1.153** in good to high yields using either PCy_3 or SIPr as ligand. The latter was usually superior to PCy_3 in the case of 6-substituted imidoyl chlorides. The alkenylation of C(sp^3)−H bonds from alkenyl(pseudo-)halide precursors is an attractive alternative to the arylation reactions as the double bond in the formed products can be easily reduced. Acyclic alkenyl bromide substrates **1.155** were efficiently converted to γ-lactams by the Baudoin group in 2016.[87] It was found that the substituent in α-position to the nitrogen is essential for high yields, presumably by inducing a significant Thorpe-Ingold effect that is necessary for the ring contraction. In the same year, the Takemoto group demonstrated the synthesis of tetrahydro-2*H*-fluorenes **1.157** by alkenylation of a bezylic methyl group.[88]

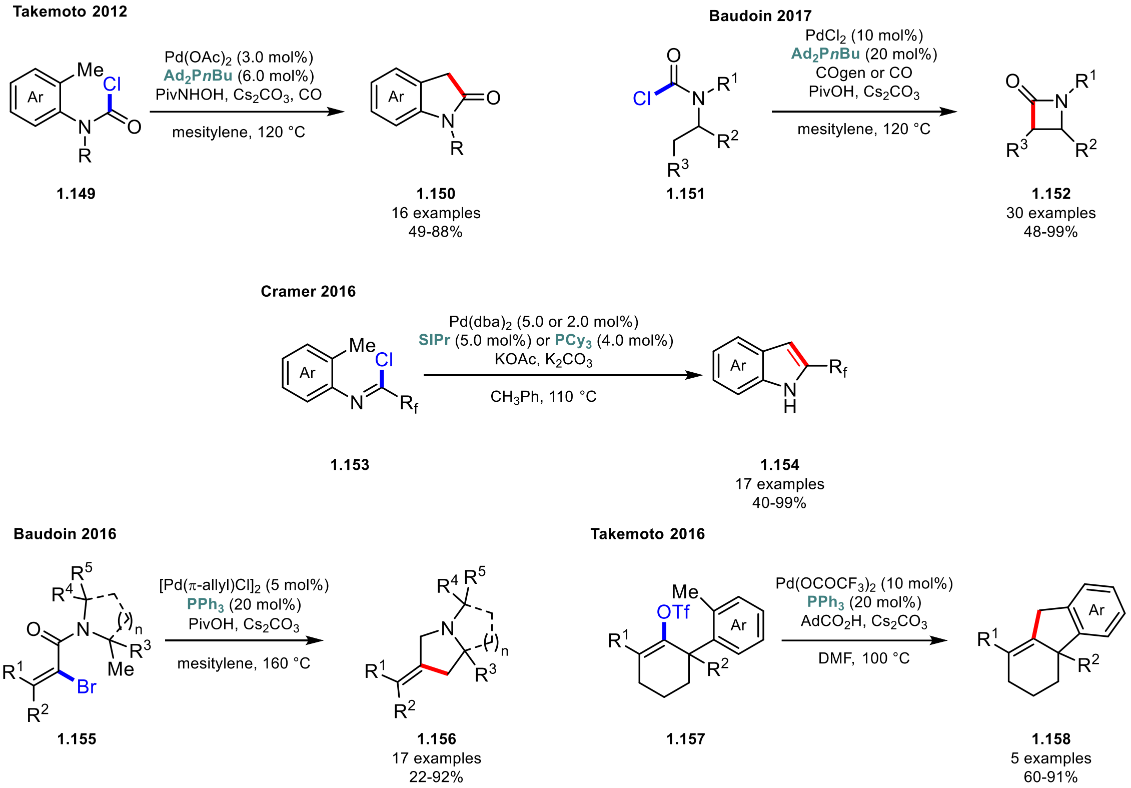
Takemoto 2012
Pd(OAc)2 (3.0 mol%)
Ad2PnBu (6.0 mol%)
PivNHOH, Cs2CO3, CO
mesitylene, 120 °C
1.149
1.150
16 examples
49-88%
Baudoin 2017
PdCl2 (10 mol%)
Ad2PnBu (20 mol%)
COgen or CO
PivOH, Cs2CO3
mesitylene, 120 °C
1.151
1.152
30 examples
48-99%
Cramer 2016
Pd(dba)2 (5.0 or 2.0 mol%)
SIPr (5.0 mol%) or PCy3 (4.0 mol%)
KOAc, K2CO3
CH3Ph, 110 °C
1.153
1.154
17 examples
40-99%
Baudoin 2016
[Pd(π-allyl)Cl]2 (5 mol%)
PPh3 (20 mol%)
PivOH, Cs2CO3
mesitylene, 160 °C
1.155
1.156
17 examples
22-92%
Takemoto 2016
Pd(OCOCF3)2 (10 mol%)
PPh3 (20 mol%)
AdCO2H, Cs2CO3
DMF, 100 °C
1.157
1.158
5 examples
60-91%

Scheme 1.21: Synthesis of 5-membered rings by cyclization of carbamoyl chlorides or alkenyl(pseudo-)halides.

1.2.2.1 Application in the total synthesis of natural products

Although the synthetic relevance of newly described arlyation/alkenylation methodologies has been demonstrated by disclosing concise syntheses of natural products, active ingredients or core structures thereof,[87–91] significant efforts towards total syntheses of natural products featuring a Pd(0)-catalyzed C(sp^3)−H activation key step to form small rings were made by the Baudoin group.

As a part of the newly reported methodology for the formation of hexahydroindoles **1.160** from alkenylbromide precursors of type **1.159**, the core structure of aeruginosins (**1.161**) was constructed in 2 additional steps.[92] Aeruginosins (**1.170**) are marine natural products that have shown *in vitro* inhibition of serine proteases.[93] Their structure consists of a 2-carboxy-6-hydroxyoctahydroindole (Choi) and hydroxyphenyllactic (Hpla) subunits (Scheme 1.23a). Motivated by these results, two congeners of this family of natural products were prepared a few years later.[94] The synthesis of the Choi fragment began with alcohol **1.162** from which the alkenyl bromide substrate **1.159a** was prepared in 6 steps. Pd(0)-catalyzed C(sp^3)−H alkenylation using Pd(Cy$_3$)$_2$ furnished hexahydroindole **1.160a** in gram-scale with yields ranging between 68-71%. Hydrogenation and further functional group transformations led to the Choi fragment in 1.2 g with a yield of 15% over 9 steps. For the Hpla fragment they applied a Pd(II)-catalyzed intermolecular C(sp^3)−H arylation method reported by the Daugulis group.[95,96] The substrate **1.165** for the intermolecular arylation reaction was obtained from **1.164** by benzyl protection, hydrolysis to the acid and installation of the 2-(pyridine-2-yl)isopropyl (PIP) amine directing group. Subjecting **1.165** to Pd(OAc)$_2$ with aryl iodide **1.166** in presence of K$_2$CO$_3$ led to the formation of **1.167** without racemization of the labile stereogenic center. Removal of the directing group and amide coupling gave fragments **1.168a** and **1.168b** bearing a D-allo-Ile-OMe and D-Leu-OMe hydrophobic amino acid respectively in high yields (Scheme 1.23b).

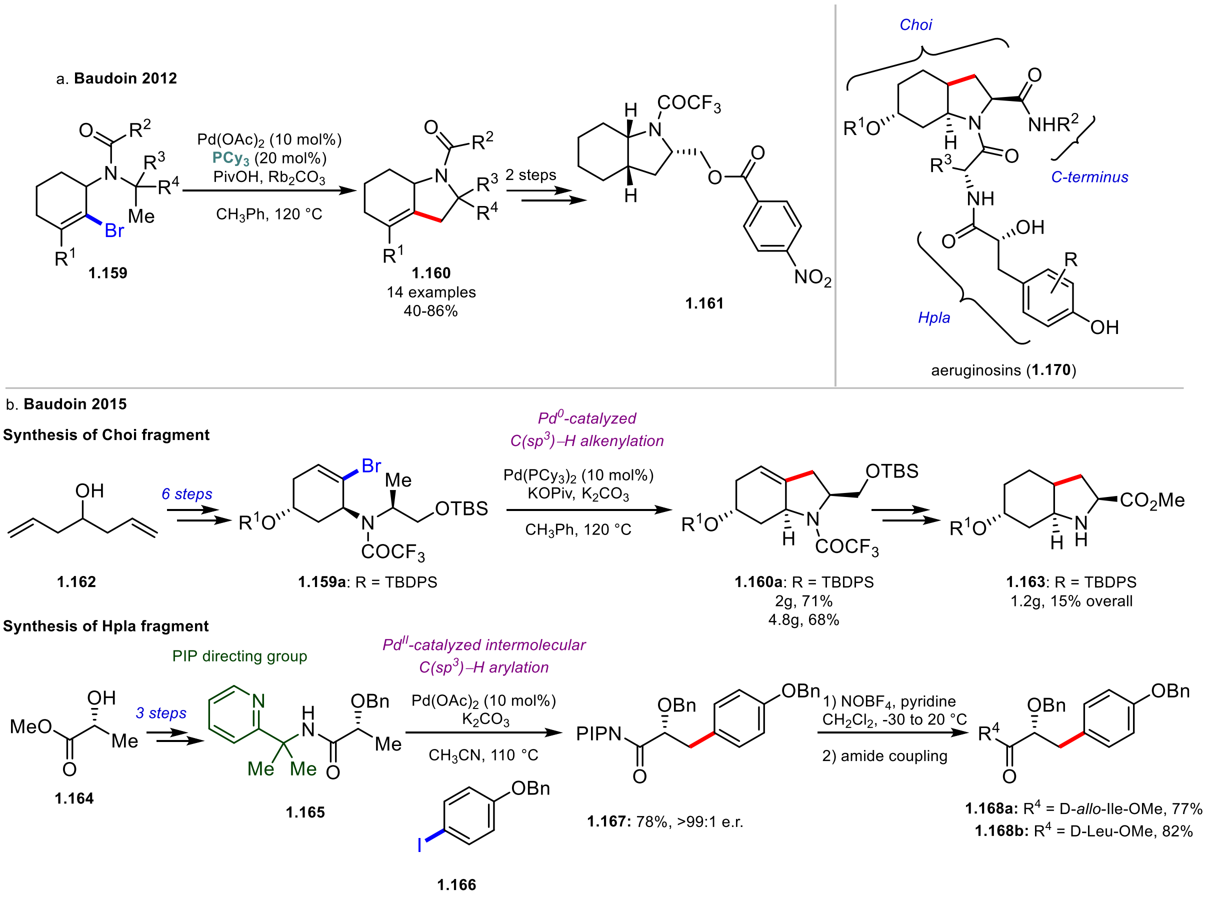
a. Baudoin 2012
1.159
Br
Pd(OAc)2 (10 mol%)
PCy3 (20 mol%)
PivOH, Rb2CO3
CH3Ph, 120 °C
1.160
14 examples
40-86%
2 steps
1.161
NO2
Choi
C-terminus
Hpla
aeruginosins (1.170)
b. Baudoin 2015
Synthesis of Choi fragment
1.162
6 steps
1.159a: R = TBDPS
Pd0-catalyzed
C(sp3)–H alkenylation
Pd(PCy3)2 (10 mol%)
KOPiv, K2CO3
CH3Ph, 120 °C
1.160a: R = TBDPS
2g, 71%
4.8g, 68%
1.163: R = TBDPS
1.2g, 15% overall
Synthesis of Hpla fragment
PIP directing group
1.164
3 steps
1.165
PdII-catalyzed intermolecular
C(sp3)–H arylation
Pd(OAc)2 (10 mol%)
K2CO3
CH3CN, 110 °C
1.166
1.167: 78%, >99:1 e.r.
1) NOBF4, pyridine
CH2Cl2, -30 to 20 °C
2) amide coupling
1.168a: R4 = D-allo-Ile-OMe, 77%
1.168b: R4 = D-Leu-OMe, 82%

Scheme 1.23: a Pd(0)-catalyzed C(sp^3)–H alkenylation to form hexahydroindoles **1.160**. b. Syntheses of Choi and Hpla cores of aeruginosins.

The two fragments were then combined by hydrolysis of the methyl ester on the Hpla fragment followed by peptide coupling to give intermediates **1.169a** and **1.169b** (Scheme 1.24).

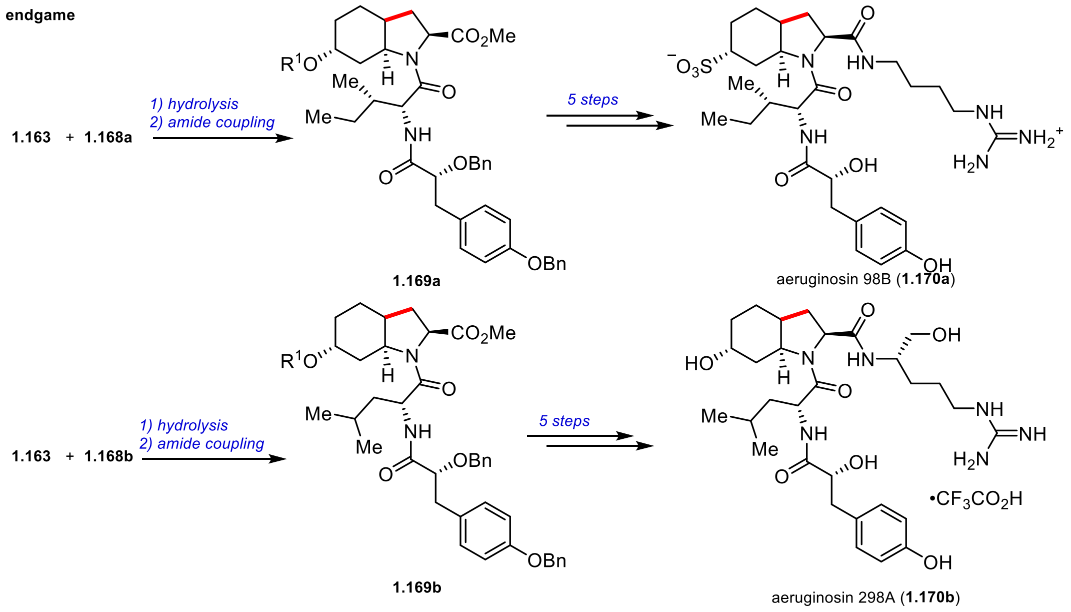
endgame
1.163 + 1.168a
1) hydrolysis
2) amide coupling
1.169a
5 steps
aeruginosin 98B (1.170a)
1.163 + 1.168b
1) hydrolysis
2) amide coupling
1.169b
5 steps
•CF3CO2H
aeruginosin 298A (1.170b)

Scheme 1.24: Coupling of Choi and Hpla fragments and installation of C-termini.

Finally, installation of the c-terminus and global deprotection gave the natural products aeruginosin 98B (**1.170a**) and 298A (**1.170b**) in 5.1% and 8.2% overall yield respectively. Later, other members of the same family with halogen substituents on the aromatic ring were reported by the same group.[97]

Another major application of Pd(0)-catalyzed C(sp^3)−H alkenylation was the divergent total synthesis of dithiodiketopiperazine (DTP) natural products (−)-epicoccin G (**1.176**) and (−)-rostratin A (**1.177**) very recently disclosed by the Baudoin group (Scheme 2.25).[98,99] Starting from cheap and abundant cyclohexenone (**1.171**), enantioselective organocatalyzed epoxidation reported by the List group[100,101] gave **1.172** in 97:3 e.r. Subsequent triflation followed by regioselective and stereospecific epoxide opening with alanine-*t*Bu ester and acetylation gave intermediate **1.173**. The free acid derivative of **1.173** obtained by deprotection of the *t*Bu group was recrystallized to further improve the d.r. to >99:1 and was then dimerized furnishing dialkenyl triflate **1.174** in decagram scale. The key two-fold C(sp^3)−H alkenylation was performed by subjecting **1.174** to 4 mol% of $Pd(PCy_3)_2$ catalyst. The addition of 20 mol% of free PCy_3 proved essential to avoid mixtures of substrate **1.174**, mono-cyclized product and detriflated byproducts. Overall, the common intermediate **1.175** could be prepared in 51% yield over 7 steps in multigram scale. A 7 step sequence including the oxidation of the double bonds, the introduction of sulfur substituents on the diketopiperazine core and deprotections led to (−)-epicoccin G (**1.176**) in 19.6% over 14 steps in the longest linear sequence which is a major improvement compared to the first synthesis (1.5% over 15 steps).[102,103] For (−)-rostratin A (**1.177**) 3 additional steps from common intermediate **1.175** were required due to the highly challenging installation of the *trans*,*trans* ring junction. Nevertheless, the first total synthesis of (−)-rostratin A (**1.177**) was completed in 12.7% yield over the longest linear sequence of 17 steps (Scheme 1.25). Moreover, the high efficiency of the presented route allowed the synthesis of the natural products and derivatives in significant amounts which allowed for cytotoxicity assessments of these structures in the leukemia cell line K562.

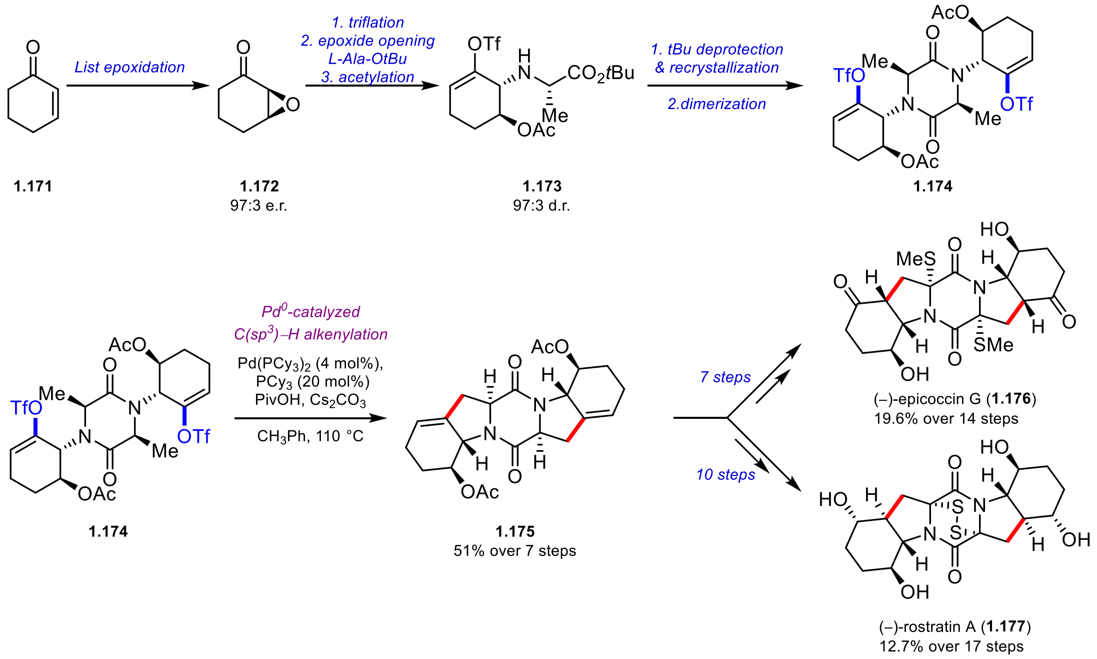
List epoxidation
1. triflation
2. epoxide opening
L-Ala-OtBu
3. acetylation
1. tBu deprotection
& recrystallization
2.dimerization
1.171
1.172
97:3 e.r.
1.173
97:3 d.r.
1.174
Pd0-catalyzed
C(sp3)–H alkenylation
Pd(PCy3)2 (4 mol%),
PCy3 (20 mol%)
PivOH, Cs2CO3
CH3Ph, 110 °C
1.174
1.175
51% over 7 steps
7 steps
10 steps
(–)-epicoccin G (1.176)
19.6% over 14 steps
(–)-rostratin A (1.177)
12.7% over 17 steps

Scheme 1.25: Total synthesis of DTP natural products (−)-epicoccin G (**1.176**) and (−)-rostratin A (**1.177**) enabled by key two-fold Pd(0)-catalyzed C(sp^3)−H alkenylation.

In general, Pd(0)-catalyzed C(sp^3)−H enables the access to of 4-,5-,6- and 7-membered hetero- or carbocycles with 5-membered examples being by far the most studied (for an example of 7-membered ring formation see chapter 2, section 2.1.1). The activation of methyl groups is predominant with a few examples of methylene C−H bond activation, mainly attributed to higher steric encumbrance and reduced acidity of the C−H bond. Electrophiles such as alkenyl(pseudo-) halides, carbamoyl chlorides and imidoyl chlorides are compatible with the reaction giving access to non-aromatic products. Moreover, enantioselective versions, which are of high interest for the pharmaceutical and medicinal industry were developed (see chapter 2, section 2.1). Finally, a wide range of active ingredients and natural products were accessed by Pd(0)-catalyzed C(sp^3)−H activation strategies further underlining the importance of this method in synthetic organic chemistry.

Chapter 2: Palladium(0)-catalyzed enantioselective intramolecular arylation of enantiotopic secondary C−H bonds for the synthesis of chiral indanes

2.1 Introduction: Pd(0)-catalyzed enantioselective activation of C(sp^3)−H bonds

The three-dimensional shape of organic molecules is of fundamental importance as it is directly linked to their activity in biological systems.[104,105] Therefore, enantioselective transformations have been a field of constant and intensive research and in particular transition metal catalysis has been key to develop improved and more efficient methods.[106–110] In this regard, enantioselective Pd-catalyzed C(sp^3)−H activation has attracted great interest from the synthetic community.[111–113] For the Pd^0-Pd^{II} manifold three main strategies have been established over the past decades.[112] (1) The *desymmetrization of enantiotopic alkyl groups* relies on the differentiation of two identical alkyl groups on substrates such as **2.1** by the chiral catalyst. In this case, the stereogenic center is formed remote to the activated C−H bond on product **2.2** (Scheme 2.1a). (2) The *activation of enantiotopic 2^{ary} C−H bond*s of structure **2.3** leads to chiral product **2.4**. The stereogenic center is formed on the same carbon atom of the C−H activation site (Scheme 2.1b). Because of unfavorable stereoelectronic properties, this enantioselective C(sp^3)–H activation process represents an important challenge. (3) The third strategy is *kinetic resolution.* Starting from a racemic mixture of **2.5** chiral product **2.6** and enriched starting material **2.7** is obtained performing a classic kinetic resolution, whereas two different enriched products **2.8** and **2.9** are obtained by parallel kinetic resolution (Scheme 2.1c).

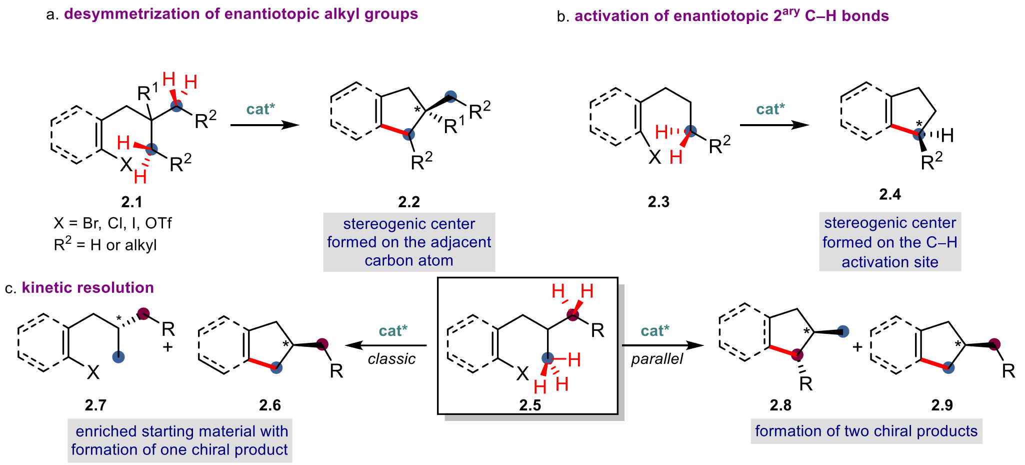
a. desymmetrization of enantiotopic alkyl groups
b. activation of enantiotopic 2ary C–H bonds
R1
H H
R2
H
X
H
R2
cat*
R1
R2
R2
2.1
X = Br, Cl, I, OTf
R2 = H or alkyl
2.2
stereogenic center formed on the adjacent carbon atom
H
X H
R2
cat*
H
R2
2.3
2.4
stereogenic center formed on the C–H activation site
c. kinetic resolution
R
+
X
R
cat*
classic
H H
R
X
H
H H
cat*
parallel
+
R
R
2.7
2.6
2.5
2.8
2.9
enriched starting material with formation of one chiral product
formation of two chiral products

Scheme 2.1: Strategies for asymmetric Pd(0)-catalyzed C(sp^3)−H activation. a. Desymmetrization of enantiotopic alkyl groups. b. Activation of enantiotopic 2^{ary} C−H bonds. c. Kinetic resolution.

2.1.1 Activation of methyl and methylene C−H bonds

The very first example of Pd(0)/Pd(II)-catalyzed enantioselective intramolecular C(sp^3)−H activation was reported by Kündig in 2011[114] for the synthesis of indolines **2.10** (Scheme 2.2). The activation of secondary C−H bonds was achieved in high yields and enantioselectivities employing chiral *N*-Heterocyclic carbene (NHC) ligands **L2.1**, reported by the same group shortly before.[115–117] Later, in addition to expanding the scope to primary C−H bonds, DFT calculations were performed to elucidate the mode of enantioinduction.[118] It was found that the reaction proceeds over a concerted metalation deprotonation mechanism which is also the rate-limiting step with an achiral NHC ligand. However, when a bulky chiral NHC ligand was used, the ligand exchange (bromide for pivalate) was rate-limiting. This change in rate-limiting step is probably attributed to high steric congestion increasing the ligand exchange barrier. Additionally, the *ortho* methyl group in ligand **L2.1a** was essential for high enantioinduction. A study on parallel kinetic resolution was presented from the same group shortly after.[119,120] Starting from a racemic mixture of substrate **2.11** two different products **2.12** and **2.13** were obtained. Using ligands **L2.1b** or ***ent*-L2.1a** up to 49% yield for both products and enantioselectivities of 99:1 and 98:2 respectively were achieved.

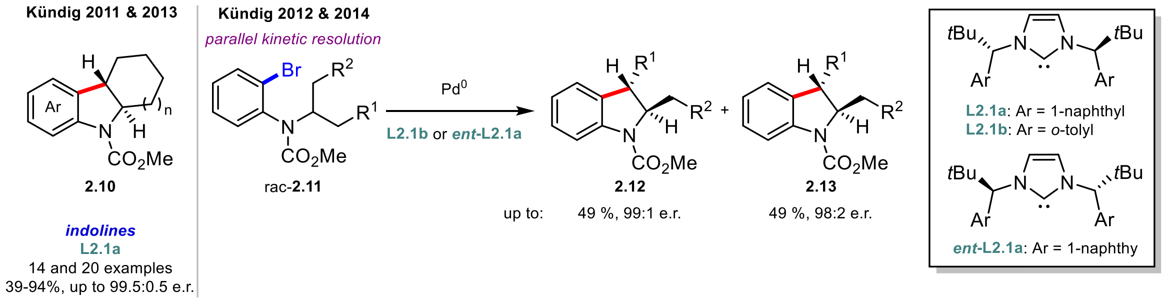
Kündig 2011 & 2013
H
Ar
n
N
H
CO2Me
2.10
indolines
L2.1a
14 and 20 examples
39-94%, up to 99.5:0.5 e.r.
Kündig 2012 & 2014
parallel kinetic resolution
Br
R2
R1
N
CO2Me
rac-2.11
Pd0
L2.1b or ent-L2.1a
H R1
R2
H
N
CO2Me
2.12
+
2.13
up to:
49 %, 99:1 e.r.
49 %, 98:2 e.r.
tBu
N
N
tBu
Ar
Ar
L2.1a: Ar = 1-naphthyl
L2.1b: Ar = o-tolyl
ent-L2.1a: Ar = 1-naphthy

Scheme 2.2: Pioneering studies on enantioselective C(sp^3)−H actvation for the synthesis of indolines.

At the same time of Kündigs first report, Kagan[121] and Cramer[122,123] disclosed enantioselective methodologies for the activation of C(sp^3)−H bonds. A limited scope of indoline structures **2.13** was presented by Kagan employing commercially available diphosphine ligand DuPhos. The more complete study on indolines **2.14** by Cramer included the activation of secondary C−H bonds in high yields and enantioselectivities, using chiral monodentate phosphine ligand **L2.2** designed for this methodology. Interestingly, with chiral trialkyl phosphine ligand **L2.3**, which shows comparable electronic properties to PCy_3, indoline **2.15** was prepared with 96% yield and 85.5:14.5 e.r. (Scheme 2.3).[123]

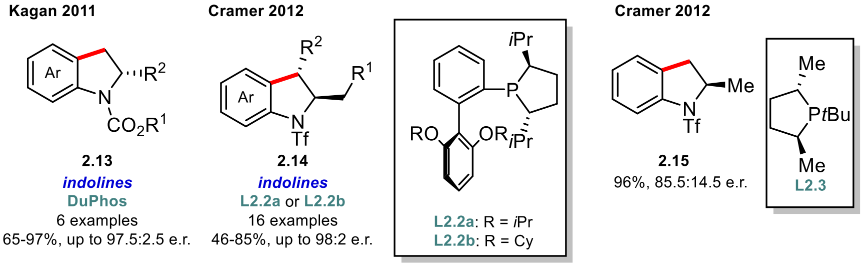
Kagan 2011
Ar
R2
N
CO2R1
2.13
indolines
DuPhos
6 examples
65-97%, up to 97.5:2.5 e.r.
Cramer 2012
R2
R1
Ar
N
Tf
2.14
indolines
L2.2a or L2.2b
16 examples
46-85%, up to 98:2 e.r.
iPr
P
RO
OR
iPr
L2.2a: R = iPr
L2.2b: R = Cy
Cramer 2012
Me
N
Tf
2.15
96%, 85.5:14.5 e.r.
Me
PtBu
Me
L2.3

Scheme 2.3: Follow-up indoline syntheses by Kagan and Cramer.

Similarly, the Baudoin group disclosed the synthesis of chiral indanes **2.16** via the desymmetrization of enantiotopic methyl groups (Scheme 2.4). Using chiral monodenate binepine ligands of type **L2.4**, originally designed for asymmetric hydrogenations,[124] high yields and enantioselectivities were observed.[125] In 2015 a more thorough study was published including the activation of secondary C−H bonds leading to indolines **2.17**, where up to three adjacent stereogenic centers are controlled at the same time with high level of diastereocontrol. Three different ligands were used for the substrate scope. Ferrocenyl-substituted **L2.4b** was the most effective for methyl activation whereas for methylene activation *o*-tolyl-substituted **L2.4c** showed the highest reactivity. Finally, ligand **L2.4d** with a 9-methylfluorenyl substituent a pyridine-based substrate could be converted to the indane product. DFT computations showed that London dispersion forces between substrate and ligand are important to stabilize the transition state.[126]

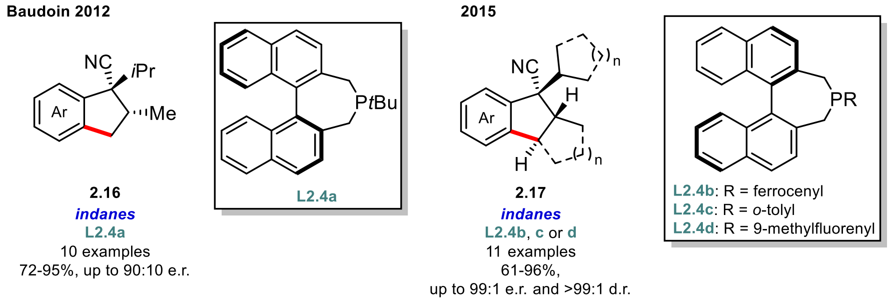
Baudoin 2012
2015
2.16
indanes
L2.4a
10 examples
72-95%, up to 90:10 e.r.
L2.4a
2.17
indanes
L2.4b, c or d
11 examples
61-96%,
up to 99:1 e.r. and >99:1 d.r.
L2.4b: R = ferrocenyl
L2.4c: R = o-tolyl
L2.4d: R = 9-methylfluorenyl

Scheme 2.4: Synthesis of chiral indanes using monodentate binepine ligands.

Besides chiral ligands, active bases can be used to induce chirality in Pd(0)-catalyzed C(sp^3)−H activation. For the synthesis of chiral indolines[122] (see Scheme 2.3) the Cramer group hypothesized that the active base relays the chiral space created by the ligand to the substrate. Indeed, a matched effect was observed when chiral base (*S*)-**A1** was used in presence of a Pd(0) catalyst and ligand **L2.2a** leading to the formation of chiral indoline (2*R*,3*S*)-**2.14a** in 75% yield and 82:18 e.r. In the mismatched combination, with chiral base (*R*)-**A1**, diastereoisomer (2*S*,3*R*)-**2.14a** was obtained with a lower 71:29 e.r. Additionally, the same substrate was subjected to reaction conditions with an achiral IPr and chiral base **A2** resulting in moderate 71:29 enantiomeric ratio (Scheme 2.5a). This result further underlined the ability of chiral bases to induce enantioselectivity. In 2017, the Baudoin group reported the synthesis of chiral indolines **2.19** using chiral phosphoric acid **A3** via desymmetrization of enantiotopic methyl groups and 27 examples were reported with high yields and enantioselectivities (Scheme 2.5b).[127] However, in the case of the less reactive methylene C−H bonds a significant decrease in reactivity was observed albeit with consistent high enantioselectivities. Kinetic resolution from rac-**2.20** featuring competing methyl and methylene groups resulted in the formation of product **2.19a** by methyl C−H activation exclusively. In contrast to the report of Kündig, product **2.19b** arising from methylene C−H bond activation was not observed.

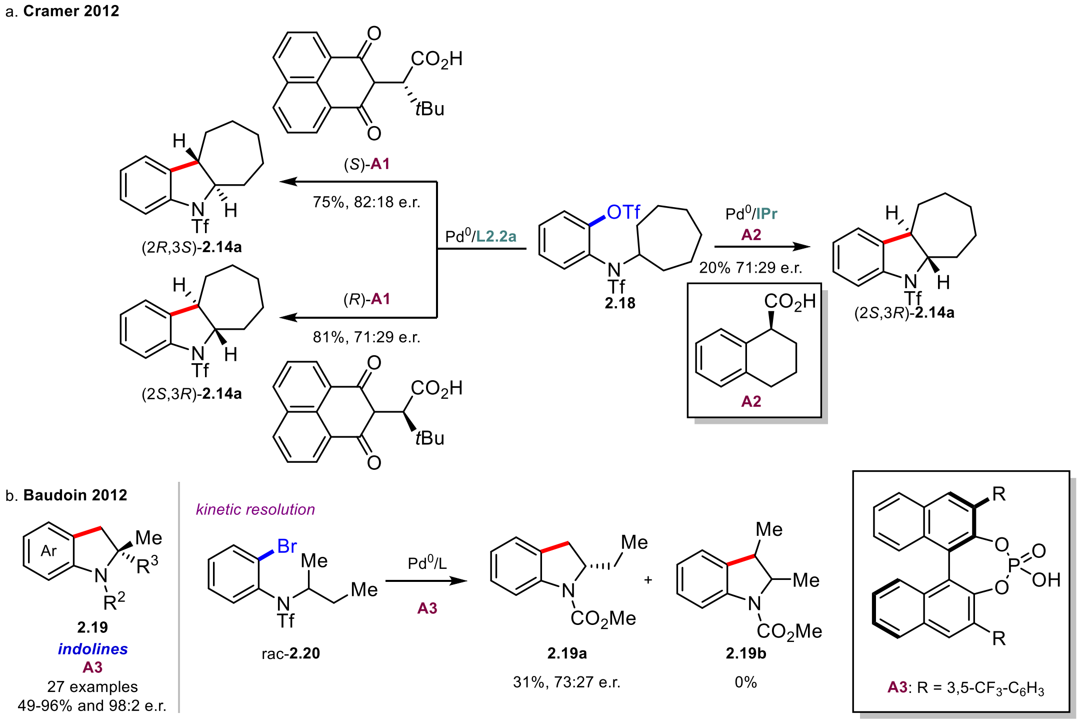
a. Cramer 2012
(S)-A1
75%, 82:18 e.r.
(2R,3S)-2.14a
Pd0/L2.2a
2.18
(R)-A1
81%, 71:29 e.r.
(2S,3R)-2.14a
Pd0/IPr
A2
20% 71:29 e.r.
(2S,3R)-2.14a
A2
b. Baudoin 2012
2.19
indolines
A3
27 examples
49-96% and 98:2 e.r.
kinetic resolution
rac-2.20
Pd0/L
A3
2.19a
31%, 73:27 e.r.
2.19b
0%
A3: R = 3,5-CF3-C6H3

Scheme 2.5: Chiral active base approach to induce chirality for the formation of indolines.

The enantioselective Pd(0)-catalyzed C−H activation reaction is a powerful tool for the synthesis of biologically active molecules. The first total synthesis of natural products including a Pd(0)-catalyzed enantioselective C(sp^3)−H activation as key step was reported by the Baudoin group in 2019 (Scheme 2.6).[128,129] The norilludalane sesquiterpene natural products (*S*)-puraquinoic (**2.25**) acid, (*S*)-deliquinone (**2.26**) and (*S*)-russujaponol F (**2.27**) share a bicyclic core with a characteristic quaternary stereogenic center. The formation of such quaternary stereogenic centers is a major challenge in synthetic organic chemistry mainly attributed to the build-up of high steric bulk in the transition state.[130–132] The C−H activation precursor **2.22** was obtained in seven steps from commercially available 2,5-dimethyl phenol **2.21**. Under the conditions reported by Kündig with the Hermann-type NHC ligand **L2.1a** (see Scheme 2.2) indane product **2.23** was obtained in 87% yield and 85:15 d.r. The proline-derived auxiliary on **2.22** with an isopropyl ester was essential to enhance selectivity as with the methyl ester derivative of **2.22** a significantly lower 66:34 e.r. was observed. Acidic removal of the auxiliary with concomitant deprotection of the methoxide led to indane **2.24**, whose enantiomeric ratio was further improved by recrystallization. Common intermediate **2.25** was prepared in two additional steps from which the three natural products **2.26**, **2.27** and **2.28** could be accessed in 14 to 15 overall steps for the longest linear sequence.

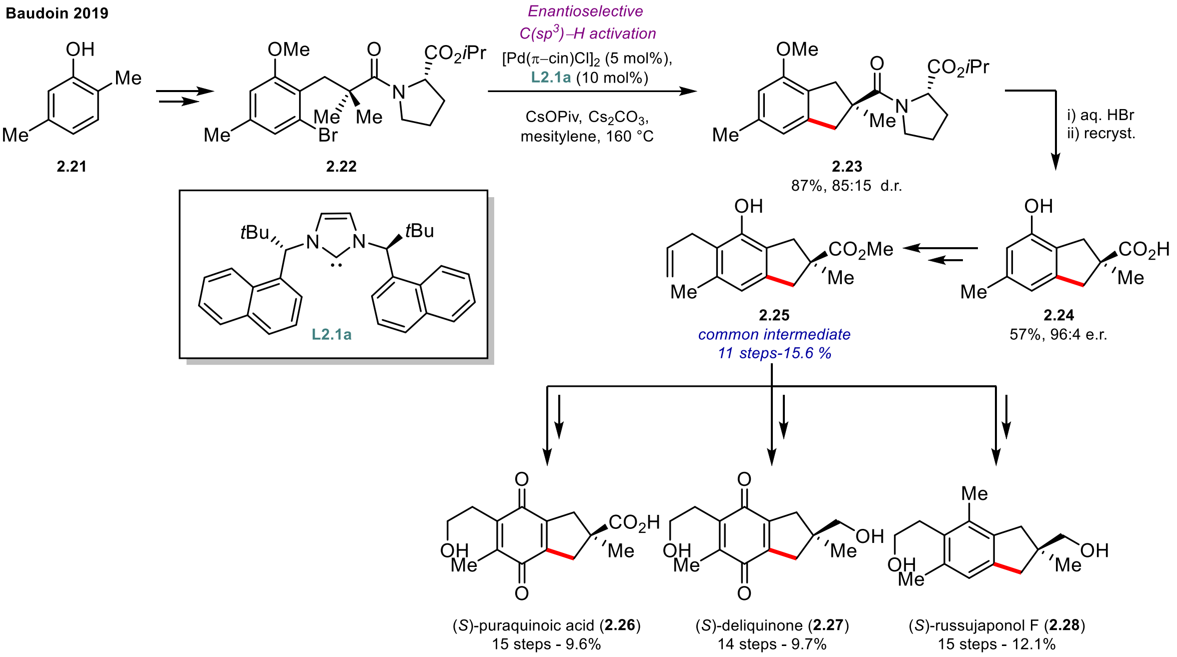
Baudoin 2019
OH
Me
Me
2.21
OMe
O
CO2iPr
N
Me
Me
Me
Br
2.22
Enantioselective
C(sp3)–H activation
[Pd(π–cin)Cl]2 (5 mol%),
L2.1a (10 mol%)
CsOPiv, Cs2CO3,
mesitylene, 160 °C
OMe
O
CO2iPr
N
Me
Me
2.23
87%, 85:15 d.r.
i) aq. HBr
ii) recryst.
tBu
N
N
tBu
L2.1a
OH
CO2Me
Me
Me
2.25
common intermediate
11 steps-15.6 %
OH
CO2H
Me
Me
2.24
57%, 96:4 e.r.
O
CO2H
OH
Me
Me
O
(S)-puraquinoic acid (2.26)
15 steps - 9.6%
O
OH
OH
Me
Me
O
(S)-deliquinone (2.27)
14 steps - 9.7%
Me
OH
OH
Me
Me
(S)-russujaponol F (2.28)
15 steps - 12.1%

Scheme 2.6: Total synthesis of (*S*)-puraquinoic (**2.25**) acid, (*S*)-deliquinone (**2.26**) and (*S*)-russujaponol F (**2.27**) by enantioselective Pd(0)-catalyzed C(sp^3)−H activation.

The enantioselective Pd(0)-catalyzed activation of cyclopropyl C–H bonds has gained great interest. The C−H bonds in cyclopropyl rings adopt a more sp^2-like character because the pronounced ring strain leads to the overlap of the C–H p-orbitals.[133–135] Thus, the C−H activation process is more facile compared to linear methylene or methyl C−H bonds. In 2012 the Cramer group reported the use of taddol derived phosphoramidite ligand **L1.2e** for the synthesis of tetraisoquinolines **2.29** in high yields and enantioselectivities (Scheme 2.7).[123] Interestingly, when R^2 = H, this methine position was activated preferentially leading to the racemic spiro-fused indoline product. Later the scope was expanded to the synthesis of dihydroquinolones and dihydroisoquinolones **2.30** and **2.31**, respectively employing the same phosphoramidite ligand **L1.2e**.[136]

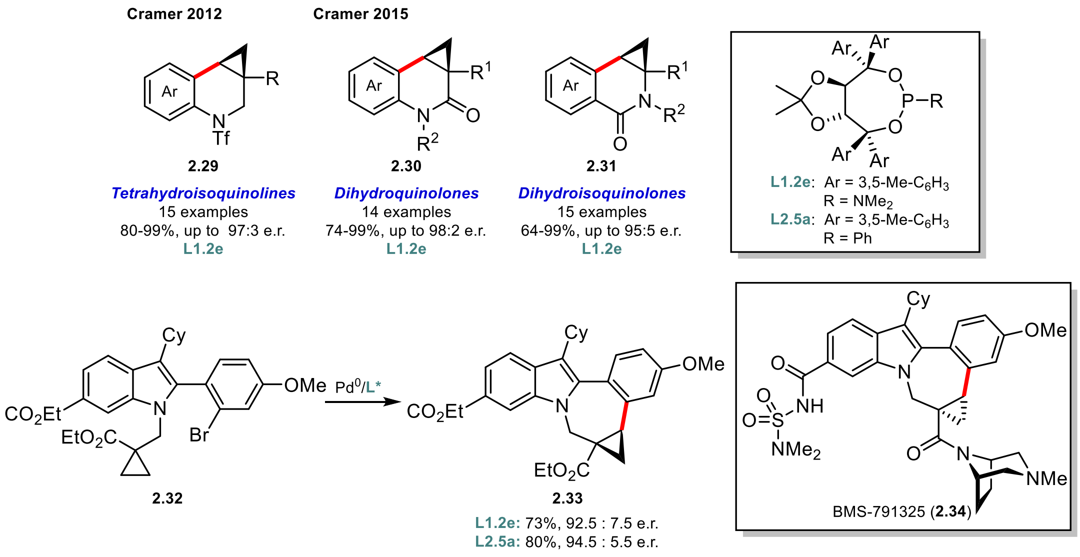
Cramer 2012
Cramer 2015
Ar
R
N
Tf
2.29
Tetrahydroisoquinolines
15 examples
80-99%, up to 97:3 e.r.
L1.2e
R^1
N
O
R^2
2.30
Dihydroquinolones
14 examples
74-99%, up to 98:2 e.r.
L1.2e
2.31
Dihydroisoquinolones
15 examples
64-99%, up to 95:5 e.r.
L1.2e
Ar
O
P–R
L1.2e: Ar = 3,5-Me-C_6H_3
R = NMe_2
L2.5a: Ar = 3,5-Me-C_6H_3
R = Ph
Cy
OMe
CO_2Et
EtO_2C
Br
2.32
Pd^0/L*
2.33
L1.2e: 73%, 92.5 : 7.5 e.r.
L2.5a: 80%, 94.5 : 5.5 e.r.
NH
O=S
NMe_2
NMe
BMS-791325 (2.34)

Scheme 2.7: Synthesis of tetrahydroisoquinolines **2.29**, dihydroquinolones **2.30** and dihydoisoquinolones **2.31** and application in the synthesis of the core structure of BMS-791325 (**2.34**).

The utility of this method was demonstrated in the synthesis of **2.33** in 73% yield and 92.5:7.5 e.r. representing the major carbon framework of BMS-791325 (**2.34**), a hepatitis C virus NS5B replicase inhibitor featuring a highly functionalized 7-membered ring.[137] The selectivity could be further increased using more electron-donating phosphonite ligand **L2.5a**.

In a similar reaction the Charette group observed enantioinduction when using hemilabile phosphine oxide ligand BozPhos for the synthesis of cyclopropane-fused azacycle **2.35** (Scheme 2.8). In this case, the palladium source played an important role.[138] With Pd_2dba_3, product **2.35** was obtained in 37% yield and 94:6 e.r. whereas with $Pd(OAc)_2$ the yield could be improved to 87% but the e.r. dropped to of 70:30. Later, the same group reported a more thorough study on the enantioselective activation of cyclopropanes to access dihydroquinolones **2.36** and dihydroisoquinolones **2.37** similar to the reports of the Cramer group (see Scheme 2.7). Using BozPhos as the ancillary ligand up to 99% yield and 99:1 e.r. was obtained.[139]

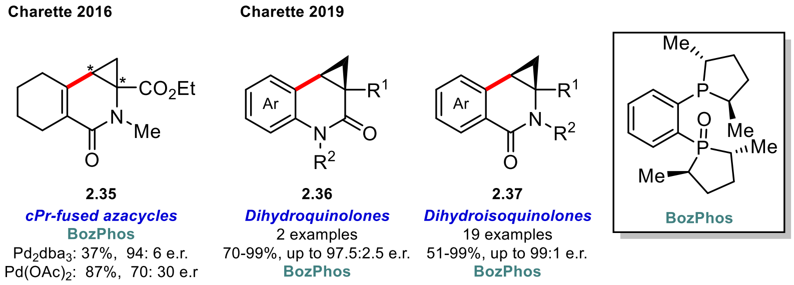
Charette 2016
Charette 2019
CO_2Et
N
Me
O
2.35
cPr-fused azacycles
BozPhos
Pd_2dba_3: 37%, 94: 6 e.r.
$Pd(OAc)_2$: 87%, 70: 30 e.r
Ar
R^1
R^2
2.36
Dihydroquinolones
2 examples
70-99%, up to 97.5:2.5 e.r.
BozPhos
2.37
Dihydroisoquinolones
19 examples
51-99%, up to 99:1 e.r.
BozPhos
Me
P
O
BozPhos

Scheme 2.8: Enantioselective activation of cyclopropane C–H bonds with chiral P,O ligand BozPhos.

Different electrophiles were used for the intramolecular C–H activation of cyclopropanes. Cyclopropyl-fused γ-lactams **2.69** were prepared from chloroacetamides **2.38**.[140] In this case high enantioselectivities were observed using taddol-derived phosphonite ligand **L2.5b** at relatively mild conditions (Scheme 2.9a). However, when R^2 = H, only starting material was recovered. The same group reported the synthesis of pyrrolidinones **2.41** from imidoyl chlorides **2.40** bearing a perfluorinated alkyl substuent in α-position to the nitrogen atom (Scheme 2.9b).[141] Previously employed phosphoramidite and phosphonite ligands of type **L1.2** and **L2.5** respectively failed to provide sufficient reactivity and enantioselectivity. Instead, chiral alkoxy diazaphospholidine **(*R*,*R*)-L1.5**,[142] with a backbone reminiscent of the NHC ligands **L2.1** described by the Kündig group (see Scheme 2.2), led to the formation of products **2.41** in excellent yields and enantioselectivities. A variety of postfunctionalizations of the pyrrolidine products were presented including a one-pot procedure for the formation of product **2.41** with subsequent nucleophilic attack on the imine moiety.

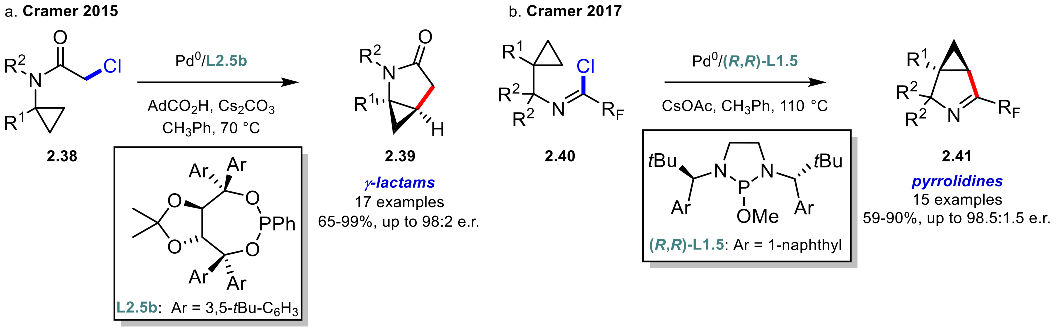
a. Cramer 2015
Pd0/L2.5b
AdCO2H, Cs2CO3
CH3Ph, 70 °C
2.38
2.39
γ-lactams
17 examples
65-99%, up to 98:2 e.r.
L2.5b: Ar = 3,5-tBu-C6H3
b. Cramer 2017
Pd0/(R,R)-L1.5
CsOAc, CH3Ph, 110 °C
2.40
2.41
pyrrolidines
15 examples
59-90%, up to 98.5:1.5 e.r.
(R,R)-L1.5: Ar = 1-naphthyl

Scheme 2.9: Enantioselective activation of cyclopropane C−H bonds from chloroacetamides **2.38** and imidoyl chlorides **2.40**. a. Synthesis γ-lactams. b. Synthesis of pyrrolidines.

The above-described methods mainly rely on the desymmetrization of methylene or methyl groups. Consequentially, the stereogenic center is formed in remote to the C−H bond undergoing activation. Examples of enantiotopic C(sp^3)−H bond activation, where the stereogenic center is formed on the carbon of the activated C−H bond are rare. The only precedent was reported by the Cramer group in 2014.[143] β-Lactams **2.42** were prepared from chloroacetamide precursors **2.43** in excellent yields and enantioselectivities using taddol derived phosphoramidite ligand **L1.2f** (Scheme 2.10). Chloroacetamides are prone to substitution reactions. Thus, one of the major challenges of this protocol was to suppress substitution reactions with nucleophilic reagents in the system such as the ligand and the active base. This limitation was overcome using a less nucleophilic phosphoramidite ligand compared to phosphines and more sterically demanding AdCO$_2$H as the active base. Additionally, a competition experiment was performed with substrate **2.43a** containing an electron-rich *p*-OMe-substituted phenyl ring electron-deficient *p*-CN-substituted phenyl ring. A product ratio of 4.8:1 in favour of structure **2.42a** arising from the activation of the more acidic benzylic position was observed.

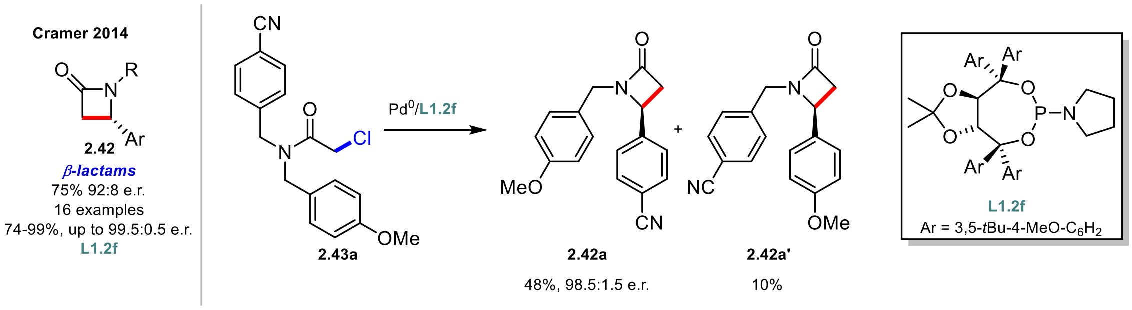
Cramer 2014
2.42
β-lactams
75% 92:8 e.r.
16 examples
74-99%, up to 99.5:0.5 e.r.
L1.2f
Pd0/L1.2f
2.43a
2.42a
48%, 98.5:1.5 e.r.
2.42a'
10%
L1.2f
Ar = 3,5-tBu-4-MeO-C6H2

Scheme 2.10: Synthesis of β-lactams by activation of enantiotopic C−H bonds.

2.2 Enantioselective Pd(0)-catalyzed intramolecular activation of methylene C−H bonds

The development of enantioselective transition metal catalyzed C−H functionalization is a long-standing challenge as it enables easy access to scalemic intermediates from readily available precursors.[111,144] The functionalization of non-activated enantiotopic methylene C(sp^3)−H bonds remains underexplored mainly due to the high bond dissociation energy of 90-110 kcal mol^{-1} and accessibility because of steric hindrance. To date, the enantioselective synthesis of β-lactams reported by the Cramer group, is the only precedent (see section 2.1.1, Scheme 2.10). However, this type of C−H bonds is easier to abstract compared to pure secondary aliphatic bonds due to the increased acidity arising from mesomeric stabilization. In this doctoral thesis we describe the development and optimization of an extremely reactive Pd(0)/NHC catalytic system, which is capable of activating secondary enantiotopic C(sp^3)−H bonds for the formation of chiral indanes. This is a rare example of enantioselective Pd(0)-catalyzed C(sp^3)−H bond activation where the stereogenic center is formed on the C−H activation site.

2.2.1 Optimization of reaction conditions

We envisioned to use substrates of type **2.44** where the modular design allows for easy exchange of the aromatic part and the alkyl chain undergoing C(sp^3)−H activation by sequential alkylation of a malonic ester. In addition, the bulkiness of the malonic esters can tune the Thorpe-Ingold effect required for the ring contraction facilitating cyclization to product **2.45** (see experimental part for substrate synthesis). We chose substrate **2.44a** featuring a fluorine atom para to the alkyl chain to monitor the reaction by ^{19}F NMR spectroscopy. An initial screening of achiral ligand classes under reported conditions for C(sp^3)−H activation was performed. Mainly dehalogenated byproduct **2.45** was observed with trialkyl and triaryl phosphine ligands under the conditions described by Ohno[79] for the synthesis of indolines (Table 1, entries 1-4). This observation indicates that the putative Pd(II) intermediate does not undergo C−H activation. Consequentially, more strongly σ-donating NHC[145] and cyclic alkyl amino carbene (CAAC)[146] ligands, that form more stable and electron-rich metal catalysts, were tested. Only starting material **2.44a** or protodehalogenation was observed under the conditions described by the Kündig group [114] with classic NHC ligands IAd, IMes and IPr (entries 5-7). In the case of CAAC ligand **L2.6** almost no conversion occurred, presumably due to its higher degree of saturation compared to the other NHC ligands, thus leading to decomposition under elevated temperatures.[114] Substantial product formation was obtained with IBiox-type ligands developed by the Glorius group.[147] With IBioxMe_4 and IBiox6 30% and 73% of the desired product was observed respectively (entries 9 and 10).

Table 2.1: Screening of achiral ligands.

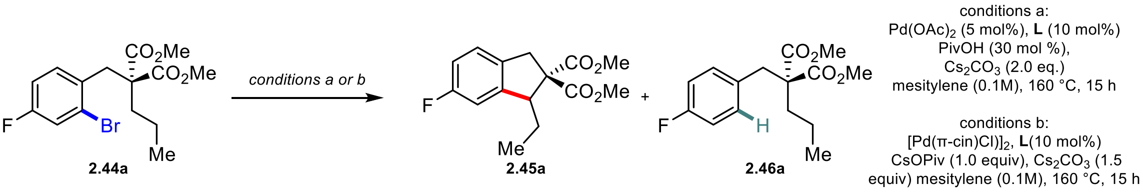
CO2Me
CO2Me
F
Br
Me
2.44a
conditions a or b
F
CO2Me
CO2Me
Me
2.45a
+
F
H
CO2Me
CO2Me
Me
2.46a
conditions a:
Pd(OAc)2 (5 mol%), L (10 mol%)
PivOH (30 mol %),
Cs2CO3 (2.0 eq.)
mesitylene (0.1M), 160 °C, 15 h
conditions b:
[Pd(π-cin)Cl)]2, L(10 mol%)
CsOPiv (1.0 equiv), Cs2CO3 (1.5 equiv) mesitylene (0.1M), 160 °C, 15 h

Entry	**conditions**[a]	**L**	**Product ratio**[a]			
			2.45a	**2.46a**	**2.44a**	**others**
1	a	PCy_3	-	75	-	25
2	a	P(*t*Bu)$_3$	5	26	69	-
3	a	CataCXium A•HCl	-	68	26	6
4	a	PPh_3	2	82	-	16
5	b	IAd•HCl	7	13	80	-
6	b	IMes•HCl	-	20	75	5
7	b	IPr•HCl	-	72	19	9
8	b	**L2.6**	-	4	96	-
9	b	IBioxMe$_4$•HOTf	30	55	-	15
10	**b**	**IBiox6•HOTf**	**73**	**14**	**-**	**13**

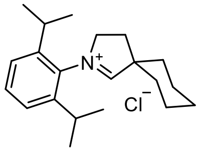

L2.6

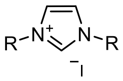

IAd•HCl: R = Ad
IPr•HCl: R = 2,6-*i*Pr-C_6H_3
IMes•HCl: R = 2,4,6-Me-C_6H_2

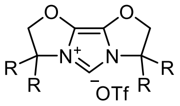
O
O
R
R
N+
N
R
R
−OTf

IBioxMe$_4$•HOTf: R = Me
IBiox6•HOTf: R,R = $(CH_2)_5$

[a]Determined by ^{19}F-NMR

Encouraged by these initial results, we turned our attention to chiral ligands. Binepine ligand **L2.4b** failed to provide any product formation in this case. Instead, Krapcho-type decarboxylation was observed as only side product (Table 2, entry 1). Phosphoramidite **L1.2b** and Phosphinite **L2.5c** were also not suitable ligands (entries 2 and 3). Surprisingly, no traces of product **2.45a** were observed with NHC ligand **L2.1a** (entry 4). Chiral IBiox ligands IBioxMenth and IBioxtBu gave product **2.45** with 41% and 33% product formation and high to excellent 86:14 and 99:1 e.r. respectively (entries 5 and 6).

Table 2.2: Screening of chiral ligands.

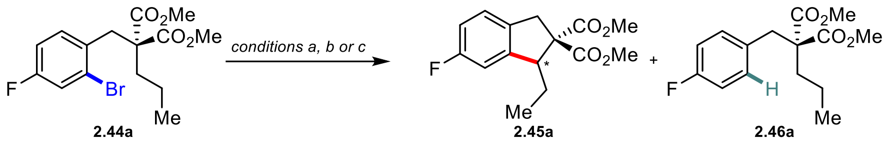
CO2Me
CO2Me
F
Br
Me
2.44a
conditions a, b or c
F
CO2Me
CO2Me
*
Me
2.45a
+
CO2Me
CO2Me
F
H
Me
2.46a

conditions a:
Pd_2dba_3 (5 mol%), **L** (15 mol%)
Cs_2CO_3 (2.0 equiv)
DMSO (0.1M), 140 °C, 15 h

conditions b:
Pd_2dba_3 (5 mol%), **L** (10 mol%)
CsOPiv (1.0 equiv), Cs_2CO_3 (1.5 equiv)
mesitylene (0.1M), 160 °C, 15 h

conditions c:
[Pd(π-cin)Cl)]$_2$, **L**(10 mol%)
CsOPiv (1.0 equiv), Cs_2CO_3 (1.5 equiv)
mesitylene (1M), 160 °C, 15 h

Entry	Conditions	L	Product ratio[a]				
			2.45a	2.46a	2.44a	others	e.r.[b]
1	a	**L2.4**•HBF_4	-	-	-	100	n.d.[c]
2	b	**L1.2b**	-	7	93	-	n.d.[c]
3	b	**L2.5c**	-	31	57	12	n.d.[c]
4	c	**L2.1a**•HI	-	10	90	-	n.d.[c]
5	**c**	**IBioxMenth•HOTf**	**41**	**34**	**19**	**6**	**86:14**
6	**c**	**IBiox*t*Bu•HOTf**	**33**	**47**	**11**	**-**	**99:1**

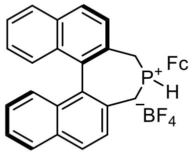

L2.4b•HBF_4

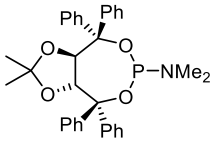
Ph
Ph
O
O
P–NMe2
O
O
Ph
Ph

L1.2b

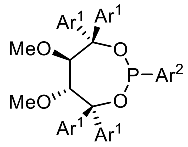
Ar1
Ar1
MeO
O
P–Ar2
MeO
O
Ar1
Ar1

L2.5c
Ar^1 = 3,5-CF_3-C_6H_3
Ar^2 = 3,5-tBu-4-OMe-C_6H_2

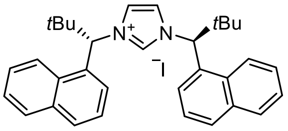

L2.1a•HI

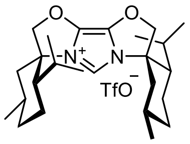

IBioxMenth•HOTf

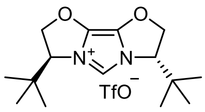

IBiox*t*Bu•HOTf

[a]Determined by ^{19}F-NMR. [b]Determined by HPLC on a chiral stationary phase. [c]n.d. = not determined.

These results prompted us to prepare chiral congeners of the same IBioxR ligand family and examine them in our reaction. Identical results were obtained with IBiox*i*Pr and IBioxCy, with 13% of product **2.45a** along with 37% of proto-dehalogenated byproduct **2.46a** (Table 2.3, entries 1 and 2). In the case of IBiox*i*Bu very poor reactivity was observed leading mainly to recovery of starting material **2.44a** (entry 3). A 1:1 ratio of product **2.45a** and byproduct **2.46a** were formed with IBioxAd as ligand (entry 4). The e.r. of 95:5 was comparable to the one obtained with IBiox*t*Bu (see Table 2.2, entry 6). Further optimization was undertaken with IBioxAd because the best reactivity/enantioselectivity compromise was obtained.

Table 2.3: Screening of chiral IBioxR-type ligands.

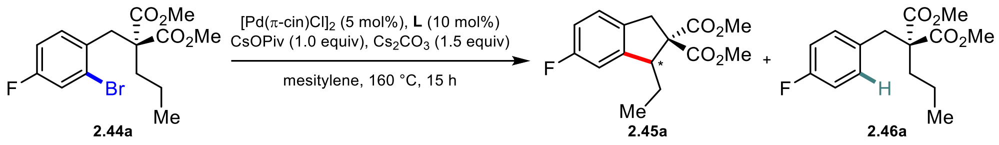

CO₂Me
CO₂Me
F
Br
Me
2.44a
[Pd(π-cin)Cl]₂ (5 mol%), L (10 mol%)
CsOPiv (1.0 equiv), Cs₂CO₃ (1.5 equiv)
mesitylene, 160 °C, 15 h
F
CO₂Me
CO₂Me
*
Me
2.45a
+
F
H
CO₂Me
CO₂Me
Me
2.46a

Entry	L	Product ratio[a]				
		2.45a	2.46a	2.44a	others	e.r.[b]
1	**IBiox*i*Pr•HOTf**	13	37	45	5	n.d.[b]
2	**IBioxCy•HOTf**	13	37	45	5	n.d.[b]
3	**IBiox*i*Bu•HOTf**	1	19	79	1	n.d.[c]
4	**IBioxAd•HOTf**	**40**	**40**	**10**	**10**	**95:5**

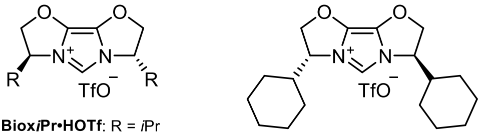

O
O
N
N
R
R
TfO⁻
O
O
N
N
TfO⁻

IBiox*i*Pr•HOTf: R = *i*Pr
IBiox*i*Bu•HOTf: R = *i*Bu
IBioxCy•HOTf: R = Ad

IBioxCy•HOTf

[a]Determined by ^{19}F-NMR. [b]Determined by HPLC on a chiral stationary phase. [c]n.d. = not determined.

Reaction parameters such as concentration, temperature and base loading were evaluated. Diluting the reaction from 0.1 M to 0.05 M gave 53% of **2.45a** and 98:2 e.r. (Table 2.4, entry 1). Conversely, a higher 0.2 M concentration led to slightly increased product formation of 60% and unchanged 98:2 e.r. (entry 2). At 120 °C only traces of product **2.45a** were observed along with 69% of starting material **2.44a** indicating that higher temperatures are required to achieve full conversion (entry 3). At 140 °C again full conversion was observed with 55% product formation (entry 4). Combining a concentration of 0.2 M with a lower temperature of 140 °C slightly increased the product formation to 59% (entry 5). At 160 °C a marginal increase in product formation to 60% and 63% was obtained with 2.0 or 3.0 equiv of Cs_2CO_3 loading (entries 6 and 7). With 2.0 equiv of Cs_2CO_3 at 140 °C resulted in lower product formation of 49% (entry 8).

Table 2.4: Effect of concentration, temperature and amount of stoichiometric base Cs_2CO_3 on the product formation.

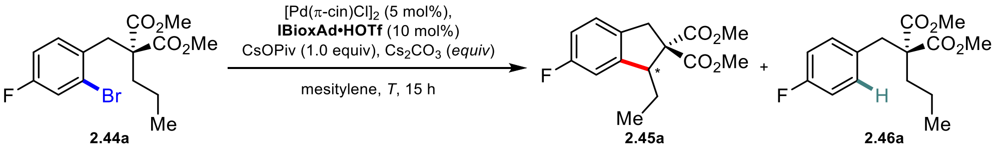

CO₂Me
CO₂Me
F
Br
Me
2.44a
[Pd(π-cin)Cl]₂ (5 mol%),
IBioxAd•HOTf (10 mol%)
CsOPiv (1.0 equiv), Cs₂CO₃ (equiv)
mesitylene, T, 15 h
F
CO₂Me
CO₂Me
*
Me
2.45a
+
F
H
CO₂Me
CO₂Me
Me
2.46a

Entry	Conc. [M]	T [°C]	Cs_2CO_3 (equiv)	Product ratio[a]				
				2.45a	2.46a	2.44a	others	e.r.[b]
1	0.05	160	1.5	53	35	6	6	98:2
2	**0.2**	**160**	**1.5**	**60**	**28**	**-**	**12**	**98:2**
3	0.1	120	1.5	7	20	69	4	n.d.[c]
4	0.1	140	1.5	55	38	-	7	98:2
5	**0.2**	**140**	**1.5**	**59**	**35**	**-**	**6**	**n.d.[b]**
6	**0.1**	**160**	**2.0**	**60**	**25**	**-**	**15**	**98:2**
7	**0.1**	**160**	**3.0**	**63**	**24**	**-**	**13**	**n.d.[b]**

8	0.1	140	2.0	49	42	-	9	n.d.[b]

[a]Determined by ^{19}F-NMR. [b]Determined by HPLC on a chiral stationary phase. [c]n.d. = not determined.

Solvent and base screenings were conducted at a 0.1 M concentration. The active base screening with 1.5 or 2.0 equiv Cs_2CO_3 at either 140 °C or 160 °C showed that pivalate derivatives were the most effective (Table 2.5, entries 1-6). Since the free pivalic acid and its cesium salt performed similarly giving 65% product formation, we decided to continue our study with CsOPiv for practicality reasons. Changing mesitylene for the more polar *n*-dibutyl ether solvent did not have any positive effect (entry 7). In xylenes, product **2.45a** was obtained with comparable product formation of 62%. (entry 8). In presence of 3Å and 4Å molecular sieves the product formation dropped significantly to 15% and 36% respectively (entries 9 and 10). Conversely, 5Å molecular sieves proved to be highly beneficial as indane **2.45a** was formed in 80% together with 18% of proto-dehalogenated byproduct **2.46** (entry 11). Different active base loading did not give improved results (entries 12 and 13). Performing the reaction in isolated isomers *o*- and *p*-xylenes was not fruitful either (entries 14 and 15).

Table 2.5: Influence of active base, amount of stoichiometric base Cs_2CO_3, temperature and solvent on the formation of product **2.45a**.

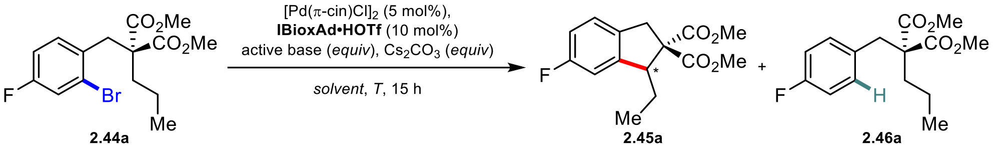

Entry	Active base (equiv)	Cs_2CO_3 (equiv)	T [°C]	Solvent	Product ratio[a]				
					2.45a	2.46a	2.44a	others	e.r.[b]
1	PivOH (0.3)	2.0	160	mesitylene	65	24	-	11	98:2
2	PivOH (0.3)	2.0	140	mesitylene	32	38	23	7	98:2
3	CsOAc (1.0)	1.5	160	mesitylene	14	41	43	2	n.d.[c]
4	CF_3CO_2Cs (1.0)	1.5	160	mesitylene	51	39	10	-	n.d.[c]
5	$AdCO_2H$ (0.3)	2.0	160	mesitylene	22	33	43	2	n.d.[c]
6	$MesCO_2H$ (0.3)	2.0	160	mesitylene	60	25	-	15	98:2
7	CsOPiv (1.0)	1.5	140	*n*Bu_2O	57	39	-	4	n.d.[c]
8	CsOPiv (1.0)	1.5	140	xylenes	62	33	-	5	98:2
9[d]	CsOPiv (1.0)	1.5	140	xylenes	15	32	18	35	n.d.[c]
10[e]	CsOPiv (1.0)	1.5	140	xylenes	36	31	4	29	n.d.[c]
11[f]	**CsOPiv (1.0)**	**1.5**	**140**	**xylenes**	**80**	**18**	**-**	**2**	**98:2**
12[f]	CsOPiv (0.3)	1.5	140	xylenes	72	20	-	8	n.d.[c]
13[f]	CsOPiv (0.3)	2.0	140	xylenes	71	26	-	3	n.d.[c]
14[f]	CsOPiv (1.0)	1.5	140	*o*-xylenes	77	20	-	3	n.d.[c]
15[f]	CsOPiv (1.0)	1.5	140	*p*-xylenes	74	24	-	2	n.d.[c]

[a]Determined by ^{19}F-NMR. [b]Determined by HPLC on a chiral stationary phase. [c]n.d. = not determined. [d]Reaction perfomed in presence of 3Å (25 mg/ 0.1 mmol). [e]Reaction perfomed in presence of 4Å (25 mg/ 0.1 mmol). [f]Reaction perfomed in presence of 5Å (25 mg/ 0.1 mmol)

Despite the high product formation of 80% (Table 2.5, entry 11), the separation from the proto-dehalogenated byproduct was very challenging. Thus, additional palladium sources were screened to suppress the dehalogenation.

Table 2.6: Screening of Pd(II) precatalysts.

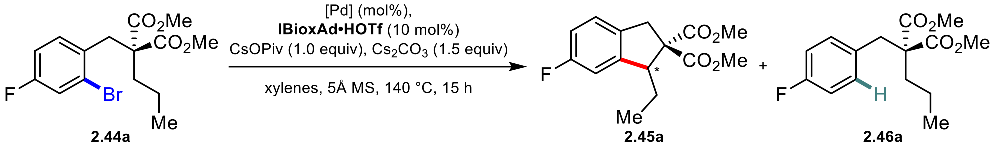
CO2Me
CO2Me
F
Br
Me
2.44a
[Pd] (mol%),
IBioxAd•HOTf (10 mol%)
CsOPiv (1.0 equiv), Cs2CO3 (1.5 equiv)
xylenes, 5Å MS, 140 °C, 15 h
F
CO2Me
CO2Me
*
Me
2.45a
+
CO2Me
CO2Me
F
H
Me
2.46a

Entry	[Pd] (mol%)	Product ratio[a]			
		2.45a	2.46a	2.44a	others
1	Pd(π-allyl)Cp (10)	15	34	14	37
2	Pd(π-cin)Cp (10)	26	35	-	39
3	**[Pd(π-allyl)Cl]$_2$ (5)**	**79**	**16**	**-**	**5**

[a]Determined by ^{19}F-NMR. [b]Determined by HPLC on a chiral stationary phase. [c]n.d. = not determined

Precatalysts Pd(π-allyl)Cp and Pd(π-cin)Cp led to poor product formation of 15% and 26% respectively (Table 2.6, entries 1 and 2). A similar reactivity was observed with [Pd(π-allyl)Cl]$_2$ giving 79% of indane **2.45a**. This precatalyst was chosen for further studies due to its straightforward preparation with high purity, thus preventing reproducibility issues.

With no major improvement after the screening of palladium sources we turned back to the active and stoichiometric bases. Keeping Cs_2CO_3 as the base, with xanthoic acid, dibenzyl phosphonate, PivNHOH only traces of product **2.45a** were observed (Table 2.7, entries 1-3).

Table 2.7: Second screening of active and stoichiometric base.

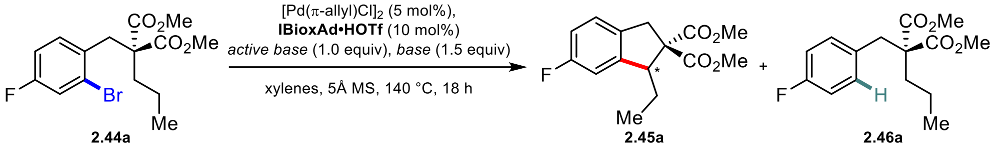
CO2Me
CO2Me
F
Br
Me
2.44a
[Pd(π-allyl)Cl]2 (5 mol%),
IBioxAd•HOTf (10 mol%)
active base (1.0 equiv), base (1.5 equiv)
xylenes, 5Å MS, 140 °C, 18 h
F
CO2Me
CO2Me
*
Me
2.45a
+
CO2Me
CO2Me
F
H
Me
2.46a

Entry	active base	base	Product ratio[a]			
			2.45a	2.46a	2.44a	others
1	xanthoic acid	Cs_2CO_3	-	11	87	2
2	dibenzyl phosphate	Cs_2CO_3	3	8	88	1
3	PivNHOH	Cs_2CO_3	4	14	66	16
4	hexanoic acid	Cs_2CO_3	61	30	2	7
5	$AdCO_2H$	Cs_2CO_3	5	3	91	1
6	$MesCO_2H$	Cs_2CO_3	14	14	67	5
7	AcOH	Cs_2CO_3	1	8	88	3
8	CsOPiv	K_2CO_3	4	17	35	44
9	CsOPiv	Rb_2CO_3	35	18	-	47
10	CsOPiv	K_3PO_4	12	18	45	25
11	CsOPiv	CsOH	3	32	57	8

[a]Determined by ^{19}F-NMR.

With hexanoic acid a significant product formation of 61% was observed however, still not outperforming CsOPiv (entry 4). Retesting $AdCO_2H$, $MesCO_2H$ and AcOH under the new conditions was not beneficial (entries 5-7). The size of the counter ion of different carbonate sources played an important role, as with the smaller K^+ and Rb^+ (compared to Cs^+) a significant lower product formation of 4% and 35% respectively was observed (entries 8 and 9). Presumably, this behaviour is attributed to increased solubility of the carbonate as the larger counter ion dissociates more easily. With K_3PO_4 only traces of indane **2.45a** were observed (entry 10). Similarly, with CsOH only 3% of the product was formed. Unfortunately, in this optimizations no increase in product formation was observed and therefore the e.r. values were not recorded.

We reevaluated the solvent effect under the new reaction conditions. With etheric solvents CPME, 1,4-dioxane and *n*Bu_2O, no improvement compared to xylenes was made (Table 2.8, entries 1-3). With t-Amyl alcohol as the reaction medium no product was observed (entry 4). Aromatic solvents such as pseudocumene, cumene and *p*-cymene, led to significant lower product formation (entries 6-7). In toluene, 76% of **2.45a** was obtained (entry 8). *α*,*α*,*α*,-Trifluorotoluene outperformed xylenes giving a product formation of 84% and 98:2 e.r. (entry 9). This result could be further improved to 95% together with only traces of dehalogenated byproduct **2.46a** using freshly distilled and degassed solvent (entry 10). The 98:2 enantiomeric ratio remained stable.

Table 2.8: Screening of solvents.

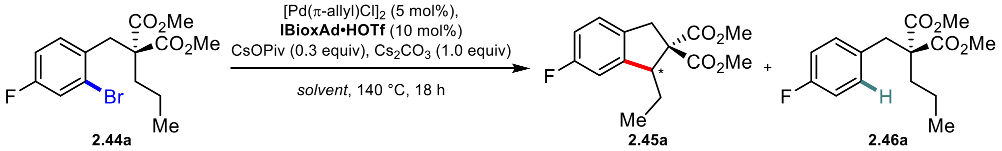

Entry	solvent	Product ratio[a]				e.r.[b]
		2.45a	2.46a	2.44a	others	
1	CPME	45	34	-	21	n.d.[c]
2	1,4-dioxane	25	23	31	21	n.d.[c]
3	*n*Bu_2O	60	33	-	7	n.d.[c]
4	*t*-amylOH	-	26	40	34	n.d.[c]
5	pseudocumene	40	36	20	4	n.d.[c]
6	cumene	24	37	7	32	n.d.[c]
7	*p*-cymene	4	55	22	19	n.d.[c]
8	toluene	76	21	-	3	n.d.[c]
9	***α*,*α*,*α*,-trifluorotoluene**	**84**	**14**	**-**	**2**	**98:2**
10[c]	***α*,*α*,*α*,-trifluorotoluene**	**95**	**2**	**-**	**3**	**98:2**

[a]Determined by ^{19}F-NMR. [b]Determined by HPLC on a chiral stationary phase. [c]n.d. = not determined. [d]Reaction run with freshly distilled and degassed solvent.

The chiral IBioxR ligands were revisited in *α*,*α*,*α*,-trifluorotoluene. IBioxMenth•HOTf gave product **2.45a** in high 89% isolated yield albeit in low 14:86 e.r. (Table 2.9, entry 1). IBiox*i*Pr•HOTf led to 14% yield and a similar 85:15 e.r. (entry 2). Slightly higher e.r. was observed with IBioxCy•HOTf despite a moderate 39% yield (entry 3). Finally, IBiox*t*Bu•HOTf and IBioxAd•HOTf performed similarly giving indane product in 88% and 91% yield respectively and 98:2 e.r. (entries 4 and 5).

Table 2.9: Screening of IBioxR ligands under optimized conditions.

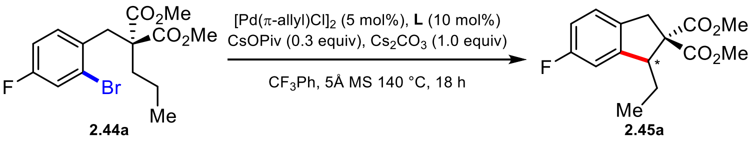

2.44a
CO2Me
CO2Me
F
Br
Me
[Pd(π-allyl)Cl]2 (5 mol%), L (10 mol%)
CsOPiv (0.3 equiv), Cs2CO3 (1.0 equiv)
CF3Ph, 5Å MS 140 °C, 18 h
F
CO2Me
CO2Me
*
Me
2.45a

Entry	L	yield (%)[a]	e.r.[b]
1	IBioxMenth•HOTf	89	14:86
2	IBiox*i*Pr•HOTf	14	85:15
3	IBioxCy•HOTf	39	7:93
4	IBiox*t*Bu•HOTf	88	98:2
5	**IBioxAd•HOTf**	**91**	**98:2**

[a]Yield of isolated product. [b]Determined by HPLC on a chiral stationary phase.

2.2.2 Scope of the Pd(0)-catalyzed asymmetric synthesis of indanes

The reaction scope was investigated under the finalized conditions. Precursors **2.44b-e** with aliphatic chains varying in length and steric bulk were suitable substrates giving indane products **2.45b-e** in good to high yields and high enantioselectivities (Scheme 2.11). Additionally, product **2.45c** could be prepared from both the corresponding aryl bromide and aryl chloride precursor, demonstrating the compatibility of the protocol with more economical and readily available aryl chlorides. Alkyl chains with a terminal fluorine atom (**2.45f**) and functional groups such as esters (**2.45g**), protected alcohols (**2.45h, 2.45i**) and protected amides (**2.45j**) were well tolerated. To demonstrate the robustness of the method, product **2.45j** was prepared in a 2.0 mmol scale in slightly lower 63% yield but high >99:1 e.r. after recrystallization. The malonic ester moiety plays a fundamental role for the cyclization of the products as it induces a Thorpe-Ingold effect that contracts the bond angle bringing the targeted C−H bond closer to the Pd-catalyst.[148] More sterically demanding ethyl and isopropyl esters were employed (**2.45k**, **2.45l**). The latter was obtained with moderate 34% isolated yield due to the difficult separation from the protodehalogenated byproduct. Products with fluorine substituents *meta* or *para* to the newly formed C−C bond were obtained in high yields and enantioselectivity (**2.45m**, **2.45a**). Notably, **2.45a** was prepared with the well-defined [Pd(IBioxAd)(π-allyl)Cl] complex in comparable yield and selectivity. Electron withdrawing substituents on the aromatic ring such as NO_2, CF_3, CO_2Me an SO_2Me were also compatible with the protocol (**2.45n**, **2.45o**, **2.45p**, **2.45q**). Despite the moderate yield, substrate **2.44r** featuring a strongly electron donating 1,3-dioxolan substituent was converted into the product in comparable enantioselectivity. Finally, tricyclic product **2.45s** arising from two-fold C−H activation was prepared by doubling the catalyst loading.

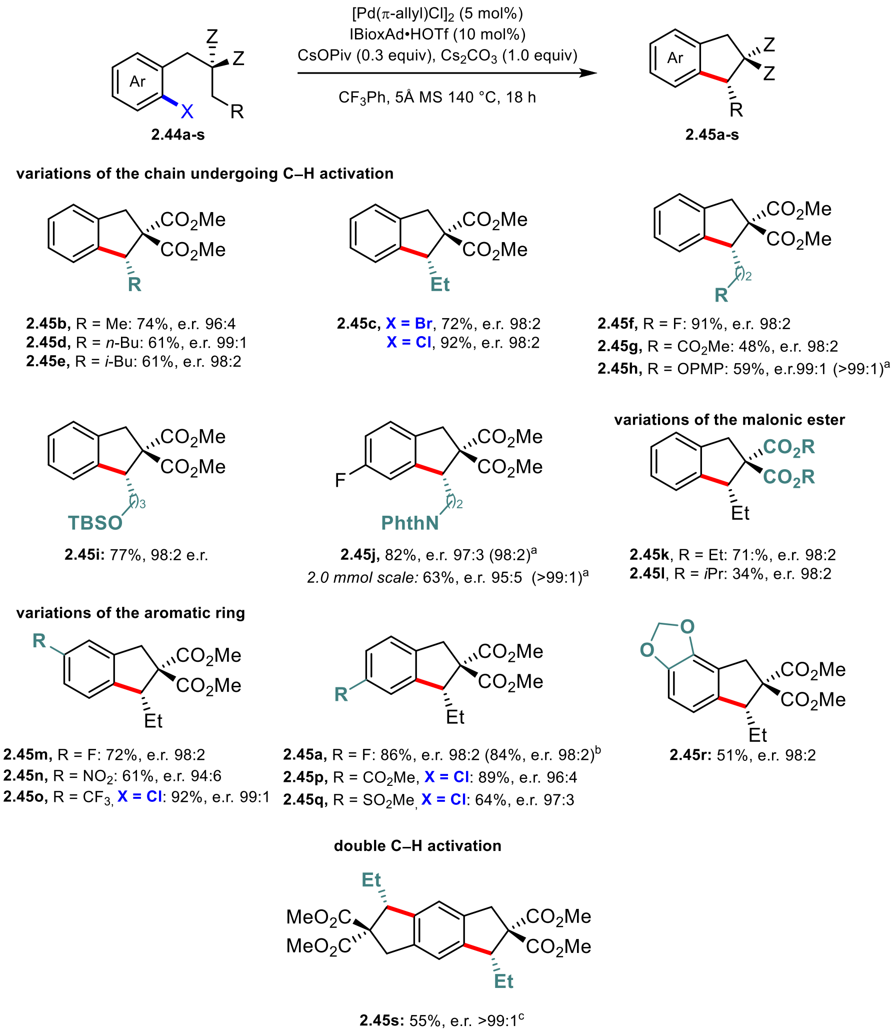
[Pd(π-allyl)Cl]2 (5 mol%)
IBioxAd•HOTf (10 mol%)
CsOPiv (0.3 equiv), Cs2CO3 (1.0 equiv)
CF3Ph, 5Å MS 140 °C, 18 h
2.44a-s
2.45a-s
variations of the chain undergoing C–H activation
2.45b, R = Me: 74%, e.r. 96:4
2.45d, R = n-Bu: 61%, e.r. 99:1
2.45e, R = i-Bu: 61%, e.r. 98:2
2.45c, X = Br, 72%, e.r. 98:2
X = Cl, 92%, e.r. 98:2
2.45f, R = F: 91%, e.r. 98:2
2.45g, R = CO2Me: 48%, e.r. 98:2
2.45h, R = OPMP: 59%, e.r.99:1 (>99:1)a
2.45i: 77%, 98:2 e.r.
2.45j, 82%, e.r. 97:3 (98:2)a
2.0 mmol scale: 63%, e.r. 95:5 (>99:1)a
variations of the malonic ester
2.45k, R = Et: 71:%, e.r. 98:2
2.45l, R = iPr: 34%, e.r. 98:2
variations of the aromatic ring
2.45m, R = F: 72%, e.r. 98:2
2.45n, R = NO2: 61%, e.r. 94:6
2.45o, R = CF3, X = Cl: 92%, e.r. 99:1
2.45a, R = F: 86%, e.r. 98:2 (84%, e.r. 98:2)b
2.45p, R = CO2Me, X = Cl: 89%, e.r. 96:4
2.45q, R = SO2Me, X = Cl: 64%, e.r. 97:3
2.45r: 51%, e.r. 98:2
double C–H activation
2.45s: 55%, e.r. >99:1c

Scheme 2.11: Scope of the reaction. [a]After recrystallization. [b]Reaction performed with [Pd(IBIoxAd)(π-allyl)Cl] complex. [c]Reaction performed in presence of 10 mol% [Pd(π-allyl)Cl]$_2$ and 20 mol% of IBioxAd•HOTf.

Chiral tertiary amides are highly desirable motifs found in natural and synthetic molecules with numerous applications in the pharmaceutical industry.[149–151] However, due to its acidic stereogenic center in α-position of the carbonyl they are very challenging to access. We therefore attempted the synthesis of product **2.45t** by activating the methylene C−H bond in α-position of a dimethyl amide substituent. Surprisingly, the product was obtained in almost quantitative yield and a high 95:5 e.r. (Table 2.10, entry 1). With substrate **2.44u** bearing a morpholine amide functional group lower yield and a decrease in enantioselectivity to 68:32 e.r. was observed (entry 2). We hypothesized that racemization occurred after the reaction went to full completion and therefore reduced the reaction time from 18 to 8 h. Indeed, enantioselectivity was restored to 97:3 (entry 3). Similarly, product **2.45v** was obtained in 80% yield and 70:30 e.r. (entry 4) after 18 h and reducing the reaction time to 4 h increased the enantioselectivity again to 98:2 e.r. (entry 5). Methyl ester **2.44w** however, gave only racemic product **2.45w** before full completion. This suggests, that the racemization process is faster than the C−H activation reaction. Nevertheless, we prepared three tertiary amides **2.45t-v** by enantioselective Pd(0)-catalyzed C(sp^3)−H bond activation, which, to our knowledge, is the first report of this kind of transformation.

Table 2.10: Synthesis of 3^{ary} amides.

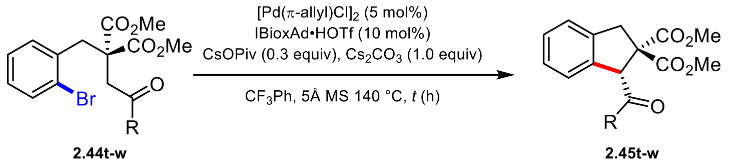

CO2Me
CO2Me
Br
O
R
2.44t-w
[Pd(π-allyl)Cl]2 (5 mol%)
IBioxAd•HOTf (10 mol%)
CsOPiv (0.3 equiv), Cs2CO3 (1.0 equiv)
CF3Ph, 5Å MS 140 °C, t (h)
CO2Me
CO2Me
R
O
2.45t-w

Entry	Product	R	t [h]	Yield [%][a]	e.r.[b]
1	**2.45t**	NMe_2	18	94	95:5
2	**2.45u**	NC_4H_8O	18	87	68:32
3	**2.45u**	NC_4H_8O	8	95	97:3
4	**2.45v**	N(Me)OMe	18	80	70:30
5	**2.45v**	N(Me)OMe	4	75	98:2
6	**2.45w**	OMe	2	n.d.[c]	55:45

[a]Yield of isolated product. [b]Determined by HPLC on a chiral stationary phase. [c]n.d. = not determined.

Heteroaromatic substrates were less efficient, displaying low product formation or no reactivity at all. For pyridine derived substrates **2.44x** and **2.44y**, the reaction did not reach full conversion and only a product formation of 55% was observed for both entries (Scheme 2.12). The product could not be separated by column chromatography because the reaction mixture contained substantial amounts of starting aryl bromide and dehalogenated byproduct. In the case of pyrazine- and quinolone- based substrates **2.44z** and **2.44aa** only traces of the product were observed. Presumably, coordination of the nitrogen to Pd led to catalyst sequestration. For thiazole-derived substrates **2.44ab** and **2.44ac** similar results were obtained. High amounts of proto-dehalogenation and starting material were observed, presumably due to the challenging reductive elimination to form the strained 5,5-fused ring system. Substrates featuring strongly electron-donating substituents in *para* and *meta* position to the bromine on the aromatic ring (**2.44ad**, **2.44ae** and **244af**) were not efficient leading to mainly proto-dehalogenation. Finally, the modification of the ring-contracting substituents from a malonic ester to a dimethyl ether (**2.44ag**) to tune the Thorpe-Ingold effect had a negative impact on the reaction outcome. Also in this case, mostly proto-dehalogenation together with non-converted starting material was observed.

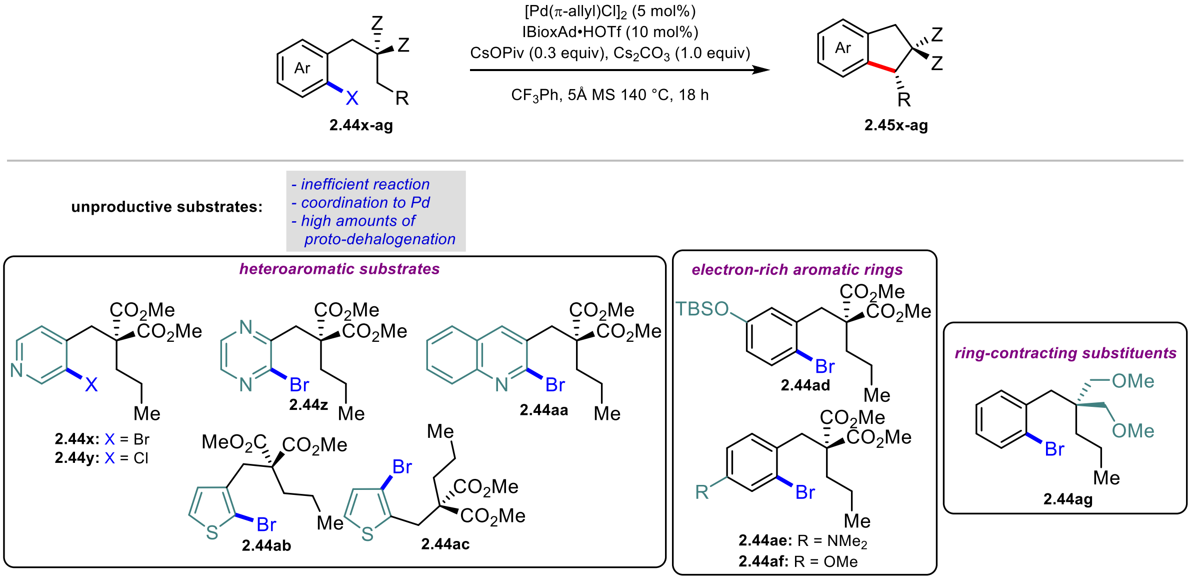

Z
Z
Ar
X
R
2.44x-ag
[Pd(π-allyl)Cl]2 (5 mol%)
IBioxAd•HOTf (10 mol%)
CsOPiv (0.3 equiv), Cs2CO3 (1.0 equiv)
CF3Ph, 5Å MS 140 °C, 18 h
Ar
Z
Z
R
2.45x-ag
unproductive substrates:
- inefficient reaction
- coordination to Pd
- high amounts of proto-dehalogenation
heteroaromatic substrates
CO2Me
CO2Me
N
X
Me
2.44x: X = Br
2.44y: X = Cl
N
N
Br
2.44z
Me
N
Br
2.44aa
Me
MeO2C
CO2Me
S
Br
2.44ab
Me
Me
Br
S
CO2Me
CO2Me
2.44ac
electron-rich aromatic rings
TBSO
Br
2.44ad
Me
R
Br
Me
2.44ae: R = NMe2
2.44af: R = OMe
ring-contracting substituents
OMe
OMe
Br
Me
2.44ag

Scheme 2.12: Unsuccessful C−H activation substrates.

To demonstrate the utility of the chiral indanes **2.45** we aimed to derivatize representative examples. Based on recent literature reports converting malonic acids to gem-difluoro and fully decarboxylated derivatives,[152,153] we envisaged to prepare products **2.45cb** and **2.45cc** (Scheme 2.13a). However, subjecting starting material **2.45ca**, which was obtained from racemic **2.45c** by saponification, to Ag-catalyzed gem-difluorination conditions was unsuccessful. Similarly, product **2.45cc** was not observed under photoinduced decarboxylation conditions. These results prompted us to select substrate **2.45j** featuring a heavy phthalimide functional group and change our functionalization strategies (Scheme 2.12b). Deprotection of the phthalimide moiety with hydrazine hydrate and concomitant cyclization led to *cis*-configured tricyclic structure **2.45ja** in very high yield and as single observable diastereoisomer. Additionally, spirocyclic dimethyl-barbiturate derivative **2.45jb** was prepared from **2.45j** by condensation with urea and subsequent methylation.

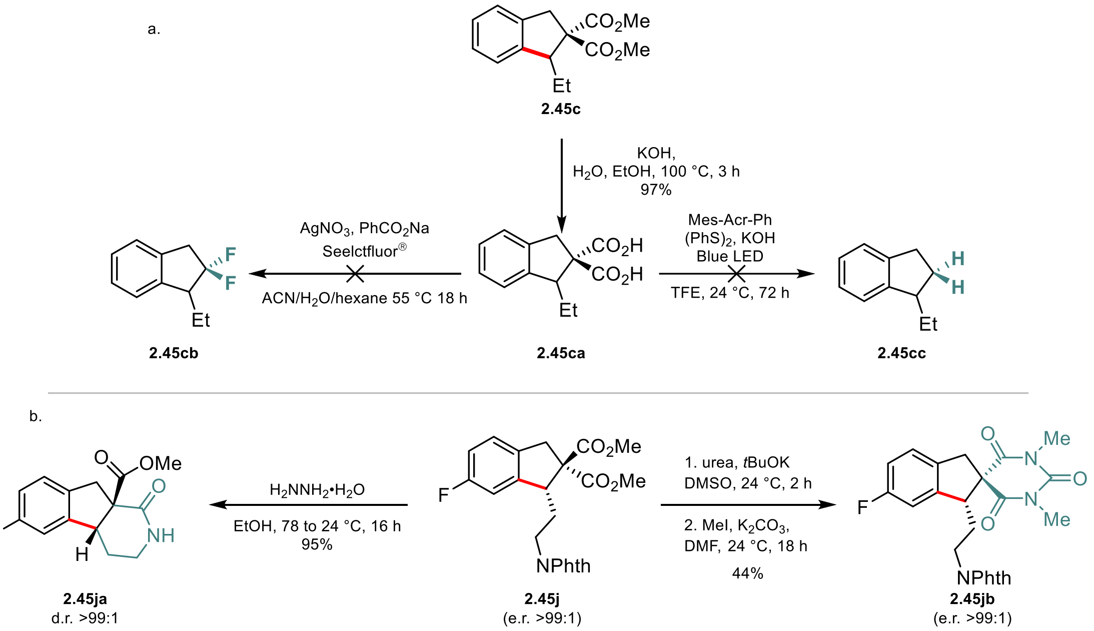
a.
2.45c
KOH,
H2O, EtOH, 100 °C, 3 h
97%
AgNO3, PhCO2Na
Seelctfluor®
ACN/H2O/hexane 55 °C 18 h
Mes-Acr-Ph
(PhS)2, KOH
Blue LED
TFE, 24 °C, 72 h
2.45cb
2.45ca
2.45cc
b.
H2NNH2•H2O
EtOH, 78 to 24 °C, 16 h
95%
1. urea, tBuOK
DMSO, 24 °C, 2 h
2. MeI, K2CO3,
DMF, 24 °C, 18 h
44%
2.45ja
d.r. >99:1
2.45j
(e.r. >99:1)
2.45jb
(e.r. >99:1)

Scheme 2.13: Derivatizations of indane products **2.45**.

Efforts to grow crystals suitable for X-ray analysis were unsuccessful. Therefore, the stereogenic center was determined to have the *R* configuration based on the vibrational circular dichroism (VCD) spectroscopy analysis of products **2.45c**, **2.45t** and **2.45ja** performed in collaboration with Prof. Dr. Thomas Bürgi (see experimental section for further details).

In order to determine the kinetic isotope effect (KIE) protiated **2.44ah** and deuterated **2.44ah-d5** were prepared and parallel kinetic experiments were performed using the well-defined [Pd(IBioxtBu)(π-allyl)Cl] complex. The observed induction period is attributed to the reduction of the Pd(II) precatalyst to the Pd(0) active species[154] and therefore an exact value could not be determined. Nevertheless, a clear isotope effect is visible as the reaction profile for protiated **2.44ah** (deep blue curve) is steeper than the one of deuterated **2.44ah-*d*$_5$** (deep red curve). This result suggests that the C−H activation step is rate-limiting.

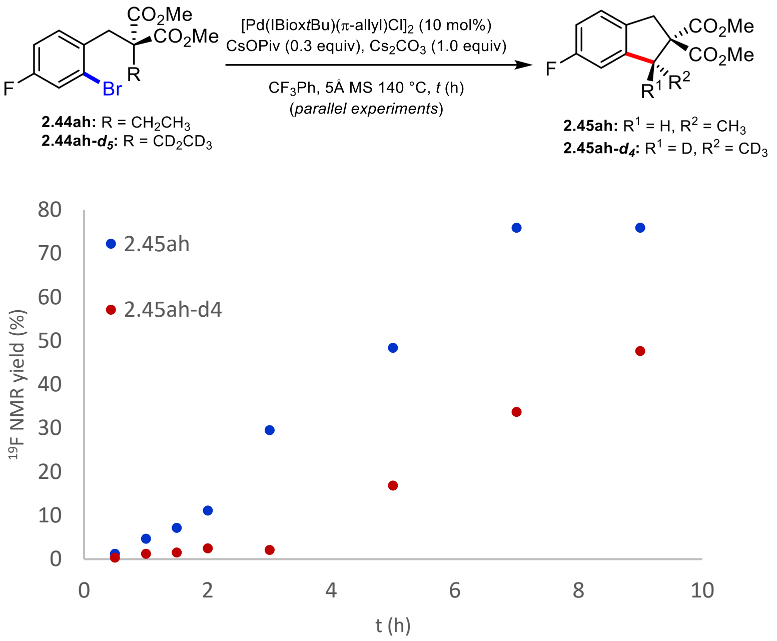

Figure 2.1: Parallel KIE experiments with **2.45ah** and **2.45ah-d$_5$**.

2.2.3 Evaluation of steric properties of IBioxR ligands

In parallel to this study, investigations on new modifications of IBiox-type ligands were ongoing in our group. IBioxMe$_4$*t*Bu was designed and prepared by introducing methyl groups in α-position of the oxygen in the bioxazoline scaffold in collaboration with Diana Cavalli. This would bring the substituents on the stereogenic centers closer to each other leading to a tighter chiral space enhancing the enantioinduction. Satisfyingly, using IBioxMe$_4$*t*Bu under our optimized conditions led to product **2.45a** in almost enantiopure form although in slightly lower 78% yield (Scheme 2.14). Additionally, we could improve the e.r. of product **2.45n**, with the lowest e.r. in the scope, from 94:6 to 98.5:1.5 with the newly synthesized ligand.

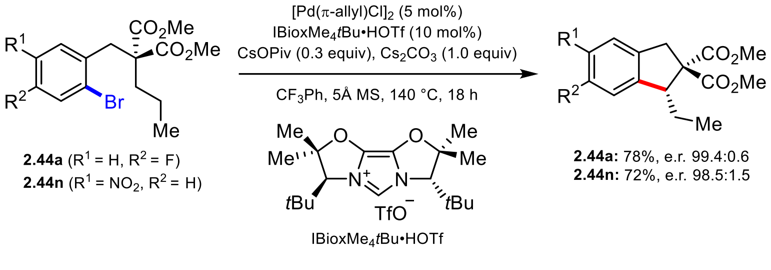
R1
R2
CO2Me
CO2Me
Br
Me
2.44a (R1 = H, R2 = F)
2.44n (R1 = NO2, R2 = H)
[Pd(π-allyl)Cl]2 (5 mol%)
IBioxMe4tBu•HOTf (10 mol%)
CsOPiv (0.3 equiv), Cs2CO3 (1.0 equiv)
CF3Ph, 5Å MS, 140 °C, 18 h
Me
Me
O
O
Me
Me
N
N
tBu
TfO−
tBu
IBioxMe4tBu•HOTf
R1
R2
CO2Me
CO2Me
Me
2.44a: 78%, e.r. 99.4:0.6
2.44n: 72%, e.r. 98.5:1.5

Scheme 2.14: Influence of gem-dimethyl substitution on the bioxazoline scaffold of IBioxMe$_4$tBu on the enantioinduction.

We studied the correlation between enantioinduction and the structure of the ligand. A typical model to describe sterics for NHC ligands is the percentage of buried volume (%V_{Bur}), originally presented by Nolan and Cavallo.[155] The %V_{Bur} value is defined as the percentage of the total volume of a sphere occupied by the ligand. The metal center is thereby positioned at the core of the sphere with a defined radius r (Figure 2.2a). The potential coordination sphere of the metal is represented by the volume of the sphere. We calculated the %V_{Bur} values of IBioxAd, IBiox*t*Bu, IBiox*i*Pr, IBioxCy, IBioxMenth and IBioxMe$_4$*t*Bu entering the parameters of the [Pd(NHC)(π-allyl)Cl] complexes obtained by DFT structure optimization in the samb*V*ca (Salerno molecular buried volume calculation) online tool (Figure 2.2b).[156]

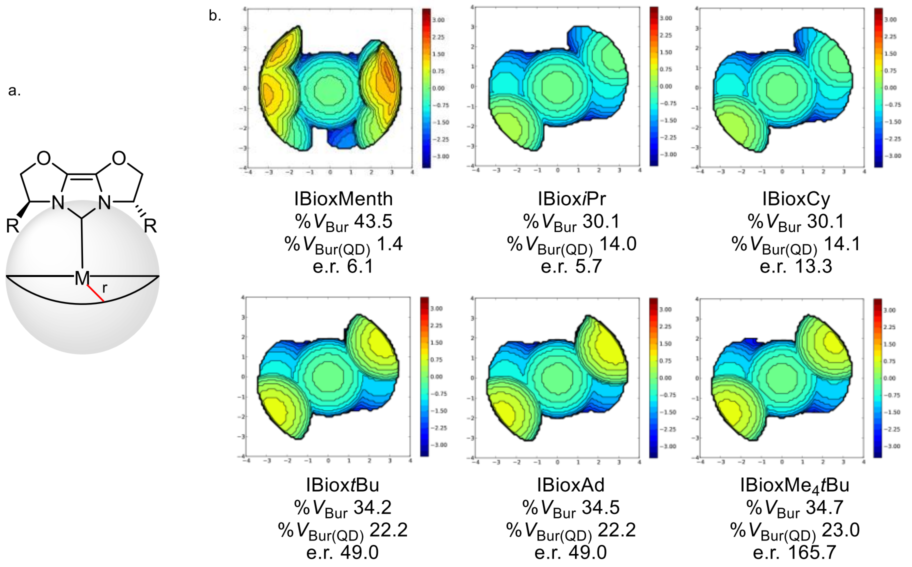
a.
b.
O
O
N
N
R
R
M
r
IBioxMenth
$\%V_{\text{Bur}}$ 43.5
$\%V_{\text{Bur(QD)}}$ 1.4
e.r. 6.1
IBioxiPr
$\%V_{\text{Bur}}$ 30.1
$\%V_{\text{Bur(QD)}}$ 14.0
e.r. 5.7
IBioxCy
$\%V_{\text{Bur}}$ 30.1
$\%V_{\text{Bur(QD)}}$ 14.1
e.r. 13.3
IBioxtBu
$\%V_{\text{Bur}}$ 34.2
$\%V_{\text{Bur(QD)}}$ 22.2
e.r. 49.0
IBioxAd
$\%V_{\text{Bur}}$ 34.5
$\%V_{\text{Bur(QD)}}$ 22.2
e.r. 49.0
IBioxMe$_4$tBu
$\%V_{\text{Bur}}$ 34.7
$\%V_{\text{Bur(QD)}}$ 23.0
e.r. 165.7

Figure 2.2: a. Schematic representation of $\%V_{\text{Bur}}$. b. Heat maps of the IBioxR-type NHC ligands and their $\%V_{\text{Bur}}/\%V_{\text{Bur(QD)}}$ values. $\%V_{\text{Bur(QD)}} = [\%V_{\text{Bur}}(\text{NE quadrant}) + \%V_{\text{Bur}}(\text{SWquadrant}) - \%V_{\text{Bur}}(\text{NW quadrant}) - \%V_{\text{Bur}}(\text{SE quadrant})]/2$.

The quadrant difference buried volume ($\%V_{\text{Bur(QD)}}$) is then obtained by adding the $\%V_{\text{Bur}}$ of the more occupied quadrants of the heat map and substracting the $\%V_{\text{Bur}}$ of the less populated quadrants.

No direct correlation between the enantiomeric ratio and the $\%V_{\text{Bur}}$ was observed when plotting the enantiomeric ratio as a function of the $\%V_{\text{Bur}}$, (Figure 2.3a). However, the enantiomeric ratio clearly increases with the $\%V_{\text{Bur(QD)}}$ (Figure 2.3b). This provides an explanation why the more congested cage-like structure of IBioxMenth is the least effective in terms of enantioinduction compared to the IBioxR ligands featuring a tertiary stereogenic center on the bisoxazoline backbone.

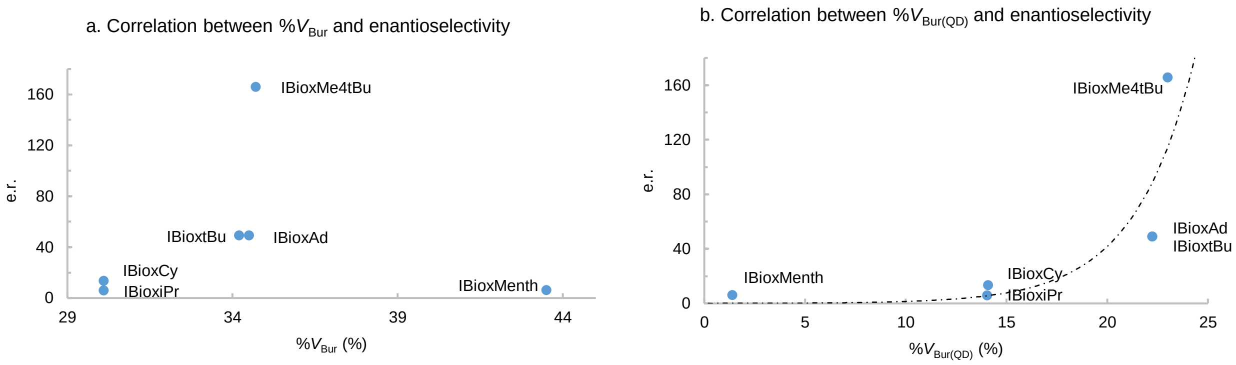

Figure 2.3: Study of ligand structure and enantioselectivity. a. $\%V_{\text{Bur}}$ as a function of enantioselectivity. b. $\%V_{\text{Bur(QD)}}$ as a function of enantioselectivity

2.2.4 Application of enantioselective Pd(0)-catalyzed C(sp^3)−H bond activation in total synthesis of natural products

Because chiral indanes are common motives in natural products,[157] we thought of demonstrating the utility of our methodology in the total synthesis of prenylated flavonoids indidene A-C (**2.47-2.49**) and Renifolin D-H (**2.50-2.54**) (Scheme 2.15a).[158,159] Indidene A-C (**2.47-2.49**) were isolated from the bark of the *Streblus indicus* tree, and exhibit cytotoxic activity against human lung epithelial A549 and human breast adenocarcinoma MCF-7 cell lines with IC$_{50}$ values ranging from 2.2 ± 0.1 to 7.2 ± 0.9 µM making them desirable targets for drug development. We envisioned that the synthesis of representative structures indidenene A (**2.47**), renifolin D (**2.50**) and indidene C (**2.49**) could be realized in a divergent fashion via common intermediate **2.56** (Scheme 2.15b).

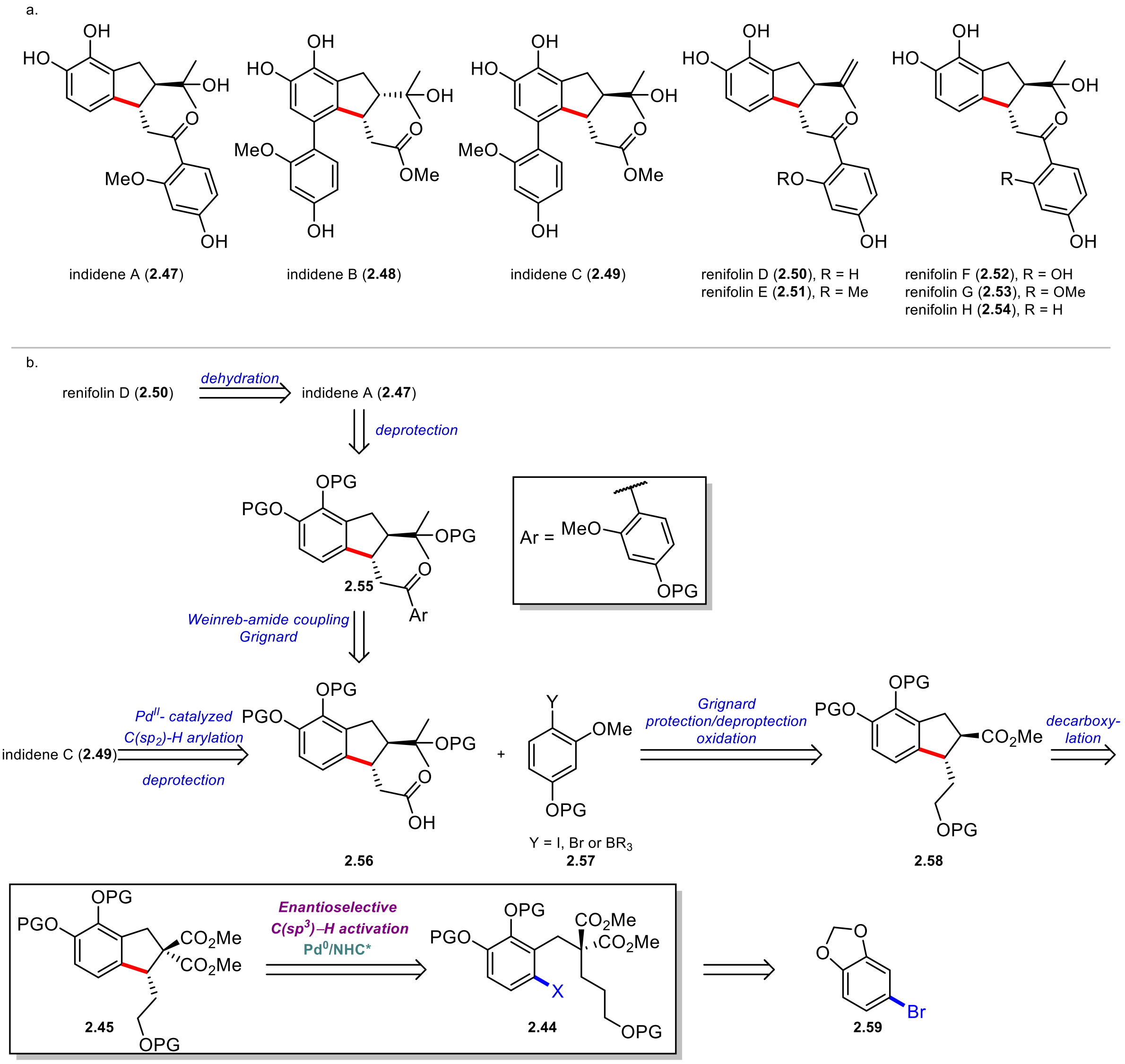
a.
indidene A (2.47)
indidene B (2.48)
indidene C (2.49)
renifolin D (2.50), R = H
renifolin E (2.51), R = Me
renifolin F (2.52), R = OH
renifolin G (2.53), R = OMe
renifolin H (2.54), R = H
b.
renifolin D (2.50)
dehydration
indidene A (2.47)
deprotection
2.55
Ar =
Weinreb-amide coupling
Grignard
Pd^II- catalyzed
C(sp2)-H arylation
indidene C (2.49)
deprotection
2.56
Y = I, Br or BR3
2.57
Grignard
protection/deprotection
oxidation
2.58
decarboxy-
lation
Enantioselective
C(sp3)–H activation
Pd0/NHC*
2.45
2.44
2.59

Scheme 2.152: Application of enantioselective Pd(0)-catalyzed C(sp^3)−H activation of secondary C−H bonds. a. Prenylated flavonoids natural products featuring a chiral indane core. b. Representative retrosynthetic analysis of indidenene A (**2.47**), renifolin D (**2.50**) and indidene C (**2.49**).

Weinreb-amide formation followed by nucleophilic addition of Grignard reagent derived from **2.57** would give intermediate **2.55**. Global deprotection would directly lead to the first natural product, indinedine A (**2.47**), and further dehydration of the tertiary alcohol would form Renifolin D (**2.50**) featuring an isopropenyl substituent on the 5-membered ring. The biaryl scaffold of indidene C (**2.49**) is envisioned to be constructed by employing a

Pd(II)-catalyzed directed C(sp^2)−H arylation strategy[160] between structure **2.57** and common intermediate **2.56** using the carboxylic acid substituent as traceless directing group. Following deprotection reactions would then grant access to the natural product. Common intermediate **2.56** is traced back to structure **2.58** by attack of the methyl ester with an excess of MeMgBr followed by deprotection of the aliphatic alcohol and oxidation to the corresponding carboxylic acid. *Trans* configured **2.58** would be prepared by krapcho-type monodecarboxylation of **2.45** which in turn is accessed by our developed enantioselective Pd(0)/NHC catalyzed arylation of secondary C(sp^3)−H bonds. Substrate **2.44** for the enantioselective C−H activation could be prepared from cheap and readily available benzodioxole **2.59** via a sequence of functional group manipulations including lithiathion/formylation, reduction to the benzylic alcohol, Appel-type reaction and sequential alkylation of dimethyl malonate.

We started the forward synthesis of natural products indidene A (**2.47**), renifolin D (**2.50**) and indidene C (**2.49**) with commercially available dioxolane **2.59** (Scheme 2.16). Following a literature procedure,[161] intermediate **2.60** was obtained over 3 steps in 83% overall yield. Alkylation of methyl malonate at room temperature afforded benzylic malonate **2.61**. Then, alkylation with the desired alkylbromide allowed for the installation of chains bearing protected alcohols in good yields. We selected benzyl (Bn) (**2.44ai**) and *tert*-butyldimethylsilyl (TBS) (**2.44aj**) protecting groups due to their orthogonality to the protected catechol moiety.

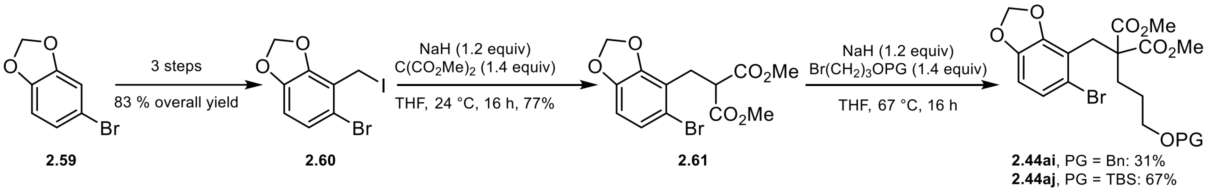

Scheme 2.16: Synthetic route to model substrates **2.44ai** and **2.44aj** for the enantioselective Pd(0)-catalyzed C(sp^3)−H activation.

Subsequently, substrates **2.44ai** and **2.44aj** were subjected to our optimized conditions. The reaction was monitored by GC-MS and 83% of product **2.45ai** was observed along with 12% proto-dehalogenation byproduct **2.46ai** (Table 2.11, entry 1). The product could not be isolated due to difficulties in separation from the proto-dehalogenated byproduct. Nevertheless, the e.r. of the crude mixture could be determined to be 98:2. Less product formation and increased proto-dehalogenation was observed with TBS protected substrate **2.44aj**, presumably due to higher steric hindrance interfering with the C−H activation process (entry 2).

Table 2.11: Test of modelsubstrates for the enantioselective Pd(0)-catalyzed C(sp^3)−H activation key step of the total synthesis.

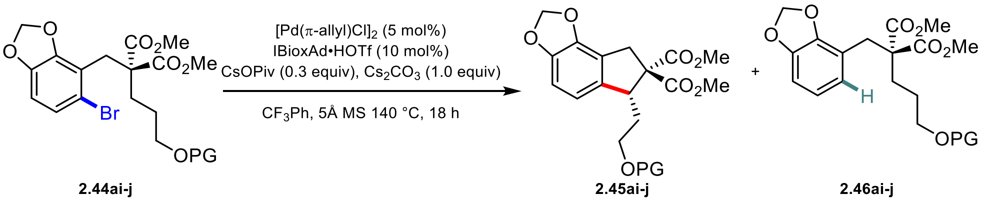
[Pd(π-allyl)Cl]2 (5 mol%)
IBioxAd•HOTf (10 mol%)
CsOPiv (0.3 equiv), Cs2CO3 (1.0 equiv)
CF3Ph, 5Å MS 140 °C, 18 h
Br
H
CO2Me
OPG
+
2.44ai-j
2.45ai-j
2.46ai-j

Entry	Substrate	PG	Product ratio[a]				e.r.[b]
			2.45	2.46	2.44	others	
1	**2.45ai**	**Bn**	**83**	**12**	**-**	**5**	**98:2**
2	**2.45aj**	TBS	62	31	-	7	n.d.[c]

[a]Determined by GC-MS. [b]Determined by HPLC on a chiral stationary phase. [c]n.d. = not determined.

With these preliminary results, the fundament for the total synthesis was layed as it was proven that the key enantioselective C(sp^3)−H activation occurs in high product formation and excellent enantioselectivity. Efforts to complete the total syntheses are currently ongoing in the group.

2.3 Expansion of enantioselective Pd(0)-catalyzed activation of secondary C−H bonds to different substrate families

To explore chemical diversity, we prepared new substrates for our developed enantioselective Pd(0)-catalyzed methodology including sulfonamide **2.62** amide **2.63** and biaryl-based substrates **2.64** and **2.65** (Scheme 2.17). A brief screening under our optimized conditions with achiral ligand IBiox6•HOTf showed that sulfonamide **2.62** and amide **2.63** were not compatible with our protocol as mostly starting material and proto-dehalogenation were observed by GC-MS. With the biaryl substrates the possibility of forming larger 6- or 7-membered rings was interrogated. With **2.64** again no product was observed. Although GC-MS analysis showed the presence of product **2.65** ^{1}H NMR spectrum of the crude mixture was not insightful and the isolation of the compound for characterization was not successful due to the low amount observed and the presence of the proto-dehalogenated byproduct.

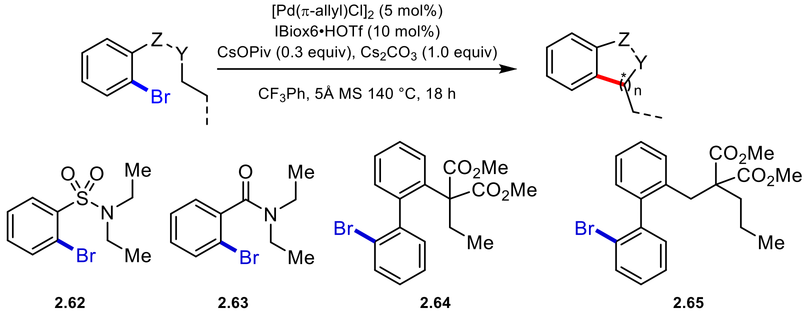
[Pd(π-allyl)Cl]$_2$ (5 mol%)
IBiox6•HOTf (10 mol%)
CsOPiv (0.3 equiv), Cs$_2$CO$_3$ (1.0 equiv)
CF$_3$Ph, 5Å MS 140 °C, 18 h
Z
Y
Br
n
O
S
N
Me
CO$_2$Me
2.62
2.63
2.64
2.65

Scheme 2.17: Substrate screening for Pd(0)-catalyzed enantioselective activation of secondary C−H bonds.

We turned our attention to the enantioselective synthesis of benzocyclobutenes of type **2.67** from aryl bromides **2.66**. Chiral benzocyclobutenes are highly desirable motifs found in several bioactive and pharmaceutical compounds. In this context, we also thought of targeting the long-standing challenge that is the formation of tertiary stereogenic centers in α-position to an amide with our substrate design. Moreover, since the first report from the Baudoin group in 2008 on the racemic synthesis of benzocyclobutenes by Pd(0)-catalyzed C(sp^3)−H activation,[74,75] no enantioselective version has been published to date. Thus, structure **2.66a** was subjected to the reported conditions for the formation of benzocyclobutenes by Pd(0) catalysis. With trialkylphosphine ligand P*t*Bu$_3$ at 140 °C in the presence of Cs$_2$CO$_3$ in DMF only Krapcho-type monodecarboxylation of the starting material was observed (Table 2.12, entry 1). Using our optimized conditions with achiral NHC ligand IBiox6•HOTf a complex mixture of different products was observed on GC-MS and NMR analysis of the crude mixture was not conclusive (entry 2). We then tested substrate **2.66b** bearing a more acidic C−H bond in α-position to an ester group. Similarly, with P*t*Bu$_3$ decarboxylation of the malonate occurred and with the NHC ligand a complex mixture was obtained.

Table 2.12: Screening of conditions for the formation of benzocyclobutenes.

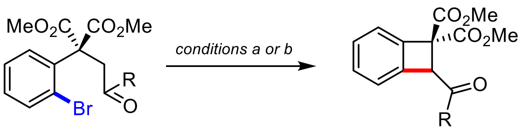

2.66a, R = NMe$_2$
2.66b, R = OMe

2.67a, R = NMe$_2$
2.67b, R = OMe

Conditions a:
Pd(OAc)$_2$ (10 mol%), P*t*Bu$_3$ (20 mol%)
Cs$_2$CO$_3$ (1.3 eq.)
DMF (0.1M) 140 °C, 18 h

Conditions b:
[Pd(π-allyl)Cl)]$_2$, IBiox6•HOTf (10 mol%)
CsOPiv (0.3 equiv), Cs$_2$CO$_3$ (1.5 equiv)
CF$_3$Ph (0.1M), 5Å MS, 140 °C, 18 h

Entry	R	conditions	observation
1	NMe$_2$	a	mono decarboxylated **2.66a**
2	NMe$_2$	b	complex mixture of products
3	OMe	a	mono decarboxylated **2.66b**
4	OMe	b	complex mixture of products

To further expand and establish the synthesis of chiral tertiary amides by Pd(0)-catalyzed C(sp^3)−H activation, we prepared glycine derived substrates of type **2.68**. Subjecting substrate **2.68a** to our optimized conditions led to recovery of starting material. Based on this result we modified the substrate changing the protecting group from COCF$_3$ to COAd to increase steric bulk at this position and therefore enhance the Thorpe-Ingold effect. Additionally, we introduced a methyl ester in place of the *t*Bu ester to reduce the steric hindrance, thus making the C−H bond in α-position more accessible for activation. Under the same conditions, with substrate **2.68b** mainly starting material with traces of proto-dehalogenated byproduct **2.70b** was obtained. Changing to a more classical catalytic system with phosphine ligands PCy$_3$ and PPh$_3$ was not fruitful either as mainly starting material and other not identifiable byproducts by both GC-MS and NMR spectroscopy, were observed (entries 3 and 4).

Table 2.13: Screening of conditions for the formation of indolines.

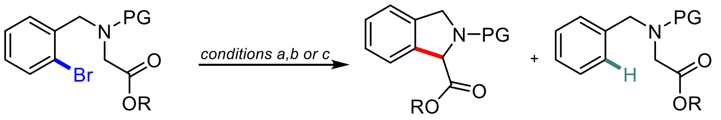

2.68a, PG = COCF$_3$, R = *t*Bu
2.68b, PG = COAd, R = OMe

2.69a-b

2.70a-b

conditions a:
[Pd(π-allyl)Cl)]$_2$, IBiox6•HOTf (10 mol%)
CsOPiv (0.3 equiv), Cs$_2$CO$_3$ (1.5 equiv)
CF$_3$Ph (0.1M), 5Å MS, 140 °C, 18 h

conditions b:
Pd(PCy$_3$)$_2$ (10 mol%)
AdCO$_2$H (0.3 equiv), Cs$_2$CO$_3$ (1.0
equiv) CH$_3$Ph (0.1M), 140 °C, 18 h

conditions c:
Pd(dba)$_2$ (10 mol%), PPh$_3$ (10 mol%)
Cs$_2$CO$_3$ (1.5 equiv),
CH$_3$Ph (0.1M), 140 °C, 18 h.

Entry	Substrate	PG	R	conditions[a]	Product ratio[a]			
					2.69	2.70	2.68	others
1	2.68a	COCF$_3$	*t*Bu	a	-	6	94	-
2	2.68b	COAd	OMe	a	-	2	98	-
3	2.68b	COAd	OMe	b	-	-	78	-
4	2.68b	COAd	OMe	c	-	-	62	38

[a] Determined by GC-MS.

Finally, we engaged sulfonamide **2.71** to our optimized conditions with achiral IBiox6•HOTf. The mass of a C−H activation product, along with not identifiable traces of other byproducts, was observed by GC-MS analysis. NMR analysis of the crude mixture indicated the formation of product **2.72** arising from the activation of the C(sp^2)−H bond of the aromatic ring on the sulfone (Scheme 2.18).

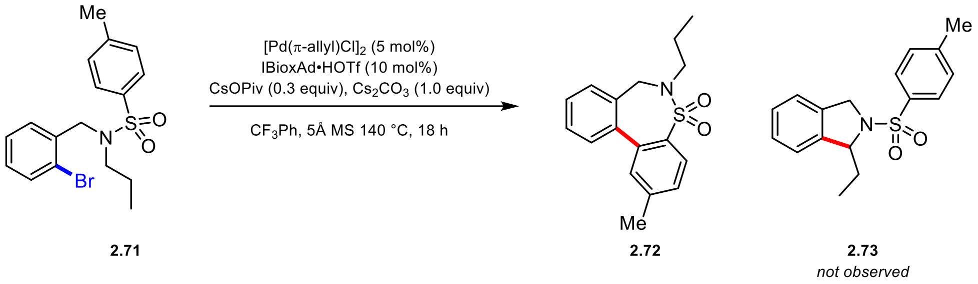
Me
Br
2.71
[Pd(π-allyl)Cl]$_2$ (5 mol%)
IBioxAd•HOTf (10 mol%)
CsOPiv (0.3 equiv), Cs$_2$CO$_3$ (1.0 equiv)
CF$_3$Ph, 5Å MS 140 °C, 18 h
2.72
Me
2.73
not observed

Scheme 2.18: Construction of 8-membered ring (**2.72**) via methyl C(sp^3)−H activation.

Interestingly, the formation of a thermodynamically unfavored 8-membered palladacycle by activation of the C(sp^2)−H bond was preferred over the activation of a secondary C(sp^3)−H bond to form **2.73**. Future efforts will focus on the suppression of this pathway by blocking this position.

2.4 Conclusion

The enantioselective synthesis of chiral indanes by Pd(0)-catalyzed arylation of secondary C−H bonds was developed. Key for the realization of this project was the design of an Pd/IBioxR catalytic system which outperformed previously applied phosphine based ligands in the activation of C(sp^3)−H bonds. The reaction proved to be tolerant to numerous functional groups as a broad variety of chiral indanes were obtained in high yields and enantioselectvities (up to 95% and >99:1 e.r.). Moreover, the first synthesis of chiral 3^{ary} amides featuring a labile stereogenic center was achieved by Pd(0)-catalyzed C(sp^3)−H activation with consistent high enantioselectivities. Additionally, with a steric analysis of IBioxR ligands the correlation between the ligand structure and enantioselectivity could be elucidated. The e.r. does not correlate directly with the $\%V_{\mathrm{Bur}}$ however it was found to increase as a function of $\%V_{\mathrm{Bur(QD)}}$. The total synthesis of prenylated chalcones natural products featuring a chiral indane core is envisaged as an application for the developed method. Preliminary results showed that the key enantioselective C(sp^3)−H activation step in high product formation and consistent high e.r. of 98:2. To date, attempts to expand the protocol to new substrates for the formation of smaller or bigger rings and tertiary stereogenic centers in α-position to carbonyls were unsuccessful.

Chapter 3: The effect of α-substitution on the reactivity of Pd(0)-catalyzed C(sp^3)−H activation for the formation of indanes

3.1 Introduction

Mechanistic studies are central to the development of synthetic organic chemistry as they allow for the understanding of previously unknown features of reaction mechanisms and can enable rational design for the development of new reactions or the improvement of existing methods. In this context, DFT calculations have been demonstrated to be a powerful computational tool to support such studies in C−H bond activation, providing insights that would otherwise be difficult or impossible to obtain experimentally.[162] For the Pd(0)-catalyzed oxidative addition induced C(sp^3)−H activation important developments towards understanding the operational mechanism have been made over the past two decades. In this context, the Fagnou group reported the synthesis of benzohydrofurans **1.140** from aryl bromide precursors **3.1** (Scheme 3.1).[78] With DFT methods the C−H bond insertion pathway proceeding through a Pd(IV) intermediate could be excluded based on the calculated energy of 47.7 kcal mol^{-1}. Instead, intramolecular carboxylate assisted transition state **3.3** was found to have a $\Delta G^{\ddagger}_{298\text{K}}$ value of 27.7 kcal mol^{-1} in benzene. The kinetic isotope effect was determined both experimentally and computationally resulting in 5.4 and 3.6 respectively. This is in accordance with the proton abstraction being the rate-limiting step.[163] Additionally, during the study of the reaction scope important site-selectivity trends were observed. Methyl groups were preferentially activated over methylene groups (**1.140b** and **1.140c**) however, the formation of a 6-membered ring arising from the activation of the terminal methyl C−H bond on the ethyl substituents was not observed. With a substrate bearing a C(sp^2)−H bond that could compete in the reaction, this position was favored, forming a 7-membered palladacycle to give structure **3.4** rather than the activation of the methyl C−H bond.

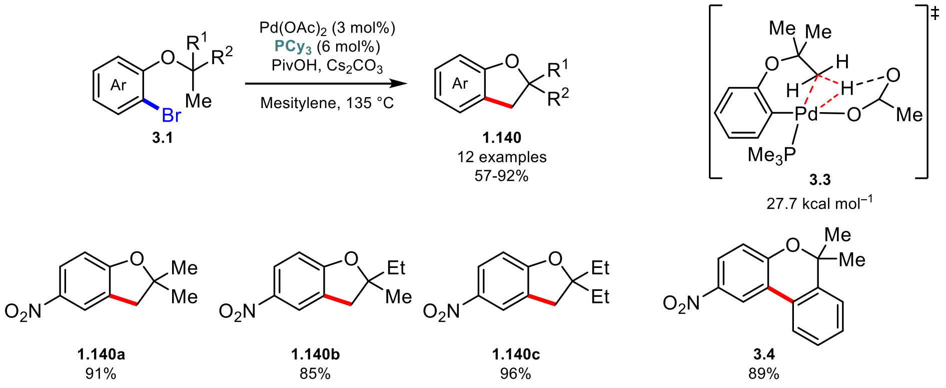

Scheme 3.1: Synthesis of benzohydrofurans **1.140** by Pd(0)-catalyzed C(sp^3)−H activation.

To rationalize the observed site selectivity, the transition states for the activation of the three different C(sp^3)−H bonds on substrate **3.1b** were calculated (Scheme 3.2). The lowest energy-barrier of 27.0 kcal mol^{-1} was obtained for transition state **3.5**, derived from the activation of the methyl C−H bond followed by transition state **3.6** with 32.5 kcal mol^{-1} arising from the activation of the methylene C−H bond on the ethyl substituent. The activation of the terminal methyl group C−H bond of the ethyl substituent requires an activation energy of 33.1 kcal mol^{-1} further underlining the greater ease with which the activation of the C(sp^2)−H bond occurs to form product **3.4** over a 7-membered palladacycle.

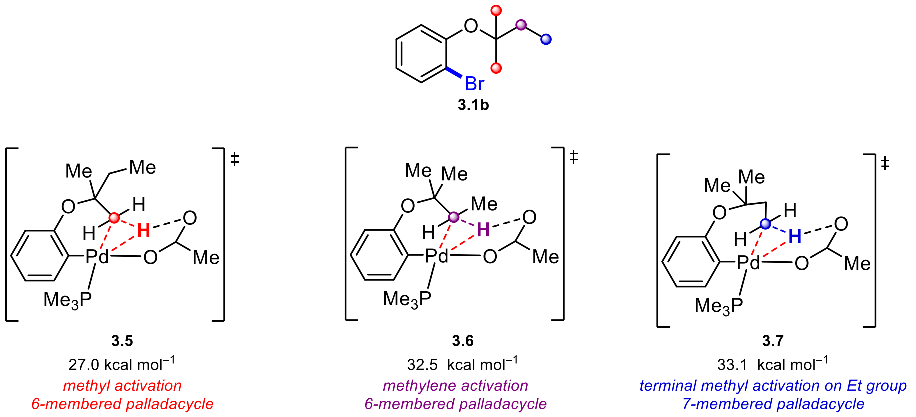
Br
3.1b
Me
Me
O
H
H
H
Pd
O
O
Me
Me3P
‡
3.5
27.0 kcal mol−1
methyl activation
6-membered palladacycle
3.6
32.5 kcal mol−1
methylene activation
6-membered palladacycle
3.7
33.1 kcal mol−1
terminal methyl activation on Et group
7-membered palladacycle

Scheme 3.2: Calculated transition states for the activation C−H bond of the methyl group (**3.5**), methylene C−H bond (**3.6**) and terminal methyl C−H bond (**3.7**) of the ethyl substituent.

In 2008 the Baudoin group disclosed a thorough mechanistic study based on the formation of benzocyclobutenes **1.131** from aryl bromide precursors **3.8** (Scheme 3.3).[74] To gain a complete mechanistic picture of the reaction, the authors computationally interrogated the critical mechanistic steps: 1) oxidative addition, 2) C−H bond activation and 3) reductive elimination. It was found that the oxidative addition proceeds through transition state **3.9** with a low activation barrier of 4.7 kcal mol^{-1} forming an oxidative addition complex with the aryl substituent in the *trans* position relative to the phosphine ligand. Following ligand exchange with carbonate, proton transfer perpendicular to the Ph−Pd−P plane via CMD transition state **3.10** takes place with an activation barrier of 27.6 kcal mol^{-1}. This result is in line with the value obtained by the Fagnou group although the aryl and the ligand were arranged in a *cis* fashion during the transition state in their case (see Scheme 3.1). Finally, reductive elimination was found to proceed through transition state **3.11** lacking the protonated active base, as no minima could be located with the base still coordinated. Although, a high ring strain builds up during the C−C coupling process the calculated energy of 22.5 kcal mol^{-1} is lower than for the proton abstraction process. Thus, the C−H activation is rate-limiting, which is supported by a significant primary KIE being observed.

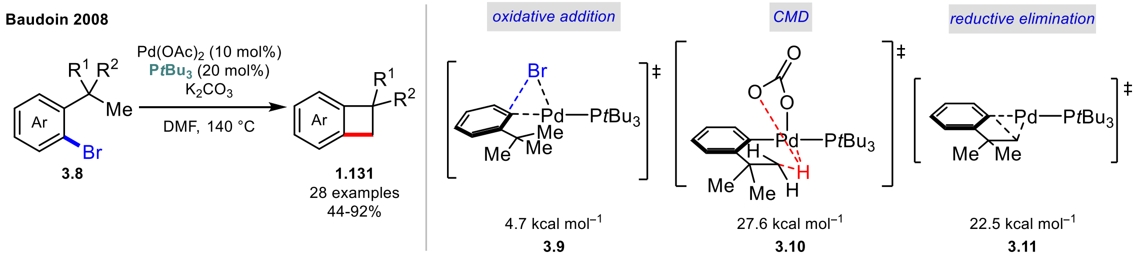
Baudoin 2008
R1 R2
Me
Ar
Br
3.8
Pd(OAc)2 (10 mol%)
PtBu3 (20 mol%)
K2CO3
DMF, 140 °C
R1
R2
Ar
1.131
28 examples
44-92%
oxidative addition
CMD
reductive elimination
Pd
PtBu3
Me
Me
‡
4.7 kcal mol−1
3.9
27.6 kcal mol−1
3.10
22.5 kcal mol−1
3.11

Scheme 3.3: Synthesis of benzocyclobutenes **1.131** and computational investigation of oxidative addition, CMD and reductive elimination.

The synthesis of amides **1.142** and sulfonamides **1.143** from substrates of type **3.12** and **3.13** respectively was used by the Fagnou group to further elucidate the mechanism of the Pd(0)-catalyzed C(sp^3)−H activation by both, experimental and DFT methods (Scheme 3.4).[80] For the formation of amides **1.142** an energy barrier of 29.1 kcal mol^{-1} was obtained for the proton abstraction via CMD transition state **3.14**. This step was proven to be rate-limiting by the measurement of an intra- and intermolecular KIE of 3.4 and 6.5 respectively, which are in the range of previously disclosed KIE values.

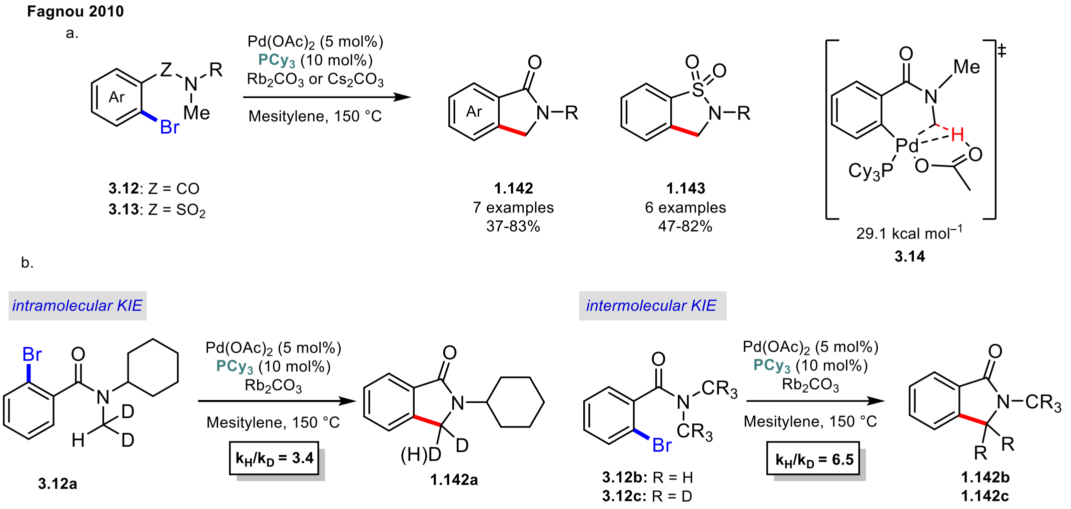
Fagnou 2010
a.
Ar
Br
Z
N
R
Me
Pd(OAc)2 (5 mol%)
PCy3 (10 mol%)
Rb2CO3 or Cs2CO3
Mesitylene, 150 °C
3.12: Z = CO
3.13: Z = SO2
1.142
7 examples
37-83%
1.143
6 examples
47-82%
Cy3P
Pd
H
29.1 kcal mol−1
3.14
b.
intramolecular KIE
intermolecular KIE
kH/kD = 3.4
kH/kD = 6.5
3.12a
1.142a
(H)D
3.12b: R = H
3.12c: R = D
1.142b
1.142c
CR3

Scheme 3.4: a. Synthesis of amides and sulfonamides by intramolecular C(sp^3)−H arylation. b. Measurement of intra- and intermolecular KIE.

To show that pivalate is directly involved in the proton abstraction step, stoichiometric experiments with the oxidative addition complexes **3.15b** and **3.16b** derived from **3.12b** and **3.13b** in the absence of either Cs_2CO_3 or CsOPiv were performed (Scheme 3.5a). Interestingly, no product was observed when only Cs_2CO_3 (10 equiv) was added to the reaction mixture. Even though amide **1.142b** and sulfonamide **1.143b** were obtained in 28% and 35% respectively in the presence of only CsOPiv (10 equiv), high yields could only be obtained with a mixture of Cs_2CO_3 (10 equiv) and CsOPiv (3.0 equiv). Therefore, the authors concluded that the Cs_2CO_3 is involved in the deprotonation of the PivOH ligand on **3.17** after CMD to render the process irreversible by impeding the reopening of the palladacycle and pushing the equilibrium towards **3.18** (Scheme 3.5b). This conclusion was further supported by DFT calculations as acetate derivative of **3.17** was calculated to be a highly energetic ground state structure and could readily revert to the starting material.

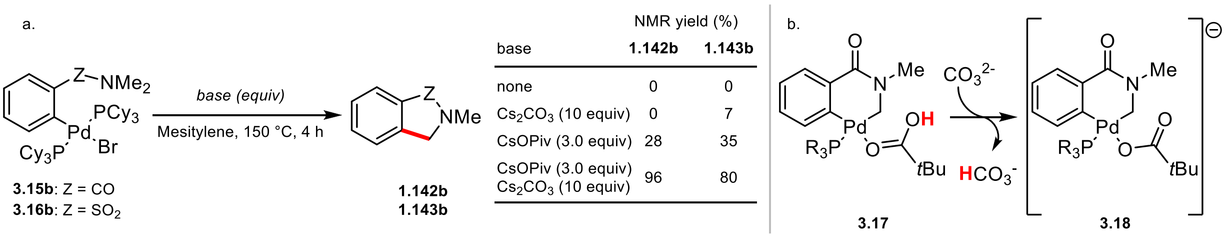
a.
Z
NMe2
PCy3
Pd
Br
Cy3P
base (equiv)
Mesitylene, 150 °C, 4 h
3.15b: Z = CO
3.16b: Z = SO2
1.142b
1.143b
b.
Me
CO3 2-
OH
R3P
tBu
HCO3-
3.17
3.18
⊖

base	NMR yield (%) 1.142b	NMR yield (%) 1.143b
none	0	0
Cs_2CO_3 (10 equiv)	0	7
CsOPiv (3.0 equiv)	28	35
CsOPiv (3.0 equiv) Cs_2CO_3 (10 equiv)	96	80

Scheme 3.5: Stoichiometric experiments to elucidate the role of CsOPiv and Cs_2CO_3.

Following this, kinetic studies were performed to obtain the order in substrate, catalyst, ligand and active base. The reaction was found to be of zeroth order in substrate indicating that the oxidative addition is not rate-limiting. The reaction is first order in catalyst. Excess of PCy_3 did not interfere with catalysis as even with a ratio of 12:1 ligand to Pd the reaction rate remained unchanged. Finally, the order in pivalate was found to be 1 for ratios of pivalate/Pd < 3:1. In the case of pivalate/Pd > 3:1 ratio, the zeroth order in pivalate was likely obtained due to saturation kinetics. Additionally, DFT calculations and experimental analysis indicated that pivalate promotes phosphine dissociation by κ^2-coordination, which is essential for the C−H activation to occur.

3.2 The effect of α-substitution on the reactivity of Pd(0)-catalyzed C(sp^3)−H arylation

The field of intramolecular Pd(0)-catalyzed C(sp^3)−H activation has experienced significant development over the past two decades as it constitutes a straightforward method to introduce molecular complexity from simple precursors. Consequently, many reports of both enantioselective and non-enantioselective Pd(0)-catalyzed C(sp^3)−H activation methodologies have been disclosed with impressive applications in natural product synthesis and other active compounds.[36,164] Throughout these studies, general trends for the activation of different types of C(sp^3)−H bonds have been observed. For instance, methyl C−H bonds are preferentially activated when in competition with methylene bonds and the presence of a heteroatom in α-position increasing the acidity of the C−H bond may facilitate the activation process.[78] For C(sp^2)−H activation this effects are well understood as Hammet plots constitute a reliable tool for quantification of the influence of arene substitution.[50,165–167] However, for C(sp^3)−H activation these effects remain unexplored as there is no comparable system for alkyl substituents. Consequently, the design and development of new methods is reliant upon experience and chemical intuition rather than accurate data. This lack of quantitative data in C(sp^3)−H activation might be attributed to the significant challenge that was until recently the activation of methylene C−H bonds. Recently, we reported a highly reactive Pd/NHC system for the enantioselective activation of methylene bonds (see chapter 2), which enabled the present study.[168] In this doctoral thesis we report on the effect of α-substitution on the reactivity of Pd(0)-catalyzed methylene C(sp^3)−H activation by measurement and comparison of relative initial rates accompanied by experimental and DFT studies for a complete mechanistic picture.

3.2.1 Optimization of the catalytic system.

At the outset of this study the previously disclosed Pd/NHC catalytic system had to be re-optimized as a substantial induction period was observed during the KIE studies (see chapter 2, Figure 2.1). This induction period, presumably originating from the reduction of the Pd(II) precatalyst to the Pd(0) active species, significantly interfered with the reliable evaluation of the kinetic curves. To overcome this challenge we decided to use Pd/NHC complex **3.19** similar to the ones reported by the Hazari group (Figure 3.1).[169,170] The sterically demanding 1-*t*Bu-indenyl ancillary ligand on this catalyst prevents the formation of off-cycle dimeric Pd(I) species by disproportionation, which slows down the generation of the Pd(0) active species. We tested this new catalyst under our optimized conditions with previously synthesized substrate **2.44ah** and stopped parallel experiments at different reaction times. The formation of product **2.45ah** was monitored by ^{19}F NMR spectroscopy using fluorobenzene as external standard (see experimental section for more details). Pleasingly, when this complex was employed as the catalyst, an induction period was not observed, confirming that catalyst **3.19** is compatible for this study.

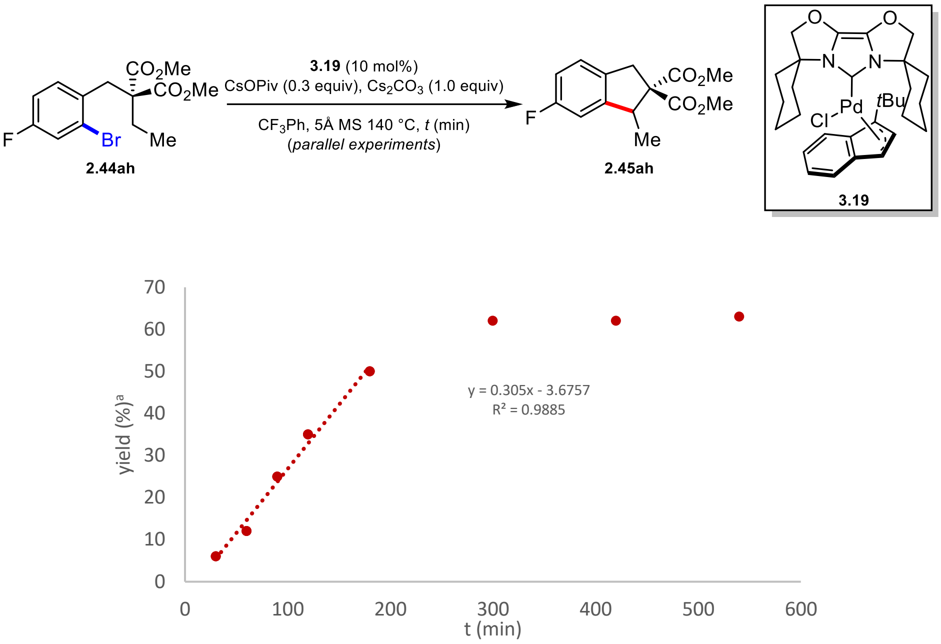

Figure 3.1: Initial rate experiment of C(sp^3)-H activation of with substrate **2.44ah** employing new catalyst **3.19**. ^{a}Determined by ^{19}F NMR using fluoronobenzene as external standard.

We began this study by examining the effects of different activators which play the role of reducing the Pd(II) precatalyst **3.19** by attacking the 1-*t*Bu-indenyl ligand. The reactions were stopped at t = 120 min as a point of reference in order to observe any effect on the rate of the reaction. With the standard conditions product **2.45ah** is formed in 35% yield (Table 3.1, entry 1). Increasing the equivalents of CsOPiv from 0.3 to 0.6 led to a comparable yield of 36% (entry 2). We therefore further increased the loading of CsOPiv to 1.5 equivalents but in this case the yield was decreased probably because the high amount of solids in the reaction mixture interfered with the stirring (entry 3). When KOPiv was used as an additive, a much lower yield was observed. This is consistent with the use of a more sparingly soluble carboxylate salt (entry 4). With the less sterically demanding CsOAc only traces of the product were observed (entry 5). The addition of 1,3-dimethylbarbituric acid (DMBA) was not fruitful and with PivNHOH again only traces of the product were observed (entries 6 and 7).

Table 3.1: Screening of activators

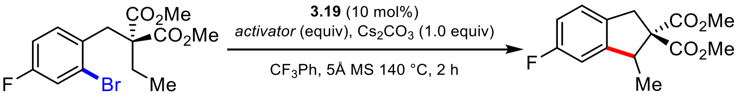

2.44ah **2.45ah**

Entry	activator (equiv)	yield (%)^a
1	**CsOPiv (0.3)**	**35**
2	CsOPiv (0.6)	36
3	CsOPiv (1.5)	30
4	KOPiv (0.3)	19
5	CsOAc (0.3)	9
6	DMBA (0.3)	-
7	PivNHOH (0.3)	2

^{a}Determined by ^{19}F NMR using fluoronobenzene as external standard.

Subsequently we turned our attention to different temperatures and concentrations. When the concentration was increased from 0.1 M to 0.2 M, a marginally higher yield of 38% was observed. However, dilution to 0.05 M almost completely shut down the reaction, as only trace amounts of the product was observed (Table 3.2, entries 1 and 2). Increasing the temperature to 150 °C and 160 °C could have led to catalyst decomposition as only traces of the product was observed (entries 3 and 4).

Table 3.2: influence of concentration and temperature on the formation of product **2.145ah.**

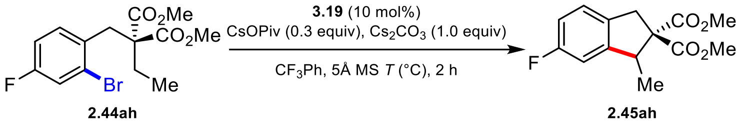

Entry	concentration (M)	Temperature (°C)	yield (%)[a]
1	0.2	140	38
2	0.05	140	4
3	0.1	150	3
4	0.1	160	4

[a]Determined by ^{19}F NMR using fluoronobenzene as external standard.

3.2.2 Mechanistic aspects of the Pd(0)-catalyzed methylene C(sp^3)−H bond activation: KIE, orders in reaction components and stirring rate experiments

Having established a robust catalytic system, we had to ensure that the C−H activation step is rate-limiting before examining the reactivity of different C−H bonds. This would enable us to conclude that differences in the rate could be attributed to differences in the C−H bonds, rather than a different process in the reaction. Thus, we performed intermolecular parallel KIE experiments with substrates **2.44ah** and **2.44ah-*d*$_5$** and obtained a value of 3.5, which confirms that the proton abstraction process is rate-limiting (Figure 3.2). Additionally, the calculated value of 4.8 is in accordance with our experimental observation. Based on these results, it is likely that the C−H activation is the rate-limiting step and that differences in the observed initial rates will be correlated to the differences in the reactivity of C−H bonds with differing α-substituents.

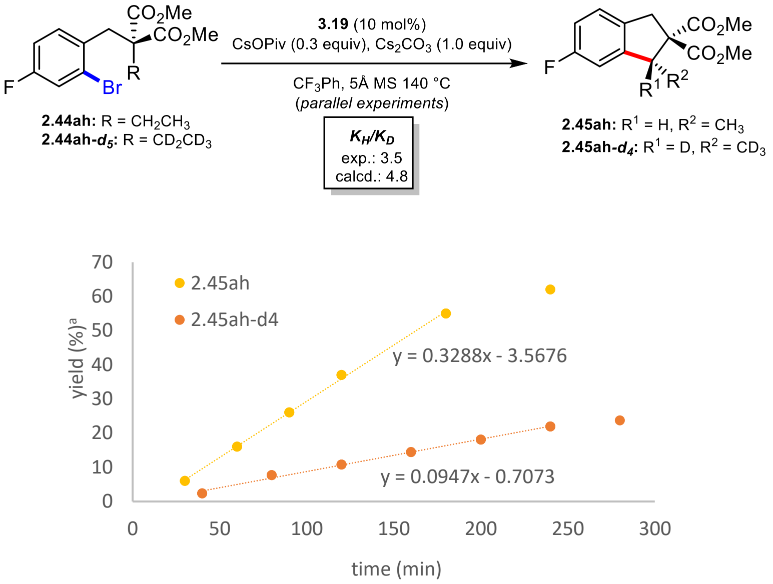

Figure 3.2: Parallel KIE experiments with substrates **2.44ah** and **2.44ah-d$_5$**. ^{a}Determined by ^{19}F NMR using fluoronobenzene as external standard.

To obtain deeper insights into the reaction mechanism the order of each reaction component was determined using the Variable Time Normalization Analysis (VTNA) developed by Burés in collaboration with Dr. Matthew Wheatley.[171] This method enables kinetic data to be gathered using relatively few data points and is determined by the overlay of the graphs.

Initially we examined the order in substrate, as this was reported to be zero order by Fagnou. Initial rate experiments at 0.1 M (black squares) and 0.2 M (red triangles) of **2.44ah** led to overlay of the curves when the exponent was set to 0 (Figure 3.3a). Zeroth order in substrate suggests that oxidative addition is not rate-limiting which is in accordance to the positive KIE. As expected, the reaction is first order in catalyst as observed with experiments at 0.01 M (black triangles) and 0.02 M (red squares) catalyst concentration. This supports the KIE suggesting that C−H activation is the rate-limiting step as it means that this step is on-cycle. In the study of the Baudoin group, Cs_2CO_3 acted as the active base. In this case, zeroth order was observed in Cs_2CO_3, however this can be explained by poor solubility of this component in CF_3Ph. Finally, the order in pivalate was found to be 0 for concentrations of 0.015 M (blue triangles) 0.03 M (orange squares) and 0.06 M (black circles) (Figure 3.3d). This is in contrast to the report of Fagnou employing a Pd(0)/phosphine catalytic system where an order of 1 was observed for ratios of pivalate/Pd < 3:1 whereas saturation kinetics were observed for a ratio of pivalate/Pd > 3:1. Zeroth order in pivalate for our case could be explained by the pivalate being involved in the off-cycle activation of the Pd(II) precatalyst but not in the C−H activation step. However, upon examining the solubility of CsOPiv in CF_3Ph, it was found to be insoluble at even low concentrations. This means that it is possible that the zero order kinetics we observe are as a direct result of saturation with respect to the concentration of CsOPiv, whereby adding more of this component does not increase the amount of this species in solution.

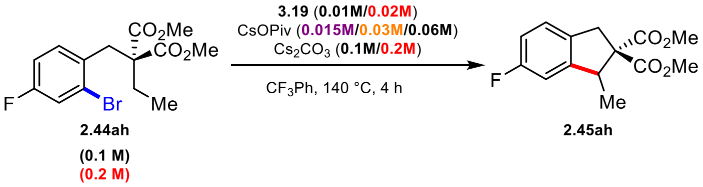
3.19 (0.01M/0.02M)
CsOPiv (0.015M/0.03M/0.06M)
Cs2CO3 (0.1M/0.2M)
CF3Ph, 140 °C, 4 h
CO2Me
CO2Me
F
Br
Me
2.44ah
(0.1 M)
(0.2 M)
CO2Me
CO2Me
F
Me
2.45ah

Figure 3.3: Determination of order in a. substrate, b. catalyst, c. Cs_2CO_3 and d. CsOPiv by VTNA.

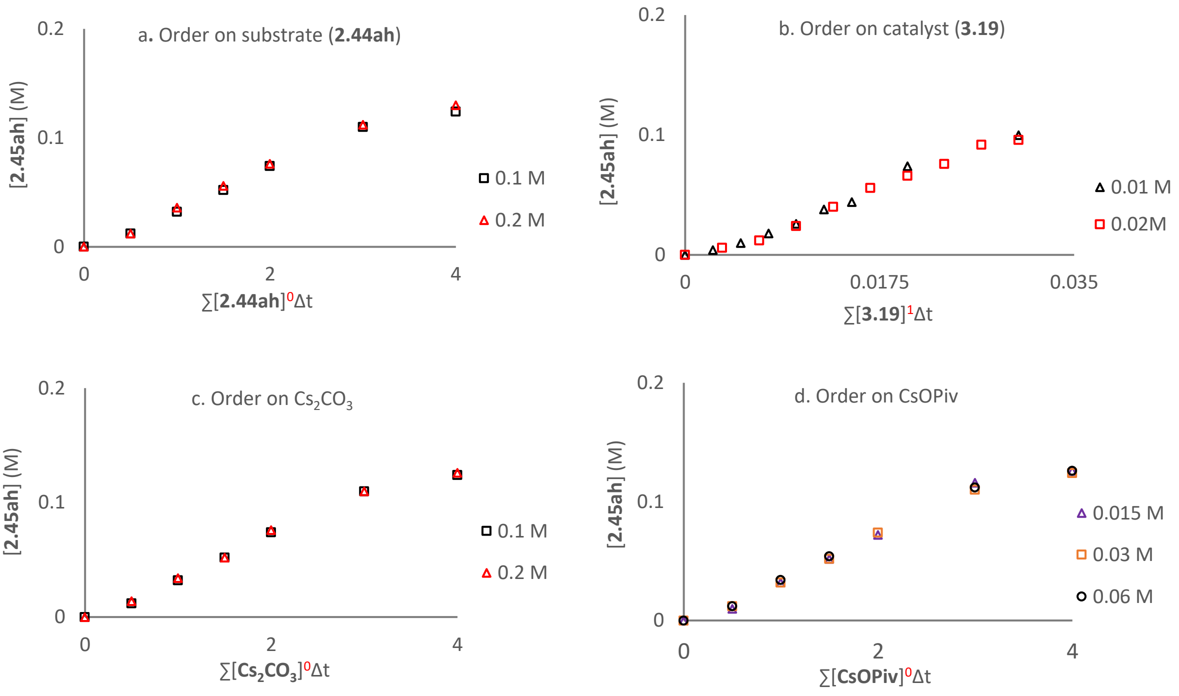

Next, we examined the influence of the stirring on the rate of the reaction. Since the reaction set up is heterogeneous, the stirring rate might affect the concentration of a component which is involved in the rate-limiting step such as CsOPiv or Cs_2CO_3.[172,173] Indeed, when the reaction was stirred at a rate of 250 rpm (blue crosses) almost no product was observed (Figure 3.4). When comparing these results with the standard stirring rate for these reactions (1000 rpm, purple squares) it is clear that there is a significant difference in the reaction due to the stirring rate. This is a result of the Gibbs-Thomson effect, as smaller particles have a higher chemical potential and therefore more of the compound is solvated. The increase in reaction rate with higher concentration of the species in solution, suggests that one or both scarcely soluble reaction components (Cs_2CO_3 or CsOPiv) play an important role in the C−H abstraction process.

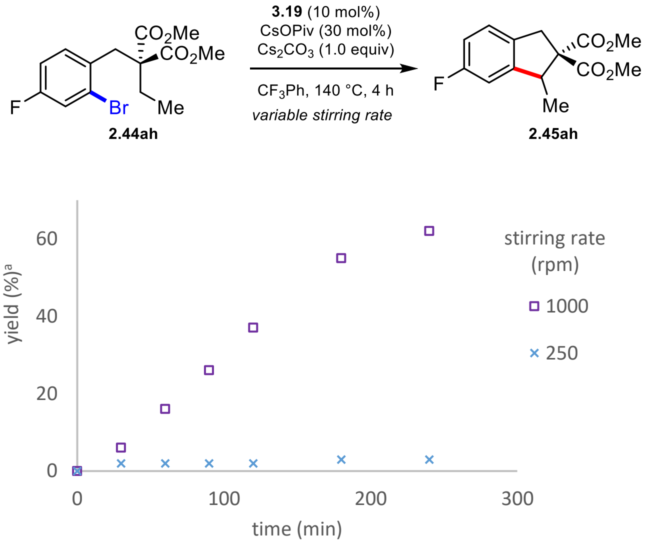

Figure 3.4: influence of stirring on reaction rate. aDetermined by ^{19}F NMR using fluoronobenzene as external standard.

Based on the obtained data supported by DFT calculations (see section 3.2.4) and on the results of previous mechanistic studies, we propose the following catalytic cycle for the Pd(0)-catalyzed methylene $C(sp^3)$−H bond activation shown in Scheme 3.6. First, precatalyst **3.19** is reduced to the Pd(0) active species. Reports by the Nolan group for similar Pd/NHC systems suggest that this process occurs by nucleophilic attack of an activator species on the alkenyl ancillary ligand.[174,175] Unfortunately, stoichiometric experiments with only precatalyst **3.19** and CsOPiv as activator have as yet failed to give structure **3.20**. However, this is perhaps due to a challenging ligand exchange being required. After generating the active Pd(0) species, it oxidatively inserts into the C−Br bond to give complex **3.21**. Subsequent ligand exchange with a carboxylate ligand gives intermediate **3.22** from which C−H bond activation via a CMD transition state (**3.23**) takes place leading to palladacycle **3.24**. Finally, reductive elimination closes the new 5-membered ring giving indanes **2.45** and restores the Pd(0) active species.

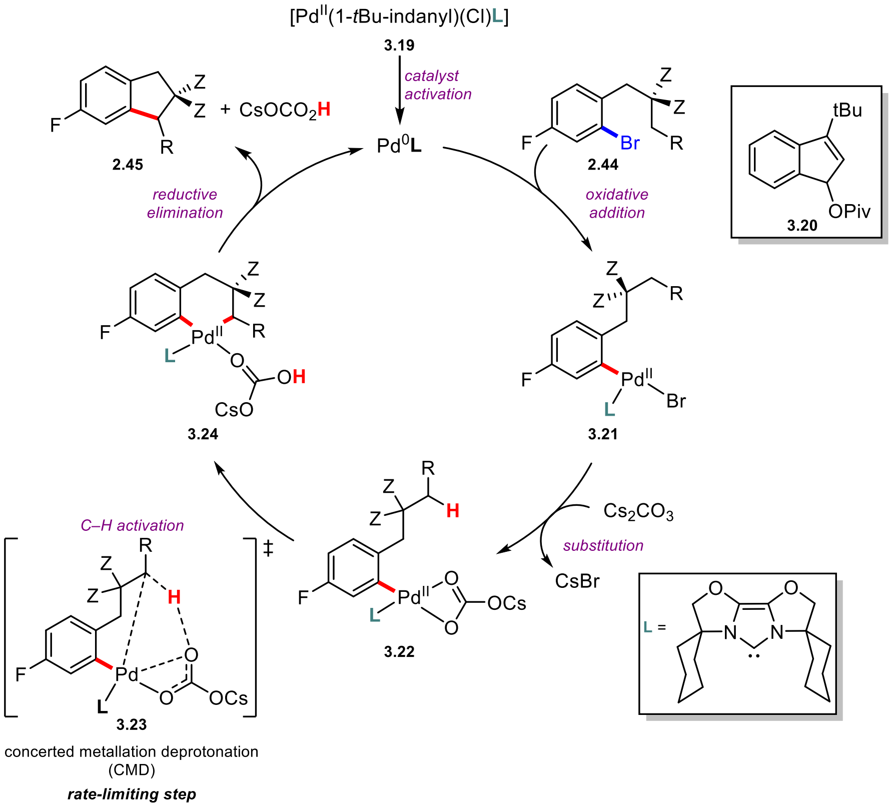
[Pd^{II}(1-tBu-indanyl)(Cl)L]
3.19
catalyst activation
Pd^{0}L
2.45
+ CsOCO$_2$H
reductive elimination
2.44
oxidative addition
3.20
tBu
OPiv
3.24
3.21
Cs$_2$CO$_3$
substitution
CsBr
C–H activation
3.22
3.23
L =
concerted metallation deprotonation (CMD)
rate-limiting step

Scheme 3.6: Proposed catalytic cycle for the Pd(0)-catalyzed activation of methylene C−H bonds.

3.2.3 Influence of α-substitution on the reactivity of methylene C(sp^3)−H bonds

Having studied the general aspects of the mechanism and showed that the C−H activation step is likely to be rate-limiting, we turned our attention to the influence of α-substitution on the reaction rate. We envisioned using substrate **2.44ah** as the base line and set the obtained relative rate to 1 (Figure 3.5). Consequently, the rates obtained with the other substrates are set on scale compared to the base line rate of 1. The substrate featuring the most acidic C−H bond (**2.44ak**, R = CO_2Me) displayed the fastest rate with a reaction 22.1 times faster than the standard reaction. On the other side of the scale, substrate **2.44ap** bearing a OMe group in α-position reacted much more slowly with a relative rate of 0.583. In between these two substrates, the observed trends were not trivial. For instance, the activation of a cyclopropyl C−H bond on substrate **2.44al** occurs 15.8 times faster than the standard reaction. In this particular case, spirocyclic product **2.45al** was obtained by activation of the most hindered position, underlining the preference for the formation of a 6-membered palladacycle. The observed high rate is presumably attributed to the increased sp^2 character of the C−H bond associated with strained cyclopropane rings.[176] Substrate **2.44am**, where R = $CONMe_2$ reacted 15.2 times faster. When compared to substrate **2.44ak** the slower reaction rate is in line with the lesser electron-withdrawing ability of amides relative to esters, which is translated in lower acidity of the C−H bond. For the activation of the methyl C−H bond on substrate **2.44an** a higher reaction rate was observed compared to the activation of the benzylic C−H bond (**2.44ao**) although the pKa value of a methyl proton is significantly higher than that of a benzylic proton (~56 vs.~43). This suggests that the rate of activation is not solely dependent on the electronic nature of the C−H bond but steric effects have a significant impact. In summary, this leads to the following overall order of activation: CO_2Me (**2.44ak**) > *c*Pr (**2.44al**) > $CONMe_2$ (**2.44am**) > H (**2.44an**) >> Ph (**2.44ao**) > Me (**2.44ah**) > OMe (**2.44ap**).

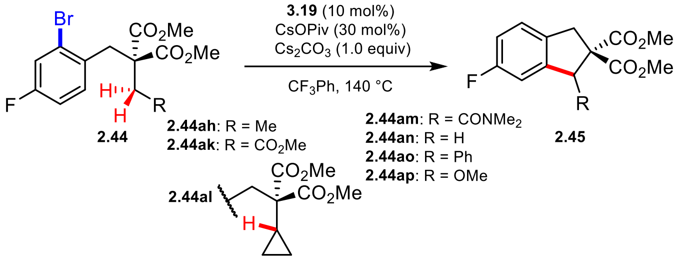

	2.44ak	**2.44al**	**2.44am**	**2.44an**	**2.44ao**	**2.44ah**	**2.44ap**
k_{rel}	22.1	15.8	15.2	10.2	2.22	1.00	0.583

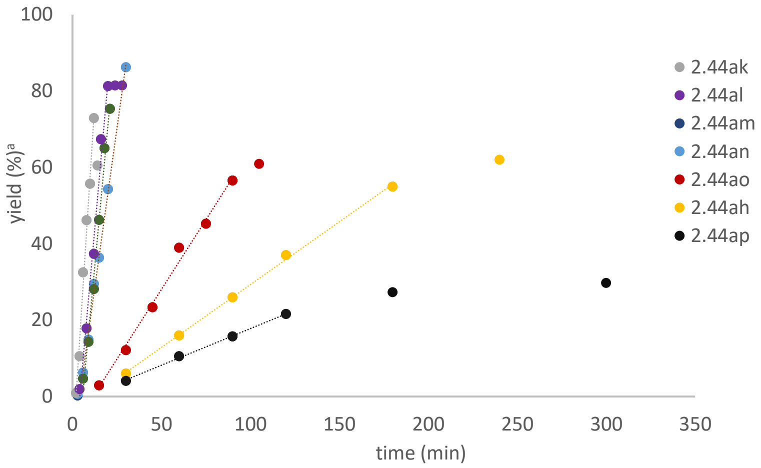

Figure 3.5: Initial rate experiments to determine the relative rate constants k_{rel}. [a]Determined by ^{19}F NMR using fluoronobenzene as external standard.

3.2.4 DFT calculations

To support our experimental data, DFT calculations were performed using the BP86 functional in collaboration with Prof. Dr. Stuart A. Macgregor. As experimental evidence for the role of CsOPiv and Cs_2CO_3 has thus far proven to be elusive, both reaction profiles were calculated individually using our model substrate **2.44ah** (R = Me group) at 413 K. Setting oxidative addition complex **3.25** as the zero point, an energy barrier of 26.7 kcal mol^{-1} was calculated for the C−H activation step via transition state **TS(3.25-3.26)** (Scheme 3.7a). From palladacycle **3.26**, reductive elimination with the protonated carbonate base still coordinated to the Pd center goes through the highly energetic transition state **TS(3.26-3.28)** with an energy barrier of 24.3 kcal mol^{-1}. However, from intermediate **3.27**, formed after dissociation of HCO_3^-, reductive elimination is energetically more favorable leading to the product **2.45ah** over transition state **TS(3.27-2.45ah)** which lies 12.5 kcal mol^{-1} lower in energy. Overall, the C−H activation process is computed to be rate-limiting which is in accordance to our experimentally obtained positive KIE value. With CsOPiv as the active base, the proton abstraction process takes place from intermediate **I(3.28-3.29)** (Scheme 3.7b). Again, reductive elimination with coordinated PivOH (**3.29**) is less favorable than from palladacycle **3.30** ($\Delta G^{\ddagger}$ 15.0 vs 11.5 kcal mol^{-1}). However, in this reaction profile the reductive elimination step lies higher in energy than the C−H activation.

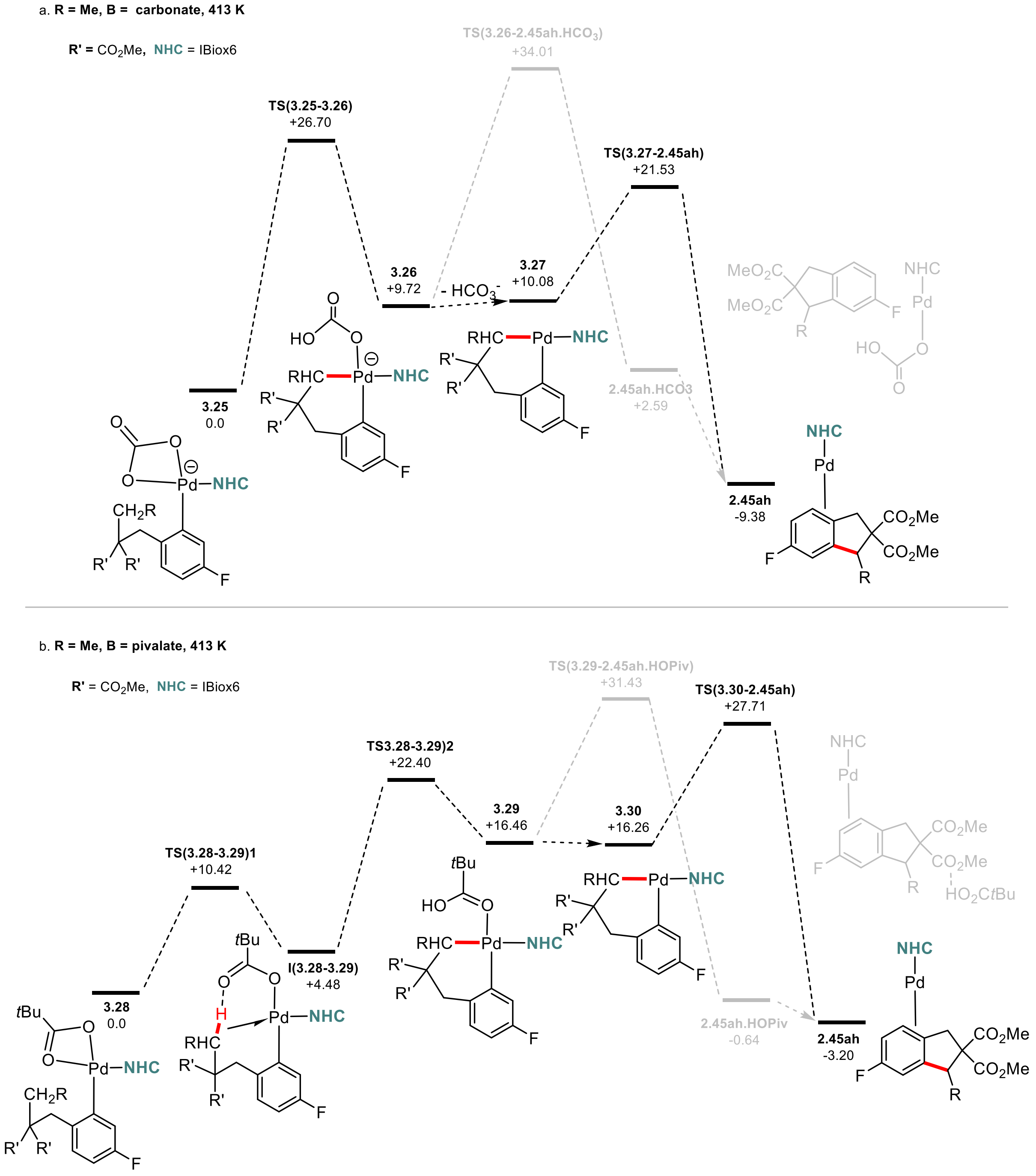
a. R = Me, B = carbonate, 413 K
R' = CO2Me, NHC = IBiox6
TS(3.26-2.45ah.HCO3)
+34.01
TS(3.25-3.26)
+26.70
TS(3.27-2.45ah)
+21.53
3.26
+9.72
- HCO3-
3.27
+10.08
3.25
0.0
2.45ah.HCO3
+2.59
2.45ah
-9.38
b. R = Me, B = pivalate, 413 K
R' = CO2Me, NHC = IBiox6
TS(3.29-2.45ah.HOPiv)
+31.43
TS(3.30-2.45ah)
+27.71
TS3.28-3.29)2
+22.40
3.29
+16.46
3.30
+16.26
TS(3.28-3.29)1
+10.42
I(3.28-3.29)
+4.48
3.28
0.0
2.45ah.HOPiv
-0.64
2.45ah
-3.20
NHC
Pd
RHC
R'
F
CH2R
CO2Me
MeO2C
HO
HO2CtBu
tBu
H

Scheme 3.7: Calculated reaction profiles for a. Cs_2CO_3 and b. CsOPiv as the active base.

3.3 Conclusion

We have studied the influence of α-substitution on the activation rate of methylene C−H bond. Key for the realization of this study was our previously disclosed Pd/NHC catalytic system capable of activating unreactive secondary C−H bonds in ring forming reactions. A significant KIE for the proton abstraction process and kinetic analysis by VTNA showed an order 1 in catalyst and 0 in substrate, which are in line with the C−H activation being rate-limiting. In contrast to previous reports, order 0 in pivalate was observed suggesting that this species is not involved in the rate-limiting step. However, due to the poor solubility of this component in CF_3Ph, the observed zero order might be a consequence of saturation kinetics. DFT calculations indicate that the carbonate base is promoting the C−H bond abstraction rather than the pivalate. Having disclosed the fundamental information suggesting that the comparison of different C−H bonds would be relevant to the overall rate of the reaction, we performed initial rate experiments to construct a reactivity scale quantifying the effect of α-substituents on the C−H activation rate. This allowed us to categorically order the substituents in a series of most to least reactive. From the obtained data, it can be concluded that the rate of activation is not only affected by the electronic properties (pKa) of the C−H bond but also by its steric environment. Overall, the presented scale represents a fundamental tool for the design of future $C(sp^3)$−H activation studies where the reaction outcome can be directed by judicious choice of the α-substituent influencing the electronic and steric properties of the targeted C−H bond.

Chapter 4: Enantioselective remote C(sp^3)−H activation by 1,4-Pd shift

4.1 Introduction

Intramolecular 1,4-Pd shift has strongly gained importance over the past decades as it constitutes an elegant and straightforward strategy to functionalize C−H bonds in remote positions to the initial C−Pd site. This has enabled the synthesis of important value added small molecules which would be otherwise difficult to access.[177–179] The ability of Pd to undergo a 1,4-shift was initially reported by Heck in 1972. The reaction of σ-Pd complex **4.1** formed in situ from (2-methyl-2-phenyl)mercury acetate and Pd(OAc)$_2$, led to a 65:35 mixture of products **4.2** and **4.3** (Scheme 4.1). Product **4.2** was formed through direct migratory insertion of methyl acrylate into the Pd–C bond followed by β-H elimination. Compound **4.3** however, was formed through intermediate **4.5** arising from *ortho*-C(sp^2)−H activation and reopening of the palladacycle (proposed mechanism). Following this observation, the first example of C(sp^3)−H activation shifting Pd on an alkyl substituent was reported by Dyker in 1992 (see chapter 1, section 1.2.2).[71]

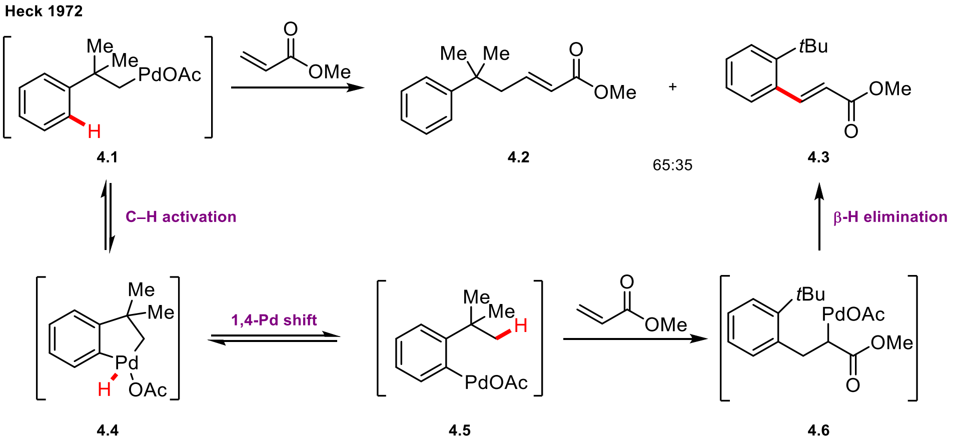

Scheme 4.1: First report of 1,4-Pd shift.

Based on this pioneering work numerous reports followed on the formation of new remote C(sp^2)−C(sp^2), C(sp^3)−C(sp^2) and C−X (X= heteroatom) bonds exploiting cross-coupling reactions such as Mizoroki-Heck, Suzuki-Miyaura, Buchwald-Hartwig, trapping of the nucleophilic aryl- or alkyl-palladium intermediate with alkynes or by termination of the reaction by β-H elimination.[178,180,181] The first example of Pd(0)-catalyzed tandem 1,4-shift/C(sp^2)−H activation was reported by Larock in 2003 (Scheme 4.2).[182] Fused polycycles of type **4.9** were prepared from biaryl iodide precursors **4.7**. In this case Pd migrates to the second aromatic ring by C(sp^2)−H activation and subsequent opening of the palladacycle leading to intermediate **4.8** from which a second C(sp^2)−H activation and reductive elimination forms the 5-membered ring.

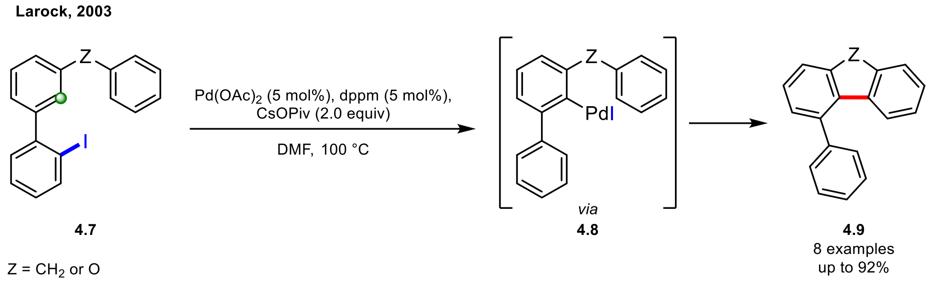
Larock, 2003
Z
I
Pd(OAc)$_2$ (5 mol%), dppm (5 mol%),
CsOPiv (2.0 equiv)
DMF, 100 °C
Z
PdI
Z
4.7
via
4.8
4.9
8 examples
up to 92%
Z = CH$_2$ or O

Scheme 4.2: First example of ring forming 1,4-Pd shift/C(sp^2)−H activation reaction.

As part of the long-standing research interest in the Pd(0)-catalyzed C(sp^3)−H activation, the Baudoin group focused on the formation of small rings remote to the original oxidative addition site exploiting Pd-mediated 1,4-shifts. In 2019, the synthesis of α-arylidene γ-lactams **4.11** and indanones **4.12** was disclosed in good to high yields (Scheme 4.3a).[183] Similar to the report of Larock, the Pd shifted to a sp^2 hybridized carbon via C−H bond activation and subsequent opening of the palladacycle, however in this case the ring was closed by the abstraction of the less reactive C(sp^3)−H bond. The usefulness of the method was demonstrated in the total synthesis of the pyrrolizidine alkaloid (−)-pyrrolam A (**4.15**) (Scheme 4.3b). Precursor **4.10a** for the Pd(0)-catalyzed 1,4-Pd shift/C(sp^3)−H activation reaction was prepared by amide coupling from 2-bromocinammic acid (**4.13**) and (*S*)-2-methyl-pyrrolidine (**4.14**) in quantitative yield. Subjecting **4.10a** to the optimized conditions gave α-arylidene γ-lactam product **4.11a** in moderate 50% yield. From this intermediate, the natural product was previously prepared in three additional steps.[184] Thus, the reported approach allows for the synthesis of pyrrolam A (**4.15**) in five steps, which is two steps shorter than the first total synthesis.[184]

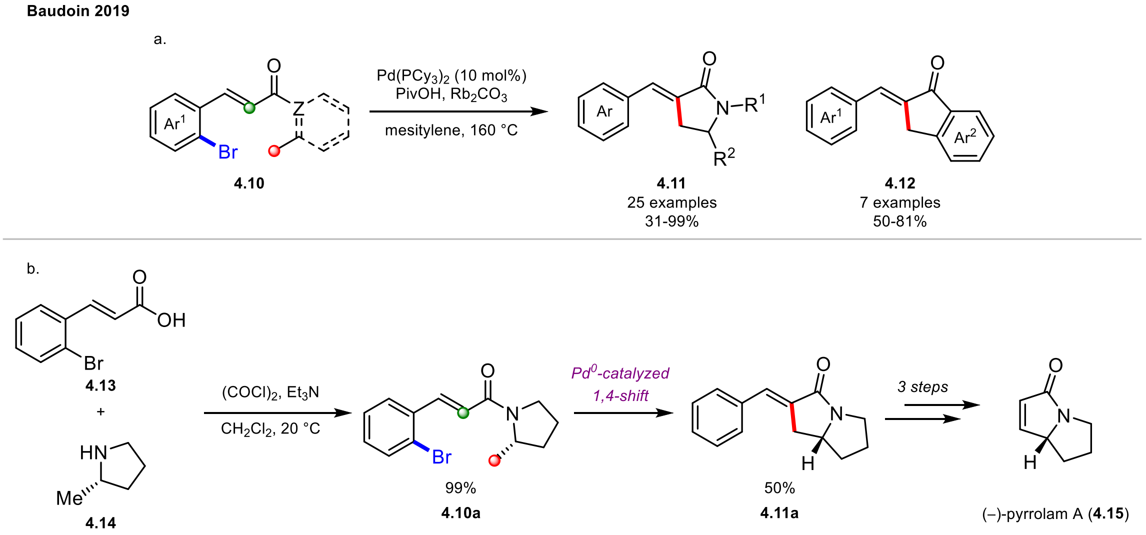
Baudoin 2019
a.
O
Ar^1
Br
Z
Pd(PCy$_3$)$_2$ (10 mol%)
PivOH, Rb$_2$CO$_3$
mesitylene, 160 °C
Ar
O
N−R^1
R^2
Ar^1
O
Ar^2
4.10
4.11
25 examples
31-99%
4.12
7 examples
50-81%
b.
O
OH
Br
4.13
+
HN
Me
4.14
(COCl)$_2$, Et$_3$N
CH$_2$Cl$_2$, 20 °C
O
N
Br
99%
4.10a
Pd^0-catalyzed
1,4-shift
O
N
H
50%
4.11a
3 steps
O
N
H
(−)-pyrrolam A (4.15)

Scheme 4.3: a. Synthesis of α-arylidene γ-lactams **4.11** and indanones **4.12** by 1,4-Pd shift/C(sp^3)−H activation. b. Application in the total synthesis of (−)-pyrrolam A (**4.15**)

Later, the same group reported the 1,4-shift of Pd onto a C(sp^3) site prior to C(sp^3)−H bond activation.[185] With this strategy dihydrobenzofurans **4.18** and indolines **4.19** could be accessed from the corresponding aryl bromide precursors **4.16** and **4.17** respectively in good to high yields (Scheme 4.4). In this case, the preparation of structures **4.18** and **4.19** can be realized without the need of a quaternary carbon otherwise required for ring contraction in direct intramolecular C(sp^3)−H activation (Scheme 4.4a). Moreover, the method could be applied to form 6-membered rings by activating a highly acidic secondary C(sp^3)−H bond. Chromanones of type **4.21** were accessed from aryl bromides **4.20** with modified reaction conditions (Scheme 4.4b). Additionally, a different type of C(sp^3)−C(sp^3) bond formation was explored using benzophenone substrates **4.22** lacking an enolizable position.

Products **4.23** featuring tertiary alcohols were prepared by a tandem 1,4-Pd shift/nucleophilic attack of the carbonyl moiety. However, these products were prone to elimination as benzofurans **4.24** were observed when left in CDCl$_3$ at room temperature for an extended period of time (Scheme 4.4c).

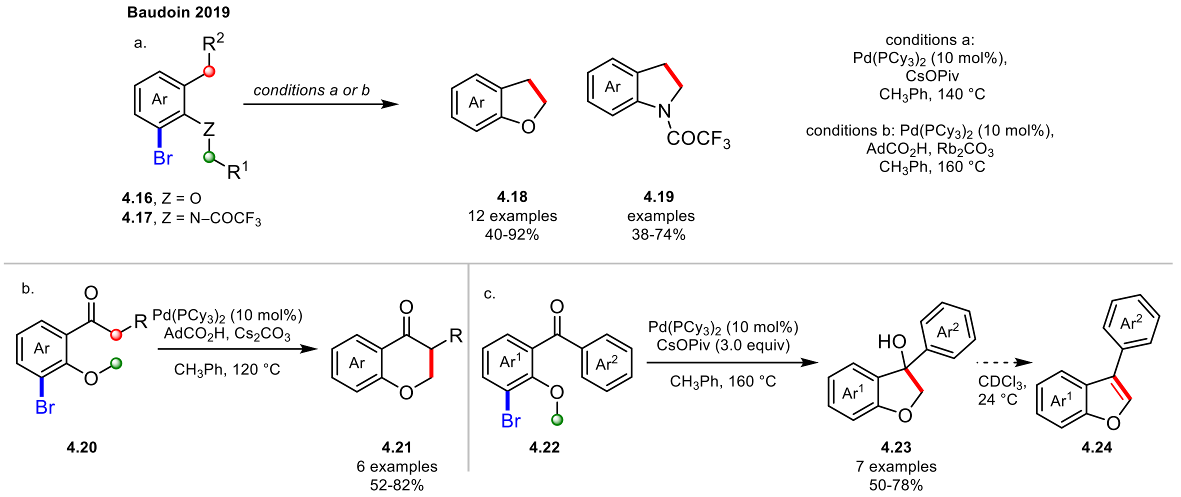
Baudoin 2019
a.
R2
Ar
Br
Z
R1
conditions a or b
Ar
O
Ar
N
COCF3
conditions a:
Pd(PCy3)2 (10 mol%),
CsOPiv
CH3Ph, 140 °C
conditions b: Pd(PCy3)2 (10 mol%),
AdCO2H, Rb2CO3
CH3Ph, 160 °C
4.16, Z = O
4.17, Z = N–COCF3
4.18
12 examples
40-92%
4.19
examples
38-74%
b.
O
R
Ar
O
Br
Pd(PCy3)2 (10 mol%)
AdCO2H, Cs2CO3
CH3Ph, 120 °C
O
R
Ar
O
4.20
4.21
6 examples
52-82%
c.
O
Ar1
Ar2
O
Br
Pd(PCy3)2 (10 mol%)
CsOPiv (3.0 equiv)
CH3Ph, 160 °C
HO
Ar2
Ar1
O
CDCl3,
24 °C
Ar2
Ar1
O
4.22
4.23
7 examples
50-78%
4.24

Scheme 4.4: First report of 1,4-Pd shift on a C(sp^3) site to form new C(sp^3)−C(sp^3) bonds. a. Synthesis of dihydrobenzofurans **4.18** and indolines **4.19**. b. Preparation of chromanones **4.21** by 6-membered ring formation. c. Formation of quaternary alcohols by tandem 1,4-Pd shift and nucleophilic attack of the carbonyl.

One year later the same group disclosed the first protocol for the formation of highly strained cyclopropanes by sequential Pd(0)-catalyzed C(sp^3)−H activation reactions.[186] When aryl bromides or triflates **4.25** were subjected to catalytic amounts of Pd(PPh$_3$)$_4$, benzylic cyclopropanes **4.26** were formed over 1,4-palladium shift (Scheme 4.5). In this case, the shift could occur on both, methyl or methylene positions. Interestingly, the nature of the active base played a fundamental role in this particular reaction. For instance, in presence of K$_2$CO$_3$ direct C−H activation product **4.27a** was observed from arylbromide **4.25a** in 46%. However, using KOPiv favors formation of **4.26a** without any traces of benzocyclobutene **4.27a**.

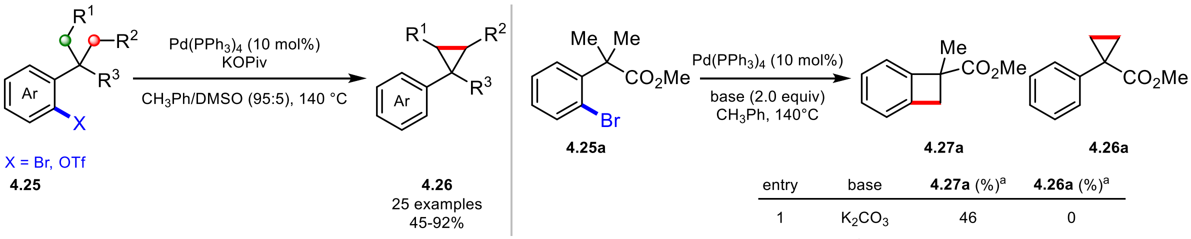
R1
R2
R3
Ar
X
X = Br, OTf
4.25
Pd(PPh3)4 (10 mol%)
KOPiv
CH3Ph/DMSO (95:5), 140 °C
R1
R2
R3
Ar
4.26
25 examples
45-92%
Me
Me
CO2Me
Br
4.25a
Pd(PPh3)4 (10 mol%)
base (2.0 equiv)
CH3Ph, 140°C
Me
CO2Me
4.27a
CO2Me
4.26a

entry	base	**4.27a** (%)[a]	**4.26a** (%)[a]
1	K$_2$CO$_3$	46	0
2	KOPiv	0	75

Scheme 4.5: Synthesis of cyclopropanes by 1,4-Pd shift.

The method was applied in the synthesis of bioactive molecules containing cyclopropyl moieties and the total synthesis of lemborexant (**4.34**) that is used for the treatment of insomnia (Scheme 4.6).[187] Substrate **4.29** was prepared from commercially available **4.28** in 5 steps. The key cyclopropanation over 1,4-Pd shift gave product **4.30**, that was subsequently elaborated to structure **4.32** by amidation with aminopyridine **4.31** as described by the Szostak group.[188] Finally, Mitsunobu reaction with parimidinol **4.33** led to (±)-lemborexant (**4.34**) in 28% overall yield over 8 steps.

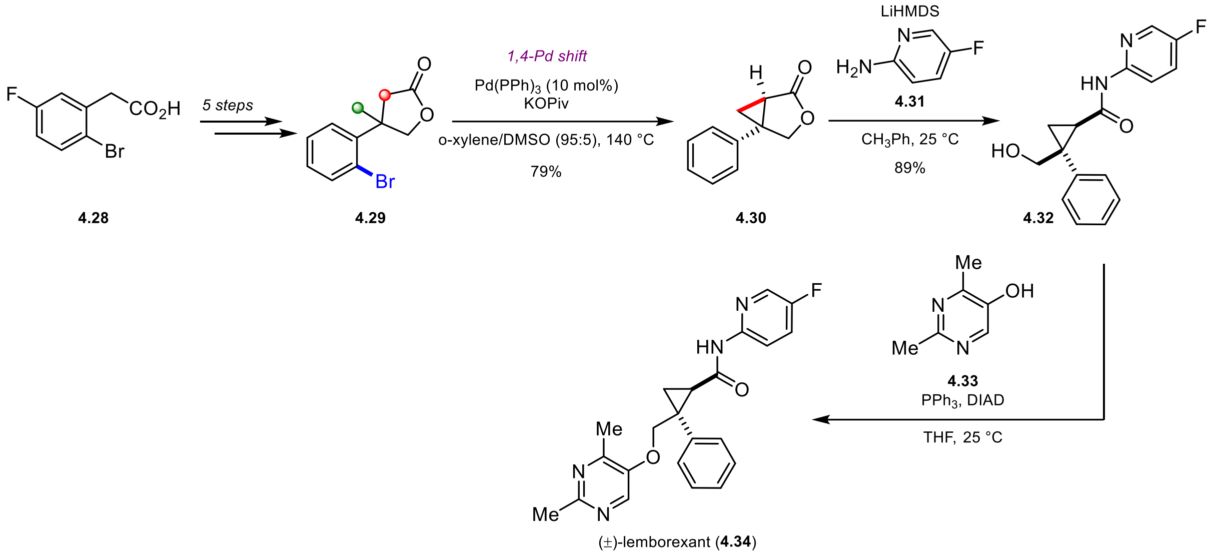
4.28
5 steps
4.29
1,4-Pd shift
Pd(PPh3)3 (10 mol%)
KOPiv
o-xylene/DMSO (95:5), 140 °C
79%
4.30
LiHMDS
4.31
CH3Ph, 25 °C
89%
4.32
4.33
PPh3, DIAD
THF, 25 °C
(±)-lemborexant (4.34)

Scheme 4.6: Total synthesis of (±)-lemborexant (**4.34**) by 1,4-Pd shift.

Very recently, the Baudoin group designed and optimized a Pd(0)/NHC catalytic system for the formation of isoindolines **4.36** and γ-lactams **4.38** by 1,4-Pd shift (Scheme 4.7).[189] After oxidative addition on aryl bromide substrates **4.35** and **4.37**, the Pd atom migrates to the methyl substituent on the nitrogen forming a σ-alkylpalladium intermediate, that subsequently undergoes C(sp^2)−H or C(sp^3)−H bond activation, respectively. In both cases the NHC ligand was key to obtain the remote C−H activation product as with phosphine based ligands mainly direct C−H activation was observed.

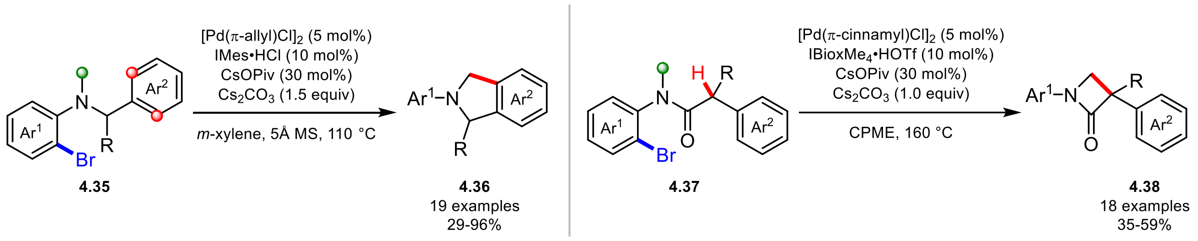
[Pd(π-allyl)Cl]2 (5 mol%)
IMes•HCl (10 mol%)
CsOPiv (30 mol%)
Cs2CO3 (1.5 equiv)
m-xylene, 5Å MS, 110 °C
4.35
4.36
19 examples
29-96%
[Pd(π-cinnamyl)Cl]2 (5 mol%)
IBioxMe4•HOTf (10 mol%)
CsOPiv (30 mol%)
Cs2CO3 (1.0 equiv)
CPME, 160 °C
4.37
4.38
18 examples
35-59%

Scheme 4.7: Synthesis of isoindolines **4.36** and γ-lactams **4.38** by 1,4-Pd shift and trapping with C(sp^2)−H or C(sp^3)−H activation respectively.

4.2 Studies on Pd(0)-catalyzed enantioselective remote C(sp^3)−H activation

The activation of remote C(sp^3)−H bonds by 1,4-Pd shift allows for the preparation of structurally distinct molecules relevant to the pharmaceutical and agrochemical industry that would otherwise not be accessible by direct C−H activation methods.[183,185,186,189] This enables the direct access of target compounds avoiding additional steps to remove undesired structural motifs. The design and development of new enantioselective methods is a long-standing challenge in synthetic organic chemistry as the activity in biological systems of such compounds is directly linked to their three dimensional arrangement.[104,105] We therefore envisioned that the design of enantioselective activation of remote C(sp^3)−H bonds would strongly contribute to the progress of the development of new and more effective drugs and other active compounds. Herein, we report on our studies on the construction of a Pd(0)-catalyzed system for the activation of remote C(sp^3)−H bonds by 1,4-Pd shift.

4.2.1 Enantioselective synthesis of oxygen containing heterocycles.

We began our investigations on enantioselective tandem 1,4-Pd shift/C(sp^3)−H activation by reevaluating the previously disclosed reaction to form benzofurans **4.18** from arylbromides **4.16**.[185] We were pleased to see that product **4.18a** was formed in 49% employing our previously disclosed Pd/NHC conditions for the activation of methylene C(sp^3)−H bonds in presence of racemic ligand IBiox6 (Table 4.1, entry 1).

Table 4.1: Screening of ligands for enantioselective 1,4-Pd shift.

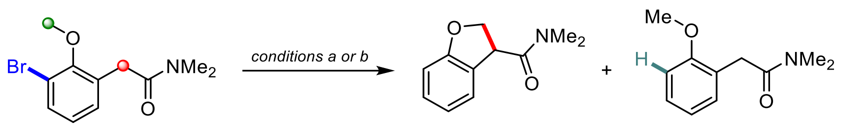

4.16a **4.18a** **4.39a**

conditions a:
[Pd(π-allyl)Cl)]$_2$ (5 mol%), **L** (10 mol%)
CsOPiv (0.3 equiv), Cs$_2$CO$_3$ (1.0 equiv)
CF$_3$Ph (0.1M), 5Å MS, 140 °C

conditions b:
Pd$_2$(dba)$_3$ (10 mol%), **L** (10 mol%)
CsOPiv (0.3 equiv), Cs$_2$CO$_3$ (1.0 equiv)
CH$_3$Ph (0.1M), 140 °C, 18 h

Entry	conditions[a]	L	Product ratio[a]				
			4.18a	4.39a	4.16a	others	e.r.[b]
1	a	IBiox6•HOTf	49	2	49	-	-
2	**a**	**IBioxAd•HOTf**	**22**	**11**	**67**	**-**	**48:52**
3	a	IBiox*t*Bu•HOTf	10	6	69	15	n.d.[c]
4	b	**L2.5d**	-	8	92	-	n.d.[c]
5	b	**L4.1**	-	13	87	-	n.d.[c]

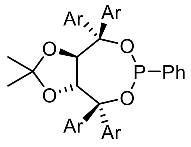

L2.5d: Ar = 3,5-*i*Pr-C$_6$H$_3$

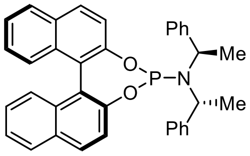

L4.1

[a]Determined by GC-MS. [b]Determined by HPLC on a chiral stationary phase. [c] n.d. = not determined.

With chiral ligand IBioxAd however, only 22% of the product were formed with 11% of proto-dehalogenated byproduct **4.39a** and 75% of starting material **4.16a**. Analysis by HPLC on a chiral stationary phase gave an e.r. of 48:52 (entry 2). With IBiox*t*Bu only traces of the product were observed and therefore the enantioinduction could not be analyzed (entry 3). Chiral phosphonite **L2.5d** and binol-derived phosphoramidite **L4.1** were not productive leading to the observation of mainly starting material **4.16a** in both cases (entries 4 and 5).

Focusing on the most efficient conditions, we evaluated a different Pd source, solvent and removed the additive to improve the previously obtained e.r. When [Pd($^{1\text{-tBu}}$Ind)Cl]$_2$ as the Pd(0) was used, a decrease in reactivity was observed, giving a product formation of only 11% (Table 4.2, entry 1). Changing the solvent to CH_3Ph or removing the 5Å molecular sieves from the reaction mixture was not fruitful as in both cases no product formation was observed (entries 2 and 3)

Table 4.2: Influence of different Pd-source, solvent and removal of additives.

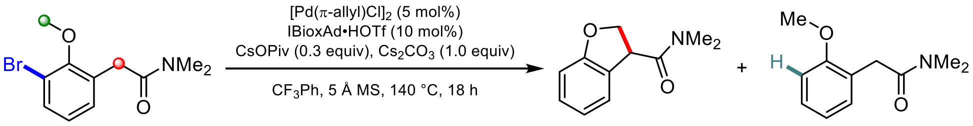
[Pd(π-allyl)Cl]2 (5 mol%)
IBioxAd•HOTf (10 mol%)
CsOPiv (0.3 equiv), Cs2CO3 (1.0 equiv)
CF3Ph, 5 Å MS, 140 °C, 18 h
Br
O
NMe2
O
O
NMe2
O
+
Me
O
H
NMe2
O

4.16a **4.18a** **4.39a**

Entry	Deviation from standard conditions	Product ratio^a				e.r.^{b}
		4.18a	4.39a	4.16a	others	
1	[Pd($^{1\text{-tBu}}$ind)Cl]$_2$ (5 mol%)	11	6	69	14	n.d.^{c}
2	CH_3Ph	-	9	91	-	n.d.^{c}
3	without 5Å MS	-	7	93	-	n.d.^{c}

^{a}Determined by GC-MS. ^{b}Determined by HPLC on a chiral stationary phase. ^{c} n.d. = not determined.

Presumably, the poor e.r. might be derived from the higher acidity of the doubly activated C(sp^3)−H bond in substrate **4.16a**. We tested substrates **4.16b-d** with different α-substituents to tune the electronic properties of the targeted C(sp^3)−H bond. We therefore subjected substrate **4.16b** featuring a pivalate group in α-position to the target methylene C(sp^3)−H bond to the previously reported conditions for 1,4-Pd shift.[185] Unfortunately, only proto-dehalogenation byproduct **4.39b** along with unreacted starting material was observed (Table 4.3, entry 1). Changing the α-substituent to a less sterically congested acetate group (**4.16c**) did not give the corresponding product (entry 2). Finally, with substrate **4.16c** bearing a NPhth group adjacent to the C−H bond, no reaction occurred after 18 h reaction time and only starting material was recovered (entry 3).

Table 4.3: Screening of substrates with different α-substituent on the second C−H bond.

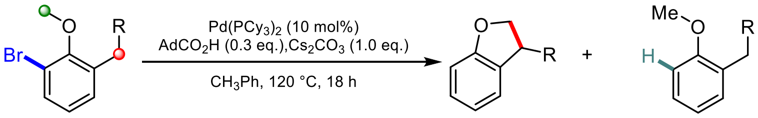

4.16b, R = OPiv
4.16c, R = OAc
4.16d, R = NPhth

4.18b-d **4.39b-d**

Entry	R	Product ratio^a			
		4.18	4.39	4.16	others
1	OPiv	-	15	85	-
2	OAc	-	34	66	-
3	NPhth	-	-	100	-

^{a}Determined by GC-MS.

We turned our attention to the alkylation of cylopropanes. Due to their unique electronic properties, [133,135,190]cyclopropane C−H bonds have been easily functionalized by means of Pd(0)-catalyzed C−H activation in the past (see chapters 1 and 2). Under the optimized 1,4-Pd shift conditions with substrate **4.16e** no product was observed (Table 4.4, entry 1). Subjecting starting material **4.16e** to our racemic Pd/NHC conditions in presence of IBiox6 was not fruitful (entry 2). With Pd(dba)$_2$ and PCy$_3$ forming the catalytic active Pd(0)(PCy$_3$)$_2$ species in situ in presence of PivOH in CH$_3$Ph no reaction occurred (entry 3). The same outcome was observed in *p*-xylene instead of CH$_3$Ph (entries 4).

Table 4.4 screening of condition sets previously employed in direct C−H activation.

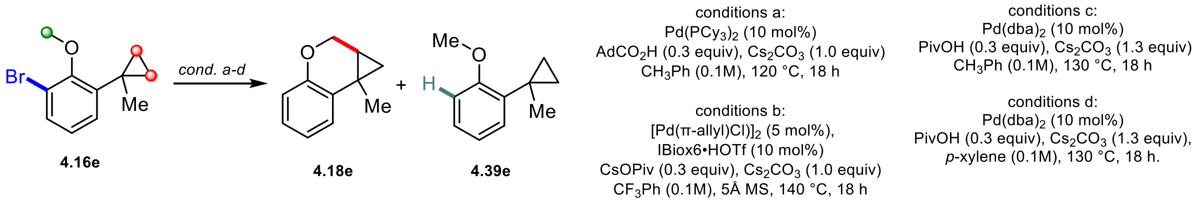
Br
O
Me
4.16e
cond. a-d
O
Me
4.18e
+
H
Me
O
Me
4.39e
conditions a:
Pd(PCy3)2 (10 mol%)
AdCO2H (0.3 equiv), Cs2CO3 (1.0 equiv)
CH3Ph (0.1M), 120 °C, 18 h
conditions b:
[Pd(π-allyl)Cl)]2 (5 mol%),
IBiox6•HOTf (10 mol%)
CsOPiv (0.3 equiv), Cs2CO3 (1.0 equiv)
CF3Ph (0.1M), 5Å MS, 140 °C, 18 h
conditions c:
Pd(dba)2 (10 mol%)
PivOH (0.3 equiv), Cs2CO3 (1.3 equiv)
CH3Ph (0.1M), 130 °C, 18 h
conditions d:
Pd(dba)2 (10 mol%)
PivOH (0.3 equiv), Cs2CO3 (1.3 equiv),
p-xylene (0.1M), 130 °C, 18 h.

Entry	conditions[a]	Product ratio[a]			
		4.18e	4.39e	4.16e	others
1	a	-	56	44	-
2	b	-	15	85	-
3	c	-	-	100	-
4	d	-	-	100	-

[a]Determined by GC-MS

4.2.2 Synthesis of chromanones

Since with substrates **4.16b-d** no product was observed, we concluded that the pKa of the target C−H bonds was too high. This hypothesis is further supported by occurring proto-dehalogenation meaning that oxidative addition takes place but then dehalogenation is favored over C−H activation. Therefore, in parallel to the studies with substrate **4.16e**, we examined the previously disclosed reaction to form chromanones **4.21** from arylbromides **4.20**.[185] Subjecting substrate **4.20a** to the reported conditions with Pd(PCy$_3$)$_2$ as catalyst to obtain a racemic reference led to a product formation of 31% along with 12% proto-dehalogenation product **4.40a** (Table 4.5, entry 1). Using the well-defined Pd(PCy$_3$)$_2$ complex led to a similar product formation of 32% (entry 2). Nevertheless, enough material in acceptable purity was obtained for HPLC analysis on a chiral stationary phase. Subsequently, we turned our attetntion to the screening of chiral ligands. In presence of phsophoramidite ligands **L4.1** and **L1.2b** no product or only traces were obtained (entries 3 and 4). A similar outcome was observed with binepine **L2.4b** and phosphonite **L4.2** (entries 5 and 6).

Table 4.5: Screening of chiral ligands for the synthesis of chromanone **4.21a**.

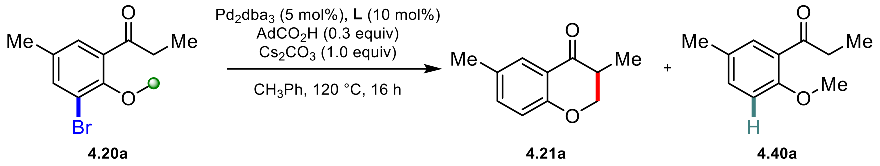
Me
O
Me
O
Br
4.20a
Pd$_2$dba$_3$ (5 mol%), **L** (10 mol%)
AdCO$_2$H (0.3 equiv)
Cs$_2$CO$_3$ (1.0 equiv)
CH$_3$Ph, 120 °C, 16 h
Me
O
Me
O
4.21a
+
Me
O
Me
O
Me
H
4.40a

Entry	L	Product ratio[a]				e.r.[c]
		4.21a	4.40a	4.20a	others	
1[b]	-	31	12	9	48	-
2[b]	-	32	5	-	63	-
3	**L4.1**	-	-	68	32	n.d.[d]
4	**L1.2b**	7	12	60	21	n.d.[d]
5	**L2.4b**	-	7	66	27	n.d.[d]
6	**L4.2**	3	7	54	36	n.d.[d]
7	**L4.3**	45	19	-	36	49:51

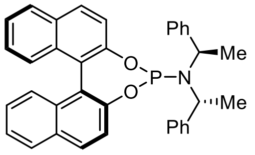
Ph
Me
O
P
N
O
Me
Ph

L4.1

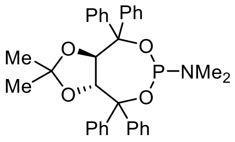
Ph
Ph
Me
O
O
Me
O
P–NMe$_2$
O
Ph
Ph

L1.2b

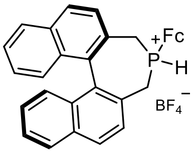

L2.4b•HBF$_4$

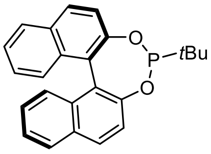

L4.2

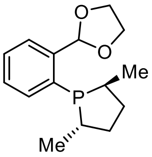

L4.3

[a] Determined by GC-MS. [b] Reaction performed with the well-defined Pd(PCy$_3$)$_2$ (10 mol%) catalyst. [c] Determined by HPLC on a chiral stationary phase. [d] n.d. = not determined.

Pleasingly, in presence of monodentate chiral phosphine **L4.3** 45% of product **4.21a** was formed. However, analysis of the enantioselectivity gave an e.r. of 49:51 (entry 7).

4.3 Conclusion

The Pd(0)-catalyzed activation of remote C(sp^3)−H bonds exploiting the ability of the catalyst to migrate in a 1,4 fashion has experienced great momentum in the past five years. To date, highly desirable enantioselective protocols remain unexplored. To this end, we conducted preliminary studies on enantioselective activation of remote C(sp^3)−H activation by designing and preparing new substrates and reevaluating racemic reactions previously reported by our group for the formation of oxygen containing heterocycles and chromanones. Preliminary evaluation of chiral ligand classes previously employed in asymmetric Pd(0)-catalyzed C−H activation were not fruitful leading in most cases to recovery of the starting material or only traces of the product. Tweaking the acidity of the C−H bond to trap the σ-alkylpalladium intermediate by changing the α-substituent did not lead to any improvement. However, with a strongly electron donating chiral NHC and a monodentate phosphine ligand substantial product formation was observed albeit in poor enantioselectivity. In conclusion our preliminary results show that chiral ligands are able to promote the ring closure by activation of the second C−H bond but the two important points have to be addressed for high levels of enantioselectivities. (1) The second C−H bond must not be too acidic to prevent racemization after forming the product and (2) a reactive chiral ligand with suitable steric properties to favor one enantiomer over the other has to be found.

5. General conclusions

This doctoral thesis presents the development of a new, highly reactive Pd(0)/NHC* catalytic system for the activation of enantiotopic secondary C−H bonds to form chiral indanes. The stereogenic center was thereby created at the C−H activation site in contrast to the desymmetrization of prochiral alkyl groups, which dominates the field. After a thorough screening of ligand families previously applied in enantioselective C−H activation methods, the IBioxR NHC ligands showed a unique reactivity towards the activation of methylene C−H bonds, outperforming other carbene and phosphorus containing ligands. Employing the IBioxAd derivative, a variety of substituted chiral indanes could be accessed in high yields and enantioselectivities including 3^{ary} amides substituted products featuring a labile stereogenic center. An analysis of the sterical properties of the IBiox-type ligands revealed that the $\%V_{\mathrm{Bur}}$ is not directly correlated with the observed enantioinduction. However, it was found that the e.r. value increases as a function of the $\%V_{\mathrm{Bur(QD)}}$. Moreover, the developed enantioselective methodology was proven compatible for the formation of the chiral indane core structure of prenylated flavonoid natural products indidene A-C and renifolin D-H in consistent high enantioselectivity.

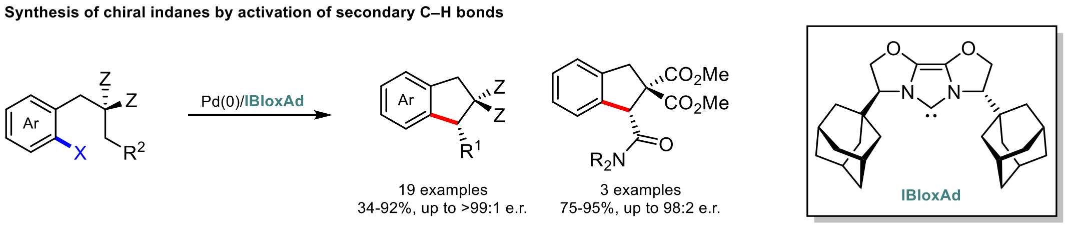

The developed methodology for the activation of methylene C−H bonds set the stage for mechanistic studies on the influence of α-substitution on the reactivity of C(sp^3)–H bonds. Initial kinetic analysis of the reaction and a significant primary KIE confirmed the C−H abstraction step to be rate-limiting ensuring that the comparison of different C−H bonds was significant. Thus, initial rate experiments with substrates featuring C–H bonds differing in electronic and steric properties were performed to construct a scale, ranking them from most to least reactive. It was found that the C(sp^3)−H bond in α-position to an ester reacts the fastest and, on the other side of the spectrum, OMe substituted C−H bond was the slowest with an overall 37.8-fold difference in initial rate. The order within the series however, proved to not be trivial leading to the following complete series α-substituted C−H bonds with R = CO_2Me > cC_2H_4 > $CONMe_2$ > H >> Ph > Me > OMe. Additionally, the calculation of the energy barrier for the different C−H bonds by DFT methods on a simplified model partially support the experimental trend. In general, the rate of C(sp^3)−H bond is not solely dependent on electronic properties (acidity) but the steric environment has a significant impact. The disclosed reactivity scale quantifying the effect of α-substitution on the reactivity of C(sp^3)−H bonds can be used as a guide for the development of new Pd(0)-catalyzed methylene C−H bond activation methods.

Construction of a reactivity scale for Pd(0)-catalyzed C(sp^3)–H activation

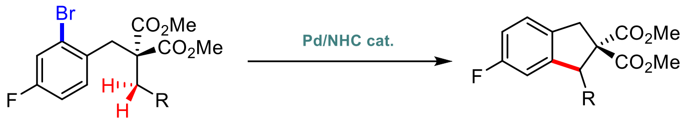
Br
CO2Me
CO2Me
F
H
H
R
Pd/NHC cat.
CO2Me
CO2Me
F
R

R	CO_2Me	cC_2H_4	$CONMe_2$	H	Ph	Me	OMe
k_{rel}	22.1	15.8	15.2	10.2	2.22	1.00	0.583

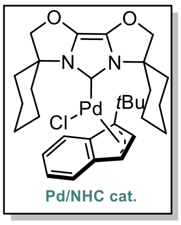
O
O
N
N
Pd
Cl
tBu
Pd/NHC cat.

Finally, initial progress was made on the development of an enantioselective methodology for the activation of remote C(sp^3)−H bonds enabled by 1,4-Pd shift. A preliminary screening of chiral ligands led to the observation of the product featuring a new 5-or 6-membered ring in poor selectivity. This suggests that the geometry of the ligand backbone is not ideal for high enantioinduction.

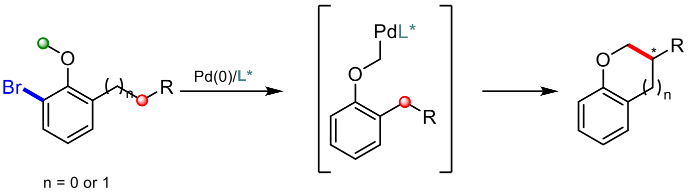
O
Br
n
R
Pd(0)/L*
n = 0 or 1
PdL*
O
R
O
*
R
n

6. Experimental part

General methods

Techniques:

All reactions involving air-sensitive compounds were carried out in pre-dried glassware under an argon atmosphere by using Schlenk techniques employing double-line argon-vacuum lines and working in an argon-filled glove box. Analytical thin layer chromatography (TLC) was performed using pre-coated Merck silica gel 60 F254 plates (0.25 mm). Visualization of the developed chromatogram was performed by UV absorbance (254 nm) or TLC stains ($KMnO_4$ and Phosphomolybdic acid). Flash chromatography was performed using Silicycle SiliaFlash P60 (230-400 mesh) with the indicated solvent system, using gradients of increasing polarity in most cases.

Chemicals:

Anhydrous solvents were purchased from Acros Organics or Sigma-Aldrich. The solvents were degassed by three cycles of freeze-pump-thaw and storing in single-necked flasks equipped with a J-Young PTFE valve when necessary. Palladium complexes were purchased from Sigma-Aldrich or Strem. All other chemical reagents were purchased from Sigma-Aldrich, Acros Organics, Alfa Aesar Apollo scientific and Fluorochem and used as received without further purification unless otherwise stated.

Instrumentation:

GCMS analyses were performed with a Shimadzu QP2010SB GCMS apparatus on a Rtx®-5ms-Low-Bleed column lined with a mass (EI) detection system. HPLC analyses was performed using a Shimadzu Prominence system with SIL-20A auto sampler, CTO-20AC column oven, LC-20AD pump system, DGU-20A3 degasser and SPD-M20A Diode Array or UV/VIS detector. The following chiral columns from Daicel Chemical Industries were used: OD-H (Chiralcel®), OJ-H (Chiralcel®), IA (Chiralpak®) in 4.6 x 250 mm size. Melting points were obtained on a Büchi melting point M-565, and are uncorrected. IR spectra were recorded on an ATR Varian Scimitar 800 and are reported in reciprocal centimeters (cm^{-1}). Nuclear magnetic resonance spectra were recorded on a Bruker Advance 400 (400 MHz), Advance 500 (500 MHz) and Advance 600 (600 MHz) in deuterated chloroform (residual peaks ^1H δ 7.26 ppm, ^{13}C δ 77.16 ppm) unless otherwise noted. ^{19}F NMR spectra were referenced to external $CFCl_3$. Both, ^{13}C and ^{19}F NMR spectra are ^1H ($\{^1H\}$) decoupled unless otherwise stated. Data are reported in parts per million (ppm) as follows: chemical shift, multiplicity (s = singlet, d = doublet, t = triplet, q = quartet, quint = quintuplet, sept = septuplet, m = multiplet and brs = broad singlet), coupling constant in Hz and integration. High resolution mass spectra were recorded by Dr. M. Pfeffer and S. Mittelheisser (Department of Chemistry, University of Basel) on a Bruker maXis 4G QTOF ESI mass spectrometer. Optical rotations were measured on a Anton Paar MCP 100 Polarimeter in a 0.7 mL micro cuvette (cell length 100mm) with NaD-Line (λ = 589 nm). The concentration (c) was given in g/100 mL.

6.1 Palladium(0)-catalyzed enantioselective intramolecular arylation of enantiotopic secondary C−H bonds for the synthesis of chiral indanes

6.1.1 Synthesis of IBioxR ligands and well-defined Pd-complexes

All IBiox-type ligands were prepared as reported[147,191,192] from different amino acids according to the following sequence:

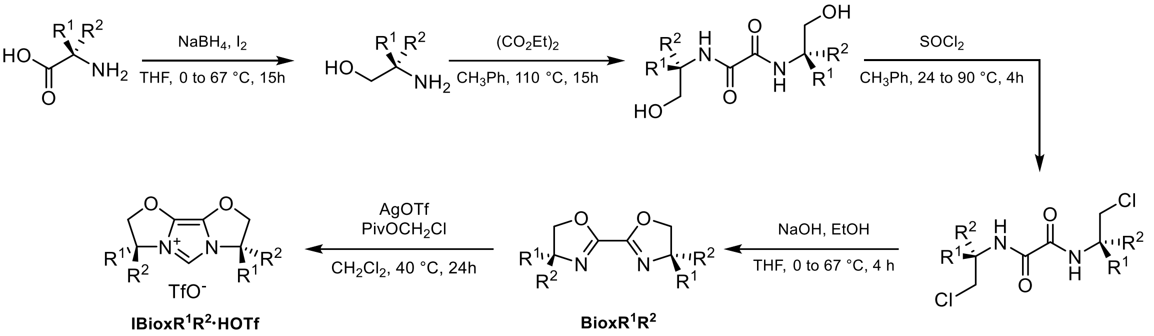

General procedure A: reduction of the amino acids

The amino acid (1 equiv), and $NaBH_4$ (3 equiv), and THF (4 mL/mmol of amino acid) were added to a dry round-bottom flask and cooled to 0 °C. A solution I_2 (1 equiv) in THF (2 mL/mmol of I_2) was added dropwise, allowing the mixture to turn whiteafter each drop. Following the addition, the mixture was heated to reflux for 15 hours. The reaction mixture was then cooled to 0 °C and quenched slowly with MeOH. The solvents were removed in vacuo, and the remaining solid was dissolved in 20% aqueous solution of KOH and stirred at 50 °C for 1.5 hours. The mixture was cooled to room temperature, extracted with EtOAc, and the combined organic extracts were dried over $MgSO_4$ and filtered. The solvent was removed in vacuo, and the crude aminoalcohol taken forward.

General procedure B: bisoxazoline synthesis

Aminoalcohol (2.1 equiv) and diethyloxalate (1.0 equiv) were stirred at reflux in toluene (2.5 mL/mmol of aminoalcohol) overnight. The reaction was then concentrated. The obtained solid was washed with petroleum ether and dried to afford the desired oxalamide which was used without further purification. $SOCl_2$ (2.9 equiv) was added to a suspension of the previously obtained oxalamide (1 equiv) in toluene (10 mL/mmol of oxalamide) at 60 °C. The solution was stirred at this temperature for 1 h and then 3 h at 90 °C. After this time, the reaction was quenched with methanol and concentrated. The residue was taken up in CH_2Cl_2 and vigorously washed with a 20% (w/v) aqueous solution of KOH. Layers were separated and the aqueous layer was extracted with CH_2Cl_2. The combined organic phases were washed with brine, dried over $MgSO_4$ and concentrated to yield the desired chlorooxalamide taken forward. To a solution of the previously obtained chlorooxalamide (1 equiv) in THF (20 mL/mmol of chlorooxalamide) a solution of NaOH (2.1 equiv) in ethanol (3 mL/mmol of NaOH) was added. After stirring at ambient temperature for 30 min the mixture was heated at 90 °C for 3 h. The solvent was evaporated, and the residue taken up in MTBE, washed with a saturated aqueous solution of Na_2CO_3 and dried over $MgSO_4$. After concentration, the crude mixture was purified by flash column chromatography (cyclohexane/EtOAc) to yield the desired bisoxazoline.

General procedure C: cyclization for NHC formation

To a suspension of AgOTf (1.45 equiv) in CH_2Cl_2 (4.5 mL/mmol of bisoxazoline) was added chloromethyl pivalate (1.45 equiv) and the resulting suspension was stirred for 45 min in the dark. The supernatant was transferred via syringe to the bioxazoline (1 equiv) and the resulting solution was stirred in a sealed tube in the dark at 40 °C for 24 h. After the solution was cooled to room temperature, the solvent was evaporated in vacuo. The resulting oil was chromatographed on silica gel (CH_2Cl_2/MeOH) to afford the corresponding IBiox·HOTf.

(3*S*,7*S*)-3,7-diisobutyl-2,3,7,8-tetrahydroimidazo[4,3-b:5,1-b']bis(oxazole)-4-ium triflate (IBiox*ⁱ*Bu·HOTf):

From **Biox*ⁱ*Bu** using **General procedure C. IBiox*ⁱ*Bu·HOTf** was obtained as a wax (178 mg, 0.43 mmol, 15%).

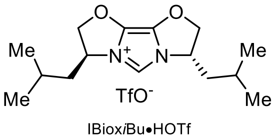

IBiox*i*Bu•HOTf
$C_{16}H_{25}F_3N_2O_5S$
M= 414,44 g.mol^{-1}

^{1}H NMR (500 MHz, $CDCl_3$): δ (ppm) 8.57 (s, 1H), 5.15 (dd, *J* = 8.8, 7.4 Hz, 2H), 4.98-4.92 (m, 2H), 4.66 (dd, *J* = 8.8, 6.2 Hz, 2H), 2.10-2.02 (m, 2H), 1.76-1.66 (m, 4H), 1.00 (d, *J* = 6.4 Hz, 6H), 1.00 (d, *J* = 6.4 Hz, 6H)

^{13}C NMR (126 MHz, $CDCl_3$): δ (ppm) 125.7, 120.8 (q, *J* = 320.2 Hz), 115.3, 82.2, 58.0, 41.7, 25.3, 22.5, 22.2

^{19}F NMR (471 MHz, $CDCl_3$): δ (ppm) -78.4.

IR (neat): ν (cm^{-1}) 2962, 1731, 1525, 1469, 1253, 1153, 1028, 635.

HRMS (ESI): Calcd for $C_{15}H_{25}N_2O_2^+$ [M]$^+$: 265.1911, found 265.1912

$[\alpha]_D^{20}$: +51.8° (c = 0.75, $CHCl_3$)

(4*R*,4'*R*)-4,4'-dicyclohexyl-4,4',5,5'-tetrahydro-2,2'-bioxazole (BioxCy):

From ***D*-cyclohexylglycine** using **General procedures A and B**. **BioxCy·HOTf** was obtained as a colorless solid (2.91 g, 9.56 mmol, 72%).

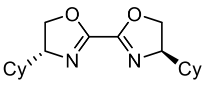

BioxCy
$C_{18}H_{28}N_2O_2$
M= 304,22 g.mol^{-1}

^{1}H NMR (500 MHz, $CDCl_3$): δ (ppm) 4.42 (dd, *J* = 9.8, 8.3 Hz, 2H), 4.14 (dd, *J* = 9.8, 8.3 Hz, 2H), 4.08 (td, *J* = 9.4, 6.7 Hz, 2H), 2.00-1.93 (m, 2H), 1.78-1.64 (m, 6H), 1.59-1.47 (m, 4H), 1.29-1.14 (m, 6H), 1.11-0.98 (m, 4H)

^{13}C NMR (126 MHz, $CDCl_3$): δ (ppm) 154.6, 72.4, 71.4, 42.5, 29.7, 29.1, 26.5, 26.4, 26.0.

IR (neat): ν (cm^{-1}) 3285, 2922, 2851, 1611, 1449, 1104, 949, 889, 719, 627

HRMS (ESI): Calcd for $C_{18}H_{28}NaO_2$ [M+Na]$^+$: 327.2043, found 327.2044

Rf: 0.63 in pure ethyl acetate

Mp: 104 °C

$[\alpha]_D^{20}$: +138 ° (c = 0.70, $CHCl_3$)

(3*R*,7*R*)-3,7-dicyclohexyl-2,3,7,8-tetrahydroimidazo[4,3-b:5,1-b']bis(oxazole)-4-ium triflate (IBioxCy·HOTf):

From **BioxCy** using **General procedure C. IBioxCy·HOTf** was obtained as a colorless solid (367 mg, 0.78 mmol, 24%).

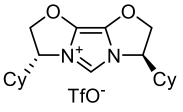

IBioxCy•HOTf
$C_{20}H_{29}F_3N_2O_5S$
M= 466,52 g.mol^{-1}

^{1}H NMR (250 MHz, $CDCl_3$): δ (ppm) 8.72 (s, 1H), 5.05 (dd, *J* = 10.1, 8.8 Hz, 2H), 4.91-4.80 (m, 4H), 2.03-1.89 (m, 2H), 1.87-1.66 (m, 9H), 1.36-1.09 (m, 9H), 1.04-0.86 (m, 2H)

^{13}C NMR (126 MHz, $CDCl_3$): δ (ppm) 125.8, 120.8 (q, *J* = 320.3 Hz), 116.4, 79.5, 63.8, 40.68, 28.3, 27.5, 25.8, 25.5, 25.4

^{19}F NMR (376 MHz, $CDCl_3$): δ (ppm) -78.5

IR (neat): ν (cm^{-1}) 2928, 2855, 1730, 1432, 1254, 1151, 1029, 635

HRMS (ESI): Calcd for $C_{19}H_{29}N_2O_2^+$ $[M]^+$: 317.2224, found 317.2219

Rf: 0.37 (CH_2Cl_2/MeOH 95:5)

Mp: 86 °C

$[\alpha]_D^{20}$: -67.2 ° (c = 0.93, $CHCl_3$)

(4*S*,4'*S*)-4,4'-diadamantyl-4,4',5,5'-tetrahydro-2,2'-bioxazole (**BioxAd**):

From ***L*-adamantylglycine,** prepared as described in the literature,[193] using **General procedures A and B**. **BioxAd·HOTf** was obtained as a colorless solid (1.54 g, 3.77 mmol, 65%).

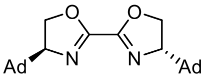

BioxAd
$C_{26}H_{36}N_2O_2$
M= 408,59 g.mol^{-1}

^{1}H NMR (500 MHz, $CDCl_3$): δ (ppm) 4.31 (dd, *J* = 9.9, 8.8 Hz, 2H) 4.29 (dd, *J* = 9.9, 8.8 Hz, 2H), 3.90 (t, *J* = 9.9 Hz, 2H), 2.02-1.97 (m, 6H), 1.74-1.63 (m, 18H), 1.46-1.40 (m, 6H)

^{13}C NMR (126 MHz, $CDCl_3$): δ (ppm) 154.5, 77.0, 68.2, 38.7, 37.1, 35.6, 28.3

IR (neat): ν (cm^{-1}) 2899, 1614, 1449, 1114, 945, 870, 655

HRMS (ESI): Calcd for $C_{52}H_{72}N_4O_4$ $[2M+Na]^+$: 839.5446, found 839.5447

Rf: 0.75 (EtOAc)

Mp: 199-202 °C

$[\alpha]_D^{20}$: -159 ° (c = 0.68, $CHCl_3$)

(3*S*,7*S*)-3,7-diadamantyl-2,3,7,8-tetrahydroimidazo[4,3-b:5,1-b']bis(oxazole)-4-ium triflate (IBioxAd·HOTf):

From **BioxAd** using **General procedure C**. **IBioxAd·HOTf** was obtained as a colorless solid (1.45 g, 2.54 mmol, 65%).

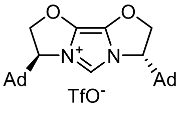

IBioxAd•HOTf
$C_{28}H_{37}F_3N_2O_5S$
M= 570,67 g.mol^{-1}

^{1}H NMR (400 MHz, $CDCl_3$): δ (ppm) 8.65 (s, 1H), 5.05 (dd, *J* = 9.4, 3.4 Hz, 2H), 4.99 (dd, *J* = 9.4, 7.5 Hz, 2H), 4.60 (dd, *J* = 7.5, 3.4 Hz, 2H), 2.13-2.07 (m, 6H), 1.77-1.64 (m, 18H), 1.57-1.49 (m, 6H)

^{13}C NMR (126 MHz, $CDCl_3$): δ (ppm) 126.0, 120.8 (q, *J* = 320.1, Hz) 117.8, 77.5, 68.7, 37.6, 36.3, 35.8, 27.7

^{19}F NMR (471 MHz, $CDCl_3$): δ (ppm) -78.4

IR (neat): ν (cm^{-1}) 2903, 2851, 1731, 1612, 1517, 1451, 1256, 1151, 1029, 635

HRMS (ESI): Calcd for $C_{27}H_{37}N_2O_2^+$ $[M]^+$: 421.2850, found 421.2847

Rf: 0.40 (CH_2Cl_2/MeOH 95:5)

Mp: 188 °C

$[\alpha]_D^{20}$: +69.7° (c = 0.34, $CHCl_3$)

General procedure D: [Pd(IBioxR)(π-allyl)Cl] complex synthesis

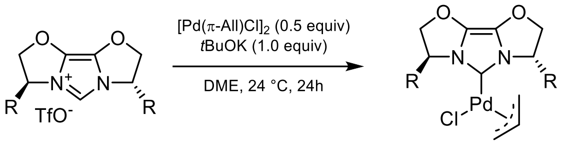

IBioxR·HOTf **Pd(IBioxR)(π-All)Cl**

The **[Pd(IBioxR)(π-allyl)Cl]** complexes were prepared according a procedure disclosed by Kündig.[114] In the glovebox, $[Pd(\pi\text{-allyl})Cl]_2$ (1.0 equiv.), **IBioxR·HOTf** (2.0 equiv.) and sodium *tert*-butoxide (2.0 equiv.) were placed into a dried catalysis tube. Dimethoxyethane (DME) (0.025 M, freshly distilled over Na and benzophenone) was added and the mixture was stirred at rt for 24 h and then quenched with aqueous NH_4Cl and extracted with CH_2Cl_2. The combined organic phases were washed with water, brine, and dried over $MgSO_4$. The resulting crude mixture was purified by flash column chromatography (EtOAc/pentane)

[Pd(IBioxAd)(π-allyl)Cl]:

Using **IBioxAd·HOTf** (100 mg, 0.175 mmol, 2.0 equiv.) and $Pd(\pi\text{- allyl})Cl]_2$ (32.0 mg, 0.088 mmol, 1.0 equiv) following **general procedure D**, **[Pd(IBioxAd)(π-allyl)Cl]** (82.0 mg, 0.136 mmol, 78%) was obtained as a colorless solid. As observed by ^1H NMR, this complex was obtained as a 1: 0.7 mixture of *endo*- and *exo*-isomers. Description of major isomer:

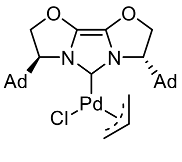

[Pd(IBioxAd)(π-All)Cl]
$C_{30}H_{41}ClN_2O_2Pd$
M= 603,54 g.mol^{-1}

^{1}H NMR (600 MHz, $CDCl_3$): δ (ppm) 5.17-5.08 (m, 1H), 4.96 (d, *J* = 9.1 Hz, 1H), 4.85 (d, *J* = 9.0 Hz, 1H), 4.75 (dd, *J* = 9.0, 7.0 Hz, 1H), 4.69 (dd, *J* = 9.0, 7.0 Hz, 1H), 4.65 (d, *J* = 6.8 Hz, 1H), 4.09 (dd, *J* = 7.4, 1.9 Hz, 1H), 3.74 (d, *J* = 6.8 Hz, 1H), 3.37 (d, *J* = 6.7 Hz, 1H), 3.17 (d, *J* = 13.4 Hz, 1H), 2.48 (d, *J* = 11.6 Hz, 1H), 2.23-1.34 (m, 30H).

^{13}C NMR (151 MHz, $CDCl_3$): δ (ppm) 158.4, 125.7, 125.4, 113.4, 77.0, 76.2, 70.5, 67.9, 66.0, 47.8, 38.9, 36.8, 36.7, 36.6, 36.5, 28.2, 28.2, 28.1, 27.1

IR (neat): ν (cm^{-1}) 2900, 2848, 1759, 1448, 1418, 1346, 1223, 1202, 913, 861

HRMS (ESI): Calcd for $C_{30}H_{41}ClN_2NaO_2Pd^+$ $[M+Na]^+$: 625.1792, found 625.1772

HRMS (ESI): Calcd for $C_{30}H_{41}N_2O_2Pd^+$ $[M-Cl]^+$: 567.2209, found 567.2201

Rf: 0.12 (pentane/EtOAc 75:25)

Mp: decomposition upon heating

$[\alpha]_D^{20}$: +214.3° (c = 0.81, $CHCl_3$)

[Pd(IBioxR)(*π*-allyl)Cl]:

Using **IBioxR·HOTf** (200 mg, 0.483 mmol, 2.0 equiv.) and Pd(π- allyl)Cl]$_2$ (88.2 mg, 0.241 mmol, 1.0 equiv) following **general procedure D**, [**Pd(IBiox*t*Bu)(*π*-allyl)Cl]** (175.0 mg, 0.390 mmol, 81%) was obtained as a colorless solid. As observed by ^{1}H NMR, this complex was obtained as a 1: 0.8 mixture of *endo*- and *exo*-isomers. Description of major isomer:

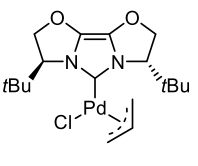

[Pd(IBiox*t*Bu)(π-allyl)Cl]
$C_{18}H_{29}ClN_2O_2Pd$
M= 447,10 g.mol^{-1}

^{1}H NMR (500 MHz, CDCl$_3$): δ (ppm) 5.18-5.08 (m, 1H), 4.91-4.74 (m, 5H), 4.10 (dd, *J* = 7.5, 2.4 Hz, 1H), 3.90 (dd, *J* = 6.8, 1.4 Hz, 1H), 3.44-3.39 (m, 1H), 3.18 (d, *J* = 13.0 Hz, 1H), 2.48-2.43 (m, 1H), 1.20 (s, 9H), 1.05 (s, 9H).

^{13}C NMR (151 MHz, CDCl$_3$): δ (ppm) 158.2, 125.6, 125.2, 113.7, 78.2, 77.8, 70.9, 67.2, 47.5, 27.3, 27.0.

IR (neat): ν (cm^{-1}) 2955, 1754, 1476, 1415, 1361, 1186, 905, 818

HRMS (ESI): Calcd for $C_{18}H_{29}N_2O_2Pd^+$ [M-Cl]$^+$: 411.1265, found 411.1271

Rf: 0.32 (pentane/EtOAc 70:30)

Mp: decomposition upon heating

$[\alpha]_D^{20}$: +128.8° (c = 1.09, CHCl$_3$)

Synthesis of IBiox*t*BuMe$_4$

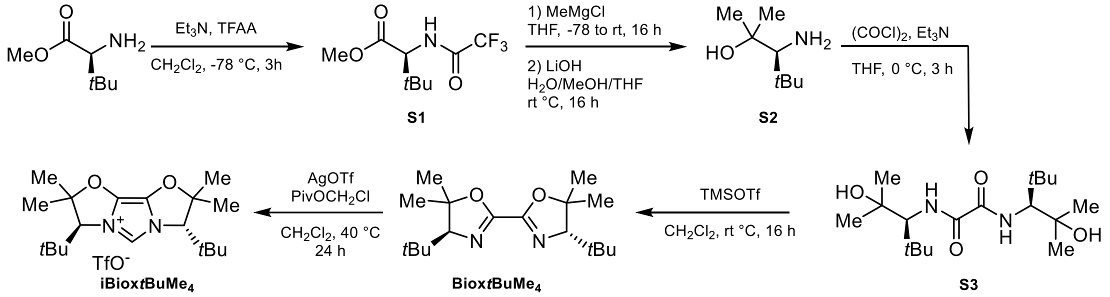

Methyl *N*-TFA L-tert-Leucinate (S1)

Under argon atmosphere, triethylamine (3.8 mL, 27.7 mmol, 3.0 equiv) was added to a solution of L-*tert*-Leucine methyl ester hydrochloride (1.68 g, 9.23 mmol, 1.0 equiv) in dry CH$_2$Cl$_2$ (20 mL) and the reaction mixture was cooled to -78 °C. Trifluoroacetic anhydride (1.3 mL, 9.23 mmol, 1.0 equiv) was added dropwise over a period of 30 min and the solution was stirred at -78 °C for 3 h. The reaction mixture was quenched with sat. NaHCO$_3$ at -78 °C and was allowed to warm to room temperature. The aqueous phase was extracted with CH$_2$Cl$_2$ (3 X 20 mL), the combined organic phase was washed with water, dried over Na$_2$SO$_4$ and concentrated under reduced pressure affording the crude *N*-TFA L-*tert*-Leucine as a yellow oil (2.23 g, 9.23 mmol, quant.).

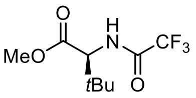

S1
$C_9H_{14}F_3NO_3$
M= 241.21 g.mol^{-1}

^{1}H NMR (400 MHz, CDCl$_3$): δ (ppm) 6.81 (s, 1H), 4.49 (d, *J* = 9.5 Hz, 1H), 3.78 (s, 3H), 1.00 (s, 10H).

^{13}C NMR (126 MHz, CDCl$_3$): δ (ppm) 170.7, 157.0 (q, *J* = 37.5 Hz), 115.9 (q, *J* = 287.9 Hz), 60.5, 52.5, 35.5, 26.5.

^{19}F NMR (471 MHz, CDCl$_3$): δ (ppm) -75.8.

IR (neat): ν (cm^{-1}) 3331, 2970, 1717, 1210, 1154

HRMS (ESI): Calcd for $C_9H_{15}F_3NO_3^+$ [M+H]$^+$: 242.0999, found 242.0998

Rf: 0.69 (CH_2Cl_2)

$[\alpha]_D^{20}$: + 27.3 ° (c = 1.00, $CHCl_3$)

(*S*)-3-Amino-2,4,4-trimethylpentan-2-ol (S2)

From **S1** (*S*)-3-Amino-2,4,4-trimethylpentan-2-ol as a yellow oil (1.62 g, 11.2 mmol, 90 %) was prepared according to a known procedure.[194] The analytical data is in full agreement with the reported one.

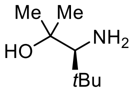

S2
$C_8H_{19}NO$
M= 145,25 g.mol^{-1}

^{1}H NMR (500 MHz, $CDCl_3$): δ (ppm) 2.34 (s, 1H), 1.30 (s, 3H), 1.13 (s, 3H), 1.00 (s, 9H).
^{13}C NMR (126 MHz, $CDCl_3$): δ (ppm) 72.4, 68.5, 35.1, 30.1, 28.9, 25.9.

(*S*)-N,N'-Bis[2-hydroxy-2,4,4-trimethylpentan-3-yl]oxalamide (S3)

Under argon atmosphere triethylamine (3.8 mL, 27.5 mmol, 4.0 equiv) was added to a solution of (*S*)-3-amino-2,4,4-trimethylpentan-2-ol (2.00 g, 13.8 mmol, 2.0 equiv) in dry THF (100 mL) and the reaction mixture was cooled to 0 °C. A solution of oxalyl chloride (0.65 mL, 6.88 mmol, 1.0 equiv) in dry THF (50 mL) was added dropwise and stirred for 3 h. The formed triethylamine salt was filtered off and the solvent removed under reduced pressure. The resulting solid was washed with hexane and diethyl ether to afford (*S*)-*N*,*N'*-Bis[2hydroxy-2,4,4-trimethylpentan-3-yl]oxalamide as a colorless powder (1.61 g, 4.67 mmol, 68 %).

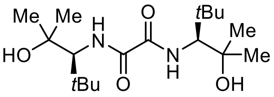

S3
$C_{18}H_{36}N_2O_4$
M= 344,50 g.mol^{-1}

^{1}H NMR (500 MHz, $CDCl_3$): δ (ppm) 7.86 (d, J = 11.0 Hz, 2H), 3.66 (d, J = 11.0 Hz, 2H), 1.81 (s, 2H), 1.39 (s, 6H), 1.26 (s, 6H), 1.07 (s, 18H).
^{13}C NMR (126 MHz, $CDCl_3$): δ (ppm) 160.1, 74.7, 64.6, 36.1, 30.4, 29.7, 28.9.
IR (neat): ν (cm^{-1}) 3371, 2972, 2605, 1666, 1504, 1377, 1159.
HRMS (ESI): Calcd for $C_{18}H_{36}N_2O_4$ [M+Na]$^+$: 367.2567 found: 367.2568.
Rf: 0.20 (CH_2Cl_2/MeOH 95:5)
Sublimation Point: 192.5 °C
$[\alpha]_D^{20}$: -36.3° (c = 1.00, $CHCl_3$)

(4*S*,4'*S*)-4,4'-Di-*tert*-butyl-5,5,5',5'-tetramethyl-4,4',5,5'-tetrahydro-2,2'-bioxazole (Biox*t*BuMe$_4$)

Under argon atmosphere a solution of Trimethylsilyl trifluoromethanesulfonate (1.05 mL, 5.8 mmol, 2.0 eq.) in dry CH_2Cl_2 (43 mL) was added dropwise to (*S*)-*N*,*N'*-Bis[2-hydroxy-2,4,4-trimethylpentan-3-yl]oxalamide (1.00 g, 2.9 mmol, 1.0 eq.) in dry CH_2Cl_2 (140 mL, 20 mM). The resulting reaction mixture was stirred at 24 °C overnight. The reaction was quenched with sat. $NaHCO_3$ and the aqueous phase was extracted with CH_2Cl_2 (3 X 140 mL). The combined organic phase was washed with brine, dried over Na_2SO_4, filtered, and concentrated under reduced pressure. The crude was purified by flash chromatography affording (4*S*,4'*S*)-4,4'-di-*tert*-butyl-5,5,5',5'-tetramethyl-4,4',5,5'-tetrahydro-2,2'-bioxazole (480 mg, 1.56 mmol, 54%) as a colorless powder.

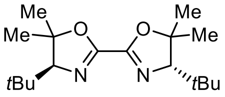

Biox*t*BuMe$_4$
$C_{18}H_{32}N_2O_2$
M= 308,47 g.mol^{-1}

1H NMR (500 MHz, CDCl3): δ (ppm) 3.56 (s, 2H), 1.52 (s, 6H), 1.50 (s, 6H), 1.09 (s, 18H)

^{13}C NMR (126 MHz, $CDCl_3$): δ (ppm) 154.0, 89.2, 83.3, 34.1, 30.7, 28.0, 23.2

IR (neat): ν (cm^{-1}) 2961, 2358, 1615, 1365, 1197, 1093

HRMS (ESI): Calcd for $C_{18}H_{32}N_2O_2$ [M+H]$^+$: 309.2537 found: 309.2541

Rf: 0.31 (cyclohexane/EtOAc 90:10)

Mp: 174.3 °C

$[\alpha]_D^{20}$: -40.2° (c = 1.00, $CHCl_3$)

(3*S*,7*S*)-3,7-di-*tert*-butyl-2,2,8,8-tetramethyl-2,3,7,8-tetrahydroimidazo[4,3-b:5,1-b']bis(oxazole)-4-ium triflate (IBiox*t*BuMe$_4$ HOTf)

From **Biox*t*BuMe$_4$** using **General procedure D**. **IBiox*t*BuMe$_4$·HOTf** was obtained as a colorless solid (70 mg, 149 μmol, 66%).

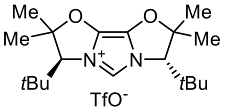

IBiox*t*BuMe$_4$•HOTf
$C_{20}H_{33}F_3N_2O_5S$
M= 470,55 g.mol^{-1}

^{1}H NMR (500 MHz, CDCl3): δ (ppm) 8.77 (s, 1H), 4.42 (s, 2H), 1.78 (s, 6H), 1.56 (s, 6H), 1.17 (s, 18H)

^{13}C NMR (126 MHz, $CDCl_3$): δ (ppm) 125.1, 119.5, 99.6, 76.1, 34.6, 29.4, 27.1, 23.7

^{19}F NMR (471 MHz, $CDCl_3$): δ (ppm) -78.25.

^{13}C NMR (126 MHz, $CDCl_3$): 125.0, 119.5, 99.6, 76.1, 34.6, 29.4, 27.1, 23.7

IR (neat): ν (cm^{-1}) 3125, 2979, 2360, 1738, 1512, 1258, 1168, 1030

HRMS (ESI): Calcd for $C_{19}H_{33}N_2O_2^+$ [M]$^+$: 321.2537 found: 321.2542

Rf: 0.27 (CH_2Cl_2/MeOH 97:3)

Mp:136.4 °C

$[\alpha]_D^{20}$: + 48.12 ° (c = 0.66, $CHCl_3$)

6.1.2 Substrates synthesis

General procedure E: benzylation of dimethyl malonate

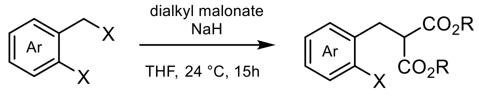

S4

Dimethyl malonate (1.4 equiv) was diluted in THF (1 mL/mmol of dimethyl malonate) and added to a suspension of 100% sodium hydride (1.2 equiv) in THF (1 mL/mmol of sodium hydride) and the mixture was stirred for 30 min at room temperature. Then, a solution of the benzyl bromide (1.0 equiv) in THF (2 mL/mmol of benzyl halide) was added dropwise and the mixture was stirred overnight at room temperature. The reaction was then quenched by addition of H_2O and brine. The phases were separated, and the aqueous layer was extracted with diethyl ether. The combined organic phases were washed with brine and dried over Na_2SO_4. After evaporation of the volatiles the crude mixture was purified by distillation under high vacuum to yield the corresponding dimethyl benzylmalonate.

Dimethyl 2-(2-bromo-4-fluorobenzyl)malonate (S4a):

From **dimethyl malonate** and **2-bromo-4-fluorobenzyl bromide** using **General procedure E**. **S4a** was obtained as a colorless solid (8.00 g, 25.08 mmol, 84%).

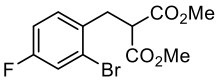

S4a

$C_{12}H_{12}BrFO_4$

M= 319,13 g.mol^{-1}

^{1}H NMR (500 MHz, $CDCl_3$): δ (ppm) 7.29 (dd, $^3J_{HF}$ = 8.2, 2.6 Hz, 1H), 7.22 (dd, J = 8.6, 6.0 Hz, 1H), 6.94 (ddd, J = 8.2, 8.3, 2.6 Hz, 1H), 3.83 (t, J = 7.8 Hz, 1H), 3.70 (s, 6H) 3.31 (d, J = 7.8 Hz, 2H)

^{13}C NMR (126 MHz, $CDCl_3$): δ (ppm) 169.0, 161.6 (d, J = 250.2 Hz), 133.0 (d, J = 3.6 Hz), 132.4 (d, J = 8.3 Hz), 124.5 (d, J = 9.5 Hz), 120.3 (d, J = 24.4 Hz), 114.7 (d, J = 20.9 Hz), 52.8, 51.4, 34.5

^{19}F NMR (471 MHz, $CDCl_3$): δ (ppm) -113.4

IR (neat): ν (cm^{-1}) 3007, 2955, 1731, 1596, 1277, 1226, 1153, 856, 777

HRMS (ESI): Calcd for $C_{12}H_{12}{}^{79}BrFNaO_4$ $[M+Na]^+$: 340.9795, found 340.9796

Rf: 0.17 (pentane/EtOAc 95:5)

Mp: 61-62°C

Dimethyl 2-(2-bromobenzyl)malonate (S4b-Br):

From **dimethyl malonate** and **2-bromobenzyl bromide** using **General procedure E**. **S4b-Br** was obtained as a colorless liquid (15.44 g, 51.27 mmol, 86%). The measured spectrometric data was in full accordance with the reported data.[195]

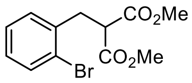

S4b-Br

$C_{12}H_{13}BrO_4$

M= 301,14 g.mol^{-1}

^{1}H NMR (400 MHz, $CDCl_3$): δ (ppm) 7.56-7.52 (m, 1H), 7.25-7.19 (m, 2H), 7.12-7.07 (m, 1H), 3.88 (t, J = 7.8 Hz, 1H), 3.70 (s, 6H), 3.34 (d, J = 7.8 Hz, 2H)

^{13}C NMR (101 MHz, $CDCl_3$): δ (ppm) 169.2, 137.1, 133.1, 131.5, 128.8, 127.6, 124.7, 52.8, 51.4, 35.3

Dimethyl 2-(2-chlorobenzyl)malonate (S4b-Cl):

From **dimethyl malonate** and **2-chlorobenzyl bromide** using **General procedure E**. **S4b-Cl** was obtained as a colorless liquid (4.62 g, 18.01 mmol, 74%). The measured spectrometric data was in full accordance with the reported data.[196]

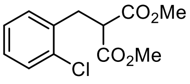

S4b-Cl
$C_{12}H_{13}ClO_4$
M= 256,68 g.mol^{-1}

^{1}H NMR (500 MHz, $CDCl_3$): δ (ppm) 7.37-7.32 (m, 1H), 7.25-7.21 (m, 1H), 7.20-7.14 (m, 2H), 3.85 (t, *J* = 7.8 Hz, 1H), 3.69 (s, 6H), 3.34 (d, *J* = 7.8 Hz, 2H)

^{13}C NMR (126 MHz, $CDCl_3$): δ (ppm) 169.2, 135.4, 134.3, 131.5, 129.8, 128.6, 127.0, 52.7, 51.3, 32.9

Diisopropyl 2-(2-bromobenzyl)malonate (S4c):

From **diisopropyl malonate**and **1-bromo-2-(bromomethyl)benzene** using **General procedure E**. **S4c** was obtained as a transparent liquid (2.70 g, 7.56 mmol, 63%).

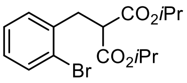

S4c
$C_{16}H_{21}BrO_4$
M= 357,24 g.mol^{-1}

^{1}H NMR (500 MHz, $CDCl_3$): δ (ppm) 7.53 (dd, *J* = 8.0, 1.3 Hz, 1H), 7.26-7.24 (m, 1H), 7.20 (td, *J* = 7.4, 1.3 Hz, 1H), 7.08 (ddd, *J* = 7.9, 7.3, 1.8 Hz, 1H), 5.01 (hept, *J* = 6.3 Hz, 2H), 3.78 (t, *J* = 7.8 Hz, 1H), 3.31 (d, *J* = 7.8 Hz, 2H), 1.22 (d, *J* = 6.3 Hz, 6H), 1.16 (d, *J* = 6.3 Hz, 6H).

^{13}C NMR (126 MHz, $CDCl_3$): δ (ppm) 168.4, 137.4, 133.1, 131.6, 128.6, 127.5, 124.8, 69.2, 52.0, 35.1, 21.7, 21.7.

IR (neat): ν (cm^{-1}) 2982, 2955, 2938, 1727, 1469, 1292, 1231, 1102, 908, 731

HRMS (ESI): Calcd for $C_{16}H_{21}{}^{79}BrNaO_4$ $[M+Na]^+$: 379.0515, found 379.0516

Rf: 0.62 (pentane/EtOAc 90:10)

Dimethyl 2-(2-bromo-5-fluorobenzyl)malonate (S4d):

From **dimethyl malonate** and **2-bromo-5-fluorobenzyl bromide** using **General procedure E**. **S4d** was obtained as a colorless liquid (3.88 g, 12.17 mmol, 77%).

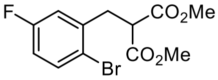

S4d
$C_{12}H_{12}BrFO_4$
M= 319,13 g.mol^{-1}

^{1}H NMR (500 MHz, $CDCl_3$): δ (ppm) 7.48 (dd, *J* = 8.8, 5.3 Hz, 1H), 6.98 (dd, *J* = 9.2, 3.1 Hz, 1H), 6.84 (ddd, *J* = 8.3, 8.3, 3.1 Hz, 1H), 3.84 (t, *J* = 7.7 Hz, 1H), 3.72 (s, 6H), 3.31 (d, *J* = 7.7 Hz, 2H)

^{13}C NMR (126 MHz, $CDCl_3$): δ (ppm) 168.9, 161.9 (d, *J* = 247.3 Hz), 139.2 (d, *J* = 7.7 Hz), 134.2 (d, *J* = 8.2 Hz), 118.7 (d, *J* = 3.2 Hz), 118.5 (d, *J* = 23.0 Hz), 116.0 (d, *J* = 22.3 Hz), 52.9, 51.26, 35.2 (d, *J* = 1.4 Hz)

^{19}F NMR (471 MHz, $CDCl_3$): δ (ppm) -114.6

IR (neat): ν (cm^{-1}) 2955, 1734, 1470, 1236, 1150, 1030, 875, 811

HRMS (ESI): Calcd for $C_{12}H_{12}{}^{79}BrFNaO_4$ $[M+Na]^+$: 340.9795, found 340.9796

Rf: 0.22 (pentane/EtOAc 95:5)

General procedure F: alkylation of dimethyl benzylmalonate

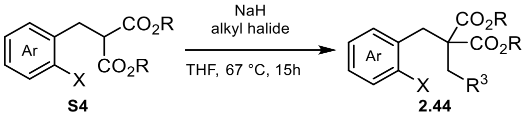

In a 10-20 mL microwave reaction vial, **S4** (1 equiv) was diluted in THF (3 mL/mmol of dimethyl benzylmalonate), then sodium hydride (60% in mineral oil, 1.2 equiv) was added in one portion and the mixture was stirred for 30 min at room temperature. Then, the choose alkyl halide (1.4 equiv) was added. If solid, the alkyl halide was added as a solution in THF. The vial was then sealed and transferred in an 80°C preheated aluminum block. After overnight stirring at this temperature, the reaction was quenched by addition of H_2O and brine. The phases were separated, and the aqueous layer was extracted with diethyl ether or ethyl acetate. The combined organic phases were washed with brine and dried over Na_2SO_4. After evaporation of the volatiles the crude mixture was purified by flash column chromatography (pentane/EtOAc) to yield the corresponding product **2.44**.

General procedure G: alkylation of dialkyl *n*-propylmalonate

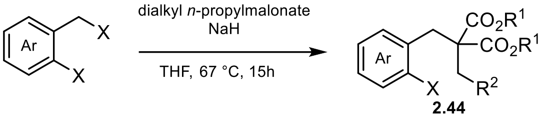

In a 10-20 mL microwave reaction vial, dialkyl *n*-propylmalonate (1 equiv) was diluted in THF (3 mL/mmol of dimethyl *n*-propylmalonate), then sodium hydride (60% in mineral oil, 1.1 equiv) was added in one portion and the mixture was stirred for 30 min at room temperature. Then, the choose benzyl bromide (1.2 equiv) was added. If solid, the alkyl halide was added as a solution in THF. The vial was then sealed and transferred in an 80°C preheated aluminum block. After overnight stirring at this temperature, the reaction was quenched by addition of H_2O and brine. The phases were separated, and the aqueous layer was extracted with diethyl ether or ethyl acetate. The combined organic phases were washed with brine and dried over Na_2SO_4. After evaporation of the volatiles the crude product was purified by flash column chromatography (pentane/EtOAc) to yield the corresponding product **1**.

Dimethyl 2-(2-bromo-4-fluorobenzyl)-2-propylmalonate (2.44a):

From **S4a** and ***n*-propyl iodide** using **General procedure F**. **2.44a** was obtained as a colorless oil (842 mg, 2.42 mmol, 82%).

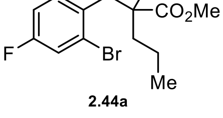

2.44a
$C_{15}H_{18}BrFO_4$
M= 361,21 g.mol^{-1}

^{1}H NMR (500 MHz, $CDCl_3$): δ (ppm) 7.30-7.26 (m, 1H), 7.15 (dd, *J* = 8.7, 6.0 Hz, 1H), 6.94 (ddd, *J* = 8.7, 7.8, 2.7 Hz, 1H), 3.70 (s, 6H), 3.42 (s, 2H), 1.85-1.78 (m, 2H), 1.36-1.25 (m, 2H), 0.92 (t, *J* = 7.3 Hz, 3H)

^{13}C NMR (126 MHz, $CDCl_3$): δ (ppm) 171.7, 161.2 (d, *J* = 250.3 Hz), 132.5 (d, *J* = 3.7 Hz), 132.2 (d, *J* = 8.3 Hz), 125.9 (d, *J* = 9.3 Hz), 120.2 (d, *J* = 24.2 Hz), 114.6 (d, *J* = 20.9 Hz), 59.1, 52.5, 37.1, 35.3, 18.2, 14.4

^{19}F NMR (471 MHz, $CDCl_3$): δ (ppm) -113.7

IR (neat): ν (cm^{-1}) 2958, 1730, 1599, 1487, 1211, 1120, 857, 731

HRMS (ESI): Calcd for $C_{15}H_{18}{}^{79}BrFNaO_4$ $[M+Na]^+$: 383.0265, found 383.0266

Rf: 0.17 (pentane/EtOAc 95:5)

Dimethyl 2-(2-bromobenzyl)-2-ethylmalonate (2.44b):

From **S4b-Br** and **ethyl iodide** using **General procedure F**. **2.44b** was obtained as a colorless oil (2.85 g, 8.66 mmol, 87%).

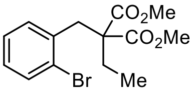

2.44b
$C_{14}H_{17}BrO_4$
M= 329,19 g.mol^{-1}

^{1}H NMR (400 MHz, $CDCl_3$): δ (ppm) 7.53 (dd, *J* = 8.0, 1.4 Hz, 1H) 7.23-7.14 (m, 2H), 7.09-7.04 (m, 1H), 3.71 (s, 6H), 3.47 (s, 2H), 1.93 (q, *J* = 7.5 Hz, 2H), 0.93 (t, *J* = 7.5 Hz, 3H)

^{13}C NMR (101 MHz, $CDCl_3$): δ (ppm) 171.7, 136.4, 133.22, 131.4, 128.6, 127.4, 126.1, 59.5, 52.5, 37.4, 26.1, 9.4

IR (neat): ν (cm^{-1}) 2951, 1729, 1435, 1223, 1125, 1026, 745

HRMS (ESI): Calcd for $C_{14}H_{17}{}^{79}BrNaO_4$ [M+Na]$^+$: 351.0202, found 351.0206

Rf: 0.31(pentane/EtOAc 95:5)

Dimethyl 2-(2-bromobenzyl)-2-propylmalonate (2.44c-Br):

From **S4b-Br** and ***n*-propyl iodide** using **General procedure F**. **2.44c-Br** was obtained as a colorless solid (1.90 g, 5.54 mmol, 82%).

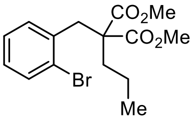

2.44c-Br
$C_{15}H_{19}BrO_4$
M= 343,22 g.mol^{-1}

^{1}H NMR (500 MHz, $CDCl_3$): δ (ppm) 7.53 (dd, *J* = 8.0, 1.2 Hz, 1H), 7.20 (td, *J* = 7.5, 1.3 Hz, 1H), 7.14 (dd, *J* = 7.8, 1.8 Hz, 1H), 7.07 (ddd, *J* = 8.0, 7.3, 1.8 Hz, 1H), 3.70 (s, 6H), 3.47 (s, 2H), 1.85-1.79 (m, 2H), 1.37-1.26 (m, 2H), 0.92 (t, *J* = 7.3 Hz, 3H)

^{13}C NMR (126 MHz, $CDCl_3$): δ (ppm) 171.8, 136.5, 133.2, 131.4, 128.6, 127.4, 126.1, 59.1, 52.5, 37.8, 35.1, 18.2, 14.4

IR (neat): ν (cm^{-1}) 2956, 2874, 1731, 1436, 1200, 754

HRMS (ESI): Calcd for $C_{15}H_{19}{}^{79}BrNaO_4$ [M+Na]$^+$: 365.0359, found 365.0363

Rf: 0.34 in a 90:10 mixture of pentane and ethyl acetate

Mp: 71-73°C

Dimethyl 2-(2-chlorobenzyl)-2-propylmalonate (2.44c-Cl):

From **S4b-Cl** and ***n*-propyl iodide** using **General procedure F**. **2.44c-Cl** was obtained as a colorless oil (432 mg, 1.44 mmol, 74%).

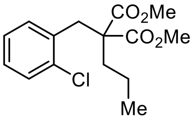

2.44c-Cl
$C_{15}H_{19}ClO_4$
M= 298,76 g.mol^{-1}

^{1}H NMR (500 MHz, $CDCl_3$): δ (ppm) 7.36-7.31 (m, 1H), 7.18-7.11 (m, 3H), 3.71 (s, 6H), 3.44 (s, 2H), 1.82-1.77 (m, 2H), 1.37-1.26 (m, 2H), 0.92 (t, *J* = 7.3 Hz, 3H)

^{13}C NMR (126 MHz, $CDCl_3$): δ (ppm) 171.8, 135.3, 134.6, 131.6, 129.8, 128.4, 126.7, 59.0, 52.5, 35.2, 34.8, 18.1, 14.4

IR (neat): ν (cm^{-1}) 2956, 2874, 1732, 1439, 1211, 1120, 1048, 751

HRMS (ESI): Calcd for $C_{15}H_{19}{}^{35}ClNaO_4$ [M+Na]$^+$: 321.0864, found 321.0867

Rf: 0.35 (pentane/EtOAc 90:10)

Dimethyl 2-(2-bromobenzyl)-2-pentylmalonate (2.44d):

From **S4b-Br** and ***n*-pentyl iodide** using **General procedure F**. **2.44d** was obtained as a slightly yellow oil (506 mg, 1.36 mmol, 82%).

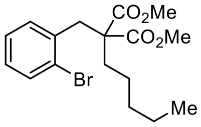

2.44d
$C_{17}H_{23}BrO_4$
M= 371,27 g.mol^{-1}

^{1}H NMR (500 MHz, CDCl$_3$): δ (ppm) 7.53 (dd, *J* = 8.0, 1.3 Hz, 1H), 7.20 (td, *J* = 7.5, 1.3 Hz, 1H), 7.15 (dd, *J* = 7.8, 1.8 Hz, 1H), 7.06 (ddd, *J* = 8.0, 7.3, 1.8 Hz, 1H), 3.70 (s, 6H), 3.48 (s, 2H), 1.87-1.81 (m, 2H), 1.33-1.25 (m, 6H), 0.87 (t, J = 6.7 Hz, 3H)

^{13}C NMR (126 MHz, CDCl$_3$): δ (ppm) 171.9, 136.5, 133.2, 131.4, 128.6, 127.3, 126.1, 59.0, 52.5, 37.8, 33.0, 32.1, 24.4, 22.5, 14.1

IR (neat): ν (cm^{-1}) 2954, 2862, 1731, 1435, 1255, 1199, 1125, 1030, 750

HRMS (ESI): Calcd for $C_{17}H_{23}{}^{79}BrNaO_4$ [M+Na]$^+$: 393.0672, found 393.0672

Rf: 0.36 (pentane/EtOAc 90:10)

Dimethyl 2-(2-bromobenzyl)-2-isopentylmalonate (2.44e):

From **S4b-Br** and **isopentyl iodide** using **General procedure F**. **2.44e** was obtained as a slightly yellow oil (515 mg, 1.39 mmol, 84%).

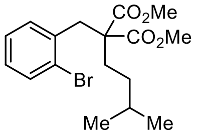

2.44e
$C_{17}H_{23}BrO_4$
M= 371,27 g.mol^{-1}

^{1}H NMR (500 MHz, CDCl$_3$): δ (ppm) 7.53 (dd, *J* = 8.0, 1.2 Hz, 1H), 7.22-7.18 (m, 1H), 7.16 (dd, *J* = 7.8, 2.0 Hz, 1H), 7.06 (ddd, *J* = 8.0, 7.1, 2.0 Hz, 1H), 3.70 (s, 6H), 3.48 (s, 2H), 1.90-1.84 (m, 2H), 1.57-1.45 (m, 1H), 1.19-1.12 (m, 2H), 0.87 (d, *J* = 6.6 Hz, 6H)

^{13}C NMR (126 MHz, CDCl$_3$): δ (ppm) 171.9, 136.5, 133.2, 131.4, 128.6, 127.3, 126.1, 59.0, 52.5, 37.8, 33.5, 31.2, 28.5, 22.6

IR (neat): ν (cm^{-1}) 2954, 2871, 1731, 1435, 1265, 1239, 1205, 1133, 1030, 750

HRMS (ESI): Calcd for $C_{17}H_{23}{}^{79}BrNaO_4$ [M+Na]$^+$: 393.0672, found 393.0674

Rf: 0.36 (pentane/EtOAc 90:10)

Dimethyl 2-(2-bromobenzyl)-2-(3-fluoropropyl)malonate (2.44f):

From **S4b-Br** and **1-fluoro-3-iodopropane** using **General procedure F**. **2.44f** was obtained as a colorless solid (435 mg, 1.20 mmol, 73%).

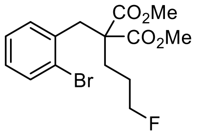

2.44f
$C_{15}H_{18}BrFO_4$
M= 361,21 g.mol^{-1}

^{1}H NMR (500 MHz, CDCl$_3$): δ (ppm) 7.54 (dd, *J* = 8.0, 1.3 Hz, 1H), 7.21 (td, *J* = 7.5, 1.3 Hz, 1H), 7.15 (dd, *J* = 7.8, 1.8 Hz, 1H), 7.08 (ddd, *J* = 8.0, 7.3, 1.8 Hz, 1H), 4.42 (dt, *J* = 47.2, 6.0 Hz, 2H), 3.73 (s, 6H), 3.50 (s, 2H), 2.00-1.92 (m, 2H), 1.79-1.66 (m, 2H)

^{13}C NMR (126 MHz, CDCl$_3$): δ (ppm) 171.5, 136.1, 133.3, 131.4, 128.8, 127.5, 126.1, 83.8 (d, *J* = 166.1 Hz), 58.7, 52.7, 38.0, 28.9 (d, *J* = 5.9 Hz), 26.1 (d, *J* = 20.1 Hz)

^{19}F NMR (235 MHz, CDCl$_3$): δ (ppm) -218.7

IR (neat): ν (cm^{-1}) 2955, 2904, 1730, 1436, 1201, 1027, 752

HRMS (ESI): Calcd for $C_{15}H_{18}{}^{79}BrFNaO_4$ [M+Na]$^+$: 383.0265, found 383.0270

Rf: 0.22 (pentane/EtOAc 90:10)

Mp: 66-68°C

Trimethyl 5-(2-bromophenyl)pentane-1,4,4-tricarboxylate (2.44g):

From **S4b-Br** and **methyl 4-iodobutyrate** using **General procedure F**. **2.44g** was obtained as a slightly yellow oil (514 mg, 1.28 mmol, 77%).

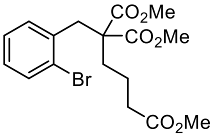

2.44g
$C_{17}H_{21}BrO_6$
M= 401,25 g.mol^{-1}

^{1}H NMR (500 MHz, $CDCl_3$): δ (ppm) 7.53 (dd, *J* = 8.0, 1.3 Hz, 1H), 7.20 (td, *J* = 7.5, 1.3 Hz, 1H), 7.15 (dd, *J* = 7.8, 1.8 Hz, 1H), 7.07 (ddd, *J* = 8.0, 7.3, 1.9 Hz, 1H), 3.71 (s, 6H), 3.65 (s, 3H), 3.48 (s, 2H), 2.31 (t, *J* = 7.5 Hz, 2H), 1.90-1.84 (m, 2H), 1.69-1.60 (m, 2H)

^{13}C NMR (126 MHz, $CDCl_3$): δ (ppm) 173.5, 171.5, 136.2, 133.3, 131.4, 128.7, 127.4, 126.1, 58.9, 52.6, 51.7, 37.8, 34.2, 32.4, 20.5

IR (neat): ν (cm^{-1}) 2953, 1729, 1435, 1199, 1166, 1026, 751

HRMS (ESI): Calcd for $C_{17}H_{231}{}^{79}BrNaO_6$ [M+Na]$^+$: 423.0414, found 423.0416

Rf: 0.34 (pentane/EtOAc 75:25)

Dimethyl 2-(2-bromobenzyl)-2-(3-((4-methoxybenzyl)oxy)propyl)malonate (2.44h):

From **S4b-Br** and **3-(4-methoxyphenoxy)-1-iodopropane** using **General procedure F**. **2.44h** was obtained as a slightly yellow oil (590 mg, 1.27 mmol, 76%).

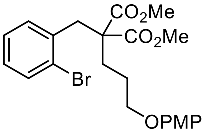

2.44h
$C_{25}H_{25}BrO_6$
M= 465,34 g.mol^{-1}

^{1}H NMR (500 MHz, $CDCl_3$): δ (ppm) 7.54 (dd, *J* = 8.0, 1.1 Hz, 1H), 7.23-7.17 (m, 2H), 7.08 (ddd, *J* = 8.0, 6.7, 2.3 Hz, 1H), 6.86-6.78 (m, 4H), 3.90 (t, *J* = 6.4 Hz, 2H), 3.76 (s, 3H), 3.72 (s, 6H), 3.52 (s, 2H), 2.06-2.00 (m, 2H), 1.82-1.74 (m, 2H)

^{13}C NMR (126 MHz, $CDCl_3$): δ (ppm) 171.6, 153.9, 153.1, 136.2, 133.3, 131.5, 128.7, 127.4, 126.1, 115.6, 114.8, 68.4, 58.8, 55.9, 52.6, 37.8, 29.6, 25.0

IR (neat): ν (cm^{-1}) 2951, 1730, 1507, 1227, 1032, 824, 749

HRMS (ESI): Calcd for $C_{22}H_{25}{}^{79}BrNaO_6$ [M+Na]$^+$: 487.0727, found 487.0729

Rf: 0.12 (pentane/EtOAc 90:10)

Dimethyl 2-(2-bromobenzyl)-2-(4-((tert-butyldimethylsilyl)oxy)butyl)malonate (2.44i):

From **S4b-Br** and ***tert*-butyl(4-iodobutoxy)dimethylsilane** using **General procedure F**. **2.44i** was obtained as a slightly yellow oil (610 mg, 1.25 mmol, 75%).

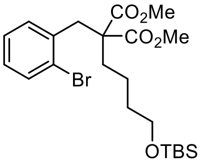

2.44i
$C_{22}H_{35}BrO_5Si$
M= 487,51 g.mol^{-1}

^{1}H NMR (500 MHz, $CDCl_3$): δ (ppm) 7.53 (dd, *J* = 8.0, 1.3 Hz, 1H), 7.22-7.17 (m, 1H), 7.15 (dd, *J* = 7.8, 1.9 Hz, 1H), 7.06 (ddd, *J* = 8.0, 7.2, 1.9 Hz, 1H), 3.70 (s, 6H), 3.59 (t, *J* = 6.3 Hz, 2H), 3.48 (s, 2H), 1.89-1.82 (m, 2H), 1.55-1.47 (m, 2H), 1.40-1.30 (m, 2H), 0.88 (s, 9H), 0.03 (s, 6H)

^{13}C NMR (126 MHz, $CDCl_3$): δ (ppm) 171.8, 136.4, 133.2, 131.4, 128.6, 127.4, 126.1, 62.8, 59.0, 52.5, 37.7, 33.1, 32.7, 26.1, 21.2, 18.4, -5.2

IR (neat): ν (cm^{-1}) 2952, 2858, 1735, 1436, 1252, 1099, 835, 775, 750

HRMS (ESI): Calcd for $C_{22}H_{35}{}^{79}BrNaO_{5Si}$ [M+Na]$^+$: 509.1329, found 509.1330l

Rf: 0.37 (pentane/EtOAc 90:10)

Dimethyl 2-(2-bromo-4-fluorobenzyl)-2-(3-(1,3-dioxoisoindolin-2-yl)propyl)malonate (2.44j):

From **4a** and ***N*-(3-iodopropyl)phtalimide** using **General procedure F**. **2.44j** was obtained as a colorless solid (1.37 g, 2.7 mmol, 86%).

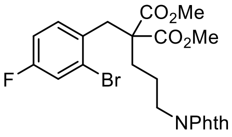

2.44j
$C_{23}H_{21}BrFNO_6$
M= 506,32 g.mol^{-1}

^{1}H NMR (500 MHz, $CDCl_3$): δ (ppm) 7.86-7.79 (m, 2H), 7.76-7.68 (m, 2H), 7.24 (dd, *J* = 8.3, 2.7 Hz, 1H), 7.13 (dd, *J* = 8.7, 6.0 Hz, 1H), 6.90 (ddd, *J* = 8.7, 7.8, 2.7 Hz, 1H), 3.69 (s, 6H), 3.67 (t, *J* = 7.3 Hz, 2H), 3.41 (s, 2H), 1.92-1.85 (m, 2H), 1.72-1.64 (m, 2H)

^{13}C NMR (126 MHz, $CDCl_3$): δ (ppm) 171.2, 168.3, 161.3 (d, *J* = 250.6 Hz), 134.1, 132.3, 132.2, 132.0 (d, *J* = 3.7 Hz), 126.0 (d, *J* = 9.3 Hz), 123.3, 120.3 (d, *J* = 24.1 Hz), 114.7 (d, *J* = 20.8 Hz), 58.7 (d, *J* = 1.1 Hz), 52.7, 37.9, 37.1, 30.1, 24.1

^{19}F NMR (235 MHz, $CDCl_3$): δ (ppm) -113.3

IR (neat): ν (cm^{-1}) 2952, 2869, 1721, 1487, 1262, 1219, 1052, 863, 719

HRMS (ESI): Calcd for $C_{23}H_{21}{}^{79}BrFNaO_6$ $[M+Na]^+$: 528.0428, found 528.0429

Rf: 0.14 (pentane/EtOAc 80:20)

Mp: 118.1-122.4 °C

Diethyl 2-(2-bromobenzyl)-2-propylmalonate (2.44k):

From **diethyl *n*-propylmalonate** and **2-bromobenzyl bromide** using **General procedure G**. **2.44k** was obtained as a colorless liquid (679 mg, 1.83 mmol, 91%).

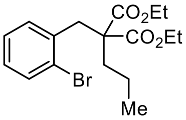

2.44k
$C_{17}H_{23}BrO_4$
M= 371,27 g.mol^{-1}

^{1}H NMR (500 MHz, $CDCl_3$): δ (ppm) 7.54-7.50 (m, 1H), 7.21-7.16 (m, 2H), 7.10-7.02 (m, 1H), 4.22-4.10 (m, 4H), 3.47 (s, 2H), 1.85-1.79 (m, 2H), 1.40-1.28 (m, 2H), 1.21 (t, *J* = 7.1 Hz, 3H), 0.92 (t, *J* = 7.3 Hz, 3H)

^{13}C NMR (126 MHz, $CDCl_3$): δ (ppm) 171.4, 136.8, 133.2, 131.5, 128.5, 127.3, 126.2, 61.4, 58.9, 37.6, 35.1, 18.1, 14.4, 14.1

IR (neat): ν (cm^{-1}) 2964, 2874, 1728, 1469, 1442, 1209, 1185, 1121, 1031, 861, 750

HRMS (ESI): Calcd for $C_{17}H_{23}{}^{79}BrNaO_4$ $[M+Na]^+$: 393.0672, found 393.0673

Rf: 0.42 (pentane/EtOAc 90:10)

Diisopropyl 2-(2-bromobenzyl)-2-propylmalonate (2.44l):

From **S4c** and ***n*-propyl iodide** using **General procedure F**. **2.44l** was obtained as a colorless solid (720 mg, 1.80 mmol, 81%).

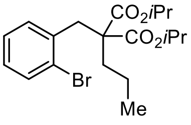

2.44l
$C_{19}H_{27}BrO_4$
M= 399,33 g.mol^{-1}

^{1}H NMR (500 MHz, $CDCl_3$): δ (ppm) 7.51 (dd, *J* = 8.0, 1.3 Hz, 1H), 7.25 (dd, *J* = 7.7, 1.7 Hz, 1H), 7.17 (td, *J* = 7.5, 1.3 Hz, 1H), 7.04 (ddd, *J* = 8.0, 7.3, 1.8 Hz, 1H), 5.02 (hept, *J* = 6.3 Hz, 2H), 3.45 (s, 2H), 1.87-1.69 (m, 2H), 1.37-1.27 (m, 2H), 1.20 (d, *J* = 6.3 Hz, 6H), 1.18 (d, *J* = 6.3 Hz, 6H), 0.90 (t, *J* = 7.3 Hz, 3H)

^{13}C NMR (126 MHz, $CDCl_3$): δ (ppm) 171.0, 137.0, 133.1, 131.4, 128.3, 127.2, 126.3, 68.9, 58.8, 37.6, 35.3, 21.7, 21.6, 18.0, 14.5.

IR (neat): ν (cm^{-1}) 2976, 2870, 1725, 1469, 1100, 749

HRMS (ESI): Calcd for $C_{19}H_{27}{}^{79}BrNaO_4$ $[M+Na]^+$: 421.0985, found 421.0988

Rf: 0.68 (pentane/EtOAc 90:10)

Mp: 54-59°C

Dimethyl 2-(2-bromo-5-fluorobenzyl)-2-propylmalonate (2.44m):

From **S4d** and ***n*-propyl iodide** using **General procedure F**. **2.44m** was obtained as a colorless oil (900 mg, 2.49 mmol, 80 %).

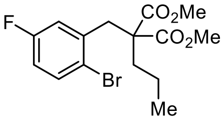

2.44m

$C_{15}H_{18}BrFO_4$

M= 361,21 g.mol^{-1}

^{1}**H NMR** (400 MHz, $CDCl_3$): δ (ppm) 7.48 (dd, J = 8.8, 5.5 Hz, 1H), 6.92 (dd, J = 9.8, 3.1 Hz, 1H), 6.82 (ddd, J = 8.8, 7.6, 3.1 Hz, 1H), 3.71 (s, 6H), 3.43 (s, 2H), 1.88-1.79 (m, 2H), 1.37-1.22 (m, 2H), 0.93 (t, J = 7.3 Hz, 3H)

^{13}**C NMR** (101 MHz, $CDCl_3$): δ (ppm) δ 171.5, 161.7 (d, J = 246.6 Hz), 138.7 (d, J = 7.7 Hz), 134.1 (d, J = 8.1 Hz), 120.2 (d, J = 3.2 Hz), 118.4 (d, J = 23.0 Hz), 115.9 (d, J = 22.4 Hz), 59.0, 52.6, 38.0 (d, J = 1.5 Hz), 35.4, 18.2, 14.4

^{19}**F NMR** (376 MHz, $CDCl_3$): δ (ppm) -114.8

IR (neat): ν (cm^{-1}) 2957, 1731, 1579, 1469, 1213, 1155, 1032, 812, 701

HRMS (ESI): Calcd for $C_{15}H_{18}{}^{79}BrFNaO_4$ [M+Na]$^+$: 388.0265, found 388.0261

Rf: 0.20 (pentane/EtOAc 95:5)

Dimethyl 2-(2-bromo-5-nitrobenzyl)-2-propylmalonate (2.44n):

From **dimethyl *n*-propylmalonate** and **2-bromo-5-nitrobenzyl bromide** using **General procedure G**. **2.44n** was obtained as a colorless solid (690 mg, 1.78 mmol, 89%).

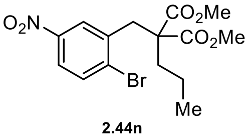

2.44n

$C_{15}H_{18}BrNO_6$

M= 388,21 g.mol^{-1}

^{1}**H NMR** (500 MHz, $CDCl_3$): δ (ppm) 8.08 (d, J = 2.7 Hz, 1H), 7.93 (dd, J = 8.8, 2.7 Hz, 1H), 7.72 (d, J = 8.8 Hz, 1H), 3.74 (s, 6H), 3.53 (s, 2H), 1.84-1.80 (m, 2H), 1.39-1.29 (m, 2H), 0.95 (t, J = 7.3 Hz, 3H)

^{13}**C NMR** (126 MHz, $CDCl_3$): δ (ppm) 171.2, 147.1, 138.8, 134.0, 133.3, 126.2, 123.1, 59.0, 52.8, 38.0, 35.5, 18.2, 14.3

IR (neat): ν (cm^{-1}) 2965, 2877, 1737, 1527, 1338, 1216, 1040, 809, 738

HRMS (ESI): Calcd for $C_{15}H_{18}{}^{79}BrNNaO_6$ [M+Na]$^+$: 410.0210, found 410.0210

Rf: 0.28 (pentane/EtOAc 90:10)

Mp: 79-81°C

Dimethyl 2-(2-chloro-5-(trifluoromethyl)benzyl)-2-propylmalonate (2.44o):

From **dimethyl *n*-propylmalonate** and **2-chloro-5-(trifluoromethyl)benzyl bromide** using **General procedure G**. **2.44o** was obtained as a colorless oil (689 mg, 1.88 mmol, 94%).

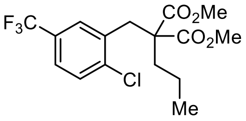

2.44o

$C_{16}H_{18}ClF_3O_4$

M= 366,76 g.mol^{-1}

^{1}**H NMR** (500 MHz, $CDCl_3$): δ (ppm) 7.48-7.45 (m, 1H), 7.44-7.40 (m, 2H), 3.71 (s, 6H), 3.47 (s, 2H), 1.82-1.75 (m, 2H), 1.40-1.26 (m, 2H), 0.93 (t, J = 7.3 Hz, 3H)

^{13}**C NMR** (126 MHz, $CDCl_3$): δ (ppm) 171.4, 139.1 (q, J = 1.5 Hz), 135.8, 130.3, 129.2 (q, J = 32.8 Hz), 128.7 (q, J = 3.8 Hz), 125.2 (q, J = 3.7 Hz), 123.8 (q, J = 272.2 Hz), 59.0, 52.6, 35.2, 34.9, 18.1, 14.2

^{19}**F NMR** (235 MHz, $CDCl_3$): δ (ppm) -62.7

IR (neat): ν (cm^{-1}) 2960, 2877, 1734, 1326, 1122, 1083, 828

HRMS (ESI): Calcd for $C_{16}H_{18}{}^{35}ClF_3NaO_4$ [M+Na]$^+$: 389.0738, found 389.0744

Rf: 0.44 (pentane/EtOAc 90:10)

Dimethyl 2-(2-chloro-4-(methoxycarbonyl)benzyl)-2-propylmalonate (2.44p):

From **dimethyl *n*-propylmalonate** and **2-chloro-4-(methoxycarbonyl)benzyl bromide** using **General procedure G**. **2.44p** was obtained as a colorless solid (565 mg, 1.58 mmol, 79%).

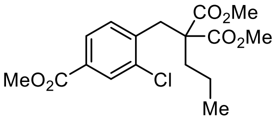

2.44p

$C_{17}H_{21}ClO_6$

M= 356,80 g.mol^{-1}

^{1}H NMR (500 MHz, $CDCl_3$): δ (ppm) 8.01 (d, *J* = 1.7 Hz, 1H), 7.81 (dd, *J* = 8.1, 1.7 Hz, 1H), 7.24 (d, *J* = 8.1 Hz, 1H), 3.90 (s, 3H), 3.69 (s, 6H), 3.47 (s, 2H), 1.84-1.76 (m, 2H), 1.36-1.25 (m, 2H), 0.92 (t, *J* = 7.3 Hz, 3H)

^{13}C NMR (126 MHz, $CDCl_3$): δ (ppm) 171.5, 165.9, 140.0, 135.6, 131.7, 130.8, 130.4, 127.7, 58.9, 52.6, 52.5, 35.4, 35.2, 18.1, 14.3

IR (neat): ν (cm^{-1}) 2969, 2875, 1736, 1712, 1285, 1215, 1122, 1051, 761

HRMS (ESI): Calcd for $C_{17}H_{21}{}^{35}ClNaO_6$ $[M+Na]^+$: 379.0919, found 379.0926

Rf: 0.20 (pentane/EtOAc 90:10)

Mp: 70-72°C

Dimethyl 2-(2-chloro-4-(methylsulfonyl)benzyl)-2-propylmalonate (2.44q):

From **dimethyl *n*-propylmalonate** and **1-(bromomethyl)-2-chloro-4-(methylsulfonyl) benzene** using **General procedure G**. **2.44q** was obtained as a colorless solid (1.30 g, 3.50 mmol, 76%).

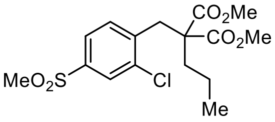

2.44q

$C_{16}H_{21}ClO_6S$

M= 376,85 g.mol^{-1}

^{1}H NMR (500 MHz, $CDCl_3$): δ (ppm) 7.92 (d, *J* = 2.0 Hz, 1H), 7.72 (dd, *J* = 8.2, 2.0 Hz, 1H), 7.41 (d, *J* = 8.2 Hz, 1H), 3.70 (s, 6H), 3.48 (s, 2H), 3.06 (s, 3H), 1.84-1.77 (m, 2H), 1.37-1.26 (m, 2H), 0.93 (t, *J* = 7.3 Hz, 3H)

^{13}C NMR (126 MHz, $CDCl_3$): δ (ppm) 171.3, 141.4, 140.5, 136.6, 132.7, 128.6, 125.4, 58.8, 52.7, 44.6, 35.5, 35.5, 18.1, 14.3

IR (neat): ν (cm^{-1}) 3020, 2958, 1725, 1457, 1301, 1213, 1150, 959, 728, 651

HRMS (ESI): Calcd for $C_{16}H_{21}{}^{35}ClNaO_6S$ $[M+Na]^+$: 399.0640, found 399.0640

Rf: 0.12 (pentane/EtOAc 80:20)

Mp: 86-91°C

Dimethyl 2-((5-bromobenzo[d][1,3]dioxol-4-yl)methyl)-2-propylmalonate (2.44r):

From **dimethyl *n*-propylmalonate** and **5-bromo-4-(iodomethyl)benzo[d][1,3]dioxole** using **General procedure G**. **2.44r** was obtained as a colorless solid (790 mg, 2.04 mmol, 83%).

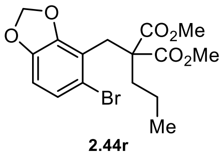

2.44r

$C_{16}H_{19}BrO_6$

M= 387,23 g.mol^{-1}

^{1}H NMR (500 MHz, $CDCl_3$): δ (ppm) 7.03 (d, *J* = 8.3 Hz, 1H), 6.59 (d, *J* = 8.3 Hz, 1H), 5.90 (s, 2H), 3.71 (s, 6H), 3.46 (s, 2H), 1.81-1.71 (m, 2H), 1.36-1.27 (m, 2H), 0.88 (t, *J* = 7.2 Hz, 3H)

^{13}C NMR (126 MHz, $CDCl_3$): δ (ppm) 171.8, 147.9, 146.6, 125.9, 118.8, 117.6, 108.7, 101.4, 58.0, 52.5, 34.8, 33.0, 18.2, 14.4

IR (neat): ν (cm^{-1}) 2959, 2908, 1727, 1451, 1295, 1055, 932, 670

HRMS (ESI): Calcd for $C_{16}H_{19}{}^{79}BrNaO_6$ $[M+Na]^+$: 409.0257, found 409.0255

Rf: 0.21 (pentane/EtOAc 90:10)

Mp: 65-69.5°C

Tetramethyl 2,2'-((2,5-dibromo-1,4-phenylene)bis(methylene))bis(2-propylmalonate) (2.44s):

From **dimethyl *n*-propylmalonate** and **1,4-dibromo-2,5-bis(bromomethyl)benzene** using **General procedure G**. **2.44s** was obtained as a colorless solid (805 mg, 1.32 mmol, 66%).

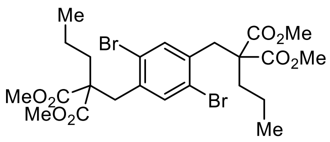

2.44s
$C_{24}H_{32}Br_2O_8$
M= 608,32 g.mol^{-1}

^{1}H NMR (500 MHz, $CDCl_3$): δ (ppm) 7.33 (s, 2H), 3.70 (s, 12H), 3.36 (s, 4H), 1.93-1.68 (m, 4H), 1.42-1.20 (m, 4H), 0.93 (t, *J* = 7.3 Hz, 6H)

^{13}C NMR (126 MHz, $CDCl_3$): δ (ppm) 171.5, 137.1, 135.4, 124.6, 59.1, 52.6, 37.2, 35.3, 18.2, 14.3.

IR (neat): ν (cm^{-1}) 2959, 2872, 1735, 1433, 1213, 1157, 1059, 852, 680

HRMS (ESI): Calcd for $C_{24}H_{32}{}^{79}BrNaO_8$ $[M+Na]^+$: 629.0356, found 629.0360

Rf: 0.32 (pentane/EtOAc 90:10)

Mp: 121-123 °C

Dimethyl 2-(2-bromobenzyl)-2-(2-(dimethylamino)-2-oxoethyl)malonate (2.44t):

From **S4b-Br** and **2-chloro-*N,N*-dimethylacetamide** using **General procedure F**. **2.44t** was obtained as a withe solid (566 mg, 1.47 mmol, 88 %).

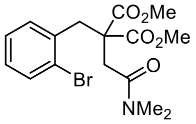

2.44t
$C_{16}H_{20}BrNO_5$
M= 386,24 g.mol^{-1}

^{1}H NMR (500 MHz, $CDCl_3$): δ (ppm) 7.53 (dd, *J* = 8.0, 1.3 Hz, 1H), 7.19 (td, *J* = 7.5, 1.3 Hz, 1H), 7.08 (td, *J* = 7.6, 1.7 Hz, 1H), 7.03 (dd, *J* = 7.7, 1.8 Hz, 1H), 3.76 (s, 6H), 3.71 (s, 2H), 2.92 (s, 3H), 2.90 (s, 3H), 2.88 (s, 2H).

^{13}C NMR (126 MHz, $CDCl_3$): δ (ppm) δ 171.3, 169.7, 136.6, 133.4, 131.9, 128.8, 127.4, 125.9, 56.7, 52.9, 37.7, 37.2, 36.4, 35.6

IR (neat): ν (cm^{-1}) 2951, 1737, 1650, 1433, 1208, 1176, 1034, 767, 658

HRMS (ESI): Calcd for $C_{16}H_{20}{}^{79}BrNNaO_5$ $[M+Na]^+$: 408.0417, found 408.0411

Rf: 0.30 (pentane/EtOAc 50:50)

Mp: 95-99 °C

Dimethyl 2-(2-bromobenzyl)-2-(2-morpholino-2-oxoethyl)malonate (2.44u):

From **S4b-Br** and **2-chloro-1-morpholinoethan-1-one** using **General procedure F**. **2.44u** was obtained as a withe solid (579 mg, 1.47 mmol, 81 %).

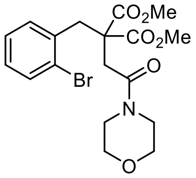

2.44u
$C_{18}H_{22}BrNO_6$
M= 428,28 g.mol^{-1}

^{1}H NMR (500 MHz, $CDCl_3$): δ (ppm) 7.54 (dd, *J* = 8.1, 1.3 Hz, 1H), 7.21 (td, *J* = 7.5, 1.3 Hz, 1H), 7.09 (ddd, *J* = 8.0, 7.4, 1.8 Hz, 1H), 7.04 (dd, *J* = 7.7, 1.7 Hz, 1H), 3.77 (s, 6H), 3.72 (s, 2H), 3.68-3.65 (m, 2H), 3.65-3.61 (m, 2H), 3.59-3.55 (m, 2H), 3.39-3.34 (m, 2H), 2.87 (s, 2H)

^{13}C NMR (126 MHz, $CDCl_3$): δ (ppm) δ 171.2, 168.5, 136.5, 133.5, 131.9, 129.0, 127.5, 126.0, 66.9, 66.4, 56.6, 53.0, 45.8, 42.0, 37.8, 36.0

IR (neat): ν (cm^{-1}) 2864, 1730, 1638, 1441, 1246, 1199, 1034, 848, 777

HRMS (ESI): Calcd for $C_{18}H_{22}{}^{79}BrNNaO_6$ $[M+Na]^+$: 450.0523, found 450.0520

Rf: 0.28 (pentane/EtOAc 50:50)

Mp: 155-160 °C

Dimethyl 2-(2-bromobenzyl)-2-(2-(methoxy(methyl)amino)-2-oxoethyl)malonate (2.44v):

From **S4b-Br** and **2-chloro-*N*-methoxy-*N*-methylacetamide** using **General procedure F**. **2.44v** was obtained as a withe solid (550 mg, 1.37 mmol, 82 %).

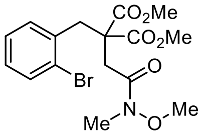

2.44v
$C_{16}H_{20}BrNO_6$
M= 402,24 g.mol^{-1}

^{1}H NMR (500 MHz, $CDCl_3$): δ (ppm) 7.53 (dd, *J* = 7.9, 1.4 Hz, 1H), 7.20 (td, *J* = 7.5, 1.3 Hz, 1H), 7.13-7.04 (m, 2H), 3.76 (s, 6H), 3.71 (s, 2H), 3.61 (s, 3H), 3.16 (s, 3H), 3.07 (s, 2H)

^{13}C NMR (126 MHz, $CDCl_3$): δ (ppm) δ 171.69, 171.1, 136.4, 133.4, 131.9, 128.9, 127.4, 126.1, 61.2, 56.2, 53.0, 37.9, 35.2, 32.4

IR (neat): ν (cm^{-1}) 2951, 1738, 1661, 1431, 1278, 1198, 1175, 880, 765

HRMS (ESI): Calcd for $C_{16}H_{20}{}^{79}BrNNaO_6$ [M+Na]$^+$: 424.0366, found 424.0367

Rf: 0.47 (pentane/EtOAc 50:50)

Mp: 60-69 °C

Dimethyl 2-(2-chloro-4-(methylsulfonyl)benzyl)-2-propylmalonate (2.44w):

From **trimethyl ethane-1,1,2-tricarboxylate** and **1-bromo-2-(bromomethyl)benzene** using **General procedure G**. **2.44w** was obtained as a colorless solid (500 mg, 1.34 mmol, 55%).

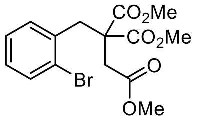

2.44w
$C_{15}H_{17}BrO_6$
M= 372,02 g.mol^{-1}

^{1}H NMR (500 MHz, $CDCl_3$): δ (ppm) 7.57-7.49 (m, 1H), 7.23-7.18 (m, 1H), 7.11-7.06 (m, 2H), 3.76 (s, 6H), 3.67 (s, 3H), 3.65 (s, 2H), 2.93 (s, 2H)

^{13}C NMR (126 MHz, $CDCl_3$): δ (ppm) 171.3, 170.5, 135.7, 133.4, 131.7, 129.0, 127.6, 126.1, 56.5, 53.1, 52.0, 38.0, 36.8

IR (neat): ν (cm^{-1}) 2948, 1755, 1727, 1427, 1226, 1195, 1168, 1038, 767

HRMS (ESI): Calcd for $C_{15}H_{17}{}^{79}BrNaO_6$ [M+Na]$^+$: 395.0101, found 395.0103

Rf: 0.17 (pentane/EtOAc 90:10)

Mp: 67.5-73.3°C

Dimethyl 2-((2-bromopyridin-3-yl)methyl)-2-propylmalonate (2.44x):

According to **general procedure F**, dimethyl 2-((2-bromopyridin-3-yl)methyl)malonate (800 mg, 2.65 mmol, 1.0 eq.) was reacted with *n*-propyliodide (631 mg, 3.71 mmol, 1.4 eq.) to give the title compound (390 mg, 1.13 mmol, 43%) as a yellow oil.

Exact Mass: 343.04

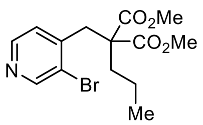

2.44x
$C_{14}H_{18}BrNO_4$
M= 344,20 g.mol^{-1}

^{1}H NMR (500 MHz, $CDCl_3$): δ (ppm) 8.70 (s, 1H), 8.40 (s, 1H), 7.18 (d, *J* = 5.1 Hz, 1H), 3.71 (s, 6H), 3.44 (s, 2H), 1.91 – 1.76 (m, 2H), 1.48 – 1.25 (m, 2H), 0.93 (t, *J* = 7.3 Hz, 3H).

^{13}C NMR (126 MHz, $CDCl_3$): δ (ppm) 171.3, 152.1, 147.8, 146.0, 126.1, 124.8, 58.6, 52.8, 37.7, 35.7, 18.1, 14.3.

GC-MS (EI): Calcd for $C_{14}H_{18}{}^{79}BrO_4$ [M]$^{+\bullet}$: 343, found 343

Dimethyl 2-((3-chloropyridin-4-yl)methyl)-2-propylmalonate (2.44y):

According to **general procedure F**, dimethyl 2-((2-chloropyridin-3-yl)methyl)malonate (1.00 g, 5.43 mmol, 1.0 eq.) was reacted with *n*-propyliodide (791 mg, 4.66 mmol, 1.4 eq.) to give the title compound (600 mg, 2.00 mmol, 52%) as a yellow oil.

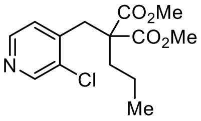

2.44y

$C_{14}H_{18}ClNO_4$

M= 299,75 g.mol^{-1}

^{1}H NMR (500 MHz, $CDCl_3$): δ (ppm) 8.54 (s, 1H), 8.36 (d, *J* = 5.0 Hz, 1H), 7.10 (d, *J* = 5.0 Hz, 1H), 3.71 (s, 6H), 3.41 (s, 2H), 1.83 – 1.78 (m, 2H), 1.29 (ddt, *J* = 14.6, 12.0, 6.0 Hz, 2H), 0.92 (t, *J* = 7.2 Hz, 3H).

^{13}C NMR (126 MHz, $CDCl_3$): δ (ppm) 171.3, 149.8, 147.6, 143.7, 133.3, 125.9, 58.5, 52.7, 35.4, 34.7, 18.0, 14.3.

GC-MS (EI): Calcd for $C_{14}H_{18}{}^{35}ClO_4$ $[M]^{+\bullet}$: 299, found 299

Dimethyl 2-((3-bromopyrazin-2-yl)methyl)-2-propylmalonate (2.44z):

According to **general procedure G**, dimethyl 2-propylmalonate (728 mg, 4.18 mmol, 1.0 eq.) was reacted with 2-(bromomethyl)-3-chloropyrazine (1.04 g, 5.01 mmol, 1.2 eq.) to give the title compound (956 mg, 3.18 mmol, 76 %) as a brown oil.

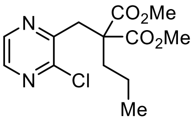

2.44z

$C_{13}H_{17}ClN_2O_4$

M= 345,19 g.mol^{-1}

^{1}H NMR (500 MHz, $CDCl_3$): δ (ppm) 8.35 (d, *J* = 2.5 Hz, 1H), 8.21 (d, *J* = 2.5 Hz, 1H), 3.73 (s, 6H), 3.64 (s, 2H), 1.97 – 1.88 (m, 2H), 1.32 – 1.21 (m, 2H), 0.88 (t, *J* = 7.3 Hz, 3H).

^{13}C NMR (126 MHz, $CDCl_3$): δ (ppm) 171.6, 152.1, 149.4, 141.74, 141.6, 57.0, 52.7, 36.3, 35.1, 18.1, 14.4.

GC-MS (EI): Calcd for $C_{13}H_{17}{}^{35}ClO_4$ $[M]^{+\bullet}$: 300, found 300

Dimethyl 2-((2-chloroquinolin-3-yl)methyl)-2-propylmalonatepropylmalonate (2.44aa):

According to **general procedure G**, dimethyl 2-propylmalonate (650 mg, 4.18 mmol, 1.0 eq.) was reacted with 3-(bromomethyl)-2-chloroquinoline (1.34 g, 5.22 mmol, 1.2 eq.) to give the title compound (897 mg, 2.56 mmol, 69 %) as a brown oil.

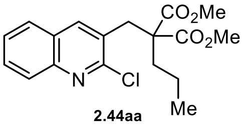

2.44aa

$C_{18}H_{20}ClNO_4$

M= 349,81 g.mol^{-1}

^{1}H NMR (500 MHz, $CDCl_3$): δ (ppm) 8.09 – 7.96 (m, 2H), 7.78 – 7.75 (m, 1H), 7.73 – 7.68 (m, 1H), 7.58 – 7.53 (m, 1H), 3.70 (s, 6H), 3.58 (d, *J* = 12.9 Hz, 2H), 1.99 – 1.84 (m, 2H), 1.44 – 1.28 (m, 2H), 0.96 (t, *J* = 7.3 Hz, 3H).

^{13}C NMR (126 MHz, $CDCl_3$): δ (ppm) 171.5, 152.1, 146.6, 145.9, 140.0, 139.0, 131.4, 130.5, 129.2, 128.3, 128.2, 127.6, 127.5, 127.4, 127.3, 127.3, 127.3, 127.1 59.1, 59.0, 37.6, 36.34, 36.1, 35.6, 18.2, 18.1, 14.4.

GC-MS (EI): Calcd for $C_{18}H_{20}{}^{35}ClO_4$ $[M]^{+\bullet}$: 349, found 349

Dimethyl 2-((2-bromothiophen-3-yl)methyl)-2-propylmalonate (2.44ab):

According to **general procedure F**, dimethyl 2-((2-bromothiophen-3-yl)methyl)malonate (800 mg, 2.60 mmol, 1.0 eq.) was reacted with *n*-propyliodide (619 mg, 3.64 mmol, 1.4 eq.) to give the title compound (717 mg, 2.05mmol, 79%) as a yellow oil.

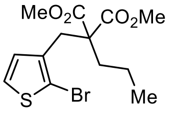

2.44ab

$C_{13}H_{17}BRO_4S$

M= 349,24 g.mol^{-1}

^{1}H NMR (500 MHz, $CDCl_3$): δ (ppm) 7.19 (d, *J* = 5.7 Hz, 1H), 6.64 (d, *J* = 5.7 Hz, 1H), 3.72 (s, 6H), 3.25 (s, 2H), 1.87 – 1.75 (m, 2H), 1.34 – 1.24 (m, 2H), 0.92 (t, *J* = 7.3 Hz, 3H).

^{13}C NMR (126 MHz, $CDCl_3$): δ (ppm) 171.7, 135.9, 128.5, 125.8, 112.3, 58.4, 52.6, 34.7, 32.2, 18.0, 14.4.

GC-MS (EI): Calcd for $C_{17}H_{21}{}^{79}BrO_6$ $[M]^{+\bullet}$: 348, found 348

Dimethyl 2-((3-chlorothiophen-2-yl)methyl)-2-propylmalonate (2.44ac):

According to **general procedure G**, dimethyl 2-propylmalonate (400 mg, 2.30 mmol, 1.0 eq.) was reacted with 2-(bromomethyl)-3-chlorothiophene (584 mg, 2.76 mmol, 1.2 eq.) to give the title compound (510 mg, 1.67 mmol, 73 %) as a brown oil.

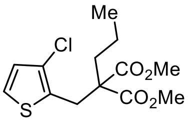

2.44ac

$C_{13}H_{17}ClO_4S$

M= 304,79 g.mol^{-1}

^{1}H NMR (500 MHz, $CDCl_3$): δ (ppm) 7.16 (d, *J* = 5.4 Hz, 1H), 6.85 (d, *J* = 5.4 Hz, 1H), 3.75 (s, 6H), 3.48 (s, 2H), 1.90 – 1.80 (m, 2H), 1.37 – 1.24 (m, 2H), 0.93 (t, *J* = 7.3 Hz, 3H).

^{13}C NMR (126 MHz, $CDCl_3$): δ (ppm) 171.3, 131.0, 127.5, 125.3, 124.3, 58.9, 52.7, 34.4, 30.7, 17.9, 14.3.

GC-MS (EI): Calcd for $C_{13}H_{17}{}^{35}ClO4$ $[M]^{+\bullet}$: 304, found 304

Dimethyl 2-(2-bromo-4-((tert-butyldimethylsilyl)oxy)benzyl)-2-propylmalonate (2.44ad):

According to **general procedure G**, dimethyl 2-propylmalonate (523 mg, 3.00 mmol, 1.0 eq.) was reacted with (4-bromo-3-(bromomethyl)phenoxy)(tert-butyl)dimethylsilane (1.60 g, 4.20 mmol, 1.4 eq.) to give the title compound (1.00 g, 2.11 mmol, 70 %) as a colorless oil.

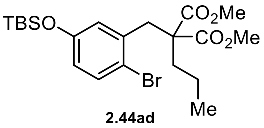

2.44ad

$C_{21}H_{33}BrO_5Si$

M= 473,48 g.mol^{-1}

^{1}H NMR (500 MHz, $CDCl_3$): δ (ppm) 7.35 (d, *J* = 8.7 Hz, 1H), 6.68 (d, *J* = 2.9 Hz, 1H), 6.57 (dd, *J* = 8.6, 2.9 Hz, 1H), 3.70 (s, 6H), 3.40 (s, 2H), 1.89 – 1.78 (m, 2H), 1.34 – 1.25 (m, 2H), 0.96 (s, 9H), 0.91 (t, *J* = 7.3 Hz, 3H), 0.17 (s, 6H).

^{13}C NMR (126 MHz, $CDCl_3$): δ (ppm) 171.8, 154.9, 137.5, 133.6, 123.2, 120.5, 117.3, 59.0, 52.5, 37.9, 35.3, 25.75, 18.2, 14.36, -4.36.

GC-MS (EI): Calcd for $C_{21}H_{33}{}^{79}BrO_6Si$ $[M]^{+\bullet}$: 472, found 472

Dimethyl 2-(2-bromo-4-(dimethylamino)benzyl)-2-propylmalonate (2.44ae):

According to **general procedure F**, dimethyl 2-(2-bromo-4-(dimethylamino)benzyl)malonate (600 mg, 1.74 mmol, 1.0 eq.) was reacted with *n*-propyliodide (355 mg, 2.09 mmol, 1.2 eq.) to give the title compound (580 mg, 1.50 mmol, 86%) as a yellow oil.

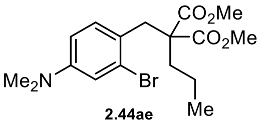

2.44ae

$C_{17}H_{24}BrNO_4$

M= 386,29 g.mol^{-1}

^{1}H NMR (500 MHz, $CDCl_3$): δ (ppm) 6.95 – 6.91 (m, 1H), 6.87 – 6.82 (m, 1H), 6.59 – 6.54 (m, 1H), 3.71 (s, 6H), 3.37 (s, 2H), 2.90 (s, 6H), 1.87 – 1.66 (m, 2H), 1.41 – 1.23 (m, 2H), 0.92 (t, *J* = 7.3 Hz, 3H).

^{13}C NMR (126 MHz, $CDCl_3$): δ (ppm) 172.1, 150.2, 131.4, 126.8, 123.1, 116.3, 111.7, 59.3, 52.4, 40.4, 36.9, 34.7, 18.2, 14.4.

GC-MS (EI): Calcd for $C_{17}H_{24}{}^{79}BrO_4$ $[M]^{+\bullet}$: 385, found 385

Dimethyl 2-(2-bromo-4-methoxybenzyl)-2-propylmalonate (2.44af):

According to **general procedure G**, dimethyl 2-propylmalonate (918 mg, 5.27 mmol, 1.0 eq.) was reacted with 2-bromo-1-(bromomethyl)-4-methoxybenzene (1.77 g, 6.32 mmol, 1.2 eq.) to give the title compound (1.82 g, 4.88 mmol, 93 %) as a colorless oil.

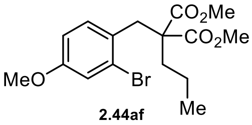

2.44af

$C_{16}H_{21}BrO_5$

M= 373,24 g.mol^{-1}

^{1}H NMR (500 MHz, $CDCl_3$): δ (ppm) 7.07 (d, *J* = 2.7 Hz, 1H), 7.03 (d, *J* = 8.6 Hz, 1H), 6.76 (dd, *J* = 8.6, 2.7 Hz, 1H), 3.76 (s, 3H), 3.70 (s, 6H), 3.40 (s, 2H), 1.85 – 1.76 (m, 2H), 1.36 – 1.24 (m, 2H), 0.92 (t, *J* = 7.3 Hz, 3H).

^{13}C NMR (126 MHz, $CDCl_3$): δ (ppm) 171.9, 158.9, 131.7, 128.2, 126.2, 118.17, 113.7, 59.2, 55.6, 52.5, 37.0, 34.9, 18.2, 14.4.

GC-MS (EI): Calcd for $C_{16}H_{21}{}^{79}BrO_5$ $[M]^{+\bullet}$: 372, found 372

1-(2,2-bis(Methoxymethyl)pentyl)-2-bromobenzene (2.44ag):

DIBAL-H (8.52 g, 10.7 mmol, 6.1 eq.) was slowly added to a solution of dimethyl 2-(2-bromobenzyl)-2-propylmalonate (**2.44c-Br**) (600 mg, 1.75 mmol, 1.0 eq.) in dry CH_2Cl_2 (11 mL) at 0°C. The mixture was stirred over night at 24 °C. The reaction was quenched by the addition of EtOAc at 0°C followed by H_2O and HCl. The aqueous phase was extracted with EtOAC (3X 10 mL) and the combined organic layers were washed with brine and dried over Na_2SO_4. After evaporation of the volatiles, the crude product was added to a suspension of NaH (221 mg. 5.52 mmol, 3.0 eq.) in DMF (3.0 mL) at 0 °C. After stirring for 30 min, MeI (1.05 g, 7.36 mmol, 4.0 eq.) was added and the mixture was stirred overnight at 24 °C. The reaction was quenched with NH_4Cl and extracted with EtOAc (3X 10 mL). The combined organic layers were washed with brine, dried over Na_2SO_4 and the volatiles were evaporated under reduced pressure. After flash column chromatography (Cyclohexane:EtOAc, 90:10) the title compound (398 mg, 1.26 mmol, 69%) was obtained as a colorless oil.

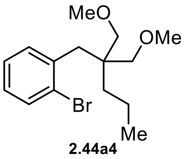

2.44a4

$C_{15}H_{23}BrO_2$

M= 315,25 g.mol^{-1}

^{1}H NMR (500 MHz, $CDCl_3$): δ (ppm) 7.53 (dd, *J* = 8.1, 1.3 Hz, 1H), 7.29 (dd, *J* = 7.7, 1.8 Hz, 1H), 7.21 (td, *J* = 7.5, 1.3 Hz, 1H), 7.04 (td, *J* = 7.7, 1.8 Hz, 1H), 3.31 (s, 6H), 3.26 (d, *J* = 9.2 Hz, 2H), 3.17 (d, *J* = 9.2 Hz, 2H), 2.89 (s, 2H), 1.40 – 1.35 (m, 4H), 1.17 – 0.74 (m, 3H).

^{13}C NMR (126 MHz, $CDCl_3$): δ (ppm) 138.7, 133.0, 132.7, 127.7, 126.9, 126.4, 75.4, 59.1, 43.7, 37.6, 35.9, 16.9, 15.1.

GC-MS (EI): Calcd for $C_{15}H_{23}{}^{79}BrO_2$ $[M]^{+\bullet}$: 314, found 314

Dimethyl 2-(2-bromo-4-fluorobenzyl)-2-ethylmalonate (2.44ah):

From **S4a** and **ethyl iodide** using **General procedure F**. **2.44x** was obtained as a colorless oil (842 mg, 2.42 mmol, 78%).

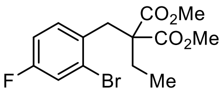

2.44ah

$C_{14}H_{16}BrFO_4$

M= 347,18

^{1}H NMR (400 MHz, $CDCl_3$): δ (ppm) 7.30-7.25 (m, 1H), 7.18 (dd, *J* = 8.7, 6.0 Hz, 1H), 6.94 (ddd, *J* = 8.7, 7.8, 2.7 Hz, 1H), 3.70 (s, 6H), 3.42 (s, 2H), 1.92 (q, *J* = 7.5 Hz, 2H), 0.93 (t, *J* = 7.5 Hz, 3H)

^{13}C NMR (126 MHz, $CDCl_3$): δ (ppm) 171.6, 161.2 (d, *J* = 250.4 Hz), 132.4 (d, *J* = 3.79 Hz) 132.2 (d, *J* = 8.2 Hz), 125.9 (d, *J* = 9.0 Hz), 120.2 (d, *J* = 24.2 Hz), 114.6 (d, *J* = 20.8 Hz), 59.5, 52.5, 36.8, 26.4, 9.4

^{19}F NMR (471 MHz, $CDCl_3$): δ (ppm) -113.7

IR (neat): ν (cm^{-1}) 2952, 1729, 1599, 1487, 1221, 1115, 1032, 879, 778

HRMS (ESI): Calcd for $C_{14}H_{16}{}^{79}BrFNaO_4$ $[M+Na]^+$: 369.0108, found 369.0111

Rf: 0.23 (pentane/EtOAc 95:5)

Dimethyl 2-(2-bromo-4-fluorobenzyl)-2-(ethyl-*d*$_5$)malonate (2.44ah-*d5*):

From **S4a** and **iodoethane-*d*$_5$** using **General procedure F**. **1y** was obtained as a slightly yellow oil (934 mg, 2.65 mmol, 83%).

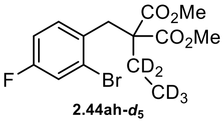

2.44ah-*d*$_5$
$C_{14}H_{11}D_5BrFO_4$
M= 352,21

^{1}H NMR (400 MHz, CDCl$_3$): δ (ppm) 7.27 (dd, *J* = 8.2, 2.6 Hz, 1H), 7.17 (dd, *J* = 8.7, 6.1 Hz, 1H), 6.97-6.90 (m, 1H), 3.70 (s, 6H), 3.41 (s, 2H)

^{13}C NMR (126 MHz, CDCl$_3$): δ (ppm) 171.6, 161.2 (d, *J* = 250.3 Hz), 132.4 (d, *J* = 3.7 Hz), 132.2 (d, *J* = 8.3 Hz), 125.9 (d, *J* = 9.3 Hz), 120.2 (d, *J* = 24.1 Hz), 114.6 (d, *J* = 20.7 Hz), 59.3, 52.5, 36.7, 26.0-25.1 (m), 8.8-7.8 (m)

^{19}F NMR (471 MHz, CDCl$_3$): δ (ppm) -113.7

IR (neat): ν (cm^{-1}) 2953, 1729, 1600, 1488, 1227, 1069, 1033, 882, 859, 831

HRMS (ESI): Calcd for $C_{14}H_{11}{}^{79}BrD5NaO_4$ [M+Na]$^+$: 374.0422, found 374.0424

Rf: 0.23 (pentane/EtOAc 95:5)

Dimethyl 2-(3-(benzyloxy)propyl)-2-((5-bromobenzo[d][1,3]dioxol-4-yl)methyl)malonate) (2.44ai):

According to **general procedure F**, dimethyl 2-(2-bromo-4-(dimethylamino)benzyl)malonate (1.69 g, 4.90 mmol, 1.0 eq.) was reacted with ((3-bromopropoxy)methyl)benzene (1.57 mg, 6.86 mmol, 1.4 eq.) to give the title compound (758 mg, 1.54 mmol, 31.4%) as a yellow oil.

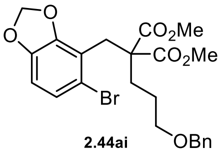

2.44ai
$C_{23}H_{25}BrO_7$
M= 493,35 g.mol^{-1}

^{1}H NMR (500 MHz, CDCl$_3$): δ (ppm) 7.37 – 7.27 (m, 5H), 7.02 (d, *J* = 8.3, 1H), 6.58 (d, *J* = 8.3 Hz, 1H), 5.80 (s, 2H), 4.47 (s, 2H), 3.71 (s, 6H), 3.48 (s, 2H), 3.44 – 3.38 (m, *J* = 6.7 Hz, 2H), 1.91 – 1.82 (m, 2H), 1.65 (p, *J* = 6.7 Hz, 2H).

^{13}C NMR (126 MHz, CDCl$_3$): δ (ppm) 171.7, 147.9, 146.6, 138.7, 128.5, 127.8, 127.7, 125.8, 118.6, 117.5, 108.7, 101.4, 72.9, 70.4, 57.8, 52.6, 33.2, 29.4, 25.3.

GC-MS (EI): Calcd for $C_{23}H_{25}{}^{79}BrO_7$ [M]$^{+\bullet}$: 492, found 492

Dimethyl 2-((5-bromobenzo[d][1,3]dioxol-4-yl)methyl)-2-(3-((tert-butyldimethylsilyl)oxy)propyl)malonate (2.44aj):

According to **general procedure F**, dimethyl 2-(2-bromo-4-(dimethylamino)benzyl)malonate (800 mg, 2.32 mmol, 1.0 eq.) was reacted with (3-bromopropoxy)(tert-butyl)dimethylsilane (831 mg, 2.78 mmol, 1.4 eq.) to give the title compound (804 mg, 1.55 mmol, 67%) as a yellow oil.

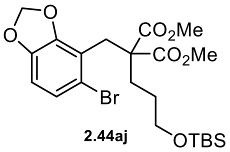

2.44aj
$C_{22}H_{33}BrO_7Si$
M= 517,49 g.mol^{-1}

^{1}H NMR (500 MHz, CDCl$_3$): δ (ppm) 7.03 (d, *J* = 8.3 Hz, 1H), 6.59 (d, *J* = 8.2 Hz, 1H), 5.90 (s, 2H), 3.71 (s, 6H), 3.60 – 3.52 (m, 2H), 3.48 (s, 2H), 1.89 – 1.77 (m, 2H), 1.59 – 1.53 (m, 2H), 0.86 (s, 9H), 0.01 (s, 6H).

^{13}C NMR (126 MHz, CDCl$_3$): δ (ppm) 171.7, 147.9, 146.6, 125.9, 118.7, 117.6, 108.7, 101.4, 63.4, 57.8, 52.5, 33.4, 29.3, 28.3, 26.1, 18.5, -5.2

GC-MS (EI): Calcd for $C_{22}H_{33}{}^{79}BrO_7Si$ [M]$^{+\bullet}$: 516, found 516

6.1.3 Enantioselective C(sp^3)–H arylation

General procedure H: Representative procedure for the asymmetric C(sp^3)–H arylation

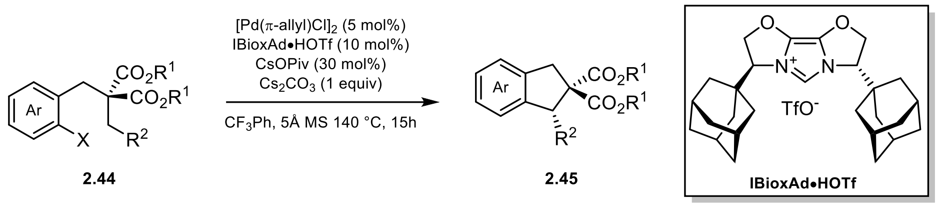

In an 2-5 mL microwave reaction vial, substrate (0.2 mmol) was introduced. Then the tube was transferred in the glovebox and [Pd(π-allyl)Cl]$_2$ (3.7 mg, 10 µmol, 5 mol%), **IBioxAd·HOTf** (11.4 mg, 20 µmol, 10 mol%), cesium pivalate (14 mg, 60 µmol, 30 mol%), caesium carbonate (65 mg, 0.2 mmol, 1 equiv) and 5Å molecular sieves powder (50 mg) were introduced and the vial was then sealed. Outside of the glovebox, *α,α,α*-trifluorotoluene (2 mL) was added. The reaction was stirred at room temperature for 10 min. The vial was then introduced in a 140°C preheated aluminum block and stirred at this temperature for 15 hours. After this period the reaction was cooled to room temperature, diluted with CH_2Cl_2 (1.0 mL), filtered over a pad of Celite (washed three times with 1 mL of CH_2Cl_2). The crude material was analyzed by GC-MS and then concentrated and purified by preparative HPLC chromatography (EtOAc/hexane) to yield the corresponding indane product. Enantiomeric ratios were then determined by HPLC using a chiral stationary phase.

Racemic materials were obtained following the same procedure, using IBioxSpiCy·HOTf as ligand.

Dimethyl (*R*)-1-ethyl-6-fluoro-1,3-dihydro-2*H*-indene-2,2-dicarboxylate (2.45a):

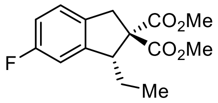

2.45a

$C_{15}H_{17}FO_4$

M= 280,30 g.mol^{-1}

From **2.44a** using **General procedure H**. **2.45a** was obtained as a colorless solid (48.2 mg, 0.172 mmol, 86%).

From **2.44a** (36.1 mg, 0.1mmol, 1.0 equiv) using **General procedure H** and **IBioxtBuMe$_4$** as the ligand. **2.45a** was obtained as a colorless oil (21.8 mg, 78.0 µmol, 78%).

^{1}H NMR (500 MHz, $CDCl_3$): δ (ppm) 7.10 (dd, *J* = 8.2, 5.2 Hz, 1H), 6.91 (dd, *J* = 8.9, 2.4 Hz, 1H), 6.85 (td, *J* = 8.8, 2.5 Hz, 1H), 3.76 (s, 3H), 3.79-3.73 (m, 2H), 3.69 (s, 3H), 3.26 (d, *J* = 16.3 Hz, 1H), 1.62-1.49 (m, 1H), 1.46-1.36 (m, 1H), 0.96 (t, J = 7.4 Hz, 3H)

^{13}C NMR (126 MHz, $CDCl_3$): δ (ppm) 172.2, 170.3, 162.2 (d, *J* = 243.6 Hz), 146.5 (d, *J* = 7.9 Hz), 134.5 (d, *J* = 2.6 Hz), 125.4 (d, *J* = 8.7 Hz), 114.1 (d, *J* = 22.4 Hz), 112.2 (d, *J* = 22.6 Hz), 66.1, 53.1, 52.7, 51.5 (d, *J* = 2.1 Hz), 38.3, 23.9, 11.7

^{19}F NMR (471 MHz, $CDCl_3$): δ (ppm) -116.6

IR (neat): ν (cm^{-1}) 2961, 2928, 1728, 1484, 1437, 1237, 1159, 875

HRMS (ESI): Calcd for $C_{15}H_{17}FNaO_4$ $[M+Na]^+$: 303.1003, found 303.1004

Rf: 0.26 (pentane/EtOAc 95:5)

Mp: 104-107°C

$[\alpha]_D^{20}$: -188.4° (c = 1.16, $CHCl_3$)

HPLC separation: Chiralcel® OD-H; 99.5:0.5 (*n*-heptane/*i*-PrOH), 0.5 ml.min^{-1}, 271 nm, t_R (minor) = 20.5 min, t_R (major) = 23.6 min, 98:2 e.r.

Dimethyl (*R*)-1-methyl-1,3-dihydro-2*H*-indene-2,2-dicarboxylate (2.45b):

From **2.44b** using **General procedure H**. **2.45b** was obtained as a colorless oil (36.7 mg, 0.145 mmol, 74%).

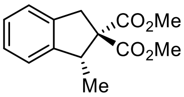

2.45b

$C_{14}H_{16}O_4$

M= 248,28 g.mol^{-1}

^{1}H NMR (400 MHz, $CDCl_3$): δ (ppm) 7.23-7.09 (m, 4H), 4.04 (q, *J* = 7.2 Hz, 1H), 3.80-3.72 (m, 7H), 1.23 (d, *J* = 7.2 Hz, 3H)

^{13}C NMR (101 MHz, $CDCl_3$): δ (ppm) 172.3, 170.9, 145.5, 139.1, 127.2, 127.2, 124.2, 123.5, 64.9, 52.9, 52.5, 45.2, 39.2, 16.7

IR (neat): ν (cm^{-1}) 2956, 1730, 1434, 1243, 1158, 1073, 1047, 754

HRMS (ESI): Calcd for C14H16NaO4 [M+Na]+ : 271.0941, found 271.0945

Rf: 0.28 (pentane/EtOAc 90:10)

[α]$_D$^{20}: -194.9° (c = 1.13, $CHCl_3$)

HPLC separation: Chiralcel® OD-H; 99:1 (*n*-heptane/*i*-PrOH), 0.5 ml.min^{-1}, 266 nm, t_R (minor) = 18.9 min, t_R (major) = 19.8 min, 95:5 e.r.

Dimethyl (*R*)-1-ethyl-1,3-dihydro-2*H*-indene-2,2-dicarboxylate (2.45c):

From **2.44c-Br** using **General procedure H**. **2.45c** was obtained as a colorless oil (38.0 mg, 0.145 mmol, 72%).

From **2.44c-Cl** using **General procedure H**. **2.45c** was obtained as a colorless oil (48.0 mg, 0.145 mmol, 92%).

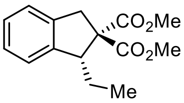

2.45c

$C_{15}H_{18}O_4$

M= 262,31 g.mol^{-1}

^{1}H NMR (400 MHz, $CDCl_3$): δ (ppm) 7.25-7.13 (m, 4H), 3.82 (d, *J* = 16.5 Hz, 1H), 3.80 (dd, *J* = 9.7, 4.9 Hz, 1H), 3.76 (s, 3H), 3.68 (s, 3H), 3.32 (d, *J* = 16.5 Hz, 1H), 1.61-1.48 (m, 1H), 1.47-1.34 (m, 1H), 0.97 (t, *J* = 7.4 Hz, 3H)

^{13}C NMR (101 MHz, $CDCl_3$): δ (ppm) 172.3, 170.7, 144.3, 139.1, 127.2, 126.7, 125.0, 124.5, 65.7, 53.0, 52.6, 51.5, 39.0, 24.1, 11.8

IR (neat): ν (cm^{-1}) 2958, 2933, 1729, 1234, 1152, 1072, 942, 759

HRMS (ESI): Calcd for $C_{15}H_{18}NaO_4$ $[M+Na]^+$: 285.1097, found 285.1103

Rf: 0.32 (pentane/EtOAc 90:10)

[α]$_D$^{20}: -208.3° (c = 1.01, $CHCl_3$)

HPLC separation: Chiralcel® OD-H; 99.5:0.5 (*n*-heptane/*i*-PrOH), 0.5 ml.min^{-1}, 266 nm, t_R (minor) = 19.3 min, t_R (major) = 23.0 min, 98:2 e.r.

Dimethyl (*R*)-1-butyl-1,3-dihydro-2*H*-indene-2,2-dicarboxylate (2.45d):

From **2.44d** using **General procedure H**. **2.45d** was obtained as a colorless oil (35.2 mg, 0.121 mmol, 61%).

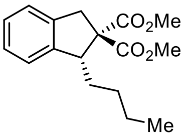

2.45d

$C_{17}H_{22}O_4$

M= 290,36 g.mol^{-1}

^{1}H NMR (500 MHz, $CDCl_3$): δ (ppm) 7.23-7.14 (m, 4H), 3.86 (dd, *J* = 9.1, 4.7 Hz, 1H), 3.81 (d, *J* = 16.4 Hz, 1H), 3.76 (s, 3H), 3.68 (s, 3H), 3.31 (d, *J* = 16.4 Hz, 1H), 1.46-1.24 (m, 6H), 0.87 (t, *J* = 7.0 Hz, 3H).

^{13}C NMR (126 MHz, $CDCl_3$): δ (ppm) 172.2, 170.5, 144.5, 138.9, 127.0, 126.6, 124.8, 124.3, 65.6, 52.8, 52.5, 49.8, 38.9, 30.6, 29.3, 22.8, 13.9.

IR (neat): ν (cm^{-1}): 2954, 2925, 1737, 1459, 1245, 1158, 754

HRMS (ESI): Calcd for $C_{15}H_{17}FNaO_4$ $[M+Na]^+$: 313.1410, found 313.1413

Rf: 0.38 (pentane/EtOAc 90:10)

[α]$_D$^{20}: -181.6° (c = 0.93, $CHCl_3$)

HPLC separation: Chiralcel® OD-H; 99.5:0.5 (*n*-heptane/*i*-PrOH), 0.5 ml.min^{-1}, 266 nm, t_R (minor) = 15.8 min, t_R (major) = 18.5 min, 98:2 e.r.

Dimethyl (*R*)-1-isobutyl-1,3-dihydro-2*H*-indene-2,2-dicarboxylate (2.45e):

From **2.44e** using **General procedure H**. **2.45e** was obtained as a colorless oil (38.5 mg, 0.133 mmol, 66%).

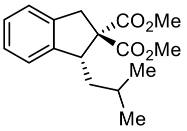

2.45e
$C_{17}H_{22}O_4$
M= 290,36 g.mol^{-1}

^{1}H NMR (500 MHz, $CDCl_3$): δ (ppm) 7.21-7.13 (m, 4H), 3.96 (dd, *J* = 10.4, 4.8 Hz, 1H), 3.79 (d, *J* = 16.4 Hz, 1H), 3.75 (s, 3H), 3.68 (s, 3H), 3.31 (d, *J* = 16.4 Hz, 1H), 1.76-1.67 (m, 1H), 1.16 (ddd, *J* = 13.2, 9.5, 4.8 Hz, 1H), 1.04 (d, *J* = 6.5 Hz, 3H), 0.89 (d, *J* = 6.5 Hz, 3H).

^{13}C NMR (126 MHz, $CDCl_3$): δ (ppm) 172.3, 170.7, 144.9, 139.0, 127.1, 126.8, 124.7, 124.5, 65.8, 53.0, 52.6, 47.8, 40.1, 39.0, 25.7, 23.9, 21.7.

IR (neat): ν (cm^{-1}): 2955, 2923, 2364, 1737, 1460, 1246, 753.

HRMS (ESI): Calcd for $C_{17}H_{22}NaO_4$ $[M+Na]^+$: 313.1410, found 313.1417

Rf: 0.45 (pentane/EtOAc 90:10)

$[\alpha]_D^{20}$: -169.3° (c = 0.94, $CHCl_3$)

HPLC separation: Chiralcel® OD-H; 99.5:0.5 (*n*-heptane/*i*-PrOH), 0.5 ml.min^{-1}, 266 nm, t_R (minor) = 14.8 min, t_R (major) = 19.7 min, 98:2 e.r.

Dimethyl (*R*)-1-(2-fluoroethyl)-1,3-dihydro-2*H*-indene-2,2-dicarboxylate (2.45f):

From **2.44f** using **General procedure H**. **2.45f** was obtained as a colorless oil (51.0 mg, 0.182 mmol, 91%).

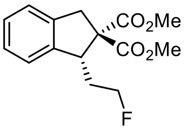

2.45f
$C_{15}H_{17}FO_4$
M= 280,30 g.mol^{-1}

^{1}H NMR (400 MHz, $CDCl_3$): δ (ppm) 7.25-7.16 (m, 4H), 4.53 (ddd, *J* = 47.0, 7.4, 5.0 Hz, 2H), 4.09 (dd, *J* = 9.8, 5.3 Hz, 1H), 3.79 (d, *J* = 16.5 Hz, 1H), 3.77 (s, 3H), 3.70 (s, 3H), 3.36 (d, *J* = 16.5 Hz, 1H), 2.05-1.88 (m, 1H), 1.86-1.65 (m, 1H)

^{13}C NMR (101 MHz, $CDCl_3$): δ (ppm) 171.9, 170.4, 143.0, 139.1, 127.6, 127.1, 124.8 (d, *J* = 1.2 Hz), 124.7, 81.7 (d, *J* = 165.4 Hz), 65.4, 53.1, 52.8, 46.0 (d, *J* = 5.8 Hz), 39.0, 31.3 (d, *J* = 20.1 Hz)

^{19}F NMR (376 MHz, $CDCl_3$): δ (ppm) -219.9

IR (neat): ν (cm^{-1}) 2962, 1736, 1713, 1438, 1241, 1071, 940, 873, 698, 649

HRMS (ESI): Calcd for $C_{15}H_{17}FNaO_4$ $[M+Na]^+$: 303.1003, found 303.1008

Rf: 0.19 (pentane/EtOAc 90:10)

Mp: 72-74°C

$[\alpha]_D^{20}$: -176.6° (c = 1.99, $CHCl_3$)

HPLC separation: Chiralcel® OD-H; 99:1 (*n*-heptane/*i*-PrOH), 0.5 ml.min^{-1}, 211 nm, t_R (minor) = 22.5 min, t_R (major) = 27.8 min, 98:2 e.r.

Dimethyl (R)-1-(2-methoxy-2-oxoethyl)-1,3-dihydro-2H-indene-2,2-dicarboxylate (2.45g):

From **2.44g** using **General procedure H**. **2.45g** was obtained as a colorless oil (30.7 mg, 0.096 mmol, 48%).

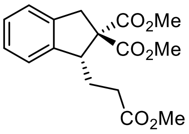

2.45g
$C_{17}H_{20}O_6$
M= 320,34 g.mol^{-1}

^{1}H NMR (500 MHz, $CDCl_3$): δ (ppm) 7.22-7.15(m, 4H), 3.92 (dd, J = 8.6, 6.1 Hz, 1H), 3.81 (d, J = 16.5 Hz, 1H), 3.77 (s, 3H), 3.69 (s, 3H), 3.66 (s, 3H), 3.32 (d, J = 16.5 Hz, 1H), 2.50 - 2.33 (m, 2H), 1.88-1.74 (m, 2H)

^{13}C NMR (126 MHz, $CDCl_3$): δ (ppm) 173.5, 171.9, 170.3, 143.2, 139.0, 127.4, 126.9, 124.5, 124.5, 65.3, 52.9, 52.7, 49.0, 39.1, 31.6, 26.1

IR (neat): ν (cm^{-1}): 3022, 2954, 1732, 1436, 1215, 749, 668

HRMS (ESI): Calcd for $C_{17}H_{20}NaO_6$ $[M+Na]^+$: 343.1152, found 343.1153

Rf: 0.19 (pentane/EtOAc 90:10)

$[\alpha]_D^{20}$: -158.3° (c = 0.975, $CHCl_3$)

HPLC separation: Chiralcel® OD-H; 98:2 (*n*-heptane/*i*-PrOH), 0.5 ml.min^{-1}, 273 nm, t_R (major) = 34.6 min, t_R (minor) = 38.4 min, 98:2 e.r.

Dimethyl (*R*)-1-(2-(4-methoxyphenoxy)ethyl)-1,3-dihydro-2*H*-indene-2,2-dicarboxylate (2.45h):

From **1h** using **General procedure H**. **2h** was obtained as a colorless oil (45.0 mg, 0.117 mmol, 59 %).

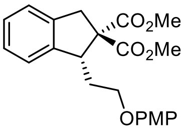

2.45
$C_{22}H_{24}O_6$
M= 384.43 g.mol^{-1}

^{1}H NMR (500 MHz, $CDCl_3$): δ (ppm) 7.22-7.11 (m, 4H), 6.89-6.81 (m, 4H), 4.20 (dd, J = 10.1, 5.1 Hz, 1H), 4.01-3.91 (m, 2H), 3.83 (d, J = 16.5 Hz, 1H), 3.78 (s, 3H), 3.76 (s, 3H), 3.69 (s, 3H), 3.37 (d, J = 16.5 Hz, 1H), 2.05-197 (m, 1H), 1.84-1.76 (m, 1H)

^{13}C NMR (126 MHz, $CDCl_3$): δ (ppm) 172.1, 170.5, 154.0, 153.0, 143.4, 139.1, 127.4, 127.0, 124.9, 124.6, 115.6, 114.8, 65. 8, 65.5, 55.9, 53.1, 52.8, 46.7, 39.0, 30.3

IR (neat): ν (cm^{-1}): 2960, 2866, 1585, 1505, 1473, 1319, 1270, 825, 757, 687

HRMS (ESI): Calcd for $C_{22}H_{24}NaO_6$ $[M+Na]^+$: 407.1465, found 407.1469

Rf: 0.41 (pentane/EtOAc 90:10)

$[\alpha]_D^{20}$: -156.7° (c = 0.30, $CHCl_3$)

HPLC separation: Chiralcel® OD-H; 95:5 (*n*-heptane/*i*-PrOH), 1.0 ml.min^{-1}, 218 nm, t_R (minor) = 10.4 min, t_R (major) = 11.7 min, >99:1 e.r.

Dimethyl (*R*)-1-(3-((tert-butyldimethylsilyl)oxy)propyl)-1,3-dihydro-2*H*-indene-2,2-dicarboxylate (2.45i):

From **2.44i** using **General procedure H**. **2.45i** was obtained as a colorless oil (62.2 mg, 0.153 mmol, 77 %).

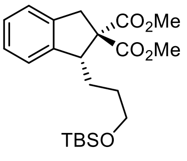

2.45i
$C_{22}H_{34}O_5Si$
M= 406.59 g.mol^{-1}

^{1}H NMR (500 MHz, $CDCl_3$): δ (ppm) 7.23-7.12 (m, 4H), 3.89 (dd, J = 9.9, 4.4 Hz, 1H), 3.82 (d, J = 16.5 Hz, 1H), 3.75 (s, 3H), 3.68 (s, 3H), 3.63-3.58 (m, 1H), 3.58-3.52 (m,1H), 3.31 (d, J = 16.5 Hz, 1H), 1.68-1.50 (m, 3H), 1.45-1.36 (m, 1H), 0.87 (s, 9H), 0.02 (s, 3H), 0.02 (s, 3H).

^{13}C NMR (126 MHz, $CDCl_3$): δ (ppm) 172.3, 170.6, 144.4, 139.1, 127.2, 126.8, 125.0, 124.5, 65.7, 63.1, 52.6, 49.8, 39.0, 30.5, 27.4, 26.1, 18.5, -5.2

IR (neat): ν (cm^{-1}): 2953, 2927, 1738, 1460, 1247, 1215, 836, 751, 668

HRMS (ESI): Calcd for $C_{22}H_{34}NaO_5Si$ $[M+Na]^+$: 429.2068, found 429.2074

Rf: 0.36 (pentane/EtOAc 90:10)

$[\alpha]_D^{20}$: -130.0° (c = 0.91, $CHCl_3$)

HPLC separation: Chiralcel® OD-H; 99.5:0.5 (*n*-heptane/*i*-PrOH), 0.5 ml.min^{-1}, 266 nm, t_R (minor) = 13.2 min, t_R (major) = 14.0 min, 98:2 e.r.

Dimethyl (*R*)-1-(2-(1,3-dioxoisoindolin-2-yl)ethyl)-6-fluoro-1,3-dihydro-2*H*-indene-2,2-dicarboxylate (2.45j):

From **2.44j** using **General procedure H**. **2.45j** was obtained as a colorless oil (69.4 mg, 0.163 mmol, 82 %).

2 mmol scale: **2.44j** (1.01 g, 2.00 mmol, 1.0 equiv) was charged In a 100 mL ACE high pressure flask and the flask was transferred into the glovebox. Then, [Pd(π-All)Cl]$_2$ (37.3 mg, 0.100 mmol, 5 mol%), **IBioxAd·HOTf** (114 mg, 0.200 mmol, 10 mol%), cesium pivalate (140 mg, 0.600 mmol, 30 mol%), caesium carbonate (650 mg, 2.00 mmol, 1 equiv), 5Å molecular sieves powder (500 mg) and *α*,*α*,*α*-trifluorotoluene (20 mL) were added. Outside the glovebox the mixture was heated at 140 °C for 18 h. The reaction mixture was allowed to cool down to room temperature, filtered over a pad of celite and the volatiles were evaporated under reduced pressure. The crude solid residue recrystallized from EtOAc/*n*-hexane yielding **2.45j** (530 mg, 1.25 mmol, 62 %) as a colorless crystalline solid.

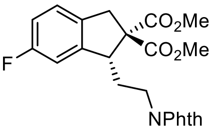

2.45j
$C_{23}H_{20}FNO_6$
M= 425.41 g.mol^{-1}

^{1}H NMR (500 MHz, CDCl$_3$): δ (ppm) 7.88-7.82 (m, 2H), 7.74-7.69 (m, 2H), 7.16 -7.10 (m, 2H), 6.88 (td, *J* = 8.7, 2.4 Hz, 1H), 3.94-3.86 (m, 2H), 3.79 (s, 3H), 3.78-3.74 (m, 1H), 3.71 (d, *J* = 16.3 Hz 1H), 3.69 (s, 3H), 3.28 (d, *J* = 16.3 Hz, 1H), 1.98-1.82 (m, 2H)

^{13}C NMR (126 MHz, CDCl$_3$): δ (ppm) 171.8, 170.2, 168.4, 162.5 (d, *J* = 244.1 Hz), 145.5 (d, *J* = 7.9 Hz), 134.54 (d, *J* = 2.6 Hz), 134.13, 132.25, 125.6 (d, *J* = 8.7 Hz), 123.4, 114.5 (d, *J* = 22.5 Hz), 111.8 (d, *J* = 23.0 Hz), 65.8, 53.1, 53.0, 47.8 (d, *J* = 2.3 Hz), 38.7, 36.4, 29.8

^{19}F NMR (471 MHz, CDCl$_3$): δ (ppm) -115.6

IR (neat): ν (cm^{-1}): 2954, 2925, 2364, 2342, 1713, 1215, 746, 669

HRMS (ESI): Calcd for $C_{23}H_{20}FNaO_6$ [M+Na]$^+$: 448.1167, found 448.1174

Rf: 0.20 (pentane/EtOAc 80:20)

Mp: 149.8-150.7 °C

$[\alpha]_D^{20}$: -124.6° (c = 0.24, CHCl$_3$)

HPLC separation: Chiralcel® IA; 95:5 (*n*-heptane/*i*-PrOH), 1.0 ml.min^{-1}, 233 nm, t_R (minor) = 22.2 min, t_R (major) = 28.0 min, 98:2 e.r.

Diethyl (R)-1-ethyl-1,3-dihydro-2H-indene-2,2-dicarboxylate (2.45k):

From **2.44k** using **General procedure H**. **2.45k** was obtained as a colorless oil (41.4 mg, 0.143 mmol, 71 %).

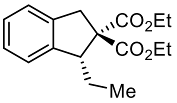

2.45k
$C_{17}H_{22}O_4$
M= 290.36 g.mol^{-1}

^{1}H NMR (500 MHz, CDCl$_3$): δ (ppm) 7.25-7.19 (m, 1H), 7.19-7.13 (m, 3H), 4.28 (dq, *J* = 10.8, 7.1 Hz, 1H), 4.23-4.13 (m, 2H), 4.08 (dq, *J* = 10.8, 7.1 Hz, 1H), 3.82 (d, *J* = 16.6 Hz, 1H), 3.80-377 m (1H), 3.29 (d, *J* = 16.6 Hz, 1H) 1.63-1.52 (m, 1H), 1.48-1.37 (m,1H), 1.28 (t, *J* = 7.1 Hz, 3H), 1.20 (t, *J* = 7.1 Hz, 3H), 0.97 (t, *J* = 7.4 Hz, 3H)

^{13}C NMR (126 MHz, CDCl$_3$): δ (ppm) 171.9, 170.3, 144.5, 139.2, 127.1, 126.6, 125.0, 124.5, 65.7, 61.6, 61.5, 51.3, 39.1, 24.0, 14.3, 14.1, 11.9

IR (neat): ν (cm^{-1}): 2961, 2926, 2363, 2340, 1733, 1461, 1247, 1155, 750

HRMS (ESI): Calcd for $C_{15}H_{17}FNaO_4$ [M+Na]$^+$: 313.1410, found 313.1412

Rf: 0.34 (pentane/EtOAc 93:7)

[α]$_D$^{20}: -164.4° (c = 0.70, $CHCl_3$)

HPLC separation: Chiralcel® OD-H; 99.5:0.5 (*n*-heptane/*i*-PrOH), 0.5 ml.min^{-1}, 272 nm, t_R (minor) = 10.4 min, t_R (major) = 16.7 min, 98:2 e.r.

Diisopropyl (*R*)-1-ethyl-1,3-dihydro-2*H*-indene-2,2-dicarboxylate (2.45l):

From **2.44l** using **General procedure H**. **2.45l** was obtained as a colorless oil (21.6 mg, 0.068 mmol, 34 %).

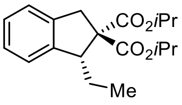

2.45l

$C_{19}H_{26}O_4$

M= 318.41 g.mol^{-1}

^{1}H NMR (500 MHz, $CDCl_3$): δ (ppm) 7.23-7.19 (m, 1H), 7.19-7.12 (m, 3H), 5.09 (hept, *J* = 6.3 Hz, 1H), 4.96 (hept, *J* = 6.3 Hz, 1H), 3.80 (d, *J* = 16.4 Hz, 1H), 3.78-3.74 (m, 1H) 3.24 (d, *J* = 16.4 Hz, 1H), 1.65-1.55 (m, 1H), 1.49-1.39 (m, 1H), 1.28 (d, *J* = 6.3 Hz, 3H), 1.25 (d, *J* = 6.3 Hz, 3H), 1.19 (d, *J* = 4.4 Hz, 3H), 1.17 (d, *J* = 4.4 Hz, 3H), 0.97 (t, *J* = 7.4 Hz, 3H)

^{13}C NMR (126 MHz, $CDCl_3$): δ (ppm) 171.4, 169.8, 144.7, 139.3, 127.0, 126.6, 124.9, 124.4, 69.1, 68.9, 65.6, 51.2, 39.3, 23.9, 21.9, 21.8, 21.7, 21.6, 11.9

IR (neat): ν (cm^{-1}): 3024, 2981, 2878, 1725, 1462, 1375, 1253, 1103, 750, 667

HRMS (ESI): Calcd for $C_{19}H_{26}NaO_4$ $[M+Na]^+$: 341.1723, found 341.1727

Rf: 0.55 (pentane/EtOAc 90:10)

[α]$_D$^{20}: -160.1° (c = 1.00, $CHCl_3$)

HPLC separation: Chiralcel® OD-H; 99.5:0.5 (*n*-heptane/*i*-PrOH), 0.5 ml.min^{-1}, 213 nm, t_R (minor) = 10.4 min, t_R (major) = 10.8 min, 98:2 e.r.

Dimethyl (*R*)-1-ethyl-5-fluoro-1,3-dihydro-2*H*-indene-2,2-dicarboxylate (2.45m):

From **2.44m** using **General procedure H**. **2.45m** was obtained as a colorless oil (40.0 mg, 0.143 mmol, 71%).

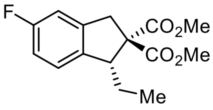

2m

$C_{15}H_{17}FO_4$

M= 280,30 g.mol^{-1}

^{1}H NMR (500 MHz, $CDCl_3$): δ (ppm) 7.15 (dd, *J* = 8.2, 5.1 Hz, 1H), 6.92 – 6.81 (m, 2H), 3.80 (d, *J* = 16.7 Hz, 1H), 3.76 (s, 3H), 3.76 – 3.73 (m, 1H), 3.69 (s, 3H), 3.29 (d, *J* = 16.7 Hz, 1H), 1.56 – 1.48 (m, 1H), 1.44 – 1.32 (m, 1H), 0.95 (t, *J* = 7.4 Hz, 3H)

^{13}C NMR (126 MHz, $CDCl_3$): δ (ppm) 172.1, 170.3, 162.5 (d, *J* = 243.8 Hz), 141.3 (d, *J* = 8.5 Hz), 139.7 (d, *J* = 2.6 Hz), 126.0 (d, *J* = 8.7 Hz), 113.6 (d, *J* = 22.3 Hz), 111.7 (d, *J* = 22.5 Hz), 66.0, 53.08, 52.7, 50.7, 39.0 (d, *J* = 2.2 Hz), 24.1, 11.7

^{19}F NMR (471 MHz, $CDCl_3$): δ (ppm) -116.3

IR (neat): ν (cm^{-1}) 2955, 2925, 2363, 1736, 1487, 1215, 747, 669

HRMS (ESI): Calcd for $C_{15}H_{17}FNaO_4$ $[M+Na]^+$: 303.1003, found 303.1008

Rf: 0.36 (pentane/EtOAc 90:10)

[α]$_D$^{20}: -136.3° (c = 0.89, $CHCl_3$)

HPLC separation: Chiralcel® OD-H; 99.5:0.5 (*n*-heptane/*i*-PrOH), 0.5 ml.min^{-1}, 276 nm, t_R (minor) = 18.5 min, t_R (major) = 21.8 min, 98:2 e.r.

Dimethyl (*R*)-1-ethyl-5-nitro-1,3-dihydro-2*H*-indene-2,2-dicarboxylate (2.45n):

From **2.44n** using **General procedure H**. **2.45n** was obtained as a colorless oil (37.5 mg, 0.122 mmol, 61%). From **1n** (38.8 mg, 0.1mmol, 1.0 equiv) using **General procedure H** and **IBioxtBuMe$_4$** as the ligand. **2.45n** was obtained as a colorless oil (22.1 mg, 72.0 µmol, 72%).

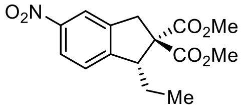

2.45n
$C_{15}H_{17}NO_6$
M= 307,30 g.mol^{-1}

^{1}H NMR (400 MHz, $CDCl_3$): δ (ppm) 8.07 (dd, *J* = 8.3, 2.1 Hz, 1H), 8.04 (s, 1H), 7.35 (d, *J* = 8.3 Hz, 1H), 3.87 (d, *J* = 16.8 Hz, 1H), 3.86 (dd, *J* = 9.6, 5.0 Hz, 1H), 3.78 (s, 3H), 3.70 (s, 3H), 3.39 (d, *J* = 16.8 Hz, 1H), 1.68-1.53 (m, 1H), 1.53-1.37 (m, 1H), 0.97 (t, *J* = 7.4 Hz, 3H)

^{13}C NMR (126 MHz, $CDCl_3$): δ (ppm) 171.6, 169.8, 152.1, 147.8, 141.0, 125.4, 122.7, 119.9, 65.6, 53.3, 52.9, 51.4, 38.7, 23.7, 11.7

IR (neat): ν (cm^{-1}) 2955, 2879, 1728, 1522, 1430, 1341, 1248, 1216, 1158, 1086, 1056, 859, 751

HRMS (ESI): Calcd for $C_{15}H_{17}NNaO_6$ $[M+Na]^+$: 330.0948, found 330.0946

Rf: 0.22 (pentane/EtOAc 93:7)

$[\alpha]_D^{20}$: -185.3° (c = 1.07, $CHCl_3$)

HPLC separation: Chiralcel® OD-H; 95:5 (*n*-heptane/*i*-PrOH), 0.5 ml.min^{-1}, 295 nm, t_R (minor) = 19.9 min, t_R (major) = 23.8 min, 94:6 e.r.

HPLC separation (with **IBiox*t*BuMe$_4$**): Chiralcel® OD-H; 95:5 (*n*-heptane/*i*-PrOH), 0.5 ml.min^{-1}, 295 nm, t_R (minor) = 20.3 min, t_R (major) = 23.9 min, 98:2 e.r.

Dimethyl (*R*)-1-ethyl-5-(trifluoromethyl)-1,3-dihydro-2*H*-indene-2,2-dicarboxylate (2.45o):

From **2.44o** using **General procedure H**. **2.45o** was obtained as a colorless oil (62.2 mg, 0.190 mmol, 95%).

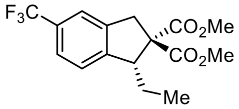

2.45o
$C_{16}H_{17}F_3O_4$
M= 330,30 g.mol^{-1}

^{1}H NMR (500 MHz, $CDCl_3$): δ (ppm) 7.44 (d, *J* = 8.5 Hz, 1H), 7.43 (s, 1H) 7.32 (d, *J* = 8.5 Hz, 1H), 3.85 (d, *J* = 16.8 Hz, 1H), 3.84 (dd, *J* = 9.8, 4.9 Hz, 1H), 3.78 (s, 3H), 3.69 (s, 3H), 3.36 (d, *J* = 16.8 Hz, 1H), 1.63-1.51 (m, 1H), 1.48-1.36 (m, 1H), 0.97 (t, *J* = 7.4 Hz, 3H)

^{13}C NMR (126 MHz, $CDCl_3$): δ (ppm) 171.9, 170.1, 148.4, 140.0, 129.7 (q, *J* = 32.1 Hz), 125.2, 124.5 (q, *J* = 272.0 Hz), 124.0 (q, *J* = 3.8 Hz), 121.5 (q, *J* = 3.7 Hz), 65.6, 53.2, 52.8, 51.4, 38.8, 23.8, 11.7

^{19}F NMR (471 MHz, $CDCl_3$): δ (ppm) -62.1

IR (neat): ν (cm^{-1}) 2975, 2877, 1731, 1436, 1327, 1252, 1153, 1114, 1065, 834

HRMS (ESI): Calcd for $C_{16}H_{17}F_3NaO_4$ $[M+Na]^+$: 353.0971, found 353.0973

Rf: 0.28 (pentane/EtOAc 95:5)

$[\alpha]_D^{20}$: -161.2° (c = 1.23, $CHCl_3$)

HPLC separation: Chiralcel® OD-H; 99.5:0.5 (*n*-heptane/*i*-PrOH), 0.5 ml.min^{-1}, 214 nm, t_R (minor) = 16.3 min, t_R (major) = 18.6 min, 98:2 e.r.

Trimethyl (*R*)-3-ethyl-1,3-dihydro-2*H*-indene-2,2,5-tricarboxylate (2.45p):

From **2.44p** using **General procedure H**. **2.45p** was obtained as a colorless oil (57.1 mg, 0.178 mmol, 89%).

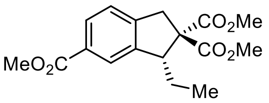

2.45p

$C_{17}H_{20}O_6$

M= 320,34 g.mol^{-1}

^{1}H NMR (500 MHz, $CDCl_3$): δ (ppm) 7.88 (s, 1H), 7.88 (d, J = 8.3 Hz, 1H), 7.24 (d, J = 8.3 Hz, 1H), 3.89 (s, 3H), 3.84 (d, J = 17.0 Hz, 1H), 3.83 (dd, J = 9.7, 5.0 Hz, 1H), 3.76 (s, 3H), 3.68 (s, 3H), 3.35 (d, J = 17.1 Hz, 1H), 1.63-1.52 (m, 1H), 1.50-1.37 (m, 1H), 0.98 (t, J = 7.4 Hz, 3H)

^{13}C NMR (126 MHz, $CDCl_3$): δ (ppm) 172.0, 170.3, 167.3, 144.8, 144.7, 129.1, 129.0, 126.1, 124.5, 65.6, 53.1, 52.7, 52.2, 51.2, 39.2, 24.0, 11.8

IR (neat): ν (cm^{-1}) 2970, 2929, 2856, 1728, 1719, 1437, 1256, 1161, 1098, 866, 759

HRMS (ESI): Calcd for $C_{17}H_{20}NaO_6$ $[M+Na]^+$: 343.1152, found 343.1158

Rf: 0.25 (pentane/EtOAc 90:10)

$[\alpha]_D^{20}$: -169.2° (c = 1.22, $CHCl_3$)

HPLC separation: Chiralcel® OD-H; 90:10 (*n*-heptane/*i*-PrOH), 0.1 ml.min^{-1}, 204 nm, t_R (minor) = 6.7 min, t_R (major) = 8.4 min, 99:1 e.r.

Dimethyl (*R*)-1-ethyl-6-(methylsulfonyl)-1,3-dihydro-*2H*-indene-2,2-dicarboxylate (2.45q):

From **2.44q** using **General procedure H**. **2.45q** was obtained as a colorless oil (43.2 mg, 0.127 mmol, 64%).

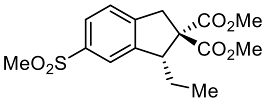

2.45q

$C_{16}H_{20}O_6S$

M= 340,39 g.mol^{-1}

^{1}H NMR (500 MHz, $CDCl_3$): δ (ppm) 7.88-7.69 (m, 2H), 7.40-7.35 (m 1H), 3.91-3.84 (m, 2H), 3.78 (s, 3H), 3.70 (s, 3H), 3.39 (d, J = 17.2 Hz, 1H), 3.04 (s, 3H), 1.65-1.57 (m, 1H), 1.51-1.40 (m, 1H), 0.98 (t, J = 7.4 Hz, 3H)

^{13}C NMR (126 MHz, $CDCl_3$): δ (ppm) 171.7, 169.9, 146.0, 139.4, 126.9, 125.4, 123.8, 65.5, 53.2, 52.9, 51.3, 44.8, 39.2, 23.9, 11.8

IR (neat): ν (cm^{-1}) 2959, 2360, 1734, 1436, 1304, 1255, 1142, 1071, 962, 765

HRMS (ESI): Calcd for $C_{16}H_{20}NaO_6S$ $[M+Na]^+$: 363.0873, found 363.0878

Rf: 0.20 (pentane/EtOAc 80:20)

$[\alpha]_D^{20}$: -116.1° (c = 0.89, $CHCl_3$)

HPLC separation: Chiralcel® AD-H; 95:5 (*n*-heptane/*i*-PrOH), 0.5 ml.min^{-1}, 210 nm, t_R (minor) = 56.9 min, t_R (major) = 63.0 min, 97:3 e.r.

Dimethyl (*R*)-6-ethyl-6,8-dihydro-7*H*-indeno[4,5-d][1,3]dioxole-7,7-dicarboxylate (2.45r):

From **2.44r** using **General procedure H**. **2.45r** was obtained as a colorless oil (31.4 mg, 0.103 mmol, 51%).

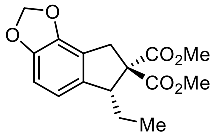

2.45r

$C_{16}H_{18}O_6$

M= 306,31 g.mol^{-1}

^{1}H NMR (500 MHz, $CDCl_3$): δ (ppm) 6.68 (d, J = 7.9 Hz, 1H), 6.65 (d, J = 7.9 Hz, 1H), 5.94-5.91 (m, 2H), 3.77 (s, 3H), 3.73-3.69 (m, 2H), 3.69 (s, 3H), 3.32 (d, J = 16.7 Hz, 1H), 1.54-144 (m, 1H), 1.41-1.29 (m, 1H), 0.94 (t, J = 7.4 Hz, 3H)

^{13}C NMR (126 MHz, $CDCl_3$): δ (ppm) 172.0, 170.3, 147.0, 143.2, 139.4, 119.5, 117.5, 107.0, 101.1, 66.3, 53.1, 52.7, 51.1, 34.9, 24.3, 11.7.

IR (neat): ν (cm^{-1}) 3020, 2975, 1737, 1655, 1215, 751, 670, 631

HRMS (ESI): Calcd for $C_{16}H_{18}NaO_6$ $[M+Na]^+$: 329.0996, found 329.0997

Rf: 0.39 (pentane/EtOAc 90:10)

[α]$_D$^{20}: -133.4° (c = 0.99, $CHCl_3$)

HPLC separation: Chiralcel® OD-H; 95:5 (*n*-heptane/*i*-PrOH), 1.0 ml.min^{-1}, 207 nm, t_R (major) = 8.7 min, t_R (minor) = 17.2 min, 98:2 e.r.

Tetramethyl (1*R*,5*R*)-1,5-diethyl-5,7-dihydro-s-indacene-2,2,6,6(1*H*,3*H*)-tetracarboxylate (2.45s):

From **2.44s** following **General procedure H with** [Pd(π-All)Cl]$_2$ (7.46 mg, 20.0 μmol, 10 mol%), **IBioxAd·HOTf** (22.8 mg, 40.0 μmol, 20 mol%), cesium pivalate (28.0 mg, 120 μmol, 60 mol%), caesium carbonate (130 mg, 0.4 mmol, 2.0 equiv) and 5Å molecular sieves powder (50 mg). **2.45s** was obtained as a colorless solid (49.1 mg, 0.110 mmol, 55%).

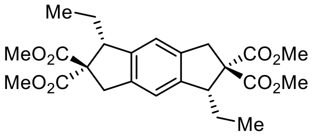

2.45s
$C_{24}H_{30}O_8$
M= 446,50 g.mol^{-1}

^{1}H NMR (500 MHz, $CDCl_3$): δ (ppm) 6.99 (s, 2H), 3.78 (d, *J* = 15.8 Hz, 2H), 3.75 (s, 6H), 3.71 (dd, *J* = 9.8, 4.8 Hz, 2H), 3.67 (s, 26), 3.24 (d, *J* = 15.8 Hz, 6H), 1.54-1.45 (m, 2H), 1.44-1.33 (m, 2H), 0.95 (t, *J* = 7.4 Hz, 6H)

^{13}C NMR (126 MHz, $CDCl_3$): δ (ppm) 172.3, 170.7, 143.2, 137.5, 121.0, 65.9, 53.0, 52.6, 51.2, 38.7, 24.2, 12.0

IR (neat): ν (cm^{-1}) 2956, 2924, 1736, 1436, 1248, 1159, 752, 668

HRMS (ESI): Calcd for $C_{24}H_{30}NaO_8$ $[M+Na]^+$: 469.1833, found 469.1841

Rf: 0.07 (pentane/EtOAc 90:10)

Mp: 51.5-53.0 °C

[α]$_D$^{20}: -248.0° (c = 0.38, $CHCl_3$)

HPLC separation: Chiralcel® OD-H; 95:5 (*n*-heptane/*i*-PrOH), 0.5 ml.min^{-1}, 282 nm, t_R (minor) = 22.3 min, t_R (minor) = 24.6 min, >99:1 e.r.

Dimethyl (*R*)-1-(dimethylcarbamoyl)-1,3-dihydro-2*H*-indene-2,2-dicarboxylate (2.45t):

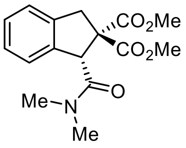

2t
$C_{16}H_{19}NO_5$
M= 305,33 g.mol^{-1}

From **2.44t** using **General procedure H**. **2.45t** was obtained as a colorless solid (57.3 mg, 0.188 mmol, 94%).

^{1}H NMR (500 MHz, $CDCl_3$): δ (ppm) 7.24- 7.13 (m, 4H), 5.25 (s, 1H), 4.21 (d, *J* = 16.3 Hz, 1H), 3.73 (s, 3H), 3.70 (s, 3H), 3.43 (d, *J* = 16.4 Hz, 0H), 3.39 (s, 1H), 2.91 (s, 3H)

^{13}C NMR (126 MHz, $CDCl_3$): δ (ppm) 172.0, 171.7, 170.2, 141.4, 140.5, 128.1, 127.1, 125.1, 123.7, 65.1, 53.4, 53.2, 52.9, 40.4, 38.7, 36.0

IR (neat): ν (cm^{-1}) 2954, 2923, 2851, 1731, 1644, 1435, 1256, 1164, 1080, 750, 616

HRMS (ESI): Calcd for $C_{16}H_{19}NaO_5$ $[M+Na]^+$: 338.1155, found 328.1159

Rf: 0.25 (pentane/EtOAc 80:20)

Mp: 113.8-115.7 °C

[α]$_D$^{20}: -155.0° (c = 0.60, $CHCl_3$)

HPLC separation: Chiralcel® IA; 85:15 (*n*-heptane/*i*-PrOH), 0.5 ml.min^{-1}, 226 nm, t_R (major) = 12.7 min, t_R (minor) = 21.4 min, 95:5 e.r.

Dimethyl (*R*)-1-(morpholine-4-carbonyl)-1,3-dihydro-2*H*-indene-2,2-dicarboxylate (2.45u):

From **2.44u** using **General procedure H**. **2.45u** was obtained as a colorless solid (57.3 mg, 0.188 mmol, 94%).

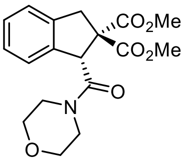

2.45u

$C_{18}H_{21}NO_6$

M= 347,37 g.mol^{-1}

^{1}H NMR (500 MHz, $CDCl_3$): δ (ppm) 7.25-7.14 (m, 3H), 7.11 (d, *J* = 7.4 Hz, 1H), 5.21 (s, 1H), 4.21 (d, *J* = 16.4 Hz, 1H), 4.03-3.87 (m, 2H), 3.85-3.79 (m, 2H), 3.74 (s, 3H), 3.71 (s, 3H), 3.69- 3.65 (m, 3H), 3.51-3.46 (m, 1H), 3.44 (d, *J* = 16.4 Hz, 1H)

^{13}C NMR (126 MHz, $CDCl_3$): δ (ppm) 171.6, 170.7, 170.0, 141.3, 140.2, 128.3, 127.3, 125.2, 123.7, 7.2, 67.1, 65.0, 53.5, 53.0, 52.6, 47.5, 42.7, 40.4

IR (neat): ν (cm^{-1}) 2962, 2867, 1584, 1508, 1473, 1270, 1215, 826, 746, 687

HRMS (ESI): Calcd for $C_{18}H_{21}NNaO_6$ $[M+Na]^+$: 370.1261, found 370.1266

Rf: 0.30 (pentane/EtOAc 50:50)

Mp: 130.3-133.7 °C

$[\alpha]_D^{20}$: -146.9° (c = 0.93, $CHCl_3$)

HPLC separation: Chiralcel® IA; 75:25 (*n*-heptane/*i*-PrOH), 1.5 ml.min^{-1}, 216 nm, t_R (major) = 6.6 min, t_R (minor) = 11.3 min, 97:3 e.r.

Dimethyl (*R*)-1-(methoxy(methyl)carbamoyl)-1,3-dihydro-2*H*-indene-2,2-dicarboxylate (2.45v):

From **2.44v** using **General procedure H**. **2.45v** was obtained as a colorless solid (48.0 mg, 0.149 mmol, 75%).

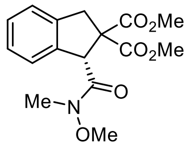

2v

$C_{16}H_{19}NO_6$

M= 321,33 g.mol^{-1}

^{1}H NMR (500 MHz, $CDCl_3$): δ (ppm) 7.34 (d, *J* = 7.3 Hzi, 1H), 7.23-7.12 (m, 3H), 5.30 (s, 1H), 4.15 (d, *J* = 16.4 Hz, 1H), 3.88 (s, 3H), 3.75 (s, 3H), 3.71 (s, 3H), 3.46 (d, *J* = 16.4 Hz, 1H), 3.16 (s, 3H).

^{13}C NMR (126 MHz, $CDCl_3$): δ (ppm) 172.4, 171.5, 170.2, 141.1, 139.96, 128.2, 127.2, 124.9, 124.9, 64.4, 61.5, 53.4, 53.4, 53.0, 40.3, 32.3

IR (neat): ν (cm^{-1}) 3020, 2955, 1737, 1655, 1215, 754, 632

HRMS (ESI): Calcd for $C_{16}H_{19}NNaO_6$ $[M+Na]^+$: 344.1105, found 344.1106

Rf: 0.20 (pentane/EtOAc 65:35)

Mp: 83.8-85.5 °C

$[\alpha]_D^{20}$: -178.4° (c = 1.20, $CHCl_3$)

HPLC separation: Chiralcel® AD-H; 75:25 (*n*-heptane/*i*-PrOH), 1.5 ml.min^{-1}, 209 nm, t_R (major) = 4.8 min, t_R (minor) = 9.1 min, 98:2 e.r.

Post-functionalizations

Methyl (4a*R*,9a*R*)-6-fluoro-1-oxo-1,2,3,4,4a,9-hexahydro-9aH-indeno[2,1-c]pyridine-9a-carboxylate (2.45ja):

2.45j (24.6 mg, 0.06 mmol, 1.0 equiv) was dissolved om EtOH (1.0 mL) and hydrazine monohydrate (17.4 mg, 0.35 mmol, 6.0 equiv) was added. The mixture was heated to reflux for 3 h and stirred at room temperature overnight. The reaction mixture was then filtered and the solvent removed under reduced pressure. The residue was taken up in EtOAc (3.0 mL), washed with brine (3x 3.0 mL) and dried over Na_2SO_4. The solvent was removed under reduced pressure to give **2.45ja** (14.4 mg, 0.058 mmol, 95%) as a single diastereoisomer without further purification.

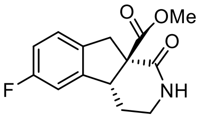

2.45ja
$C_{14}H_{14}FNO_3$
M= 263.27 g.mol^{-1}

^{1}H NMR (500 MHz, $CDCl_3$): δ (ppm) δ 7.72 (s, 1H), 6.67-6.59 (m, 2H), 6.49 – 6.42 (m, 1H), 3.96 (d, *J* = 16.4, 1H), 3.48 (d, *J* = 16.4, 1H), 3.30 (s, 3H), 3.26 (t, *J* = 5.8, 1H), 2.66-2.60 (m, 1H), 2.52-2.45 (m, 1H), 1.75-1.67 (m, 1H), 1.22-1.14 (m, 1H)

^{13}C NMR (126 MHz, $CDCl_3$): δ (ppm) 172.3, 171.3, 162.8 (d, *J* = 243.4 Hz), 144.4 (d, *J* = 7.6 Hz), 136.7 (d, *J* = 2.5 Hz), 126.3 (d, *J* = 8.6 Hz), 114.7 (d, *J* = 22.4 Hz), 110.4 (d, *J* = 22.3 Hz), 60.8, 52.4, 47.8 (d, *J* = 2.1 Hz), 39.7, 39.2, 25.2

^{19}F NMR (471 MHz, $CDCl_3$): δ (ppm) -116.5

IR (neat): ν (cm^{-1}) 3233, 2924, 1738, 1662, 1484, 1243, 1099, 1053, 872, 822

HRMS (ESI): Calcd for $C_{14}H_{14}NnaO_3$ $[M+Na]^+$: 286.0850, found 286.0853

Rf: 0.20 (pentane/EtOAc 40:60)

Mp: 123.4-126.0 °C

(*R*)-1-(2-(1,3-Dioxoisoindolin-2-yl)ethyl)-6-fluoro-1',3'-dimethyl-1,3-dihydro-2'*H*-spiro[indene-2,5'-pyrimidine]-2',4',6'(1'*H*,3'*H*)-trione (2.45jb):

To a solution of **2.45j** (60 mg, 0.141 mmol, 1.0 equiv) in DMSO urea (50 mg, 0.832 mmol, 5.9 equiv) and KO^{t}Bu (34.8 mg, 0.310 mmol, 2.2 equiv) were added and the mixture was stirred at room temperature for 2 h. Afterwards, the mixture was diluted with EtOAc (3.0 mL) and washed with HCl (0.1 M, 3.0 mL). The aqueous phase was extracted with EtOAc (3 x 3.0 mL), the combined organic layers were dried over Na_2SO_4 and evaporated under reduced pressure. The crude residue was taken up in DMF (1.0 mL) and K_2CO_3 (105 mg, 0.761 mmol, 5.4 equiv) and MeI (40.0 mg, 0.282 mmol, 2.0 equiv) were added. The reaction mixture was stirred at room temperature overnight. Then, the mixture was acidified with HCL (0.1 M) and extracted with Et_2O. The organic phase was dried over Na_2SO_4 and evaporated under reduced pressure. The crude mixture was purified by preparative HPLC to give **2.45jb** (28.0 mg, 0.06 mmol, 44%) as a colorless solid.

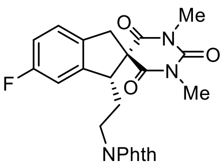

2jb
$C_{24}H_{20}FN_3O_5$
M= 449.44 g.mol^{-1}

^{1}H NMR (500 MHz, $CDCl_3$): δ (ppm) δ 7.87-7.79 (m, 2H), 7.77-7.69 (m, 2H), 7.14-7.08 (m, 1H), 6.94-6.88 (m, 2H), 3.97 (d, *J* = 8.3, 5.6 Hz, 1H), 3.71-3.64 (m, 1H), 3.61-3.56 (m, 1H), 3.51 (s, 2H), 3.38 (s, 3H), 3.35 (s, 3H), 2.30-2.22 (m, 1H), 2.06-1.99 (m, 1H)

^{13}C NMR (126 MHz, $CDCl_3$): δ (ppm) 172.0, 169.8, 168.2, 162.8 (d, *J* = 244.5 Hz), 151.2, 144.6 (d, *J* = 7.8 Hz), 134.9 (d, *J* = 2.7 Hz), 134.3, 132.1, 125.0 (d, *J* = 8.8 Hz), 123.6, 114.7 (d, *J* = 22.5 Hz), 110.8 (d, *J* = 23.5 Hz), 61.3, 53.2 (d, *J* = 2.3 Hz), 43.1, 36.2, 29.9, 29.4, 28.90

^{19}F NMR (471 MHz, $CDCl_3$): δ (ppm) -115.6

IR (neat): ν (cm^{-1}) 2927, 1710, 1673, 1438, 1372, 1264, 1093, 718, 651

HRMS (ESI): Calcd for C24H20FN$_3$NaO5 [M+Na]$^+$: 472.1279, found 472.1283

Rf: 0.24 in a (pentane/*i*PrOH 95:5)

[α]$_D^{20}$: -63.50° (c = 0.8, CHCl$_3$)

HPLC separation: Chiralcel® AS; 92:8 (*n*-heptane/*i*-PrOH), 0.5 ml.min^{-1}, 227 nm, t_R (major) = 60.9 min, t_R (minor) = 71.1 min, >99:1 e.r.

Mp: 46.4-49.9 °C

6.1.4 Effect of the ligand structure on the enantioselectivity

Determination of buried volumes

DFT calculations were performed using Gaussian 16.[197] The geometries of [Pd(NHC)(allyl)Cl] complexes were optimized with the BP86[198,199] functional and TZVP basis set[200] for non-metal atoms and with a Stuttgart effective core potential and valence basis set[201,202] taken from the Basis Set Exchange[203] for Pd, similar to the method reported by Cavallo and co-workers.[156] Frequency calculations were performed to confirm the existence of a local minimum energy geometry.

The buried volumes of NHCs were determined using the Samb*V*ca 2.1 application[204] by inputting the above optimized structures of [Pd(NHC)(allyl)Cl] complexes. IMes and IAd were used as reference NHC ligands to validate the method (calculated %V_{Bur} from DFT-optimized complexes: IMes, 32.7, IAd, 37.3, calculated %V_{Bur} from Xray structures: IMes, 32.6, IAd, 37.5).[205]

The enantiomeric ratio was obtained by HPLC analysis on a chiral stationary phase.

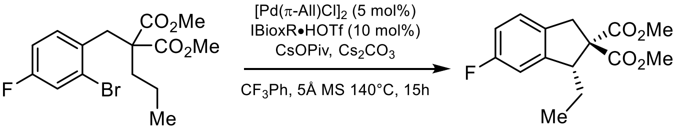

2.44a **2.45a**

IBioxR	e.r.	%V_{Bur} (3.5 Å)	Quadrant Diff %V_{Bur} [%V_{Bur}(SW+NE)–%V_{Bur}(NW+SE)]/2
Menth	6.1	43.5	1.4
iPr	5.7	30.1	14.05
*t*Bu	13.3	30.1	14.1
Cy	49.0	34.2	22.25
Ad	49.0	34.5	22.25
*t*BuMe$_4$	165.7	34.7	23

Table S1: Effect of ligand structure on enantioselectivity. Calculated %V_{Bur} and Quadrant Diff %V_{Bur}

6.1.5 Determination of absolute configuration of **2.45c**, **2.45t** and **2.45ja** by VCD spectroscopy

VCD experiments

IR and vibrational circular dichroism (VCD) spectra were recorded on a Bruker PMA 50 accessory coupled to a Tensor 27 Fourier transform infrared spectrometer. A photoelastic modulator (Hinds PEM 90) set at 1/4 retardation was used to modulate the handedness of the circular polarized light. Demodulation was performed by a lock-in amplifier (SR830 DSP). An optical low-pass filter (< 1800 cm^{-1}) in front of the photoelastic modulator was used to enhance the signal/noise ratio. Solutions of ca. 4 mg in 200 µl CD_2Cl_2 of **2.45c**, **2.45t** and **2.45ja** were prepared and measured in a transmission cell equipped with CaF_2 windows and a 200 µm spacer. The VCD spectrum of the pure solvent served as the reference and was subtracted from the VCD spectrum of the compound in order to eliminate artefacts. For both the sample and the reference, ca. 30’000 scans at 4 cm^{-1} resolution were averaged.

Calculations

Density functional theory (DFT) as implemented in Gaussian16[197] was used to study the conformation and to calculate the corresponding IR and VCD spectra. The calculations were performed using the b3pw91 functional and a 6-31+G(d,p) basis set. All calculations were performed for gas phase species. Prior to the calculation of the spectra all degrees of freedom were completely relaxed. IR and VCD spectra were constructed from calculated dipole and rotational strengths assuming Gaussian band shape with a half-width at half-maximum of 4 cm^{-1}. Frequencies were scaled by a factor of 0.97. To calculate the Boltzmann distribution of the different conformers a thermal free energy correction was applied. Only conformers with a population of at least 4% were considered.

Conformational search

A systematic conformation search was done taking into account the conformational degrees of freedom of the respective molecules. For **2.45c** the 5-ring is not flat. In addition the orientation of the ester groups and the ethyl group has to be considered. Similarly, for **2.45t** the conformation of the 5-ring, the orientation of the ester groups and the orientation of the amide group had to be considered. For **2.45ja** the conformation degrees of freedom that were considered are the 5-ring, the 6-ring (position of CH_2 group) and the orientation of the ester group.

Results for 2.45c

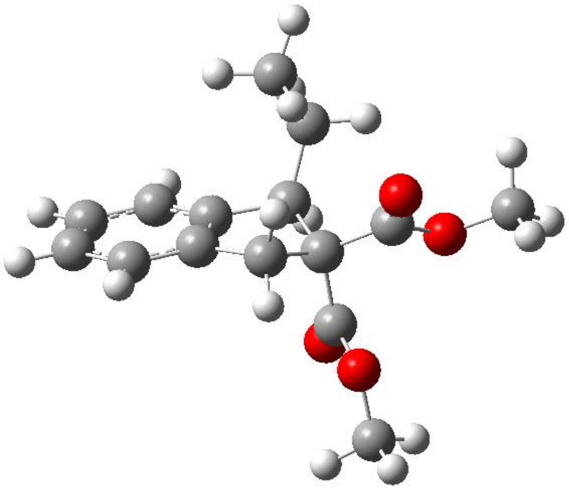

Figure S1*:* The structure shows the most stable conformer of **2.45c** found. This conformer accounts for 58% according to a Boltzmann population at room temperature.

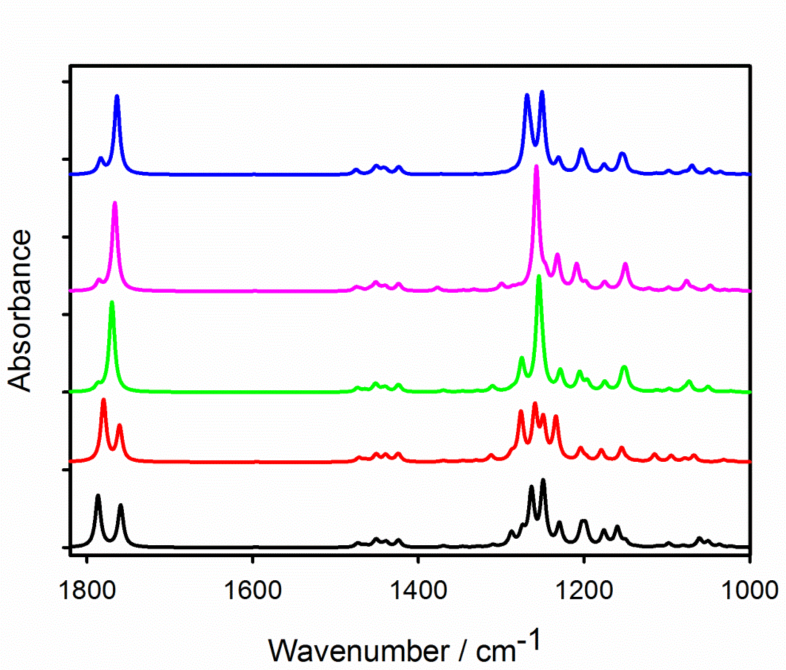

Figure S2*:* Calculated IR spectra of the five most stable conformers of **2.45c** accounting for (from bottom to top) 5%, 10%, 58%, 20% and 7% of the calculated population.

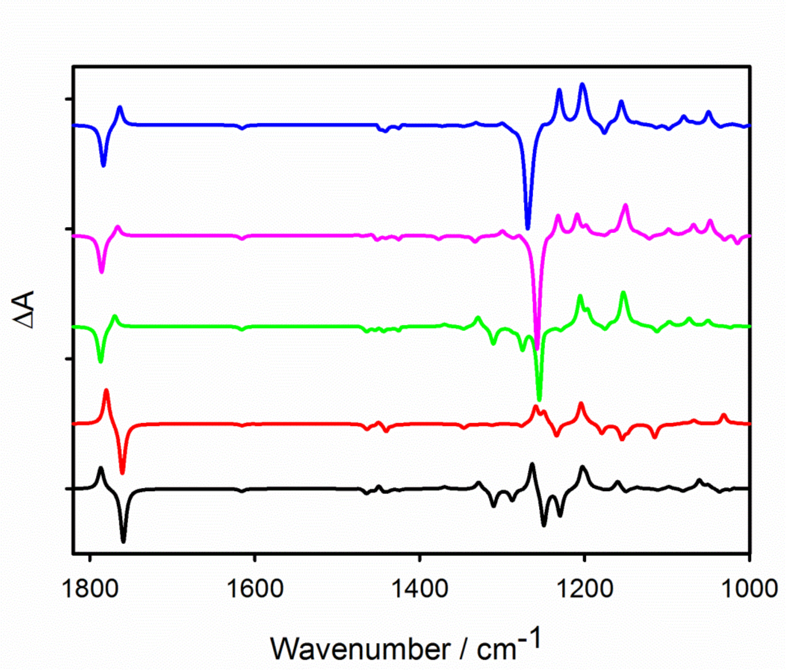

Figure S3*:* Calculated VCD spectra of the five most stable conformers of **2.45c** accounting for (from bottom to top) 5%, 10%, 58%, 20% and 7% of the calculated population.

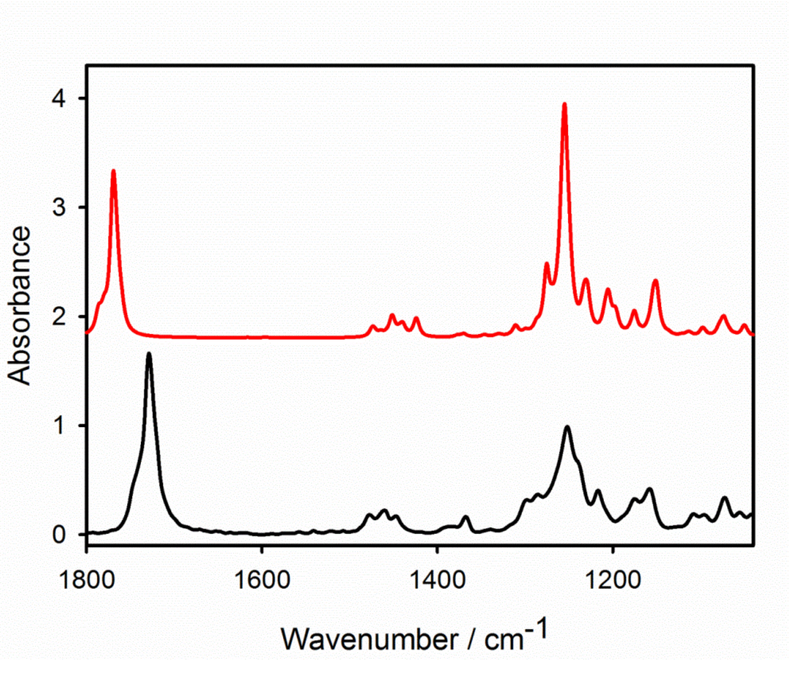

Figure S4: Comparison between experimental (black) and calculated (red) infrared spectra of **2.45c**. The calculated spectrum is the linear combination (Boltzmann weighted) of the spectra of the five most stable conformers.

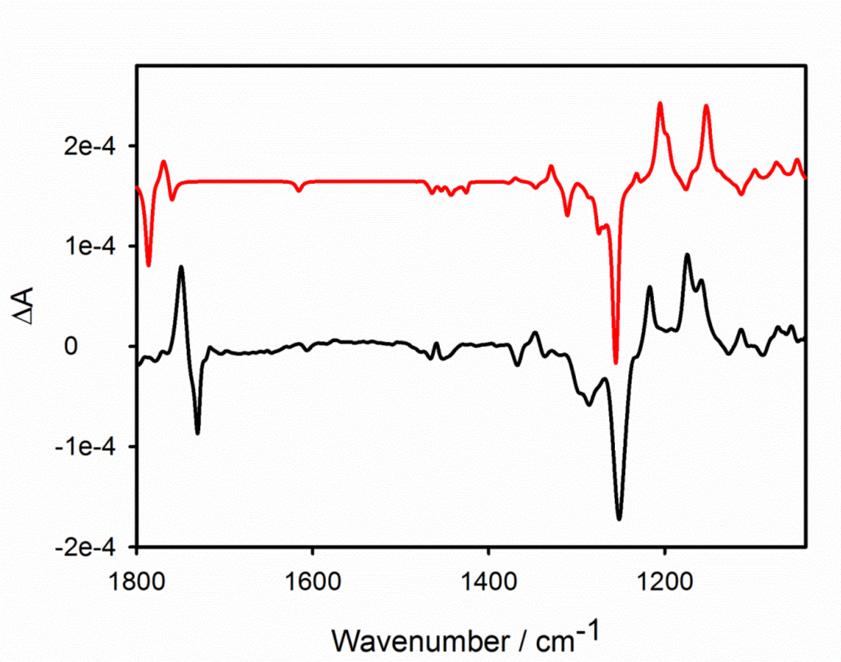

Figure S5: Comparison between experimental (black) and calculated (red) VCD spectra of **2.45c**. The calculated spectrum is the linear combination (Boltzmann weighted) of the spectra of the five most stable conformers.

Assignment of absolute configuration

Except for the carbonyl region the agreement between experimental and calculated VCD spectra is good. The absolute configuration of the sample measured and the one used for the calculation (see structure above) is therefore the same.

Results for 2.45t

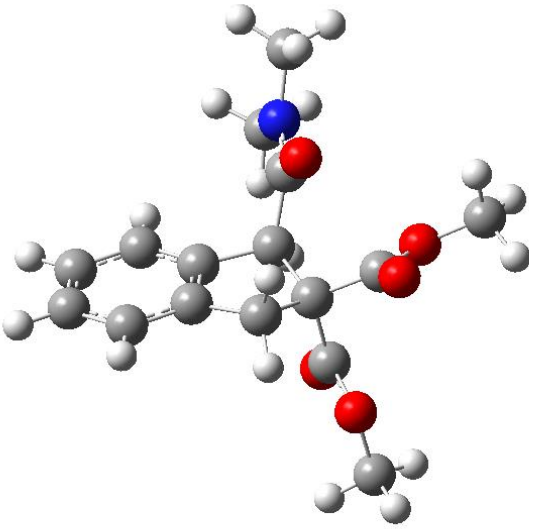

Figure S6: The structure shows the most stable conformer of **2.45t** found. This conformer accounts for 48% according to a Boltzmann population at room temperature.

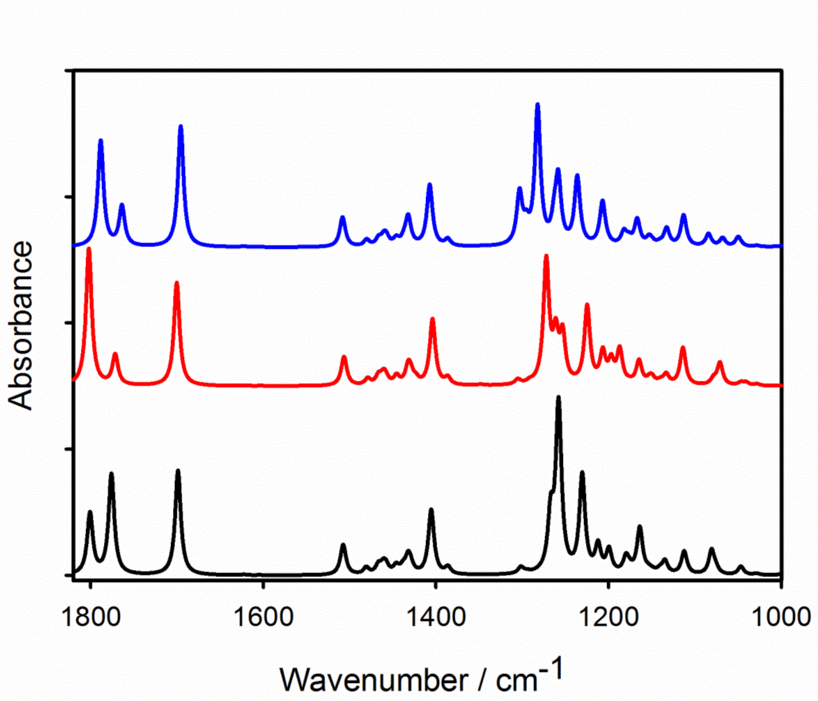

Figure S7: Calculated IR spectra of the three most stable conformers of **2.45t** accounting for (from bottom to top) 48%, 4% and 48% of the calculated population.

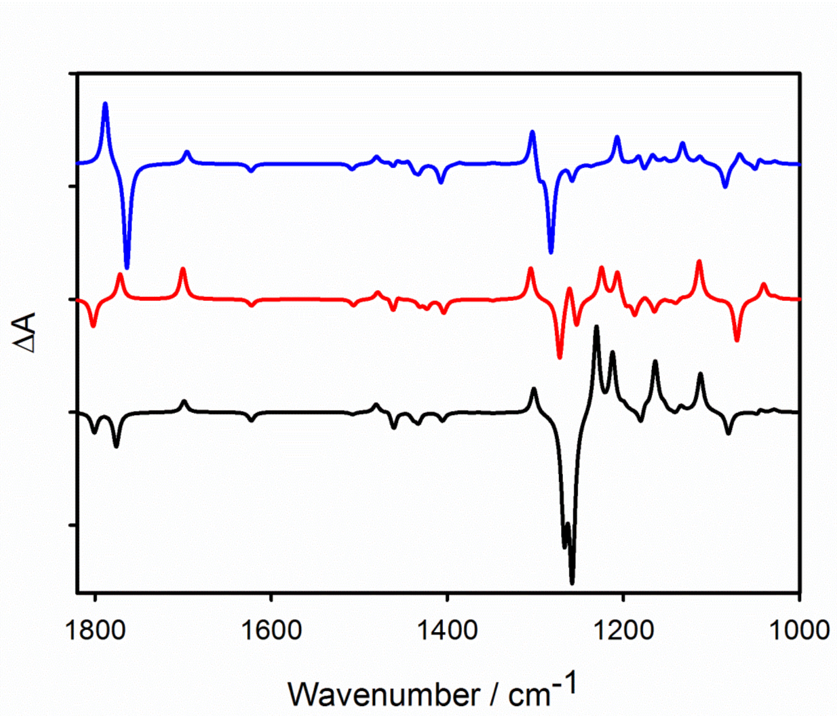

Figure S8: Calculated VCD spectra of the three most stable conformers of **2.45t** accounting for (from bottom to top) 48%, 4% and 48% of the calculated population.

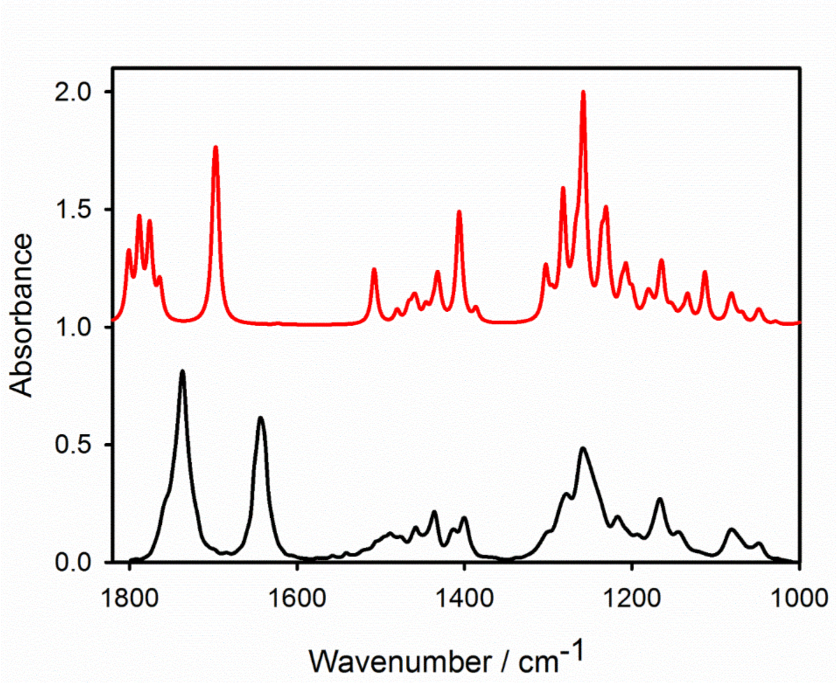

Figure S9: Comparison between experimental (black) and calculated (red) infrared spectra of **2.45t**. The calculated spectrum is the linear combination (Boltzmann weighted) of the spectra of the three most stable conformers.

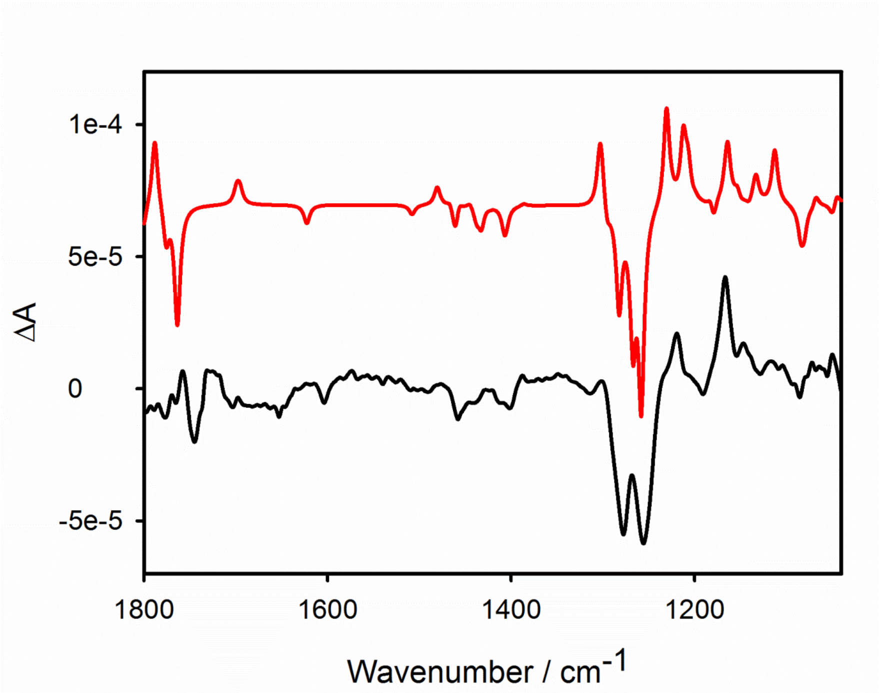

Figure S10: Comparison between experimental (black) and calculated (red) VCD spectra of **2.45t**. The calculated spectrum is the linear combination (Boltzmann weighted) of the spectra of the three most stable conformers.

Assignment of absolute configuration

Except for the carbonyl region the agreement between experimental and calculated VCD spectra is good. The absolute configuration of the sample measured and the one used for the calculation (see structure above) is therefore the same.

Results for 2.45ja

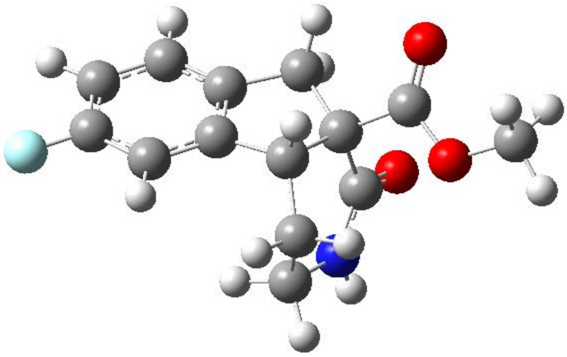

Figure S.11: The structure shows the most stable conformer of **2.45ja** found. This conformer accounts for 42% according to a Boltzmann population at room temperature.

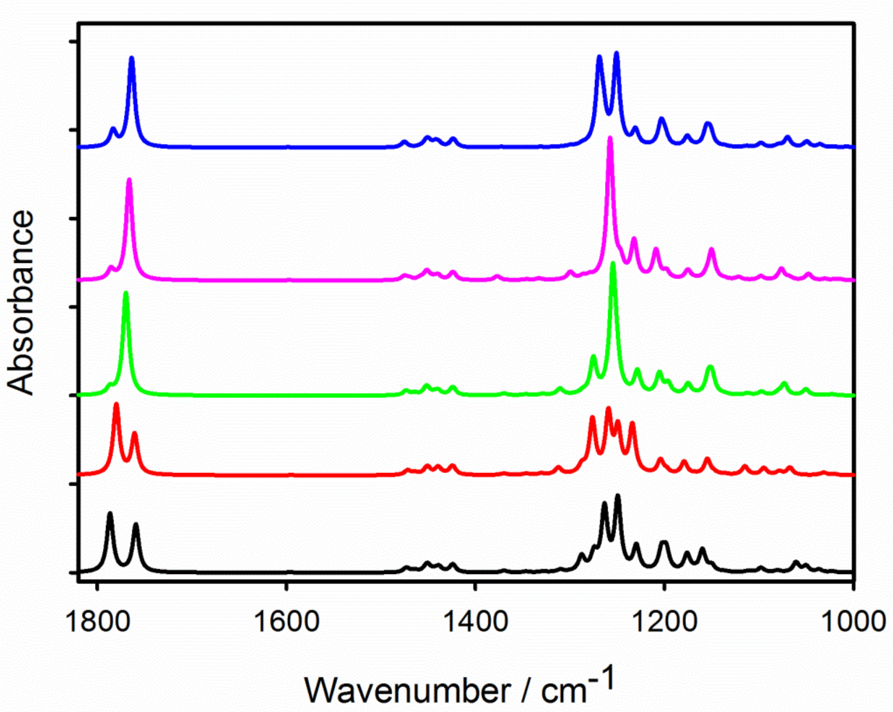

Figure S15: Calculated IR spectra of the five most stable conformers of **2.45ja** accounting for (from bottom to top) 17%, 7%, 42%, 11% and 23% of the calculated population.

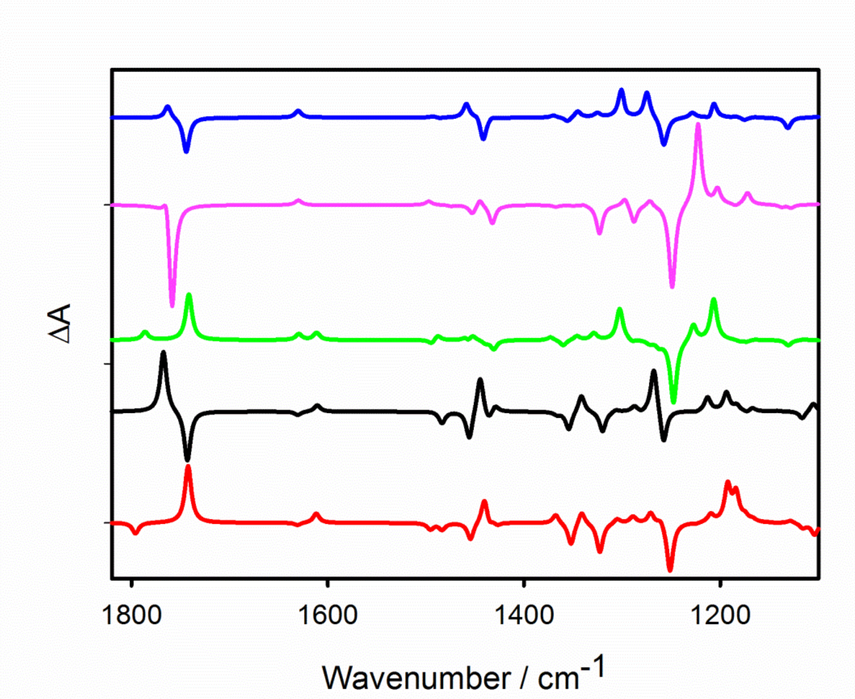

Figure S13: Calculated VCD spectra of the five most stable conformers of **2.45ja** accounting for (from bottom to top) 17%, 7%, 42%, 11% and 23% of the calculated population.

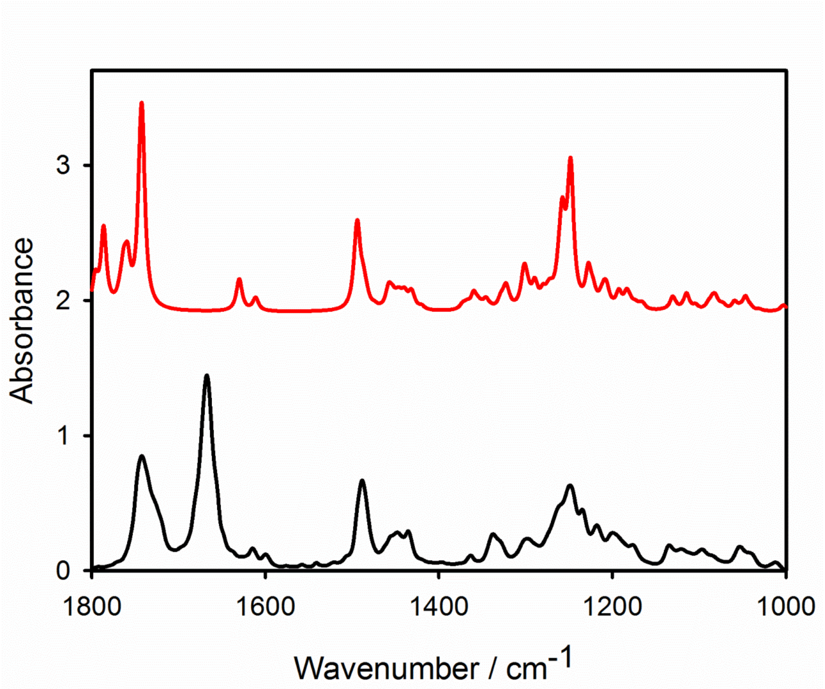

Figure S14: Comparison between experimental (black) and calculated (red) infrared spectra of **2.45ja**. The calculated spectrum is the linear combination (Boltzmann weighted) of the spectra of the five most stable conformers.

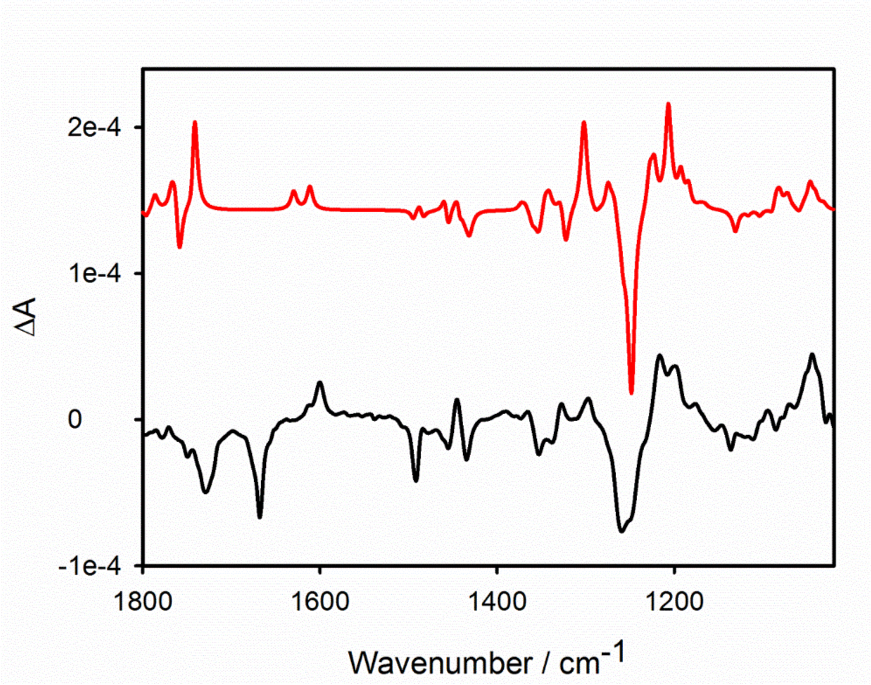

Figure S15: Comparison between experimental (black) and calculated (red) VCD spectra of **2.45ja**. The calculated spectrum is the linear combination (Boltzmann weighted) of the spectra of the five most stable conformers.

Assignment of absolute configuration

Except for the carbonyl region the agreement between experimental and calculated VCD spectra is good. The absolute configuration of the sample measured and the one used for the calculation (see structure above) is therefore the same.

6.1.6 Synthesis of new substrates for enantioselective C(sp^3)−H activation

2-Bromo-*N*,*N*-diethylbenzenesulfonamide (2.62):

2-Bromobenzenesulfonyl chloride (1.00 g, 3.91 mmol, 1.0 eq.) and diethyl amine (372 mg, 5.08 mmol, 1.30 eq.) were dissolved in CH_2Cl_2 (10 mL). Triethyl amine (1.20 g, 11.7 mmol, 3.0 eq.) was added and the reaction was stirred for 3 h. The reaction was quenched by the addition of H2O (10 mL) and the aqueous phase was extracted with EtOAc (3 x 10 mL). The combined organic layers were washed with brine, dried over Na_2SO_4 and the volatiles were evaporated under reduced pressure. The title compound was obtained as a colorless oil (837 mg, 2.86 mmol, 73%) without further purification.

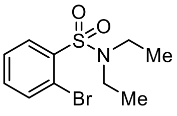

2.62
$C_{10}H_{14}BrNO_2S$
M= 292,19 g.mol^{-1}

^{1}H NMR (500 MHz, $CDCl_3$): δ (ppm) 8.13 (d, *J* = 7.8 Hz, 1H), 7.72 (d, *J* = 7.8 Hz, 1H), 7.49 – 7.31 (m, 2H), 3.39 (q, *J* = 7.1 Hz, 4H), 1.12 (t, *J* = 7.1 Hz, 6H).

^{13}C NMR (126 MHz, $CDCl_3$): δ (ppm) 140.0, 135.7, 133.4, 132.3, 127.6, 120.5, 41.3, 13.8.

GC-MS (EI): Calcd for $C_{10}H_{14}{}^{79}BrNO_2S$ $[M]^{+\bullet}$: 291, found 291

2-Bromo-*N*,*N*-diethylbenzamide (2.63):

2-Bromobenzoyl chloride (3.00 g, 13.7 mmol, 1.0 eq.) and diethylamine (1.10 g, 15.0 mmol, 1.1 eq.) were dissolved in CH_2Cl_2 (75 mL). Triethylamine (1.73 g, 17.1 mmol, 1.25 eq.) was added and the reaction was stirred for 3 h. The reaction was quenched by the addition of H2O (10 mL) and the aqueous phase was extracted with EtOAc (3 x 10 mL). The combined organic layers were washed with brine, dried over Na_2SO_4 and the volatiles were evaporated under reduced pressure. The title compound was obtained as a colorless oil (3.30 g, 12.9 mmol, 94%). Without further purification.

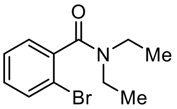

2.63
$C_{11}H_{14}BrNO$
M= 256,14 g.mol^{-1}

^{1}H NMR (500 MHz, $CDCl_3$): δ (ppm) 7.56 (d, *J* = 8.1 Hz, 1H), 7.37 – 730 (m, 1H), 7.29 – 7.14 (m, 2H), 3.83 (dq, *J* = 14.6, 7.4 Hz, 1H), 3.34 (dq, *J* = 14.4, 7.3 Hz, 1H), 3.15 (dq, *J* = 16.1, 8.4, 8.0 Hz, 2H), 1.27 (t, *J* = 7.1 Hz, 3H), 1.06 (t, *J* = 7.1 Hz, 3H).

^{13}C NMR (126 MHz, $CDCl_3$): δ (ppm) 168.6, 139.0, 132.9, 130.1, 127.7, 127.6, 119.4, 42.8, 39.1, 14.0, 12.7.

GC-MS (EI): Calcd for $C_{11}H_{14}{}^{79}BrNO$ $[M]^{+\bullet}$: 255, found 255

Dimethyl 2-(2'-bromo-[1,1'-biphenyl]-2-yl)-2-ethylmalonate) (2.64):

According to **general procedure F**, dimethyl 2-(2'-bromo-[1,1'-biphenyl]-2-yl)malonate (476 mg, 1.31 mmol, 1.0 eq.) was reacted with ethyl iodide (245 mg, 1.57 mmol, 1.2 eq.) to give the title compound (350 mg, 895 µmol, 68%) as a yellow oil.

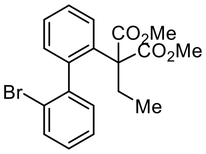

2.64
$C_{19}H_{19}BrO_4$
M= 391,26 g.mol^{-1}

^{1}H NMR (500 MHz, $CDCl_3$): δ (ppm) 7.55 (d, *J* = 8.0 Hz, 1H), 7.25 – 7.04 (m, 6H), 6.99 (d, *J* = 7.6 Hz, 1H), 3.60 (s, 3H), 3.36 (s, 3H), 2.10 (dq, *J* = 14.5, 7.3 Hz, 1H), 1.92 (dq, *J* = 14.5, 7.3 Hz, 1H), 0.78 (t, *J* = 7.3 Hz, 3H).

^{13}C NMR (126 MHz, $CDCl_3$): δ (ppm) 171.5, 170.9, 142.0, 139.9, 136.25, 133.2, 132.9, 131.7, 129.8, 129.2, 127.8, 127.0, 126.6, 124.9, 64.2, 52.7, 52.7, 29.8, 10.6.

GC-MS (EI): Calcd for $C_{19}H_{19}{}^{79}BrO_4$ $[M]^{+\bullet}$: 390, found 390

Dimethyl 2-((2'-bromo-[1,1'-biphenyl]-2-yl)methyl)-2-propylmalonate) (2.65):

According to **general procedure G**, dimethyl 2-propylmalonate (557 mg, 3.20 mmol, 1.0 eq.) was reacted with 2-bromo-2'-(bromomethyl)-1,1'-biphenyl (1.25 g, 3.83 mmol, 1.2 eq.) to give the title compound (1.00 g, 2.38 mmol, 73 %) as a brown oil.

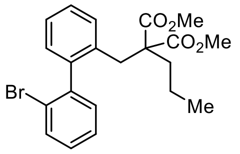

2.65
$C_{21}H_{23}BrO_4$
M= 419,31 g.mol^{-1}

^{1}H NMR (500 MHz, CDCl$_3$): δ (ppm) 7.65 (d, *J* = 8.0 Hz, 1H), 7.43 – 7.26 (m, 3H), 7.24 – 7.16 (m, 2H), 7.17 – 7.07 (m, 2H), 3.66 (s, 3H), 3.64 (s, 3H), 3.38 (d, *J* = 14.7 Hz, 1H), 3.17 – 3.08 (m, 1H), 1.65 – 1.56 (m, 1H), 1.54 – 1.45 (m, 1H), 0.69 (t, *J* = 4.8 Hz, 3H).

^{13}C NMR (126 MHz, CDCl$_3$): δ (ppm) 172.2, 172.1, 134.5, 133.0, 132., 130.78, 129.7, 128.9, 128.0, 127.3, 126.7, 124.2, 59.3, 52.4, 52.3, 35.1, 34.5, 17.7, 14.4.

GC-MS (EI): Calcd for $C_{21}H_{23}{}^{79}BrO_4$ $[M]^{+\bullet}$: 418, found 418

Dimethyl 2-(2-bromophenyl)-2-(2-(dimethylamino)-2-oxoethyl)malonateglycinate (2.66a):

According to **general procedure F**, dimethyl 2-(2-bromophenyl)malonate (502 mg, 1.76 mmol, 1.0 eq.) was reacted with 2-chloro-*N*,*N*-dimethylacetamide (300 mg, 2.46 mmol, 1.4 eq.) to give the title compound (353 mg, 947 µmol, 54%) as a colorless oil.

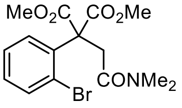

2.66a
$C_{15}H_{18}BrNO_5$
M= 372,21 g.mol^{-1}

^{1}H NMR (500 MHz, CDCl$_3$): 7.60 (dd, *J* = 8.1, 1.6 Hz, 1H), 7.56 (dd, *J* = 8.1, 1.4 Hz, 1H), 7.31 (td, *J* = 7.8, 1.4 Hz, 1H), 7.15 (td, *J* = 7.8, 1.6 Hz, 1H), 3.82 (s, 6H), 3.53 (s, 2H), 3.03 (s, 3H), 2.93 (s, 3H).

^{13}C NMR (126 MHz, CDCl$_3$): δ (ppm) 170.1, 169.6, 137.3, 134.7, 131.4, 129.3, 127.6, 123.3, 63.0, 53.5, 38.8, 37.4, 35.8.

GC-MS (EI): Calcd for $C_{17}H_{21}{}^{79}BrO_6$ $[M]^{+\bullet}$: 371, found 371

Trimethyl 1-(2-bromophenyl)ethane-1,1,2-tricarboxylate (2.66b):

According to **general procedure F**, dimethyl 2-(2-bromophenyl)malonate (1.00 g, 3.48 mmol, 1.0 eq.) was reacted with methyl 2-bromoacetate (639 mg, 4.17 mmol, 1.2 eq.) to give the title compound (620 mg, 1.73 mmol, 50%) as a yellow oil.

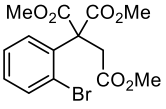

2.66b
$C_{14}H_{15}BrO_6$
M= 359,17 g.mol^{-1}

^{1}H NMR (500 MHz, CDCl$_3$): 7.58 (dd, *J* = 7.9, 1.4 Hz, 1H), 7.38 – 7.29 (m, 2H), 7.23 – 7.13 (m, 1H), 3.84 (s, 6H), 3.69 (s, 3H), 3.48 (s, 2H).

^{13}C NMR (126 MHz, CDCl$_3$): δ (ppm) 170.9, 169.7, 136.5, 135.0, 130.5, 129.6, 127.7, 123.3, 63.2, 53.6, 52.1, 39.3.

GC-MS (EI): Calcd for $C_{14}H_{15}{}^{79}BrO_6$ $[M]^{+\bullet}$: 358, found 358

Tert-butyl N-(2-bromobenzyl)-N-(2,2,2-trifluoroacetyl)glycinate (2.68a):

Titanium(IV) isopropoxide (2.11, 7.13 mmol, 1.3 eq.) was added to a solution of tert-butyl glycinate (1.42 g, 10.8 mmol, 2.0 eq.) followed by the addition of 2-bromobenzaldehyde (1.00 g, 5.40 mmol, 1.0 eq.). The reaction mixture was stirred for 3 h at 24 °C. Then, Sodium borohydride (204 mg, 5.40 mmol, 1.0 eq.) was added and the mixture was stirred for another 2 h. The reaction was quenched by the addition of H$_2$O (2.0 mL) and the precipitate was filtered and washed with tiethyl ether (20 mL). The organic layer was separated and the aqueous phase was extracted with diethyl ether (20 mL). The combined organic layers were dried over Na_2SO_4 and the volatiles were removed under reduced pressure. The crude product was then dissolved in CH_2Cl_2 (11 mL) and Et_3N (318 mg, 3.14 mmol, 1.4 eq.), DMAP (26.6 mg, 218 µmol, 0.1 eq.) and trifluoroacetic anhydride (549 mg, 2.62 mmol 1.2 eq.) were added at 0 °C. The mixture was stirred for 16 at 24 °C and the volatiles were removed under reduced pressure. Purification by flash column chromatography (Cyclohexane:EtOAc, 85:15) yield the title compound (800 mg, 2.02 mmol, 93%) as a yellow liquid.

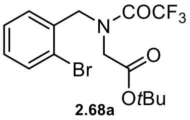

2.68a
$C_{15}H_{17}BF_3NO_3$
M= 396,20 g.mol^{-1}

^{1}H NMR (500 MHz, $CDCl_3$): δ (ppm) 7.61 – 7.51 (m, 1H), 7.38 – 7.29 (m, 1H), 7.28 – 7.25 (m, 1H), 7.25 – 7.17 (m, 1H), 4.84 (d, *J* = 26.6 Hz, 2H), 3.94 (d, *J* = 32.7 Hz, 2H), 1.46 (s, 9H).

^{13}C NMR (126 MHz, $CDCl_3$): δ (ppm) 166.85, 166.34, 157.91 (dq, *J* = 48.9, 36.5 Hz), 133.92 (d, *J* = 56.1 Hz), 133.37 (d, *J* = 16.0 Hz), 130.59, 130.01 (d, *J* = 5.3 Hz), 128.68, 128.21 (d, *J* = 2.3 Hz), 124.00 (d, *J* = 112.9 Hz), 121.95 – 111.27 (m), 83.10 (d, *J* = 39.3 Hz), 51.72 (q, *J* = 3.6 Hz), 50.92, 48.53 (q, *J* = 3.5 Hz), 28.04 (d, *J* = 11.2 Hz).

GC-MS (EI): Calcd for $C_{15}H_{17}{}^{79}BrF_3NO_3$ $[M]^{+\bullet}$: 395, found 395

Methyl N-((3r,5r,7r)-adamantane-1-carbonyl)-N-(2-bromobenzyl)glycinate (2.68b):

Titanium(IV) isopropoxide (2.11, 7.13 mmol, 1.3 eq.) was added to a solution of methyl glycinate (962 mg, 10.8 mmol, 2.0 eq.) followed by the addition of 2-bromobenzaldehyde (1.00 g, 5.40 mmol, 1.0 eq.). The reaction mixture was stirred for 3 h at 24 °C. Then, Sodium borohydride (204 mg, 5.40 mmol, 1.0 eq.) was added and the mixture was stirred for another 2 h. The reaction was quenched by the addition of H_2O (2.0 mL) and the precipitate was filtered and washed with tiethyl ether (20 mL). The organic layer was separated and the aqueous phase was extracted with diethyl ether (20 mL). The combined organic layers were dried over Na_2SO_4 and the volatiles were removed under reduced pressure. The crude product was then dissolved in CH_2Cl_2 (11 mL) and Et_3N (318 mg, 3.14 mmol, 1.4 eq.), DMAP (26.6 mg, 218 µmol, 0.1 eq.) and adamantine-1-carbonyl chloride (1.29 g, 6.48 mmol 1.2 eq.) were added at 0 °C. The mixture was stirred for 16 at 24 °C and the volatiles were removed under reduced pressure. Purification by flash column chromatography (Cyclohexane:EtOAc, 85:15) yield the title compound (662 mg, 1.57 mmol, 29%) as a yellow liquid.

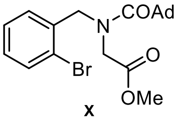

x
$C_{21}H_{26}BrNO_3$
M= 420,35 g.mol^{-1}

^{1}H NMR (500 MHz, $CDCl_3$): δ (ppm) 7.57 (d, *J* = 7.8 Hz, 1H), 7.33 (t, *J* = 7.5 Hz, 1H), 7.22 – 7.12 (m, 2H), 4.90 (s, 2H), 3.93 (s, 2H), 3.73 (s, 3H), 2.00 (s, 9H), 1.74 – 1.61 (m, 6H).

^{13}C NMR (126 MHz, $CDCl_3$): δ (ppm) 178.3, 170.2, 136.1, 133.2, 129.1, 127.9, 122.9, 53.4, 52.2, 50.1, 42.1, 39.2, 36.6, 28.5.

GC-MS (EI): Calcd for $C_{21}H_{26}{}^{79}BrNO_3$ $[M]^{+\bullet}$: 419, found 419

N-(2-bromobenzyl)-4-methyl-N-propylbenzenesulfonamide (2.71):

of 2-bromobenzaldehyde (2.00 g, 9.85 mmol, 1.00 eq.) was dissolved in CH_2Cl_2 (20 mL) and *n*-propylamine (640 mg, 10.8 mmol, 1.1 eq.) and Na_2SO_4 (4.20 g, 29.6 mmol, 3.0 eq.) was added. The mixture was stirred at roomtemperature for 3 h and sodium borohydride (186 mg, 4.93 mmol, 0.5 eq) was added. The reaction mixture was stirred for another 2 h before quenching with H_2O (2.0 mL). The aqueous phase was extracted with EtOAc (3X 20 mL) and the combined organic layers were washed with H_2O (20 mL) and brine (20 mL). The organic phase was dried over Na_2SO_4 and the volatiles were removed under reduced pressure. The crude mixture was dissolved again in CH_2Cl_2 (20 mL) and DMAP (120 mg, 985 µmol, 0.1 eq), DIPEA (3.82 g, 29.6 mmol, 3.0 eq.) and *p*-toluenesulfonyl chloride (2.82 g, 14.8 mmol, 1.5 eq.) were added. The reaction was stirred for 2 h at 24 °C and the volatiles were then removed under reduced pressure. Flash column chromatography (cyclohexane:EtOAc, 80:20) gave the title compound (1.75 g, 4.45 mmol, 45%) as colorless oil.

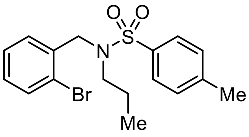

2.71

$C_{17}H_{20}BrNO_2S$

M= 382,32 g.mol^{-1}

^{1}H NMR (500 MHz, $CDCl_3$): 7.78 – 7.70 (m, 1H), 7.62 – 7.57 (m, 1H), 7.52 – 7.47 (m, 1H), 7.35 – 7.28 (m, 3H), 7.16 – 7.11 (m, 1H), 4.43 (s, 2H), 3.11 (dd, *J* = 9.0, 6.7 Hz, 2H), 2.44 (s, 3H), 1.43 – 1.31 (m, 2H), 0.74 (t, *J* = 7.4 Hz, 3H).

^{13}C NMR (126 MHz, $CDCl_3$): δ (ppm) 143.5, 137.1, 136.3, 132.7, 130.2, 129.1, 127.8, 127.3, 123.0, 51.9, 51.1, 21.7, 11.3.

GC-MS (EI): Calcd for $C_{17}H_{20}{}^{79}BrNO_2S$ $[M]^{+\bullet}$: 381, found 381

6.2 The effect of α-substitution on the reactivity of Pd(0)-catalyzed C(sp^3)−H activation for the formation of indanes

6.2.1 Catalyst preparation

^{tBuInd}Pd(IBiox6)Cl (3.19):

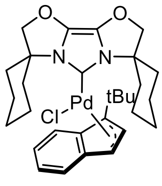

3.19
$C_{30}H_{40}ClN_2O_2Pd$
M= 602,53 g.mol^{-1}

The title compound (**10**) was prepared after a modified procedure from Kündig.[114] In the glovebox a schlenktube was charged with [^{tBuInd}PdCl]$_2$ (1.07 g, 1.71 mmol, 1.0 eq.) IBiox6.HOTf (1.50 g, 3.42 mmol, 2.0 equiv) and NaOtBu (329 mg, 3.42 mmol, 2.0 equiv) and sealed with a rubber septum. Outside the glovebox, 1,2-dimethoxyethan (70 mL) was added and the reaction was stirred at 24 °C for 18 h. The reaction was quenched with aq. NH_4Cl and extracted with CH_2Cl_2. The combined organic layers were washed with brine, dried over and evaporated under reduced pressure. The crude mixture was purified by column chromatography (cyclohexane:EtOAc, 80:20) to obtain a deep red slurry which was triturated in a diethyl ether/pentane mixture to obtain product **10** (1.25 g, 2.08 mmol, 61%) as bright yellow solid.

H NMR (500 MHz, C_6D_6): δ (ppm) 7.52 (dd, *J* = 7.7, 0.9 Hz, 1H), 6.98 (dt, *J* = 7.7, 4.3 Hz, 1H), 6.81 (d, *J* = 4.2 Hz, 2H), 6.64 (d, *J* = 2.8 Hz, 1H), 5.08 (d, *J* = 2.8 Hz, 1H), 4.03 – 3.99 (m, 3H), 3.96 (d, *J* = 8.5 Hz, 1H), 3.17 (td, *J* = 14.0, 4.1 Hz, 1H), 2.77 (td, *J* = 13.9, 4.1 Hz, 1H), 2.13 (td, *J* = 13.6, 12.9, 4.4 Hz, 1H), 1.88 – 1.83 (m, 1H), 1.83 – 1.77 (m, 2H), 1.73 (s, 9H), 1.51 – 1.41 (m, 5 H), 1.39 – 1.31 (m, 2H), 1.26 (td, *J* = 7.6, 6.9, 3.6 Hz, 1H), 1.23 – 1.17 (m, 1H), 1.10 (qt, *J* = 13.4, 3.6 Hz, 1H), 0.96 – 0.83 (m, 1H), 0.72 – 0.62 (m, 2H), 0.60 – 0.52 (m, 1H), 0.51 – 0.40 (m, 1H).

^{13}C NMR (126 MHz, C_6D_6): δ (ppm) 141.5, 141.3, 139.3, 126.5, 126.2, 124.8, 124.0, 120.8, 117.8, 116.7, 109.6, 84.4, 84.3, 65.1, 64.1, l63.1, 36.3, 35.6, 35.1, 35.0, 34.5, 29.9, 25.4, 24.2, 24.0, 24.0, 23.7, 23.4.

IR (neat): ν (cm^{-1}) 2939, 2859, 1756, 1453, 1415, 1350, 1209, 959, 853, 750

HRMS (ESI): Calcd for $C_{30}H_{39}N_2O_2$ Pd [M-Cl]$^+$: 565.2052, found 565.2061

Rf: 0.18 (cyclohexane/EtOAc 80:20)

Mp: decomposition upon heating

6.2.2 Substrate and reference for proto-dehalogenation synthesis

Dimethyl 2-ethyl-2-(4-fluorobenzyl)malonate (2.44ah-dehalo):

According to **general procedure G**, dimethyl 2-ethylmalonate (497 mg, 3.10 mmol, 1.0 equiv) 1-(bromomethyl)-4-fluorobenzene (700 mg, 3.70 mmol, 1.2 equiv) **2.44ah-dehalo** was obtained as a colorless oil (704 mg, 2.62 mmol, 85%).

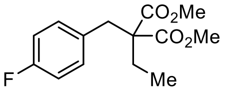

2.44ah-dehalo

$C_{14}H_{17}FO_4$

M= 268,28 g.mol^{-1}

^{1}H NMR (500 MHz, $CDCl_3$): δ (ppm) 7.08 – 7.00 (m, 2H), 6.98 – 6.92 (m, 2H), 3.71 (s, 6H), 3.20 (s, 2H), 1.84 (q, *J* = 7.6 Hz, 2H), 0.91 (t, *J* = 7.6 Hz, 2H).

^{13}C NMR (126 MHz, $CDCl_3$): δ (ppm) 171.7, 162.1 (d, *J* = 245.2 Hz), 132.0 (d, *J* = 3.2 Hz), 131.4 (d, *J* = 7.9 Hz), 115.3 (d, *J* = 21.2 Hz), 70.0 (d, *J* = 1.3 Hz), 52.5, 37.2, 25.2, 8.9.

^{19}F NMR (471 MHz, $CDCl_3$): δ (ppm) -115.9

IR (neat): ν (cm^{-1}) 2954, 1730, 1510, 1436, 1219, 1119, 841, 740

HRMS (ESI): Calcd for $C_{14}H_{17}FNaO_4$ $[M+Na]^+$: 291.1003, found 291.1007

Rf: 0.36 (cyclohexane/EtOAc 90:10)

Dimethyl 2-(ethyl-d5)-2-(4-fluorobenzyl)malonate (2.44ah-*d5*-dehalo):

According to **general procedure F**, dimethyl 2-(4-fluorobenzyl)malonate (252 mg, 1.05 mmol, 1.0 equiv) was reacted with iodoethane-*d5* (203 mg, 1.26 mmol, 1.2 equiv). **2.44ah-*d5*-dehalo** was obtained as a colorless oil (94.5 mg, 346 µmol, 33%).

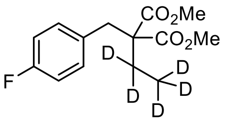

2.44ah-*d5*-dehalo

$C_{14}H_{12}D_5FO_4$

M=273,31 g.mol^{-1}

^{1}H NMR (500 MHz, $CDCl_3$): δ (ppm) 7.07 – 7.00 (m, 2H), 6.97 – 6.89 (m, 2H), 3.71 (s, 6H), 3.20 (s, 2H).

^{13}C NMR (126 MHz, $CDCl_3$): δ (ppm) 171.7, 162.1 (d, *J* = 245.2 Hz), 132.0 (d, *J* = 3.4 Hz), 131.4 (d, *J* = 7.9 Hz), 115.3 (d, *J* = 21.3 Hz), 59.5 52.4, 37.2.

^{19}F NMR (471MHz, $CDCl_3$): δ (ppm) -115.9

IR (neat): ν (cm^{-1}) 2954, 1730, 1510, 1436, 1222, 1102, 1069, 843

HRMS (ESI): Calcd for $C_{14}H_{12}D_5FNaO_4$ $[M+Na]^+$: 296.1317, found 296.1317

Rf: 0.24 (cyclohexane/EtOAc 95:5)

Trimethyl 3-(4-fluorophenyl)propane-1,2,2-tricarboxylate (2.44ak-dehalo):

According to **general procedure G**, 2-Methoxycarbonyl-succinic acid dimethyl ester (633 mg, 3.10 mmol, 1.0 equiv) was reacted with 1-(bromomethyl)-4-fluorobenzene (700 mg, 3.70 mmol, 1.2 equiv). **2.44ak-dehalo** was obtained as a colorless oil (682 mg, 2.18 mmol, 70%).

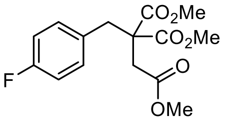

2.44ak-dehalo

$C_{15}H_{17}FO_6$

M= 312,29 g.mol^{-1}

^{1}H NMR (400 MHz, $CDCl_3$): δ 7.07 – 7.01 (m, 2H), 6.99 – 6.92 (m, 2H), 3.75 (s, 6H), 3.70 (s, 3H), 3.35 (s, 2H), 2.86 (s, 2H)

^{13}C NMR (126 MHz, $CDCl_3$): δ (ppm) 171.1, 170.4, 162.2 (d, *J* = 245.9 Hz), 131.7 (d, *J* = 8.0 Hz), 131.4 (d, *J* = 3.4 Hz), 115.5 (d, *J* = 21.2 Hz), 56.8 (d, *J* = 1.4 Hz), 53.0, 52.1, 38.1, 36.8

^{19}F NMR (376 MHz, $CDCl_3$): δ (ppm) -115.4

IR (neat): ν (cm^{-1}) 2956, 1733, 1511, 1282, 1221, 1168, 846,

HRMS (ESI): Calcd for $C_{15}H_{17}FNaO_6$ [M+Na]$^+$: 335.0901 found 335.0905

Rf: 0.19 (cyclohexane/EtOAc 90:10)

Dimethyl 2-cyclopropyl-2-(4-fluorobenzyl)malonate (2.44al-dehalo):

To a solution of **(2.44al)** (400 mg, 1.1 mmol, 1.0 eq.) and Et_3N (134 mg, 1.32 mmol, 1.2 eq.) in MeOH (X mL) under argon atmosphere Pd/C was added and the mixture was purged with H_2. The reaction was stirred for 18 h at 24 °C. The mixture was wiltered over a pad of celite and the volatiles removed under reduced pressure giving **2.44al-dehalo** (301 mg, 1.07 mmol, 97%) as a colorless liquid.

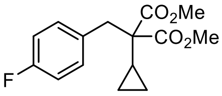

2.44al-dehalo
$C_{15}H_{17}FO_4$
M= 280,30 g.mol^{-1}

l**^{1}H NMR** (500 MHz, $CDCl_3$): δ (ppm) 7.17 – 7.11 (m, 2H), 6.97 – 6.91 (m, 2H), 3.70 (s, 6H), 3.27 (s, 2H), 1.14 (tt, *J* = 8.6, 5.6 Hz, 1H), 0.61 – 0.56 (m, 2H), 0.41 – 0.35 (m, 2H).

^{13}C NMR (126 MHz, $CDCl_3$): δ (ppm) 171.0, 162.1 (d, *J* = 245.1 Hz), 132.0 (d, *J* = 3.3 Hz), 131.8 (d, *J* = 7.9 Hz), 115.1 (d, *J* = 21.2 Hz), 60.2 (d, *J* = 1.3 Hz), 52.4, 40.7, 14.5, 2.9.

^{19}F NMR (376 MHz, $CDCl_3$): δ (ppm) -116.0

IR (neat): ν (cm^{-1}) 2954, 1729, 1510, 1436, 1245, 1199, 1048, 828

HRMS (ESI): Calcd for $C_{15}H_{17}FNaO_4$ [M+Na]$^+$: 303.1003, found 303.1004

Rf: 0.43 (cyclohexane/EtOAc 90:10)

Dimethyl 2-(2-(dimethylamino)-2-oxoethyl)-2-(4-fluorobenzyl)malonate (2.44am-dehalo):

According to **general procedure F**, dimethyl 2-(4-fluorobenzyl)malonate (500 mg, 2.08 mmol, 1.0 equiv) was reacted with 2-chloro-*N*,*N*-dimethylacetamide (354 mg, 2.91 mmol, 1.4 equiv). **2.44am-dehalo** was obtained as a colorless solid (552 mg, 2.08 mmol, 82%).

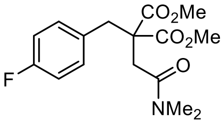

2.44am-dehalo
$C_{16}H_{20}FNO_5$
M= 325,34 g.mol^{-1}

^{1}H NMR (400 MHz, $CDCl_3$): δ 6.99 – 6.78 (m, 4H), 3.75 (s, 6H), 3.47 (s, 2H), 2.95 (s, 3H), 2.89 (s, 3H), 2.81 (s, 2H).

^{13}C NMR (126 MHz, $CDCl_3$): δ (ppm) 171.1, 169.6, 162.1 (d, *J* = 245.6 Hz), 132.5 (d, *J* = 3.4 Hz), 131.4 (d, *J* = 7.9 Hz), 115.4 (d, *J* = 21.1 Hz), 57.0 (d, *J* = 1.3 Hz), 52.9, 37.8, 37.2, 35.8, 35.6.

^{19}F NMR (376 MHz, $CDCl_3$): δ (ppm) -115.7

IR (neat): ν (cm^{-1}) 2962, 1729, 1641, 1510, 1209, 1182, 823

HRMS (ESI): Calcd for $C_{16}H_{21}FNNaO$ [M+Na]$^+$: 348.1218 found 348.1218

Rf: 0.43 (cyclohexane/EtOAc 50:50)

Dimethyl 2-(4-fluorobenzyl)-2-methylmalonate (2.44am-dehalo):

According to **general procedure G**, dimethyl 2-methylmalonate (453 mg, 3.10 mmol, 1.0 equiv) was reacted with 1-(bromomethyl)-4-fluorobenzene (700 mg, 3.70 mmol, 1.2 equiv). **2.44an-dehalo** was obtained as a colorless liquid (640 mg, 2.52 mmol, 81%).

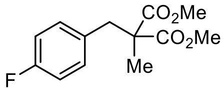

2.44an-dehalo
$C_{13}H_{15}FO_4$
M= 254,26 g.mol^{-1}

^{1}H NMR (400 MHz, $CDCl_3$): δ (ppm) 7.10–7.04 (m, 2H), 6.99 – 6.90 (m, 2H), 3.73 (s, 6H), 3.20 (s, 2H), 1.34 (s, 3H).

^{13}C NMR (126 MHz, $CDCl_3$): δ (ppm) 172.3, 162.1 (d, *J* = 245.3 Hz), 131.9 (d, *J* = 3.4 Hz), 131.8 (d, *J* = 7.9 Hz), 115.2 (d, *J* = 21.2 Hz), 55.0 (d, *J* = 1.3 Hz), 52.7, 40.64, 19.9.

^{19}F NMR (376 MHz, $CDCl_3$): δ (ppm) -115.9

IR (neat): ν (cm^{-1}) 2955, 1731, 1510, 1221, 1107, 841, 792

HRMS (ESI): Calcd for $C_{13}H_{15}FNaO_4$ [M+Na]$^+$: 277.0847, found 277.0852

Rf: 0.31 (cyclohexane/EtOAc 90:10)

Dimethyl 2-benzyl-2-(4-fluorobenzyl)malonate (2.44ao-dehalo):

According to **general procedure G**, dimethyl 2-benzylmalonate (689 mg, 3.10 mmol, 1.0 equiv) was reacted with 1-(bromomethyl)-4-fluorobenzene (700 mg, 3.70 mmol, 1.2 equiv). **2.44ao-dehalo** was obtained as a colorless oil (610 mg, 1.85 mmol, 60%).

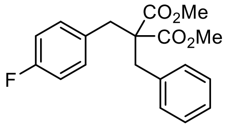

2.44ao-dehalo
$C_{19}H_{19}FO_4$
M= 330,36 g.mol^{-1}

^{1}H NMR (400 MHz, $CDCl_3$): δ (ppm) 7.33 – 7.22 (m, 3H), 7.16 – 7.09 (m, 4H), 7.00 – 6.92 (m, 2H), 3.64 (s, 6H), 3.23 (s, 2H), 3.18 (s, 3H)

^{13}C NMR (126 MHz, $CDCl_3$): δ (ppm) 171.3, 162.1 (d, *J* = 245.5 Hz), 136.1, 132.1 (d, *J* = 3.4 Hz), 131.7 (d, *J* = 7.9 Hz), 130.1, 128.48, 127.2, 115.2 (d, *J* = 21.3 Hz), 60.6 (d, *J* = 1.3 Hz), 52.4, 39.7, 38.8.

^{19}F NMR (376 MHz, $CDCl_3$): δ (ppm) -115.8

IR (neat): ν (cm^{-1}) 2952, 1728, 1510, 1201, 1173, 843, 701

HRMS (ESI): Calcd for $C_{19}H_{19}FNaO_4$ [M+Na]$^+$: 353.1160, found 353.1163

Rf: 0.42 (cyclohexane/EtOAc 90:10)

Dimethyl 2-(4-fluorobenzyl)-2-(methoxymethyl)malonate (2.44ap-dehalo):

According to **general procedure F**, dimethyl 2-(4-fluorobenzyl)malonate (500 mg, 2.08 mmol, 1.0 equiv) was reacted with MOMBr (364 mg, 2.91 mmol, 1.1 equiv). **2.44ap-dehalo** was obtained as a colorless oil (280.0 mg, 2.08 mmol, 48%).

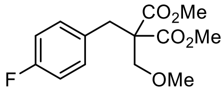

2.44ap-dehalo
$C_{14}H_{17}FO_5$
M= 284,11 g.mol^{-1}

^{1}H NMR (500 MHz, $CDCl_3$): δ 7.09 – 7.02 (m, 2H), 6.98 – 6.92 (m, 2H), 3.73 (s, 6H), 3.59 (s, 2H), 3.35 (s, 3H), 3.32 (s, 2H).

^{13}C NMR (126 MHz, $CDCl_3$): δ (ppm) 170.0, 162.1 (d, *J* = 245.2 Hz), 131.7 (d, *J* = 3.3 Hz), 131.6 (d, *J* = 7.9 Hz), 115.3 (d, *J* = 21.2 Hz), 71.1, 59.6 (d, *J* = 1.1 Hz), 52.7, 35.6.

^{19}F NMR (471 MHz, $CDCl_3$): δ (ppm) -115.9

IR (neat): ν (cm^{-1}) 2954, 1734, 1511, 1219, 1159, 1099, 848,

HRMS (ESI): Calcd for $C_{14}H_{17}FNaO_5$ [M+Na]$^+$: 307.0952 found 307.0956

Rf: 0.32 (cyclohexane/EtOAc 90:10)

Dimethyl 2-(2-bromo-4-fluorobenzyl)-2-ethylmalonate (2.44ah):

According to **general procedure F**, 2-(2-bromo-4-fluorobenzyl)malonate (1.00 g, 3.13 mmol, 1.0 equiv) was reacted with iodoethane (683 mg, 4.38 mmol, 1.4 equiv). **2.44ah** was obtained as a colorless oil (842 mg, 2.42 mmol, 78%).

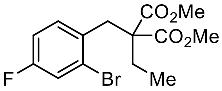

2.44ah

$C_{14}H_{16}FBrO_4$

M= 347,18 g.mol^{-1}

^{1}H NMR (400 MHz, $CDCl_3$): δ (ppm) 7.30-7.25 (m, 1H), 7.18 (dd, *J* = 8.7, 6.0 Hz, 1H), 6.94 (ddd, *J* = 8.7, 7.8, 2.7 Hz, 1H), 3.70 (s, 6H), 3.42 (s, 2H), 1.92 (q, *J* = 7.5 Hz, 2H), 0.93 (t, *J* = 7.5 Hz, 3H)

^{13}C NMR (126 MHz, $CDCl_3$): δ (ppm) 171.6, 161.2 (d, *J* = 250.4 Hz), 132.4 (d, *J* = 3.79 Hz) 132.2 (d, *J* = 8.2 Hz), 125.9 (d, *J* = 9.0 Hz), 120.2 (d, *J* = 24.2 Hz), 114.6 (d, *J* = 20.8 Hz), 59.5, 52.5, 36.8, 26.4, 9.4

^{19}F NMR (471 MHz, $CDCl_3$): δ (ppm) -113.7

IR (neat): ν (cm^{-1}) 2952, 1729, 1599, 1487, 1221, 1115, 1032, 879, 778

HRMS (ESI): Calcd for $C_{14}H_{16}{}^{79}BrFNaO_4$ $[M+Na]^+$: 369.0108, found 369.0111

Rf: 0.23 (pentane/EtOAc 95:5)

Dimethyl 2-(2-bromo-4-fluorobenzyl)-2-(ethyl-*d*$_5$)malonate (2.44ah-*d5*):

According to **general procedure F**, 2-(2-bromo-4-fluorobenzyl)malonate (1.02 g, 3.20 mmol, 1.0 equiv) was reacted with iodoethane-*d5* (721 mg, 4.48 mmol, 1.4 equiv). **2.44ah-*d5*** was obtained as a colorless oil (934 mg, 2.65 mmol, 83%).

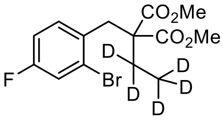

2.44ah-*d5*

$C_{14}H_{11}D_5BrFO_4$

M= 352,21 g.mol^{-1}

^{1}H NMR (400 MHz, $CDCl_3$): δ (ppm) 7.27 (dd, *J* = 8.2, 2.6 Hz, 1H), 7.17 (dd, *J* = 8.7, 6.1 Hz, 1H), 6.97-6.90 (m, 1H), 3.70 (s, 6H), 3.41 (s, 2H)

^{13}C NMR (126 MHz, $CDCl_3$): δ (ppm) 171.6, 161.2 (d, *J* = 250.3 Hz), 132.4 (d, *J* = 3.7 Hz), 132.2 (d, *J* = 8.3 Hz), 125.9 (d, *J* = 9.3 Hz), 120.2 (d, *J* = 24.1 Hz), 114.6 (d, *J* = 20.7 Hz), 59.3, 52.5, 36.7, 26.0-25.1 (m), 8.8-7.8 (m)

^{19}F NMR (471 MHz, $CDCl_3$): δ (ppm) -113.7

IR (neat): ν (cm^{-1}) 2953, 1729, 1600, 1488, 1227, 1069, 1033, 882, 859, 831

HRMS (ESI): Calcd for $C_{14}H_{11}{}^{79}BrD5NaO_4$ $[M+Na]^+$: 374.0422, found 374.0424

Rf: 0.23 (pentane/EtOAc 95:5)

Trimethyl 3-(2-bromo-4-fluorophenyl)propane-1,2,2-tricarboxylate (2.44ak):

According to **general procedure G**, 2-Methoxycarbonyl-succinic acid dimethyl ester (954 mg, 4.67 mmol, 1.0 equiv) was reacted with 2-bromo-4-fluorobenzyl bromide (1.50 g, 5.60 mmol, 1.2 equiv). **2.44ak** was obtained as a colorless oil (1.29 g, 3.30 mmol, 71%).

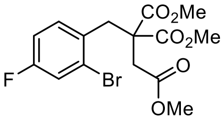

2.44ak

$C_{15}H_{16}BrFO_6$

M= 391,19 g.mol-1

^{1}H NMR (500 MHz, $CDCl_3$): δ 7.29 (dd, *J* = 8.3, 2.7 Hz, 1H), 7.10 (dd, *J* = 8.7, 6.0 Hz, 1H), 6.95 (td, *J* = 8.3, 2.7 Hz, 1H), 3.76 (s, 6H), 3.67 (s, 3H), 3.61 (s, 2H), 2.92 (s, 2H).

^{13}C NMR (126 MHz, $CDCl_3$): δ (ppm) 171.2, 170.4, 161.5 (d, *J* = 251.1 Hz), 132.5 (d, *J* = 8.3 Hz), 131.7 (d, *J* = 3.7 Hz), 126.0 (d, *J* = 9.4 Hz), 120.5 (d, *J* = 24.2 Hz), 114.9 (d, *J* = 20.9 Hz), 56.5 (d, *J* = 1.2 Hz), 53.1, 52.1, 37.2, 36.9.

^{19}F NMR (376 MHz, $CDCl_3$): δ (ppm) -112.8

IR (neat): ν (cm^{-1}) 2950, 2361, 1487, 1256, 1196, 1041, 846, 758

HRMS (ESI): Calcd for $C_{15}H_{16}{}^{79}BrFNaO_6$ [M+Na]$^+$: 413.0007, found 413.0011

Rf: 0.19 (cyclohexane/EtOAc 90:10)

Mp: 85.4 °C

Dimethyl 2-(2-bromo-4-fluorobenzyl)-2-cyclopropylmalonate (2.44al):

According to **general procedure G**, dimethyl 2-cyclopropylmalonate (1.34 g, 7.81 mmol, 1.0 equiv) was reacted with 2-bromo-4-fluorobenzyl bromide (2.72 g, 10.2 mmol, 1.3 equiv). **2.44al** was obtained as a colorless oil (1.76 g, 4.89 mmol, 63%).

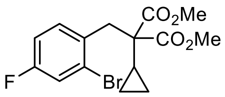

2.44al

$C_{15}H_{16}BrFO_4$

M= 359,19 g.mol^{-1}

^{1}**H NMR** (400 MHz, $CDCl_3$): δ (ppm) 7.23 (dd, *J* = 8.7, 6.1 Hz, 1H), 6.94 (ddd, *J* = 8.6, 7.7, 2.6 Hz, 1H), 3.71 (s, 6H), 3.51 (s, 2H), 1.24 – 1.13 (m, 1H), 0.62 – 0.52 (m, 2H), 0.49 – 0.36 (m, 2H).

^{13}**C NMR** (126 MHz, $CDCl_3$): δ (ppm) δ 170.9, 132.4 (d, *J* = 3.7 Hz), 132.3 (d, *J* = 8.2 Hz), 126.3 (d, *J* = 9.1 Hz), 120.2 (d, *J* = 24.2 Hz), 114.5 (d, *J* = 20.7 Hz), 59.8 (d, *J* = 1.1 Hz), 52.6, 39.1, 14.8, 3.5.

^{19}**F NMR** (376 MHz, $CDCl_3$): δ (ppm) -113.8

IR (neat): ν (cm^{-1}) 2950, 1727, 1599, 1486, 1242, 1195, 1174, 1045, 860, 698

HRMS (ESI): Calcd for $C_{15}H_{16}{}^{79}BrFNaO_4$ [M+Na]$^+$: 381.0108, found 381.0104

Rf: 0.35 (cyclohexane/EtOAc 90:10)

Dimethyl 2-(2-bromo-4-fluorobenzyl)-2-(2-(dimethylamino)-2-oxoethyl)malonate (2.44am):

According to **general procedure F**, 2-(2-bromo-4-fluorobenzyl)malonate (1.00 g, 3.13 mmol, 1.0 equiv) was reacted with 2-chloro-*N*,*N*-dimethylacetamide (533 mg, 4.38 mmol, 1.4 equiv). **2.44am** was obtained as a colorless solid (1.15 g, 2.84 mmol, 91%).

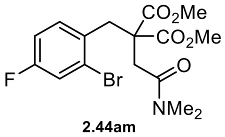

2.44am

$C_{16}H_{19}BrFNO_5$

M= 404,23 g.mol-1

^{1}**H NMR** (500 MHz, $CDCl_3$): δ (ppm) 7.28 (dd, *J* = 8.3, 2.7 Hz, 1H), 7.03 (dd, *J* = 8.6, 6.0 Hz, 1H), 6.93 (td, *J* = 8.3, 2.7 Hz, 1H), 3.75 (s, 6H), 3.68 (s, 2H), 2.92 (s, 3H), 2.92 (s, 3H), 2.87 (s, 2H).

^{13}**C NMR** (126 MHz, $CDCl_3$): δ (ppm) 171.1, 169.6, 161.4 (d, *J* = 250.7 Hz), 132.7 (d, *J* = 8.4 Hz), 132.6 (d, *J* = 3.7 Hz), 125.8 (d, *J* = 9.3 Hz), 120.4 (d, *J* = 24.1 Hz), 114.7 (d, *J* = 20.8 Hz), 56.7 (d, *J* = 1.3 Hz), 53.0, 37.3, 37.0, 36.4, 35.6.

^{19}**F NMR** (235 MHz, $CDCl_3$): δ (ppm) -113.2

IR (neat): ν (cm^{-1}) 2959, 1735, 1638 1485, 1203, 1134, 864, 674

HRMS (ESI): Calcd for $C_{16}H_{19}{}^{79}BrFNNaO_5$ [M+Na]$^+$: 426.0323, found 426.0325

Rf: 0.41 (cyclohexane/EtOAc 50:50)

Mp: 117.7 °C

Dimethyl 2-(2-bromo-4-fluorobenzyl)-2-methylmalonate (2.44an):

According to **general procedure F**, 2-(2-bromo-4-fluorobenzyl)malonate (500 mg, 1.57 mmol, 1.0 equiv) was reacted with MeI (267 mg, 1.88 mmol, 1.2 equiv). **2.44an** was obtained as a colorless solid (296 mg, 2.42, 888 µmol, 57%).

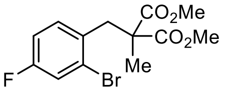

2.44an
$C_{13}H_{14}BrFO_4$
M= 333,15 g.mol^{-1}

^{1}H NMR (400 MHz, $CDCl_3$): δ (ppm) 7.30 (dd, *J* = 8.3, 2.7 Hz, 1H), 7.13 (dd, *J* = 8.7, 6.1 Hz, 1H), 6.94 (ddd, *J* = 8.7, 7.9, 2.7 Hz, 1H), 3.75 (s, 6H), 3.47 (s, 2H), 1.38 (s, 3H).

^{13}C NMR (126 MHz, $CDCl_3$): δ (ppm) 172.2, 161.3 (d, *J* = 250.5 Hz), 132.2 (d, *J* = 3.7 Hz), 132.2 (d, *J* = 8.2 Hz), 126.2 (d, *J* = 9.3 Hz), 120.3 (d, *J* = 24.2 Hz), 114.7 (d, *J* = 20.7 Hz), 55.2 (d, *J* = 1.3 Hz), 52.8, 38.9, 19.6.

^{19}F NMR (376 MHz, $CDCl_3$): δ (ppm) -113.5

IR (neat): ν (cm^{-1}) 2954, 1731, 1600, 1488, 1226, 1112, 882, 827

HRMS (ESI): Calcd for $C_{13}H_{14}{}^{79}BrFNaO_4$ $[M+Na]^+$: 354.9952, found 354.9954

Rf: 0.28 (cyclohexane/EtOAc 90:10)

Mp: 51.3 °C

Dimethyl 2-benzyl-2-(2-bromo-4-fluorobenzyl)malonate (2.44ao):

According to **general procedure B**, 2-(2-bromo-4-fluorobenzyl)malonate (500 mg, 1.57 mmol, 1.0 equiv) was reacted with benzyl bromide (376 mg, 2.20 mmol, 1.4 equiv). **2.44ao** was obtained as a colorless solid (615 mg, 1.50 mmol, 96%).

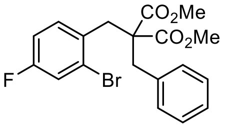

2.44ao
$C_{19}H_{18}BrFO_4$
M= 409,5 g.mol^{-1}

^{1}H NMR (500 MHz, $CDCl_3$): δ (ppm) 7.34 (dd, *J* = 8.7, 6.1 Hz, 1H), 7.31 – 7.22 (m, 4H), 7.14 – 7.10 (m, 2H), 6.98 – 6.90 (m, 1H), 3.62 (s, 6H), 3.41 (s, 2H), 3.35 (s, 2H).

^{13}C NMR (126 MHz, $CDCl_3$): δ (ppm) 171.1, 161.2 (d, *J* = 250.2 Hz), 136.0, 132.6 (d, *J* = 3.7 Hz), 132.3 (d, *J* = 8.2 Hz), 130.1, 128.4, 127.3, 126.1 (d, *J* = 9.3 Hz), 119.9 (d, *J* = 24.2 Hz), 114.5 (d, *J* = 20.6 Hz), 60.1, 52.6, 41.2, 38.3.

^{19}F NMR (235 MHz, $CDCl_3$): δ (ppm) -113.8

IR (neat): ν (cm^{-1}) 2947, 1726, 1485, 1242, 1194, 1173, 849, 698

HRMS (ESI): Calcd for $C_{19}H_{18}{}^{79}BrFNaO_4$ $[M+Na]^+$: 431.0265 found 431.0269

Rf: 0.32 (cyclohexane/EtOAc 95:5)

Mp: 70.0 °C

Dimethyl 2-(2-bromo-4-fluorobenzyl)-2-(methoxymethyl)malonate (2.44ap):

According to **general procedure F**, 2-(2-bromo-4-fluorobenzyl)malonate (700 mg, 2.19 mmol, 1.0 equiv) was reacted with MOMBr (328 mg, 2.63 mmol, 1.2 equiv). **2.44ap** was obtained as a colorless solid (710 mg, 1.96 mmol, 89%).

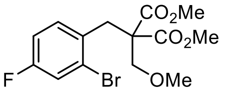

2.44ap

$C_{14}H_{16}BrFO_5$

M= 363,18 g.mol^{-1}

^{1}**H NMR** (500 MHz, $CDCl_3$): δ (ppm) δ 7.27 (dd, *J* = 8.3, 2.7 Hz, 1H), 7.23 (dd, *J* = 8.7, 6.1 Hz, 1H), 6.96 (ddd, *J* = 8.6, 7.9, 2.7 Hz, 1H), 3.74 (s, 6H), 3.64 (s, 2H), 3.53 (s, 2H), 3.34 (s, 3H).

^{13}**C NMR** (126 MHz, $CDCl_3$): δ (ppm) 169.9, 161.3 (d, *J* = 250.5 Hz), 133.0 (d, *J* = 8.3 Hz), 131.9 (d, *J* = 3.7 Hz), 125.6 (d, *J* = 9.5 Hz), 120.2 (d, *J* = 24.2 Hz), 114.6 (d, *J* = 20.8 Hz), 71.6, 59.1, 58.9, 52.8, 35.0.

^{19}**F NMR** (235 MHz, $CDCl_3$): δ (ppm) -113.5

IR (neat): ν (cm^{-1}) 2921, 2885, 1728, 1487, 1227, 1201, 1100, 872, 797

HRMS (ESI): Calcd for $C_{14}H_{16}{}^{79}BrFNaO_5$ $[M+Na]^+$: 385.0057, found 385.0056

Rf: 0.25 (cyclohexane/EtOAc 90:10)

Mp: 86.3

6.2.3 Product syntheses

General procedure H: Synthesis of indane products by Pd(0)-catalyzed C(sp^3)−H activation of methylene C−H bonds.

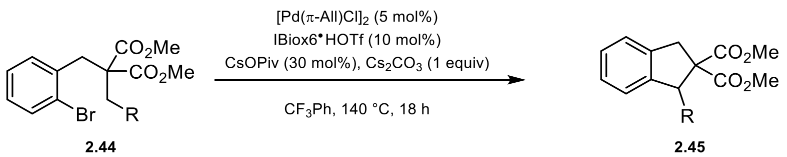

In an 2-5 mL microwave reaction vial, substrate (0.2 mmol) was introduced. Then the tube was transferred in the glovebox and [Pd(π-allyl)Cl]$_2$ (3.7 mg, 10 μmol, 5 mol%), IBiox6·HOTf (11.4 mg, 20 μmol, 10 mol%), cesium pivalate (14 mg, 60 μmol, 30 mol%), caesium carbonate (65 mg, 0.2 mmol, 1 equiv) and 5Å molecular sieves powder (50 mg) were introduced and the vial was then sealed. Outside of the glovebox, *α,α,α*-trifluorotoluene (2 mL) was added. The reaction was stirred at room temperature for 10 min. The vial was then introduced in a 140°C preheated aluminum block and stirred at this temperature for 15 hours. After this period the reaction was cooled to room temperature, diluted with CH_2Cl_2 (1.0 mL), filtered over a pad of Celite (washed three times with 1 mL of CH_2Cl_2). The crude material was analyzed by GC-MS and then concentrated and purified by preparative HPLC chromatography (EtOAc/hexane) to yield the corresponding indane product.

Dimethyl 6-fluoro-1-methyl-1,3-dihydro-2*H*-indene-2,2-dicarboxylate (2.45ah):

According to **general procedure H** the title compound (27.0 mg, 101 µmol, 51%) was obtained as a colorless oil.

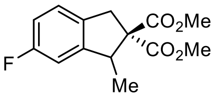

2.45ah
$C_{14}H_{15}FO_4$
M= 266,27 g.mol^{-1}

^{1}H NMR (500 MHz, CDCl$_3$): δ (ppm) 7.10 (dd, *J* = 9.0, 5.1 Hz, 1H), 6.89 – 6.80 (m, 2H), 4.00 (q, *J* = 7.2 Hz, 1H), 3.74 (s, 3H), 3.73 (s, 3H), 3.70 (d, *J* = 16.2 Hz, 1H), 3.25 (d, *J* = 16.2 Hz, 1H), 1.22 (d, *J* = 7.2 Hz, 3H).

^{13}C NMR (126 MHz, CDCl$_3$): δ (ppm) 172.1, 170.6, 162.7 (d, *J* = 243.7 Hz), 147.7 (d, *J* = 7.8 Hz), 134.4 (d, *J* = 2.6 Hz), 125.2 (d, *J* = 8.6 Hz), 114.1 (d, *J* = 22.5 Hz), 110.7 (d, *J* = 22.7 Hz), 65.4, 53.0, 52.6, 45.2 (d, *J* = 2.2 Hz), 38.5, 16.5.

^{19}F NMR (376 MHz, CDCl$_3$): δ (ppm) -116.2

IR (neat): ν (cm^{-1}) 2956, 2361, 1731, 1489, 1239, 1077, 872, 812

HRMS (ESI): Calcd for $C_{14}H_{15}FNaO_4$ [M+Na]$^+$: 289.0847, found 289.0845

Rf: 0.20 (cyclohexane/EtOAc 95:5)

Dimethyl 6-fluoro-1-(methyl-*d*$_3$)-1,3-dihydro-2*H*-indene-2,2-dicarboxylate-1-*d* (2.45ah-*d4*):

According to **general procedure H** the title compound (17.0 mg, 62.9 µmol, 32%) was obtained as a colorless oil.

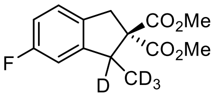

2.45ah-*d4*
$C_{14}H_{11}D_4FO_4$
M= 270,29 g.mol^{-1}

^{1}H NMR (250 MHz, CDCl$_3$): δ (ppm) 7.13 – 7.05 (m, 1H), 6.89 – 6.80 (m, 2H), 3.74 (s, 3H), 3.73 (s, 3H), 3.70 (d, *J* = 16.4 Hz, 1H), 3.25 (d, *J* = 16.4 Hz, 1H).

^{13}C NMR (126 MHz, CDCl$_3$): δ (ppm) 172.1, 170.6, 162.6 (d, *J* = 243.6 Hz), 147.6 (d, *J* = 7.9 Hz), 134.4 (d, *J* = 2.6 Hz), 125.2 (d, *J* = 8.6 Hz), 114.1 (d, *J* = 22.5 Hz), 110.7 (d, *J* = 22.6 Hz), 65.2, 53.0, 52.5, 38.5.

^{19}F NMR (376 MHz, CDCl$_3$): δ (ppm) -116.2

IR (neat): ν (cm^{-1}) 2955, 2848, 1732, 1489, 1257, 1164, 906, 729

HRMS (ESI): Calcd for $C_{14}H_{11}D_4FNaO_4$ [M+Na]$^+$: 293.1098, found 293.1102

Rf: 0.22 (cyclohexane/EtOAc 95:5)

Trimethyl 6-fluoro-1,3-dihydro-2*H*-indene-1,2,2-tricarboxylate (2.45ak):

According to **general procedure H** the title compound (52.0 mg, 168 µmol, 84%) was obtained as a colorless oil.

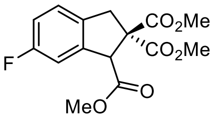

2.45ak
$C_{15}H_{15}FO_6$
M= 310,28 g.mol-1

^{1}H NMR (400 MHz, CDCl$_3$): δ (ppm) 7.16 (dd, *J* = 8.3, 5.1 Hz, 1H), 7.07 (dd, *J* = 8.6, 2.5 Hz, 1H), 6.92 (td, *J* = 8.7, 2.5 Hz, 1H), 4.80 (s, 1H), 3.93 (d, *J* = 16.0 Hz, 1H), 3.75 (s, 3H), 3.72 (s, 3H), 3.68 (s, 3H), 3.43 (d, *J* = 16.0 Hz, 1H).

^{13}C NMR (126 MHz, CDCl$_3$): δ (ppm) 171.2, 170.7, 169.5, 162.4 (d, *J* = 245.0 Hz), 140.4 (d, *J* = 8.5 Hz), 135.8 (d, *J* = 2.7 Hz), 125.9 (d, *J* = 8.6 Hz), 115.7 (d, *J* = 22.5 Hz), 112.2 (d, *J* = 23.3 Hz), 64.4, 56.3 (d, *J* = 2.2 Hz), 53.6, 53.1, 52.6, 39.1.

^{19}F NMR (376 MHz, CDCl$_3$): δ (ppm) -115.3

IR (neat): ν (cm^{-1}) 2956, 2361, 1733, 1435, 1238, 1163, 1011, 879

HRMS (ESI): Calcd for $C_{15}H_{15}FNaO_6$ [M+Na]$^+$: 333.0754, found 333.0752

Rf: 0.23 (cyclohexane/EtOAc 90:10)

Dimethyl 6'-fluorospiro[cycloprpane-1,1'-indene]-2',2'(3'H)-dicarboxylate (2.45al):

According to **general procedure H** the title compound (37.0 mg, 133 µmol, 67 %) was obtained as a colorless solid.

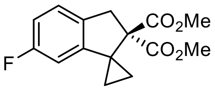

2.45al
$C_{15}H_{15}FO_4$
M= 278,28 g.mol-1

^{1}H NMR (500 MHz, $CDCl_3$): δ (ppm) δ 7.11 – 7.05 (m, 1H), 6.79 (ddd, *J* = 9.2, 8.3, 2.4 Hz, 1H), 6.37 (dd, *J* = 9.0, 2.4 Hz, 1H), 3.71 (s, 6H), 3.67 (s, 2H), 1.22 – 1.18 (m, 2H), 1.02 – 0.98 (m, 2H).

^{13}C NMR (126 MHz, $CDCl_3$): δ (ppm) 170.8, 163.1 (d, *J* = 243.4 Hz), 148.4 (d, *J* = 8.3 Hz), 133.9 (d, *J* = 2.5 Hz), 125.0 (d, *J* = 8.9 Hz), 113.3 (d, *J* = 22.7 Hz), 105.9 (d, *J* = 23.5 Hz), 64.5, 52.8, 39.7, 31.7 (d, *J* = 2.5 Hz), 15.0.

^{19}F NMR (376 MHz, $CDCl_3$): δ (ppm) -115.9

IR (neat): ν (cm^{-1}) 2958, 2361, 1730, 1493, 1251, 1155, 1059, 859

HRMS (ESI): Calcd for $C_{15}H_{15}FNaO_4$ [M+Na]$^+$: 301.0847, found 301.0853

Rf: 0.15 (cyclohexane/EtOAc 95:5)

Mp: 110.5 °C

Dimethyl 1-(dimethylcarbamoyl)-6-fluoro-1,3-dihydro-2*H*-indene-2,2-dicarboxylate (2.45am):

According to **general procedure H** the title compound (47.0 mg, 145 µmol, 73%) was obtained as a colorless oil.

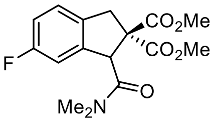

2.45am
$C_{16}H_{18}FNO_5$
M= 323,32 g.mol-1

^{1}H NMR (500 MHz, $CDCl_3$): δ 7.15 (dd, *J* = 8.3, 5.1 Hz, 1H), 6.91 – 6.84 (m, 2H), 5.21 (s, 1H), 4.14 (d, *J* = 16.1 Hz, 1H), 3.72 (s, 3H), 3.71 (s, 3H), 3.37 (s, 3H), 3.37 (d, *J* = 16.1 Hz, 1H), 2.92 (s, 3H).

^{13}C NMR (126 MHz, $CDCl_3$): δ (ppm) 171.6, 171.4, 169.9, 162.3 (d, *J* = 244.1 Hz), 142.3 (d, *J* = 8.2 Hz), 136.9 (d, *J* = 2.7 Hz), 126.1 (d, *J* = 8.9 Hz), 115.1 (d, *J* = 22.4 Hz), 111.1 (d, *J* = 23.0 Hz), 65.5, 53.5, 53.1 (d, *J* = 2.0 Hz), 53.0, 39.6, 38.6, 36.0.

^{19}F NMR (376 MHz, $CDCl_3$): δ (ppm) -116.1

IR (neat): ν (cm^{-1}) 2959, 2361, 1730, 1640, 1492, 1219, 1161, 835, 628

HRMS (ESI): Calcd for $C_{16}H_{18}FNNaO_5$ [M+Na]$^+$: 346.1061, found 346.1067

Rf: 0.36 (cyclohexane/EtOAc 50:50)

Mp: 126.4 °C

Dimethyl 5-fluoro-1,3-dihydro-2*H*-indene-2,2-dicarboxylate (2.44an):

According to **general procedure H** the title compound (39.0 mg, 155 µmol, 77%) was obtained as a colorless oil.

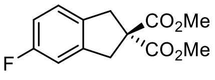

2.44an
$C_{13}H_{13}FO_4$
M= 252,24 g.mol-1

^{1}H NMR (500 MHz, $CDCl_3$): δ (ppm) 7.15 – 7.09 (m, 1H), 6.92 – 6.82 (m, 2H), 3.75 (s, 6H), 3.57 (s, 2H), 3.54 (s, 2H).

^{13}C NMR (126 MHz, $CDCl_3$): δ (ppm) 172.0, 162.5 (d, *J* = 243.7 Hz), 142.1 (d, *J* = 8.4 Hz), 135.4 (d, *J* = 2.5 Hz), 125.3 (d, *J* = 8.9 Hz), 114.1 (d, *J* = 22.5 Hz), 111.5 (d, *J* = 22.6 Hz), 60.9, 53.2, 40.7 (d, *J* = 2.3 Hz), 39.9.

^{19}F NMR (376 MHz, $CDCl_3$): δ (ppm) -116.5

IR (neat): ν (cm^{-1}) 2956, 2934, 1734, 1486, 1239, 1210, 1076, 809, 714

HRMS (ESI): Calcd for $C_{13}H_{13}FNaO_4$ [M+Na]$^+$: 275.0690, found 275.0695

Rf: 0.30 (cyclohexane/EtOAc 90:10)

Mp: 83.7 °C

Dimethyl 6-fluoro-1-phenyl-1,3-dihydro-2*H*-indene-2,2-dicarboxylatedicarboxylate (2.45ao):

Under Ar atmosphere at 0 °C dimethyl malonate (291 mg, 2.2 mmol, 1.1 eq.) was added to a suspension of NaH (264 mg, 60%, 6.60 mmol, 3.3 eq.) in THF (10 mL). After stirring for 30 min a solution of 2-(bromo(phenyl)methyl)-1-(bromomethyl)-4-fluorobenzene (715 mg, 2.00 mmol, 1.0 eq.) in THF (6.0 mL) was added. The reaction was heated to reflux for 16 h and then quenched by the addition of H_2O. The layers were separated and the aqueous phase was extracted with Et_2O (3 x 15 mL). The combined organic layers were dried over Na_2SO_4 and concentrated under reduced pressure. The crude product was purified by flash column chromatography (cyclohexane/EtOAc 90:10) to obtain the title compound (360 mg, 1.10 mmol, 55 %) as a colorless solid.

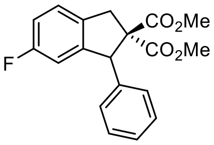

2.45ao
$C_{19}H_{17}FO_5$
M= 328,34 g.mol-1

^{1}H NMR (250 MHz, $CDCl_3$): δ (ppm) 7.25 – 7.19 (m, 4H), 7.11 – 7.01 (m, 2H), 6.96 – 6.89 (m, 1H), 6.73 (dd, *J* = 8.8, 2.5 Hz, 1H), 5.33 (s, 1H), 3.97 (d, *J* = 16.6 Hz, 1H), 3.76 (s, 3H), 3.32 (d, *J* = 16.6 Hz, 1H), 3.21 (s, 3H).

^{13}C NMR (126 MHz, $CDCl_3$): δ (ppm) 172.1, 169.6, 162.7 (d, *J* = 244.3 Hz), 145.7 (d, *J* = 8.0 Hz), 139.3, 135.6 (d, *J* = 2.5 Hz), 129.3, 128.3, 127.6, 125.4 (d, *J* = 8.7 Hz), 114.9 (d, *J* = 22.7 Hz), 112.4 (d, *J* = 22.6 Hz), 67.1, 56.8 (d, *J* = 2.3 Hz), 53.2, 52.2, 39.1

^{19}F NMR (376 MHz, $CDCl_3$): δ (ppm) -115.6

IR (neat): ν (cm^{-1}) 2951, 2361, 1727, 1487, 1248, 1206, 747, 705

HRMS (ESI): Calcd for $C_{19}H_{17}FNaO_4$ $[M+Na]^+$: 351.1003, found 351.1008

Rf: 0.25 (cyclohexane/EtOAc 90:10)

Mp: 110.7 °C

Dimethyl 6-fluoro-1-methoxy-1,3-dihydro-2*H*-indene-2,2-dicarboxylate (2.45ap):

According to **general procedure H** the title compound (9.00 mg, 31.9 µmol, 16%) was obtained as a colorless oil.

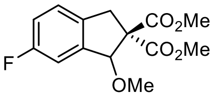

2.45ap
$C_{14}H_{15}FO_5$
M= 282,27 g.mol-1

^{1}H NMR (500 MHz, $CDCl_3$): δ (ppm) 7.16 (dd, *J* = 8.3, 5.0 Hz, 1H), 7.06 (dd, *J* = 8.4, 2.5 Hz, 1H), 6.98 (td, *J* = 8.7, 2.5 Hz, 1H), 5.30 (s, 1H), 3.86 (d, *J* = 16.4 Hz, 1H), 3.77 (s, 3H), 3.74 (s, 3H), 3.49 (s, 3H), 3.17 (d, *J* = 16.1 Hz, 1H).

^{13}C NMR (151 MHz, $CDCl_3$): δ (ppm) 171.3, 168.8, 162.3 (d, *J* = 244.7 Hz), 142.1 (d, *J* = 7.7 Hz), 135.6 (d, *J* = 2.6 Hz), 126.0(d, *J* = 8.5 Hz), 116.4 (d, *J* = 22.6 Hz), 112.3 (d, *J* = 22.5 Hz), 87.0 (d, *J* = 2.2 Hz), 66.6, 58.4, 53.1, 52.9, 37.9.

^{19}F NMR (376 MHz, $CDCl_3$): δ (ppm) -115.9

IR (neat): ν (cm^{-1}) 2954, 2842, 1735, 1436, 1243, 1120, 1087, 650

HRMS (ESI): Calcd for $C_{14}H_{15}FNaO_5$ $[M+Na]^+$: 305.0796, found 305.0801

Rf: 0.31 (cyclohexane/EtOAc 90:10)

6.2.4 Kinetic experiments

General procedure I

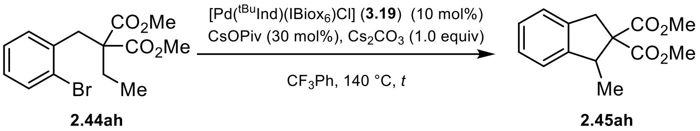

CO2Me
CO2Me
Br
Me
2.44ah
[Pd(tBuInd)(IBiox6)Cl] (3.19) (10 mol%)
CsOPiv (30 mol%), Cs2CO3 (1.0 equiv)
CF3Ph, 140 °C, t
CO2Me
CO2Me
Me
2.45ah

Inside a glovebox, CsOpiv (14.0 mg, 60 µmol, 0.3 eq.) and Cs_2CO_3 (65.2 mg, 0.2 mmol, 1.0 eq) were weighted 7 times and charged in 7 different catalysis tubes individually. Stock solutions of [Pd(^{tBu}Ind)(IBiox6)Cl] (20 µmmol/mL) and substrate (200 µmol/mL) in CF_3Ph were prepared and 1 mL of each was added in each tube to reach a concentration of 0.1 M. The tubes were capped, taken out of the glovebox and inserted in a preheated metal block at 140 °C with a stirring rate of 1000 rpm. The reactions were stopped at different times and cooled to 24 °C by inserting the tubes into another metal block. A stock solution of the internal standard (200 µmol/mL) in CF_3Ph was prepared and 1 mL was added to each tube after the reaction. The mixture was filtered over a short pad of silica and analysed by ^{19}F NMR against the standard.

Orders by VTNA

Order on Aryl bromide

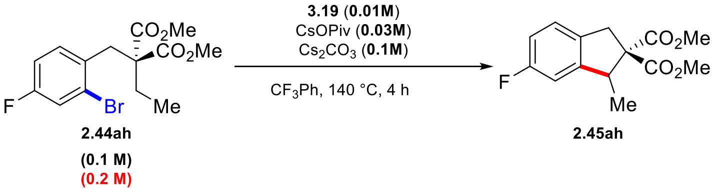

CO2Me
CO2Me
F
Br
Me
2.44ah
(0.1 M)
(0.2 M)
3.19 (0.01M)
CsOPiv (0.03M)
Cs2CO3 (0.1M)
CF3Ph, 140 °C, 4 h
F
CO2Me
CO2Me
Me
2.45ah

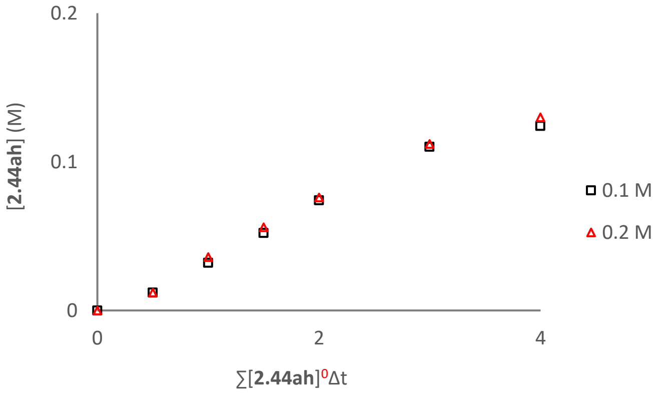

The reaction displays zero order with respect to the concentration of aryl bromide starting material. This suggests that the oxidative addition is not kinetically relevant in this reaction.

Order on catalyst

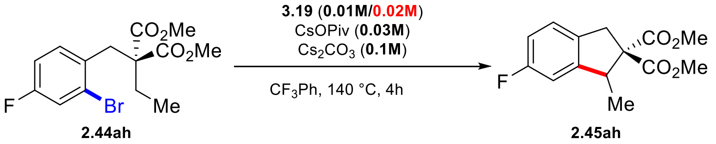
3.19 (0.01M/0.02M)
CsOPiv (0.03M)
Cs_2CO_3 (0.1M)
CF_3Ph, 140 °C, 4h
CO_2Me
CO_2Me
F
Br
Me

2.44ah
(0.1 M)

2.45ah

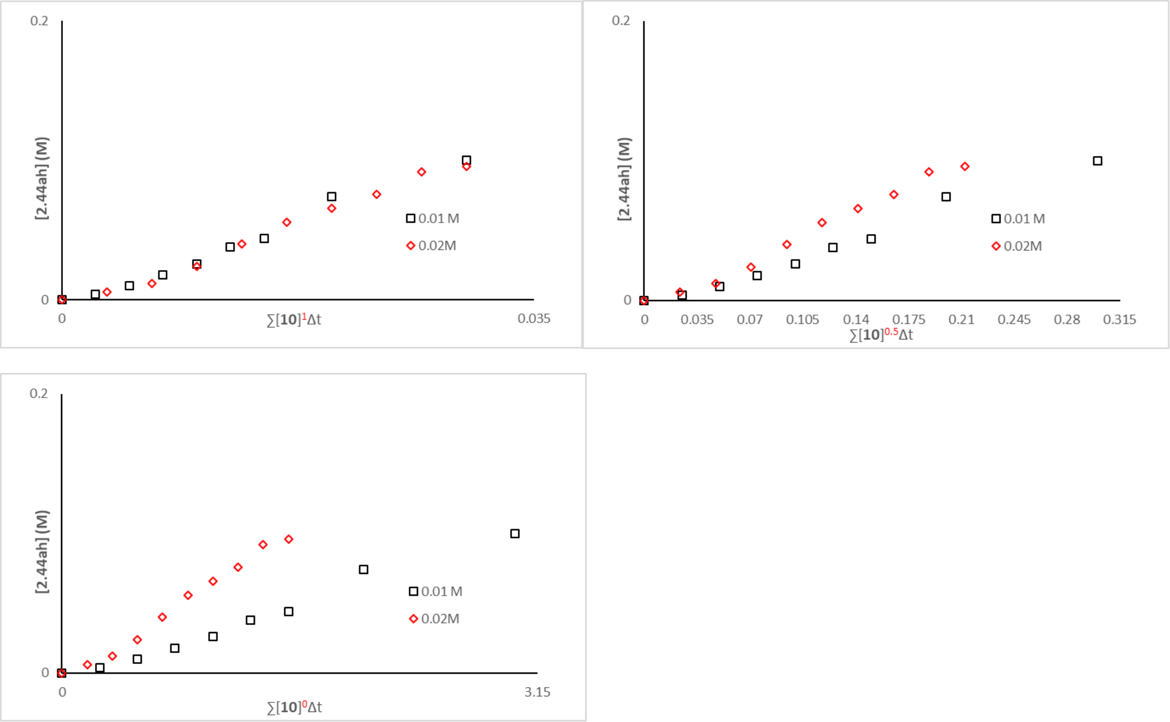

Clockwise from top left: Order 1 on catalyst, Order 0.5 on catalyst, Order 0 on catalyst. The curves overlay when the power is raised to 1, suggesting 1st order dependence on the concentration of catalyst for this reaction.

Order on Cs_2CO_3

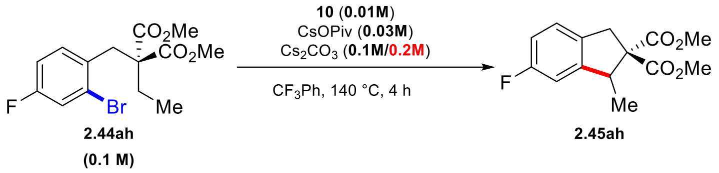
CO2Me
CO2Me
F
Br
Me
2.44ah
(0.1 M)
10 (0.01M)
CsOPiv (0.03M)
Cs2CO3 (0.1M/0.2M)
CF3Ph, 140 °C, 4 h
CO2Me
CO2Me
F
Me
2.45ah

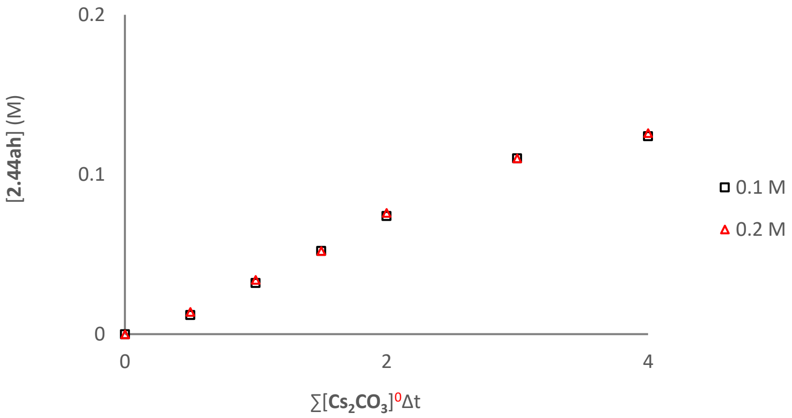

The reaction displays zero order with respect to the concentration of Cs_2CO_3. However, this is most likely as a result of saturation kinetics being observed for this inorganic base in a $PhCF_3$.

Order on CsOPiv

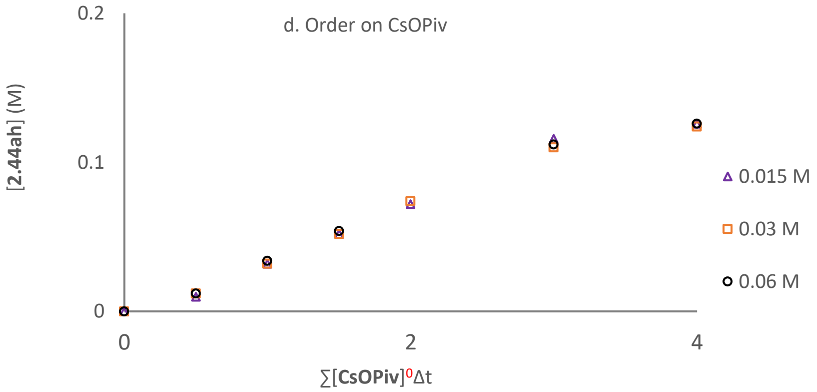

The reaction displays zero order with respect to the concentration of CsOPiv. This could suggest that the pivalate is not engaged in the C–H activation step, however due to the low solubility of CsOPiv in $PhCF_3$, it is not possible with this data to rule out the observation of zero order kinetics due to saturation.

Reaction at different stirring rates

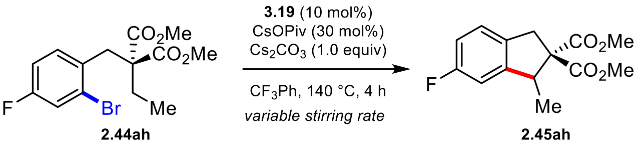
CO2Me
CO2Me
F
Br
Me
2.44ah
3.19 (10 mol%)
CsOPiv (30 mol%)
Cs2CO3 (1.0 equiv)
CF3Ph, 140 °C, 4 h
variable stirring rate
CO2Me
CO2Me
F
Me
2.45ah

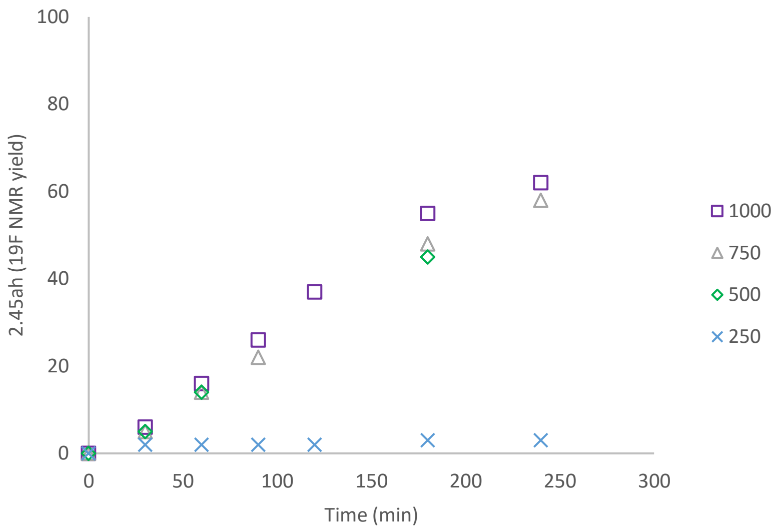

The reaction displays significant variation when the stirring rate is altered. This suggests that one of the inorganic bases in the reaction (or both) are involved in a kinetically relevant step

Reaction without Cs_2CO_3

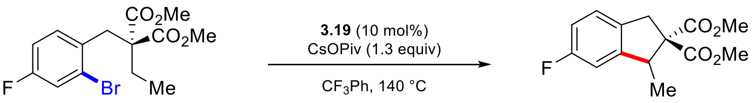
CO2Me
CO2Me
F
Br
Me
3.19 (10 mol%)
CsOPiv (1.3 equiv)
CF3Ph, 140 °C
CO2Me
CO2Me
F
Me

The reaction failed to give any product formation in the absence of Cs_2CO_3. Only the corresponding protodehalogenated starting material was detected.

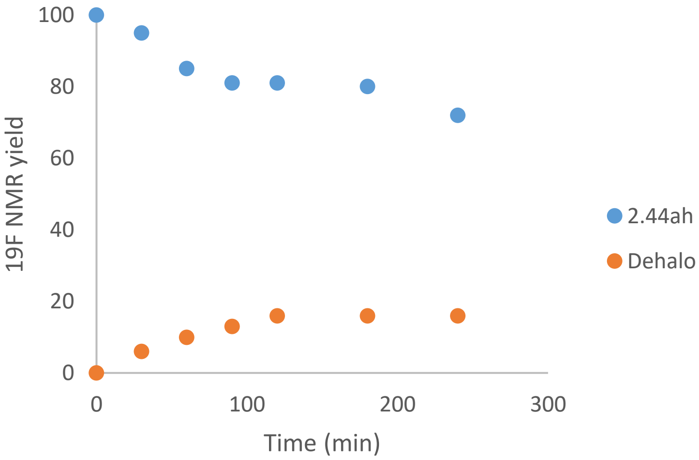

Reaction without CsOPiv

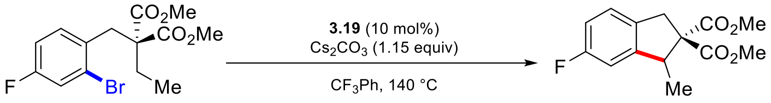

CO2Me
CO2Me
F
Br
Me
3.19 (10 mol%)
Cs2CO3 (1.15 equiv)
CF3Ph, 140 °C
F
CO2Me
CO2Me
Me

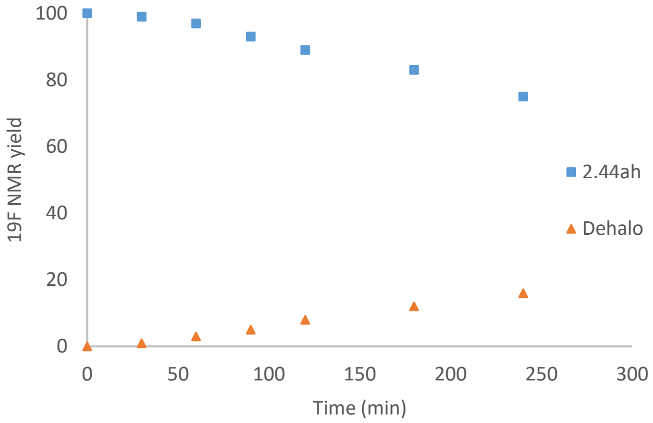

The reaction failed to give any product formation in the absence of CsOPiv. Only the corresponding protodehalogenated starting material was detected

General procedure J

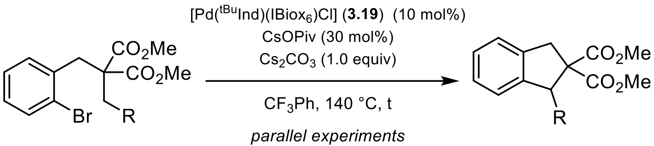
[Pd(tBuInd)(IBiox6)Cl] (3.19) (10 mol%)
CsOPiv (30 mol%)
Cs2CO3 (1.0 equiv)
CF3Ph, 140 °C, t
parallel experiments
CO2Me
CO2Me
Br
R

2.44 **2.45**

Inside a glovebox, CsOpiv (14.0 mg, 60 µmol, 0.3 eq.) and Cs_2CO_3 (65.2 mg, 0.2 mmol, 1.0 eq) were weighted 7 times and charged in 7 different catalysis tubes individually. Stock solutions of [Pd(^{tBu}Ind)(IBiox6)Cl] (20 µmmol/mL) and substrate (200 µmol/mL) in CF_3Ph were prepared and 1 mL of each was added in each tube to reach a concentration of 0.1 M. The tubes were capped, taken out of the glovebox and inserted in a preheated metal block at 140 °C. The reactions were stopped at different times and immediately cooled to 24 °C by inserting the tubes into another metal block. A stock solution of the external standard (200 µmol/mL) in CF_3Ph was prepared and 1 mL was added to each tube after the reaction. The mixture was filtered over a short pad of silica and analysed by ^{19}F NMR against the standard.

Initial rate experiments

2.44ah

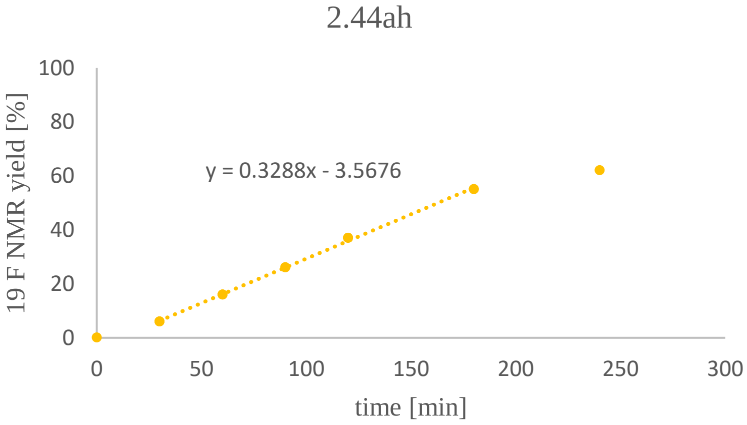

Time [min]	^{19}F NMR yield [%]
30	6
60	16
90	26
120	37
180	55
240	62

2.44ah-*d5*

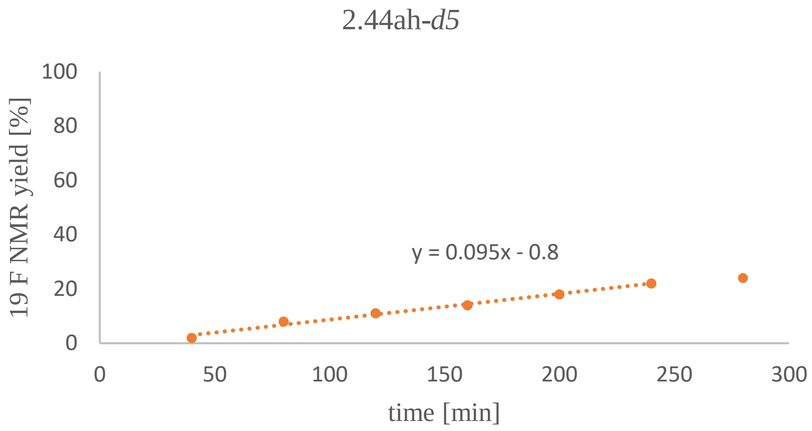

Time [min]	^{19}F NMR yield [%]
40	2
80	8
120	11
160	14
200	18
240	22
280	24

2.44ak

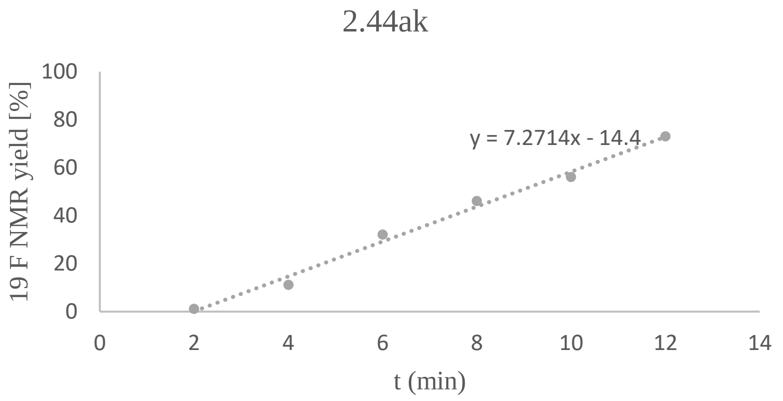

Time [min]	^{19}F NMR yield [%]
3	1
6	11
9	32
12	46
15	56
20	73

2.44al

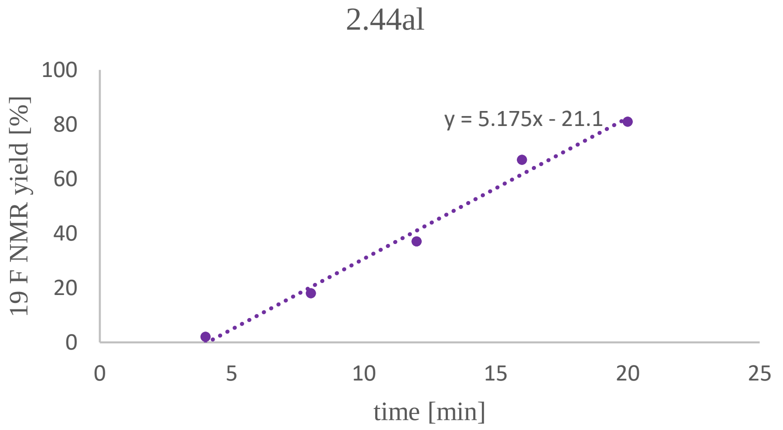

Time [min]	^{19}F NMR yield [%]
4	2
8	18
12	37
16	67
20	81

2.44am

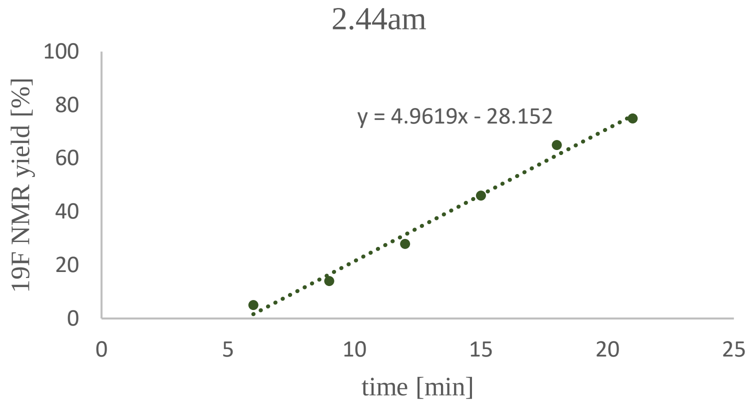

Time [min]	^{19}F NMR yield [%]
6	5
9	14
12	28
15	46
18	65
21	75

2.44an

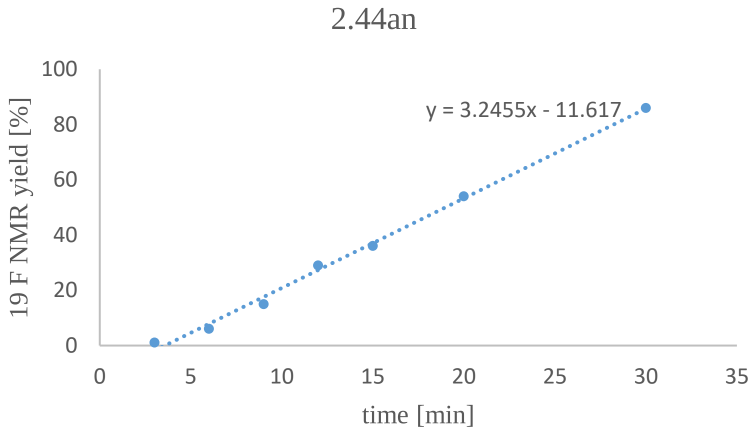

Time [min]	^{19}F NMR yield [%]
3	1
6	6
9	15
12	29
15	36
20	54
30	86

2.44ao

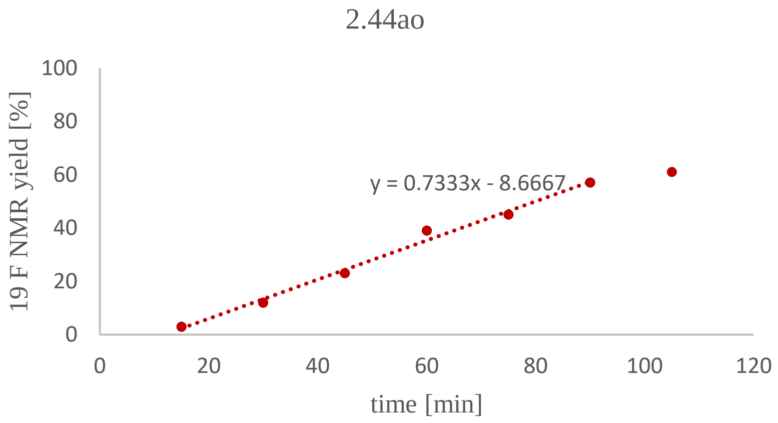

Time [min]	^{19}F NMR yield [%]
15	3
30	12
45	23
60	39
75	45
90	57
105	61

2.44ap

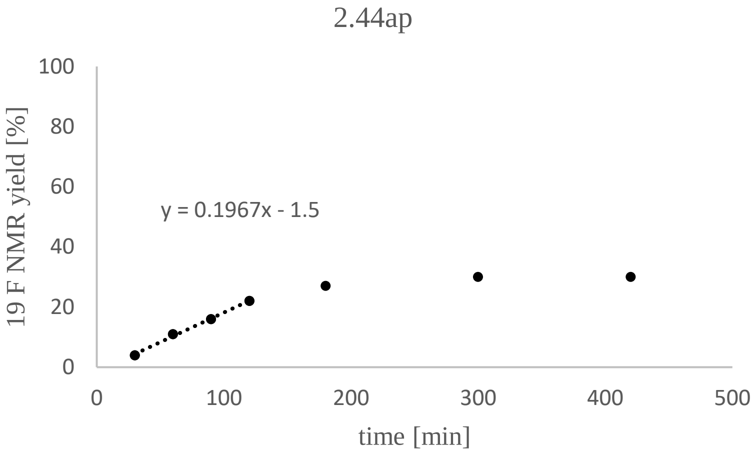

Time [min]	^{19}F NMR yield [%]
30	4
60	11
90	16
120	22
180	27
300	30
420	30

6.3 Enantioselective remote C(sp^3)−H activation by 1,4-Pd shift

6.3.1 Substrate synthesis

2-(3-Bromo-2-methoxyphenyl)-*N*,*N*-dimethylacetamide (4.16a):

The title compound (1.04 g, 3.82 mmol, 47%) was obtained following a literature procedure from 2-(3-bromo-2-methoxyphenyl)acetic acid (2.0 g, 8.16 mmol, 1.0 eq.) and dimethylamine hydrochloride (732 mg, 8.98 mmol, 1.10 eq.).[185]

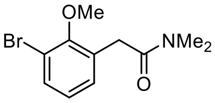

4.16a
$C_{11}H_{14}BrNO_2$
M= 272.14

^{1}H NMR (500 MHz, CDCl$_3$): δ (ppm) 7.45 (dd, *J* = 7.9, 1.6 Hz, 1H), 7.21 (dd, *J* = 7.7, 1.6 Hz, 1H), 6.95 (t, *J* = 7.8 Hz, 1H), 3.82 (s, 3H), 3.75 (s, 2H), 3.01 (s, 3H), 2.97 (s, 3H).

^{13}C NMR (126 MHz, CDCl$_3$): δ (ppm) 170.8, 155.0, 132.5, 131.0, 129.9, 125.7, 117.3, 61.1, 37.7, 35.8, 35.2.

GC-MS (EI): Calcd for $C_{11}H_{14}{}^{79}BrNO_2$ $[M]^{+•}$: 271, found 271

3-Bromo-2-methoxybenzyl pivalate (4.16b):

3-bromo-2-methoxybenzaldehyde (900 mg, 4.19 mmol, 1.0 eq.) was dissolved in MeOH (14 mL) and NaBH$_4$ (238 mg, 6.29 mmol, 1.5 eq.) was added portion wise at 0 °C. The reaction mixture was stirred at 24 °C for 3 h and quenched by the addition of H$_2$O (5.0 mL). The aqueous phase was extracted with EtOAc and the combined orgnic layers were washed with H$_2$O (15 mL), Brine (15 mL) and dried over Na$_2$SO$_4$. Afterwards the volatiles were removed under reduced pressure. The crude benzyl alcohol was dissolved in CH$_2$Cl$_2$ (8.0 mL) and pyridine (251 mg, 3.17 mmol, 0.80 eq.) and pivalyl chloride (585 mg, 4.75 mmol, 1.2 eq.) were added sequentially. The mixture was stirred at 24 °C for 3 h. The mixture was then poured into water (20 mL) and the mixture was stirred vigorously for 30 min. The aqueous phase was extracted with EtOAc (3 X 20 mL) and the combined organic layers were washed with H$_2$O (20 mL) and brine and dried over Na$_2$O$_4$. The volatiles were removed under reduced pressure and the crude mixture was purified by column chromatography (cyclohexane:EtOAc, 98:2) to give the title compound (1.02 g, 3.39 mmol, 86%) as a colorless liquid.

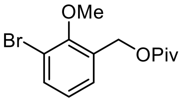

4.16b
$C_{13}H_{17}BrO_3$
M= 301.18

^{1}H NMR (500 MHz, CDCl$_3$): δ (ppm) 7.52 (dd, *J* = 8.0, 1.6 Hz, 1H), 7.31 (dd, *J* = 7.7, 1.6 Hz, 1H), 7.00 (t, *J* = 7.8 Hz, 1H), 5.19 (s, 2H), 3.89 (s, 3H), 1.23 (s, 9H).

^{13}C NMR (126 MHz, CDCl$_3$): δ (ppm) 178.5, 155.6, 133.7, 132.1, 129.1, 125.7, 117.6, 61.7, 61.6, 39.0, 27.4.

GC-MS (EI): Calcd for $C_{13}H_{17}{}^{79}BrO_3$ $[M]^{+•}$: 300, found 300

3-Bromo-2-methoxybenzyl acetate (4.16c):

3-bromo-2-methoxybenzaldehyde (900 mg, 4.19 mmol, 1.0 eq.) was dissolved in MeOH (14 mL) and NaBH$_4$ (238 mg, 6.29 mmol, 1.5 eq.) was added portion wise at 0 °C. The reaction mixture was stirred at 24 °C for 3 h and quenched by the addition of H$_2$O (5.0 mL). The aqueous phase was extracted with EtOAc and the combined orgnic layers were washed with H$_2$O (15 mL), Brine (15 mL) and dried over Na$_2$SO$_4$. Afterwards the volatiles were removed under reduced pressure. The crude benzyl alcohol was dissolved in CH$_2$Cl$_2$ (8.0 mL) and pyridine (251 mg, 3.17 mmol, 0.80 eq.) and acetic anhydride (849 mg, 8.32 mmol, 2.1 eq.) were added sequentially. The mixture was stirred at 24 °C for 3 h. The mixture was then poured into water (20 mL) and the mixture was stirred vigorously for 30 min. The aqueous phase was extracted with EtOAc (3 X 20 mL) and the combined organic layers were washed with H$_2$O (20 mL) and brine and dried over Na$_2$O$_4$. The volatiles were removed under reduced pressure and the crude mixture was purified by column chromatography (cyclohexane:EtOAc, 95:10) to give the title compound (1.00 g, 3.86 mmol, 98%) as a colorless liquid.

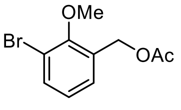

4.16c
$C_{10}H_{11}BrO_3$
M= 259.10

^{1}H NMR (500 MHz, $CDCl_3$): δ (ppm) 7.53 (dd, *J* = 8.0, 1.6 Hz, 1H), 7.32 (dd, *J* = 7.7, 1.6 Hz, 1H), 7.00 (t, *J* = 7.8 Hz, 1H), 5.18 (s, 2H), 3.89 (s, 3H), 2.11 (s, 3H).

^{13}C NMR (126 MHz, $CDCl_3$): δ (ppm) 170.9, 155.8, 134.1, 131.5, 129.6, 125.6, 117.6, 61.7, 21.2.

GC-MS (EI): Calcd for $C_{10}H_{11}{}^{79}BrO_3$ $[M]^{+\bullet}$: 258, found 258

2-(3-Bromo-2-methoxybenzyl)isoindoline-1,3-dione (4.16d):

(3-bromo-2-methoxyphenyl)methanol (1.00 g, 4.61 mmol, 1.0 eq.) (prepared as above) was dissolved in CH_2Cl_2 (45 mL) and PBr_3 (3.74 g, 13.8 mmol, 3.0 eq.) was added. The mixture was stirred at 24 °C for 3 h and then the volatiles were removed under reduced pressure. The crude mixture was redissolved in DMF (10 mL) and phtalimide potassium salt (613 mg, 3.31 mmol, 1.10 eq.) was added and the mixture was heated at 90 °C for 16 h. The volatiles were removed under reduced pressure and the residue dissolved in CH_3Cl (15 mL) and filtered. The filtrate was washed with H_2O (20 mL), brine (20 mL) and dried over Na_2SO_4. After removing the solvent under reduced pressure the crude product was passed through a short plug of silica to give the title compound (896 mg, 2.59 mmol, 86%) as a yellow oil.

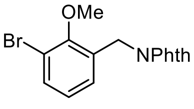

4.16d
C_8H_8BrO
M= 200.05

^{1}H NMR (500 MHz, $CDCl_3$): δ (ppm) 7.90 – 7.82 (m, 2H), 7.79 – 7.66 (m, 2H), 7.46 (dd, *J* = 8.0, 1.6 Hz, 1H), 7.20 (dd, *J* = 7.7, 1.5 Hz, 1H), 6.92 (t, *J* = 7.8 Hz, 1H), 4.94 (s, 2H), 3.98 (d, *J* = 0.7 Hz, 3H).

^{13}C NMR (126 MHz, $CDCl_3$): δ (ppm) 168.1, 155.2, 134.2, 133.3, 132.2, 131.6, 128.6, 125.5, 123.5, 117.5, 61.2, 37.0.

GC-MS (EI): Calcd for $C_8H_8{}^{79}BrO$ $[M]^{+\bullet}$: 199, found 199

1-Bromo-2-methoxy-3-(1-methylcyclopropyl)benzene (4.16e):

To a solution of methyltriphenylphosphonium bromide (3.82 mg, 10.7 mmol, 2.30 eq.) in THF (28 mL) was added KO*t*Bu (1.18 g, 10.6 mmol, 2.3 eq.) at 0 °C. After stirring for 2 h at 0 °C 1-(3-bromo-2-methoxyphenyl)ethan-1-one (1.07 g, 4.65 mmol, 1.0 eq.) and the mixture was continued to stir at 24 °C for 6 h. The reaction was quenched by the addition of HCl (10 mL, 1M) and the aqueous phase was extracted with EtOAc (3 X 10 mL). The combined combined organic layers were washed with brine (2 X 10 mL) and dried over Na_2SO_4. After removing the volatiles under reduced pressure the crude was filtered over a plug of silica.

To dry CH_2Cl_2 (5.0 mL) Et_2Zn (6.18 g, 4.06 mmol, 2.0 eq.) was added under argon atmosphere. Then, TFA (463 mg, 4.06 mmol, 2.0 eq.) was added at 0 °C. After stirring for 20 min, a solution of CH2I2 (2.18 g, 8.12 mmol, 4.0 eq.) in CH_2Cl_2 (2.9 mL) was added. After stirring for additional 20 min a solution of the olefin obtained above in CH_2Cl_2 (2.0 mL) was added slowly and the mixture stirred for 30 min at 24 °C. The reaction as quenched by the addition of HCl (5 mL, 0.1 M) and hexanes (10 mL) and the layers were separated. The aqueous layer was extracted with hexanes (3 X 10 mL) and the combined organic layers were washed with H_2O (10 mL) and brine (10 mL). After drying over Na_2SO_4, the volatiles were removed under reduced pressure. Flash column chromatography (cyclohexane:EtOAc, 98:2) gave the title compound (434 mg, 1.80 mmol, 89%) as a colorless liquid.

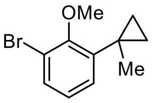

4.16e
$C_{11}H_{13}BrO$
M= 241.13

^{1}H NMR (500 MHz, $CDCl_3$): δ (ppm) 7.40 (dt, *J* = 7.9, 1.2 Hz, 1H), 7.23 (dt, *J* = 7.7, 1.2 Hz, 1H), 6.89 (t, *J* = 7.8 Hz, 1H), 3.96 (s, 3H), 1.38 (s, 3H), 0.83 (t, *J* = 3.0 Hz, 2H), 0.72 (t, *J* = 3.2 Hz, 2H).

^{13}C NMR (126 MHz, $CDCl_3$): δ (ppm) 157.1, 142.0, 131.9, 130.2, 125.2, 117.9, 61.0, 26.4, 19.2, 14.1.

GC-MS (EI): Calcd for $C_{11}H_{13}{}^{79}BrO$ $[M]^{+\bullet}$: 240, found 240

1-(3-Bromo-2-methoxy-5-methylphenyl)propan-1-one (4.20a):

The title compound (2.30 g, 8.94 mmol, 91%) was prepared after a literature procedure. The analytical data is in full agreement with the reported one. [185]

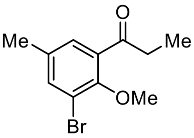

4.20a
$C_{11}H_{13}BrO_2$
M= 257.13

^{1}H NMR (400 MHz, $CDCl_3$): δ (ppm) 7.49 – 7.47 (m, 1H), 7.26 – 7.24 (m, 1H), 3.82 (s, 3H), 2.96 (q, *J* = 7.3 Hz, 2H), 2.31 (d, *J* = 0.8 Hz, 3H), 1.17 (t, *J* = 7.3 Hz, 3H).

^{13}C NMR (126 MHz, $CDCl_3$): δ (ppm) 203.8, 153.3, 136.9, 135.7, 135.2, 129.1, 117.9, 62.6, 36.3, 20.6, 8.5.

7. References

[1] C. C. C. Johansson Seechurn, M. O. Kitching, T. J. Colacot, V. Snieckus, *Angew. Chem. Int. Ed.* **2012**, *51*, 5062–5085.

[2] R. Jana, T. P. Pathak, M. S. Sigman, *Chem. Rev.* **2011**, *111*, 1417–1492.

[3] R. Dorel, C. P. Grugel, A. M. Haydl, *Angew. Chem. Int. Ed.* **2019**, *58*, 17118–17129.

[4] L. J. Cheng, N. P. Mankad, *Chem. Soc. Rev.* **2020**, *49*, 8036–8064.

[5] G. Cahiez, A. Moyeux, *Chem. Rev.* **2010**, *110*, 1435–1462.

[6] J. Q. Chen, J. H. Li, Z. B. Dong, *Adv. Synth. Catal.* **2020**, *362*, 3311–3331.

[7] C. Sambiagio, S. P. Marsden, A. J. Blacker, P. C. McGowan, *Chem. Soc. Rev.* **2014**, *43*, 3525–3550.

[8] K. C. Nicolaou, P. G. Bulger, D. Sarlah, *Angew. Chem. Int. Ed.* **2005**, *44*, 4442–4489.

[9] J. F. Hartwig, *J. Am. Chem. Soc.* **2016**, *138*, 2–24.

[10] H. X. Dai, A. F. Stepan, M. S. Plummer, Y. H. Zhang, J. Q. Yu, *J. Am. Chem. Soc.* **2011**, *133*, 7222–7228.

[11] P. Buchschacher, J. Kalvoda, O. Jeger, *J. Am. Chem. Soc.* **1958**, *80*, 2905–2906.

[12] E. J. Corey, W. R. Hertler, *J. Am. Chem. Soc.* **1958**, *80*, 2903–2904.

[13] A. R. Dick, M. S. Sanford, *Tetrahedron* **2006**, *62*, 2439–2463.

[14] K. M. Altus, J. A. Love, *Commun. Chem.* **2021**, *4*, DOI 10.1038/s42004-021-00611-1.

[15] N. D. Fessner, *ChemCatChem* **2019**, *11*, 2226–2242.

[16] Y. Yan, J. Wu, G. Hu, C. Gao, L. Guo, X. Chen, L. Liu, W. Song, *Synth. Syst. Biotechnol.* **2022**, *7*, 887–899.

[17] M. P. Doyle, R. Duffy, M. Ratnikov, L. Zhou, *Chem. Rev.* **2010**, *110*, 704–724.

[18] H. M. L. Davies, D. Morton, *Chem. Soc. Rev.* **2011**, *40*, 1857–1869.

[19] F. Collet, R. H. Dodd, P. Dauban, *Chem. Commun.* **2009**, 5061–5074.

[20] J. L. Roizen, M. E. Harvey, J. du Bois, *Acc. Chem. Res.* **2012**, *45*, 911–922.

[21] D. Mansuy, *Coord. Chem. Rev.* **1993**, *125*, 129–142.

[22] B. Meunier, *Chem. Rev.* **1992**, *92*, 1411–1456.

[23] J. A. Labinger, J. E. Bercaw Arnold, M. Beckman, *Nature* **2002**, *417*, 507–514.

[24] T. Rogge, N. Kaplaneris, N. Chatani, J. Kim, S. Chang, B. Punji, L. L. Schafer, D. G. Musaev, J. Wencel-Delord, C. A. Roberts, R. Sarpong, Z. E. Wilson, M. A. Brimble, M. J. Johansson, L. Ackermann, *Nature Reviews Methods Primers* **2021**, *1*, DOI 10.1038/s43586-021-00041-2.

[25] D. Alberico, M. E. Scott, M. Lautens, *Chem. Rev.* **2007**, *107*, 174–238.

[26] D. Lapointe, K. Fagnou, *Chem. lett.* **2010**, *39*, 1118–1126.

[27] D. L. Davies, S. A. Macgregor, C. L. McMullin, *Chem. Rev.* **2017**, *117*, 8649–8709.

[28] T. Dalton, T. Faber, F. Glorius, *ACS Cent. Sci.* **2021**, *7*, 245–261.

[29] C. Sambiagio, D. Schönbauer, R. Blieck, T. Dao-Huy, G. Pototschnig, P. Schaaf, T. Wiesinger, M. F. Zia, J. Wencel-Delord, T. Besset, B. U. W. Maes, M. Schnürch, *Chem. Soc. Rev.* **2018**, *47*, 6603–6743.

[30] F.-L. Zhang, K. Hong, T.-J. Li, H. Park, J.-Q. Yu, *Science* **2016**, *351*, 249–252.

[31] Y. Wu, Y. Q. Chen, T. Liu, M. D. Eastgate, J. Q. Yu, *J. Am. Chem. Soc.* **2016**, *138*, 14554–14557.

[32] X.-H. Liu, H. Park, J.-H. Hu, Y. Hu, Q.-L. Zhang, B.-L. Wang, B. Sun, K.-S. Yeung, F.-L. Zhang, J.-Q. Yu, *J. Am. Chem. Soc.* **2017**, *139*, 888–896.

[33] J.-T. Cheng, L.-J. Xiao, S.-Q. Qian, Z. Zhuang, A. Liu, J.-Q. Yu, *Angew. Chem. Int. Ed.* **2022**, *61*, DOI 10.1002/anie.202117233.

[34] F. Mo, G. Dong, *Science* **2014**, *345*, 68–72.

[35] C.-H. Jun, H. Lee, J.-B. Hong, *J. Org. Chem.* **1997**, *62*, 1200–1201.

[36] O. Baudoin, *Acc. Chem. Res.* **2017**, *50*, 1114–1123.

[37] X. Chen, K. M. Engle, D. H. Wang, Y. Jin-Quan, *Angew. Chem. Int. Ed.* **2009**, *48*, 5094–5115.

[38] T. W. Lyons, M. S. Sanford, *Chem. Rev.* **2010**, *110*, 1147–1169.

[39] G. Dyker, *Chem. Rev.* **2017**, *117*, 8754–8786.

[40] D. E. Ames, D. Bull, *Tetrahedron* **1982**, *38*, 383–387.

[41] D. E. Ames, A. Opalko, *Synthesis* **1983**, *3*, 234–235.

[42] D. E. Ames, A. Opalko, *Tetrahedron* **1984**, *40*, 1919–1925.

[43] G. Bringmann, J. Holenz, R. Weirich, M. Riibenacker, C. Funke, M. R. Boyd, R. J. Gulakowski, G. Francois, *Tetrahedron* **1998**, *54*, 497–512.

[44] G. Bringmann, J. Holenz, R. Weirich, M. Riibenacker, C. Funke, M. R. Boyd, R. J. Gulakowski, G. Francois, *Angew. Chem. Int. Ed.* **2001**, *40*.

[45] L. C. Campeau, M. Parisien, M. Leblanc, K. Fagnou, *J. Am. Chem. Soc.* **2004**, *126*, 9186–9187.

[46] M. Lafrance, N. Blaquière, K. Fagnou, *Chem. Commun.* **2004**, 2874–2875.

[47] M. Lafrance, N. Blaquiere, K. Fagnou, *Eur. J. Org. Chem.* **2007**, 811–825.

[48] F. Bellina, R. Rossi, *Tetrahedron* **2009**, *65*, 10269–10310.

[49] D. García-Cuadrado, A. A. C. Braga, F. Maseras, A. M. Echavarren, *J. Am. Chem. Soc.* **2006**, *128*, 1066–1067.

[50] D. García-Cuadrado, P. de Mendoza, A. A. C. Braga, F. Maseras, A. M. Echavarren, *J. Am. Chem. Soc.* **2007**, *129*, 6880–6886.

[51] M. R. Albicker, N. Cramer, *Angew. Chem. Int. Ed.* **2009**, *48*, 9139–9142.

[52] D. Grosheva, N. Cramer, *ACS Catal.* **2017**, *7*, 7417–7420.

[53] D. Grosheva, N. Cramer, *Angew. Chem. Int. Ed.* **2018**, *57*, 13644–13647.

[54] W. Dong, G. Xu, W. Tang, *Tetrahedron* **2019**, *75*, 3239–3247.

[55] J. Diesel, N. Cramer, *ACS Catal.* **2019**, *9*, 9164–9177.

[56] R. Shintani, H. Otomo, K. Ota, T. Hayashi, *J. Am. Chem. Soc.* **2012**, *134*, 7305–7308.

[57] Z.-Q. Lin, W.-Z. Wang, S.-B. Yan, W.-L. Duan, *Angew. Chem. Int. Ed.* **2015**, *54*, 6265–6265.

[58] L. Liu, A. A. Zhang, Y. Wang, F. Zhang, Z. Zuo, W. X. Zhao, C. L. Feng, W. Ma, *Org. Lett.* **2015**, *17*, 2046–2049.

[59] G. Xu, M. Li, S. Wang, W. Tang, *Org. Chem. Front.* **2015**, *2*, 1342–1345.

[60] Y. Lin, W. Y. Ma, Q. Y. Sun, Y. M. Cui, L. W. Xu, *Synlett* **2017**, *28*, 1432–1436.

[61] Z. Li, Z. Q. Lin, C. G. Yan, W. L. Duan, *Organometallics* **2019**, *38*, 3916–3920.

[62] X. Ma, Z. Gu, *RSC Adv.* **2014**, *4*, 36241–36244.

[63] L. Liu, A. A. Zhang, R. J. Zhao, F. Li, T. J. Meng, N. Ishida, M. Murakami, W. X. Zhao, *Org. Lett.* **2014**, *16*, 5336–5338.

[64] D. W. Gao, Q. Yin, Q. Gu, S. L. You, *J. Am. Chem. Soc.* **2014**, *136*, 4841–4844.

[65] R. Deng, Y. Huang, X. Ma, G. Li, R. Zhu, B. Wang, Y. B. Kang, Z. Gu, *J. Am. Chem. Soc.* **2014**, *136*, 4472–4475.

[66] D. W. Gao, C. Zheng, Q. Gu, S. L. You, *Organometallics* **2015**, *34*, 4618–4625.

[67] D. W. Gao, Y. Gu, S. B. Wang, Q. Gu, S. L. You, *Organometallics* **2016**, *35*, 3227–3233.

[68] C. Nottingham, H. Müller-Bunz, P. J. Guiry, *Angew. Chem. Int. Ed.* **2016**, *55*, 1115–1119.

[69] B. bin Xu, J. Ye, Y. Yuan, W. L. Duan, *ACS Catal.* **2018**, *8*, 11735–11740.

[70] C. G. Newton, E. Braconi, J. Kuziola, M. D. Wodrich, N. Cramer, *Angew. Chem. Int. Ed.* **2018**, *130*, 11206–11210.

[71] G. Dyker, *Angew. Chem. Int. Ed. Engl.* **1992**, *31*, 1023–1025.

[72] O. Baudoin, A. Herrbach, F. Guéritte, *Angew. Chem. Int. Ed.* **2003**, *42*, 5736–5740.

[73] J. Hitce, P. Retailleau, O. Baudoin, *Chem. Eur. J.* **2007**, *13*, 792–799.

[74] M. Chaumontet, R. Piccardi, N. Audic, J. Hitce, J. L. Peglion, E. Clot, O. Baudoin, *J. Am. Chem. Soc.* **2008**, *130*, 15157–15166.

[75] S. Rousseaux, M. Davi, J. Sofack-Kreutzer, C. Pierre, C. E. Kefalidis, E. Clot, K. Fagnou, O. Baudoin, *J. Am. Chem. Soc.* **2010**, *132*, 10706–10716.

[76] R. Rocaboy, D. Dailler, F. Zellweger, M. Neuburger, C. Salomé, E. Clot, O. Baudoin, *Angew. Chem. Int. Ed.* **2018**, *130*, 12307–12311.

[77] H. Ren, P. Knochel, *Angew. Chem. Int. Ed.* **2006**, *45*, 3462–3465.

[78] M. Lafrance, S. I. Gorelsky, K. Fagnou, *J. Am. Chem. Soc.* **2007**, *129*, 14570–14571.

[79] T. Watanabe, S. Oishi, N. Fujii, H. Ohno, *Org. Lett.* **2008**, *10*, 1759–1762.

[80] S. Rousseaux, S. I. Gorelsky, B. K. W. Chung, K. Fagnou, *J. Am. Chem. Soc.* **2010**, *132*, 10692–10705.

[81] J. X. Yan, H. Li, X. W. Liu, J. L. Shi, X. Wang, Z. J. Shi, *Angew. Chem. Int. Ed.* **2014**, *53*, 4945–4949.

[82] R. Rocaboy, D. Dailler, O. Baudoin, *Org. Lett.* **2018**, *20*, 772–775.

[83] C. Tsukano, M. Okuno, Y. Takemoto, *Angew. Chem. Int. Ed.* **2012**, *51*, 2763–2766.

[84] D. Dailler, R. Rocaboy, O. Baudoin, *Angew. Chem. Int. Ed.* **2017**, *56*, 7218–7222.

[85] S. D. Friis, A. T. Lindhardt, T. Skrydstrup, *Acc. Chem. Res.* **2016**, *49*, 594–605.

[86] J. Pedroni, N. Cramer, *Org. Lett.* **2016**, *18*, 1932–1935.

[87] P. M. Holstein, D. Dailler, J. Vantourout, J. Shaya, A. Millet, O. Baudoin, *Angew. Chem. Int. Ed.* **2016**, *128*, 2855–2859.

[88] S. Suetsugu, N. Muto, M. Horinouchi, C. Tsukano, Y. Takemoto, *Chem. Eur. J.* **2016**, *22*, 8059–8062.

[89] S. Janody, R. Jazzar, A. Comte, P. M. Holstein, J. P. Vors, M. J. Ford, O. Baudoin, *Chem. Eur. J.* **2014**, *20*, 11084–11090.

[90] O. Baudoin, *Chimia* **2021**, *75*, 967–971.

[91] M. Chaumontet, P. Retailleau, O. Baudoin, *J. Org. Chem.* **2009**, *74*, 1774–1776.

[92] J. Sofack-Kreutzer, N. Martin, A. Renaudat, R. Jazzar, O. Baudoin, *Angew. Chem. Int. Ed.* **2012**, *51*, 10399–10402.

[93] K. Ersmark, J. R. del Valle, S. Hanessian, *Angew. Chem. Int. Ed.* **2008**, *47*, 1202–1223.

[94] D. Dailler, G. Danoun, O. Baudoin, *Angew. Chem. Int. Ed.* **2015**, *54*, 4919–4922.

[95] V. G. Zaitsev, D. Shabashov, O. Daugulis, *J. Am. Chem. Soc.* **2005**, *127*, 13154–13155.

[96] D. Shabashov, O. Daugulis, *J. Am. Chem. Soc.* **2010**, *132*, 3965–3972.

[97] D. Dailler, G. Danoun, B. Ourri, O. Baudoin, *Chem. Eur. J.* **2015**, *21*, 9370–9379.

[98] P. Thesmar, O. Baudoin, *J. Am. Chem. Soc.* **2019**, *141*, 15779–15783.

[99] P. Thesmar, S. Coomar, A. Prescimone, D. Häussinger, D. Gillingham, O. Baudoin, *Chem. Eur. J.* **2020**, *26*, 15298–15312.

[100] X. Wang, C. M. Reisinger, B. List, *J. Am. Chem. Soc.* **2008**, *130*, 6070–6071.

[101] O. Lifchits, M. Mahlau, C. M. Reisinger, A. Lee, C. Farès, I. Polyak, G. Gopakumar, W. Thiel, B. List, *J. Am. Chem. Soc.* **2013**, *135*, 6677–6693.

[102] K. C. Nicolaou, S. Totokotsopoulos, D. Giguère, Y. P. Sun, D. Sarlah, *J. Am. Chem. Soc.* **2011**, *133*, 8150–8153.

[103] K. C. Nicolaou, M. Lu, S. Totokotsopoulos, P. Heretsch, D. Giguère, Y. P. Sun, D. Sarlah, T. H. Nguyen, I. C. Wolf, D. F. Smee, C. W. Day, S. Bopp, E. A. Winzeler, *J. Am. Chem. Soc.* **2012**, *134*, 17320–17332.

[104] L. A. Nguyen, H. He, C. Pham-Huy, *Int. J. Biomed. Sci.* **2006**, 85–100.

[105] N. C. P. de Albuquerque, D. B. Carrão, M. D. Habenschus, A. R. M. de Oliveira, *J. Pharm. Biomed. Anal.* **2018**, *147*, 89–109.

[106] C. Bolm, J. A. Gladysz, *Chem. Rev.* **2003**, *103*, 2761–2762.

[107] K. E. Poremba, S. E. Dibrell, S. E. Reisman, *ACS Catal.* **2020**, *10*, 8237–8246.

[108] X. Y. Liu, Y. Qin, *Green Synthesis and Catalysis* **2022**, *3*, 25–39.

[109] B. Su, J. F. Hartwig, *Angew. Chem. Int. Ed.* **2022**, *61*, ASAP.

[110] G. J. Mei, W. L. Koay, C. X. A. Tan, Y. Lu, *Chem. Soc. Rev.* **2021**, *50*, 5985–6012.

[111] T. G. Saint-Denis, R. Y. Zhu, G. Chen, Q. F. Wu, J. Q. Yu, *Science* **2018**, *359*, eaao4798.

[112] O. Vyhivskyi, A. Kudashev, T. Miyakoshi, O. Baudoin, *Chem. Eur. J.* **2021**, *27*, 1231–1257.

[113] E. L. Lucas, N. Y. S. Lam, Z. Zhuang, H. S. S. Chan, D. A. Strassfeld, J. Q. Yu, *Acc. Chem. Res.* **2022**, *55*, 537–550.

[114] M. Nakanishi, D. Katayev, C. Besnard, E. P. Kündig, *Angew. Chem. Int. Ed.* **2011**, *50*, 7438–7441.

[115] E. P. Kündig, T. M. Seidel, Y. X. Jia, G. Bernardinelli, *Angew. Chem. Int. Ed.* **2007**, *46*, 8484–8487.

[116] Y. X. Jia, J. M. Hillgren, E. L. Watson, S. P. Marsden, E. P. Kündig, *Chem. Commun.* **2008**, 4040–4042.

[117] Y. X. Jia, D. Katayev, G. Bernardinelli, T. M. Seidel, E. P. Kündig, *Chem. Eur. J.* **2010**, *16*, 6300–6309.

[118] E. Larionov, M. Nakanishi, D. Katayev, C. Besnard, E. P. Kündig, *Chem. Sci.* **2013**, *4*, 1995–2005.

[119] D. Katayev, M. Nakanishi, T. Bürgi, E. P. Kündig, *Chem. Sci.* **2012**, *3*, 1422–1425.

[120] D. Katayev, E. Larionov, M. Nakanishi, C. Besnard, E. P. Kündig, *Chem. Eur. J.* **2014**, *20*, 15021–15030.

[121] S. Anas, A. Cordi, H. B. Kagan, *Chem. Commun.* **2011**, *47*, 11483–11485.

[122] T. Saget, S. J. Lemouzy, N. Cramer, *Angew. Chem. Int. Ed.* **2012**, *51*, 2238–2242.

[123] P. A. Donets, T. Saget, N. Cramer, *Organometallics* **2012**, *31*, 8040–8046.

[124] S. Gladiali, E. Alberico, K. Junge, M. Beller, *Chem. Soc. Rev.* **2011**, *40*, 3744–3763.

[125] N. Martin, C. Pierre, M. Davi, R. Jazzar, O. Baudoin, *Chem. Eur. J.* **2012**, *18*, 4480–4484.

[126] P. M. Holstein, M. Vogler, P. Larini, G. Pilet, E. Clot, O. Baudoin, *ACS Catal.* **2015**, *5*, 4300–4308.

[127] L. Yang, R. Melot, M. Neuburger, O. Baudoin, *Chem. Sci.* **2017**, *8*, 1344–1349.

[128] R. Melot, M. v. Craveiro, T. Bürgi, O. Baudoin, *Org. Lett.* **2019**, *21*, 812–815.

[129] R. Melot, M. v. Craveiro, O. Baudoin, *J. Org. Chem.* **2019**, *84*, 12933–12945.

[130] K. Fuji, *Chem. Rev.* **1993**, *93*, 2037–2066.

[131] E. J. Corey, A. Guzman-Perez, *Angew. Chem. Int. Ed.* **1998**, *37*, 388–401.

[132] E. v. Prusov, *Angew. Chem. Int. Ed.* **2017**, *56*, 14356–14358.

[133] A. D. Walsh, *Trans. Faraday Soc.* **1949**, *45*, 179–190.

[134] H. A. Skinner, *Nature* **1947**, *160*, 902.

[135] L. Klasinc, Z. Maksic, M. Randic, *J. Chem. Soc. A* **1966**, 755–757.

[136] J. Pedroni, T. Saget, P. A. Donets, N. Cramer, *Chem. Sci.* **2015**, *6*, 5164–5171.

[137] X. Zheng, T. W. Hudyma, S. W. Martin, C. Bergstrom, M. Ding, F. He, J. Romine, M. A. Poss, J. F. Kadow, C. H. Chang, J. Wan, M. R. Witmer, P. Morin, D. M. Camac, S. Sheriff, B. R. Beno, K. L. Rigat, Y. K. Wang, R. Fridell, J. Lemm, D. Qiu, M. Liu, S. Voss, L. Pelosi, S. B. Roberts, M. Gao, J. Knipe, R. G. Gentles, *Bioorg. Med. Chem. Lett.* **2011**, *21*, 2925–2929.

[138] C. L. Ladd, A. B. Charette, *Org. Lett.* **2016**, *18*, 6046–6049.

[139] C. Mayer, C. L. Ladd, A. B. Charette, *Org. lett.* **2019**, *21*, 2639–2644.

[140] J. Pedroni, N. Cramer, *Angew. Chem. Int. Ed.* **2015**, *127*, 11992–11995.

[141] J. Pedroni, N. Cramer, *J. Am. Chem. Soc.* **2017**, *139*, 12398–12401.

[142] P. A. Donets, N. Cramer, *J. Am. Chem. Soc.* **2013**, *135*, 11772–11775.

[143] J. Pedroni, M. Boghi, T. Saget, N. Cramer, *Angew. Chem. Int. Ed.* **2014**, *53*, 9064–9067.

[144] C. G. Newton, S. G. Wang, C. C. Oliveira, N. Cramer, *Chem. Rev.* **2017**, *117*, 8908–8976.

[145] T. Dröge, F. Glorius, *Angew. Chem. Int. Ed.* **2010**, *49*, 6940–6952.

[146] M. Melaimi, R. Jazzar, M. Soleilhavoup, G. Bertrand, *Angew. Chem. Int. Ed.* **2017**, *56*, 10046–10068.

[147] G. Altenhoff, R. Goddard, C. W. Lehmann, F. Glorius, *J. Am. Chem. Soc.* **2004**, *126*, 15195–15201.

[148] R. M. Beeskey, C. K. Ingold, J. F. Thorpe, *J. Chem. Soc., Trans.* **1915**, *107*, 1080–1106.

[149] H. Wang, Y. Yu, X. Xie, C. Wang, Y. Zhang, Y. Yuan, X. Zhang, J. Liu, P. Wang, · Minjun Chen, *J. Infect. Chemother.* **2000**, *6*, 81–85.

[150] N. A. Magnus, T. M. Braden, J. Y. Buser, A. C. Debaillie, P. C. Heath, C. P. Ley, J. R. Remacle, D. L. Varie, T. M. Wilson, *Org. Process Res. Dev.* **2012**, *16*, 830–835.

[151] S. C. Lu, *Biochim Biophys Acta* **2013**, 3143–3153.

[152] Z. Wang, C. Y. Guo, C. Yang, J. P. Chen, *J. Am. Chem. Soc.* **2019**, *141*, 5617–5622.

[153] J. D. Griffin, M. A. Zeller, D. A. Nicewicz, *J. Am. Chem. Soc.* **2015**, *137*, 11340–11348.

[154] N. Marion, O. Navarro, J. Mei, E. D. Stevens, N. M. Scott, S. P. Nolan, *J. Am. Chem. Soc.* **2006**, *128*, 4101–4111.

[155] H. Clavier, S. P. Nolan, *Chem. Commun.* **2010**, *46*, 841–861.

[156] A. Poater, B. Cosenza, A. Correa, S. Giudice, F. Ragone, V. Scarano, L. Cavallo, *Eur. J. Inorg. Chem.* **2009**, 1759–1766.

[157] B. Gabriele, R. Mancuso, L. Veltri, *Chem. Eur. J.* **2016**, *22*, 5056–5094.

[158] R. He, X. Huang, Y. Zhang, L. Wu, H. Nie, D. Zhou, B. Liu, S. Deng, R. Yang, S. Huang, Z. Nong, J. Li, Y. Huang, *J. Nat. Prod.* **2016**, *79*, 2472–2478.

[159] Y. P. Li, Y. C. Yang, Y. K. Li, Z. Y. Jiang, X. Z. Huang, W. G. Wang, X. M. Gao, Q. F. Hu, *Fitoterapia* **2014**, *95*, 214–219.

[160] D.-H. Wang, K. M. Engle, B.-F. Shi, J.-Q. Yu, *Science* **2010**, *327*, 315–319.

[161] H. Weinstabl, M. Suhartono, Z. Qureshi, M. Lautens, *Angew. Chem. Int. Ed.* **2013**, *52*, 5305–5308.

[162] Y. Boutadla, D. L. Davies, S. A. Macgregor, A. A. Poblador-Bahamonde, *Dalton Trans.* **2009**, 5820–5831.

[163] E. M. Simmons, J. F. Hartwig, *Angew. Chem. Int. Ed.* **2012**, *51*, 3066–3072.

[164] J. He, M. Wasa, K. S. L. Chan, Q. Shao, J. Q. Yu, *Chem. Rev.* **2017**, *117*, 8754–8786.

[165] J. Li, L. Ackermann, *Angew. Chem. Int. Ed.* **2015**, *54*, 3635–3638.

[166] S. Nakanowatari, R. Mei, M. Feldt, L. Ackermann, *ACS Catal.* **2017**, *7*, 2511–2515.

[167] D. E. Stephens, J. Lakey-Beitia, G. Chavez, C. Ilie, H. D. Arman, O. v. Larionov, *Chem. Commun.* **2015**, *51*, 9507–9510.

[168] R. Melot, M. Zuccarello, D. Cavalli, N. Niggli, M. Devereux, B. Thomas, O. Baudoin, *Angew. Chem. Int. Ed.* **2021**, *60*, 7245–7250.

[169] P. R. Melvin, D. Balcells, N. Hazari, A. Nova, *ACS Catal.* **2015**, *5*, 5596–5606.

[170] M. R. Espinosa, A. Doppiu, N. Hazari, *Adv. Synth. Catal.* **2020**, *362*, 5062–5078.

[171] J. Burés, *Angew. Chem. Int. Ed.* **2016**, *55*, 16084–16087.

[172] R. E. Plata, D. E. Hill, B. E. Haines, D. G. Musaev, L. Chu, D. P. Hickey, M. S. Sigman, J. Q. Yu, D. G. Blackmond, *J. Am. Chem. Soc.* **2017**, *139*, 9238–9245.

[173] Q. Lin, T. Diao, *J. Am. Chem. Soc.* **2019**, *141*, 17937–17948.

[174] M. S. Viciu, R. F. Germaneau, O. Navarro-Fernandez, E. D. Stevens, S. P. Nolan, *Organometallics* **2002**, *21*, 5470–5472.

[175] N. Marion, O. Navarro, J. Mei, E. D. Stevens, N. M. Scott, S. P. Nolan, *J. Am. Chem. Soc.* **2006**, *128*, 4101–4111.

[176] A. Veillard, G. del Re, *Theoret. Chim. Acta* **1964**, *2*, 55–62.

[177] S. Ma, Z. Gu, *Angew. Chem. Int. Ed.* **2005**, *44*, 7512–7517.

[178] F. Shi, R. F. Larock, *Top. Curr. Chem.* **2010**, *292*, 123–164.

[179] A. Rahim, J. Feng, Z. Gu, *Chin. J. Chem.* **2019**, *37*, 929–945.

[180] T. Čarný, R. Rocaboy, A. Clemenceau, O. Baudoin, *Angew. Chem. Int. Ed.* **2020**, *59*, 18980–18984.

[181] J. Pan, M. Su, S. L. Buchwald, *Angew. Chem. Int. Ed.* **2011**, *50*, 8647–8651.

[182] M. A. Campo, Q. Huang, T. Yao, Q. Tian, R. C. Larock, *J. Am. Chem. Soc.* **2003**, *125*, 11506–11507.

[183] R. Rocaboy, O. Baudoin, *Org. Lett.* **2019**, *21*, 1434–1437.

[184] Y. Aoyagi, T. Manabe, A. Ohta, T. Kuriharat, G.-L. Pangt, T. Yuharat, *Tetrahedron* **1996**, *52*, 869–876.

[185] R. Rocaboy, I. Anastasiou, O. Baudoin, *Angew. Chem. Int. Ed.* **2019**, *58*, 14625–14628.

[186] A. Clemenceau, P. Thesmar, M. Gicquel, A. le Flohic, O. Baudoin, *J. Am. Chem. Soc.* **2020**, *142*, 15355–15361.

[187] Y. Yoshida, Y. Naoe, T. Terauchi, F. Ozaki, T. Doko, A. Takemura, T. Tanaka, K. Sorimachi, C. T. Beuckmann, M. Suzuki, T. Ueno, S. Ozaki, M. Yonaga, *J. Med. Chem.* **2015**, *58*, 4648–4664.

[188] G. Li, C. L. Ji, X. Hong, M. Szostak, *J. Am. Chem. Soc.* **2019**, *141*, 11161–11172.

[189] T. Miyakoshi, N. E. Niggli, O. Baudoin, *Angew. Chem. Int. Ed.* **2022**, *61*, DOI 10.1002/anie.202116101.

[190] H. A. Skinner, *Nature* **1947**, *160*, 902.

[191] S. Würtz, C. Lohre, R. Fröhlich, K. Bergander, F. Glorius, *J. Am. Chem. Soc.* **2009**, *131*, 8344–8345.

[192] F. Glorius, G. Altenhoff, R. Goddard, C. Lehmann, *Chem. Commun.* **2002**, *2*, 2704–2705.

[193] D. J. Augeri, J. A. Robl, D. A. Betebenner, D. R. Magnin, A. Khanna, J. G. Robertson, A. Wang, L. M. Simpkins, P. Taunk, Q. Huang, S. P. Han, B. Abboa-Offei, M. Cap, L. Xin, L. Tao, E. Tozzo, G. E. Welzel, D. M. Egan, J. Marcinkeviciene, S. Y. Chang, S. A. Biller, M. S. Kirby, R. A. Parker, L. G. Hamann, *J. Med. Chem.* **2005**, *48*, 5025–5037.

[194] Y. Kohari, Y. Okuyama, E. Kwon, T. Furuyama, N. Kobayashi, T. Otuki, J. Kumagai, C. Seki, K. Uwai, G. Dai, T. Iwasa, H. Nakano, *J. Org. Chem.* **2014**, *79*, 9500–9511.

[195] N. Nella, E. Parker, J. Hitce, P. Larini, R. Jazzar, O. Baudoin, *Chem. Eur. J.* **2014**, *20*, 13272–13278.

[196] T. Takuwa, J. Y. Onishi, J. I. Matsuo, T. Mukaiyama, *Chem. Lett.* **2004**, *33*, 8–9.

[197] Gaussian 16 Revision A.03, M. J. Frisch, G. W. Trucks, H. B. Schlegel, G. E. Scuseria, M. A. Robb, J. R. Cheeseman, G. Scalmani, V. Barone, G. A. Petersson, H. Nakatsuji, X. Li, M. Caricato, A. v. Marenich, J. Bloino, B. G. Janesko, R. Gomperts, B. Mennucci, H. P. Hratchian, J. v. Ortiz, A. F. Izmaylov, J. L. Sonnenberg, D. Williams-Young, F. Ding, F. Lipparini, F. Egidi, J. Goings, B. Peng, A. Petrone, T. Henderson, D. Ranasinghe, V. G. Zakrzewski, J. Gao, N. Rega, G. Zheng, W. Liang, M. Hada, M. Ehara, K. Toyota, R. Fukuda, J. Hasegawa, M. Ishida, T. Nakajima, Y. Honda, O. Kitao, H. Nakai, T. Vreven, K. Throssell, J. A. , Jr. Montgomery, J. E. Peralta, F. Ogliaro, M. J. Bearpark, J. J. Heyd, E. N. Brothers, K. N. Kudin, V. N. Staroverov, T. A. Keith, R. Kobayashi, J. Normand, K. Raghavachari, A. P. Rendell, J. C. Burant, S. S. Iyengar, J. Tomasi, M. Cossi, J. M. Millam, M. Klene, C. Adamo, R. Cammi, J. W. Ochterski, R. L. Martin, K. Morokuma, O. Farkas, J. B. Foresman, D. J. Fox, Gaussian Inc., Wallingtonford CT, **2016**.

[198] A. D. Becke, *Phys. Rev. A* **1988**, *38*, 3098–3100.

[199] J. P. Perdew, K. Burke, M. Ernzerhof, *Phys. Rev. Lett.* **1996**, *77*, 3865–3868.

[200] A. Schäfer, C. Huber, R. Ahlrichs, *J. Chem. Phys.* **1994**, *100*, 5829–5835.

[201] J. M. L. Martin, A. Sundermann, *J. Chem. Phys.* **2001**, *114*, 3408–3420.

[202] D. Andrae, U. H. Iubermann, M. Dolg, H. Stoll, H. Preub, *Theor. Chim. Acta.* **1990**, *77*, 123–141.

[203] B. P. Pritchard, D. Altarawy, B. Didier, T. D. Gibson, T. L. Windus, *J. Chem. Inf. Model.* **2019**, *59*, 4814–4820.

[204] L. Falivene, Z. Cao, A. Petta, L. Serra, A. Poater, R. Oliva, V. Scarano, L. Cavallo, *Nat. Chem.* **2019**, *11*, 872–879.

[205] M. S. Viciu, O. Navarro, R. F. Germaneau, R. A. Kelly, W. Sommer, N. Marion, E. D. Stevens, L. Cavallo, S. P. Nolan, *Organometallics* **2004**, *23*, 1629–1635.

8. Spectra

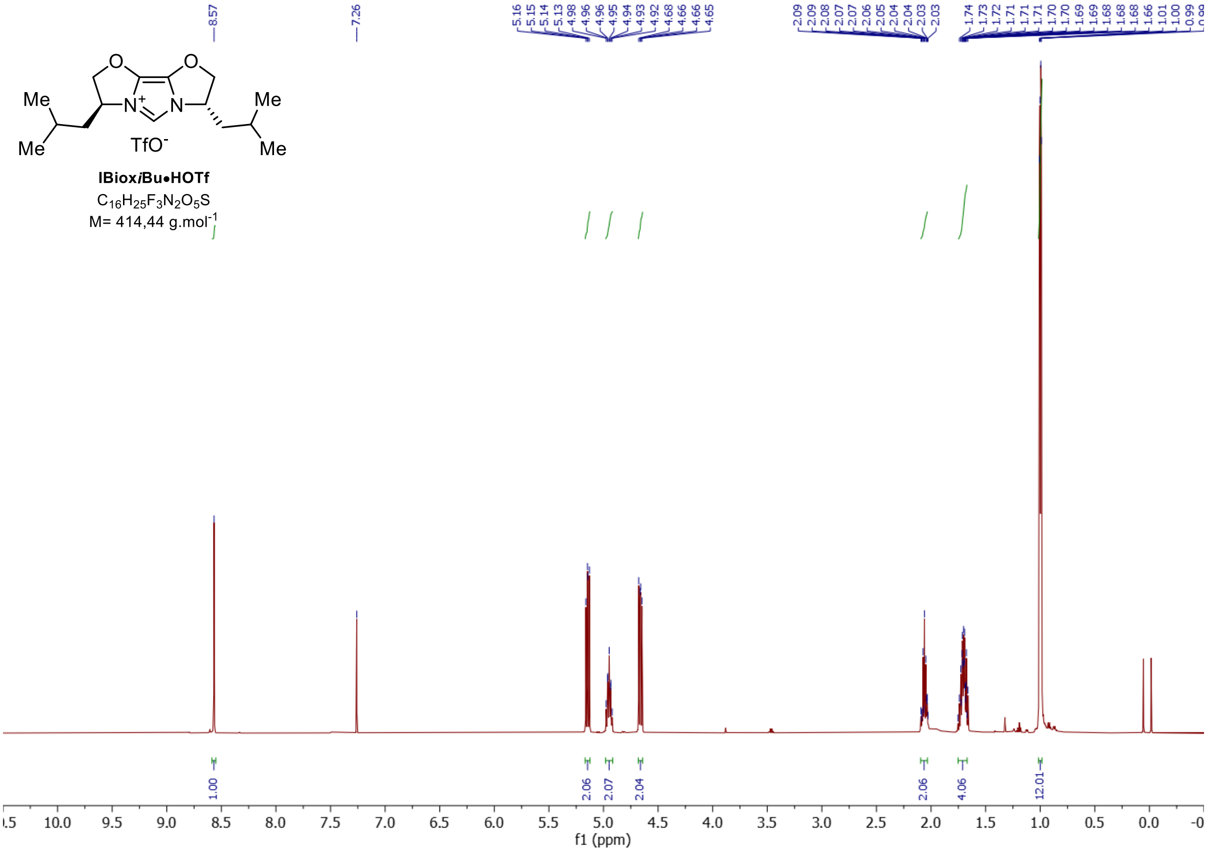

IBiox*i*Bu•HOTf

$C_{16}H_{25}F_3N_2O_5S$

M= 414,44 g.mol^{-1}

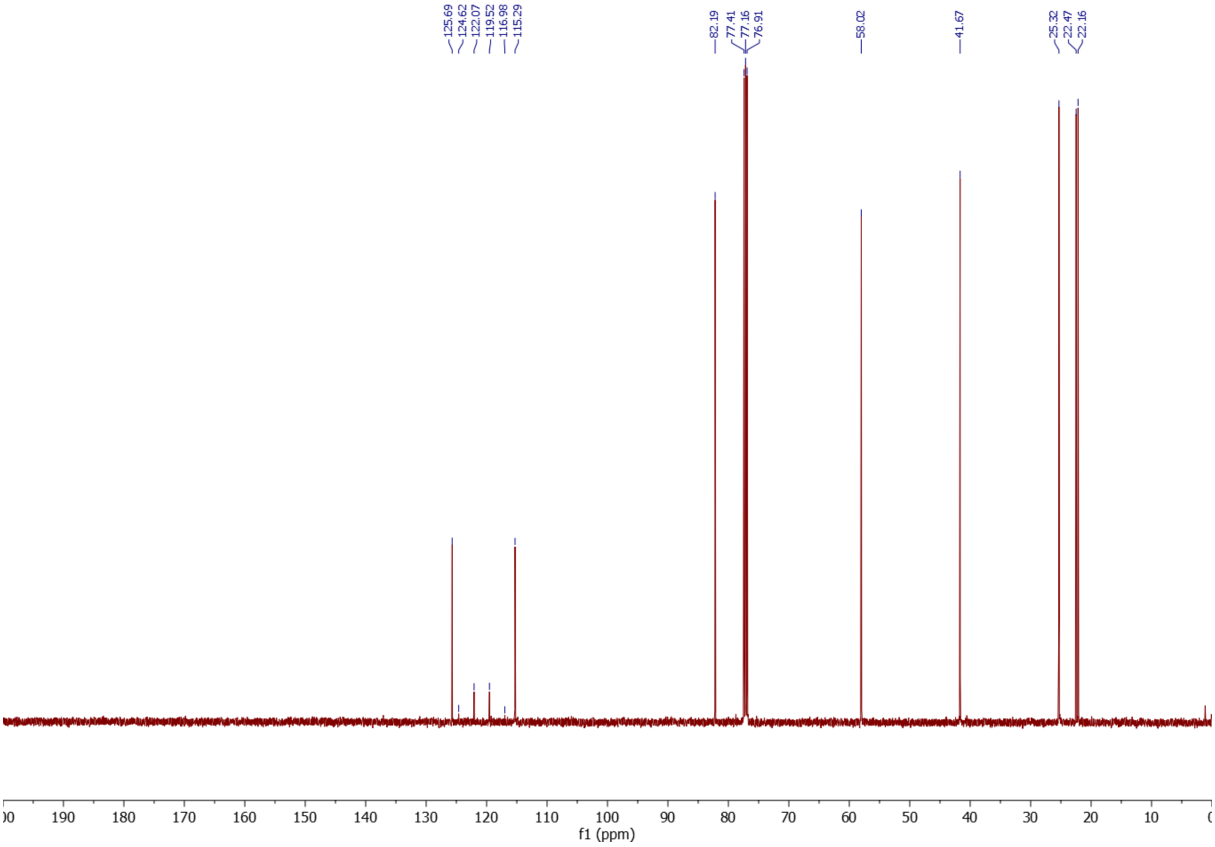

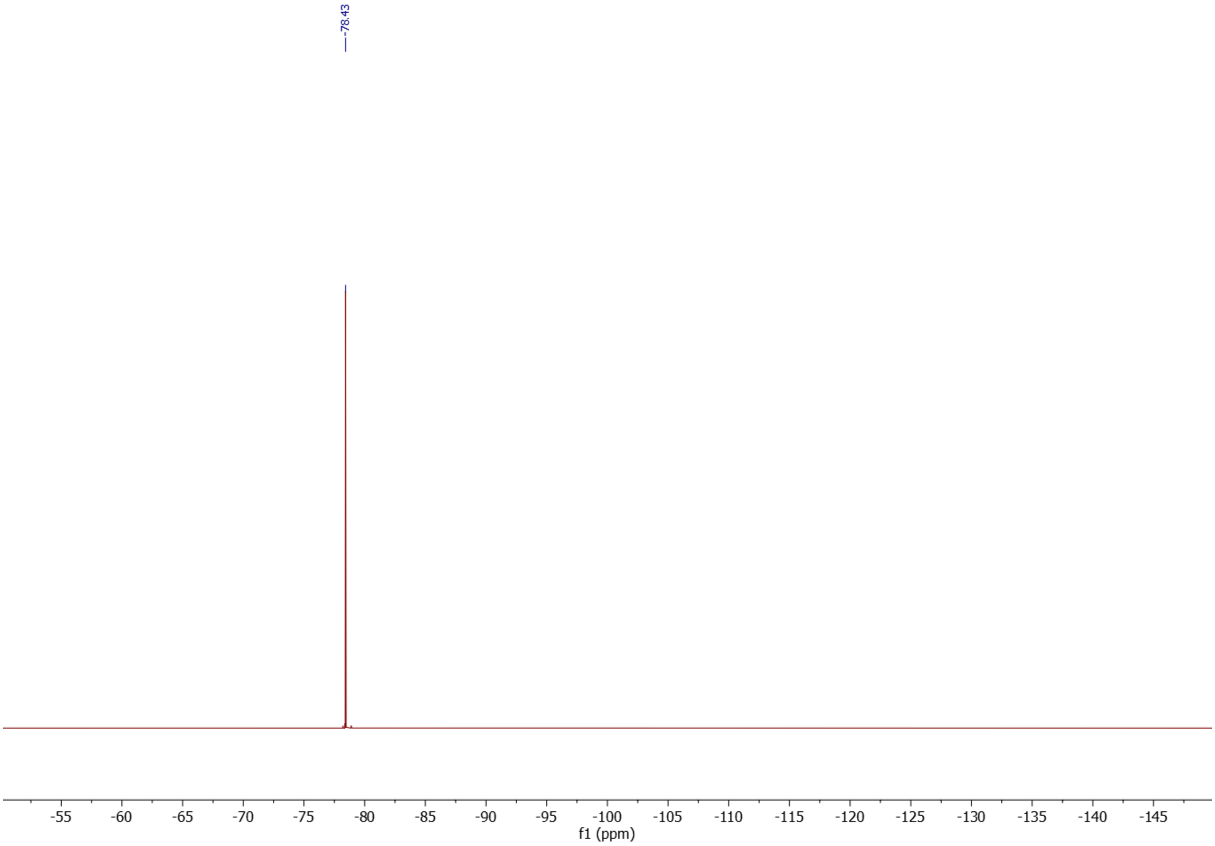
-78.43
-55
-60
-65
-70
-75
-80
-85
-90
-95
-100
-105
-110
-115
-120
-125
-130
-135
-140
-145
f1 (ppm)

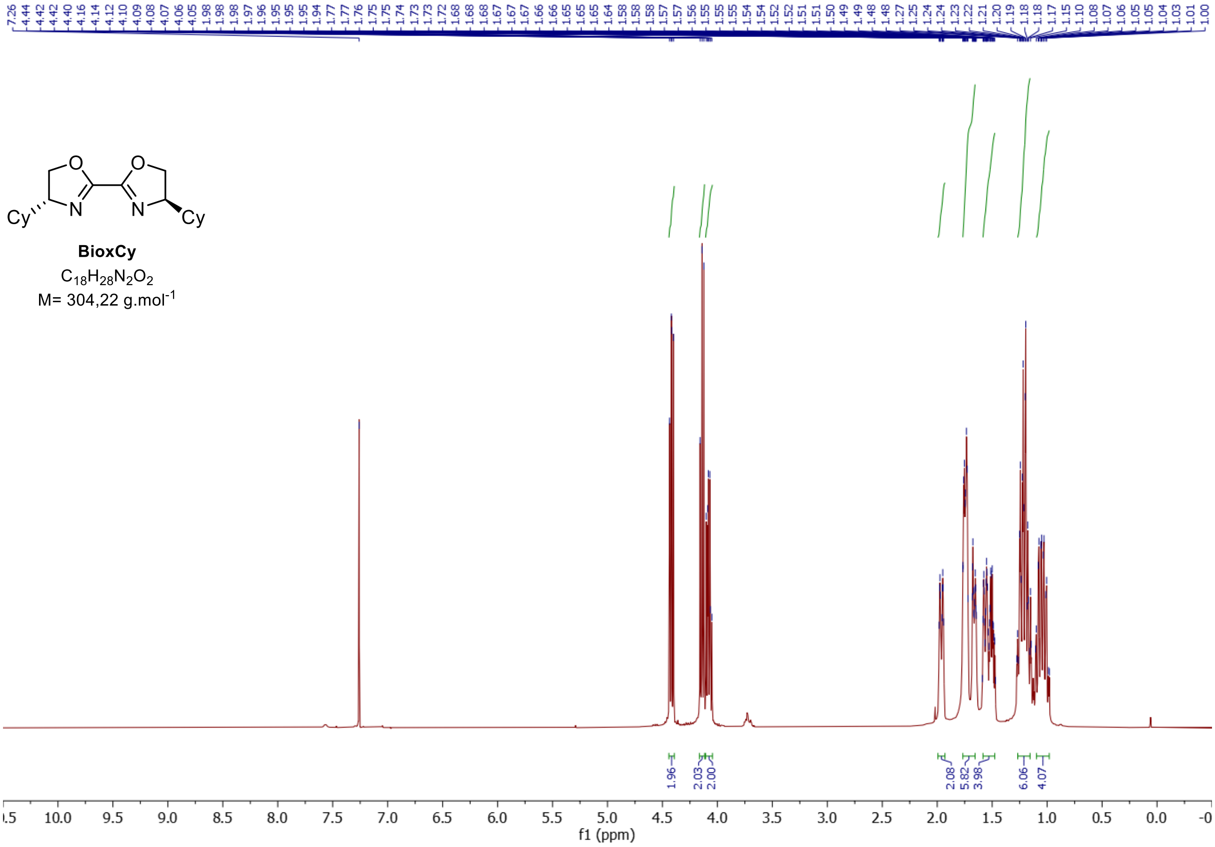

BioxCy

$C_{18}H_{28}N_2O_2$

M= 304,22 g.mol^{-1}

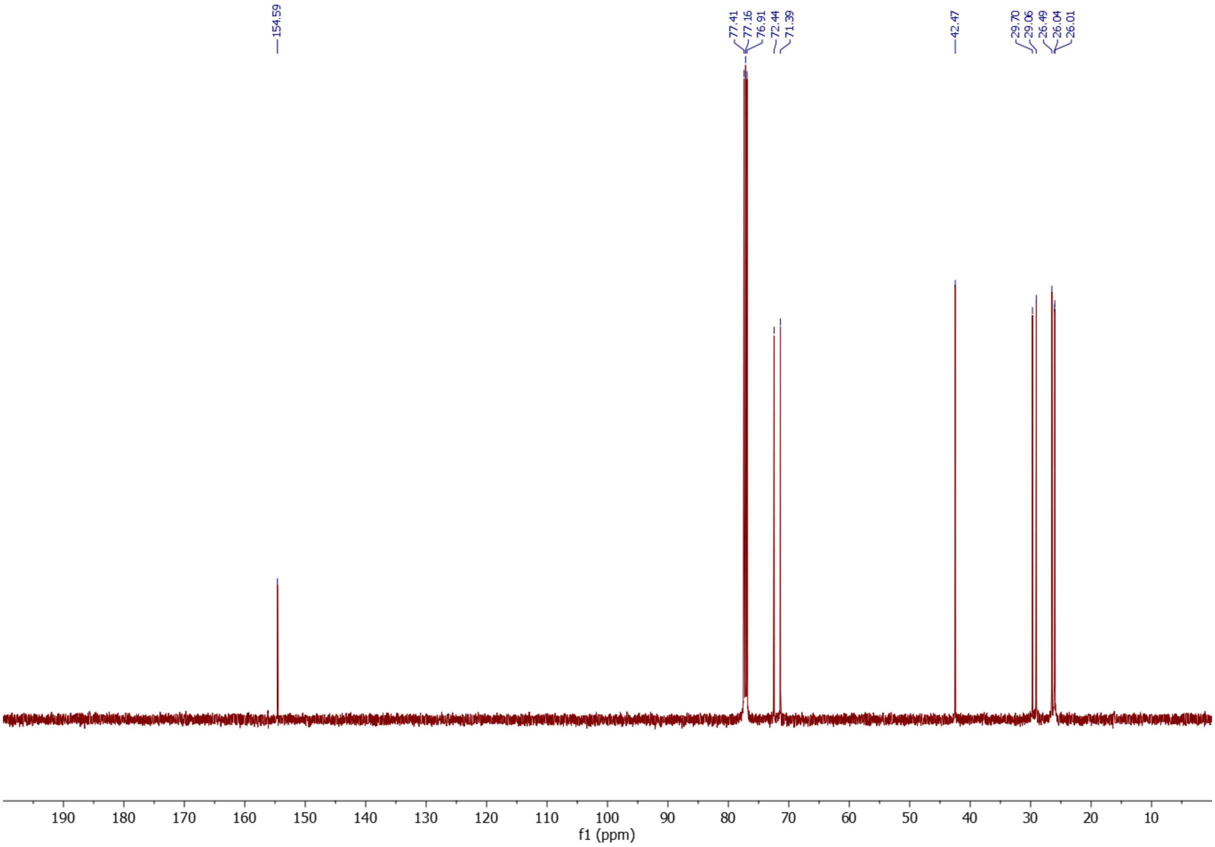

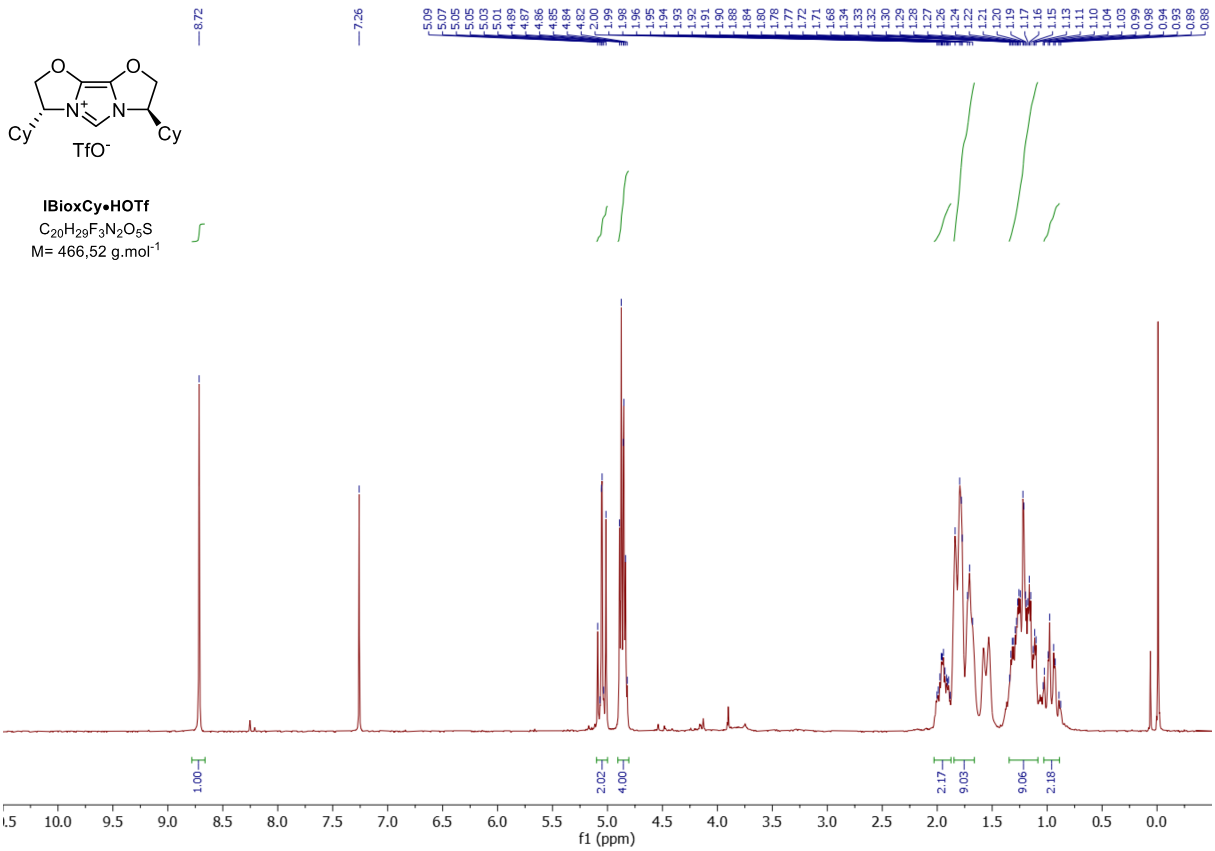

IBioxCy•HOTf

$C_{20}H_{29}F_3N_2O_5S$

M= 466,52 g.mol^{-1}

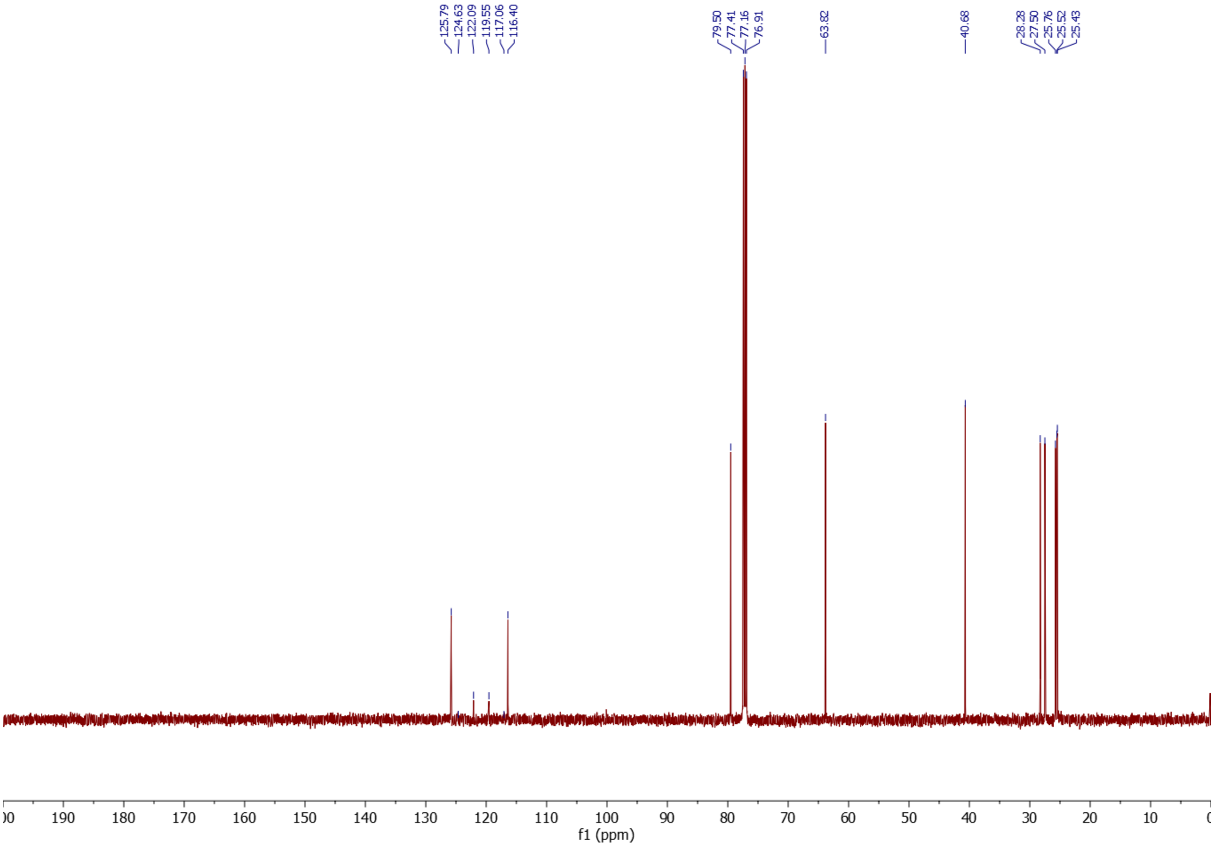

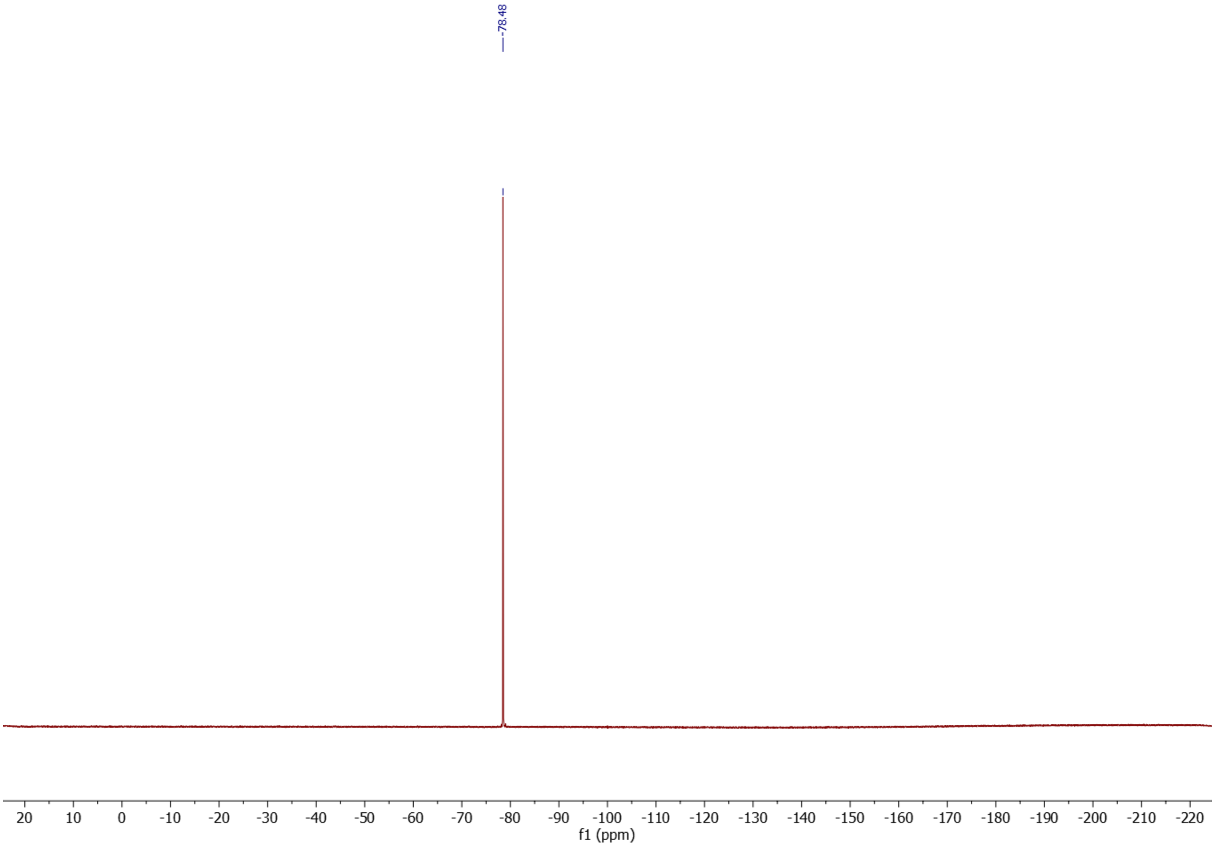
-78.48
20
10
0
-10
-20
-30
-40
-50
-60
-70
-80
-90
-100
-110
-120
-130
-140
-150
-160
-170
-180
-190
-200
-210
-220
f1 (ppm)

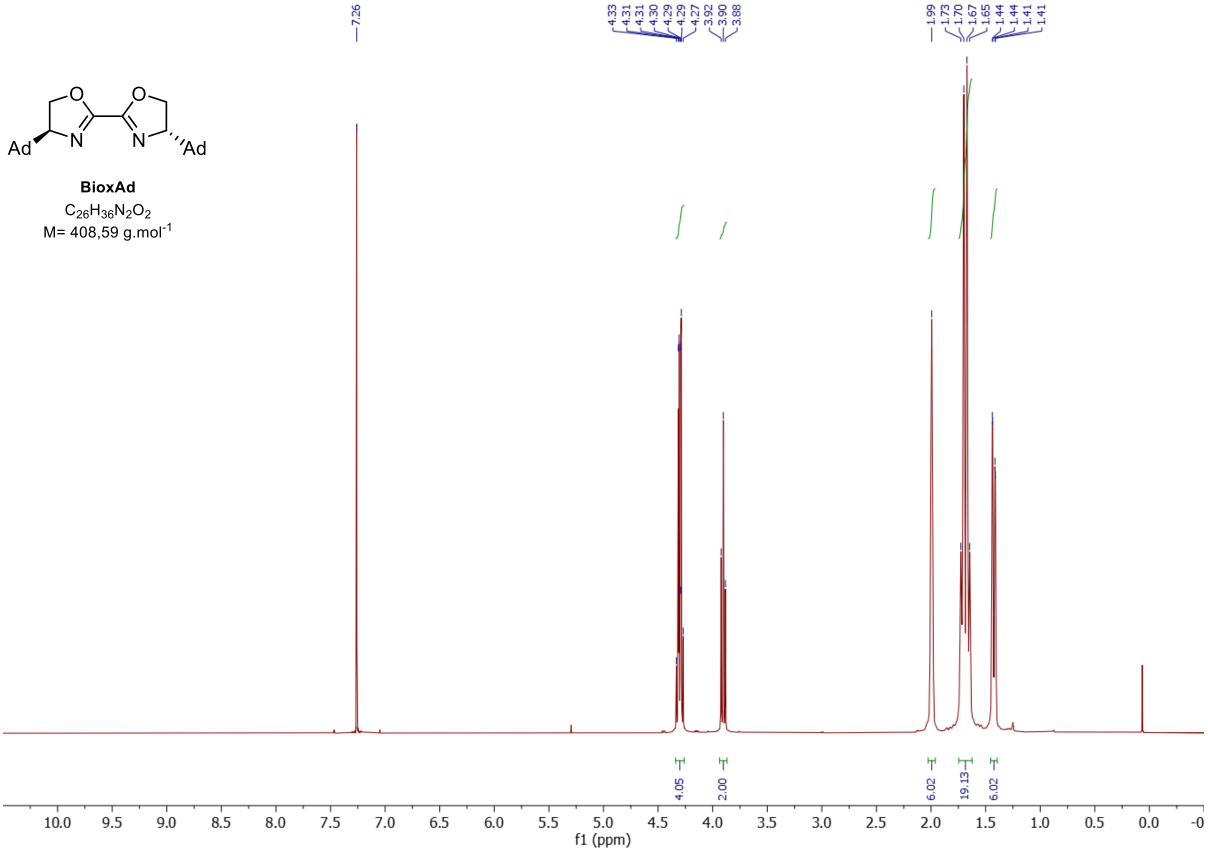

BioxAd

$C_{26}H_{36}N_2O_2$

M= 408,59 g.mol^{-1}

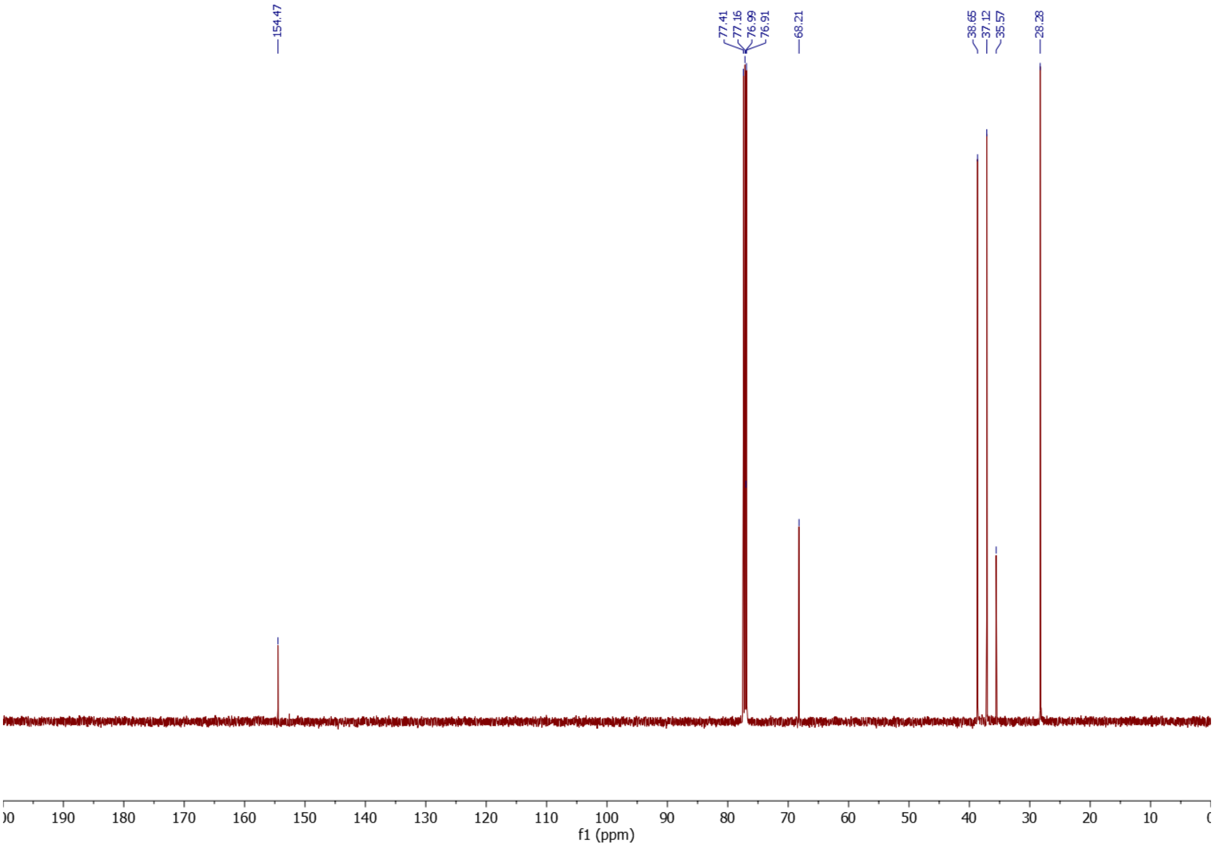

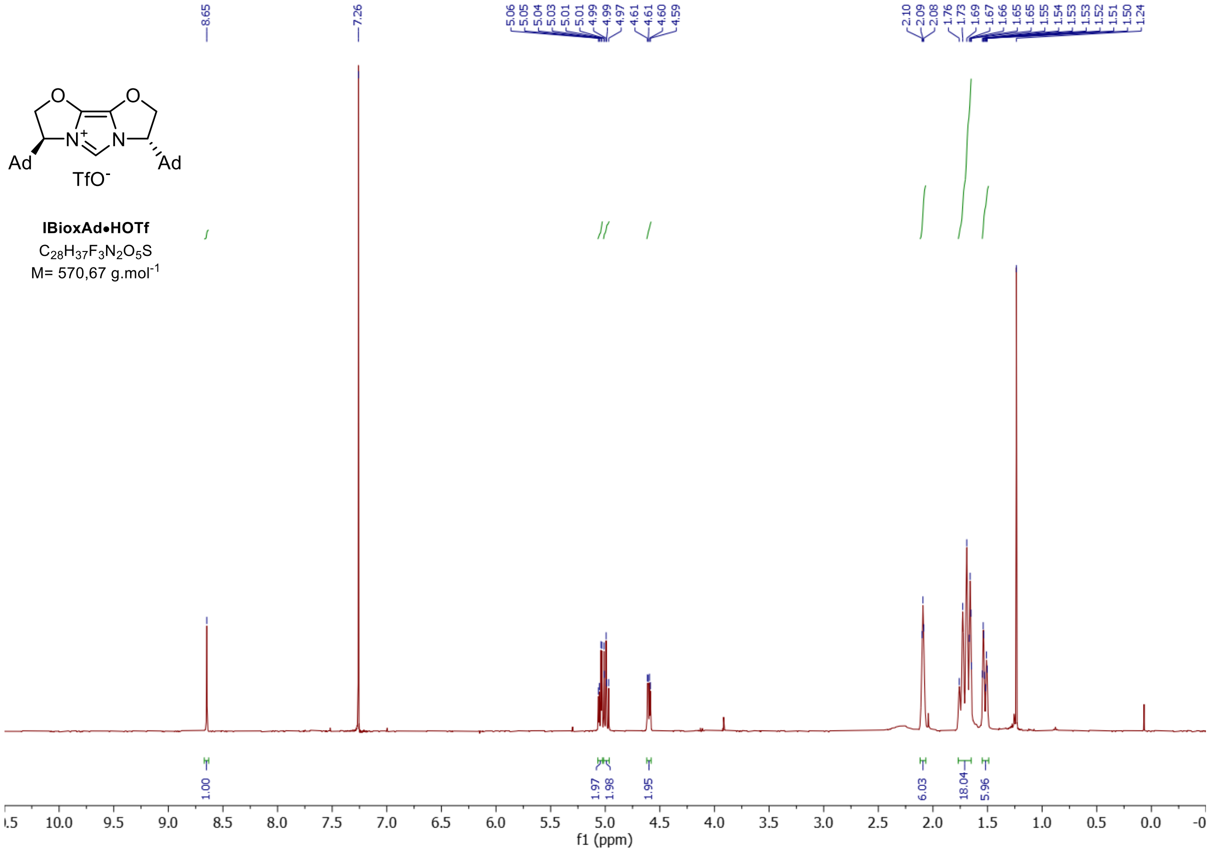

IBioxAd•HOTf

$C_{28}H_{37}F_3N_2O_5S$

M= 570,67 g.mol^{-1}

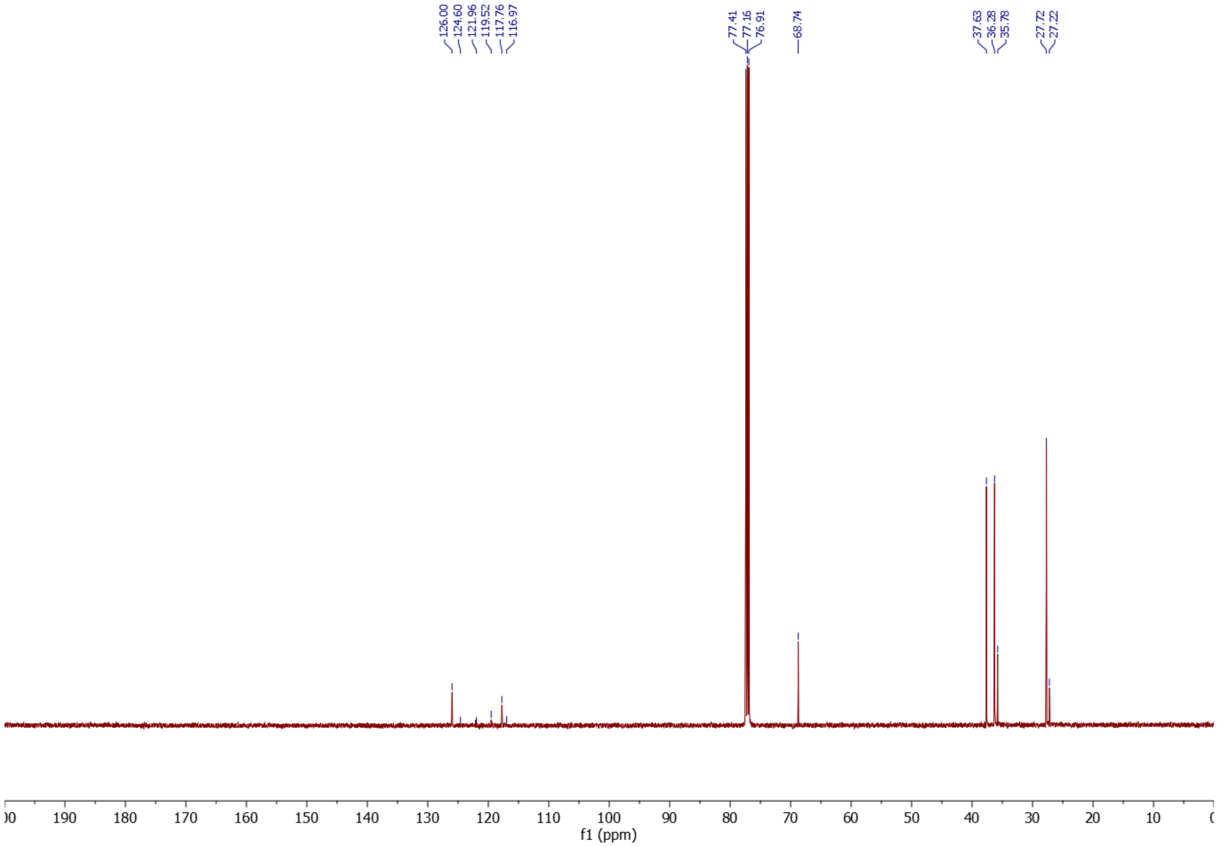

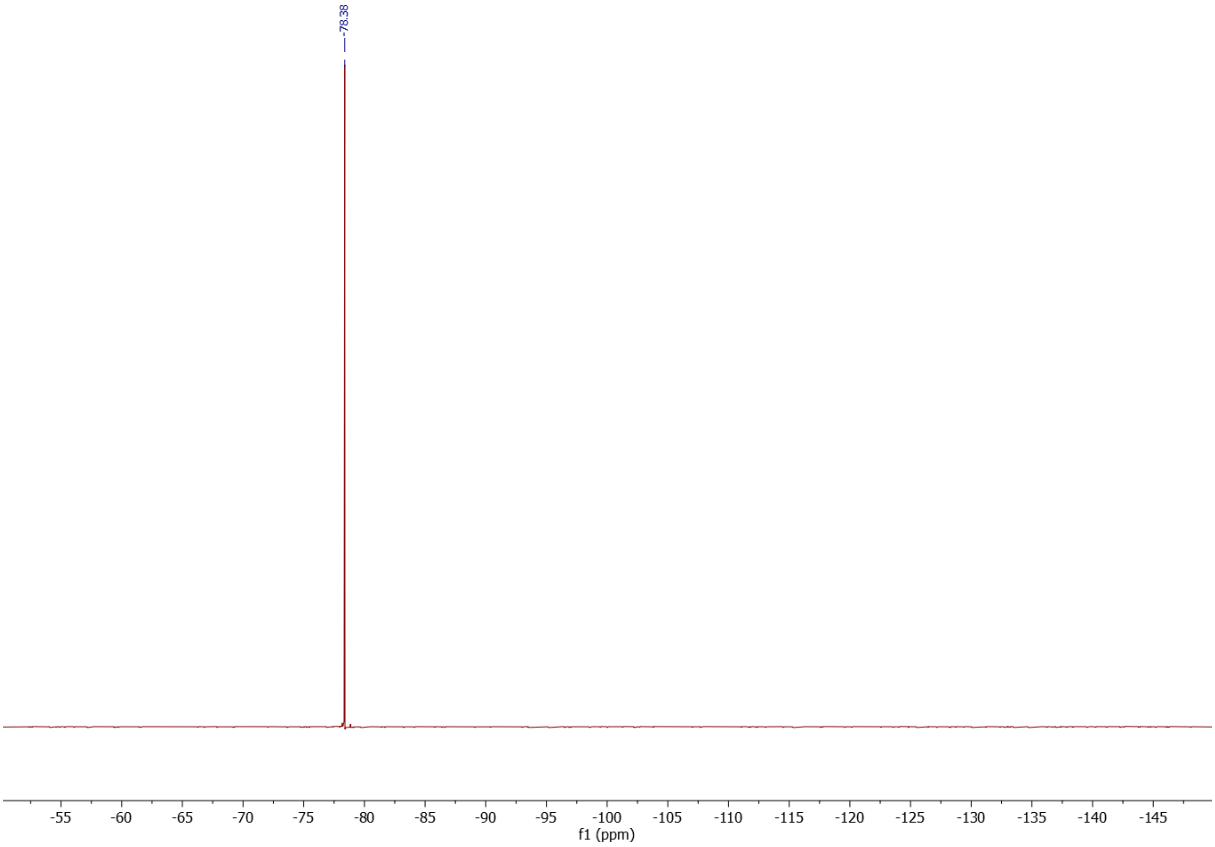
-78.38
-55
-60
-65
-70
-75
-80
-85
-90
-95
-100
-105
-110
-115
-120
-125
-130
-135
-140
-145
f1 (ppm)

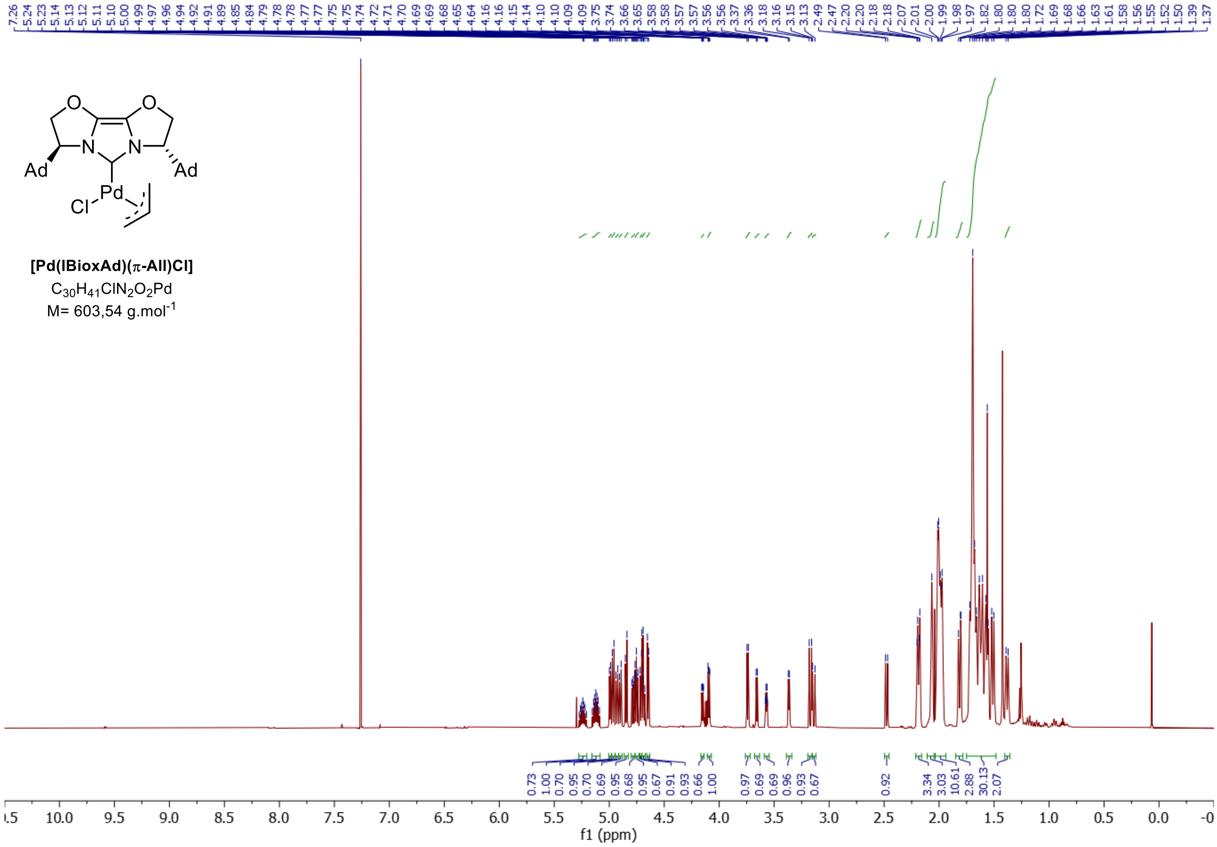

[Pd(IBioxAd)(π-All)Cl]

$C_{30}H_{41}ClN_2O_2Pd$

M= 603,54 g.mol^{-1}

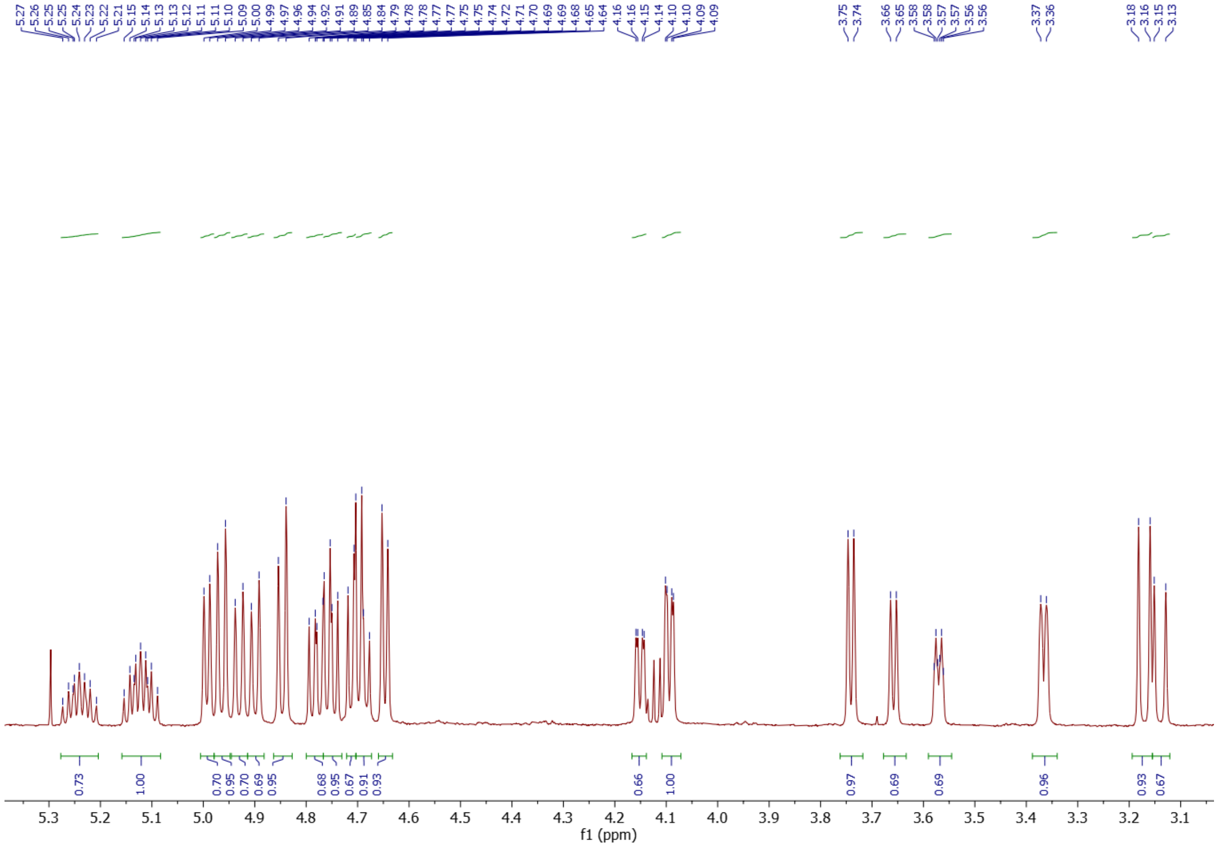

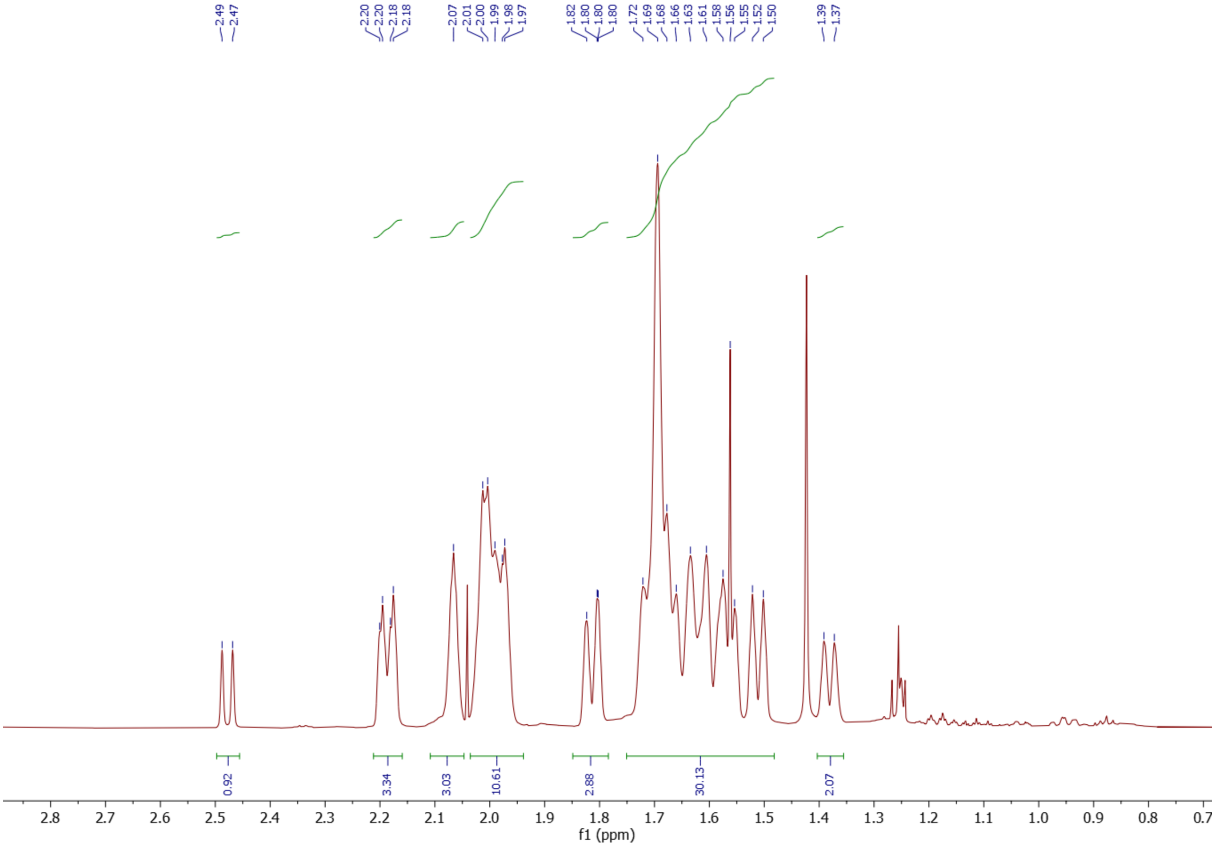
2.49
2.47
2.20
2.20
2.18
2.18
2.07
2.01
2.00
1.99
1.98
1.97
1.82
1.80
1.80
1.80
1.72
1.69
1.68
1.66
1.63
1.61
1.58
1.56
1.55
1.52
1.50
1.39
1.37
0.92
3.34
3.03
10.61
2.88
30.13
2.07
2.8
2.7
2.6
2.5
2.4
2.3
2.2
2.1
2.0
1.9
1.8
1.7
1.6
1.5
1.4
1.3
1.2
1.1
1.0
0.9
0.8
0.7
f1 (ppm)

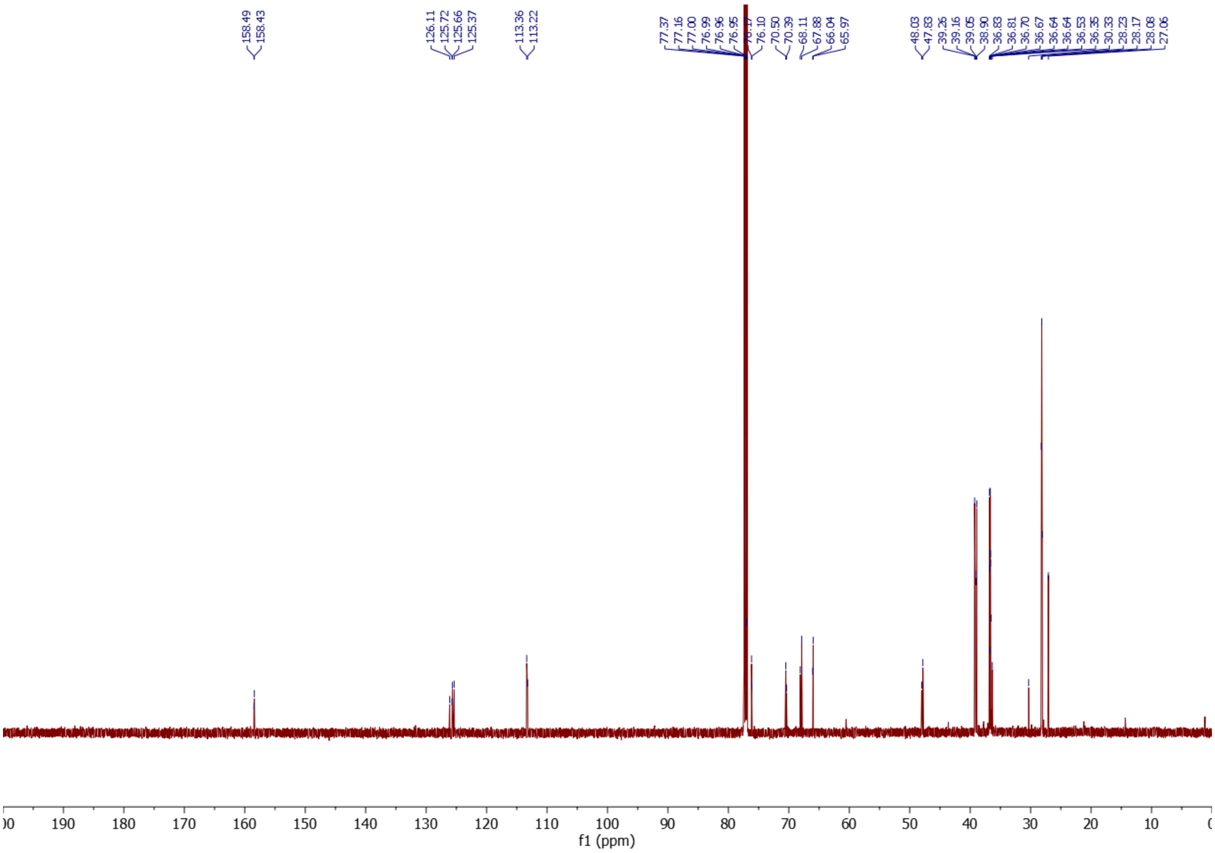
158.49
158.43
126.11
125.72
125.66
125.37
113.36
113.22
77.37
77.16
77.00
76.99
76.96
76.95
76.17
76.10
70.50
70.39
68.11
67.88
66.04
65.97
48.03
47.83
39.26
39.16
39.05
38.90
36.83
36.81
36.70
36.67
36.64
36.64
36.53
36.35
30.33
28.23
28.17
28.08
27.06
190
180
170
160
150
140
130
120
110
100
90
80
70
60
50
40
30
20
10
f1 (ppm)

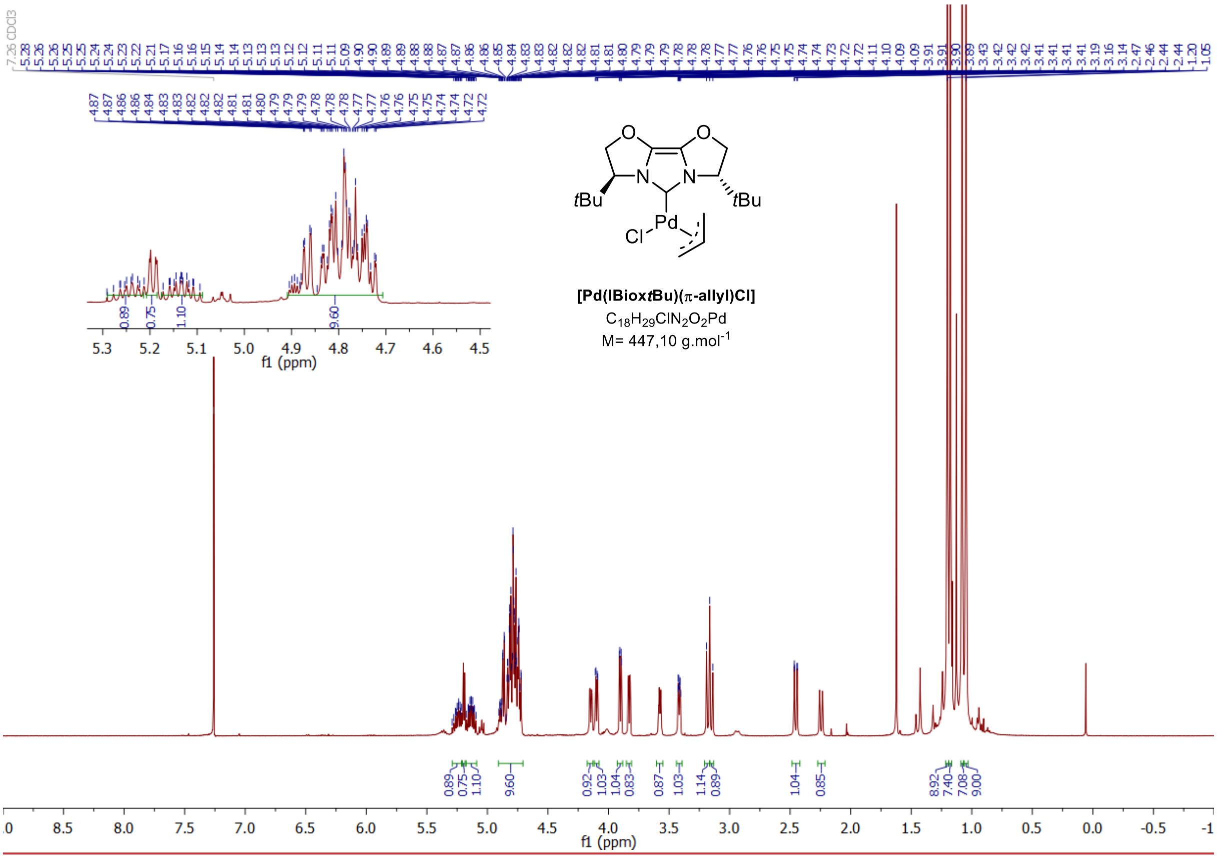

[Pd(IBiox*t*Bu)(π-allyl)Cl]

$C_{18}H_{29}ClN_2O_2Pd$

M= 447,10 g.mol^{-1}

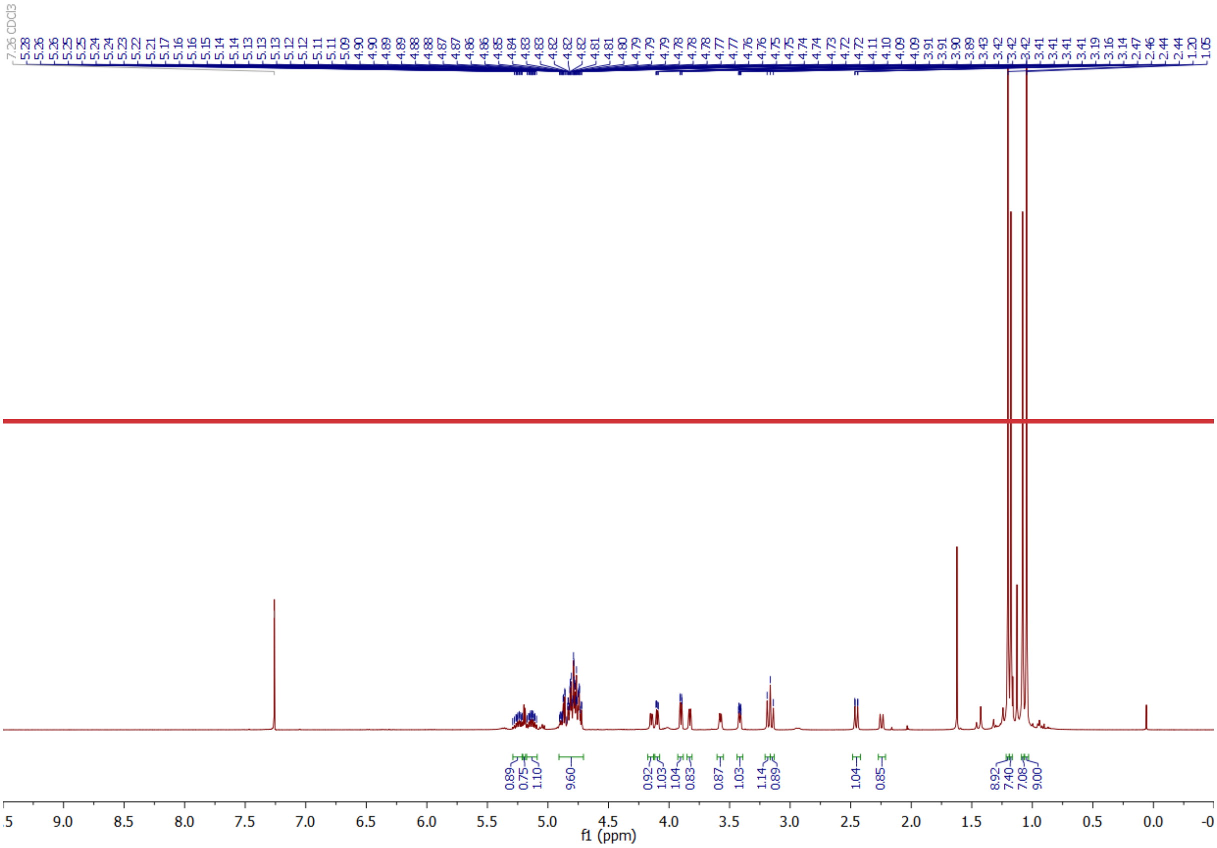

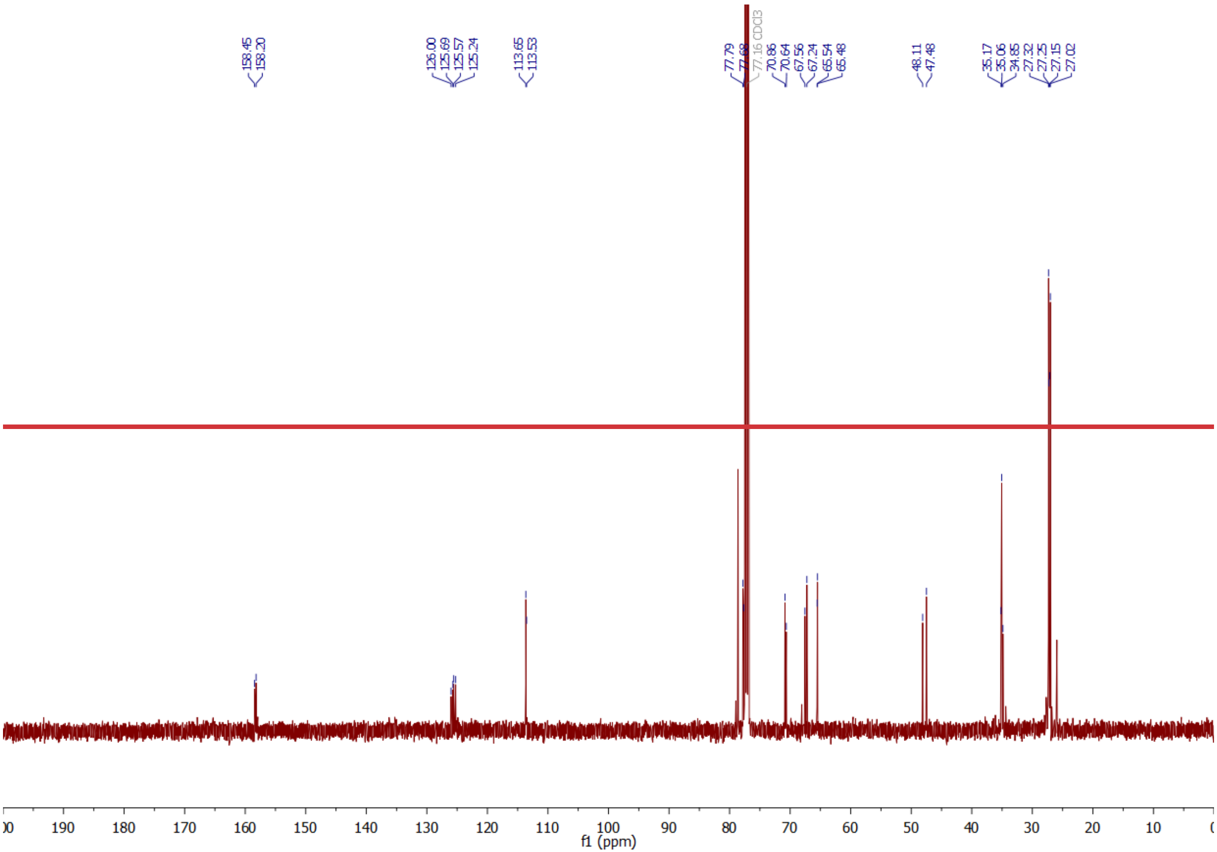
158.45
158.20
126.00
125.69
125.57
125.24
113.65
113.53
77.79
77.68
77.16 CDCl3
70.86
70.64
67.56
67.24
65.54
65.48
48.11
47.48
35.17
35.06
34.85
27.32
27.25
27.15
27.02
190
180
170
160
150
140
130
120
110
100
90
80
70
60
50
40
30
20
10
f1 (ppm)

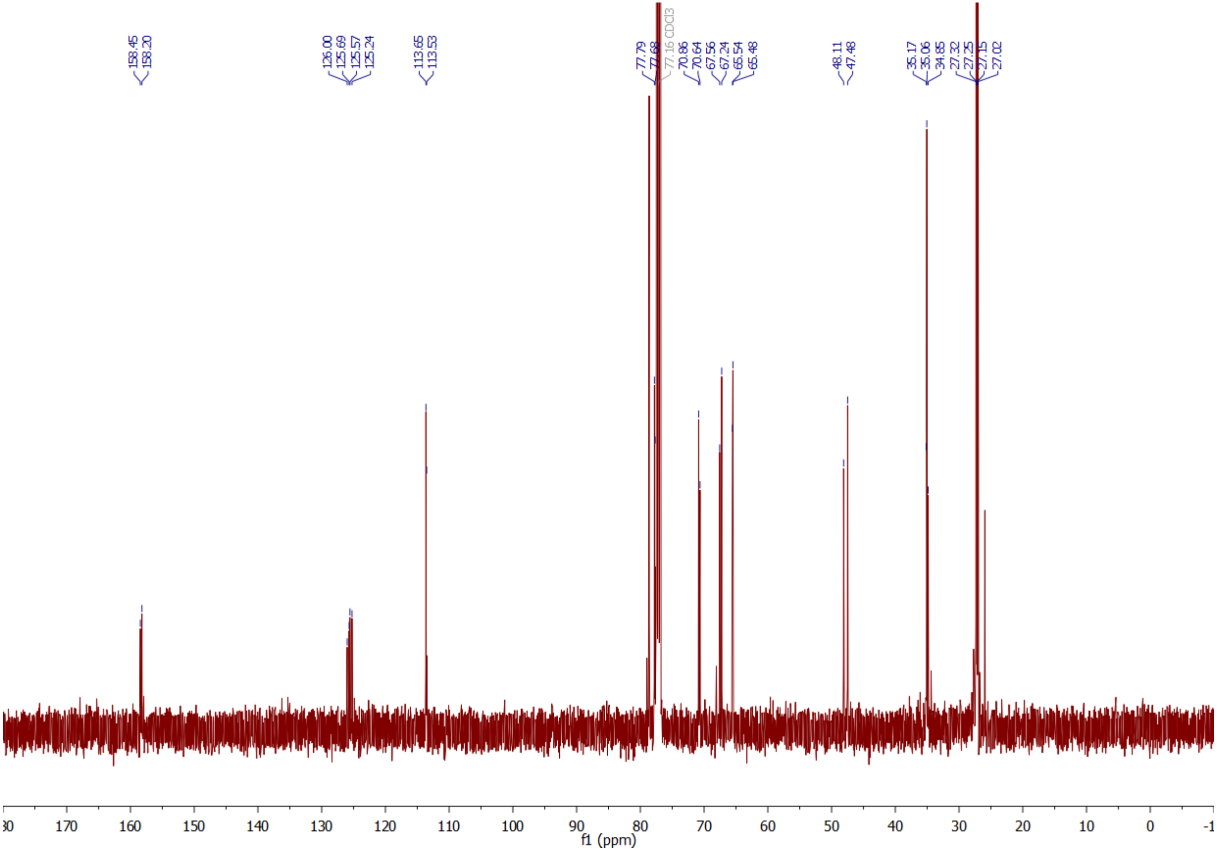
158.45
158.20
126.00
125.69
125.57
125.24
113.65
113.53
77.79
77.68
77.16 CDCl3
70.86
70.64
67.56
67.24
65.54
65.48
48.11
47.48
35.17
35.06
34.85
27.32
27.25
27.15
27.02
170
160
150
140
130
120
110
100
90
80
70
60
50
40
30
20
10
0
f1 (ppm)

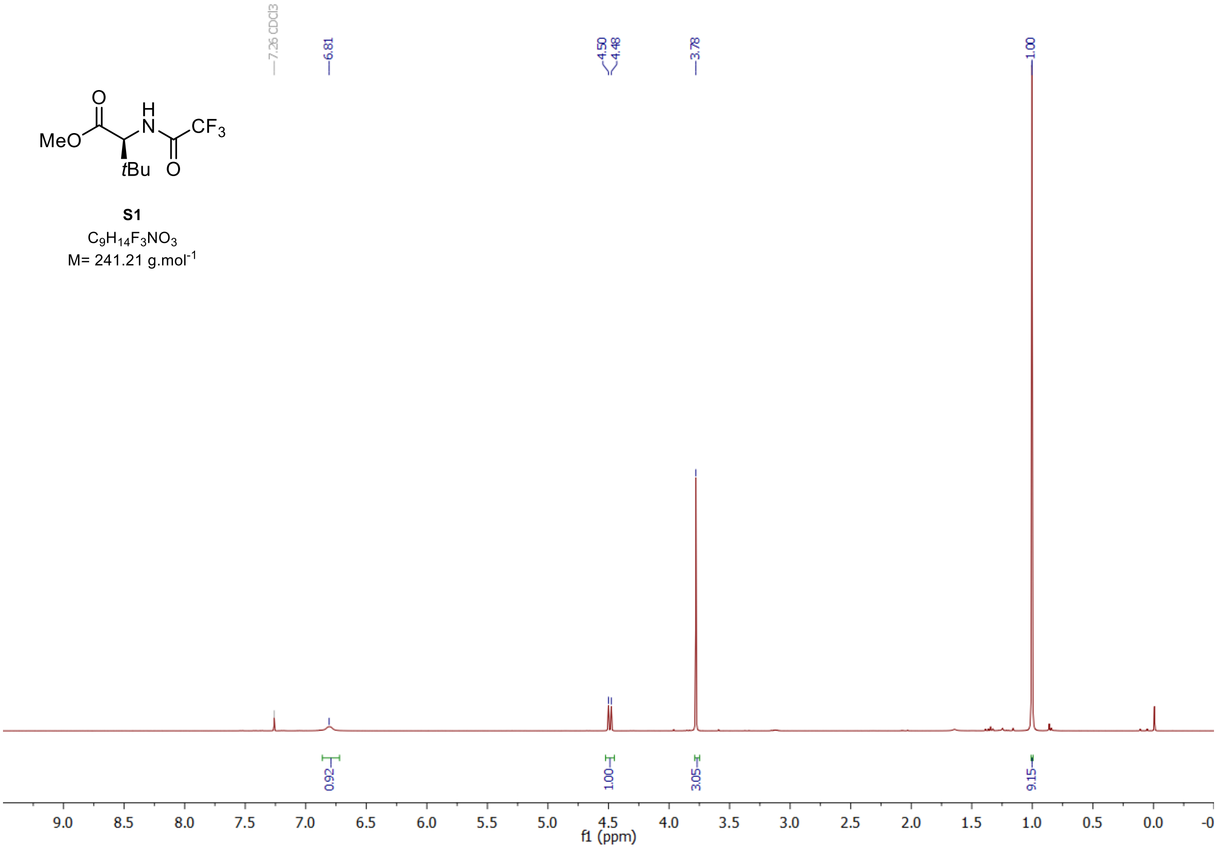

S1

$C_9H_{14}F_3NO_3$

M= 241.21 g.mol^{-1}

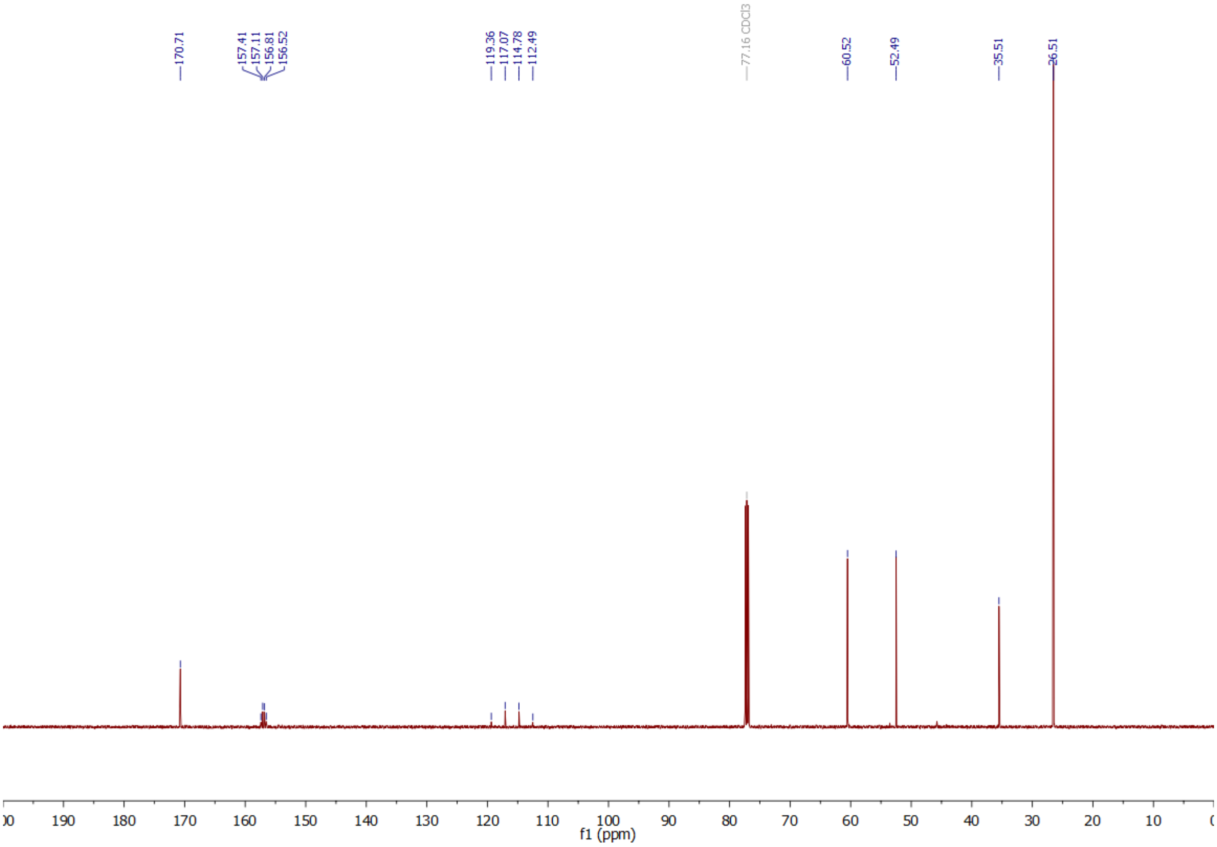

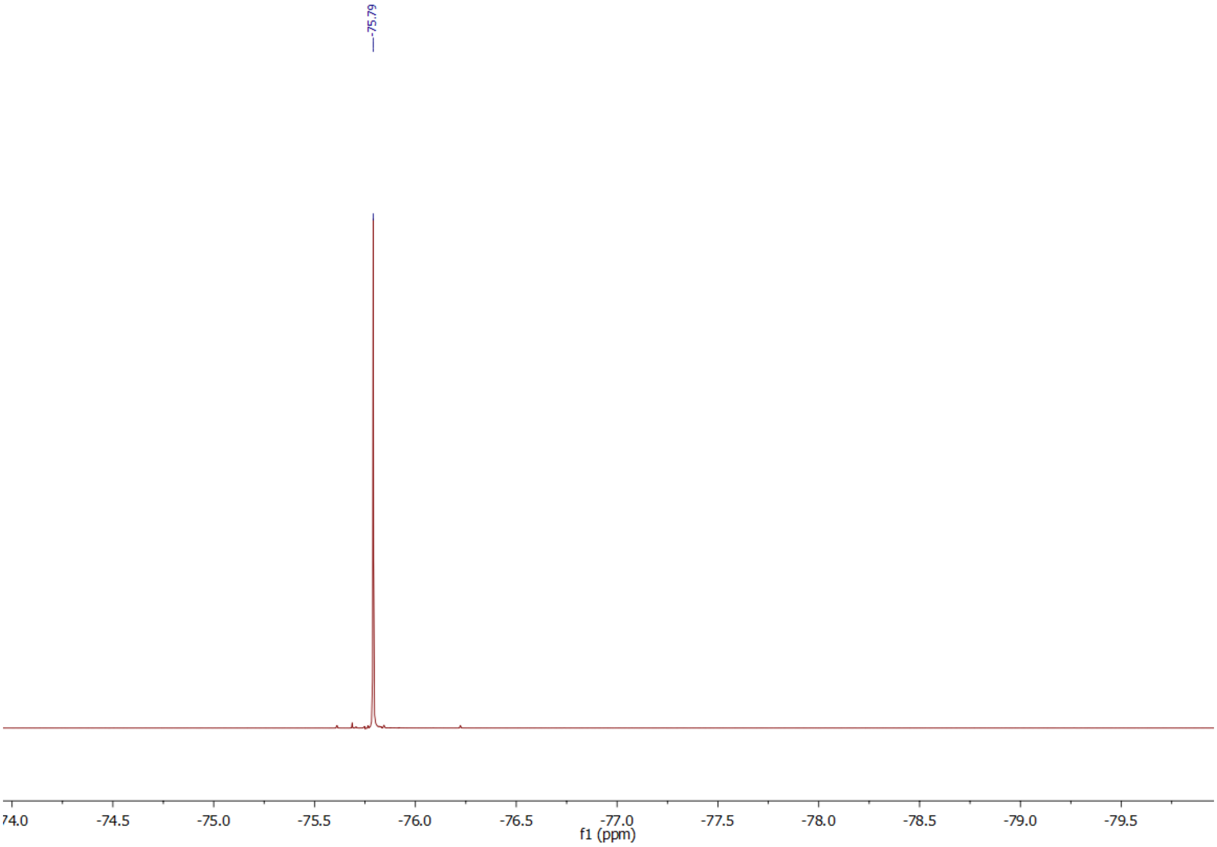
-75.79
74.0
-74.5
-75.0
-75.5
-76.0
-76.5
-77.0
-77.5
-78.0
-78.5
-79.0
-79.5
f1 (ppm)

Me
Me
HO
NH2
tBu

S2

$C_8H_{19}NO$

M= 145,25 g.mol^{-1}

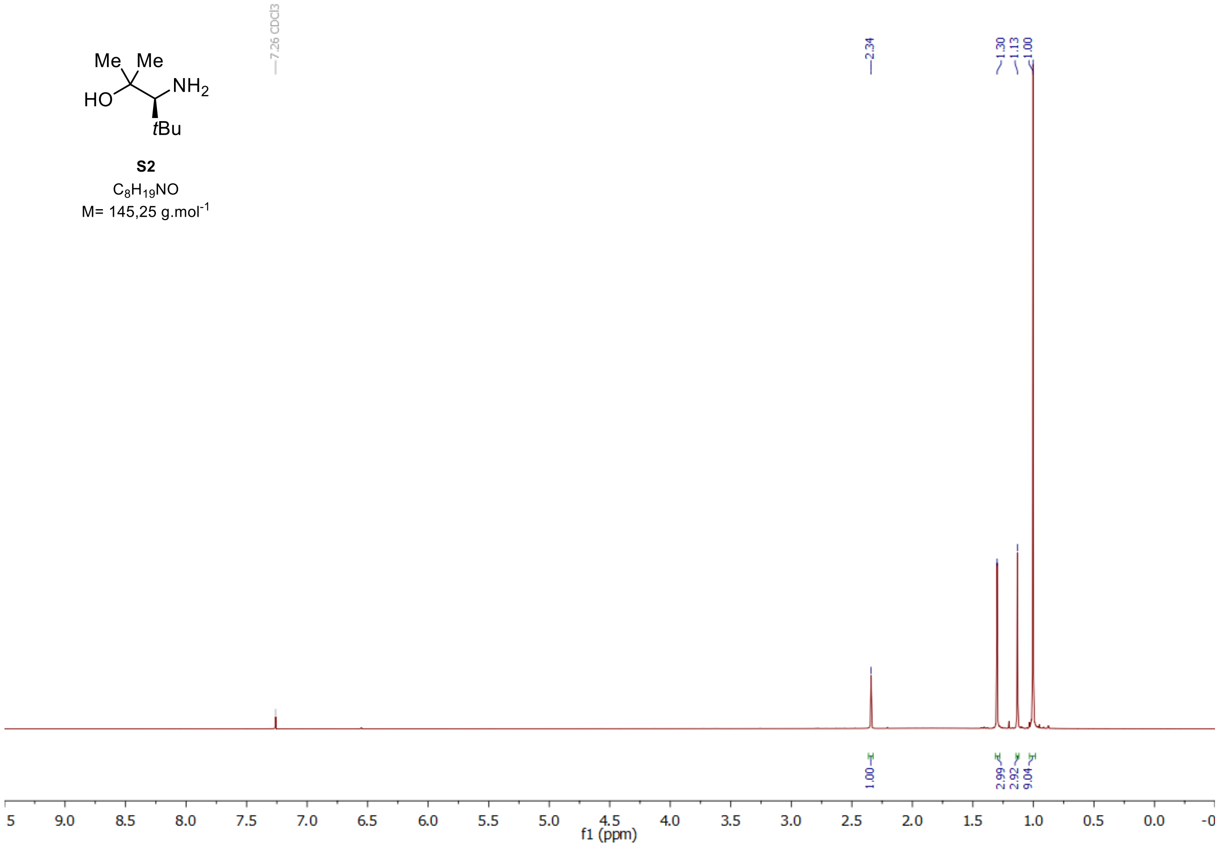

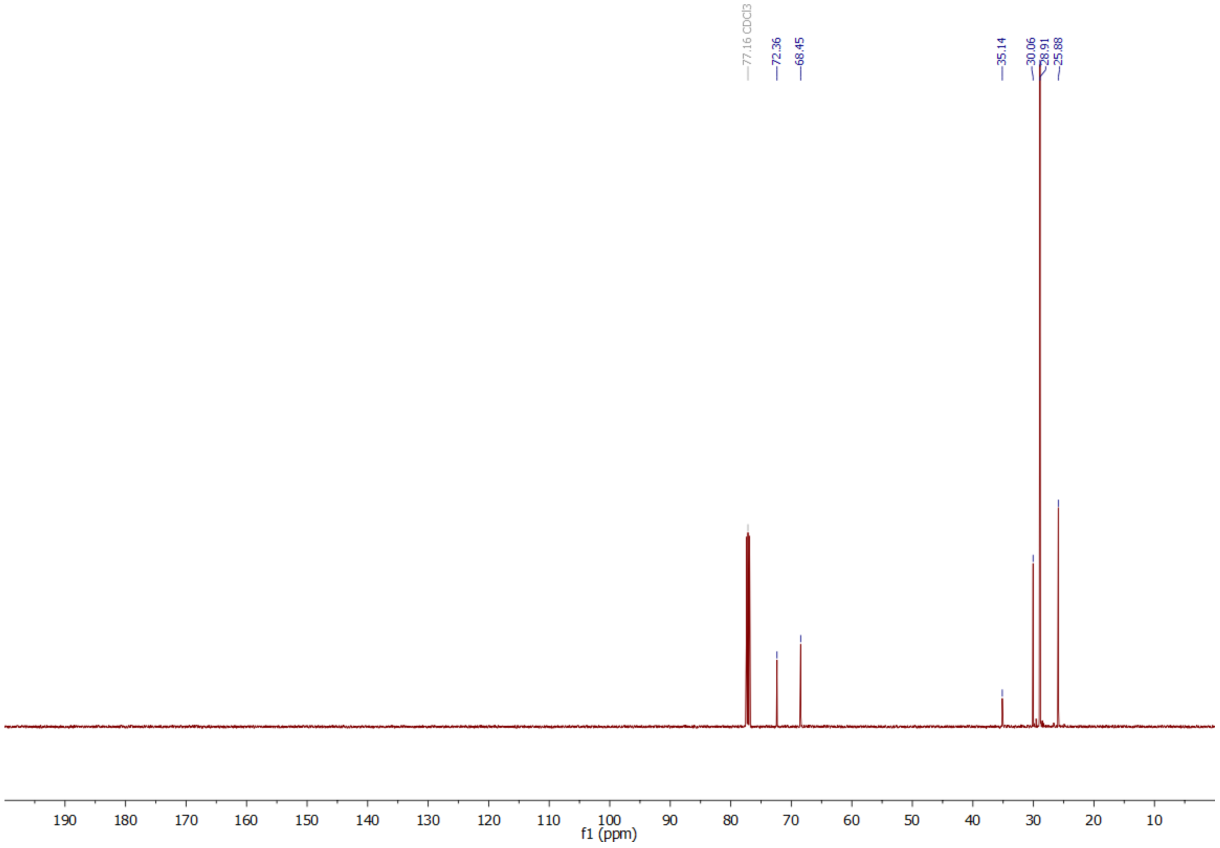

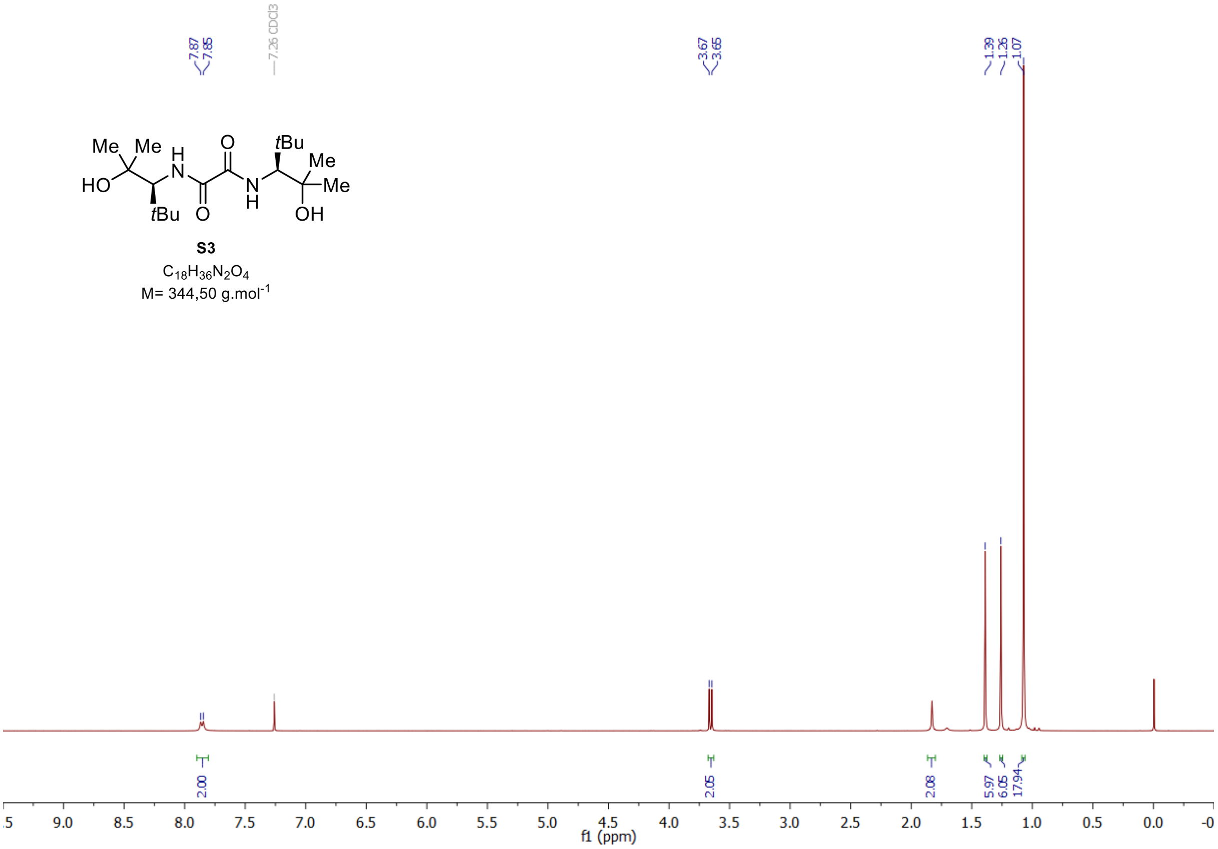

S3

$C_{18}H_{36}N_2O_4$

M= 344,50 g.mol^{-1}

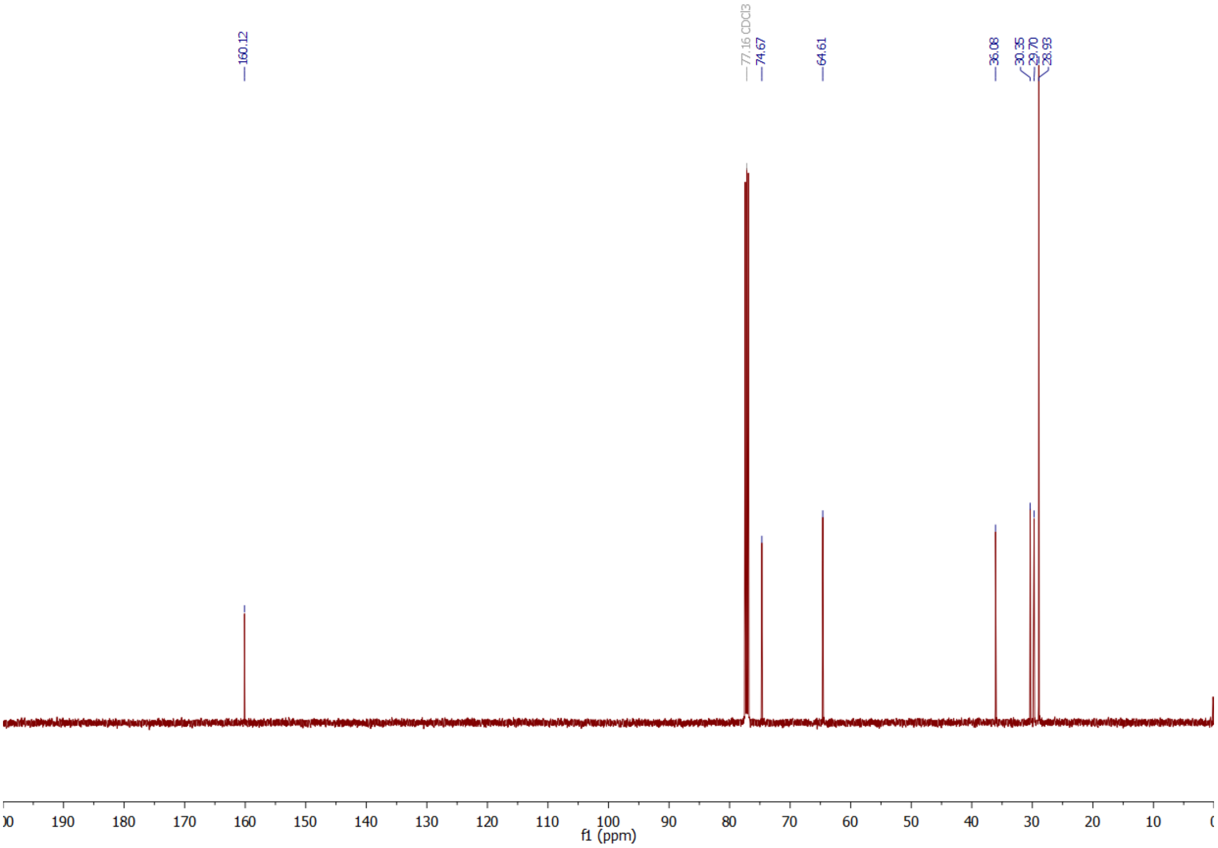

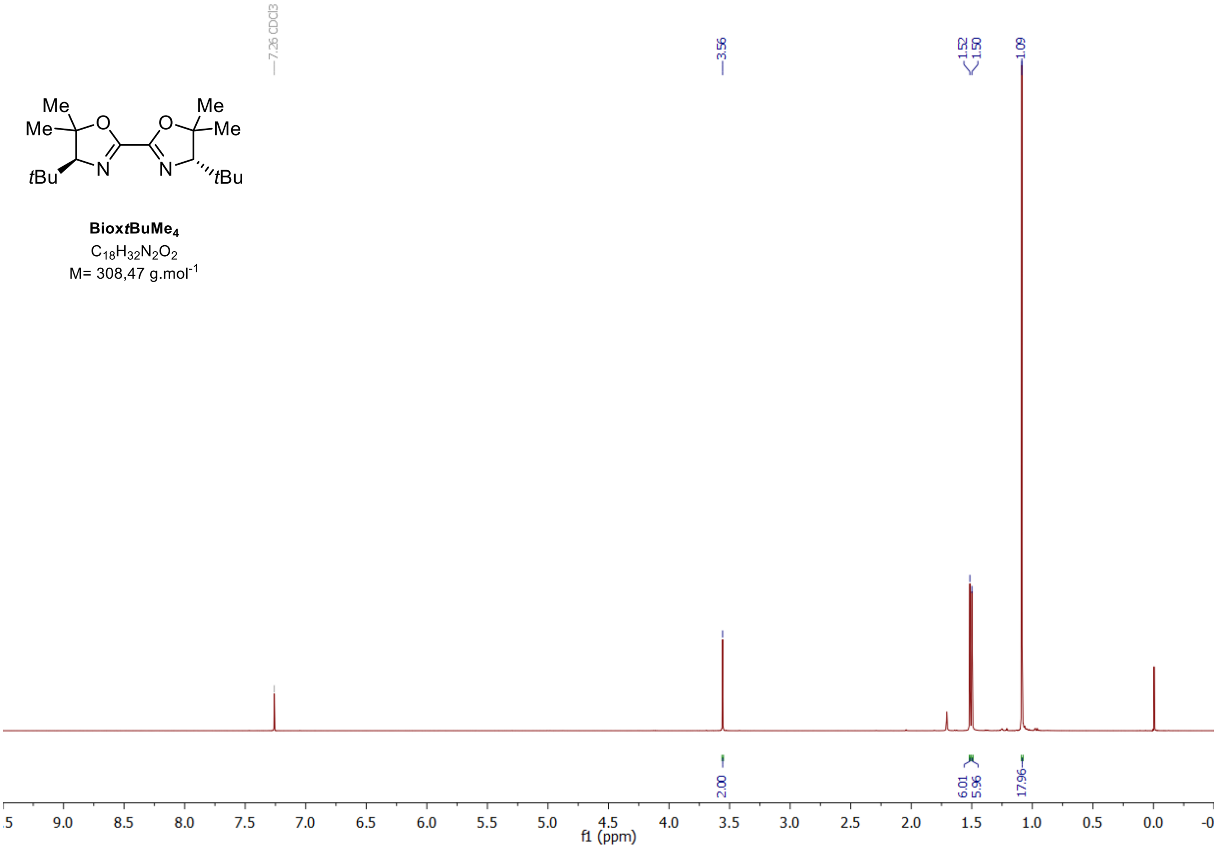

Biox*t*BuMe$_4$
$C_{18}H_{32}N_2O_2$
M= 308,47 g.mol^{-1}

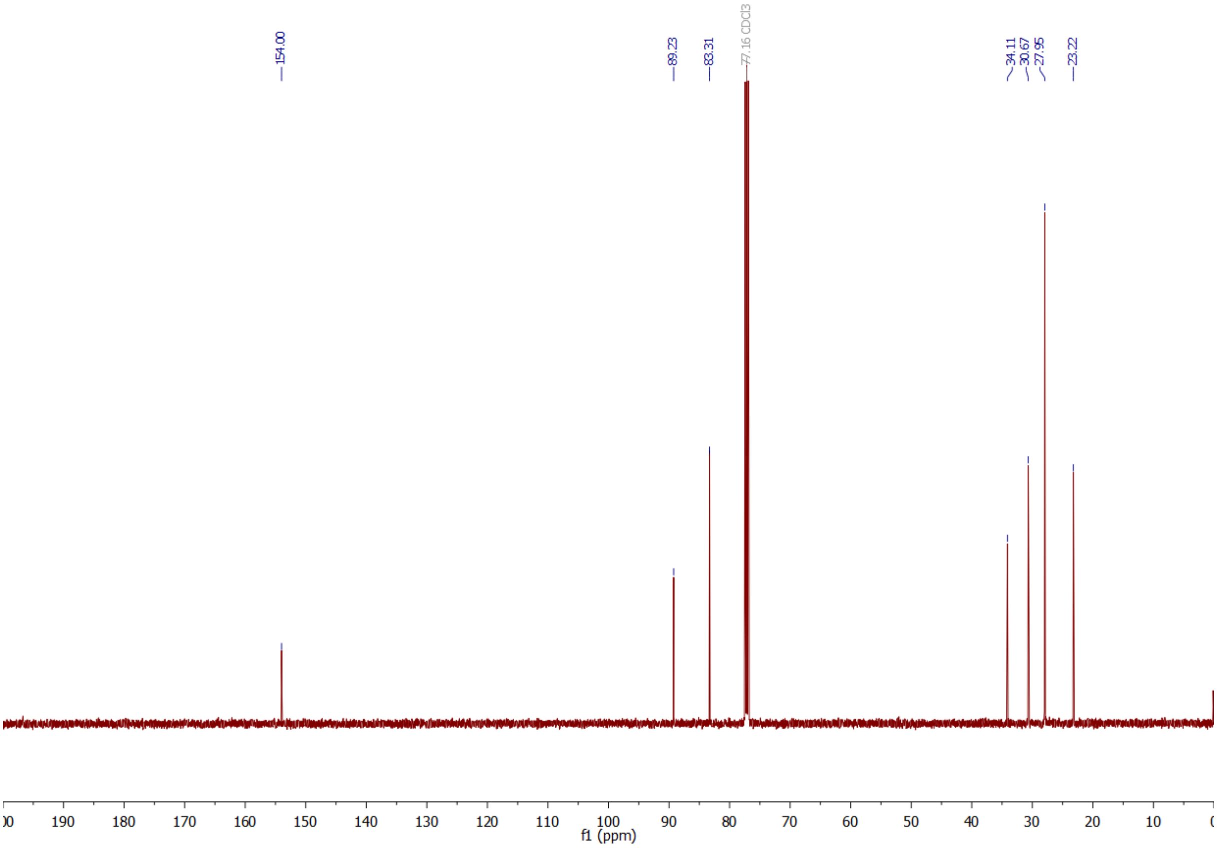

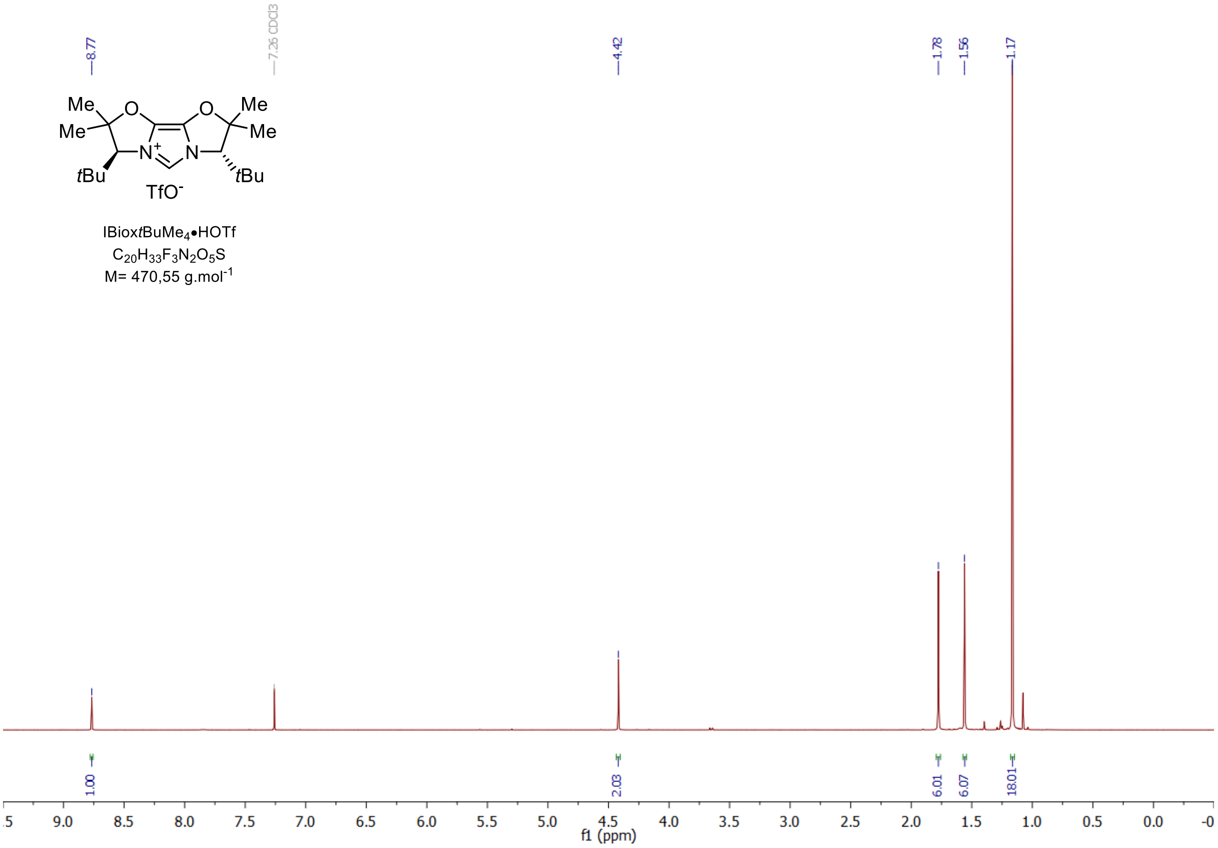

IBiox*t*BuMe$_4$•HOTf
$C_{20}H_{33}F_3N_2O_5S$
M= 470,55 g.mol^{-1}

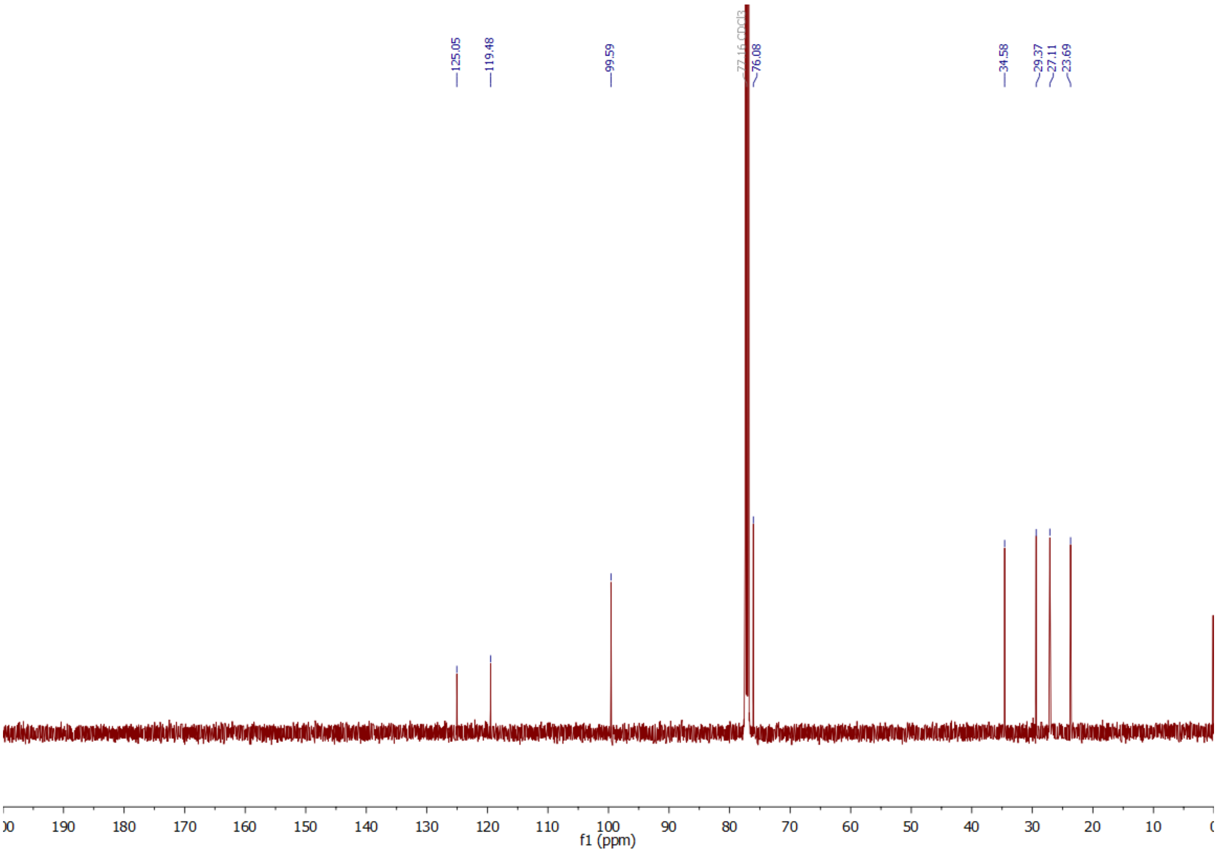

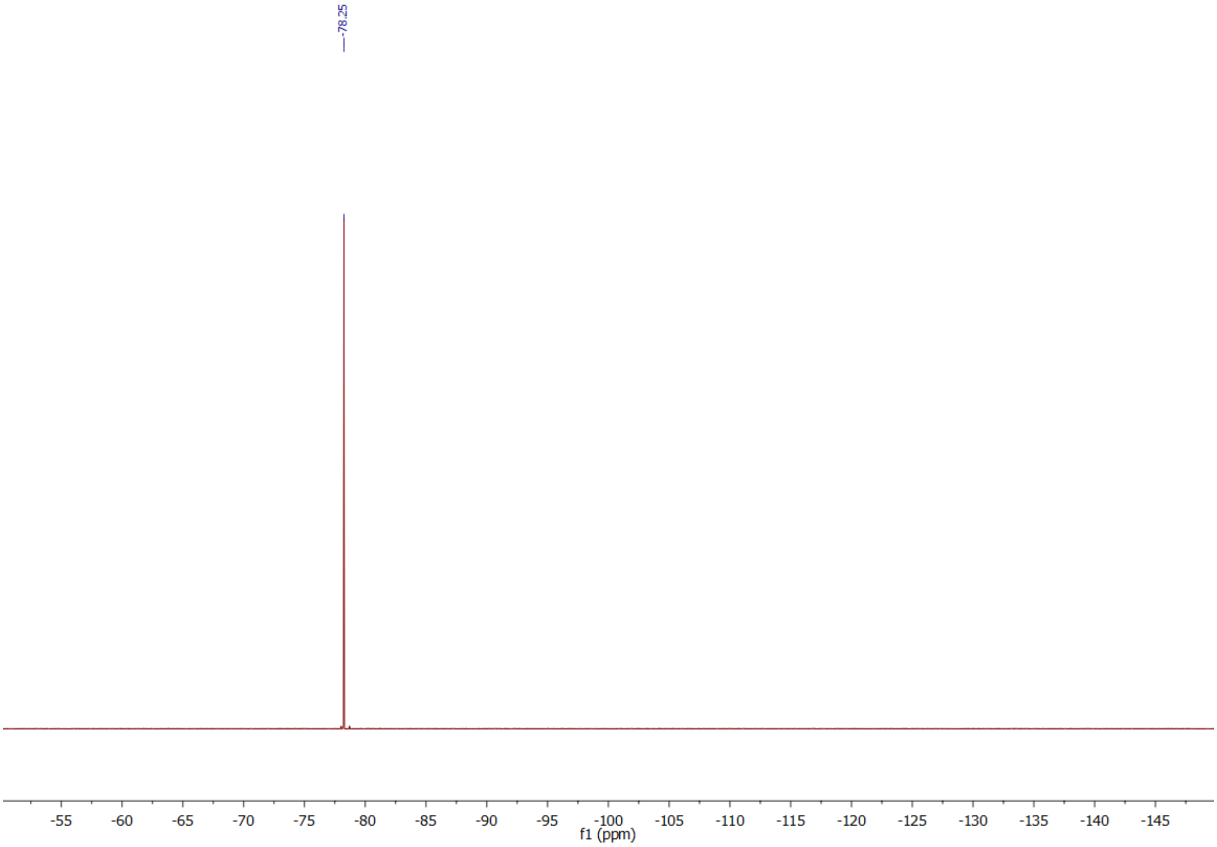
-78.25
-55
-60
-65
-70
-75
-80
-85
-90
-95
-100
-105
-110
-115
-120
-125
-130
-135
-140
-145
f1 (ppm)

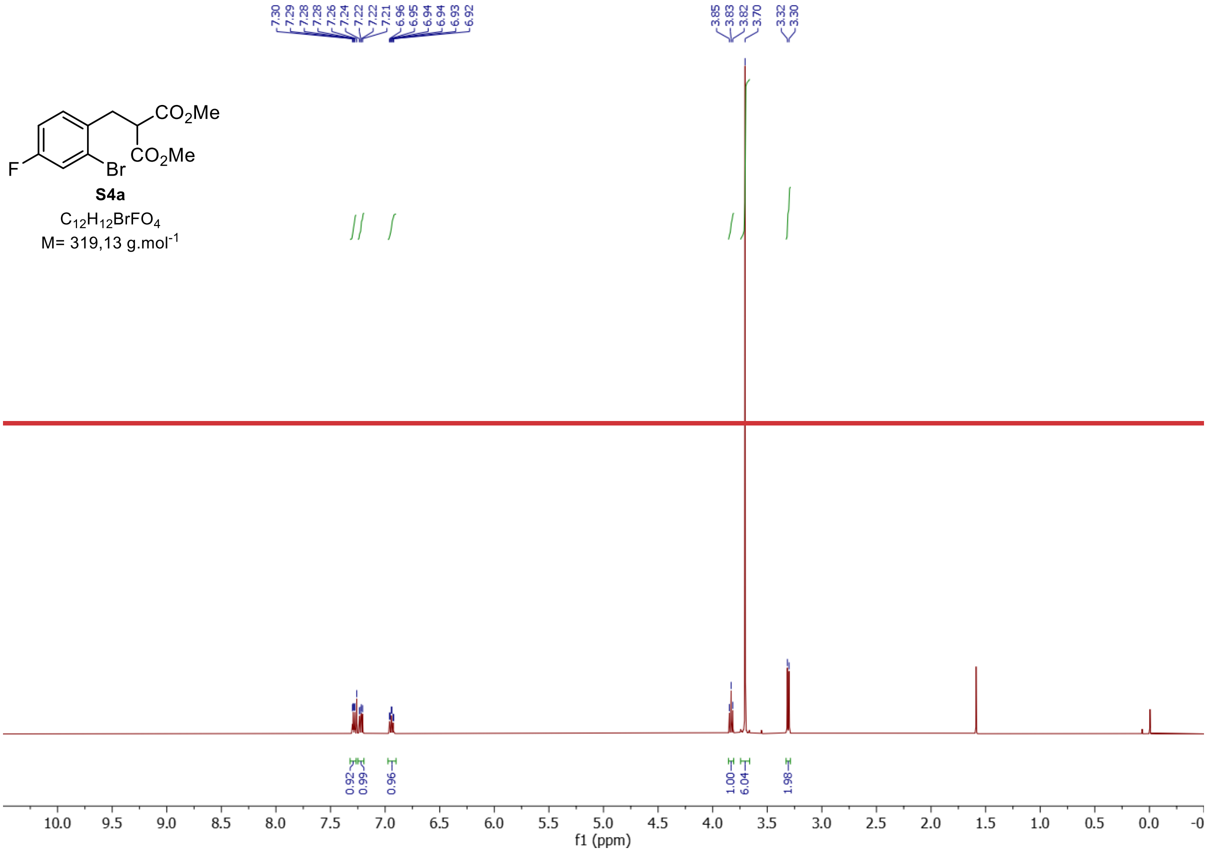
S4a
$C_{12}H_{12}BrFO_4$
M= 319,13 g.mol^{-1}
CO2Me
CO2Me
F
Br
7.30 7.29 7.28 7.28 7.26 7.24 7.22 7.22 7.21 6.96 6.95 6.94 6.94 6.93 6.92
3.85 3.83 3.82 3.70 3.32 3.30
0.92 0.99 0.96 1.00 6.04 1.98
10.0 9.5 9.0 8.5 8.0 7.5 7.0 6.5 6.0 5.5 5.0 4.5 4.0 3.5 3.0 2.5 2.0 1.5 1.0 0.5 0.0 -0
f1 (ppm)

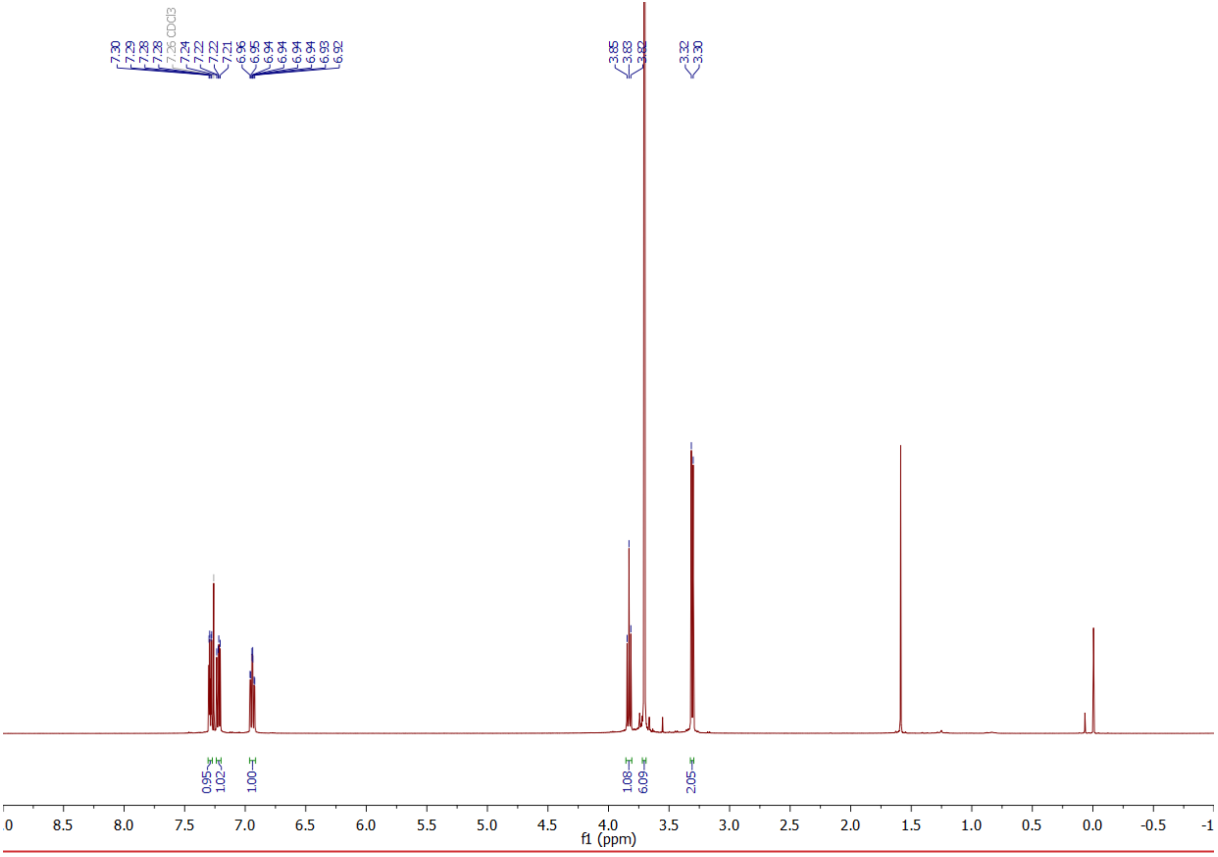
7.30 7.29 7.28 7.28 7.26 CDCl3 7.24 7.22 7.22 7.21 6.96 6.95 6.94 6.94 6.94 6.94 6.93 6.92
3.85 3.83 3.82 3.32 3.30
0.95 1.02 1.00 1.08 6.09 2.05
0 8.5 8.0 7.5 7.0 6.5 6.0 5.5 5.0 4.5 4.0 3.5 3.0 2.5 2.0 1.5 1.0 0.5 0.0 -0.5 -1
f1 (ppm)

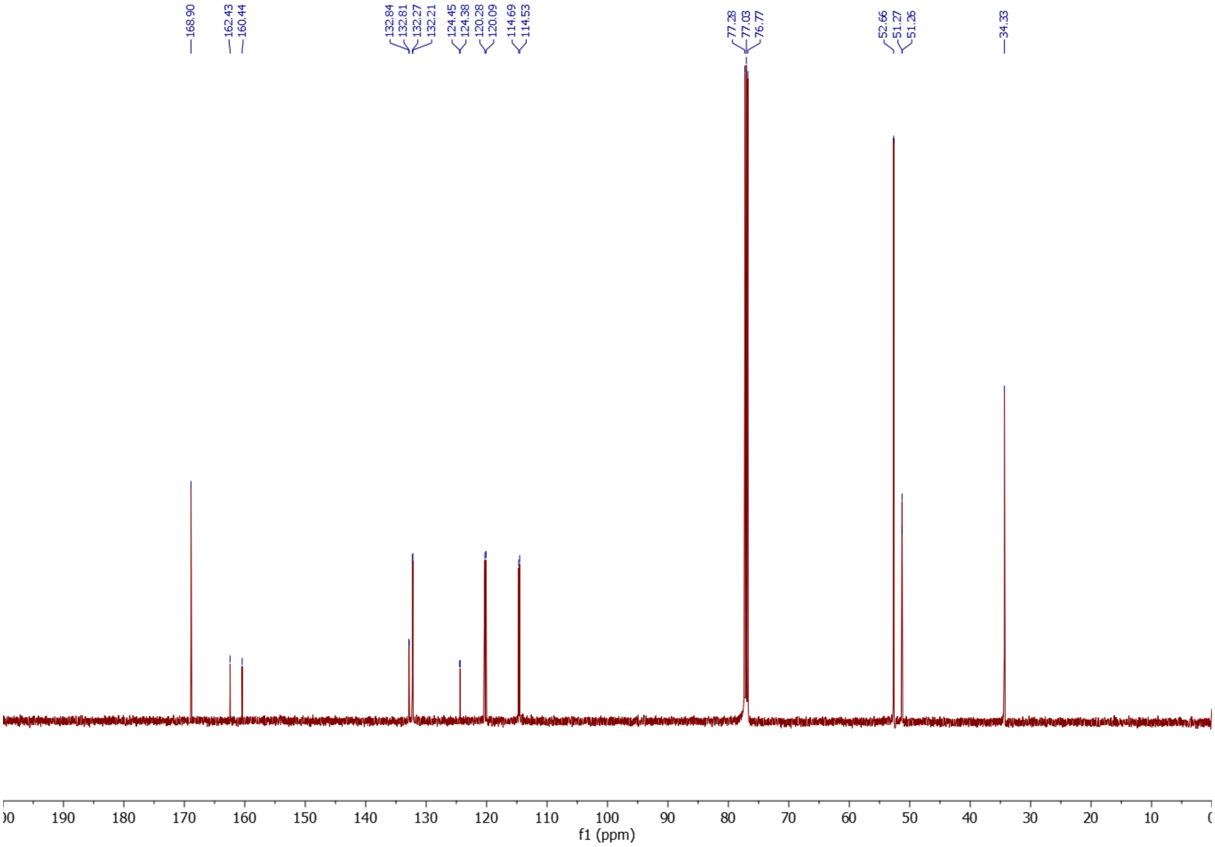
168.90
162.43
160.44
132.84
132.81
132.27
132.21
124.45
124.38
120.28
120.09
114.69
114.53
77.28
77.03
76.77
52.66
51.27
51.26
34.33
190
180
170
160
150
140
130
120
110
100
90
80
70
60
50
40
30
20
10
f1 (ppm)

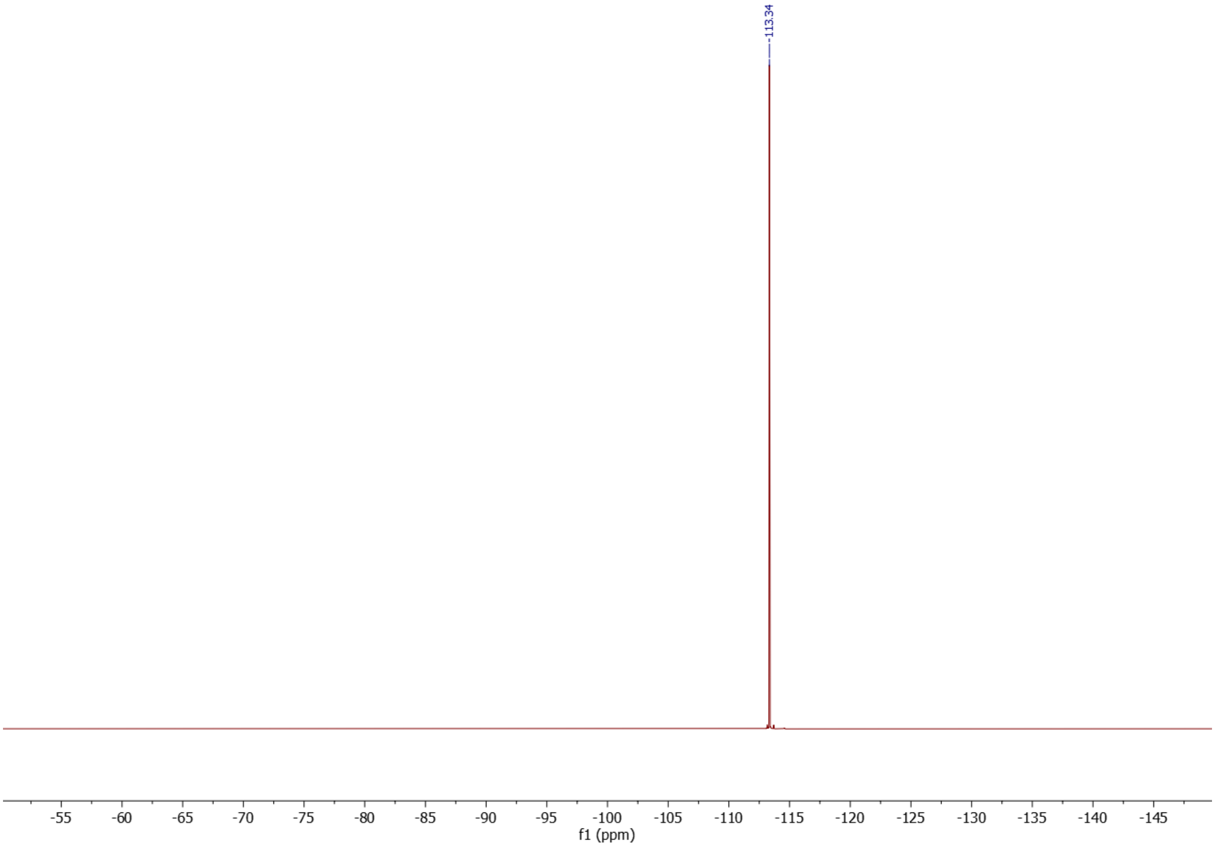
-113.34
-55
-60
-65
-70
-75
-80
-85
-90
-95
-100
-105
-110
-115
-120
-125
-130
-135
-140
-145
f1 (ppm)

CO$_2$*i*Pr
CO$_2$*i*Pr
Br

S4c

$C_{16}H_{21}BrO_4$

M= 357,24 g.mol^{-1}

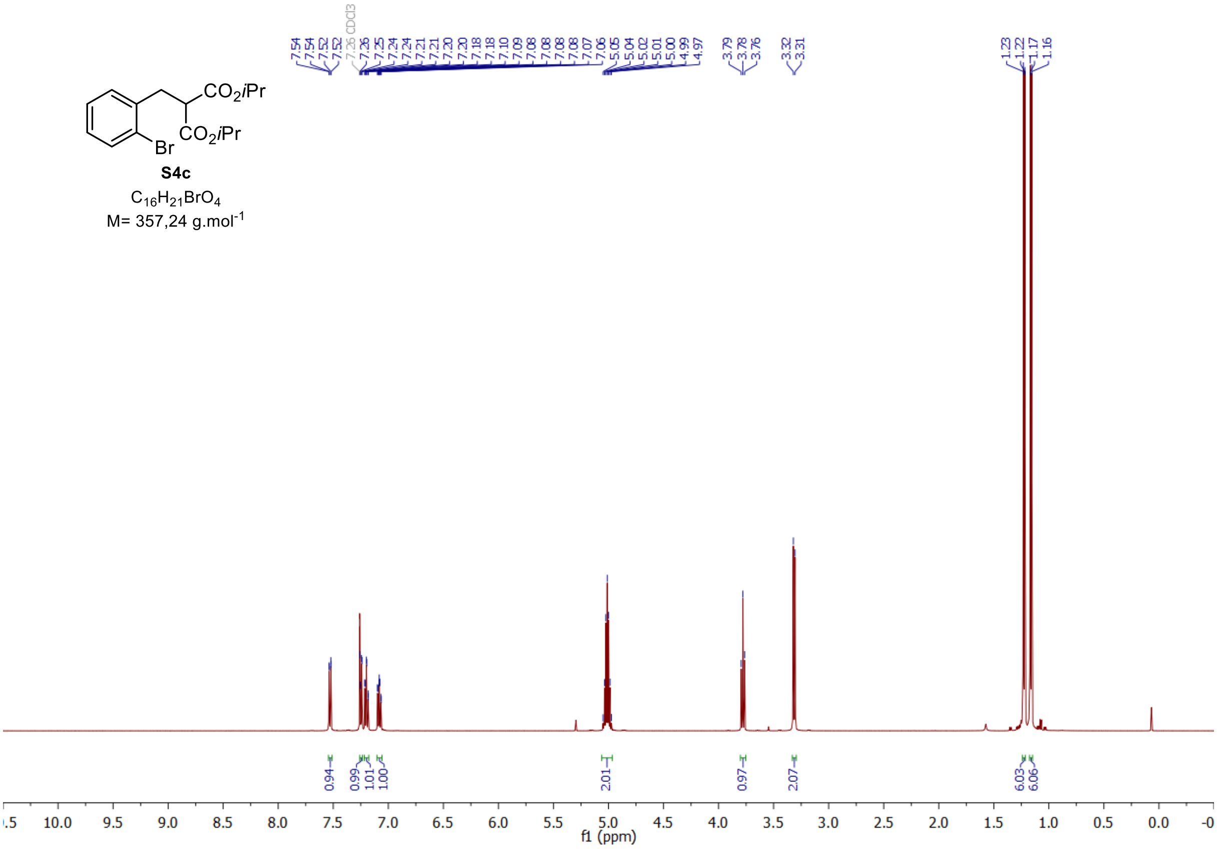

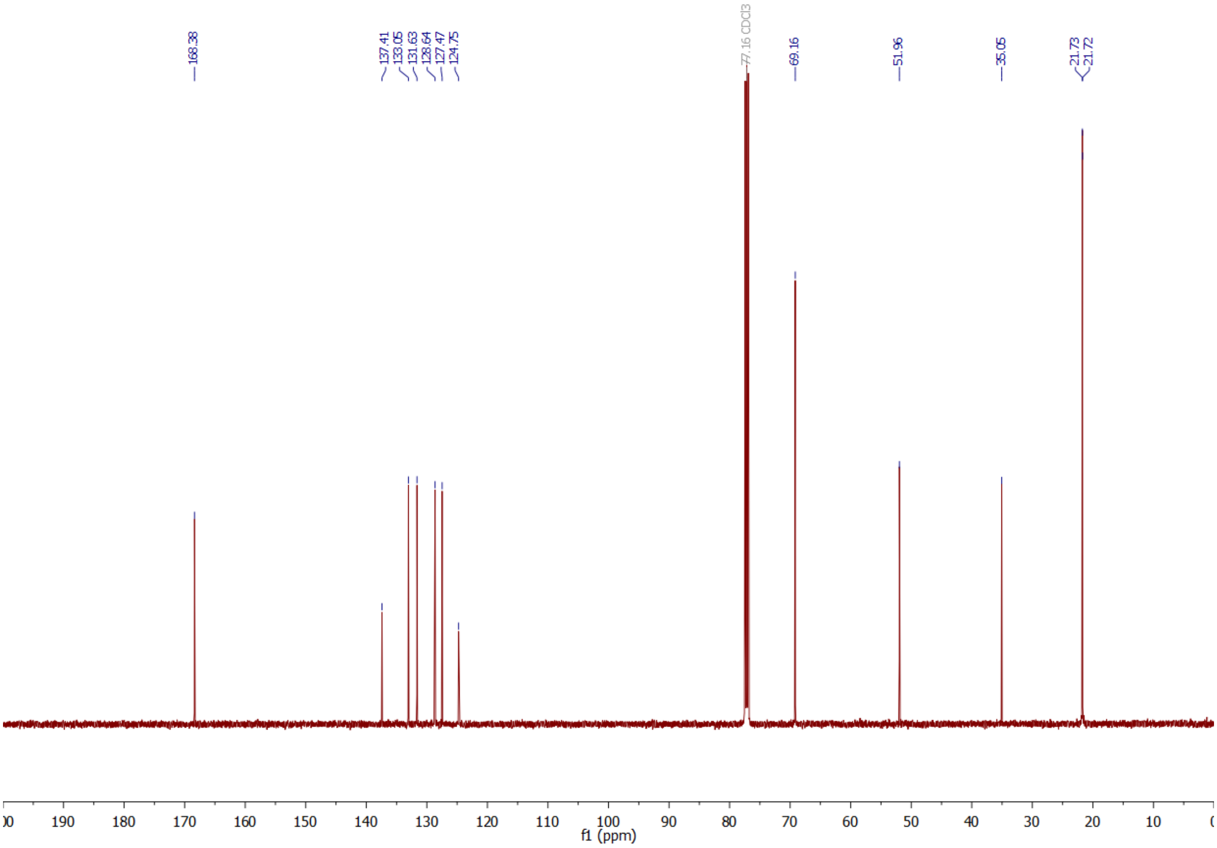

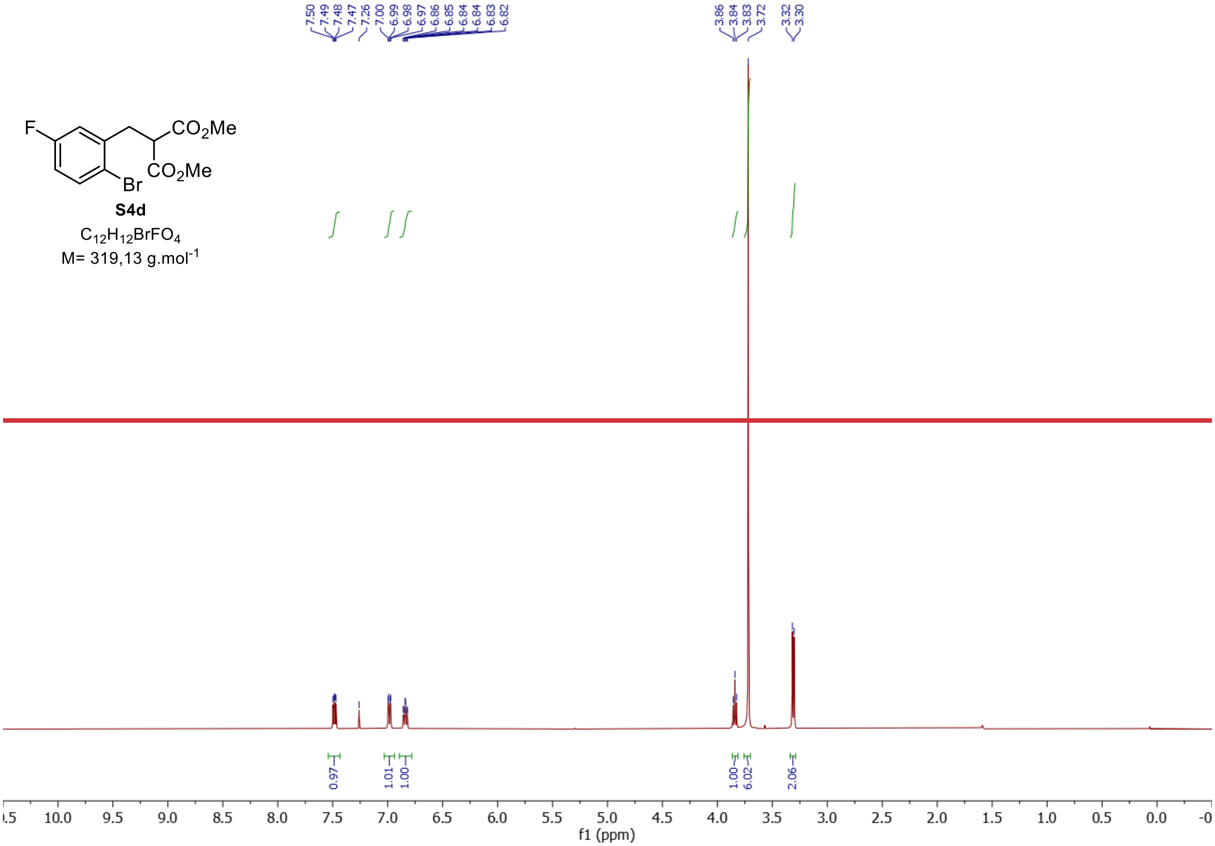

S4d

$C_{12}H_{12}BrFO_4$

M= 319,13 g.mol^{-1}

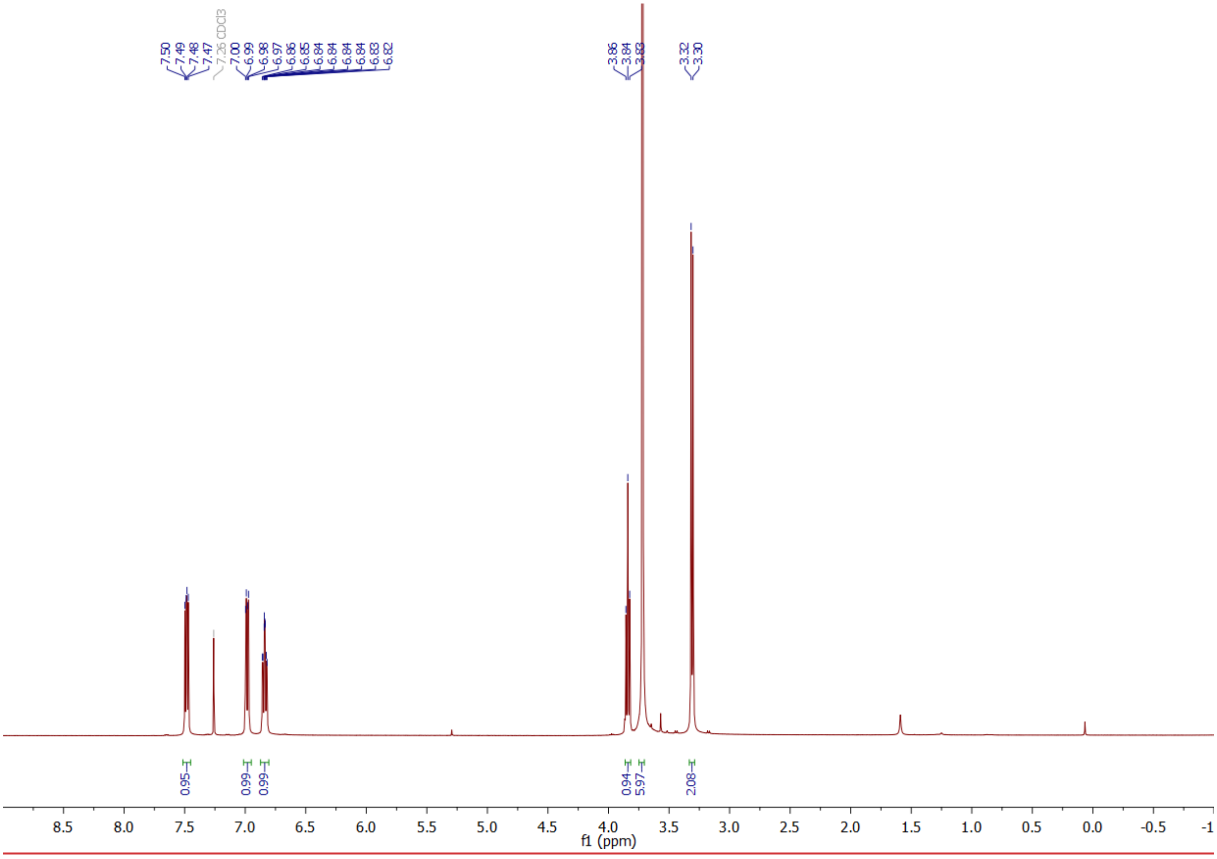

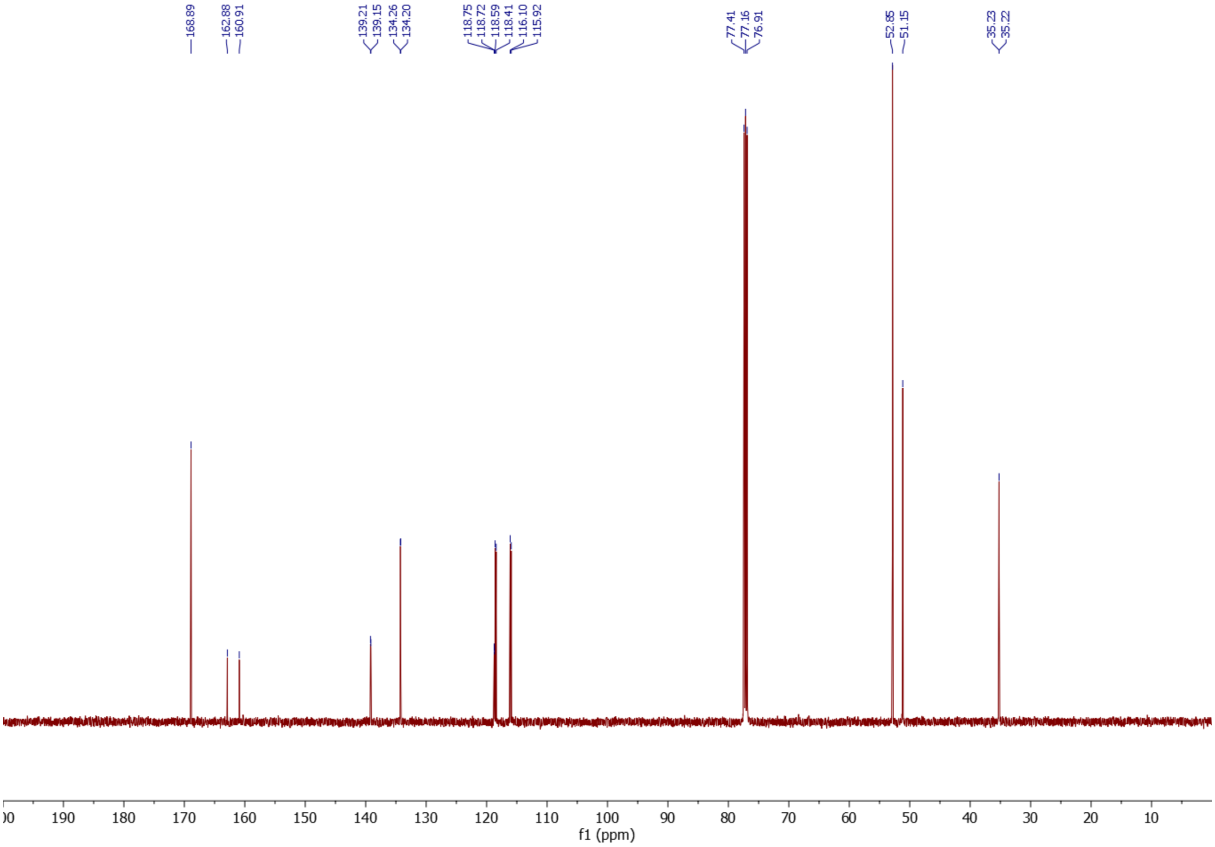
168.89
162.88
160.91
139.21
139.15
134.26
134.20
118.75
118.72
118.59
118.41
116.10
115.92
77.41
77.16
76.91
52.85
51.15
35.23
35.22
00
190
180
170
160
150
140
130
120
110
100
90
80
70
60
50
40
30
20
10
f1 (ppm)

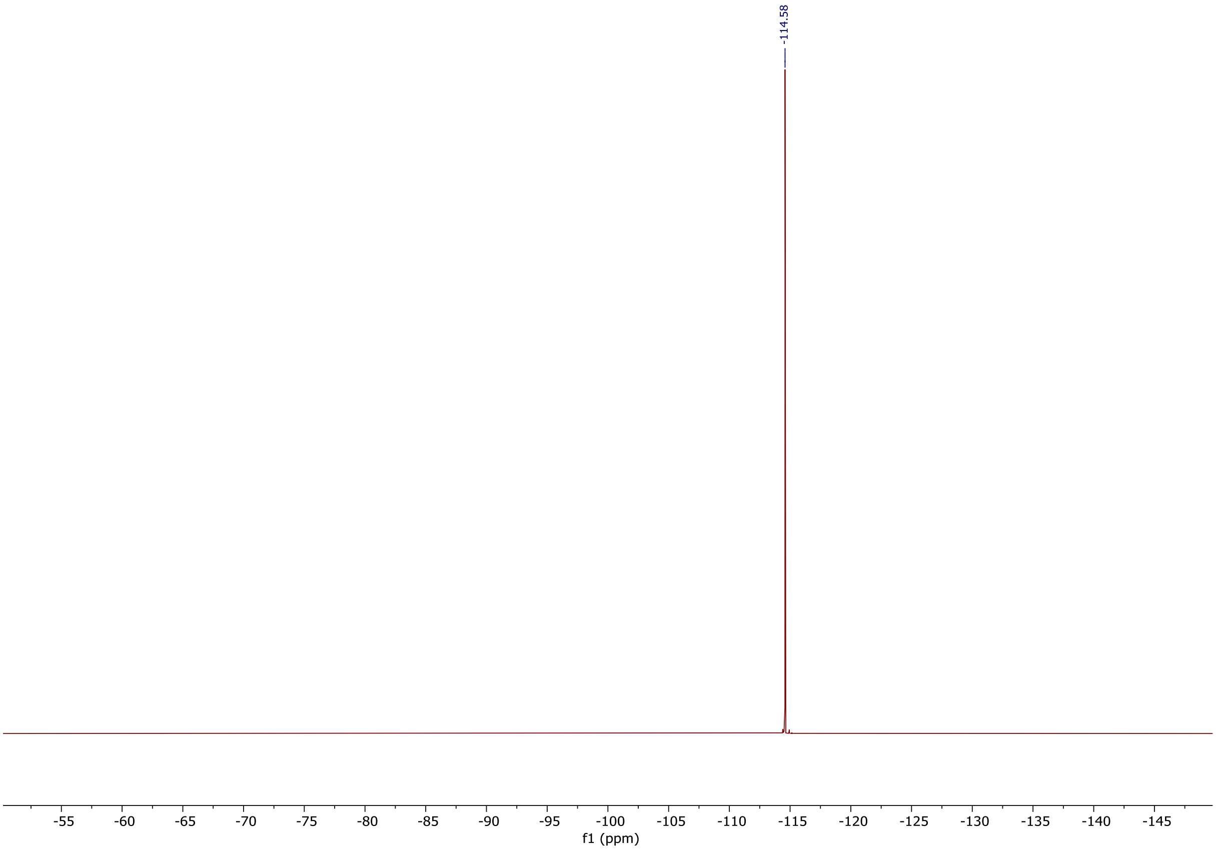
-114.58
-55
-60
-65
-70
-75
-80
-85
-90
-95
-100
-105
-110
-115
-120
-125
-130
-135
-140
-145
f1 (ppm)

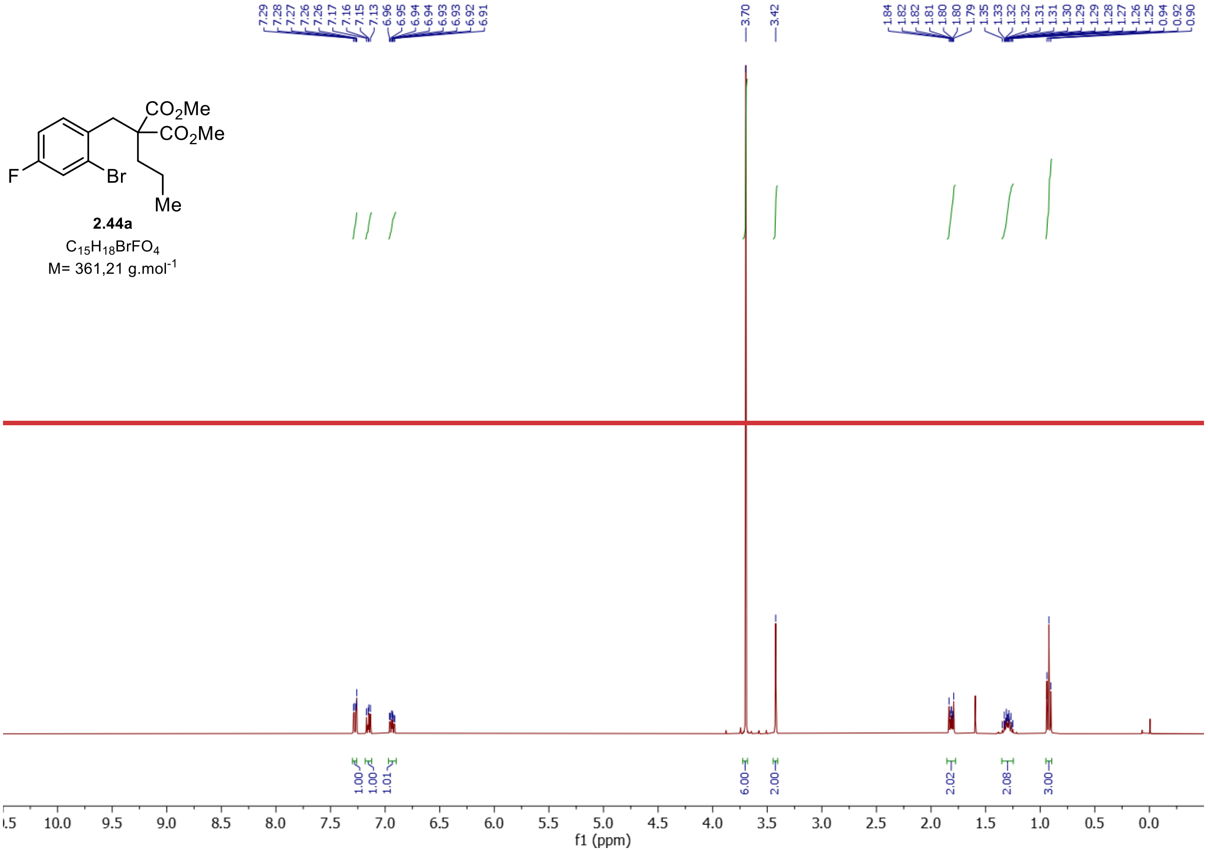

2.44a

$C_{15}H_{18}BrFO_4$

M= 361,21 g.mol^{-1}

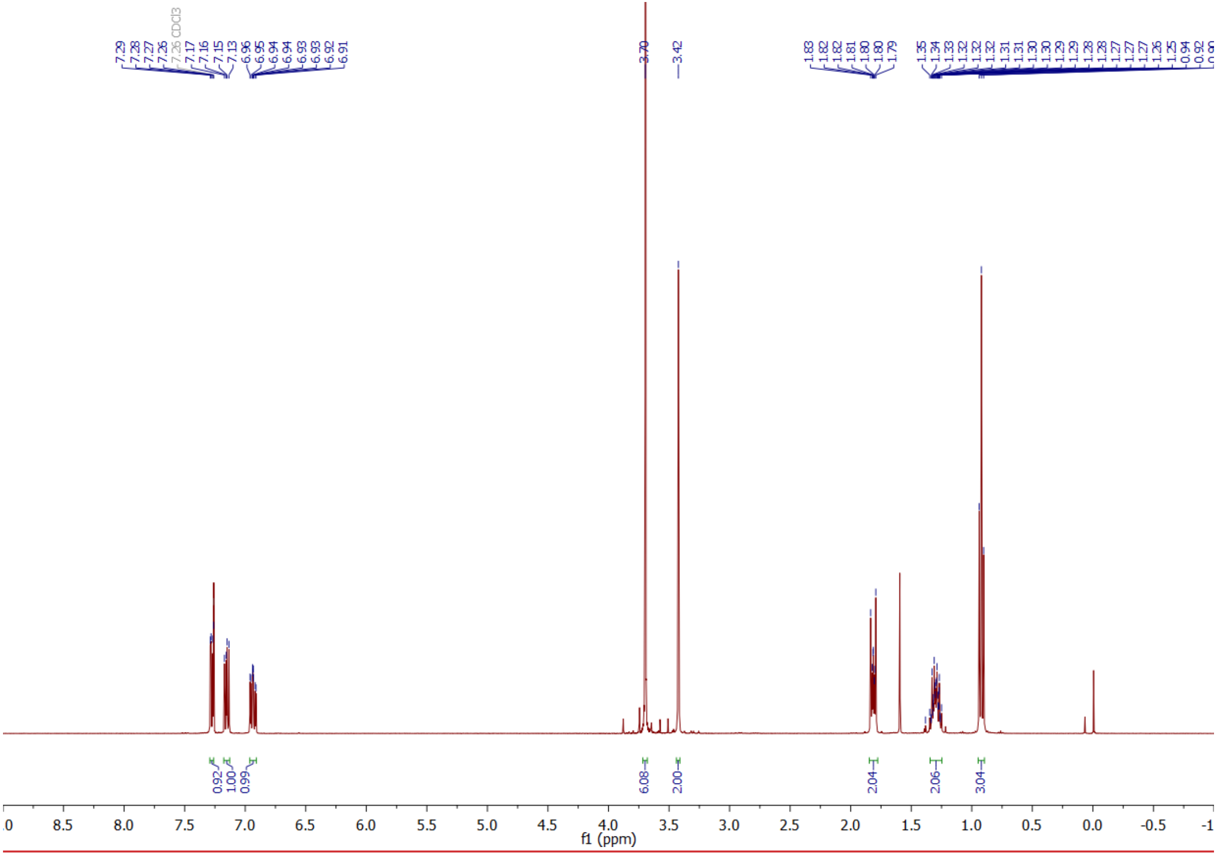

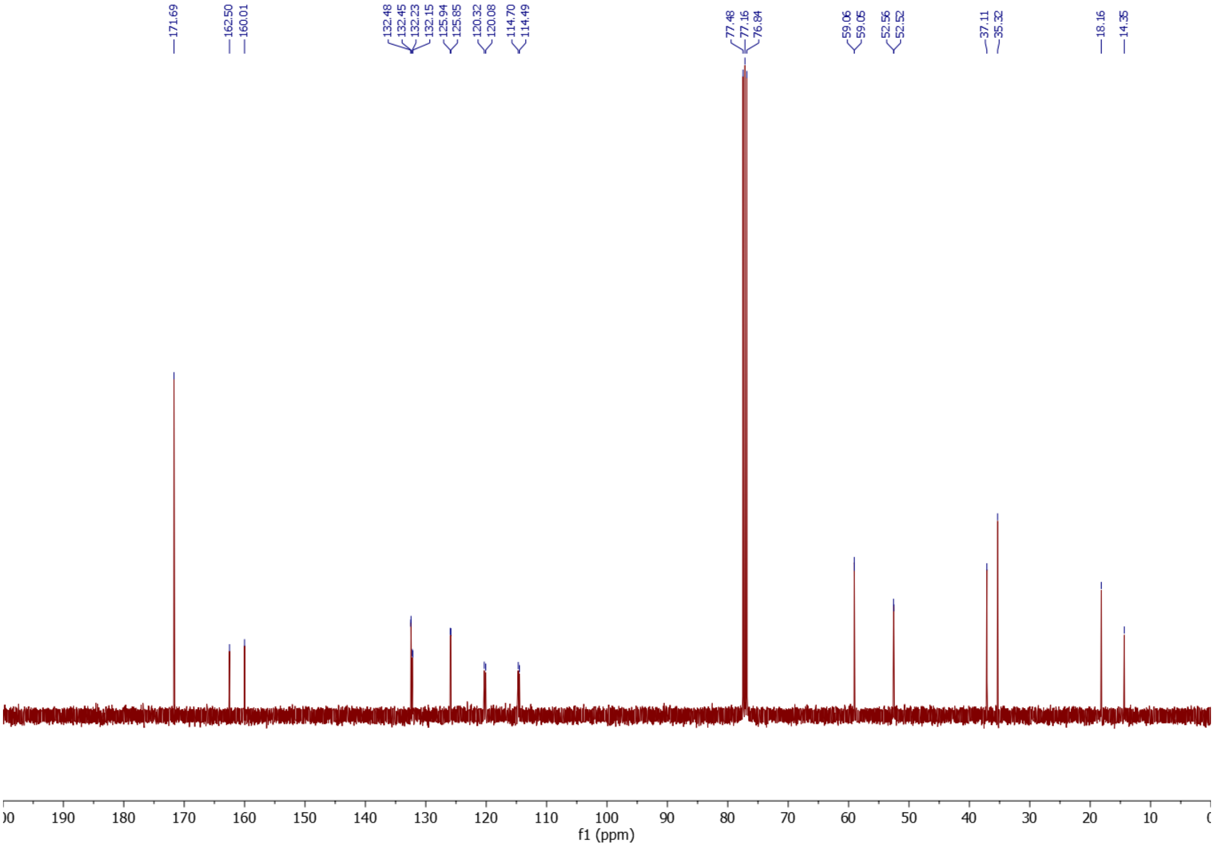
171.69
162.50
160.01
132.48
132.45
132.23
132.15
125.94
125.85
120.32
120.08
114.70
114.49
77.48
77.16
76.84
59.06
59.05
52.56
52.52
37.11
35.32
18.16
14.35
190
180
170
160
150
140
130
120
110
100
90
80
70
60
50
40
30
20
10
f1 (ppm)

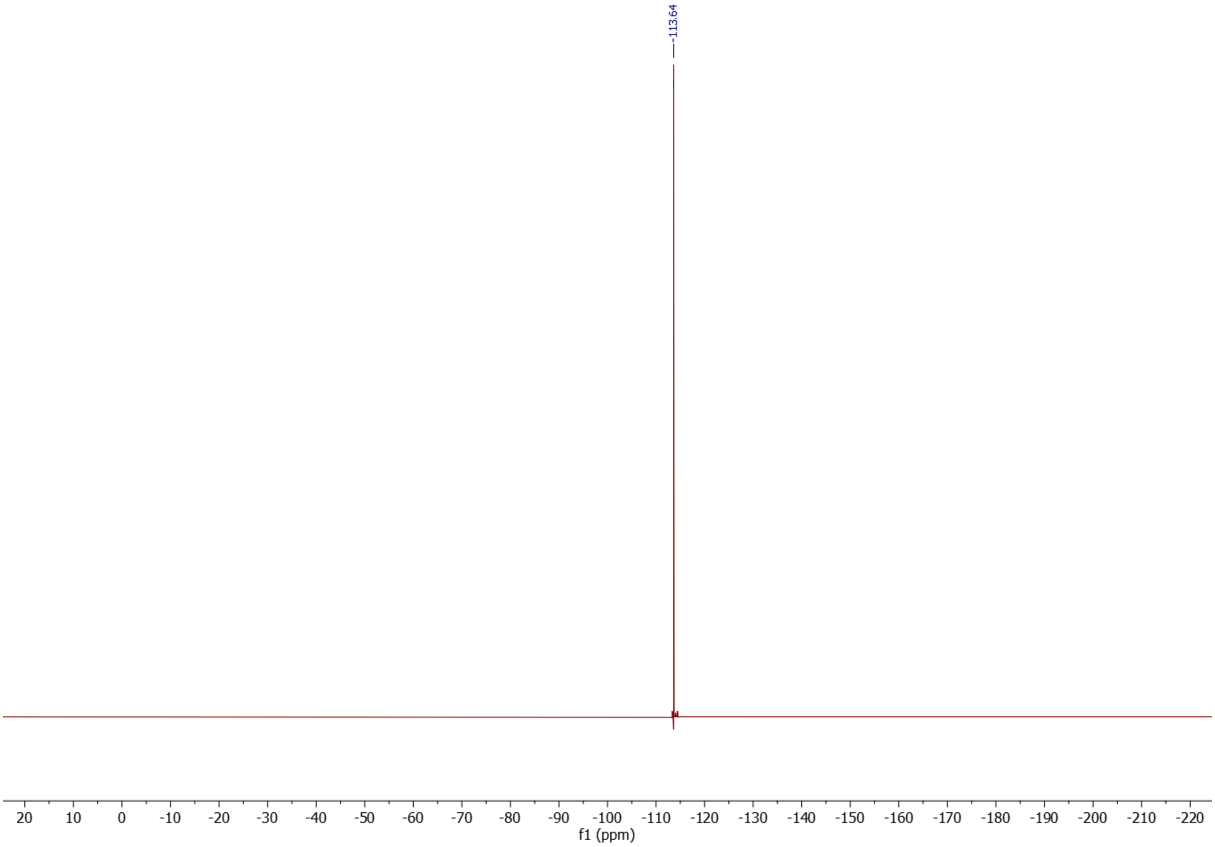
-113.64
20
10
0
-10
-20
-30
-40
-50
-60
-70
-80
-90
-100
-110
-120
-130
-140
-150
-160
-170
-180
-190
-200
-210
-220
f1 (ppm)

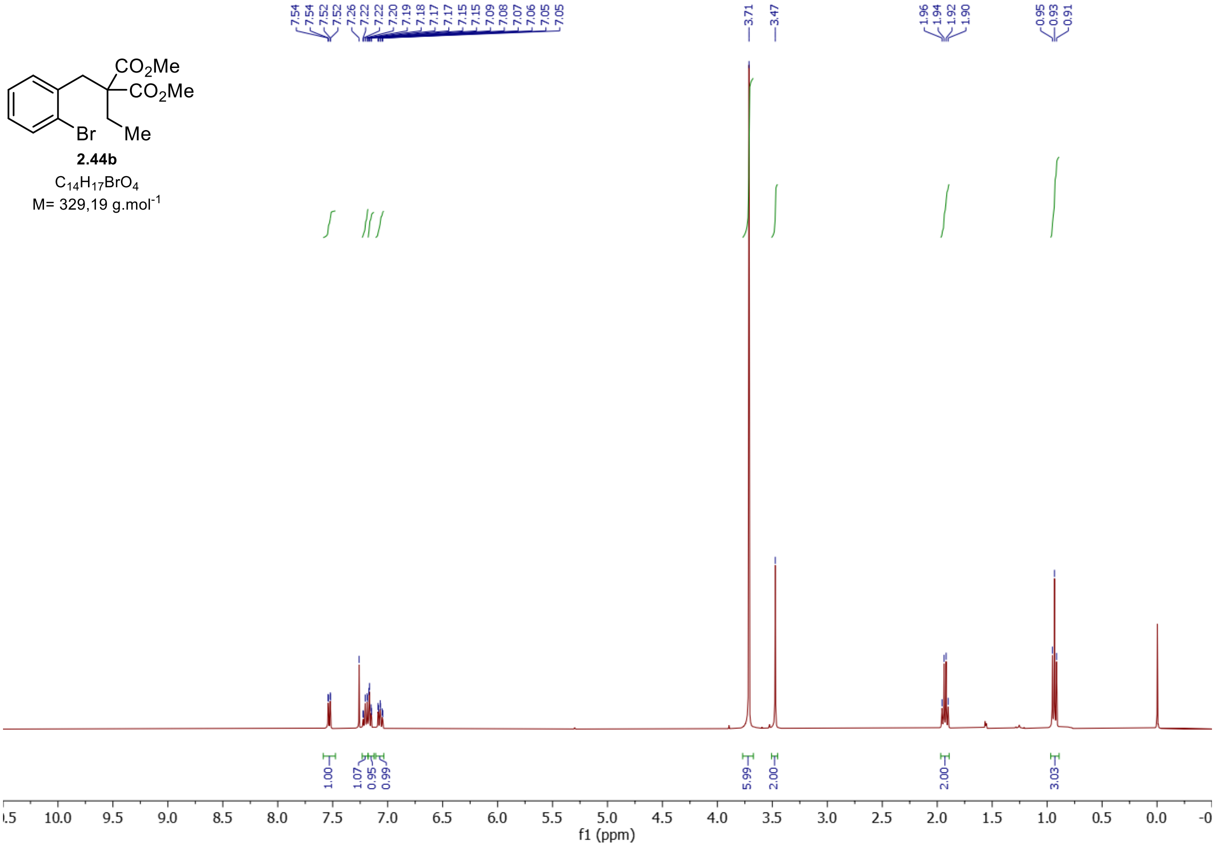

2.44b

$C_{14}H_{17}BrO_4$

M= 329,19 g.mol^{-1}

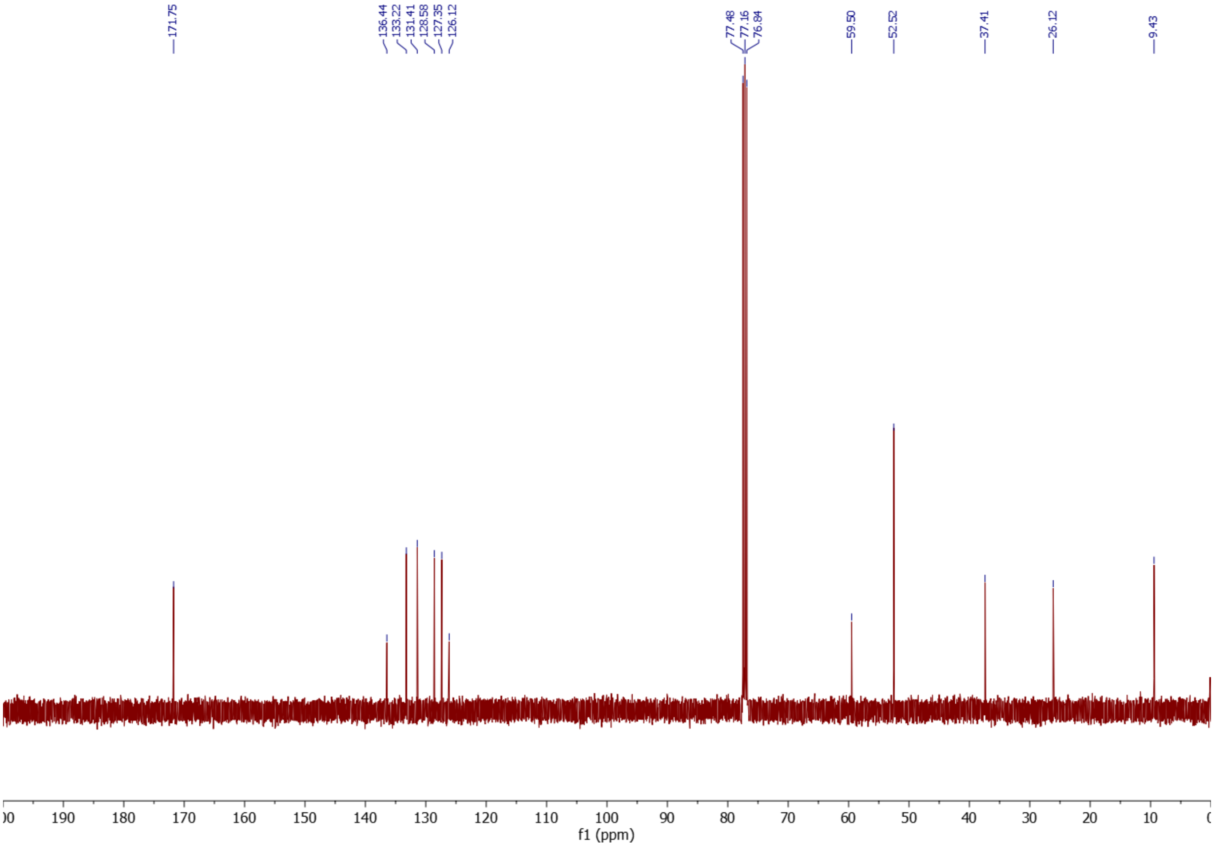

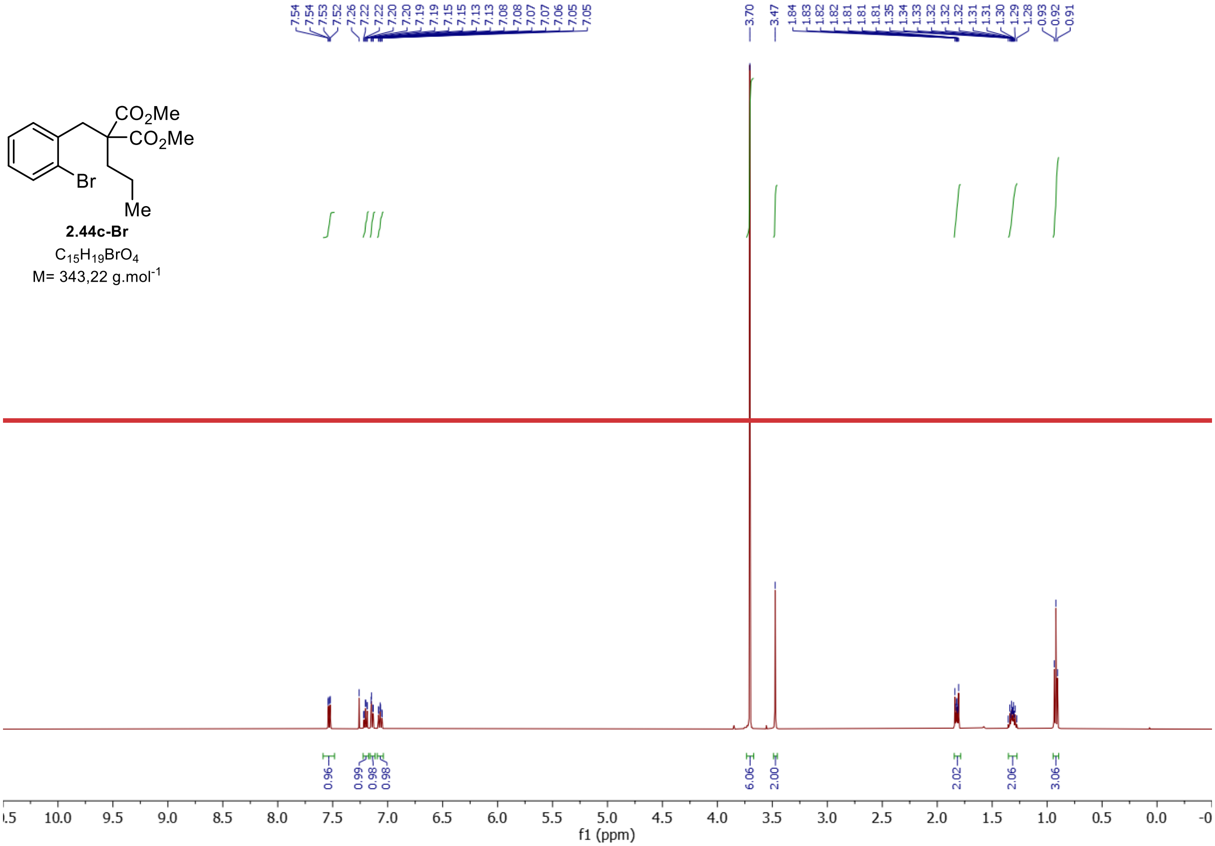

2.44c-Br

$C_{15}H_{19}BrO_4$

M= 343,22 g.mol^{-1}

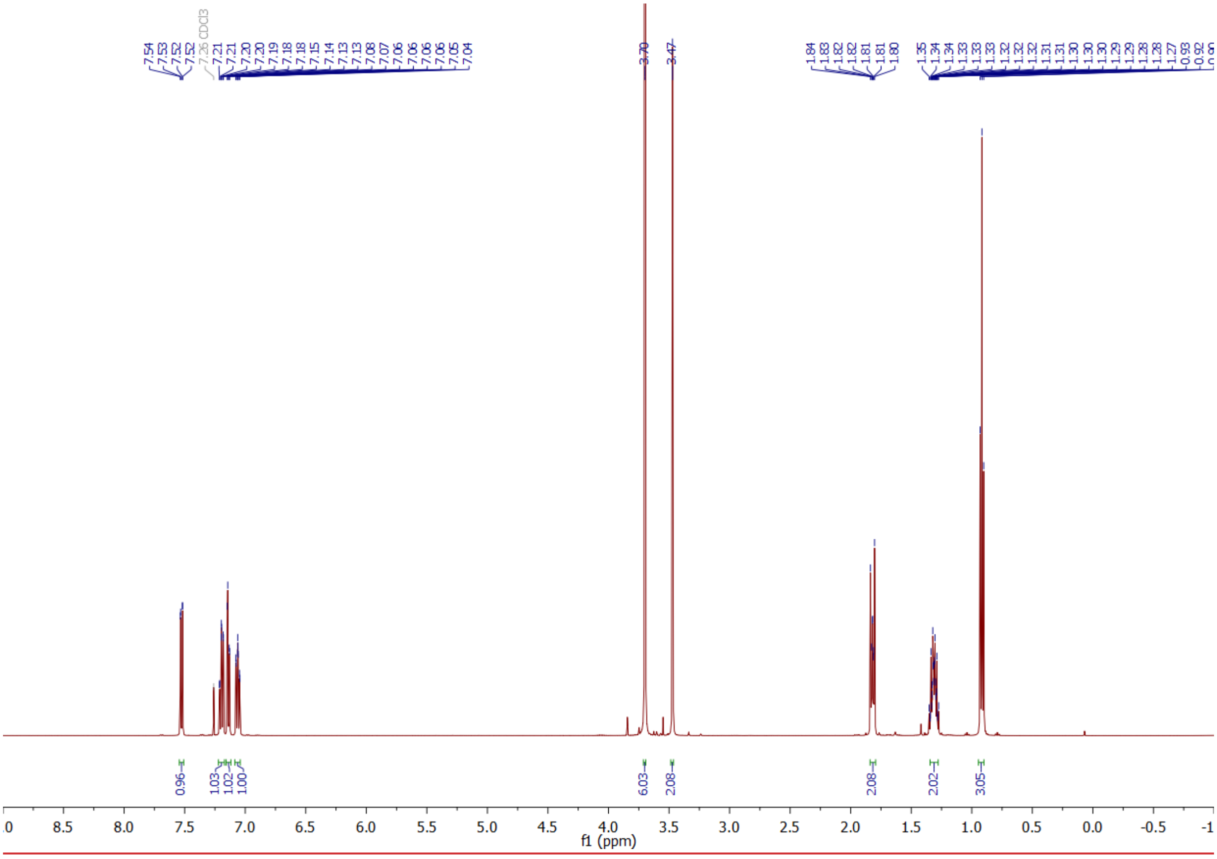

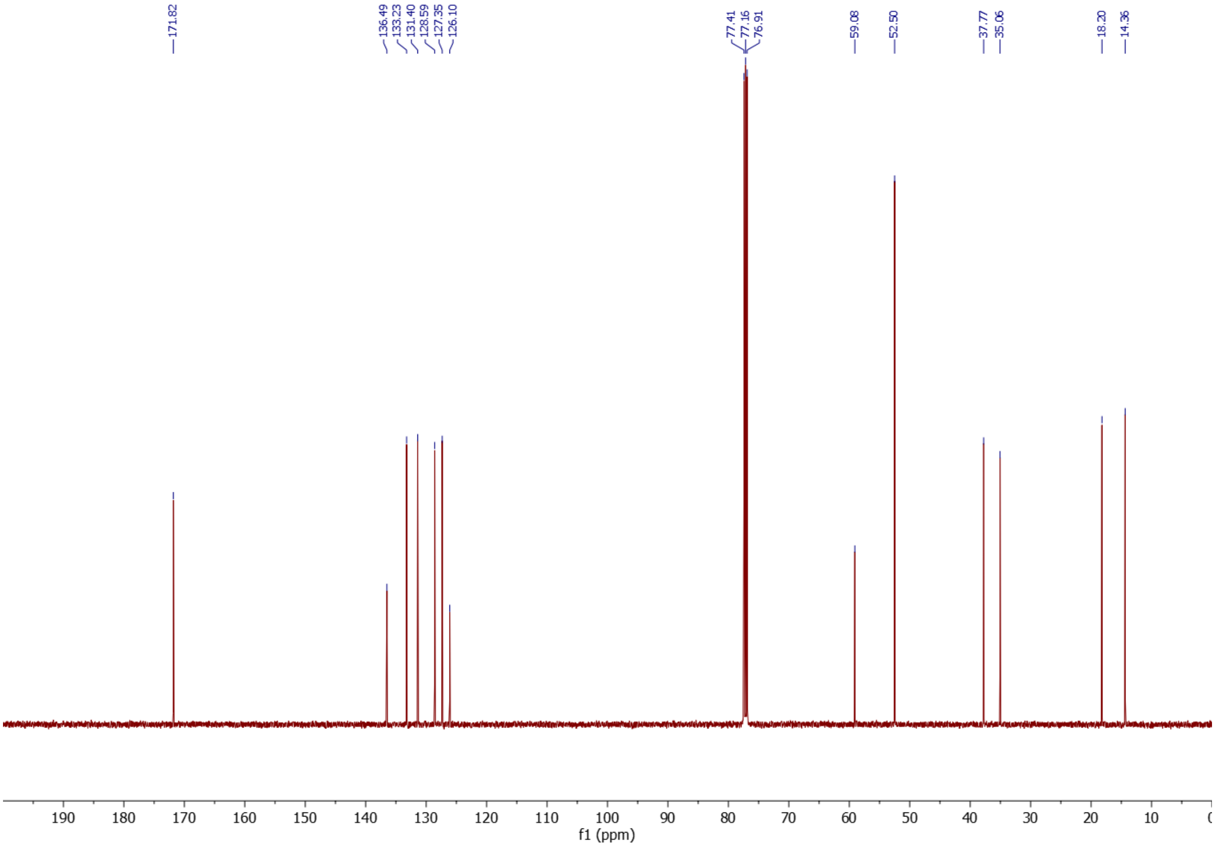
171.82
136.49
133.23
131.40
128.59
127.35
126.10
77.41
77.16
76.91
59.08
52.50
37.77
35.06
18.20
14.36
190
180
170
160
150
140
130
120
110
100
90
80
70
60
50
40
30
20
10
0
f1 (ppm)

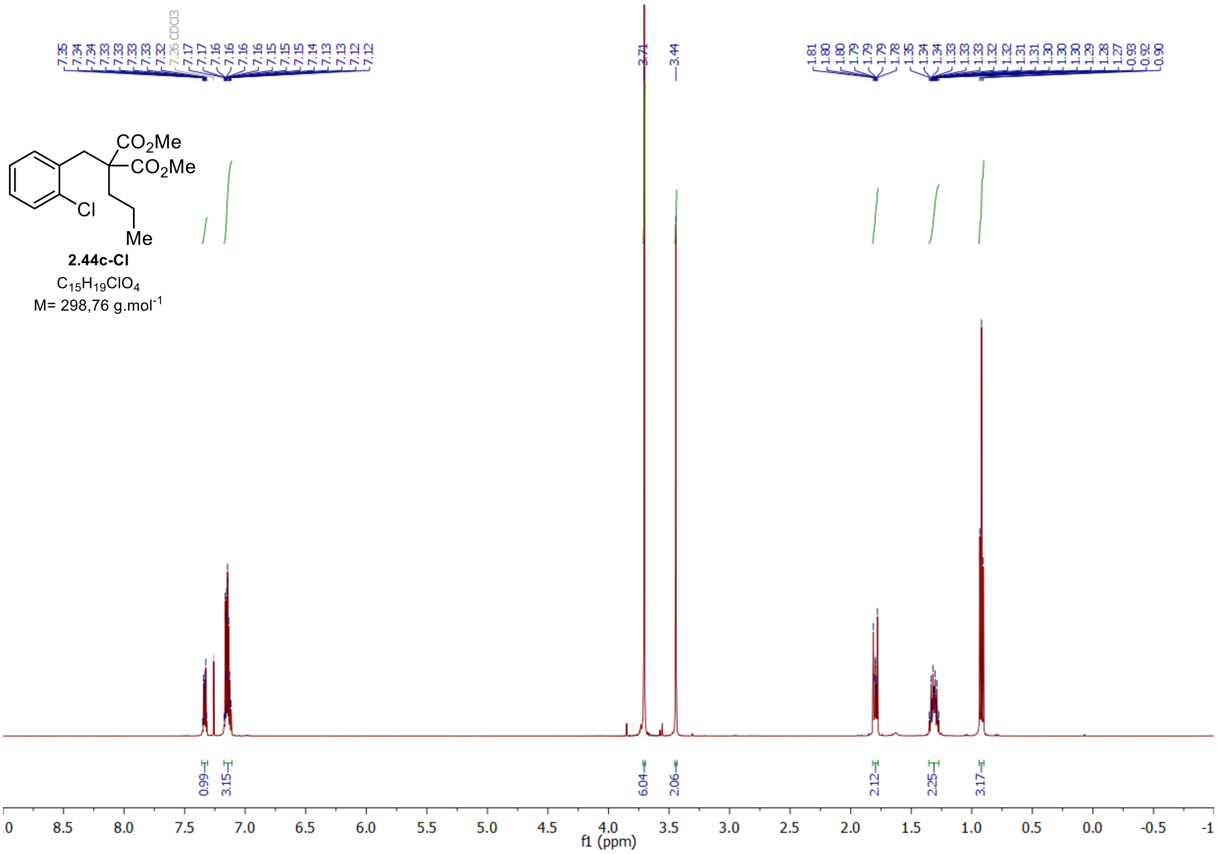

2.44c-Cl

$C_{15}H_{19}ClO_4$

M= 298,76 g.mol^{-1}

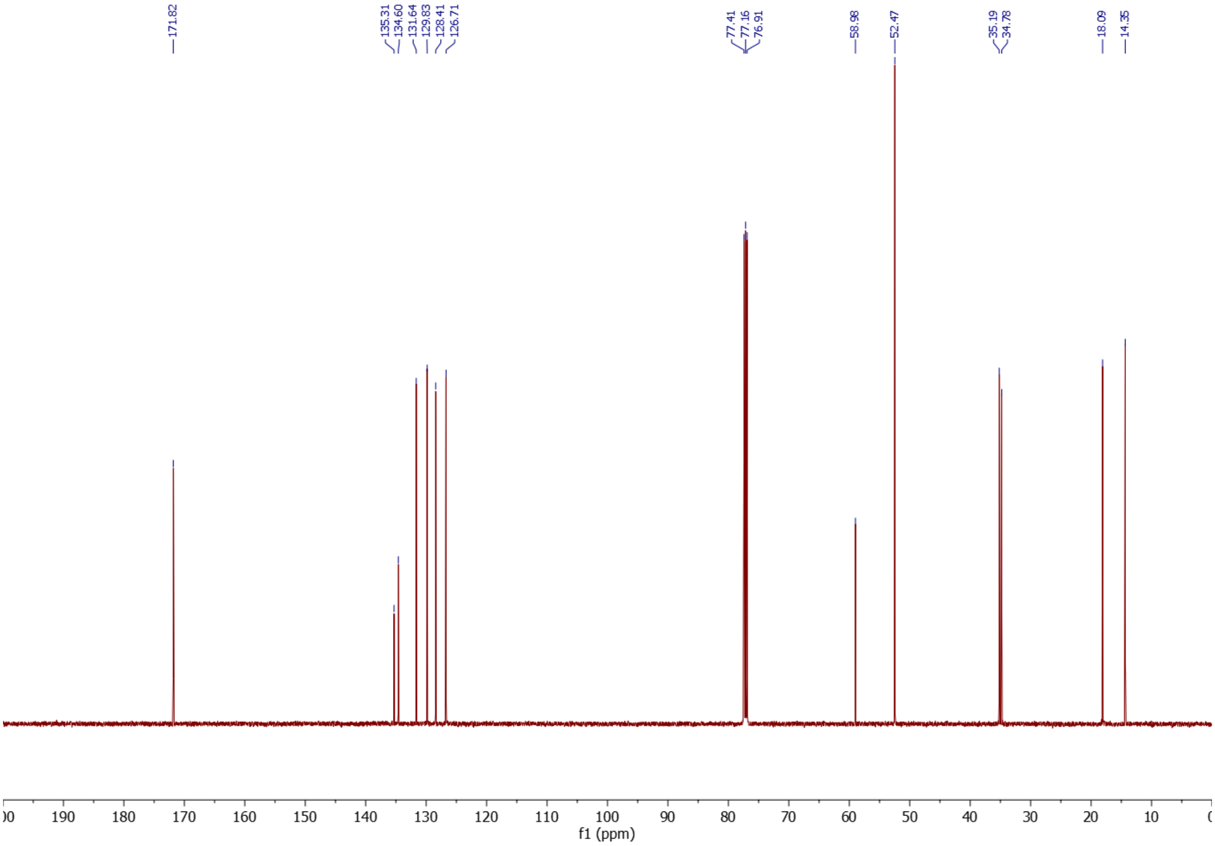

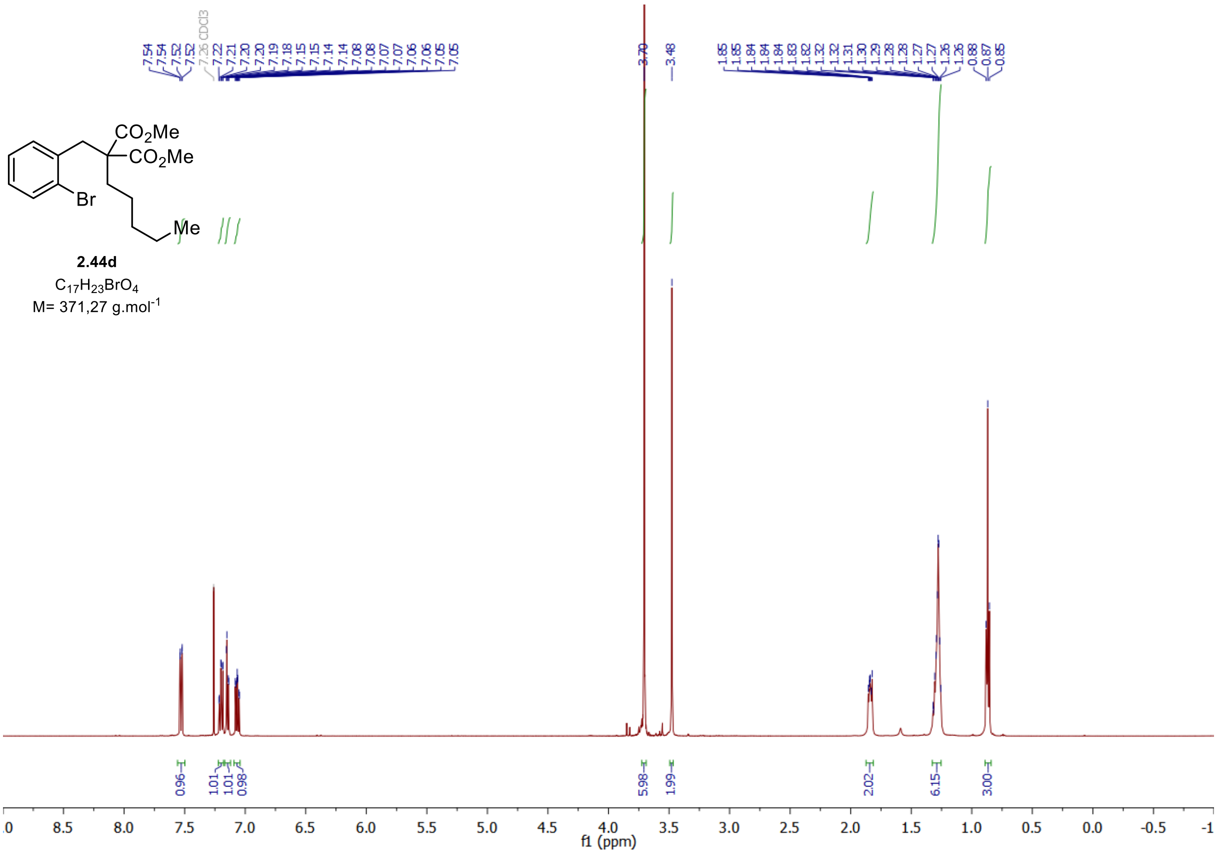

2.44d

$C_{17}H_{23}BrO_4$

M= 371,27 g.mol^{-1}

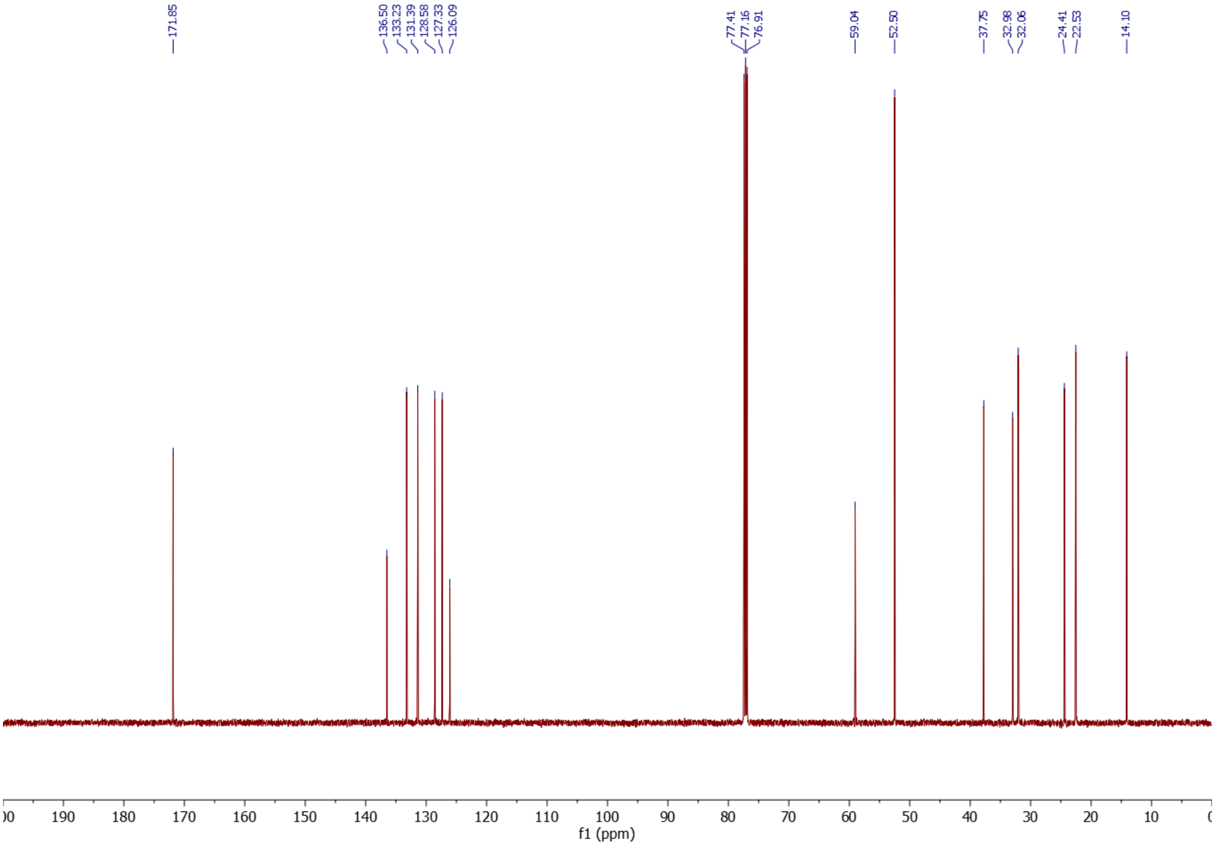

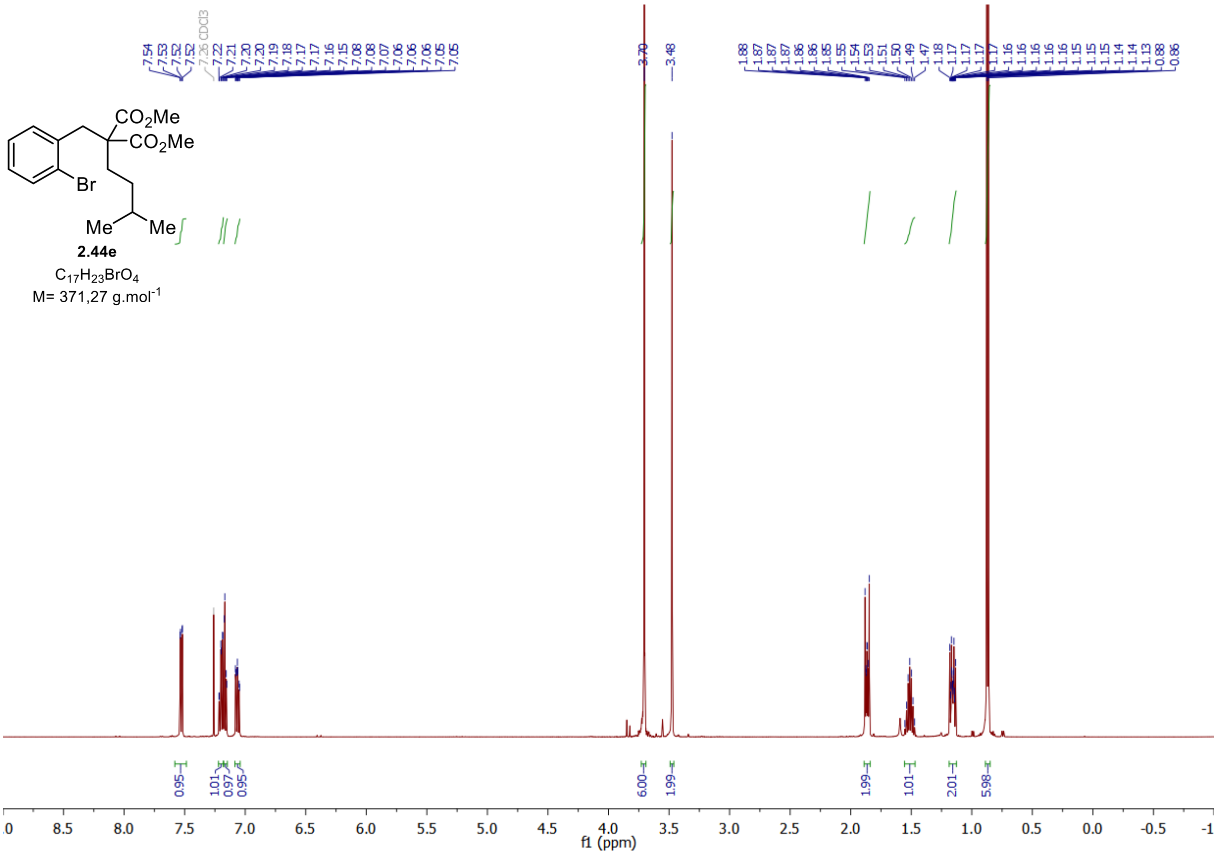

2.44e

$C_{17}H_{23}BrO_4$

M= 371,27 g.mol^{-1}

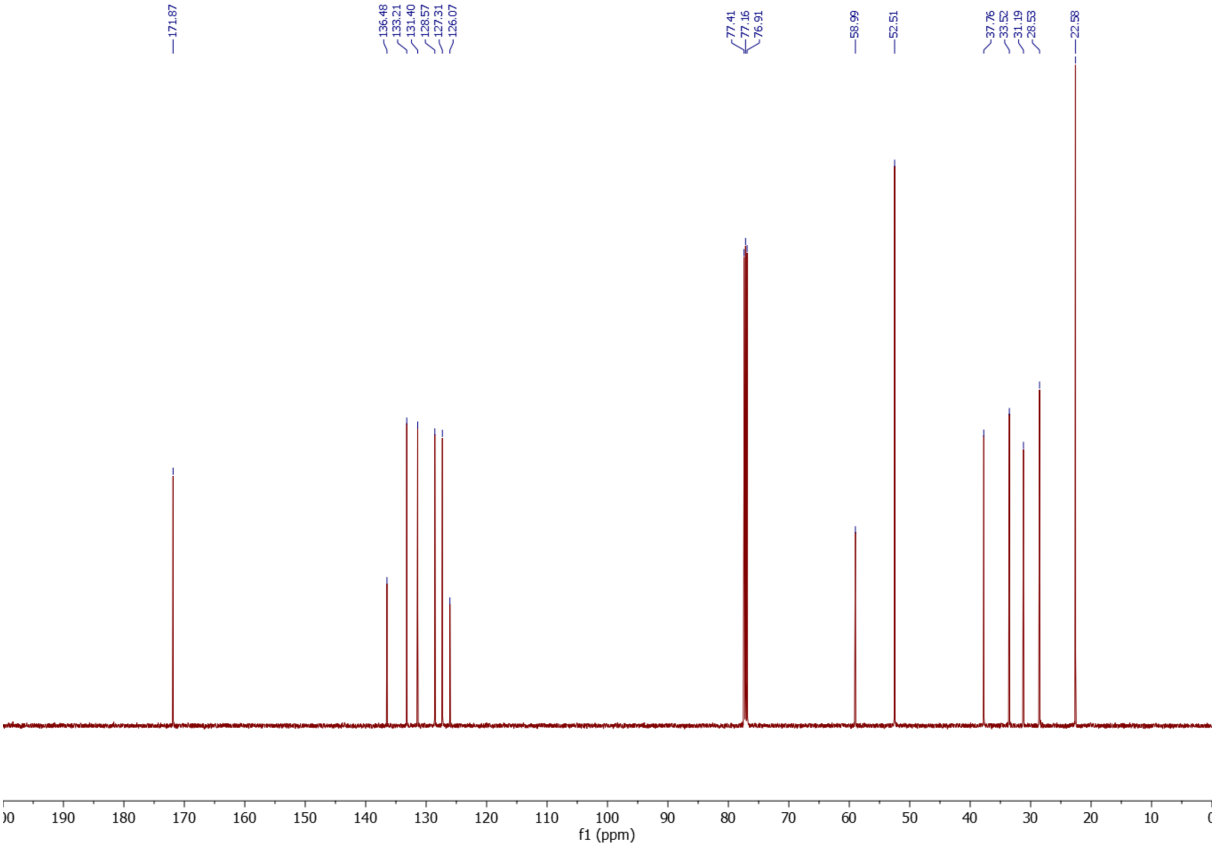

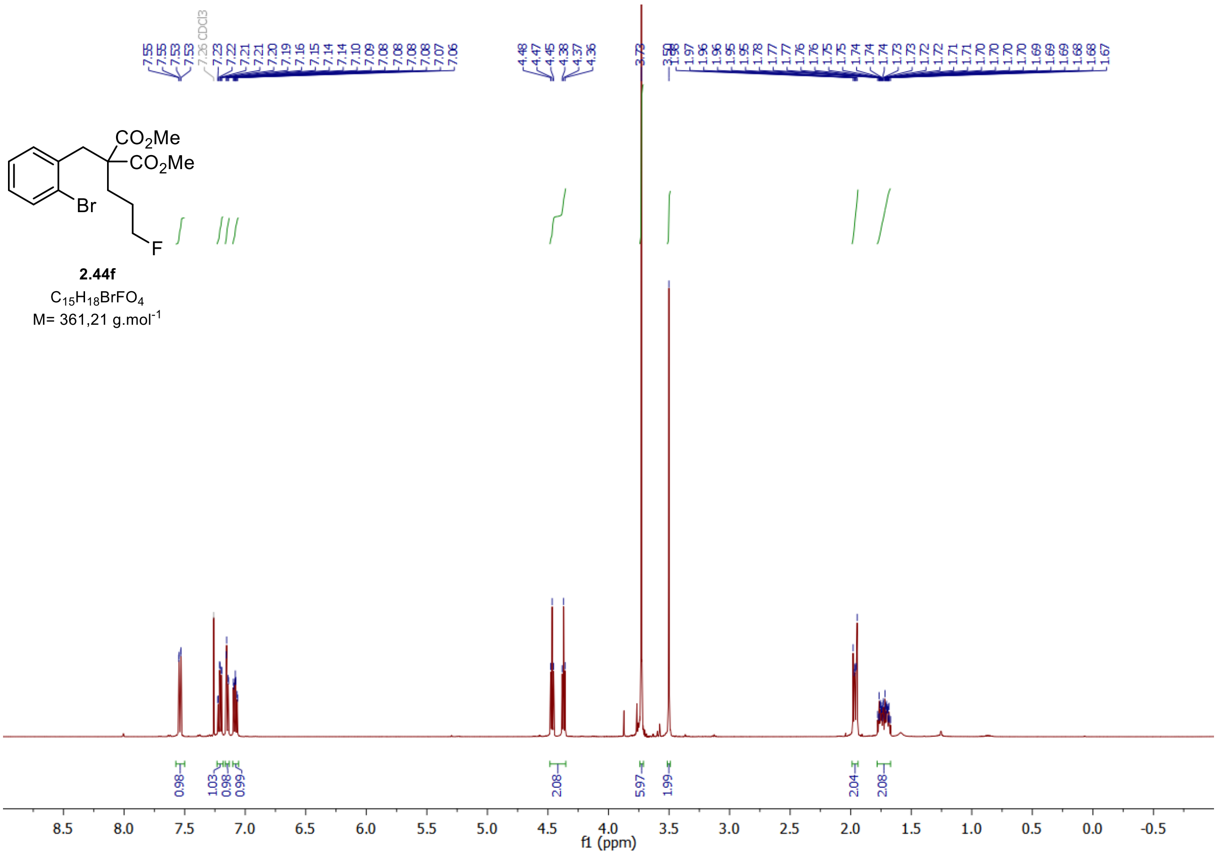

2.44f

$C_{15}H_{18}BrFO_4$

M= 361,21 g.mol^{-1}

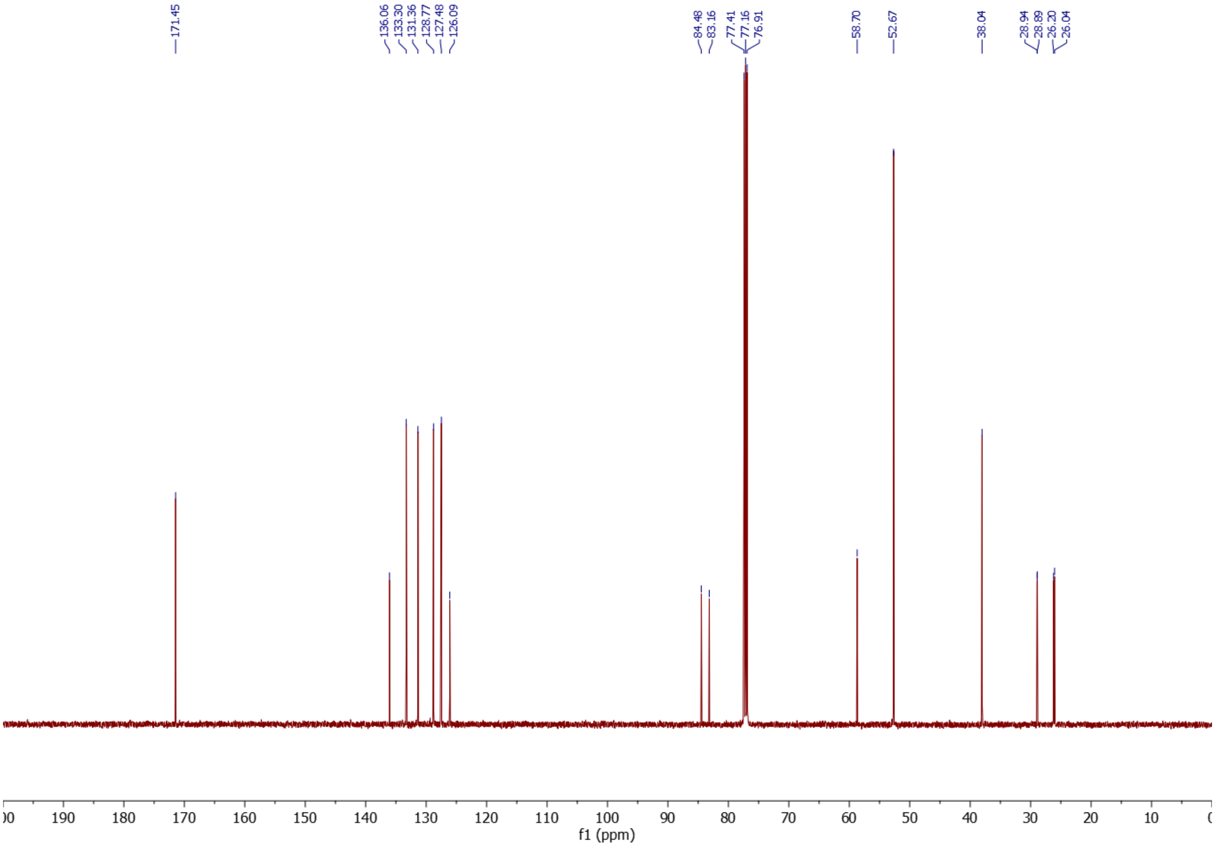

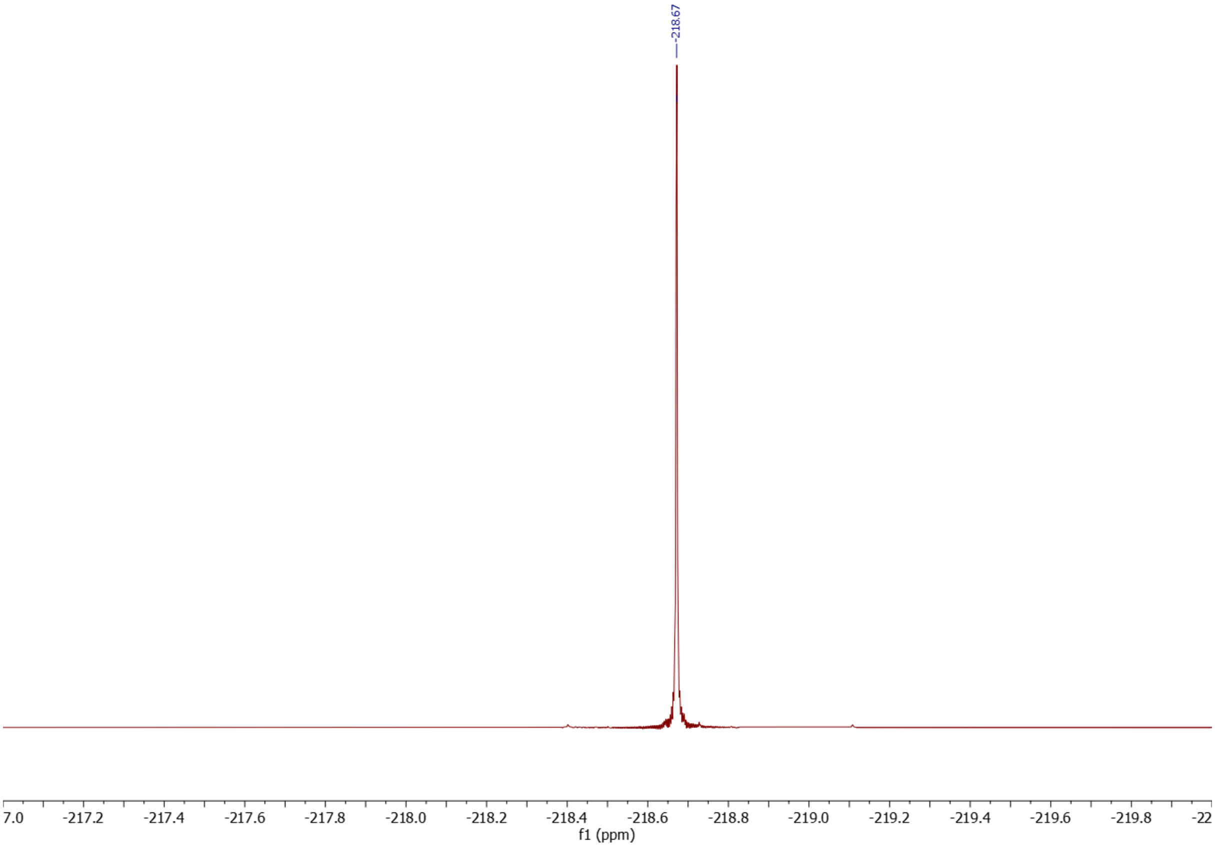
-218.67
7.0
-217.2
-217.4
-217.6
-217.8
-218.0
-218.2
-218.4
-218.6
-218.8
-219.0
-219.2
-219.4
-219.6
-219.8
-22
f1 (ppm)

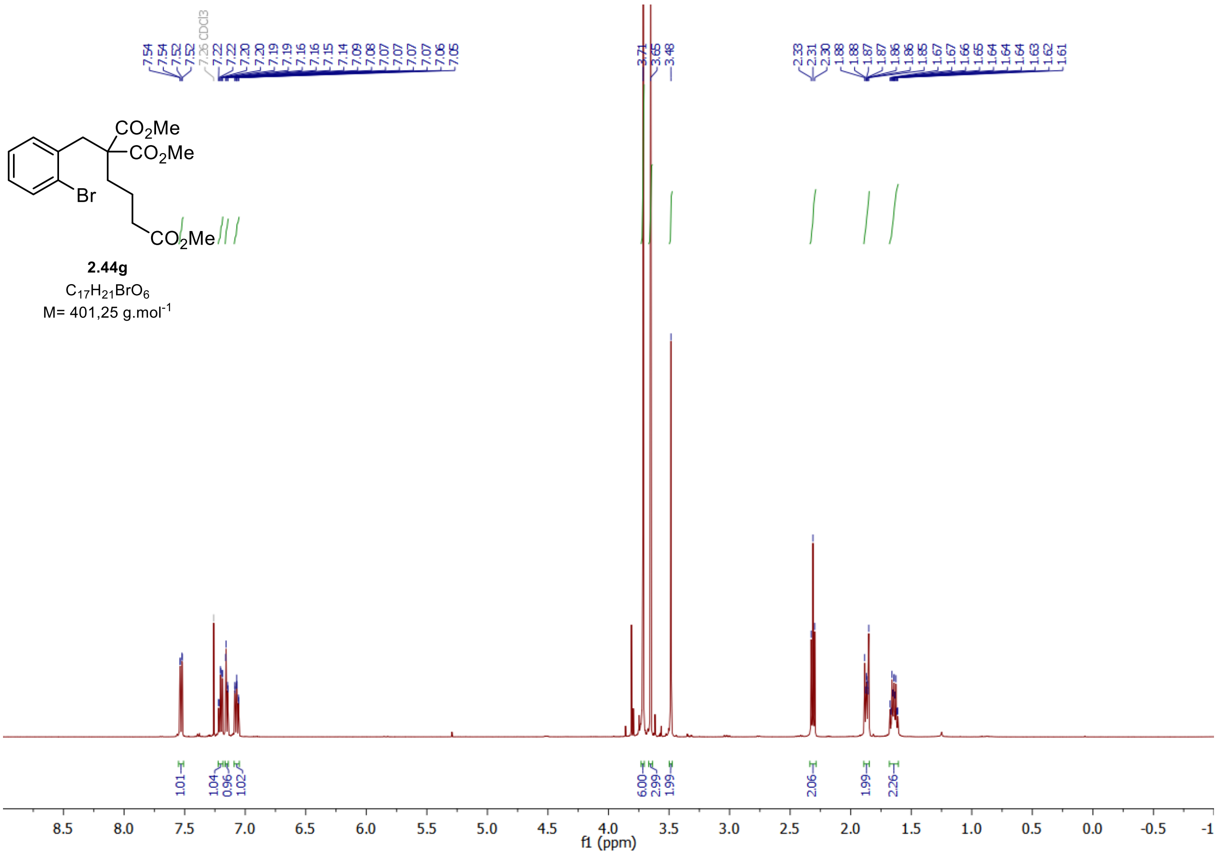

2.44g

$C_{17}H_{21}BrO_6$

M= 401,25 g.mol^{-1}

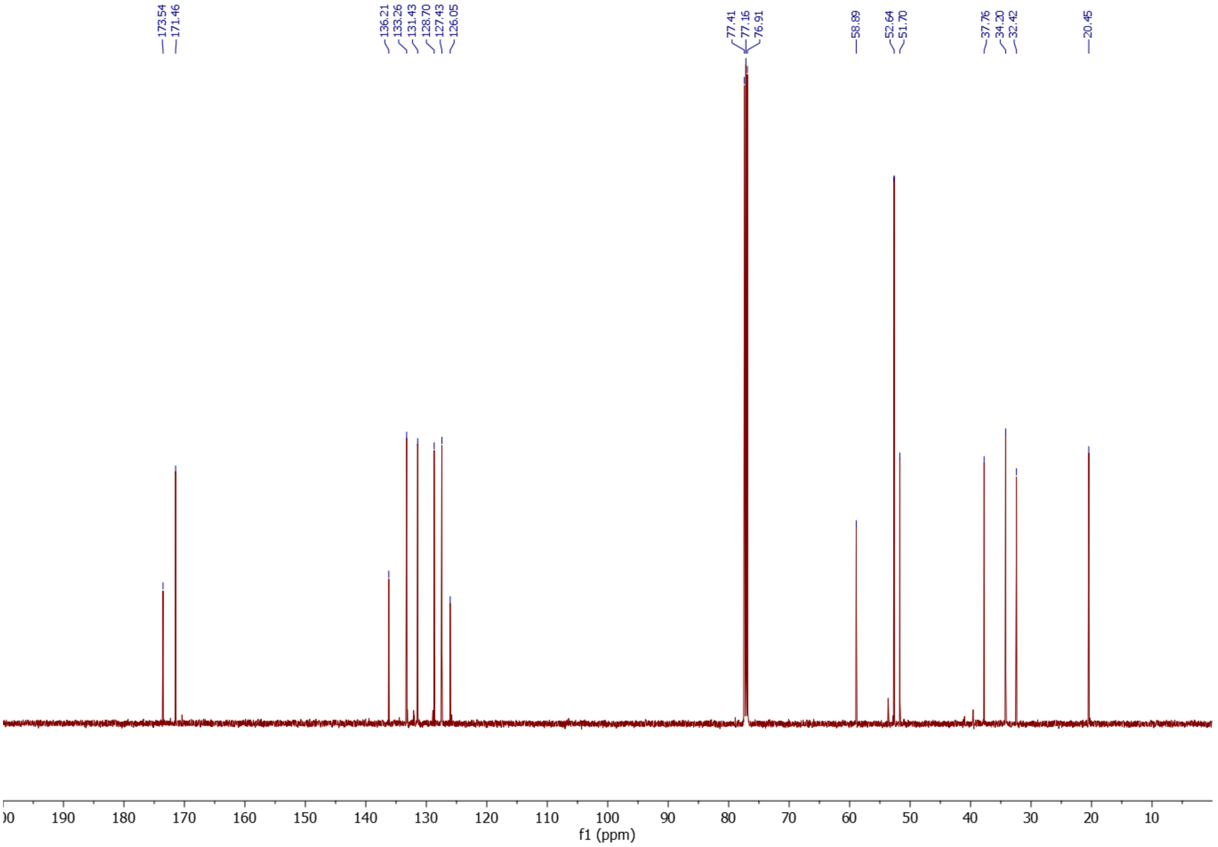

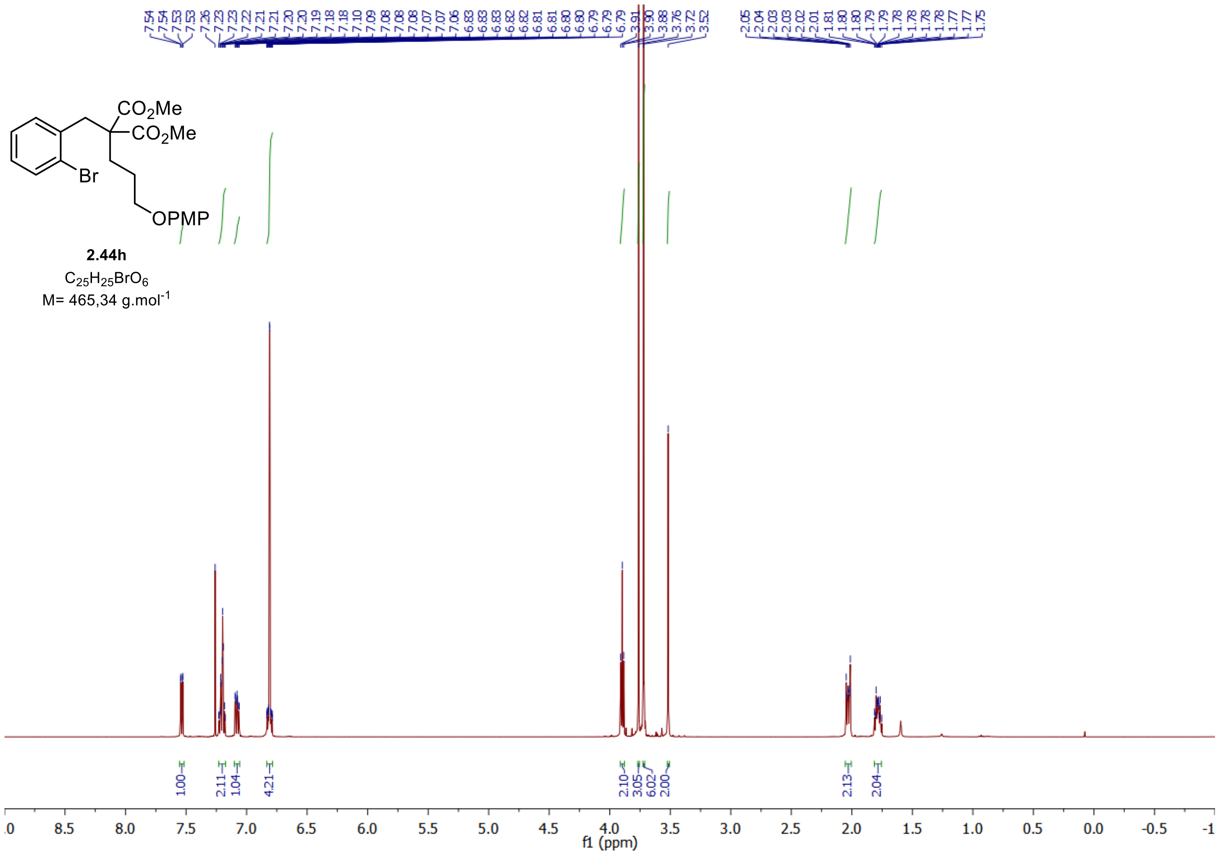

2.44h

$C_{25}H_{25}BrO_6$

M= 465,34 g.mol^{-1}

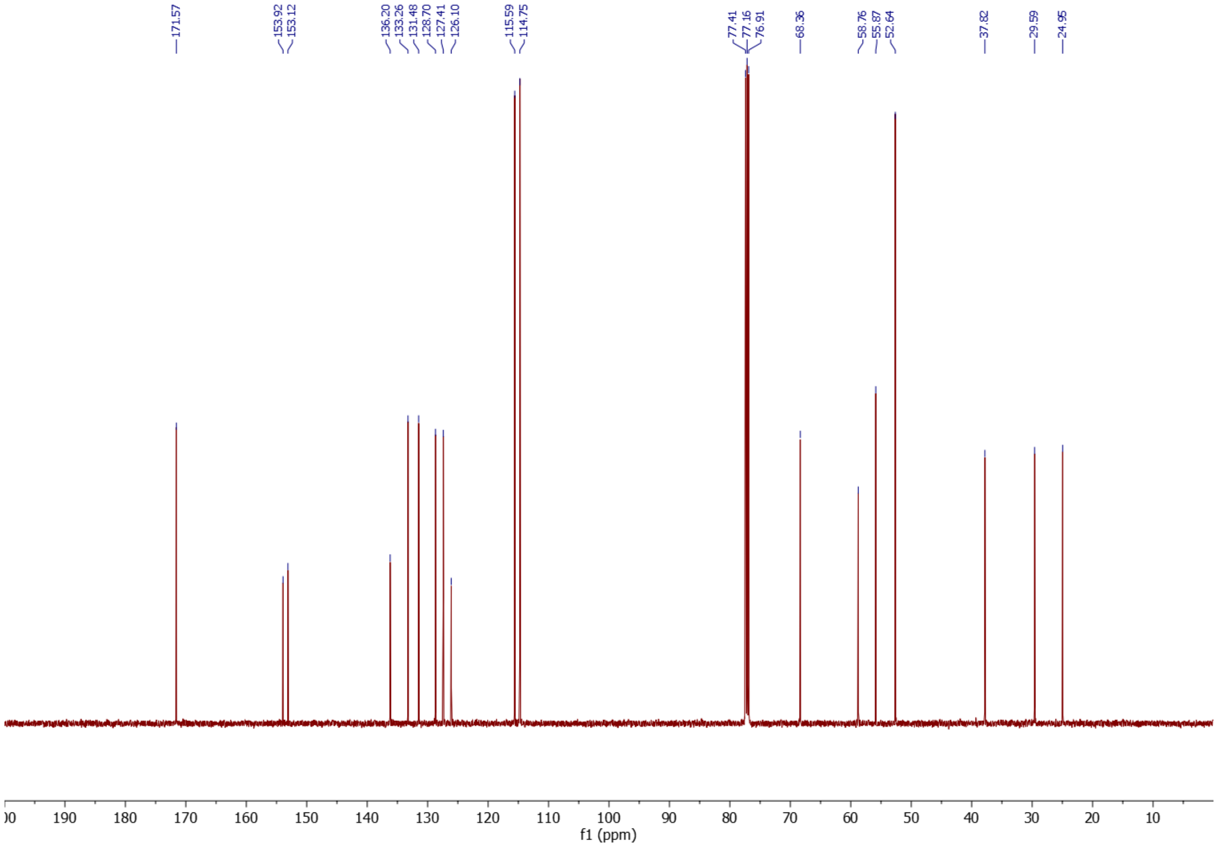

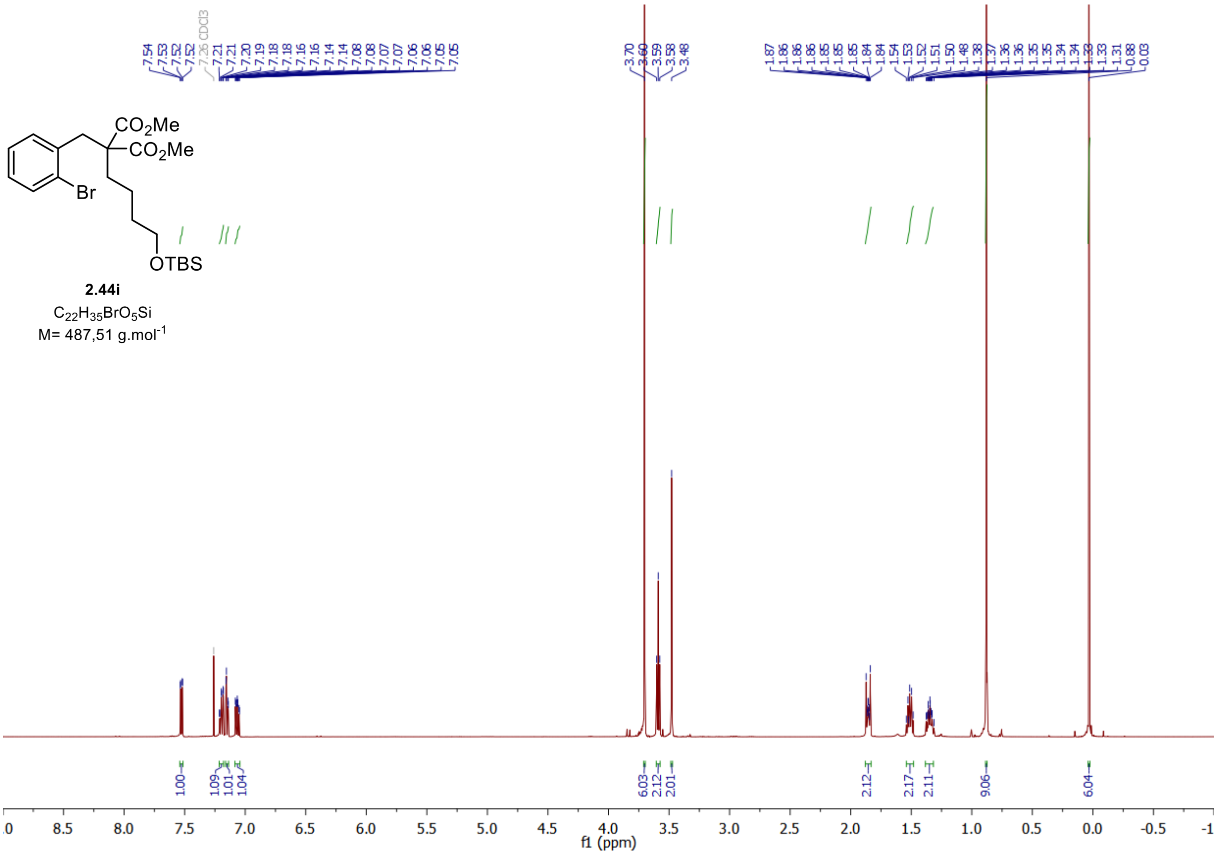

2.44i

$C_{22}H_{35}BrO_5Si$

M= 487,51 g.mol^{-1}

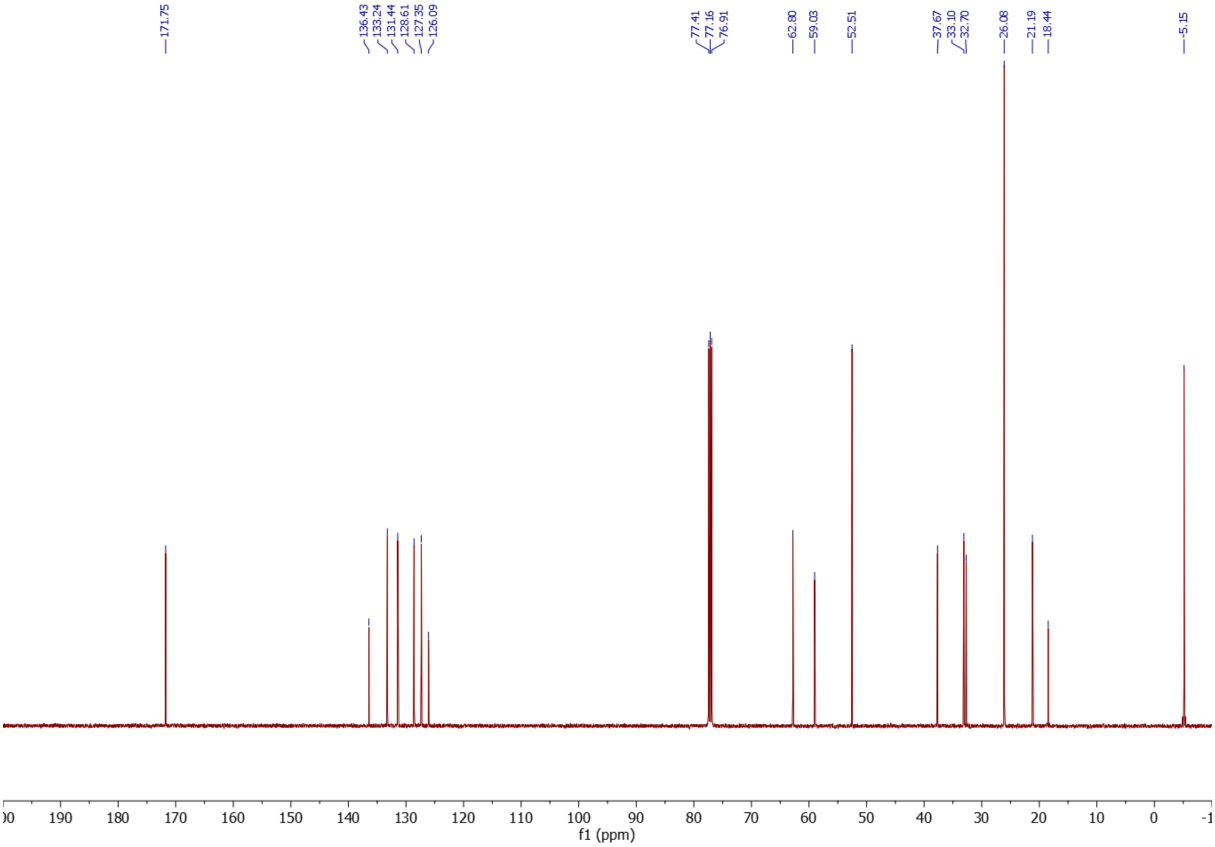

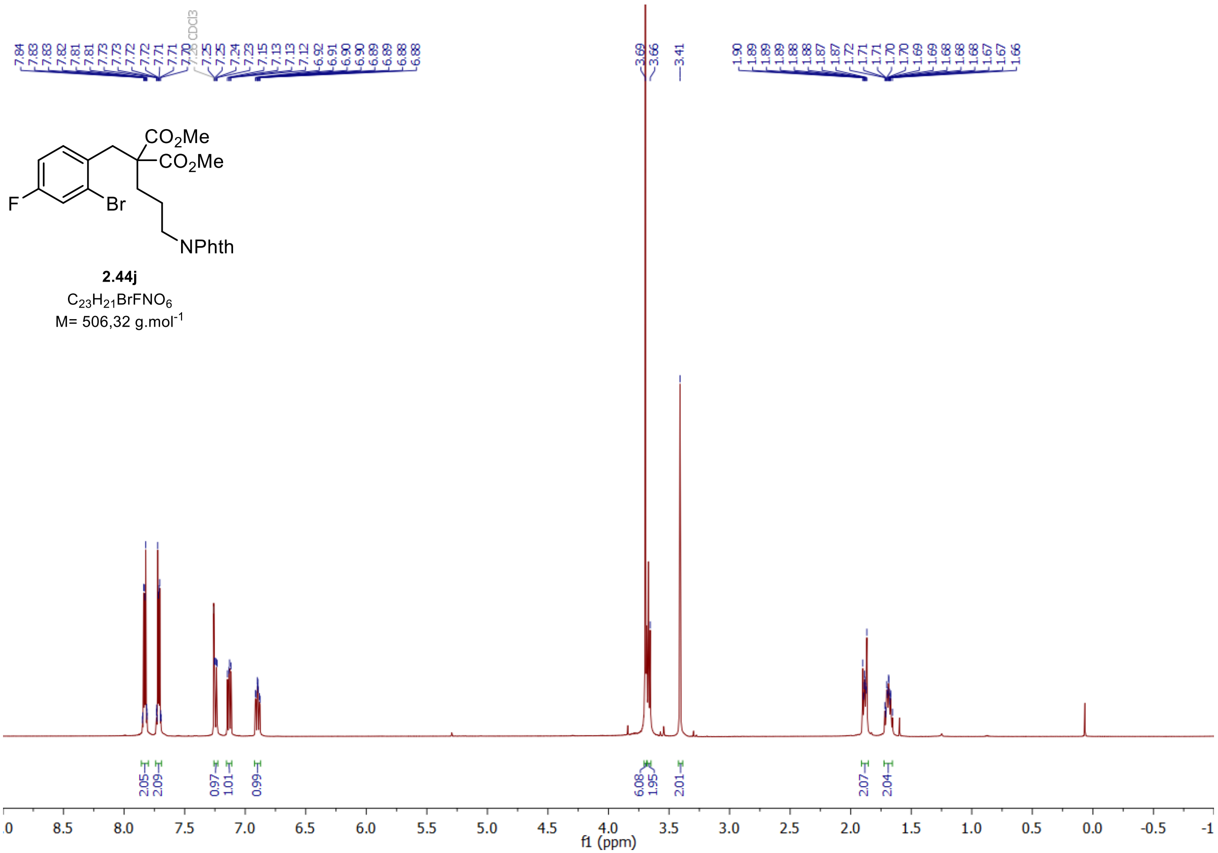

2.44j

$C_{23}H_{21}BrFNO_6$

M= 506,32 g.mol^{-1}

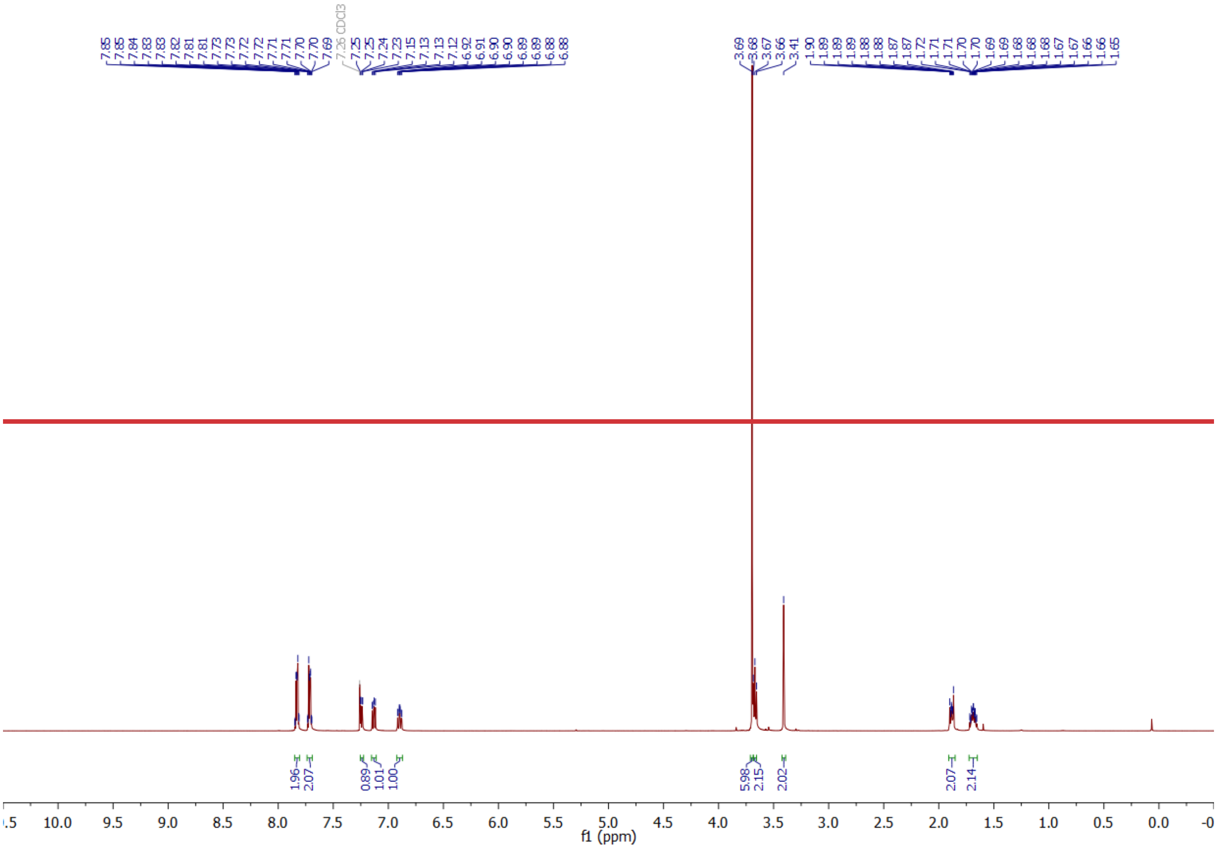

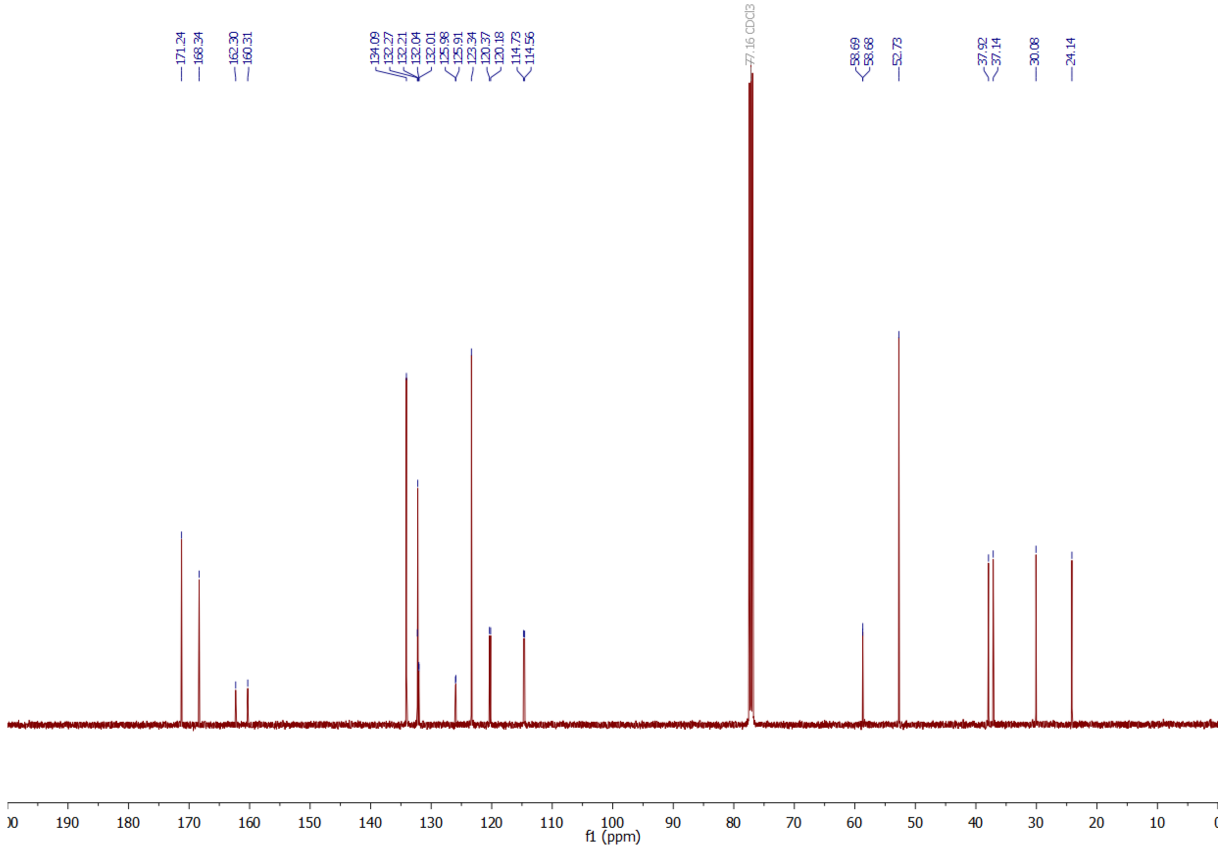
171.24
168.34
162.30
160.31
134.09
132.27
132.21
132.04
132.01
125.98
125.91
123.34
120.37
120.18
114.73
114.56
77.16 CDCl3
58.69
58.68
52.73
37.92
37.14
30.08
24.14
190
180
170
160
150
140
130
120
110
100
90
80
70
60
50
40
30
20
10
f1 (ppm)

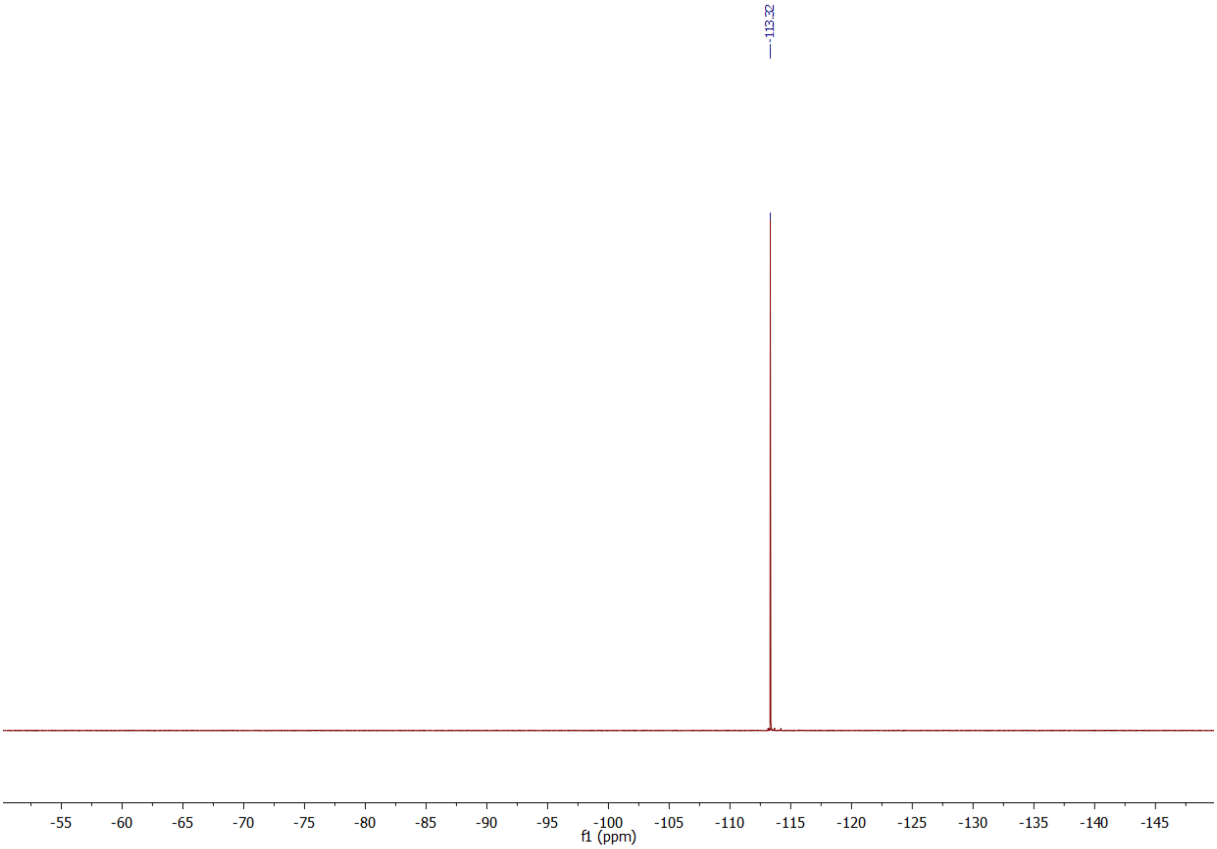
-113.32
-55
-60
-65
-70
-75
-80
-85
-90
-95
-100
-105
-110
-115
-120
-125
-130
-135
-140
-145
f1 (ppm)

CO2Et
CO2Et
Br
Me

2.44k

$C_{17}H_{23}BrO_4$

M= 371,27 g.mol^{-1}

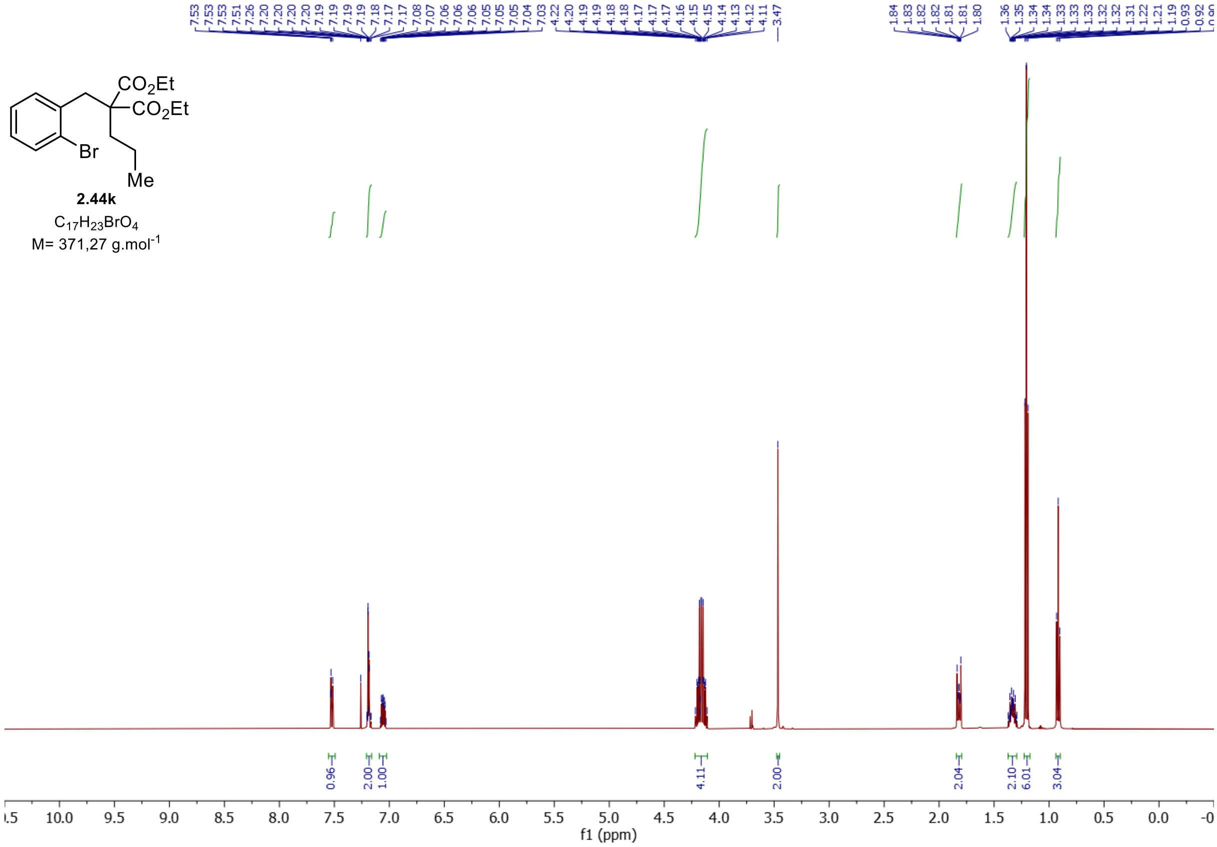

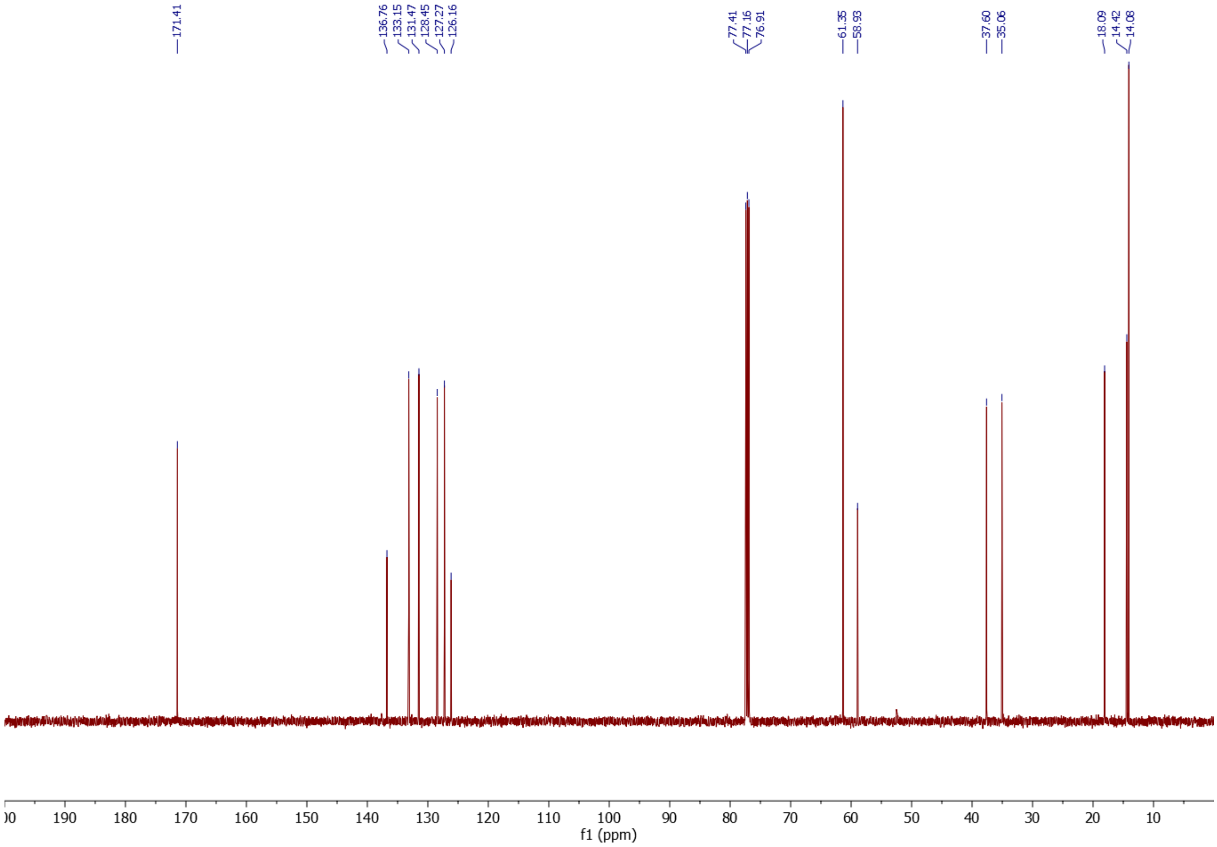

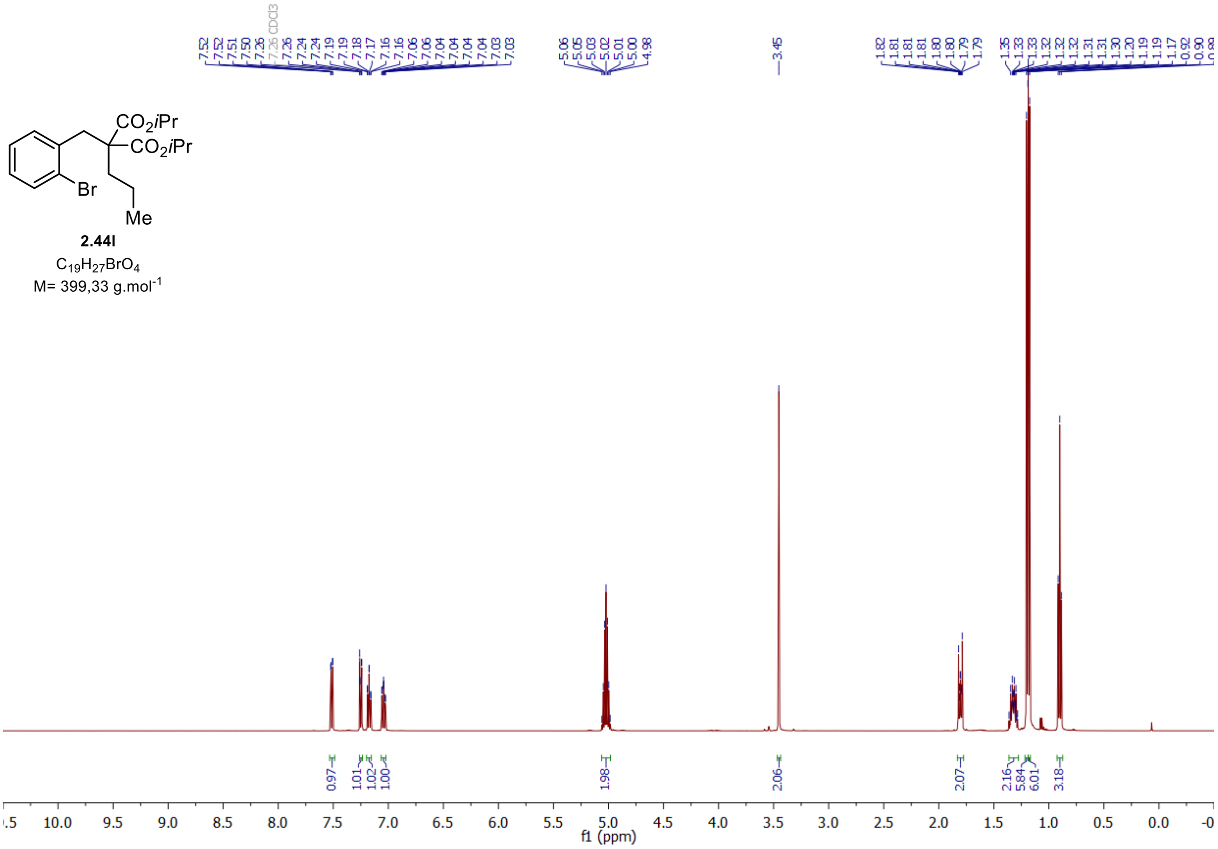

2.44l

$C_{19}H_{27}BrO_4$

M= 399,33 g.mol^{-1}

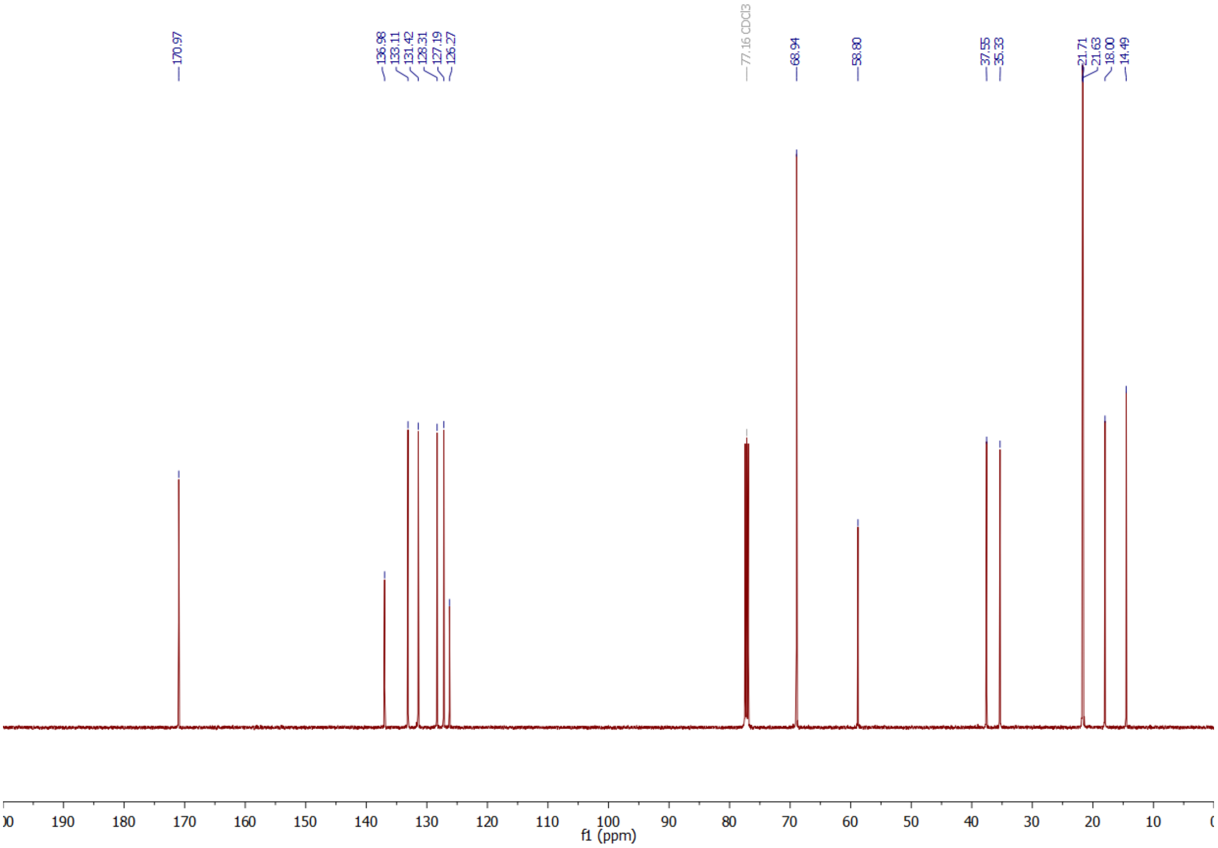

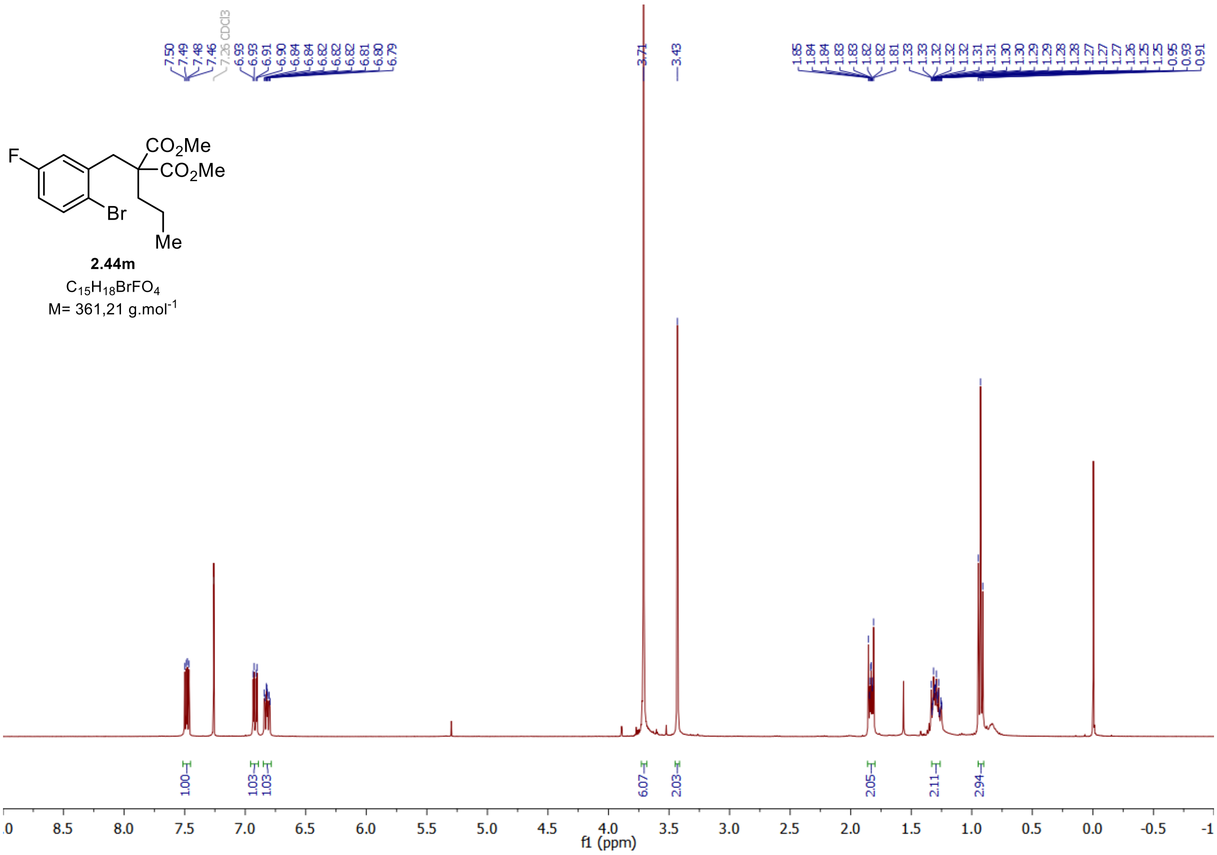

2.44m

$C_{15}H_{18}BrFO_4$

M= 361,21 g.mol^{-1}

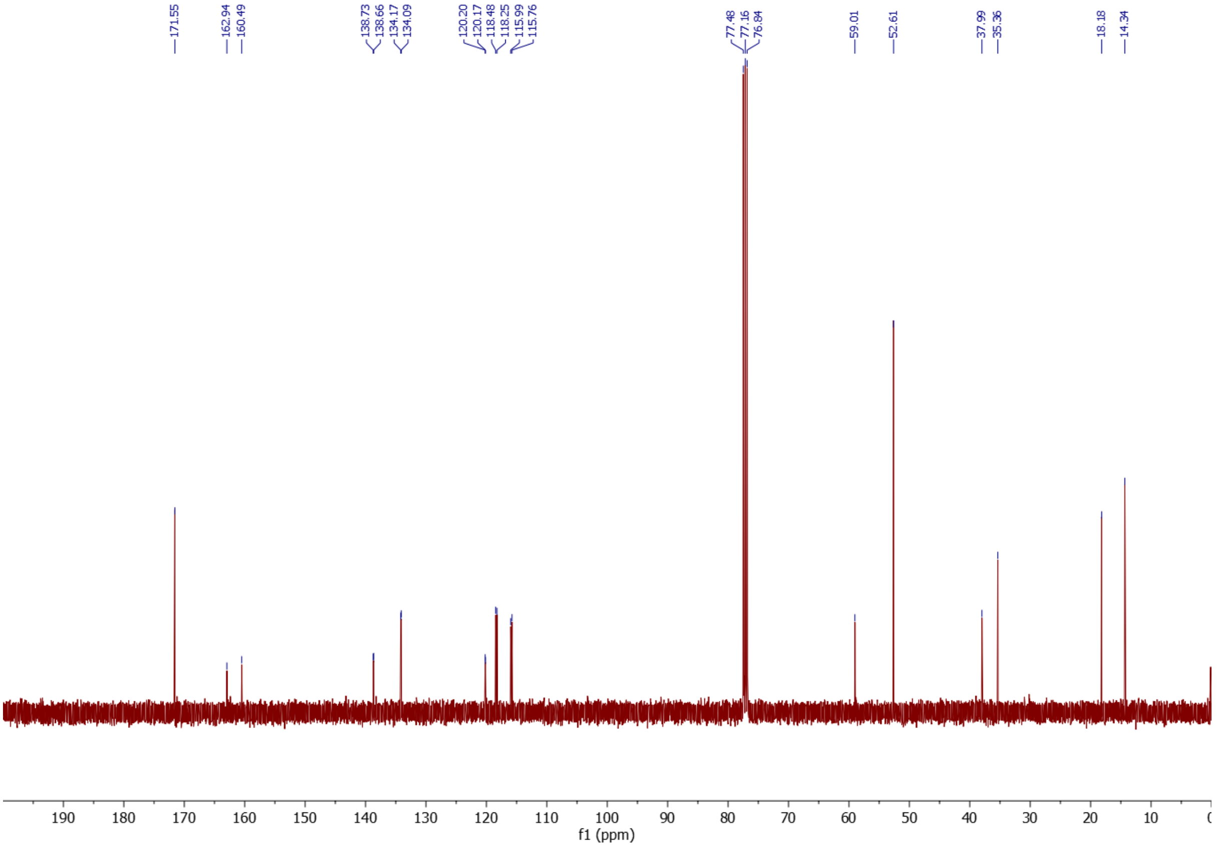

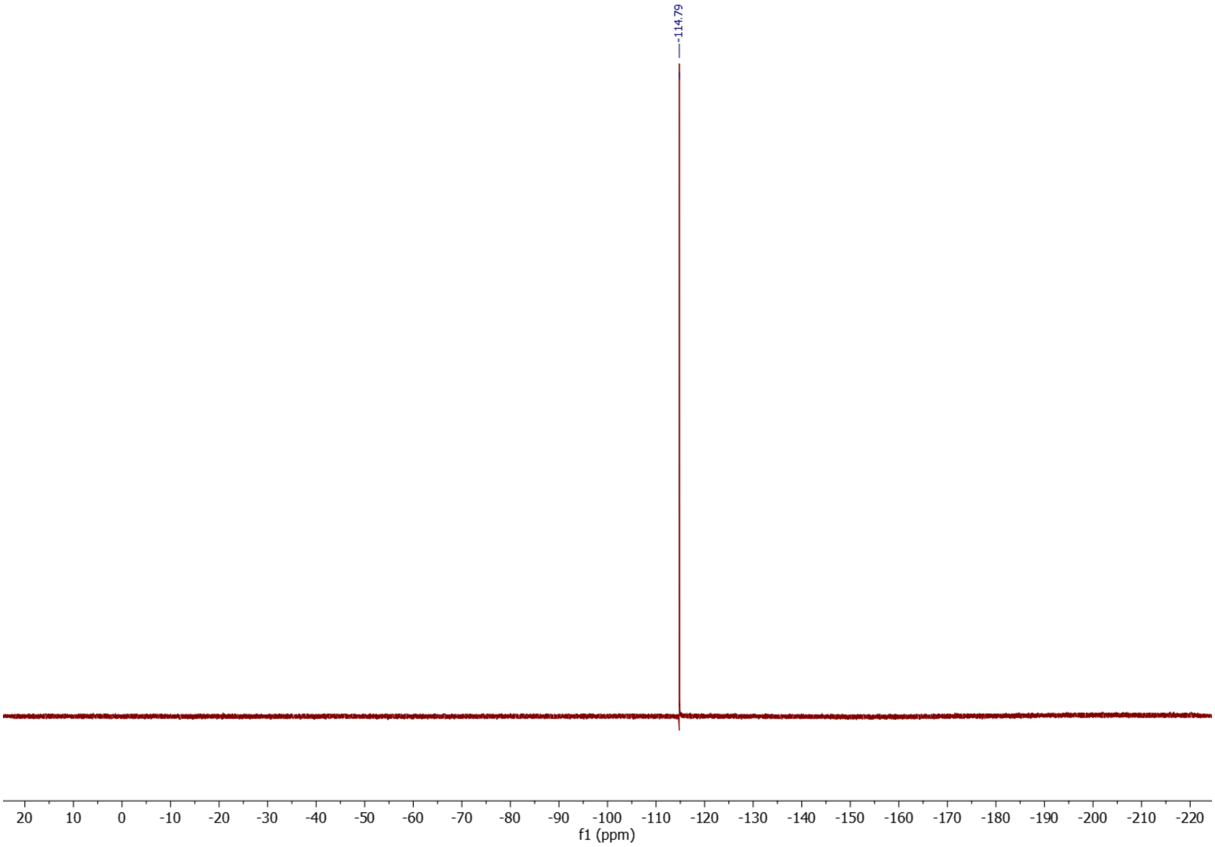
-114.79
20
10
0
-10
-20
-30
-40
-50
-60
-70
-80
-90
-100
-110
-120
-130
-140
-150
-160
-170
-180
-190
-200
-210
-220
f1 (ppm)

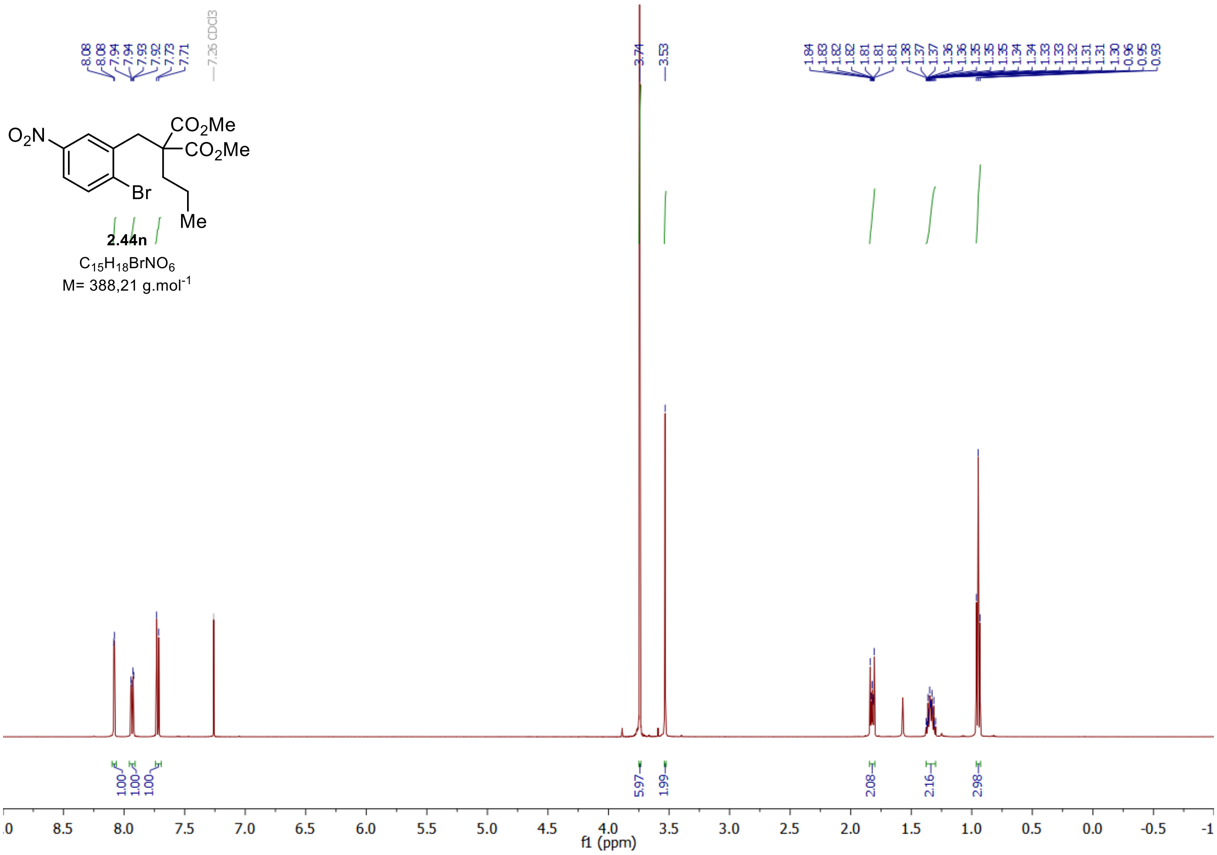

2.44n

$C_{15}H_{18}BrNO_6$

M= 388,21 g.mol^{-1}

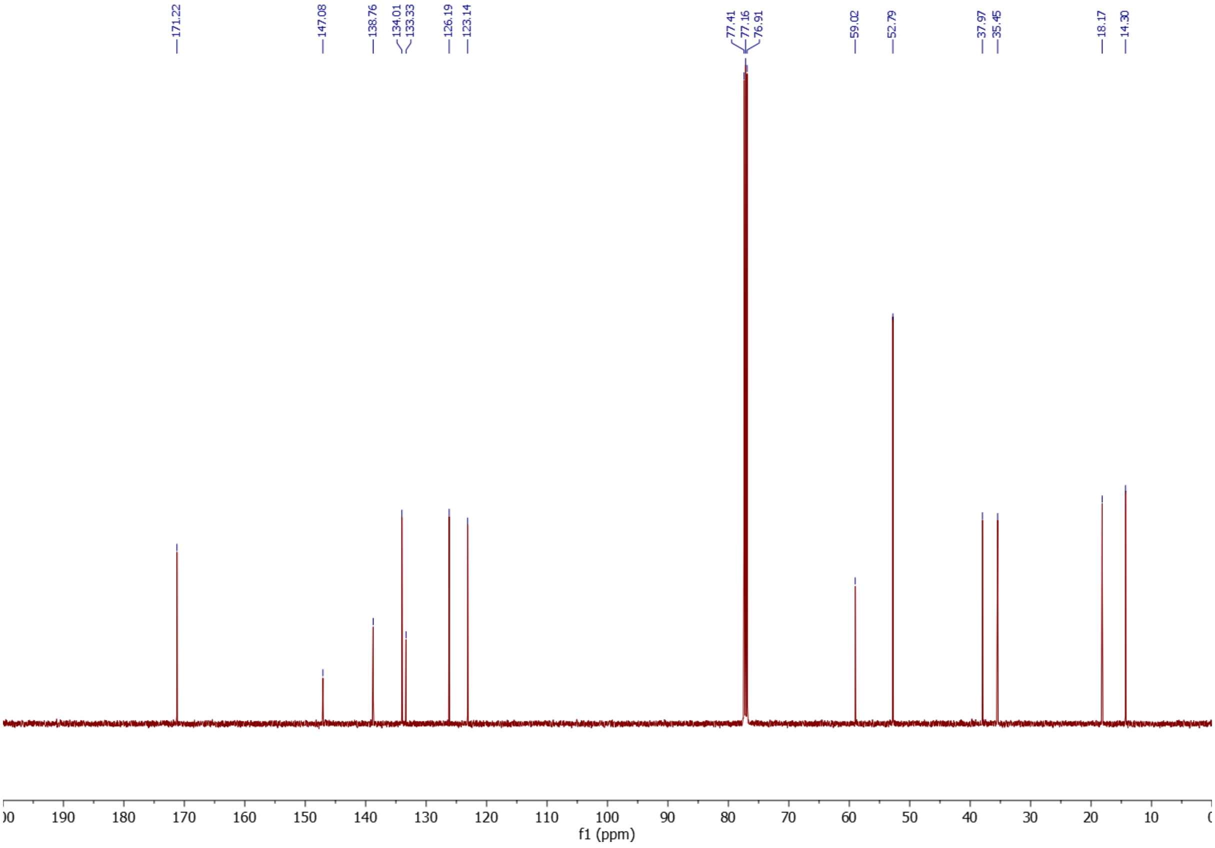

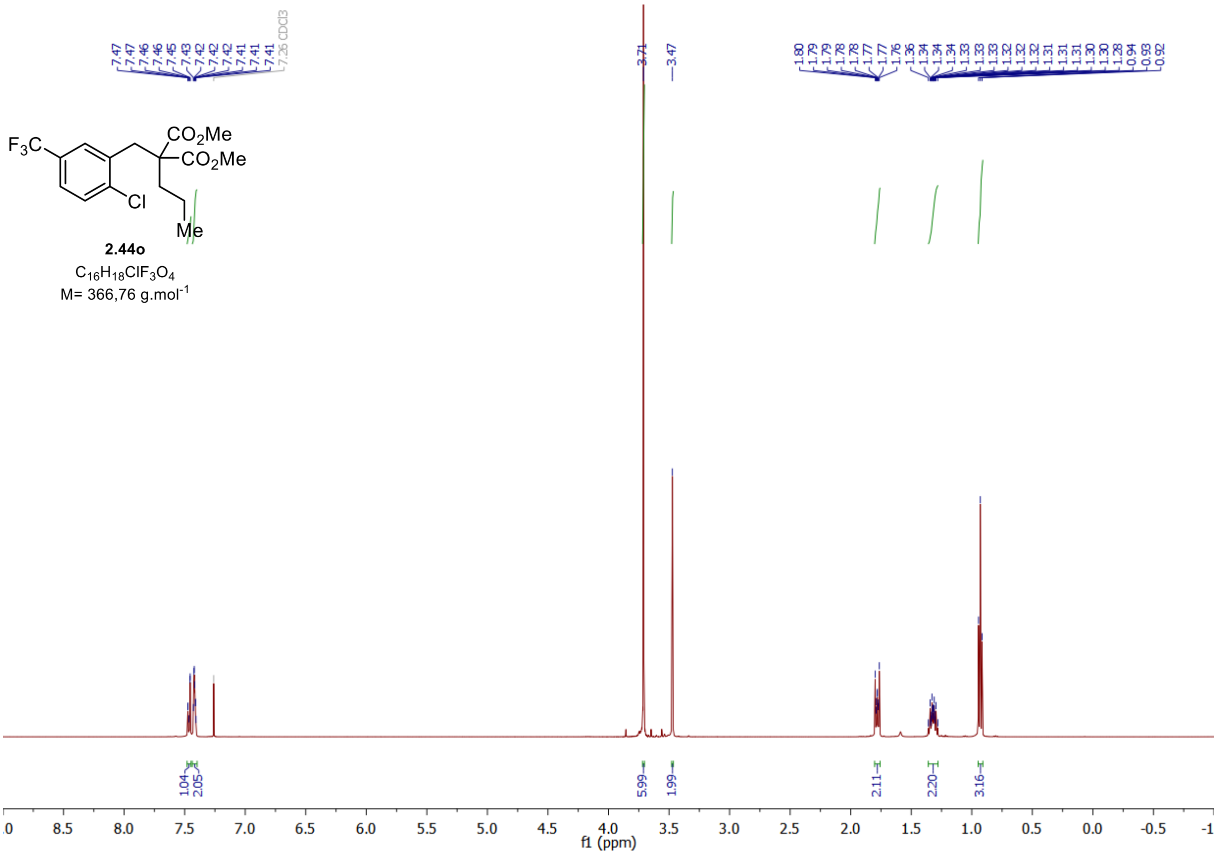

2.44o

$C_{16}H_{18}ClF_3O_4$

M= 366,76 g.mol^{-1}

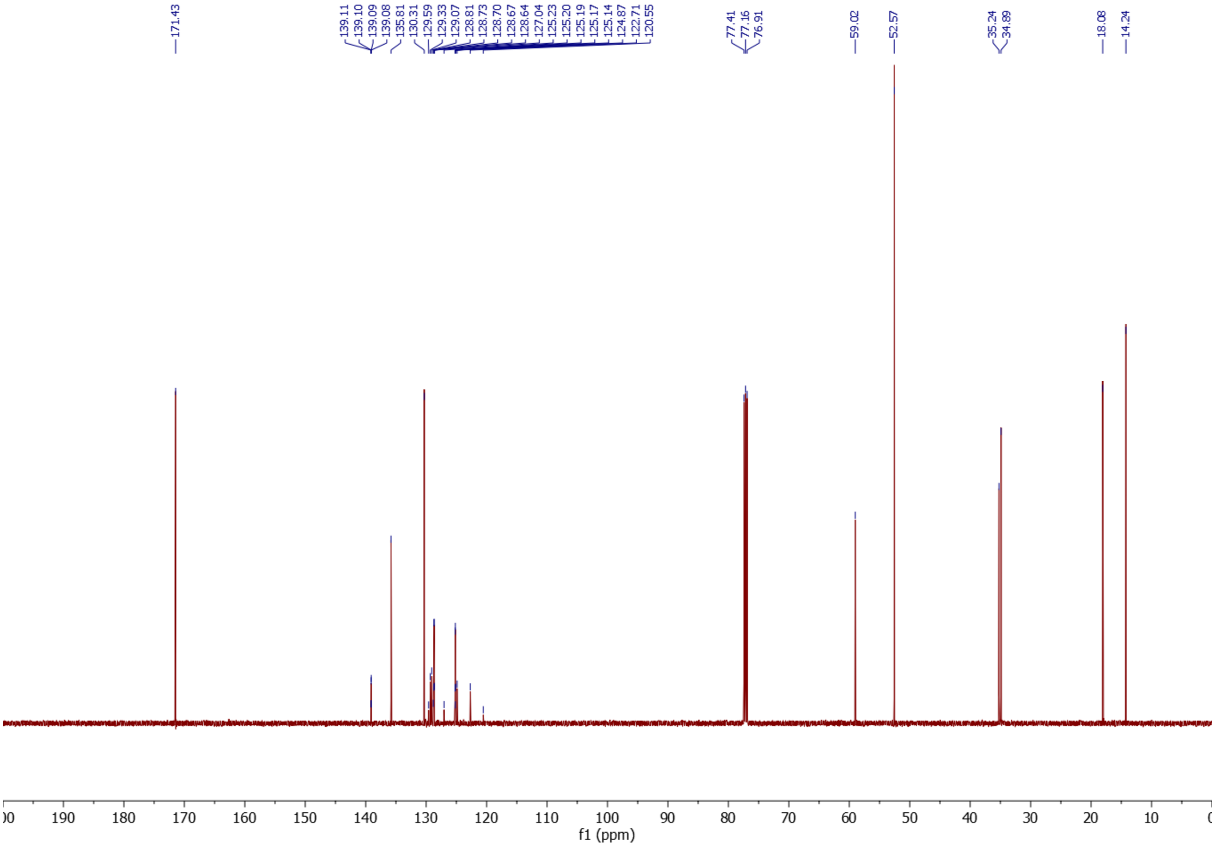

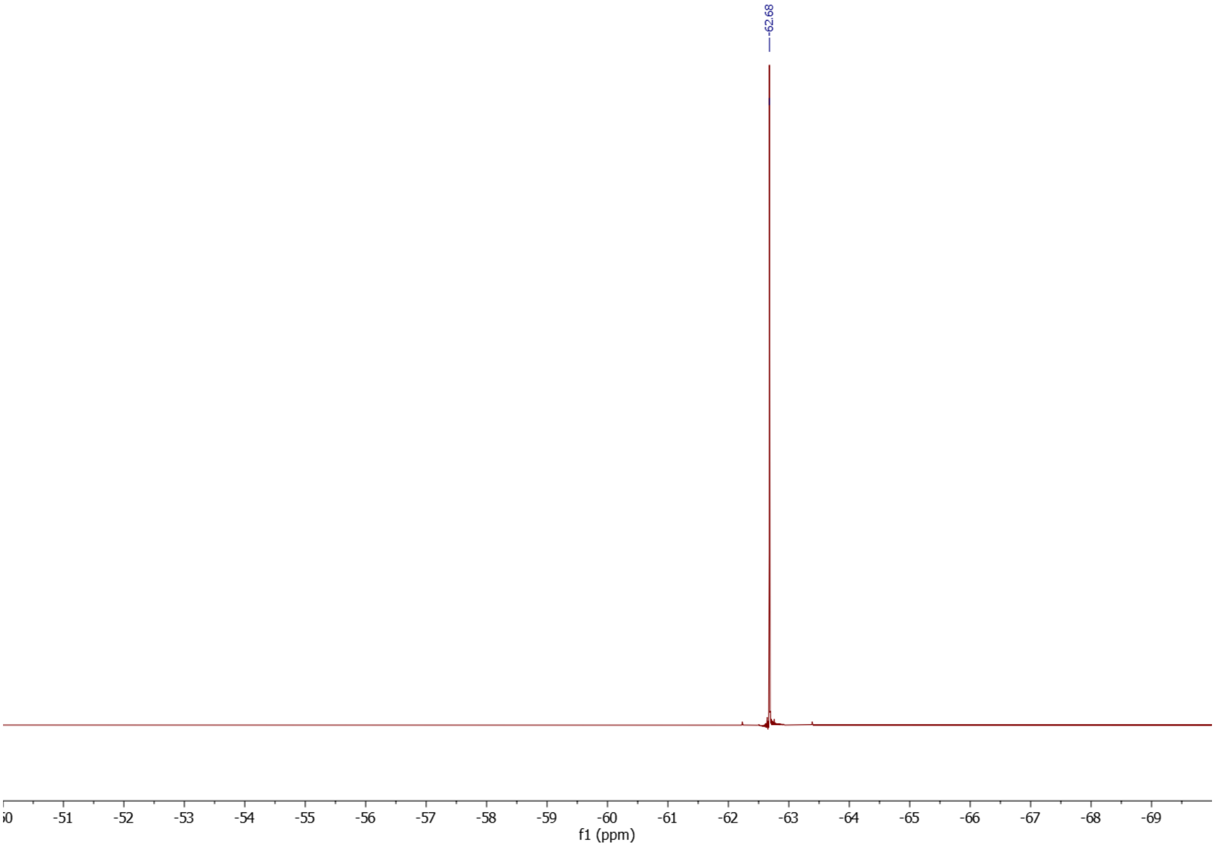
-62.68
-51
-52
-53
-54
-55
-56
-57
-58
-59
-60
-61
-62
-63
-64
-65
-66
-67
-68
-69
f1 (ppm)

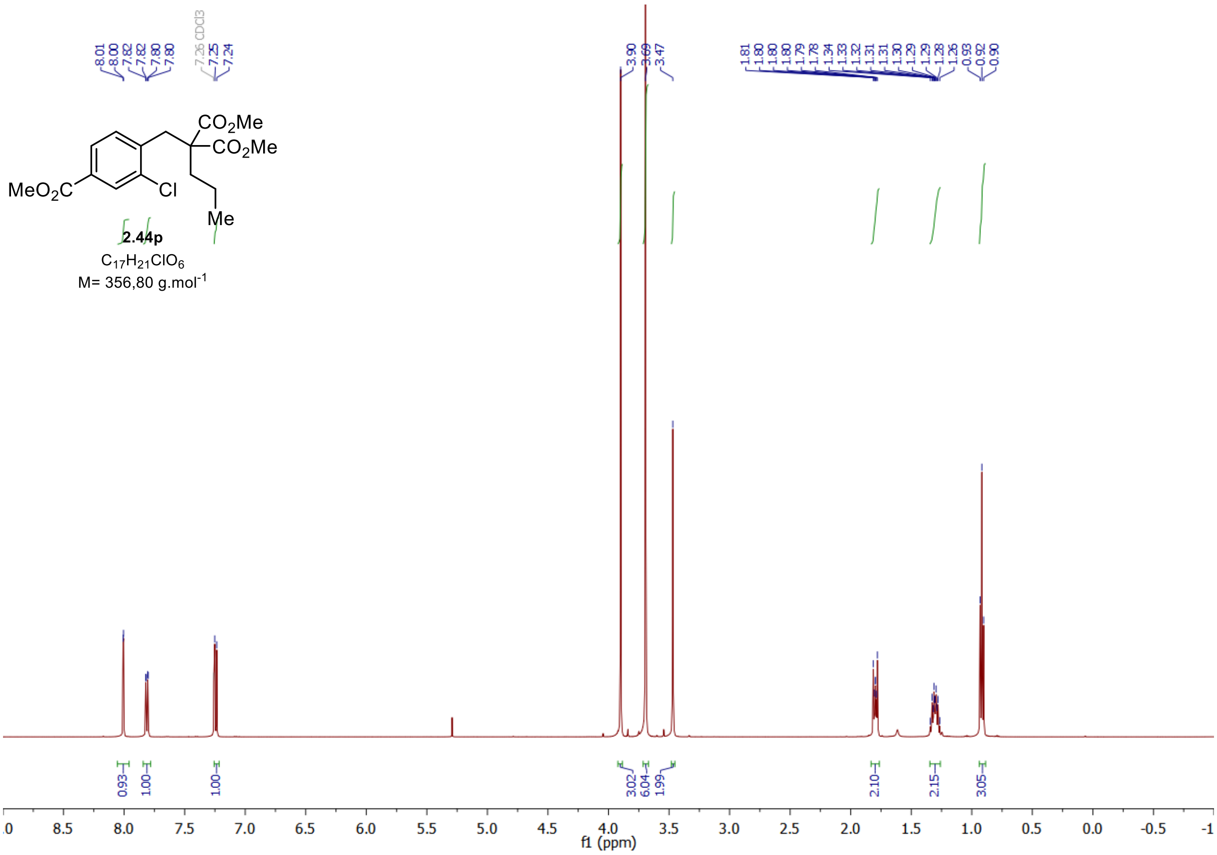

2.44p

$C_{17}H_{21}ClO_6$

M= 356,80 g.mol^{-1}

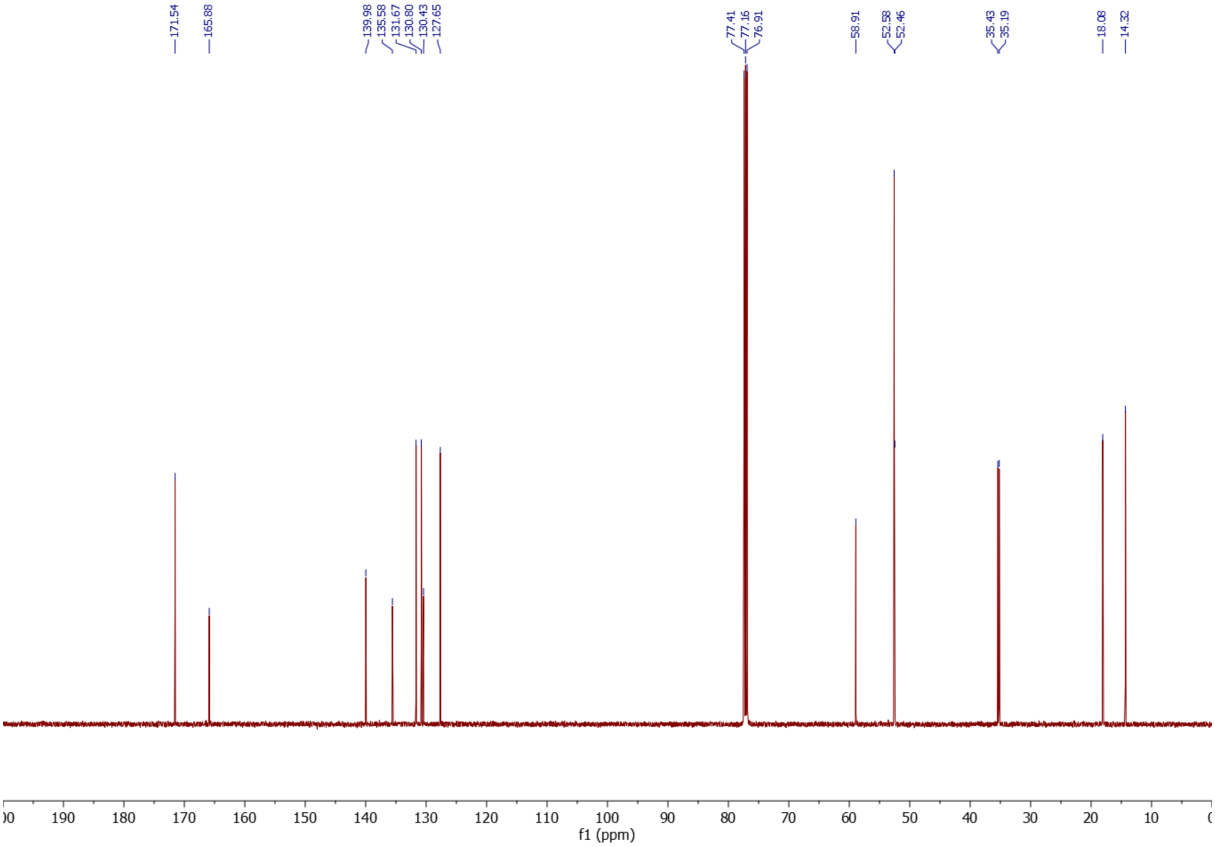

CO2Me
CO2Me
MeO2S
Cl
Me

2.44q

$C_{16}H_{21}ClO_6S$

M= 376,85 g.mol^{-1}

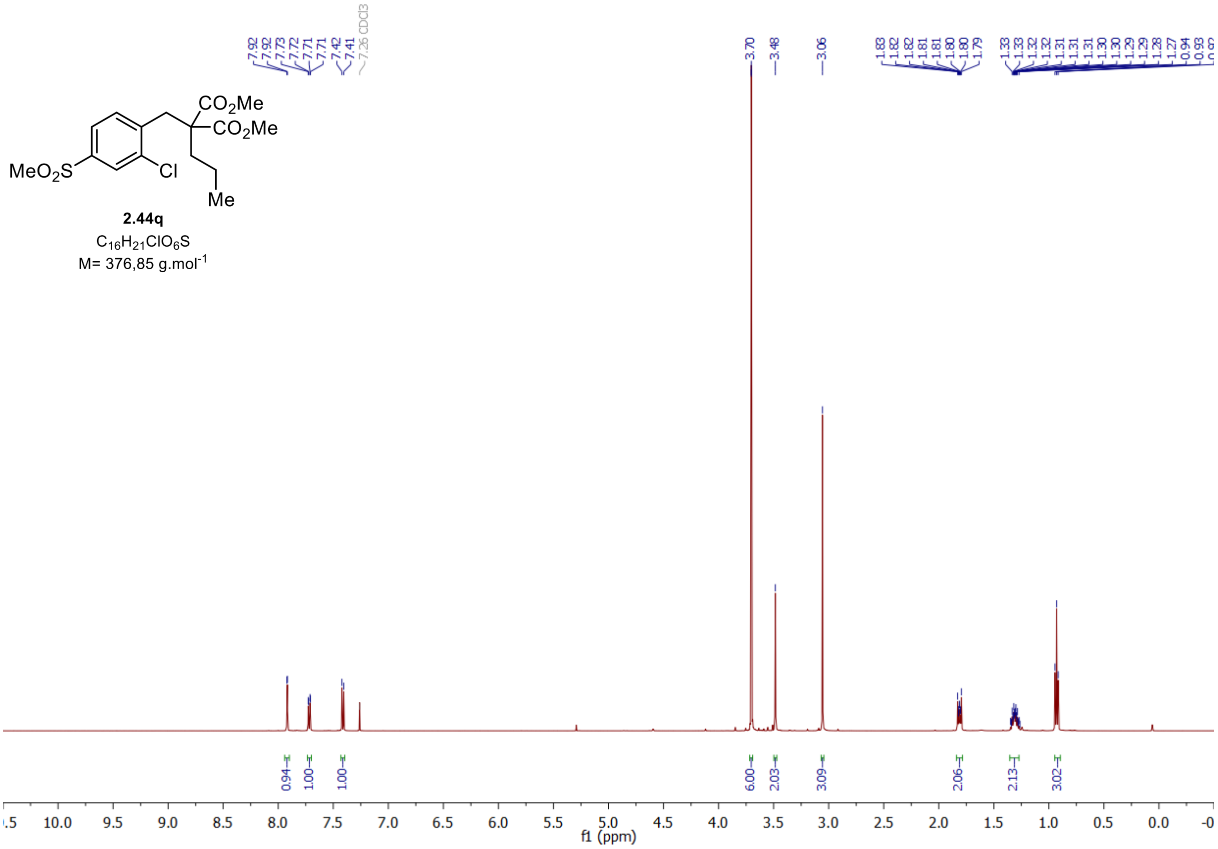

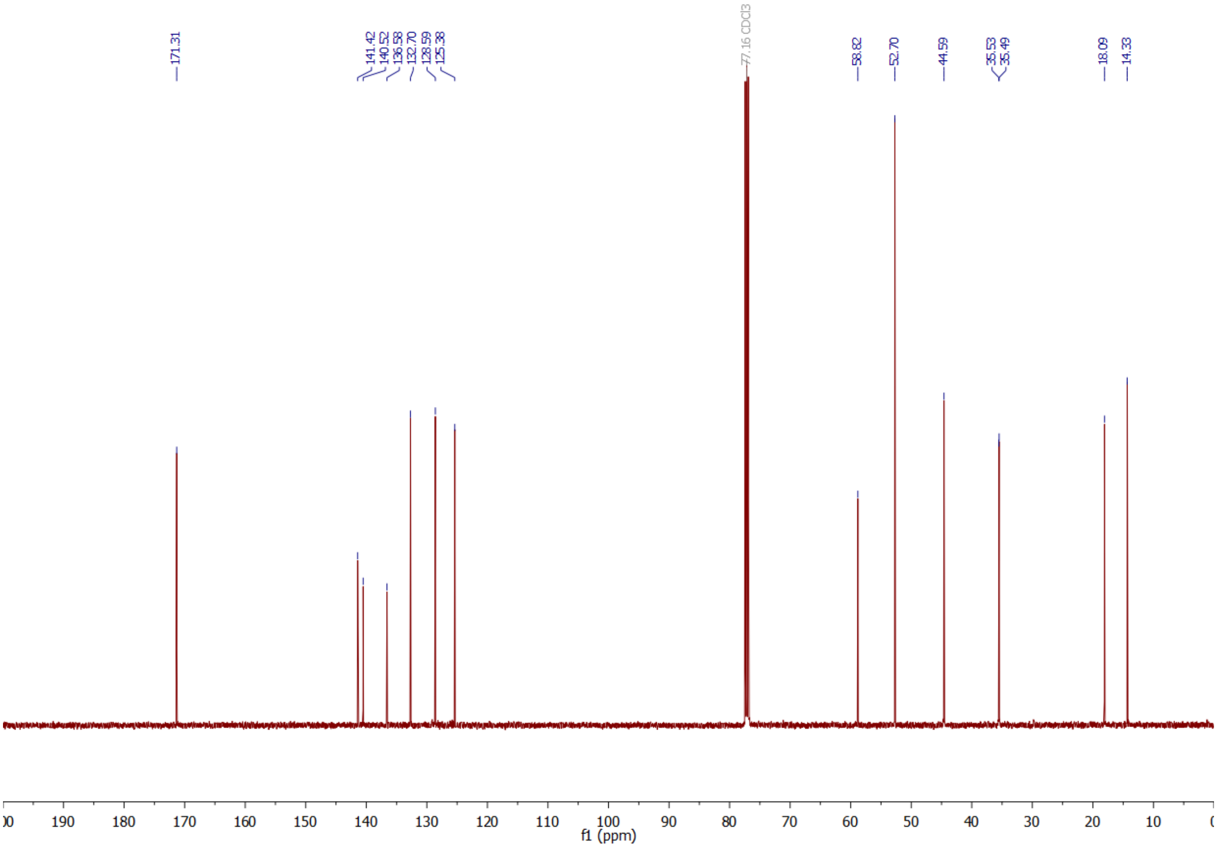

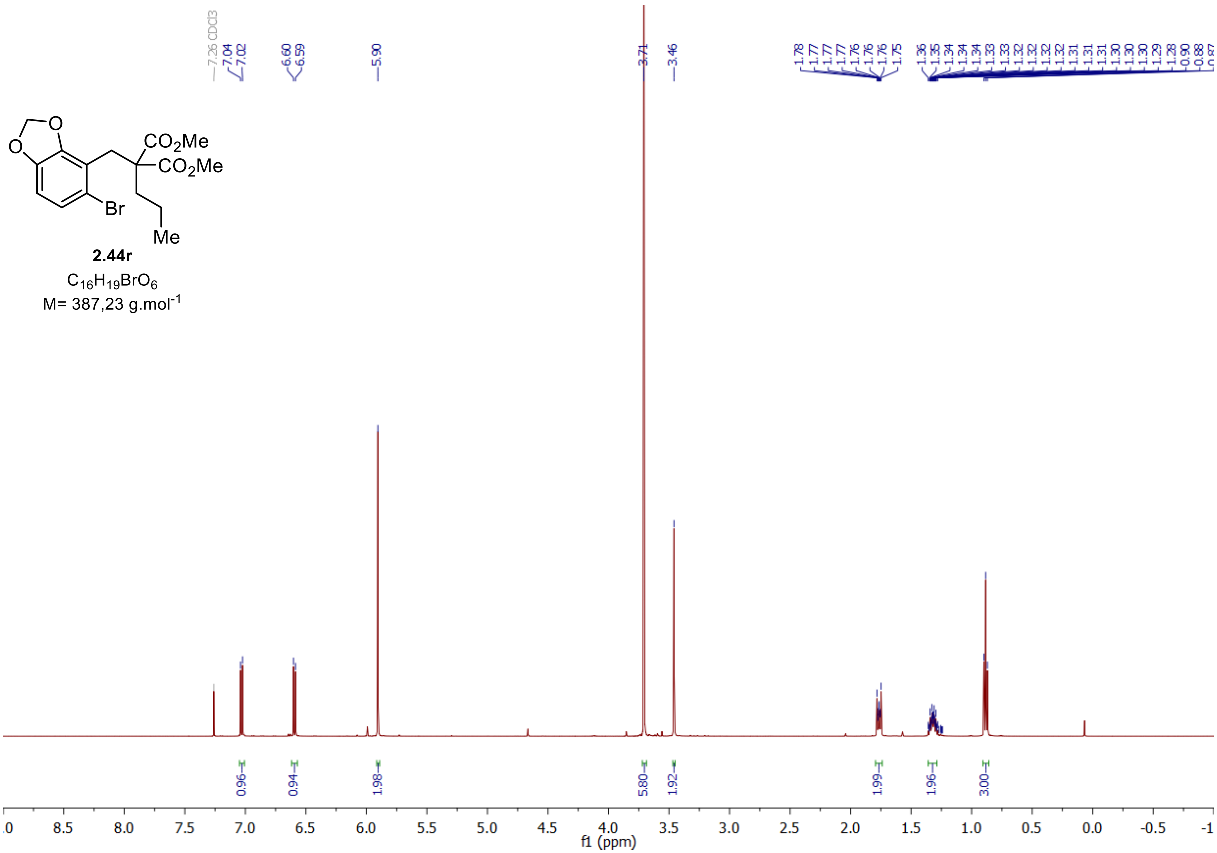

2.44r

$C_{16}H_{19}BrO_6$

M= 387,23 g.mol^{-1}

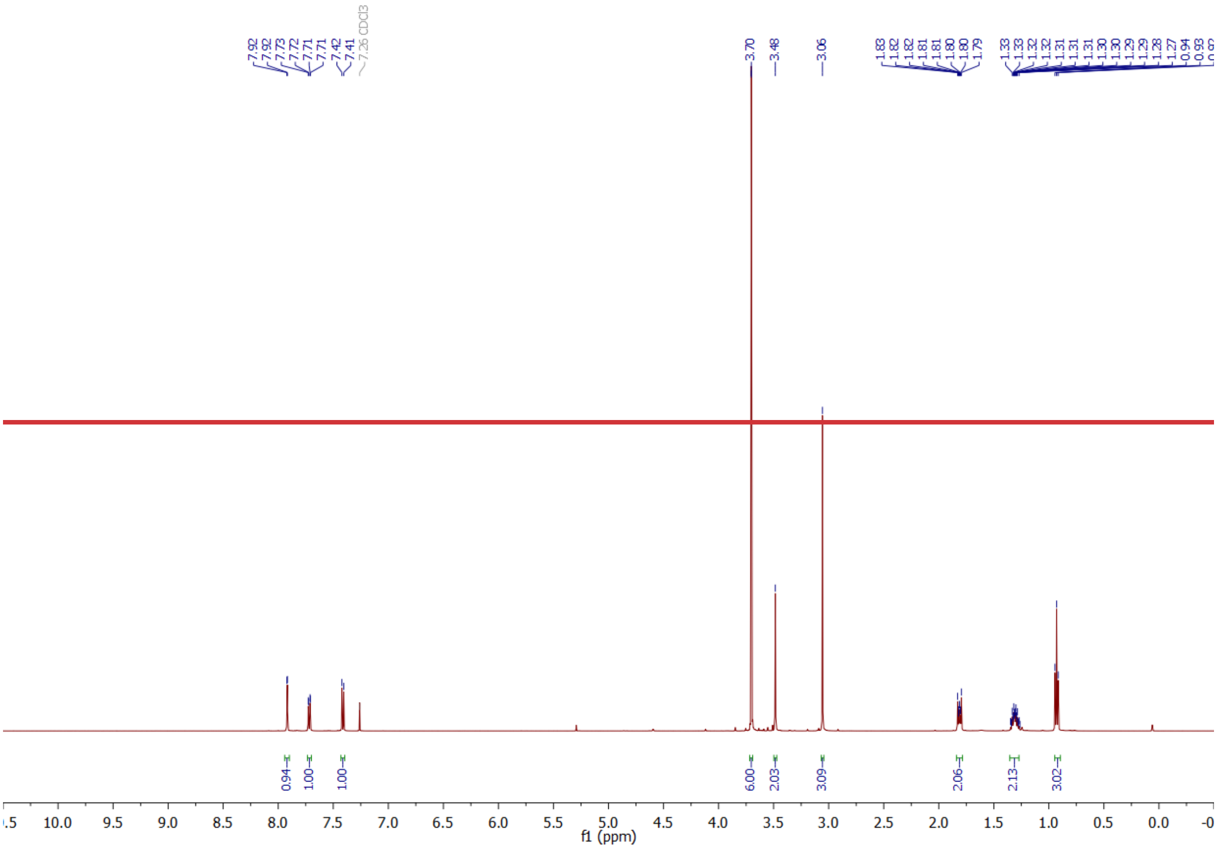

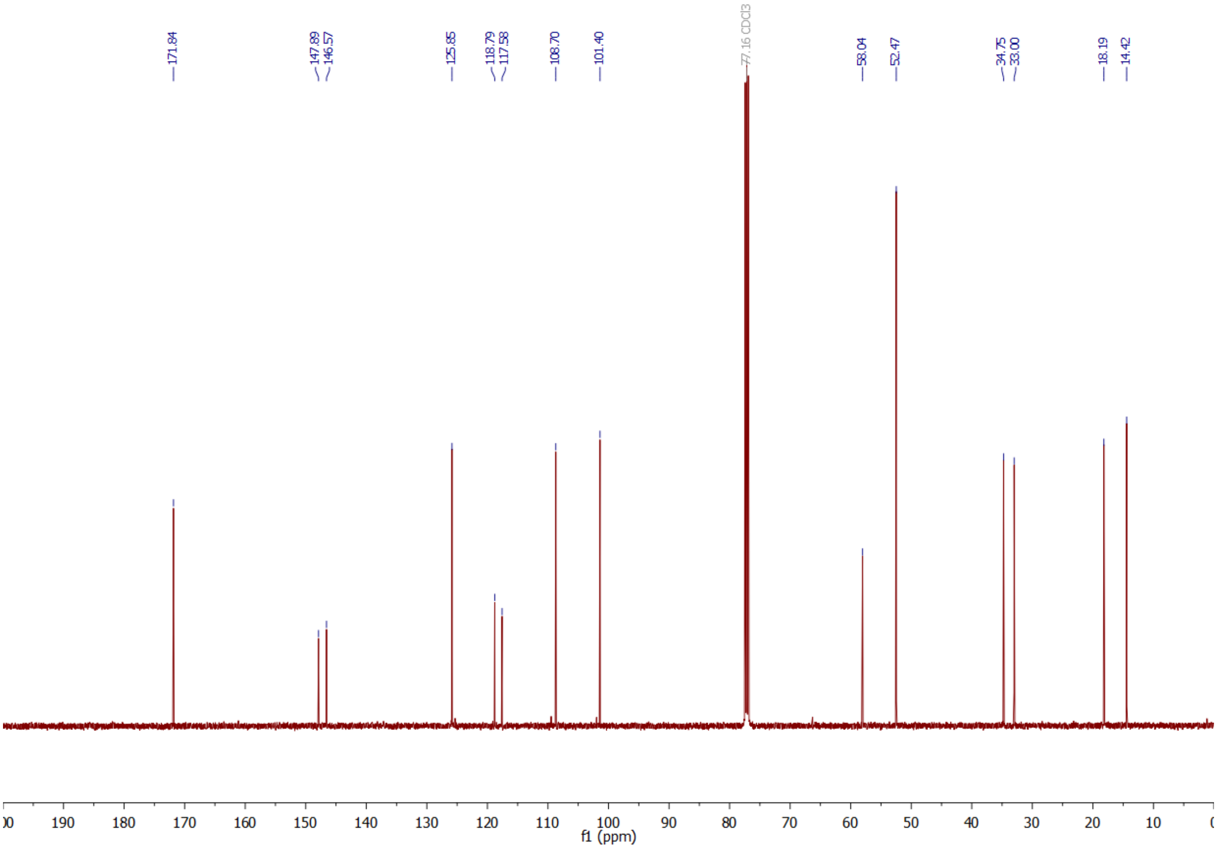
171.84
147.89
146.57
125.85
118.79
117.58
108.70
101.40
77.16 CDCl3
58.04
52.47
34.75
33.00
18.19
14.42
190
180
170
160
150
140
130
120
110
100
90
80
70
60
50
40
30
20
10
f1 (ppm)

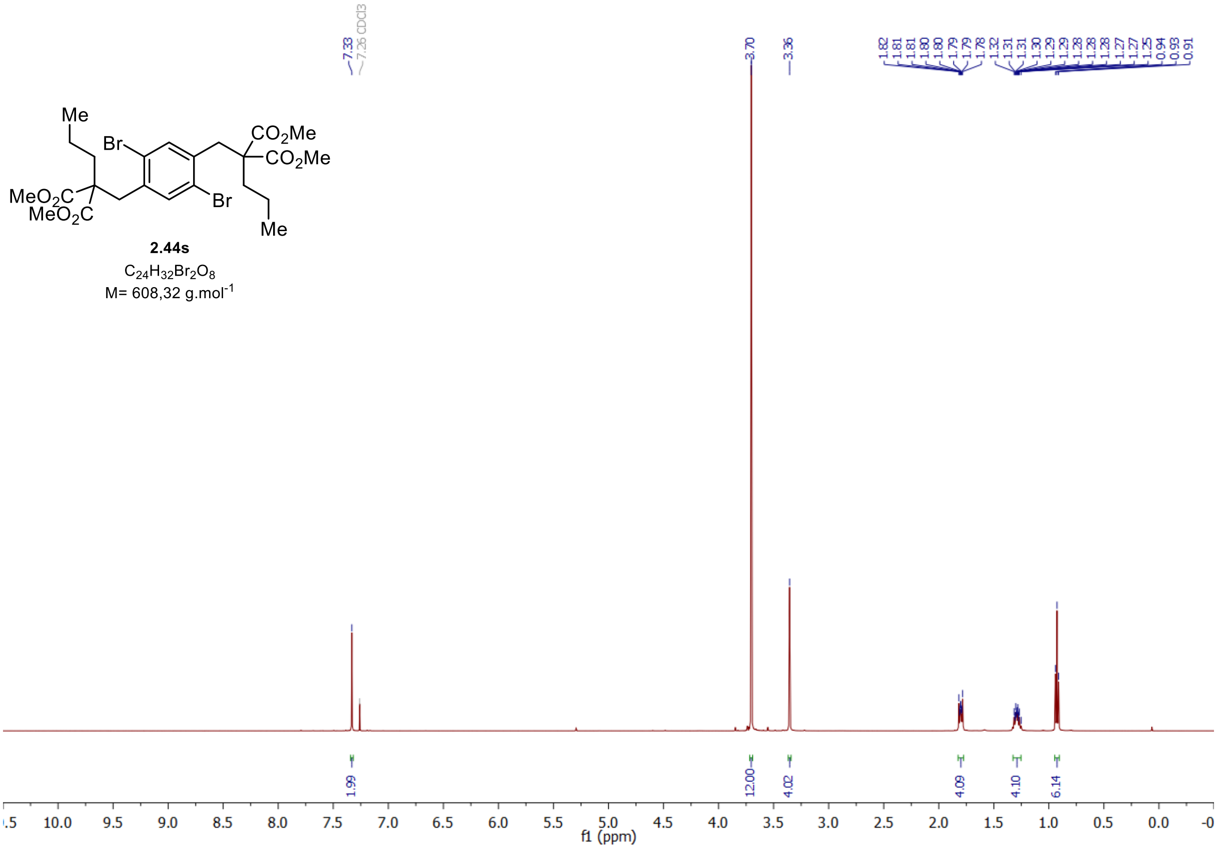

2.44s

$C_{24}H_{32}Br_2O_8$

M= 608,32 g.mol^{-1}

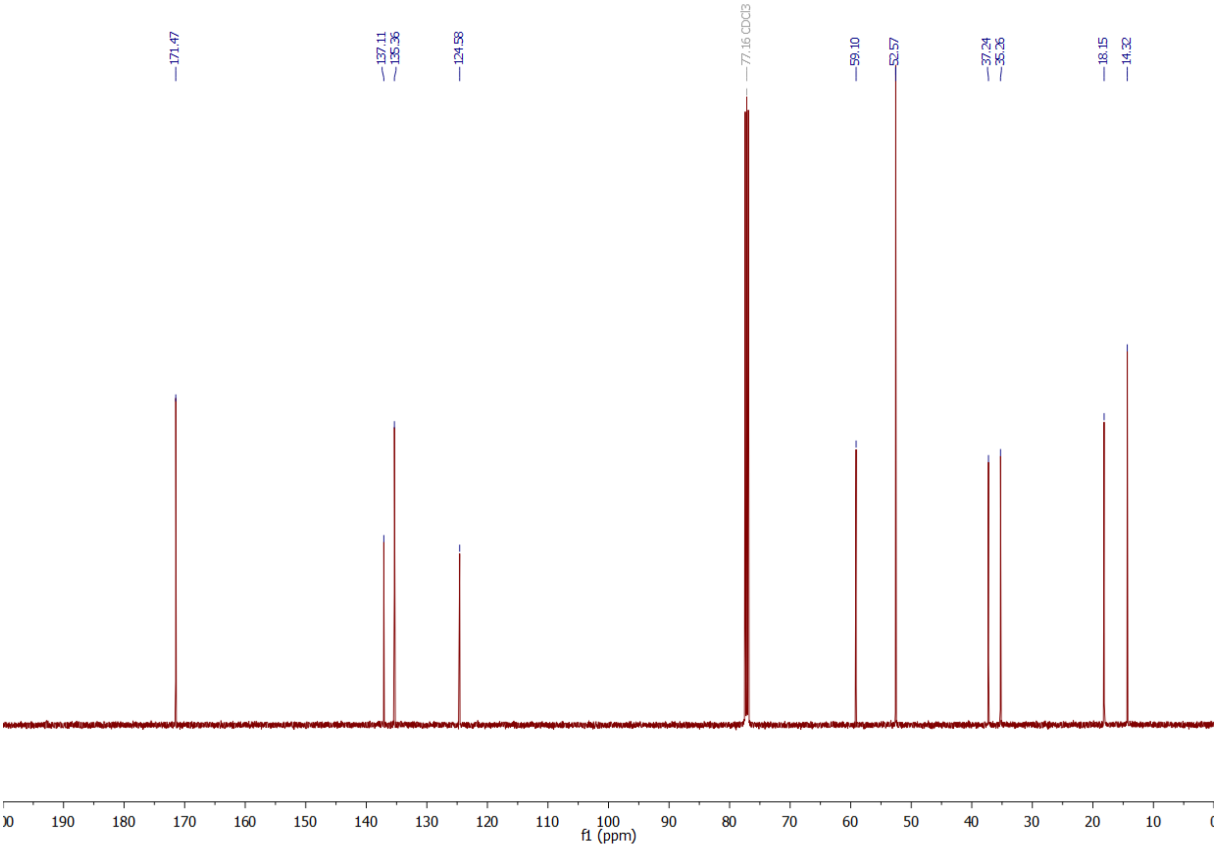

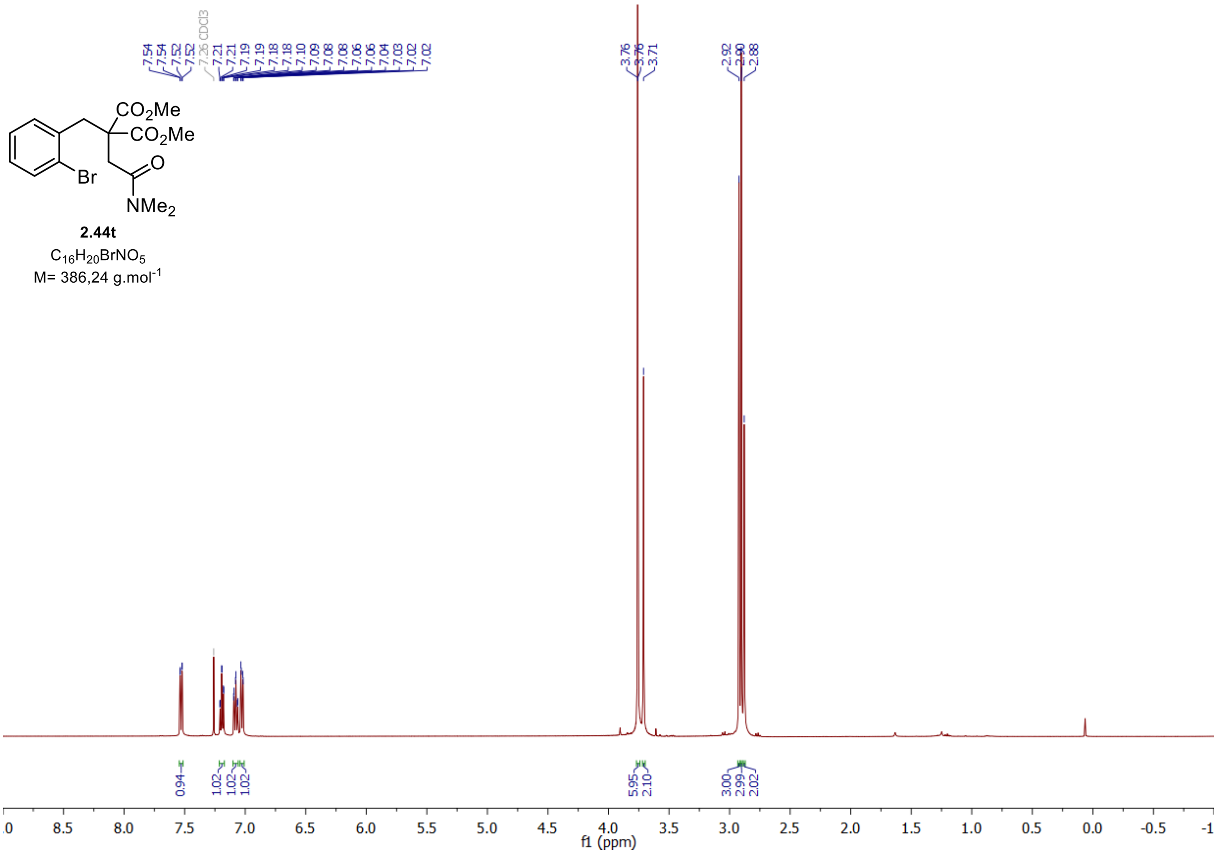

2.44t

$C_{16}H_{20}BrNO_5$

M= 386,24 g.mol^{-1}

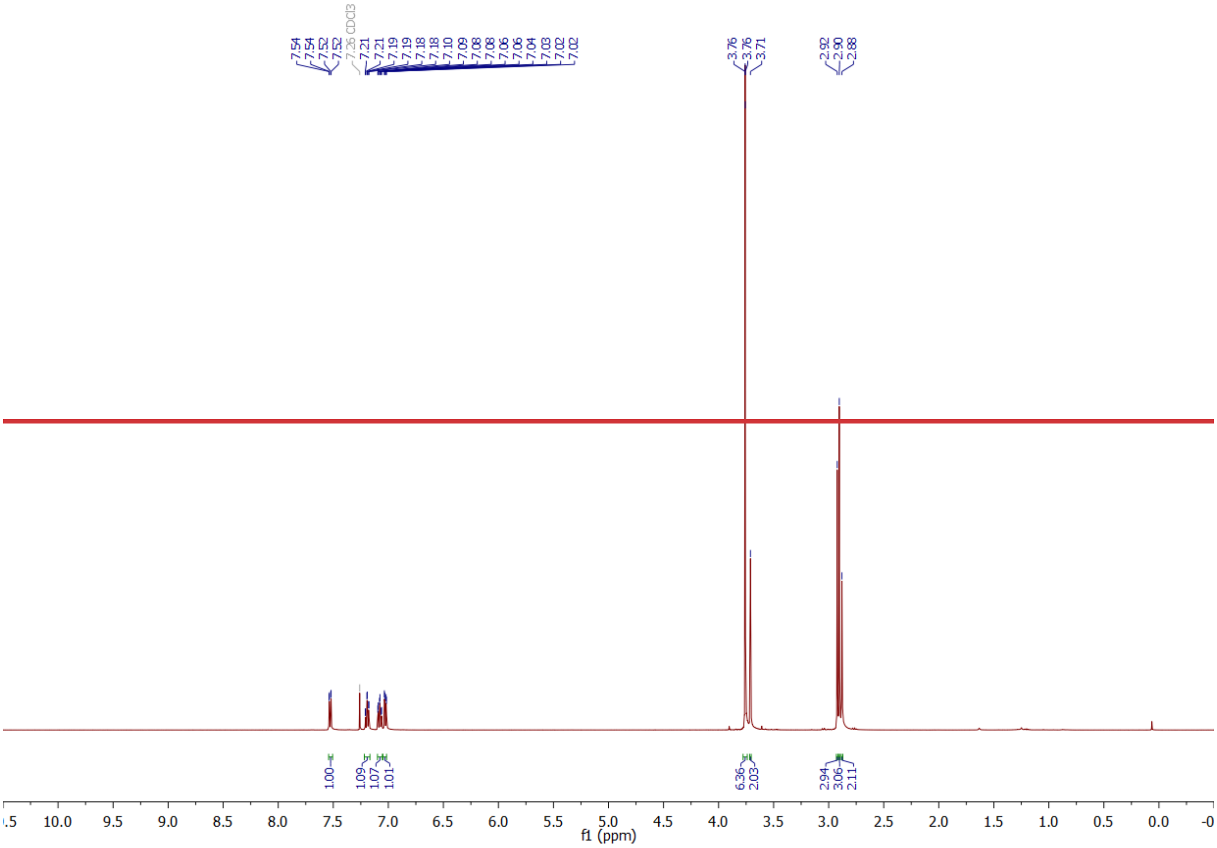

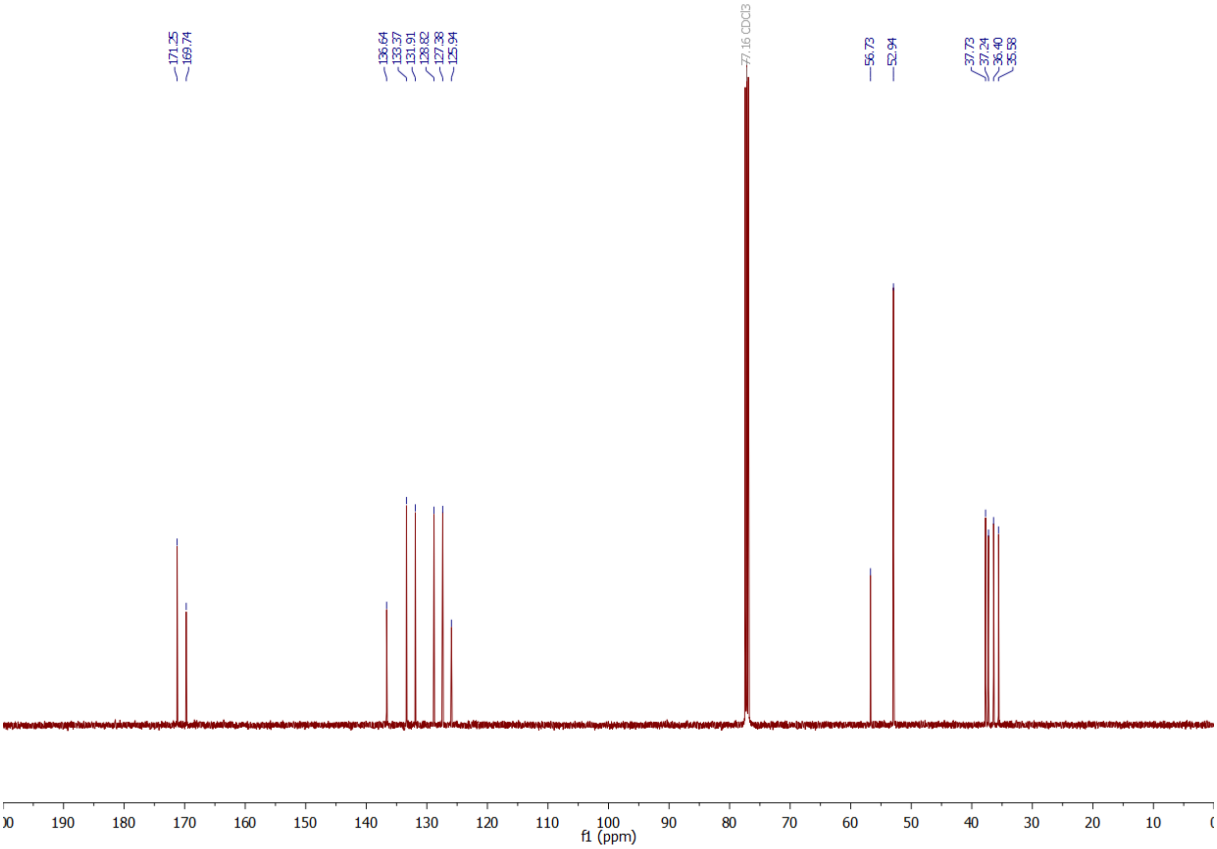
171.25
169.74
136.64
133.37
131.91
128.82
127.38
125.94
77.16 CDCl3
56.73
52.94
37.73
37.24
36.40
35.58
00
190
180
170
160
150
140
130
120
110
100
90
80
70
60
50
40
30
20
10
0
f1 (ppm)

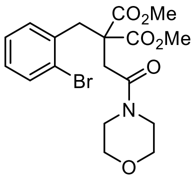

2.44u

$C_{18}H_{22}BrNO_6$

M= 428,28 g.mol^{-1}

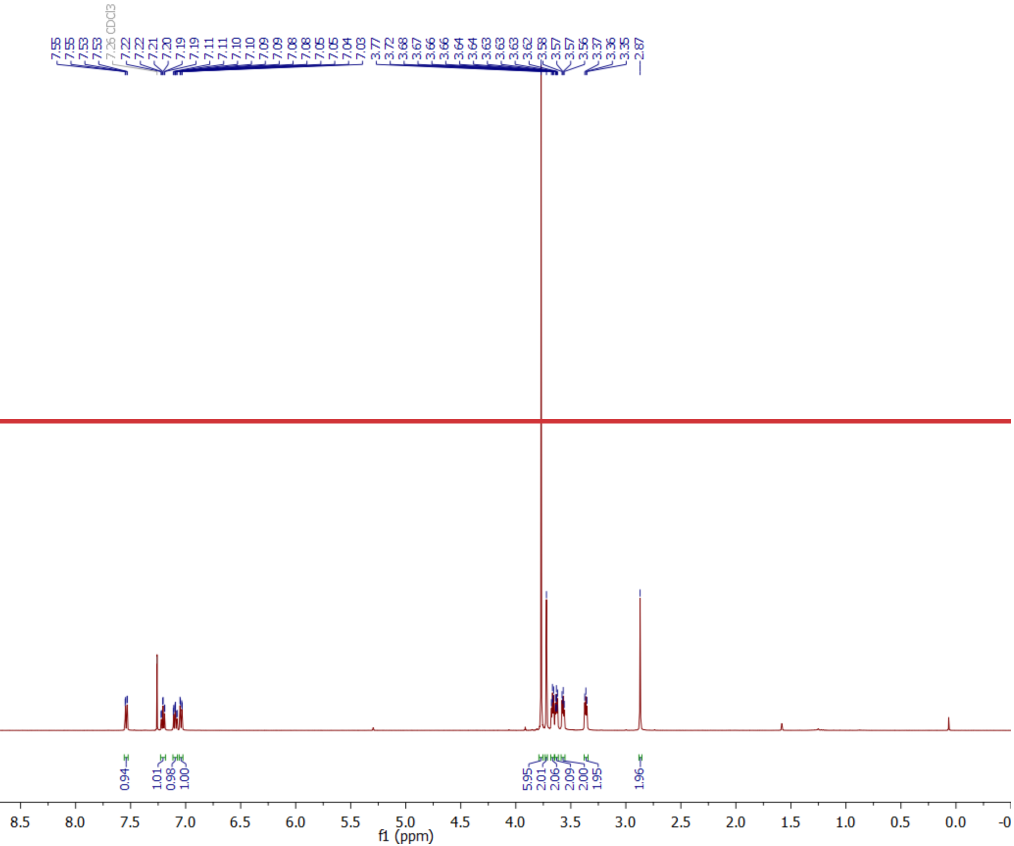

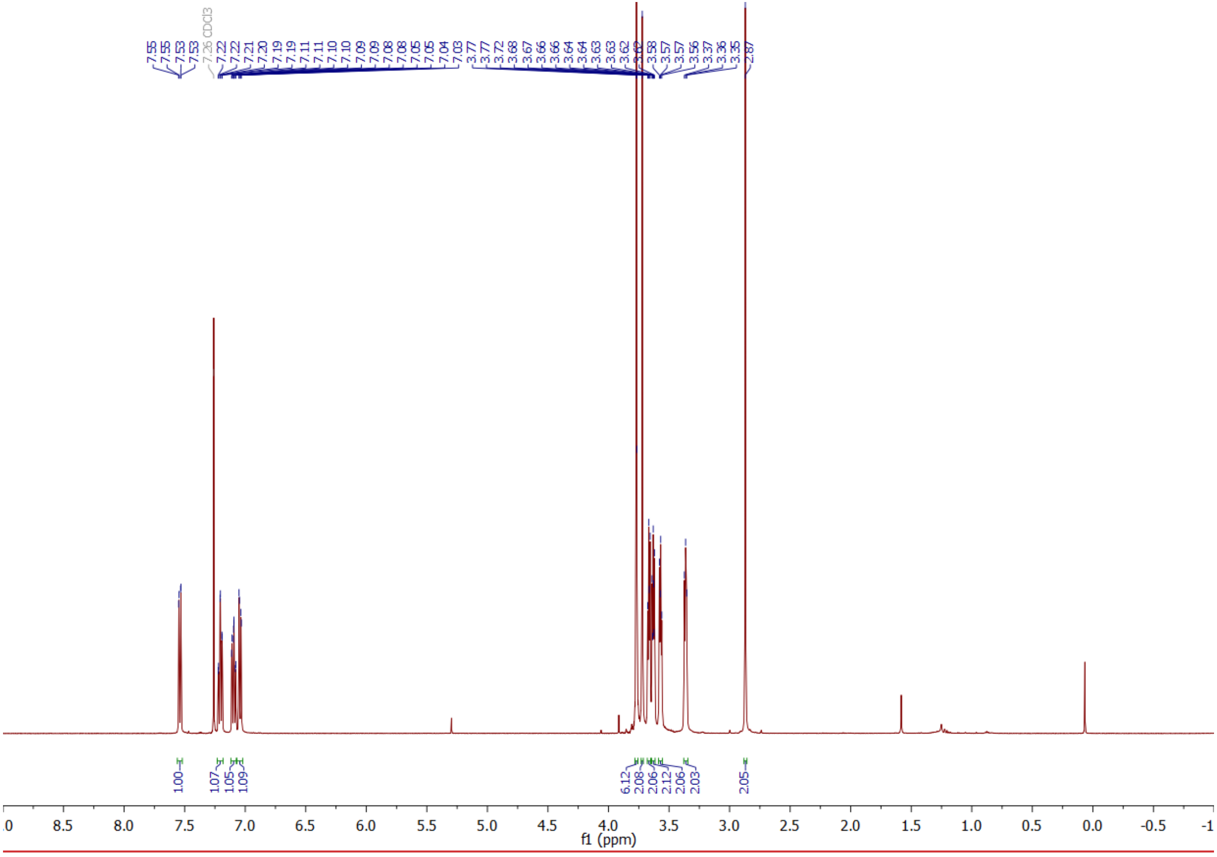

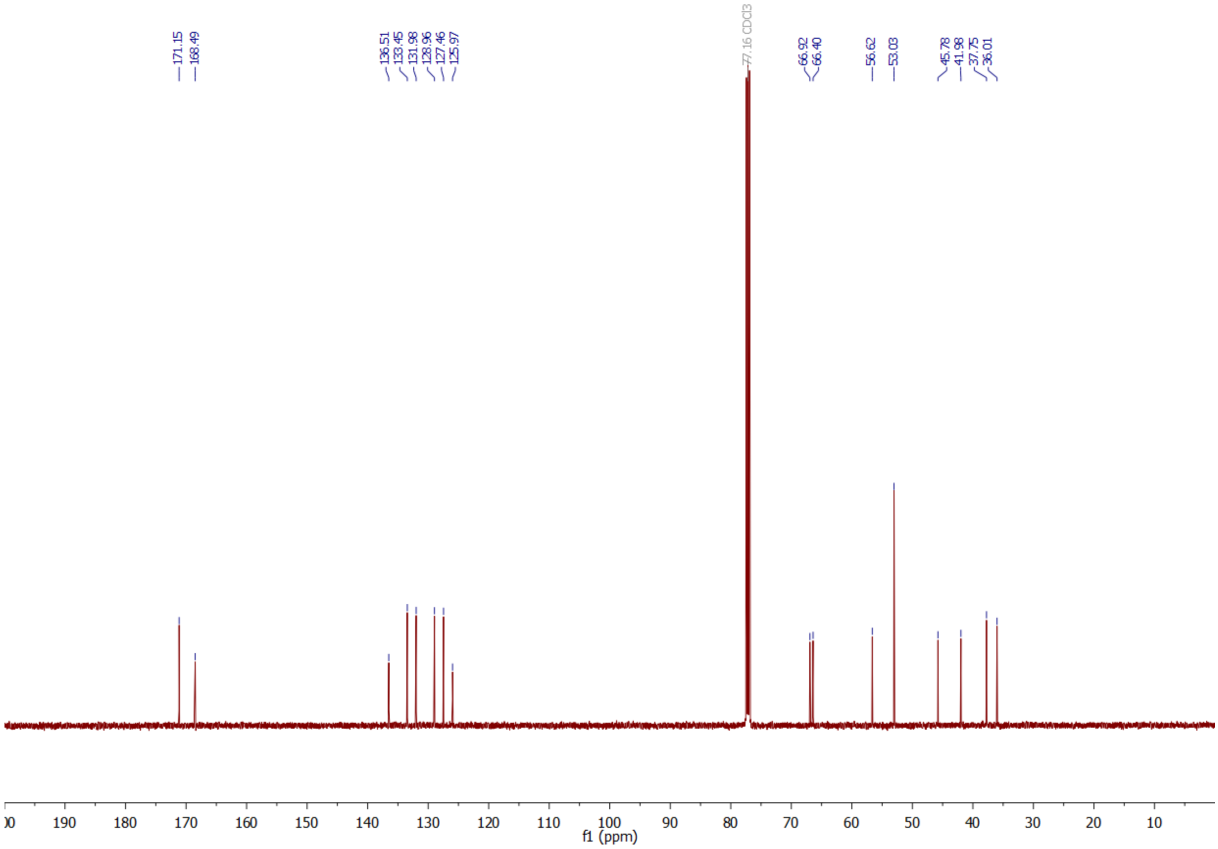
171.15
168.49
136.51
133.45
131.98
128.96
127.46
125.97
77.16 CDCl3
66.92
66.40
56.62
53.03
45.78
41.98
37.75
36.01
190
180
170
160
150
140
130
120
110
100
90
80
70
60
50
40
30
20
10
f1 (ppm)

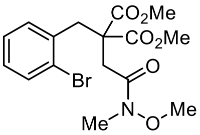
CO2Me
CO2Me
Br
O
N
Me
O
Me

2.44v

$C_{16}H_{20}BrNO_6$

M= 402,24 g.mol^{-1}

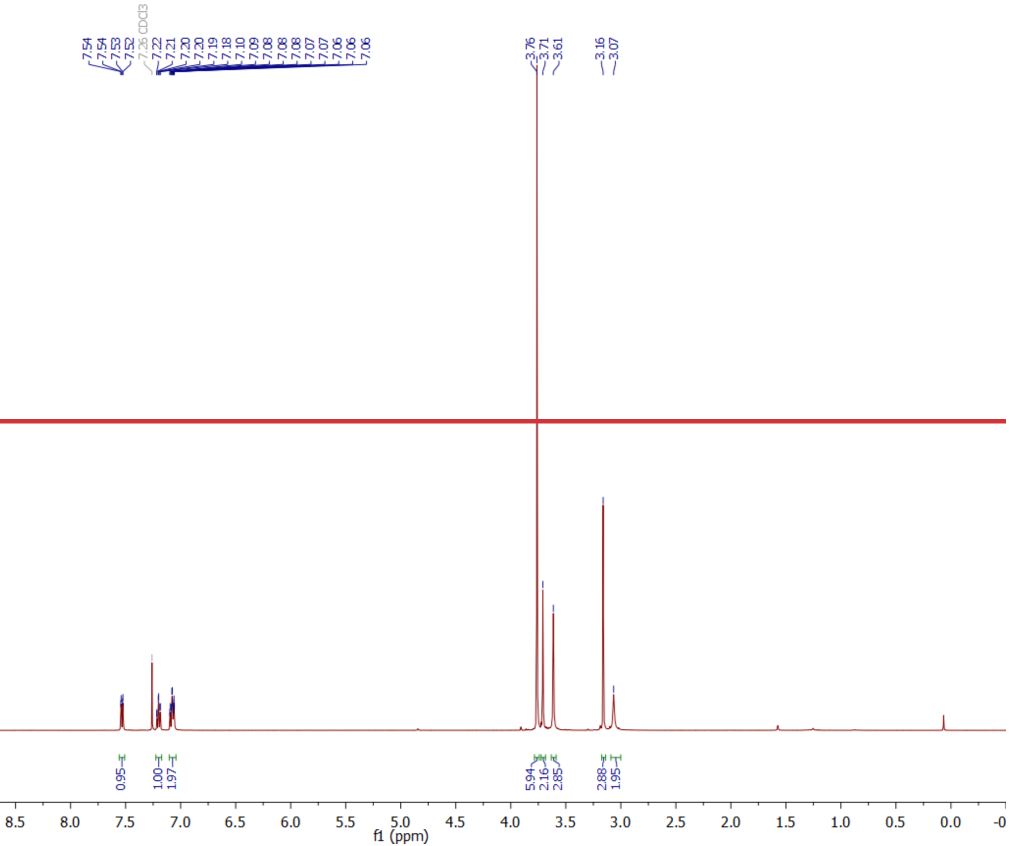

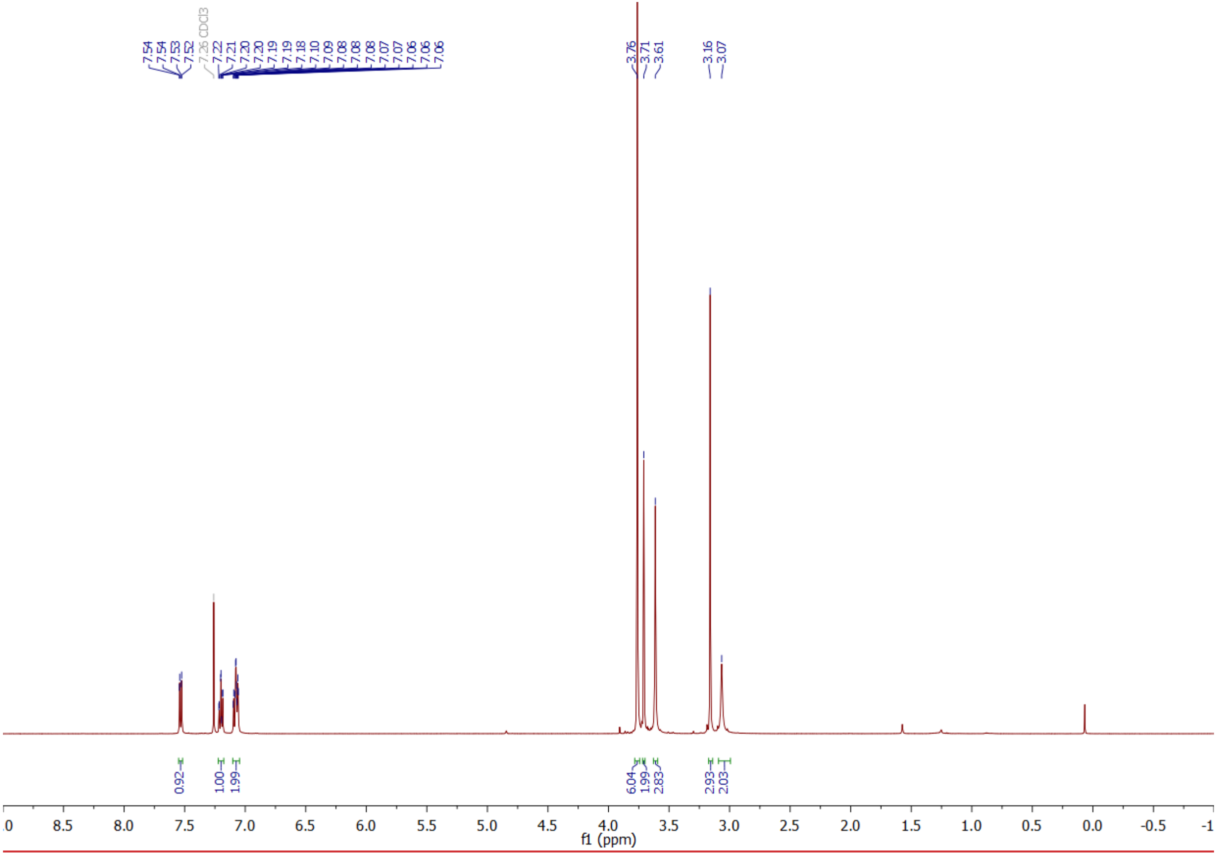

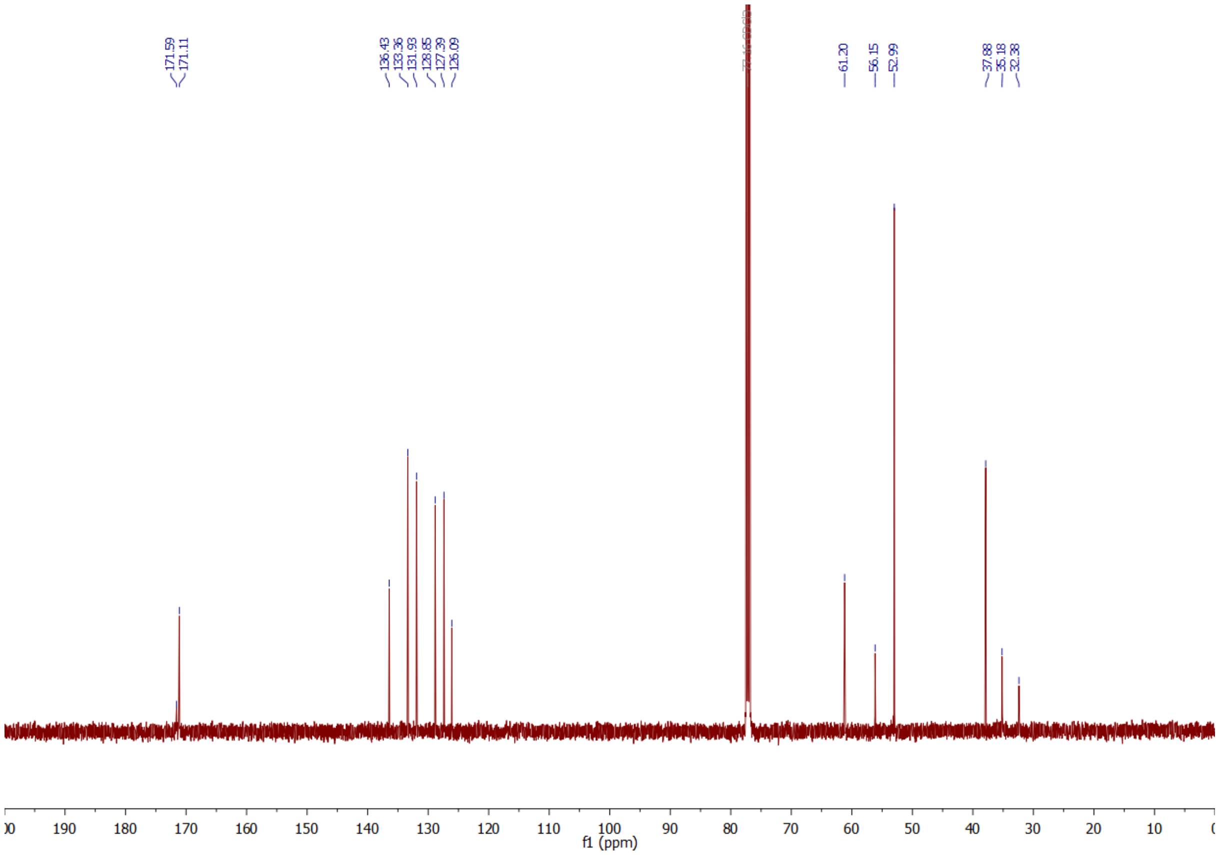
171.59
171.11
136.43
133.36
131.93
128.85
127.39
126.09
77.16 cdcl3
61.20
56.15
52.99
37.88
35.18
32.38
190
180
170
160
150
140
130
120
110
100
90
80
70
60
50
40
30
20
10
f1 (ppm)

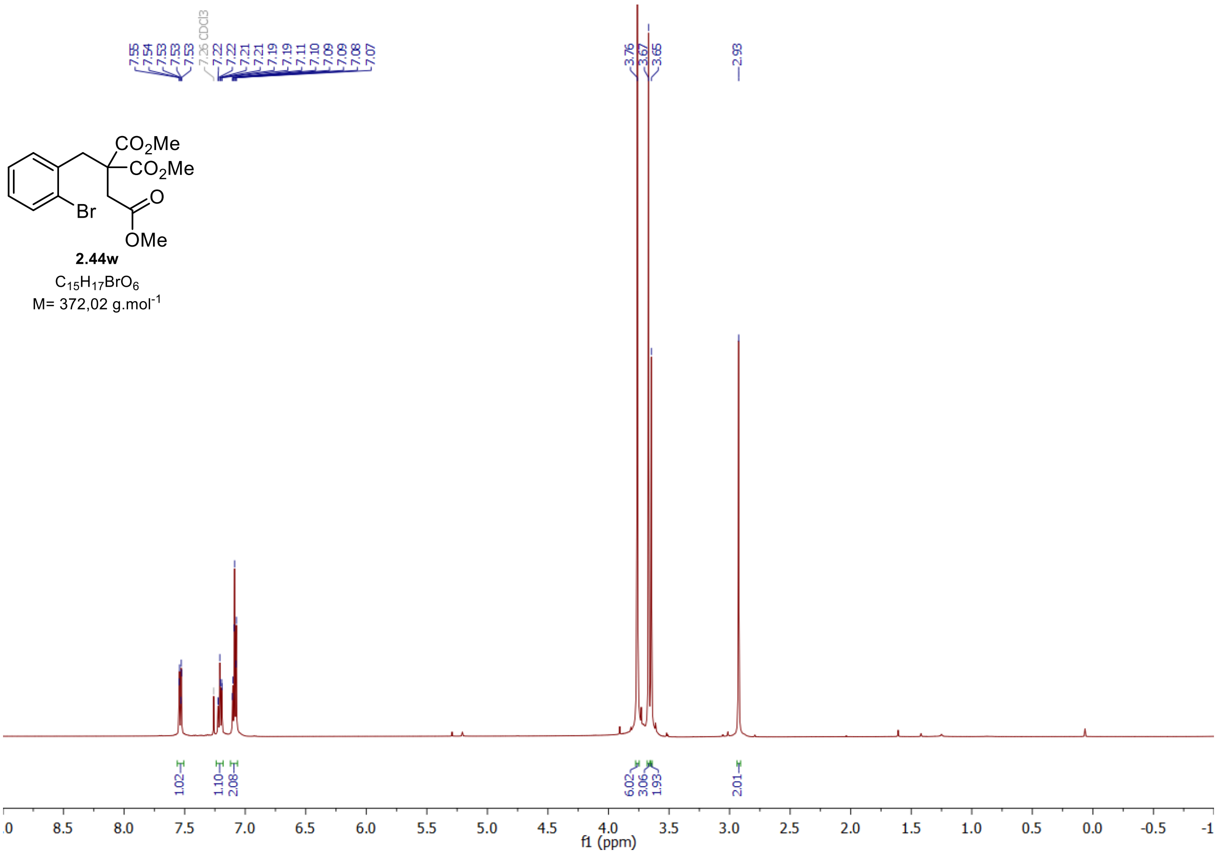

2.44w

$C_{15}H_{17}BrO_6$

M= 372,02 g.mol^{-1}

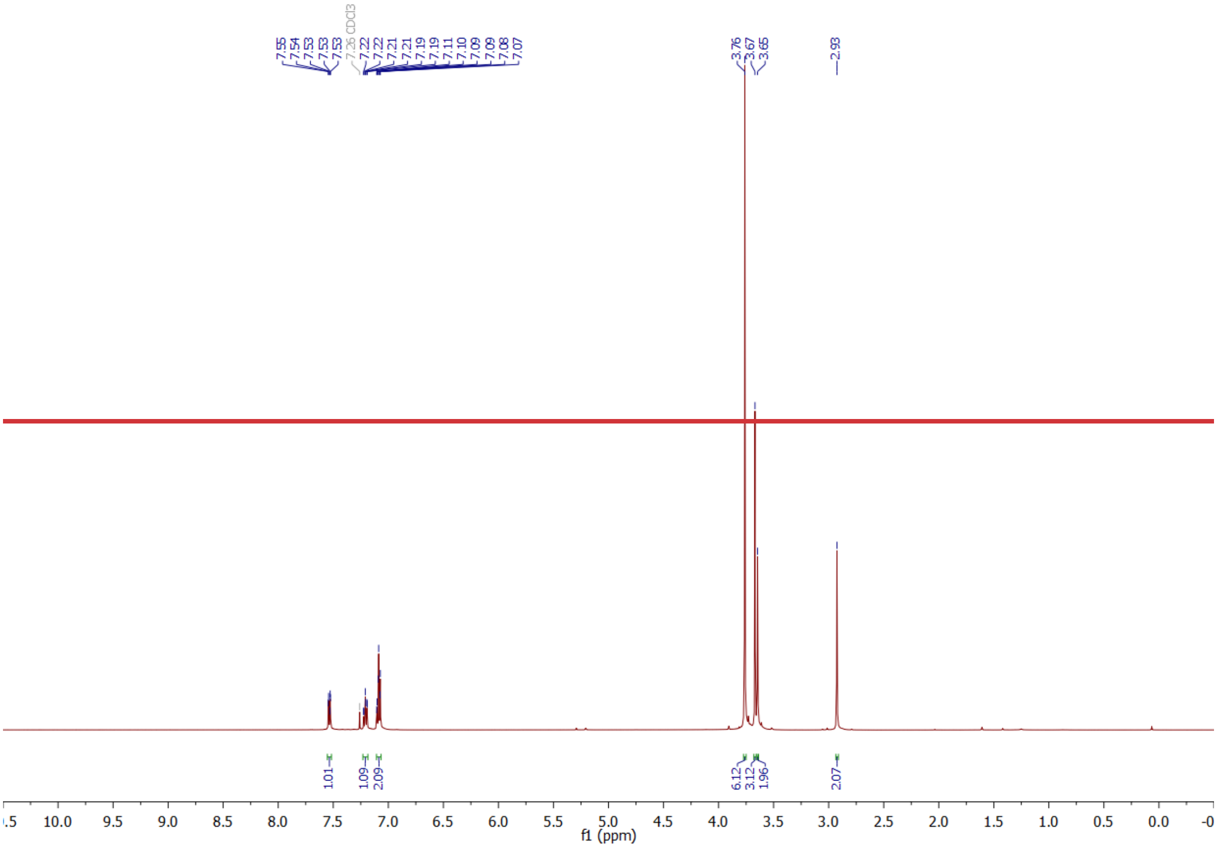

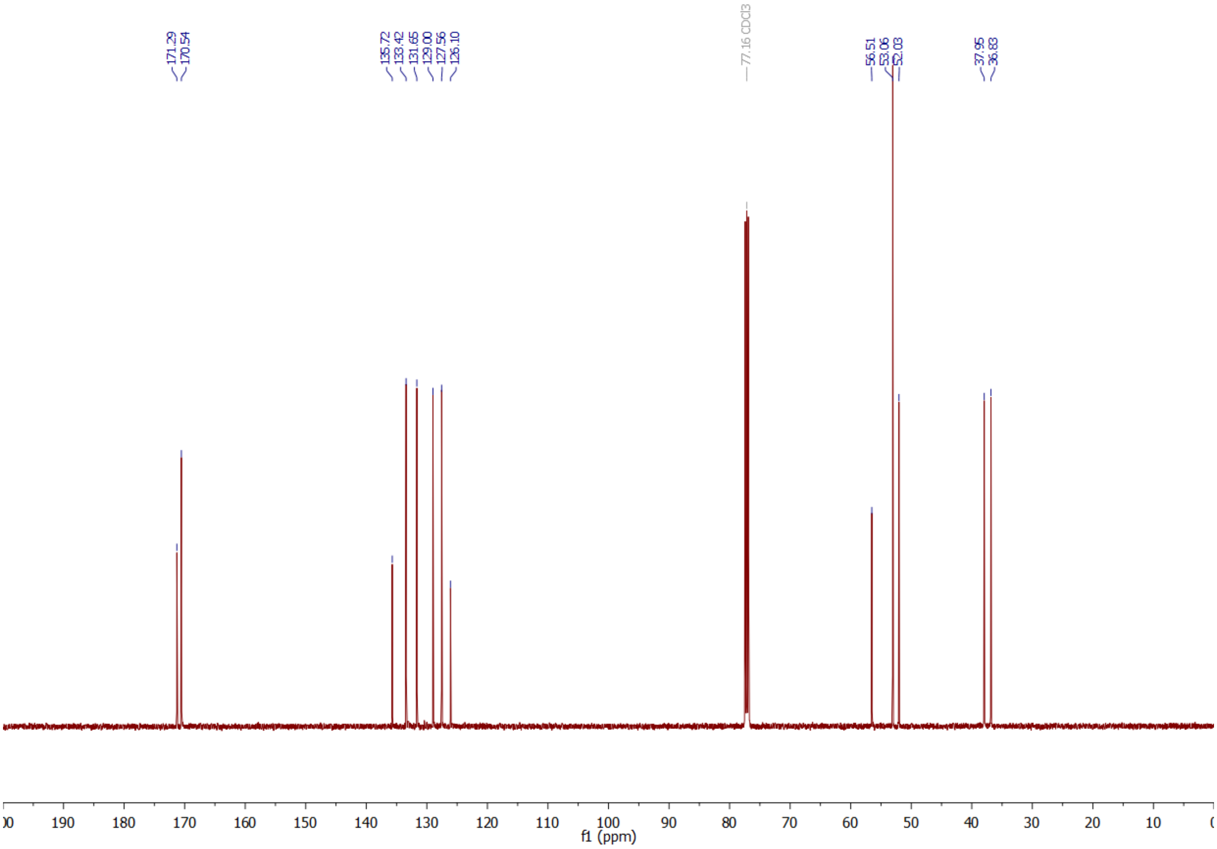
171.29
170.54
135.72
133.42
131.65
129.00
127.56
126.10
77.16 CDCl3
56.51
53.06
52.03
37.95
36.83
190
180
170
160
150
140
130
120
110
100
90
80
70
60
50
40
30
20
10
f1 (ppm)

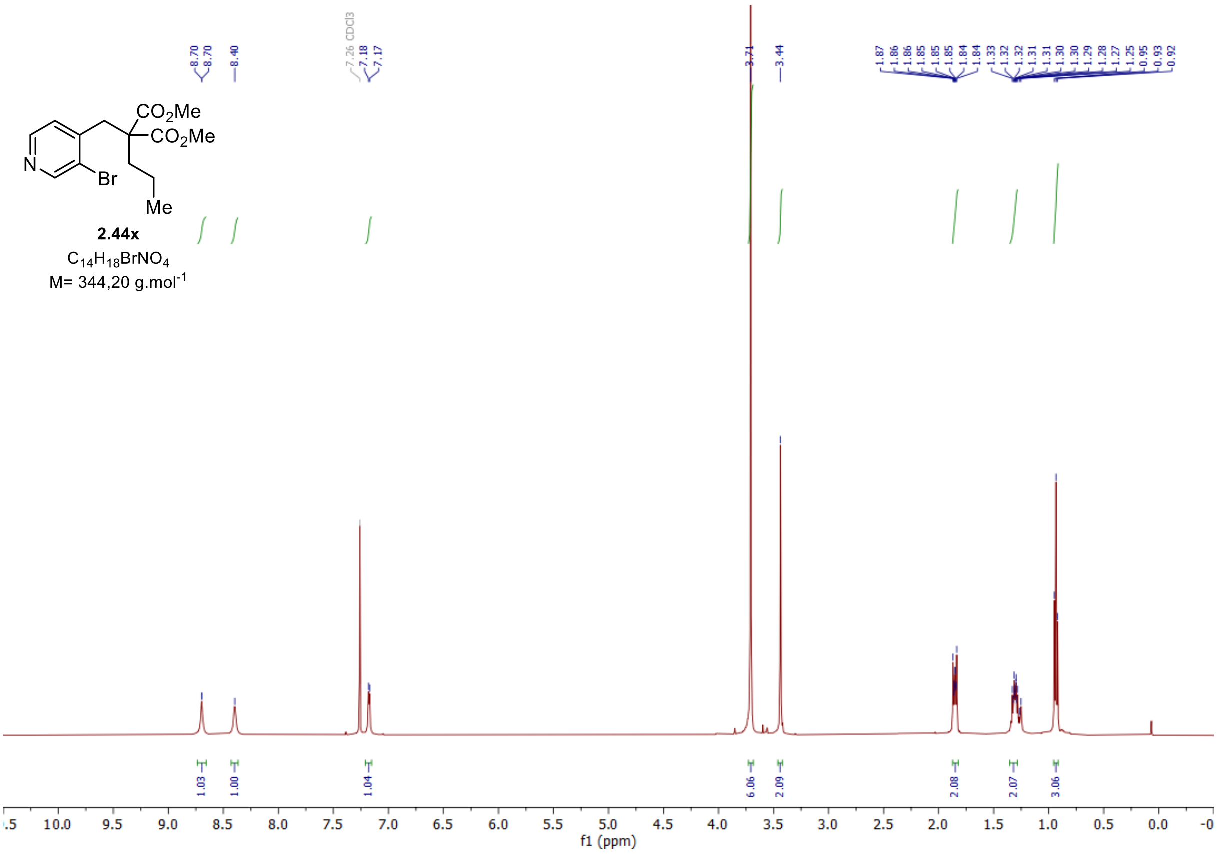

2.44x

$C_{14}H_{18}BrNO_4$

M= 344,20 g.mol^{-1}

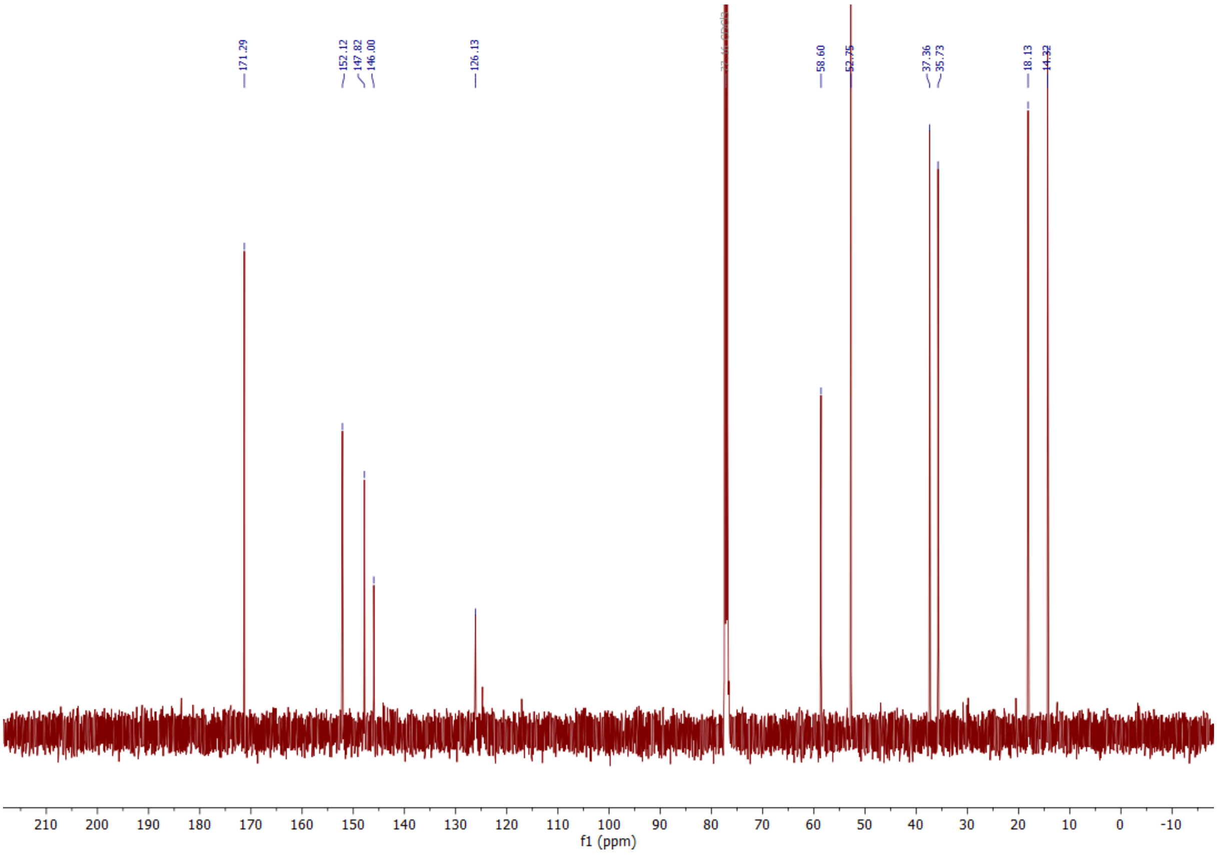

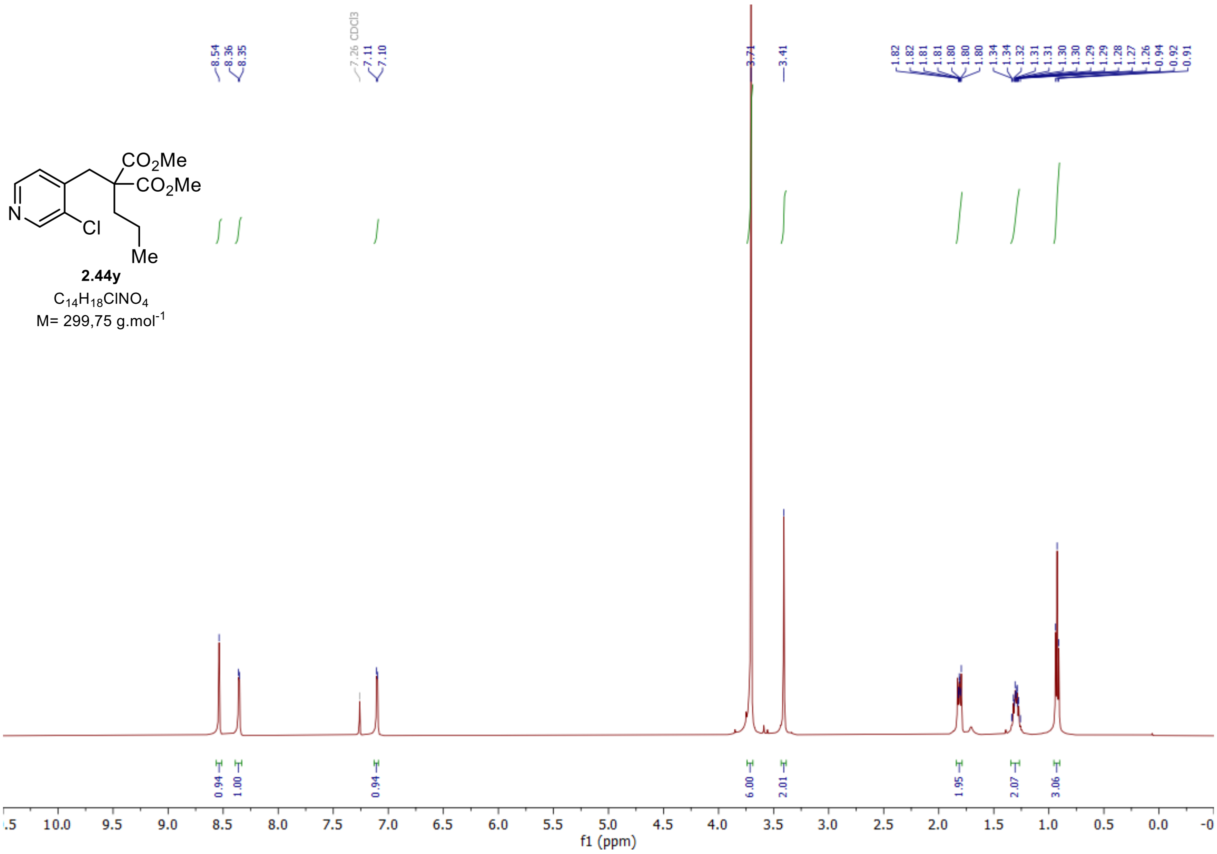

2.44y

$C_{14}H_{18}ClNO_4$

M= 299,75 g.mol^{-1}

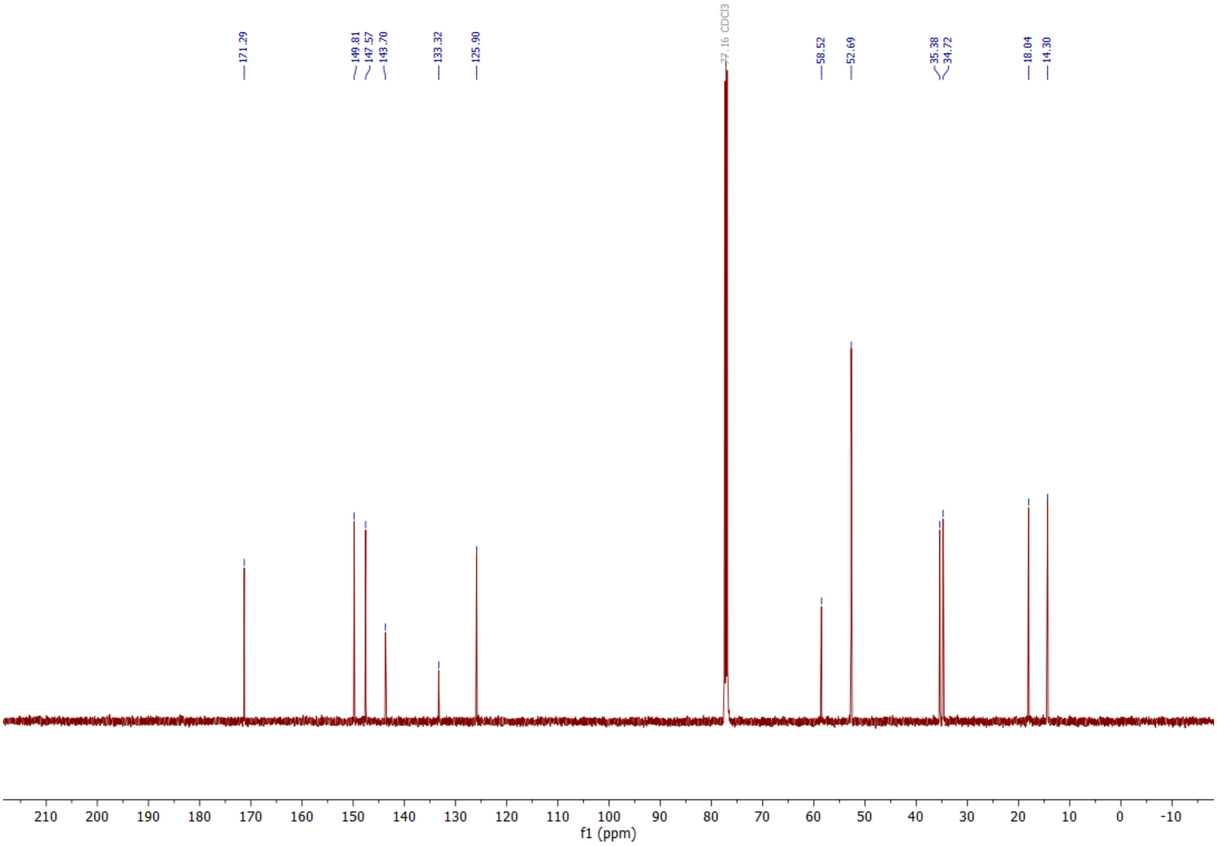

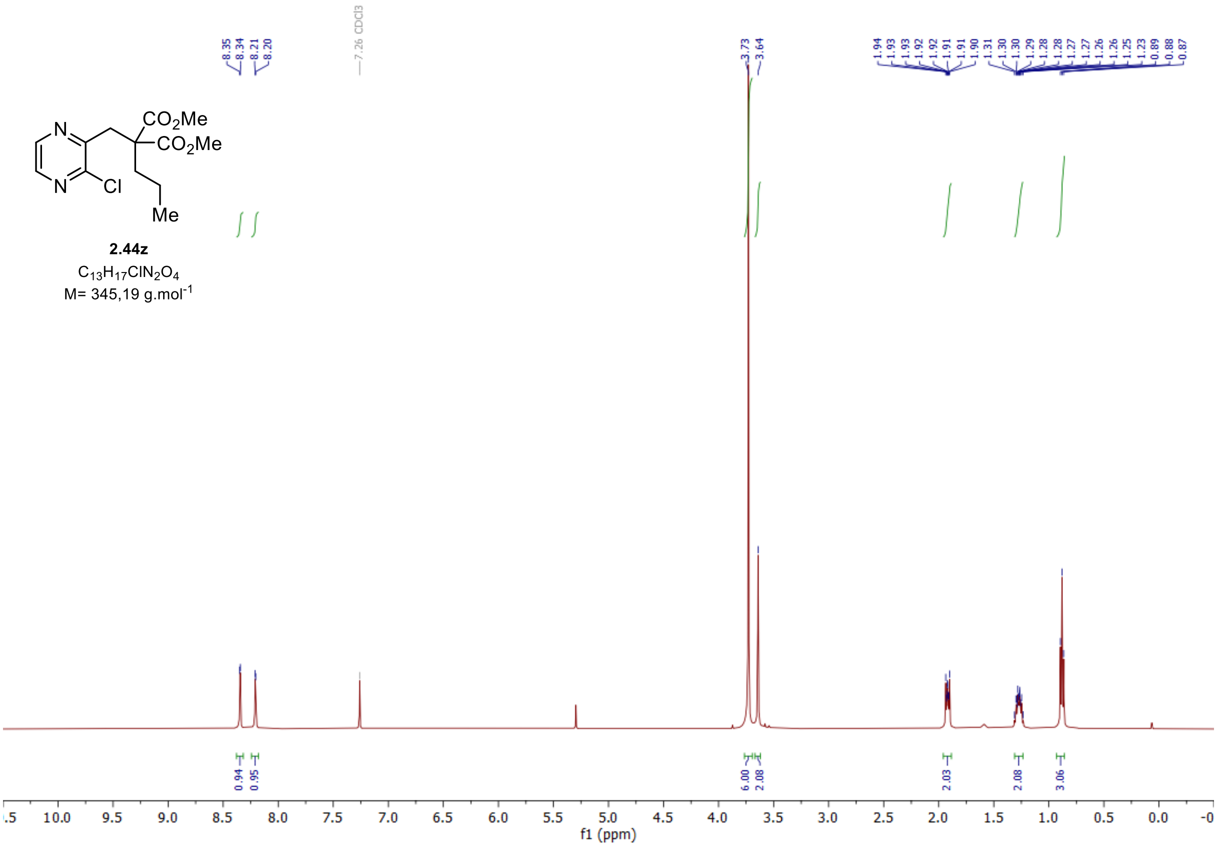

2.44z

$C_{13}H_{17}ClN_2O_4$

M= 345,19 g.mol^{-1}

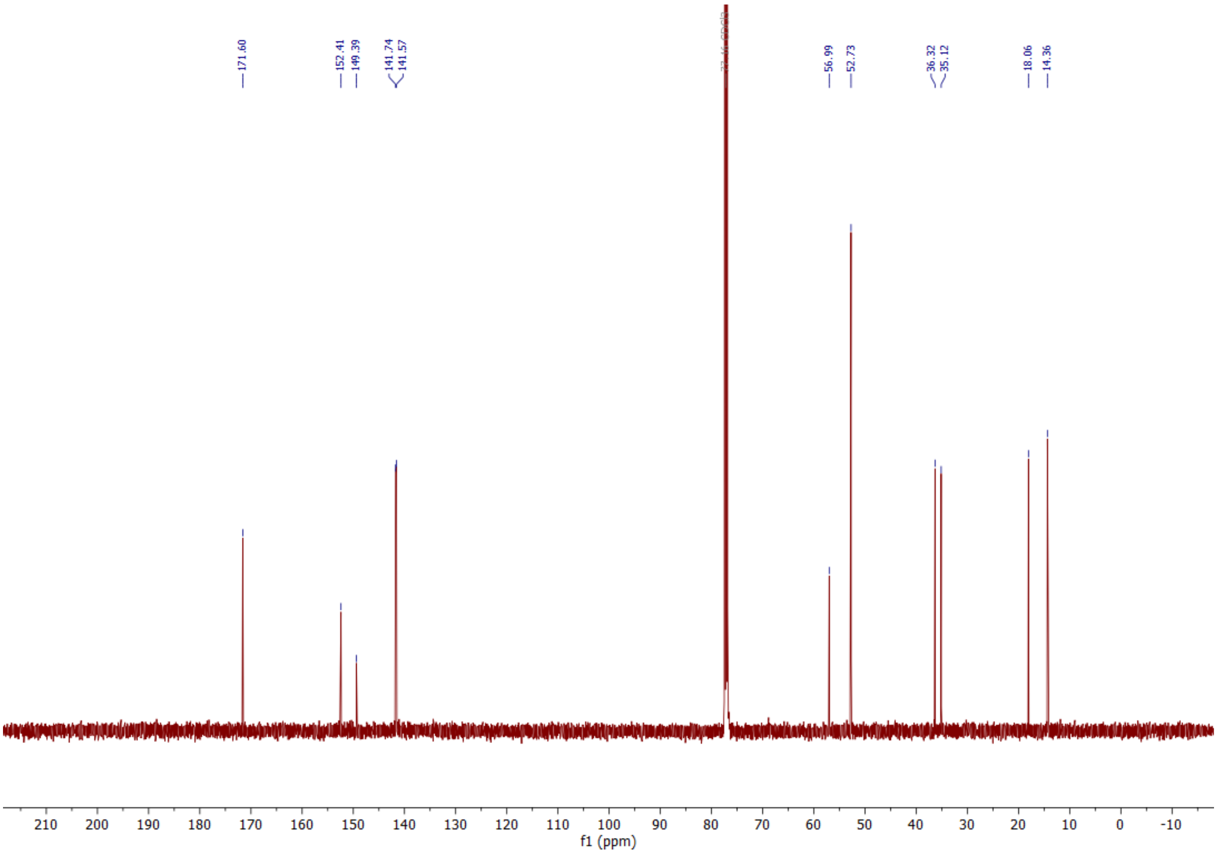

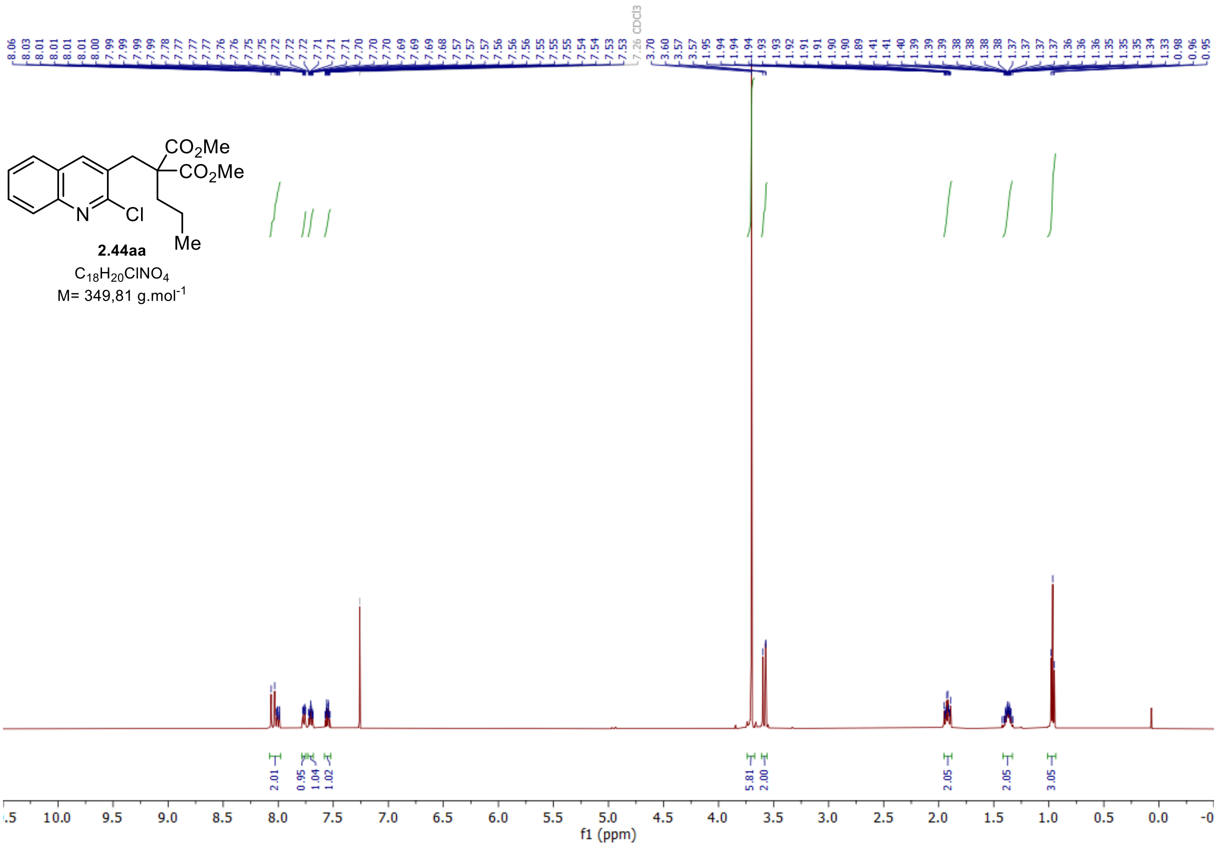

2.44aa

$C_{18}H_{20}ClNO_4$

M= 349,81 g.mol^{-1}

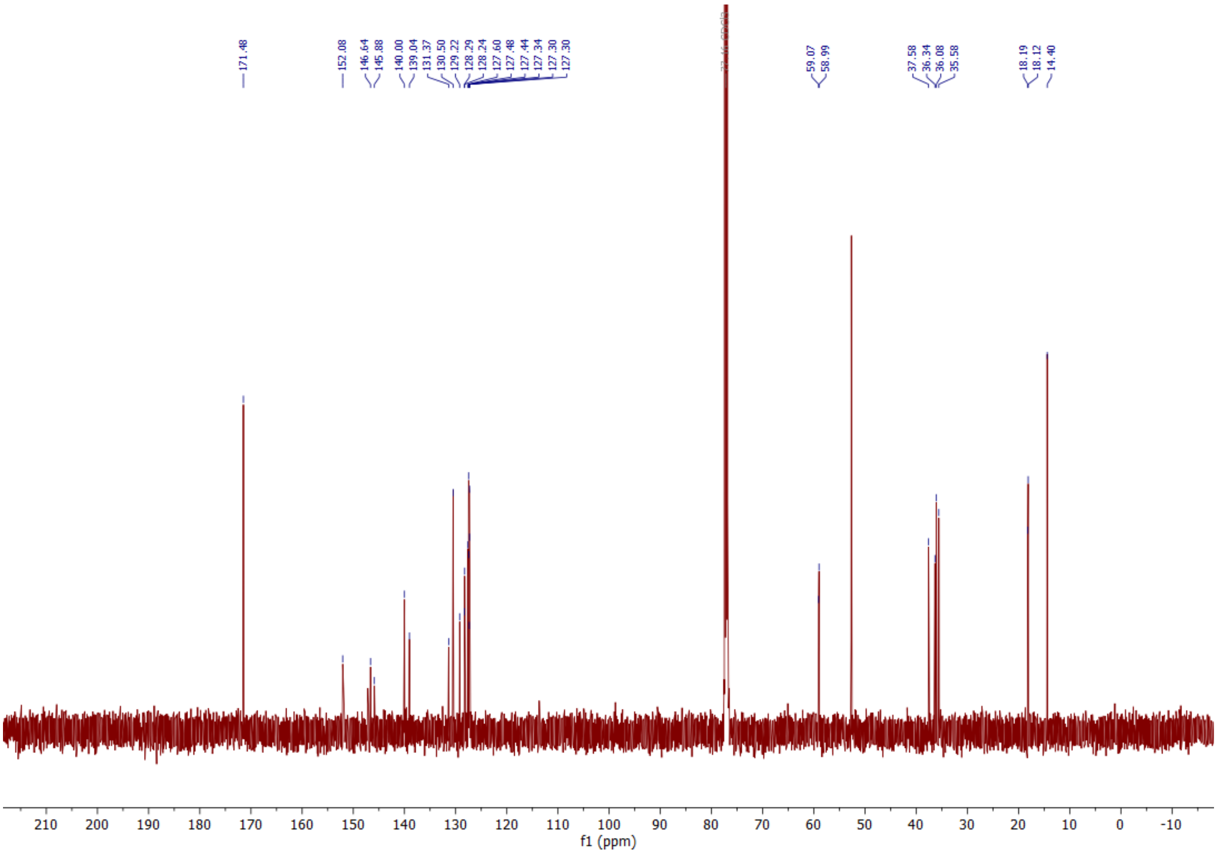

MeO2C
CO2Me
S
Br
Me

2.44ab

$C_{13}H_{17}BRO_4S$

M= 349,24 g.mol^{-1}

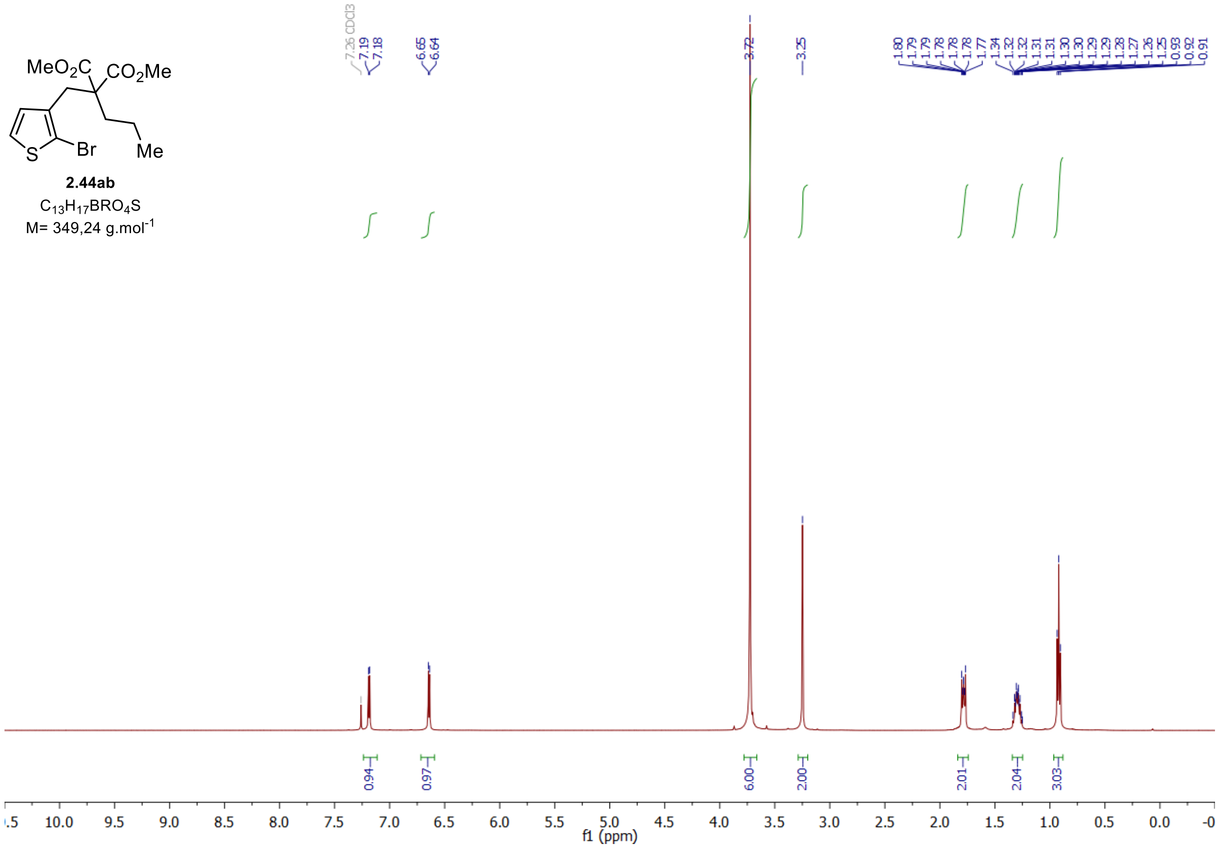

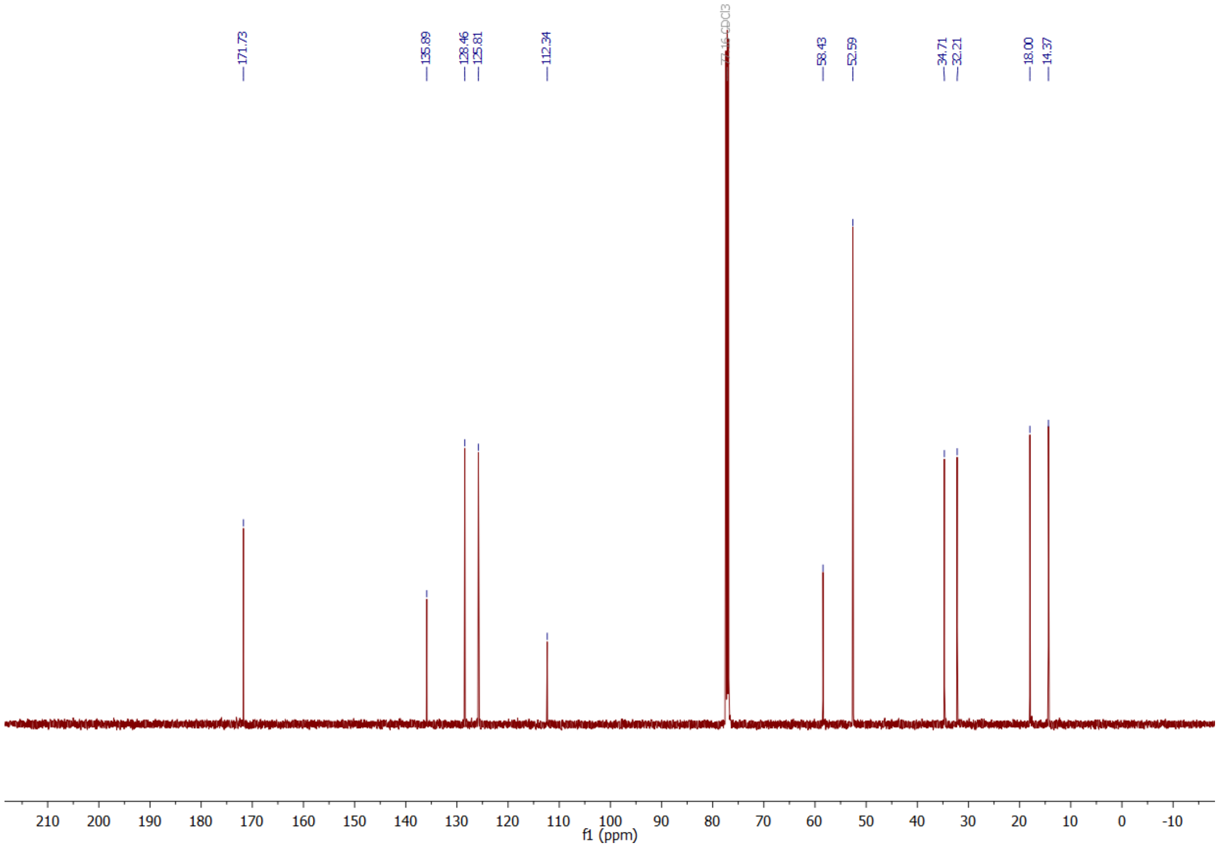

2.44ac

$C_{13}H_{17}ClO_4S$

M= 304,79 g.mol^{-1}

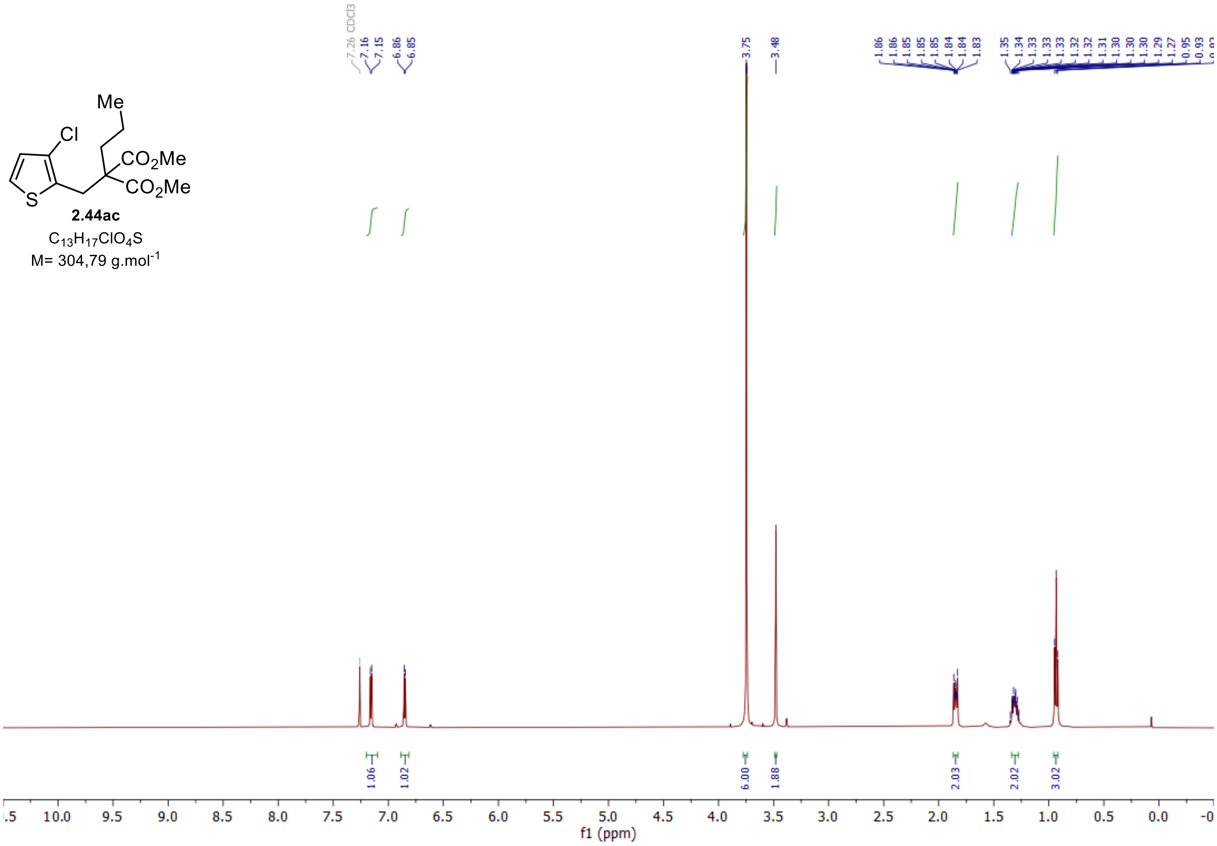

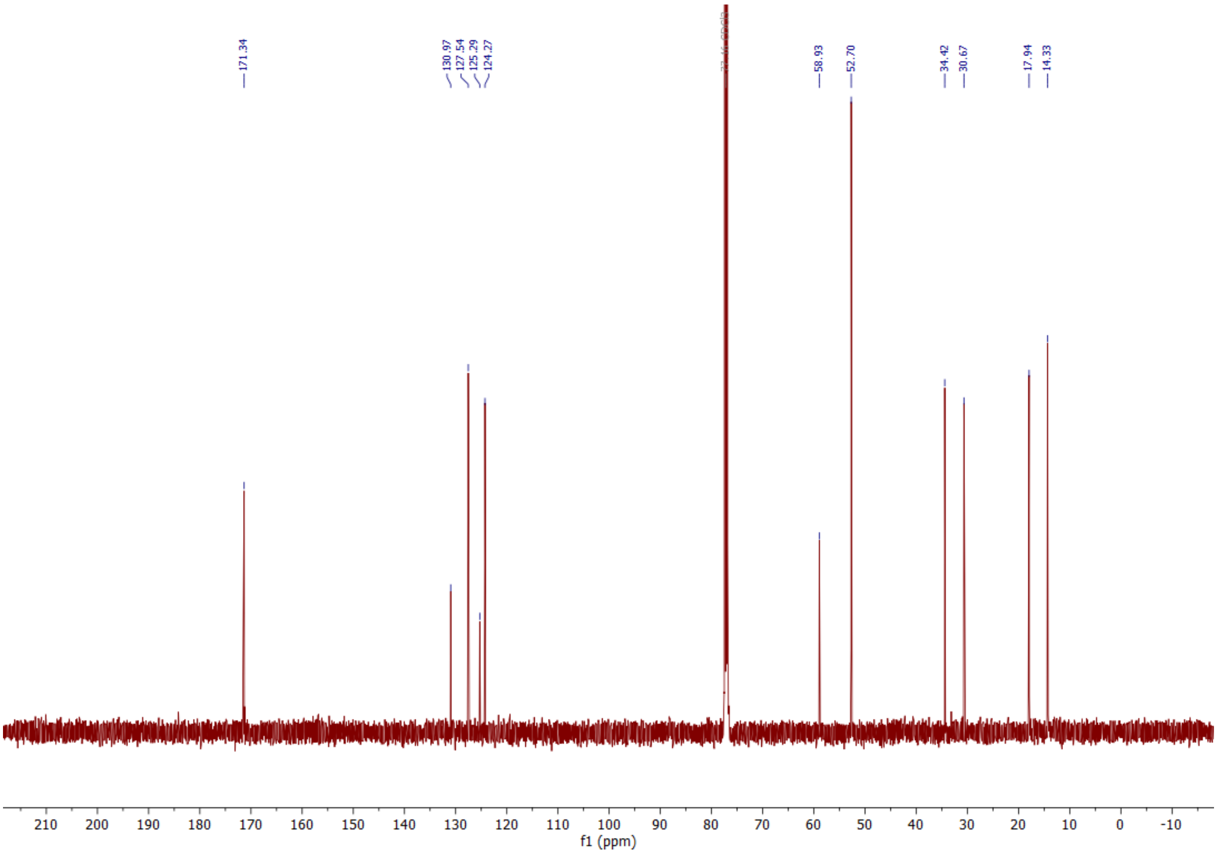

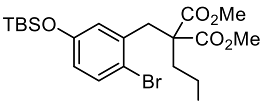
TBSO
CO2Me
CO2Me
Br
Me

2.44ad

$C_{21}H_{33}BrO_5Si$

M= 473,48 g.mol^{-1}

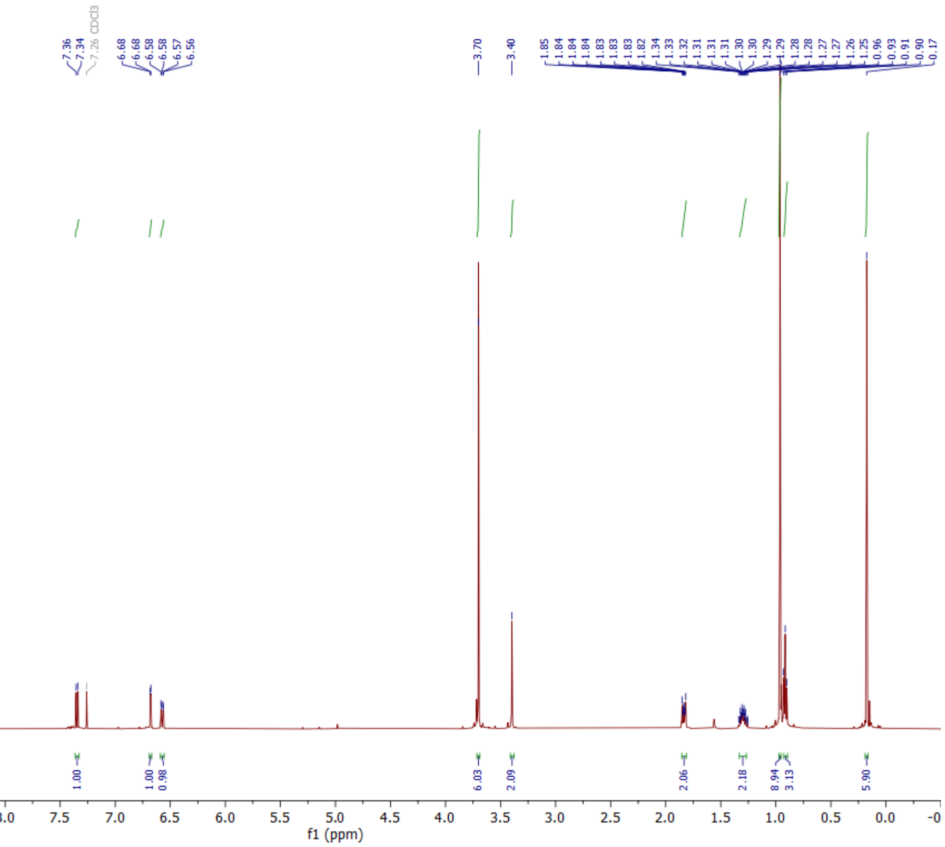

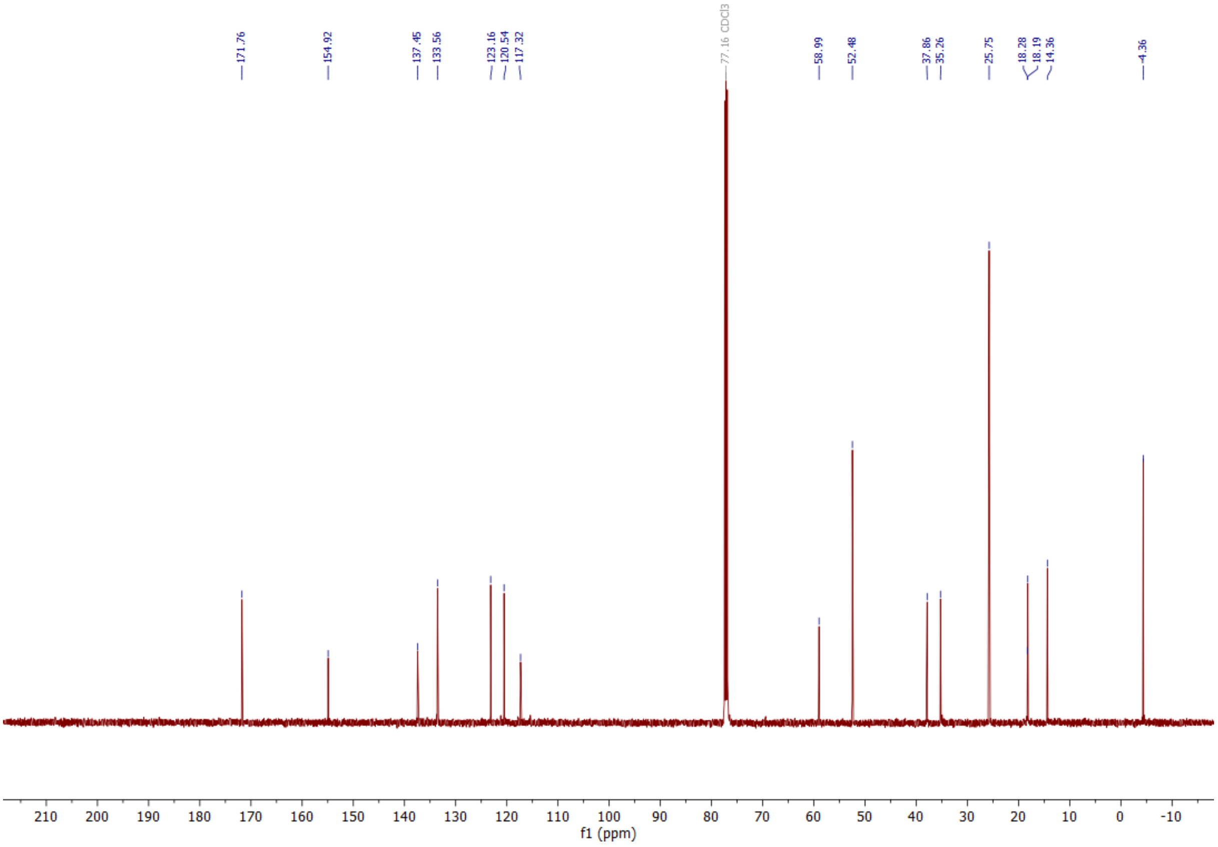

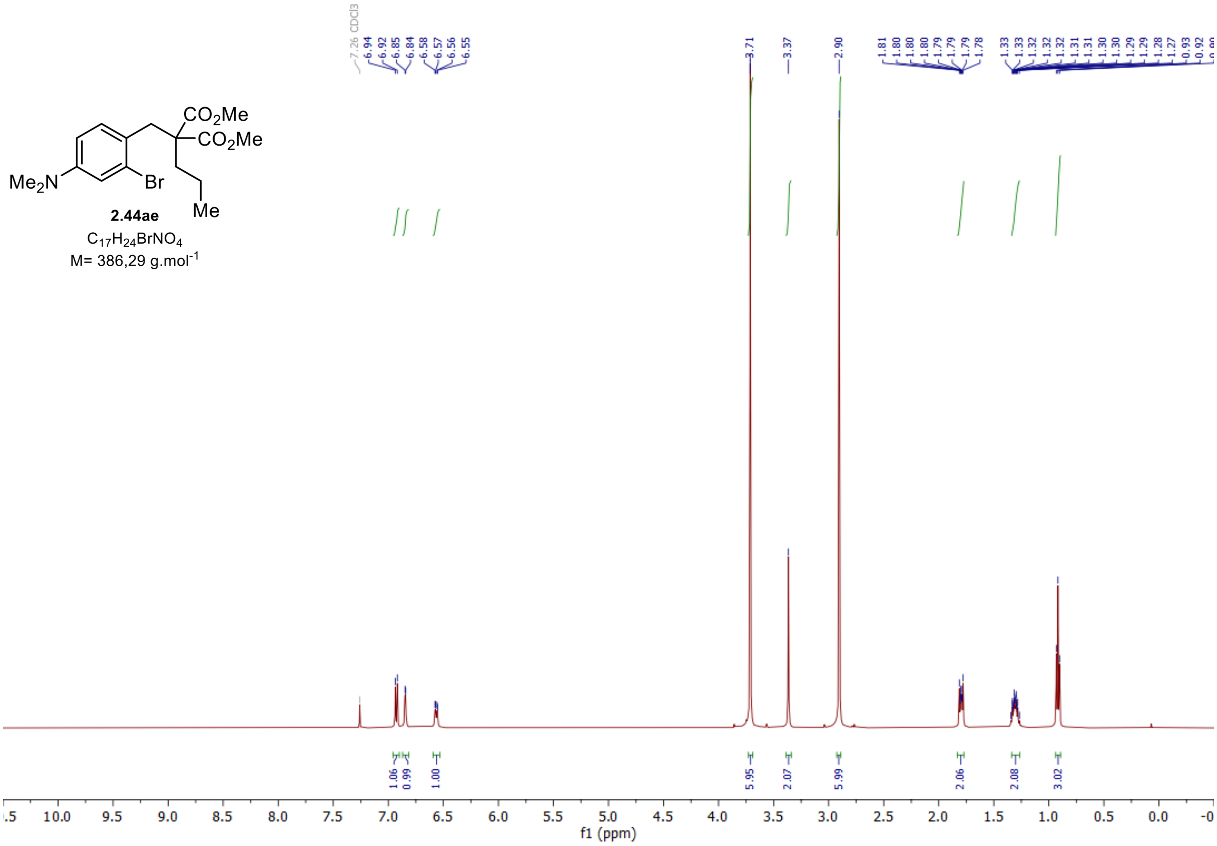

2.44ae

$C_{17}H_{24}BrNO_4$

M= 386,29 g.mol^{-1}

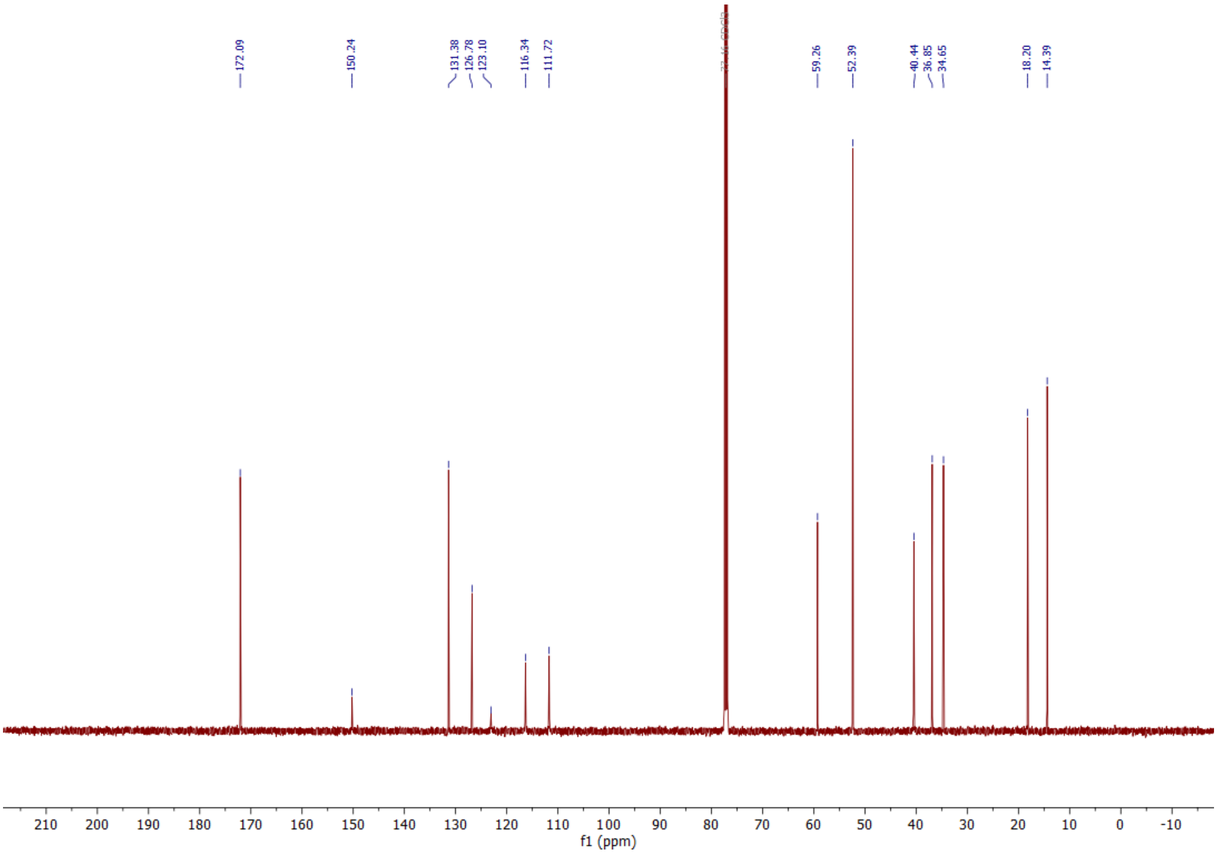

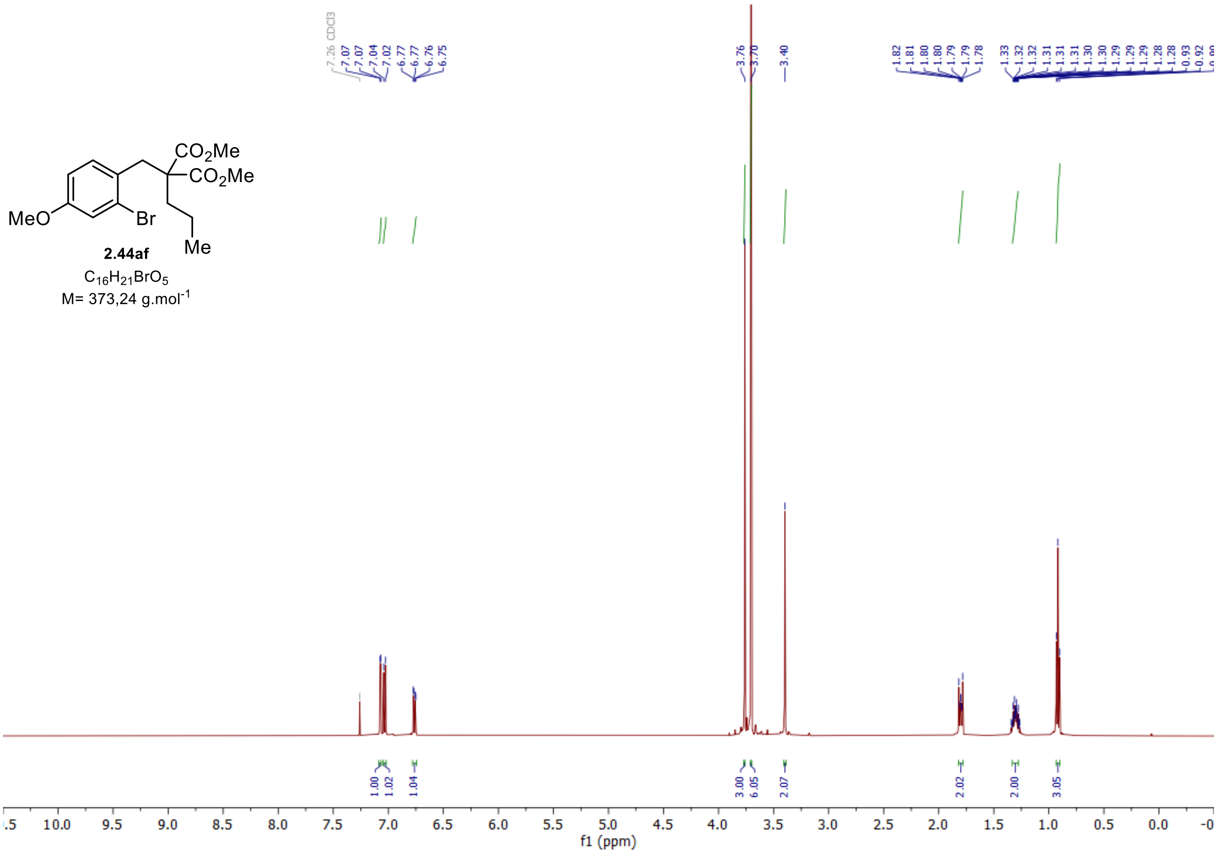

2.44af

$C_{16}H_{21}BrO_5$

M= 373,24 g.mol^{-1}

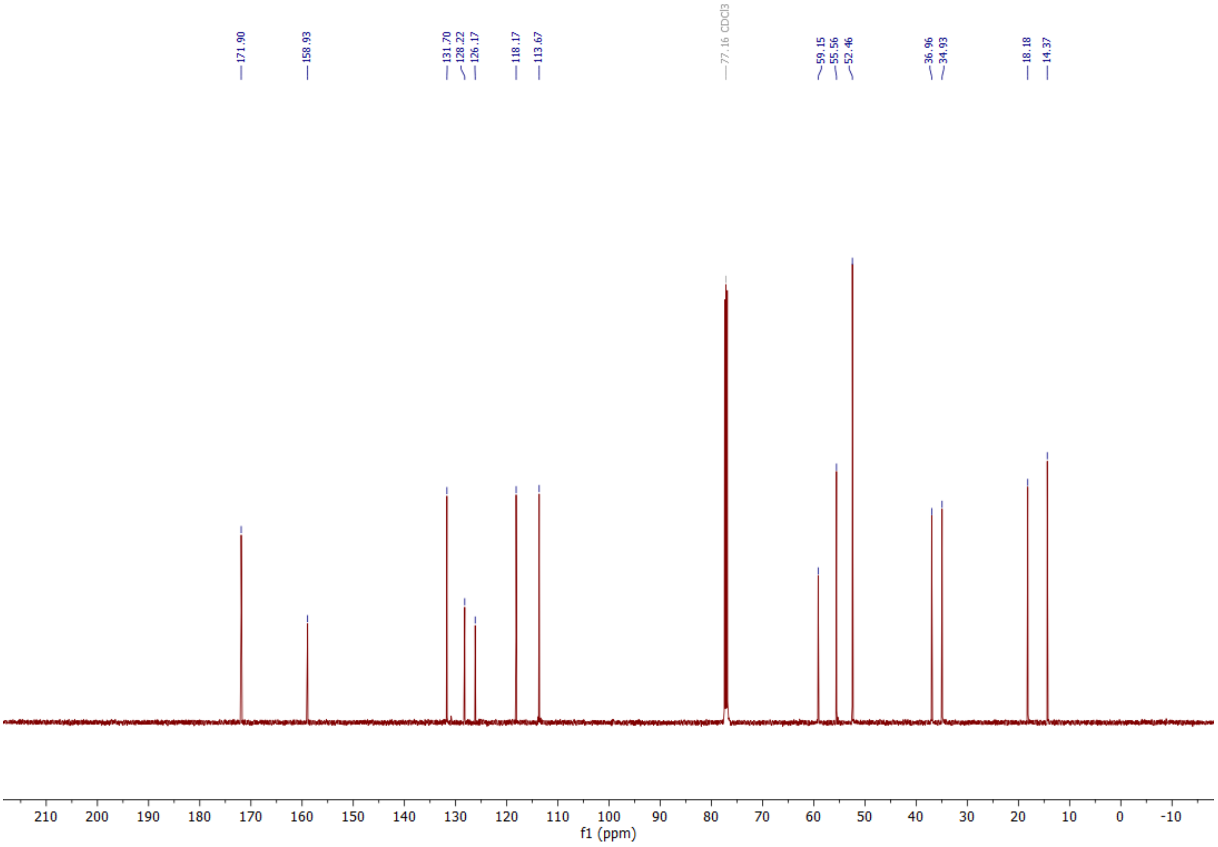

MeO
OMe
Br
Me

2.44a4

$C_{15}H_{23}BrO_2$

M= 315,25 g.mol^{-1}

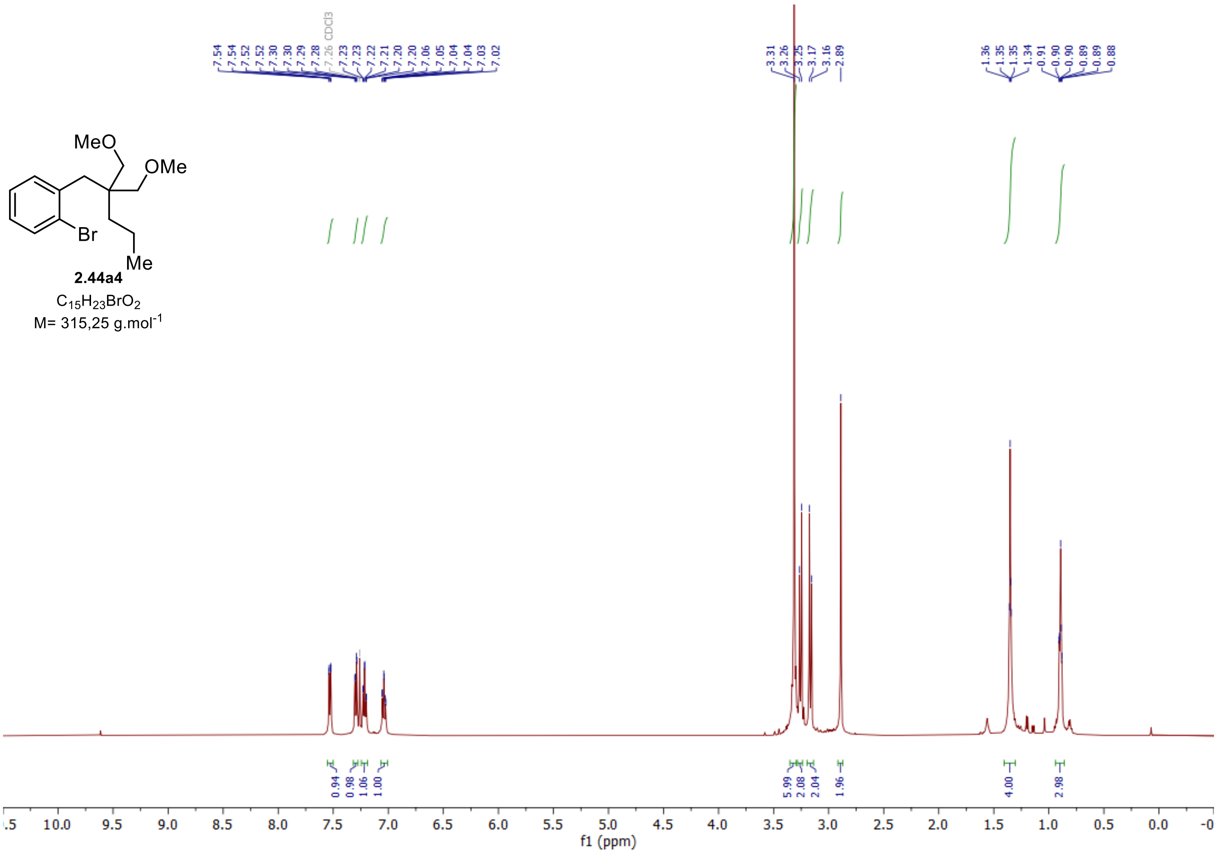

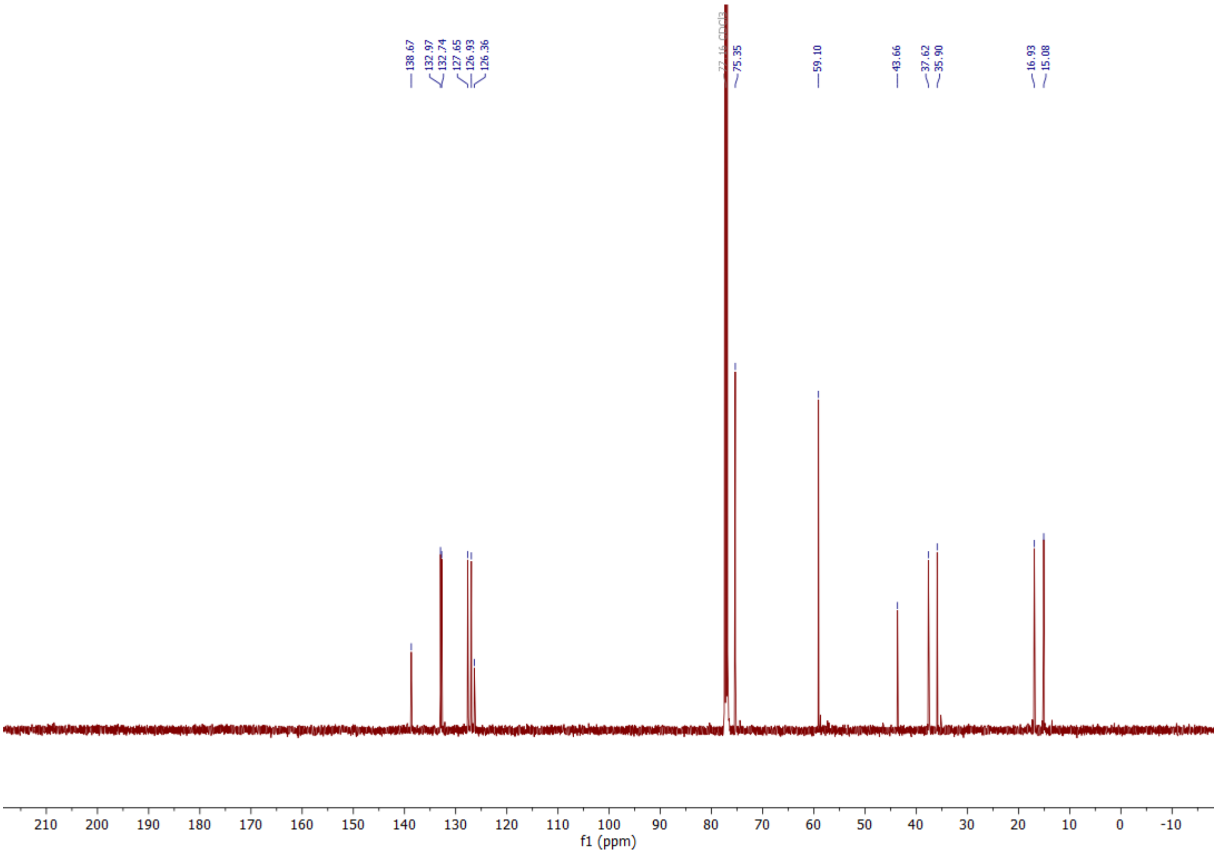

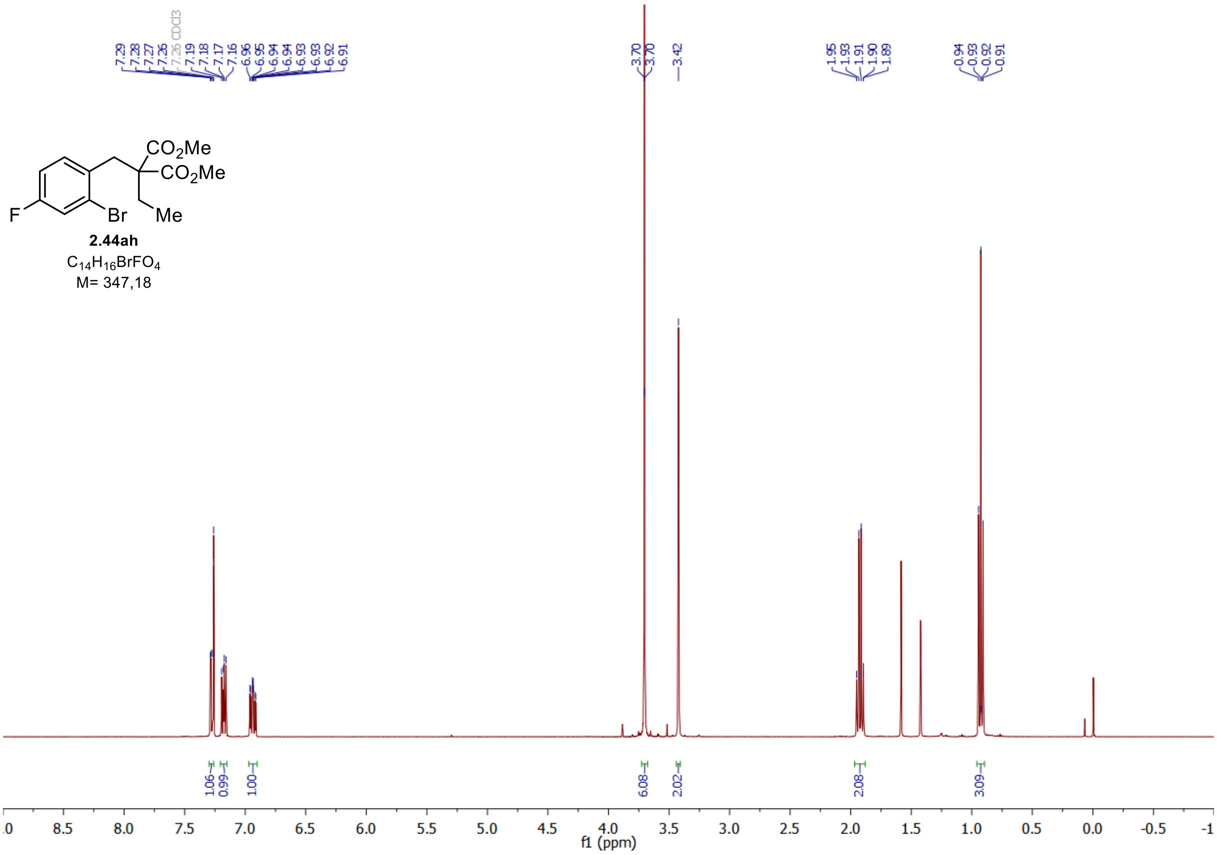

2.44ah

$C_{14}H_{16}BrFO_4$

M= 347,18

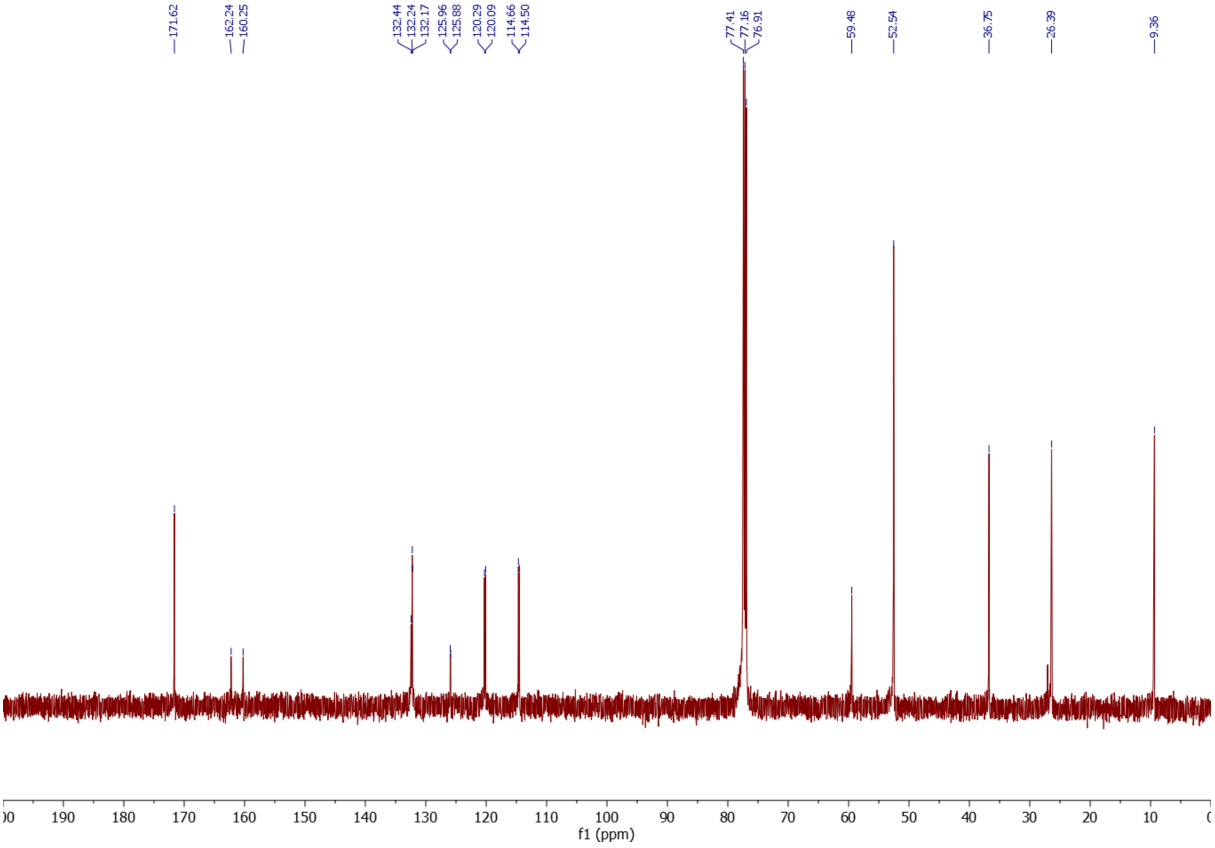

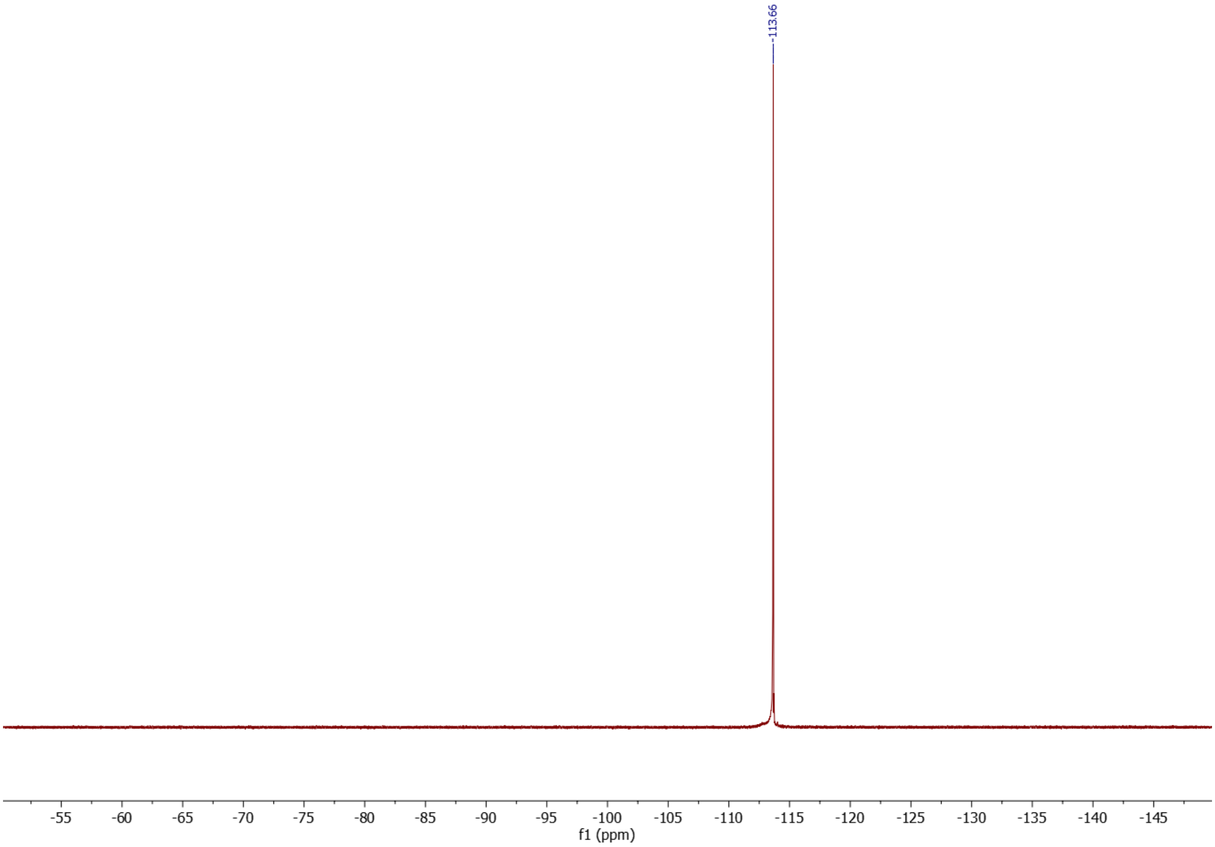
-113.66
-55
-60
-65
-70
-75
-80
-85
-90
-95
-100
-105
-110
-115
-120
-125
-130
-135
-140
-145
f1 (ppm)

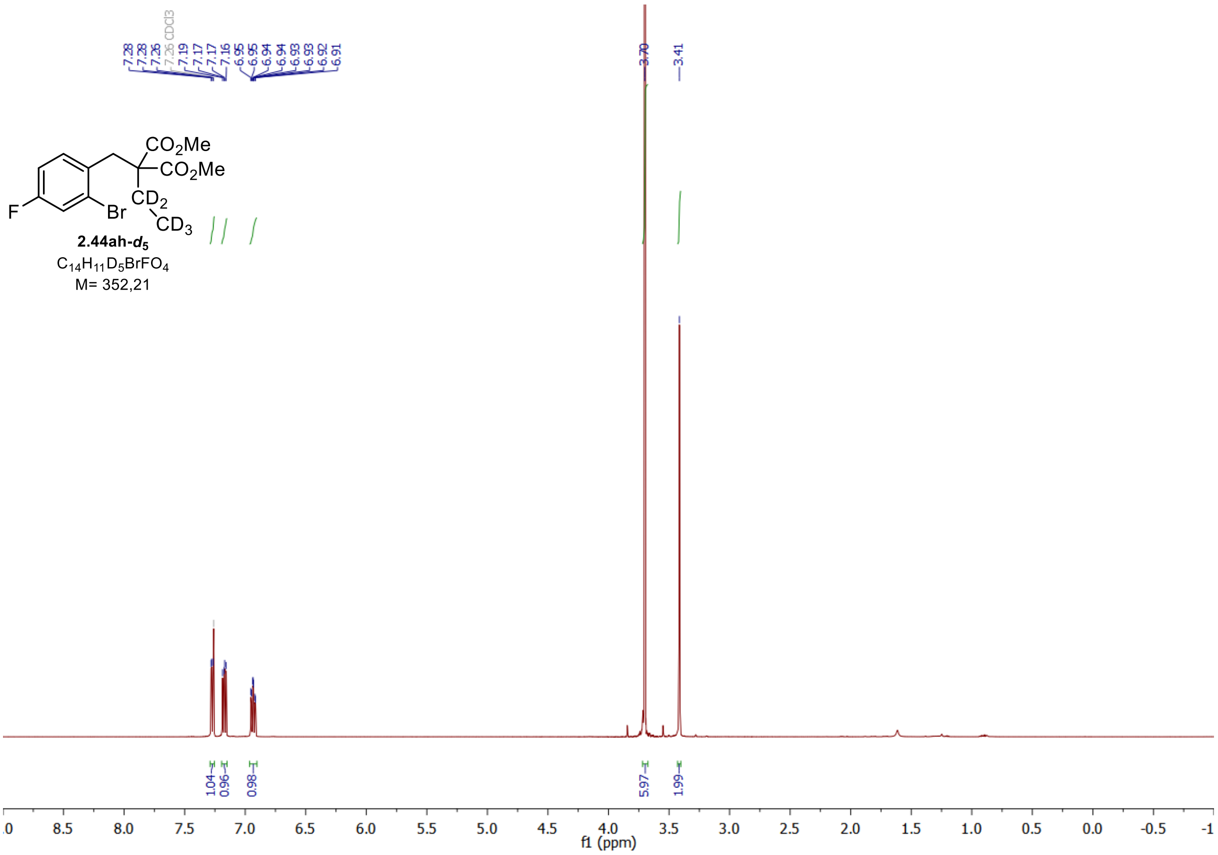

2.44ah-*d*$_5$

$C_{14}H_{11}D_5BrFO_4$

M= 352,21

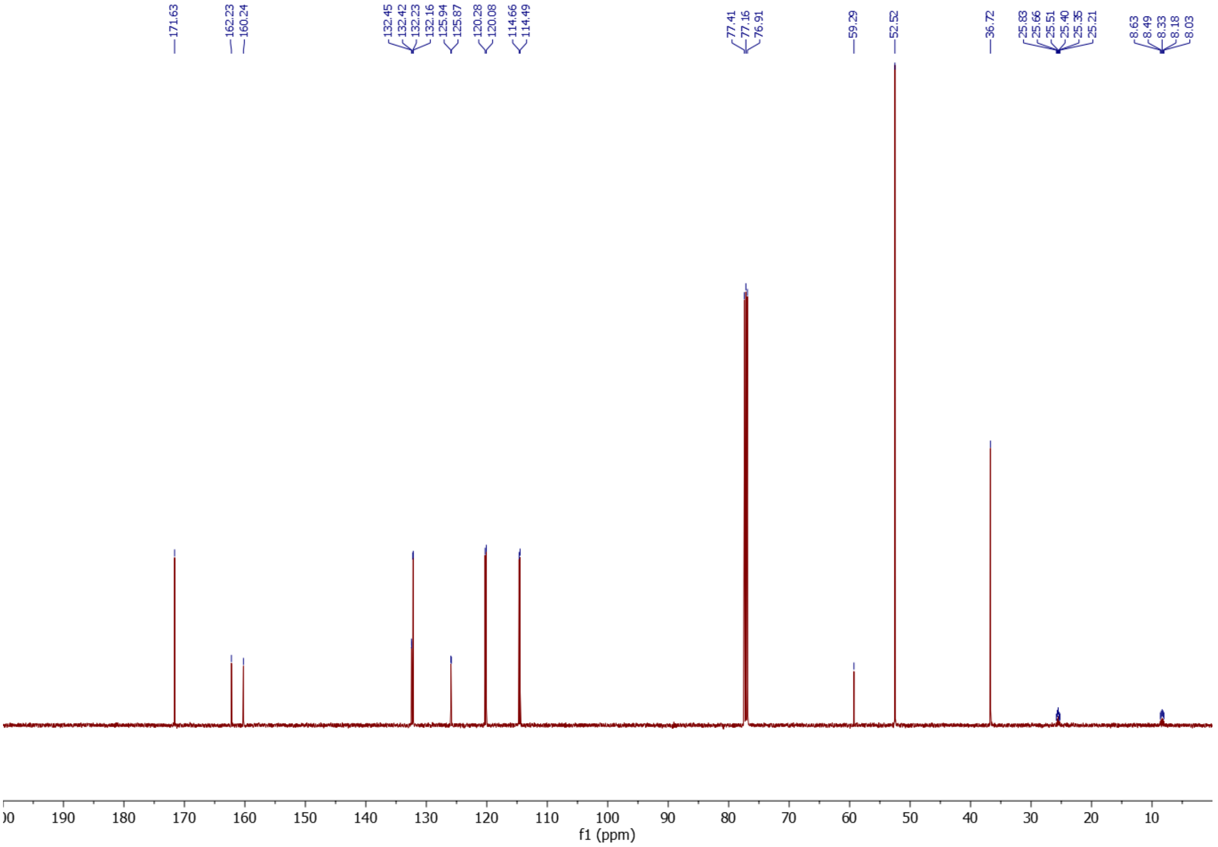

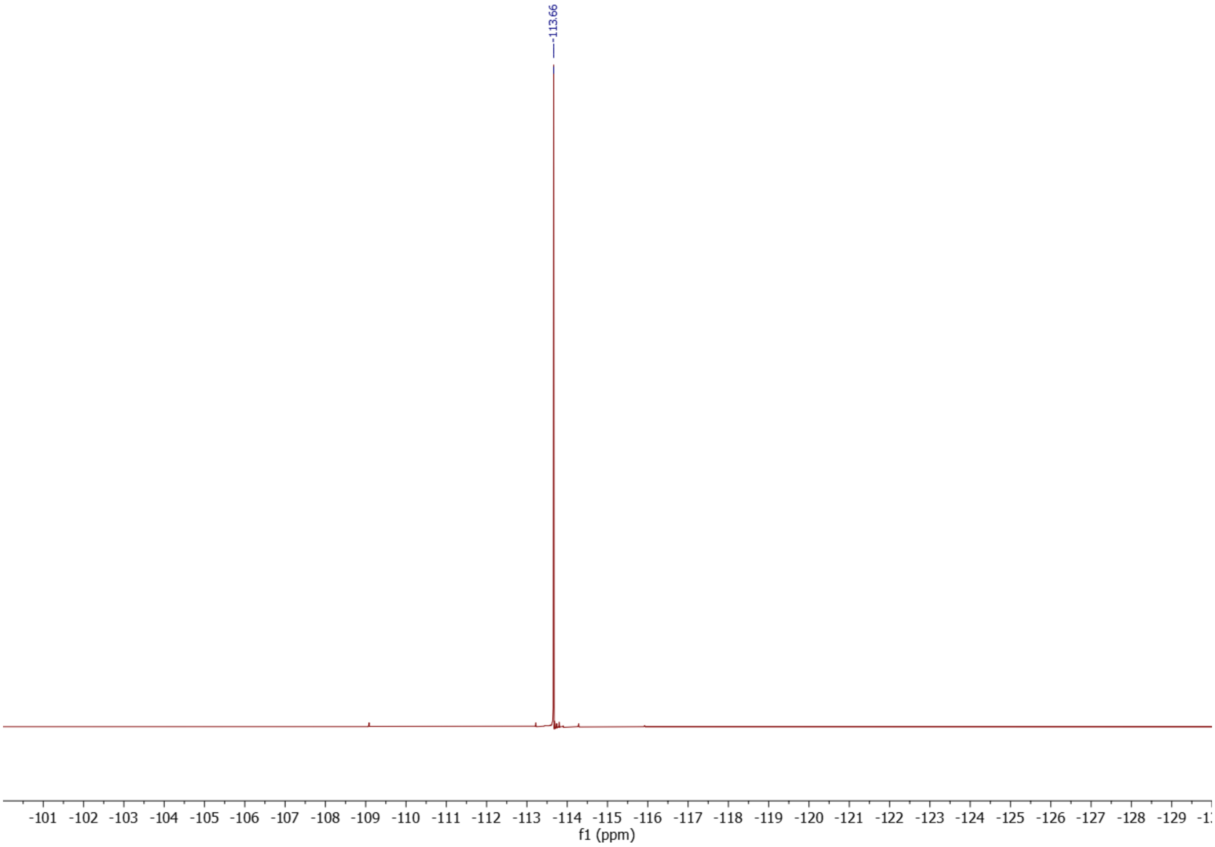
-113.66
-101 -102 -103 -104 -105 -106 -107 -108 -109 -110 -111 -112 -113 -114 -115 -116 -117 -118 -119 -120 -121 -122 -123 -124 -125 -126 -127 -128 -129
f1 (ppm)

O
O
CO2Me
CO2Me
Br
OBn

2.44ai

$C_{23}H_{25}BrO_7$

M= 493,35 g.mol^{-1}

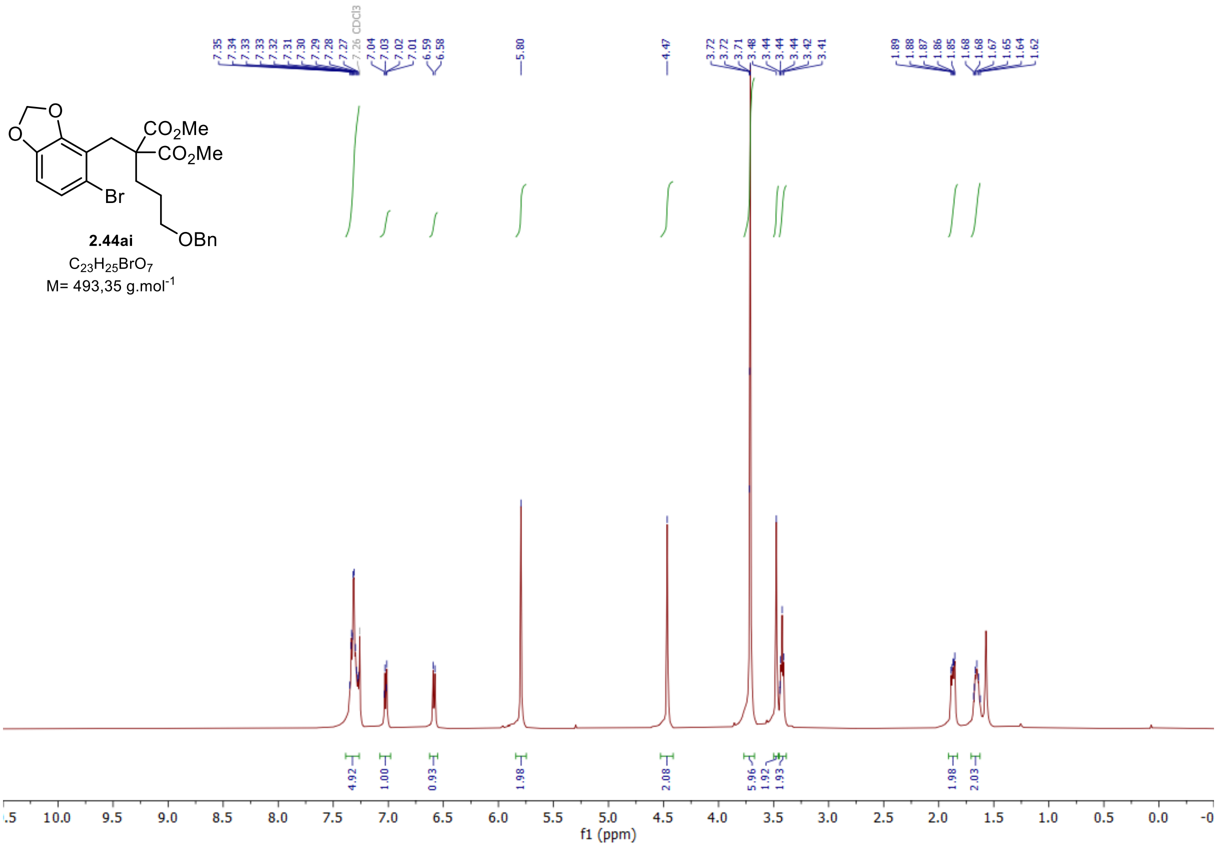

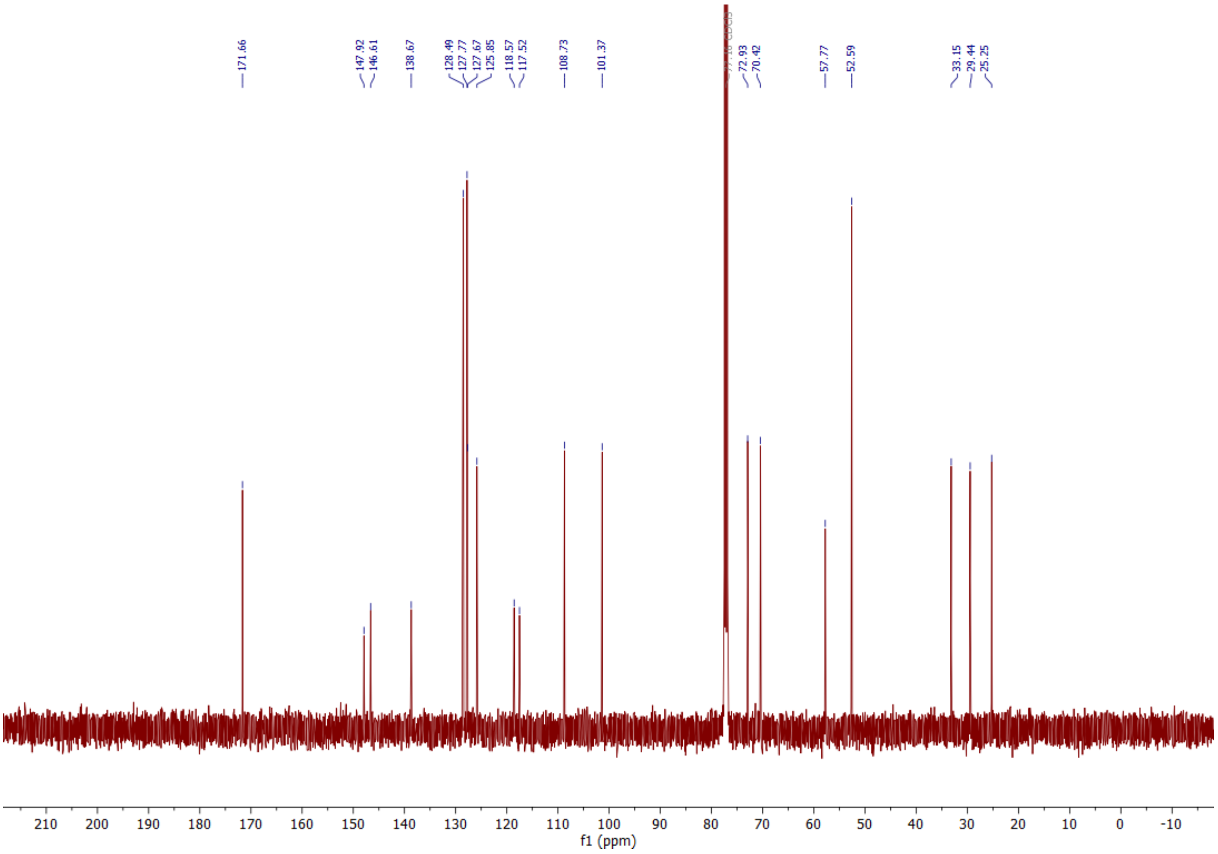

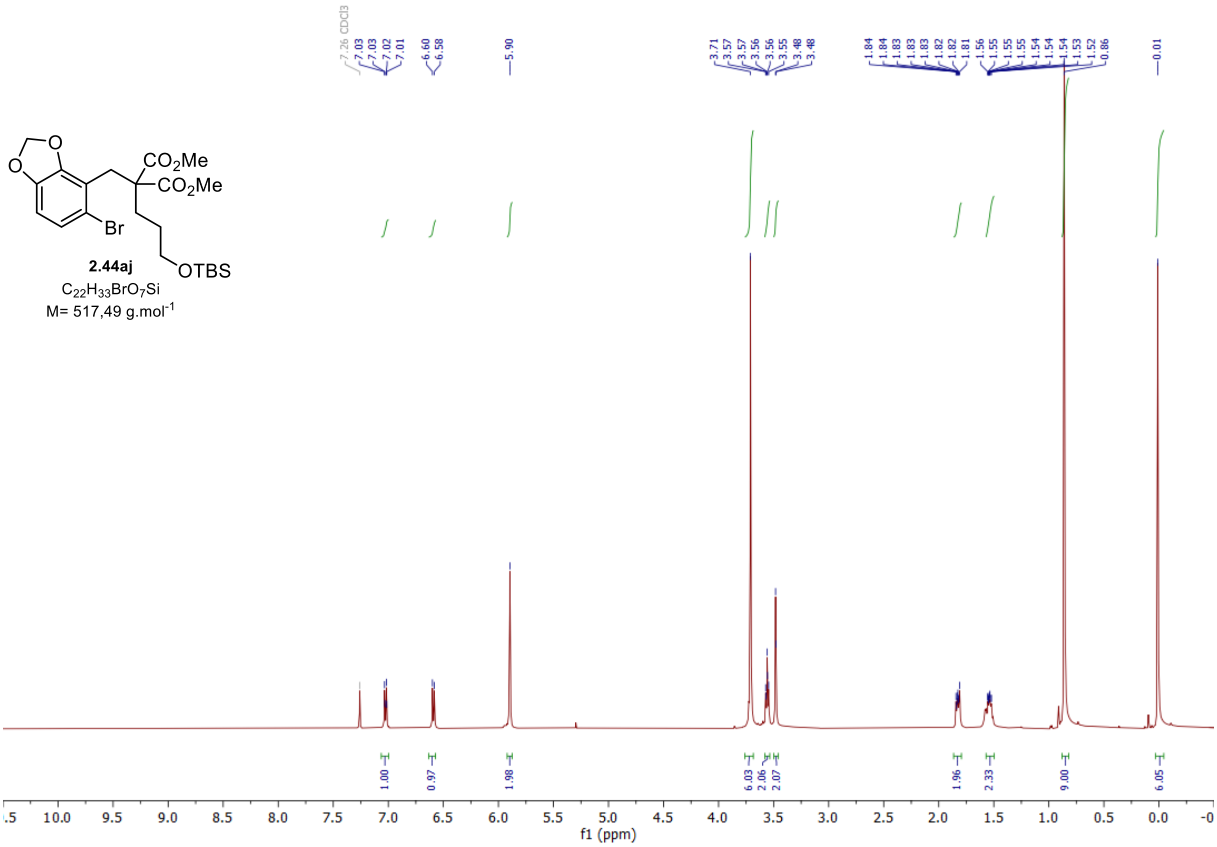

2.44aj

$C_{22}H_{33}BrO_7Si$

M= 517,49 g.mol^{-1}

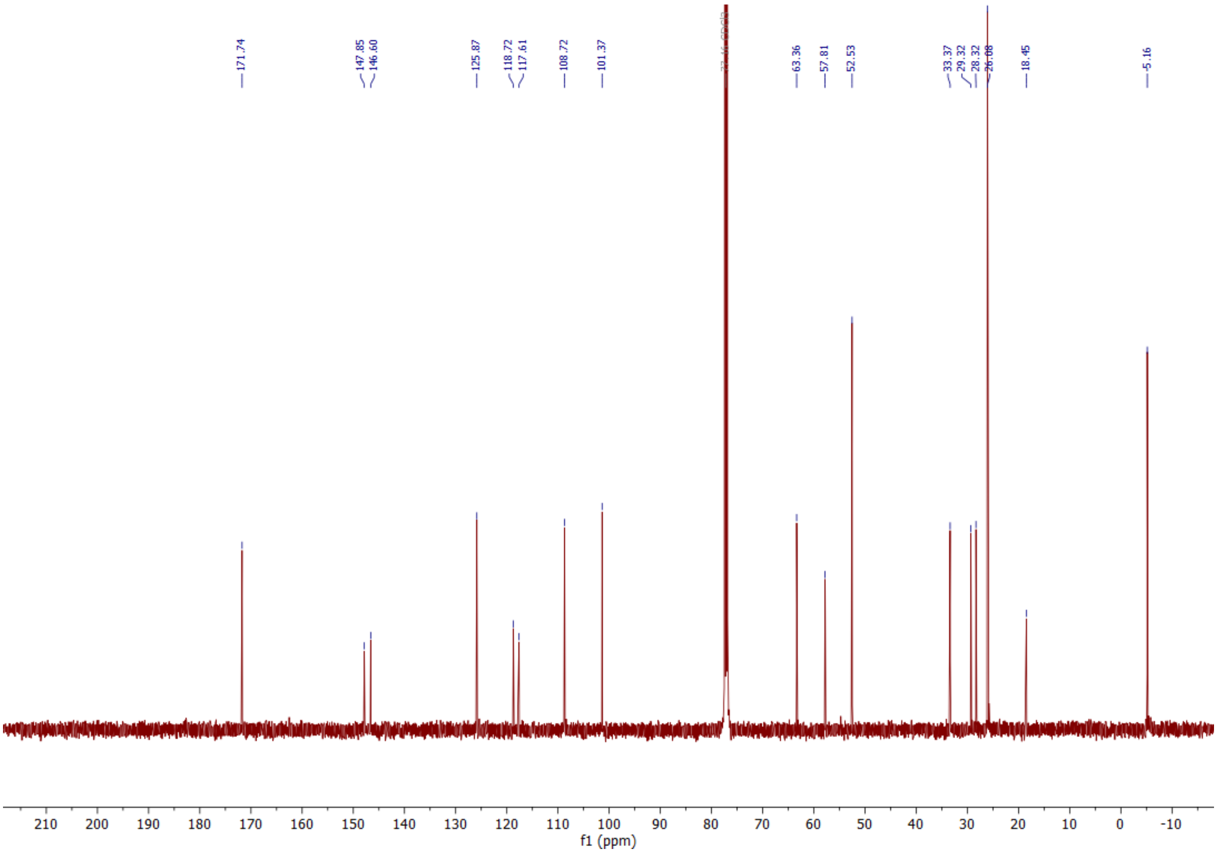

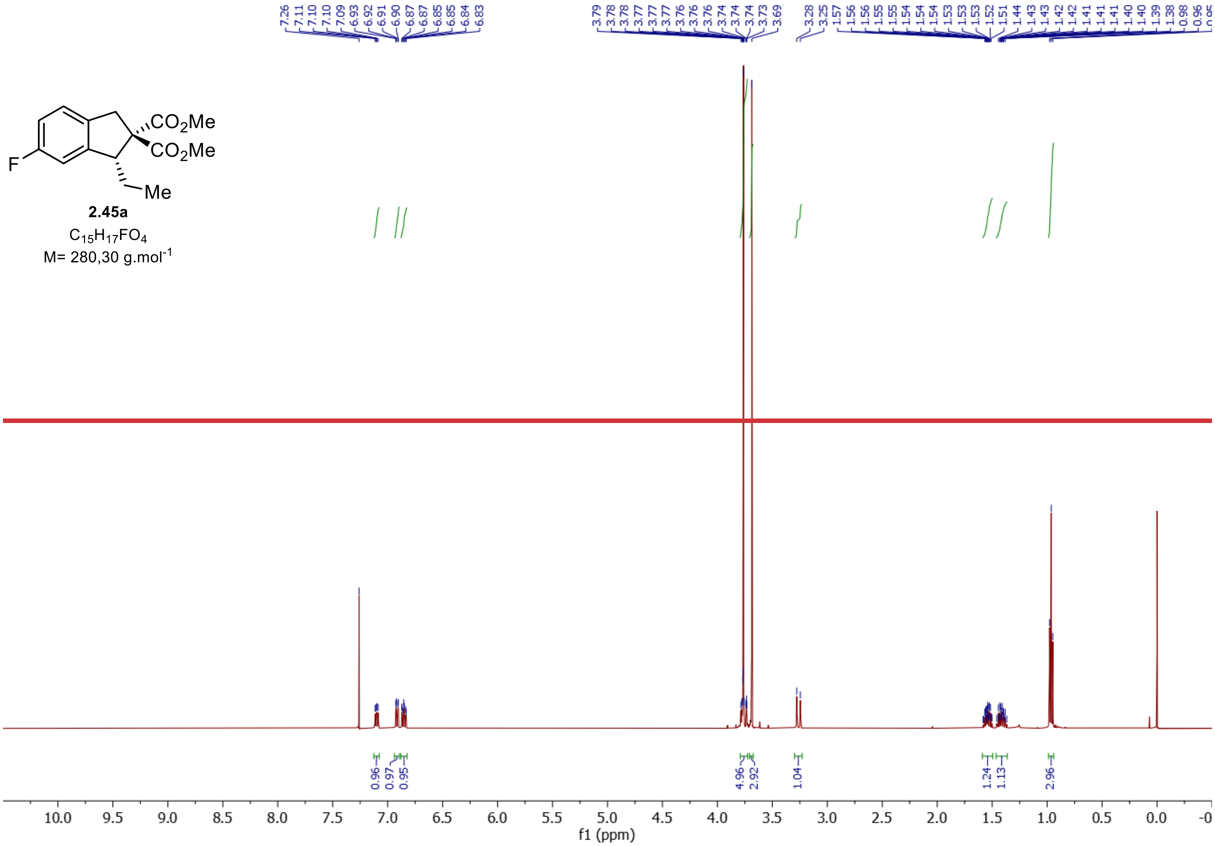

2.45a

$C_{15}H_{17}FO_4$

M= 280,30 g.mol^{-1}

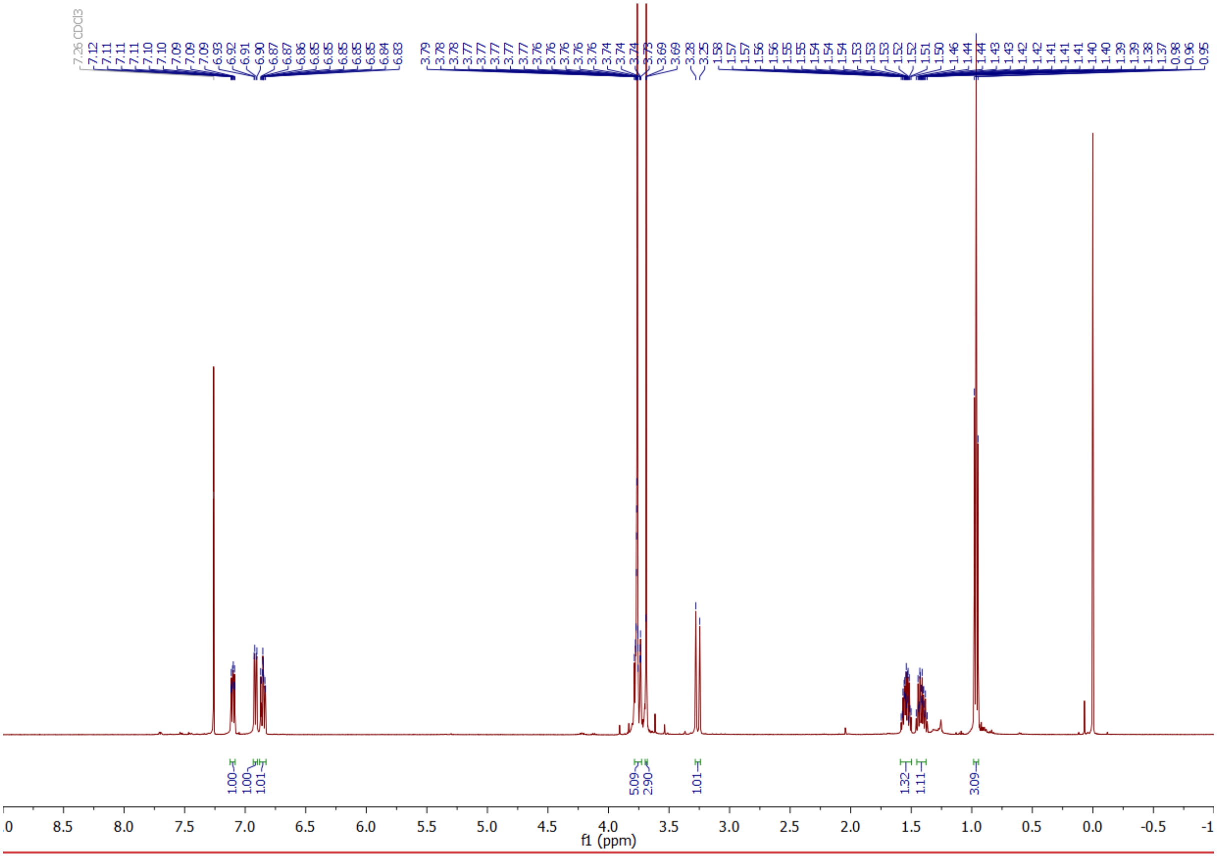

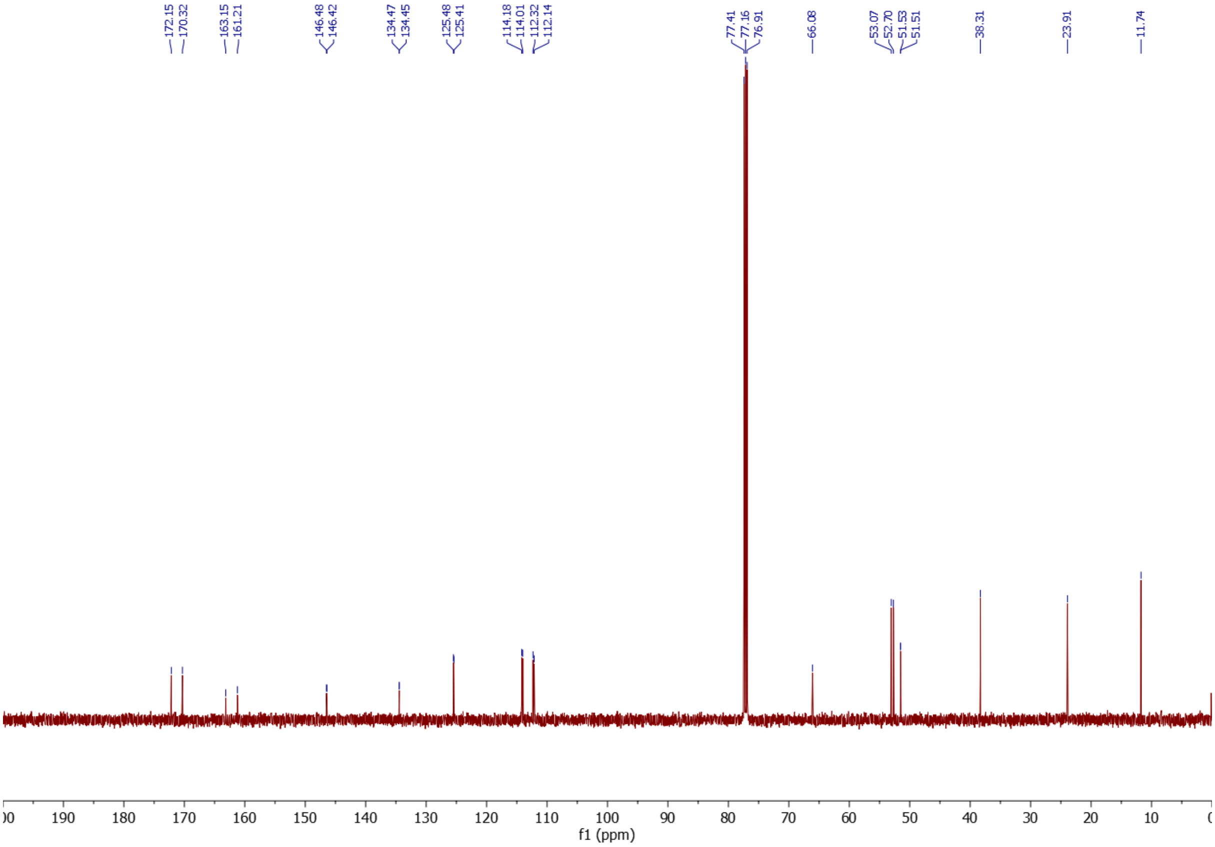
172.15
170.32
163.15
161.21
146.48
146.42
134.47
134.45
125.48
125.41
114.18
114.01
112.32
112.14
77.41
77.16
76.91
66.08
53.07
52.70
51.53
51.51
38.31
23.91
11.74
190
180
170
160
150
140
130
120
110
100
90
80
70
60
50
40
30
20
10
f1 (ppm)

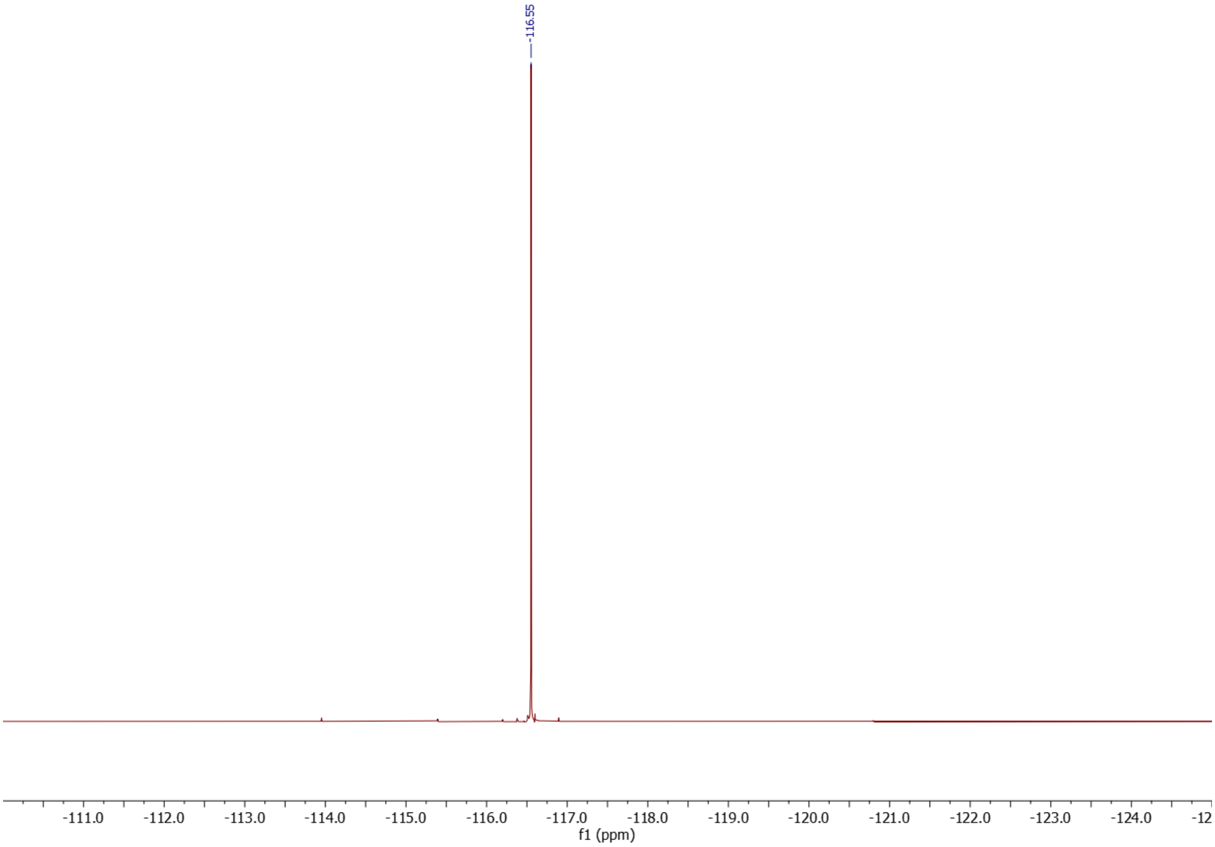
-116.55
-111.0
-112.0
-113.0
-114.0
-115.0
-116.0
-117.0
-118.0
-119.0
-120.0
-121.0
-122.0
-123.0
-124.0
f1 (ppm)

<Chromatogram>

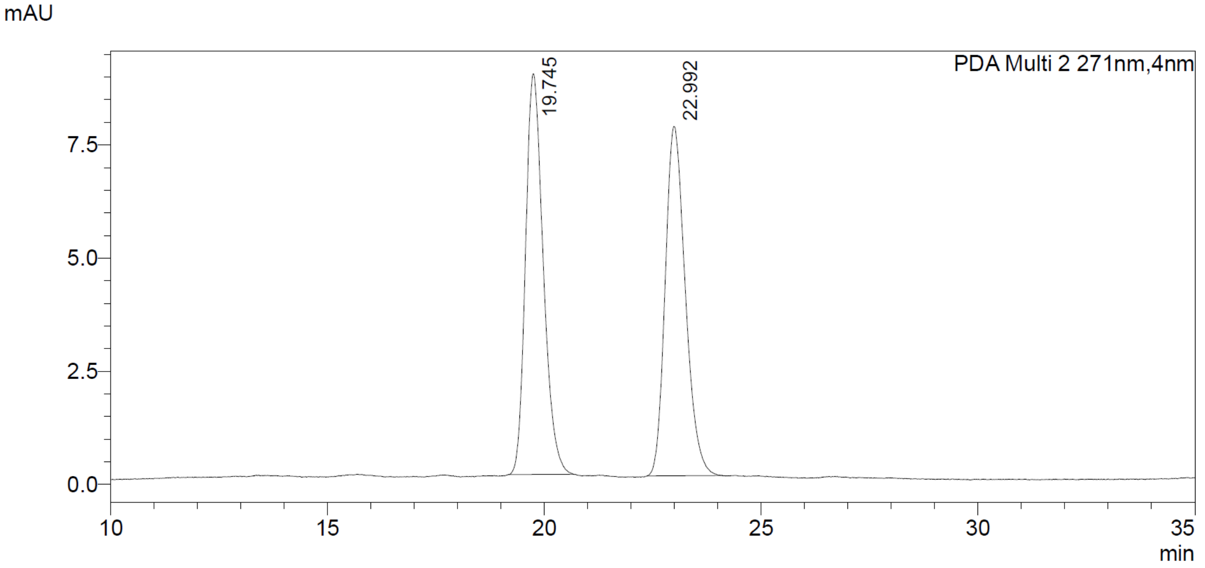

<Peak Table>

PDA Ch2 271nm

Peak#	Ret. Time	Area	Area%
1	19.745	251628	50.261
2	22.992	249015	49.739
Total		500643	100.000

<Chromatogram>

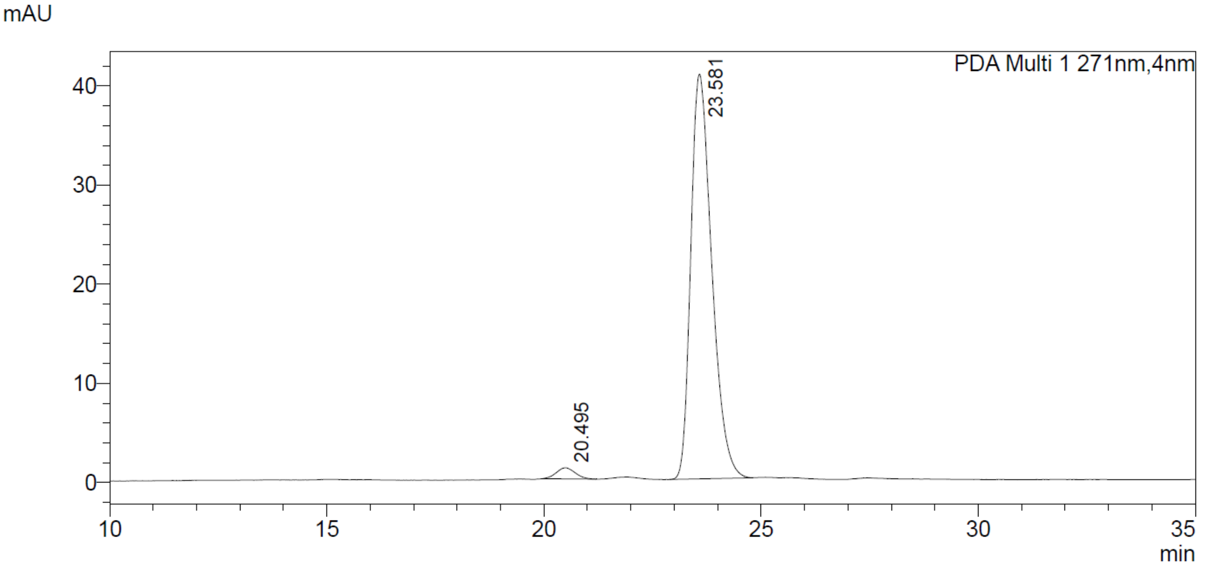

<Peak Table>

PDA Ch1 271nm

Peak#	Ret. Time	Area	Area%
1	20.495	33920	2.415
2	23.581	1370586	97.585
Total		1404507	100.000

<Chromatogram>

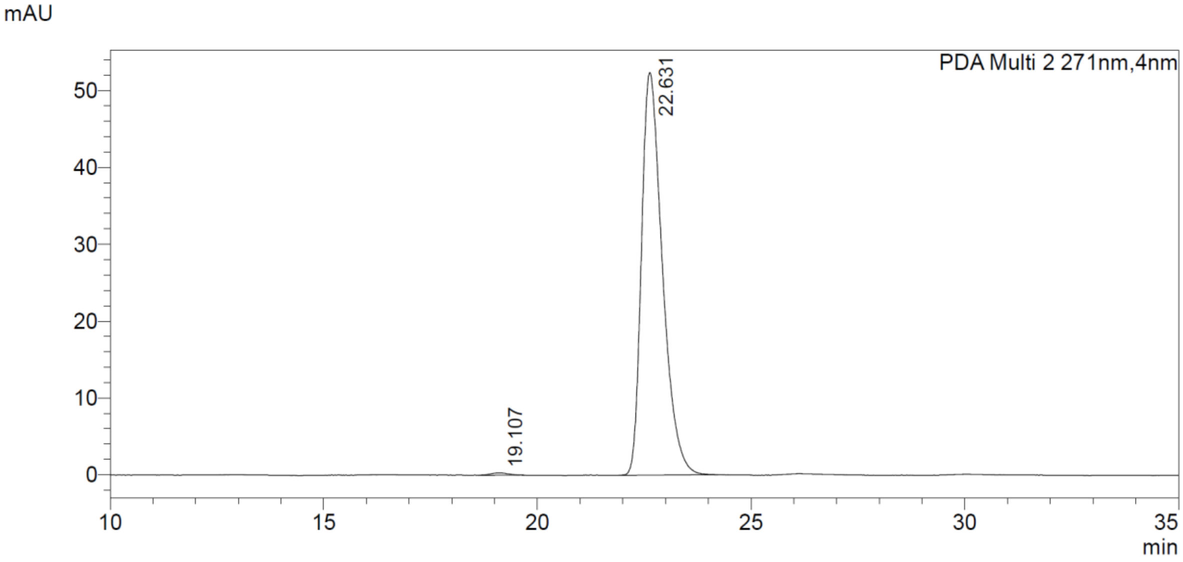

<Peak Table>

PDA Ch2 271nm

Peak#	Ret. Time	Area	Area%
1	19.107	9175	0.512
2	22.631	1782595	99.488
Total		1791771	100.000

CO2Me
CO2Me
Me

2.45b

$C_{14}H_{16}O_4$

M= 248,28 g.mol^{-1}

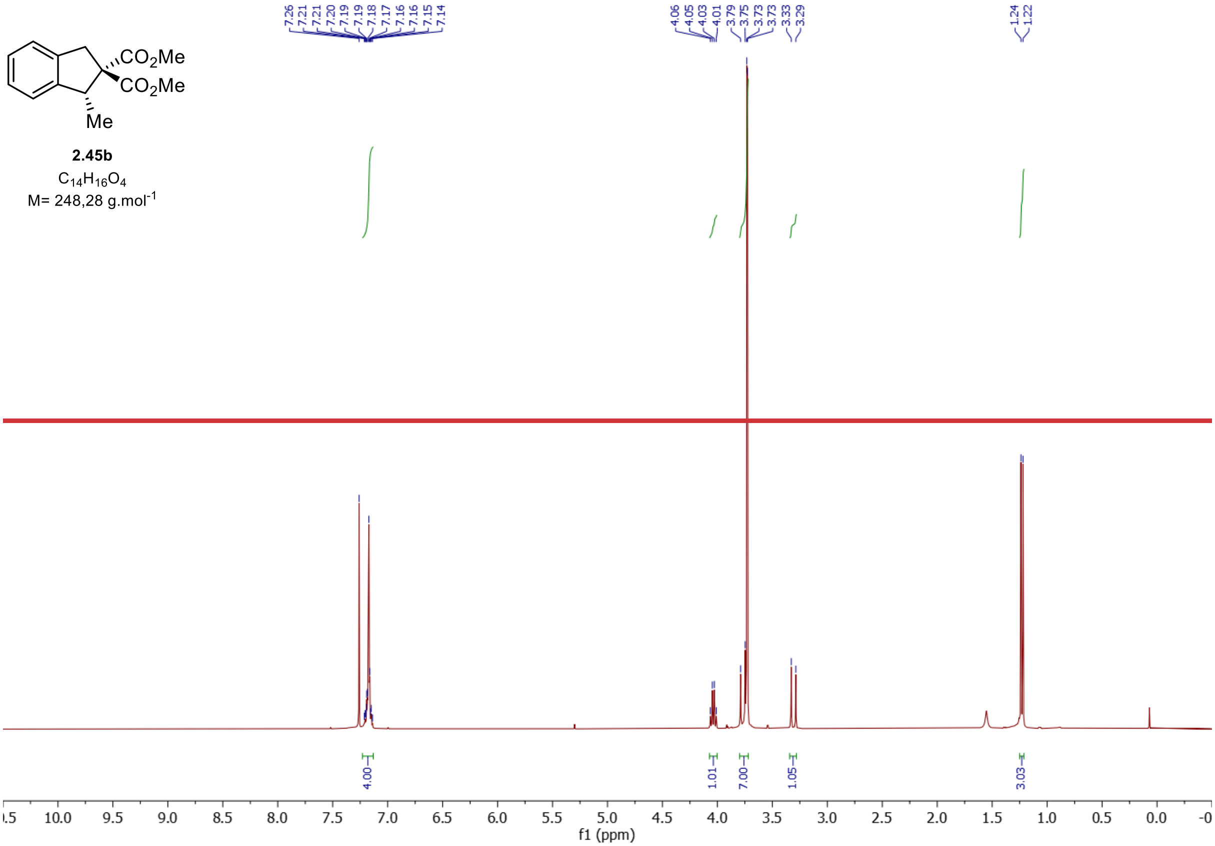

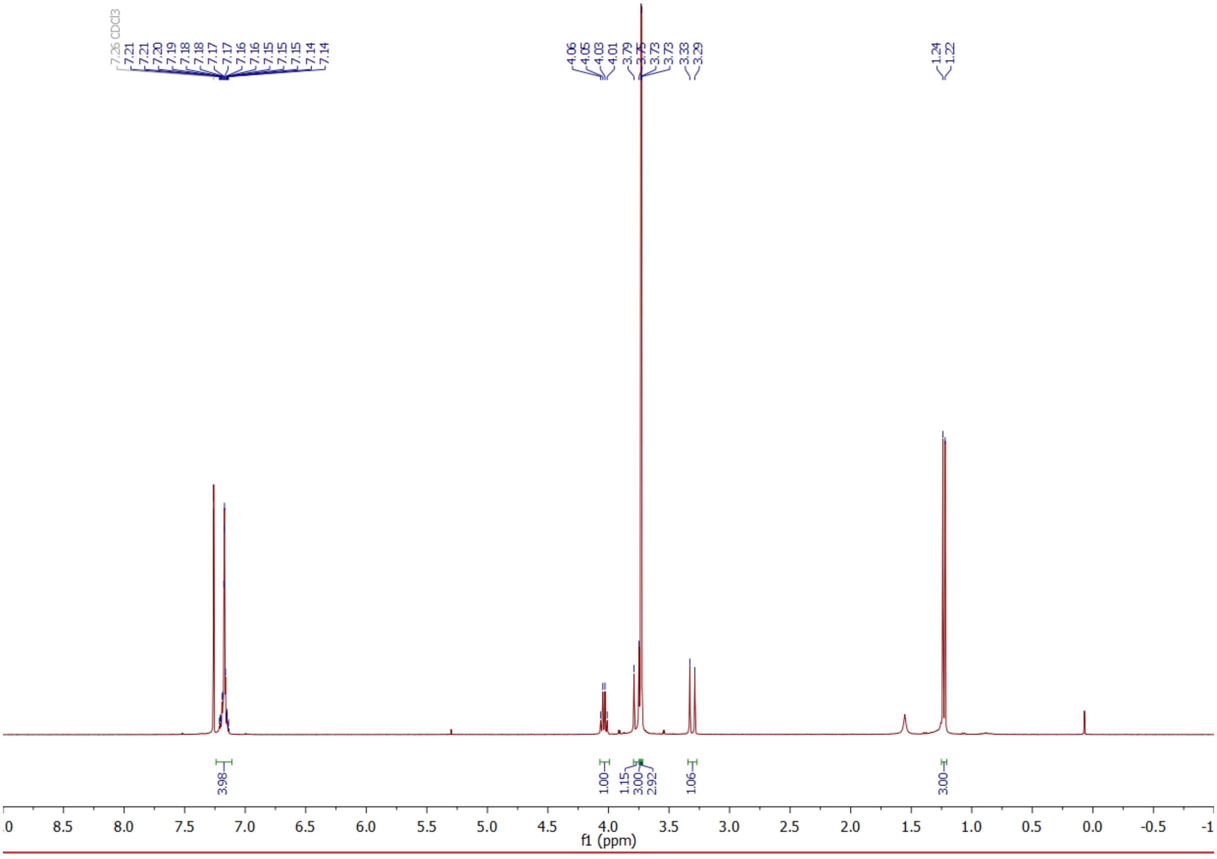

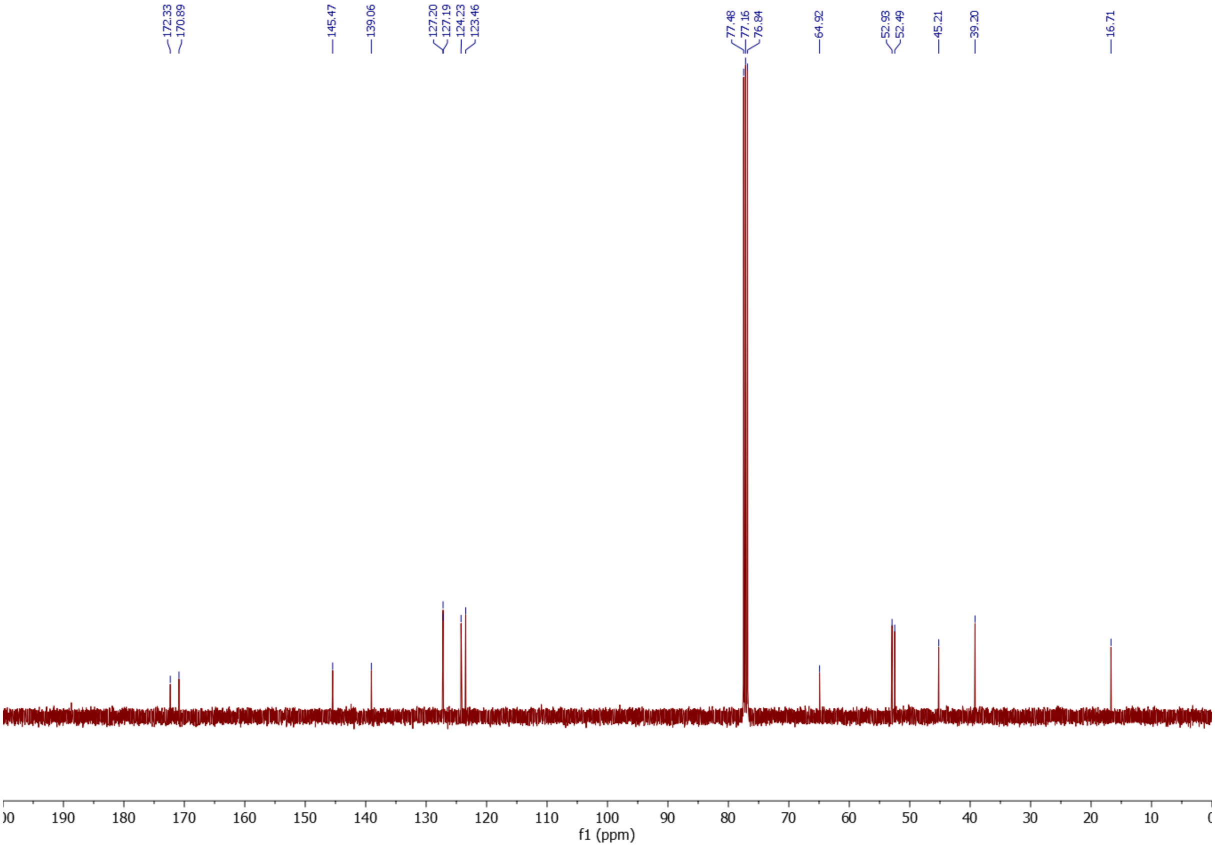
172.33
170.89
145.47
139.06
127.20
127.19
124.23
123.46
77.48
77.16
76.84
64.92
52.93
52.49
45.21
39.20
16.71
190
180
170
160
150
140
130
120
110
100
90
80
70
60
50
40
30
20
10
f1 (ppm)

<Chromatogram>

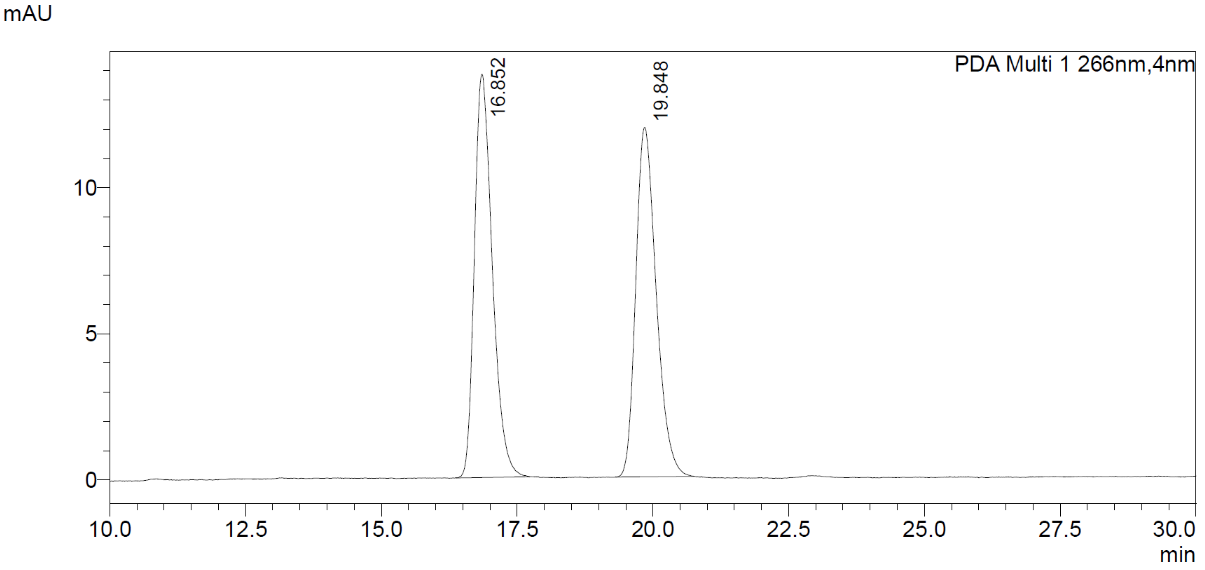

<Peak Table>

PDA Ch1 266nm

Peak#	Ret. Time	Area	Area%
1	16.852	316995	50.293
2	19.848	313305	49.707
Total		630301	100.000

<Chromatogram>

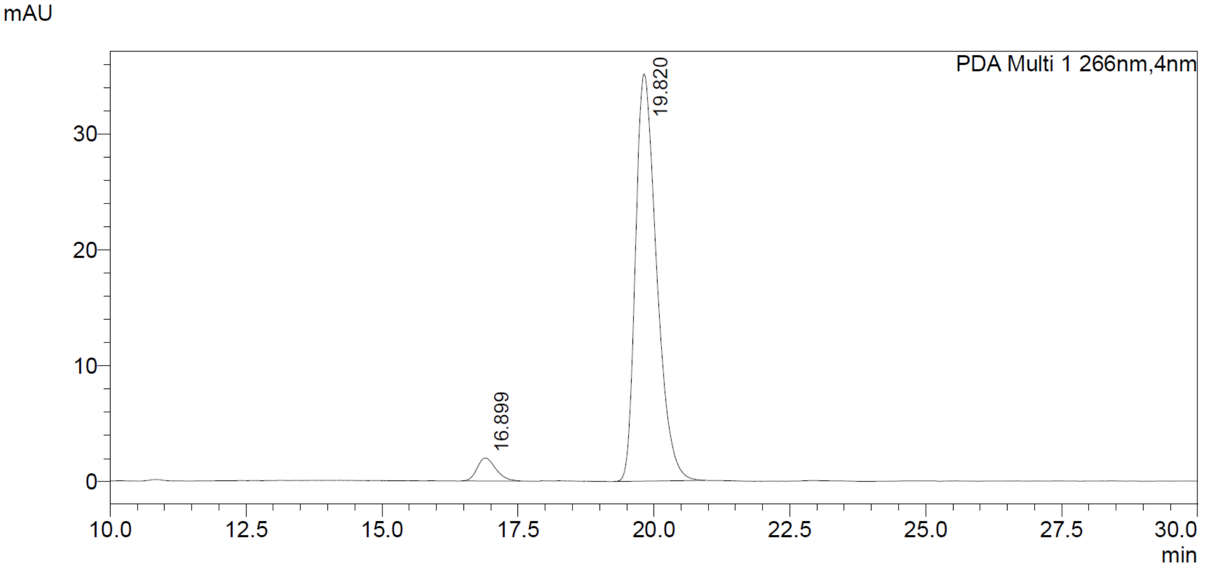

<Peak Table>

PDA Ch1 266nm

Peak#	Ret. Time	Area	Area%
1	16.899	47679	4.779
2	19.820	950060	95.221
Total		997738	100.000

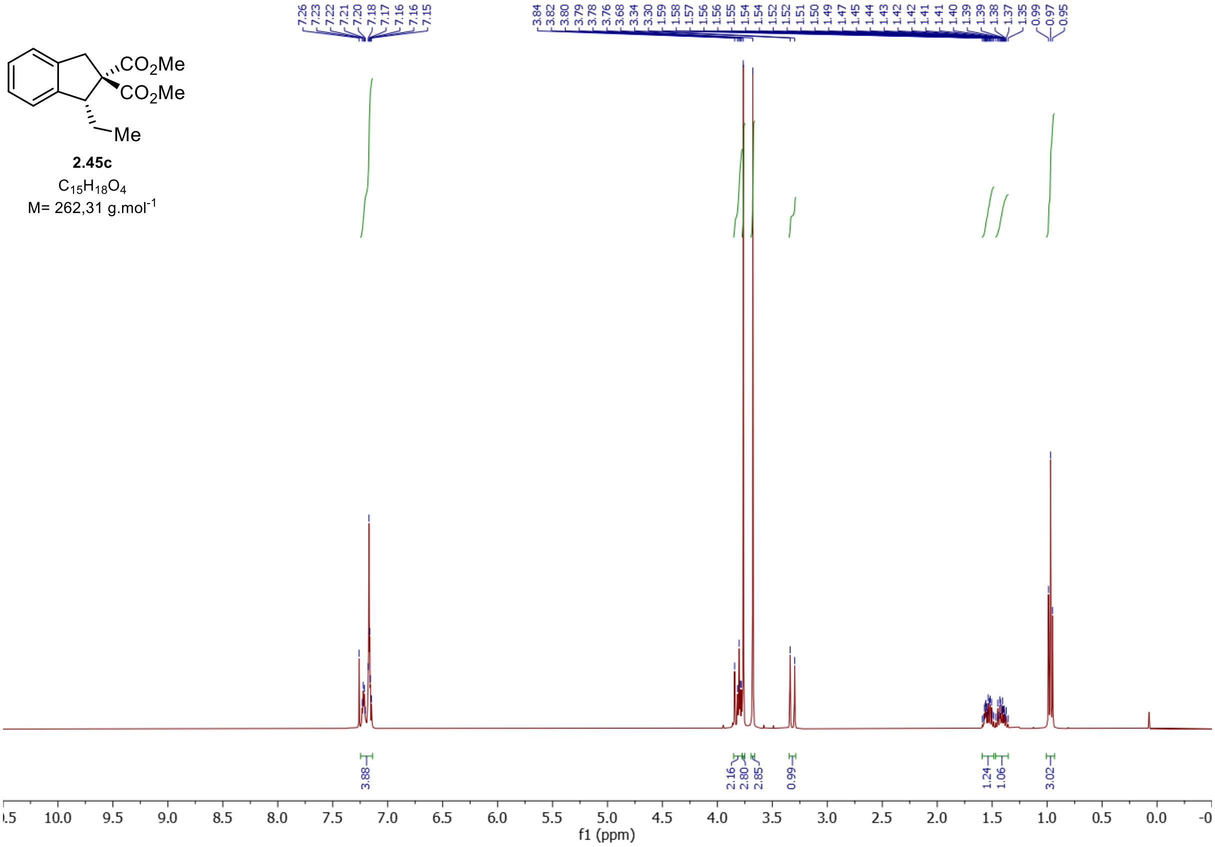

2.45c

$C_{15}H_{18}O_4$

M= 262,31 g.mol^{-1}

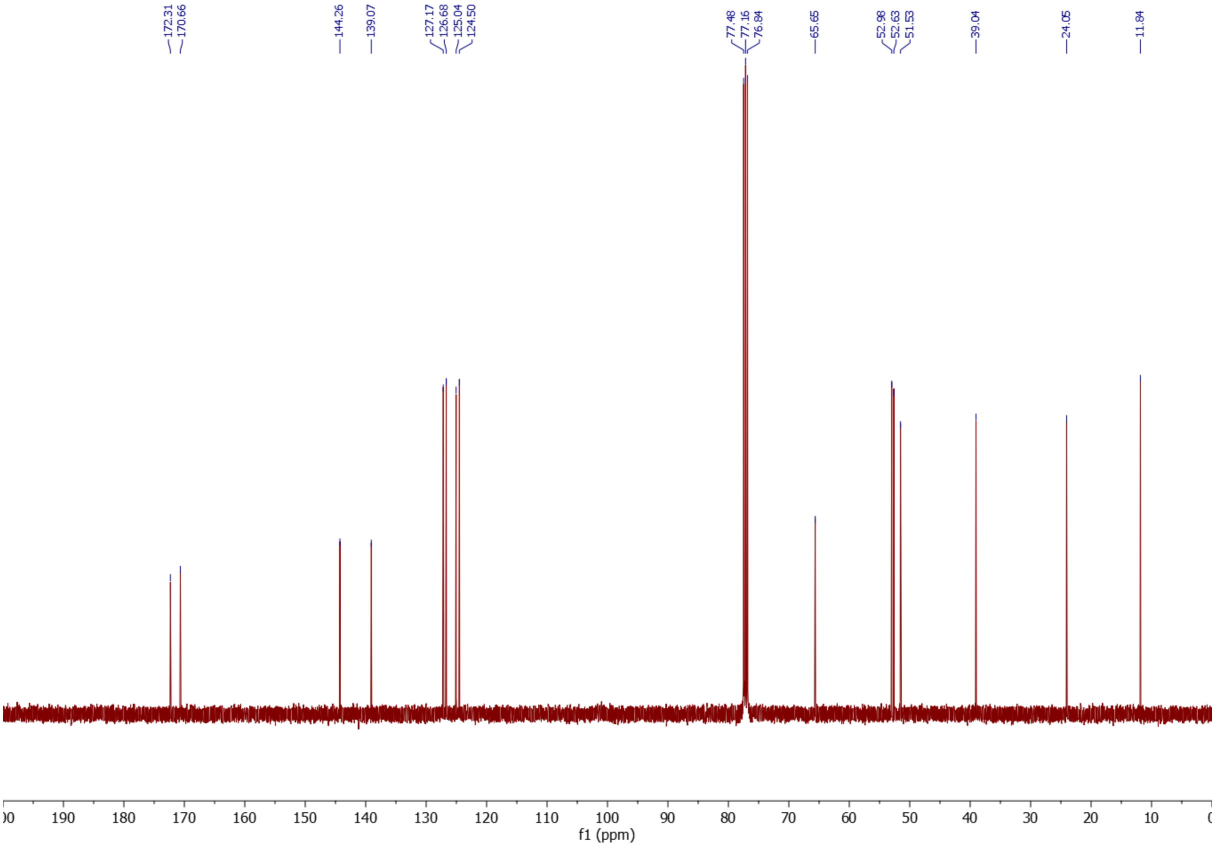

<Chromatogram>

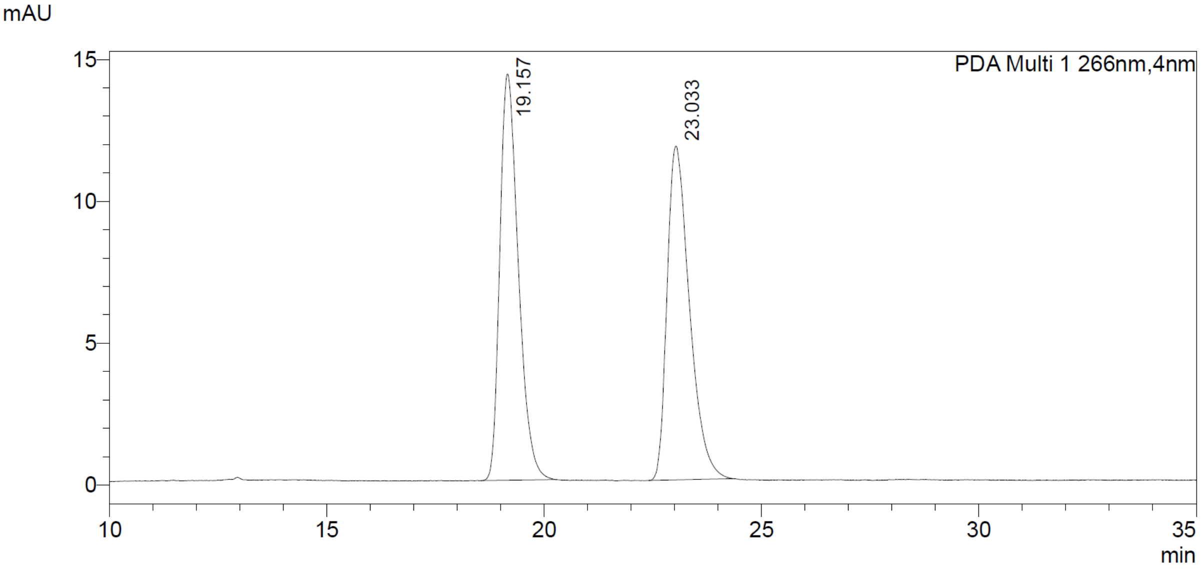

<Peak Table>

PDA Ch1 266nm

Peak#	Ret. Time	Area	Area%
1	19.157	424363	50.131
2	23.033	422141	49.869
Total		846504	100.000

<Chromatogram>

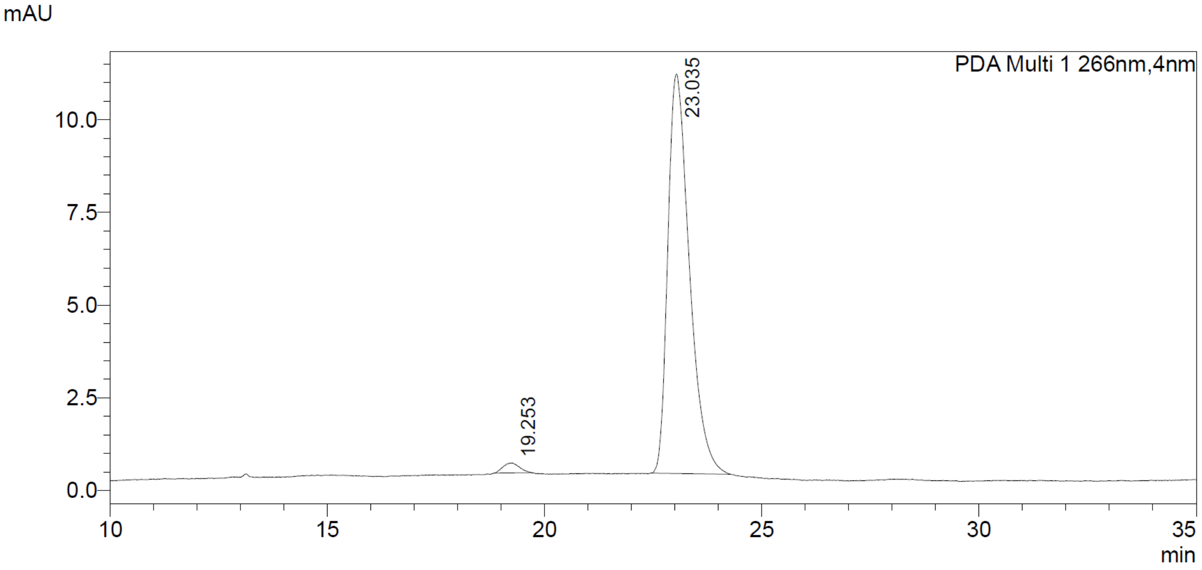

<Peak Table>

PDA Ch1 266nm

Peak#	Ret. Time	Area	Area%
1	19.253	7030	1.852
2	23.035	372496	98.148
Total		379526	100.000

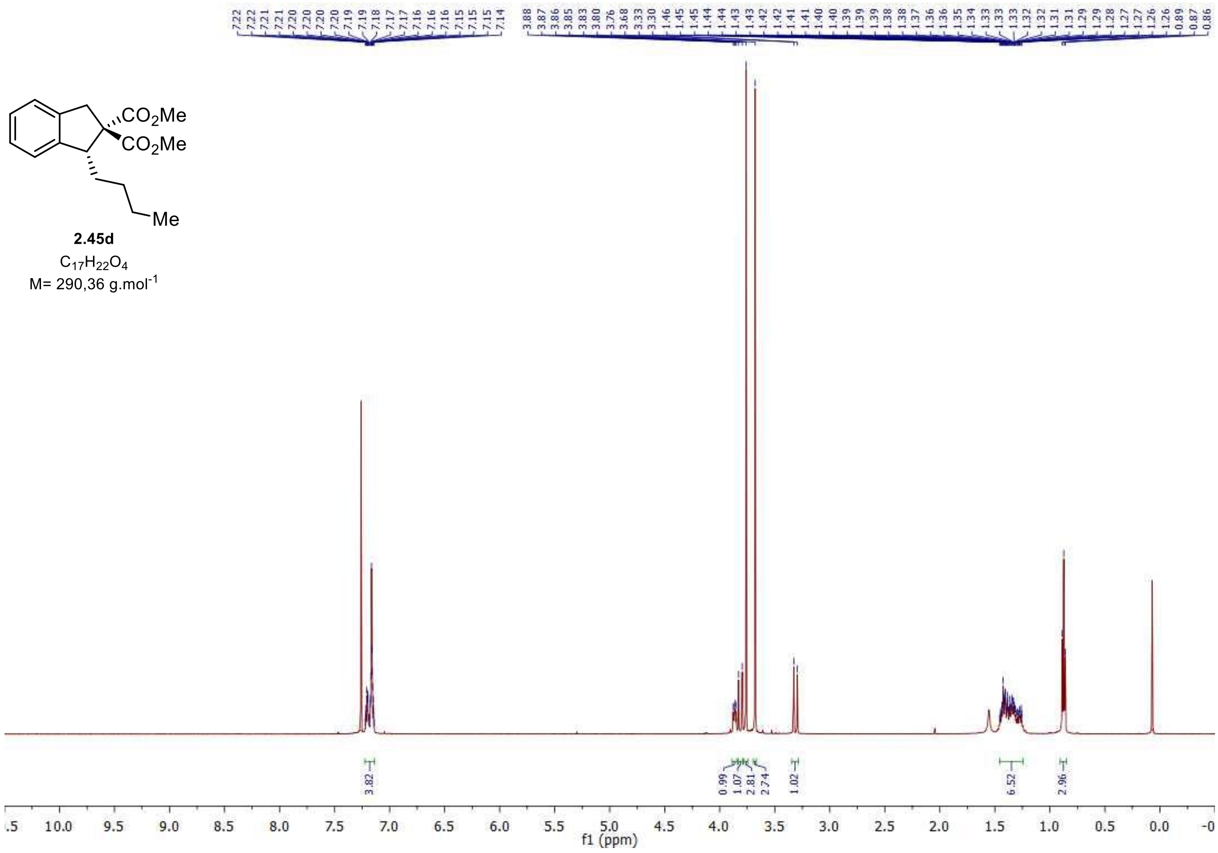

2.45d

$C_{17}H_{22}O_4$

M= 290,36 g.mol^{-1}

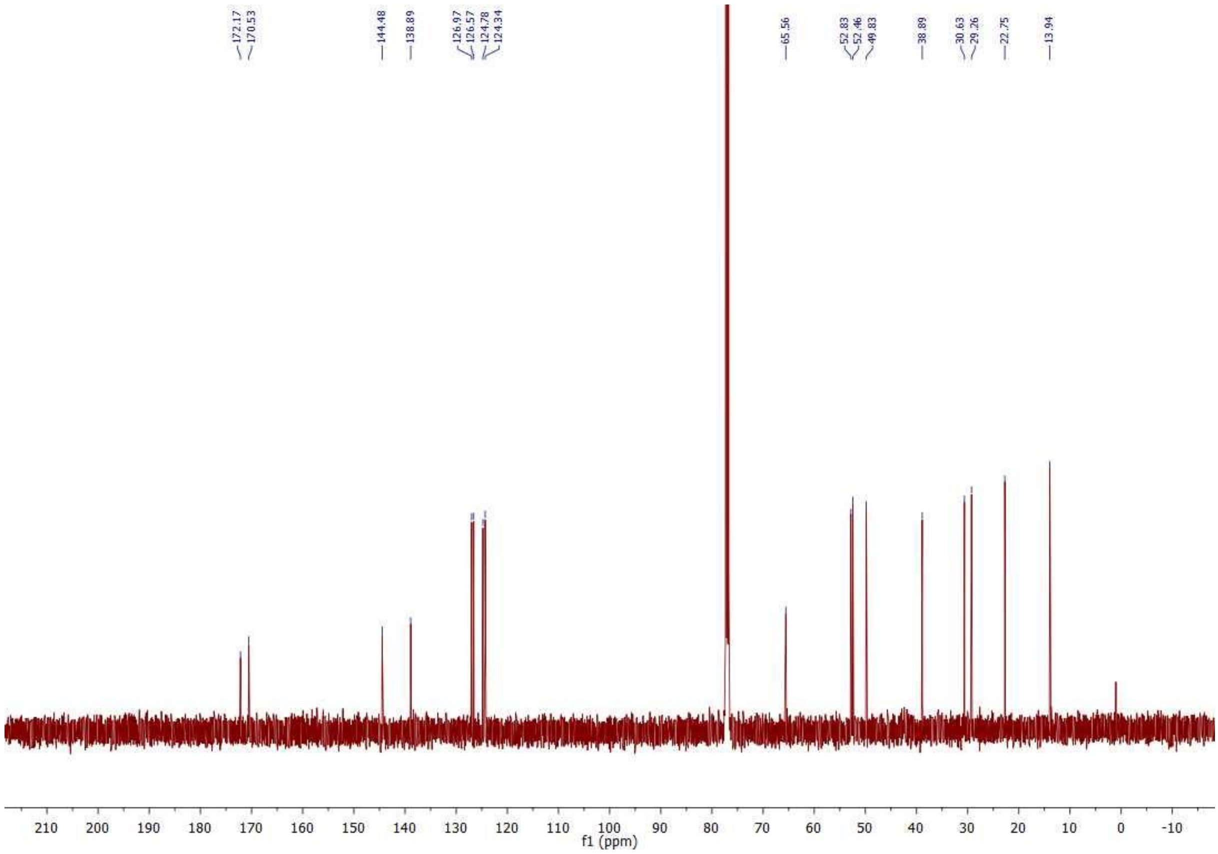

<Chromatogram>

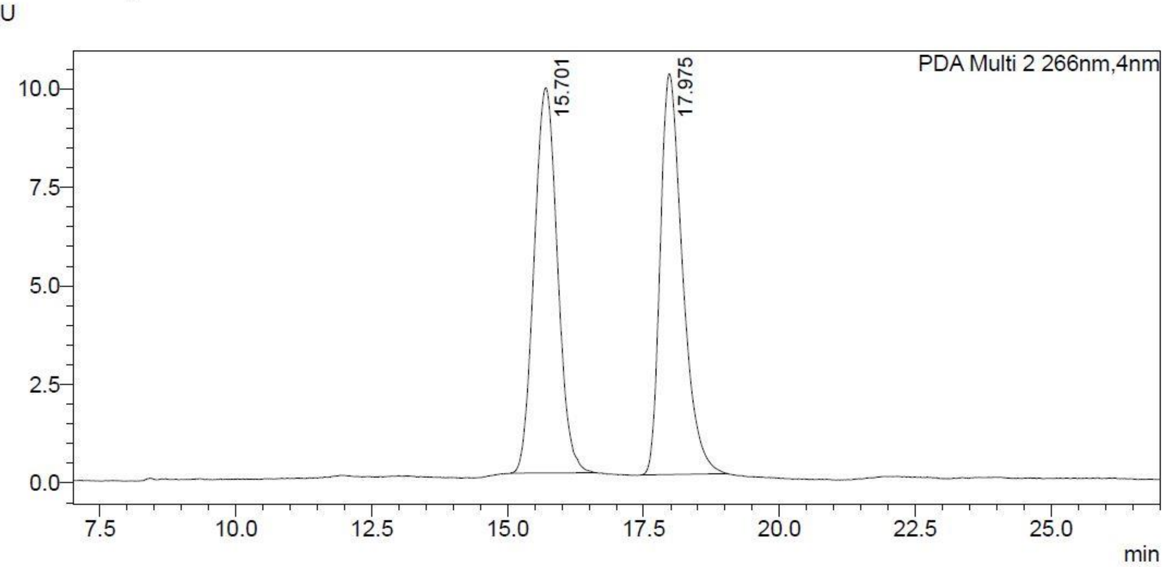

<Peak Table>

PDA Ch2 266nm

Peak#	Ret. Time	Area	Area%
1	15.701	291898	50.120
2	17.975	290505	49.880
Total		582403	100.000

<Chromatogram>

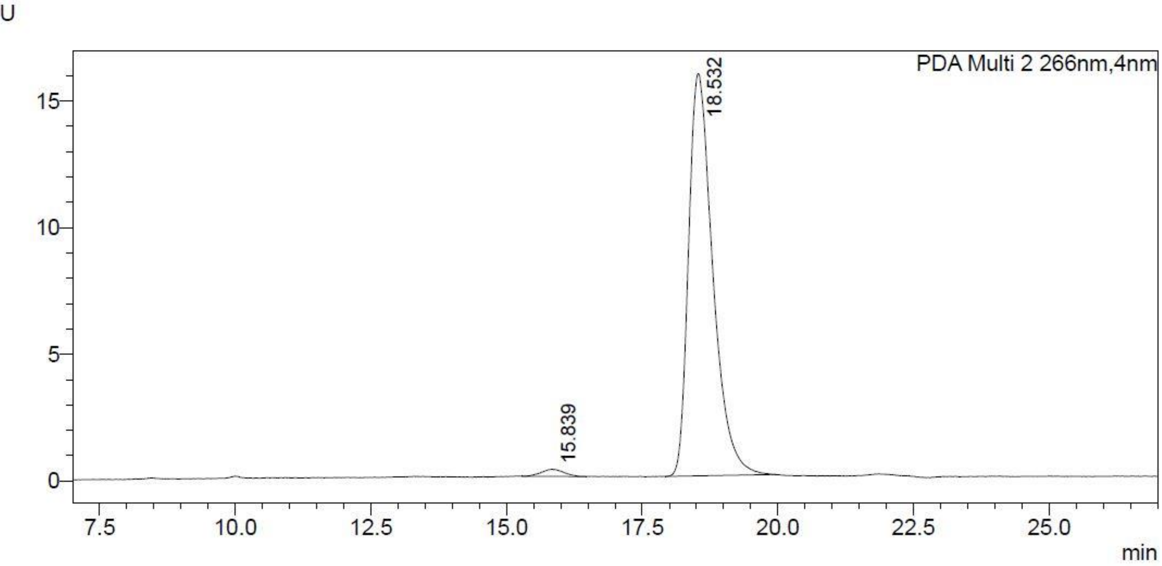

<Peak Table>

PDA Ch2 266nm

Peak#	Ret. Time	Area	Area%
1	15.839	8030	1.600
2	18.532	493856	98.400
Total		501886	100.000

CO$_2$Me
CO$_2$Me
Me
Me

2.45e

$C_{17}H_{22}O_4$

M= 290,36 g.mol^{-1}

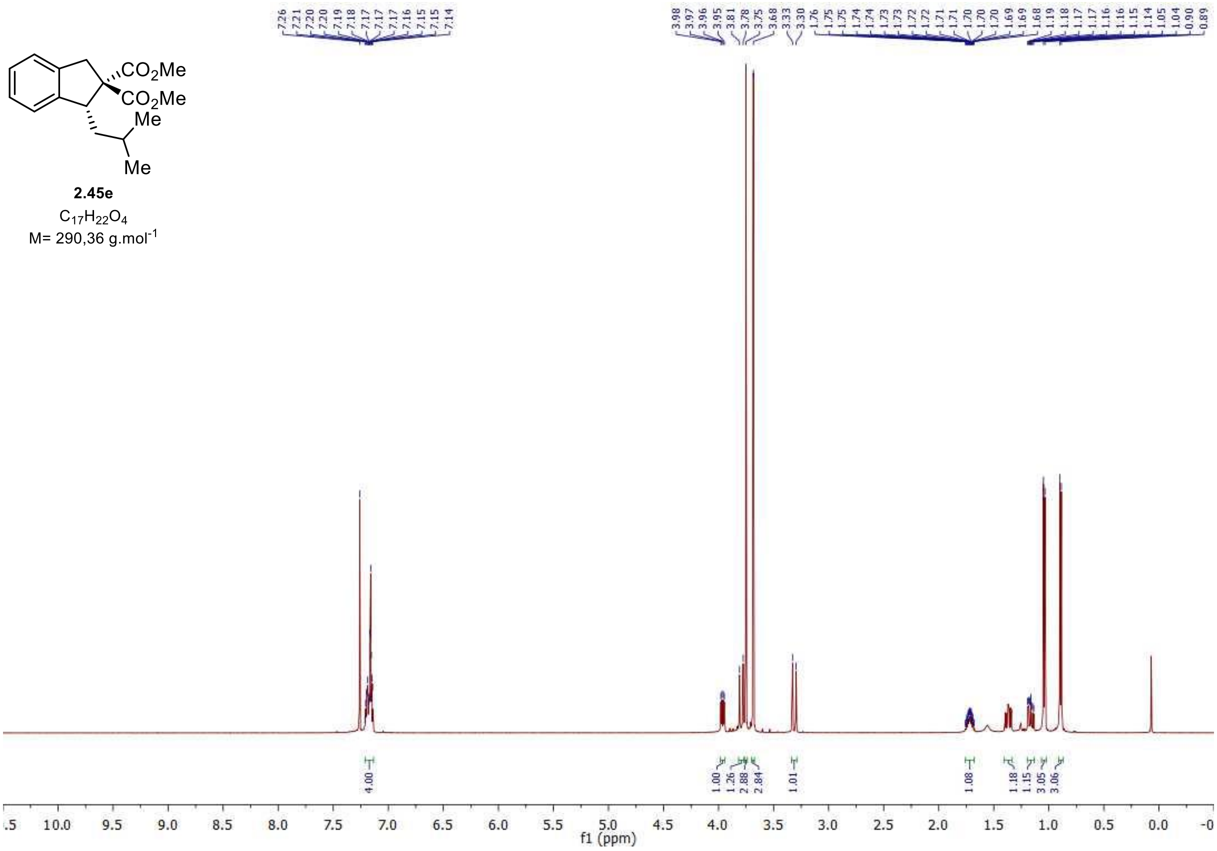

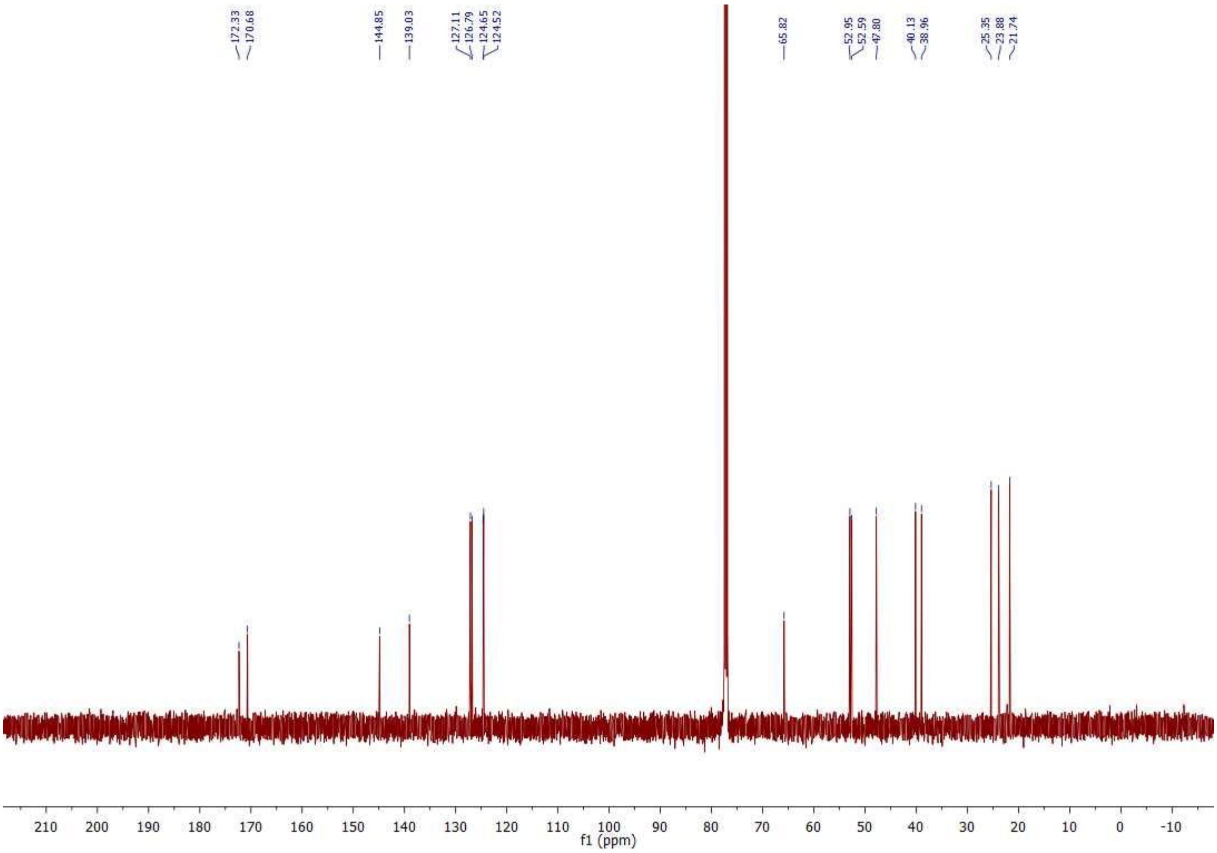

<Chromatogram>

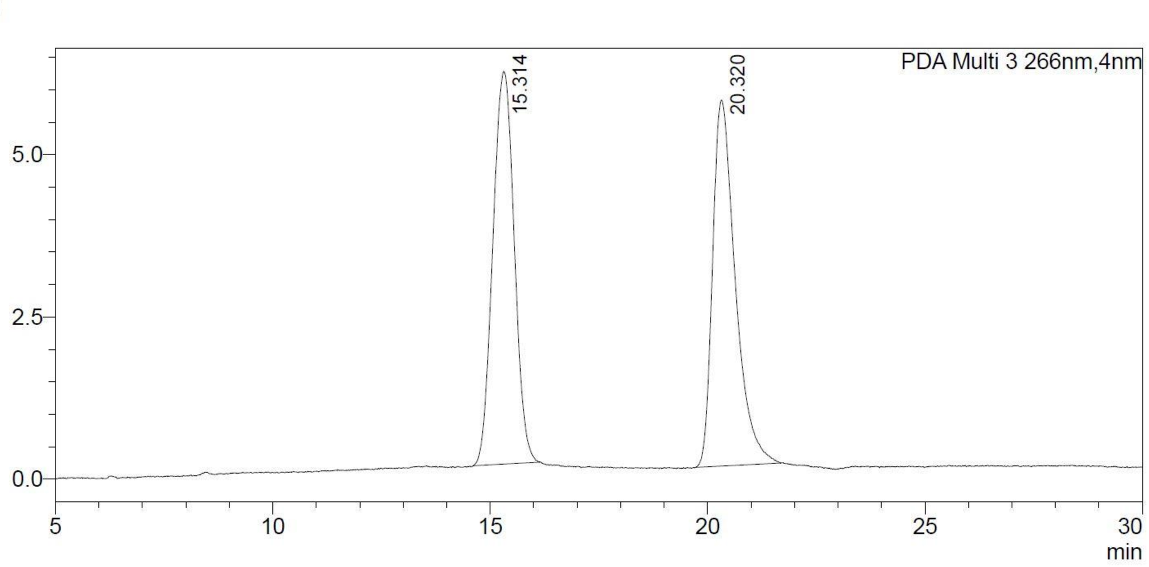

<Peak Table>

PDA Ch3 266nm

Peak#	Ret. Time	Area	Area%
1	15.314	207070	50.264
2	20.320	204895	49.736
Total		411965	100.000

<Chromatogram>

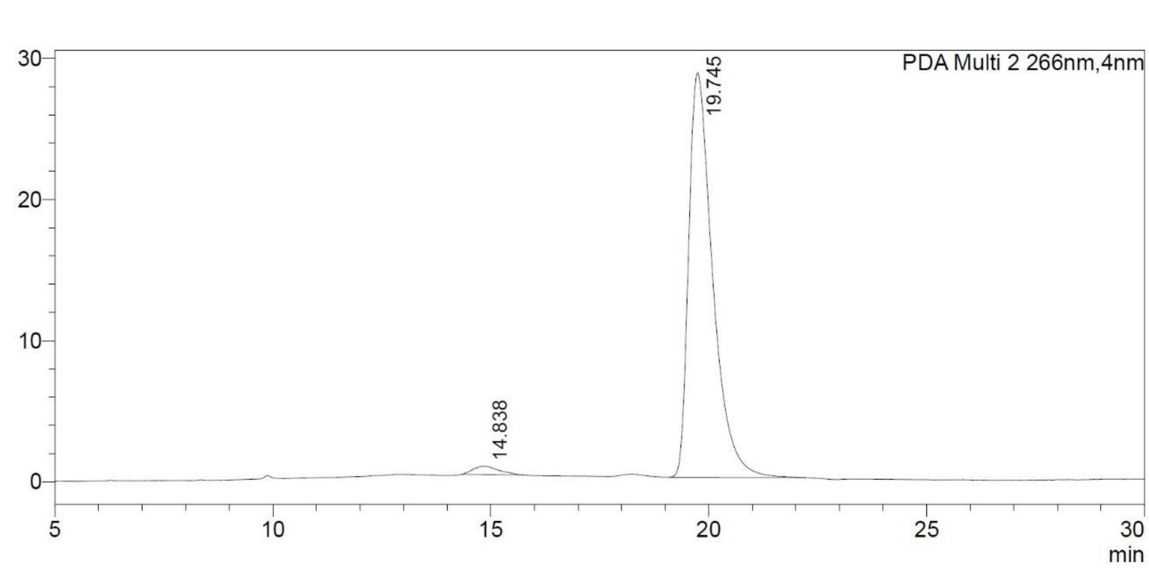

<Peak Table>

PDA Ch2 266nm

Peak#	Ret. Time	Area	Area%
1	14.838	24129	2.153
2	19.745	1096799	97.847
Total		1120928	100.000

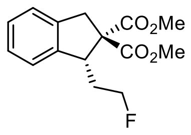
CO2Me
CO2Me
F

2.45f
$C_{15}H_{17}FO_4$
M= 280,30 g.mol^{-1}

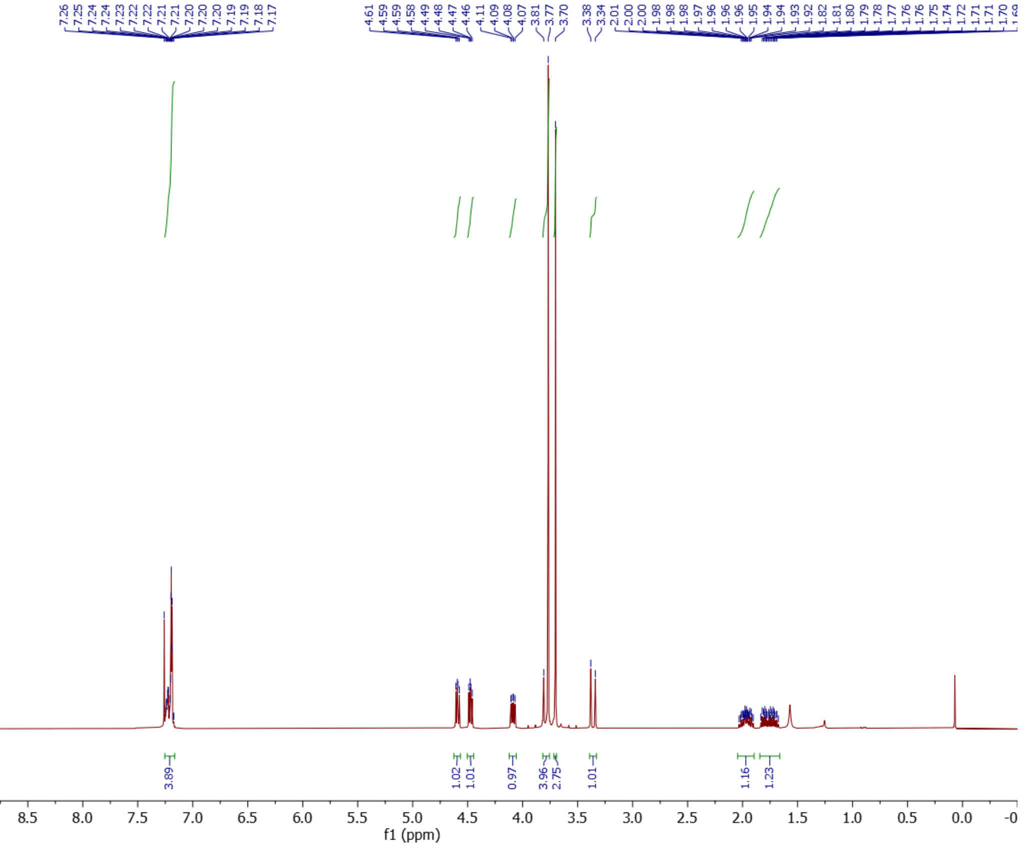

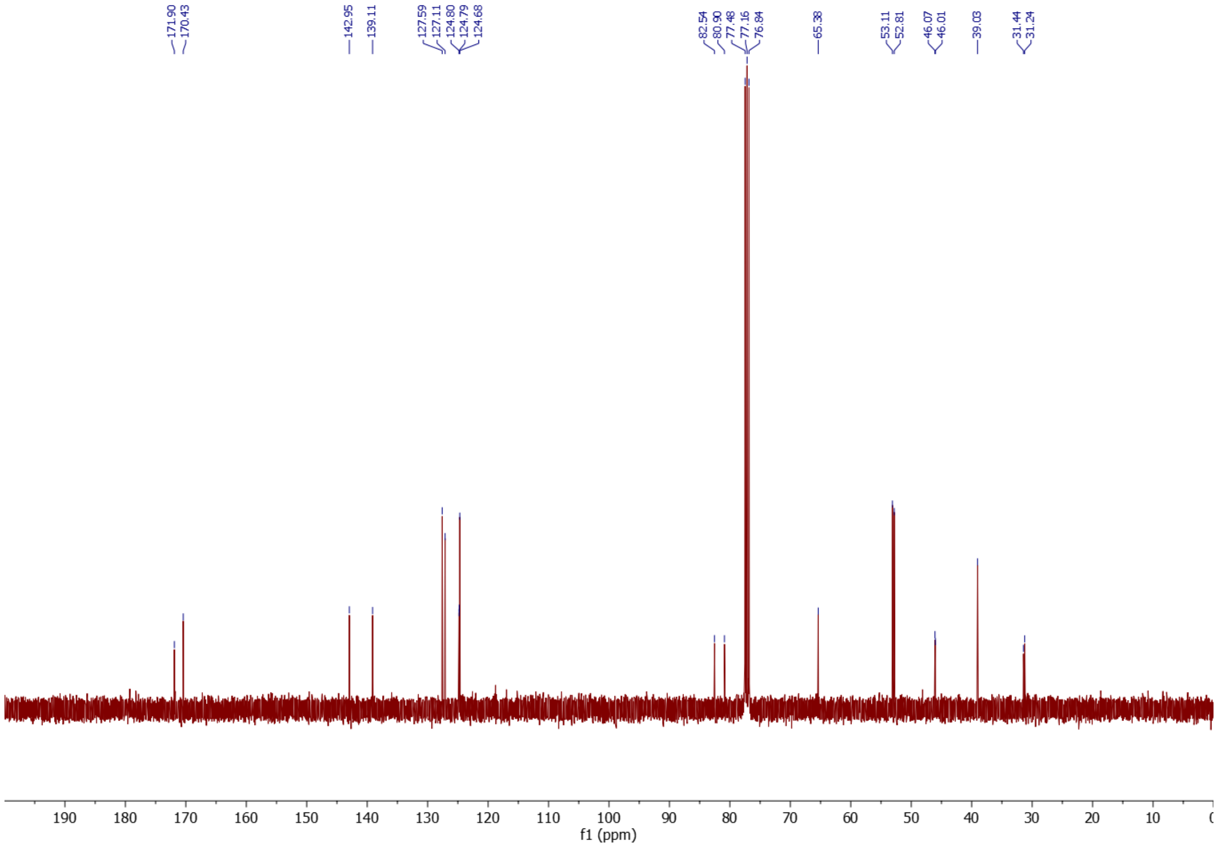

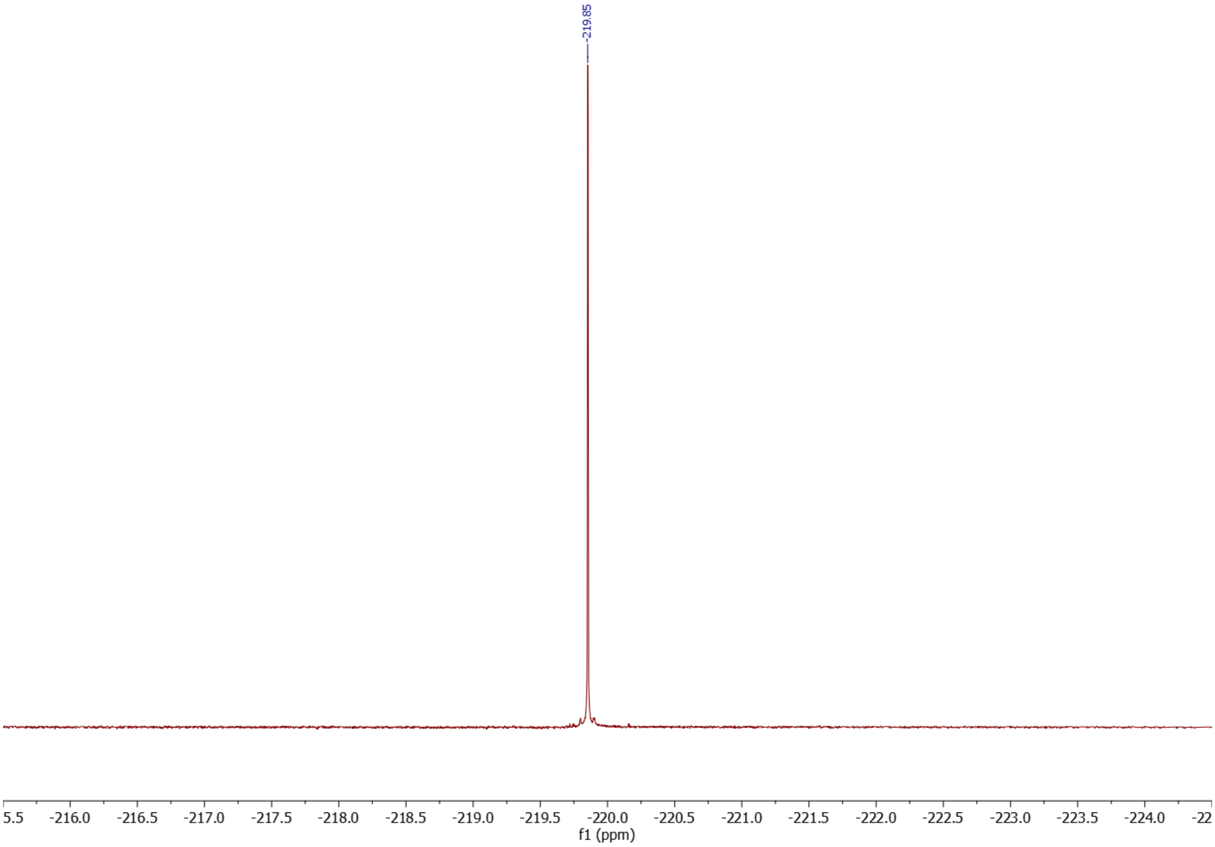
-219.85
5.5
-216.0
-216.5
-217.0
-217.5
-218.0
-218.5
-219.0
-219.5
-220.0
-220.5
-221.0
-221.5
-222.0
-222.5
-223.0
-223.5
-224.0
-22
f1 (ppm)

<Chromatogram>

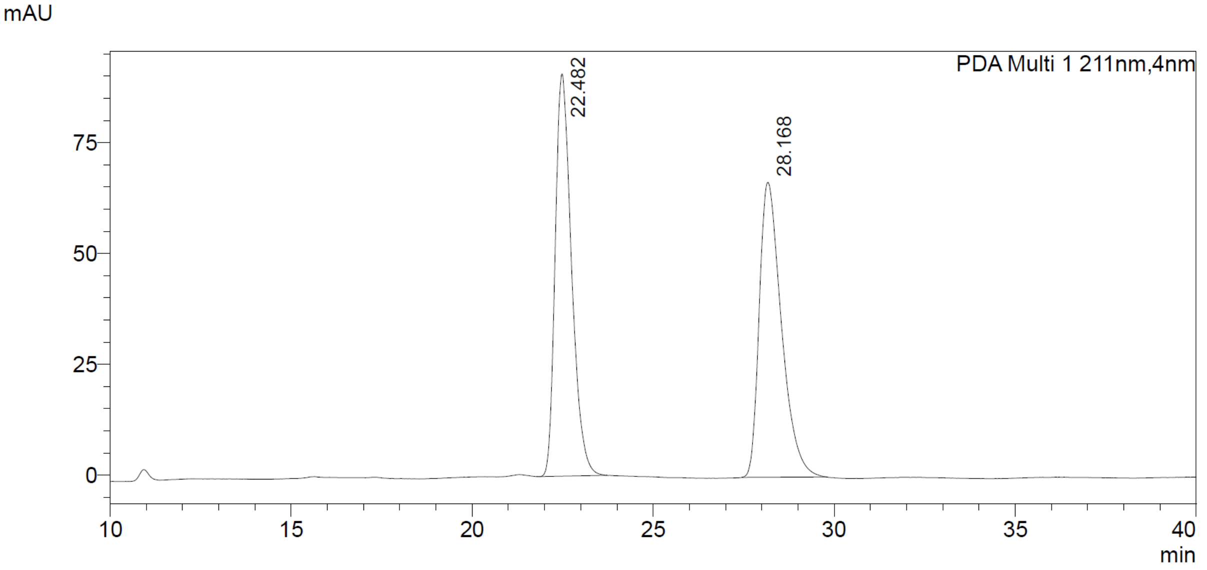

<Peak Table>

PDA Ch1 211nm

Peak#	Ret. Time	Area	Area%
1	22.482	2849460	50.106
2	28.168	2837403	49.894
Total		5686863	100.000

<Chromatogram>

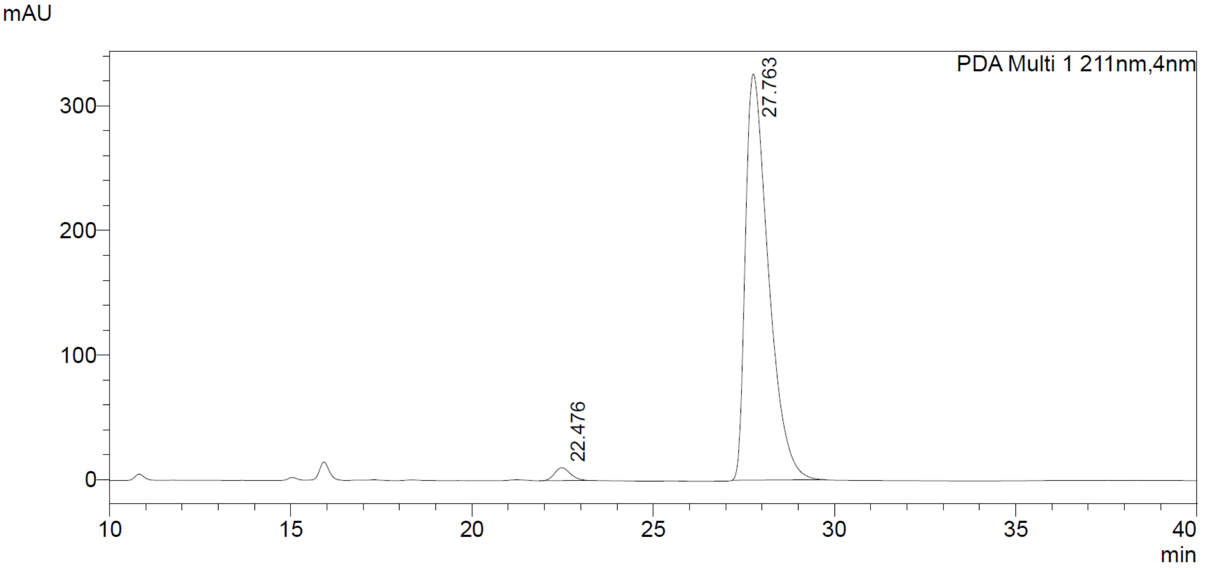

<Peak Table>

PDA Ch1 211nm

Peak#	Ret. Time	Area	Area%
1	22.476	313085	2.128
2	27.763	14398888	97.872
Total		14711973	100.000

CO2Me
CO2Me
CO2Me

2.45g

$C_{17}H_{20}O_6$

M= 320,34 g.mol^{-1}

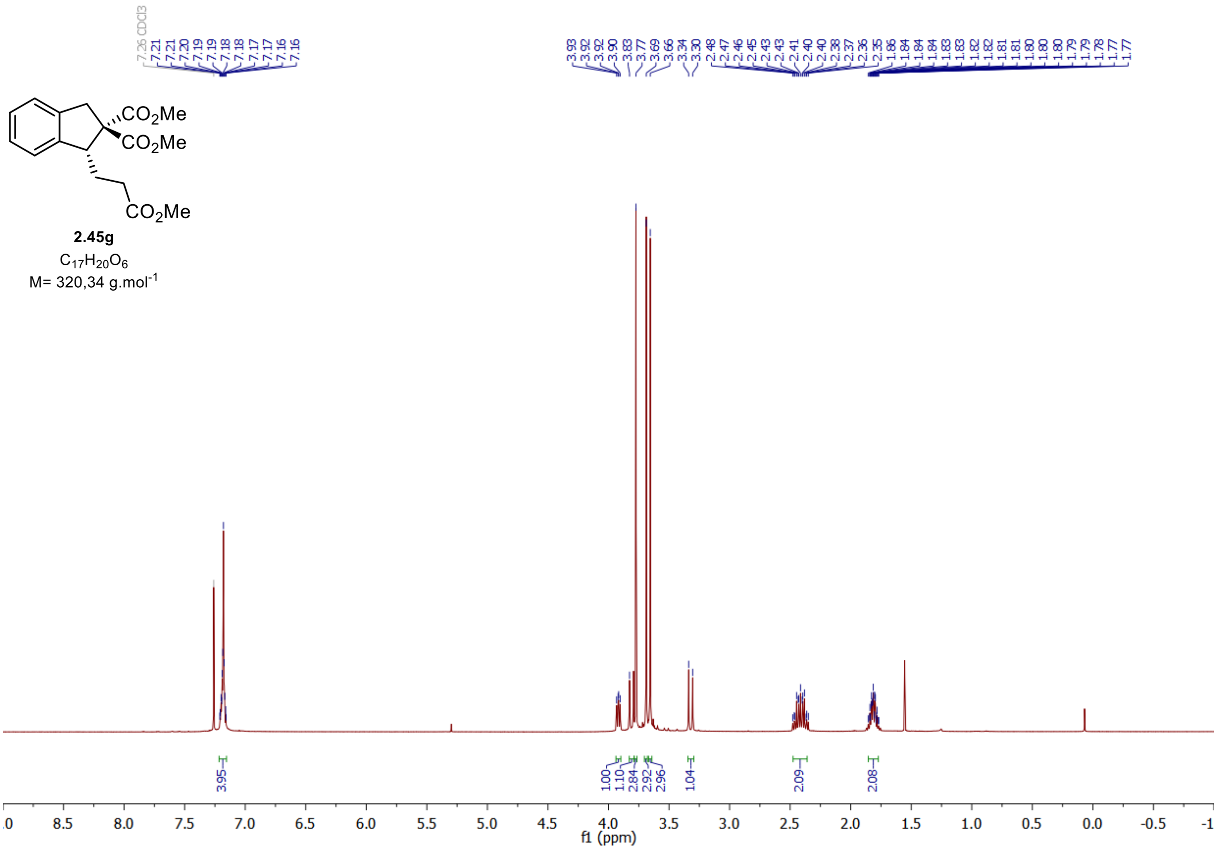

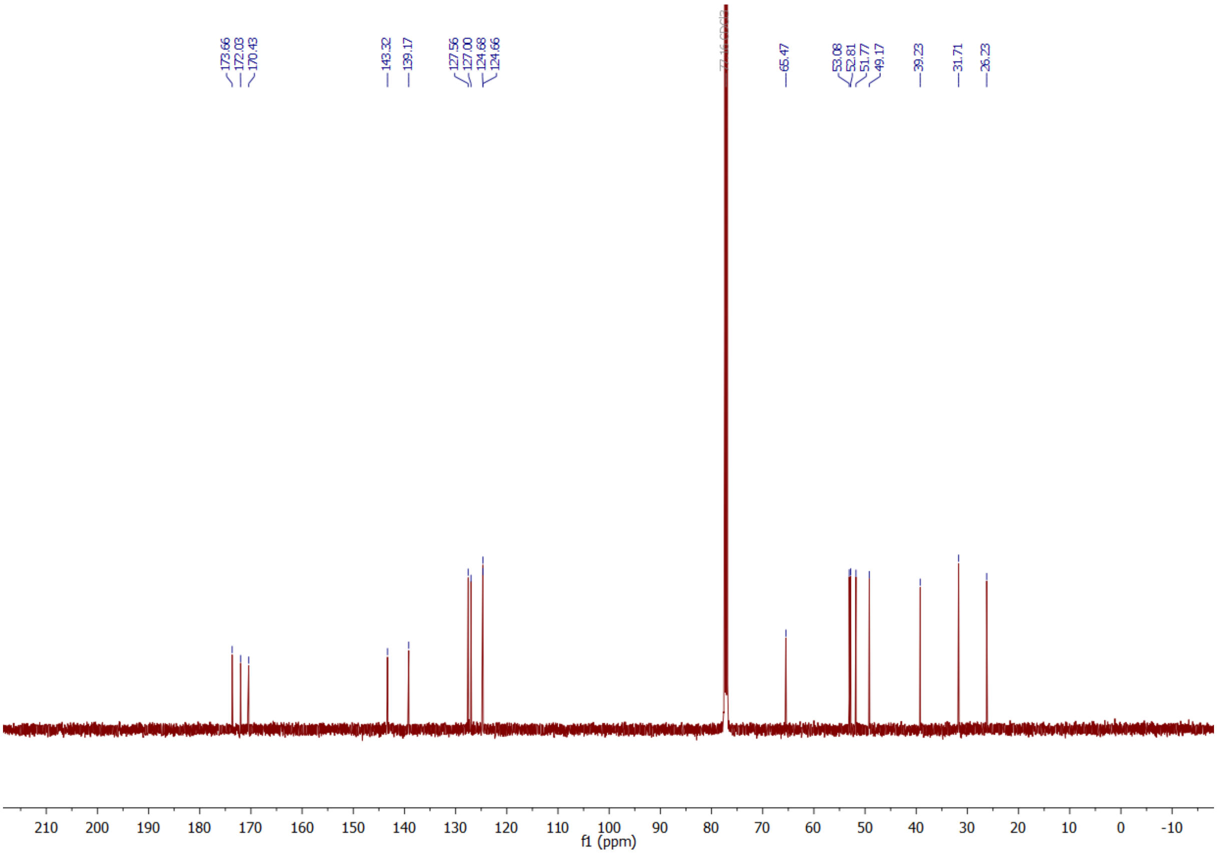

<Chromatogram>

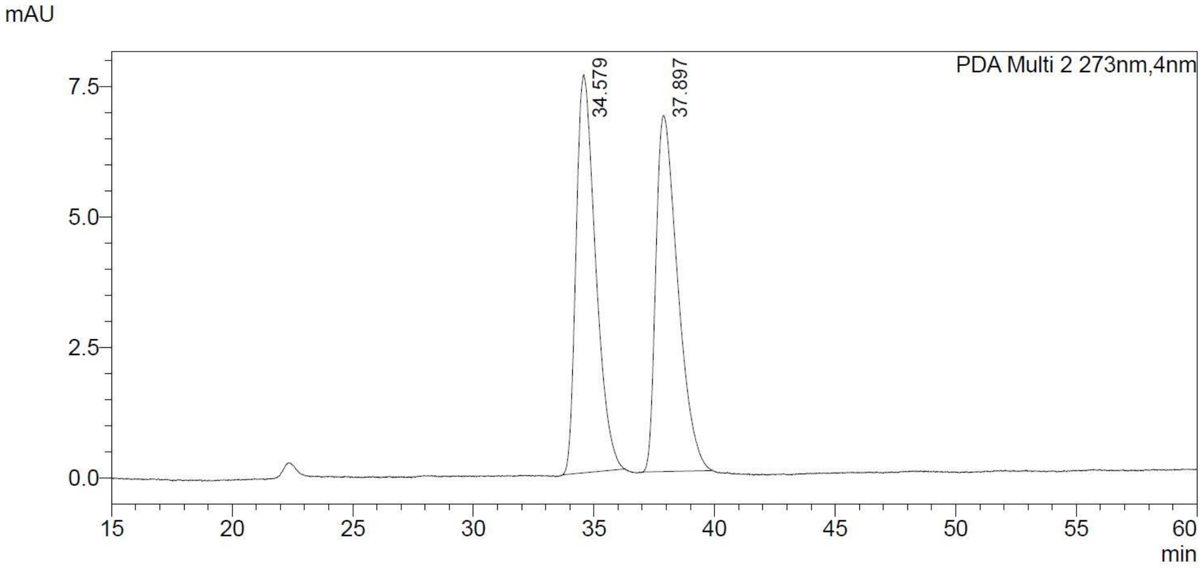

<Peak Table>

PDA Ch2 273nm

Peak#	Ret. Time	Area	Area%
1	34.579	429333	49.906
2	37.897	430958	50.094
Total		860291	100.000

<Chromatogram>

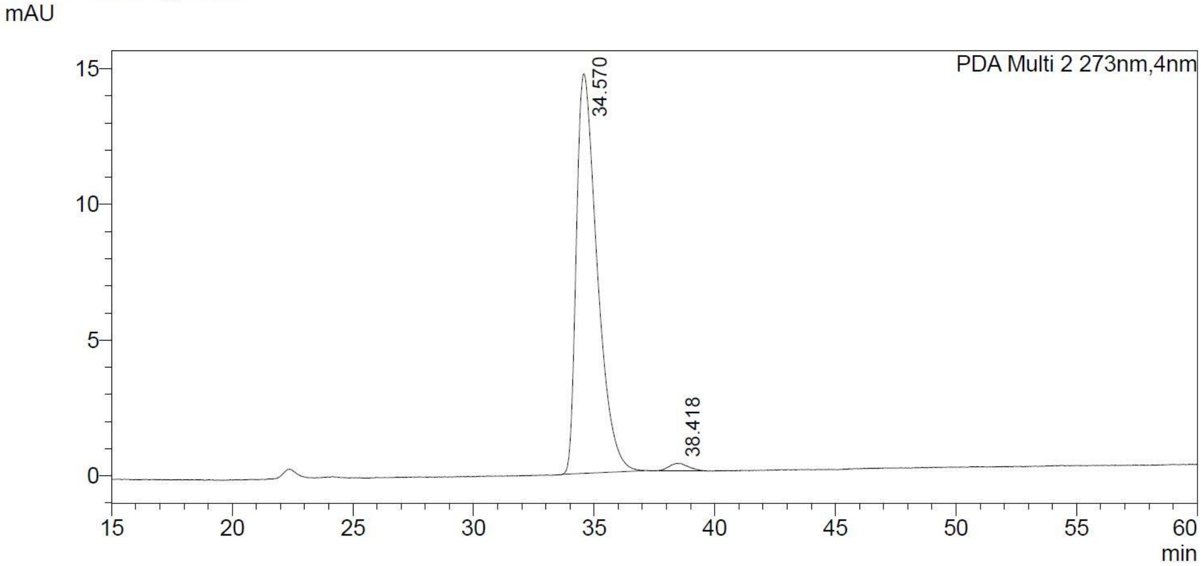

<Peak Table>

PDA Ch2 273nm

Peak#	Ret. Time	Area	Area%
1	34.570	884027	98.403
2	38.418	14351	1.597
Total		898378	100.000

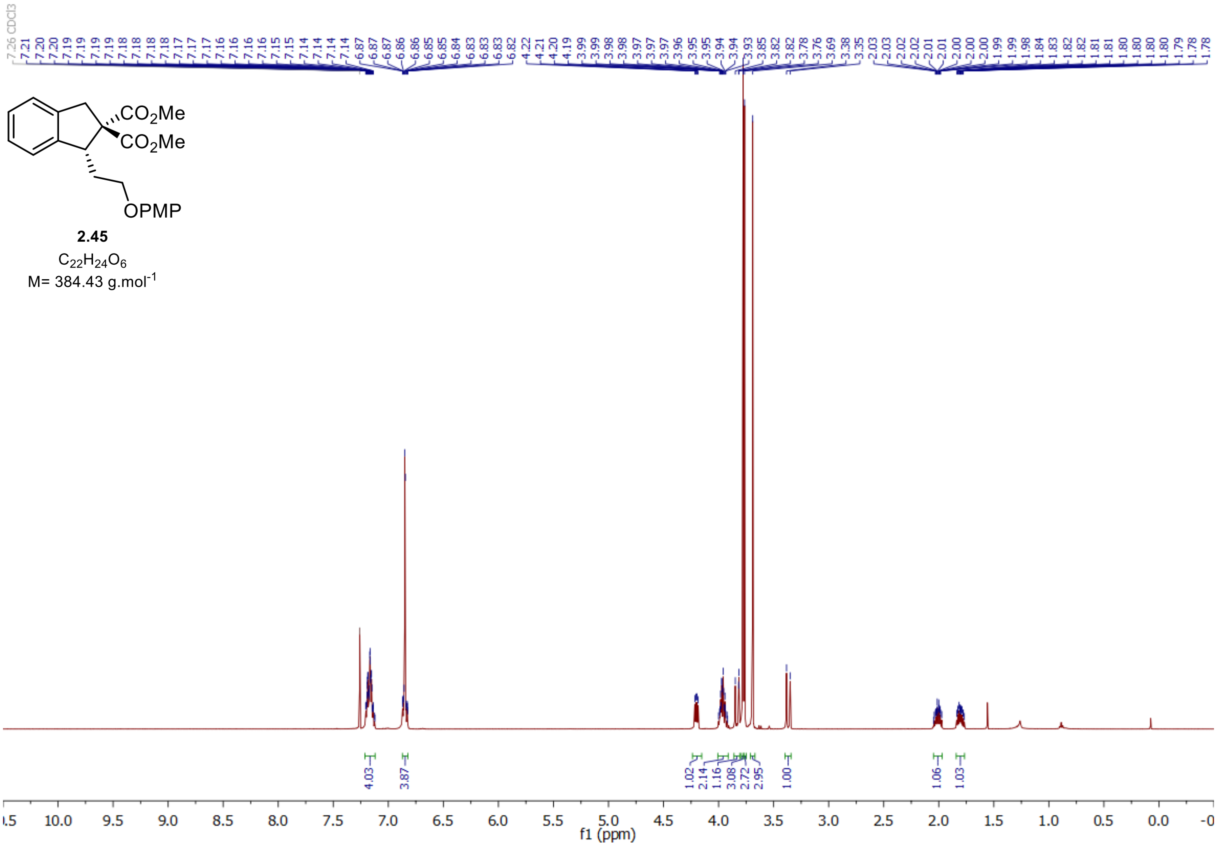

2.45

$C_{22}H_{24}O_6$

M= 384.43 g.mol^{-1}

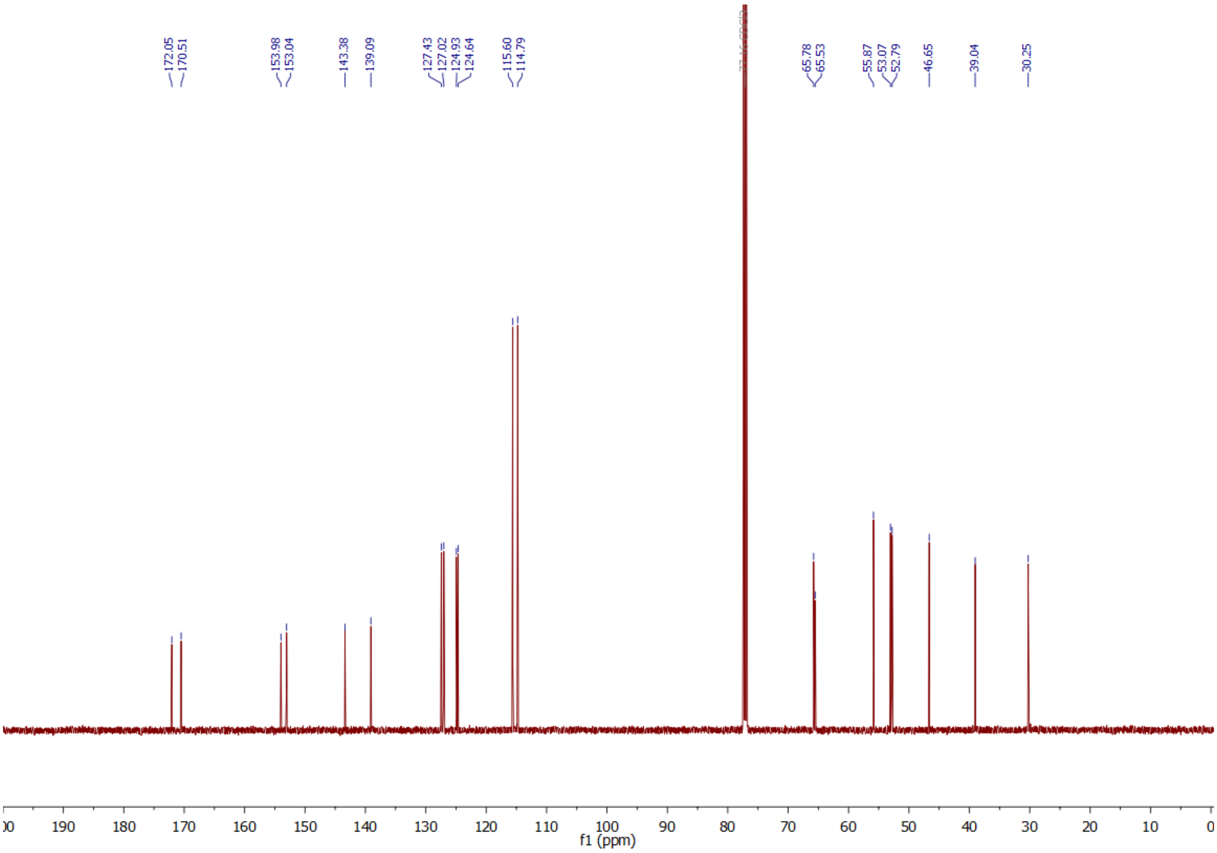

<Chromatogram>

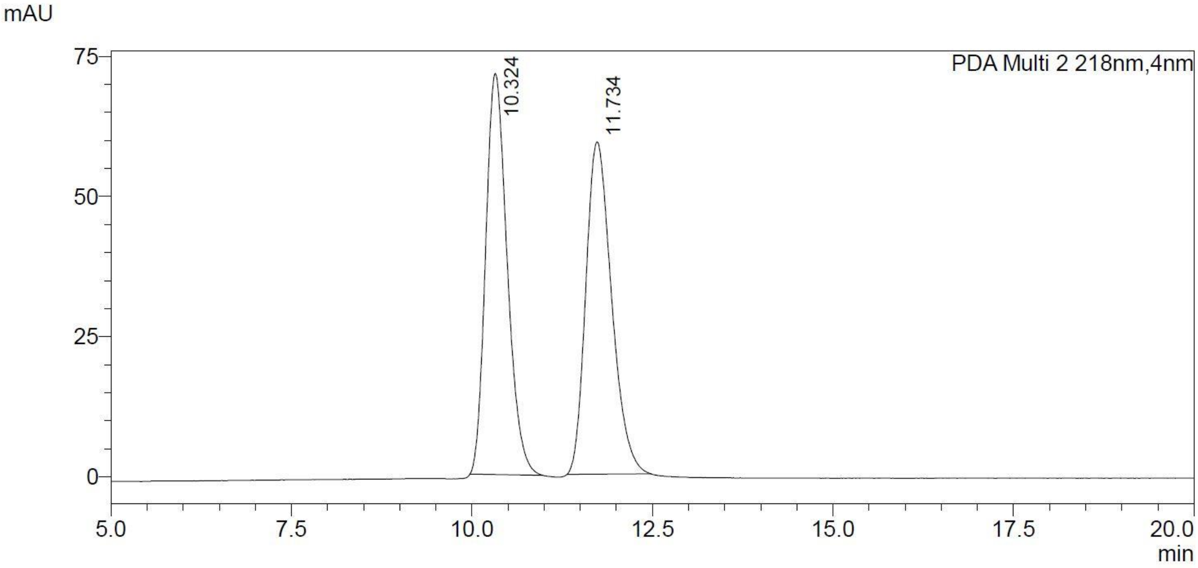

<Peak Table>

PDA Ch2 218nm

Peak#	Ret. Time	Area	Area%
1	10.324	1479813	50.152
2	11.734	1470832	49.848
Total		2950645	100.000

<Chromatogram>

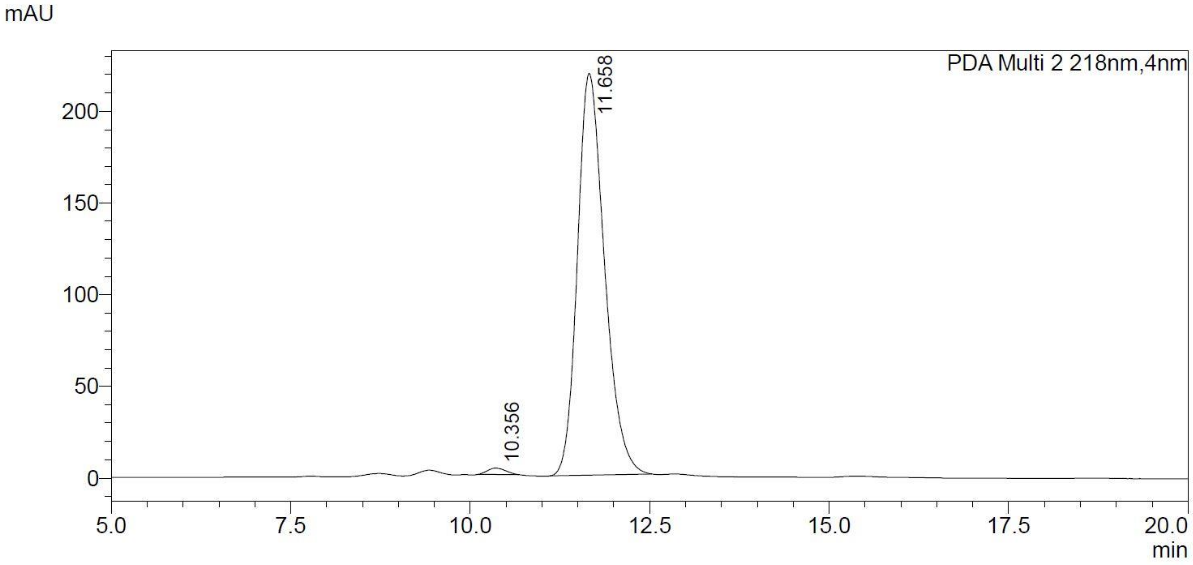

<Peak Table>

PDA Ch2 218nm

Peak#	Ret. Time	Area	Area%
1	10.356	61372	1.056
2	11.658	5749455	98.944
Total		5810828	100.000

<Chromatogram>

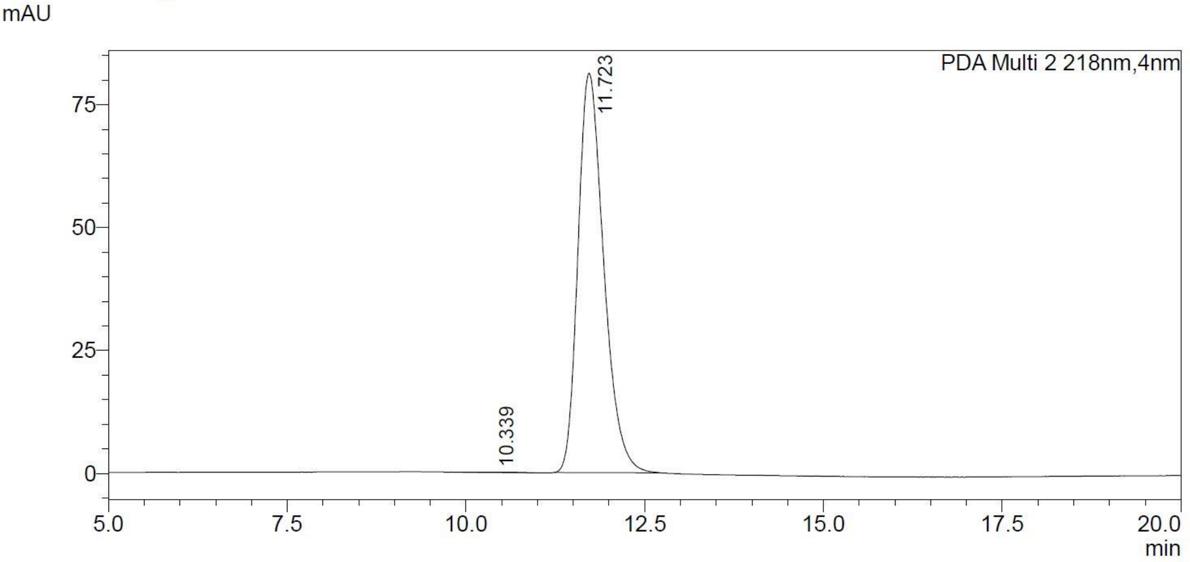

<Peak Table>

PDA Ch2 218nm

Peak#	Ret. Time	Area	Area%
1	10.339	2229	0.109
2	11.723	2037827	99.891
Total		2040057	100.000

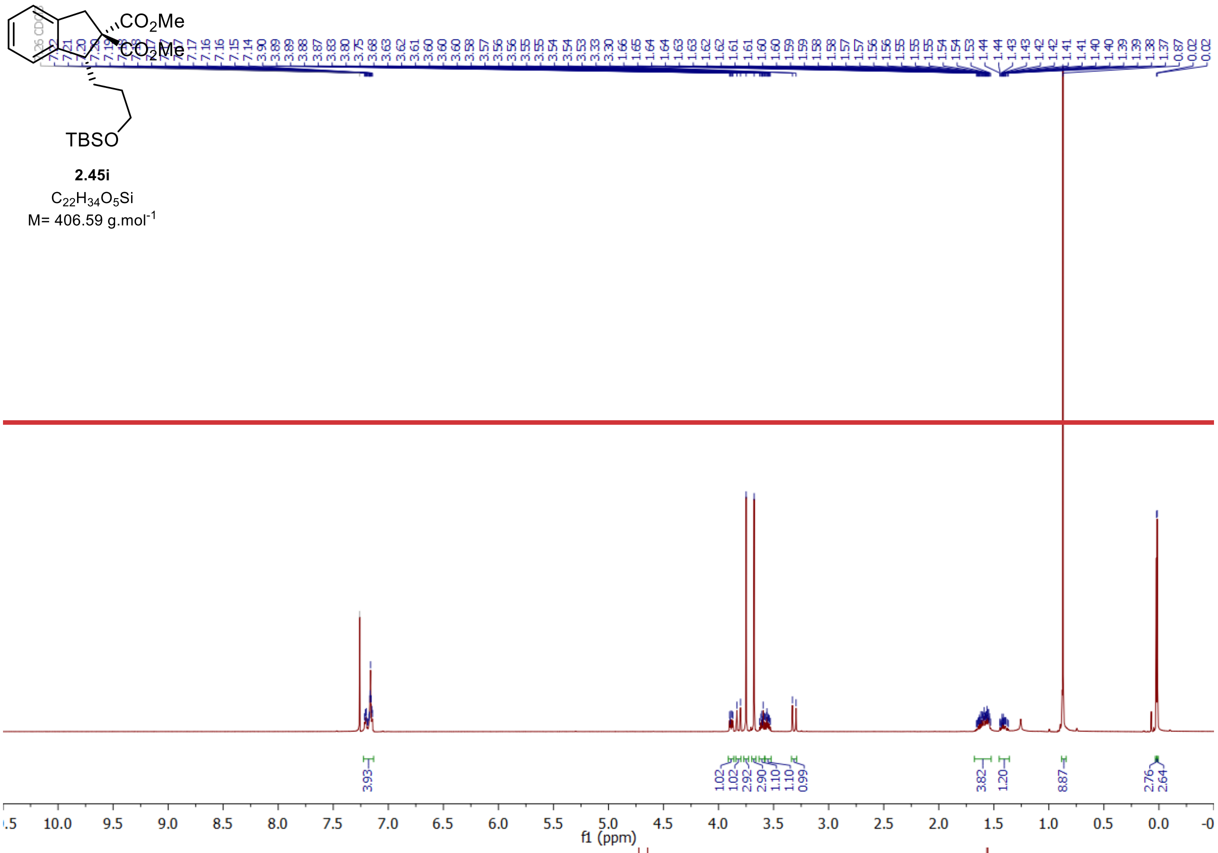

2.45i

$C_{22}H_{34}O_5Si$

M= 406.59 g.mol^{-1}

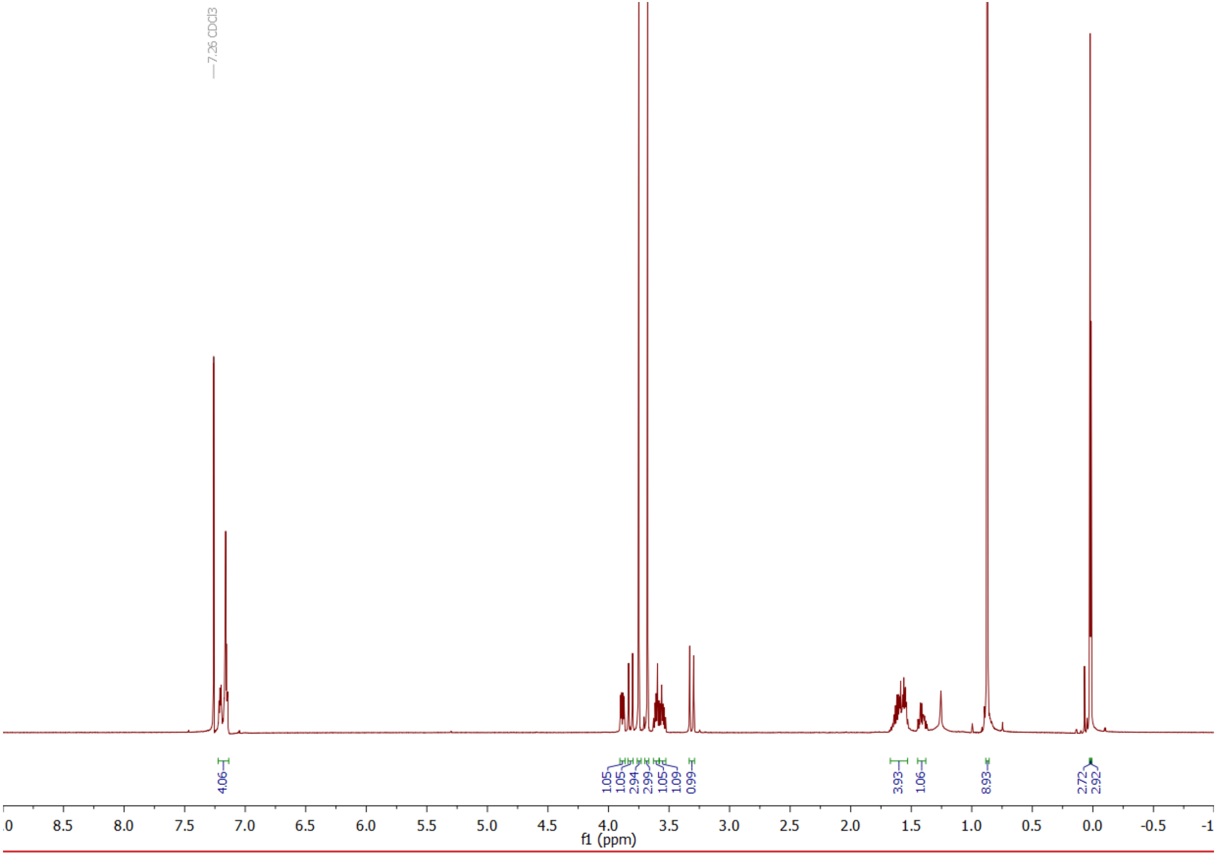

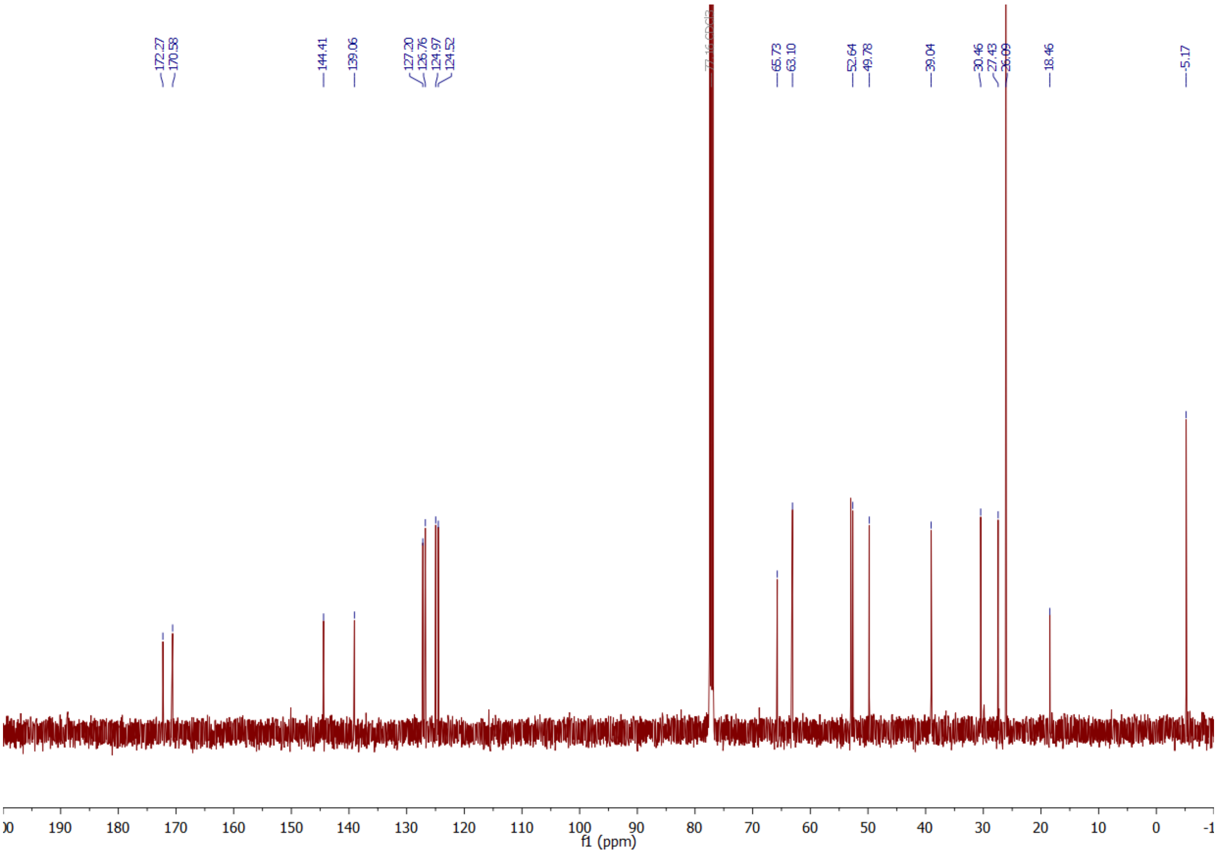
172.27
170.58
144.41
139.06
127.20
126.76
124.97
124.52
77.16 CDCl3
65.73
63.10
52.64
49.78
39.04
30.46
27.43
26.09
18.46
-5.17
190
180
170
160
150
140
130
120
110
100
90
80
70
60
50
40
30
20
10
0
-1
f1 (ppm)

<Chromatogram>

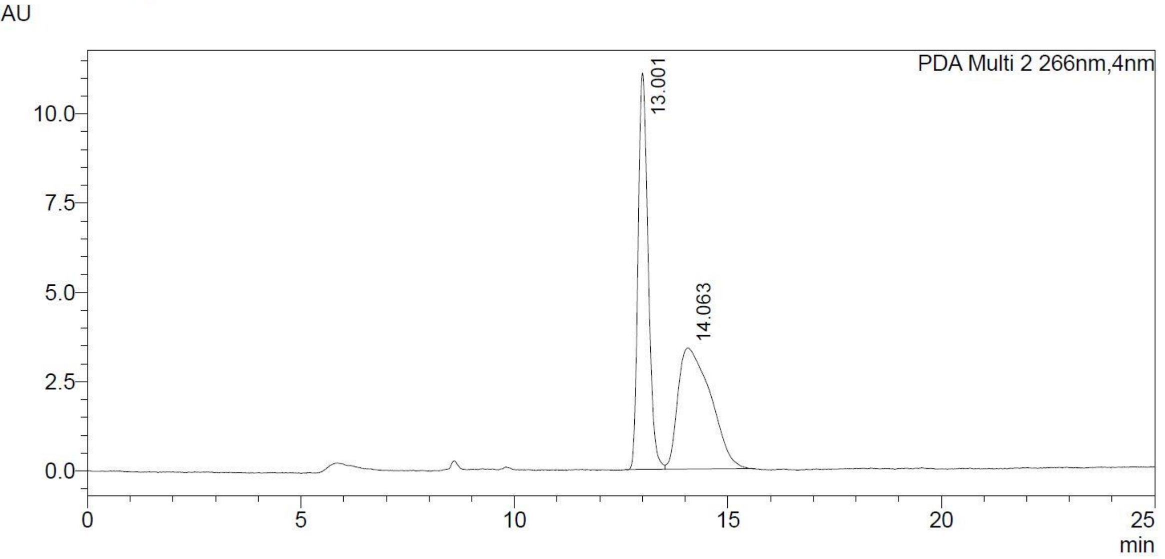

<Peak Table>

PDA Ch2 266nm

Peak#	Ret. Time	Area	Area%
1	13.001	182022	50.235
2	14.063	180318	49.765
Total		362340	100.000

<Chromatogram>

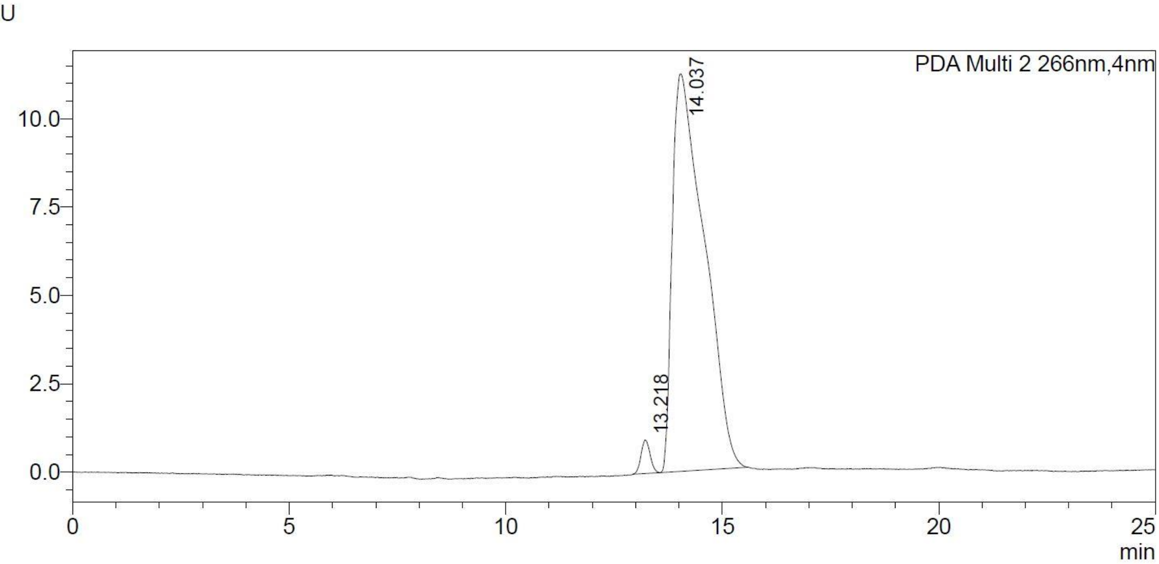

<Peak Table>

PDA Ch2 266nm

Peak#	Ret. Time	Area	Area%
1	13.218	13914	2.354
2	14.037	577191	97.646
Total		591105	100.000

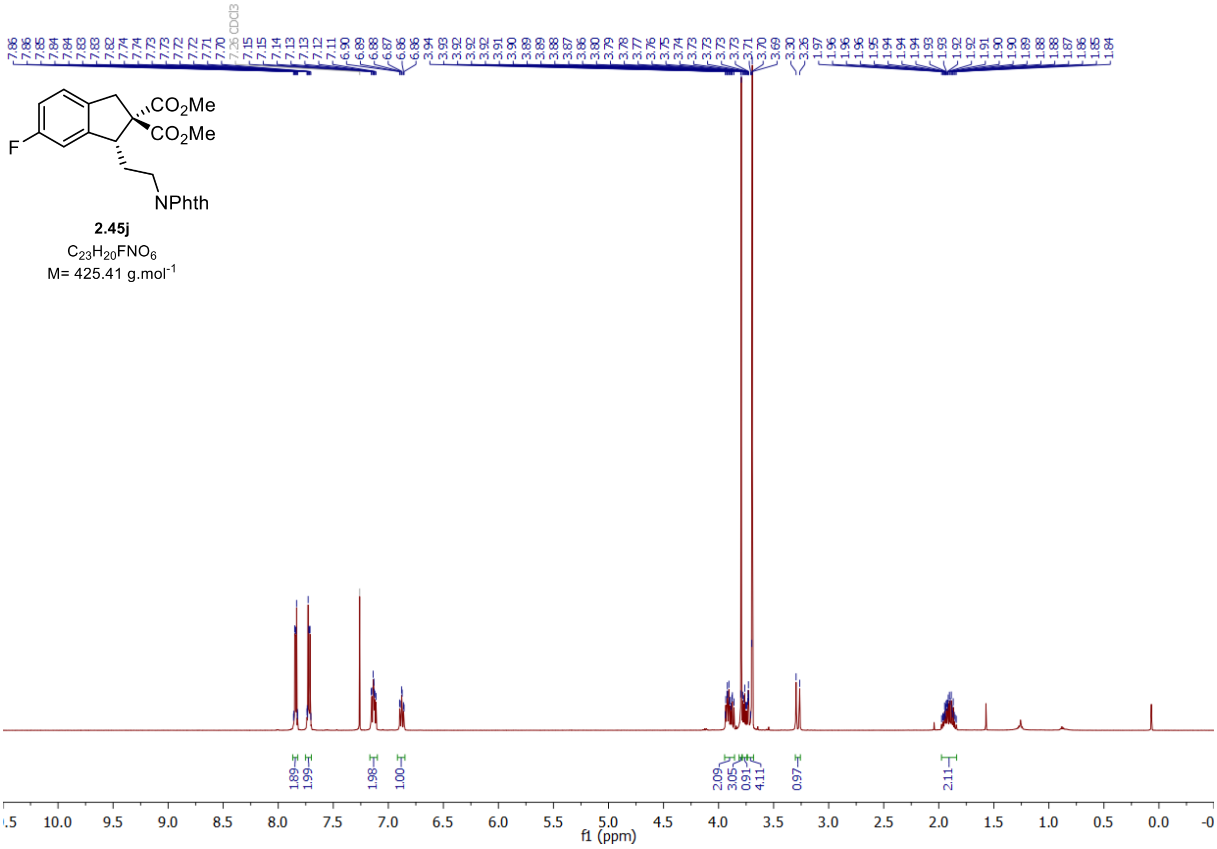

2.45j

$C_{23}H_{20}FNO_6$

M= 425.41 g.mol^{-1}

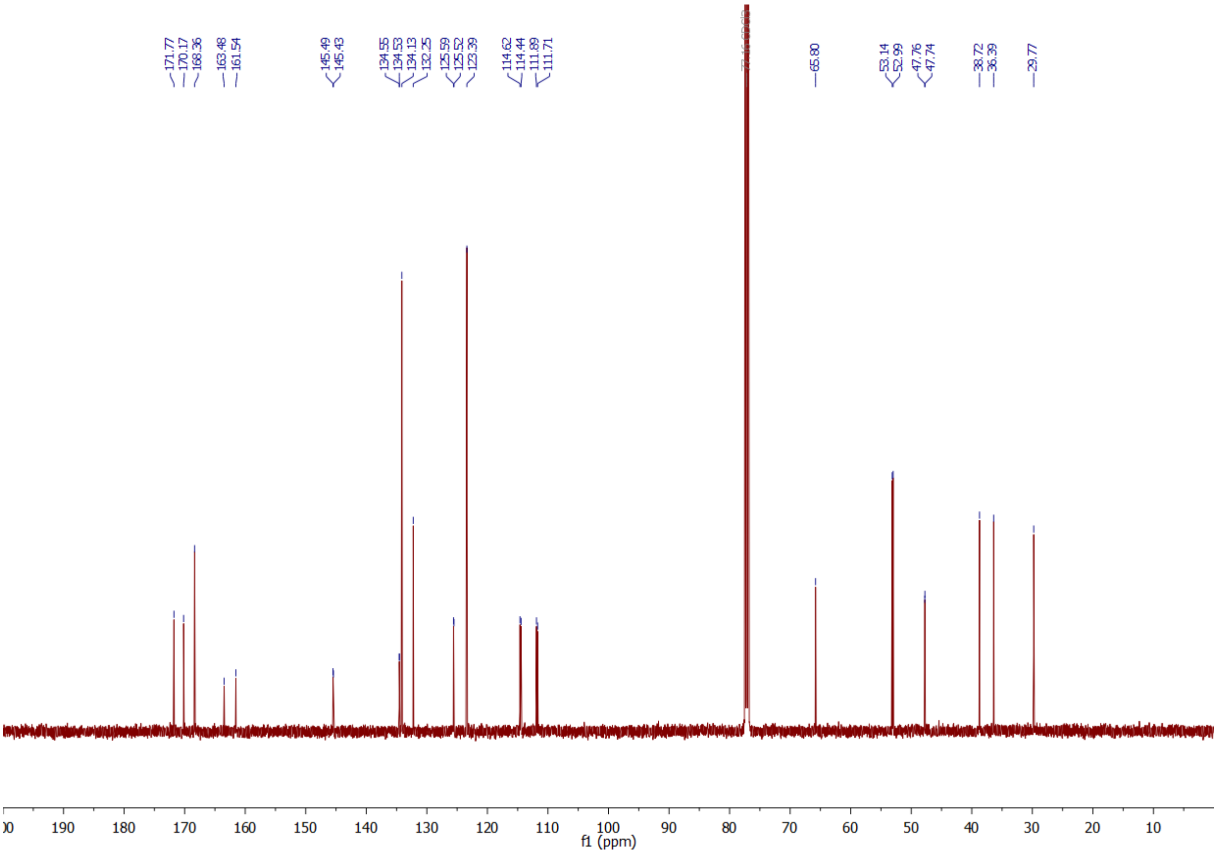

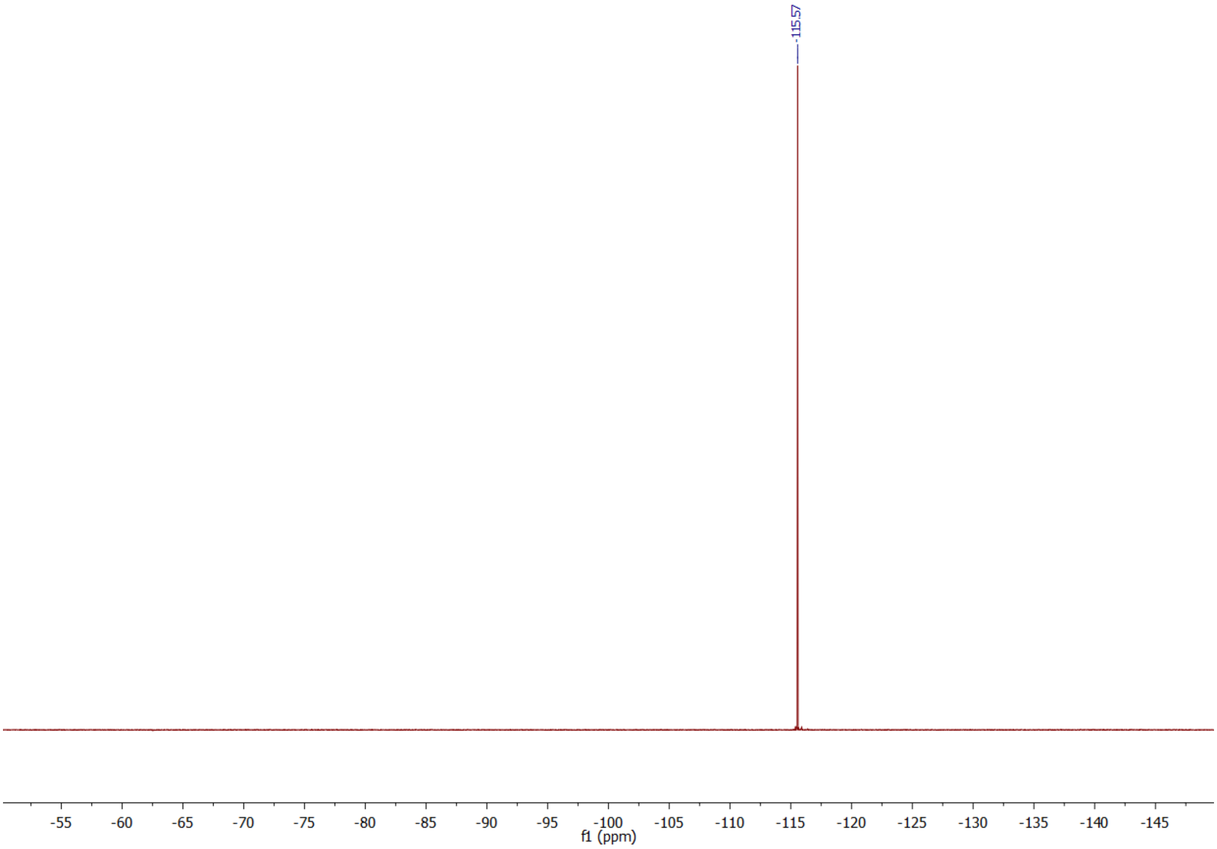
-115.57
-55
-60
-65
-70
-75
-80
-85
-90
-95
-100
-105
-110
-115
-120
-125
-130
-135
-140
-145
f1 (ppm)

<Chromatogram>

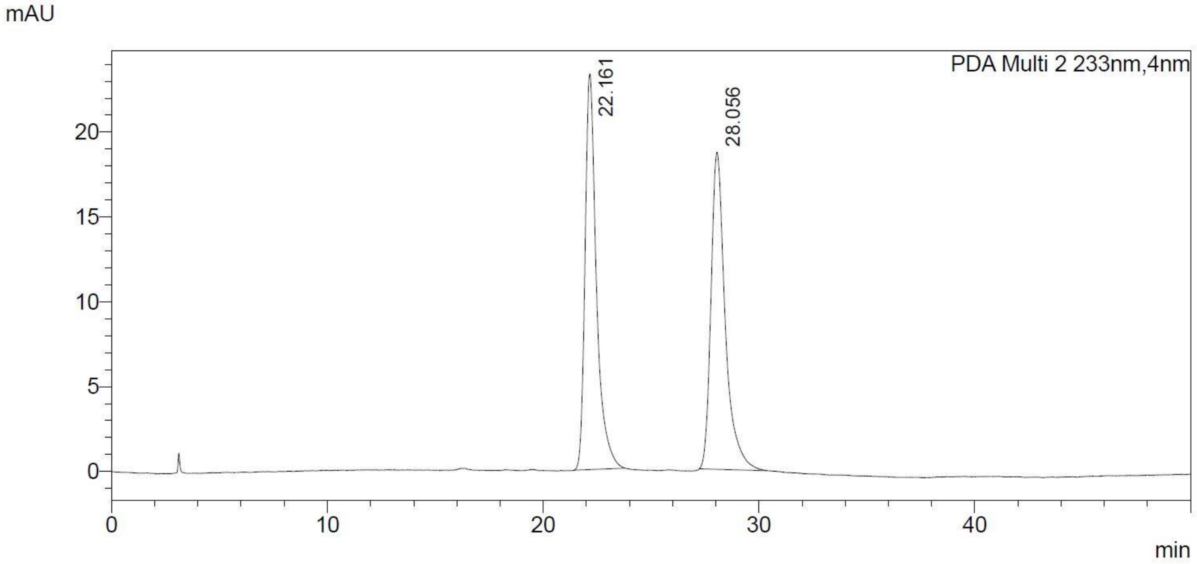

<Peak Table>

PDA Ch2 233nm

Peak#	Ret. Time	Area	Area%
1	22.161	852634	49.833
2	28.056	858348	50.167
Total		1710982	100.000

<Chromatogram>

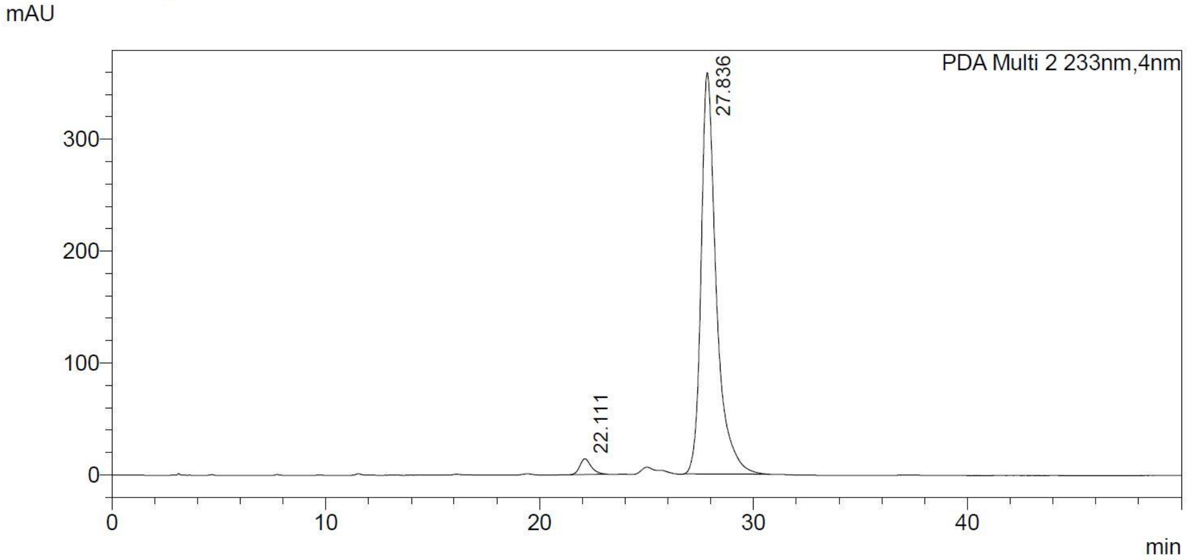

<Peak Table>

PDA Ch2 233nm

Peak#	Ret. Time	Area	Area%
1	22.111	510996	2.801
2	27.836	17733284	97.199
Total		18244280	100.000

<Chromatogram>

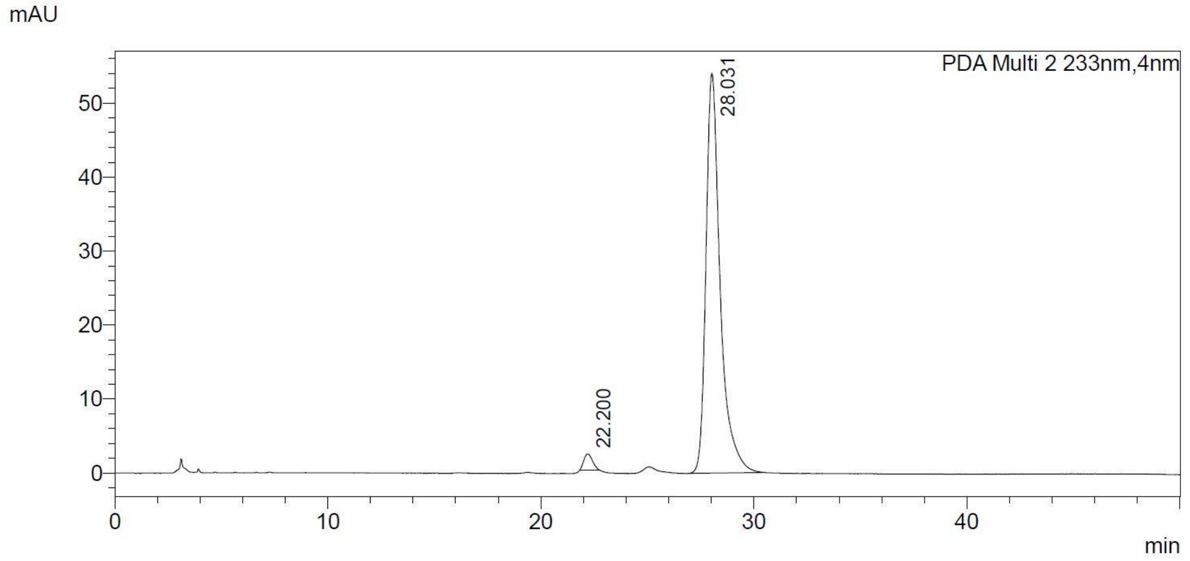

<Peak Table>

PDA Ch2 233nm

Peak#	Ret. Time	Area	Area%
1	22.200	62571	2.435
2	28.031	2506791	97.565
Total		2569362	100.000

2.00 mmol scale **:**

<Chromatogram>

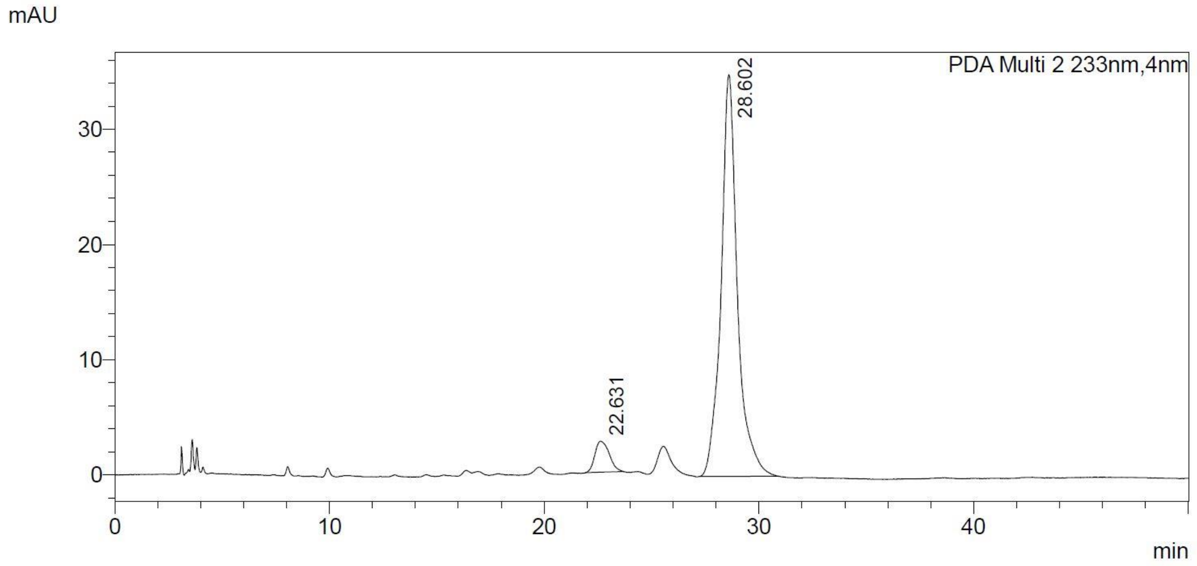

<Peak Table>

PDA Ch2 233nm

Peak#	Ret. Time	Area	Area%
1	22.631	125586	6.375
2	28.602	1844341	93.625
Total		1969926	100.000

<Chromatogram>

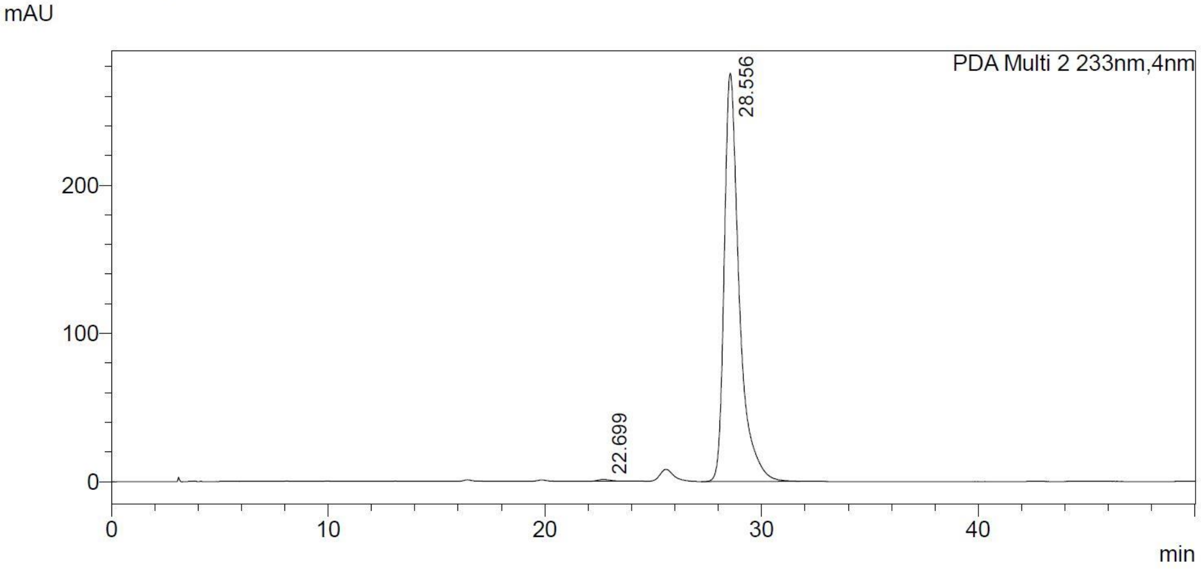

<Peak Table>

PDA Ch2 233nm

Peak#	Ret. Time	Area	Area%
1	22.699	38989	0.294
2	28.556	13214100	99.706
Total		13253089	100.000

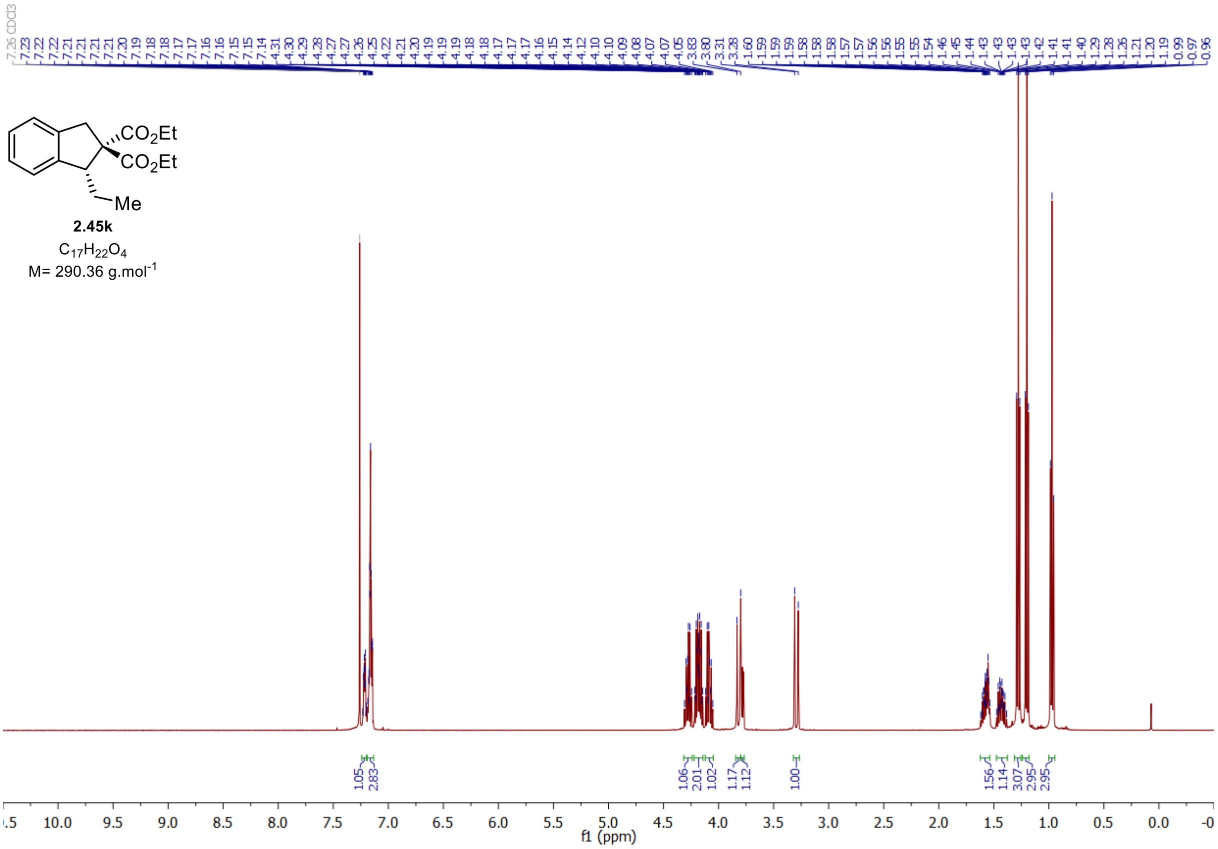

CO2Et
CO2Et
Me
2.45k
C17H22O4
M= 290.36 g.mol-1
7.26 CDCl3
7.23
7.22
7.22
7.21
7.21
7.21
7.21
7.20
7.19
7.18
7.17
7.17
7.16
7.16
7.15
7.15
7.14
4.31
4.30
4.29
4.28
4.27
4.27
4.26
4.25
4.22
4.21
4.20
4.19
4.19
4.19
4.18
4.18
4.17
4.17
4.17
4.16
4.15
4.14
4.12
4.10
4.10
4.09
4.08
4.07
4.07
4.05
3.83
3.80
3.31
3.28
1.60
1.59
1.59
1.59
1.59
1.58
1.58
1.58
1.57
1.57
1.56
1.56
1.55
1.55
1.54
1.46
1.45
1.44
1.43
1.43
1.43
1.43
1.42
1.41
1.41
1.40
1.29
1.28
1.26
1.21
1.20
1.19
0.99
0.97
0.96
1.05
2.83
1.06
2.01
1.02
1.17
1.12
1.00
1.56
1.14
3.07
2.95
2.95
10.0
9.5
9.0
8.5
8.0
7.5
7.0
6.5
6.0
5.5
5.0
4.5
4.0
3.5
3.0
2.5
2.0
1.5
1.0
0.5
0.0
f1 (ppm)

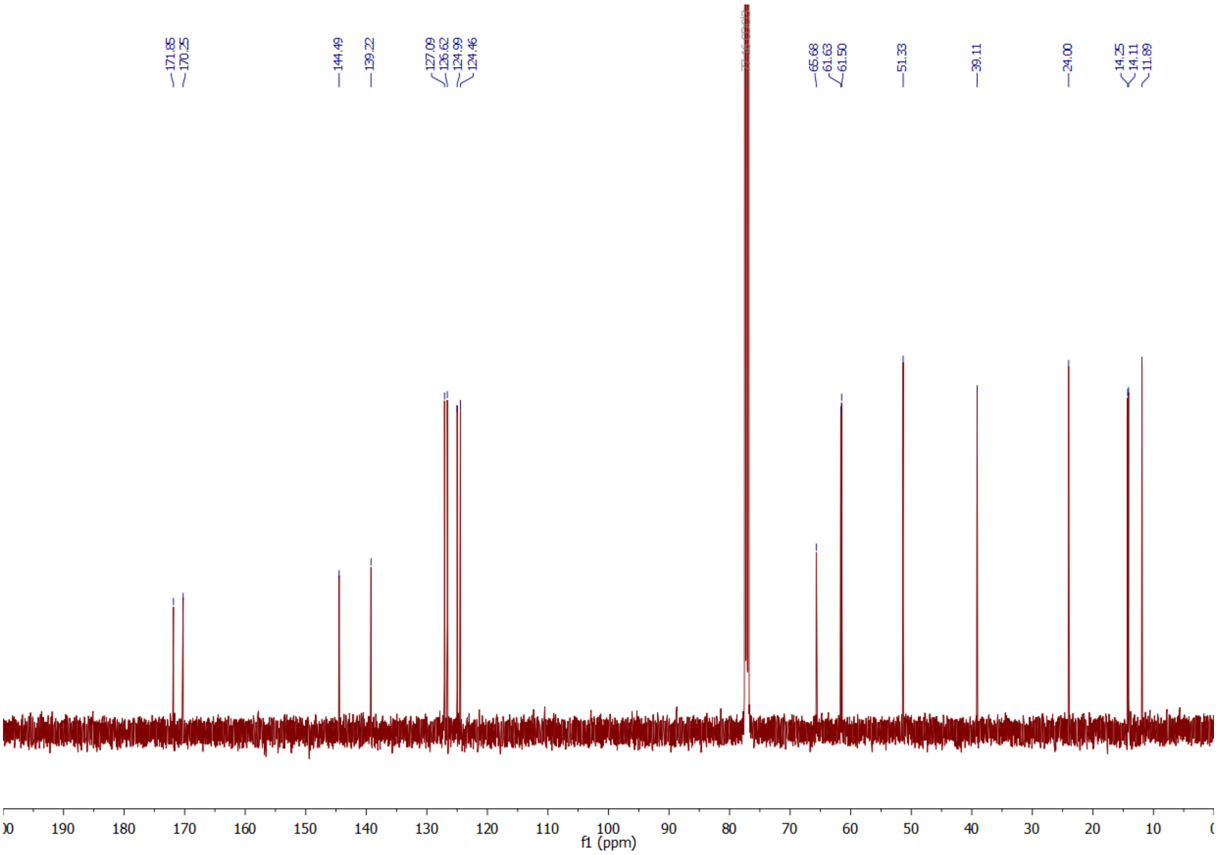

171.85
170.25
144.49
139.22
127.09
126.62
124.99
124.46
77.16 CDCl3
65.68
61.63
61.50
51.33
39.11
24.00
14.25
14.11
11.89
190
180
170
160
150
140
130
120
110
100
90
80
70
60
50
40
30
20
10
f1 (ppm)

<Chromatogram>

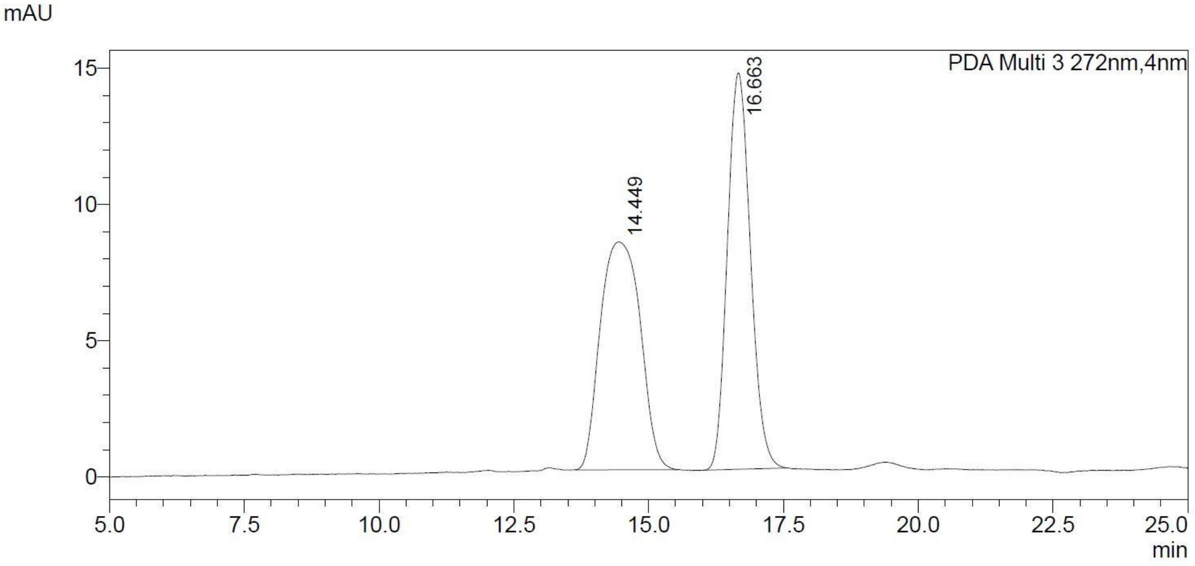

<Peak Table>

PDA Ch3 272nm

Peak#	Ret. Time	Area	Area%
1	14.449	433702	49.959
2	16.663	434421	50.041
Total		868123	100.000

<Chromatogram>

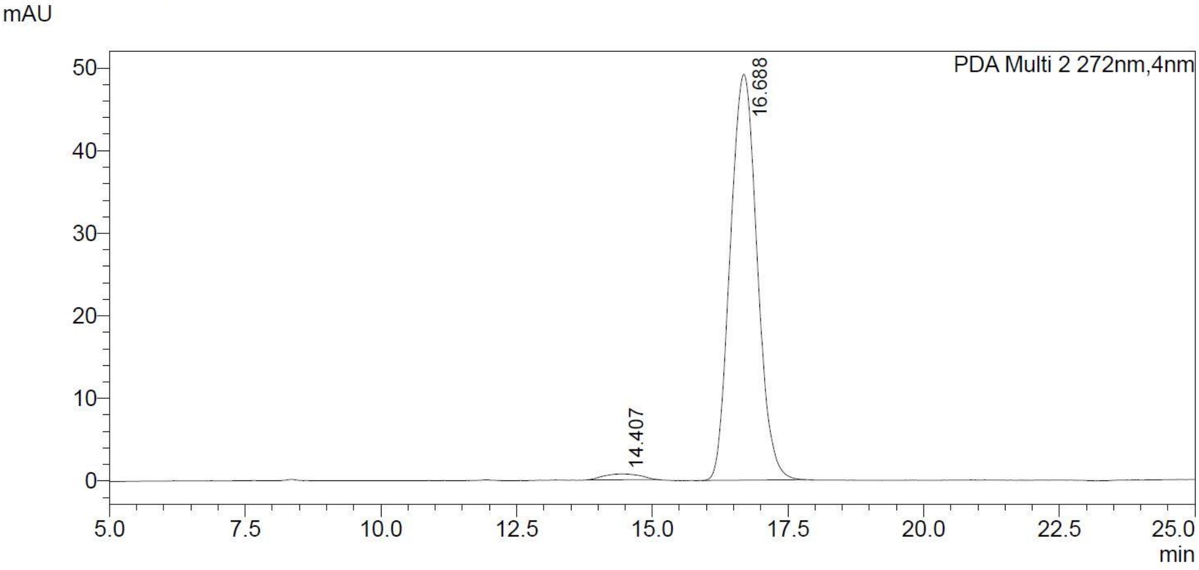

<Peak Table>

PDA Ch2 272nm

Peak#	Ret. Time	Area	Area%
1	14.407	33559	1.944
2	16.688	1692427	98.056
Total		1725986	100.000

CO2iPr
CO2iPr
Me

2.45l

$C_{19}H_{26}O_4$

M= 318.41 g.mol^{-1}

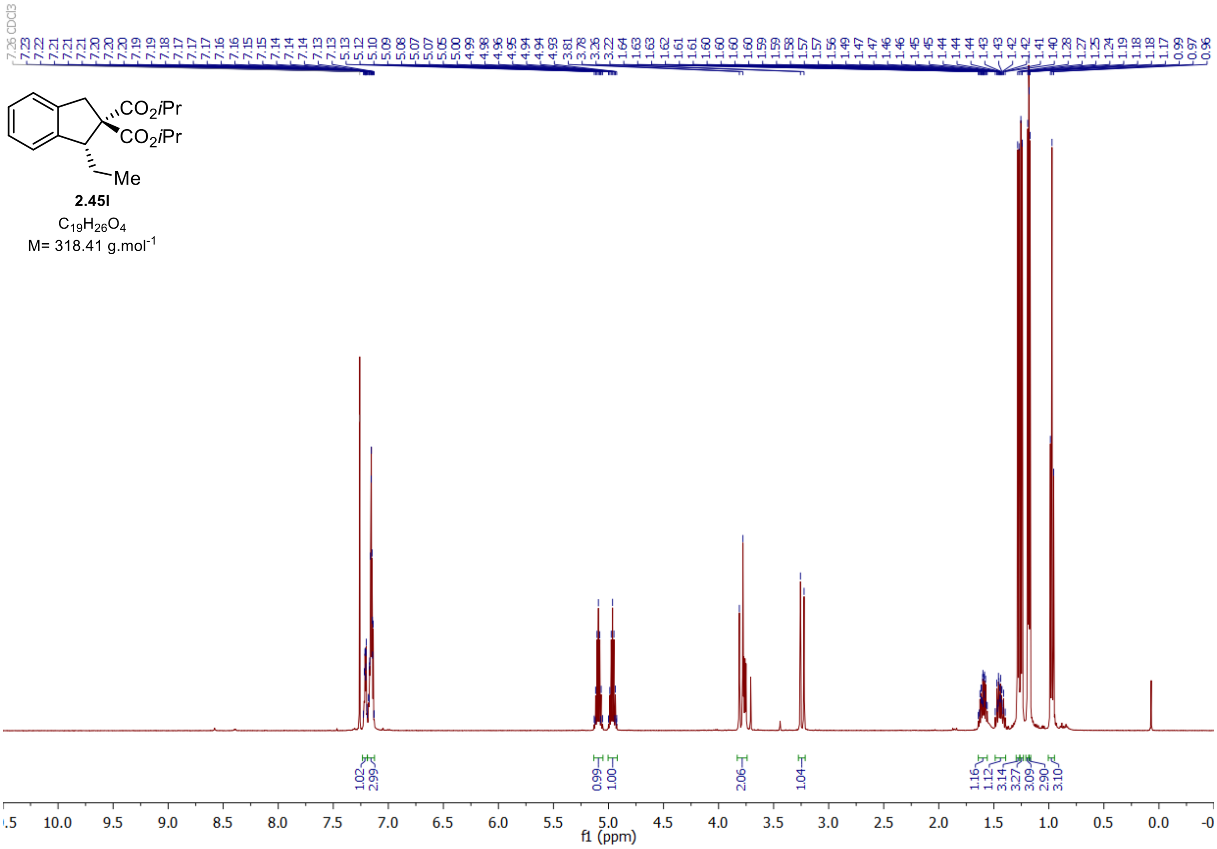

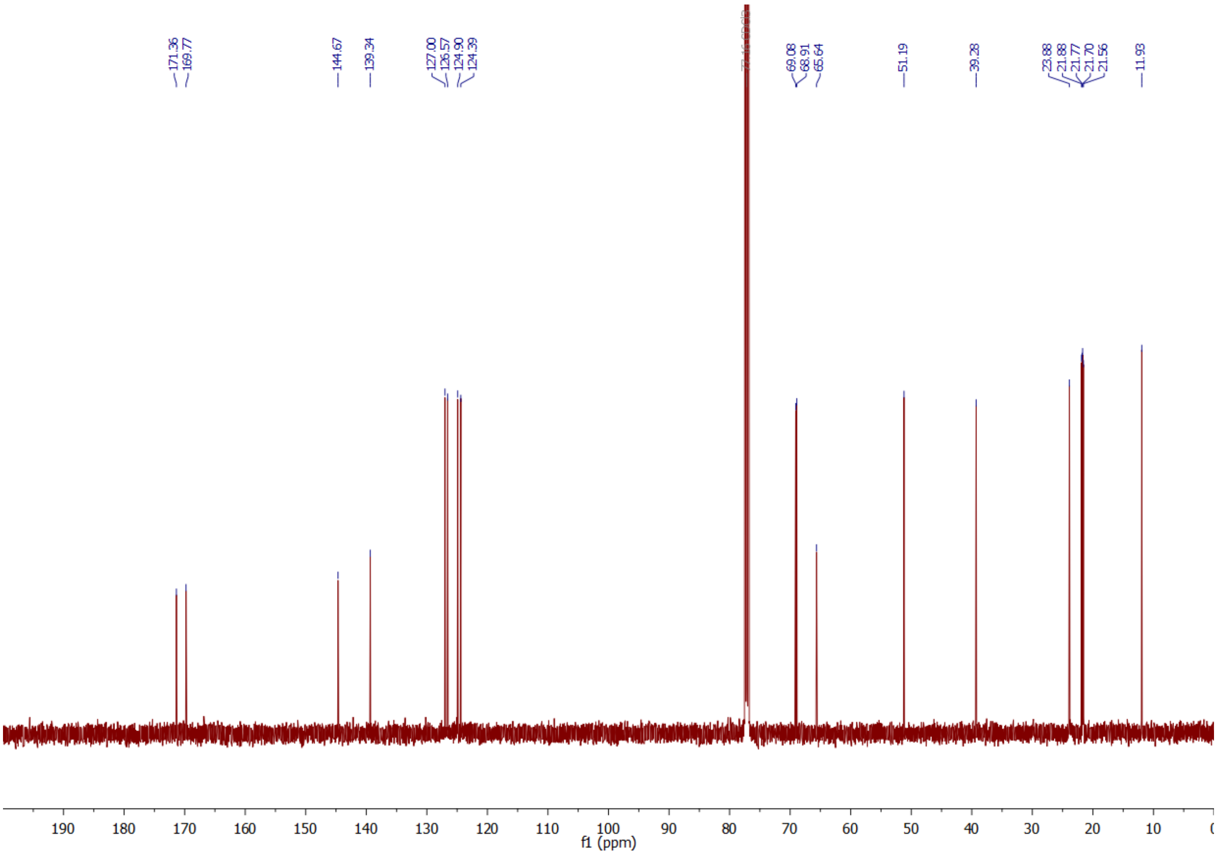

<Chromatogram>

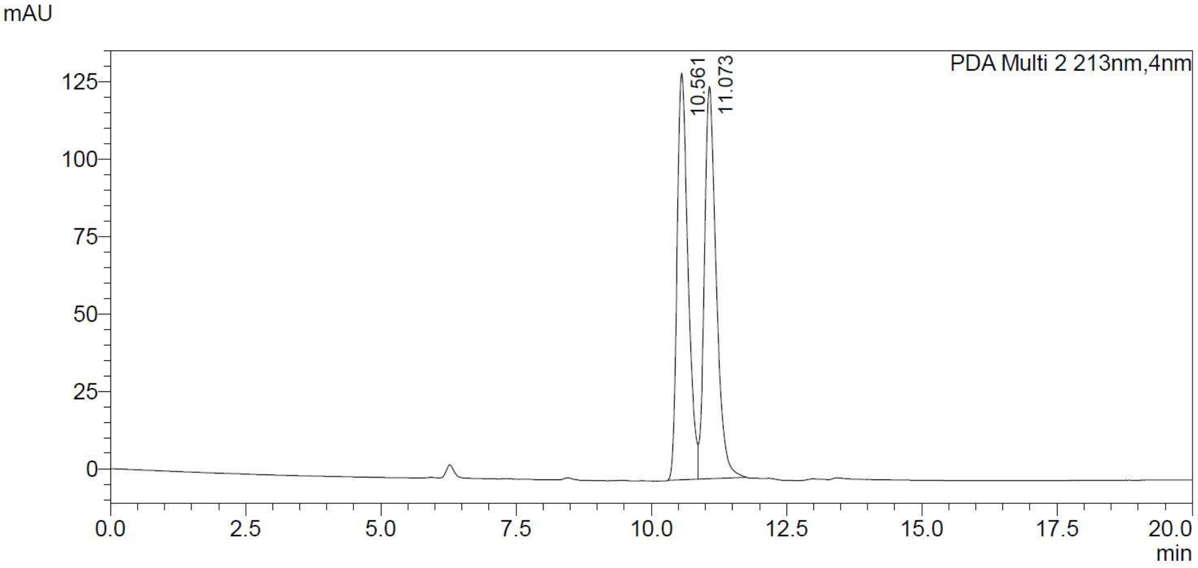

<Peak Table>

PDA Ch2 213nm

Peak#	Ret. Time	Area	Area%
1	10.561	1850668	48.976
2	11.073	1928037	51.024
Total		3778705	100.000

<Chromatogram>

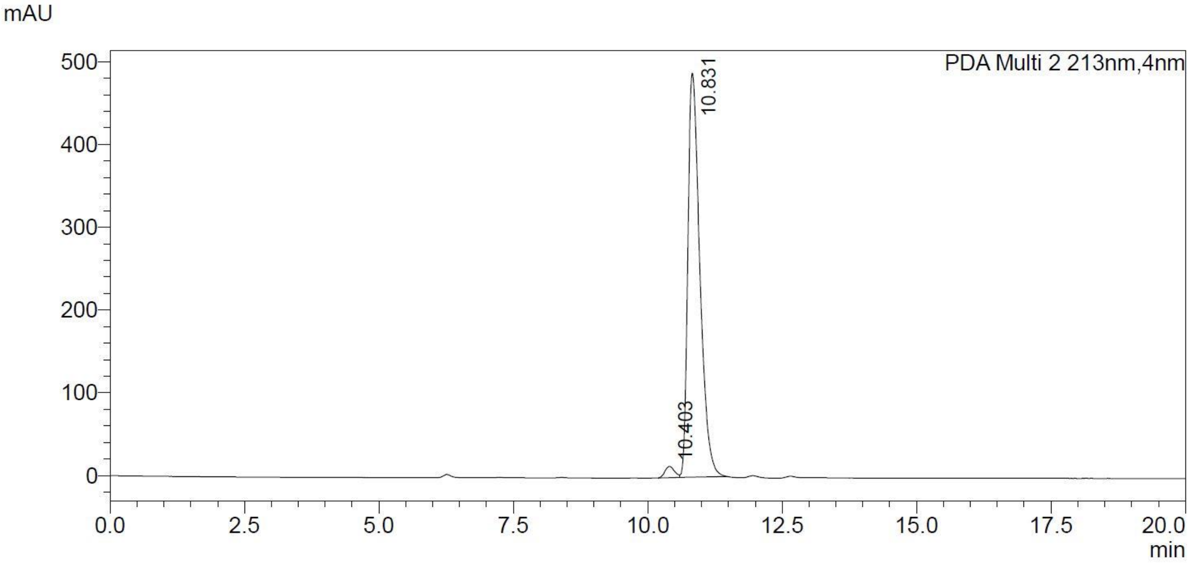

<Peak Table>

PDA Ch2 213nm

Peak#	Ret. Time	Area	Area%
1	10.403	168719	2.181
2	10.831	7568306	97.819
Total		7737025	100.000

F
CO2Me
CO2Me
Me

2m

$C_{15}H_{17}FO_4$

M= 280,30 g.mol^{-1}

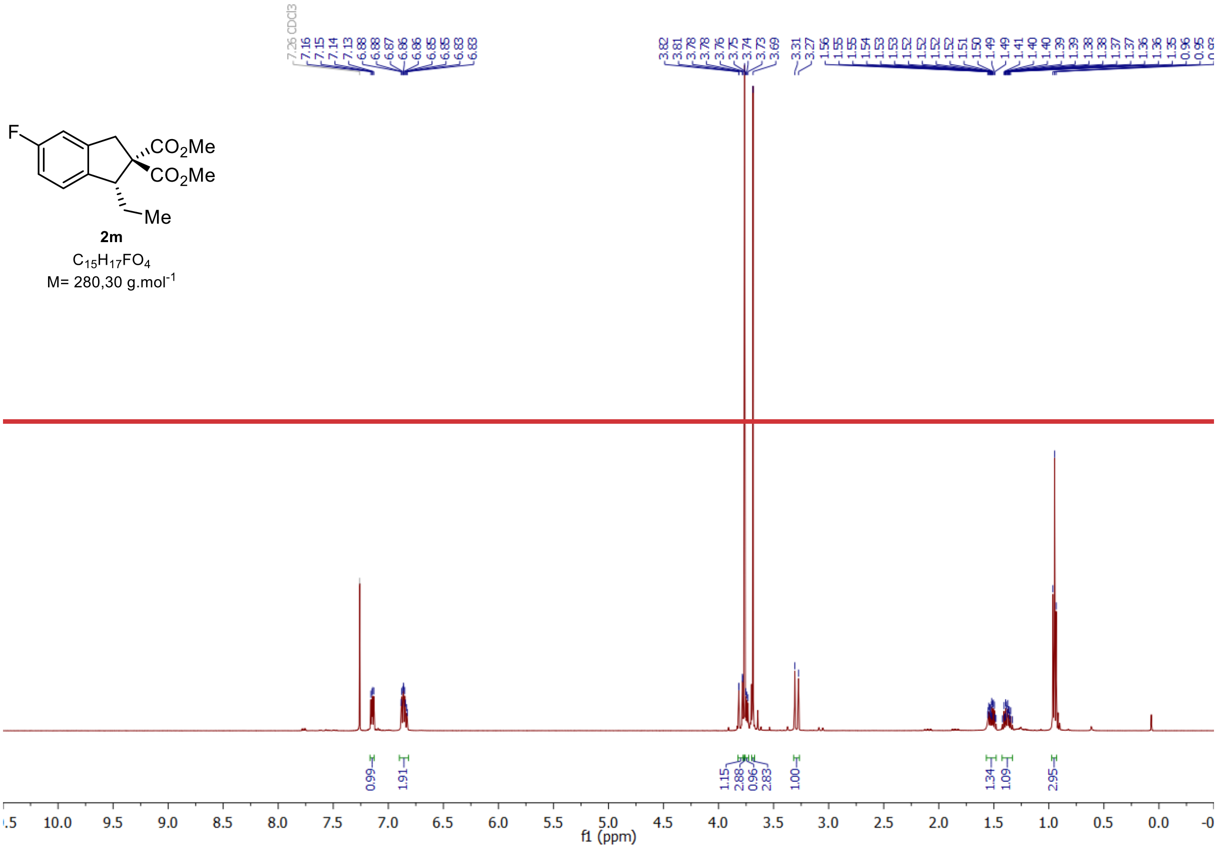

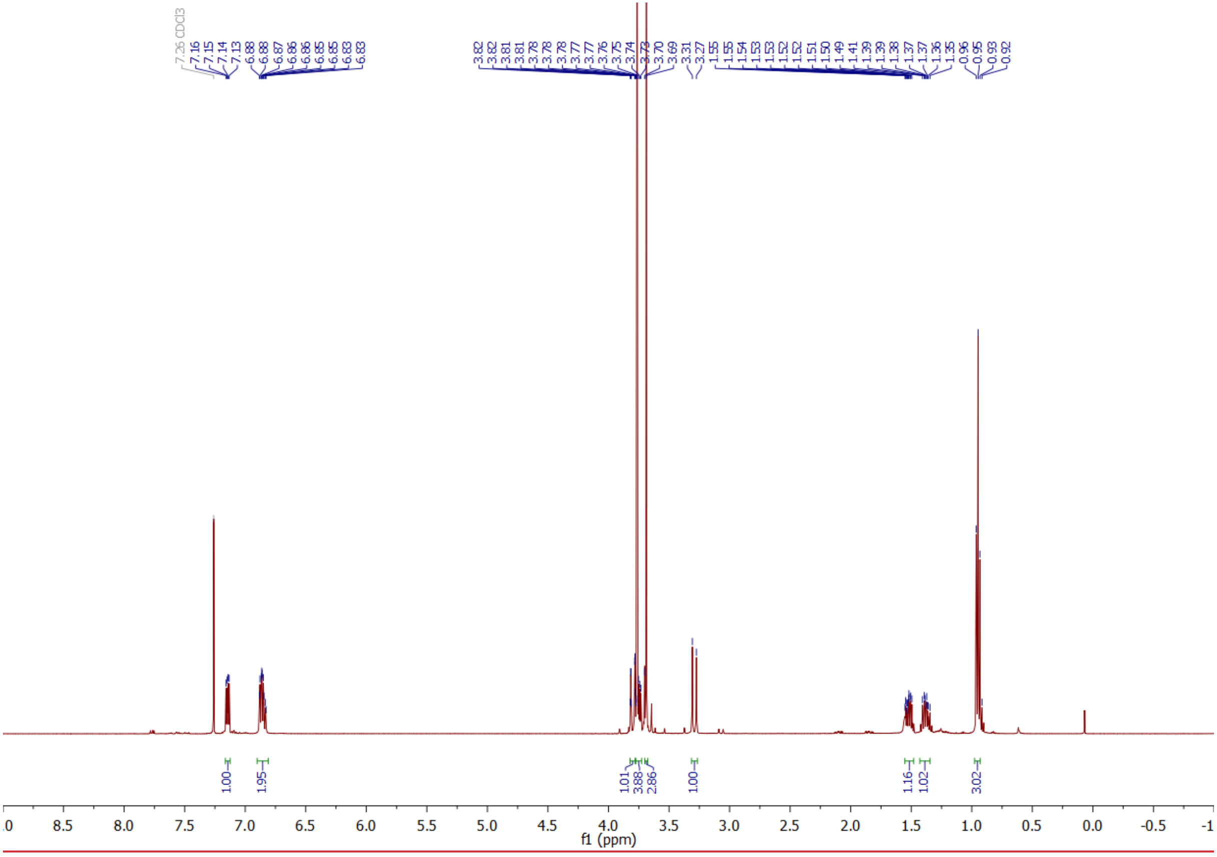

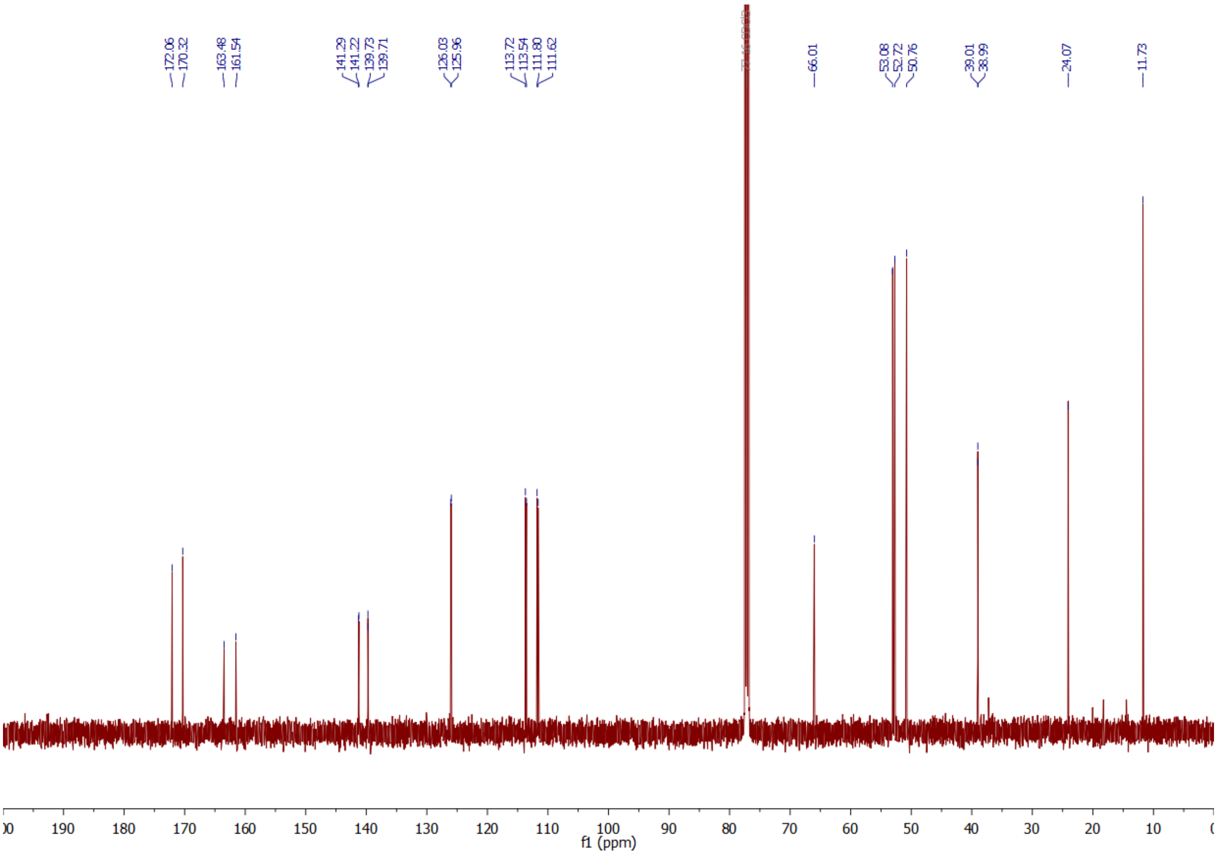
172.06
170.32
163.48
161.54
141.29
141.22
139.73
139.71
126.03
125.96
113.72
113.54
111.80
111.62
66.01
53.08
52.72
50.76
39.01
38.99
24.07
11.73
190
180
170
160
150
140
130
120
110
100
90
80
70
60
50
40
30
20
10
f1 (ppm)

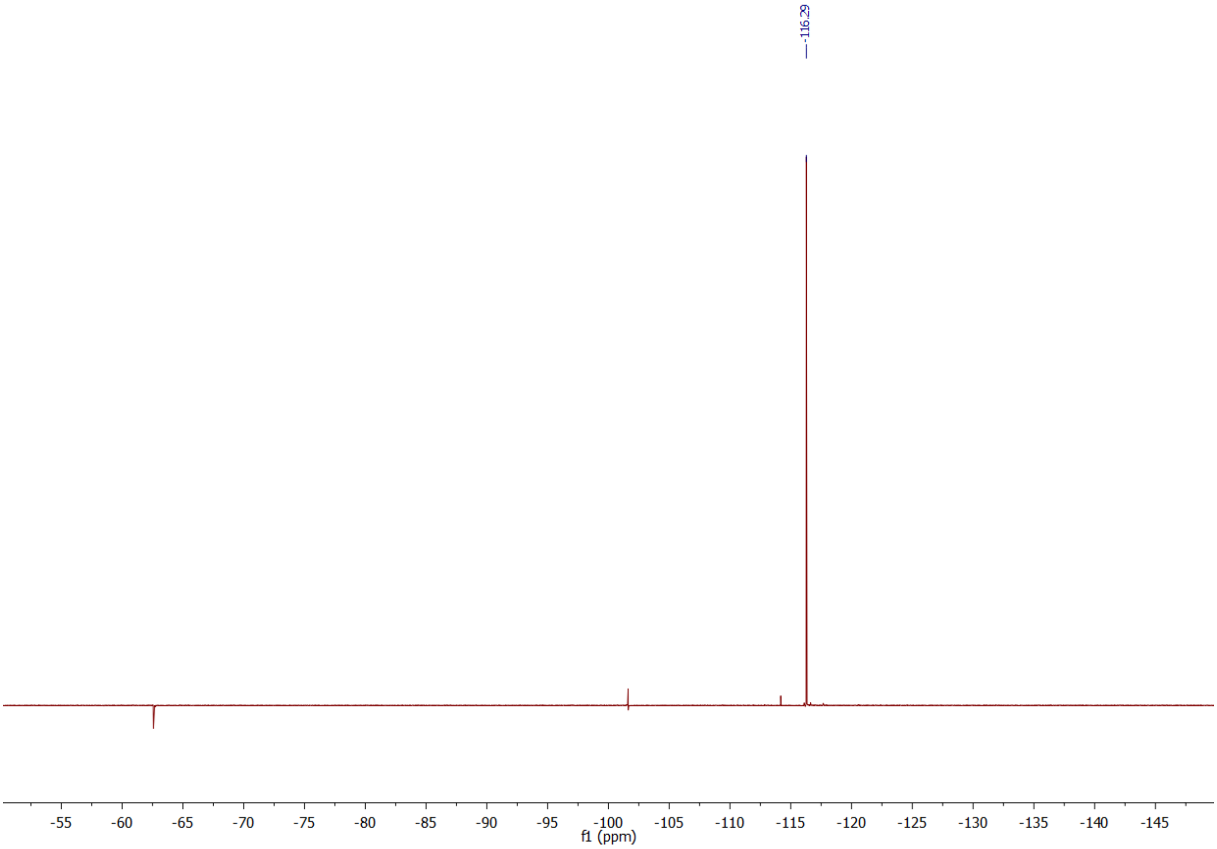
-116.29
-55
-60
-65
-70
-75
-80
-85
-90
-95
-100
-105
-110
-115
-120
-125
-130
-135
-140
-145
f1 (ppm)

<Chromatogram>

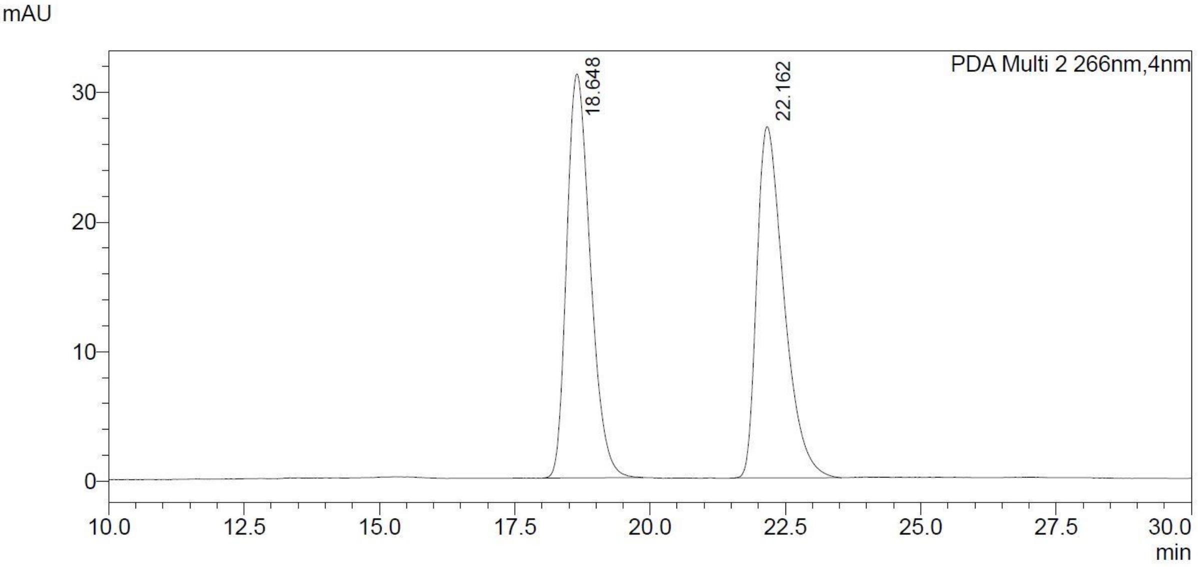

<Peak Table>

PDA Ch2 266nm

Peak#	Ret. Time	Area	Area%
1	18.648	945842	50.030
2	22.162	944704	49.970
Total		1890546	100.000

<Chromatogram>

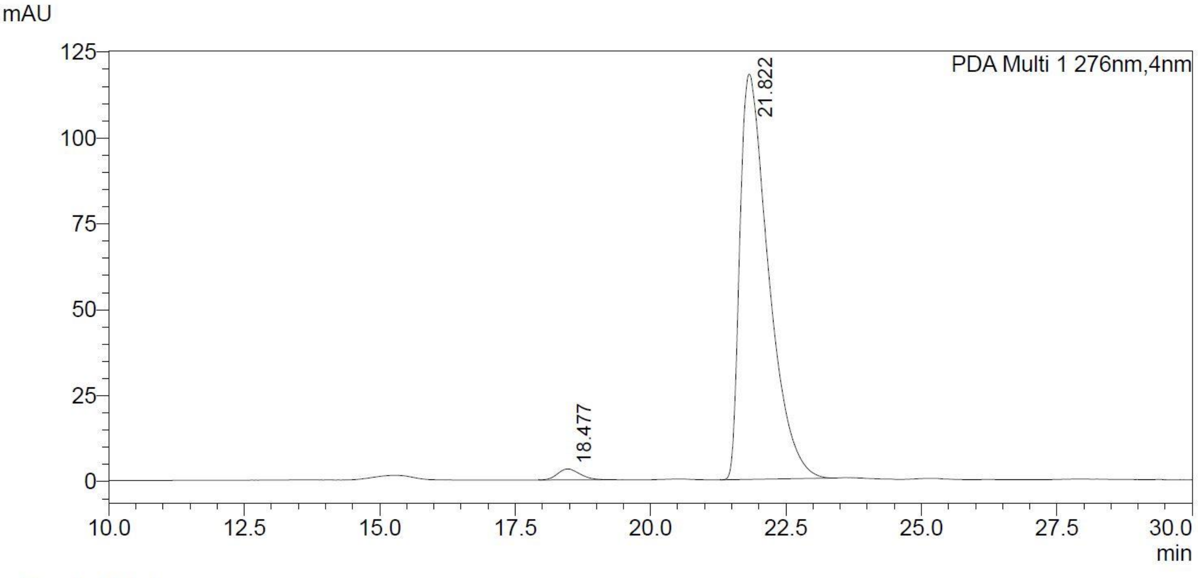

<Peak Table>

PDA Ch1 276nm

Peak#	Ret. Time	Area	Area%
1	18.477	91613	2.068
2	21.822	4337618	97.932
Total		4429231	100.000

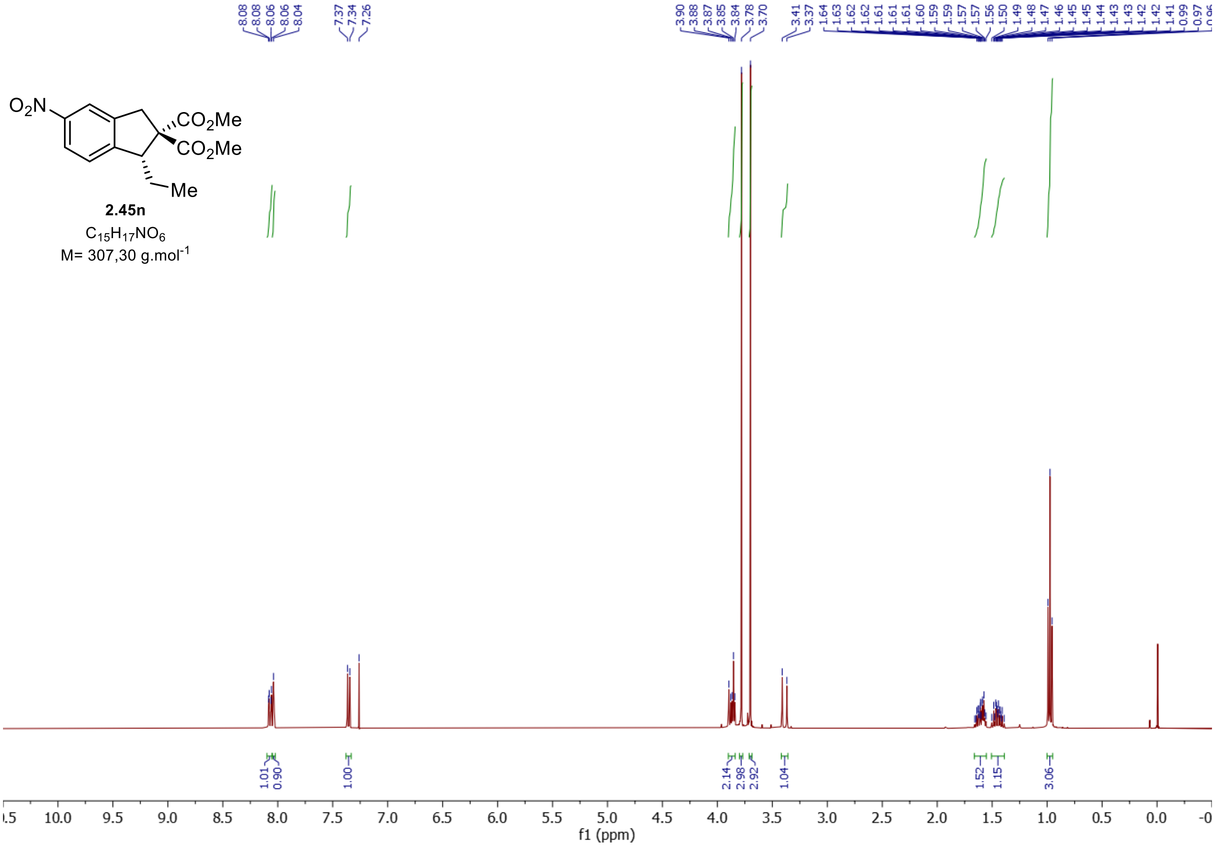

2.45n

$C_{15}H_{17}NO_6$

M= 307,30 g.mol^{-1}

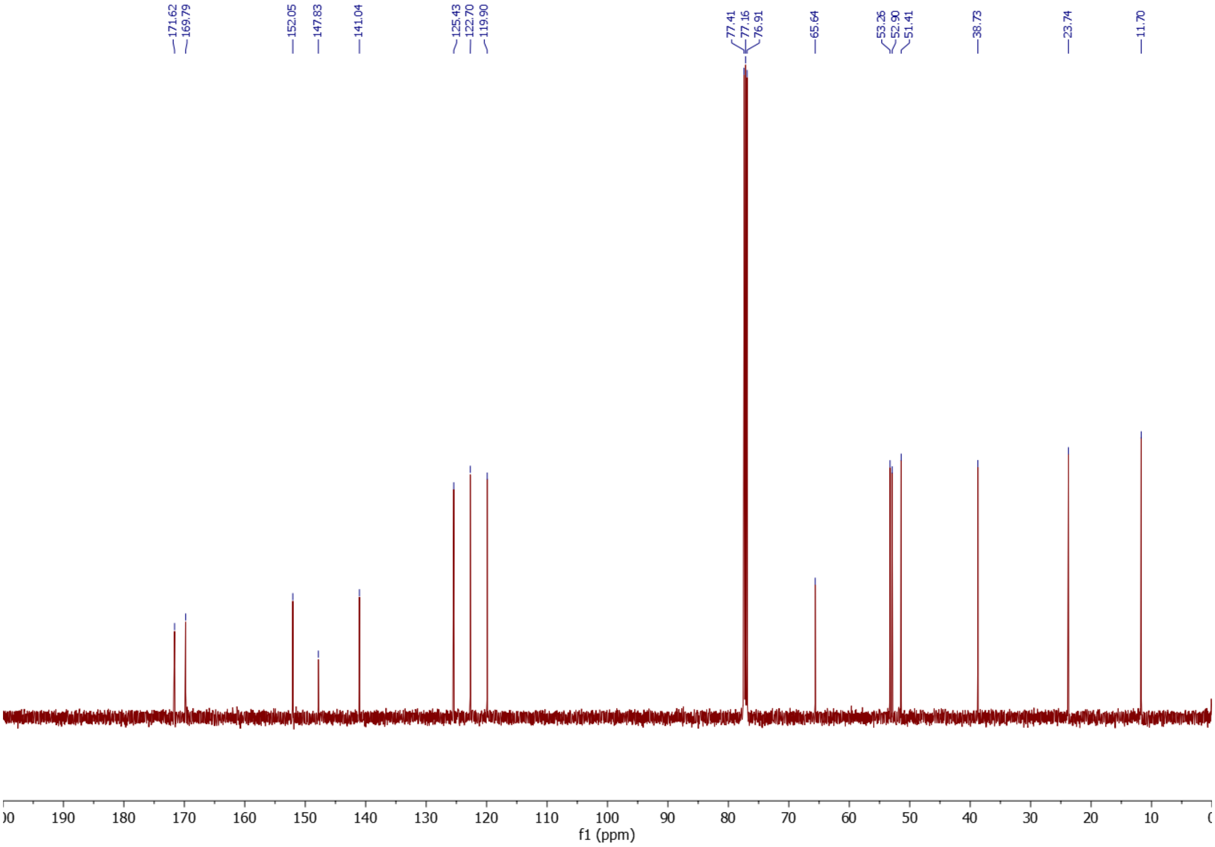

<Chromatogram>

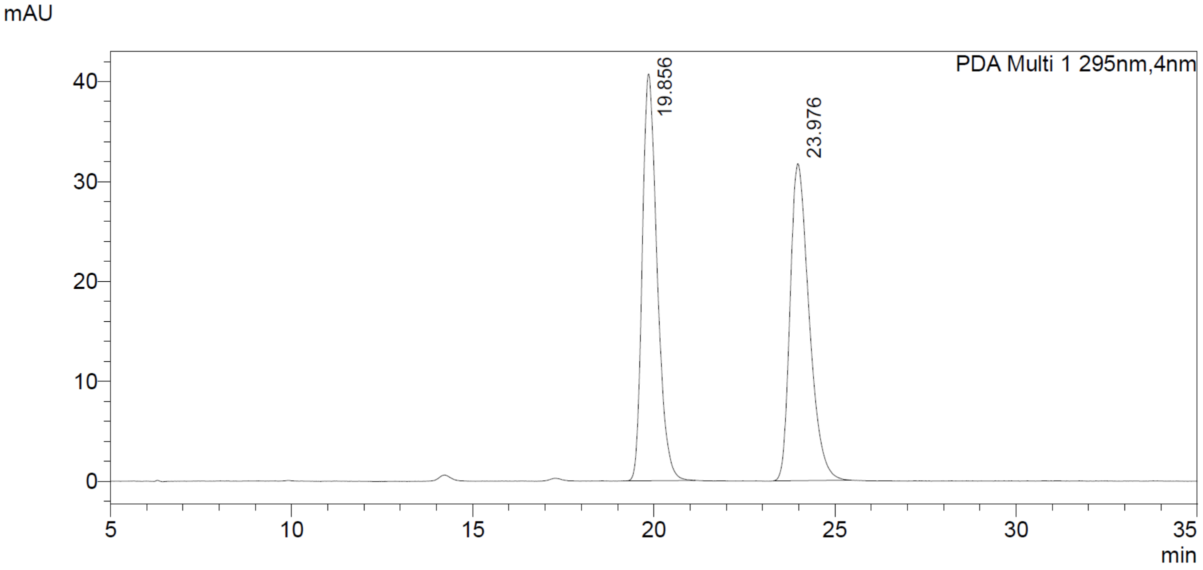

<Peak Table>

PDA Ch1 295nm

Peak#	Ret. Time	Area	Area%
1	19.856	1163701	50.094
2	23.976	1159338	49.906
Total		2323039	100.000

<Chromatogram>

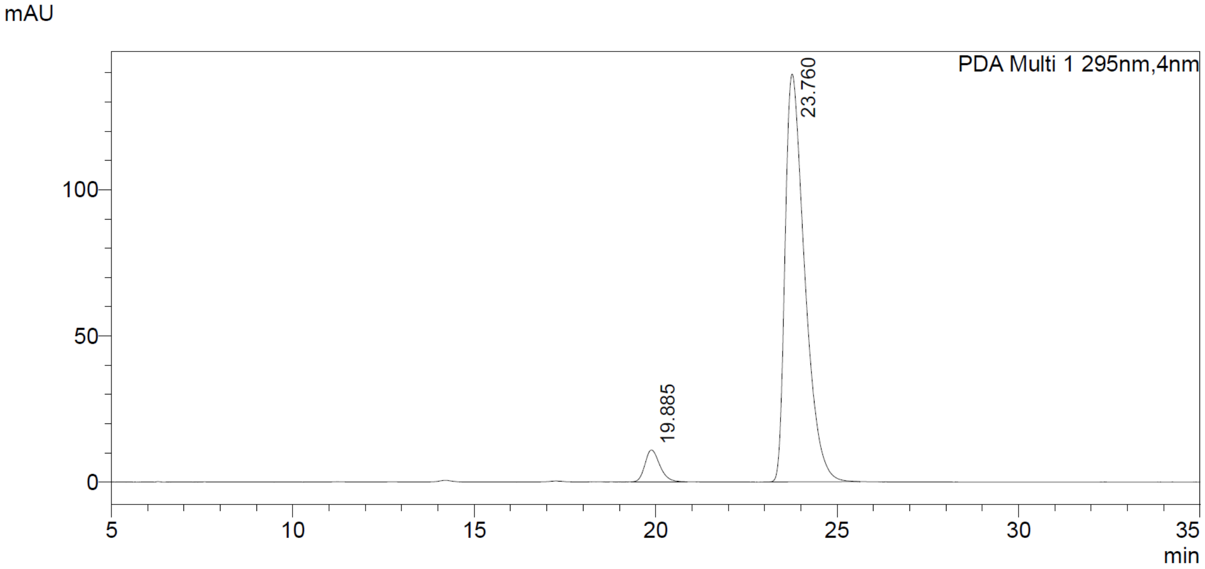

<Peak Table>

PDA Ch1 295nm

Peak#	Ret. Time	Area	Area%
1	19.885	309244	5.581
2	23.760	5231662	94.419
Total		5540906	100.000

<Chromatogram>

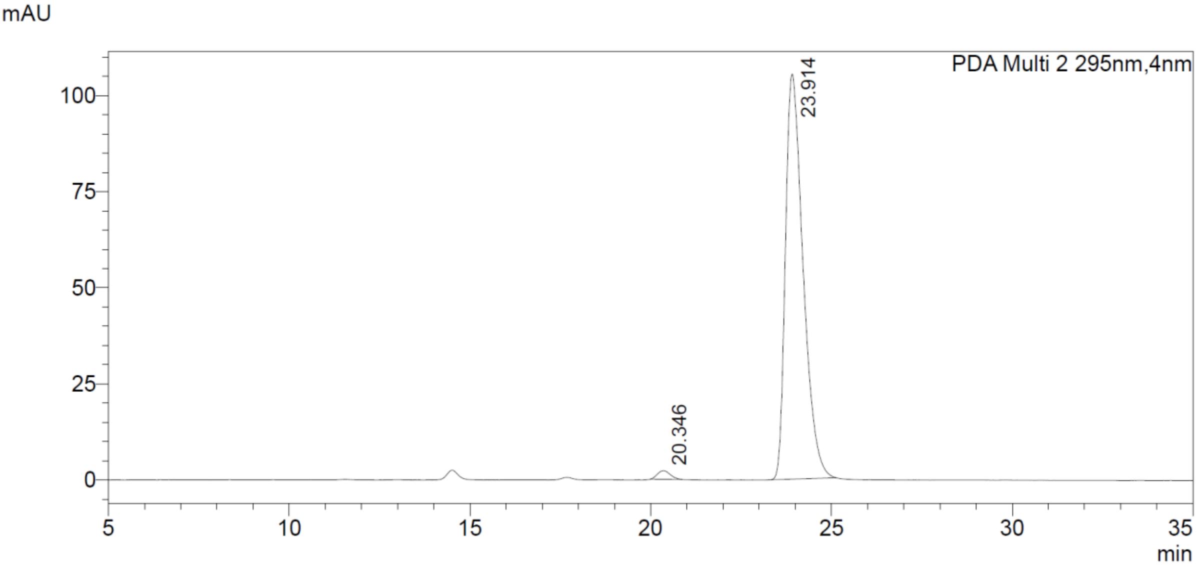

<Peak Table>

PDA Ch2 295nm

Peak#	Ret. Time	Area	Area%
1	20.346	55259	1.520
2	23.914	3580187	98.480
Total		3635445	100.000

F3C
CO2Me
CO2Me
Me

2.45o

$C_{16}H_{17}F_3O_4$

M= 330,30 g.mol^{-1}

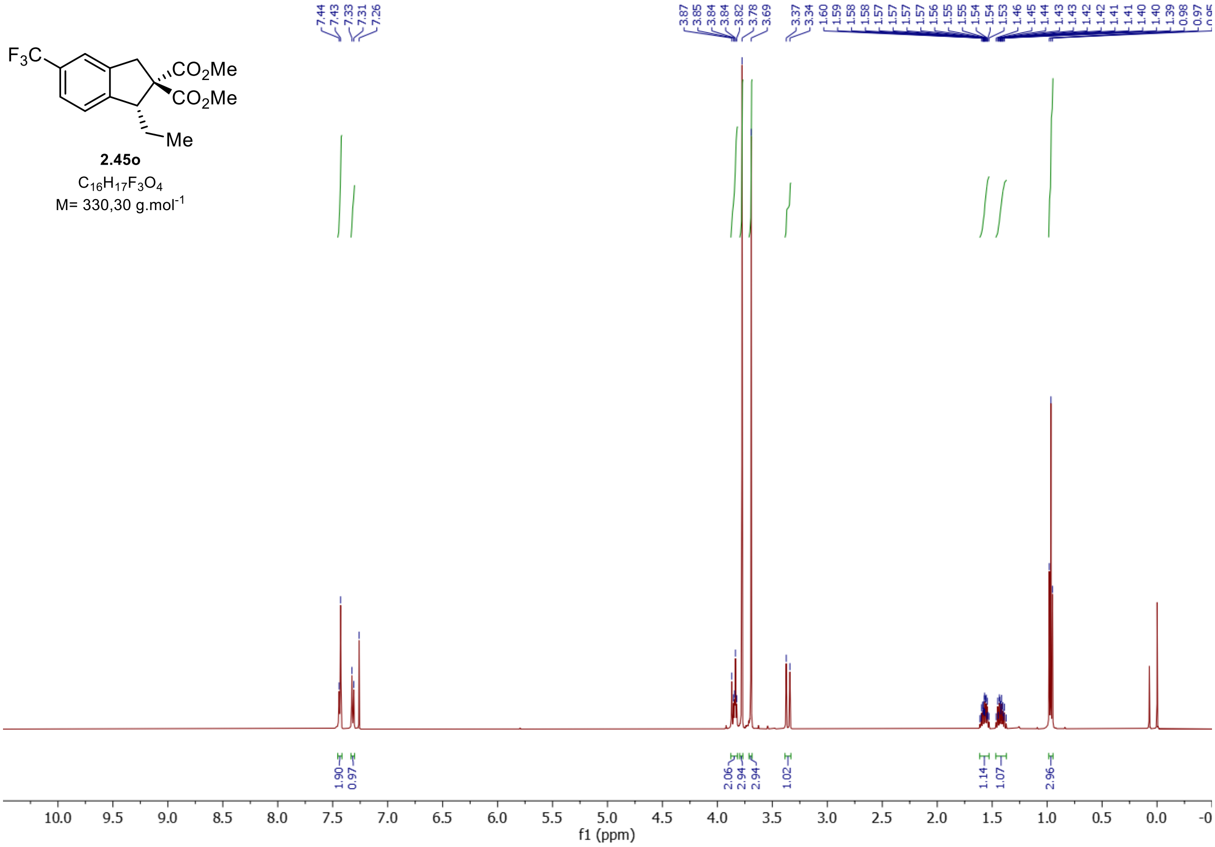

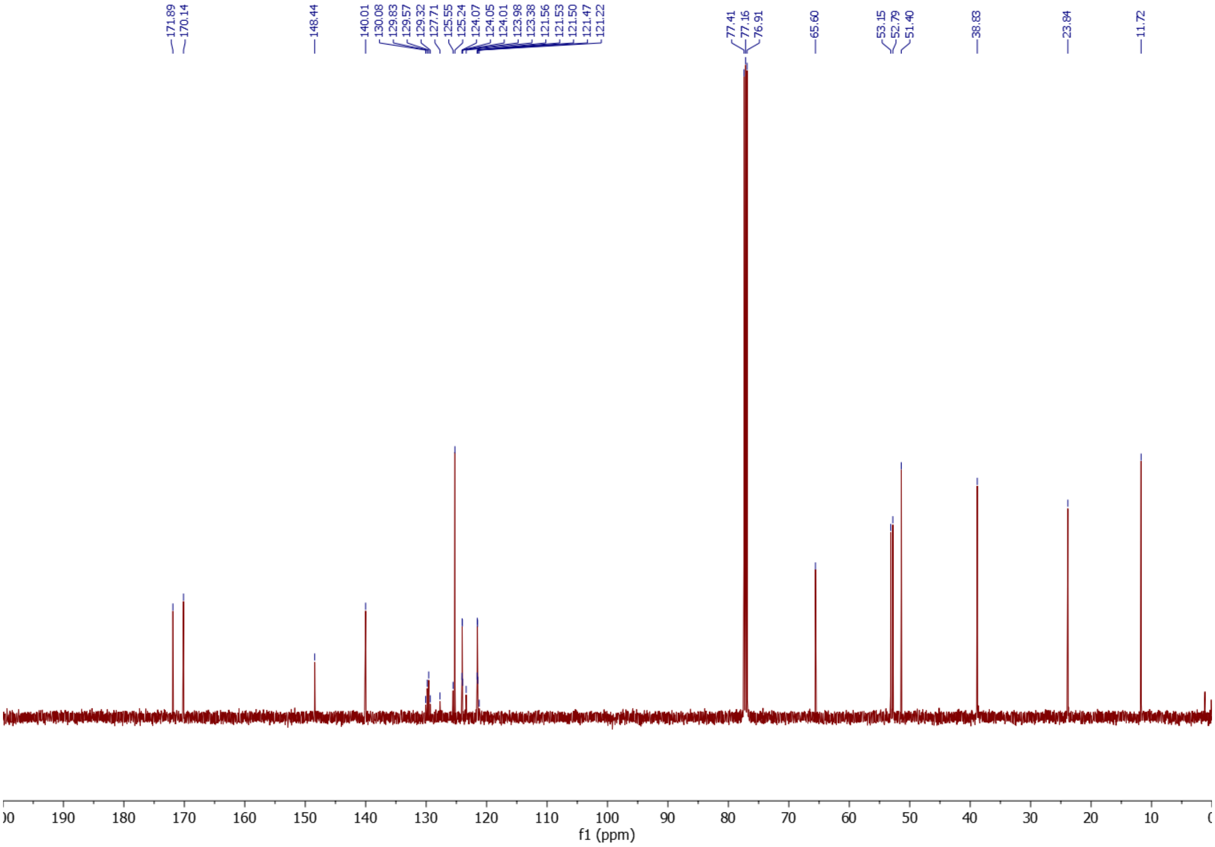

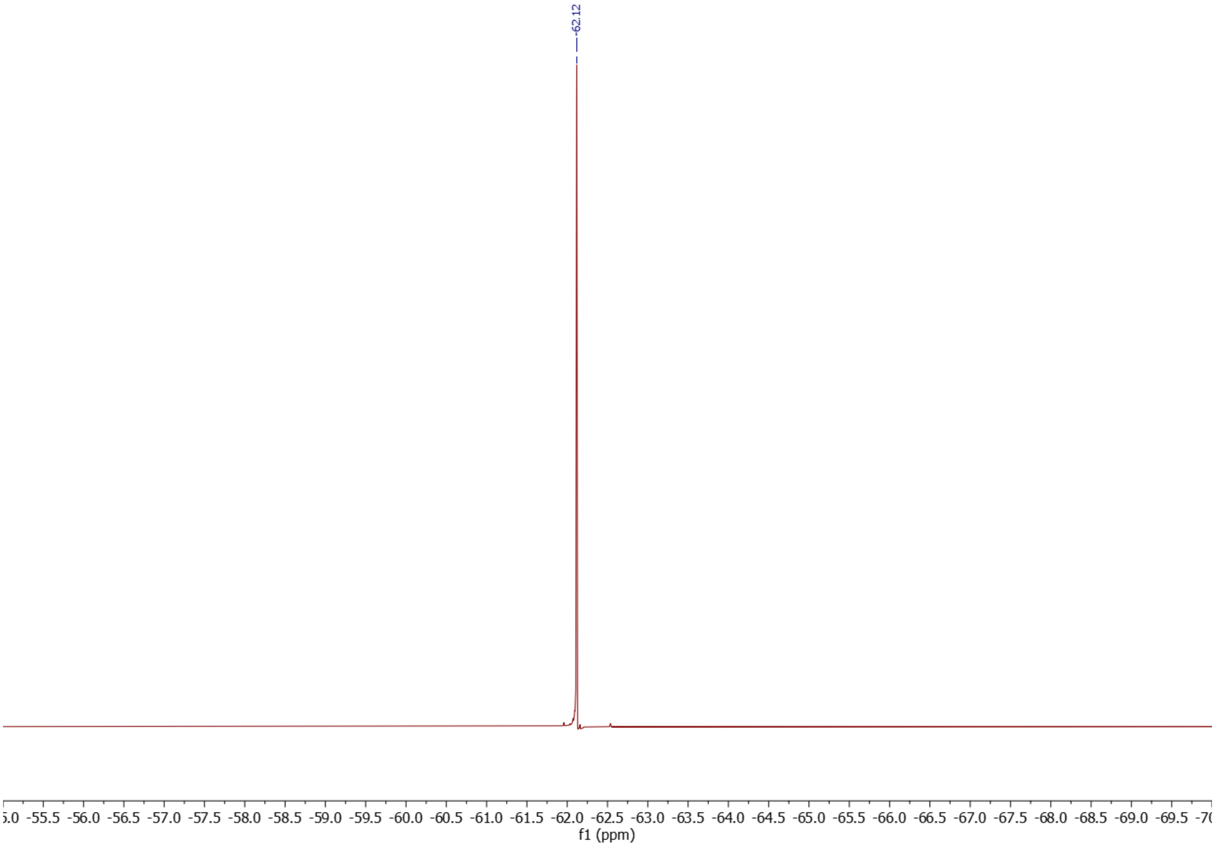
-62.12
-55.0 -55.5 -56.0 -56.5 -57.0 -57.5 -58.0 -58.5 -59.0 -59.5 -60.0 -60.5 -61.0 -61.5 -62.0 -62.5 -63.0 -63.5 -64.0 -64.5 -65.0 -65.5 -66.0 -66.5 -67.0 -67.5 -68.0 -68.5 -69.0 -69.5 -70
f1 (ppm)

<Chromatogram>

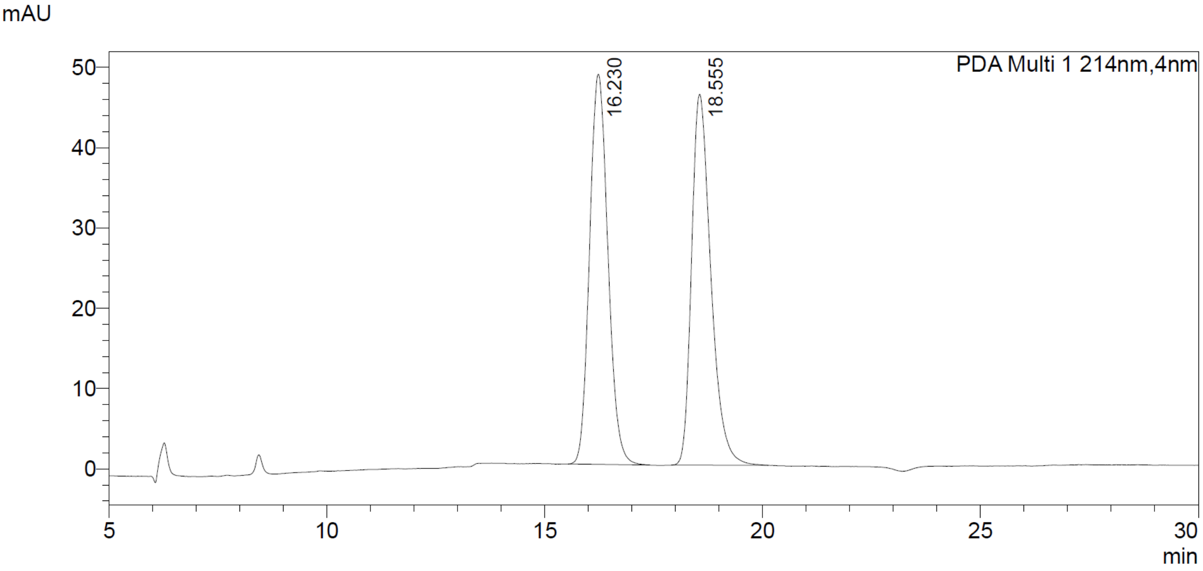

<Peak Table>

PDA Ch1 214nm

Peak#	Ret. Time	Area	Area%
1	16.230	1426260	50.032
2	18.555	1424463	49.968
Total		2850723	100.000

<Chromatogram>

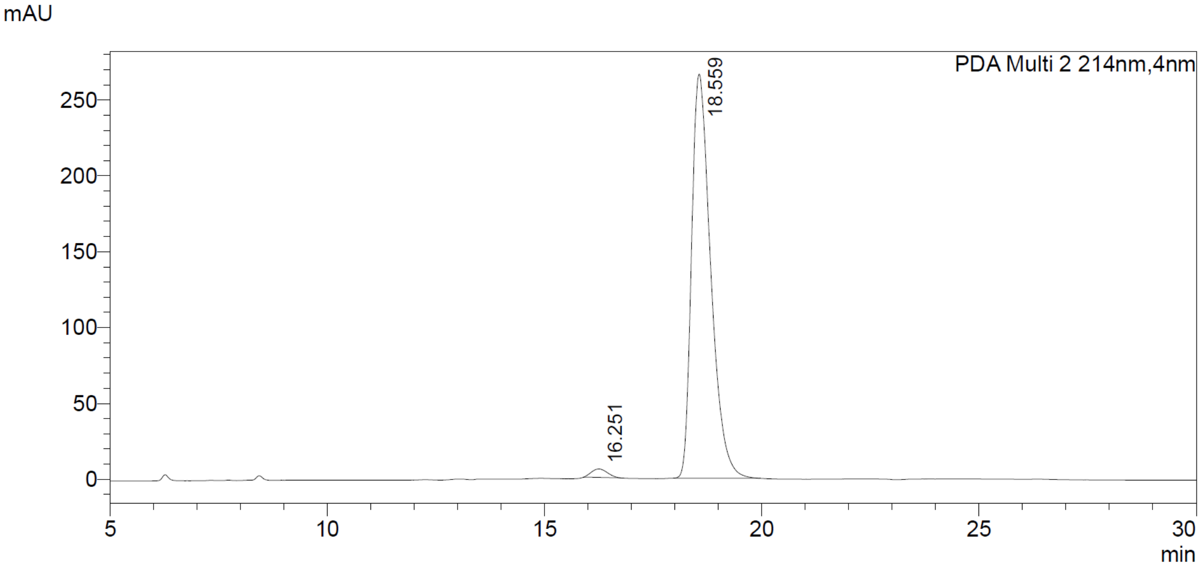

<Peak Table>

PDA Ch2 214nm

Peak#	Ret. Time	Area	Area%
1	16.251	142760	1.718
2	18.559	8167949	98.282
Total		8310709	100.000

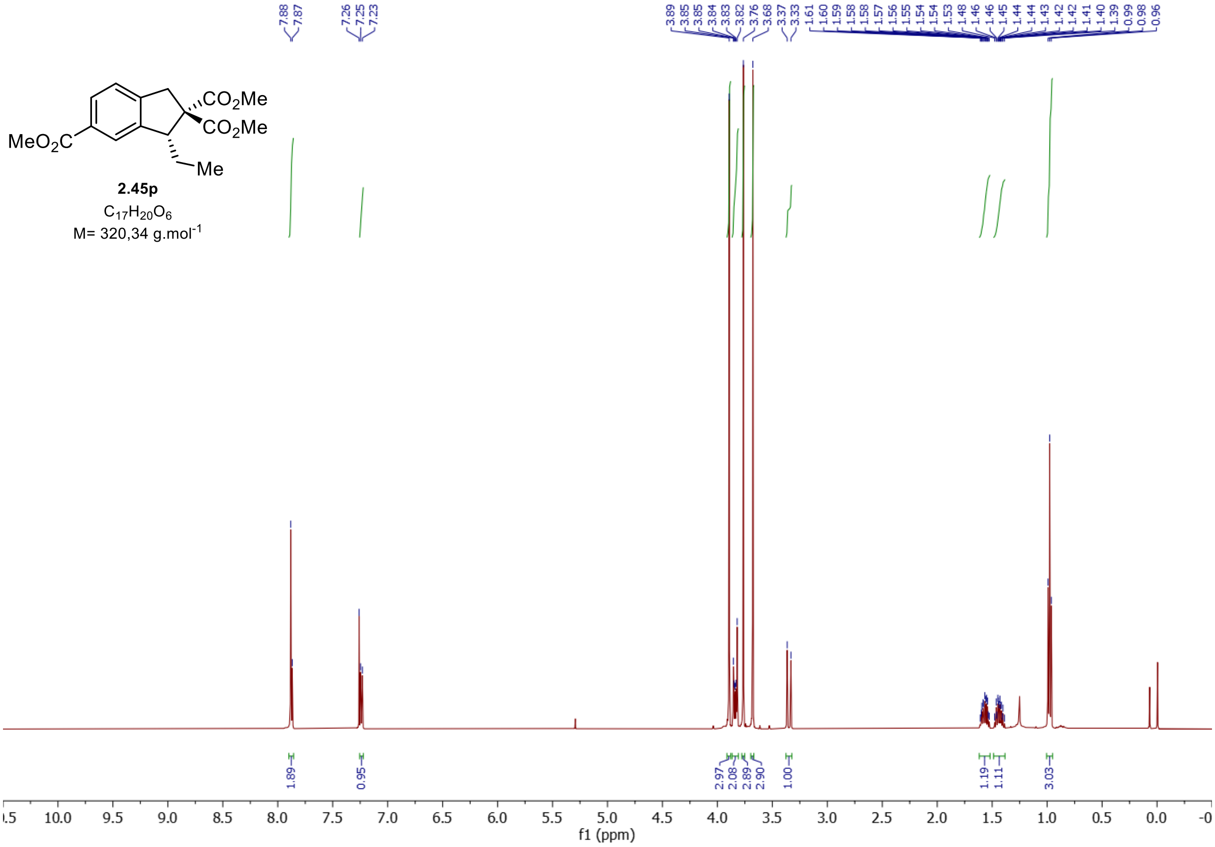

2.45p

$C_{17}H_{20}O_6$

M= 320,34 g.mol^{-1}

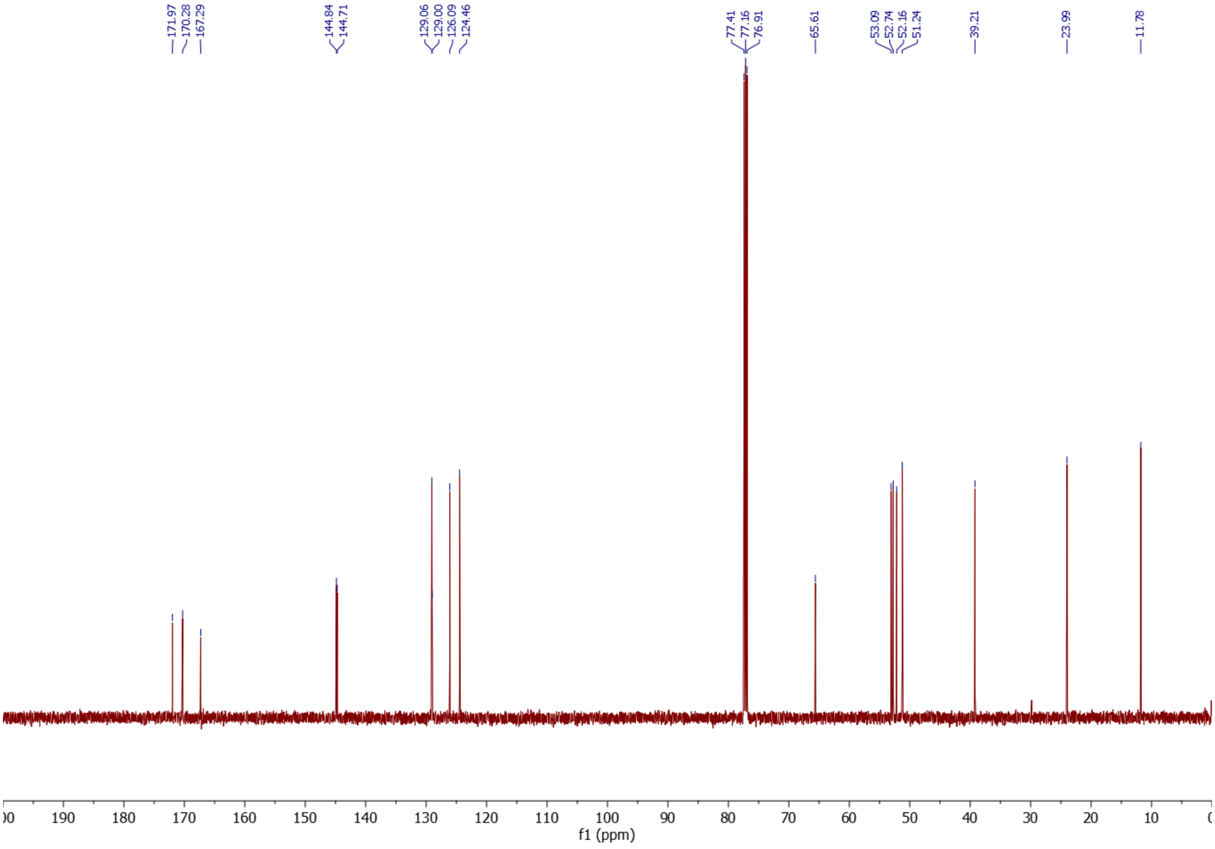

<Chromatogram>

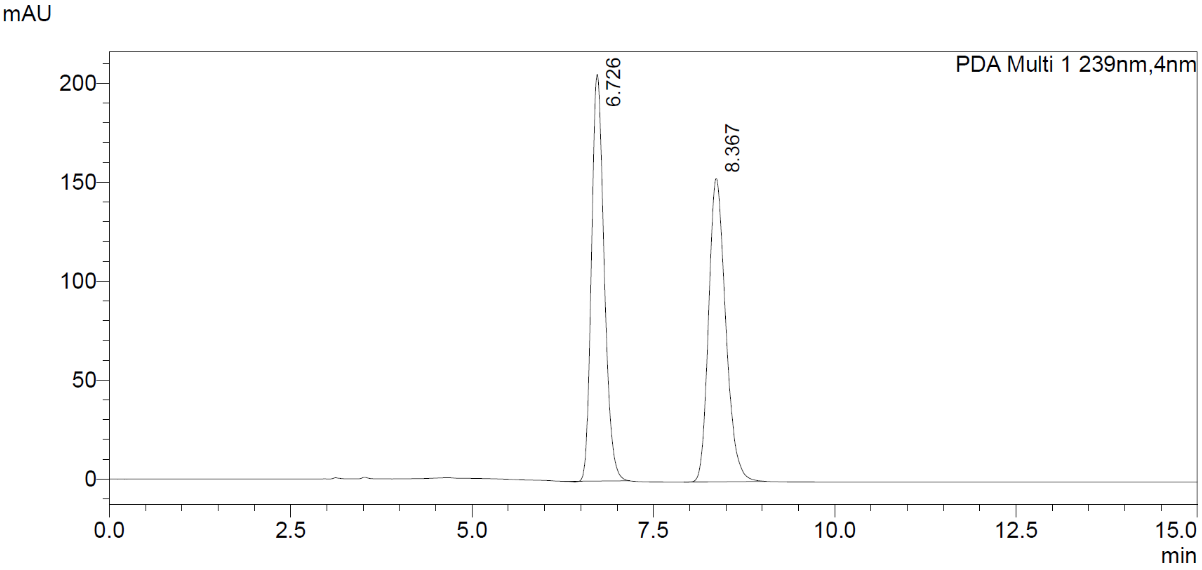

<Peak Table>

PDA Ch1 239nm

Peak#	Ret. Time	Area	Area%
1	6.726	2504582	49.929
2	8.367	2511716	50.071
Total		5016298	100.000

<Chromatogram>

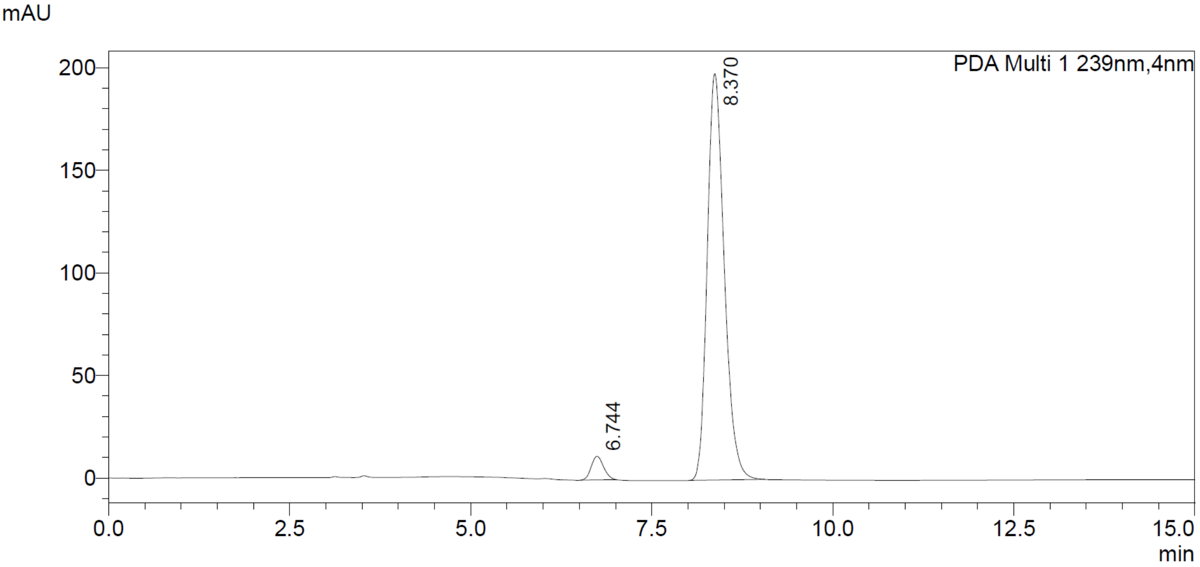

<Peak Table>

PDA Ch1 239nm

Peak#	Ret. Time	Area	Area%
1	6.744	136318	4.037
2	8.370	3239989	95.963
Total		3376307	100.000

MeO2S
CO2Me
CO2Me
Me

2.45q

$C_{16}H_{20}O_6S$

M= 340,39 g.mol^{-1}

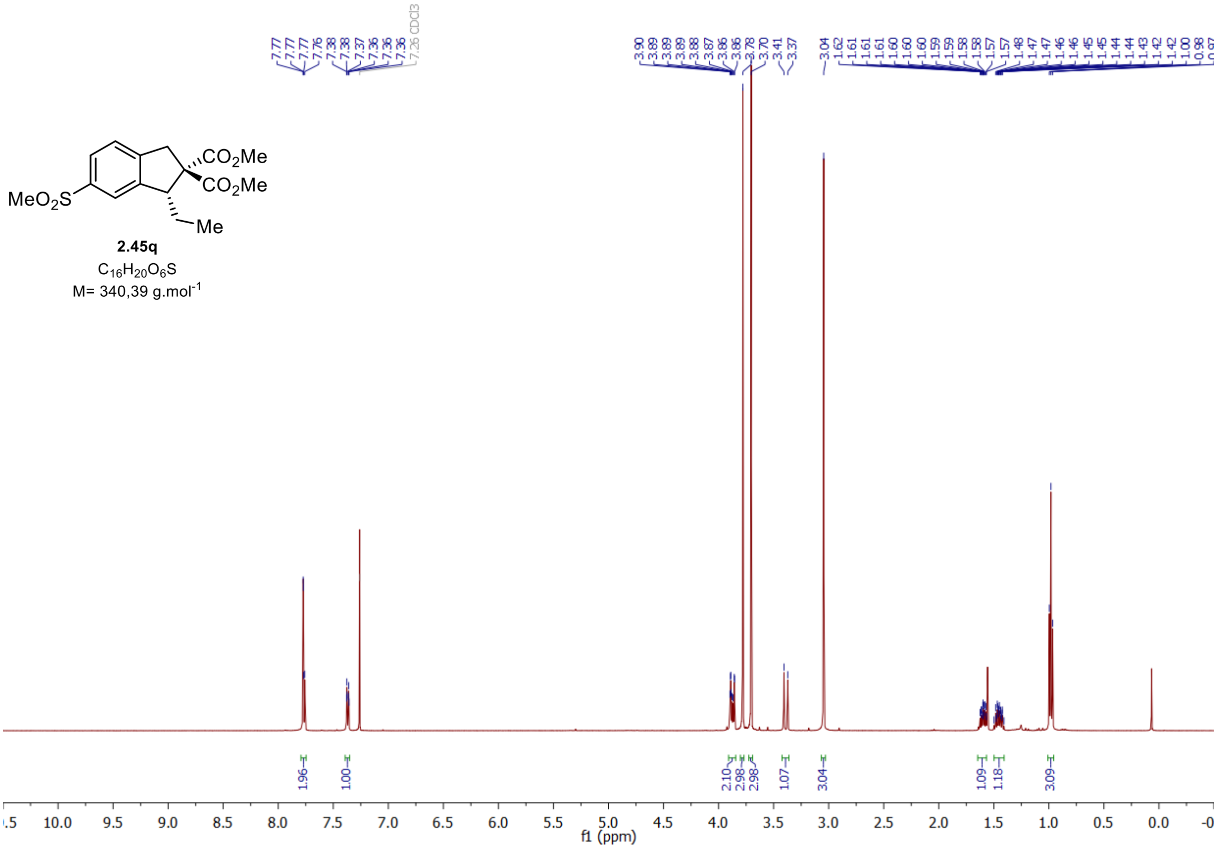

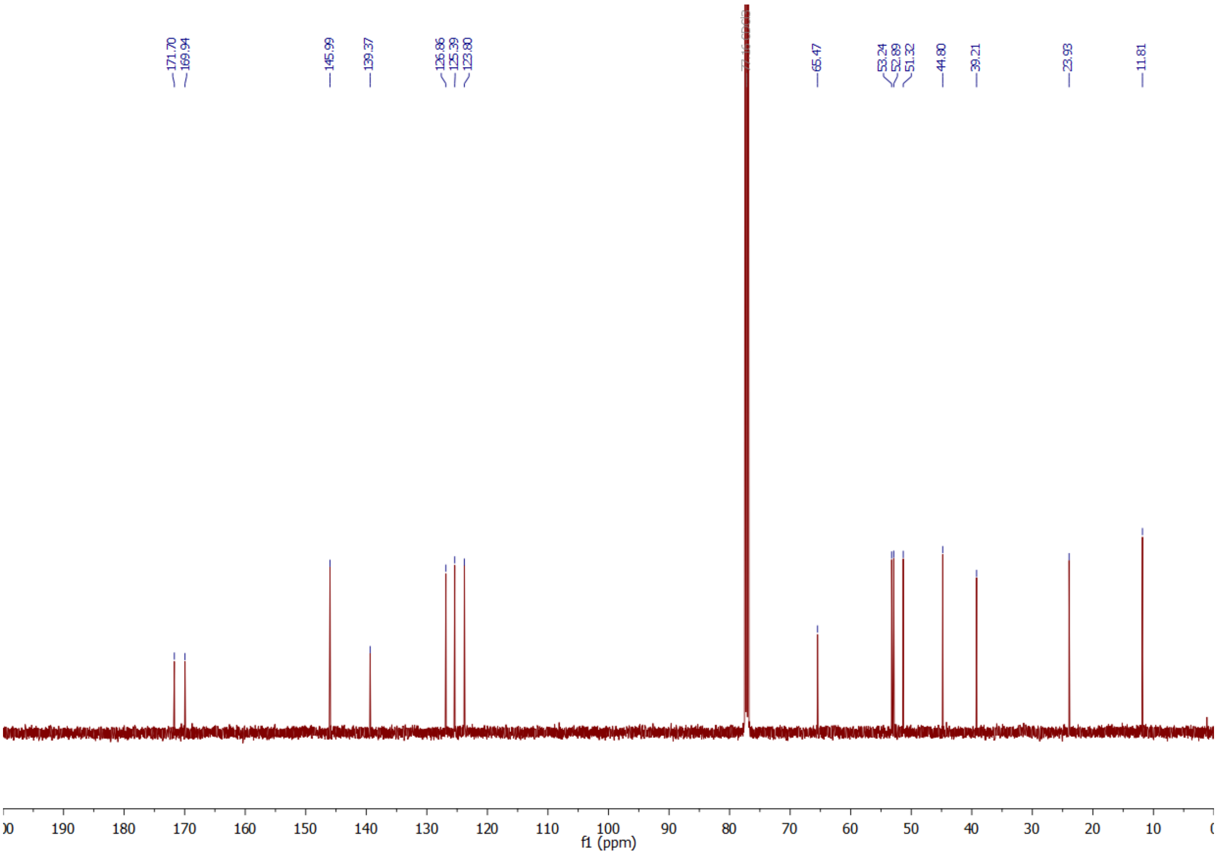

<Chromatogram>

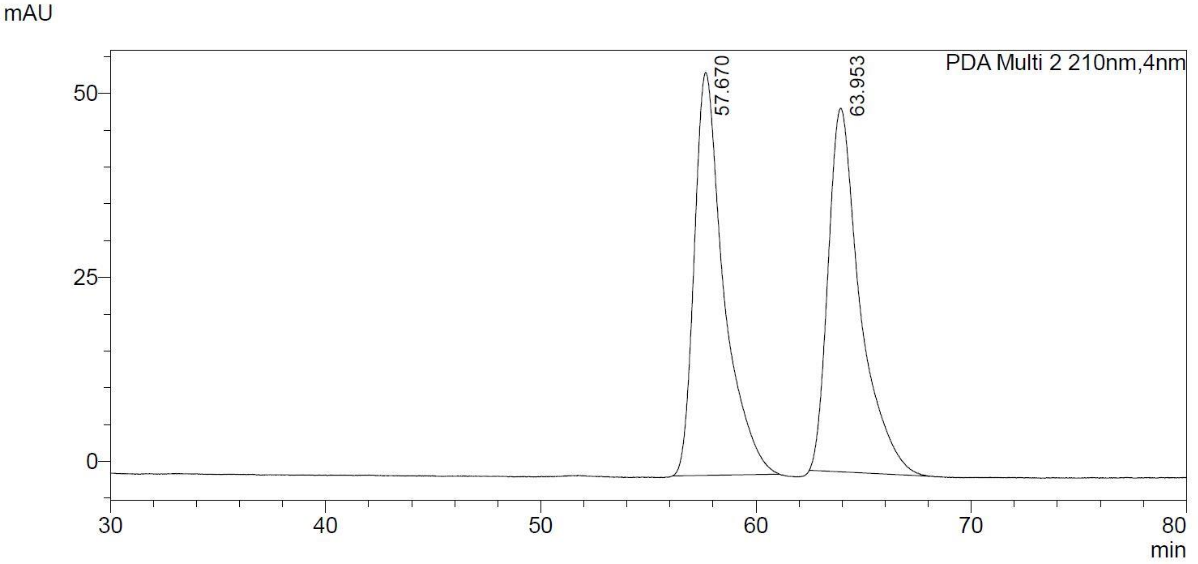

<Peak Table>

PDA Ch2 210nm

Peak#	Ret. Time	Area	Area%
1	57.670	5195367	50.416
2	63.953	5109636	49.584
Total		10305003	100.000

<Chromatogram>

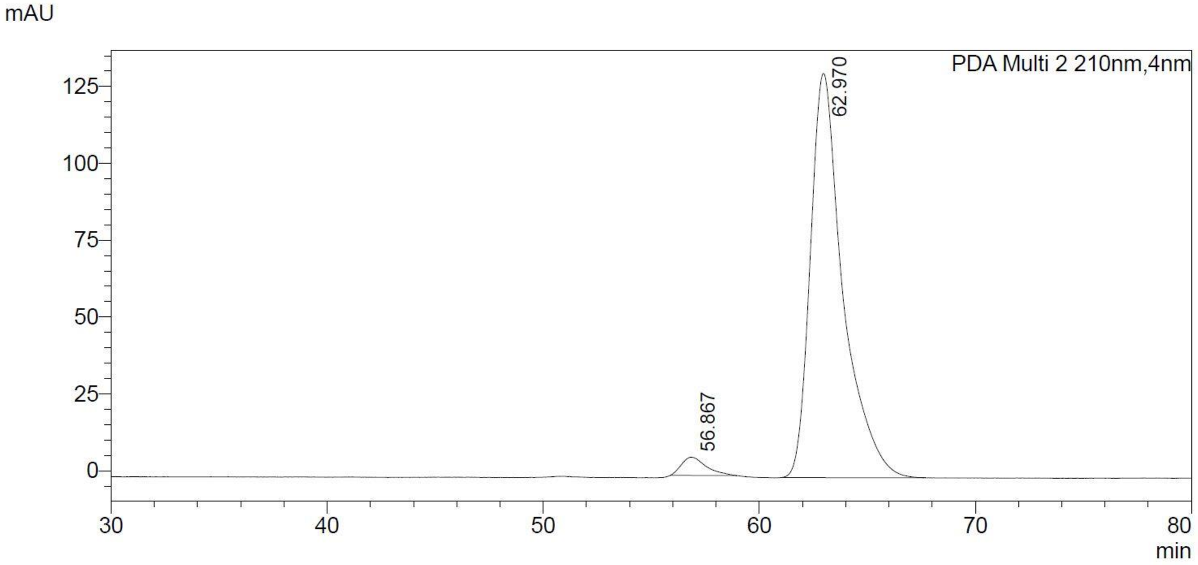

<Peak Table>

PDA Ch2 210nm

Peak#	Ret. Time	Area	Area%
1	56.867	472198	3.310
2	62.970	13794384	96.690
Total		14266582	100.000

O
O
CO2Me
CO2Me
Me

2.45r

$C_{16}H_{18}O_6$

M= 306,31 g.mol^{-1}

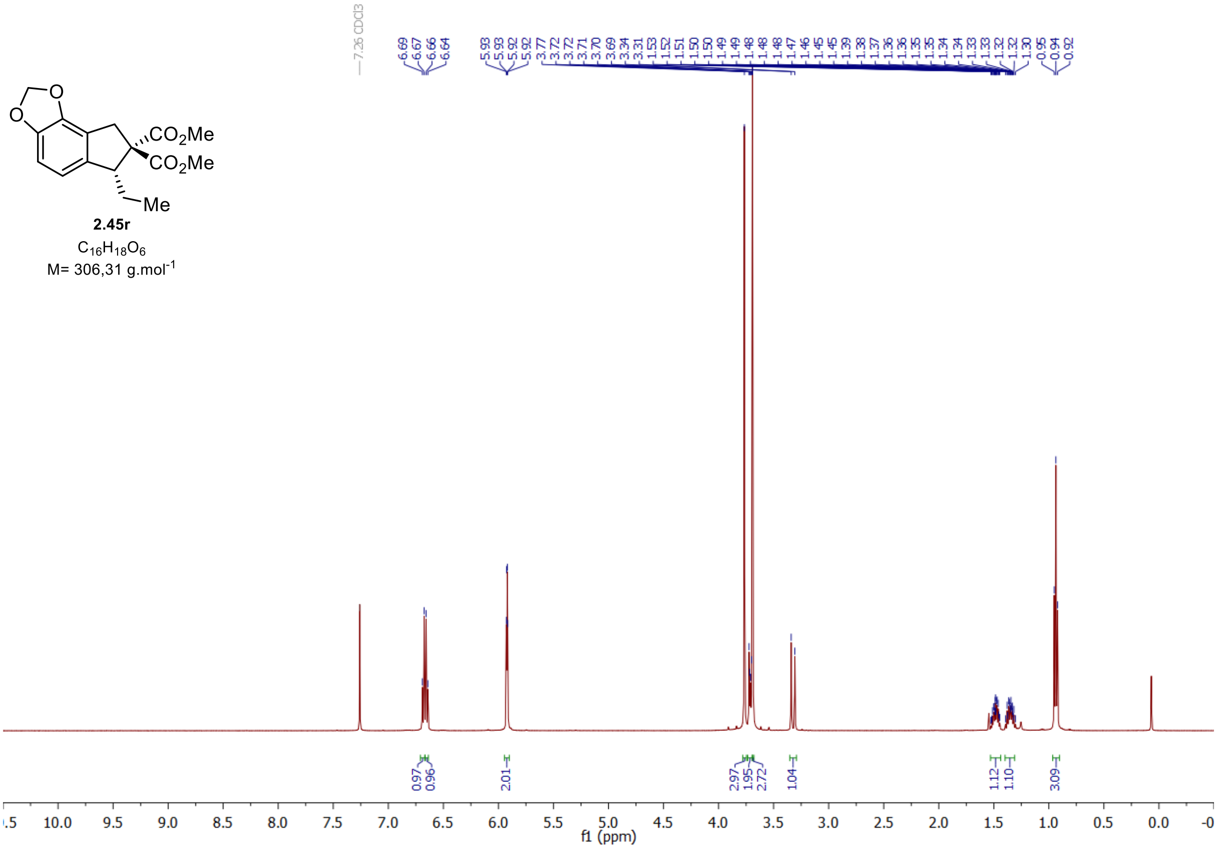

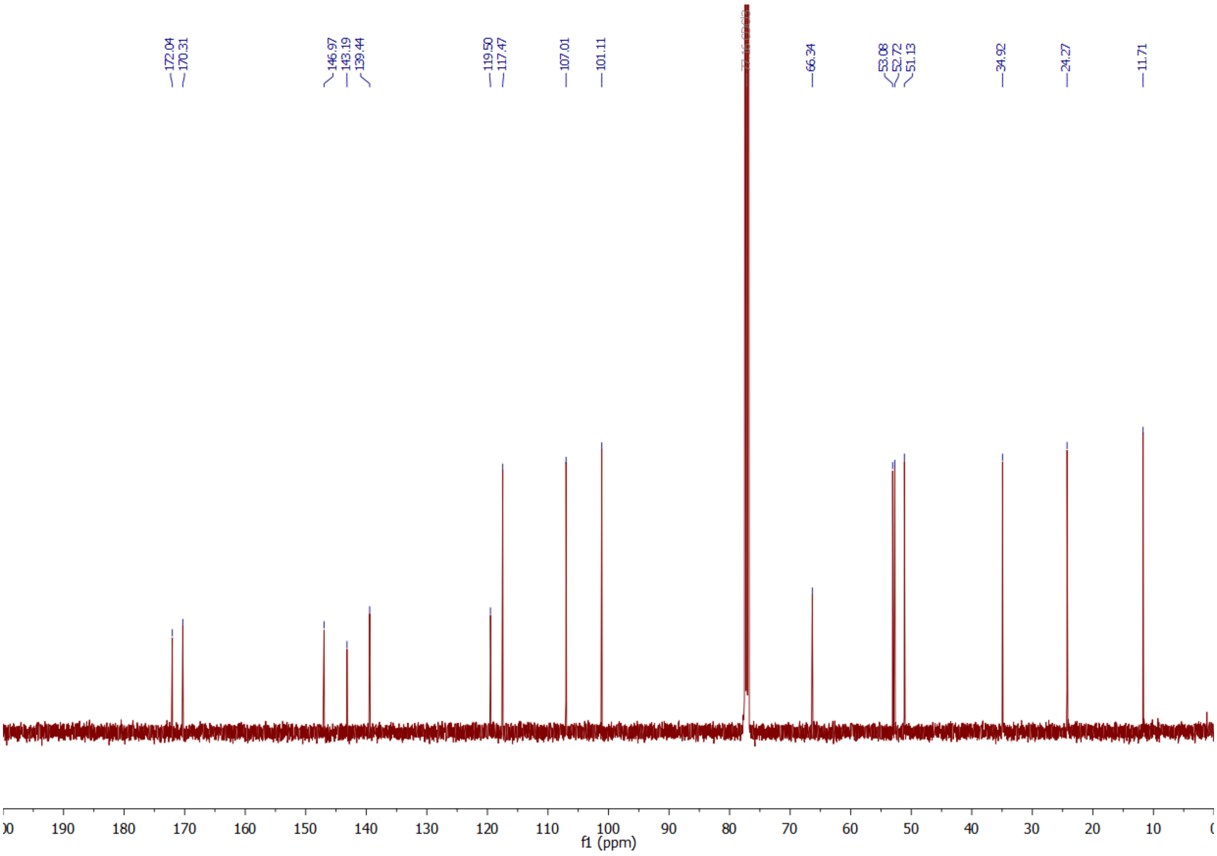

<Chromatogram>

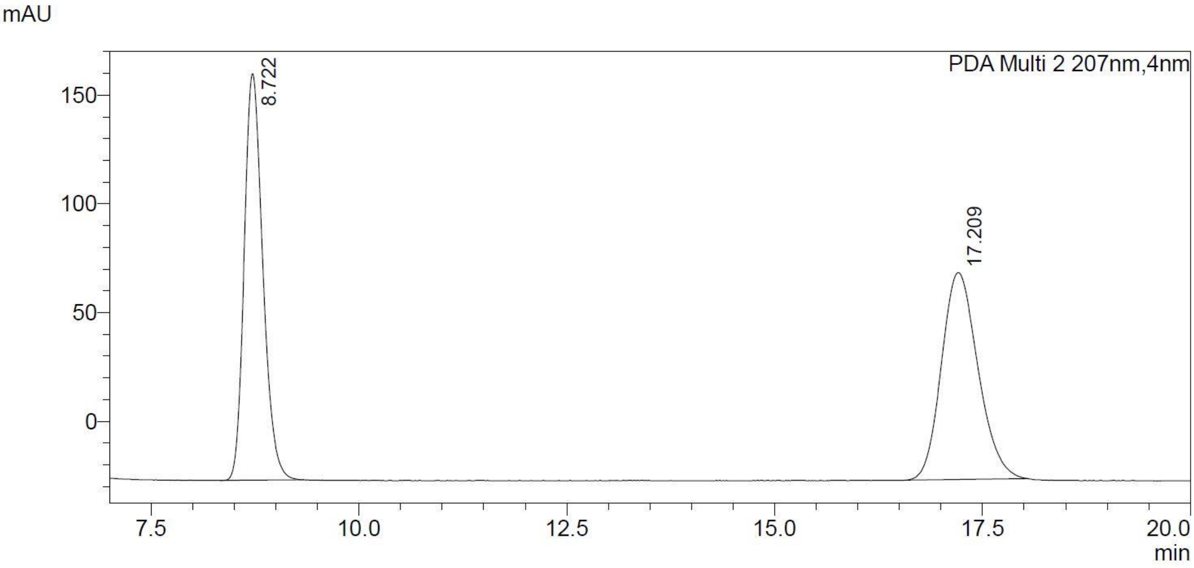

<Peak Table>

PDA Ch2 207nm

Peak#	Ret. Time	Area	Area%
1	8.722	2913940	50.049
2	17.209	2908284	49.951
Total		5822224	100.000

<Chromatogram>

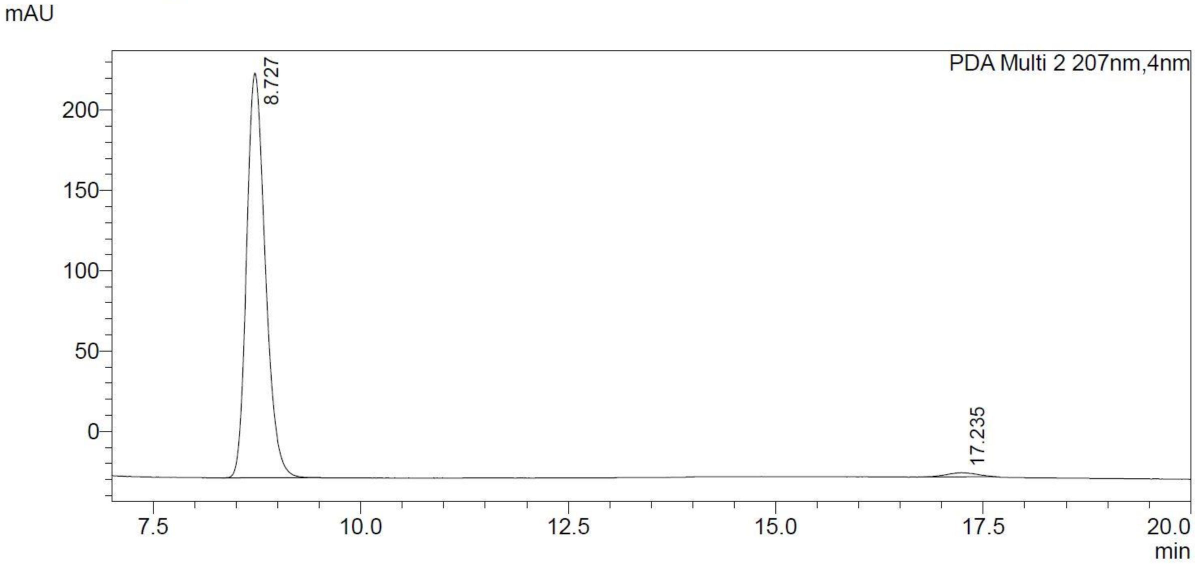

<Peak Table>

PDA Ch2 207nm

Peak#	Ret. Time	Area	Area%
1	8.727	3944522	98.336
2	17.235	66760	1.664
Total		4011282	100.000

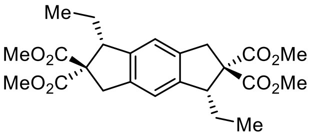
Me
MeO2C
MeO2C
CO2Me
CO2Me
Me

2.45s

$C_{24}H_{30}O_8$

M= 446,50 g.mol^{-1}

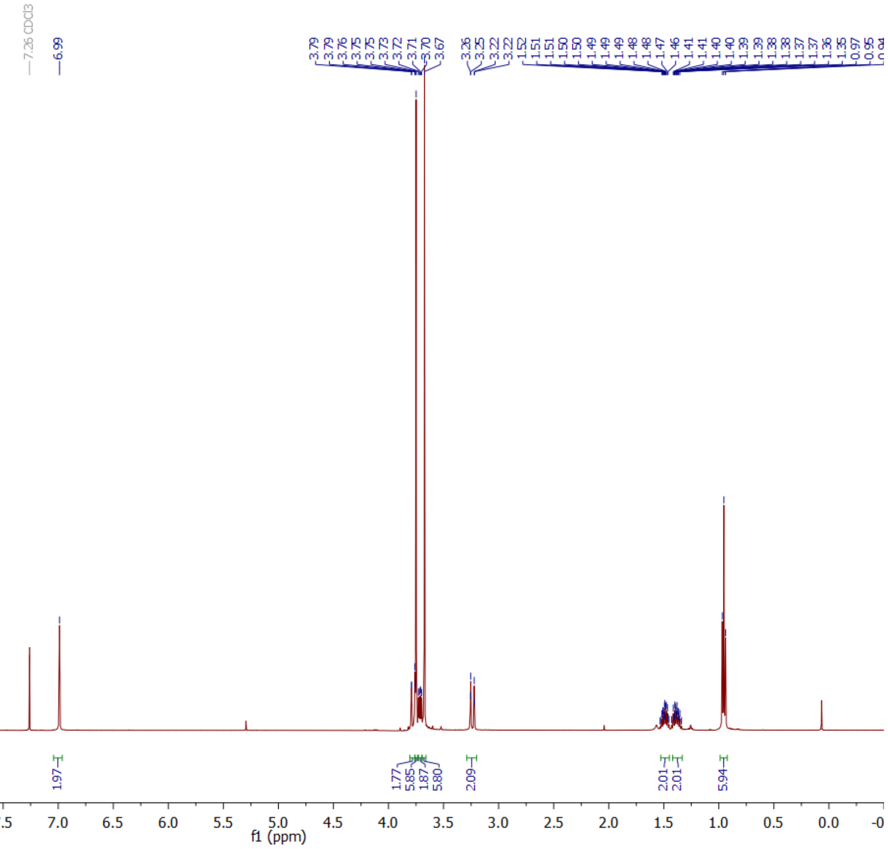

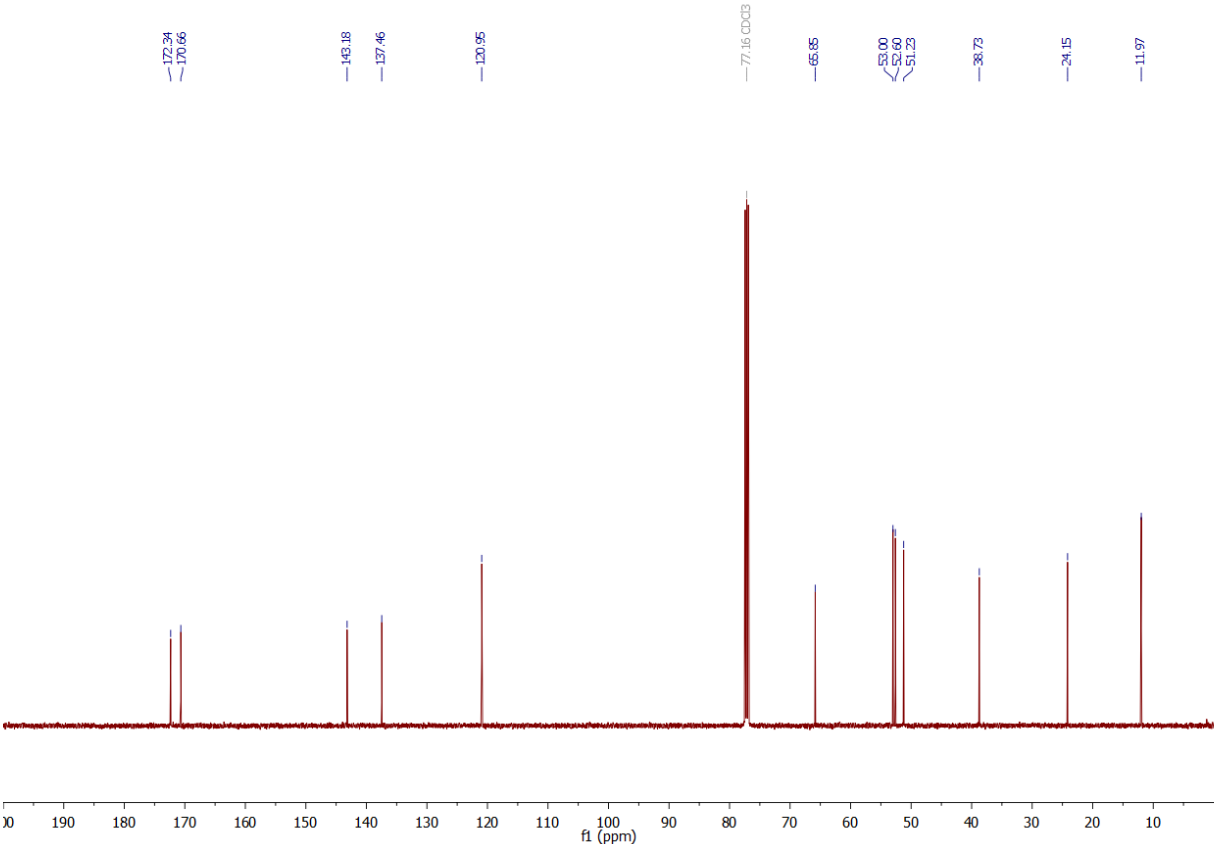

<Chromatogram>

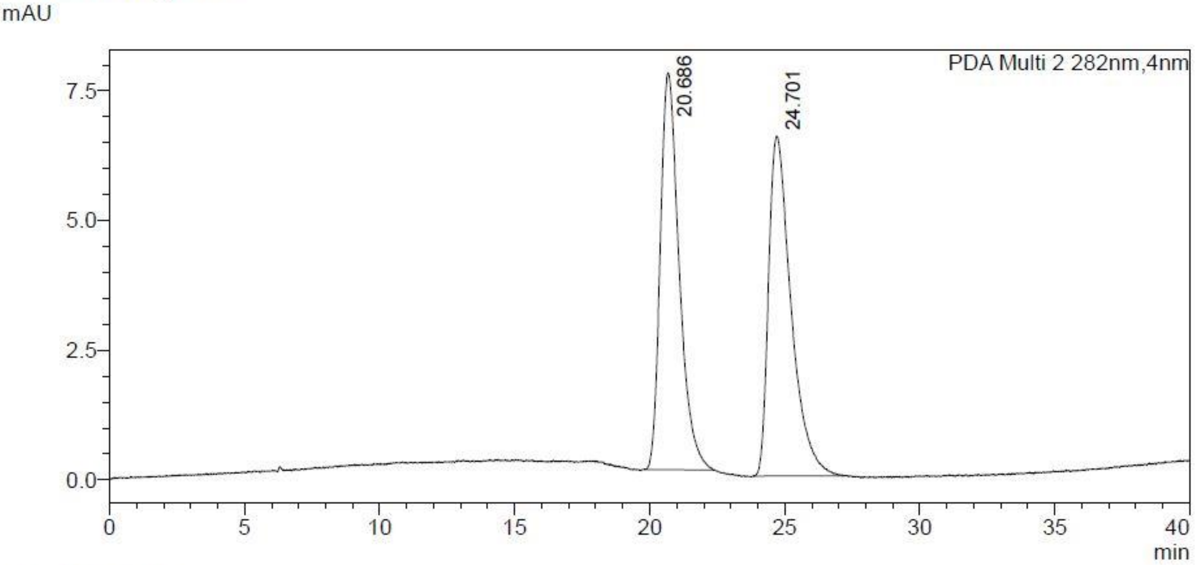

<Peak Table>

PDA Ch2 282nm

Peak#	Ret. Time	Area	Area%
1	20.686	372721	49.603
2	24.701	378682	50.397
Total		751403	100.000

<Chromatogram>

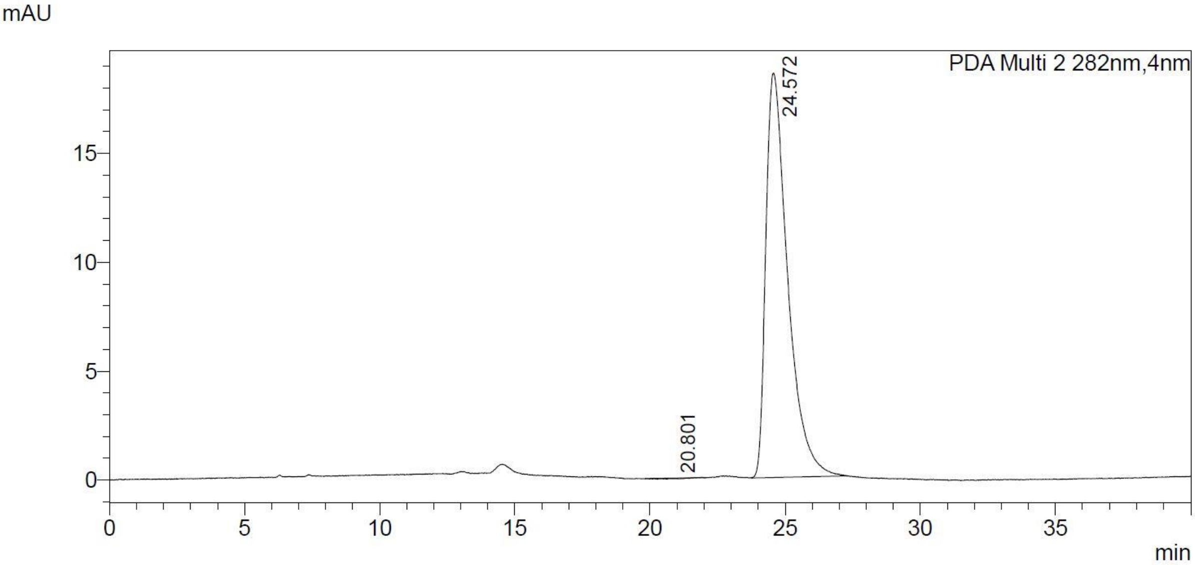

<Peak Table>

PDA Ch2 282nm

Peak#	Ret. Time	Area	Area%
1	20.801	-1677	-0.161
2	24.572	1042030	100.161
Total		1040352	100.000

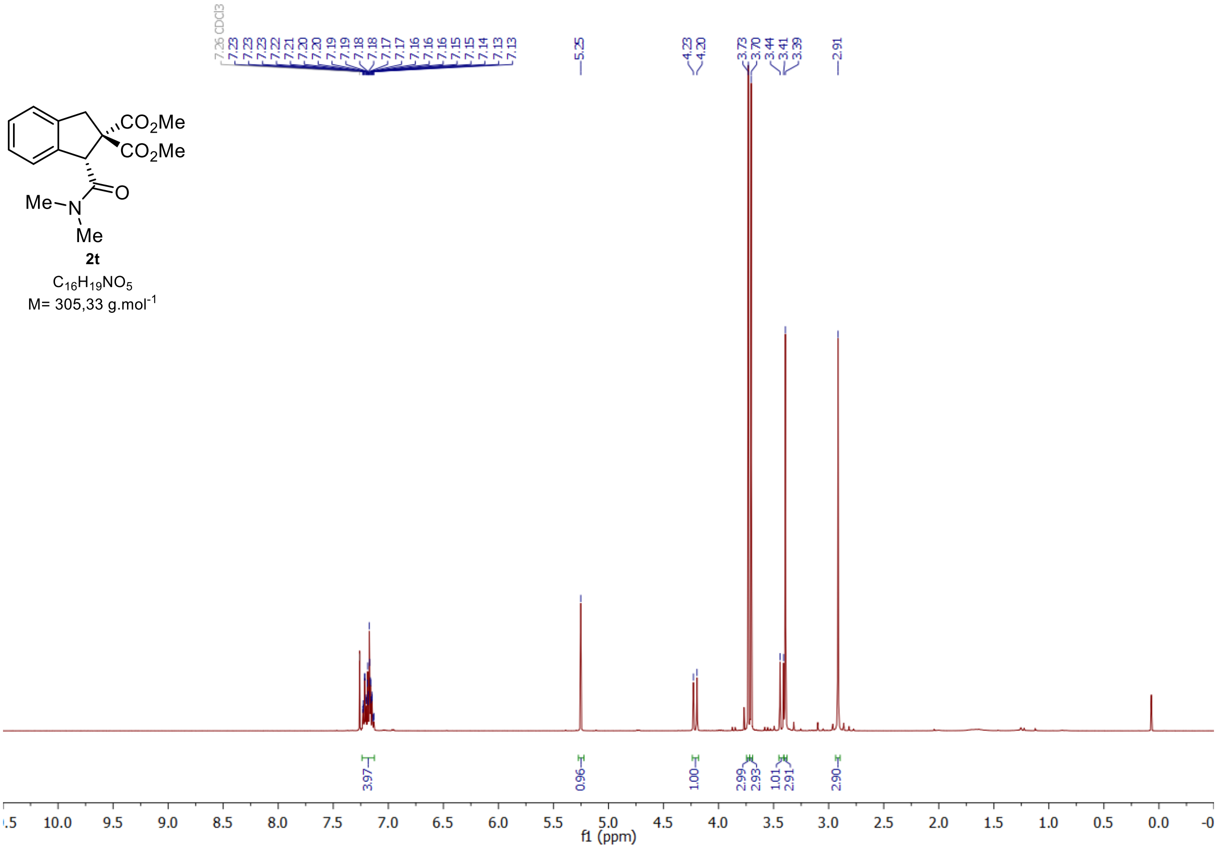

2t

$C_{16}H_{19}NO_5$
M= 305,33 g.mol^{-1}

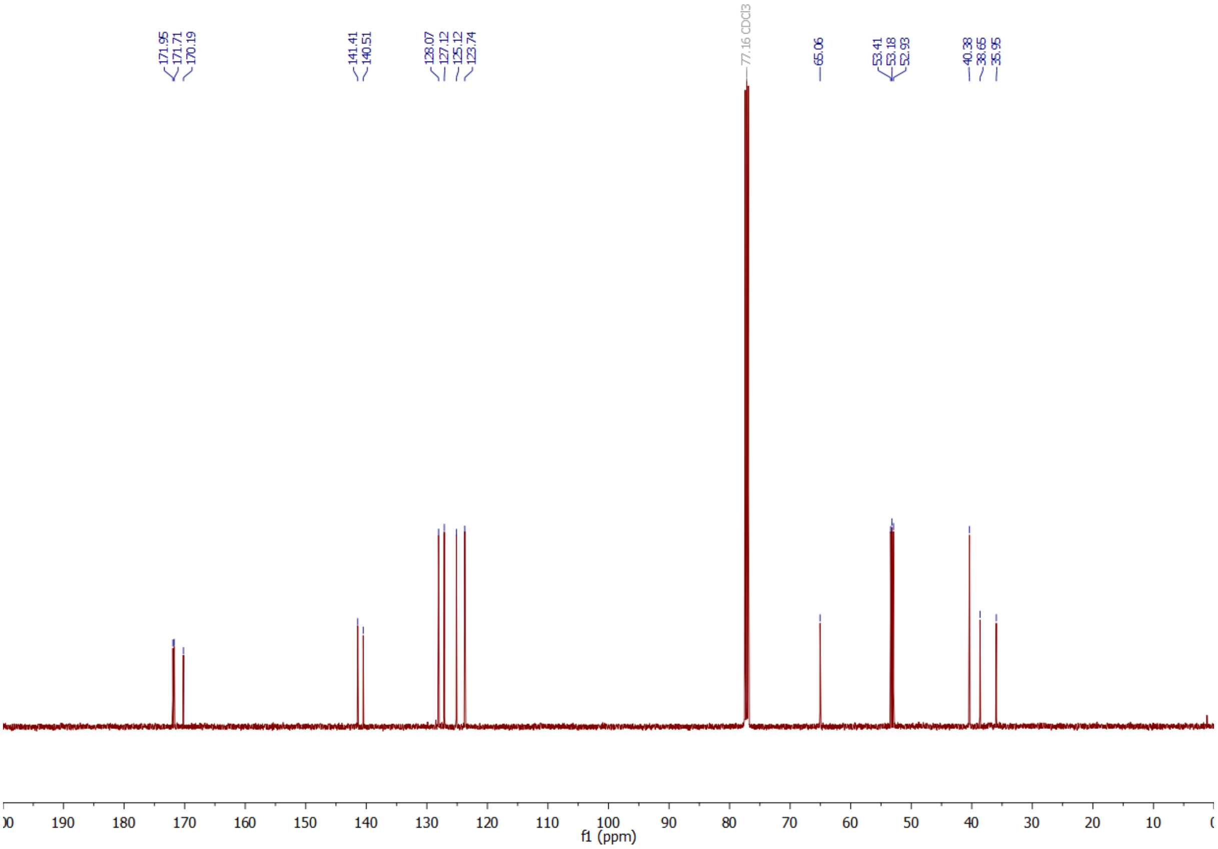

<Chromatogram>

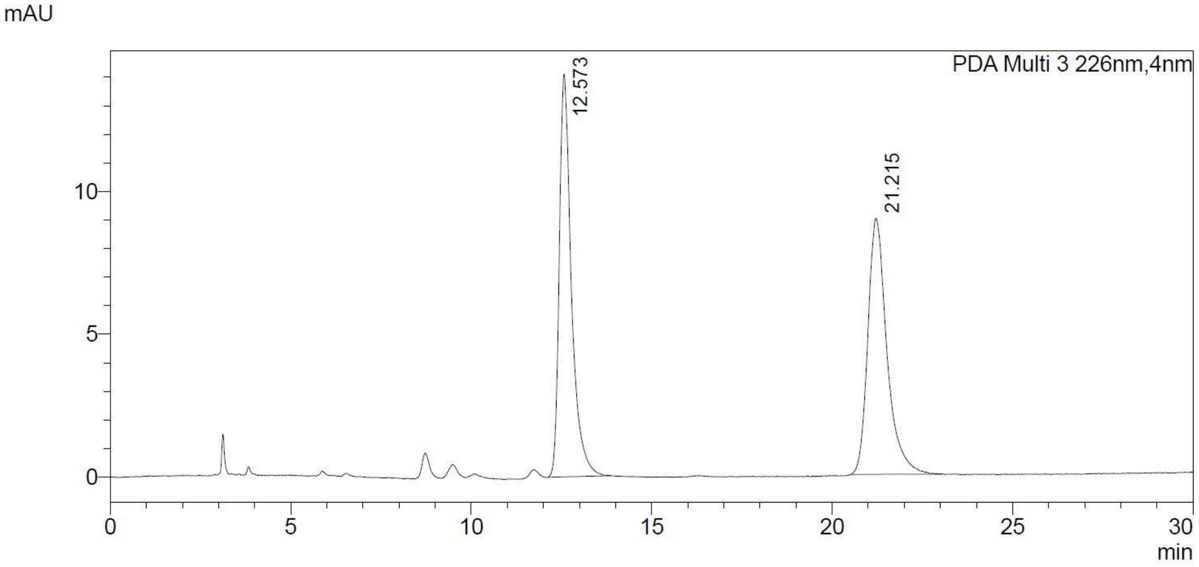

<Peak Table>

PDA Ch3 226nm

Peak#	Ret. Time	Area	Area%
1	12.573	328982	49.967
2	21.215	329418	50.033
Total		658400	100.000

<Chromatogram>

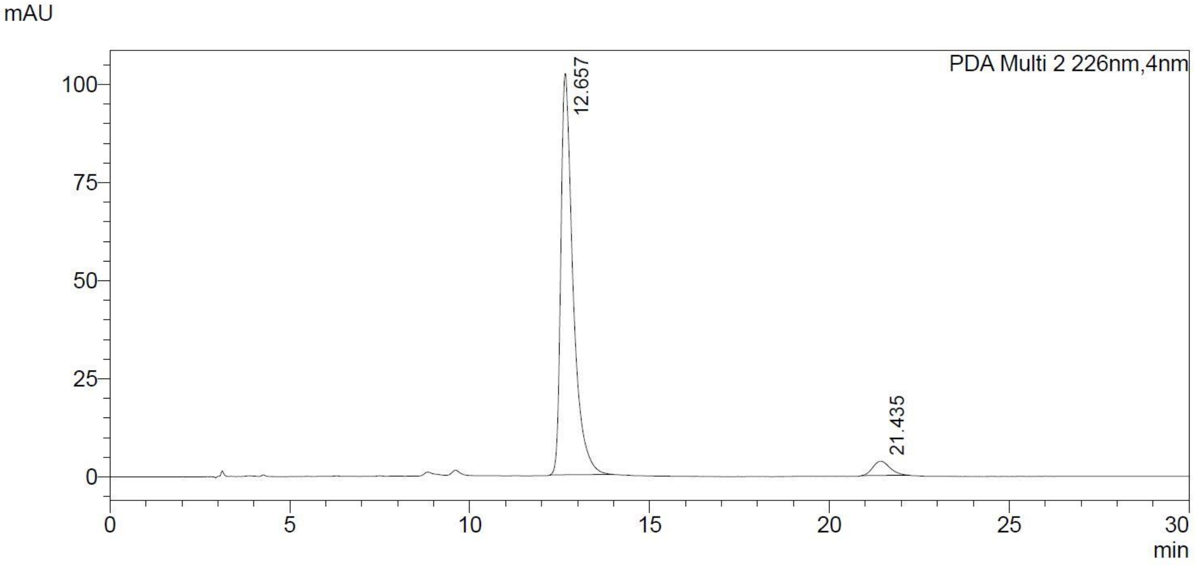

<Peak Table>

PDA Ch2 226nm

Peak#	Ret. Time	Area	Area%
1	12.657	2411760	95.257
2	21.435	120082	4.743
Total		2531842	100.000

CO2Me
CO2Me
N
O
O

2.45u

$C_{18}H_{21}NO_6$

M= 347,37 g.mol^{-1}

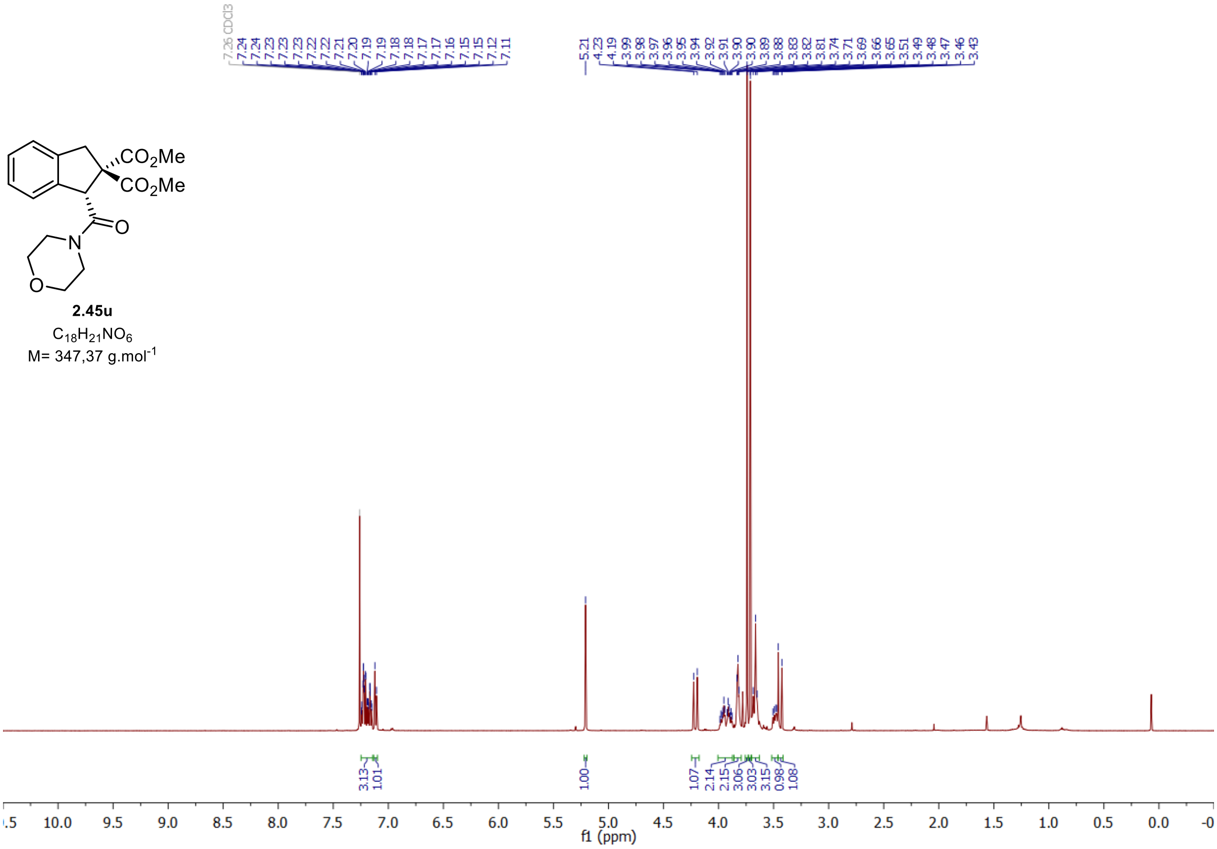

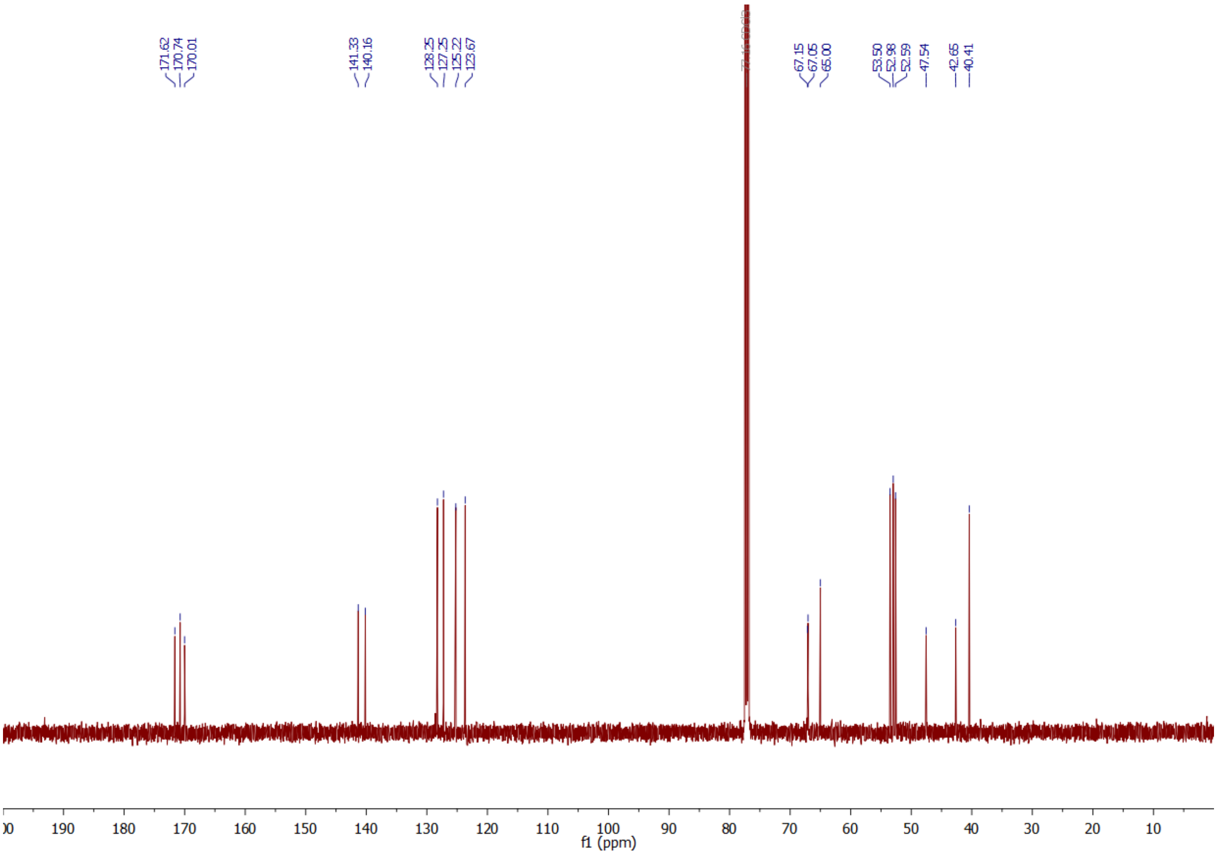

<Chromatogram>

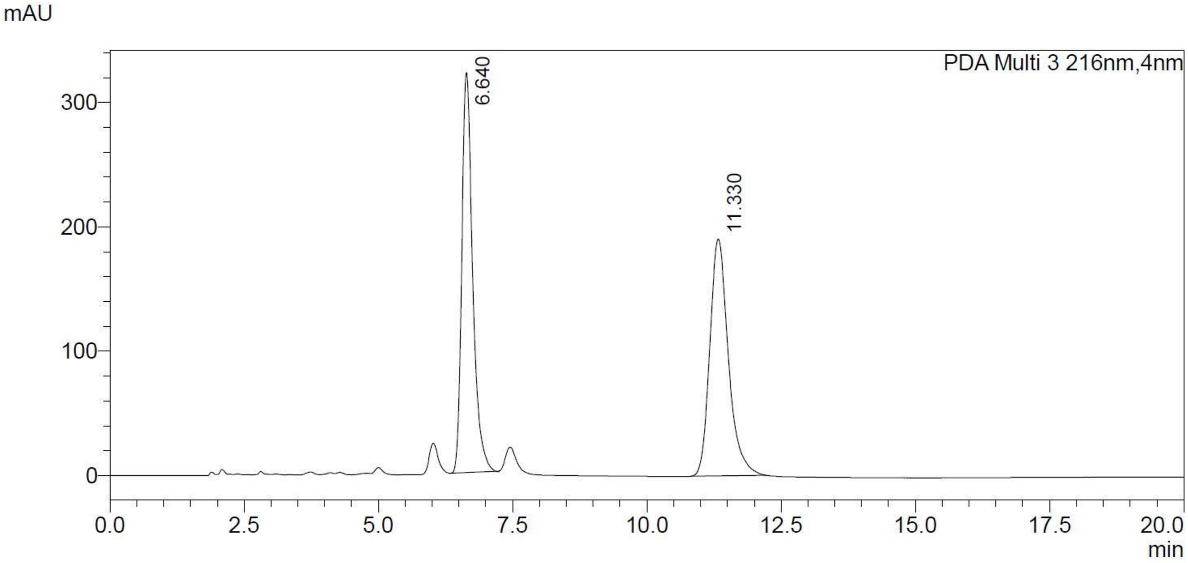

<Peak Table>

PDA Ch3 216nm

Peak#	Ret. Time	Area	Area%
1	6.640	4527380	49.717
2	11.330	4578923	50.283
Total		9106304	100.000

<Chromatogram>

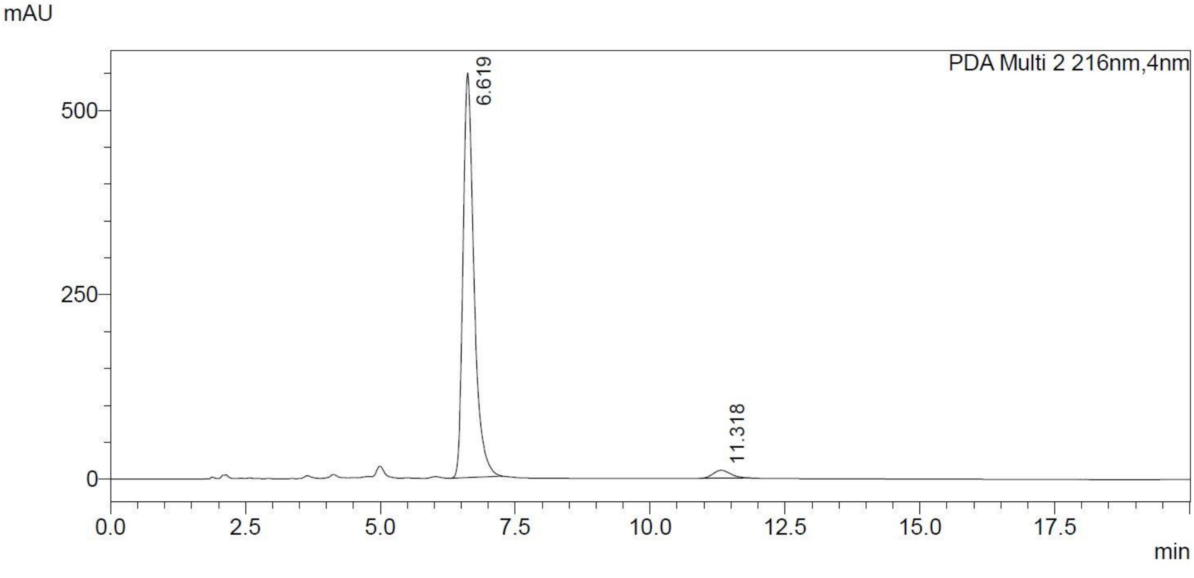

<Peak Table>

PDA Ch2 216nm

Peak#	Ret. Time	Area	Area%
1	6.619	7757982	96.996
2	11.318	240246	3.004
Total		7998228	100.000

CO$_2$Me
CO$_2$Me
O
Me
N
OMe

2v

$C_{16}H_{19}NO_6$

M= 321,33 g.mol^{-1}

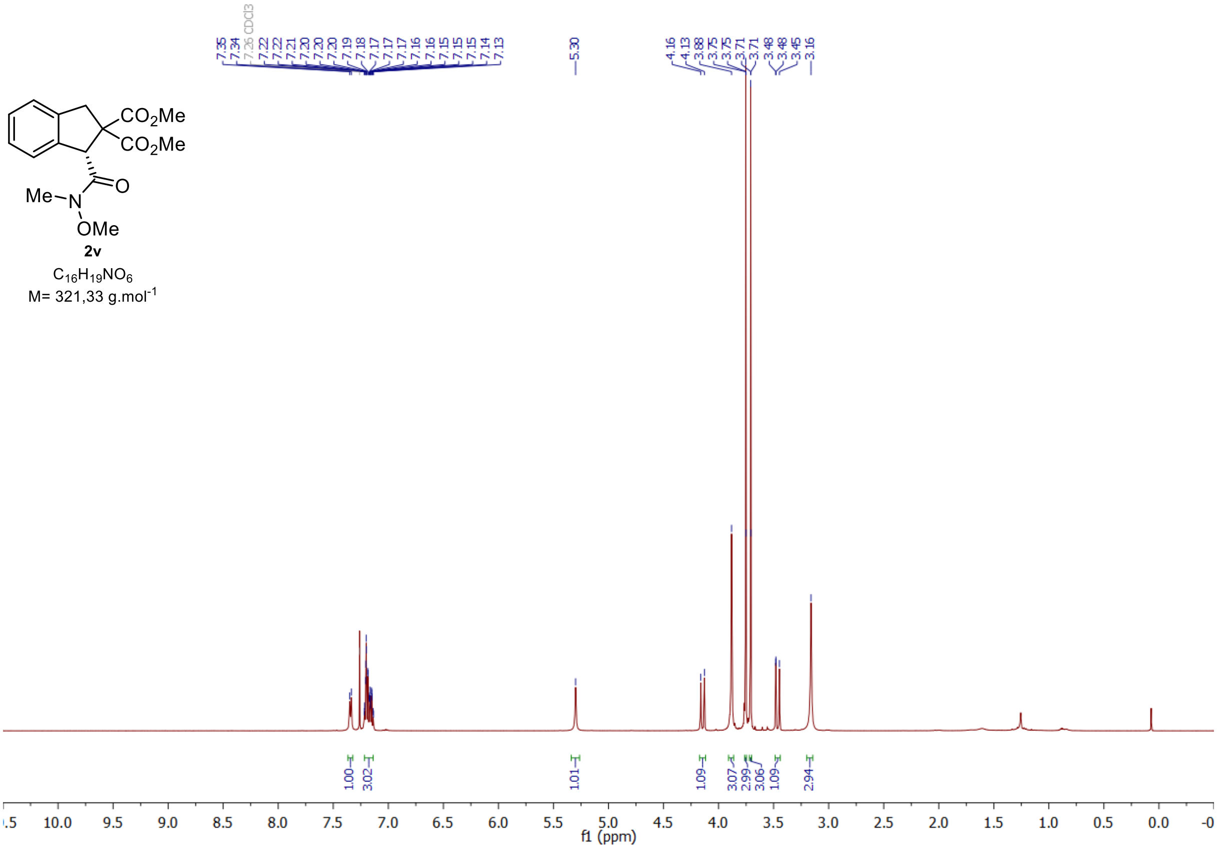

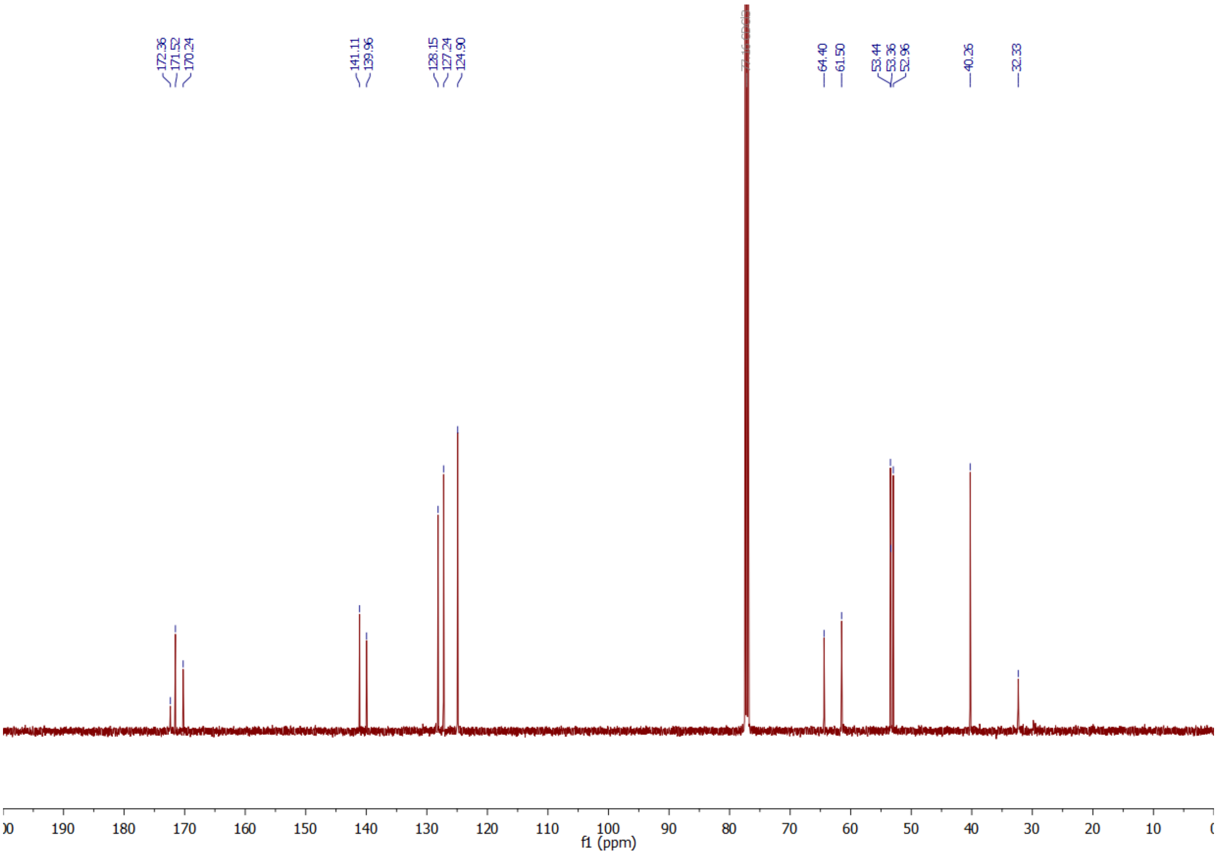

<Chromatogram>

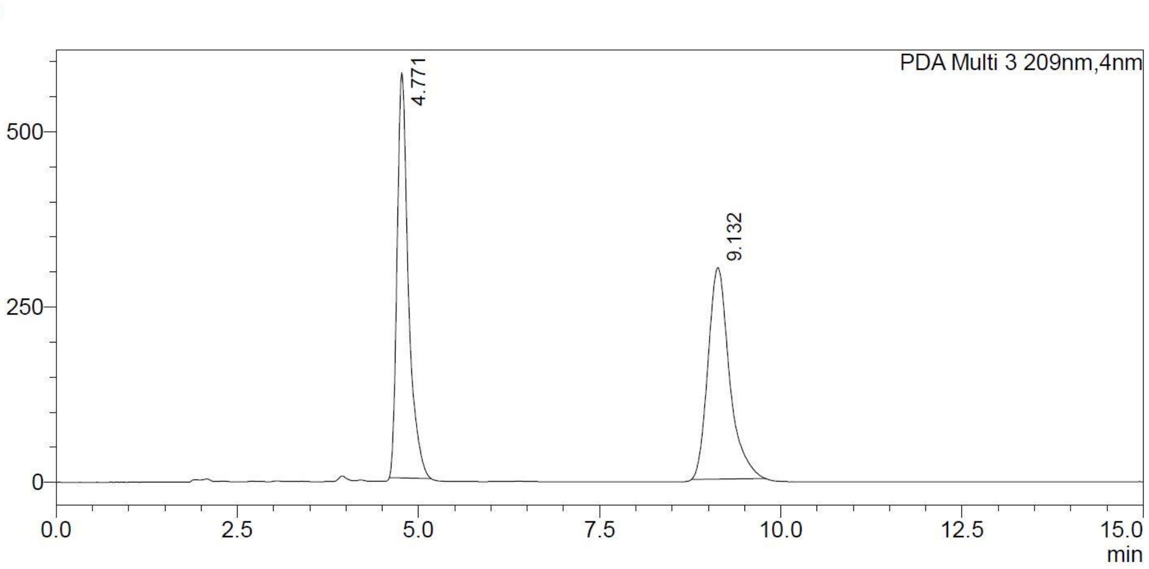

<Peak Table>

PDA Ch3 209nm

Peak#	Ret. Time	Area	Area%
1	4.771	6269119	50.148
2	9.132	6232155	49.852
Total		12501274	100.000

<Chromatogram>

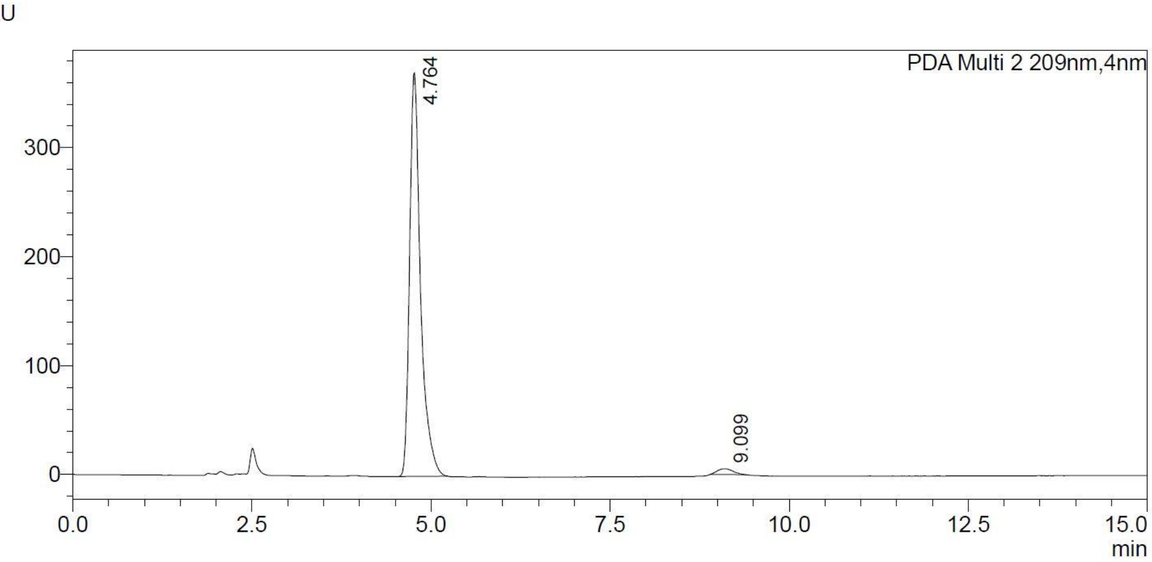

<Peak Table>

PDA Ch2 209nm

Peak#	Ret. Time	Area	Area%
1	4.764	3938708	97.909
2	9.099	84127	2.091
Total		4022835	100.000

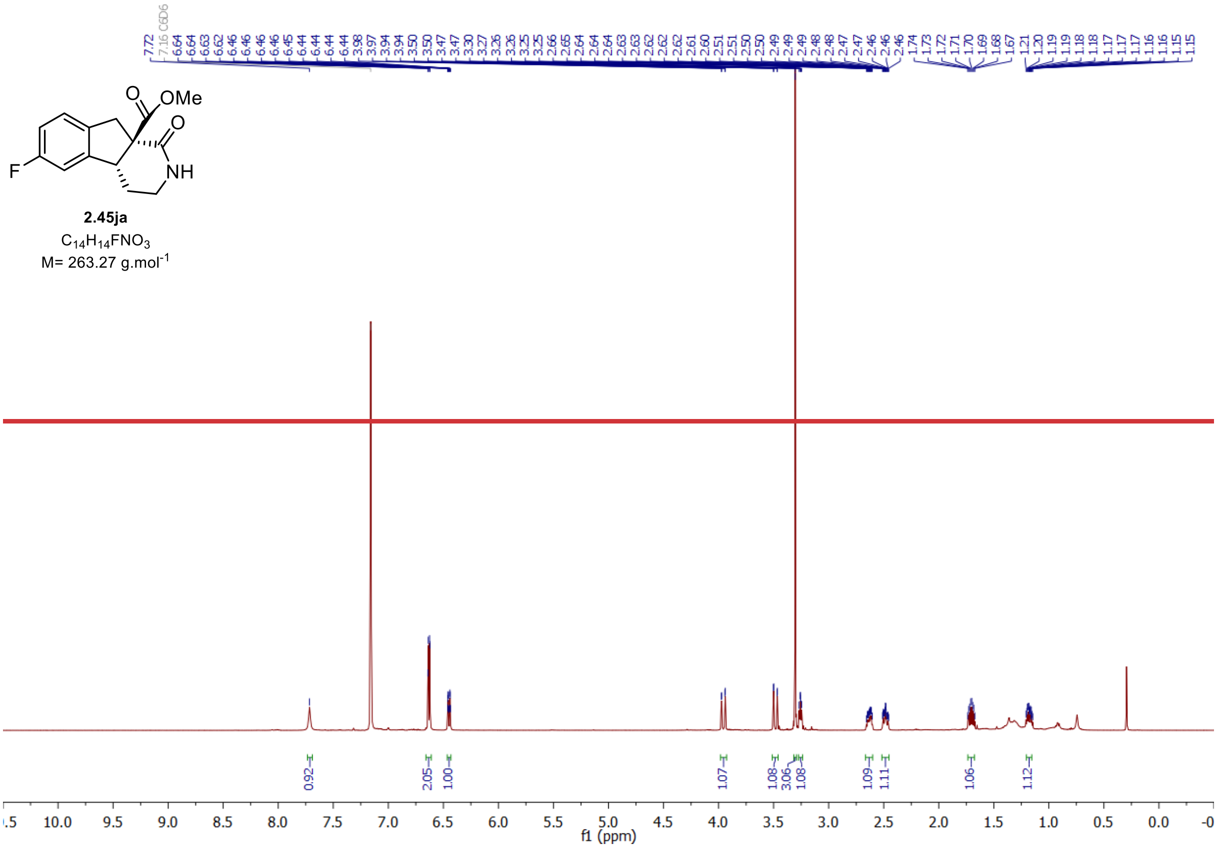

2.45ja

$C_{14}H_{14}FNO_3$

M= 263.27 g.mol^{-1}

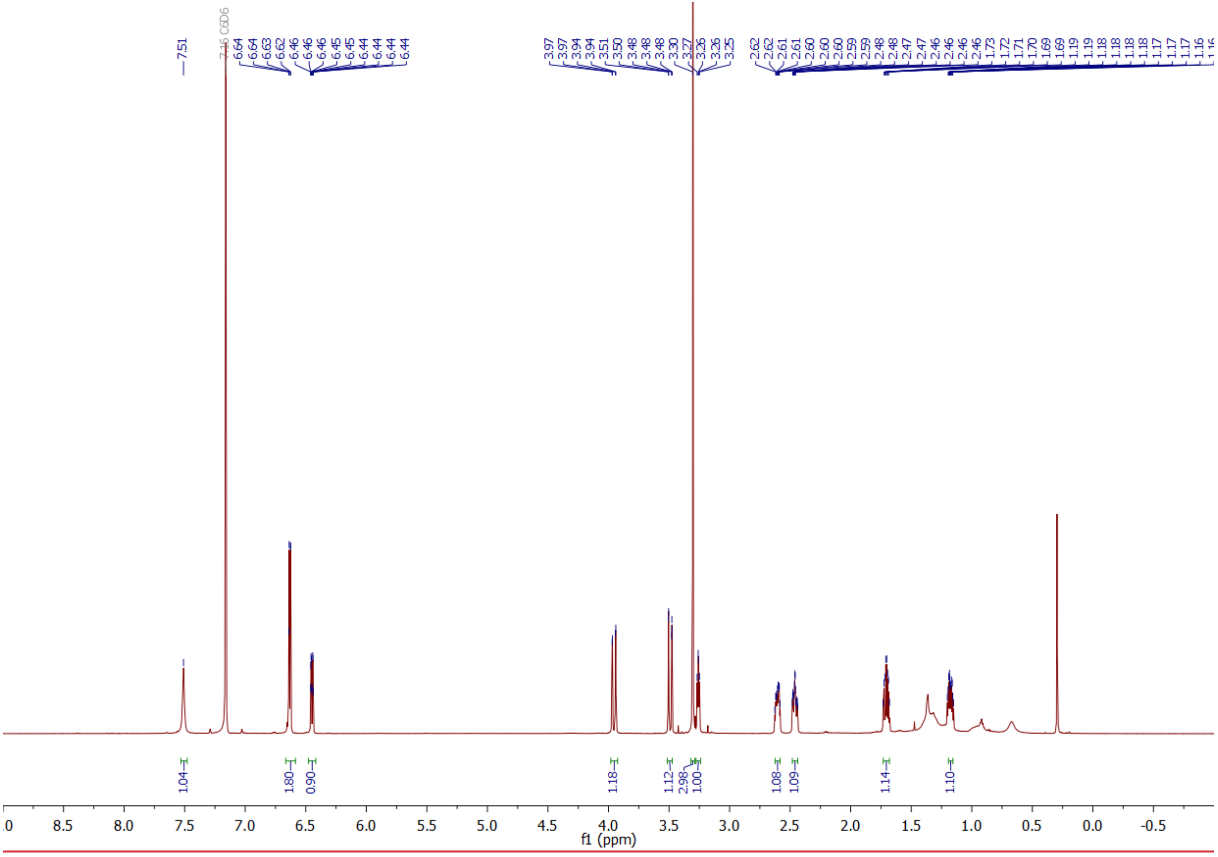

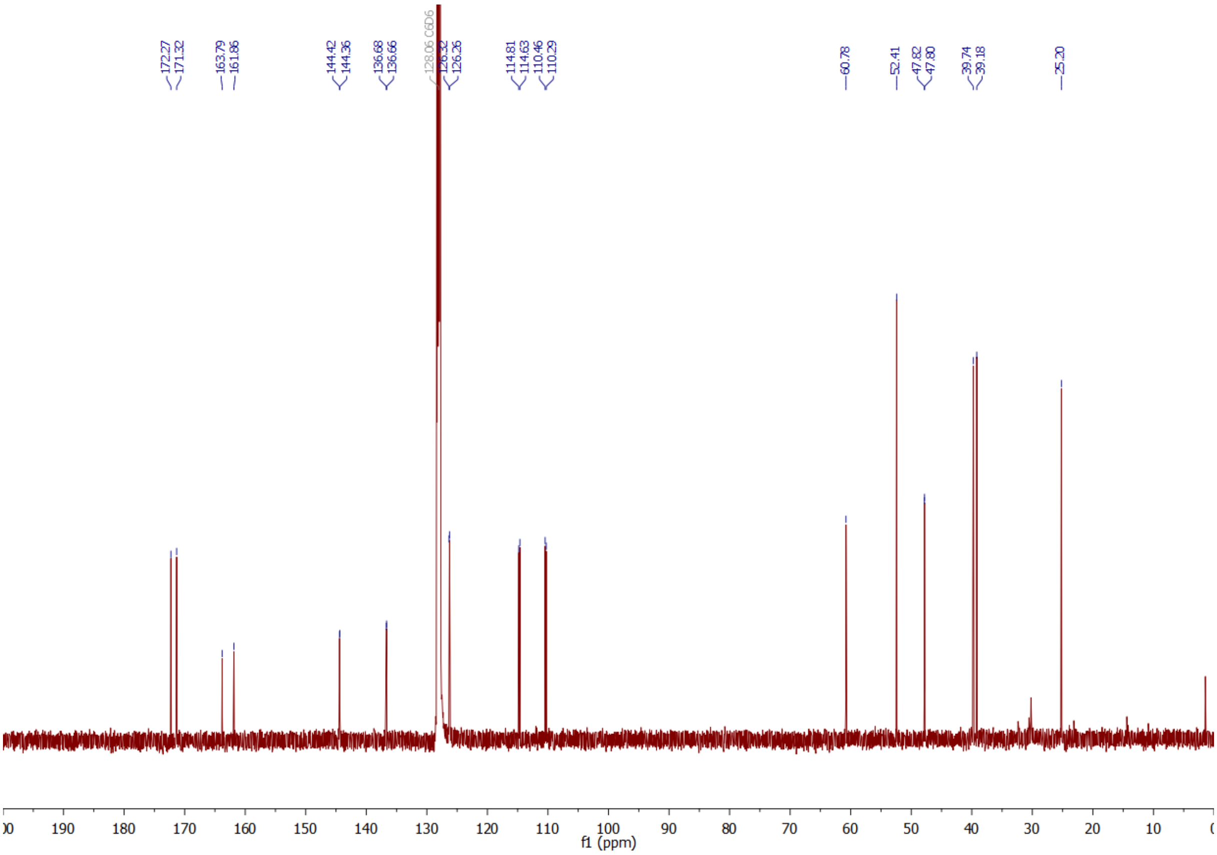
172.27
171.32
163.79
161.86
144.42
144.36
136.68
136.66
128.06 C6D6
126.32
126.26
114.81
114.63
110.46
110.29
60.78
52.41
47.82
47.80
39.74
39.18
25.20
190
180
170
160
150
140
130
120
110
100
90
80
70
60
50
40
30
20
10
f1 (ppm)

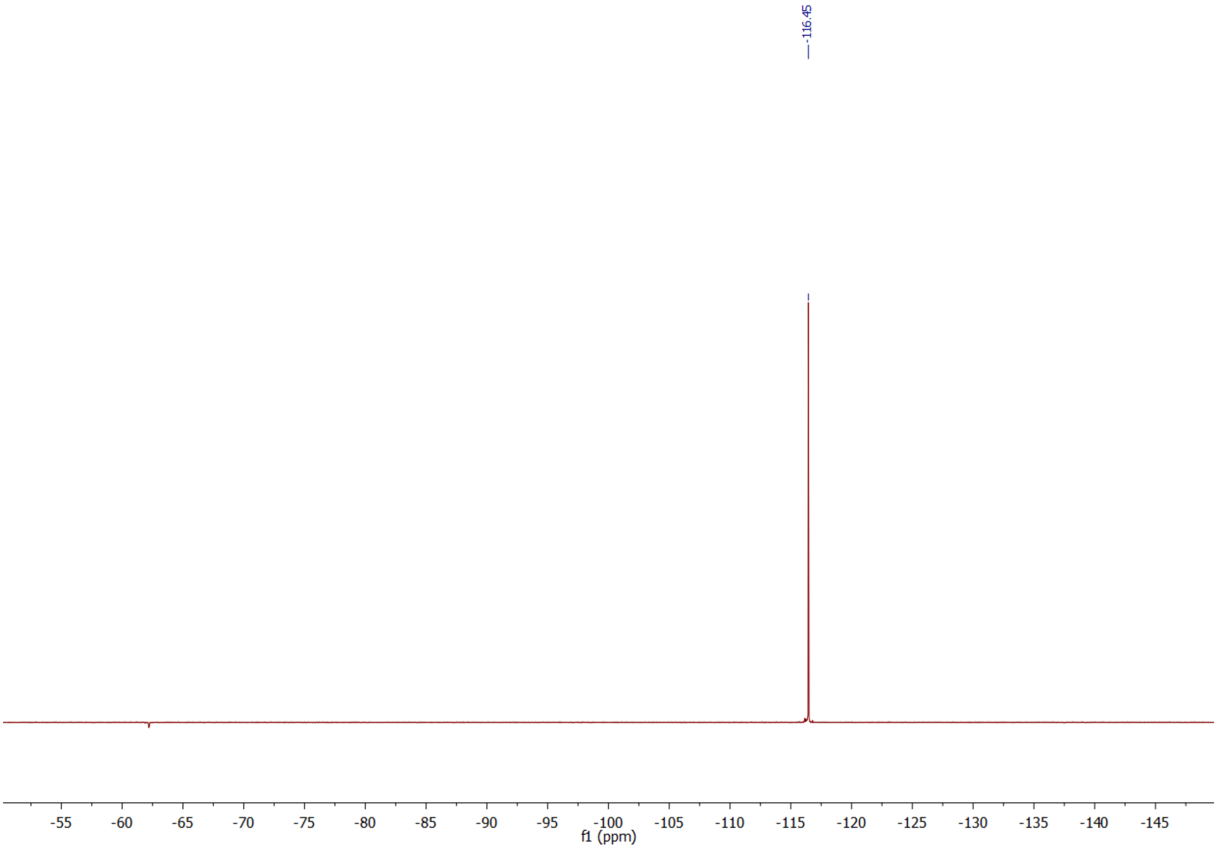
-116.45
-55
-60
-65
-70
-75
-80
-85
-90
-95
-100
-105
-110
-115
-120
-125
-130
-135
-140
-145
f1 (ppm)

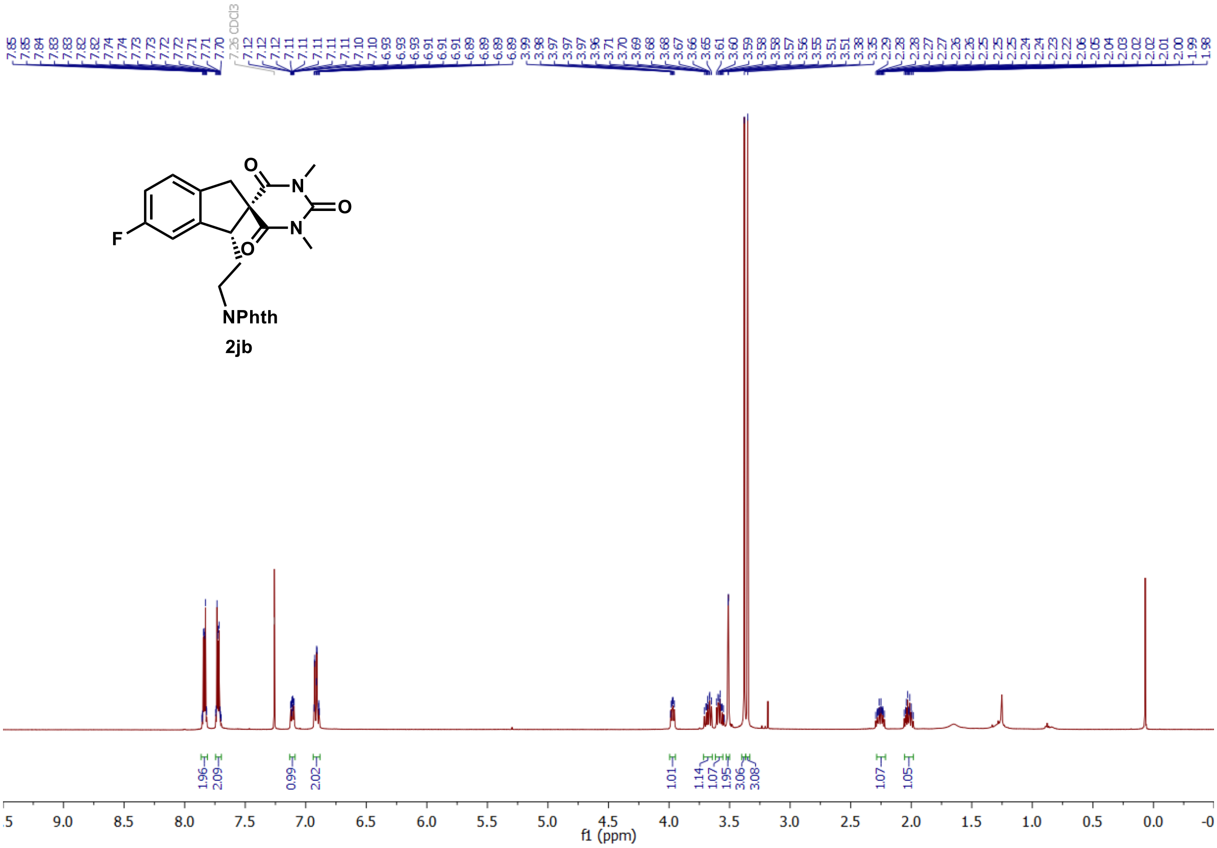
7.85
7.85
7.84
7.83
7.83
7.82
7.82
7.74
7.74
7.73
7.73
7.72
7.72
7.71
7.71
7.70
7.26 CDCl3
7.12
7.12
7.12
7.11
7.11
7.11
7.11
7.11
7.10
7.10
6.93
6.93
6.93
6.91
6.91
6.91
6.89
6.89
6.89
6.89
3.99
3.98
3.97
3.97
3.97
3.96
3.71
3.70
3.69
3.68
3.68
3.67
3.66
3.65
3.61
3.60
3.59
3.58
3.58
3.57
3.56
3.55
3.51
3.51
3.38
3.35
2.29
2.28
2.28
2.27
2.27
2.26
2.26
2.25
2.25
2.25
2.24
2.24
2.23
2.22
2.06
2.05
2.04
2.03
2.02
2.02
2.01
2.00
1.99
1.98
O
N
O
N
F
O
O
NPhth
2jb
1.96
2.09
0.99
2.02
1.01
1.14
1.07
1.95
3.06
3.08
1.07
1.05
.5
9.0
8.5
8.0
7.5
7.0
6.5
6.0
5.5
5.0
4.5
4.0
3.5
3.0
2.5
2.0
1.5
1.0
0.5
0.0
-0
f1 (ppm)

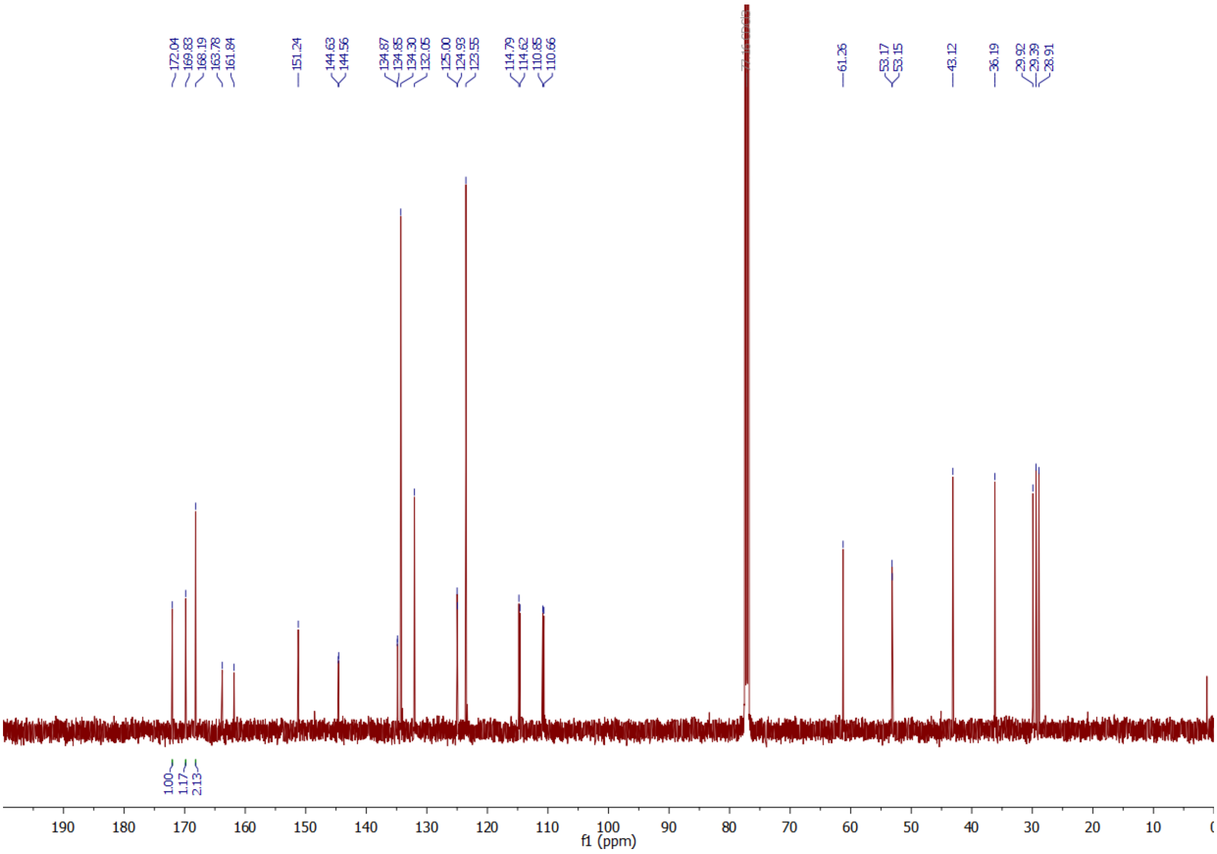
172.04
169.83
168.19
163.78
161.84
151.24
144.63
144.56
134.87
134.85
134.30
132.05
125.00
124.93
123.55
114.79
114.62
110.85
110.66
77.16 CDCl3
61.26
53.17
53.15
43.12
36.19
29.92
29.39
28.91
1.00
1.17
2.13
190
180
170
160
150
140
130
120
110
100
90
80
70
60
50
40
30
20
10
f1 (ppm)

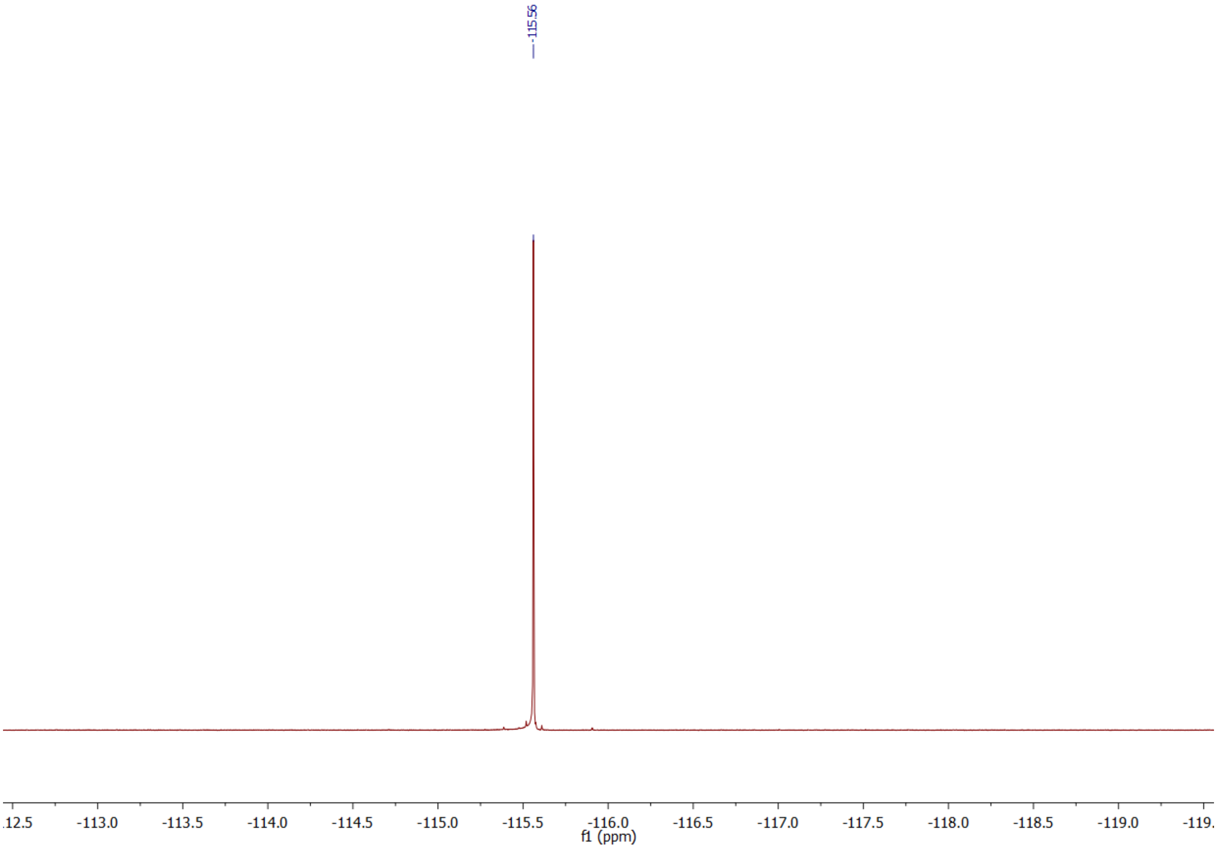
-115.56
.12.5
-113.0
-113.5
-114.0
-114.5
-115.0
-115.5
-116.0
f1 (ppm)
-116.5
-117.0
-117.5
-118.0
-118.5
-119.0
-119.

<Chromatogram>

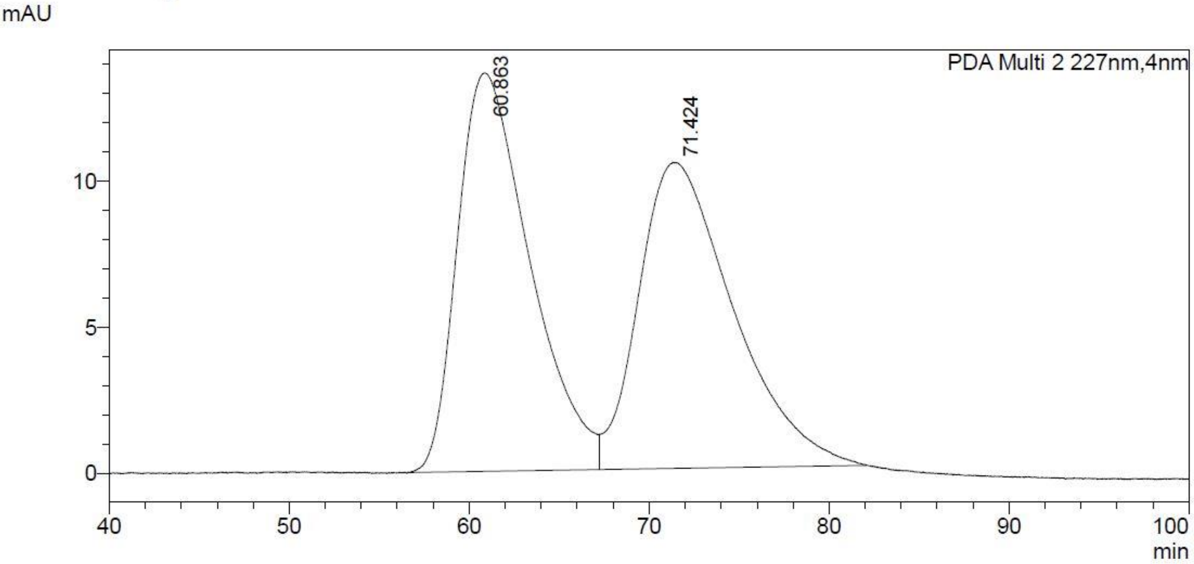

<Peak Table>

PDA Ch2 227nm

Peak#	Ret. Time	Area	Area%
1	60.863	3815913	49.927
2	71.424	3827050	50.073
Total		7642963	100.000

<Chromatogram>

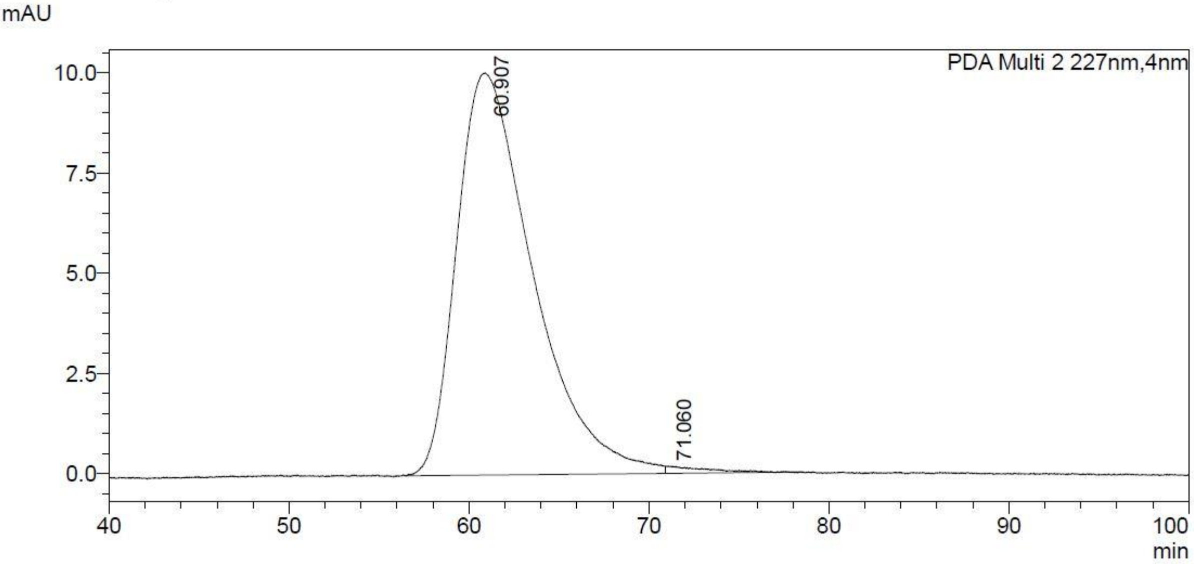

<Peak Table>

PDA Ch2 227nm

Peak#	Ret. Time	Area	Area%
1	60.907	2952636	99.029
2	71.060	28940	0.971
Total		2981576	100.000

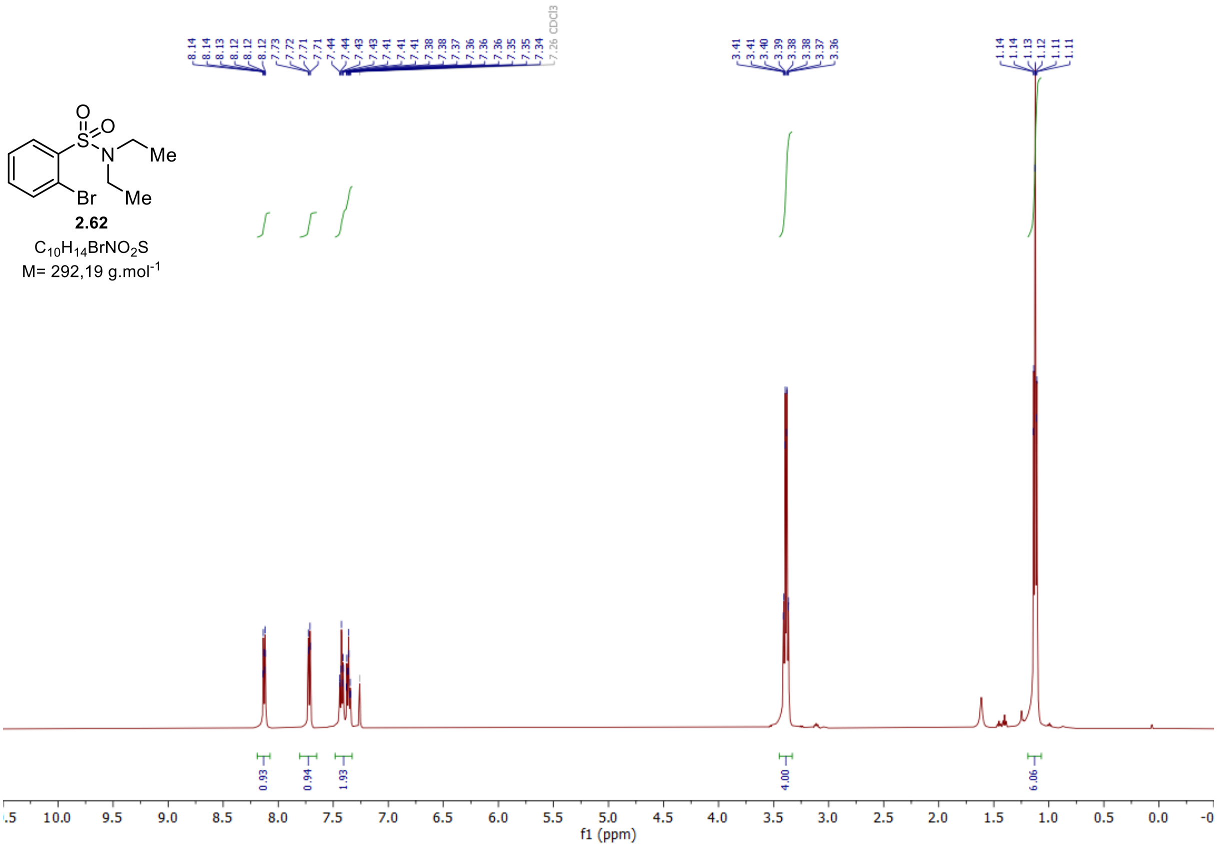

2.62

$C_{10}H_{14}BrNO_2S$

M= 292,19 g.mol^{-1}

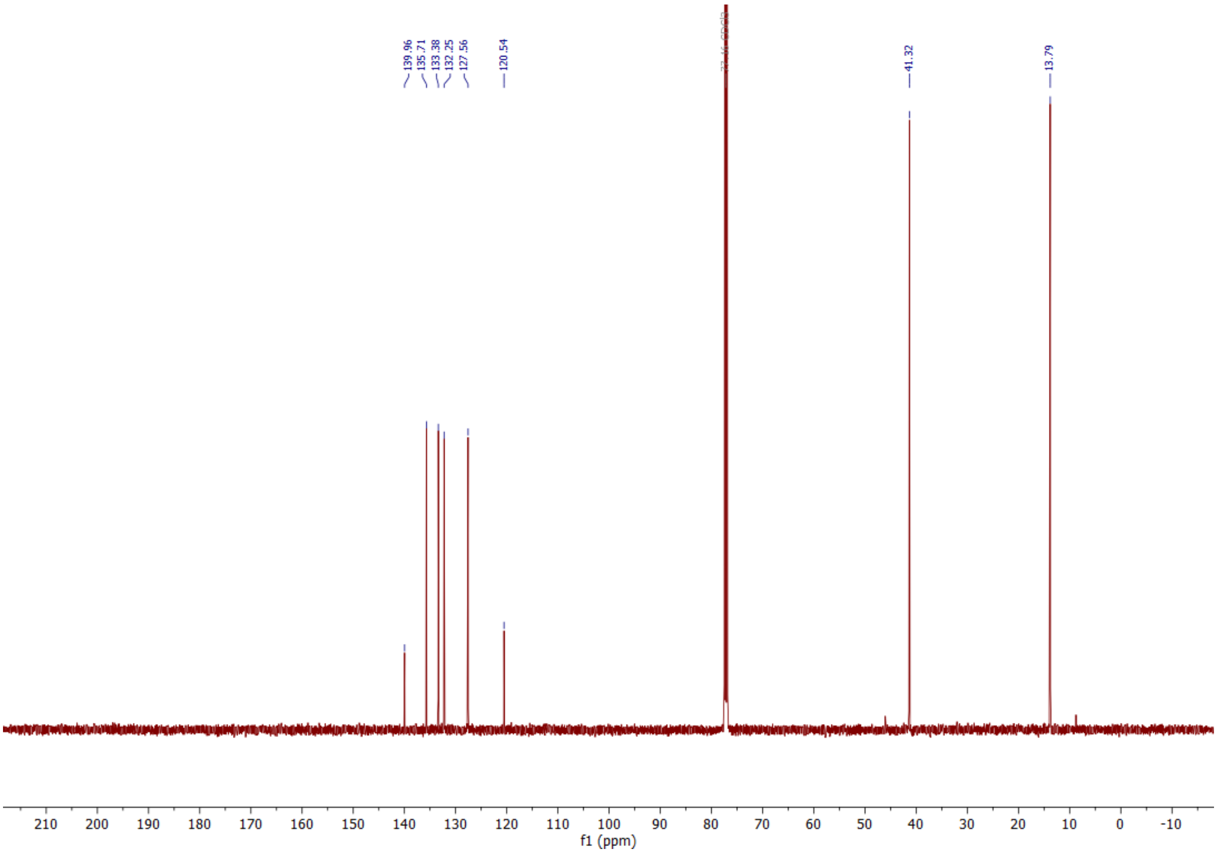

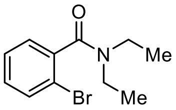

2.63
$C_{11}H_{14}BrNO$
M= 256,14 g.mol^{-1}

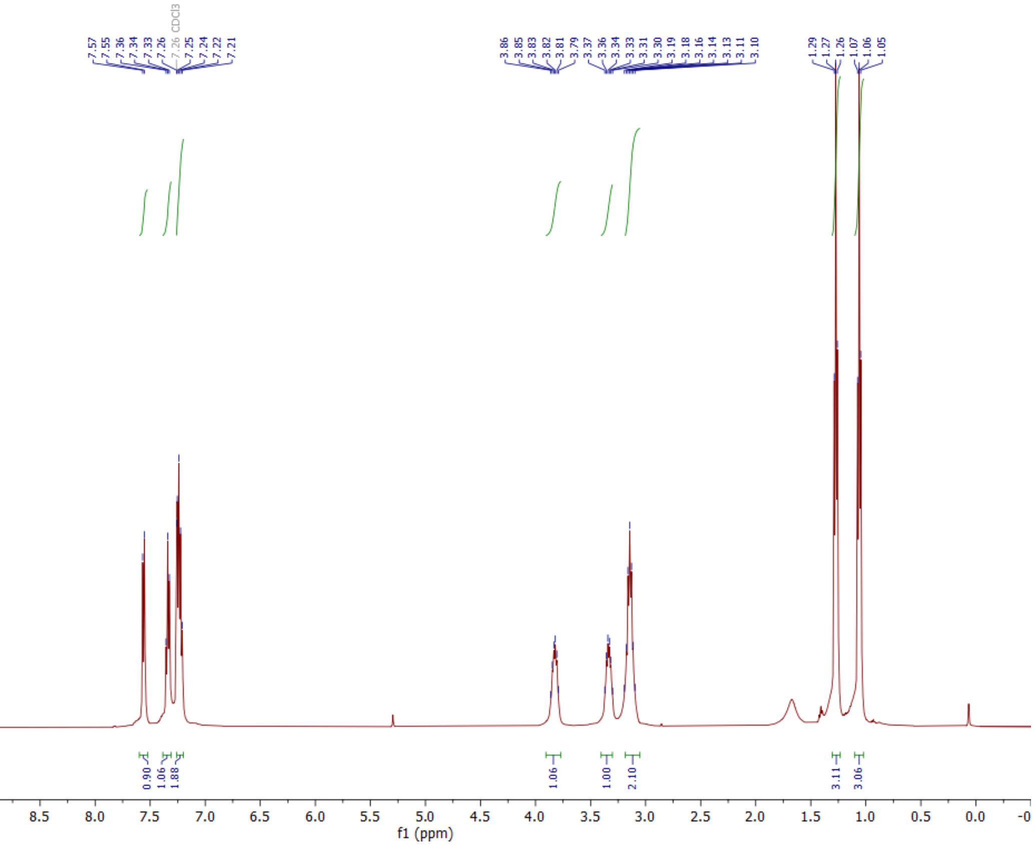

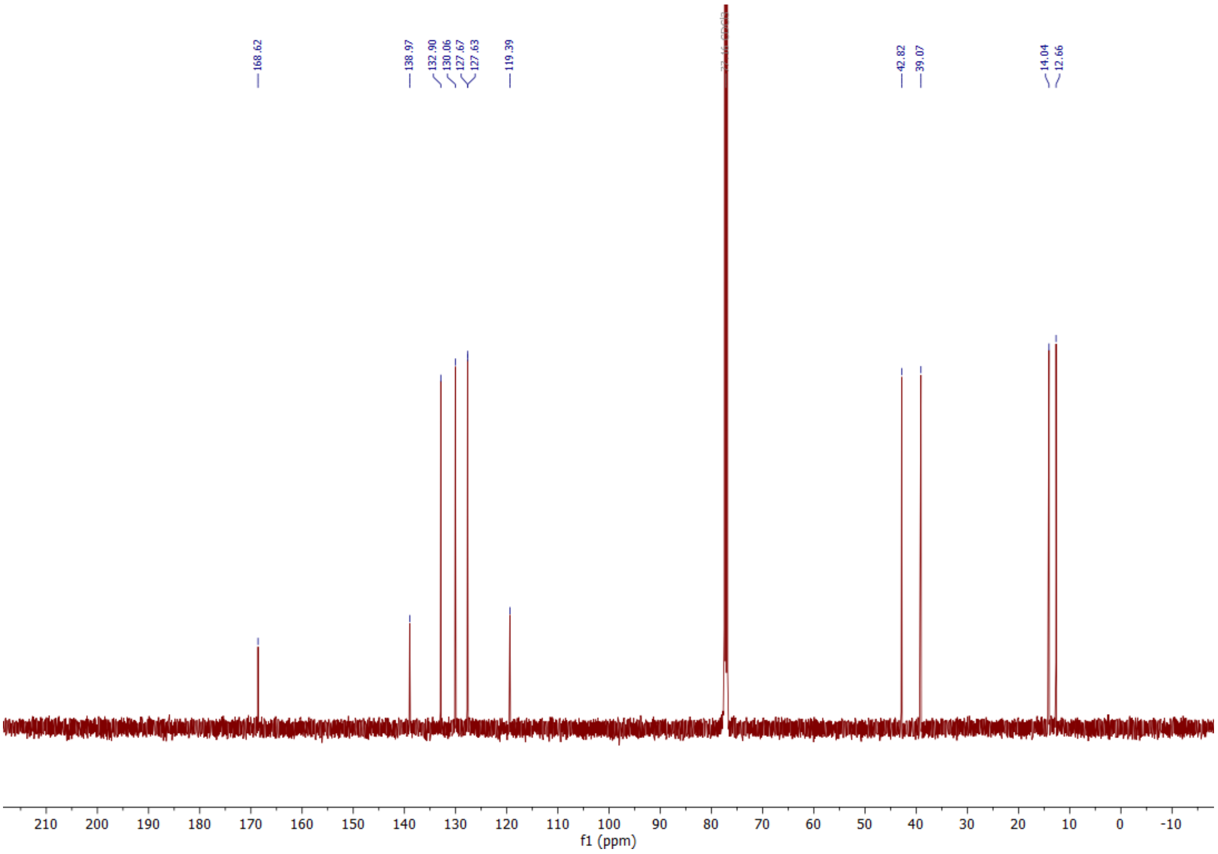

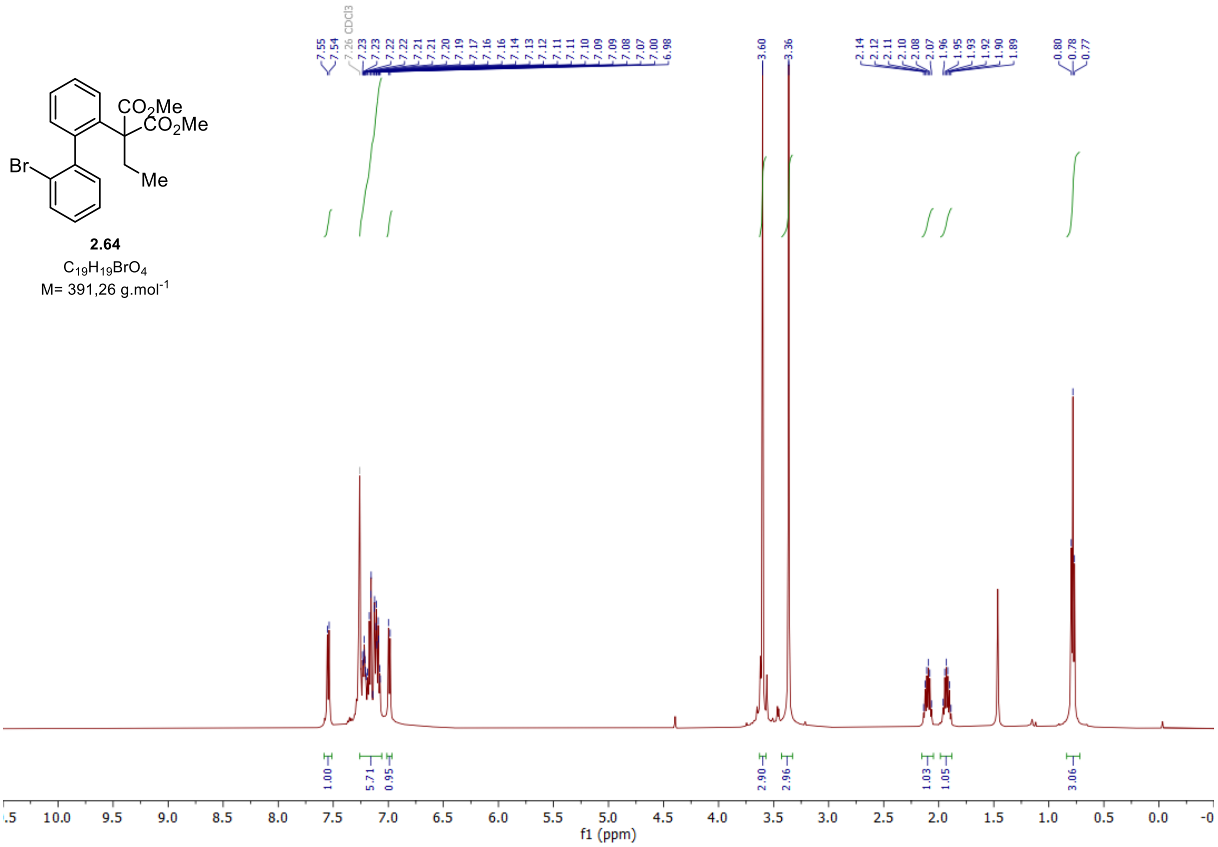

2.64

$C_{19}H_{19}BrO_4$

M= 391,26 g.mol^{-1}

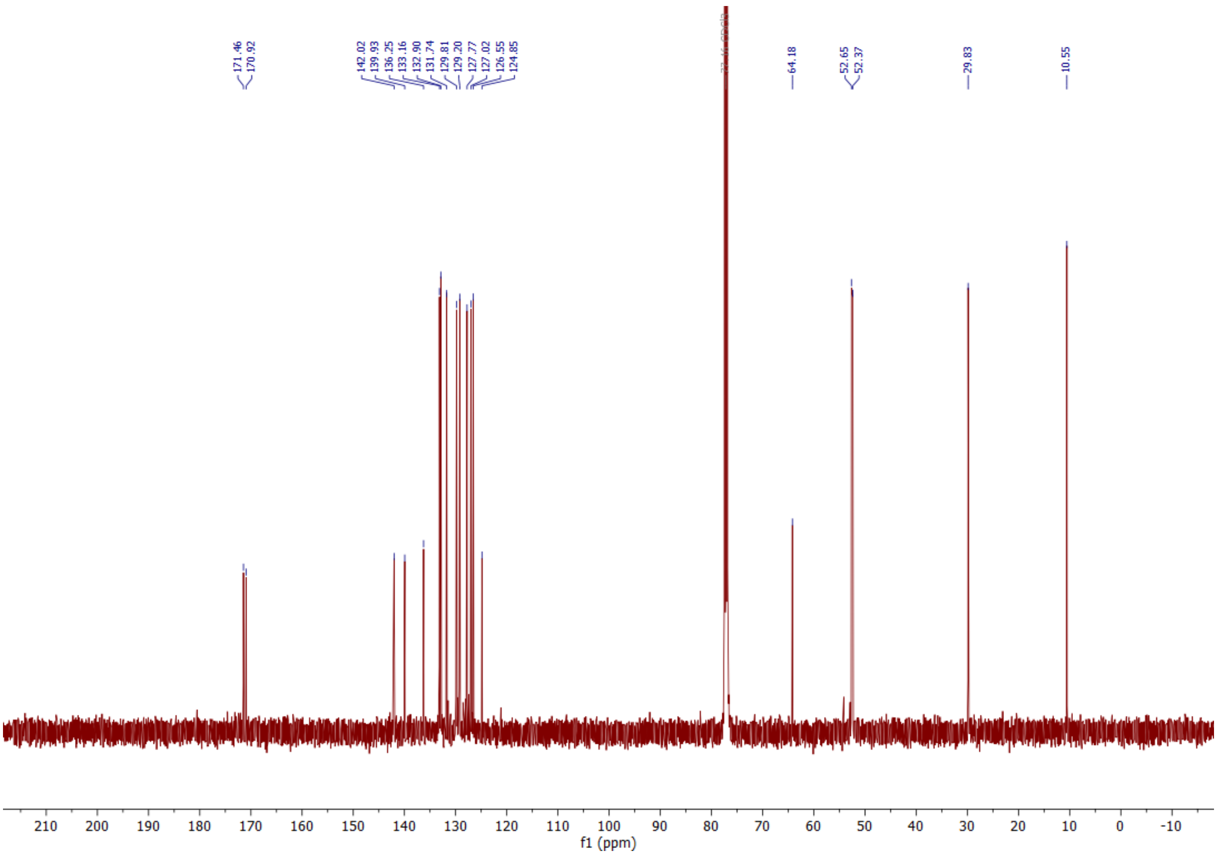

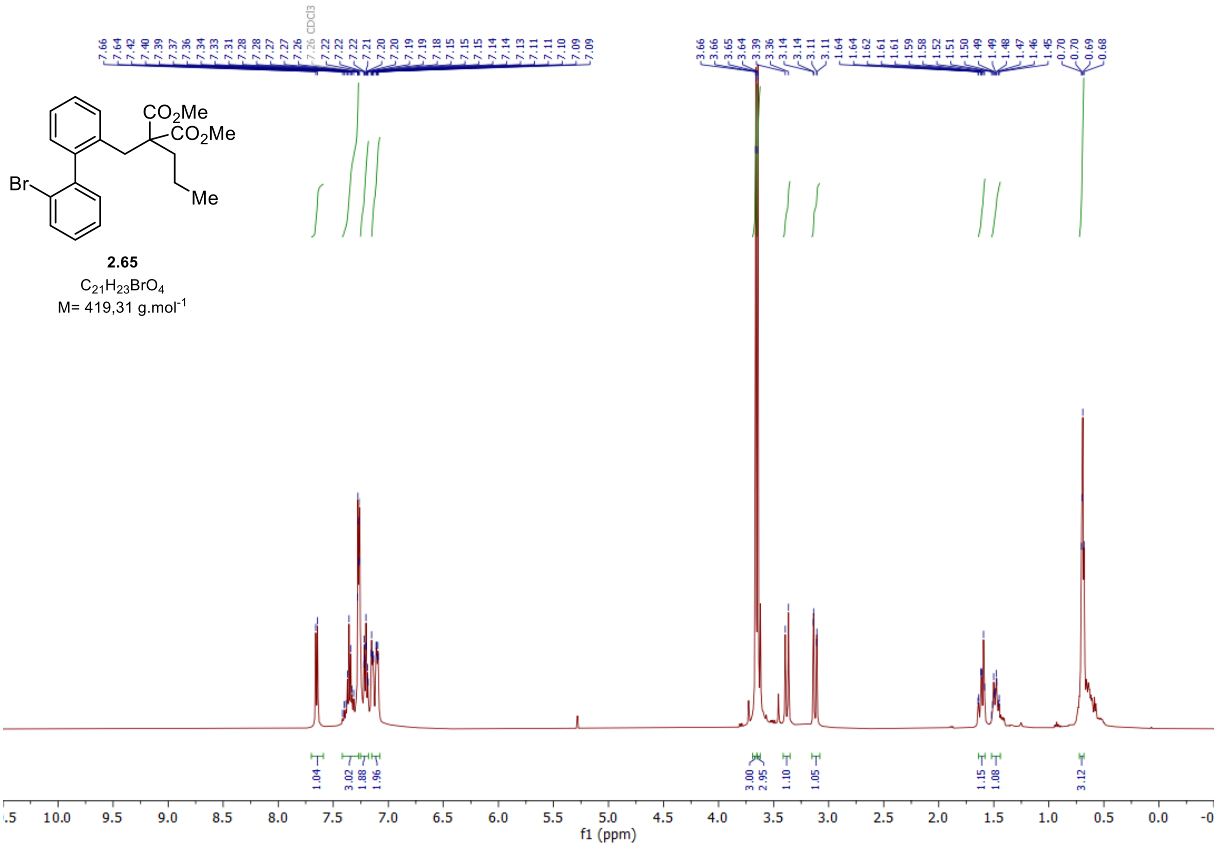

2.65

$C_{21}H_{23}BrO_4$

M= 419,31 g.mol^{-1}

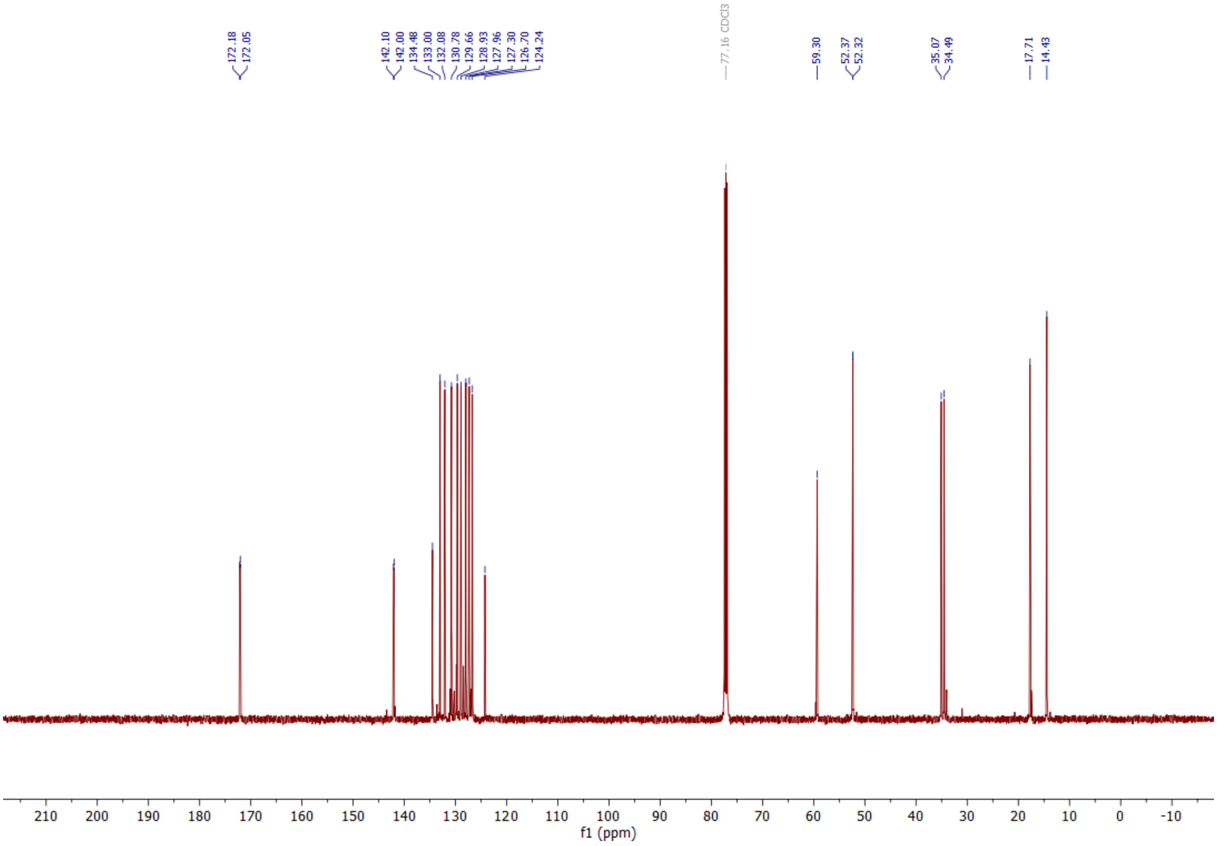

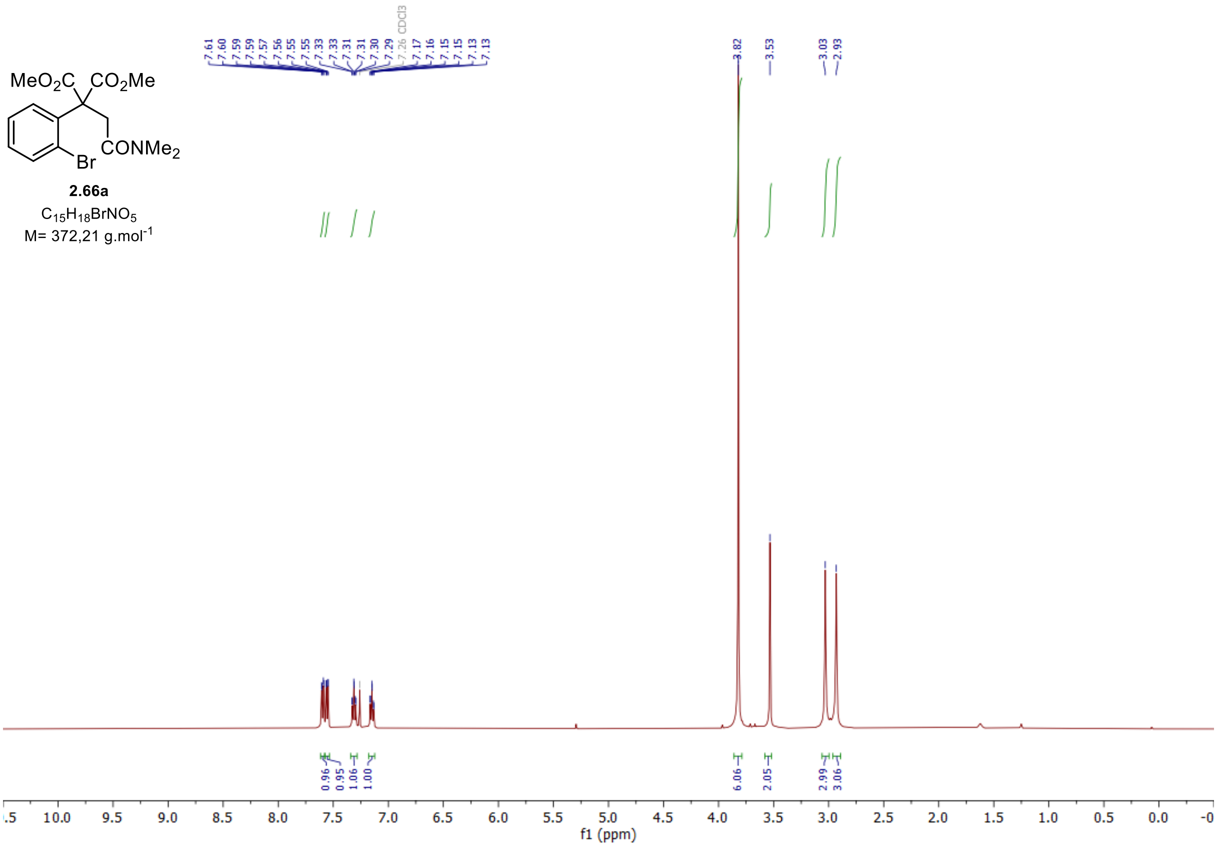

2.66a

$C_{15}H_{18}BrNO_5$

M= 372,21 g.mol^{-1}

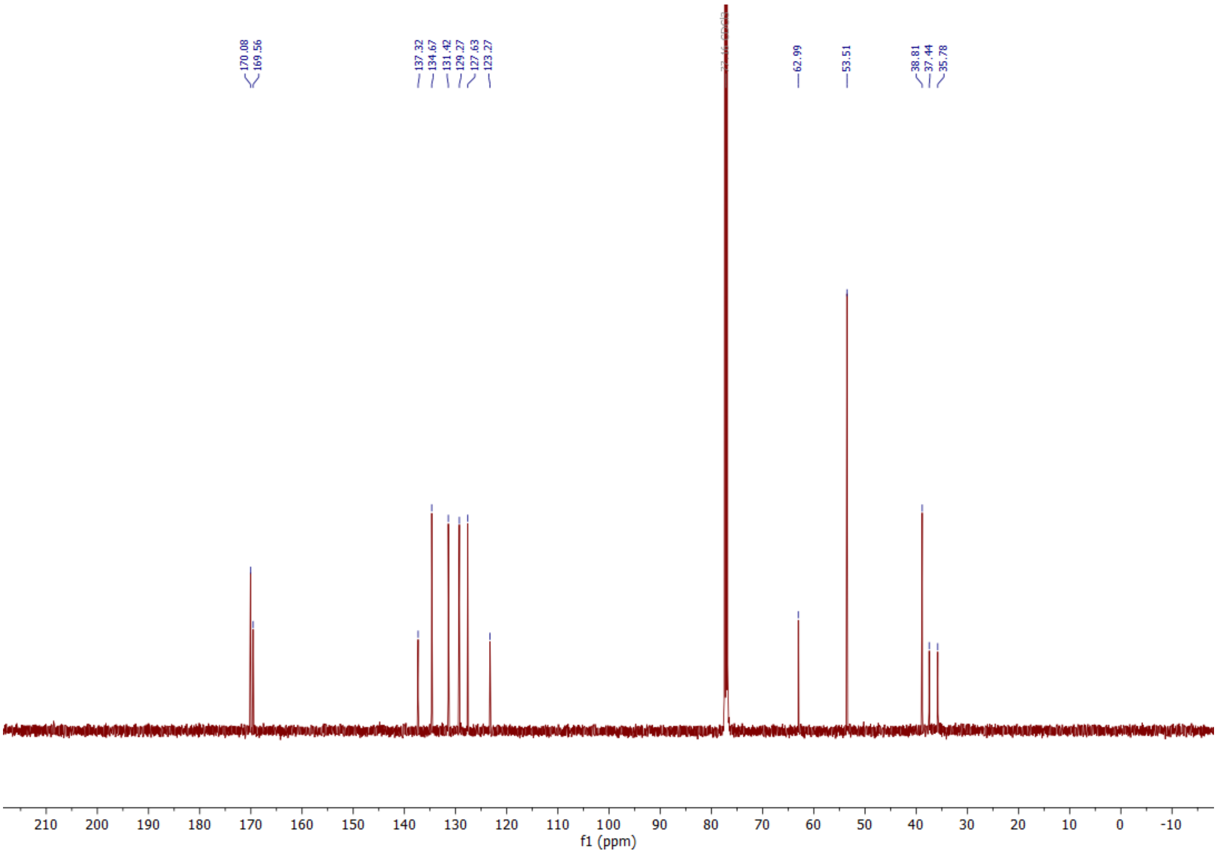

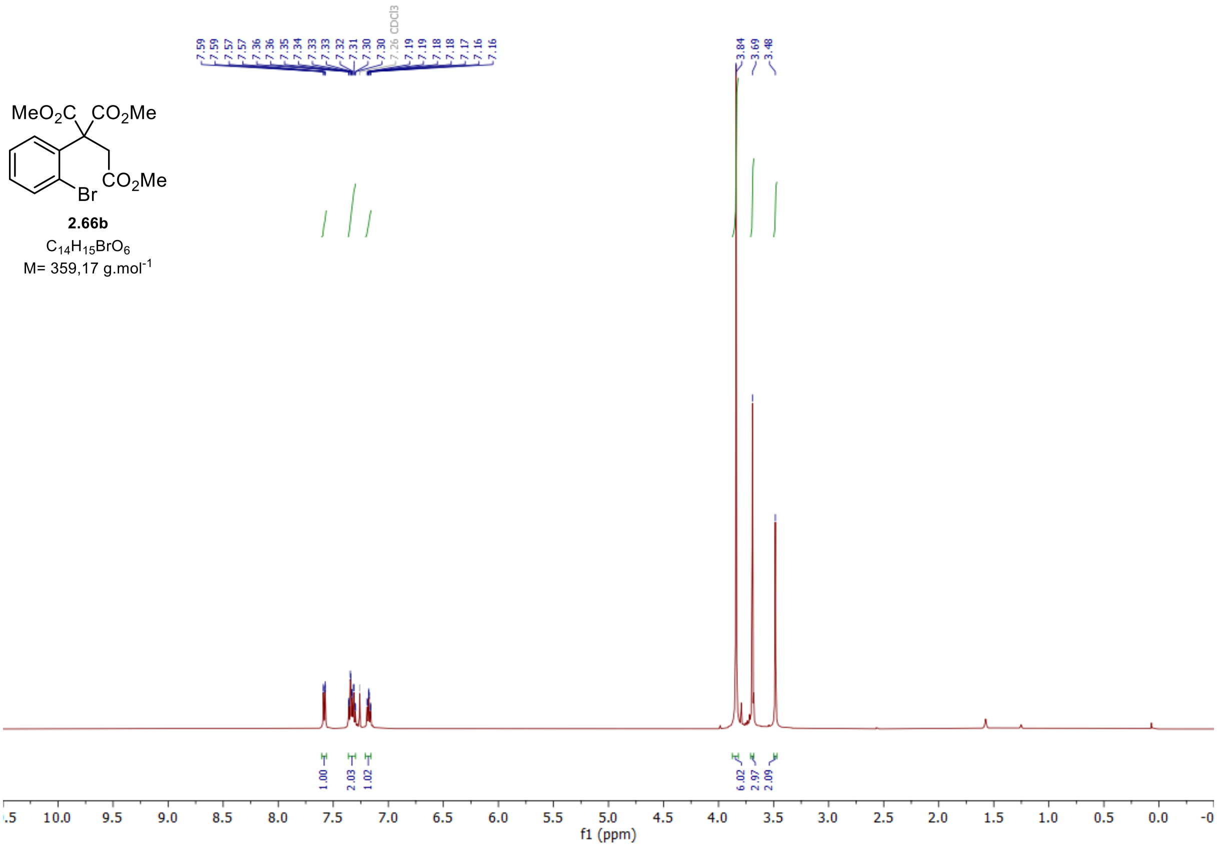

2.66b

$C_{14}H_{15}BrO_6$

M= 359,17 g.mol^{-1}

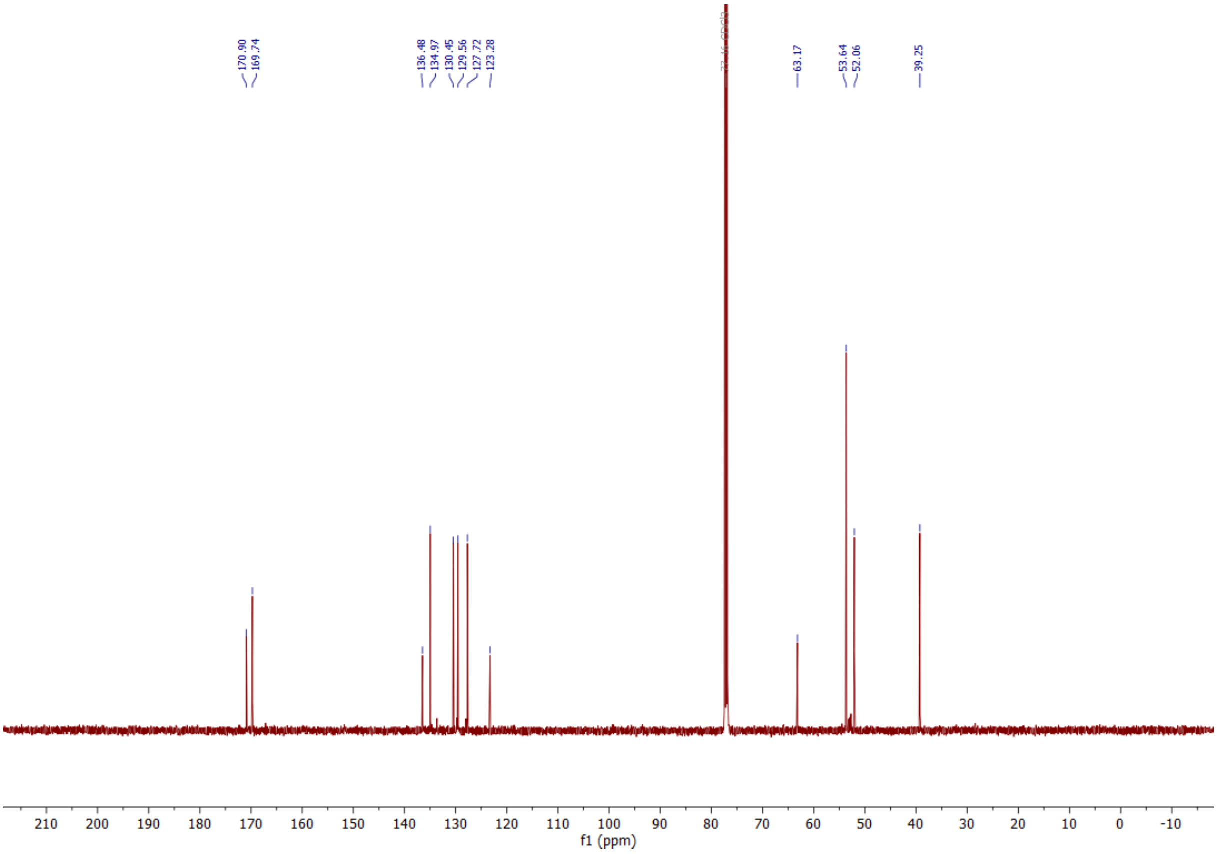

COCF3
N
O
Br
OtBu

2.68a

$C_{15}H_{17}BF_3NO_3$

M= 396,20 g.mol^{-1}

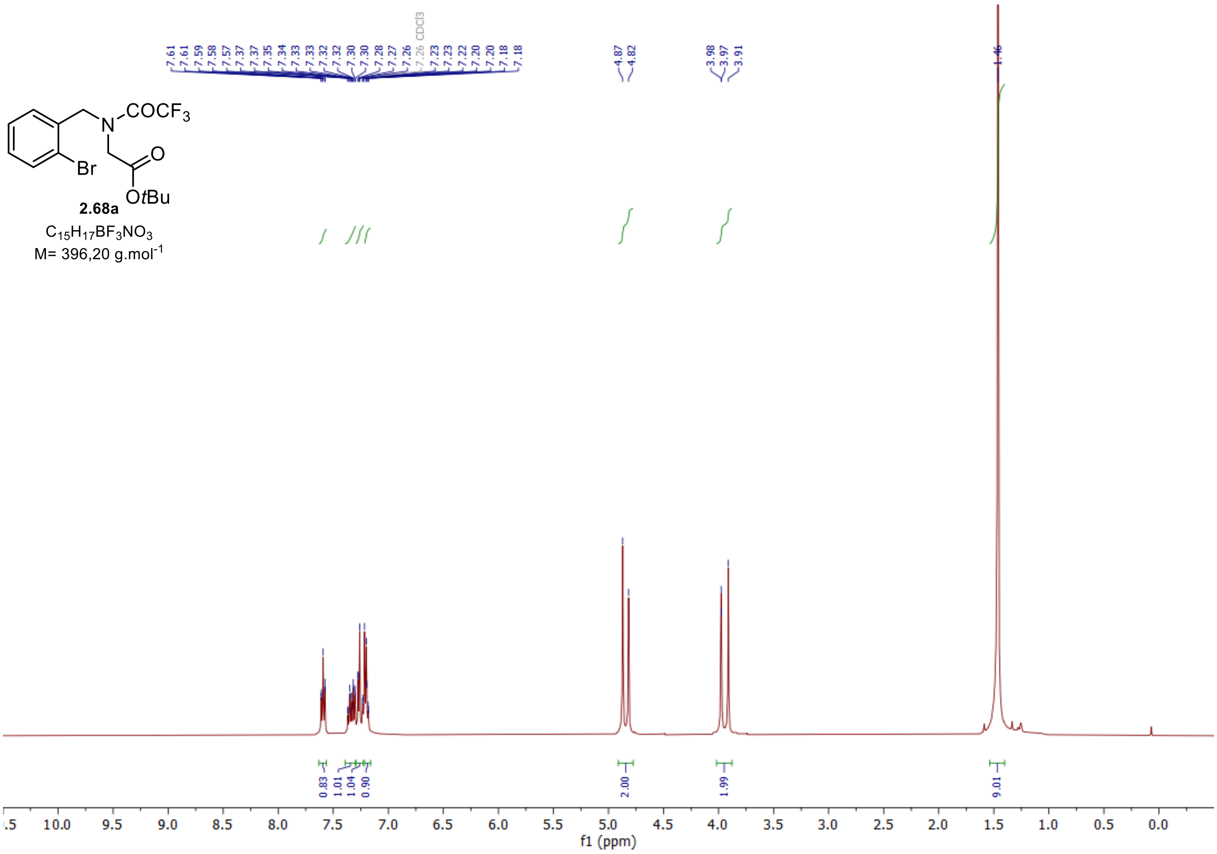

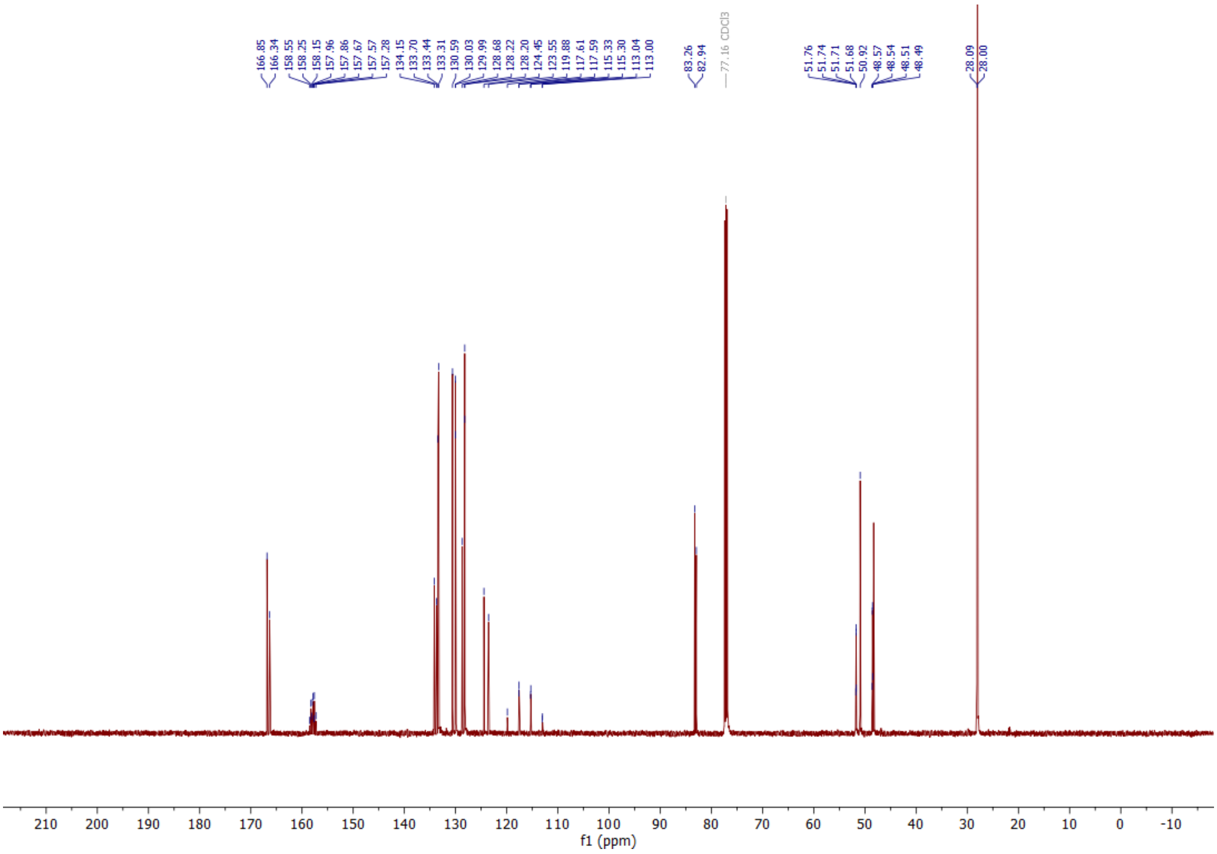

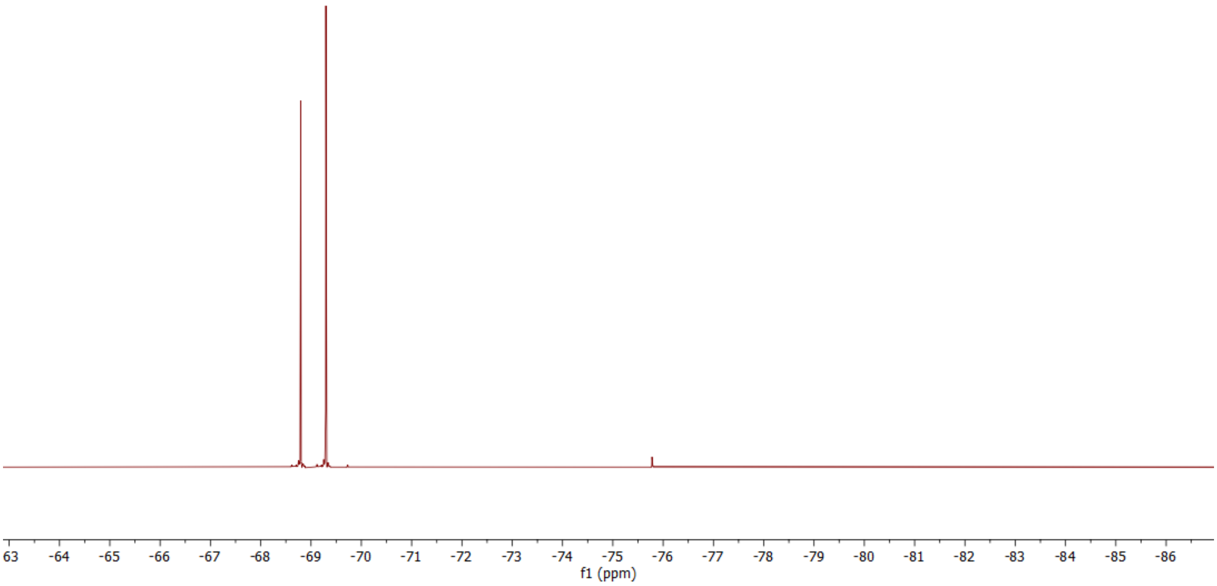
63
-64
-65
-66
-67
-68
-69
-70
-71
-72
-73
-74
-75
-76
-77
-78
-79
-80
-81
-82
-83
-84
-85
-86
f1 (ppm)

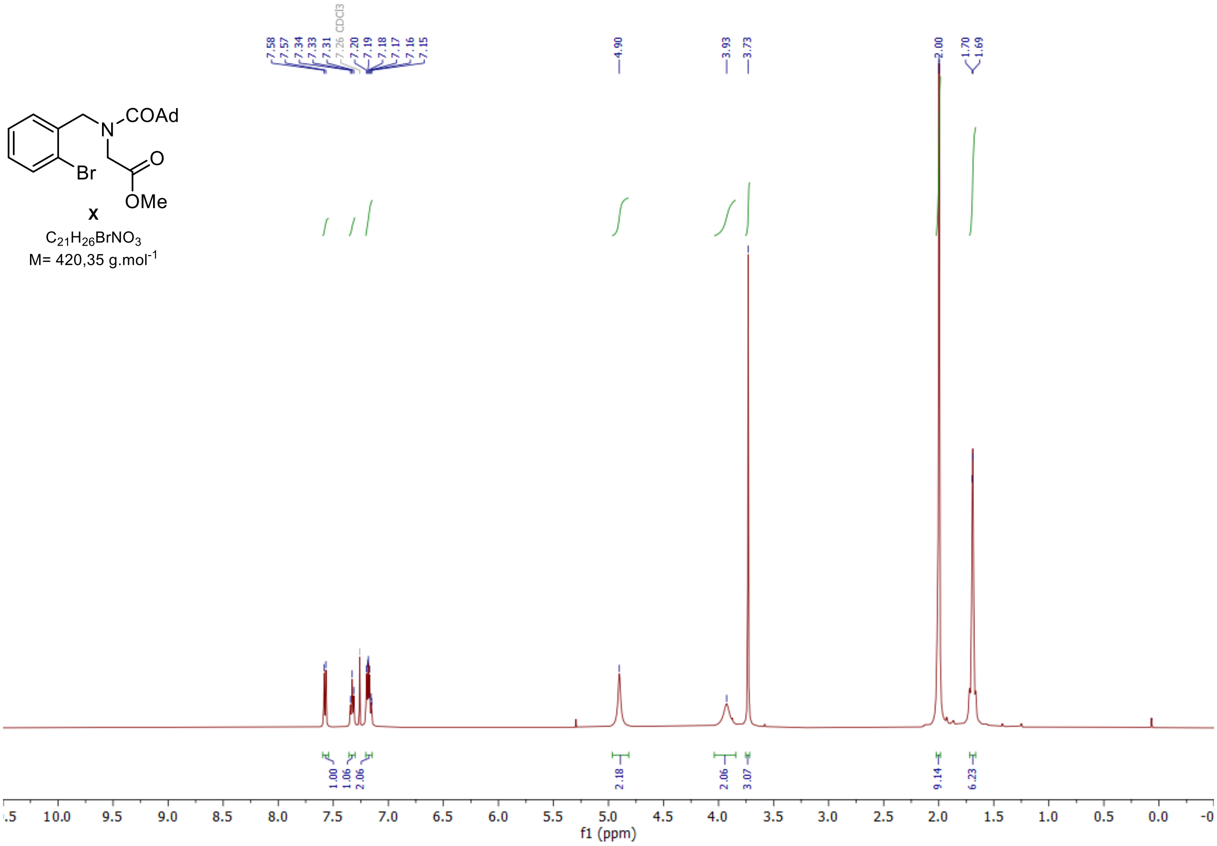

x

$C_{21}H_{26}BrNO_3$
M= 420,35 g.mol^{-1}

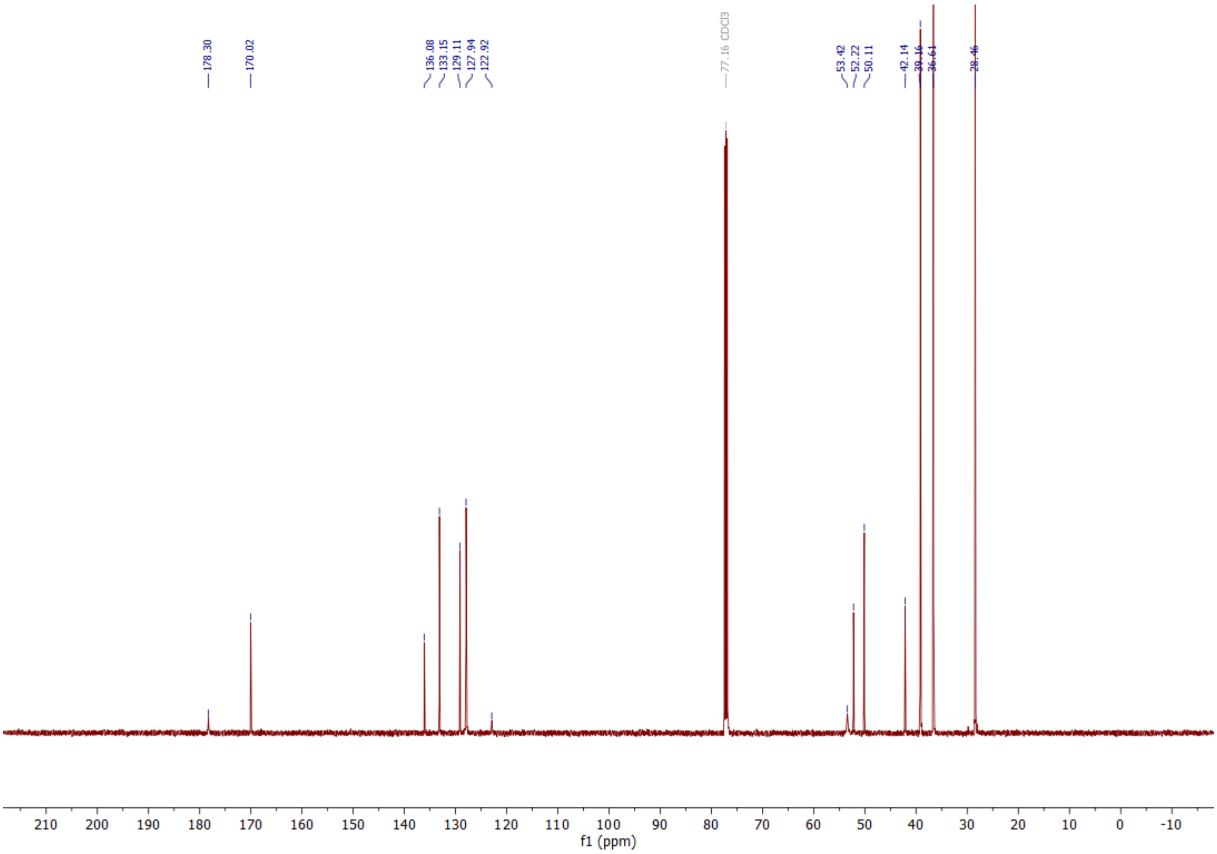

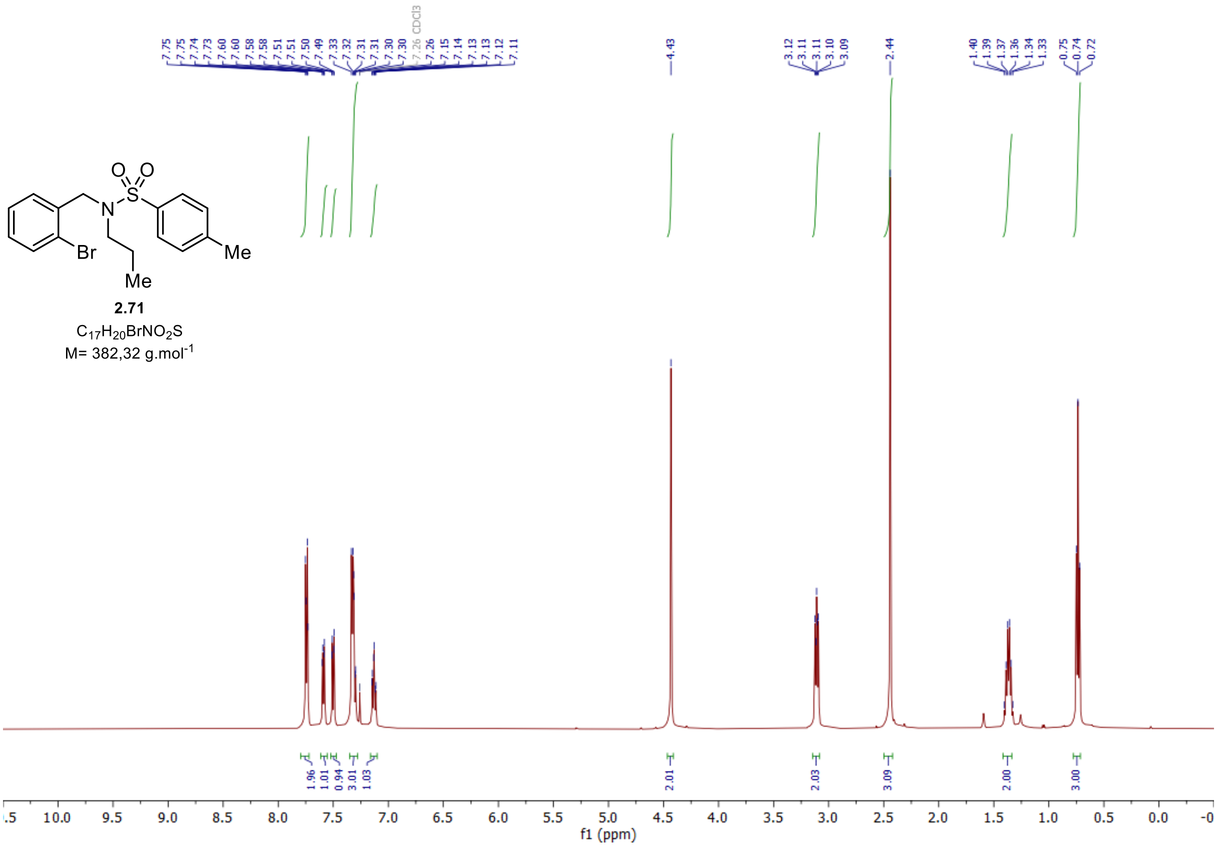

2.71

$C_{17}H_{20}BrNO_2S$

M= 382,32 g.mol^{-1}

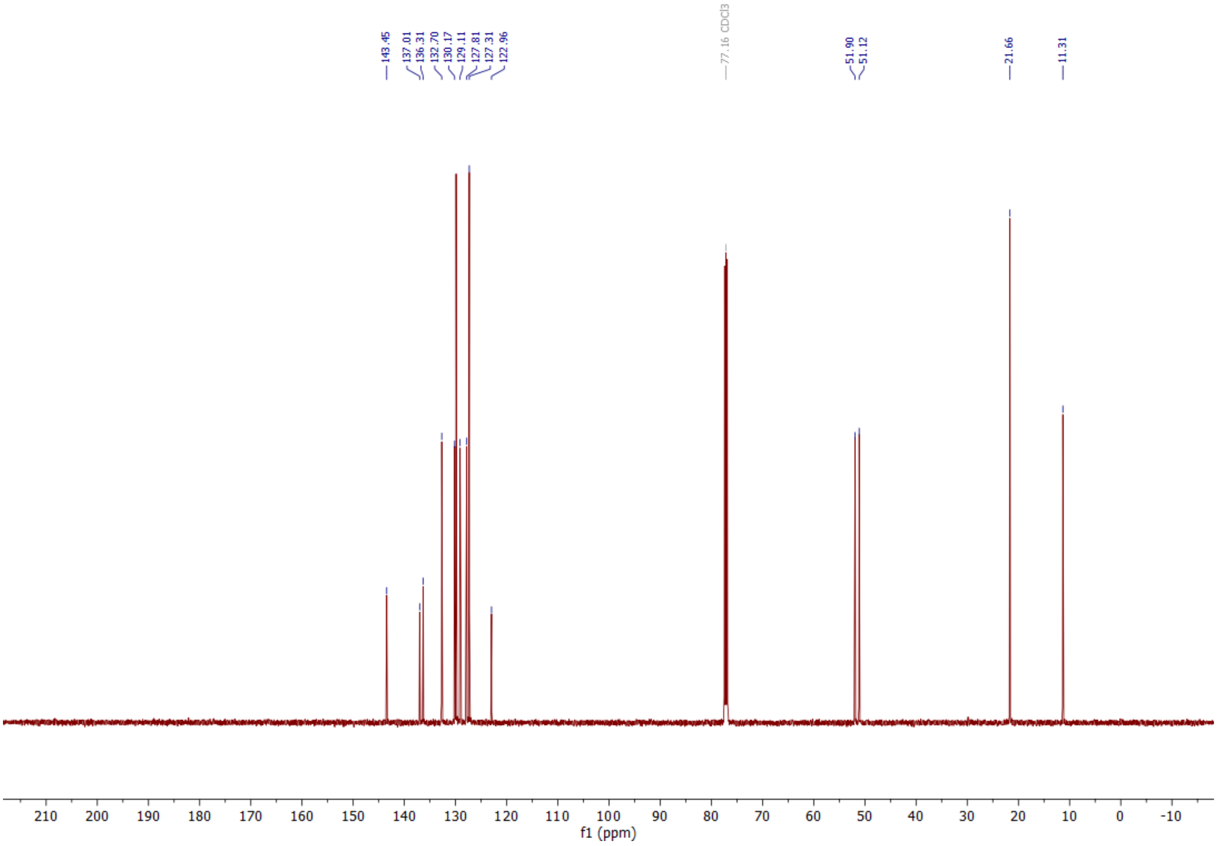

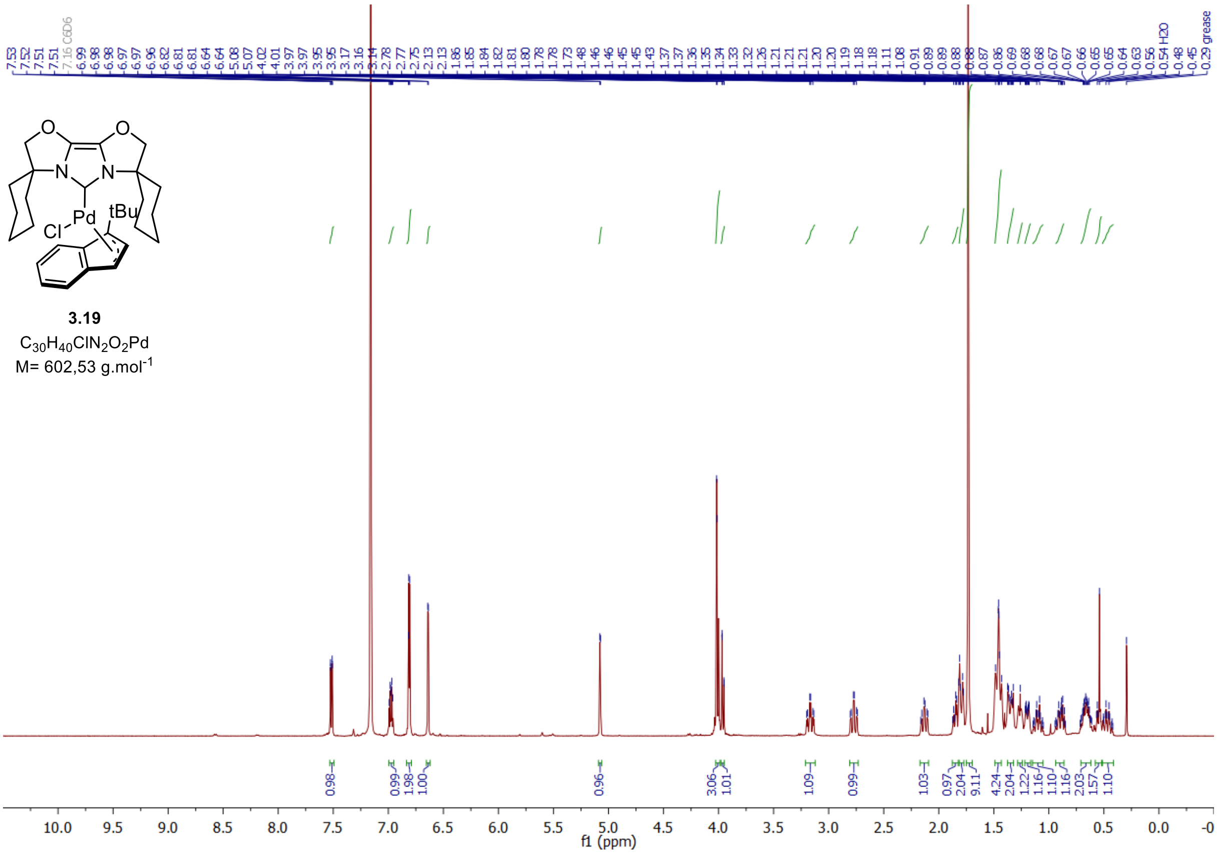

3.19

$C_{30}H_{40}ClN_2O_2Pd$

M= 602,53 g.mol^{-1}

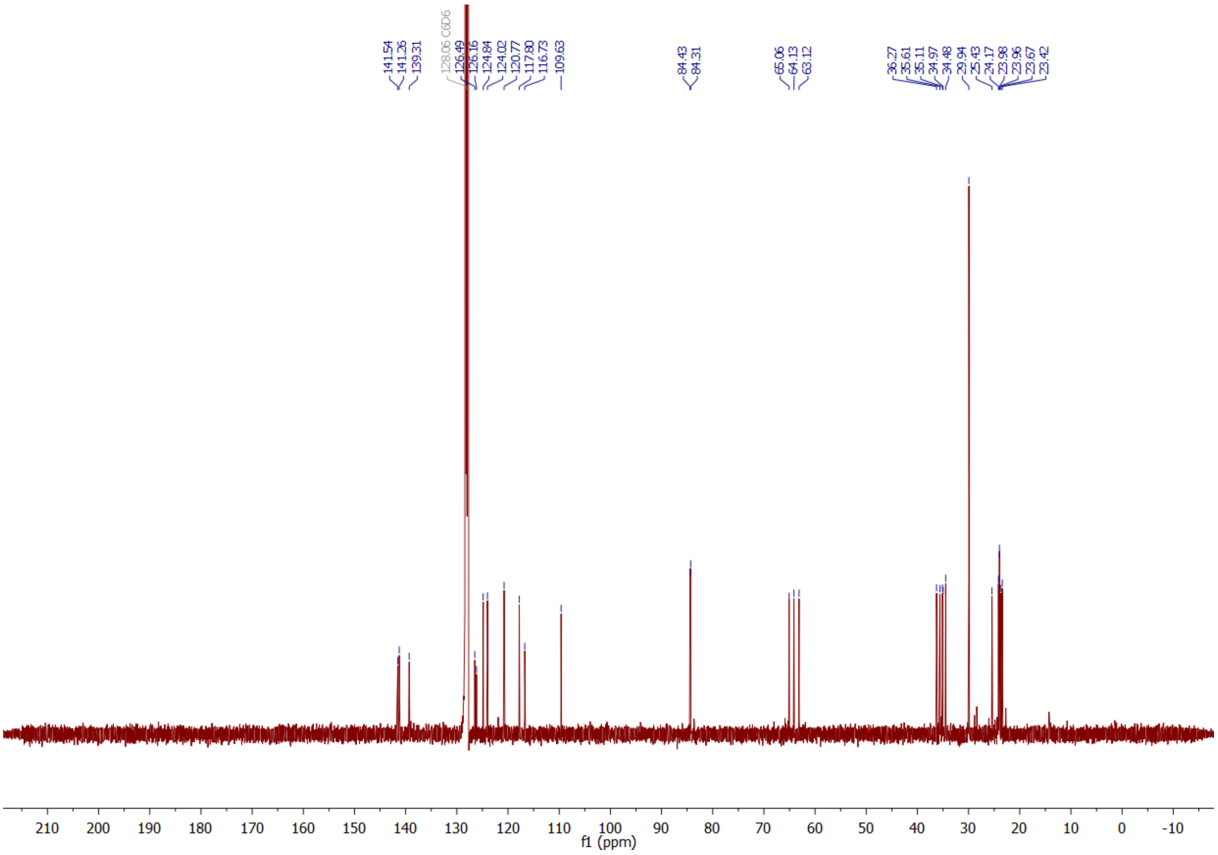

CO2Me
CO2Me
F
Me

2.44ah-dehalo

$C_{14}H_{17}FO_4$

M= 268,28 g.mol^{-1}

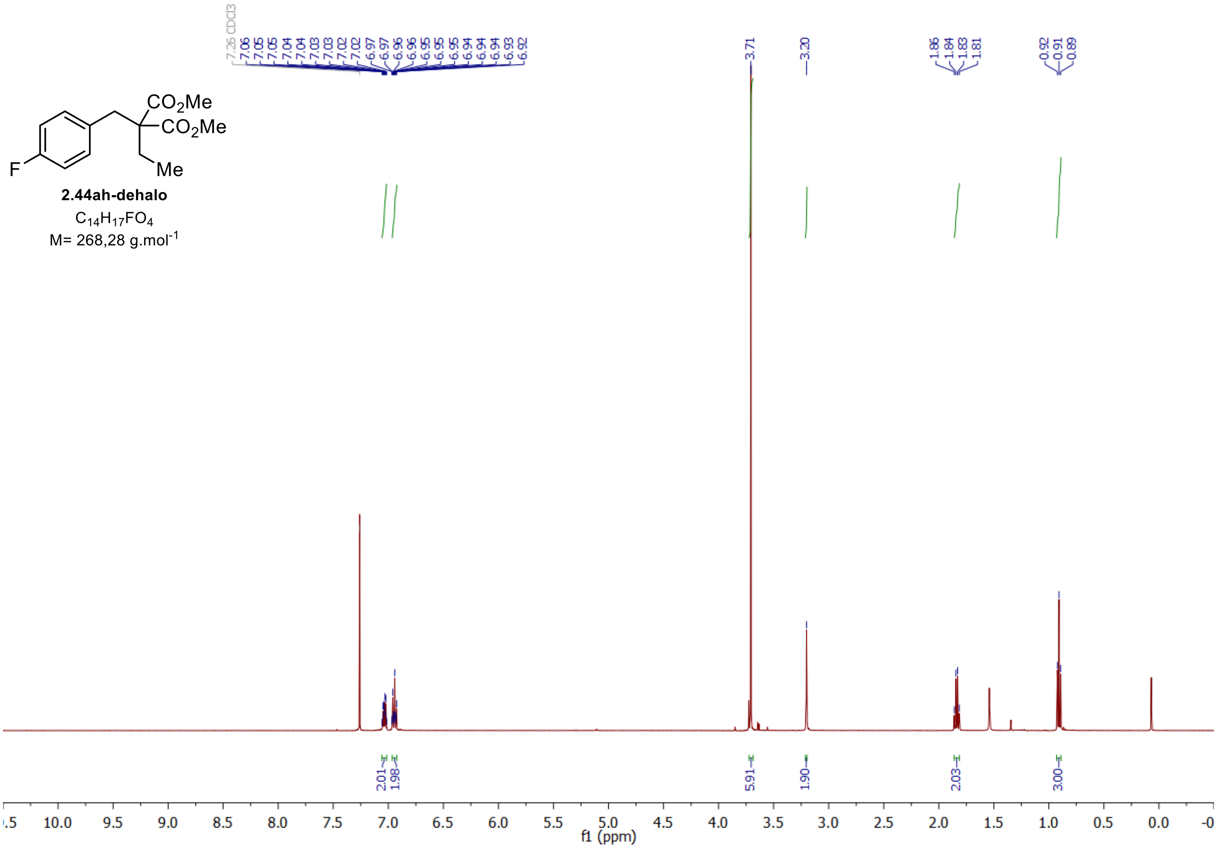

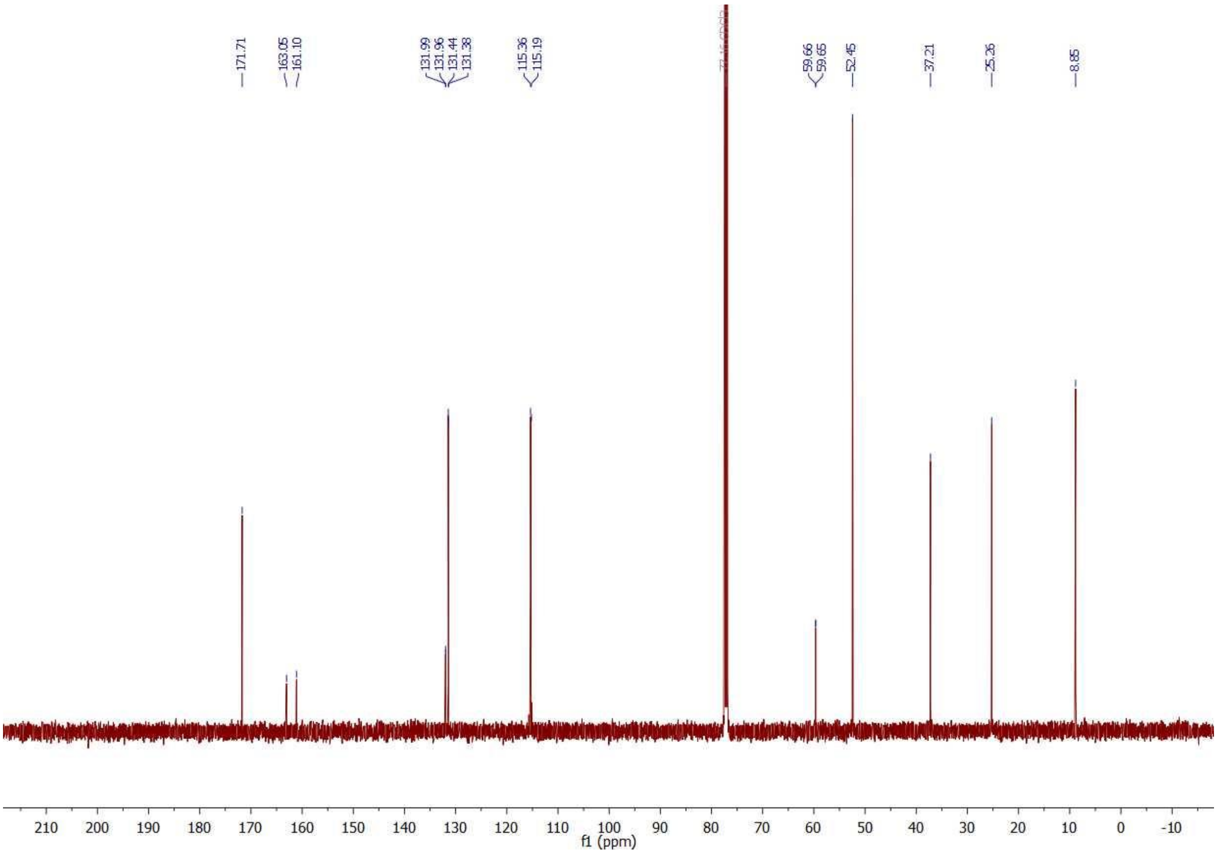

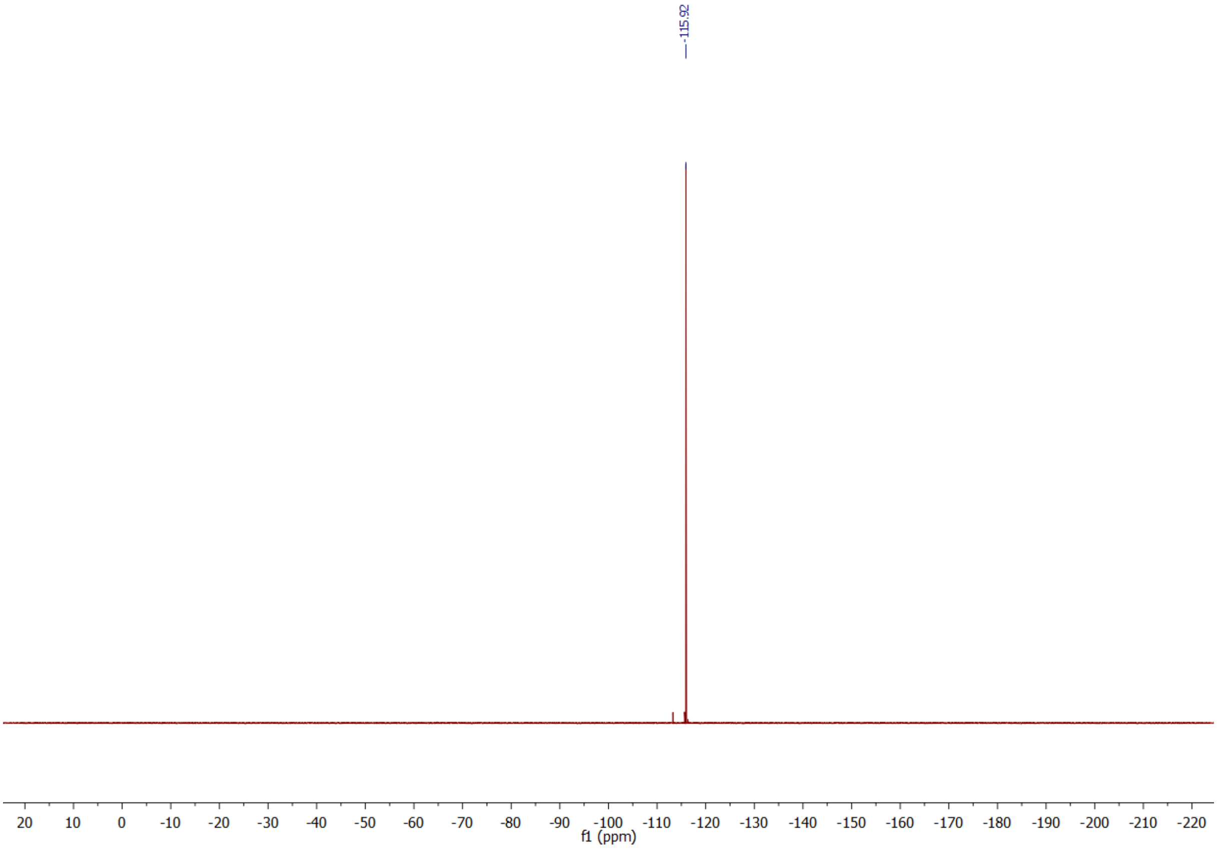
-115.92
20
10
0
-10
-20
-30
-40
-50
-60
-70
-80
-90
-100
-110
-120
-130
-140
-150
-160
-170
-180
-190
-200
-210
-220
f1 (ppm)

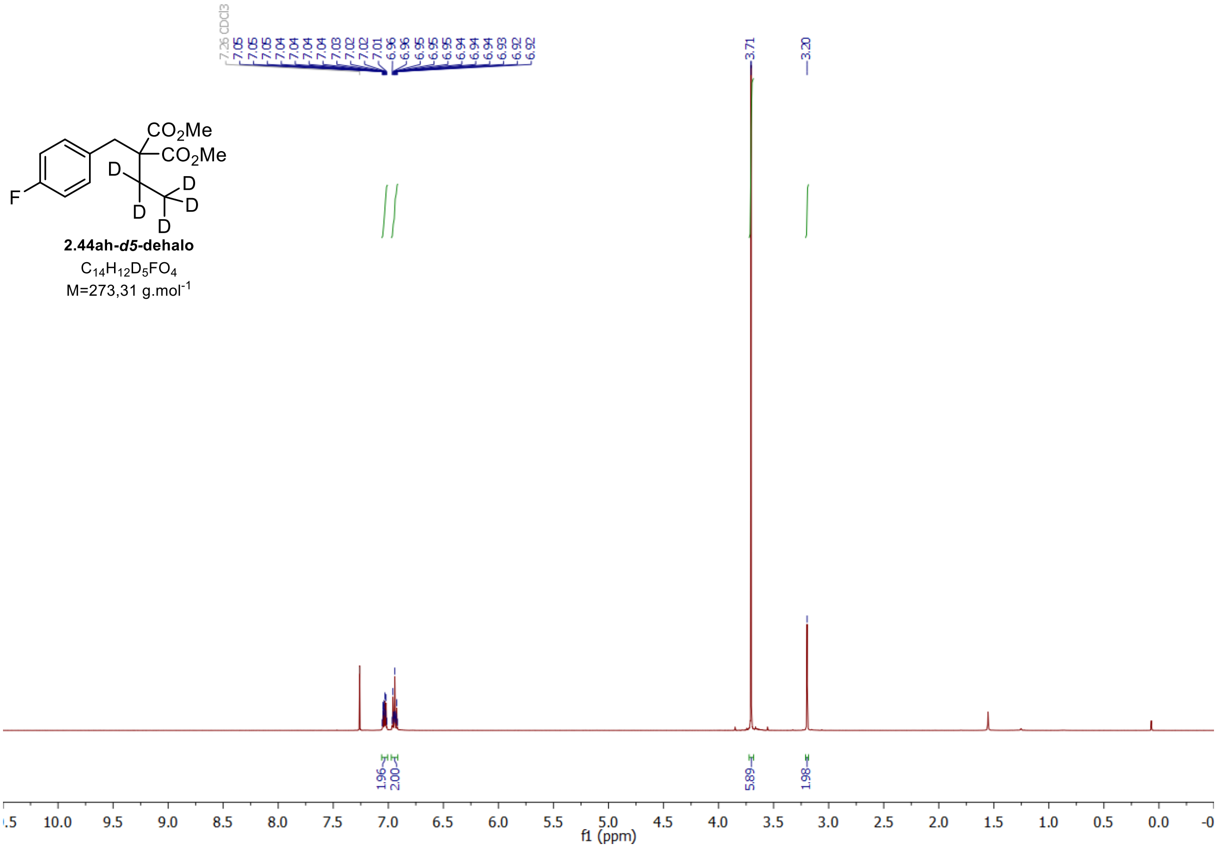

2.44ah-*d5*-dehalo

$C_{14}H_{12}D_5FO_4$

M=273,31 g.mol^{-1}

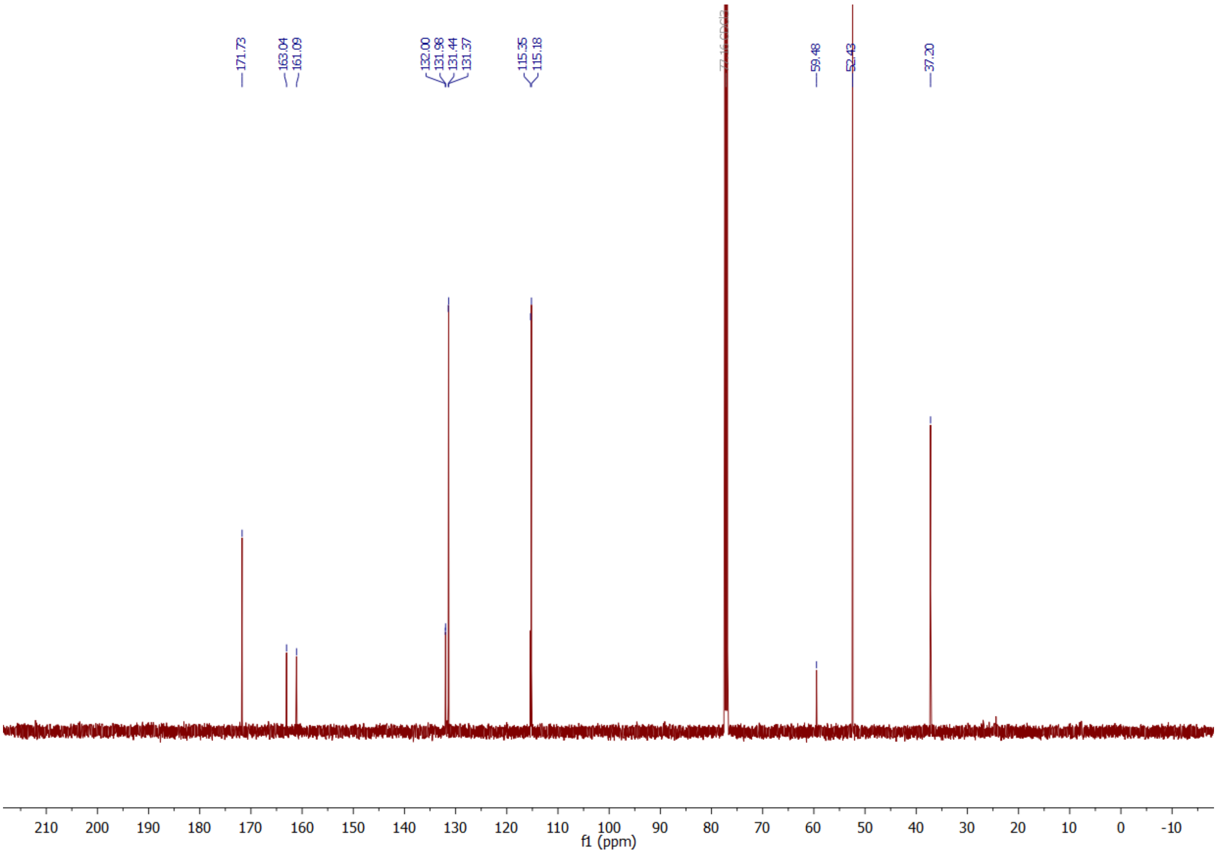

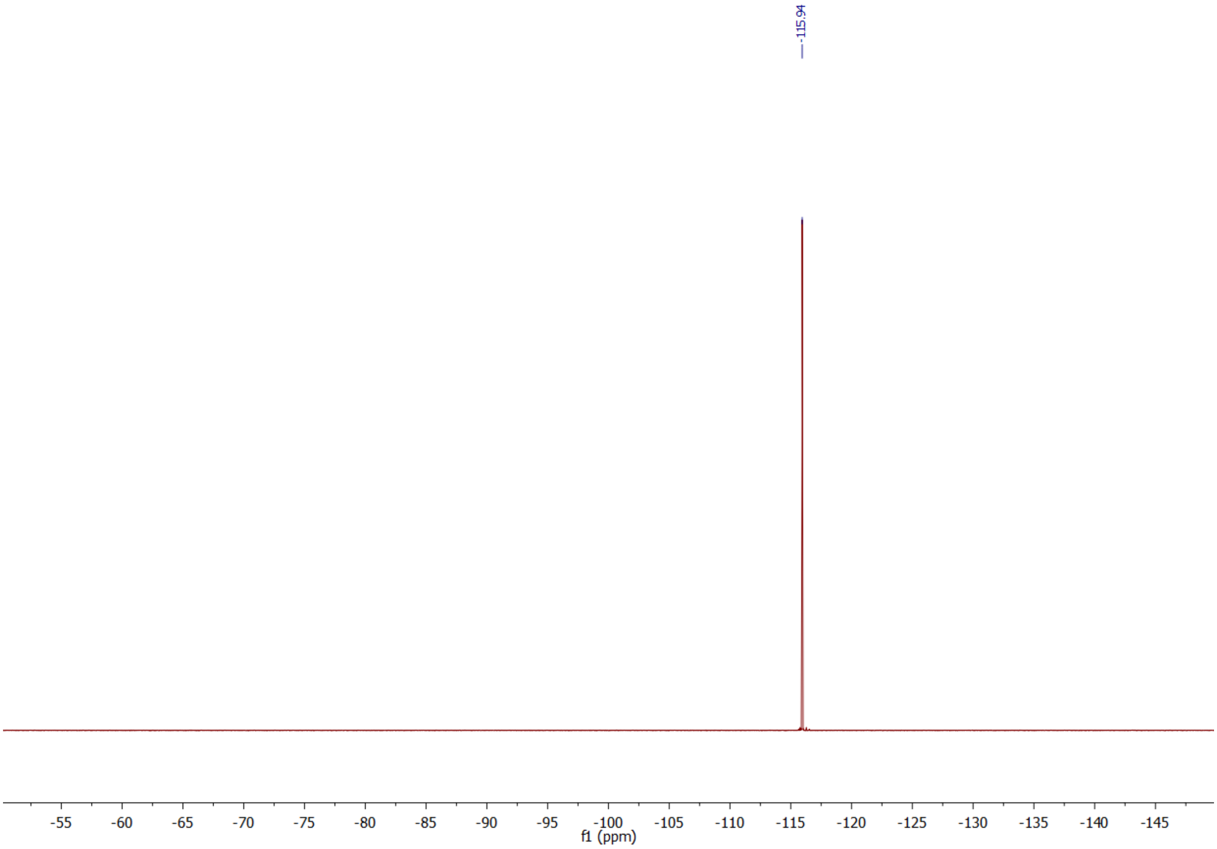
-115.94
-55
-60
-65
-70
-75
-80
-85
-90
-95
-100
-105
-110
-115
-120
-125
-130
-135
-140
-145
f1 (ppm)

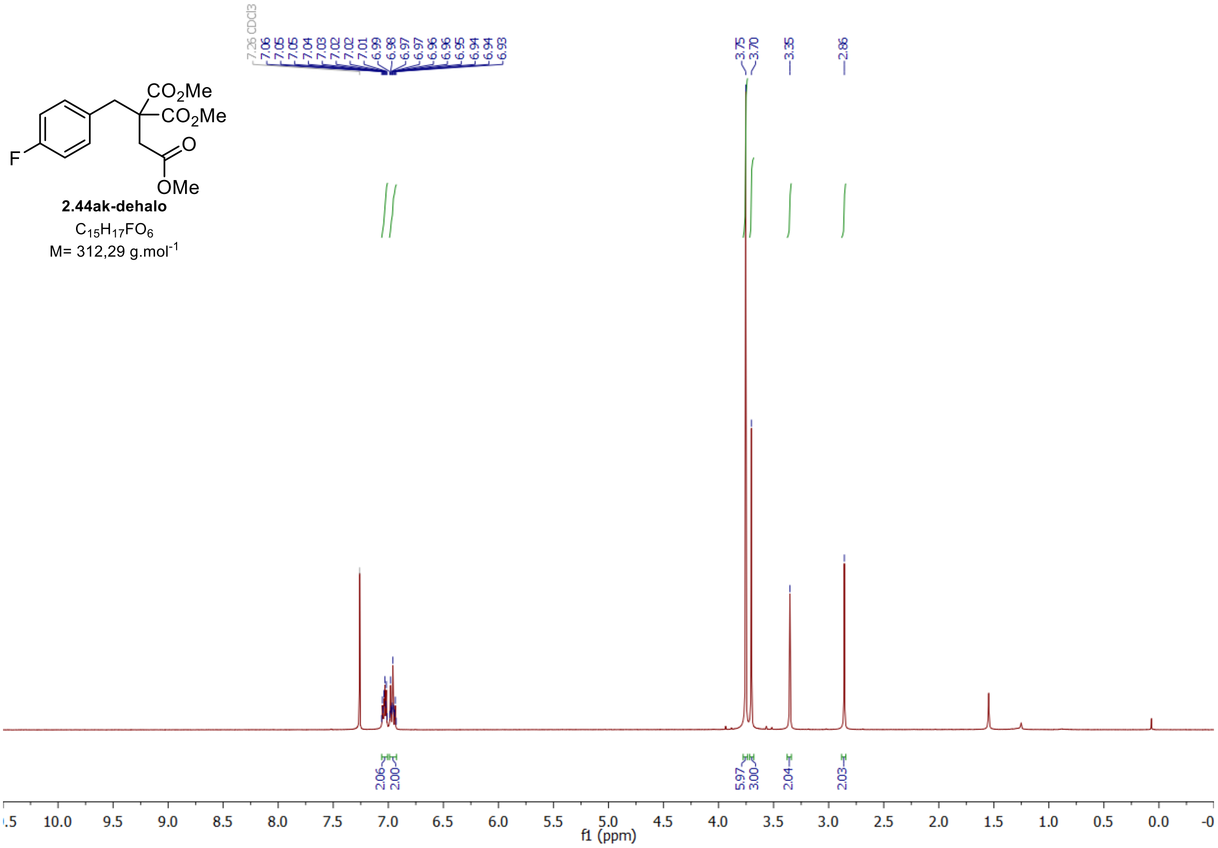

2.44ak-dehalo

$C_{15}H_{17}FO_6$

M= 312,29 g.mol^{-1}

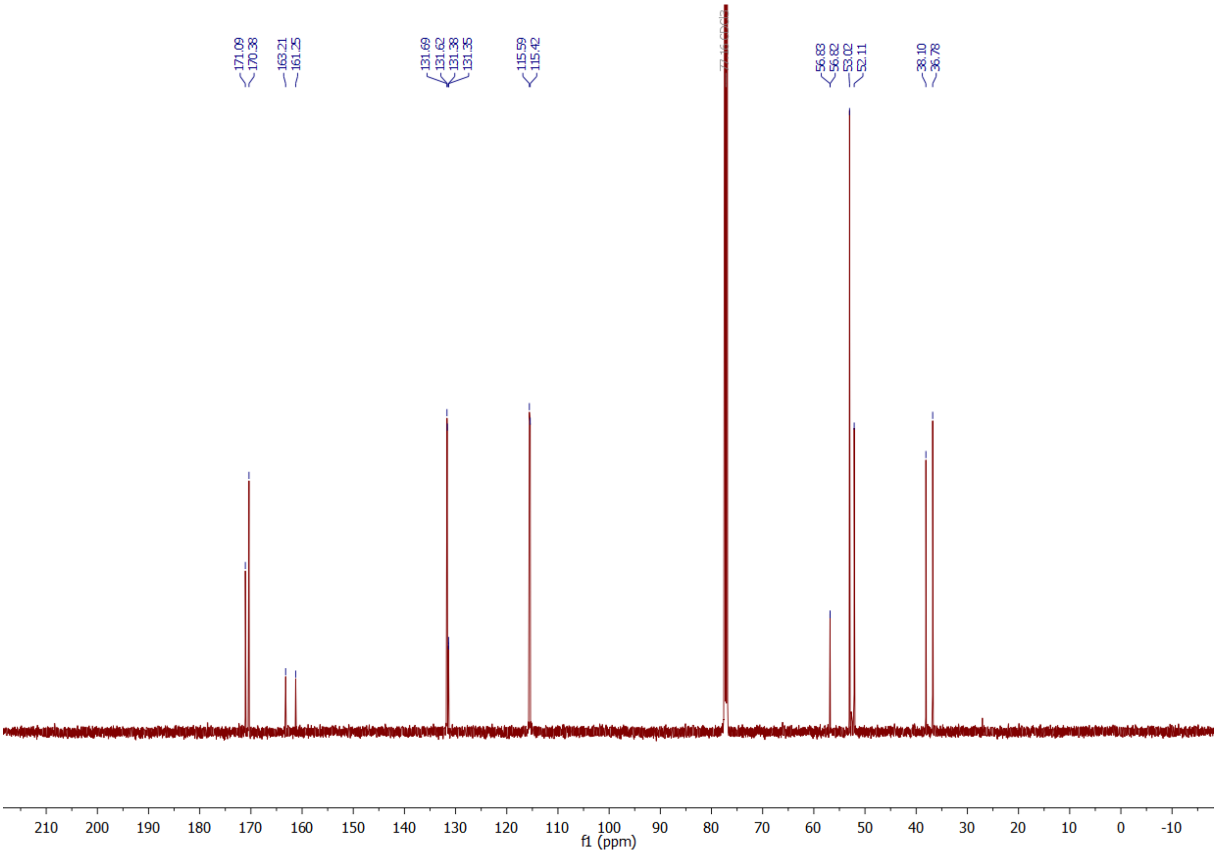

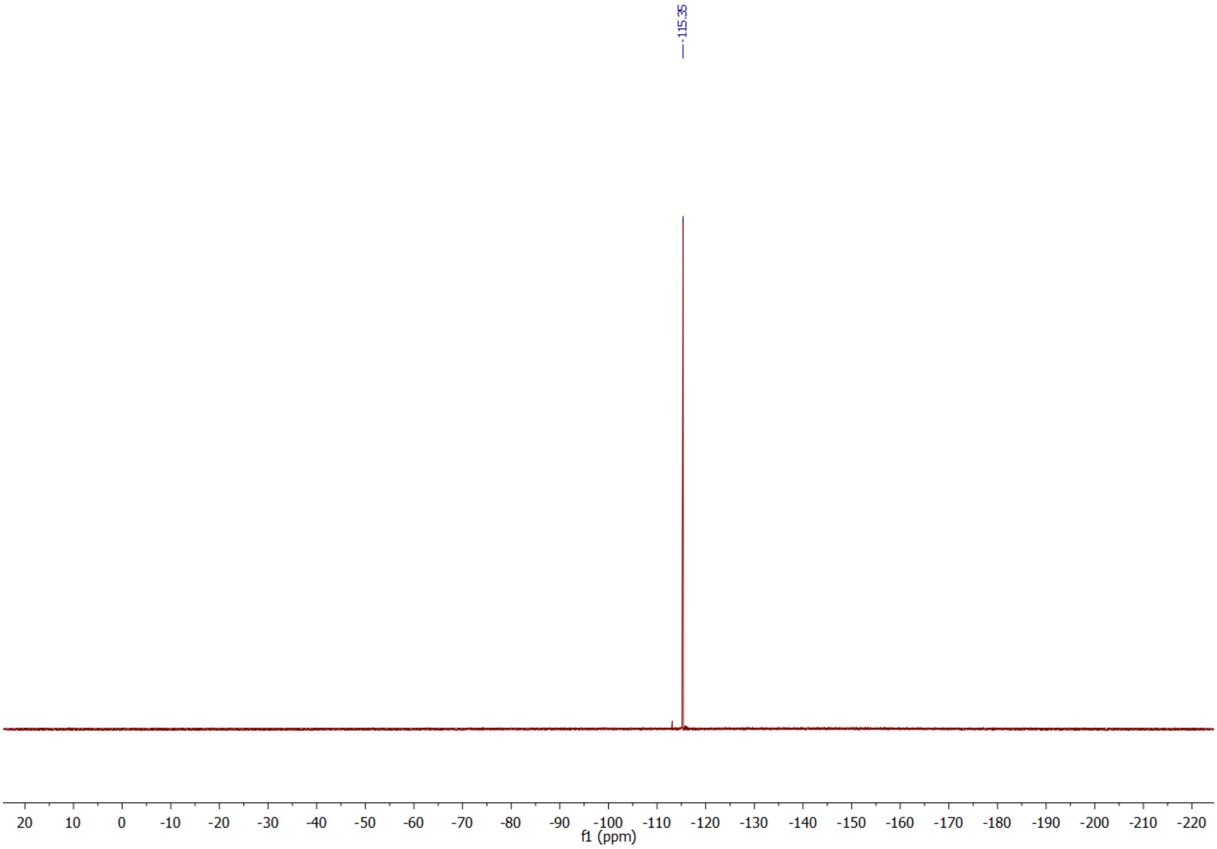
-115.35
20
10
0
-10
-20
-30
-40
-50
-60
-70
-80
-90
-100
-110
-120
-130
-140
-150
-160
-170
-180
-190
-200
-210
-220
f1 (ppm)

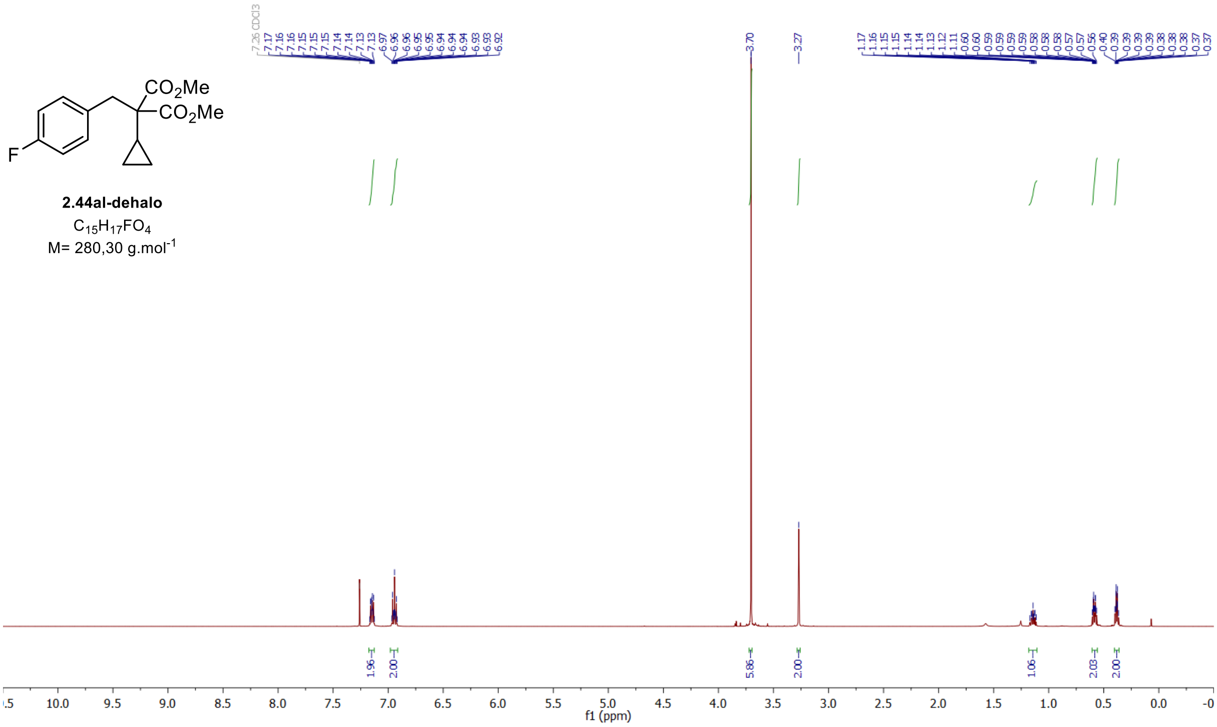

2.44al-dehalo

$C_{15}H_{17}FO_4$

M= 280,30 g.mol^{-1}

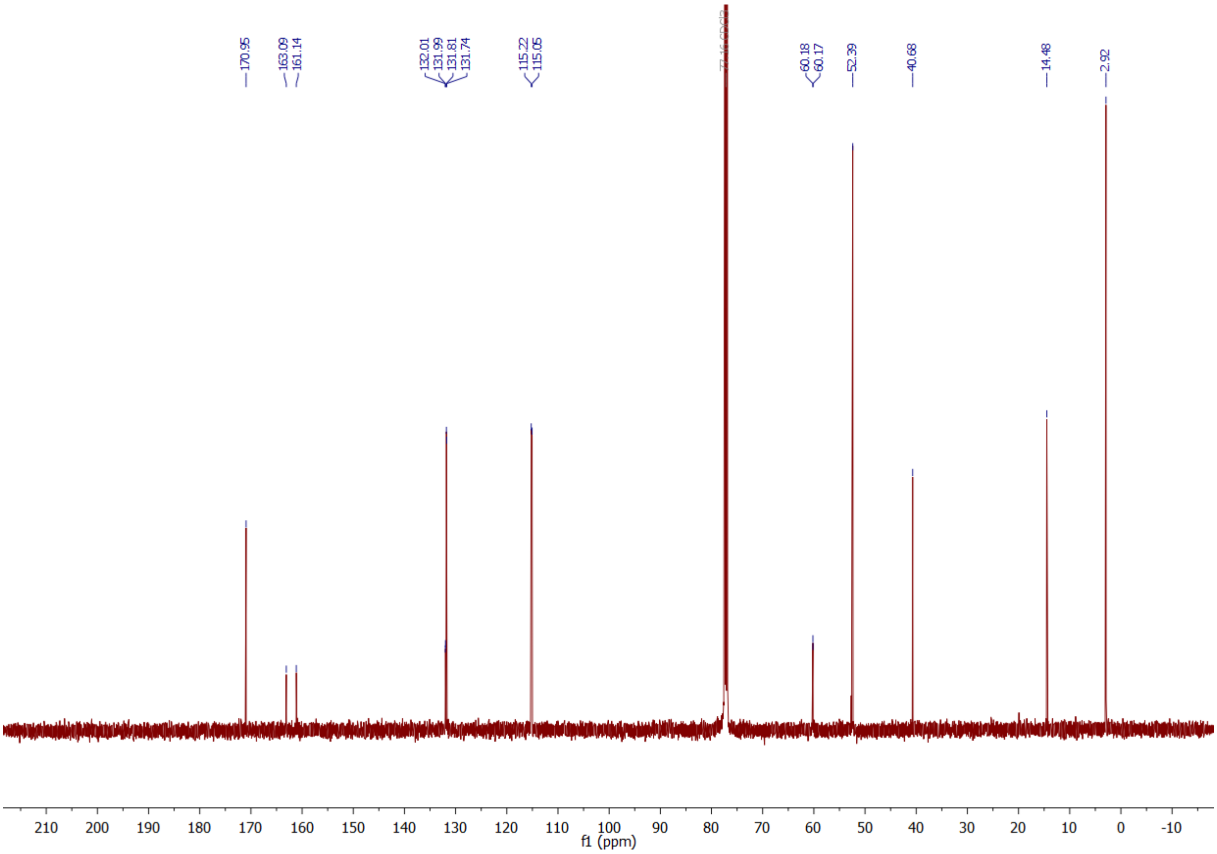

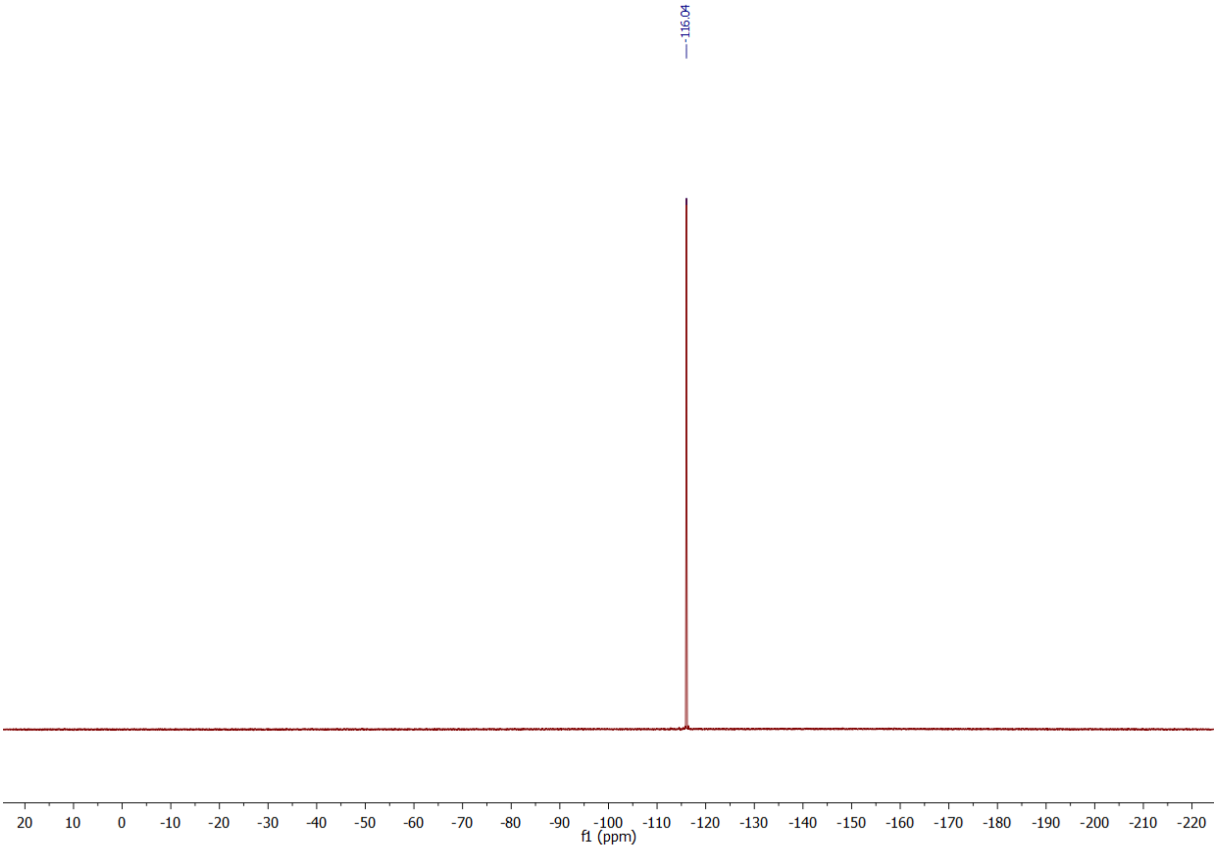
-116.04
20
10
0
-10
-20
-30
-40
-50
-60
-70
-80
-90
-100
-110
-120
-130
-140
-150
-160
-170
-180
-190
-200
-210
-220
f1 (ppm)

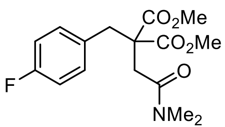
CO2Me
CO2Me
O
NMe2
F

2.44am-dehalo

$C_{16}H_{20}FNO_5$

M= 325,34 g.mol^{-1}

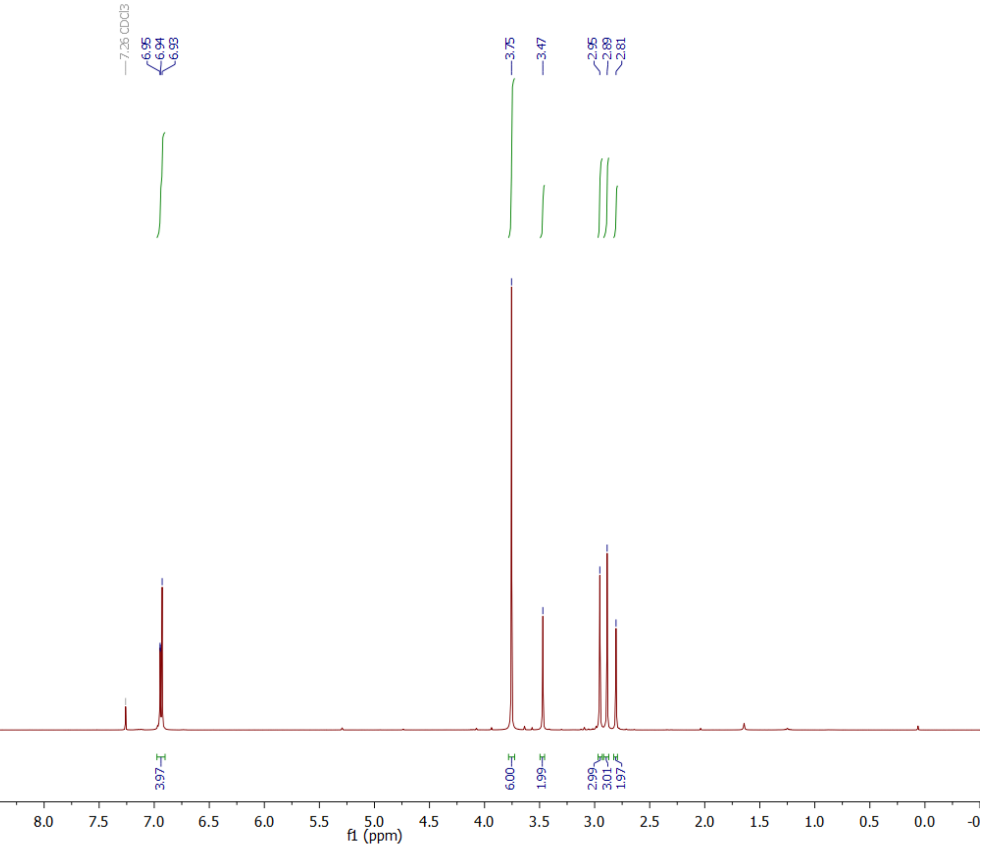

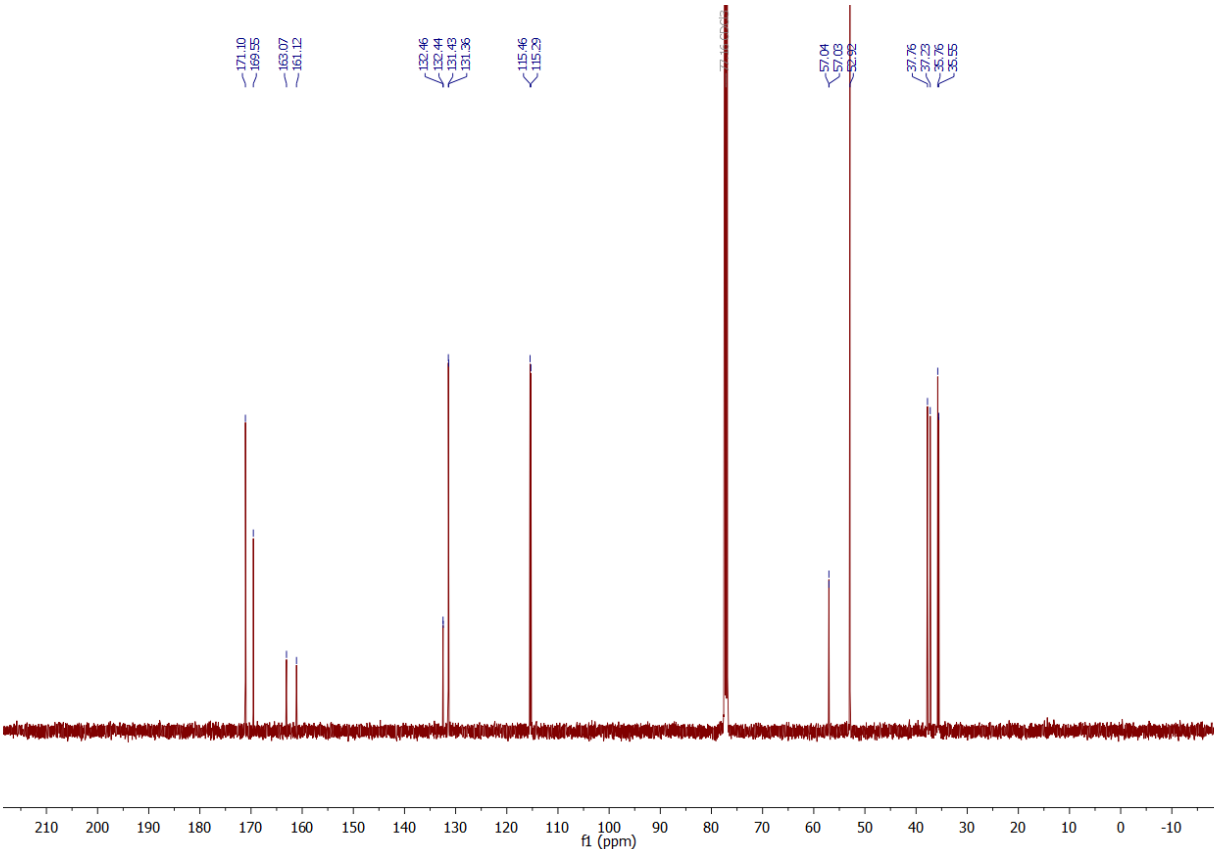

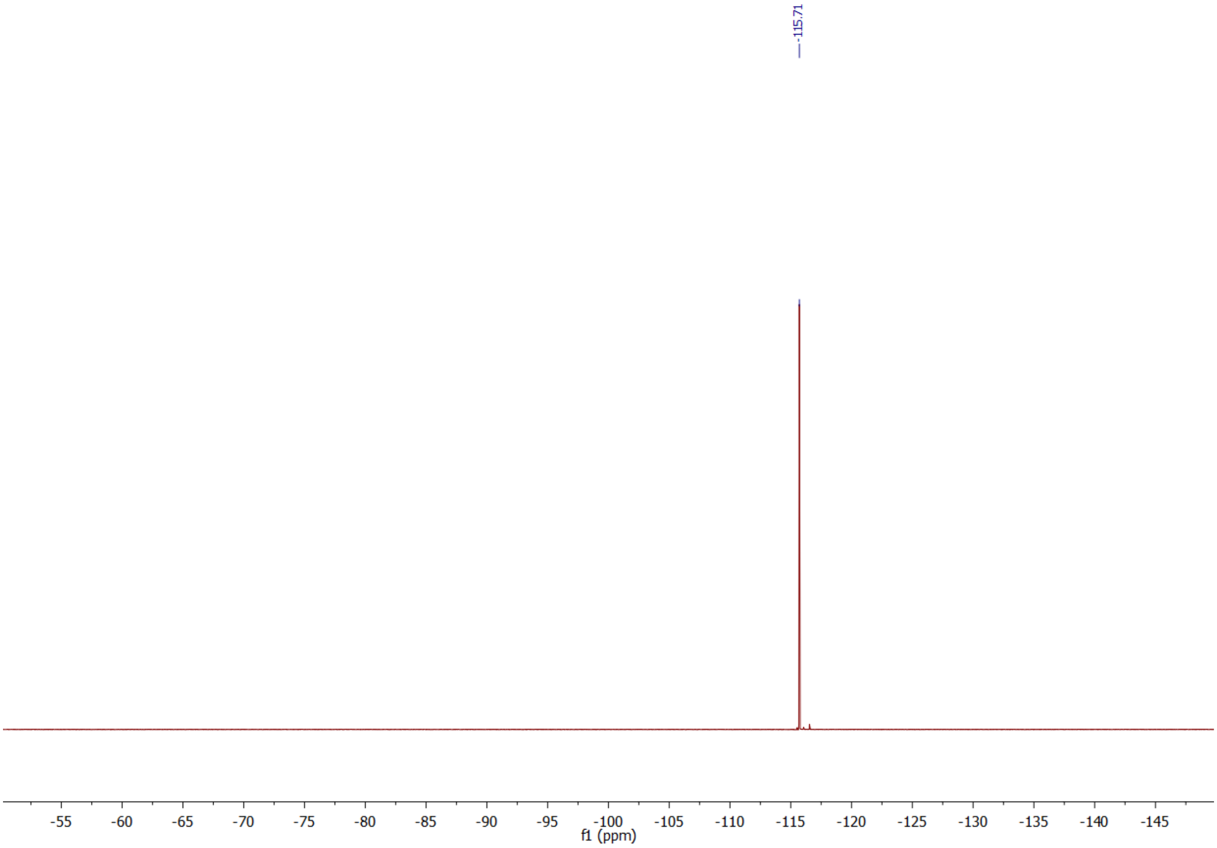
-115.71
-55
-60
-65
-70
-75
-80
-85
-90
-95
-100
-105
-110
-115
-120
-125
-130
-135
-140
-145
f1 (ppm)

CO2Me
CO2Me
Me
F

2.44an-dehalo

$C_{13}H_{15}FO_4$

M= 254,26 g.mol^{-1}

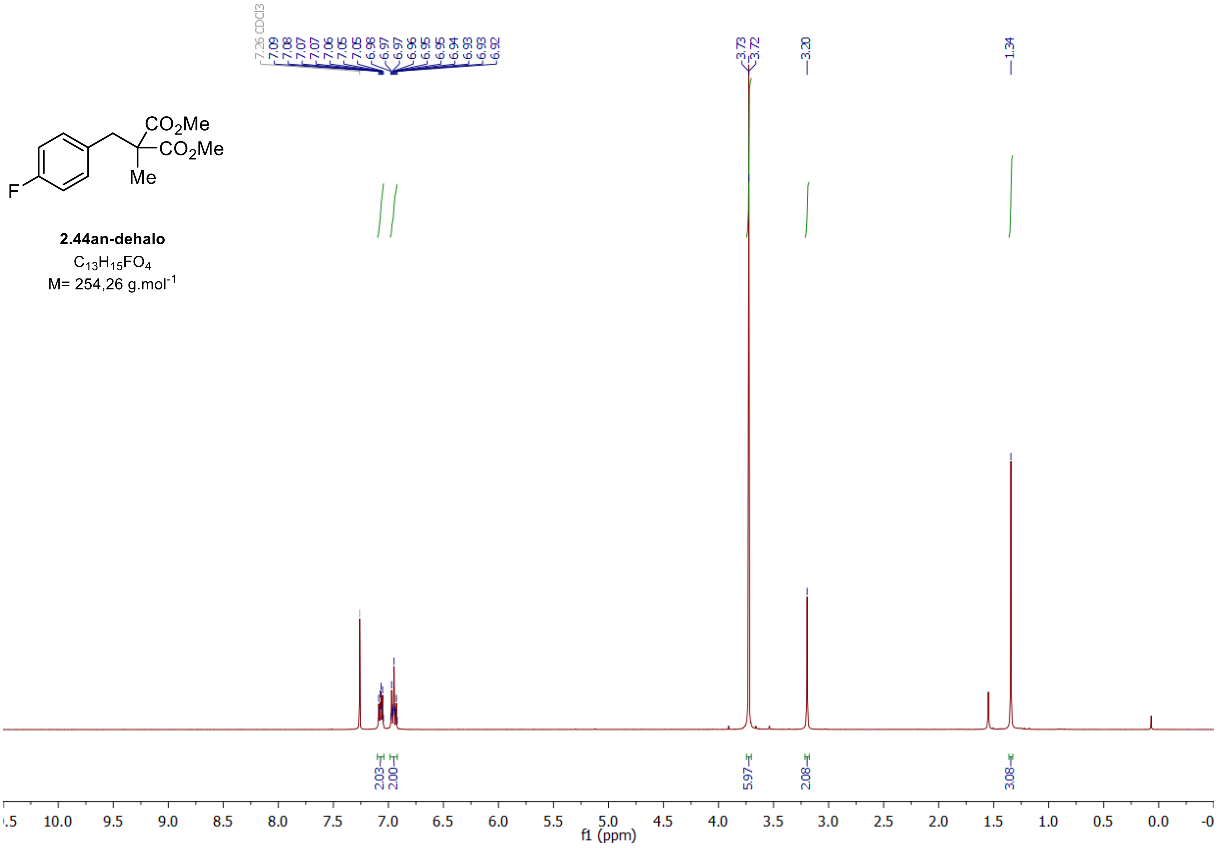

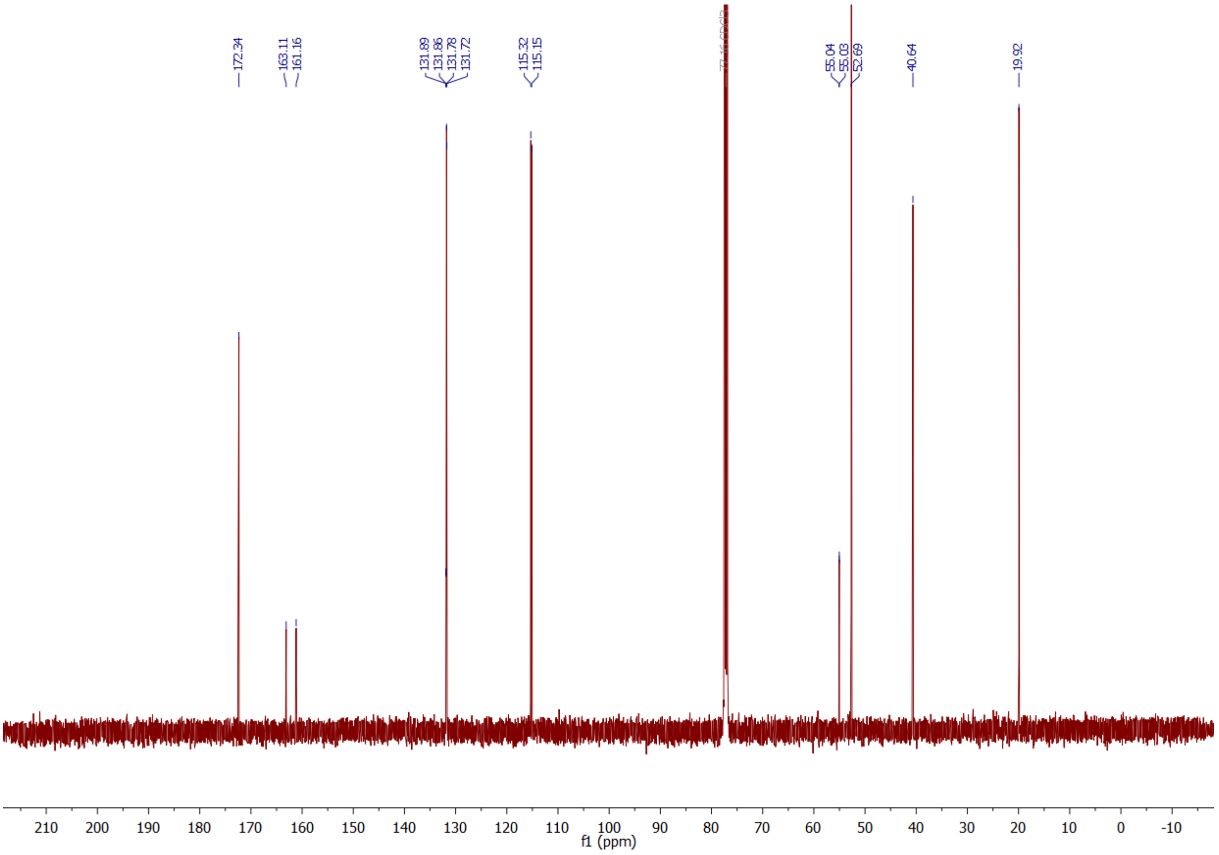

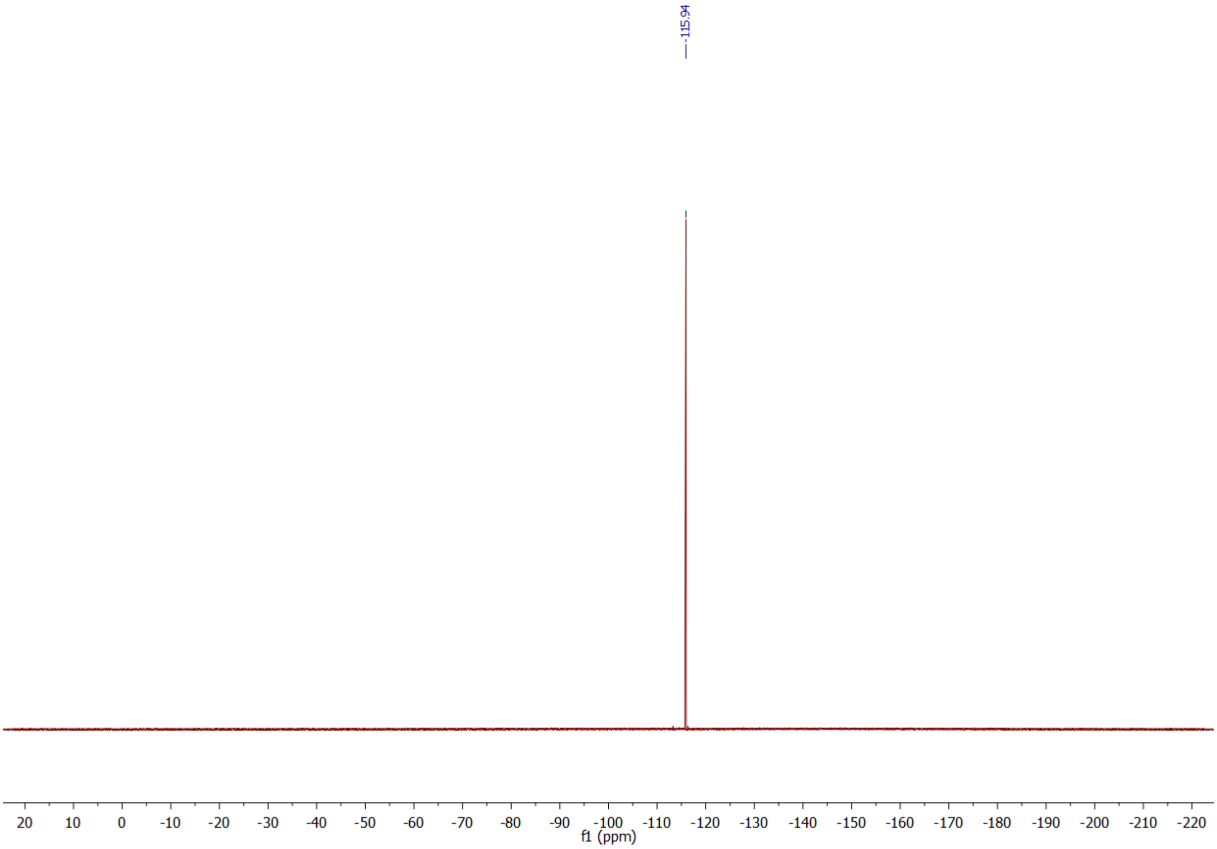
-115.94
20
10
0
-10
-20
-30
-40
-50
-60
-70
-80
-90
-100
-110
-120
-130
-140
-150
-160
-170
-180
-190
-200
-210
-220
f1 (ppm)

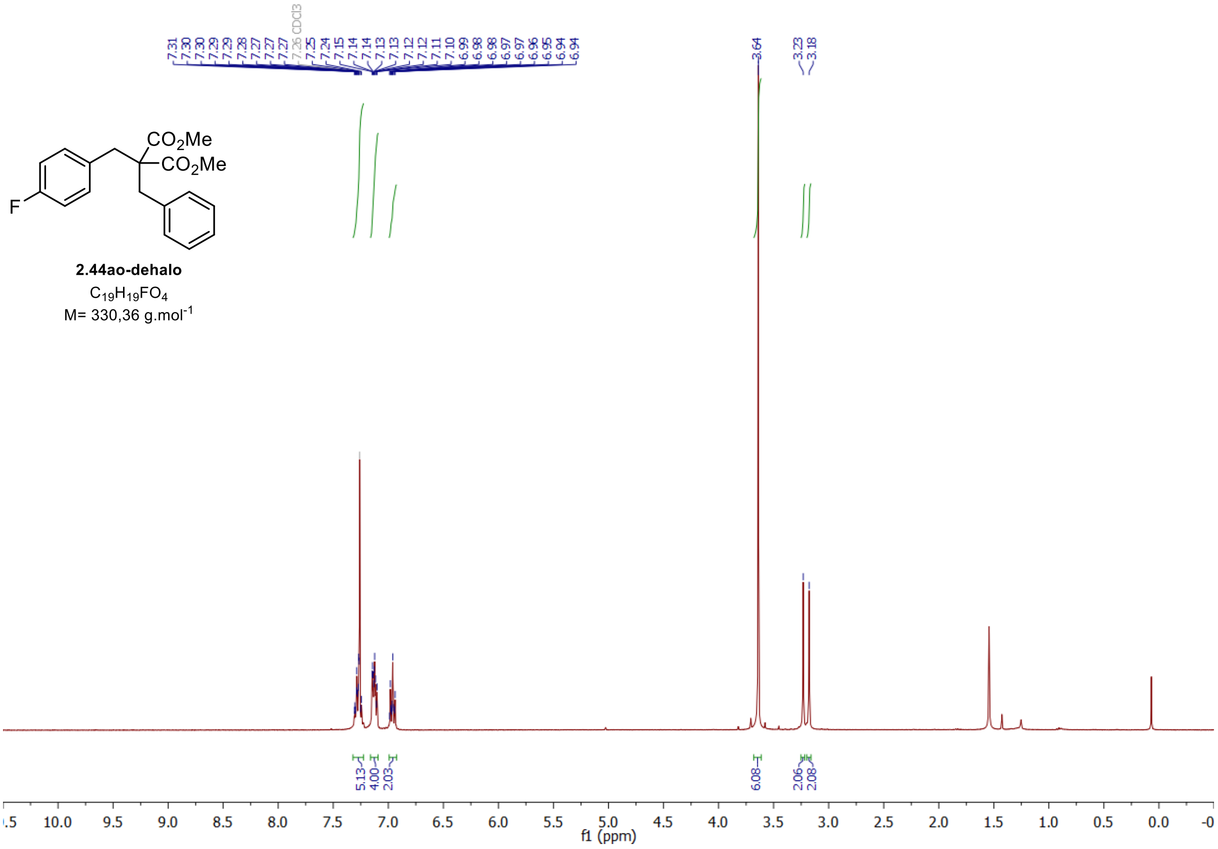

2.44ao-dehalo

$C_{19}H_{19}FO_4$

M= 330,36 g.mol^{-1}

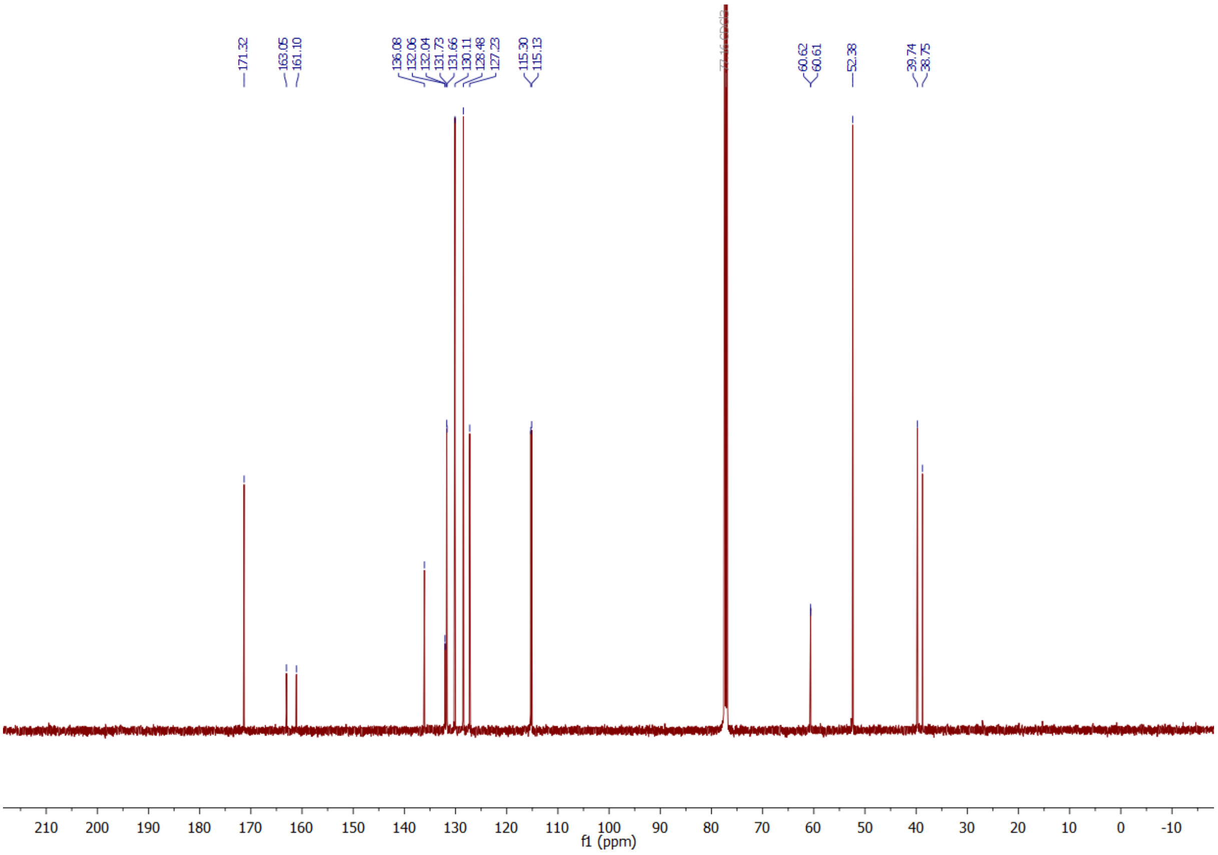

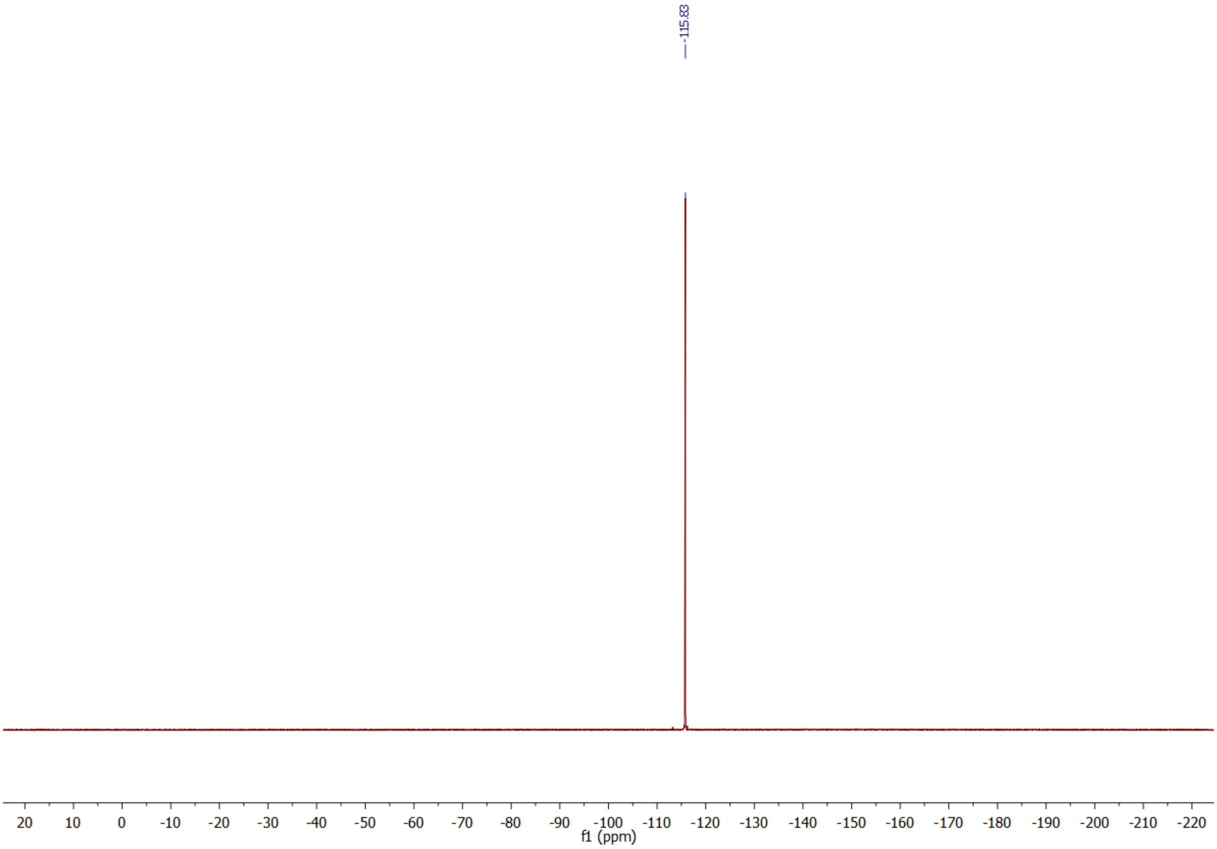
-115.83
20
10
0
-10
-20
-30
-40
-50
-60
-70
-80
-90
-100
-110
-120
-130
-140
-150
-160
-170
-180
-190
-200
-210
-220
f1 (ppm)

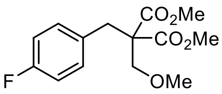
CO2Me
CO2Me
OMe
F

2.44ap-dehalo
$C_{14}H_{17}FO_5$
M= 284,11 g.mol^{-1}

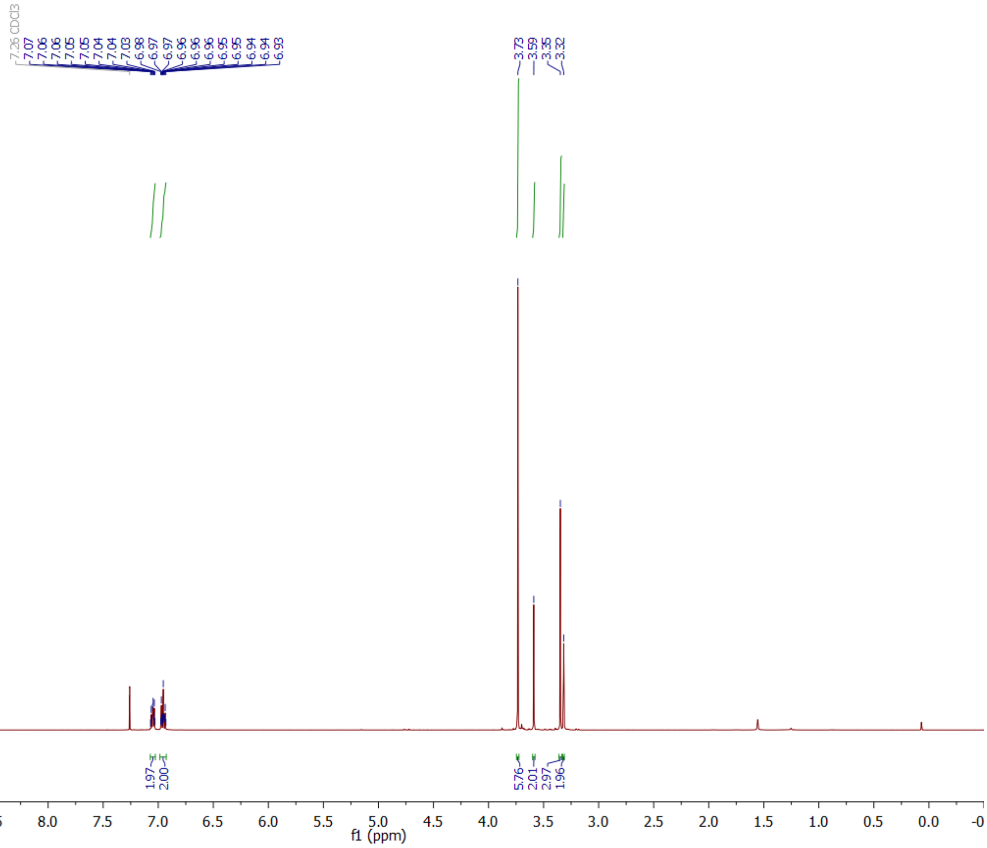

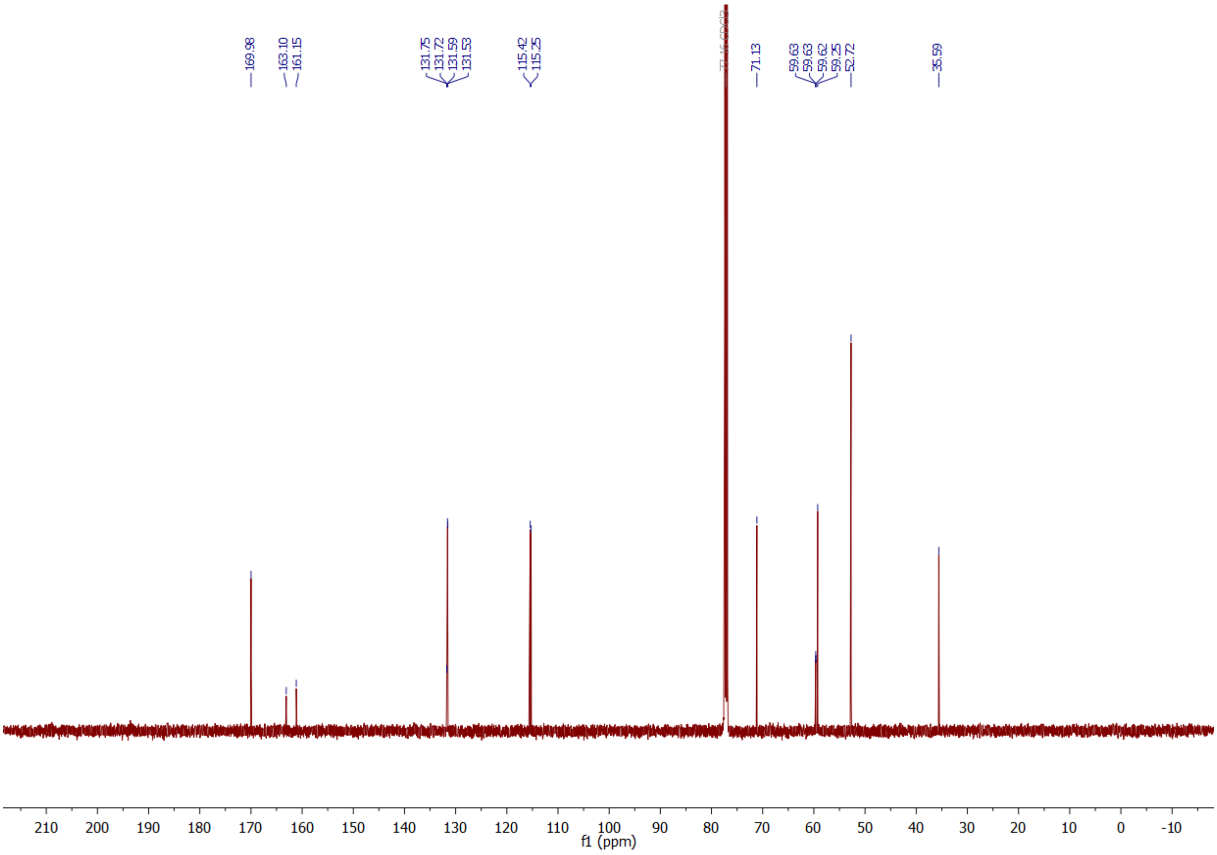

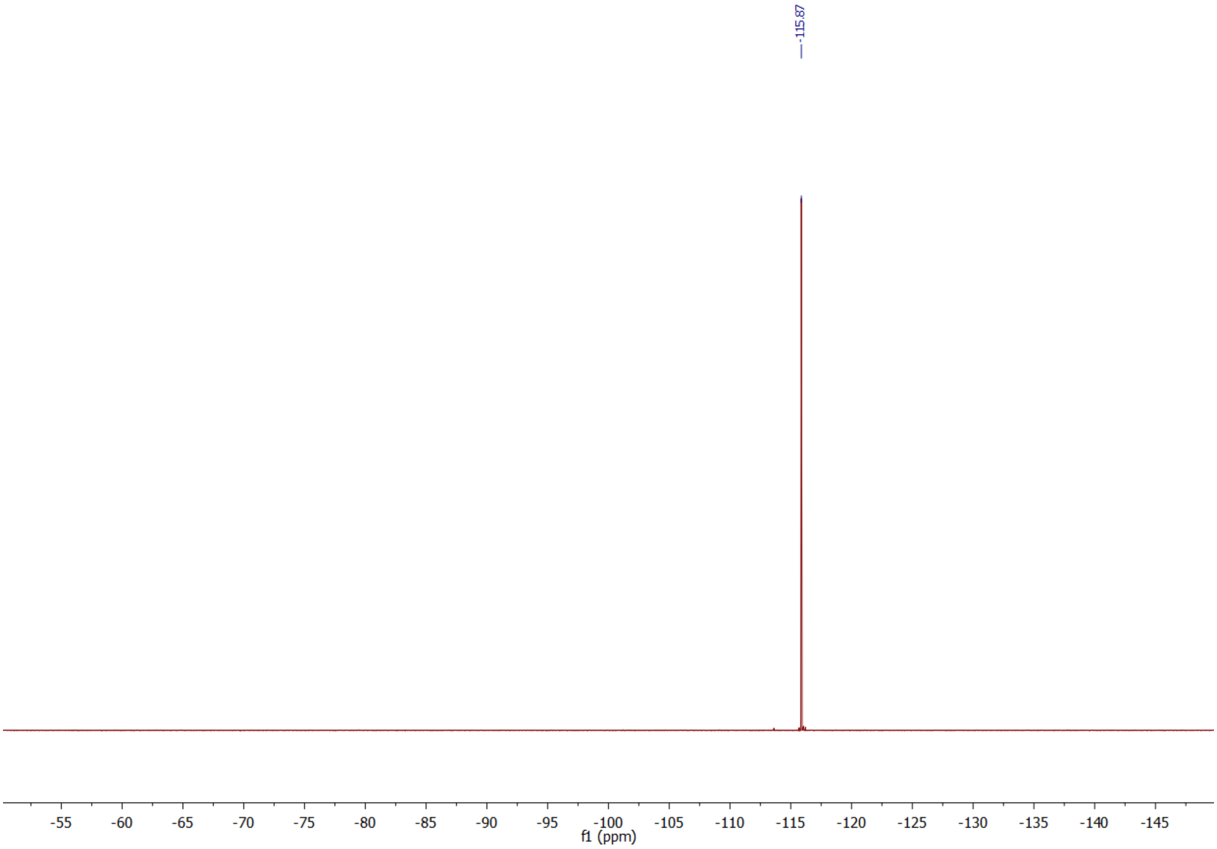
-115.87
-55
-60
-65
-70
-75
-80
-85
-90
-95
-100
-105
-110
-115
-120
-125
-130
-135
-140
-145
f1 (ppm)

CO2Me
CO2Me
F
Br
Me

2.44ah

$C_{14}H_{16}FBrO_4$

M= 347,18 g.mol^{-1}

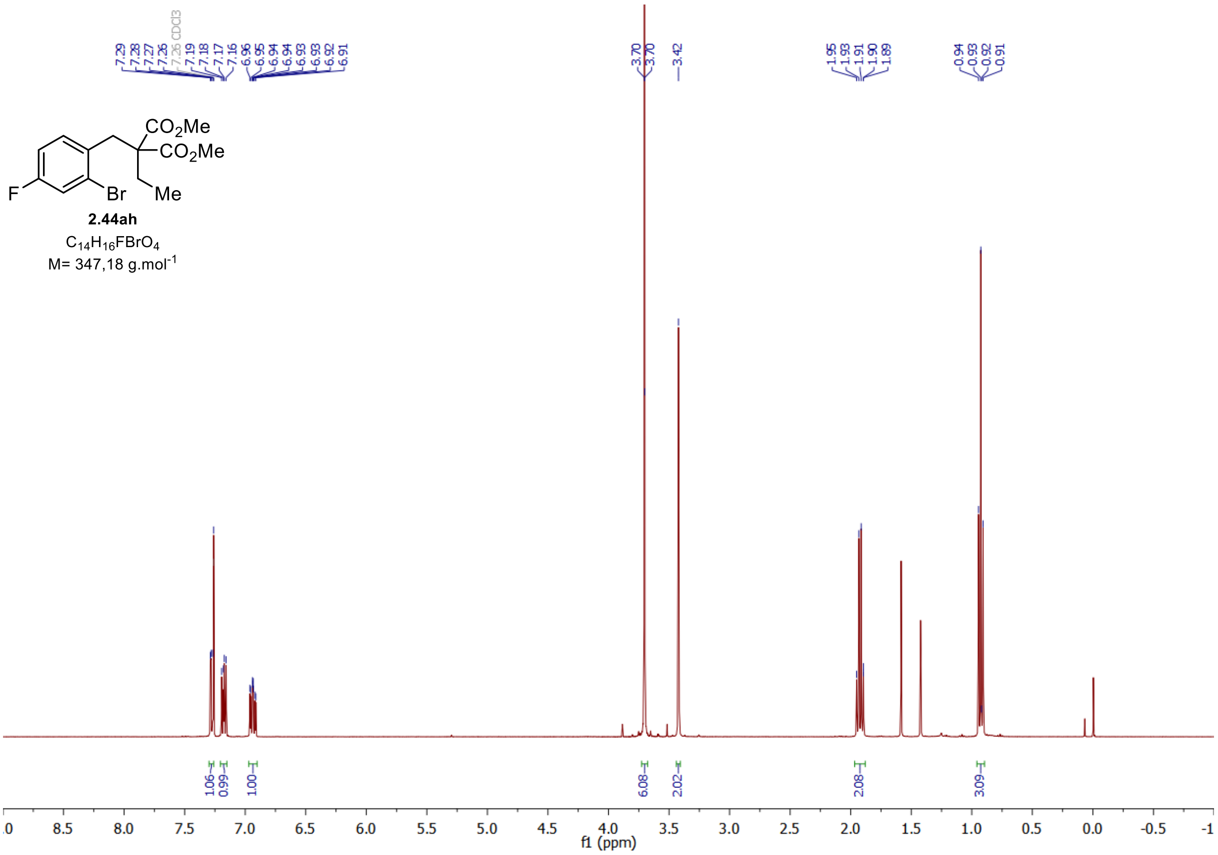

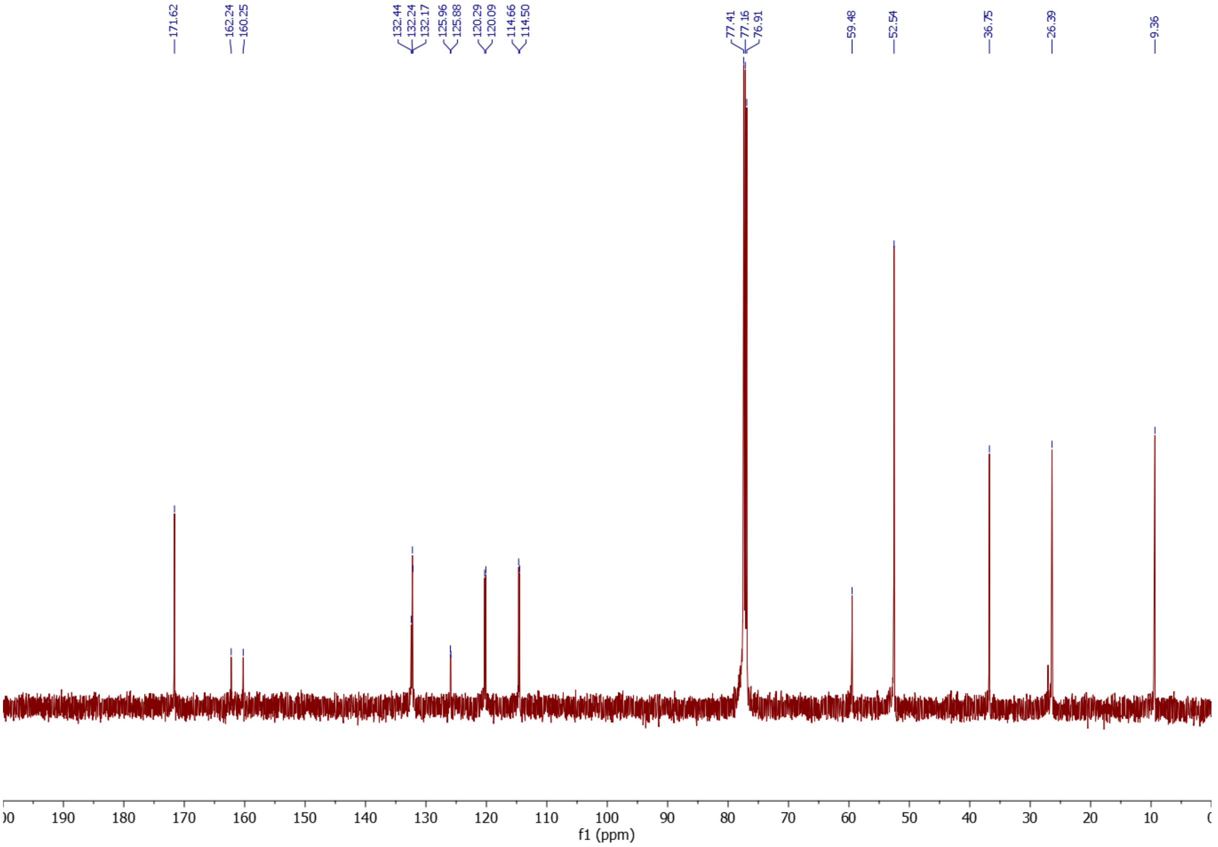

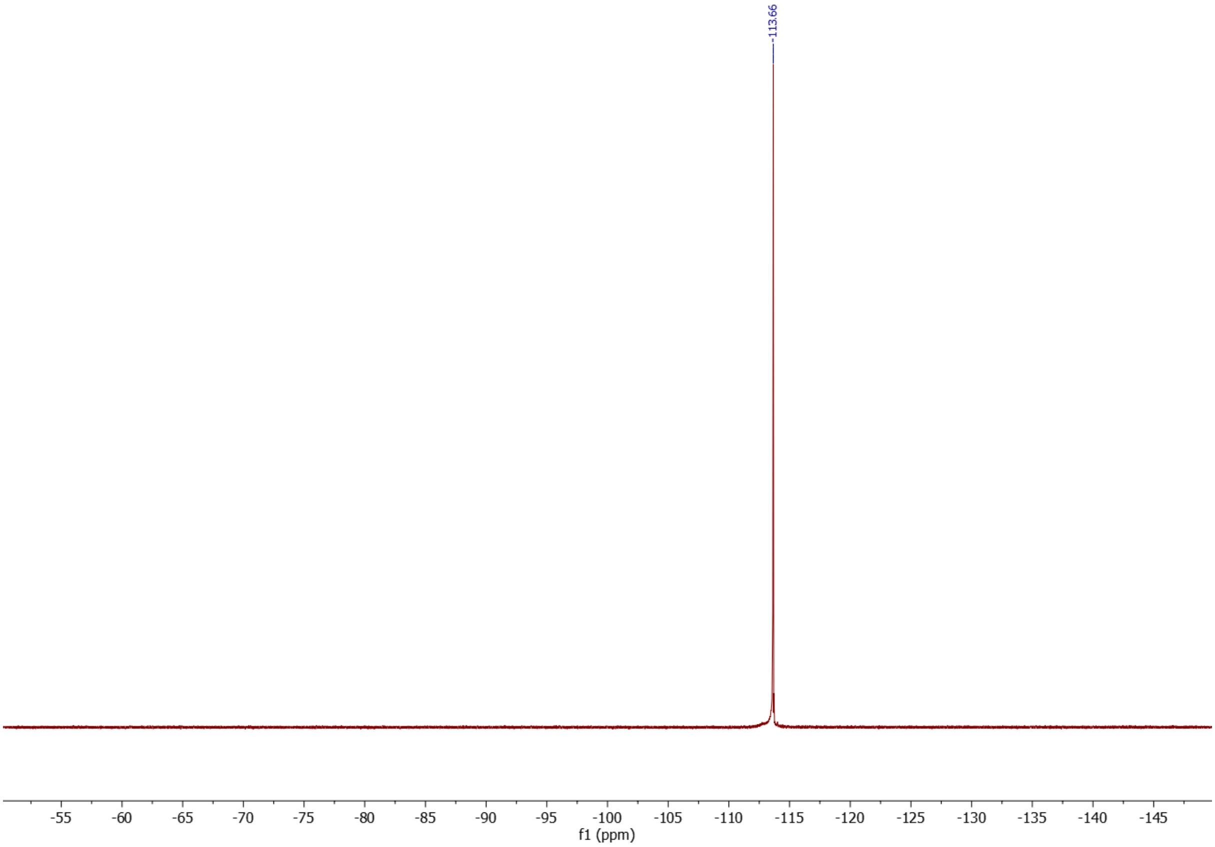
-113.66
-55
-60
-65
-70
-75
-80
-85
-90
-95
-100
-105
-110
-115
-120
-125
-130
-135
-140
-145
f1 (ppm)

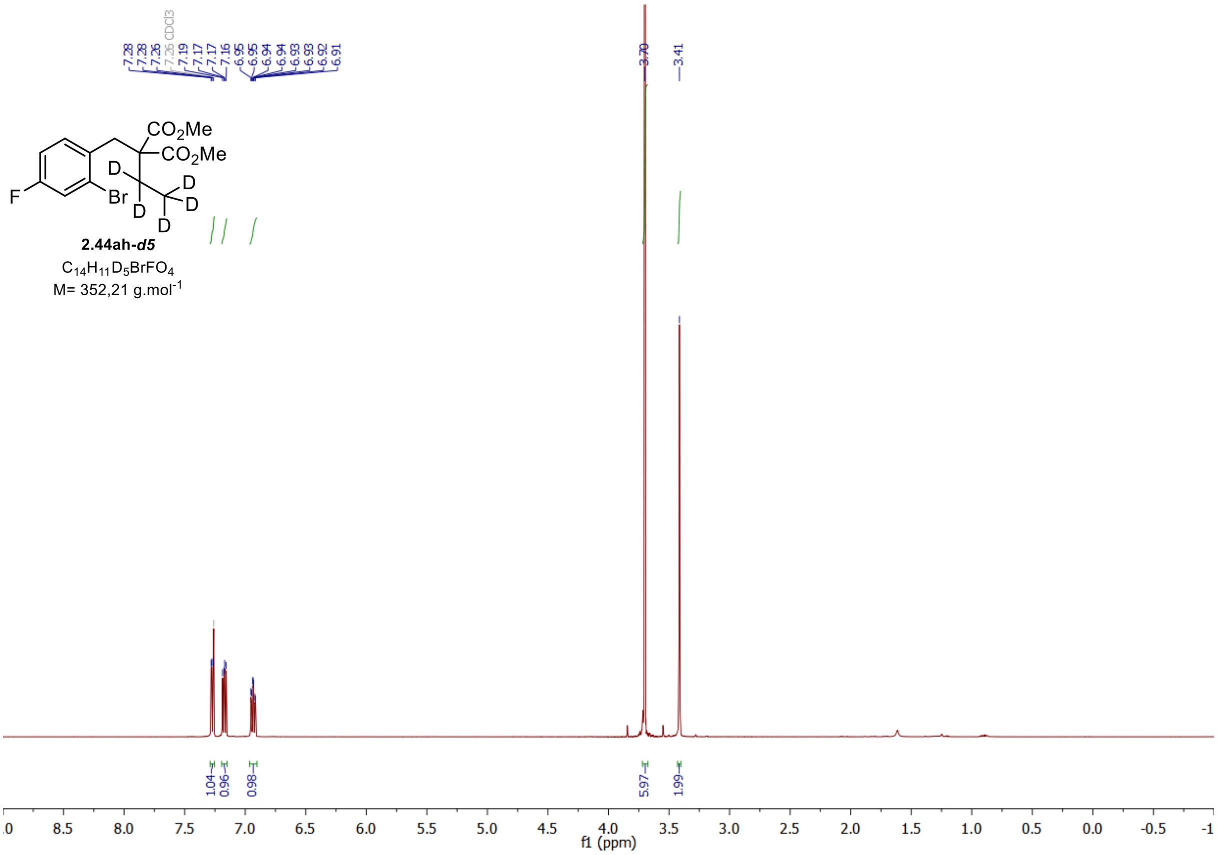

2.44ah-*d5*

$C_{14}H_{11}D_5BrFO_4$

M= 352,21 g.mol^{-1}

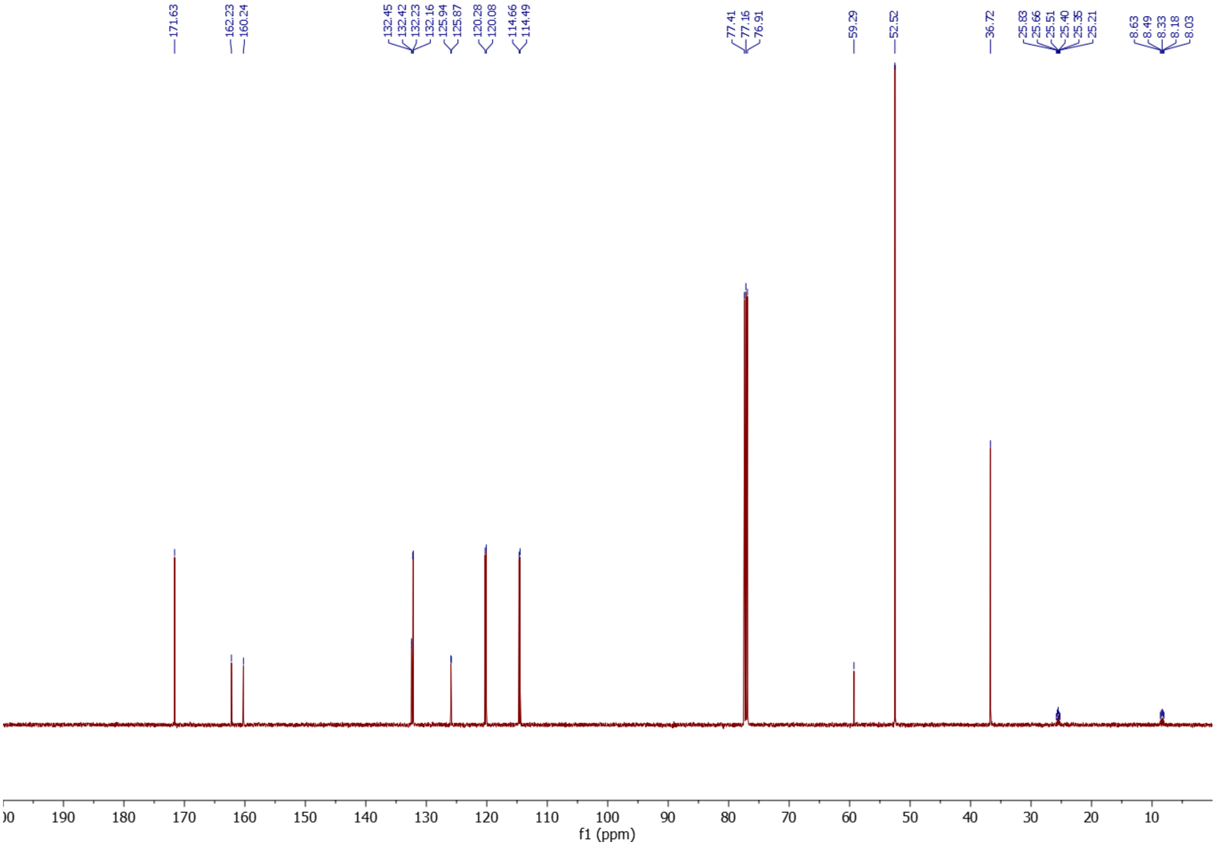

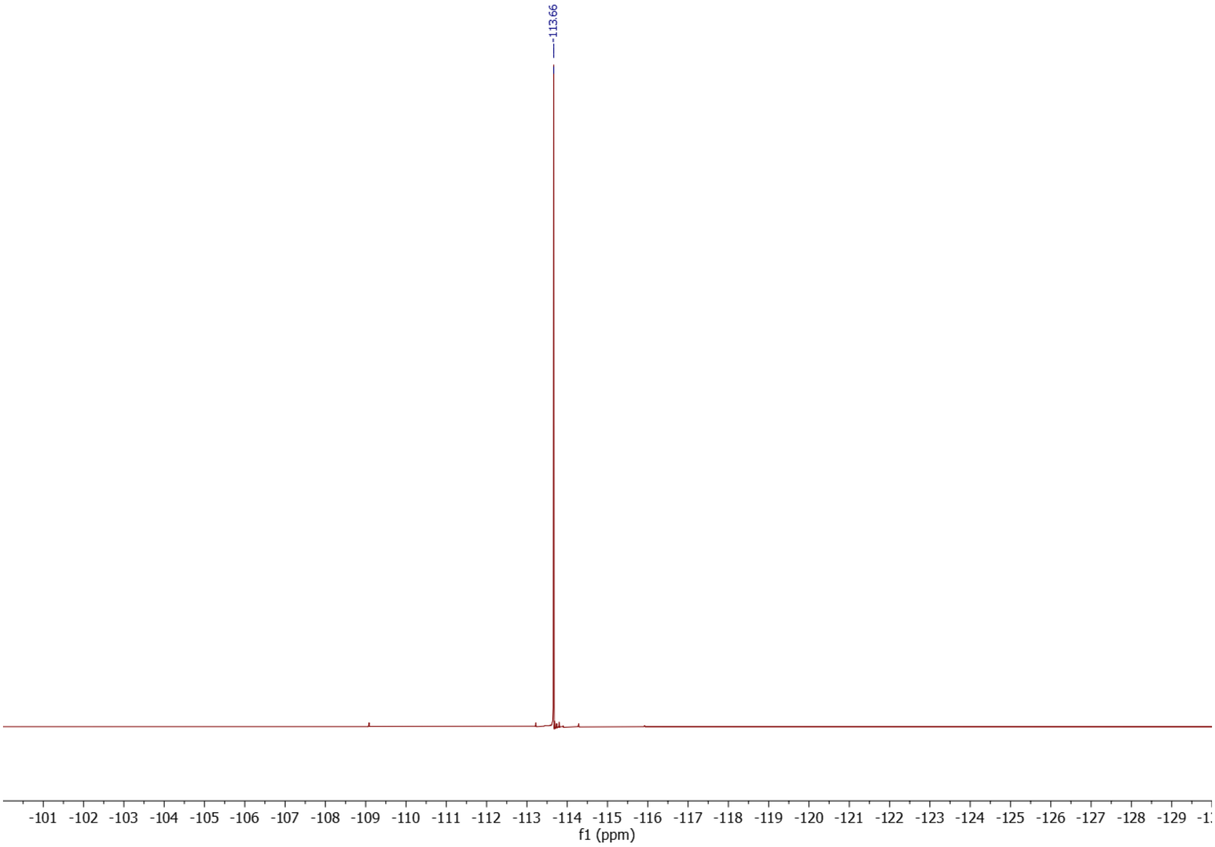
-113.66
-101
-102
-103
-104
-105
-106
-107
-108
-109
-110
-111
-112
-113
-114
-115
-116
-117
-118
-119
-120
-121
-122
-123
-124
-125
-126
-127
-128
-129
f1 (ppm)

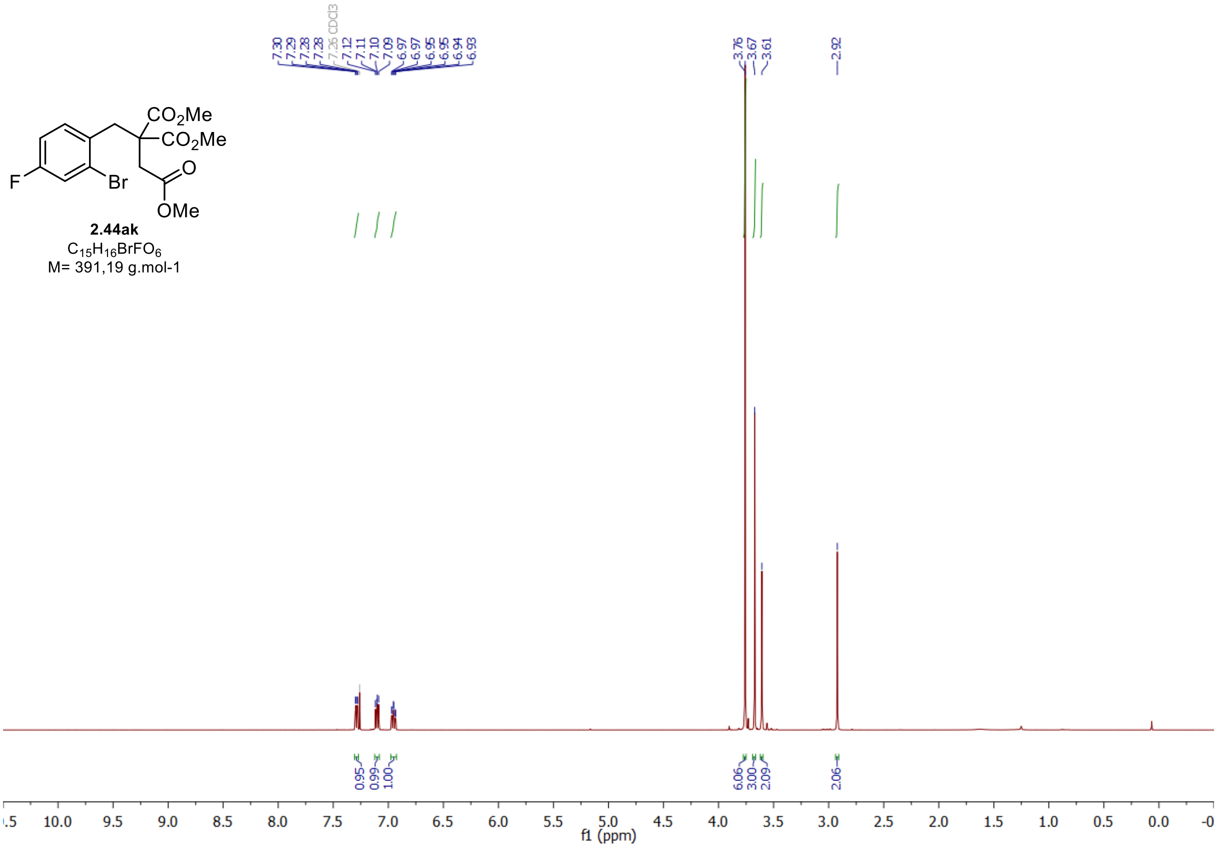

2.44ak
$C_{15}H_{16}BrFO_6$
M= 391,19 g.mol-1

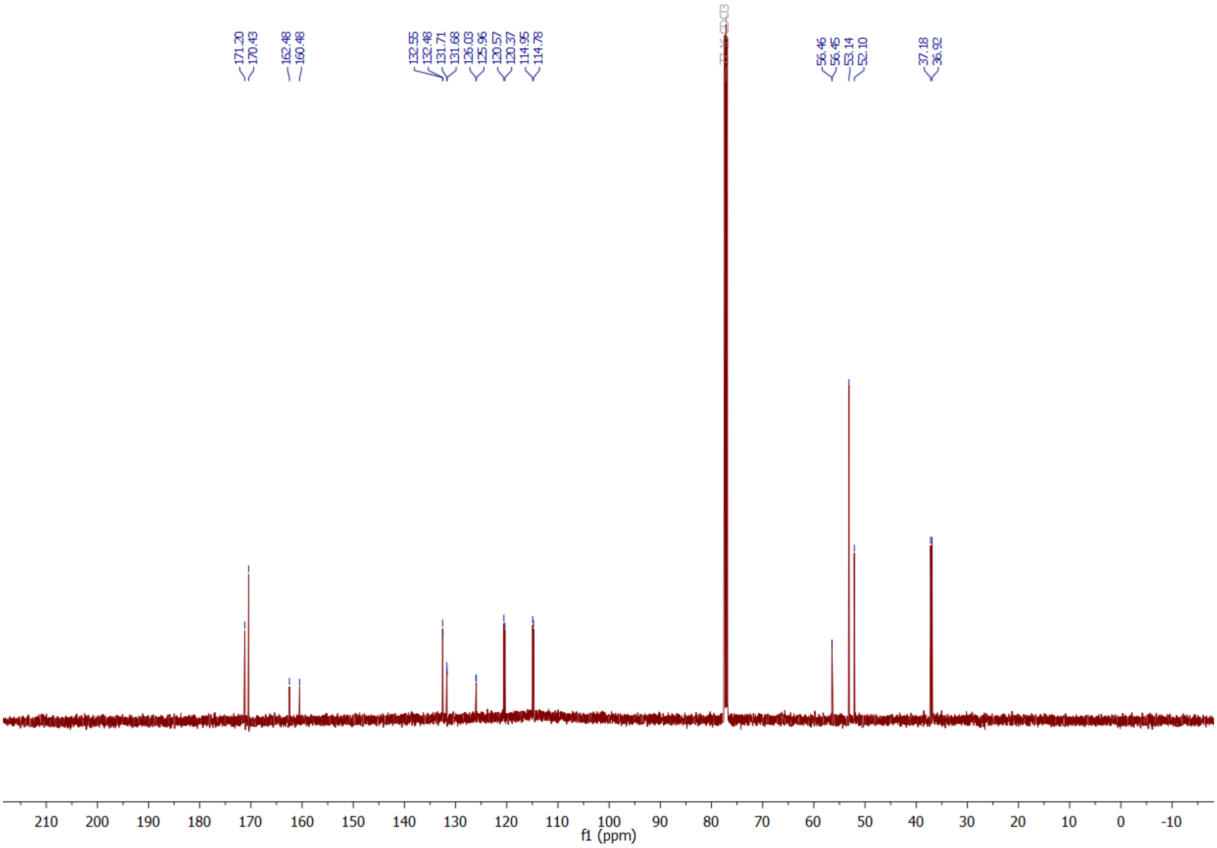

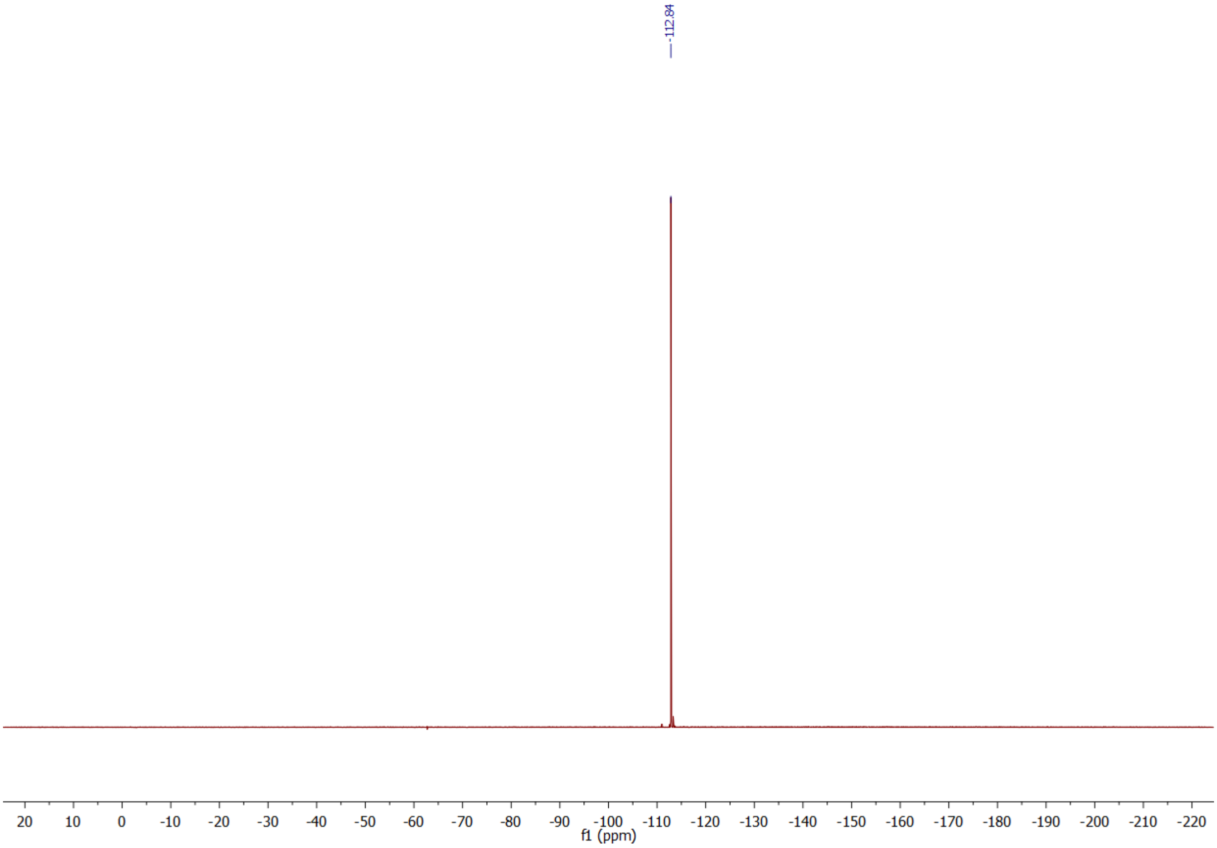
-112.84
20
10
0
-10
-20
-30
-40
-50
-60
-70
-80
-90
-100
-110
-120
-130
-140
-150
-160
-170
-180
-190
-200
-210
-220
f1 (ppm)

CO2Me
CO2Me
F
Br

2.44al

$C_{15}H_{16}BrFO_4$

M= 359,19 g.mol^{-1}

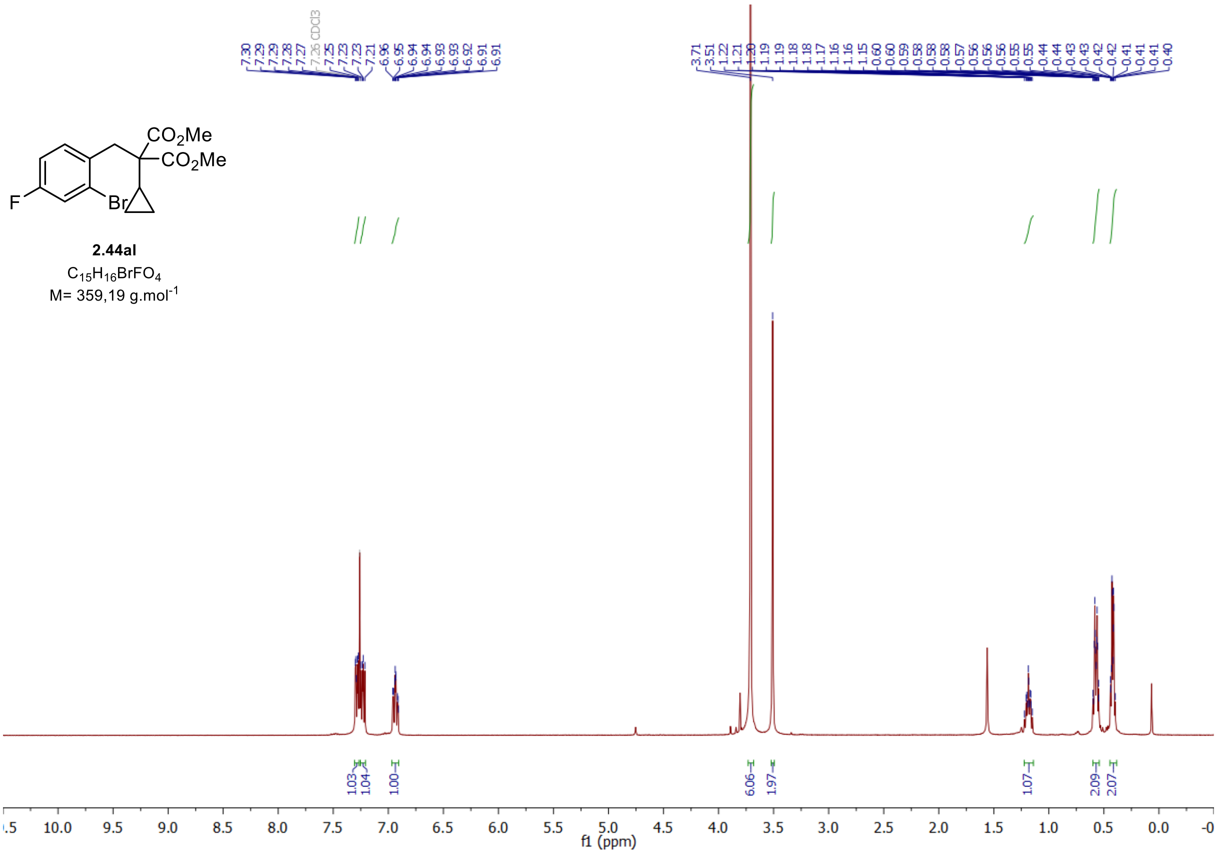

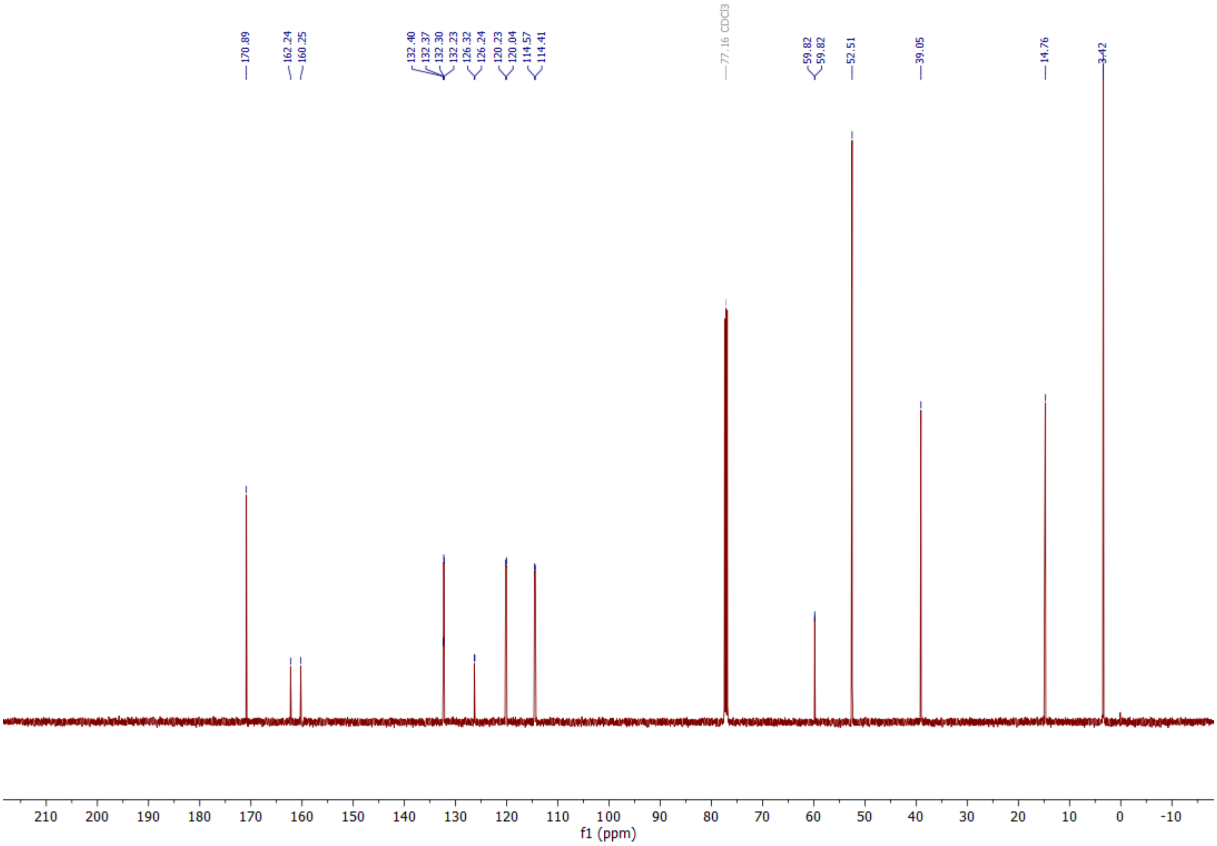

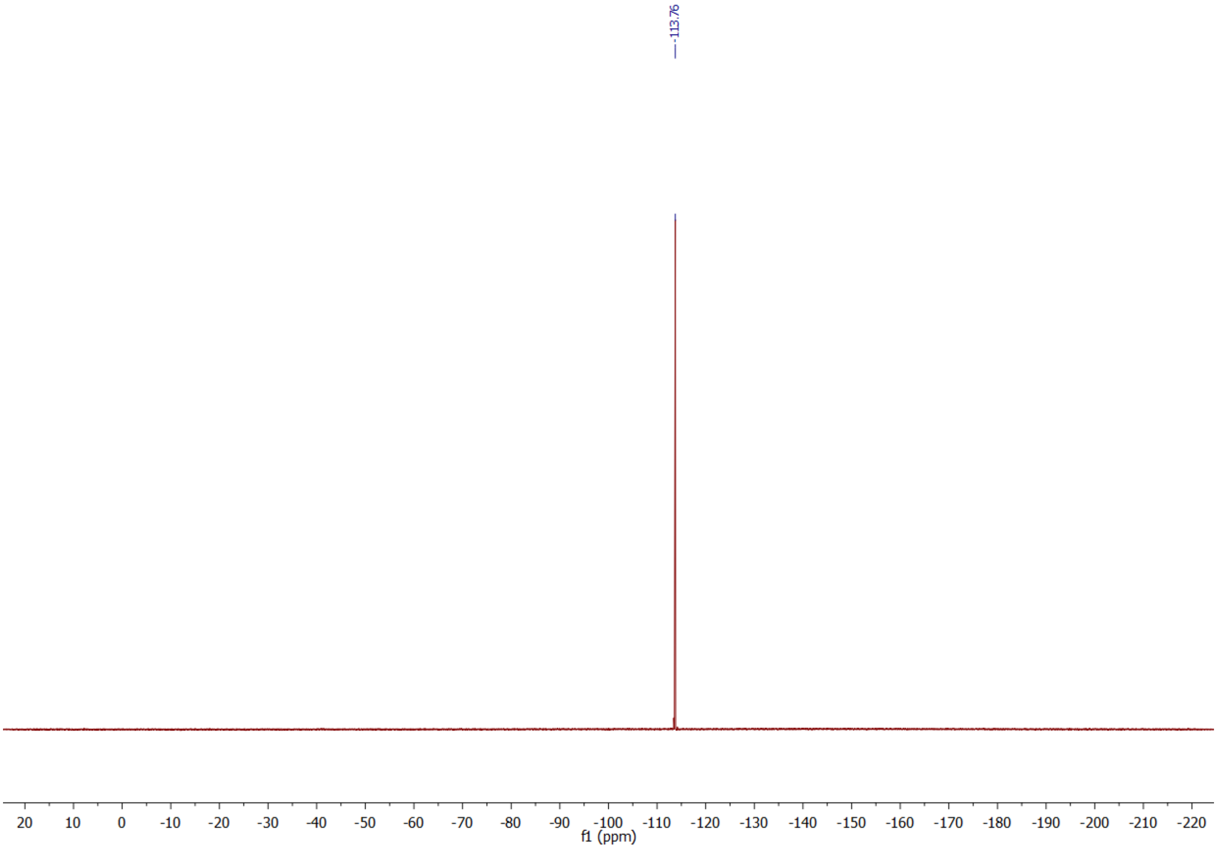
-113.76
20
10
0
-10
-20
-30
-40
-50
-60
-70
-80
-90
-100
-110
-120
-130
-140
-150
-160
-170
-180
-190
-200
-210
-220
f1 (ppm)

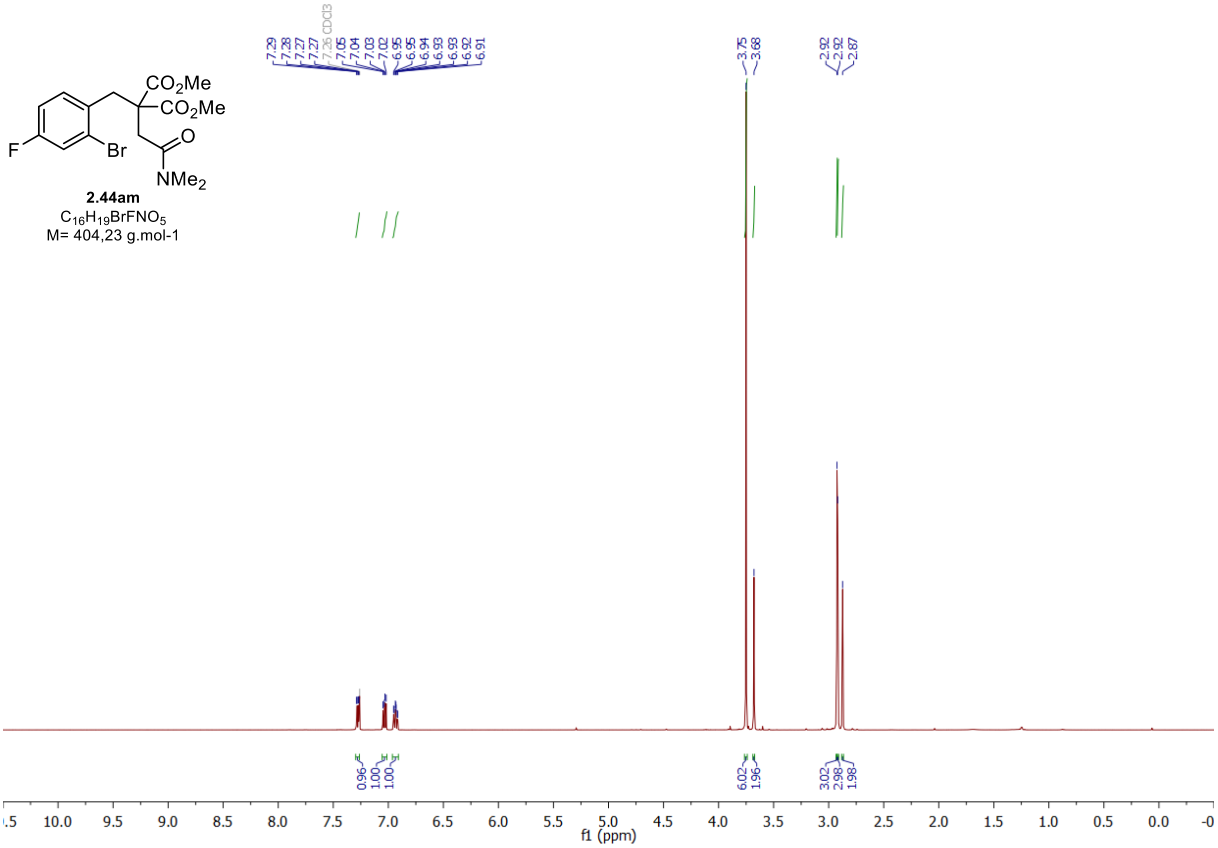

2.44am

$C_{16}H_{19}BrFNO_5$

M= 404,23 g.mol-1

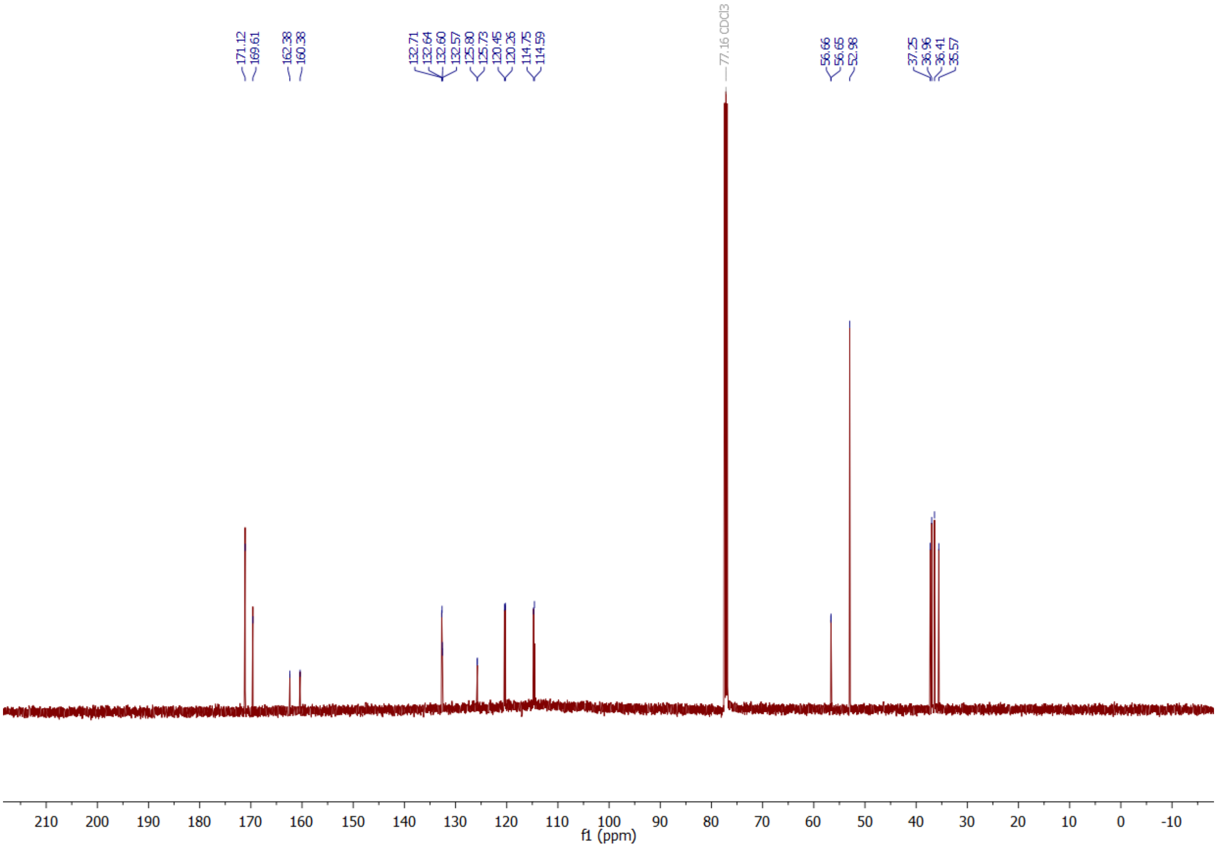

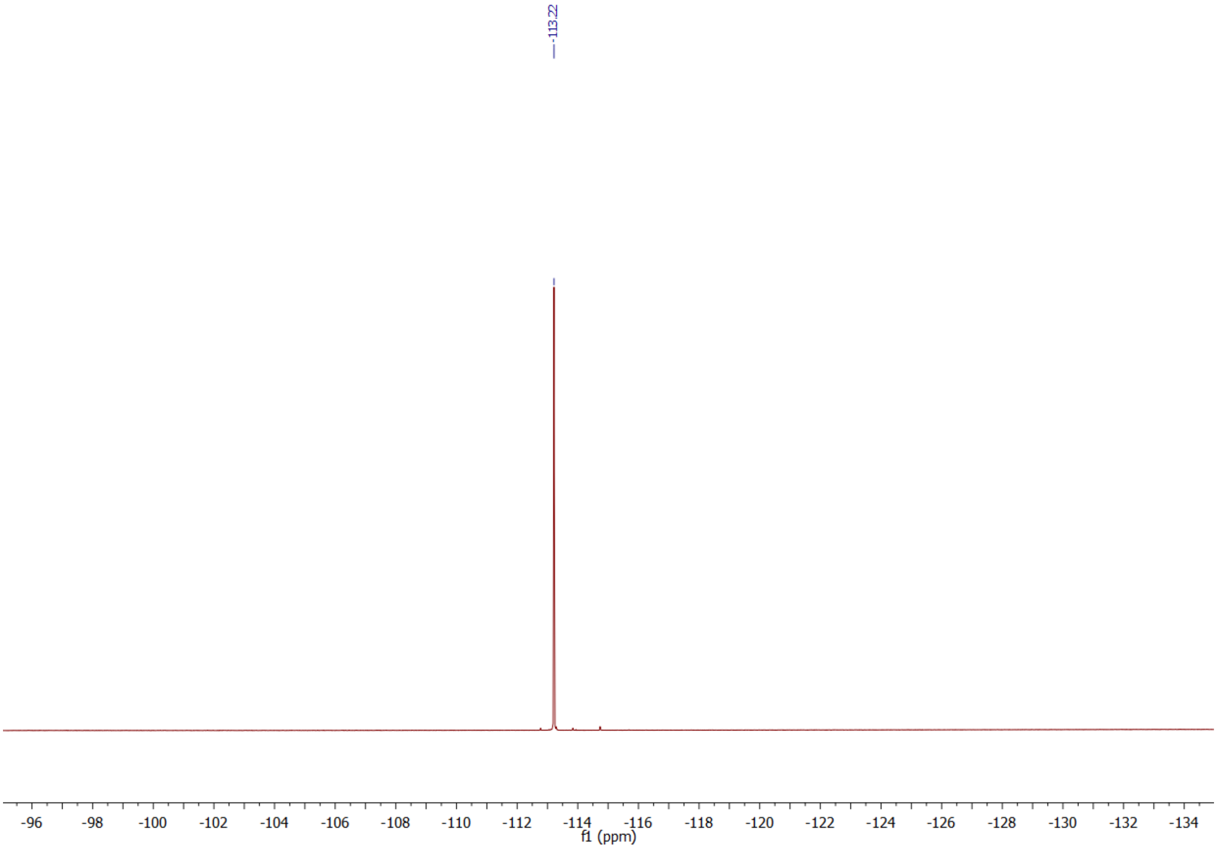
-113.22
-96
-98
-100
-102
-104
-106
-108
-110
-112
-114
-116
-118
-120
-122
-124
-126
-128
-130
-132
-134
f1 (ppm)

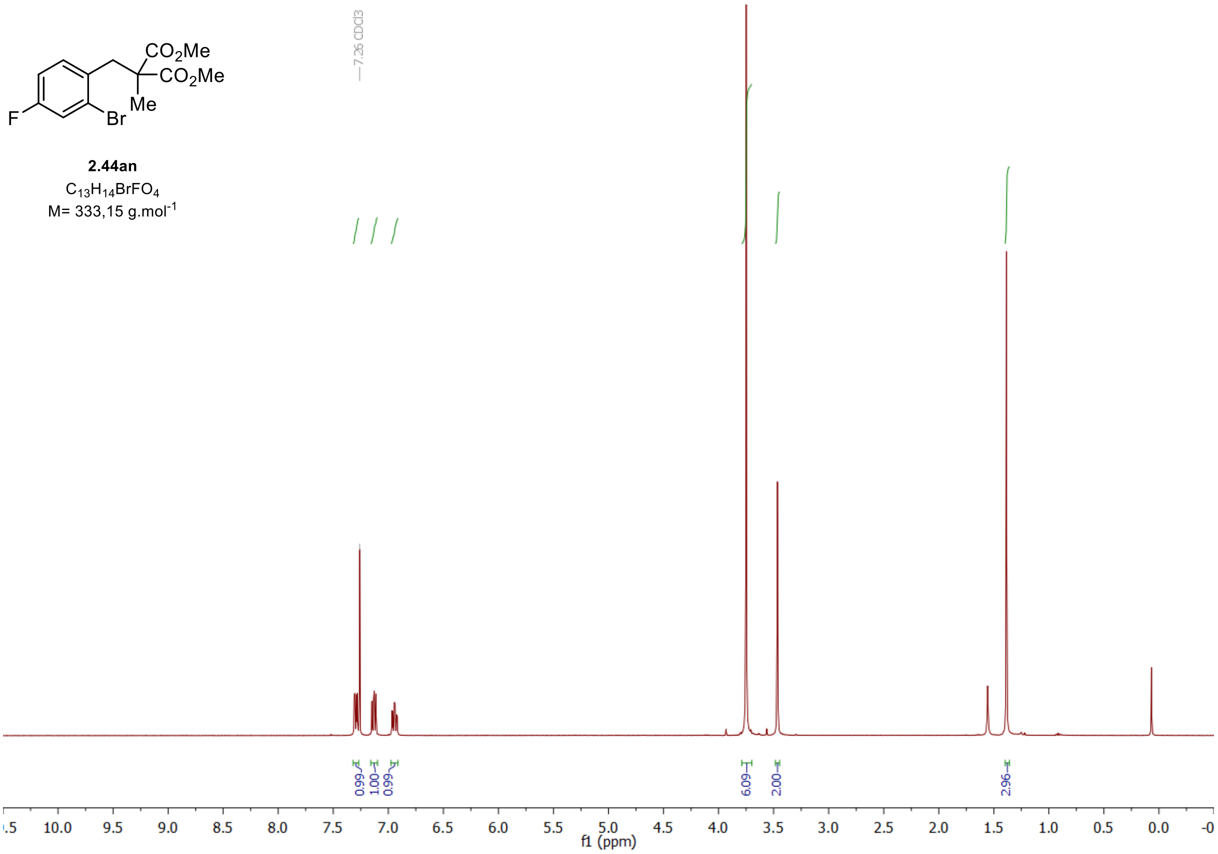

2.44an

$C_{13}H_{14}BrFO_4$

M= 333,15 g.mol^{-1}

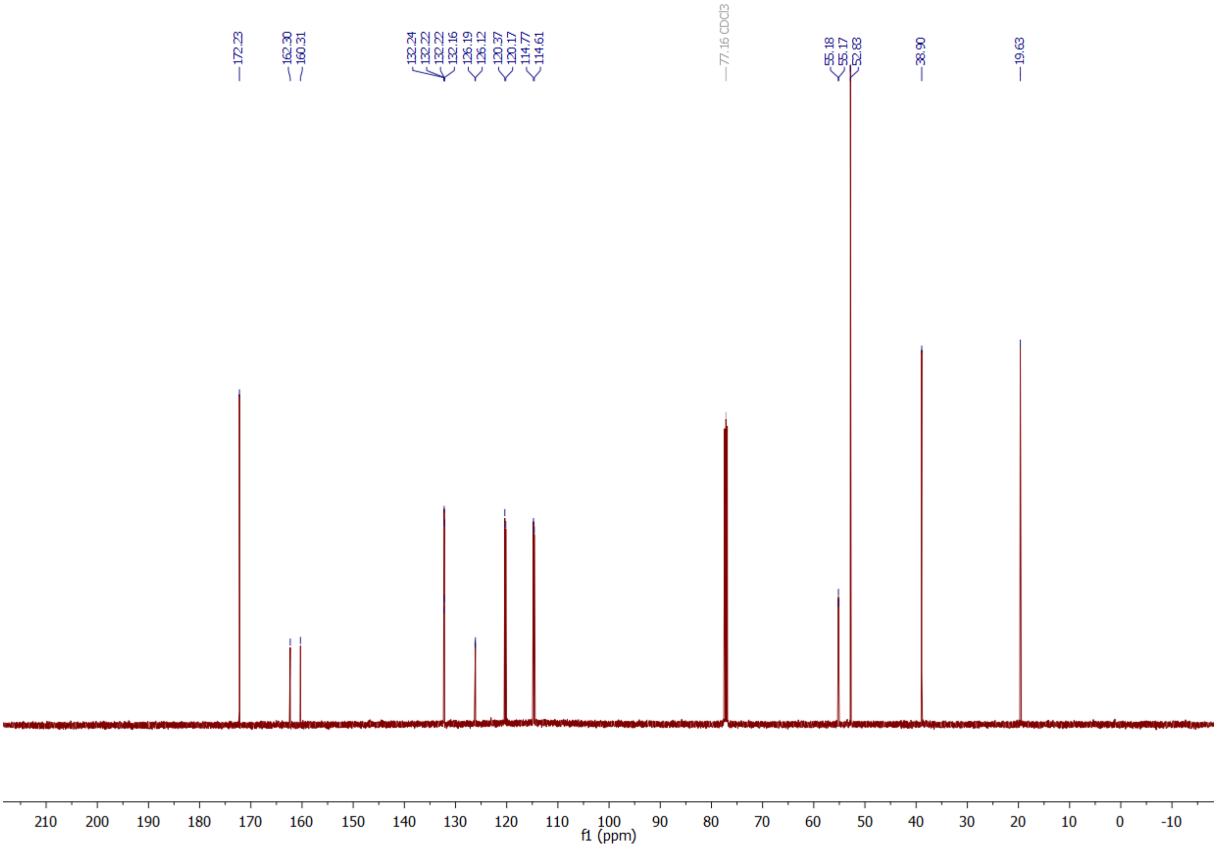

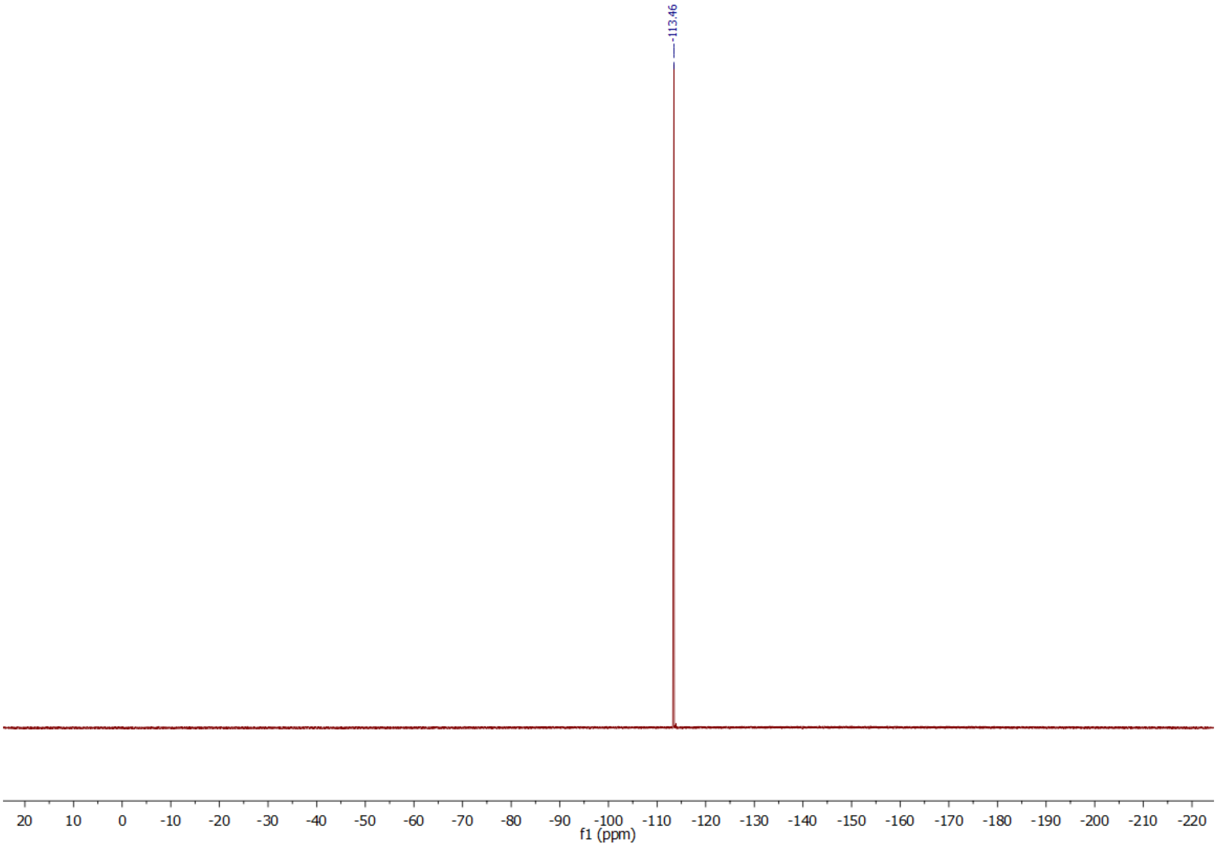
-113.46
20
10
0
-10
-20
-30
-40
-50
-60
-70
-80
-90
-100
-110
-120
-130
-140
-150
-160
-170
-180
-190
-200
-210
-220
f1 (ppm)

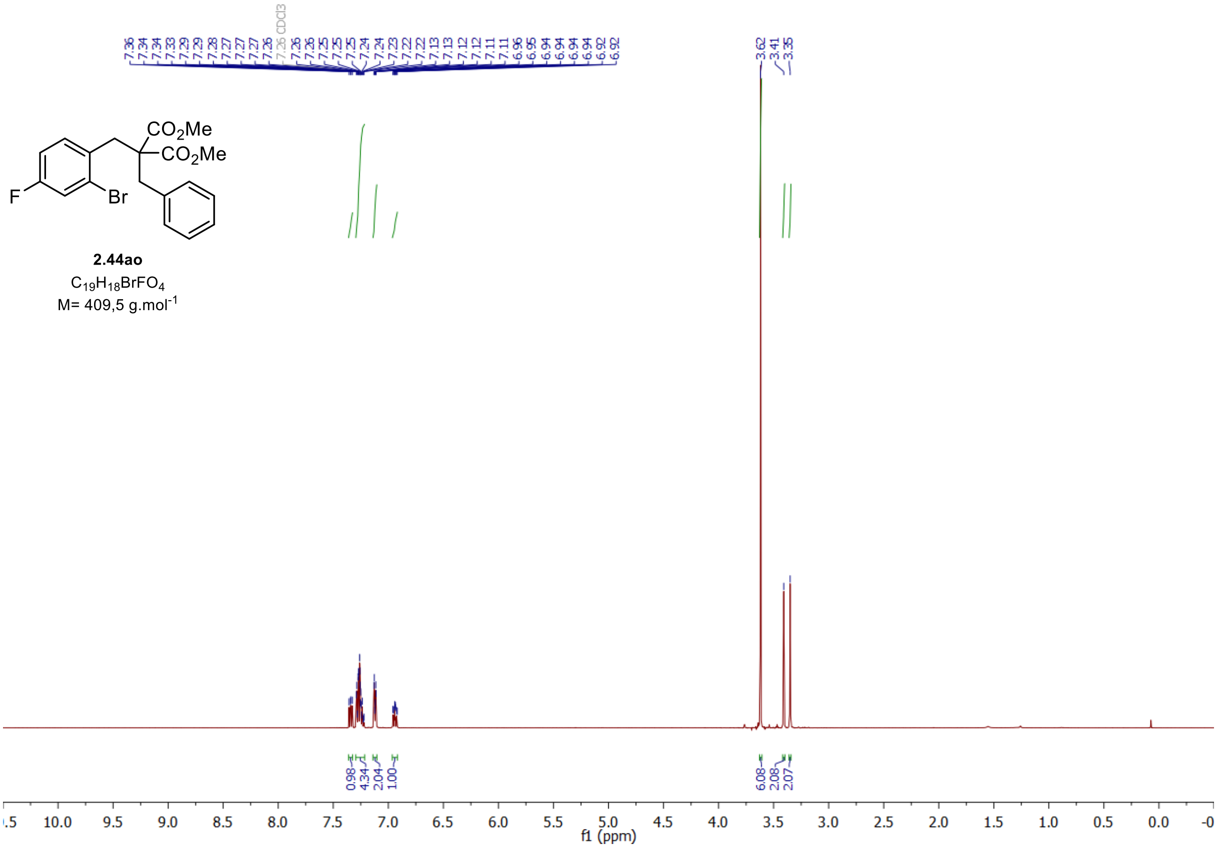

2.44ao

$C_{19}H_{18}BrFO_4$

M= 409,5 g.mol^{-1}

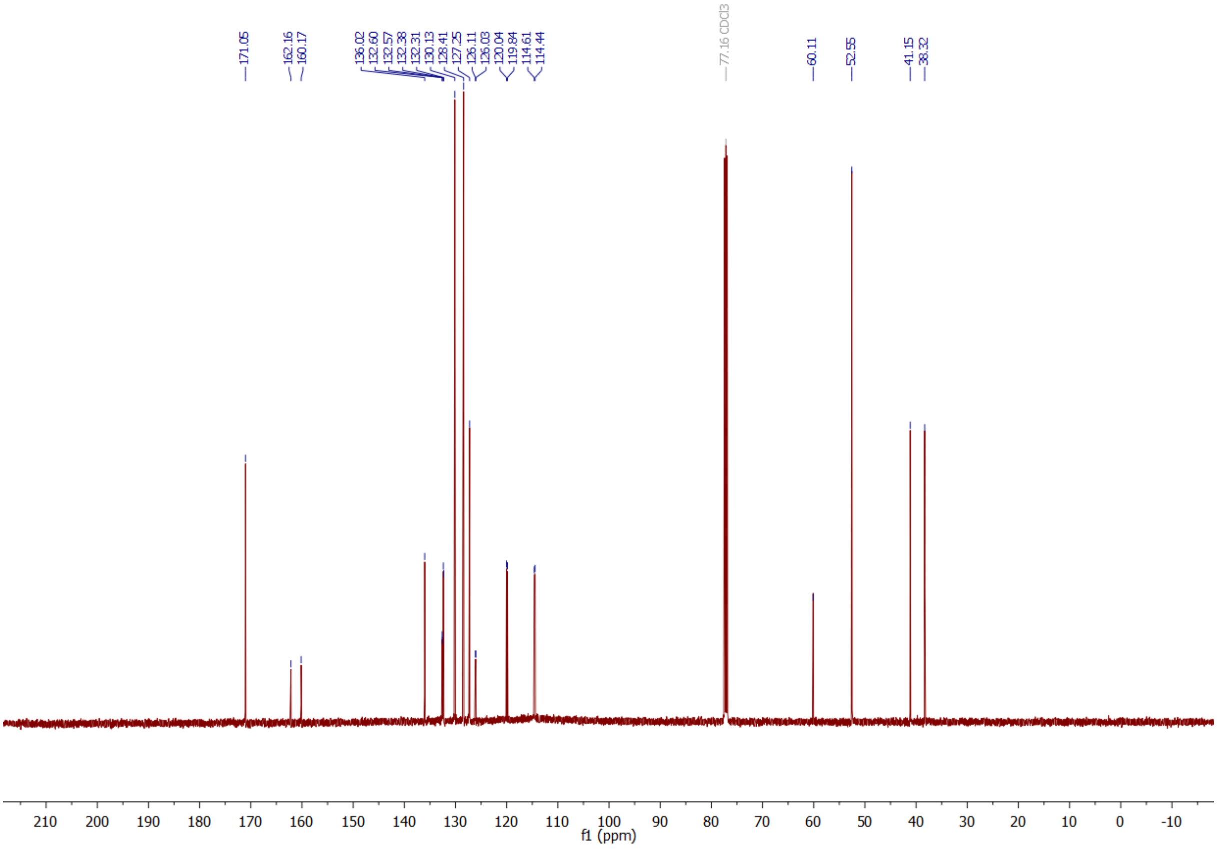

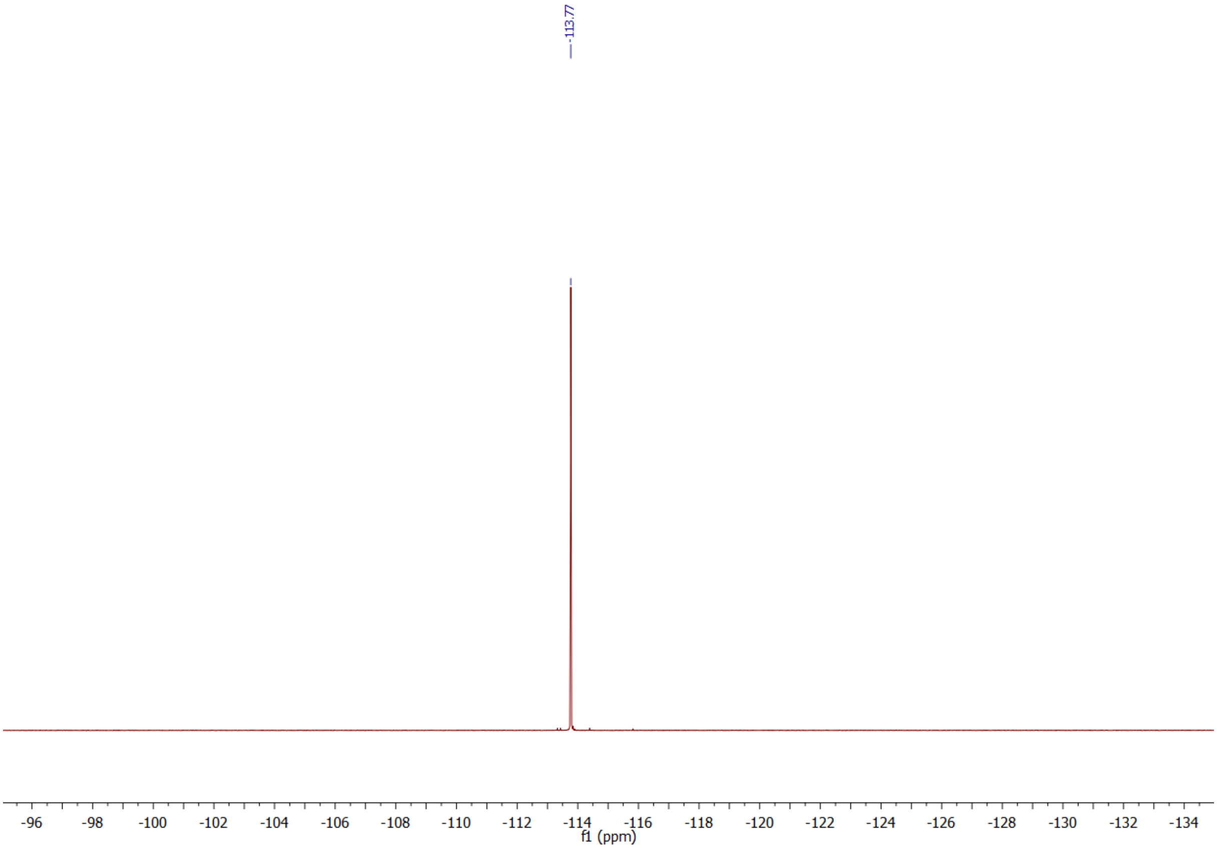
-113.77
-96
-98
-100
-102
-104
-106
-108
-110
-112
-114
-116
-118
-120
-122
-124
-126
-128
-130
-132
-134
f1 (ppm)

CO2Me
CO2Me
F
Br
OMe

2.44ap

$C_{14}H_{16}BrFO_5$

M= 363,18 g.mol^{-1}

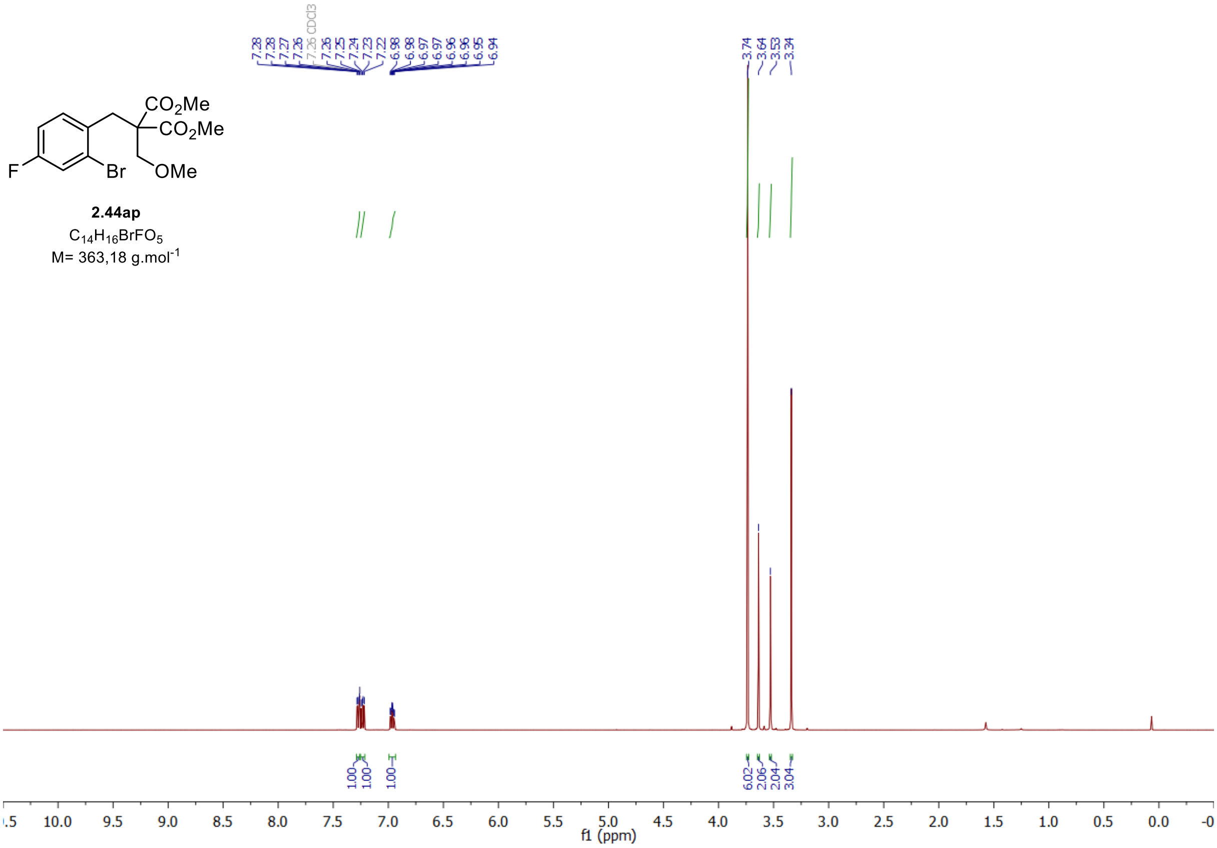

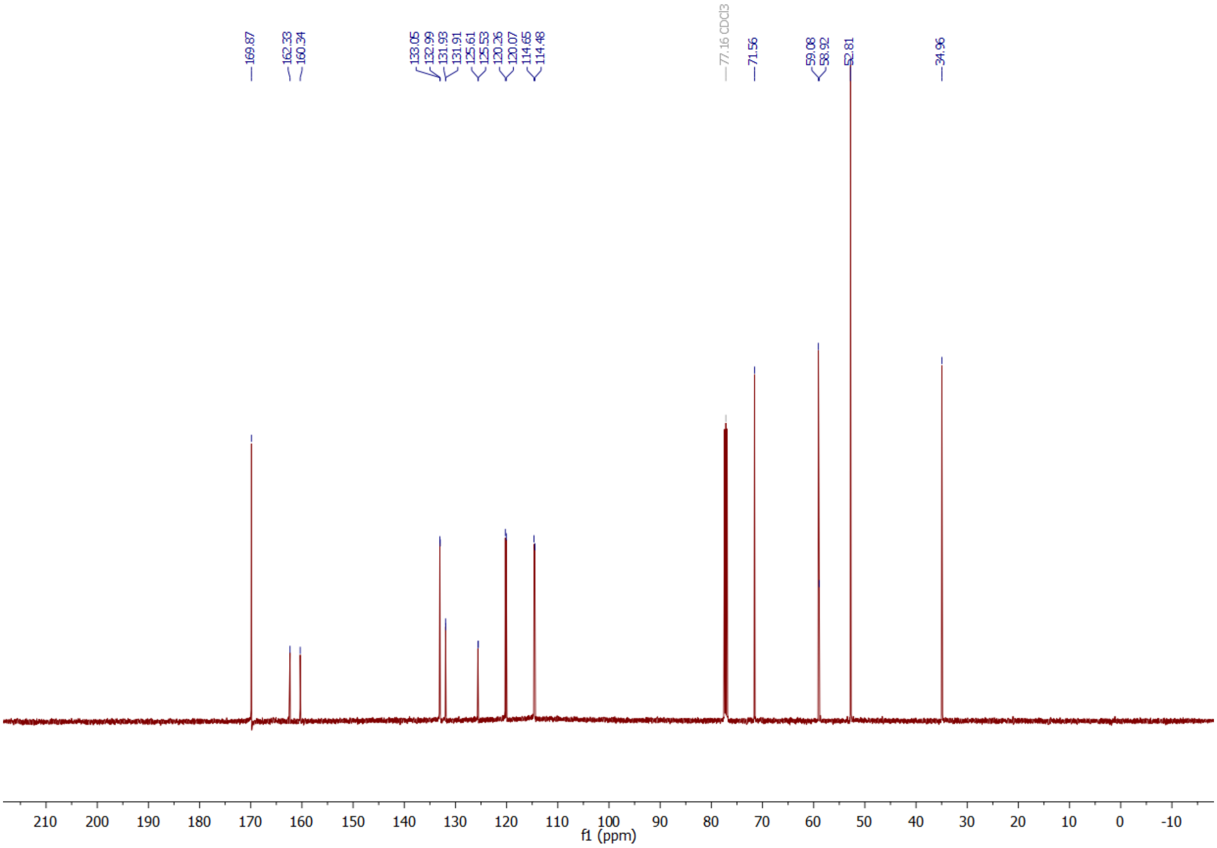

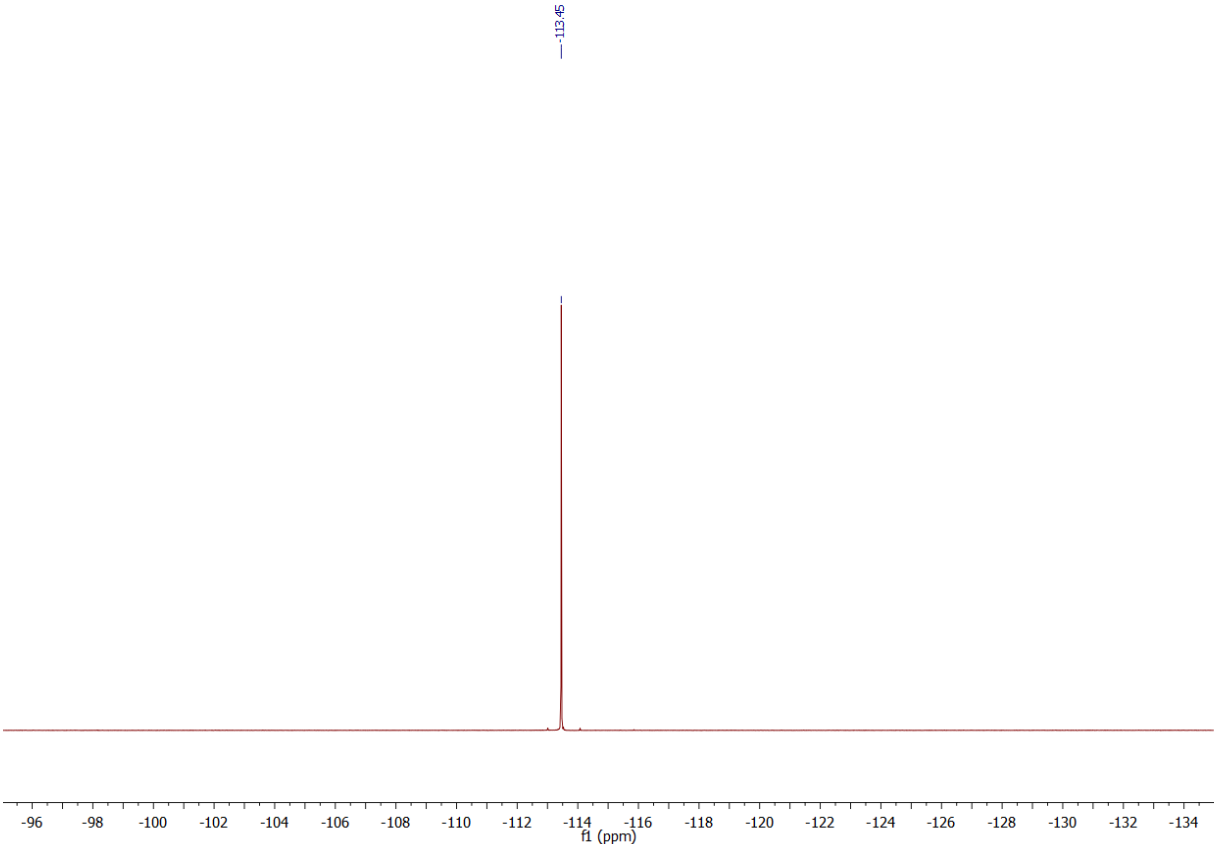
-113.45
-96
-98
-100
-102
-104
-106
-108
-110
-112
-114
-116
-118
-120
-122
-124
-126
-128
-130
-132
-134
f1 (ppm)

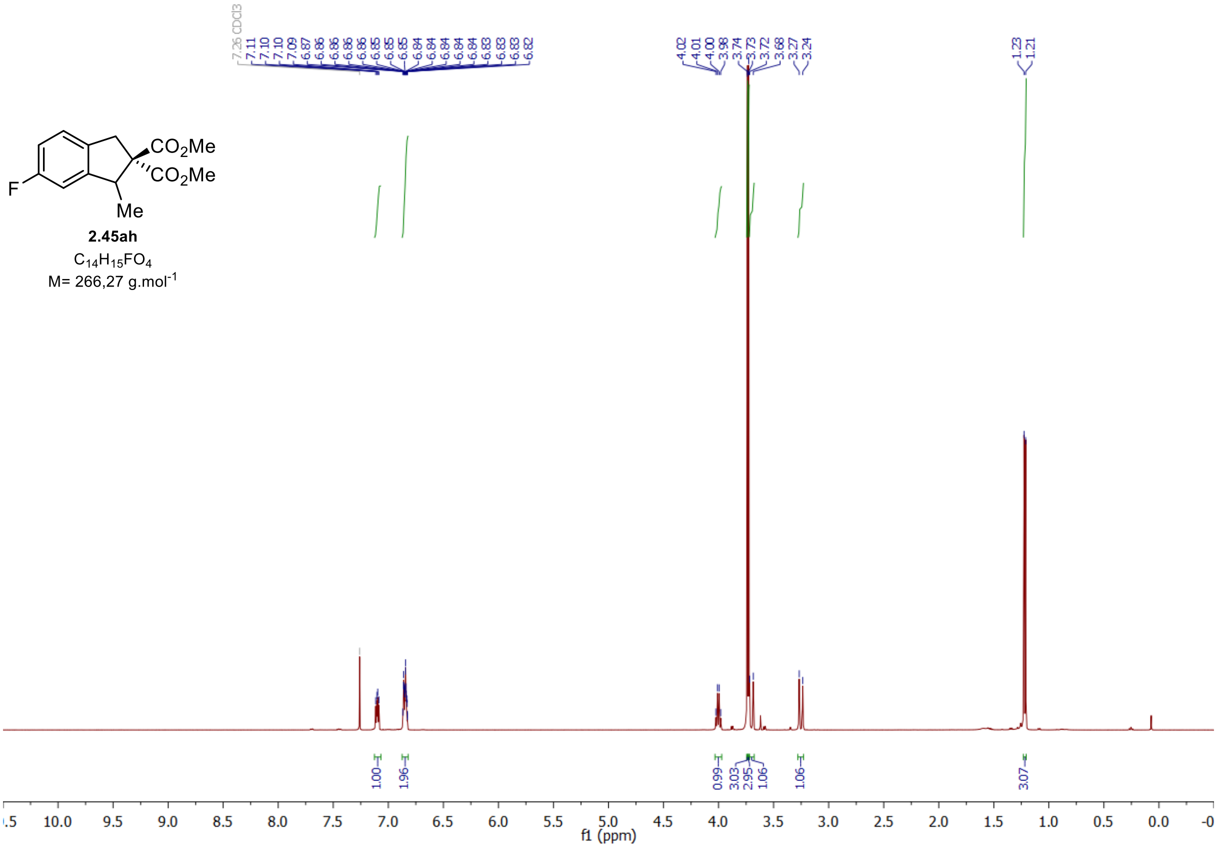

2.45ah

$C_{14}H_{15}FO_4$

M= 266,27 g.mol^{-1}

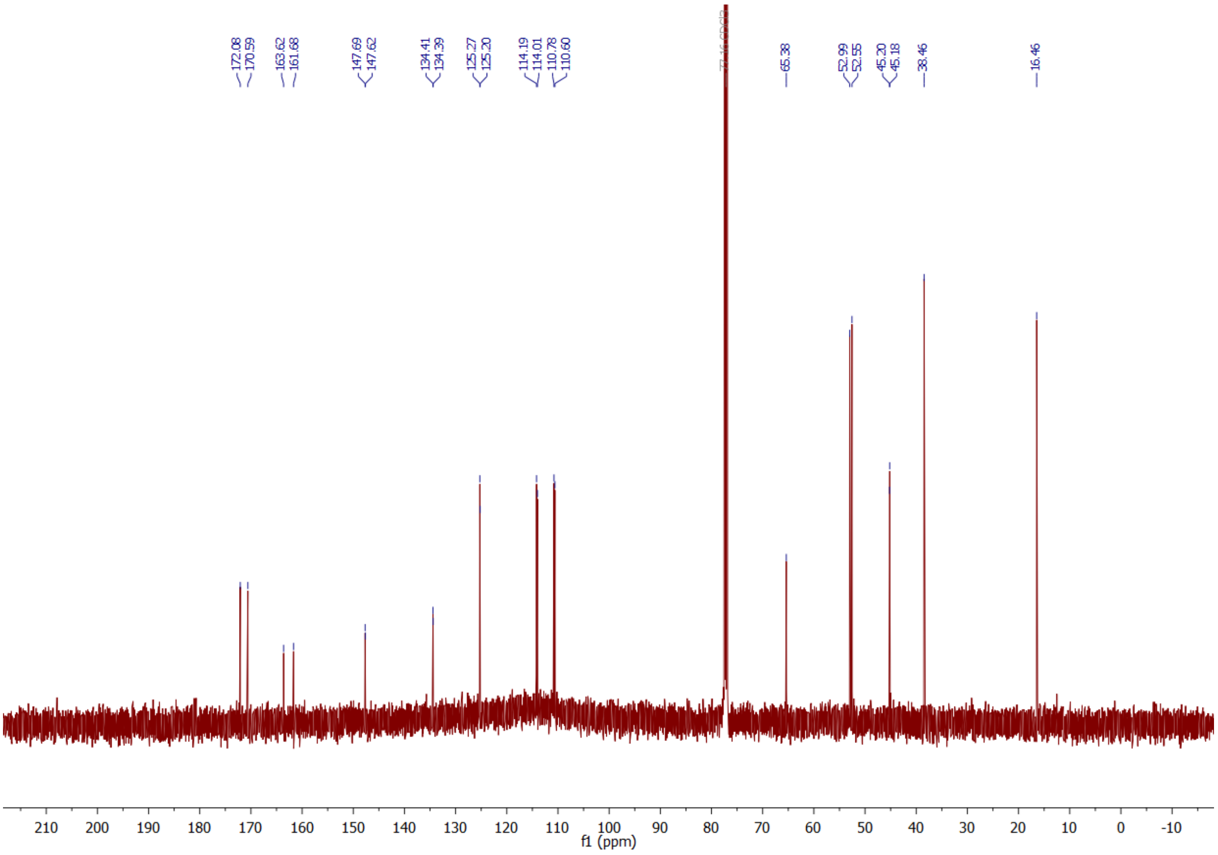

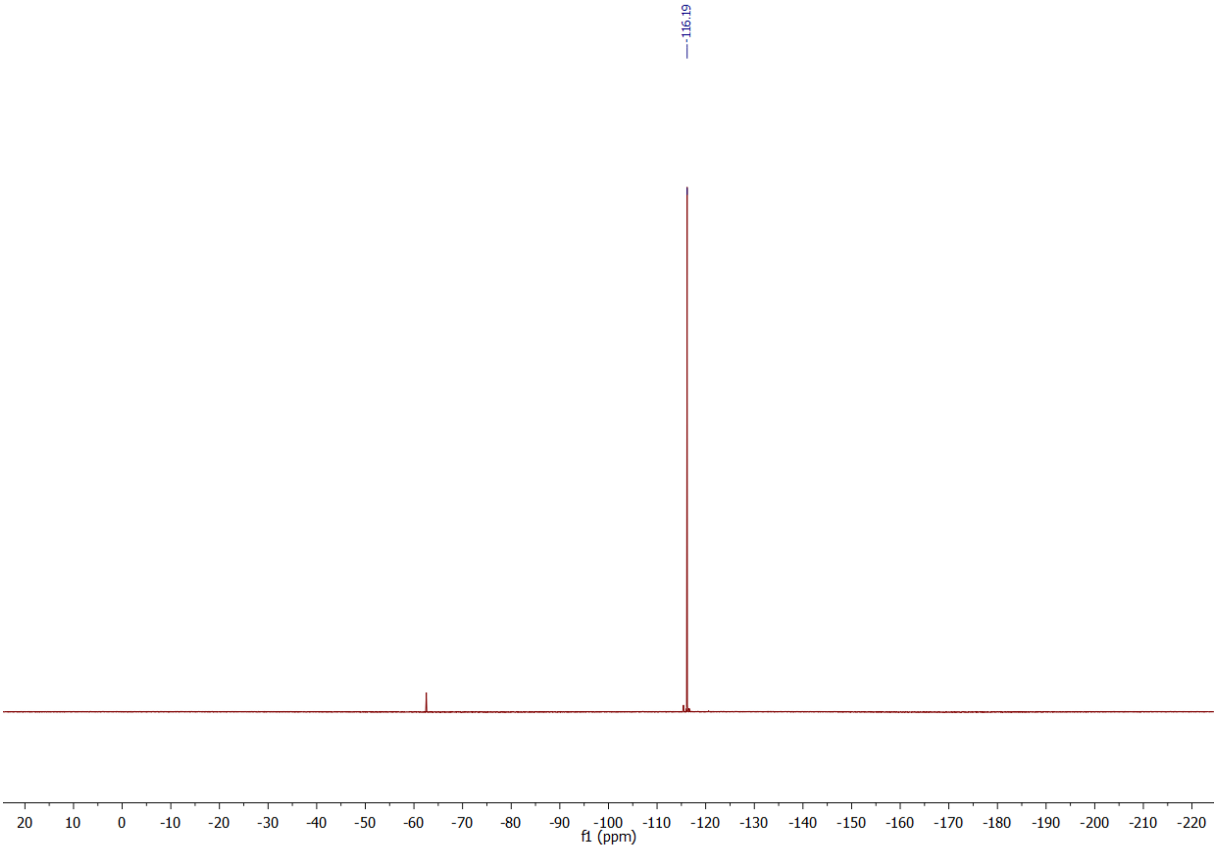
-116.19
20
10
0
-10
-20
-30
-40
-50
-60
-70
-80
-90
-100
-110
-120
-130
-140
-150
-160
-170
-180
-190
-200
-210
-220
f1 (ppm)

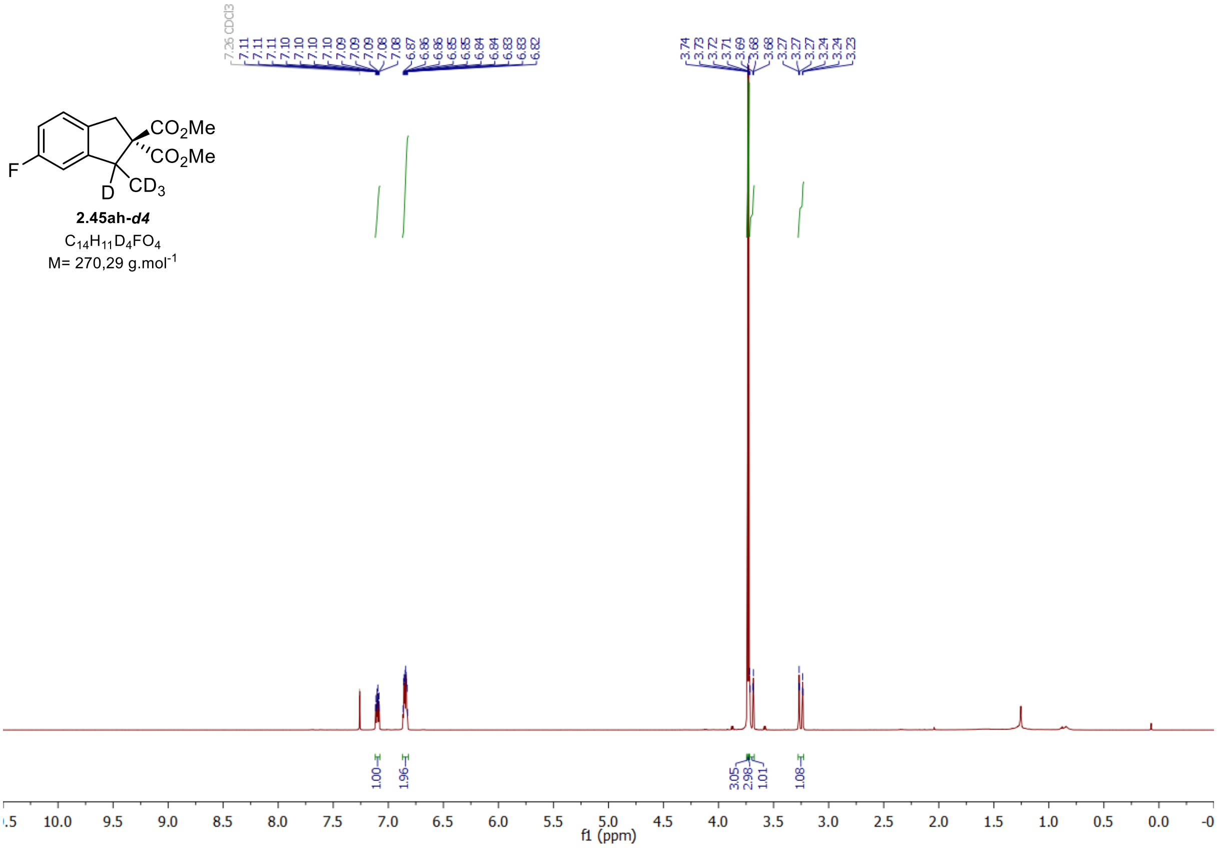

2.45ah-*d4*

$C_{14}H_{11}D_4FO_4$

M= 270,29 g.mol^{-1}

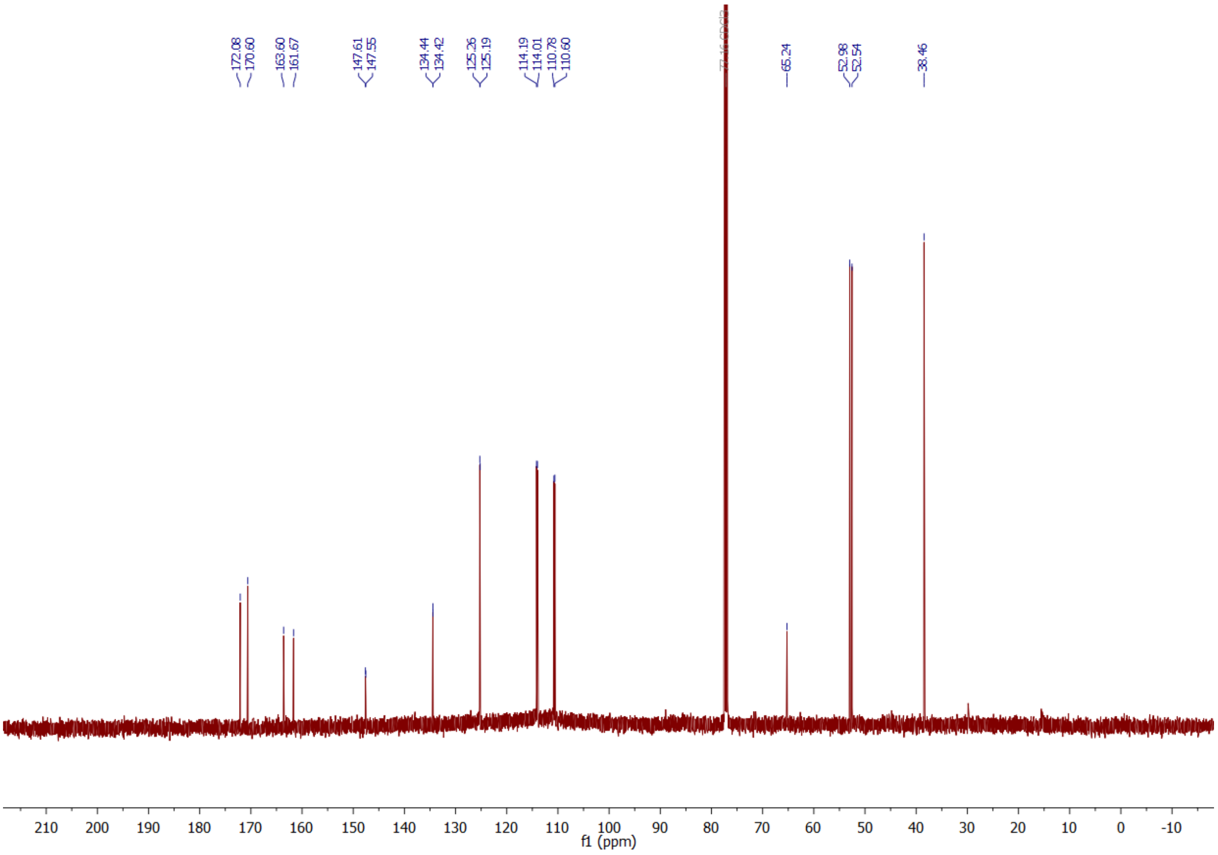

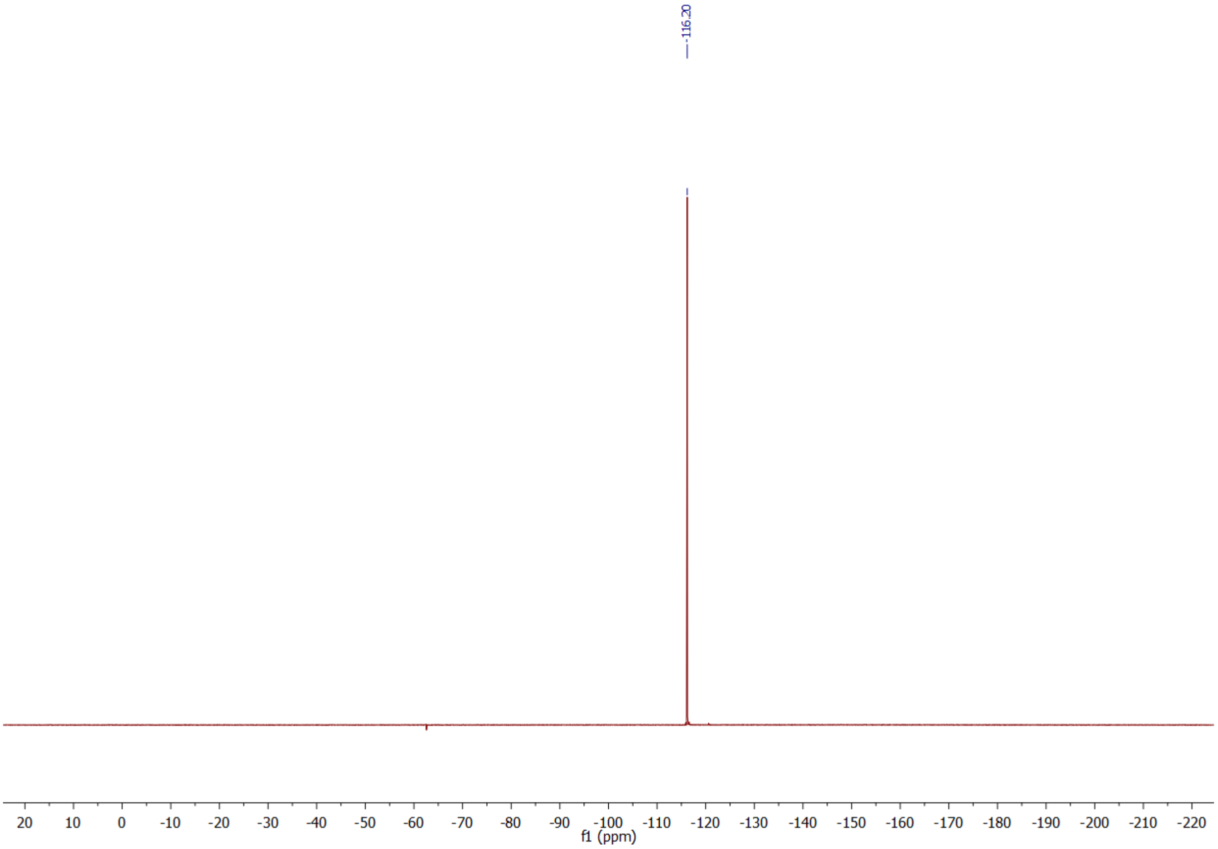
-116.20
20
10
0
-10
-20
-30
-40
-50
-60
-70
-80
-90
-100
-110
-120
-130
-140
-150
-160
-170
-180
-190
-200
-210
-220
f1 (ppm)

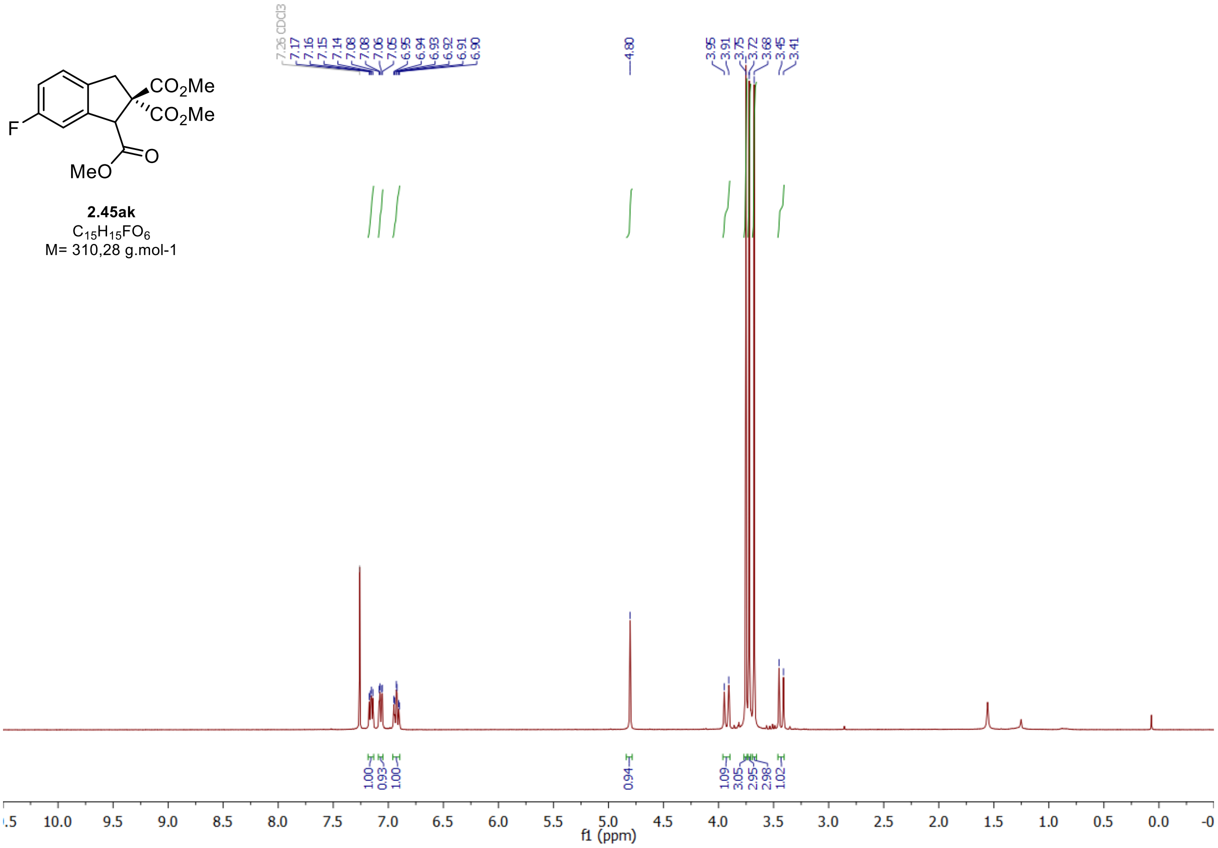

2.45ak

$C_{15}H_{15}FO_6$

M= 310,28 g.mol-1

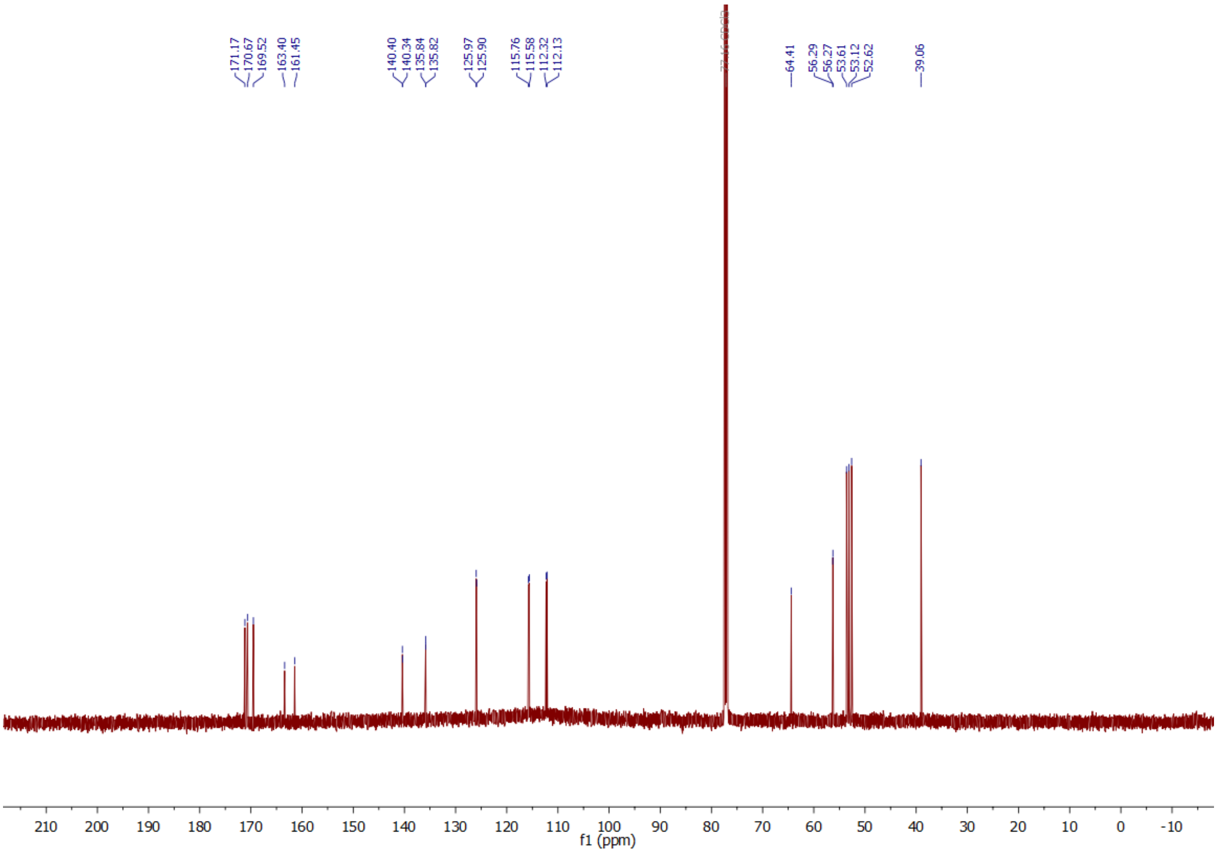

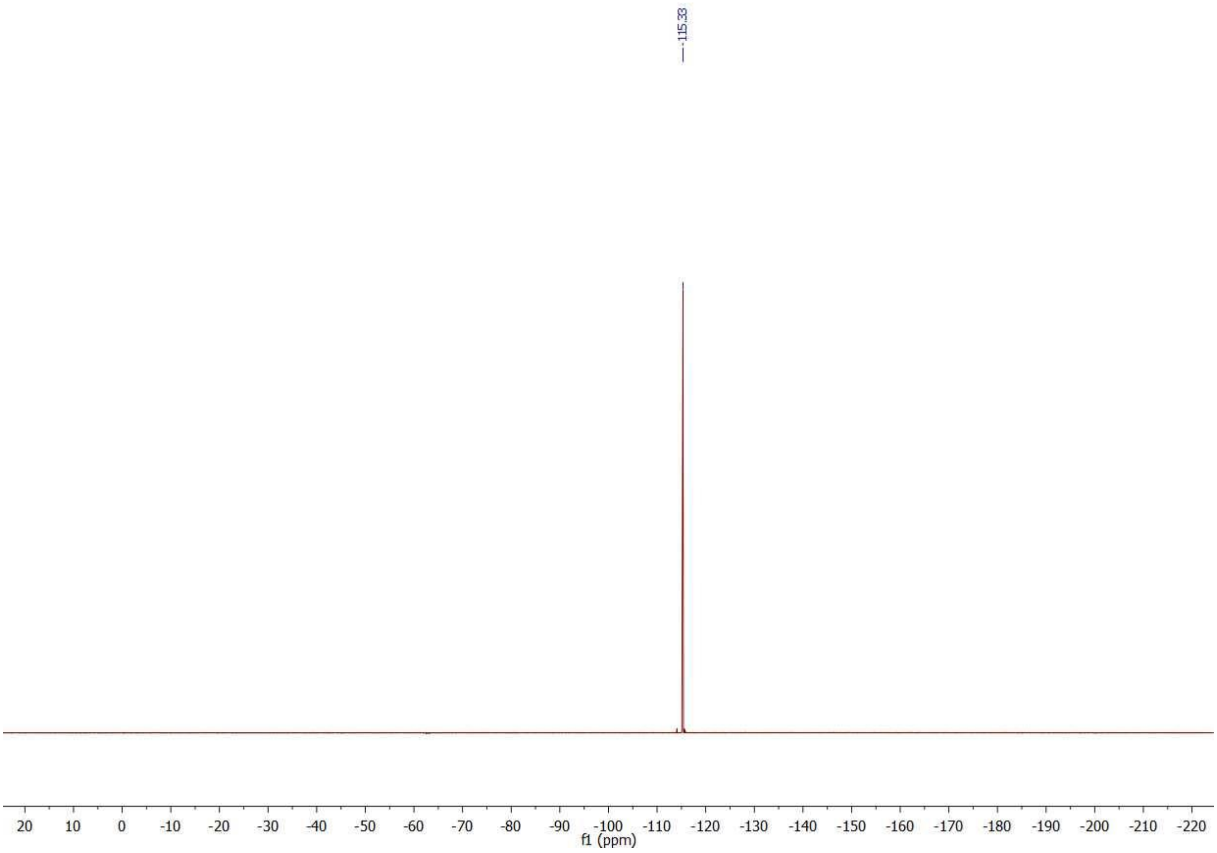
-115.33
20
10
0
-10
-20
-30
-40
-50
-60
-70
-80
-90
-100
-110
-120
-130
-140
-150
-160
-170
-180
-190
-200
-210
-220
f1 (ppm)

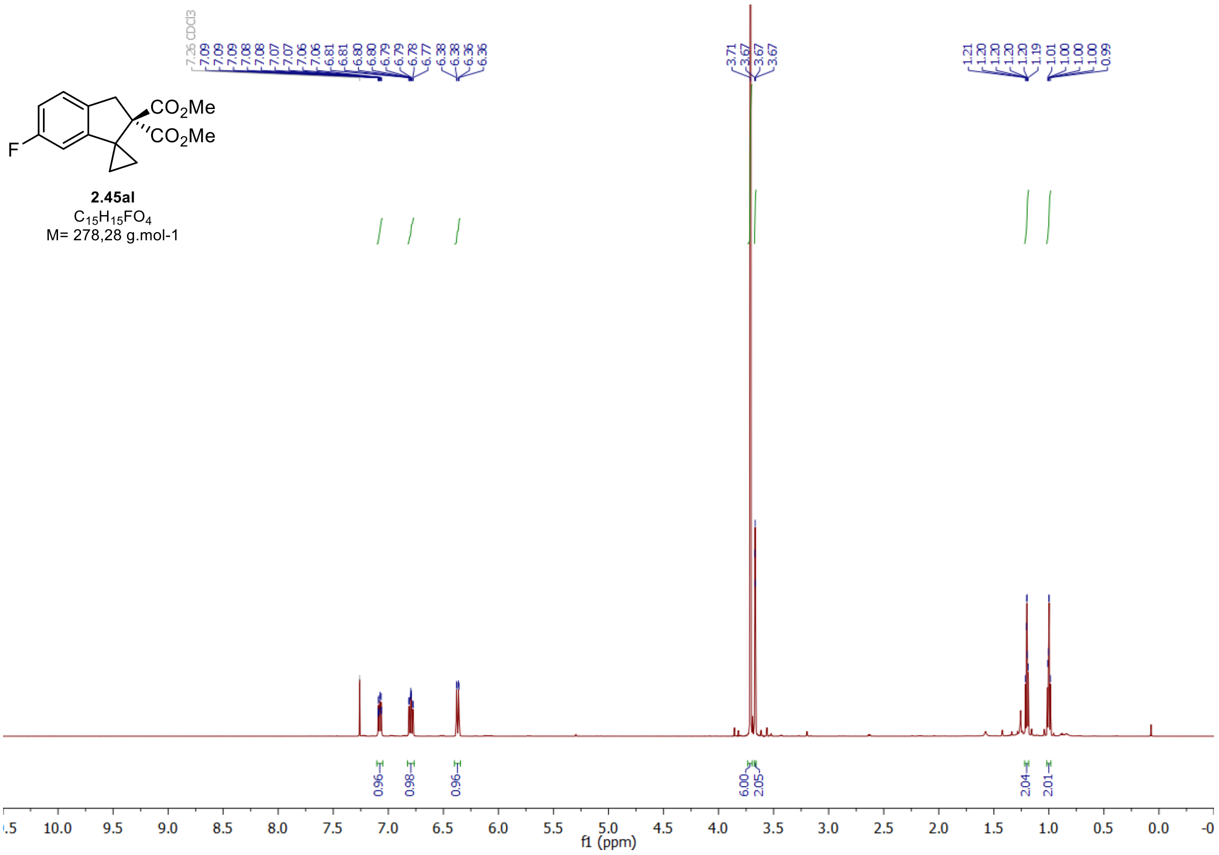

2.45al

$C_{15}H_{15}FO_4$

M= 278,28 g.mol-1

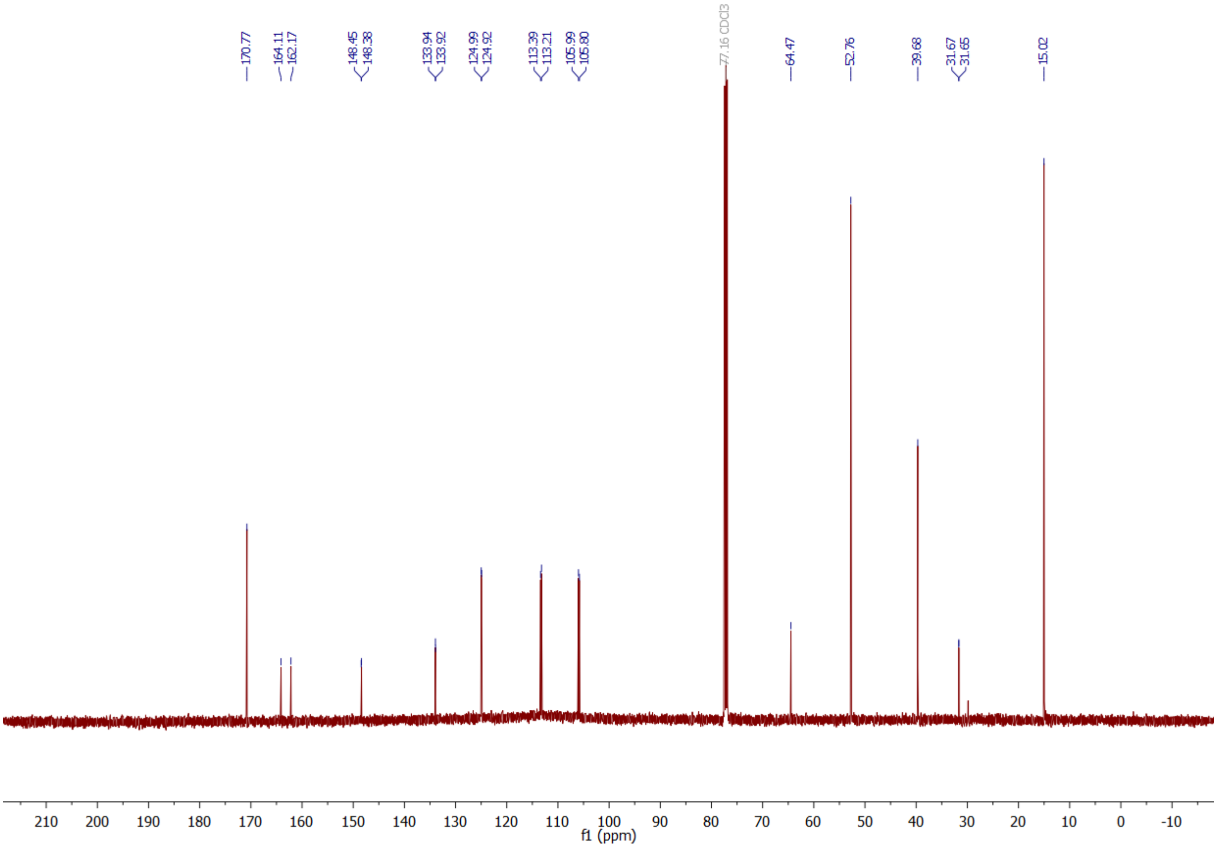

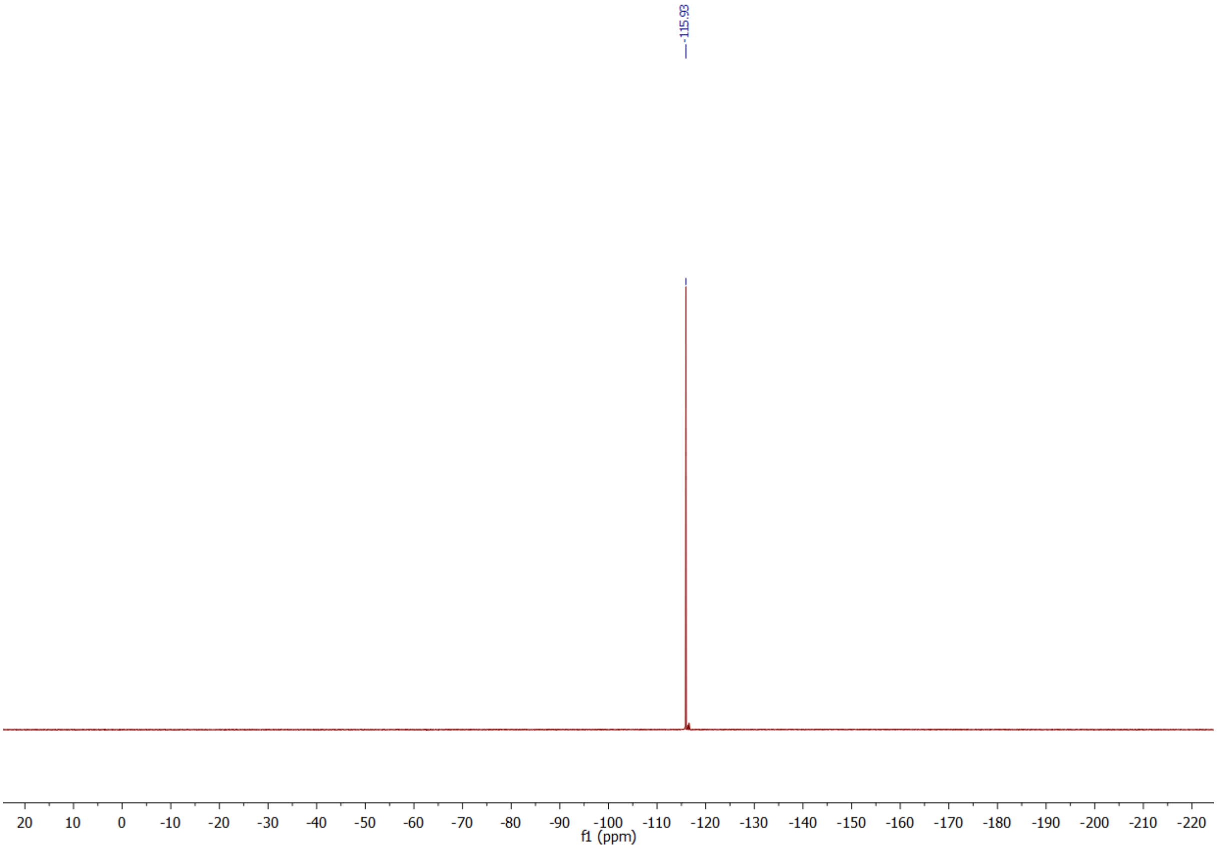
-115.93
20
10
0
-10
-20
-30
-40
-50
-60
-70
-80
-90
-100
-110
-120
-130
-140
-150
-160
-170
-180
-190
-200
-210
-220
f1 (ppm)

CO2Me
CO2Me
F
Me2N
O

2.45am
$C_{16}H_{18}FNO_5$
M= 323,32 g.mol-1

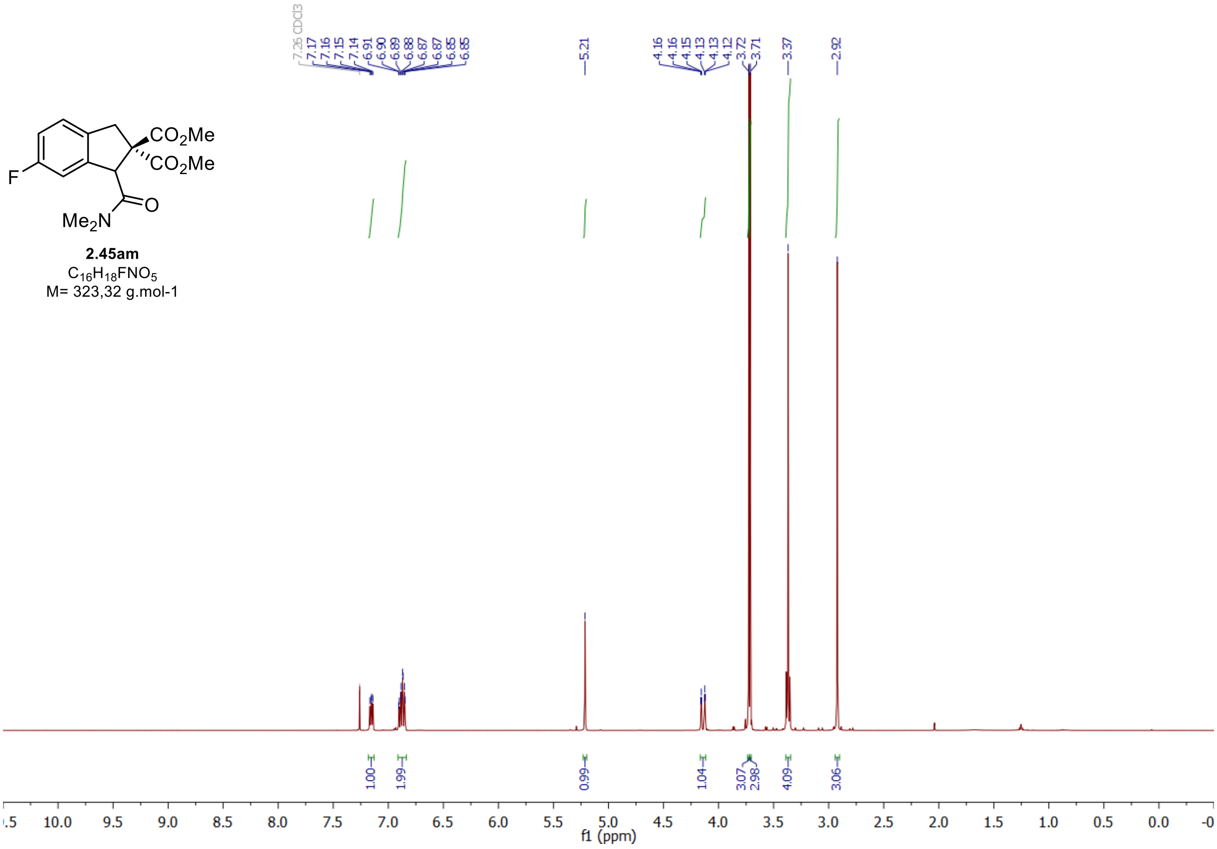

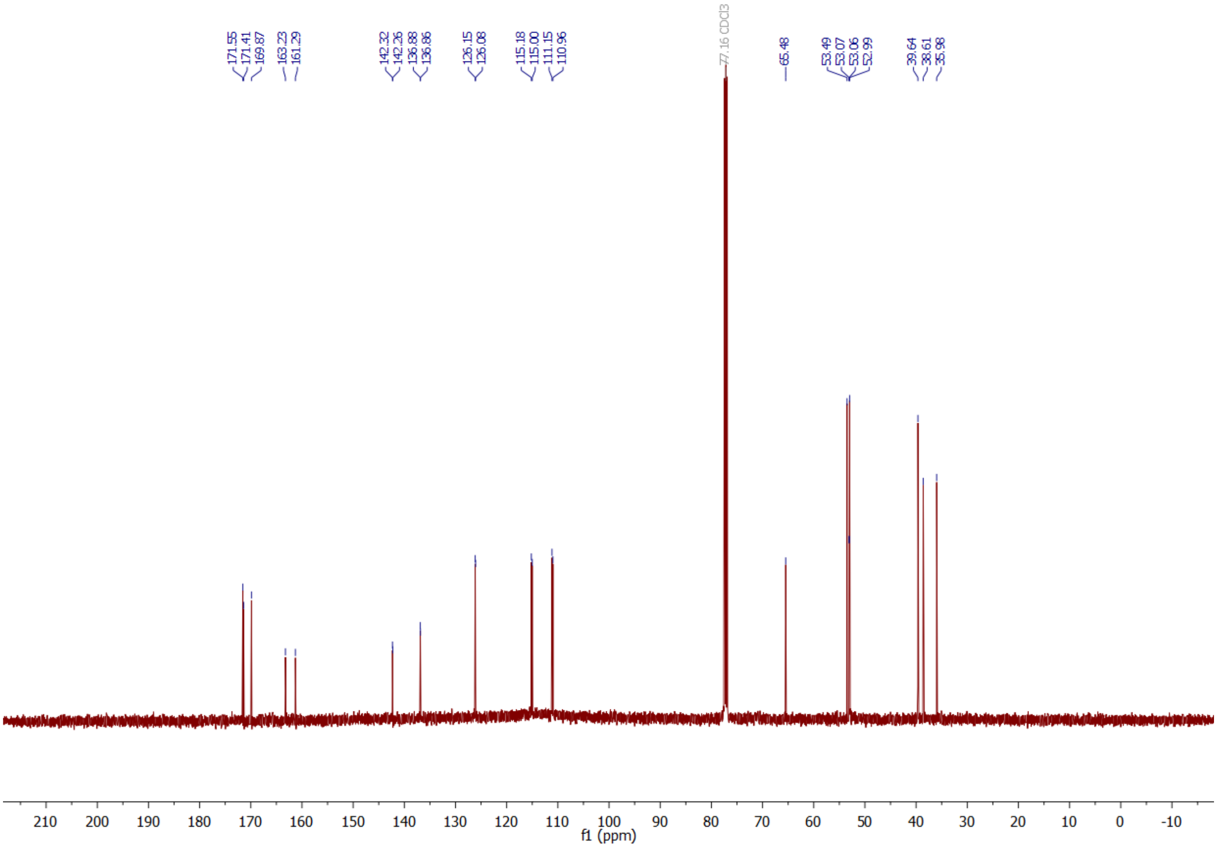

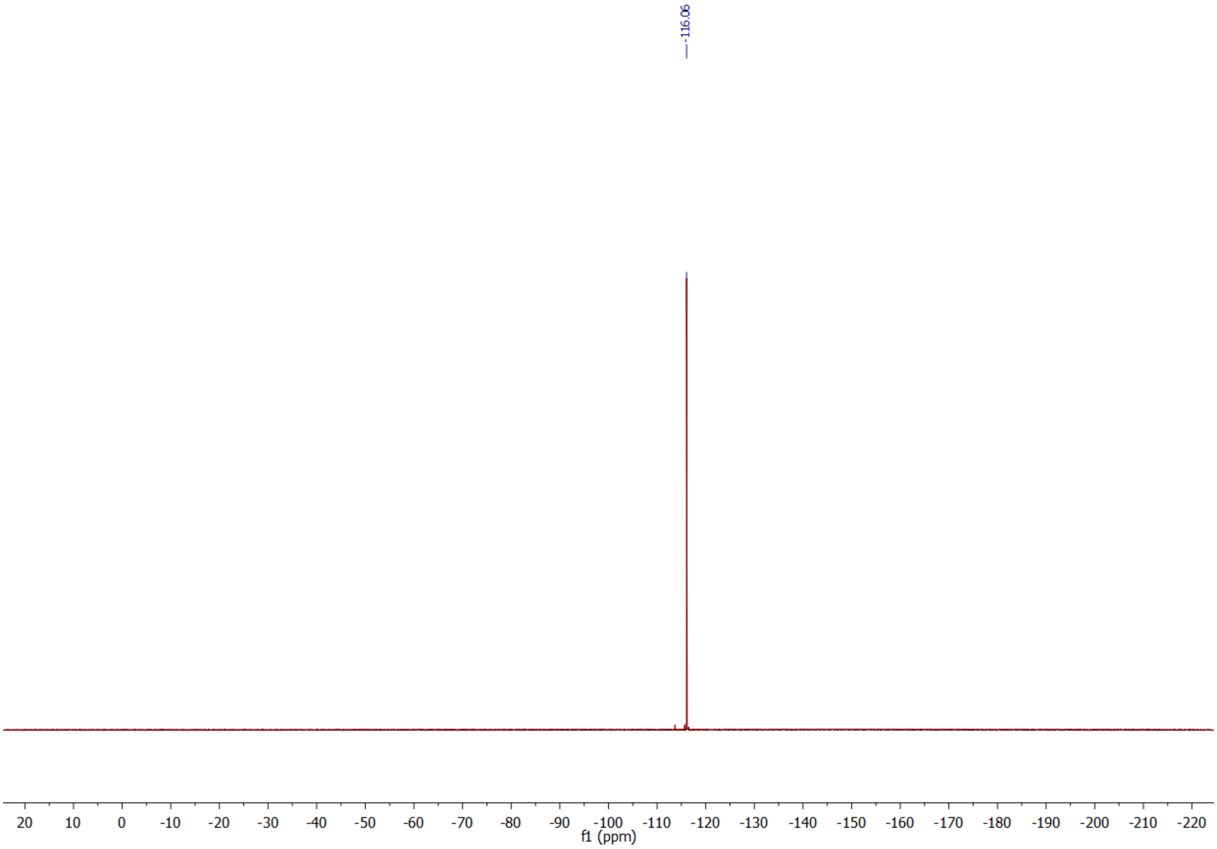
-116.06
20
10
0
-10
-20
-30
-40
-50
-60
-70
-80
-90
-100
-110
-120
-130
-140
-150
-160
-170
-180
-190
-200
-210
-220
f1 (ppm)

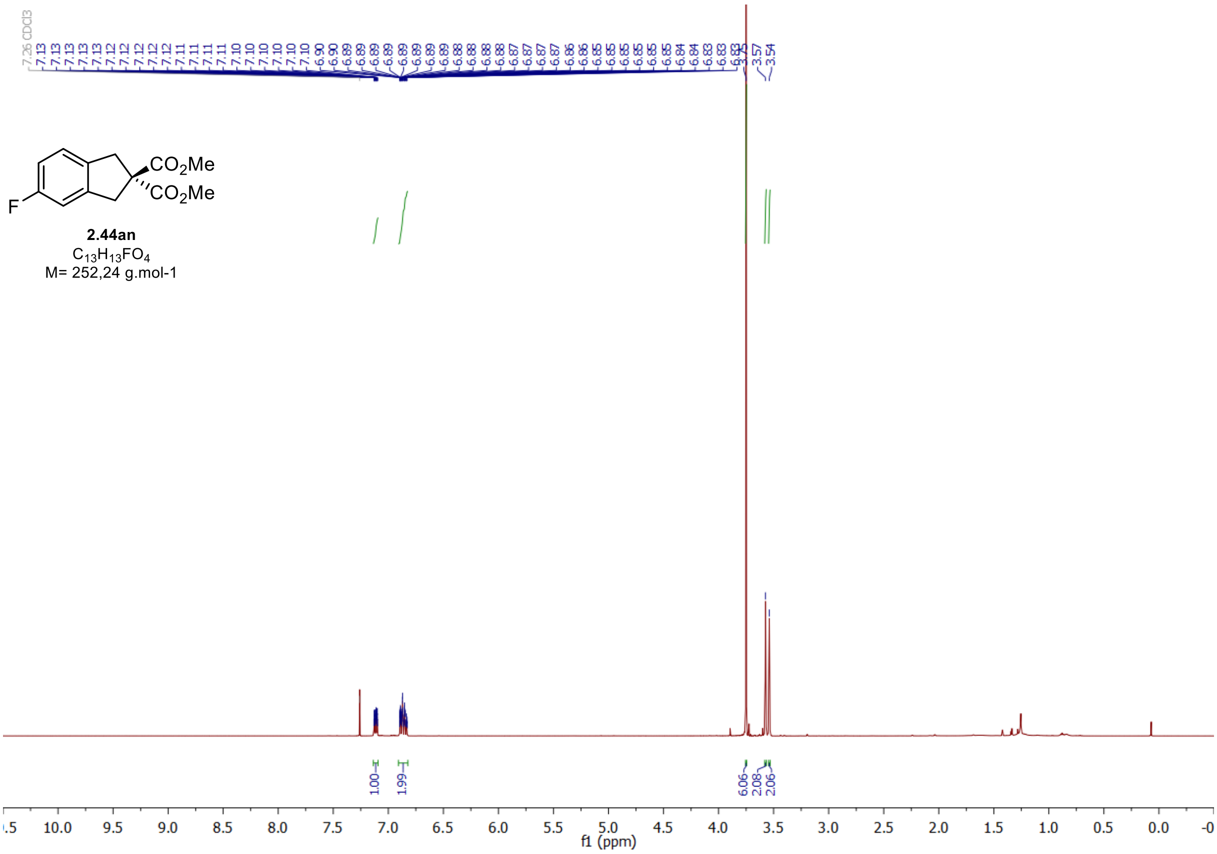

2.44an

$C_{13}H_{13}FO_4$

M= 252,24 g.mol-1

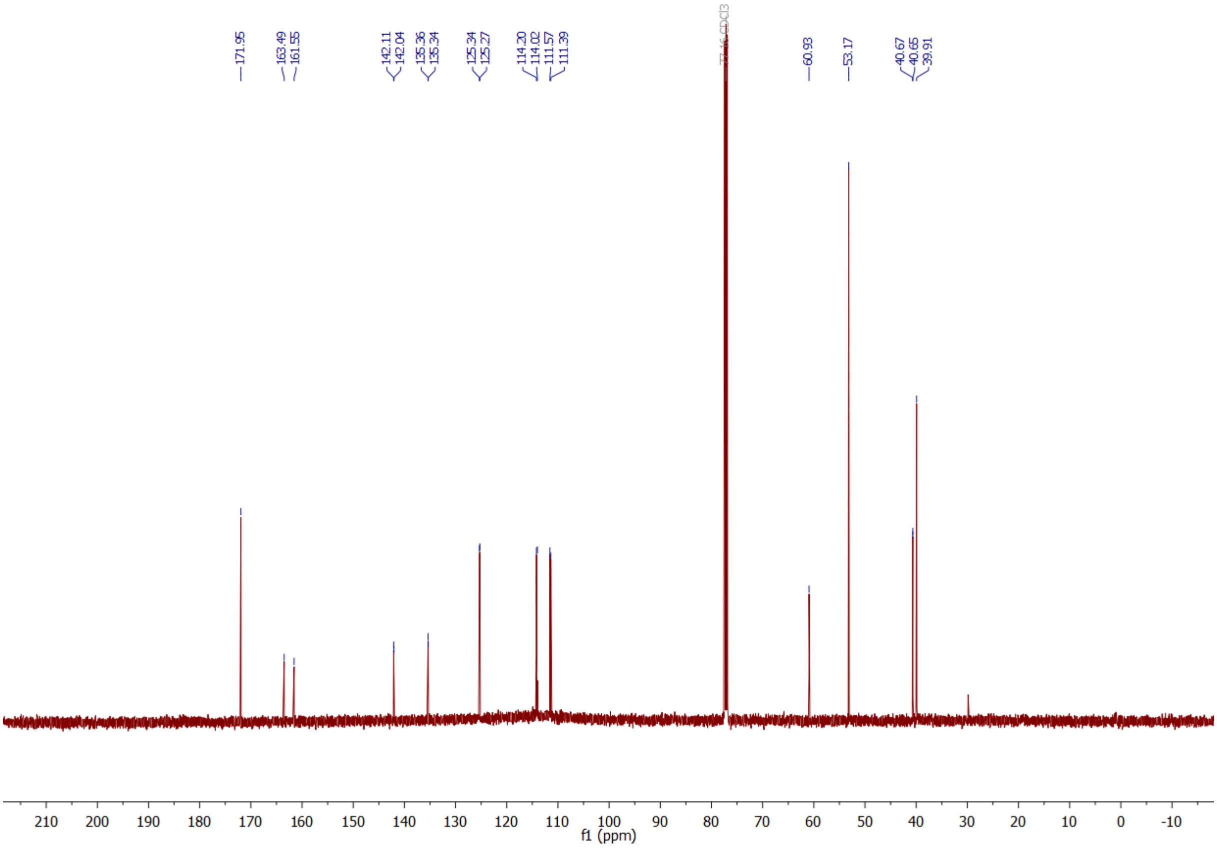

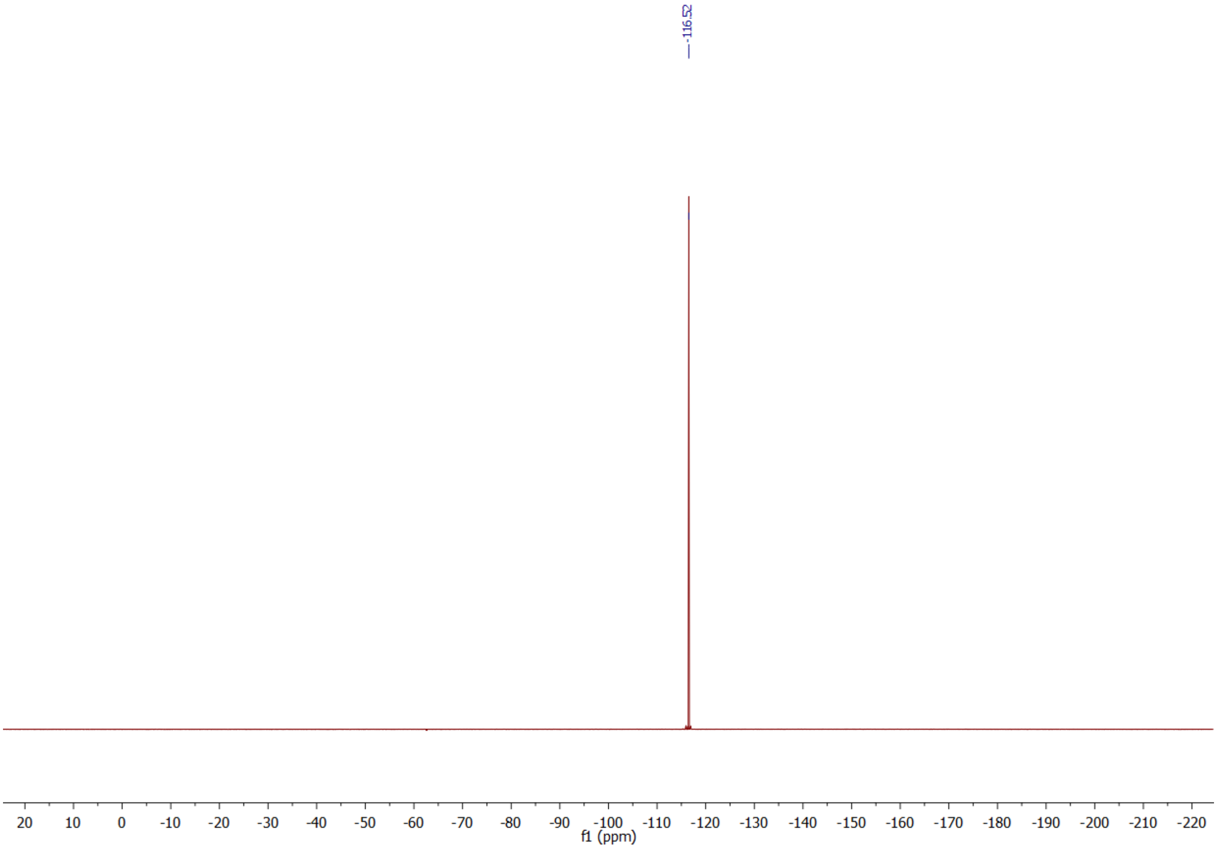
-116.52
20
10
0
-10
-20
-30
-40
-50
-60
-70
-80
-90
-100
-110
-120
-130
-140
-150
-160
-170
-180
-190
-200
-210
-220
f1 (ppm)

CO2Me
CO2Me
F

2.45ao
$C_{19}H_{17}FO_5$
M= 328,34 g.mol-1

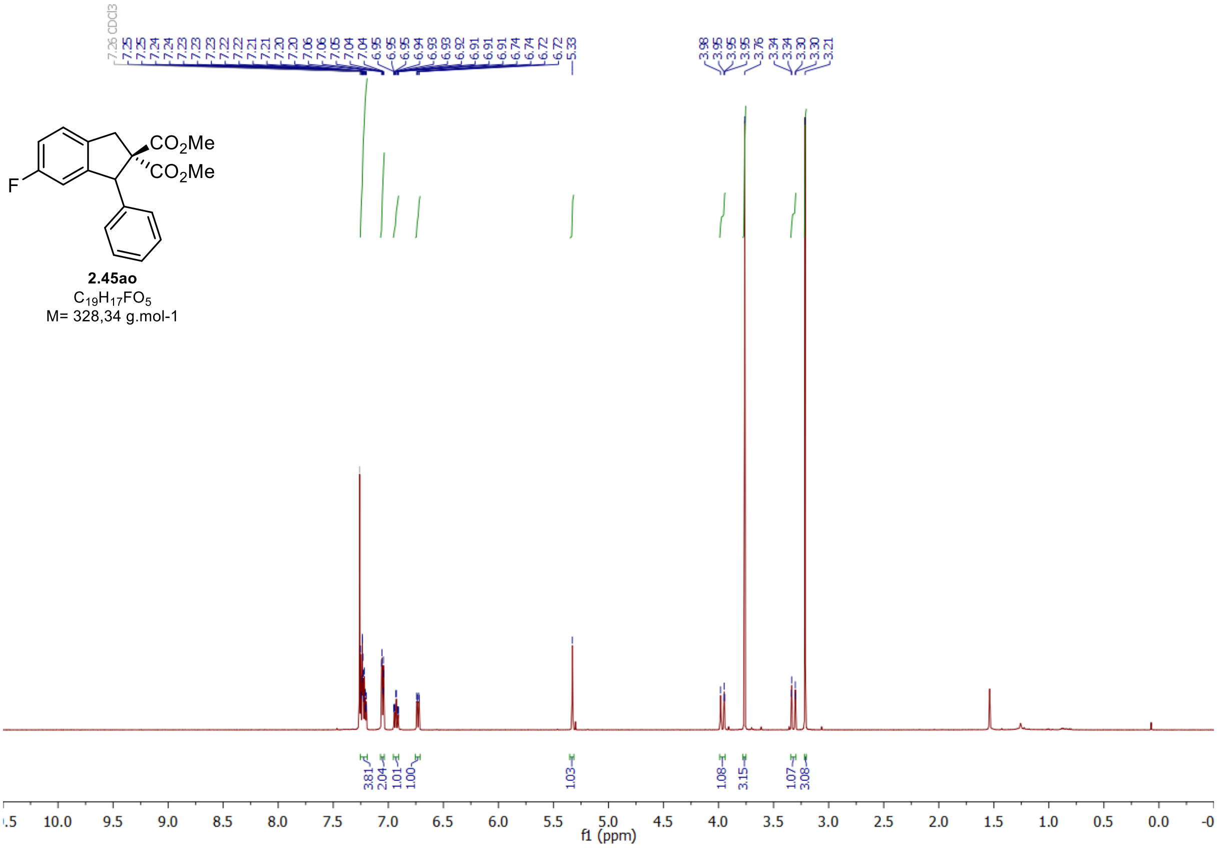

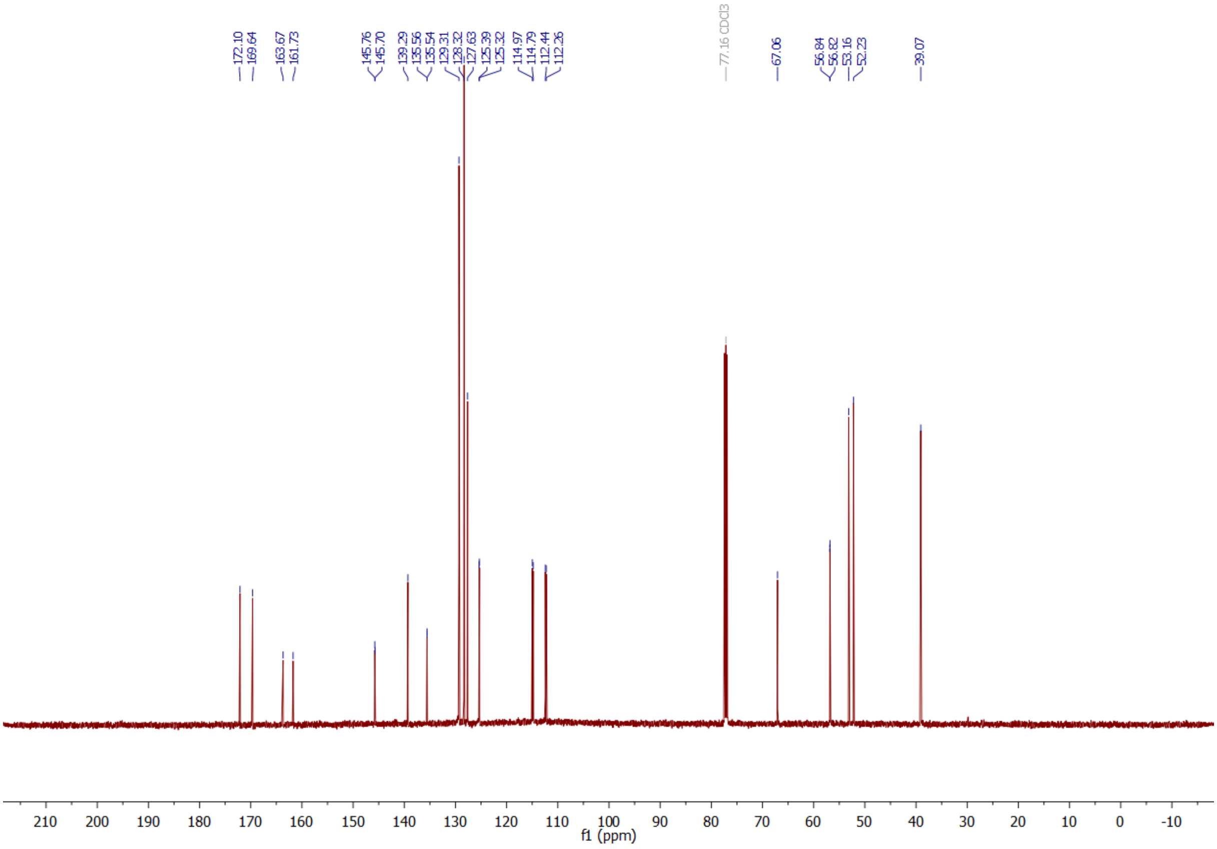

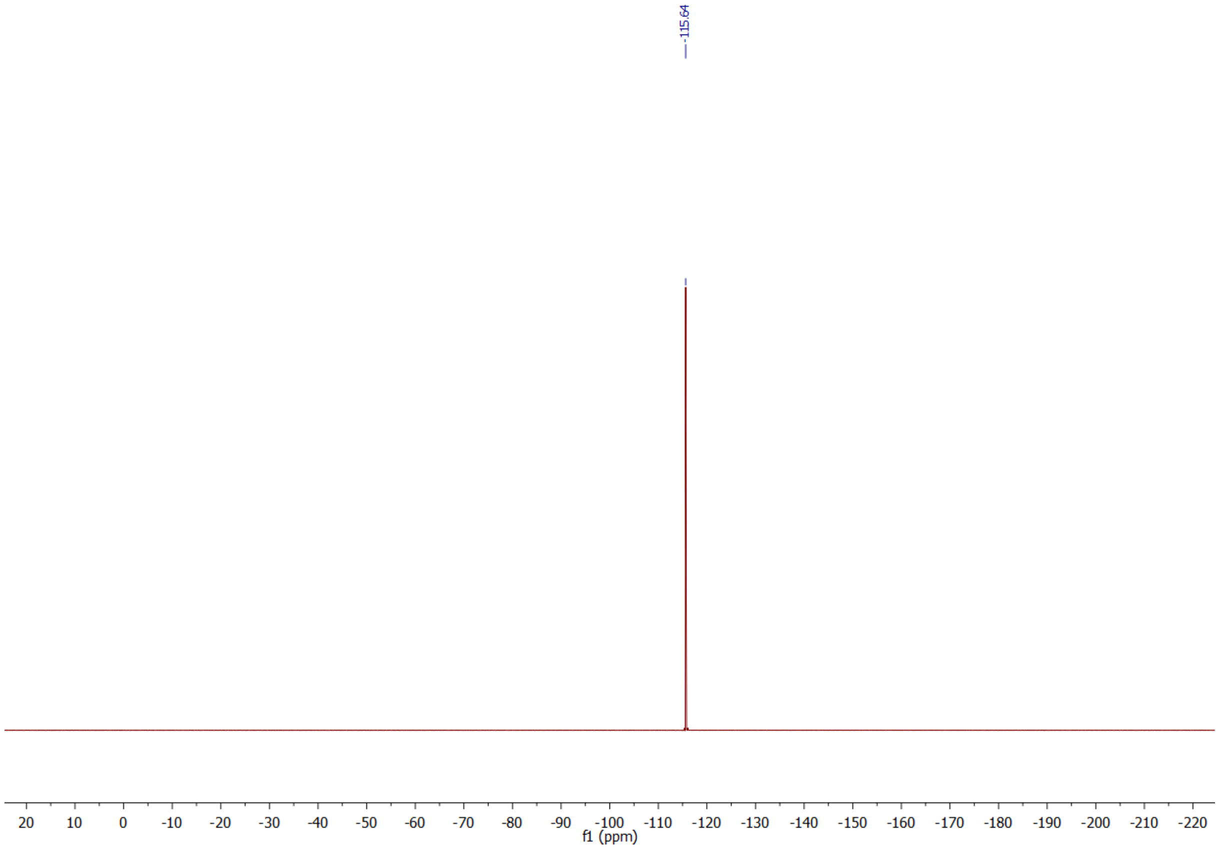
-115.64
20
10
0
-10
-20
-30
-40
-50
-60
-70
-80
-90
-100
-110
-120
-130
-140
-150
-160
-170
-180
-190
-200
-210
-220
f1 (ppm)

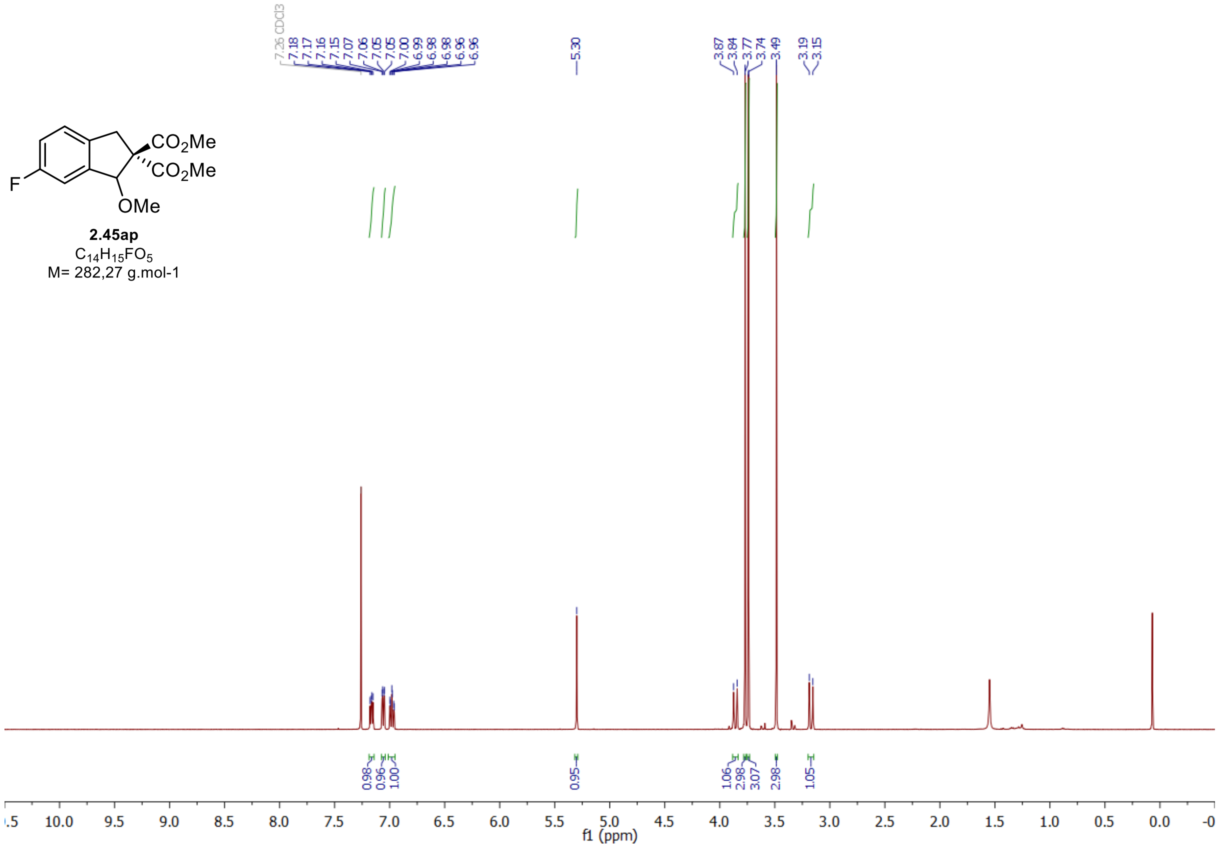

2.45ap
$C_{14}H_{15}FO_5$
M= 282,27 g.mol-1

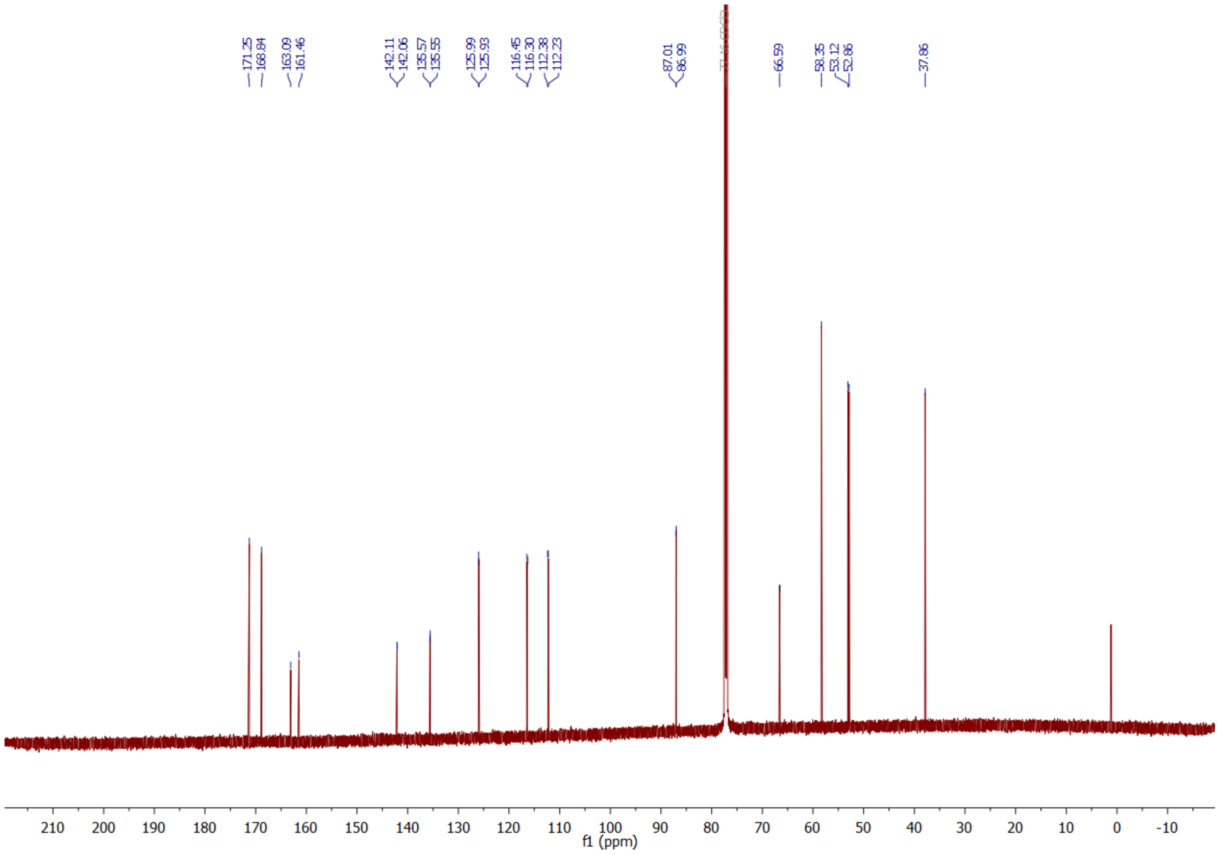

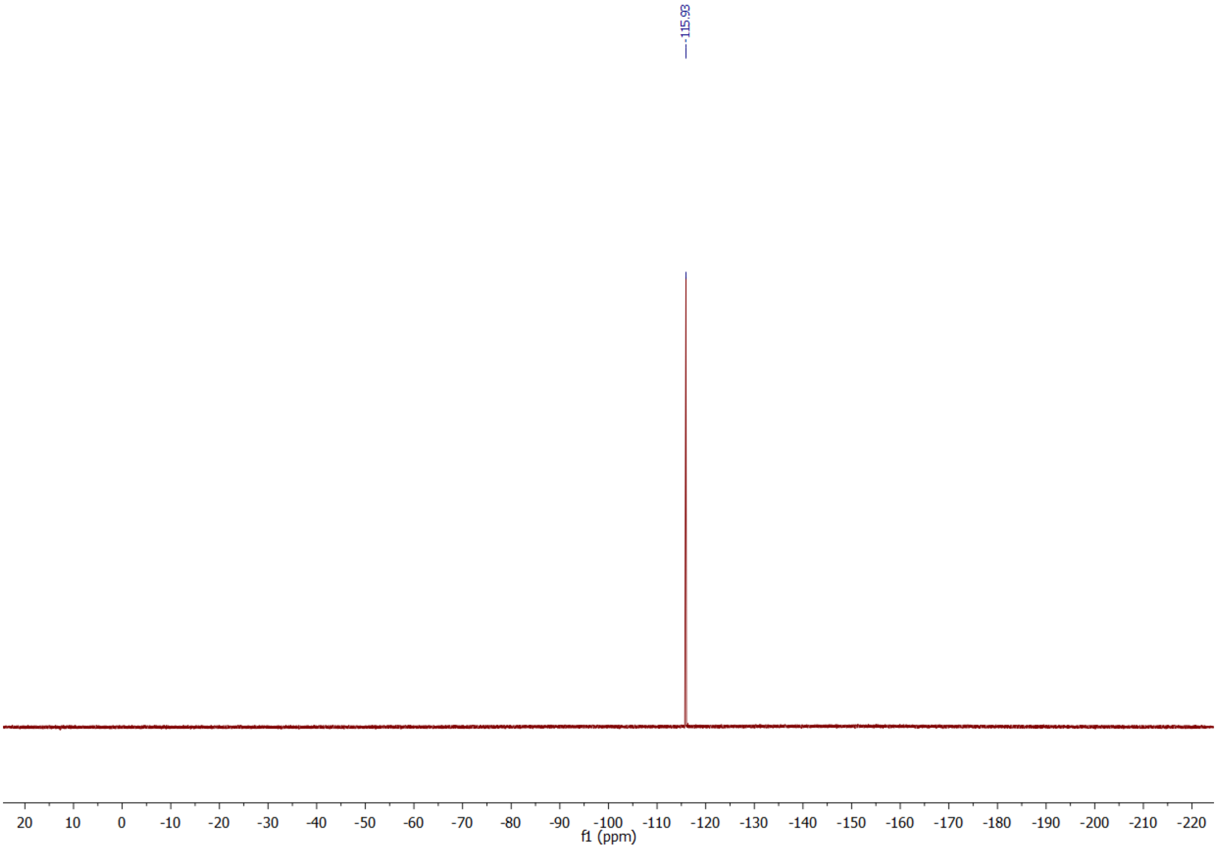
-115.93
20
10
0
-10
-20
-30
-40
-50
-60
-70
-80
-90
-100
-110
-120
-130
-140
-150
-160
-170
-180
-190
-200
-210
-220
f1 (ppm)

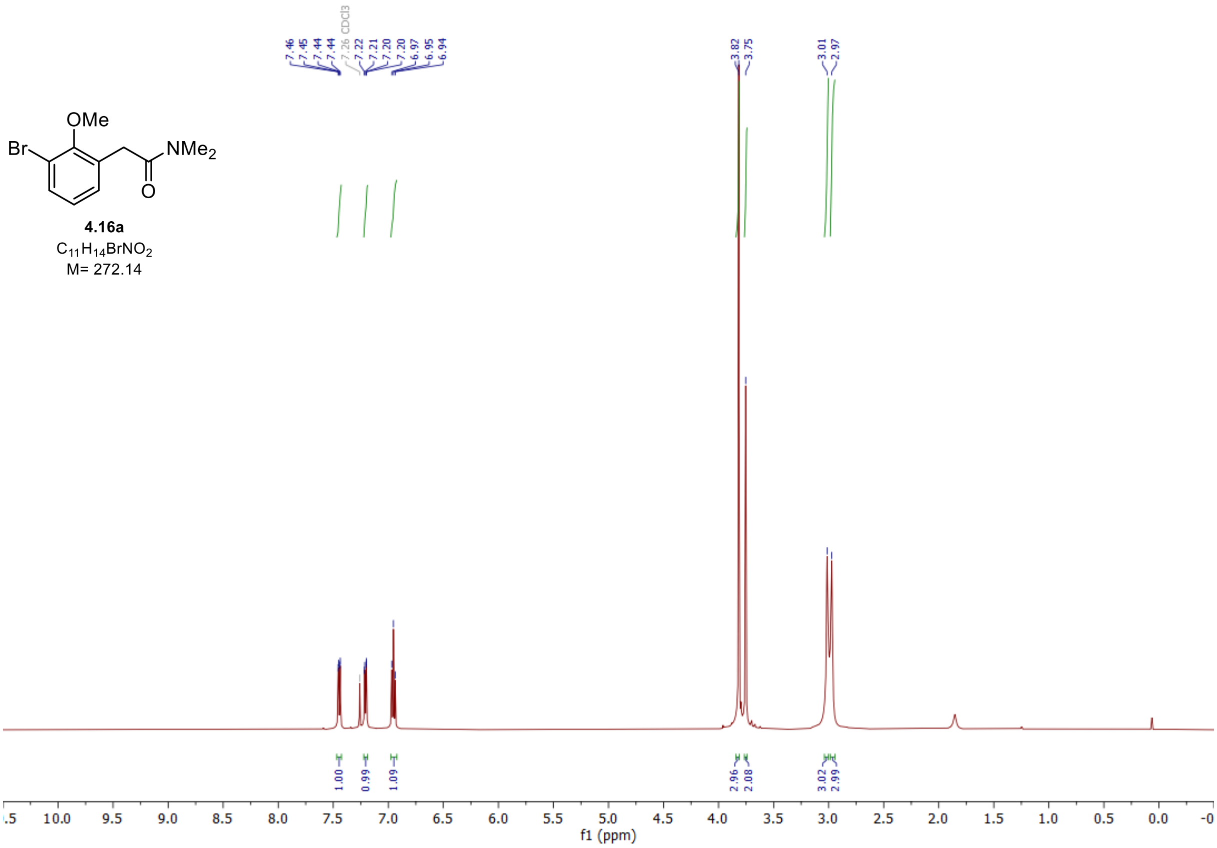

4.16a
$C_{11}H_{14}BrNO_2$
M= 272.14

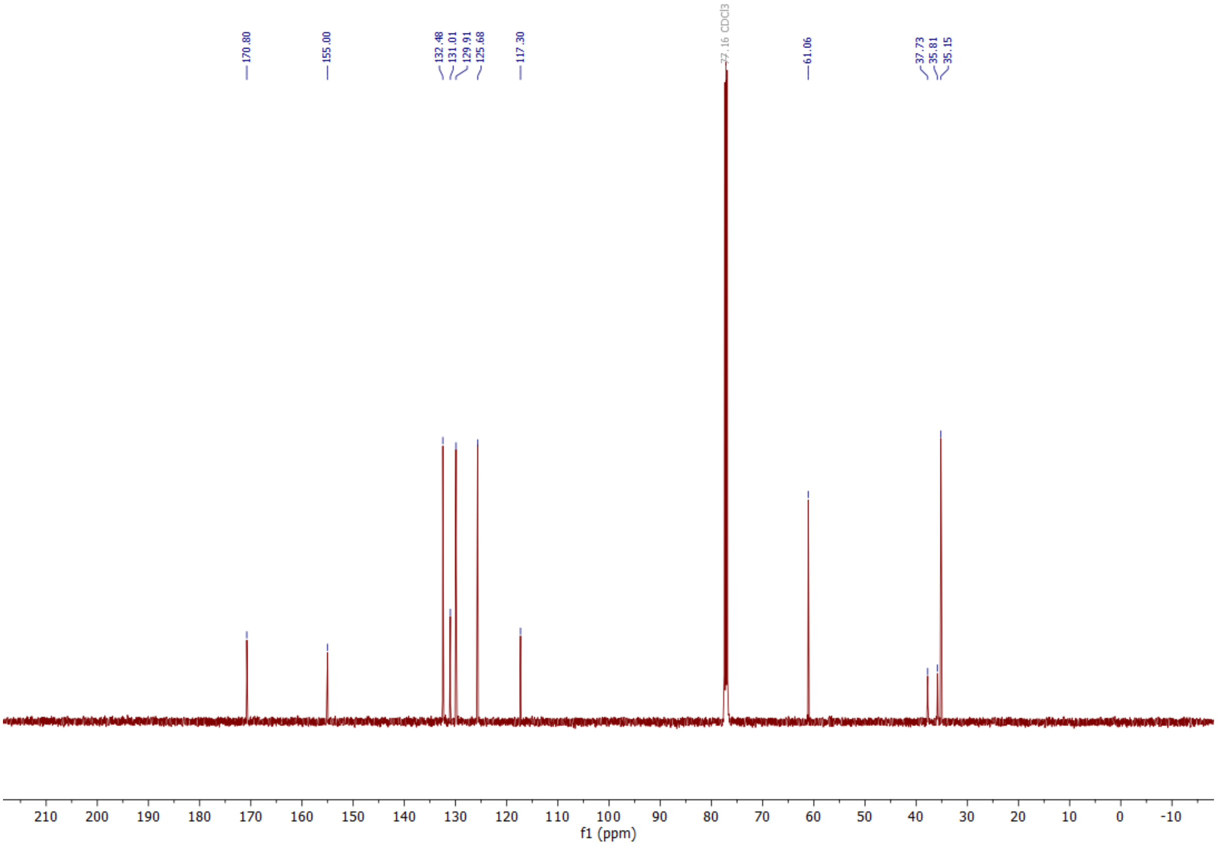

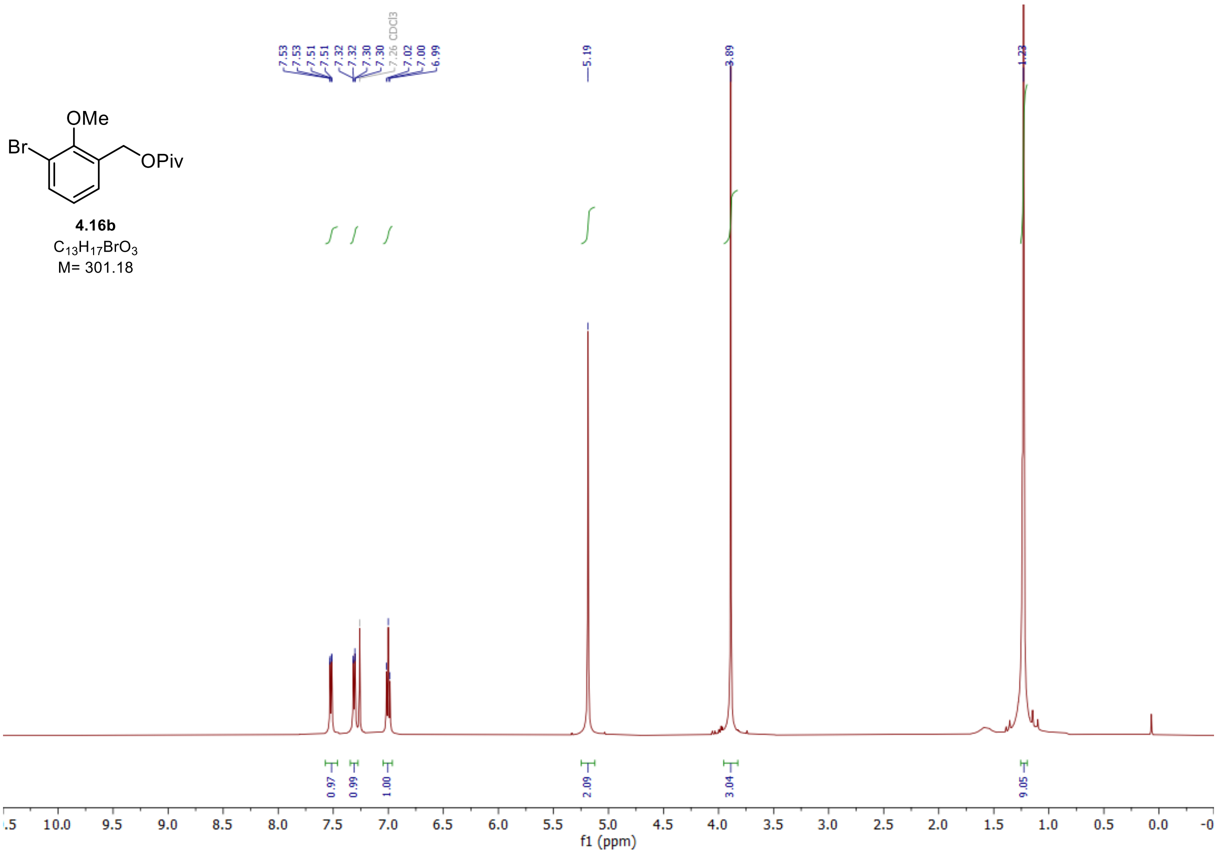

4.16b
$C_{13}H_{17}BrO_3$
M= 301.18

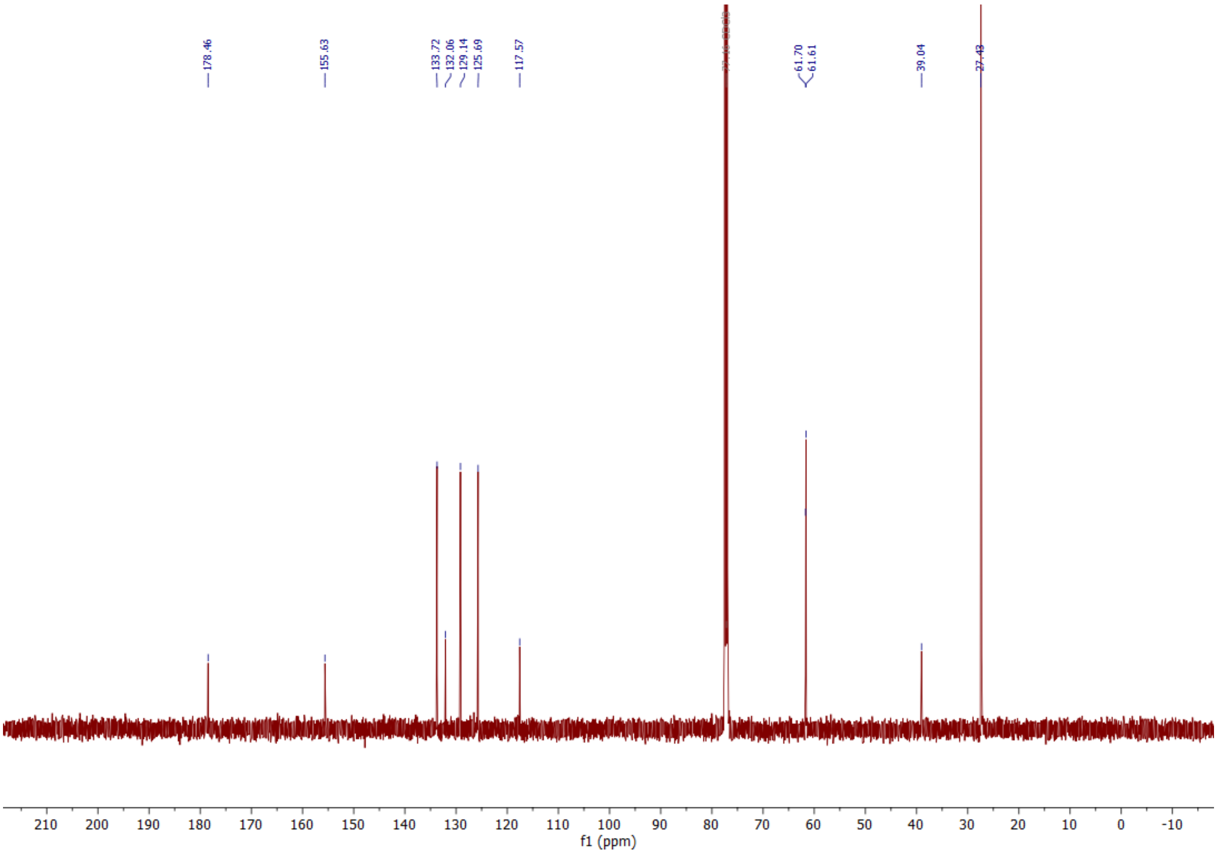

4.16c
$C_{10}H_{11}BrO_3$
M= 259.10

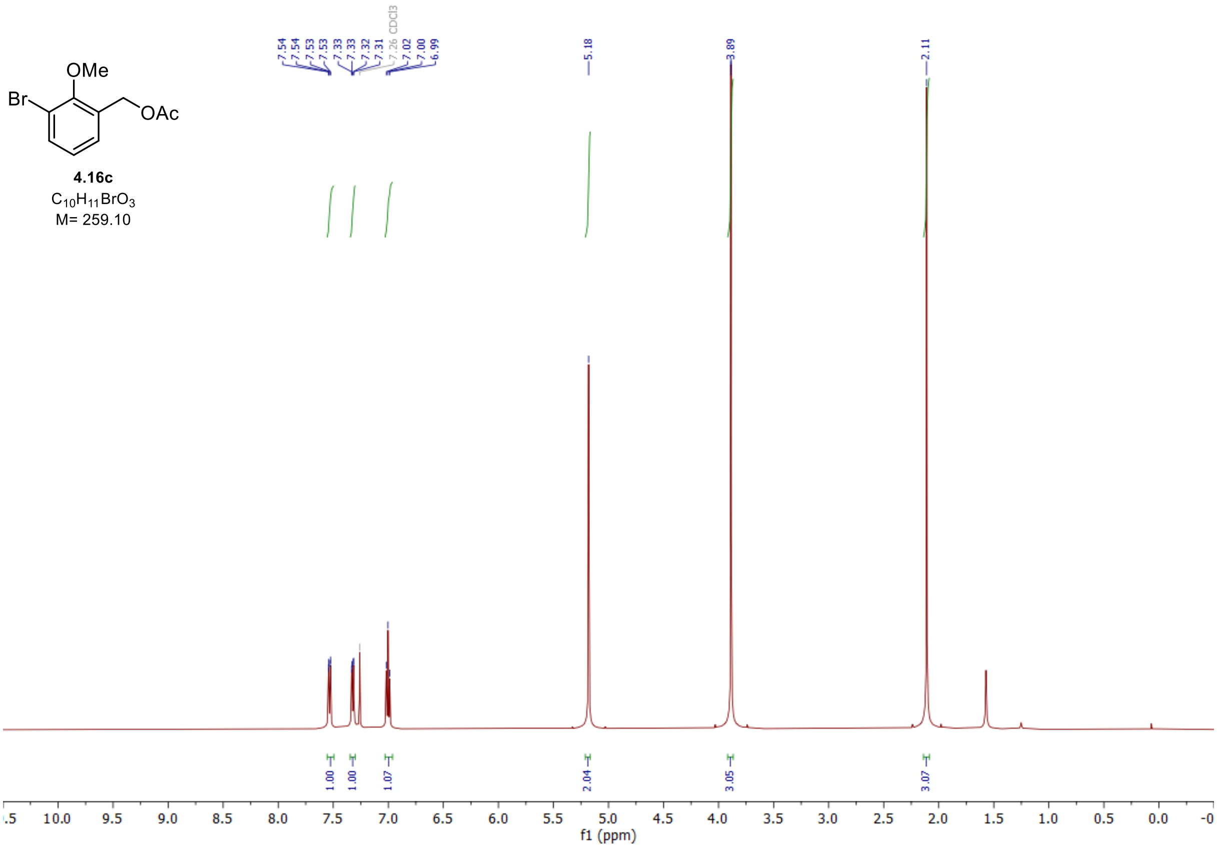

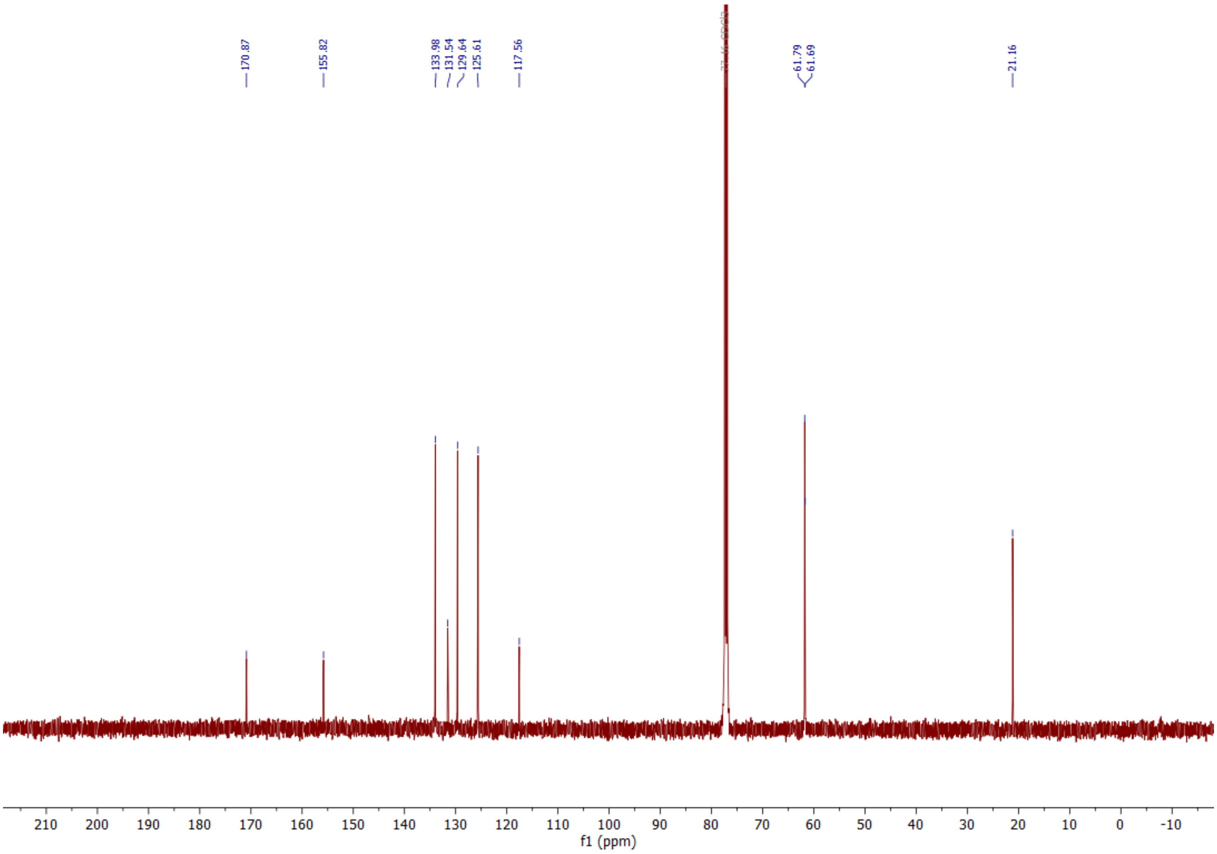

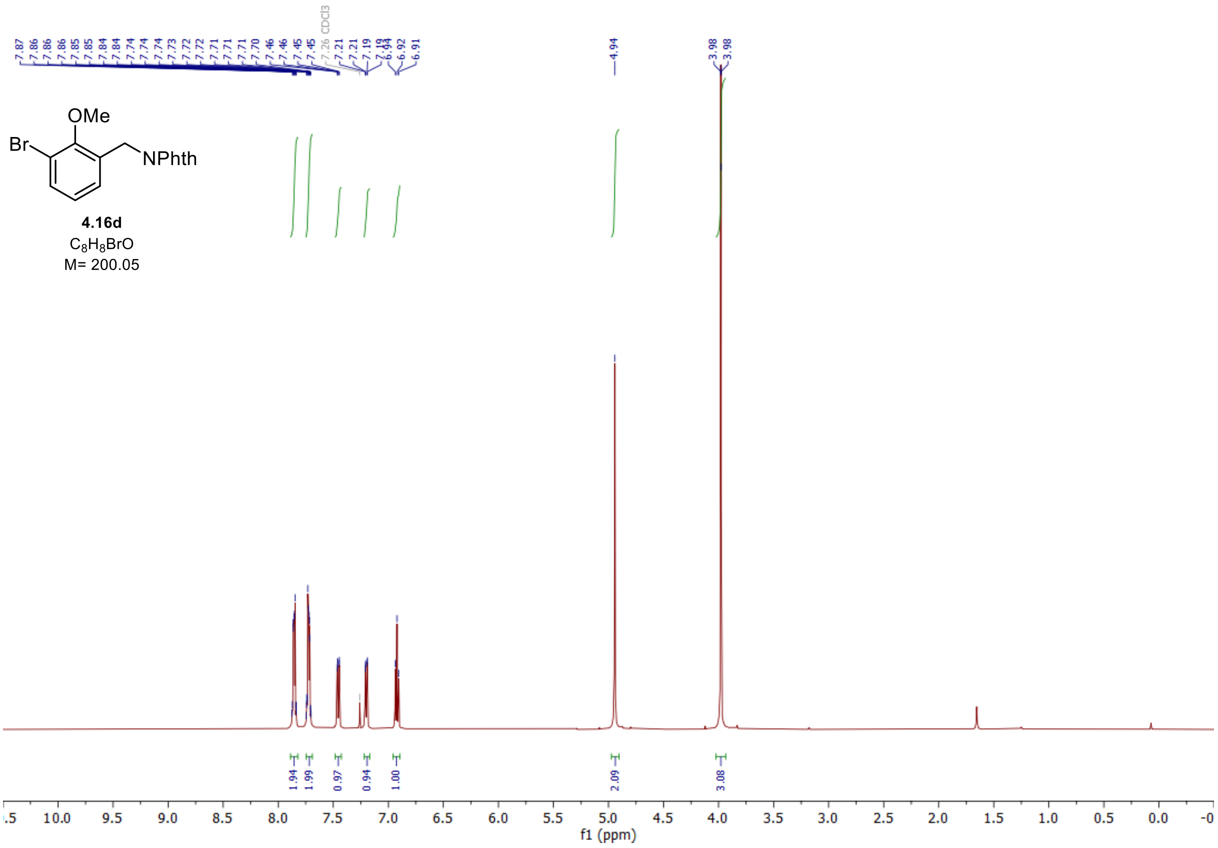

4.16d

C_8H_8BrO

M= 200.05

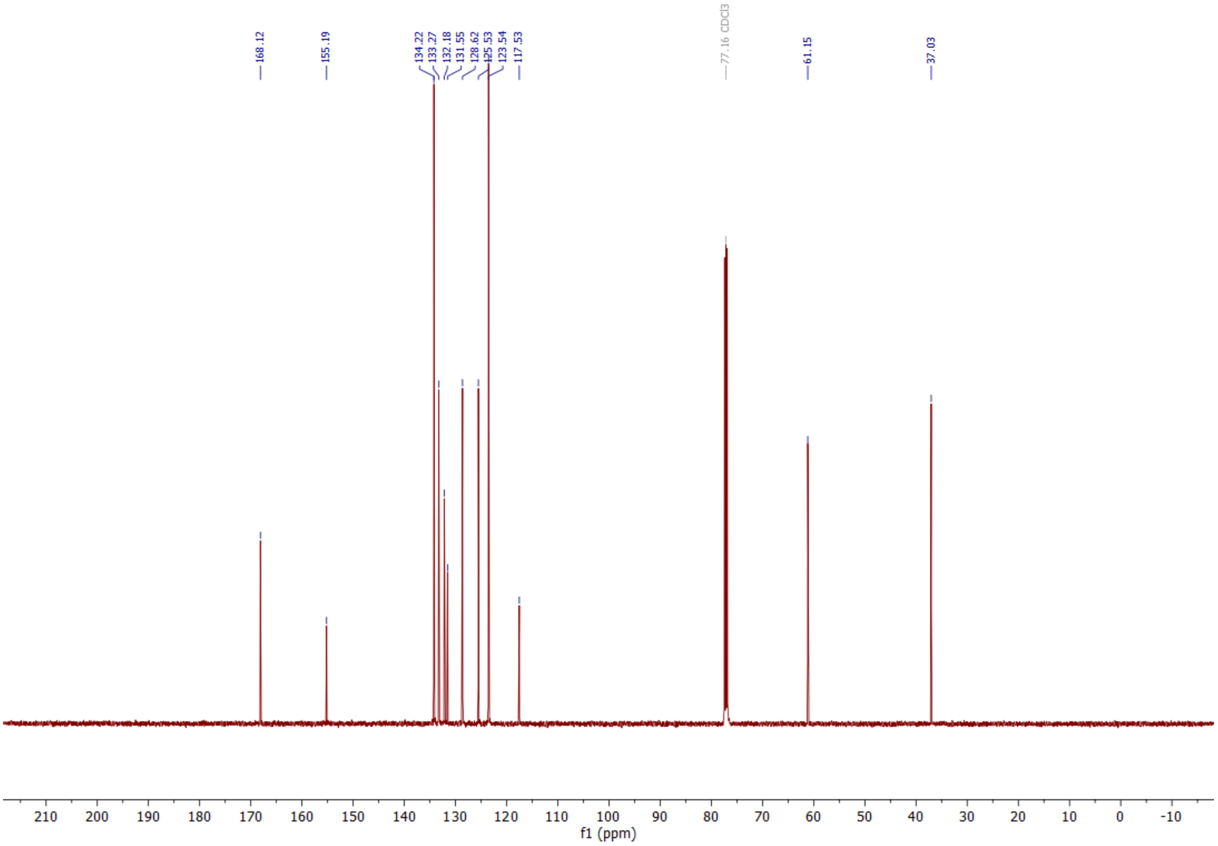

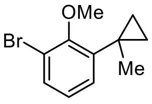

4.16e
$C_{11}H_{13}BrO$
M= 241.13

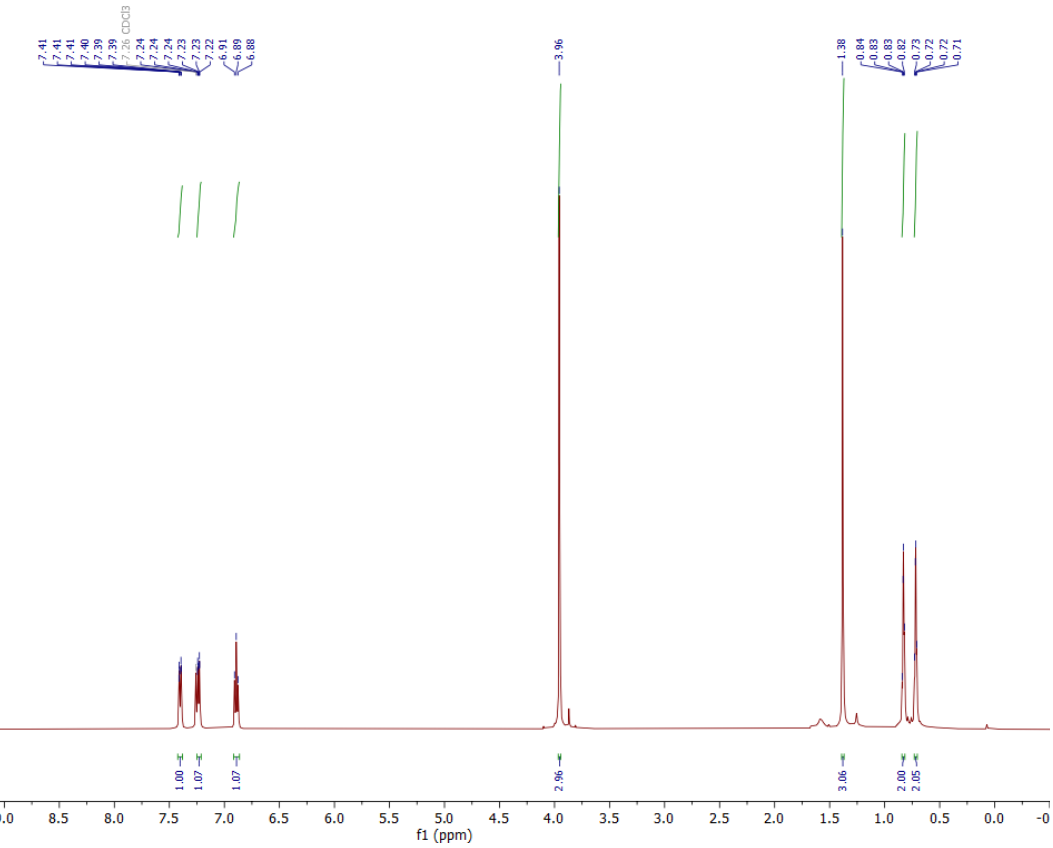

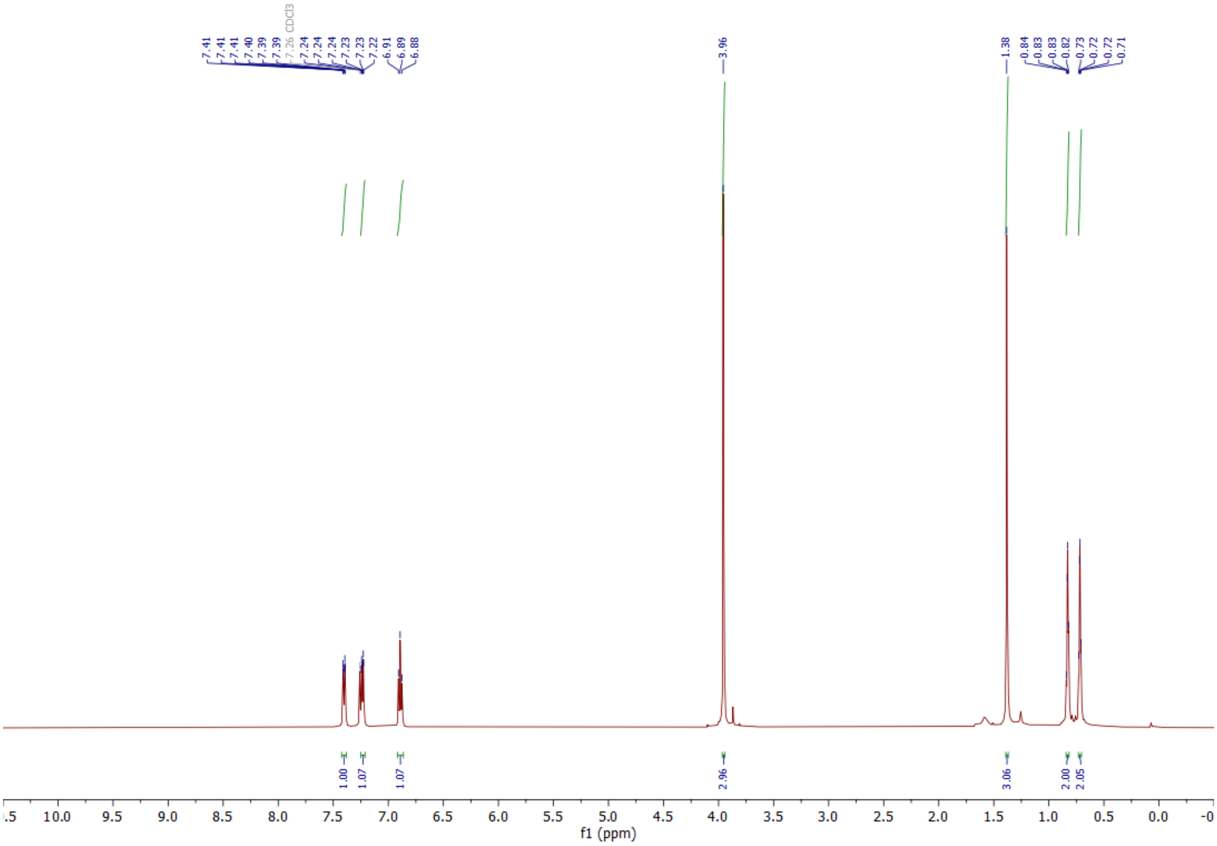

4.20a

$C_{11}H_{13}BrO_2$

M= 257.13

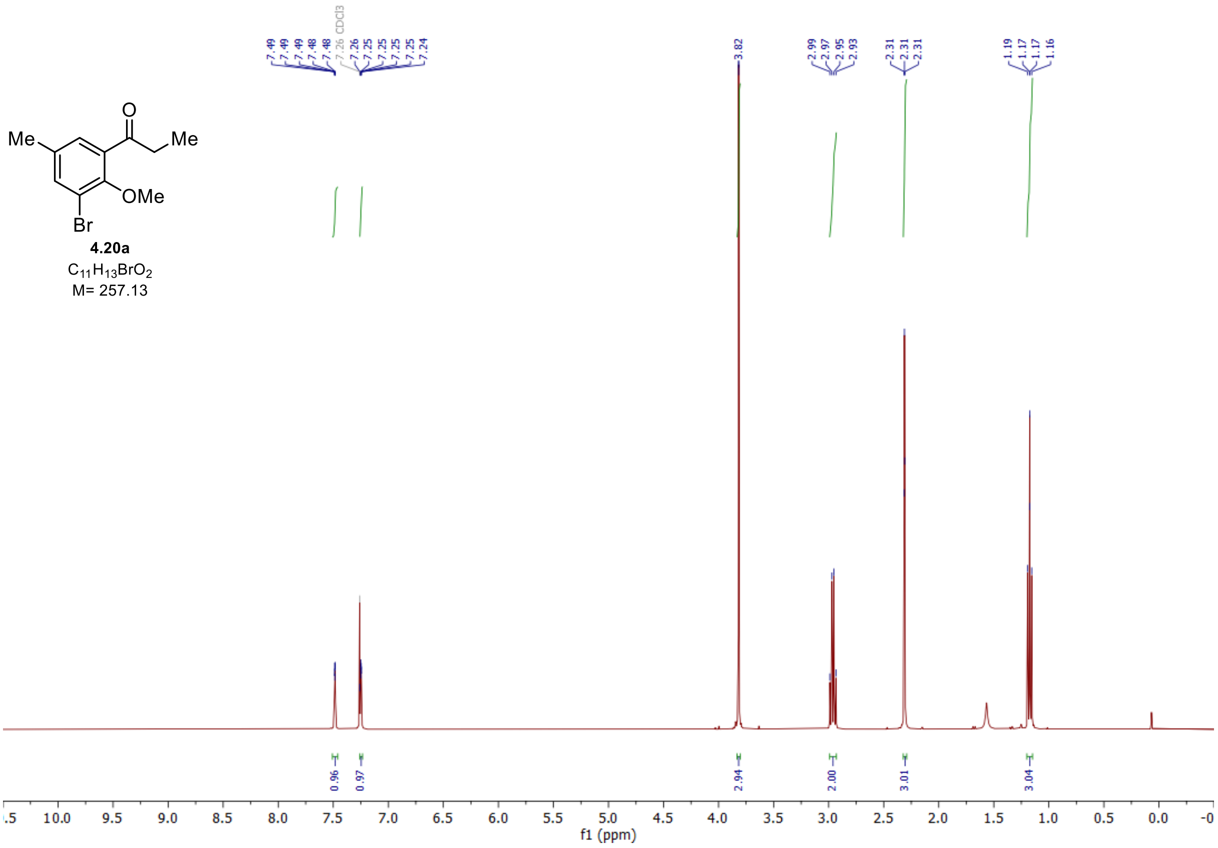

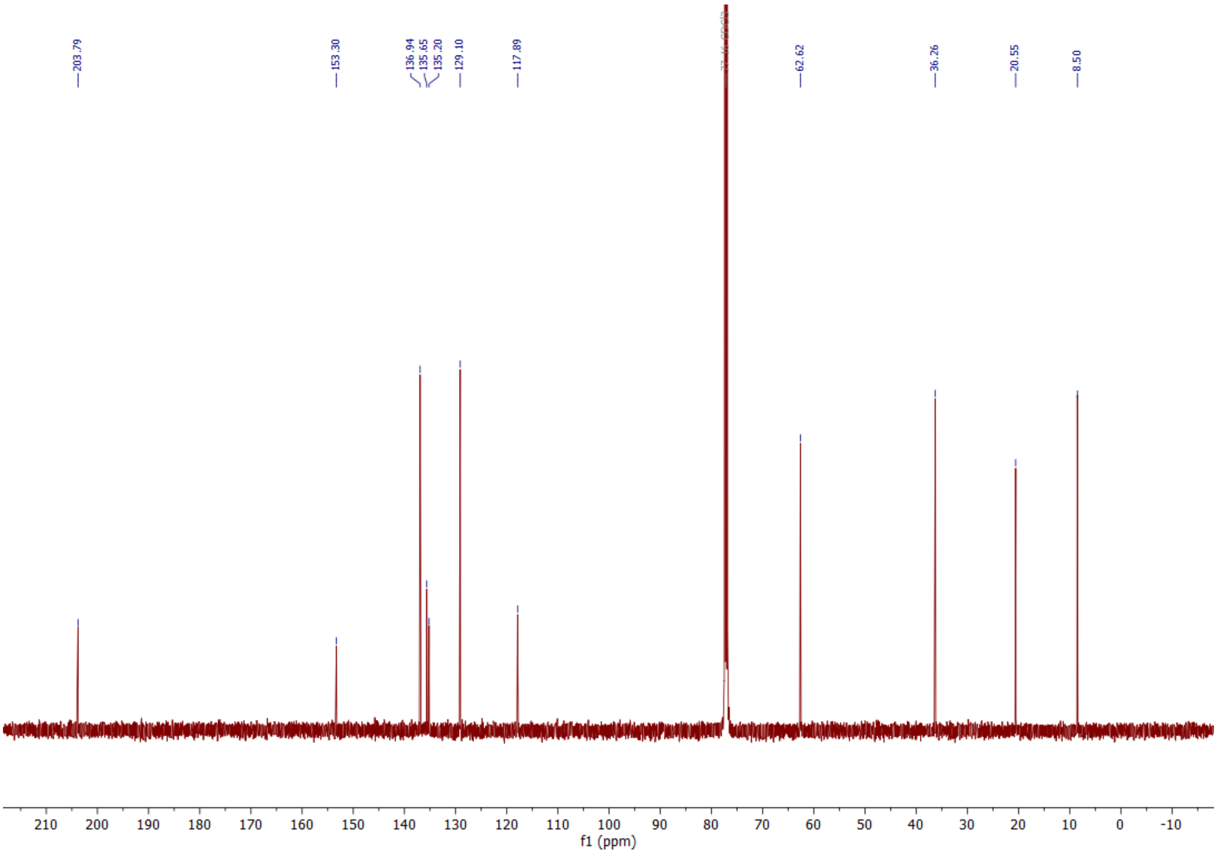

Marco Zuccarello

Personal Information

Place of birth: Basel-Stadt, Switzerland

Current address: University of Basel, St. Johanns-Ring 19, 4056 Basel (work affiliation)
Wasgenring 155, 4055 Basel (private affiliation)
Phone: +41 76 569 95 93
E-mail: marco.zuccarello@unibas.ch (work)
zuccarello.marco@gmail.com (private)
OrcID orcid.org/0000-0002-6081-8731
Nationality: Swiss/Italian

Research Experience

Oct 2018	**Doctoral Study at University of Basel** Supervision by Prof. Dr. Olivier Baudoin (olivier.baudoin@unibas.ch) Enantioselective Pd^0-Catalyzed methylene C(sp^3)–H activation reactions and mechanistic studies.
Feb – Sep 2018	**Master Thesis** Supervision by Prof. Dr. Olivier Baudoin Dr. Romain Melot (melot@kofo.mpg.de) Title: Enantioselective Synthesis of Substituted Indanes via Pd(0)-Catalyzed Methylene C(sp^3)–H Bond Activation
Aug – Sep 2017	**Research Project II** Supervision by Prof. Dr. Olivier Baudoin Title: Towards a Novel Family of Bifunctional NHC Ligands for Enantioselective C–H Activation
Aug – Sep 2016	**Research Project I** Supervision by Prof. Dr. Christof Sparr (christof.sparr@unibas.ch) Title: Synthesis of Electron-Deficient Tetra-Ketones for Atroposelective Arene-Forming Aldol Condensation

Education

Oct 2018 –	**Ph.D. studies** University of Basel, Switzerland Advisor: Prof. Dr. O. Baudoin
Sep 2017 – Aug 2018	**M.Sc. in Chemistry** University of Basel Chemistry, Switzerland Supervisors: Dr. R. Melot and Prof. Dr. O. Baudoin Final grade 5.7 out of 6

Feb 2014 – Jul 2017	**B.Sc in Chemistry** University of Basel, Switzerland Final grade 5.2 out of 6

Employment history

Oct 2018 –	**University of Basel** Doctoral candidate Advisor*:* Prof. Dr. O. Baudoin

Institutional responsibilities

Oct 2018 –	Floor evacuation responsible
Dec 2016 – Oct 2018	Vice president of the “Verband Basler Chemiestudierender (VBC)”

Supervision of Junior Researchers

Feb – Apr 2022	**Research Mentor** Domenic Kronenberg (internship on M.Sc. level)
Sep – Dec 2020	**Research Mentor** Géraldine Kiechler (internship on M.Sc. level)
Aug – Nov 2019	**Research Mentor** Alex Cavadini (internship on M.Sc. level)
May – June 2019	**Research Mentor** Andreas Ostertag (internship on B.Sc. level)

Teaching

Feb – June 2021	**Supervision of Advanced Chemistry Practical Course** Laboratory course for 6th semester Bachelor students
Feb – June 2020	**Supervision of Advanced Chemistry Practical Course** Laboratory course for 6th semester Bachelor students
Feb – June 2019	**Supervision of Advanced Chemistry Practical Course** Laboratory course for 6th semester Bachelor students

Memberships in Panels

Jan 2020 – Jan 2021	Co-Author of the “Swiss Science Concentrates” published in *Chimia*

Active Memberships

Oct 2018	Member of the Swiss Chemical Society

Personal Skills

Languages:

Italian (Mother tongue)	**Swissgerman** (fluent)	**Spanish** (basic level)
German (fluent)	**English** (fluent)	**French** (basic level)

Instruments:

- Operation and maintenance of high-pressure liquid chromatography (HPLC) systems on analytical and preparative scale.
- Operation of GC-MS, TLC-MS, Glovebox

Publications in Peer-Reviewed Scientific Journals

Melot, R.†; **Zuccarello, M.†**; Cavalli, D.; Niggli, N.; Baudoin, O. "Pd^0-catalyzed Enantioselective Intramolecular Arylation of Enantiotopic Secondary C–H Bonds", *Angew. Chem. Int. Ed.* **2021**, *60*, 7245–7250. († denotes equal contribution). Link

Contribution to Conferences

25th Aug. 2020	Melot, R.†; **Zuccarello, M.†**; Cavalli, D.; Niggli, N.; Baudoin, O. "Pd^0-catalyzed Enantioselective Intramolecular Arylation of Enantiotopic Secondary C–H Bonds" *Poster presentation*, SCS Fall Meeting 2020 (online conference), Bern, Switzerland, 2020.
30th Oct. 2020	Melot, R.†; **Zuccarello, M.†**; Cavalli, D.; Niggli, N.; Baudoin, O. "Pd^0-catalyzed Enantioselective Intramolecular Arylation of Enantiotopic Secondary C–H Bonds" *Poster presentation*, SCS 3rd Swiss Industrial Chemistry Symposium (online conference), Switzerland, 2020.
10th Sep. 2021	Melot, R.†; **Zuccarello, M.†**; Cavalli, D.; Niggli, N.; Baudoin, O. "Pd^0-catalyzed Enantioselective Intramolecular Arylation of Enantiotopic Secondary C–H Bonds" *Poster presentation* SCS Fall Meeting 2021 (online conference), Switzerland, 2021.
3-8th Jul. 2022	Melot, R.†; **Zuccarello, M.†**; Cavalli, D.; Niggli, N.; Baudoin, O. "Pd^0-catalyzed Enantioselective Intramolecular Arylation of Enantiotopic Secondary C–H Bonds" *Poster presentation*, 17th Belgian Organic Synthesis Symposium (BOSS XVII), Namur, Belgium, 2022.